



This document was produced  
by scanning the original publication.

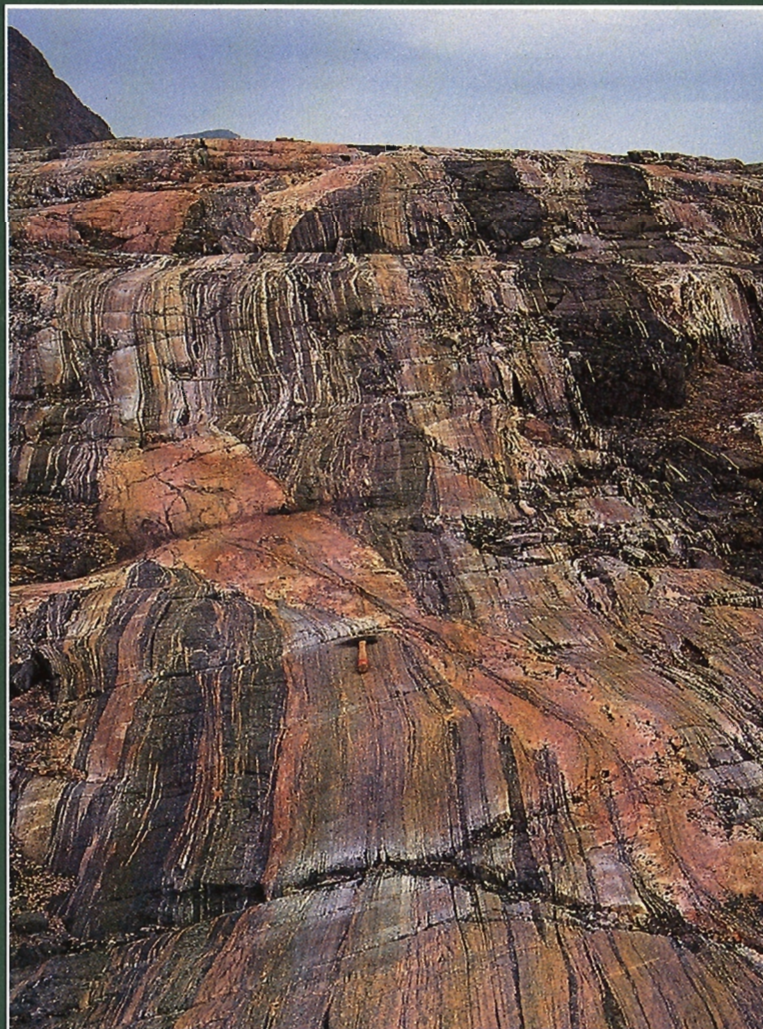
Ce document est le produit d'une  
numérisation par balayage  
de la publication originale.

GEOLOGICAL SURVEY OF CANADA  
COMMISSION GÉOLOGIQUE DU CANADA

**CURRENT RESEARCH 1994-C  
CANADIAN SHIELD**

---

**RECHERCHES EN COURS 1994-C  
BOUCLIER CANADIEN**



1994



Natural Resources  
Canada

Ressources naturelles  
Canada

Canada



## **NOTICE TO LIBRARIANS AND INDEXERS**

The Geological Survey's Current Research series contains many reports comparable in scope and subject matter to those appearing in scientific journals and other serials. Most contributions to Current Research include an abstract and bibliographic citation. It is hoped that these will assist you in cataloguing and indexing these reports and that this will result in a still wider dissemination of the results of the Geological Survey's research activities.

## **AVIS AUX BIBLIOTHÉCAIRES ET PRÉPARATEURS D'INDEX**

La série Recherches en cours de la Commission géologique contient plusieurs rapports dont la portée et la nature sont comparables à ceux qui paraissent dans les revues scientifiques et autres périodiques. La plupart des articles publiés dans Recherches en cours sont accompagnés d'un résumé et d'une bibliographie, ce qui vous permettra, on l'espère, de cataloguer et d'indexer ces rapports, d'où une meilleure diffusion des résultats de recherche de la Commission géologique.



GEOLOGICAL SURVEY OF CANADA  
COMMISSION GÉOLOGIQUE DU CANADA

**CURRENT RESEARCH 1994-C**  
**CANADIAN SHIELD**

---

**RECHERCHES EN COURS 1994-C**  
**BOUCLIER CANADIEN**

**1994**



©Minister of Energy, Mines and Resources Canada 1994

Available in Canada through  
authorized bookstore agents and other bookstores

or by mail from

Canada Communication Group - Publishing  
Ottawa, Canada K1A 0S9

and from

Geological Survey of Canada offices:

601 Booth Street  
Ottawa, Canada K1A 0E8

3303-33rd Street N.W.,  
Calgary, Alberta T2L 2A7

100 West Pender Street  
Vancouver, B.C. V6B 1R8

A deposit copy of this publication is also available for reference  
in public libraries across Canada

Cat. No. M44-1994/1  
ISBN 0-660-58982-6

Price subject to change without notice

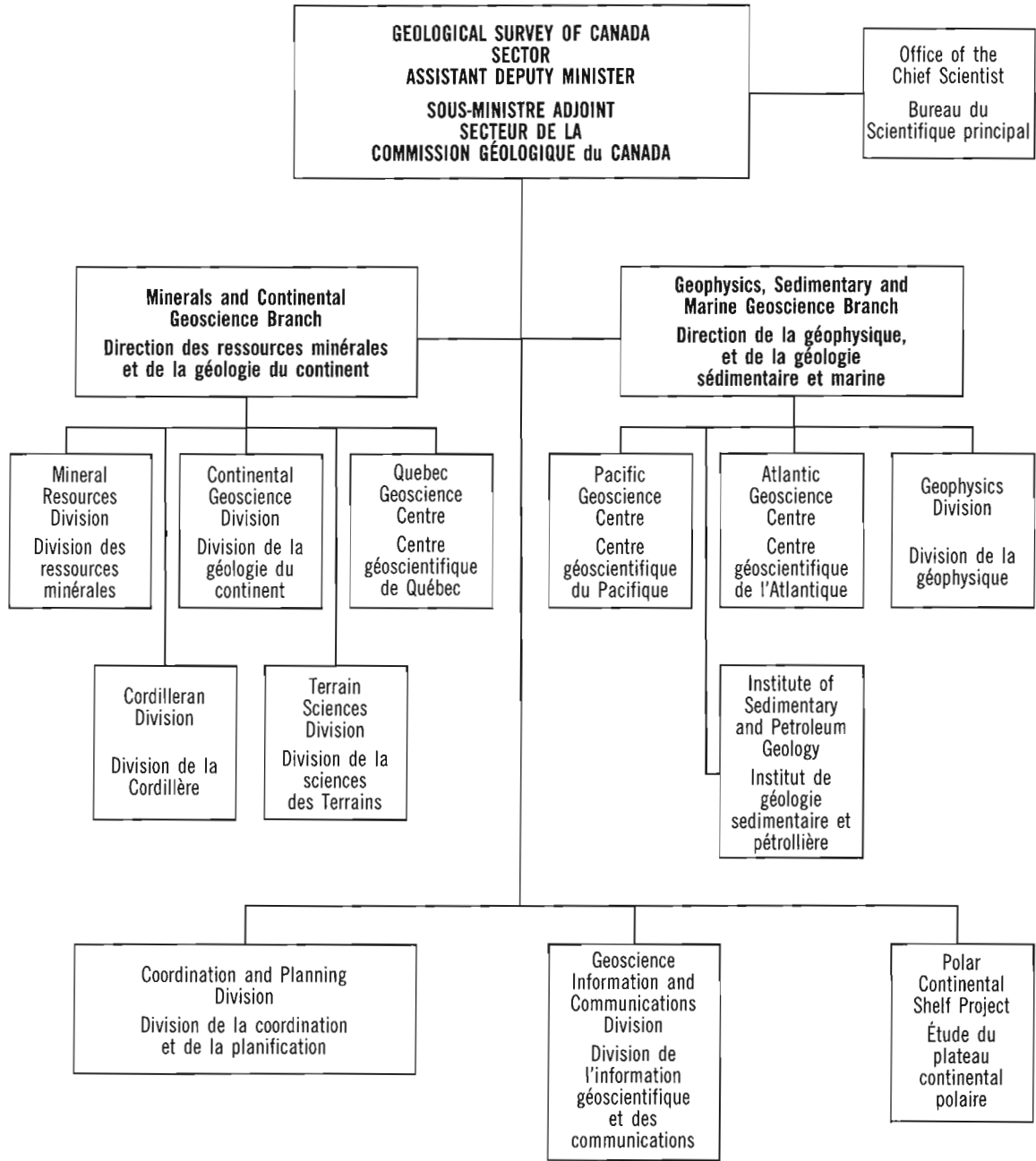
**Cover description**

Strongly sheared Archean gneisses, transposed Paleoproterozoic mafic dykes, and synkinematic pegmatite veins in the Paleoproterozoic Komaktorvik shear zone, Torngat Orogen, Labrador. See paper by Van Kranendonk et al., p. 321-332. (photo by M. Van Kranendonk. GSC 1993-305L)

**Description de la photo couverture**

Gneiss fortement cisailés de l'Archéen, dykes mafiques transposés du Paléoprotérozoïque et veines de pegmatite syncinématiques à l'intérieur de la zone de cisaillement de Komaktorvik, orogène de Torngat, Labrador. Voir l'article de Van Kranendonk et al., p. 321-332. (photo de M. Van Kranendonk, GSC 1993-305-L)







## Separates

A limited number of separates of the papers that appear in this volume are available by direct request to the individual authors. The addresses of the Geological Survey of Canada offices follow:

601 Booth Street  
OTTAWA, Ontario  
K1A 0E8  
(FAX: 613-996-9990)

Institute of Sedimentary and Petroleum Geology  
3303-33rd Street N.W.  
CALGARY, Alberta  
T2L 2A7  
(FAX: 403-292-5377)

Cordilleran Division  
100 West Pender Street  
VANCOUVER, B.C.  
V6B 1R8  
(FAX: 604-666-1124)

Pacific Geoscience Centre  
P.O. Box 6000  
9860 Saanich Road  
SIDNEY, B.C.  
V8L 4B2  
(Fax: 604-363-6565)

Atlantic Geoscience Centre  
Bedford Institute of Oceanography  
P.O. Box 1006  
DARTMOUTH, N.S.  
B2Y 4A2  
(FAX: 902-426-2256)

Québec Geoscience Centre  
2700, rue Einstein  
C.P. 7500  
Ste-Foy (Québec)  
G1V 4C7  
(FAX: 418-654-2615)

When no location accompanies an author's name in the title of a paper, the Ottawa address should be used.

## Tirés à part

On peut obtenir un nombre limité de «tirés à part» des articles qui paraissent dans cette publication en s'adressant directement à chaque auteur. Les adresses des différents bureaux de la Commission géologique du Canada sont les suivantes:

601, rue Booth  
OTTAWA, Ontario  
K1A 0E8  
(facsimilé : 613-996-9990)

Institut de géologie sédimentaire et pétrolière  
3303-33rd St. N.W.,  
CALGARY, Alberta  
T2L 2A7  
(facsimilé : 403-292-5377)

Division de la Cordillère  
100 West Pender Street  
VANCOUVER, British Columbia  
V6B 1R8  
(facsimilé : 604-666-1124)

Centre géoscientifique du Pacifique  
P.O. Box 6000  
9860 Saanich Road  
SIDNEY, British Columbia  
V8L 4B2  
(facsimilé : 604-363-6565)

Centre géoscientifique de l'Atlantique  
Institut océanographique Bedford  
B.P. 1006  
DARTMOUTH, Nova Scotia  
B2Y 4A2  
(facsimilé : 902-426-2256)

Centre géoscientifique de Québec  
2700, rue Einstein  
C.P. 7500  
Ste-Foy (Québec)  
G1V 4C7  
(facsimilé : 418-654-2615)

Lorsque l'adresse de l'auteur ne figure pas sous le titre d'un document, on doit alors utiliser l'adresse d'Ottawa.



---

# CONTENTS

---

Regional geology of the Winter Lake-Lac de Gras area, central Slave Province, District of Mackenzie, Northwest Territories <b>P.H. Thompson, D. Ross, and A. Davidson</b> . . . . .	1
Geology of the northern half of the Winter Lake supracrustal belt, Slave Province, Northwest Territories <b>R.B. Hrabi, J.W. Grant, A. Berclaz, D. Duquette, and M.E. Villeneuve</b> . . . . .	13
Geology of Paul Lake area, Lac de Gras-Lac du Sauvage region of the central Slave Province, District of Mackenzie, Northwest Territories <b>B.A. Kjarsgaard and R.J.S. Wyllie</b> . . . . .	23
Glacial geology and implications for drift prospecting in the Lac de Gras, Winter Lake, and Aylmer Lake map areas, central Slave Province, Northwest Territories <b>L.A. Dredge, B.C. Ward, and D.E. Kerr</b> . . . . .	33
The sedimentology and provenance of the Et-Then Group as a record of deformation on the McDonald fault zone, East Arm, Great Slave Lake, Northwest Territories <b>B.D. Ritts</b> . . . . .	39
Contact relationships between the Anialik River volcanic belt and the Kangguyak gneiss belt, northwestern Slave Province, Northwest Territories <b>C. Relf, A. Chouinard, H. Sandeman, and M. Villeneuve</b> . . . . .	49
The Shaler Supergroup and revision of Neoproterozoic stratigraphy in Amundsen Basin, Northwest Territories <b>R.H. Rainbird, C.W. Jefferson, R.S. Hildebrand, and J.K. Worth</b> . . . . .	61
Geology of the Wijinnedi Lake area – a Paleoproterozoic(?) asymmetric uplift of Archean rocks in the southwestern Slave Province, District of Mackenzie, Northwest Territories <b>J.B. Henderson</b> . . . . .	71
Geology and mineral occurrences of the central part of High Lake greenstone belt, Archean Slave Province, Northwest Territories: a preliminary account of an unconformity between two volcanic sequences <b>J.R. Henderson, M.N. Henderson, and J.A. Kerswill</b> . . . . .	81
Preliminary report on the geology of the Indin Lake supracrustal belt, western Slave Province, Northwest Territories <b>S.J. Pehrsson and C. Beaumont-Smith</b> . . . . .	91

Disseminated gold mineralization in the Stewart River area, La Ronge Domain, Saskatchewan <b>K.H. Poulsen and F. Robert</b> . . . . .	103
Structural relationships across the Tabbernor Fault, Nielson Lake area, Trans-Hudson Orogen, Saskatchewan <b>C.G. Elliott</b> . . . . .	113
Structural investigation of high-grade rocks of the Kramanituar complex, Baker Lake area, Northwest Territories <b>M. Sanborn-Barrie</b> . . . . .	121
Geology of the Early Proterozoic gold metallotect, Hurwitz Group in the Cullaton-Griffin lakes area, central Churchill Structural Province, Northwest Territories <b>A.R. Miller, M.J. Balog, B.A. Barham, and K.L. Reading</b> . . . . .	135
Geology of the Sandhill Zn-Cu showing in the Gibson Lake area, District of Keewatin, Northwest Territories <b>A.E. Armitage, A.R. Miller, and N.D. MacRae</b> . . . . .	147
Archean and Lower Proterozoic geology of western Dubawnt Lake, Northwest Territories <b>T.D. Peterson and P. Born</b> . . . . .	157
Geology of Archean and Proterozoic supracrustal rocks in the Otter and Ducker lakes area, southern District of Keewatin, Northwest Territories <b>L.B. Aspler, J.R. Chiarenzelli, D.L. Ozarko, and K.B. Powis</b> . . . . .	165
Ice flow events in the Cormorant Lake-Wekusko Lake area, northern Manitoba <b>I. McMartin</b> . . . . .	175
Transition between the Flin Flon and Kisseynew domains of the Trans-Hudson Orogen, File Lake-Limestone Point Lake area, northern Manitoba <b>K.A. Connors and K.M. Ansdell</b> . . . . .	183
Lithological and structural relationships in Paleoproterozoic rocks in the east Wekusko Lake area, Trans-Hudson Orogen, Manitoba <b>K.M. Ansdell and K.A. Connors</b> . . . . .	193
Glacial dispersal and drift composition, Rice Lake Greenstone Belt, southeastern Manitoba <b>P.J. Henderson</b> . . . . .	205
Regional geology and geophysics of the sub-Phanerozoic Precambrian basement south of the Flin Flon-Snow Lake-Hanson Lake Belt, Manitoba-Saskatchewan <b>A.D. Leclair, S.B. Lucas, R.G. Scott, D. Viljoen, and J. Broome</b> . . . . .	215

Geological, geochemical, and age constraints on base metal mineralization in the Manitouwadge greenstone belt, northwestern Ontario <b>E. Zaleski, V.L. Peterson, and O. van Breemen</b> . . . . .	225
Structure and tectonics of the Manitouwadge greenstone belt and Wawa-Quetico subprovince boundary, Superior Province, northwestern Ontario <b>V.L. Peterson and E. Zaleski</b> . . . . .	237
Till composition in the vicinity of the Manitouwadge greenstone belt, Ontario <b>I.M. Kettles and J.B. Murton</b> . . . . .	249
An interim report on geological, structural, and geochronological investigations of granitoid rocks in the vicinity of the Swayze greenstone belt, southern Superior Province, Ontario <b>K.B. Heather and O. van Breemen</b> . . . . .	259
Geology of the Levack gneiss complex, the northern footwall of the Sudbury structure, Ontario <b>K.D. Card</b> . . . . .	269
Acoustic velocity logging at the McConnell nickel deposit, Sudbury area, Ontario: preliminary in situ measurements <b>K.A. Pflug, P.G. Killeen, and C.J. Mwenifumbo</b> . . . . .	279
Timing relationships between Cu-Au mineralization, dykes, and shear zones in the Chibougamau camp, northeastern Abitibi subprovince, Quebec <b>F. Robert</b> . . . . .	287
Vein fields in gold districts: the example of Val d'Or, southeastern Abitibi subprovince, Quebec <b>F. Robert</b> . . . . .	295
A preliminary report of porphyry Cu-Mo-Au and shear zone-hosted Cu-Au deposits in the Chibougamau area, Quebec <b>W.D. Sinclair, P. Pilote, R.V. Kirkham, F. Robert, and R. Daigneault</b> . . . . .	303
Oceanic allochthons in an Archean continental margin sequence, Vizion greenstone belt, northern Quebec <b>T. Skulski, J.A. Percival, and R.A. Stern</b> . . . . .	311
New results and summary of the Archean and Paleoproterozoic geology of the Burwell domain, northern Torngat Orogen, Labrador, Quebec, and Northwest Territories <b>M.J. Van Kranendonk, R.J. Wardle, F.C. Mengel, L.M. Campbell, and L. Reid</b> . . . . .	321
Tholeiitic and weakly alkalic basaltic volcanism of the Mugford Group, northern Labrador: preliminary geochemical results <b>M.A. Hamilton</b> . . . . .	333



Combining field observations and remote sensing to map the Grenville Front along the Pascagama River, Quebec <b>D.F. Graham and A. Ciesielski</b> . . . . .	343
Géologie et cibles d'exploration de la partie centre est de la ceinture métasédimentaire du Québec, Province de Grenville <b>L. Corriveau, D. Morin et L. Madore</b> . . . . .	355
Comparison of trace element distributions in lake sediments and waters from the Florence Lake area, Labrador <b>P.W.B. Friske, G.E.M. Hall, and S.J.A. Day</b> . . . . .	367
Author Index . . . . .	377

# Regional geology of the Winter Lake-Lac de Gras area, central Slave Province, District of Mackenzie, Northwest Territories

P.H. Thompson, D. Ross<sup>1</sup>, and A. Davidson  
Continental Geoscience Division

*Thompson, P.H., Ross, D., and Davidson, A., 1994: Regional geology of the Winter Lake-Lac de Gras area, central Slave Province, District of Mackenzie, Northwest Territories; in Current Research 1994-C; Geological Survey of Canada, p. 1-12.*

---

**Abstract:** In the Winter Lake-Lac de Gras area, narrow belts of metavolcanic rocks occur between a northeastern metasedimentary domain and a southwestern migmatitic, gneissic granitoid domain containing subordinate supracrustal rocks. Homogeneous late plutons intrude both domains. Supracrustal rocks are assigned to the Yellowknife Supergroup.

Complex fold interference patterns in the metasedimentary domain contrast with subrhombic geometry outlined by thin supracrustal belts surrounding large blocks of metagranitoid and gneiss. Lowest grade of low pressure regional metamorphism in supracrustal rocks is associated with migmatitic, foliated granitoid and gneiss. The lithological transition and differences in structure and metamorphic grade are attributed to a higher proportion of pre-Yellowknife sialic crust to the southwest.

Base metal and gold deposits occur within the metasedimentary domain and volcanic rocks. Supracrustal rocks are less mineralized where they are subordinate to pre-Yellowknife rocks. Diamondiferous kimberlites occur just east of the area in the metasedimentary domain.

**Résumé :** Dans la région des lacs Winter et de Gras, des ceintures étroites de roches métavolcaniques se trouvent entre un domaine métasédimentaire, au nord-est, et un domaine de métagranitoïdes foliés, gneissiques et migmatitiques, au sud-ouest, où les roches supracrustales occupent un volume très réduit. Des plutons homogènes tardifs sont intrusifs dans les deux domaines. Les roches supracrustales sont attribuées au Supergroupe de Yellowknife.

Les figures d'interférence complexes formées dans le domaine métasédimentaire par la superposition de plis régionaux contrastent avec les formes subrhomboïdales définies par des ceintures de roches supracrustales étroites entourant de vastes blocs de métagranitoïdes et de gneiss dans l'autre domaine. Le plus bas degré du métamorphisme régional de basse pression dans les roches supracrustales est associé aux granitoïdes foliés et gneiss migmatitiques. La transition lithologique et les différences de style structural et d'intensité du métamorphisme à travers la carte sont attribués à une plus grande proportion de croûte sialique plus ancienne que le Supergroupe de Yellowknife vers le sud-ouest.

Des gisements de métaux de base et d'or sont présents dans le domaine métasédimentaire ou dans les roches métavolcaniques contiguës. Les roches supracrustales sont moins minéralisées lorsque leur volume est moindre que celui des lithologies antérieures au Supergroupe de Yellowknife. Des kimberlites diamantifères se trouvent juste à l'est de la région cartographiée, dans le domaine métasédimentaire.

---

<sup>1</sup> College of Geographical Science, Lawrencetown, Nova Scotia

## INTRODUCTION

Bedrock mapping at 1:250 000 scale during the second of three field seasons advanced knowledge of the origin, evolution, and economic potential of the central Slave Province. The area, located 200 km north of Yellowknife (Fig. 1), includes parts of three supracrustal domains with high gold and base metal potential (Yellowknife-Beaulieu River, Courageous Lake-Lac de Gras, and Winter Lake-Contwoyto Lake) and the western third of the BHP-Diamet diamond property. Mapping focused on interrelationships of Archean supracrustal and granitoid domains. The area is large enough (11 000 km<sup>2</sup>) that associations between deposition, magmatism, deformation, regional metamorphism, and metallogeny can be studied and the results extrapolated to other parts of the Slave Province.

Scientific and logistical collaboration with exploration companies, DIAND, Government of Northwest Territories, and colleagues in CGD and other GSC divisions (Terrain Sciences, Mineral Resources, Pacific Geoscience Centre) is an important facet of the project. Thompson et al. (1993b) and Dredge et al. (1994) present new data on metallogeny and Quaternary geology, respectively. Rencz et al. (1993) integrated reconnaissance geological maps, aeromagnetic data, and LANDSAT TM imagery. Hrabi et al. (1993, 1994) elucidated the stratigraphy and structure of the Winter Lake supracrustal belt. Villeneuve (1993) published the first U/Pb zircon ages. Three undergraduate theses (Ross, 1993; Duquette, 1993; Paulen, 1993) have been completed. Ongoing studies of mafic dyke swarms (W.R. Baragar, K. Buchan, A. LeCheminant) utilized samples collected during regional mapping.

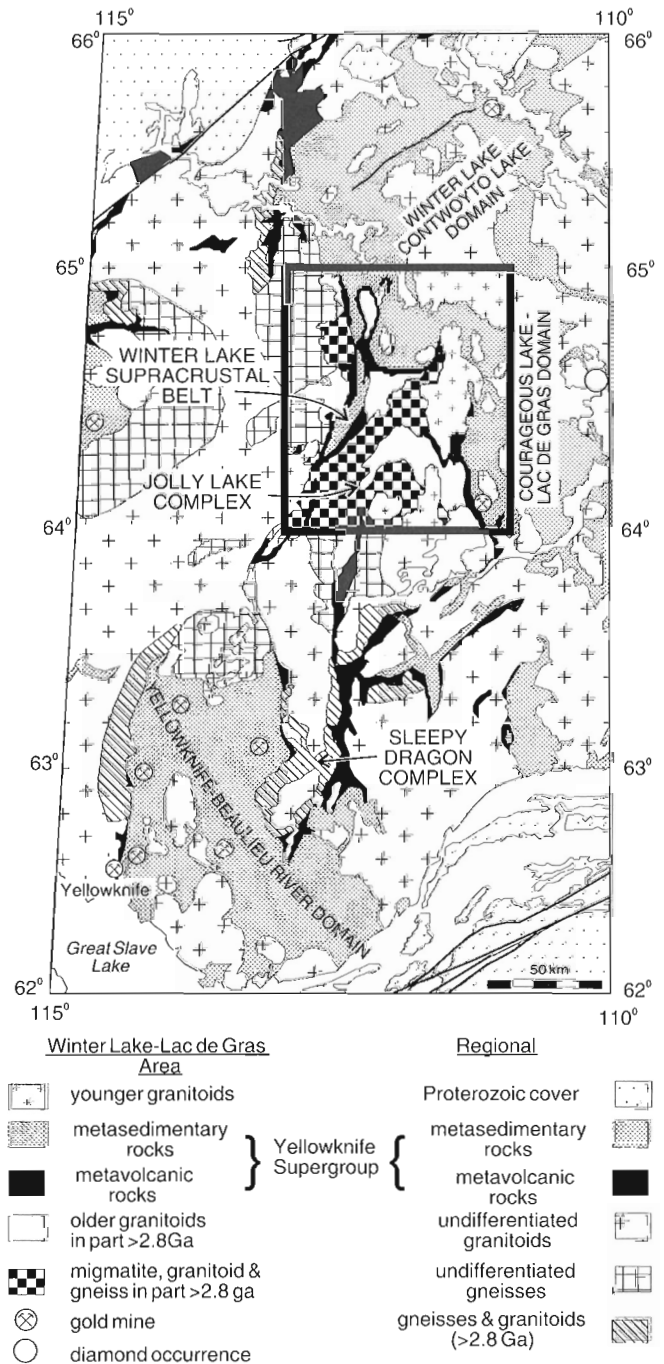
Current mapping (Thompson et al., 1993b) extends and refines the regional geological framework outlined by Fraser (1969) and Folinsbee (1949). Previous detailed mapping was limited to the Courageous Lake volcanic belt (Moore et al., 1951; Dillon-Leitch, 1981, 1984). The current map area includes the transition between extensive supracrustal rocks intruded mainly by late granitoids to the north (Bostock, 1980; King et al., 1991) and the region to the south (Moore et al., 1951; Henderson, 1944) where supracrustal rocks are subordinate to migmatitic and gneissic granitoid rocks and homogeneous plutons. Continuity across the map area of key lithotectonic elements combined with major changes in lithology, structure, and metamorphic grade make the area a prime target for further advancement of understanding of Slave Province geology.

## ROCK UNITS

This report describes five new rock units as well as modifications to those already defined (Thompson et al., 1993a). The previous two-fold division of plutonic rocks into older, variably deformed and metamorphosed granitoid units, and younger, homogeneous, mainly massive plutons is maintained. Older granitoids bounded to the west by the Winter

Lake supracrustal belt and to the north and east by the Desteffany Lake and Courageous Lake volcanic belts (Fig. 2) are here called the Jolly Lake complex.

West of the Winter Lake belt, massive to weakly-foliated biotite granite intrudes foliated metagranitoid, gneiss, and granitoid migmatite, and metasedimentary migmatite, and amphibolite gneiss. Complex granitoids to the south and north may be extensions of the Jolly Lake complex.



**Figure 1.** Location of the Winter Lake-Lac de Gras area and major supracrustal domains, southwestern Slave Structural Province.



### **Older granitoids (Jolly complex; units 1-4, Fig. 2)**

In this report, we redefine the granitoid migmatite/gneiss unit, Courageous Lake metaplutonic suite and foliated meta-granite-tonalite units of Thompson et al. (1993a). Gneissic (layered) and migmatitic components of the two composite units are grouped together in a new quartzofeldspathic gneissic unit (1) and a new granitoid migmatite unit (2). The homogeneous, foliated granitoid components of the composite units have been reassigned to unit 3, an expanded foliated metagranite-tonalite. Hornblende metagranite (4) is unchanged from Thompson et al. (1993a). "Older granitoids" is a convenient term referring to the variably-recrystallized and deformed rocks in the Jolly complex and west of the Winter Lake belt. "Younger granitoids" are massive, homogeneous plutons that postdate metamorphism and deformation in adjacent rocks.

### **Quartzofeldspathic gneisses (layered) (unit 1)**

Fine- to medium-grained, variably-folded and straight gneisses (Fig. 3a) form two broad swaths across the Jolly Lake complex. Similar rocks occur west of the Winter Lake supracrustal belt and smaller bodies are present in the cores of folds within the northern supracrustal domain. Millimetre- to decimetre-scale layering (gneissosity) is attributed to various combinations of ductile deformation and migmatization involving both injection of melt and in situ partial melting. Boudins or inclusions of amphibolite are prominent locally. Considering the wide distribution of simple mineralogy (quartz, one or two feldspars, biotite,  $\pm$ hornblende), absence of aluminosilicates, close association with granitoid rocks, and the lack of remnants of unequivocal supracrustal rocks, the protolith is assumed to have been plutonic. Hornblende in anatectic leucosomes in central Jolly Lake complex indicates that maximum metamorphic conditions reached at least upper amphibolite facies. The gneisses are intruded by two ages of granitoid (units 3 and 12-14) and are structurally both discordant and concordant with respect to adjacent supracrustal rocks (see below), in which metamorphic grade is generally markedly lower. Whether relatively high strain at this contact reflects a major structural discontinuity, or is merely a result of contrasts in lithology and metamorphic grade, remains to be demonstrated.

### **Granitoid migmatite (unit 2)**

The characteristically irregular variations of modal composition and grain size of these rocks (Fig. 3b) are attributed to magmatic injection and partial melting in granitic to tonalitic rocks. Outcrops with a nebulitic aspect containing streaky, lenticular leucosome and melanosome or wispy concentrations of biotite are typical of this unit north and west of Jolly Lake and west of the Winter Lake belt. East of Jolly Lake, most of the heterogeneity is caused by multiple phases of intrusion. Contacts between granitoid migmatite and either foliated metagranitoid or gneissic rocks are ambiguous. It is not clear if in situ partial melting formed leucosome and melanosome in a homogeneous granitoid or if a heterogeneous

rock was homogenized as the degree of melting increased. In either case, tight folding and shearing generally accompanied the process.

### **Foliated metagranite-tonalite (unit 3)**

In this report, we extend this unit to include homogeneous foliated granitoid components of "granitoid/migmatite/gneiss" and "Courageous Lake metaplutonic suite" described by Thompson et al. (1993a). Parts of the unit may be significantly older than the Yellowknife Supergroup if the deformed amphibolite dykes that cut it are synvolcanic. On the other hand, zircons from similar rocks just north of the map area yielded a synvolcanic age (Bostock, 1980).

### **Yellowknife Supergroup (units 5-8)**

All supracrustal rocks in the Winter Lake-Lac de Gras area are assigned to the Yellowknife Supergroup (Henderson, 1970).

### **Volcanic and related rocks (units 5-6)**

This heterogeneous sequence comprises metamorphosed massive, pillowed, and clastic metavolcanic rocks, gabbro, interflow sedimentary rocks, undivided thin-layered gneisses, carbonate schist, calcsilicate gneiss, ultramafic rocks, and quartz arenite. Moore (1956) and Dillon-Leitch (1981) associated dykes and sills of metagabbro and quartz porphyry with volcanism. Except for thick units of felsic volcanic rock, unit 5 is not subdivided on Figure 2. Both felsic volcanic rocks and rare quartz arenite occur below, interlayered with and on top of mafic volcanic rocks. Red-brown-weathering ultramafic rocks (Ross, 1993) are interlayered with mafic volcanic rocks in the Winter Lake and Courageous Lake belts and underlie the mafic succession at Desteffany Lake (Thompson et al., 1993a). Chemical analyses show that peridotitic komatiites are present in all three belts. This year, two more ultramafic occurrences were found south of Newbigging Lake. A new occurrence of quartz arenite interlayered with felsic volcanic rocks west of the lake extends the occurrences described by Thompson (1992) and Hradi et al. (1993) 3 km farther northeast.

Southwest of Jolly Lake (Fig. 2), the northern tip of the Beaulieu River volcanic belt contains most of the rock types characteristic of this unit elsewhere in the area. For example, the association of quartz arenite, felsic and mafic volcanic rocks, metagabbro, and calcsilicate gneiss along the eastern contact of hornblende metagranite at Lake Providence is essentially the same as the succession 80 km to the south, although it displays higher metamorphic grade.

### **Polymictic metaconglomerate (unit 7)**

The narrow belt of metaconglomerate discovered in the southwest corner of the area is correlated with those mapped to the north by Fraser (1969) and Hradi et al. (1993). This distinctive unit extends discontinuously for more than

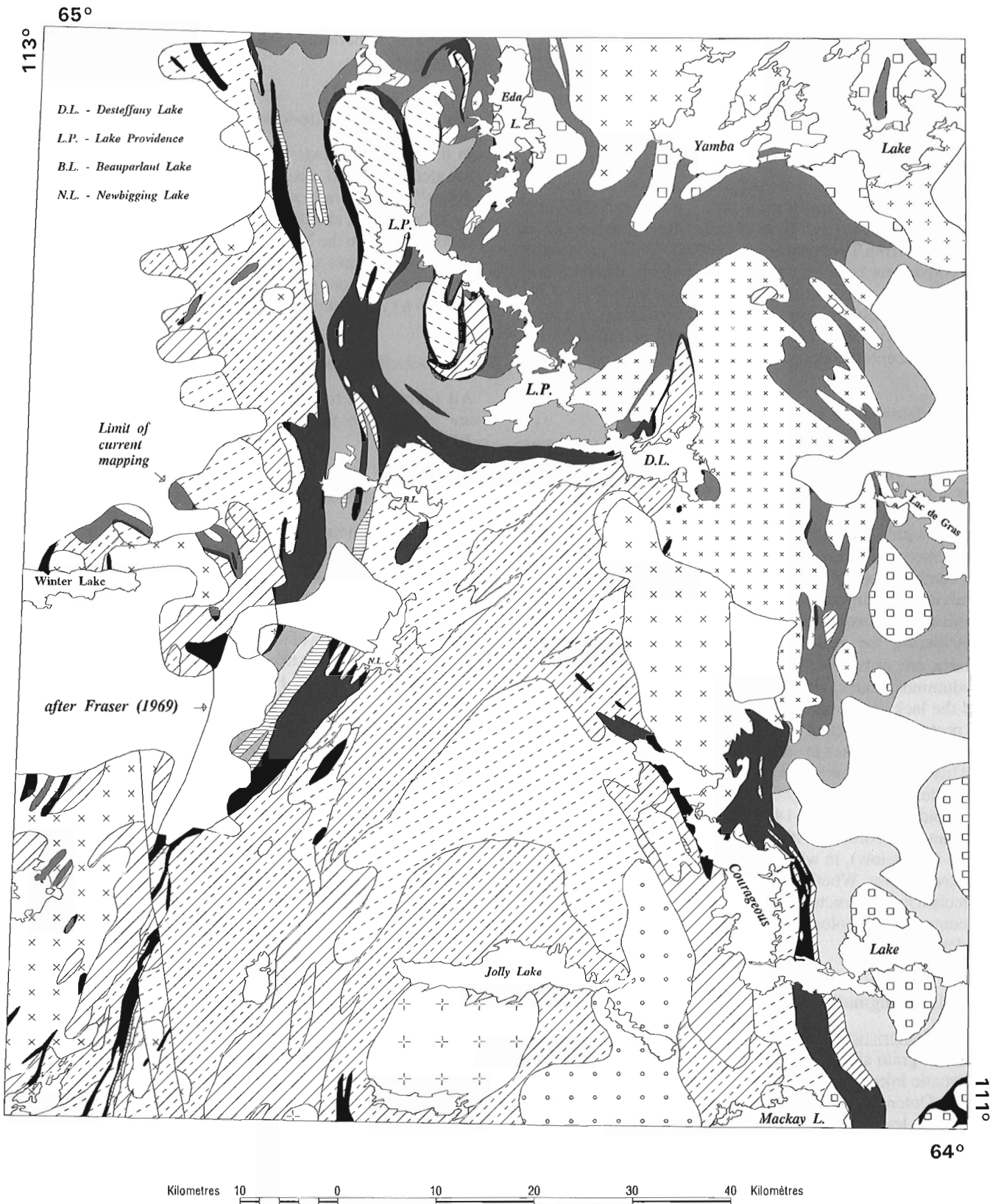
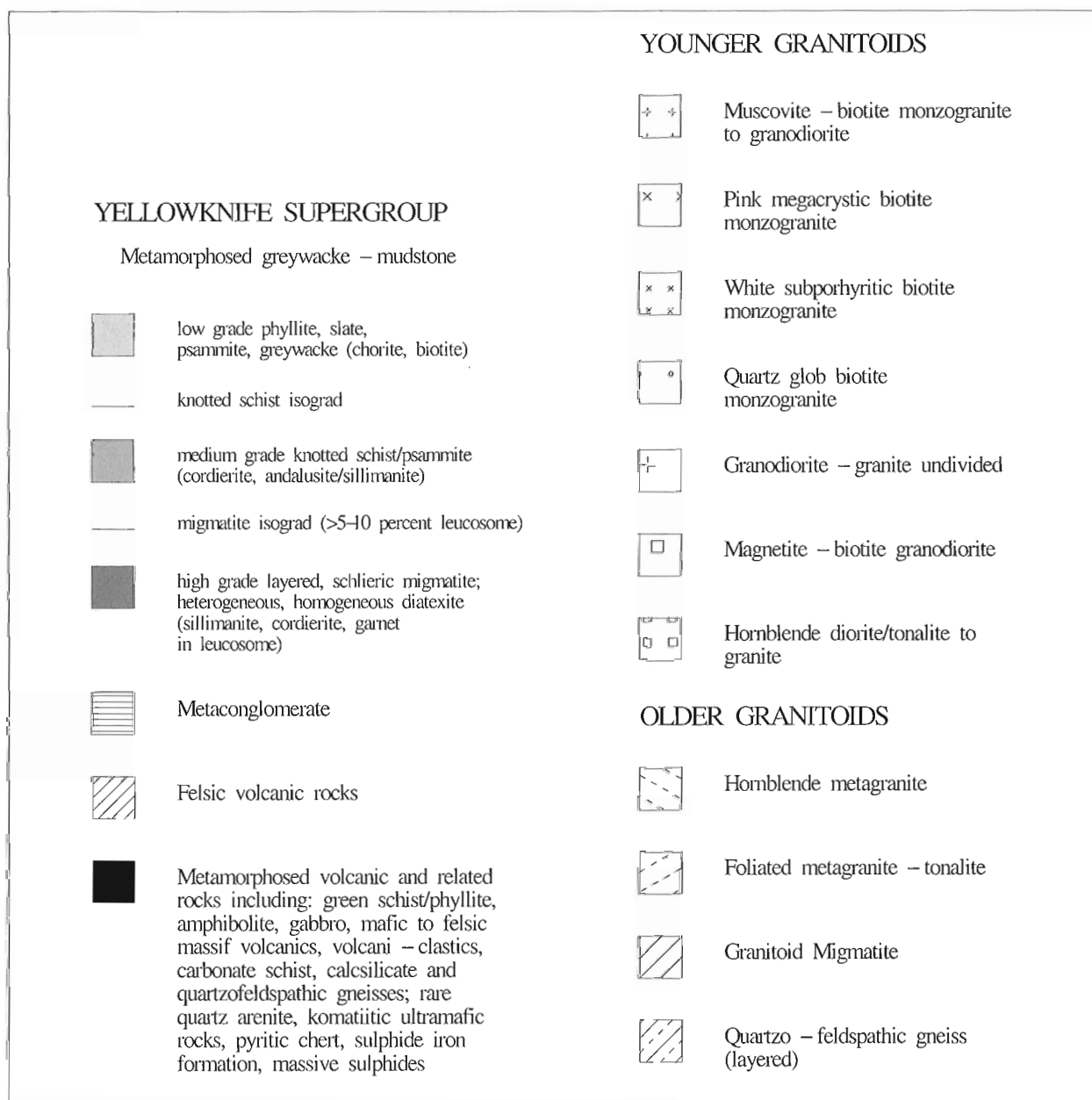
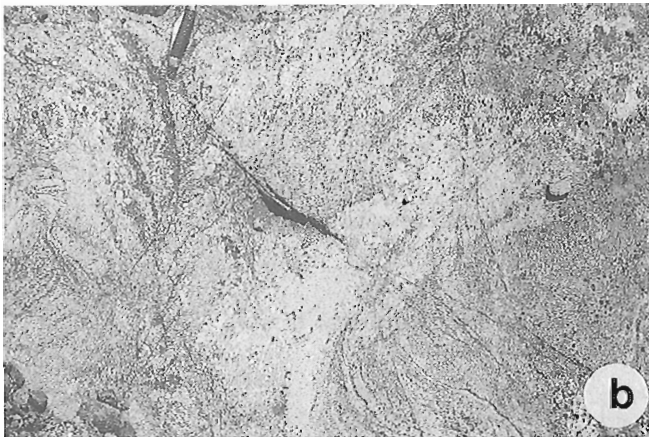
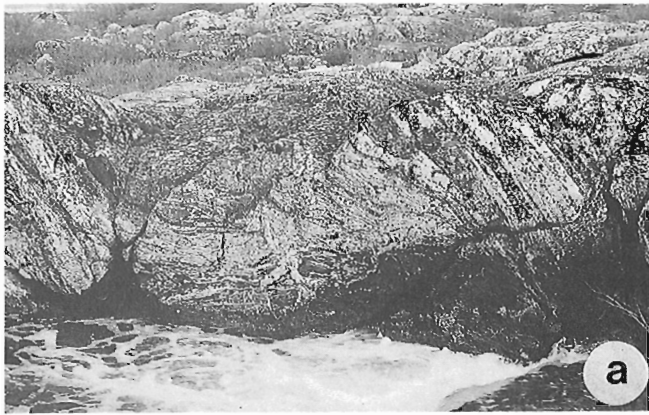


Figure 2. Preliminary geological map of the Winter Lake-Lac de Gras map area (NTS 76D-W112, 86A-E112). Mafic dykes have been omitted for clarity.

100 km. In the southwestern segment (Fig. 3c), it is generally conformable with underlying mafic metavolcanics and overlying cordierite-sillimanite schist and psammite. Strongly-deformed felsic and mafic volcanic clasts are prominent. Garnet occurs in the matrix and in moderately-deformed tonalitic cobbles and boulders. Garnet is also present in the first few centimetres of adjacent metatonalite at one locality (Fig. 3d) where metatonalite appears to intrude the conglomerate before main phase deformation and metamorphism affected both rock units. Thirty kilometres farther north, the cobbles are less deformed, and andalusite in associated pelitic

interbeds (Fig. 3e) indicates lower metamorphic grade. West of Newbigging Lake, the conglomerate is in the greenschist facies. Interlayered with the metagreywacke-mudstone and mafic volcanic rocks of the Yellowknife Supergroup and subjected to the same range of metamorphic grade and intensity of deformation, the polymictic conglomerate is probably not a Temiskaming-like sequence as was suggested by Hrabí et al. (1993). Deposition during or soon after volcanism, as proposed for the Keskarrah Formation (Bostock, 1980), 15 km north of the area, and Raquette Lake Formation (Henderson, 1985) 150 km to the south, is likely.







### Phyllite/knotted schist/metasedimentary migmatite (unit 8)

Mapping of metasedimentary rocks south of Yamba Lake and between Lac de Gras and Courageous Lake revealed rocks similar to those described by Thompson et al. (1993a). Changes in mineral assemblage and microstructure transform phyllite and slate (unit 8a) to cordierite-andalusite schist and sillimanite schist (unit 8b) to metatexite and diatexite (unit 8c). The prevalence of garnet over cordierite in metasedimentary migmatite west of the Winter Lake belt is anomalous and may indicate a more iron-rich protolith.

### Younger granitoids (units 9-15)

#### Hornblende diorite/tonalite to granite (unit 9)

The type example of this suite is the Courageous Lake pluton (Duquette, 1993) which has a core of monzogranite and an outer zone of quartz diorite/tonalite. All plutons are strongly magnetic. The teardrop-shaped pluton to the north is also zoned but only tonalitic to dioritic marginal phases are exposed in the eastern and southern plutons. Near Mackay Lake hornblende-rich phases are rare. The main schistosity and map-scale isoclinal folds outlined by bedding wrap around each igneous body. Mafic and ultramafic inclusions are common but pelitic xenoliths are absent. Strongly deformed granitic lenses or boudins in the metasedimentary rocks near the eastern pluton may be remnants of dykes related to intrusion of the body.

### Figure 3.

*a) quartzofeldspathic gneiss (unit 1) from Jolly complex. Cliff is 2 m high. (GSC 1993-250G)*

*b) granitoid migmatite (unit 2), western Jolly complex. Knife = 8 cm. (GSC 1993-250E)*

*c) tonalitic and metavolcanic cobbles in polymictic metaconglomerate, southwestern segment of Winter Lake supracrustal belt (knife = 8 cm). (GSC 1993-250C)*

*d) contact (intrusive?) between foliated metatonalite and polymictic metaconglomerate. Garnet occurs in matrix and pebbles of metaconglomerate and in metatonalite near the contact. Well-developed foliation in both rocks intersects contact near knife (8 cm). (GSC 1993-250D)*

*e) less-deformed granitoid clasts in metaconglomerate; note andalusite porphyroblasts in pelitic interbeds in finer grained part of unit. Knife = 8 cm. (GSC 1993-250B)*

*f) foliated amphibolite dyke cuts foliated metagranite (unit 3). Knife = 8 cm. (GSC 1993-250I)*

*g) deformed amphibolite dyke cuts gneissosity in unit 1. (GSC 1993-250A)*

### Magnetite-biotite granodiorite (unit 10)

Large, massive, homogeneous plutons of biotite granodiorite intrude metasedimentary migmatite. They have irregular shapes at Eda and Yamba lakes and, taken together, form an incomplete collar around younger megacrystic granite. In this unit, within a few decimetres of contacts with migmatite, grain size and modal composition may vary greatly and several phases of aplitic to pegmatitic dykes form open folds. Lenticular, fine grained, mafic inclusions define a fairly consistent orientation in the granodiorite.

### Granite to granodiorite undivided (unit 11)

The granitic pluton south of Jolly Lake is similar in composition to other younger biotite granite and granodiorite. It is weakly foliated along the western margin and conformable with the gneissosity in the surrounding gneisses. Heterogeneous zones of migmatitic granitoid (inclusions?) occur within the pluton and near the northern contact. Ten kilometres to the west, a small mass of similar foliated granodiorite is continuous with the Prang Lake granite (Stubley, 1991).

### Quartz glob granite (unit 12)

The "globular granite" of Thompson et al. (1993a) was traced farther south and west. This massive rock intrudes units 1-3.

### White biotite monzogranite (13)

White-weathering, mainly massive biotite monzogranite, characterized by relatively even grain size, subporphyritic texture and abundant inclusions, is limited mainly to the area east of Desteffany Lake. Dykes of white granite intrude the Yellowknife Supergroup in the northern part of the Winter Lake belt and, locally, northeast of Lake Providence. The granite and associated pegmatite cut across folds and planar structures in medium- to high-grade supracrustal rocks, older granitoid, and gneiss; dykes and sills of the granite, however, are boudined. Map-scale bodies of massive granite are conformable with the regional foliation trend where it defines D<sub>3</sub> folds.

### Pink megacrystic biotite granite (unit 14)

Extensive plutons of syenogranite to monzogranite occur in the southwest corner of the area, north of Courageous Lake and west of Yamba Lake. The unit intrudes supracrustal rocks, older granitoid and gneiss as well as magnetic granodiorite (unit 10). Rafts of country rock are common in the southwestern body but rare in the central and northern bodies. Locally, megacrysts of K-feldspar have a preferred orientation that is conformable with planar fabrics in the adjacent country rocks, yet the granite is clearly younger than most of the strain recorded in these rocks. Foliation in the granite is attributed to regional deformation during intrusion of a partly crystallized magma. Although magnetite occurs locally in the

northern body, in general the granite corresponds to aeromagnetic lows. The contrast is particularly well-defined between the granite and the "collar" of magnetic granodiorite near Eda and Yamba lakes.

### **Muscovite-biotite granite-granodiorite (unit 15)**

Two-mica granites form major intrusions to the east (Folinsbee, 1949; Kjarsgaard and Wylie, 1994), but in the project area are limited to a small body at the western edge of the Winter Lake belt and a larger pluton southeast of Yamba Lake. These characteristically massive to weakly-foliated, locally-porphyrific, leucocratic rocks intrude metasedimentary rocks and the Yamba magnetic granodiorite (unit 10).

### *Mafic Dykes*

There are two kinds of discordant mafic dyke in the area. Relatively unaltered Proterozoic diabase dykes cut all rock units; among these, dykes of the Mackenzie swarm are the most common, and are the cause of prominent north-northwest oriented linear magnetic anomalies. Metamorphosed and variably-deformed Archean dykes cut across foliation (Fig. 3f) and gneissosity (Fig. 3g) in the Jolly Lake complex and in similar rocks west of the Winter Lake belt (Fig. 4). There is a striking spatial relation between occurrences of discordant amphibolite dykes and overlying volcanic belts (Fig. 2,4). Moore (1956) and Dillon-Leitch (1981) related metamorphosed dykes in foliated metagranitoid (unit 3) west of Courageous Lake to mafic dykes and sills within the adjacent metavolcanic belt, which predate metamorphism and deformation of the belt. They assumed the mafic dykes to be of synvolcanic age. If the dykes are synvolcanic, the observation that metamorphosed dykes cut gneissosity in the older granitoid rocks supports the contention that the gneisses are of pre-Yellowknife Supergroup age.

## **LITHOTECTONIC DOMAINS**

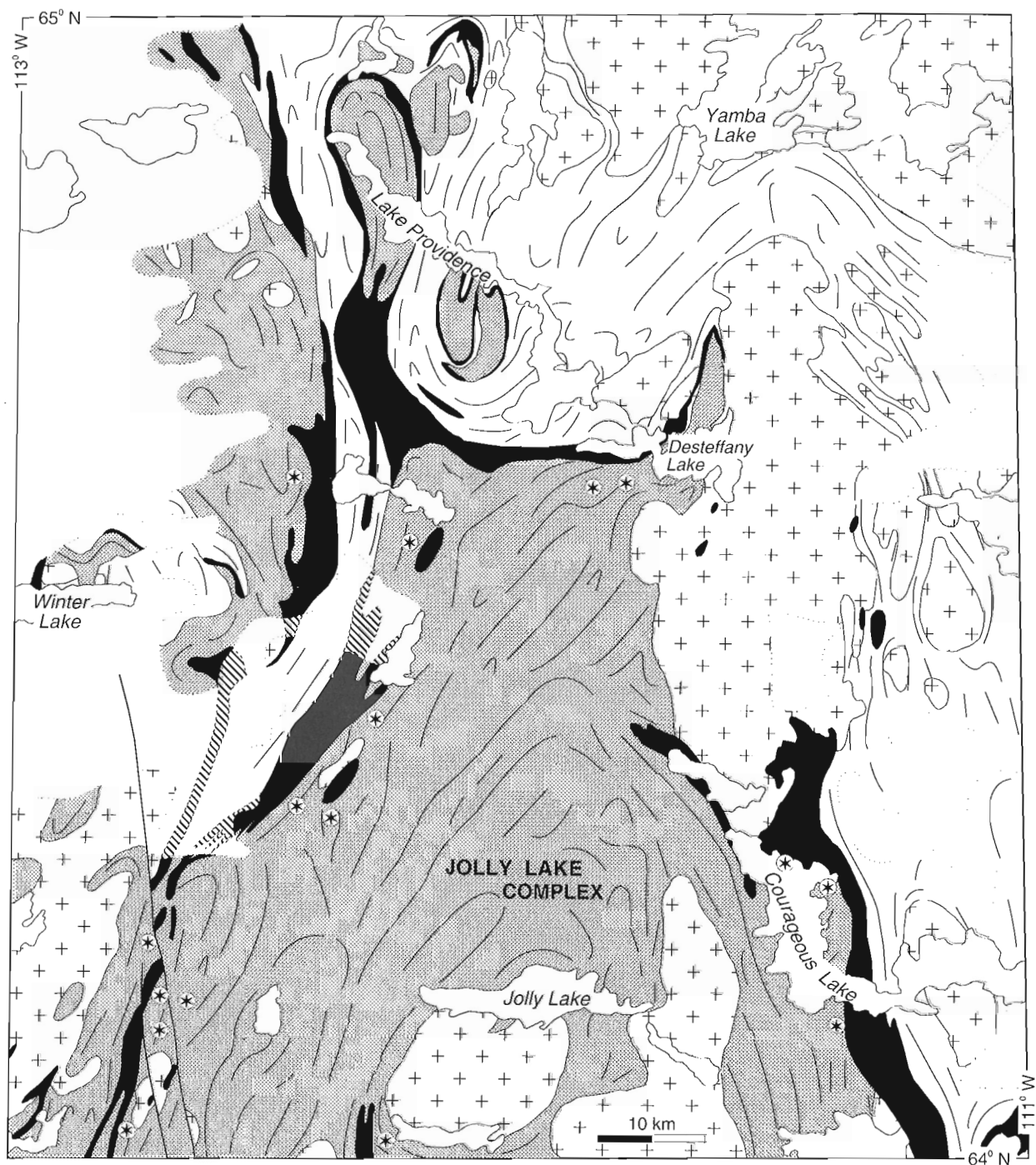
The Winter Lake-Lac de Gras area provides an opportunity to study parts of three major supracrustal domains (Yellowknife Supergroup) as well as extensive areas of granitoid and gneissic rocks (Fig. 1). Polymictic metaconglomerate and quartz arenite, rare elsewhere in the province, occur in significant volumes in the Winter Lake supracrustal belt. Our mapping shows that an isolated occurrence of undivided supracrustal rocks in the southwest corner (Fraser, 1969) is part of a narrow belt of mafic volcanic rocks, polymictic conglomerate, and pelitic schist and psammite that links the Winter Lake supracrustal belt with Yellowknife Supergroup volcanic rocks in the Squalus Lake area (Stubley and Irwin, 1992; M. Stubley, pers. comm., 1993). Discovery of felsic volcanic rocks associated with massive sulphide-bearing mafic gneisses between Lac de Gras and Courageous Lake suggests Courageous Lake and Desteffany Lake volcanic belts may have been continuous before intrusion of intervening younger granitoid bodies. New occurrences of supracrustal rocks at high metamorphic grade west of the Winter Lake belt (Fig. 2), combined with Fraser's observations, indicate

Yellowknife Supergroup rocks in the central part of the belt may have been continuous with similar rocks to the north, west (Indin Lake), and southwest (Russell Lake) (Fig. 1). The unusually high proportion of garnet in this metasedimentary migmatite is consistent with it being iron-formation-bearing Itchen Formation rather than the less iron-rich Contwoyto Formation present farther east in the map area. The Winter Lake-Contwoyto Lake and Courageous Lake-Lac de Gras domains (Fig. 1) are parts of a much larger entity divided by abundant younger plutons in the vicinity of Yamba Lake (Fig. 1, 2). This "superdomain" is now known to be linked to the Yellowknife-Beaulieu River supracrustal domain by the Winter Lake belt. The Courageous Lake volcanic belt is another link if it can be extrapolated southwestward to join the Beaulieu River volcanic belt south of the map area (Fig. 1). These narrow zones of metamorphosed sedimentary and volcanic rocks traverse a large area of the Slave Province previously assumed to contain mainly homogeneous granitoid rocks.

The central part of the map area comprises foliated and migmatitic granitoid and gneissic rocks that may be basement to the Yellowknife Supergroup. There is a striking similarity in the way volcanic belts outline the Jolly Lake complex, the volcanic rocks associated with basement at Point Lake 20 km to the northwest, and those rimming the basement-cored Sleepy Dragon Complex 125 km to the south (Fig. 1). As the proportion of supracrustal rocks decreases southward, structural geometry of volcanic rocks changes from complex curvilinear fold patterns north of the Jolly complex to a blocky, almost rhombic pattern (see below). Thompson et al. (1993a) suggested that the transition from a major supracrustal domain to an extensive granitoid domain represents an exhumed ensialic basin margin.

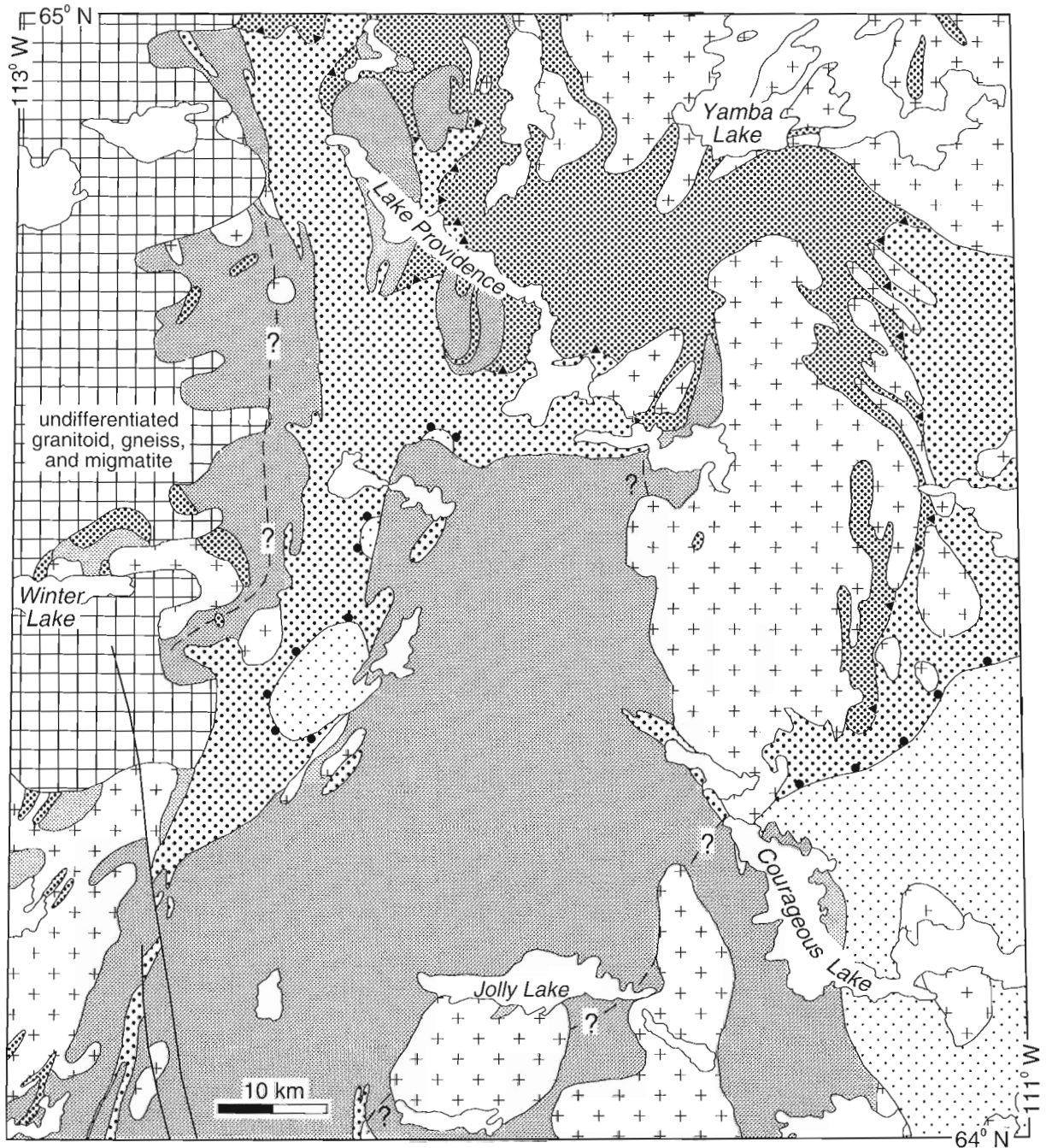
## **STRUCTURAL GEOLOGY**






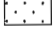

Figure 4 shows the trends of principal planar structures in both the northeastern supracrustal domain and the Jolly complex. Whereas both domains are characterized by complex folding of foliations and gneissosity, the geometry of structures involving volcanic rocks and older granitoids changes southward across the area. These rocks are involved in large-scale fold interference patterns where they are interlayered with extensive metasedimentary rocks. In the south half of the area, where supracrustal rocks are subordinate, volcanic rocks make angular bends (approximately 120°) around broad areas of older granitoids, for example, at the north end of Courageous Lake belt and on both sides of the central part of the Winter Lake belt. Twenty kilometres south of the map area, the Courageous Lake belt makes another such bend. The belt can be extrapolated southwestward to a 60° intersection with the Beaulieu River volcanic belt (Fig. 1). There appears to be a change from a domain where fold geometry is imposed on the older plutonic suite and volcanic rocks, to one where fold geometry is strongly influenced, if not controlled, by the shape of the contact with older granitoid units. Henderson (1985) related a similar rhombic geometry around the Yellowknife supracrustal domain to ensialic basin formation.



- ⊕ ⊕ younger plutons
- metasedimentary rocks
- volcanic & related rocks
- ▨ older granitoid rocks
- ⊛ discordant metamorphosed mafic dykes
- limit of current mapping

**Figure 4.** Trends of principal foliation and gneissosity. Note local discordance between structure in older granitoid rocks and that in overlying Yellowknife Supergroup volcanic rocks. Discordant metamorphosed mafic dykes occur in older granitoid units near overlying volcanic belts.



-  younger granitoids
- YELLOWKNIFE SUPERGROUP**
-  upper amphibolite facies
-  migmatite (>5-10% leucosome)
-  lower amphibolite facies
-  knotted schist isograd
-  greenschist facies
-  older granitoids, migmatite, gneiss

**Figure 5.** Distribution of grade of low-pressure regional metamorphism. Isograds are discordant to both older and younger granitoid suites; "?" indicate possible extrapolations of isograds.



Four lines of evidence support the hypothesis that structures in the Jolly Lake complex are older than those in the supracrustal rocks. 1) Structural trends in the Yellowknife Supergroup are locally discordant to the boundary and internal structural trends of the Jolly Lake complex (Fig. 4). 2) Metamorphosed and deformed mafic dykes cut gneiss and foliated metagranitoid near the volcanic belts, both in the complex and in possibly correlative rocks west of the Winter Lake belt (Fig. 4); similar mafic intrusions predate formation of the planar fabrics in adjacent volcanic belts. 3) The change in structural style noted previously is consistent with the gneisses in the Jolly complex being part of an older, stiffer sialic crust. 4) The distribution of metamorphic grade in supracrustal rocks (see below) indicates that the Jolly Lake complex, whose migmatitic and gneissic rocks record uniformly high metamorphic grade, had cooled before the onset of regional metamorphism of the Yellowknife Supergroup.

At present, it seems unlikely that formation of gneissosity and foliation in the Jolly Lake complex occurred at the same time as metamorphism and deformation in the Yellowknife Supergroup. Formation of these structures during thinning of lower crust beneath the supracrustal basins as they filled with the Yellowknife Supergroup is a hypothesis that needs to be tested. More detailed analysis of present data, together with petrography, geochronology, and more mapping are needed to confirm or deny the currently preferred hypothesis, that structures in the Jolly complex, and therefore, the gneissic rocks themselves are older than the Yellowknife Supergroup.

## REGIONAL METAMORPHISM

Isograds indicating the first appearance of cordierite "knots" (with or without andalusite) and of migmatite (>5-10% leucosome) in metamorphosed greywacke-mudstone outline variations in metamorphic grade across the map area (Fig. 5). The isograd pattern is discordant to older granitoids and is cut by the younger granitoid suite. Relations between structural elements and porphyroblasts indicate deformation and metamorphism overlapped in time and space.

Typical of low-pressure metamorphism, the range of mineral assemblages and degree of partial melting in the migmatite indicate high temperatures (400-700°C) at moderate depths (pressure = 3-5 kbar) in the crust. These high geothermal gradients were maintained during a period of crustal shortening and moderate overthickening. The magnitude of this overthickening is evident from the fact that, despite the significant crustal shortening implied by the major folds, only 10-15 km of postmetamorphism uplift and erosion has occurred.

Discordance between the isograd pattern and both younger and older granitoid suites implies the granitoids are either too old or too young to be the source of metamorphic heat. Younger plutons intrude the area of lowest metamorphic grade without producing mappable contact aureoles and plutons are absent from an extensive area of highest grade (Fig. 5). The areas of lowest grade overlap, or are adjacent to,

older granitoid rocks (Jolly Lake complex). Where homogeneous plutonic rocks intrude medium and high grade rocks they are clearly younger than the main phase of deformation and metamorphism at the present level of erosion. Thompson's (1989) model deriving heat from high geothermal gradients established before the onset of crustal thickening and from radiogenic heat produced by overthickened sialic crust is more likely.

Low grade metamorphosed supracrustal rocks in or near the Jolly Lake complex (Fig. 5) suggest that the complex was a relatively cool block of pre-Yellowknife crust when the Yellowknife Supergroup was metamorphosed. The southward change in structural style described previously is consistent with decreasing metamorphic gradients and a higher proportion of stiff crystalline basement rocks. The pre-Yellowknife age inferred for older granitoids from discordant metamorphosed mafic dykes can explain the discordance in metamorphic grade between gneisses and granitoid migmatite of the Jolly Lake complex and adjacent supracrustal rocks.

## ECONOMIC GEOLOGY

Upgrading the regional geology of the map area has enhanced its mineral potential in a number of ways. Current mapping has established lithological continuity between volcano-sedimentary sequences containing gold and base metal deposits (e.g., Courageous Lake and Beaulieu River volcanic belts) and less well-explored sequences (Winter Lake supracrustal belt, Desteffany Lake volcanic belt). Extension of the known distribution of the Yellowknife Supergroup into areas previously mapped as granitoid and gneissic rocks provides new targets for mineral exploration. Felsic volcanic rocks identified north-northeast of the Courageous Lake belt and to the north and west of Desteffany Lake (Fig. 2; see also Fig. 2 of Thompson et al., 1993a) merit further attention. Felsic volcanic rocks west of Newbigging Lake (Hrabi et al., 1993, 1994) are of particular interest. Thin belts of volcanic and related rocks north of Lake Providence comprise the same volcano-sedimentary sequence associated with the INC volcanic massive sulphide occurrence 15 km north of the area (Fall, 1979). Sulphide-bearing iron-formation, first recognized at the contact between volcanic rocks and metagreywacke in a gossan near Desteffany Lake (Thompson et al., 1993a, b), has been identified at other localities in the same stratigraphic position from west of Desteffany Lake to Mackay Lake, a distance of over 100 km (J.A. Kerswill, pers. comm., 1993). A single sample from the Desteffany Lake gossan assayed 220 ppb gold. Finally, systematic mapping of the extensive granitoid and gneissic rocks permits a more realistic evaluation of their apparent low mineral potential.

Diamondiferous kimberlite pipes are reported just east and north of the map area in the domain characterized by extensive metasedimentary rocks and late plutons. When the distribution of pipes becomes better known, it will be important to establish if their occurrence bears any relation to lithological domain boundaries such as the possible ancient basin margin described in this paper.

## ACKNOWLEDGMENTS

Field assistants Robert Johnson, Lonnie Chin, and Treena Bron did an excellent job. Katherine Venance's multi-faceted contribution to the project was much appreciated. Kevin Chiasson kept the Yellowknife logistics working smoothly. First-class flying services were provided by Ptarmigan Airways and, through Polar Continental Shelf Project, Canadian Helicopters. Sharing campsites and helicopters with John Kerswill (MRD) and with Linda Dredge, Brent Ward, and Dan Kerr of TSD was a pleasant experience and good for science. We benefitted from a working visit by Mike Stublely (Mineral Initiatives Office GNWT). Dianne Paul applied her considerable talent to the diagrams. Cameron Bowie ensured a smooth transition from field maps to published product. Bob Baragar arranged for chemical analysis of peridotitic komatiites. Contacts with Monopros Ltd., Tanquery Resources Ltd., Windspear Resources Ltd., and Brian Weir are acknowledged with thanks. Ken Card and Maurice Lambert provided helpful critical reviews.

## REFERENCES

- Bostock, H.H.**  
1980: Geology of the Itchen Lake area, District of Mackenzie; Geological Survey of Canada, Memoir 391, 101 p.
- Dillon-Leitch, H.C.H.**  
1981: Volcanic stratigraphy, structure and metamorphism in the Courageous-Mackay Lake Greenstone Belt, Slave Province, Northwest Territories; MSc thesis, University of Ottawa, Ottawa, Ontario, 169 p.  
1984: Geology of the Courageous Lake-Mackay Lake greenstone belt, NWT, parts of NTS 75M/14,15; 76D/2,3,5,6; Department of Indian Affairs and Northern Development, Northwest Territories Geology Division, EGS 1984-4a,b,c,d, scale 1:24 000.
- Dredge, L.A., Ward, B.C., and Kerr, D.E.**  
1994: Glacial geology and implications for drift prospecting in the Lac de Gras, Winter Lake, and Aylmer Lake map areas, central Slave Province, Northwest Territories; in *Current Research 1994-C*; Geological Survey of Canada.
- Duquette, D.**  
1993: Petrographie, géochimie, et classification géotectonique du pluton de Courageous Lake, T.N.O.; Thèse de Baccalauréat de Science, Université d'Ottawa, Ottawa, Ontario, 54 p.
- Fall, R.M.**  
1979: Geology and metamorphism of the INC 10 sulphide occurrence, Coppermine River area, NWT; MSc thesis, University of Western Ontario, London, Ontario, 145 p.
- Folinsbee, R.E.**  
1949: Lac de Gras, District of Mackenzie, Northwest Territories; Geological Survey of Canada, Map 977A.
- Fraser, J.A.**  
1969: Winter Lake, District of Mackenzie; Geological Survey of Canada, Map 1219A.
- Henderson, J.B.**  
1970: Stratigraphy of the Yellowknife Supergroup, Yellowknife Bay-Prosperous Lake area, District of Mackenzie; Geological Survey of Canada, Paper 70-26, 12 p.  
1985: Geology of the Yellowknife-Hearne Lake area, District of Mackenzie: a segment across an Archean basin; Geological Survey of Canada, Memoir 414, 135 p.
- Henderson, J.F.**  
1944: MacKay Lake, District of Mackenzie, NWT; Geological Survey of Canada, Map 738A.
- Hrabi, B., Grant, J.W., Godin, P.D., Helmstaedt, H., and King, J.E.**  
1993: Geology of the Winter Lake supracrustal belt, central Slave Province, District of Mackenzie, Northwest Territories; in *Current Research, Part C*; Geological Survey of Canada, Paper 93-1C, p. 71-81.
- Hrabi, R.B., Grant, J.W., Berclaz, A., Duquette, D., and Villeneuve, M.**  
1994: Geology of the northern half of the Winter Lake supracrustal belt, Slave Province, Northwest Territories; in *Current Research 1994-C*; Geological Survey of Canada.
- King, J.E., Van Nostrand, T., Bethune, K., Wingate, M.T., and Relf, C.**  
1991: Final field report on the Contwoyto-Nose Lakes map area, central Slave Province, District of Mackenzie, N.W.T.; in *Current Research, Part C*; Geological Survey of Canada, Paper 91-1C, p. 99-108.
- Kjarsgaard, B.A. and Wyllie, R.J.S.**  
1994: Geology of Paul Lake-Lac de Gras-Lac de Sauvage area, central Slave Province, District of Mackenzie, Northwest Territories; in *Current Research 1994-C*; Geological Survey of Canada.
- Moore, J.C.G., Miller, M.L., and Barnes, F.Q.**  
1951: Carp Lakes, Northwest Territories; Geological Survey of Canada, Paper 51-8.
- Moore, J.C.G.**  
1956: Courageous Lake-Matthews Lakes area, District of Mackenzie, Northwest Territories; Geological Survey of Canada, Memoir 283, 52 p.
- Paulen, R.C.**  
1993: Metallogenic studies: an investigation of gossans in the Winter Lake-Lac de Gras area, central Slave Province, District of Mackenzie, Northwest Territories; Contribution to Special Topics in Geology; Mount Allison University, 82 p.
- Rencz, A.N., Baril, D., and Thompson, P.H.**  
1993: Integrating LANDSAT, aeromagnetic, and geological data for regional bedrock mapping, Winter Lake-Lac de Gras, map area, Northwest Territories; in *Current Research, Part E*; Geological Survey of Canada, Paper 93-1E, p. 239-246.
- Ross, D.A.**  
1993: Petrology of metamorphosed ultramafic rocks at Desteffany, Newbigging, and Courageous Lakes, central Slave Province, NWT; BSc. thesis, Carleton University, 42 p.
- Stublely, M.**  
1991: Preliminary geology of the Prang Lake area, parts of NTS 85P/15,16; Department of Indian Affairs and Northern Development, NWT Geology Division, EGS 1990-19.
- Stublely, M. and Irwin, D.**  
1992: Preliminary geology of the Squalus Lake area, northcentral NTS 85P; Department of Indian Affairs and Northern Development, NWT Geology Division, EGS 1992-10.
- Thompson, P.H.**  
1989: Moderate overthickening of thinned sialic crust and the origin of granitic magmatism and regional metamorphism in low-P/high-T terranes; *Geology*, v. 17, p. 520-523.  
1992: The Winter Lake - Lac de Gras regional mapping project, central Slave Province, District of Mackenzie, Northwest Territories; in *Current Research, Part A*; Geological Survey of Canada, Paper 92-1A, p. 41-46.
- Thompson, P.H., Ross, D., Froese, E., Kerswill, J.A., and Peshko, M.**  
1993a: Regional geology in the Winter Lake-Lac de Gras area central Slave Province, District of Mackenzie, Northwest Territories; in *Current Research, Part C*; Geological Survey of Canada, Paper 93-1C, p. 61-70.
- Thompson, P.H., Ross, D.A., Davidson, A., Froese, E., Kerswill, J.A., and Pesko, M.**  
1993b: Preliminary geological map of the Winter Lake-Lac de Gras area, central Slave Province, District of Mackenzie, NWT; Geological Survey of Canada, Open File 2740.
- Villeneuve, M.**  
1993: Preliminary geochronological results from the Winter Lake-Lac de Gras Slave Province NATMAP project, N.W.T.; in *Radiogenic Age and Isotopic Studies: Report 7*; Geological Survey of Canada, Paper 93-2.

# Geology of the northern half of the Winter Lake supracrustal belt, Slave Province, Northwest Territories<sup>1</sup>

R.B. Hrabi<sup>2</sup>, J.W. Grant<sup>2</sup>, A. Berclaz<sup>3</sup>, D. Duquette<sup>4</sup>, and M.E. Villeneuve  
Continental Geoscience Division

*Hrabi, R.B., Grant, J.W., Berclaz, A., Duquette, D., and Villeneuve, M.E., 1994: Geology of the northern half of the Winter Lake supracrustal belt, Slave Province, Northwest Territories; in Current Research 1994-C; Geological Survey of Canada, p. 13-22.*

---

**Abstract:** Mapping of the northern half of the Winter Lake supracrustal belt has confirmed the basic tectonostratigraphy developed in the southern half of the belt. Older felsic volcanic rocks occur at the base of supracrustal sequence. Units of komatiitic basalt continue from the southern Winter Lake belt within the mafic volcanic sequence and are interpreted to form part of a komatiitic basalt-tholeiitic basalt volcanic assemblage. Two outcrops of well-preserved sheeted dykes with asymmetric cooling margins are present within the mafic volcanic sequence. A younger package of felsic volcanic rocks, not present in the southern half of the belt, occurs between the mafic volcanic rocks and the turbiditic sedimentary rocks. Two major phases of folding and cleavage development are inferred to be primarily responsible for the present structural geometry of the supracrustal rocks, with later near belt-parallel sinistral faults modifying this geometry.

**Résumé :** La cartographie de la partie nord de la ceinture supracrustale de Winter Lake a confirmé la tectonostratigraphie de base établie dans la partie sud de cette ceinture. Des roches volcaniques felsiques anciennes se trouvent à la base de la séquence supracrustale. Des unités de basalte komatiitique, reconnues dans la partie sud de la ceinture de Winter Lake, ont été tracées au sein de la séquence volcanique mafique. Elles sont interprétées comme faisant partie d'un assemblage volcanique de basalte komatiitique et de basalte tholéiitique. Deux affleurements montrant des dykes laminés à bordures figées asymétriques, bien préservés, sont présents au sein de la séquence volcanique mafique. Un assemblage plus jeune de roches volcaniques felsiques, non représenté dans la partie sud de la ceinture, est présent entre les roches volcaniques mafiques et les roches sédimentaires (turbidites). Deux épisodes de plissement majeurs, accompagnés de la formation de clivages, sont considérés comme étant principalement responsables de la géométrie structurale actuelle des roches supracrustales. Des failles senestres pratiquement parallèles à la ceinture ont par la suite modifiées cette géométrie.

---

<sup>1</sup> Contribution to Canada-Northwest Territories Mineral Initiative (1991-1996), an initiative under the Canada-Northwest Territories Economic Development Cooperation Agreement.

<sup>2</sup> Department of Geological Sciences, Queen's University, Kingston, Ontario K7L 3N6

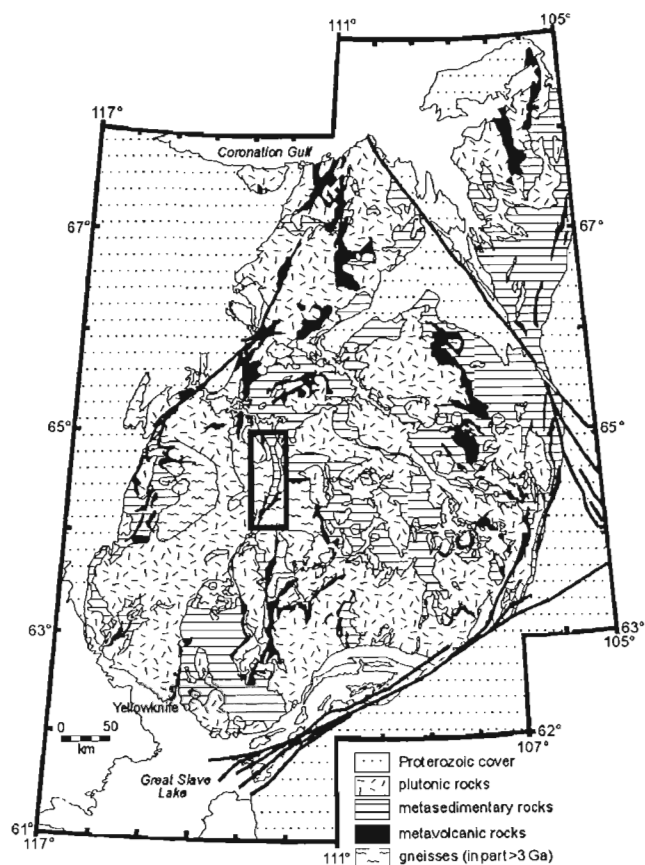
<sup>3</sup> Département de Géologie, Université Laval, Ste-Foy, Québec G1K 7P4

<sup>4</sup> Department of Geology, University of Ottawa, Ottawa, Ontario K1N 6N5

## INTRODUCTION

The purpose of the Winter Lake Mineral Initiatives Project is to conduct 1:50 000 scale mapping of the Winter Lake supracrustal belt to better define the supracrustal rock assemblages, deformation history, and geological context of mineral showings. The belt is located in the east half of the Winter Lake sheet (NTS 86A), central Slave Province (Fig. 1). Project funding is provided by the Canada-Northwest Territories Mineral Initiatives (Project C4. 120).

Previous work in the Winter Lake area includes 1:250 000 scale regional mapping by Fraser (1969), detailed mapping of the sedimentary rocks southwest of Newbigging Lake (Rice et al., 1990), and concurrent 1:250 000 scale mapping by Thompson (1992) and Thompson et al. (1993, 1994) in a complementary NATMAP project. Work this summer was mainly a northward continuation of 1992 mapping in the south half of the belt, and completes the mapping of the supracrustal belt between 64° and 65° of latitude. A simplified map of the results of this field season is presented in Figure 2.



**Figure 1.** Location of the Winter Lake supracrustal belt (outlined) in the Slave Province. Modified after Hoffman (1989).

This report concentrates on: 1) additional descriptive details of the supracrustal rock packages defined during the 1992 season (Hrabi et al., 1993); 2) description of an additional folding and cleavage forming event, not recognized in the southern half of the belt; and 3) initial results of U-Pb geochronology of the supracrustal units. All rock types have been metamorphosed under greenschist or amphibolite facies conditions, but for clarity the prefix "meta" has been omitted in this paper.

## SUPRACRUSTAL ROCK UNITS

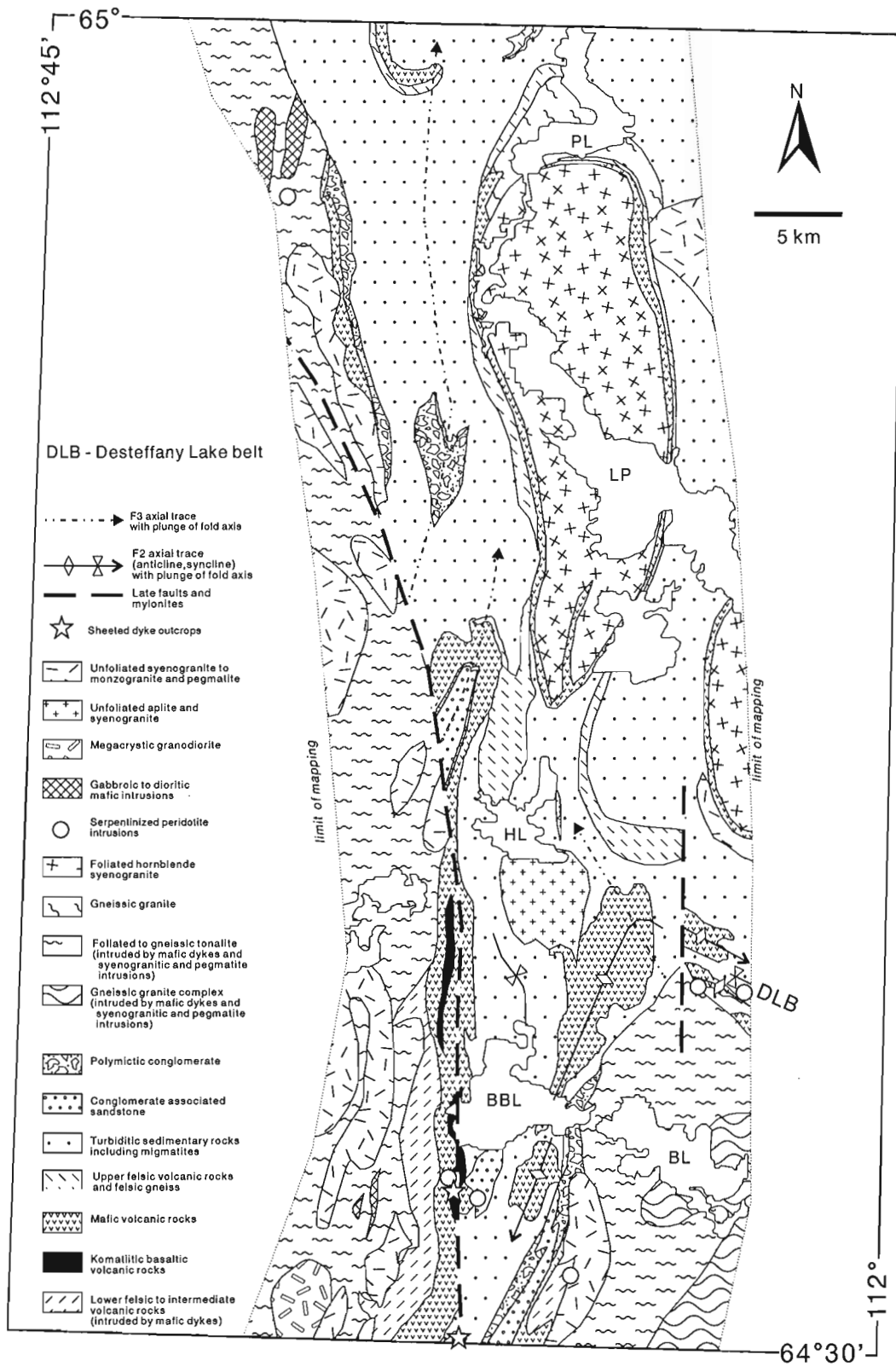
On the basis of mapping during the summer of 1992, the supracrustal units in the Winter Lake belt were tentatively subdivided into three groups (Hrabi et al., 1993). Units of felsic volcanic rock, associated quartz-rich sedimentary rock, and a unit of komatiitic basalt were grouped into a pre-Yellowknife Supergroup package. Mafic volcanic rocks and the turbiditic sedimentary rocks that generally overlie them in the map area, typical of much of the Yellowknife Supergroup (Henderson, 1970) elsewhere in the Slave Province, were grouped together. Polymictic conglomerates and associated sedimentary rocks were assigned to a post-Yellowknife Supergroup unit, believed to be analogous to the Jackson Lake Formation in the Yellowknife greenstone belt. Mapping in the northern half of the Winter Lake belt suggests that, with one important revision, the tectonostratigraphy proposed for the belt based on mapping in the south half of the belt is valid.

### *Felsic to intermediate volcanic rocks*

The felsic volcanic unit mapped on the east side at the base of the Winter Lake supracrustal belt continues to the north along the east side of the belt as a small lens and is also found along the west margin reaching a maximum width of approximately 1.5 km. On the west side of the belt, north of approximately 64°30', a unit that had been mapped as greywacke, biotite-quartz schist, nodular schist, and minor hornblende schist (Fraser, 1969) is here considered to be part of this lower felsic volcanic package (Fig. 2), because it lies stratigraphically beneath the main mafic volcanic sequence and gabbro dykes constitute a large volume of the unit, as in the lower felsic rocks on the east side. Outcrops of felsic volcanic rock are also found along strike to the north as enclaves within foliated biotite tonalite.

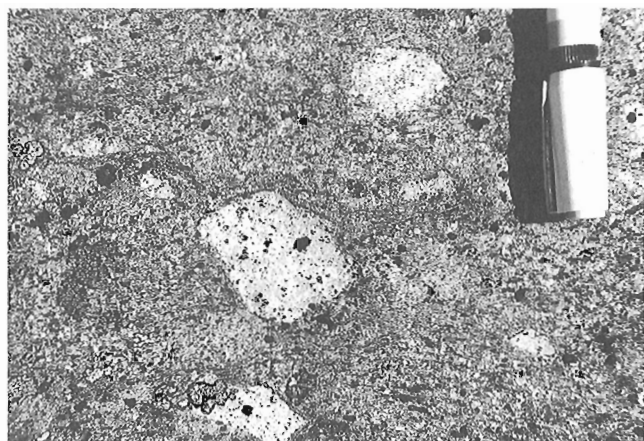
Most of the unit is composed of fine grained, light-grey-to cream-weathering, quartz-plagioclase-hornblende-biotite schist. Thin layers of lappilli-ash tuff or ash tuff breccia make up a smaller volume of the unit (Fig. 3). These contain up to 60% light grey-weathering, monomictic, quartz-phyric volcanic clasts within a matrix compositionally similar to the fine grained layers.

Based on the structural position of the felsic volcanic rocks at the base of the supracrustal rocks and observations of contacts and bedding orientations indicating it has a con-



**Figure 2.** Simplified geological map of the northern half of the Winter Lake supracrustal belt. PL – Point Lake, LP – Lake Providence, HL – Hopeless lake, BBL – Big Bear lake, BL – Beauparlant Lake.





**Figure 3.** *Monomictic, felsic lapilli ash tuff within the felsic volcanic unit at the base of the supracrustal sequence on the west side of the belt. Outcrop is located west of Big Bear lake.*

formable or disconformable upper contact with the overlying mafic volcanic rocks, the felsic volcanic unit was interpreted to be the oldest of the preserved supracrustal units (Hrabi et al., 1993). U-Pb dating of a sample of red-weathering, massive felsic volcanic rock from the south shore of Newbigging Lake resulted in a date of  $3118 \pm 11/-8$  Ma (M. Villeneuve, unpub. data, 1993). Unless all the zircons in the sample are xenocrysts, this would represent the age of formation of the lower felsic volcanic package. This date, together with one of  $3141.7 \pm 1.2/-1.1$  Ma from a quartz-eye dacite porphyry in the Napaktulik Lake area (Villeneuve et al., 1993) are the oldest identified yet from supracrustal rocks in the Slave Province.

### **Quartz-rich sedimentary rocks**

Quartz-rich sedimentary rocks are associated with the felsic volcanic rocks in the southeastern part of the belt, forming thin, discontinuous units. A few outcrops containing quartz-rich sedimentary rocks were also found further north, but they are not continuous enough to be traced as a separate unit and are included with the lower felsic volcanic rocks in Figure 2.

U-Pb dates of detrital zircons from a sample of this unit at the north shore of Sherpa lake (Hrabi et al., 1993), all fall within the range of 3140-3160 Ma (M. Villeneuve, unpub. data, 1993). Given the tight range of dates from these zircons and their similarity to the date from the felsic volcanic rocks, it is suggested that the orthoquartzite is derived from the underlying older felsic volcanic rocks.

### **Mafic and komatiitic basalt volcanic rocks**

#### **Komatiitic basalt**

The komatiitic basalt unit mapped in the southern part of the belt occurs between the felsic volcanic rocks and mafic volcanic rocks and has apparently conformable upper and lower contacts. It was tentatively grouped with the less common

pre-Yellowknife Supergroup felsic volcanic-orthoquartzite package (Hrabi et al., 1993), as komatiitic volcanic rocks had not been identified previously in the Yellowknife Supergroup.

Additional field data suggests that this interpretation should be revised. Units with a komatiitic basalt composition (but enriched  $\text{TiO}_2$ ) were found within a turbidite sequence of the Yellowknife Supergroup in the Lake of the Enemy area (Johnstone, 1992), suggesting that komatiites may be present elsewhere in the Yellowknife Supergroup. In addition, more units of pillowed komatiitic basalt (Fig. 4) were mapped in 1993 on the west side of the Winter Lake belt, both in the middle of the mafic volcanic succession and near its upper contact (Fig. 2). In areas of relatively low strain, contacts and facing directions within the komatiitic basalts and surrounding mafic units indicate that the units are conformable and interlayered. This in turn suggests that the komatiitic basalts are more likely to be associated with the mafic volcanic rocks, similar to the common komatiite-tholeiite association in other Archean supracrustal belts (Jackson and Fyon, 1991).

#### *Chemistry*

Three samples of pillowed komatiitic basalt were analyzed for major elements (XRF), trace elements (XRF, INAA, ICP-MS), and rare-earth elements (ICP-MS) at XRAL Laboratories, Toronto. Analytical results are shown in Table 1. All three samples plot in the komatiitic basalt field on a Jensen Cation plot (Fig. 5) and are LREE-enriched (Fig. 6A). Similar high-Mg volcanic rocks from the Beaulieu River Belt have been analyzed (Lambert et al., 1992). For various reasons, the results were interpreted by Lambert et al. (1992) as unrepresentative of original melt compositions. As all the samples from the Winter Lake belt were taken from pillowed flows, they are definitely extrusive and are not likely to have been affected by excessive crystal accumulation. Although Zr is slightly enriched, it falls along the same compositional trends as komatiitic basalts from other Archean terranes (Ludden and Gélinais, 1982).



**Figure 4.** *Pillowed komatiitic basalt, identified in outcrop by its light green colour, soft weathered surface, and the common presence of tremolite crystals, located near the top of the mafic volcanic sequence.*

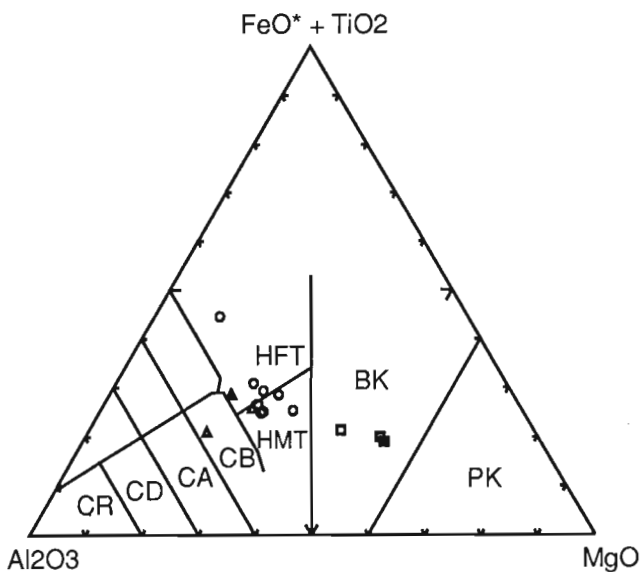
**Table 1.** Geochemical analysis of komatiitic basalts, pillowed basalts, and massive basalt flows or fine grained mafic intrusions. All samples analyzed by XRF, INAA, and ICP-MS at XRAL Laboratories, Toronto.

Sample Name	HLB-92-B0207A	HLB-92-J0684A	HLB-92-F0356B	HLB-92-B0201A	HLB-92-J0072A	HLB-92-J0560A	HLB-92-B0046B	HLB-92-B0073A	HLB-92-B0185A	HLB-92-C0024B	HLB-92-J0063A	HLB-92-J0070B	HLB-92-J0122A
Rock Type	korn. bsf	korn. bsf	korn. bsf	pH. bsf	pH. bsf	pH. bsf	mass. mafic	mass. mafic	mass. mafic	mass. mafic	mass. mafic	mass. mafic	mass. mafic
Mg Number	68.73	74.49	73.34	44.99	52.44	52.50	52.51	55.07	22.02	52.75	45.94	49.54	58.70
SiO2 (wt%)	62.40	50.00	48.90	50.90	52.00	53.90	50.00	51.50	52.70	49.10	49.70	49.20	48.20
TiO2	0.66	0.57	0.64	1.11	0.83	0.88	0.96	0.73	1.62	0.96	1.10	1.04	0.74
Al2O3	11.70	11.20	10.60	15.00	14.80	15.90	15.10	14.70	12.80	13.90	14.30	14.70	13.90
Fe2O3	10.90	11.60	11.30	12.40	11.80	8.17	12.70	11.60	18.80	14.10	14.40	14.40	12.90
MnO	0.21	0.19	0.18	0.24	0.37	0.24	0.18	0.20	0.26	0.20	0.29	0.23	0.20
MgO	12.10	17.10	15.70	5.12	6.57	4.56	7.09	7.18	2.68	7.96	6.18	7.14	9.26
CaO	8.59	5.65	8.57	12.30	10.80	13.10	11.20	10.40	7.72	11.00	11.40	10.60	12.50
Na2O	2.23	0.65	1.31	1.83	2.05	2.37	1.79	2.90	2.59	1.60	1.90	1.13	1.01
K2O	0.08	0.37	0.24	0.25	0.42	0.18	0.07	0.30	0.40	0.20	0.15	0.87	0.21
P2O5	0.06	0.06	0.06	0.10	0.09	0.08	0.08	0.06	0.13	0.07	0.10	0.09	0.07
LOI	1.15	2.40	2.40	1.05	0.70	0.75	0.50	0.55	0.30	0.85	0.40	0.95	0.60
Total	98.93	97.39	97.50	99.25	99.73	99.38	99.17	99.84	99.70	99.08	99.52	99.40	98.99
Cr (ppm)	1110	1400	1600	150	330	350	220	140	13	340	83	120	170
Ni	226	414	515	96	97	151	118	73	115	92	90	115	209
Co	57	76	70	49	40	49	49	48	42	48	50	44	53
Sc	34	38	32	32	40	40	39	40	46	46	36	38	36
V	214	216	209	227	229	260	221	202	53	254	249	237	216
Cu	82	1	56	103	64	89	142	31	234	117	115	97	96
Zn	65	75	65	88	64	80	80	166	111	91	93	97	81
Ga	22	16	17	19	14	17	17	17	24	18	19	19	16
Ge	15	154	16	8	18	10	12	16	11	10	13	72	75
Li	42	12	29	8	6	5	7	7	8	7	8	5	7
Nb	180	140	140	240	150	150	170	120	310	170	270	190	160
Hf	67	57	63	81	59	59	64	58	107	57	88	66	54
Zr	15	12	12	15	18	18	19	16	36	18	22	20	17
Y	2.8	1.4	2.0	0.4	0.4	0.2	0.2	0.9	4.8	0.2	0.7	2.0	0.5
Th	0.7	0.3	0.8	1.8	2.50	1.6	0.9	0.4	2.3	0.4	0.7	0.3	0.5
U	7.80	4.20	3.30	5.30	6.20	7.60	3.00	4.60	13.00	2.90	5.80	3.40	2.40
La	15.60	9.00	8.30	12.70	1.00	1.20	7.50	9.90	25.50	7.30	14.00	8.50	6.10
Ce	1.90	1.10	1.10	1.80	1.00	1.20	1.20	1.40	3.20	1.20	2.10	1.40	1.00
Pr	8.10	4.90	5.60	8.70	5.40	6.00	6.20	6.50	14.30	5.90	9.90	6.90	5.10
Nd	2.20	1.50	1.70	2.70	1.90	2.10	2.40	2.00	4.60	2.30	3.20	2.40	1.90
Sm	0.66	0.35	0.56	0.91	0.82	0.83	0.82	0.75	1.46	0.79	0.98	0.87	0.72
Eu	2.30	1.60	1.90	2.70	2.30	2.50	2.70	2.30	5.20	2.50	3.50	2.80	2.30
Gd	0.40	0.30	0.30	0.50	0.40	0.50	0.50	0.40	0.90	0.50	0.60	0.50	0.40
Tb	2.80	2.00	2.30	2.90	3.00	3.10	3.40	2.70	6.20	3.20	4.00	3.50	2.90
Dy	0.57	0.47	0.48	0.66	0.66	0.67	0.75	0.60	1.36	0.69	0.82	0.76	0.63
Ho	1.60	1.50	1.40	1.80	1.80	1.80	2.10	1.80	4.10	1.80	2.20	2.10	1.80
Er	0.25	0.22	0.20	0.30	0.30	0.30	0.30	0.30	0.60	0.30	0.30	0.30	0.30
Tm	1.50	1.50	1.30	1.20	1.90	1.90	2.10	1.70	4.20	1.80	2.20	2.10	1.80
Yb	0.24	0.22	0.23	0.17	0.27	0.27	0.31	0.25	0.63	0.26	0.31	0.31	0.30
Lu													

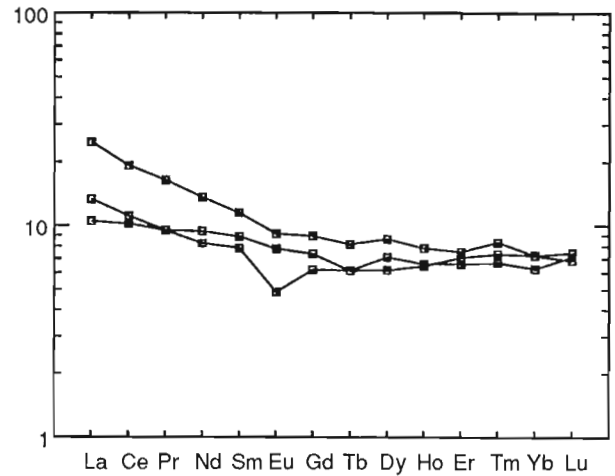
**Mafic volcanic rocks**

On the west side of the belt, the mafic volcanic rocks form an east-facing homocline that is continuous to a point northwest of Hopeless lake where it is folded about an F<sub>3</sub> fold and terminates against a late fault, and intermittently from there to the north boundary of the map area (Fig. 2). On the east side of the belt, a south-plunging, north-trending anticline, cored by mafic volcanic rocks, is refolded into the Desteffany Lake belt which strikes away from the Winter Lake supra-crustal belt (Fig. 2). Massive and pillowed facies dominate in these units, although differentiated mafic sills and serpentized peridotites were mapped within the western homocline to the west of Big Bear lake. A thin unit of amphibolite is conformable with the margins of a large foliated, hornblende+biotite syenogranite intrusion in the northeast part of the map area (Thompson et al., 1993). This unit is continuous and occurs structurally below turbiditic sedimentary rocks and a younger felsic volcanic unit, similar to less recrystallized mafic volcanic rocks elsewhere. At the northern margin of the map area a thin, folded unit of mafic rocks continues off the north edge of the map (Fig. 2).

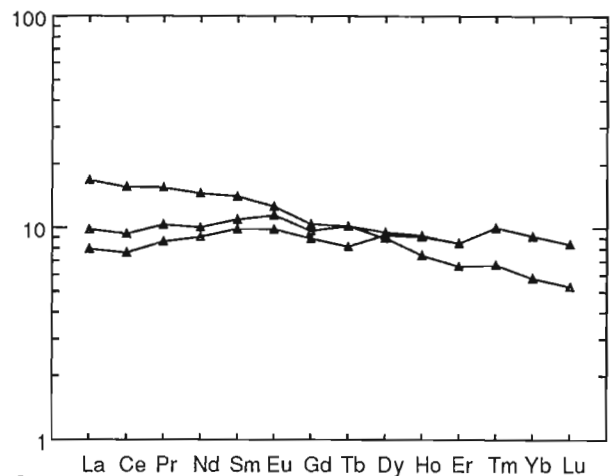
Two separate outcrops of sheeted dykes occur approximately 7 km apart at about the same stratigraphic level, near the top of the main mafic section southwest of Big Bear lake (Fig. 2). The southern dyke occurrence has mafic volcanic rocks above and below it, although the contacts were not observed. The exposed section is 15 m wide (Fig. 7a) and consists of parallel-sided dykes trending at 090°. Over the 15 m, twenty dykes are present, ranging in thickness from 25 cm to 100 cm. The northern outcrop of sheeted dykes is approximately 15 m by 35 m and also consists of parallel-sided dykes that strike between 070° and 040° (Fig. 7b). Over a 7 m measured section, twenty-one individual dykes are present, ranging in thickness from 10 cm to 75 cm. Each dyke



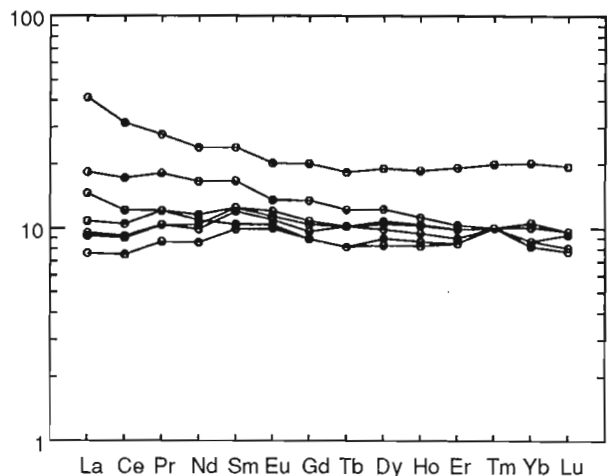
**Figure 5.** Jensen Cation Plot of analyzed pillowed komatiitic basalts (□), pillowed basalts (Δ), and fine grained massive mafic flows or intrusions (○).



A.



B.

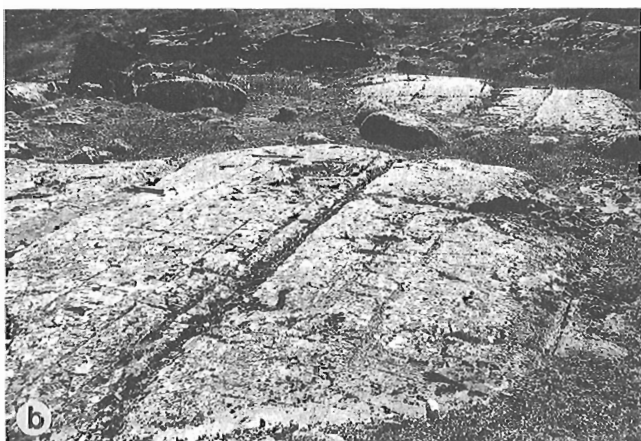


C.

**Figure 6.** Rare-earth element spidergrams of A) pillowed komatiitic basalts, B) pillowed mafic rocks, and C) fine grained massive mafic flows or intrusions. All plots normalized using Leedy chondrite values divided by 1.20 (Taylor and Gorton, 1977).

is asymmetric with a single chilled margin on the southern contact of the dykes. The mafic dyke section sits directly above a series of serpentinized peridotite intrusions, approximately 500 m thick, and stratigraphically below a thin sequence of pillowed komatiitic basalts and tholeiitic basalts. Together, the dykes and pillowed mafic rock types resemble components of typical ophiolite sequences, although their thicknesses are significantly less than Proterozoic or Paleozoic ophiolites (Helmstaedt and Scott, 1992). No feeder dykes to the sheeted complex were recognized in the ultramafic intrusions and mafic volcanic rocks below. The absence of such dykes may mean that a currently unrecognized fault has displaced the sheeted dykes from their magma source.

Small, serpentinized peridotite intrusions are found throughout the map area within most of the supracrustal rock types (Fig. 2). Although they were not shown on the simplified map of the southern half of the belt, similar peridotite bodies were also mapped south of Newbigging Lake within the older felsic volcanic rocks and near Izabeau lake within mafic volcanic rocks (Hrabi et al., 1993).



**Figure 7.** Outcrops of sheeted dykes, striking approximately east-west, perpendicular to the overall strike of the mafic volcanic sequence on the west side of the Winter Lake belt. **a)** Southern occurrence close to 64°30' latitude. **b)** Northern occurrence southwest of Big Bear lake. Rock hammer for scale in both photographs.

### Chemistry

Preliminary results of geochemical analysis of mafic volcanic rocks sampled in the south half of the map area in 1992 are presented in Table 1. The samples were taken from both pillowed and massive flows that, in outcrop, had very similar characteristics. Most samples plot as high-Mg to high-Fe tholeiites on a Jensen Cation Plot (Fig. 5), although one sample plots in the calc-alkalic basalt field. The rare-earth element (REE) profiles of the tholeiitic basalts are flat to slightly light rare-earth element (LREE) enriched with no strong Eu anomaly (Fig. 6B and 6C). Additional analyses are in progress to understand the geochemical variations in these rocks.

### Other felsic volcanic rocks

The distribution of a group of felsic volcanic rocks, identified by Thompson et al. (1993) in numerous locations within the map area, was defined in greater detail during the present mapping (Fig. 2). Although no facing directions are available, this group of felsic rocks generally occurs at or within several hundred metres of the contact between the mafic volcanic rocks and the turbiditic sedimentary rocks. The felsic rocks are light weathering, fine- to medium-grained ash tuffs, or lappilli ash tuffs with a high proportion (up to 40%) of 1-2 cm disk-shaped fragments containing or rimmed by fine grained sillimanite (Fig. 8a). At higher metamorphic grades, in the northern part of the map area, this unit is represented by a garnet-bearing quartzo-feldspathic gneiss which in places contains sillimanite (Fig. 8b). Since these rocks are found higher in the supracrustal stratigraphy and are not intruded by the great volume of gabbro found in the older felsic volcanic rocks at the base of the supracrustal assemblage, they are inferred to represent a separate and younger felsic unit.

### Polymictic conglomerate and associated sandstone

Polymictic conglomerate associated with arkosic, sometimes crossbedded, sandstones have been described in the southern part of the map area (Hrabi et al., 1993). On the basis of map-scale unconformable relationships and the absence of the earliest folding event recognized in the turbiditic sedimentary rocks, the polymictic conglomerates and associated sandstones were interpreted to be a younger group of rocks, unconformably overlying the rest of the supracrustal rocks. Additional occurrences of polymictic conglomerate and associated sandstone, most identified by previous authors (Fraser, 1969; Rice et al., 1990; Thompson et al., 1993) are outlined in the north part of the map area (Fig. 2). In the northern part of the map area, the conglomerates and their contacts are relatively highly strained and there are no clear-cut map-scale unconformities to provide additional evidence for the unconformable relationship inferred in the south (Hrabi et al., 1993). Dating of clasts and matrix of the conglomerates and cross-cutting intrusions are needed to bracket the depositional age of these rocks.

## INTRUSIVE UNITS

As in the first field season, mapping included the granitoid-gneiss rocks and plutonic rocks adjacent to and within the map area. Most of these units have been described previously (Thompson, 1992; Hrabi et al., 1993; Thompson et al., 1993). Two additional plutonic rock types were mapped this summer. The first, a foliated and recrystallized hornblende±biotite syenogranite, was described by Thompson et al. (1993) but was not found in the southern half of the supracrustal belt. The second is a poorly exposed, weakly deformed, coarse grained biotite syenogranite with a wide marginal zone of fine grained to aphanitic quartz-porphyry found in the middle of the belt, centred south of Hopeless lake (Fig. 2).

The tonalite gneiss complex and granite gneiss bounding the belt in the southern half of the map area have been described previously (Hrabi et al., 1993; Thompson et al., 1993). Foliated biotite tonalite or gneissic tonalite also bounds much of the west margin of the belt in the northern half of the map area. The granitoid gneiss, present along the eastern boundary of the belt to the south, continues to the north but is separated from the belt, near Beauparlant Lake, by a large intrusion of foliated and

recrystallized biotite±hornblende tonalite (Thompson et al., 1993). The contact of the granite gneiss and the fabric in the gneiss are deflected to an approximately easterly strike approaching the Desteffany Lake belt just north of Beauparlant Lake.

### *Hornblende±biotite syenogranite*

Two large intrusions of recrystallized and foliated hornblende±biotite syenogranite are located near the northern end of Lake Providence and were mapped by Thompson et al. (1993). Both intrusions are variably foliated, with the foliation intensity increasing strongly at the east and west margins of the intrusions. Supracrustal units, particularly thin units of amphibolite inferred to be recrystallized mafic volcanic rocks, are completely conformable with the margins of these intrusions, and are strongly deformed at the contact, although the fabric within the foliated syenogranite is not conformable with the supracrustal rocks at its northern contact.

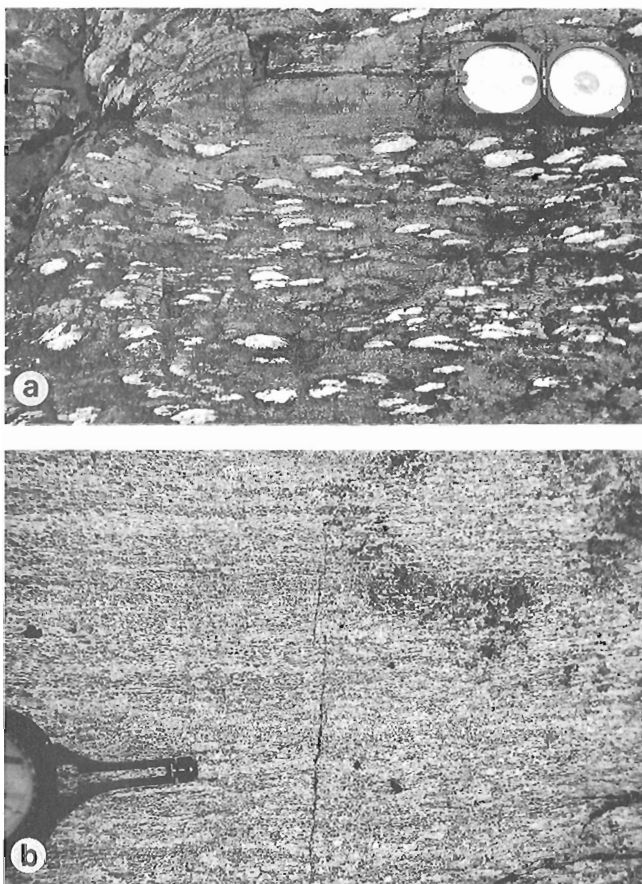
## STRUCTURES AND DEFORMATION HISTORY

Three sets of Archean structures were recognized in the first summer of mapping in the southern Winter Lake belt (Hrabi et al., 1993). Additional features of these deformation events, and evidence for a fourth important deformation event inferred from structures mapped during 1993, are described below.

The earliest structures, recognized only in the southern half of the belt, are early folds ( $F_1$ ) in the turbiditic sedimentary rocks with no recognized axial-planar cleavage (Hrabi et al., 1993). The dominant cleavage, subparallel to the belt margins cut both limbs of these folds.

Structures that are inferred to belong to the second deformation event are the dominant foliation ( $S_2$ ), which is subparallel to the margin of the belt along much of its length, and folds ( $F_2$ ) that deform the supracrustal rocks into variably plunging folds with axial planes parallel to the length of the belt in the central part of the belt (south part of Fig. 2). These  $F_2$  folds have metre- to kilometre-scale wavelengths. Southwest of Beauparlant Lake, pillows in mafic volcanic rocks and bedding in overlying turbidites wrap around a south-plunging  $F_2$  anticline. South-facing pillows can be recognized in the hinge zone of this fold, despite a strong north-striking axial planar cleavage ( $S_2$ ). To the north, these mafic volcanic rocks close, and then open again north at Big Bear lake, suggesting a dome and basin fold interference pattern. No crosscutting fabrics are associated with this apparent crossfolding and  $S_2$  foliation is not refolded, indicating that the  $F_2$  domes resulted from either periclinal  $F_2$  fold forms or  $F_2$  refolding of earlier  $F_1$  folds.

Within the Desteffany Lake belt close to its junction with the Winter Lake belt, the dominant foliation is approximately northeast-striking, parallel to the Desteffany Lake belt and axial-planar to a set of southeast-plunging folds, also cored by mafic volcanic rocks with turbiditic sedimentary rocks on the limbs. Close to the junction of the two belts a well-developed,



**Figure 8.** a) Outcrop of disc-shaped fragments within part of the upper felsic volcanic sequence. Outcrop located northwest of Hopeless lake. b) Example of quartzo-feldspathic gneiss, representing the higher grade equivalent of the upper felsic volcanic sequence. Outcrop located west of Lake Providence.



north-striking crenulation cleavage deforms the dominant northeast-striking foliation in the Desteffany Lake supracrustal belt. A north-striking fault follows the crenulation cleavage and juxtaposes Desteffany Lake mafic volcanic rocks against turbiditic sedimentary rocks (Fig. 2). A very important feature of the folds in both the Winter Lake and Desteffany Lake belts at this juncture is that both pillow-facing directions and graded bedding in the overlying turbidites indicate that the supracrustal rocks locally face outward into the belt-bounding biotite tonalite intrusion, in contrast to most of the belt where supracrustal rocks are broadly conformable with, and face away from, the belt margin.

If the dominant foliations and associated folds in both the Winter Lake and Desteffany Lake belts are continuations of the same set of structural features, these structures must have been folded about a post- $D_2$  fold ( $F_3$ ), as mapped by Thompson et al. (1993). A second possibility is that the dominant foliation in the Desteffany Lake belt predates the dominant foliation in the Winter Lake belt. A later east-west compression responsible for the dominant foliation in the Winter Lake belt would then locally crenulate the pre-existing dominant foliation in the Desteffany Lake belt where it joins the Winter Lake belt.

The dominant  $S_2$  foliation maintains its steep, belt-parallel orientation to north of Hopeless lake; north of this its orientation becomes more complicated. Foliations in the turbiditic sedimentary rocks often dip shallowly to the north, and at the north map boundary in the centre of the belt (Fig. 2), they parallel a folded package of mafic volcanic, younger felsic volcanic, and turbiditic sedimentary rocks. These foliations are mineralogically similar to  $S_2$  foliations to the south and are interpreted to belong to the same generation of structures ( $D_2$ ), suggesting that bedding and foliations are folded about a post- $D_2$  fold ( $F_3$ ) in the north half of the map area.

In addition to the  $F_3$  folds, north-trending  $S_3$  planar fabric variably overprint the shallowly-dipping  $S_2$  foliation at several locations west of Lake Providence. Where the  $S_3$  fabric is a spaced cleavage, mica in the microlithon preserves the  $S_2$  orientation. In conglomerate, flattened competent granitic clasts and quartz veins strike approximately east-west, yet less competent mafic and fine grained clasts are flattened along a north-south axis, reflecting a preserved  $S_2$  and weaker, overprinting  $S_3$ , respectively.

Strike-slip faults, postdating all other structures and metamorphism, with strike lengths of hundreds of kilometres, partially characterize a north-south corridor that includes the Winter Lake supracrustal belt (Stublely, 1990a, b; Hrabi et al., 1993). One of these faults, striking  $350^\circ$ - $000^\circ$  with a sinistral offset of approximately 15 km, was mapped in the area last year and continues to the south (Stublely, 1990a, b). An additional fault with similar orientation and sense of displacement was mapped this summer, cutting obliquely across the belt at a small angle. The extension of this fault in the south half of the belt displaces a unit of polymictic conglomerate ca. 2.5 km in a left-lateral sense. In the northern part of the

map area, it follows close to the upper contact of the mafic volcanic section west of Big Bear lake before cutting into the bounding granitoids to the west (Fig. 2). A strong foliation or mylonitic foliation, extensive hydrothermal alteration, and brecciation characterize the fault where exposed in the supracrustal belt and in the adjacent granitoids.

## DISCUSSION

Mapping in the northern half of the Winter Lake belt suggests that, with one important revision, the tectonostratigraphy proposed for the belt based on mapping in the south half of the belt is valid. A felsic volcanic sequence occupies the lowest stratigraphic position in the belt and has been dated at  $3118 \pm 11/-8$  Ma. This unit represents a supracrustal sequence significantly older than previously dated units (van Breemen et al., 1992) of the Yellowknife Supergroup. Komatiitic basalts are present at the base, in the middle and at the top of the mafic volcanic sequence that overlies the old felsic volcanic sequence. As such, the komatiitic basalts are considered part of a komatiitic-tholeiitic basalt association, rather than the bimodal felsic volcanic-komatiite association that mapping in the southern half of the belt had suggested (Hrabi et al., 1993). The mafic volcanic sequence west of Big Bear lake also includes serpentized peridotite (Thompson et al., 1993), layered mafic sills, and sheeted dykes. An additional package of younger felsic volcanic rocks, identified by Thompson et al. (1993), occurs above the mafic volcanic sequence near its contact with the overlying turbiditic sedimentary rocks. Two major phases of folding and cleavage development are inferred to be primarily responsible for the present distribution of supracrustal rock units in the map area.

The recognition of outcrops of sheeted dykes within the mafic volcanic sequence, together with the layered mafic sills and serpentized peridotite are intriguing, considering that these rock types are components of typical ophiolite sequences (Anonymous, 1972). Multiple mafic dyke intrusions within the Kam Group of the Yellowknife Supergroup (Helmstaedt et al., 1986) have been used to suggest that sea-floor spreading operated during the Archean. Given the significance of sheeted dykes in recognizing possible Archean ophiolites, detailed mapping of the mafic volcanic sequence in the area of the sheeted dykes, and the relationship of this sequence with the underlying older felsic supracrustal sequence is a prime objective of fieldwork to be conducted next summer.

## ACKNOWLEDGMENTS

Excellent assistance in the field was provided by Corrine Paul. Rod Brown and Kevin Chiasson are thanked for their expediting services. Herb Helmstaedt, Janet King, and Peter Thompson provided stimulating discussions in the field and beneficial reviews of this manuscript.

---

**REFERENCES**


---

**Anonymous.**

1972: Penrose conference field report on ophiolites; *Geotimes*, v. 17, p. 24-25.

**Fraser, J.A.**

1969: *Geology, Winter Lake, District of Mackenzie*; Geological Survey of Canada, Map 1219A, scale 1:253 440.

**Helmstaedt, H., Padgham, W.A., and Brophy, J.A.**

1986: Multiple dikes in Lower Kam Group, Yellowknife greenstone belt: evidence for Archean sea-floor spreading?; *Geology*, v. 14, p. 562-566.

**Helmstaedt, H.H. and Scott, D.J.**

1992: The Proterozoic ophiolite problem; in *Proterozoic Crustal Evolution*, (ed.) K.C. Condie; Elsevier, Amsterdam, p. 55-95.

**Henderson, J.B.**

1970: Stratigraphy of the Yellowknife Supergroup, Yellowknife Bay-Prosperous Lake area, District of Mackenzie; Geological Survey of Canada, Paper 70-26, 12 p.

**Hoffman, P.F.**

1989: Precambrian geology and tectonic history of North America; in *The Geology of North America - An Overview*, Geological Society of America, *The Geology of North America Volume A*, p. 447-512.

**Hrabi, R.B., Grant, J.W., Godin, P.D., Helmstaedt, H., and King, J.E.**

1993: *Geology of the Winter Lake supracrustal belt, central Slave Province, District of Mackenzie, Northwest Territories*; in *Current Research, Part C*; Geological Survey of Canada, Paper 93-1C, p. 71-81.

**Jackson, S.L. and Fyon, J.A.**

1991: The western Abitibi Subprovince in Ontario; in *Geology of Ontario, Ontario Geological Survey, Special Volume 4*, pt. 1, p. 405-482.

**Johnstone, R.M.**

1992: *Geology and mineral potential of the Lake of the Enemy area, south-central Slave Province (parts of 75M/9,10,15,16)*; in *Exploration Overview 1992*, (ed.) J. Brophy; Northwest Territories Geology Division, Department of Indian Affairs and Northern Development, p. 32.

**Lambert, M.B., Ernst, R.E., and Dudás, F.Ö.L.**

1992: Archean mafic dyke swarms near the Cameron River and Beaulieu River volcanic belts and their implications for tectonic modelling of the Slave Province, Northwest Territories; *Canadian Journal of Earth Sciences*, v. 29, p. 2226-2248.

**Ludden, J.N. and Gélinas, L.**

1982: Trace element characteristics of komatiites and komatiitic basalts from the Abitibi metavolcanic belt of Quebec; in *Komatiites*, (ed.) N.T. Arndt and E.G. Nisbet; George Allen and Unwin, London, p. 331-346.

**Rice, R.J., Long, D.G.F., Fyson, W.K., and Roscoe, S.M.**

1990: Sedimentological evaluation of three Archean metaquartzite- and conglomerate-bearing sequences in the Slave province, N.W.T.; in *Current Research, Part C*; Geological Survey of Canada, Paper 90-1C, p. 305-322.

**Stubley, M.P.**

1990a: Preliminary geology of the McCrea-Drybones lakes area (parts of NTS 85 P/9 and 10); Northwest Territories Geology Division, Department of Indian Affairs and Northern Development, Map EGS 1990-4, scale 1:50 000.

1990b: Preliminary geology of the Prang Lake area (parts of NTS 85P/15 and 16); Northwest Territories Geology Division, Department of Indian Affairs and Northern Development, Map EGS 1990-19, scale 1:50 000.

**Taylor, S.R. and Gorton, M.P.**

1977: Geochemical application of spark source mass spectrography. III. Element sensitivity, precision and accuracy; *Geochimica et Cosmochimica Acta*, v. 41, p. 1375-1380.

**Thompson, P.H.**

1992: The Winter Lake-Lac de Gras regional mapping project, central Slave Province, District of Mackenzie, Northwest Territories; in *Current Research, Part A*; Geological Survey of Canada, Paper 92-1A, p. 41-46.

**Thompson, P.H., Ross, D., Froese, E., Kerswill, J.A., and Peshko, M.**

1993: Regional geology in the Winter Lake-Lac de Gras area, central Slave Province, District of Mackenzie, Northwest Territories; in *Current Research, Part C*; Geological Survey of Canada, Paper 93-1C, p. 61-70.

**Thompson, P.H., Ross, D., and Davidson, A.**

1994: Regional geology of the Winter Lake-Lac de Gras area, central Slave Province, Northwest Territories; in *Current Research 1994-C*; Geological Survey of Canada.

**van Breemen, O., Davis, W.J., and King, J.E.**

1992: Temporal distribution of granitoid plutonic rocks in the Archean Slave Province, northwest Canadian Shield; *Canadian Journal of Earth Sciences*, v. 29, p. 2186-2199.

**Villeneuve, M.E., Jackson, V.A., and Thompson, P.H.**

1993: Geochronological evidence for the existence of pre-Yellowknife Supergroup supracrustal sequences in the Slave Province; Geological Association of Canada, Mineralogical Association of Canada, Joint Annual Meeting, Program and Abstracts, v. 18, p. A107.

---

Geological Survey of Canada Project 870008

# Geology of Paul Lake area, Lac de Gras-Lac du Sauvage region of the central Slave Province, District of Mackenzie, Northwest Territories<sup>1</sup>

B.A. Kjarsgaard and R.J.S. Wyllie  
Continental Geoscience Division

*Kjarsgaard, B.A. and Wyllie, R.J.S., 1994: Geology of Paul Lake area, Lac de Gras-Lac du Sauvage region of the central Slave Province, District of Keewatin, Northwest Territories; in Current Research 1994-C; Geological Survey of Canada, p. 23-32.*

---

**Abstract:** The Lac de Gras area of the Northwest Territories is currently the focus of intense exploration activity for diamondiferous kimberlite intrusions. The geology is dominated by Archean metagreywacke and granitoids. Ductile deformation has produced at least two sets of folds and related fabrics. Granitoid emplacement occurs syn- and post-tectonically. Faulting occurred during the Late Archean/Early Proterozoic. Four Proterozoic dyke swarms cut the Archean rocks in the map area. Detailed structural data were obtained for the area, along with subdivisions of the granitoid suites represented and new information on contact relationships. Possible controls on the spatial emplacement of kimberlites are considered in relation to regional structures and Proterozoic dyke swarms.

**Résumé :** La région du lac de Gras, dans les Territoires du Nord-Ouest, est en ce moment le centre d'une intense activité d'exploration ayant pour but de découvrir des intrusions de kimberlite diamantifère. La géologie de cette région est dominée par des métagrauwackes et granitoïdes archéens. Une déformation ductile a produit au moins deux ensembles de plis et les fabriques associées. L'emplacement des granitoïdes est syn- et post-tectonique. Des failles datent de la fin de l'Archéen et du début du Protérozoïque. Quatre essaims de dykes protérozoïques recoupent les roches archéennes dans la région cartographiée. Des données structurales détaillées ont été recueillies, les différentes suites de granitoïdes ont été subdivisées et de l'information nouvelle sur les relations de recoupement est présentée. Les contrôles possibles de l'emplacement des kimberlites sont étudiés en fonction des structures régionales et des essaims de dykes protérozoïques.

---

<sup>1</sup> Contribution to Canada-Northwest Territories Mineral Initiatives (1991-1996), an initiative under the Canada-Northwest Territories Economic Development Cooperation Agreement.

## INTRODUCTION

The Lac de Gras-Lac du Sauvage area, northeast NTS 76D (Fig. 1) is comprised dominantly of Archean meta-sedimentary and granitoid rocks, and transected by numerous Proterozoic diabase dykes. Recently, more than twenty kimberlite diatremes have been found in the area (Northern Miner, 1993a). Mapping is supported by the 1991-1996 Canada-NWT Mineral Initiatives Agreement and the Slave NATMAP project. Mapping was completed over the 1992 and 1993 field seasons. Objectives of the project include detailed kimberlite petrological studies, and regional geological mapping. The mapping results should assist in understanding the tectono-magmatic evolution of the Slave Province, and provide insights into geological controls on the spatial distribution of kimberlite. Mapping was completed in NTS map sheet 76D/9 and parts of 76D/10, 8 and 16.

## PREVIOUS GEOLOGICAL MAPPING

The mapping of Folinsbee (1949) resulted in the publication of GSC map #977A (1:250 000). Thompson et al. (1993) is currently remapping the western half of the Lac de Gras sheet. King et al. (1991) recently completed mapping the Contwoyto-Nose Lakes area to the north. The Aylmer Lake sheet to the east was most recently mapped by Lord (1952).

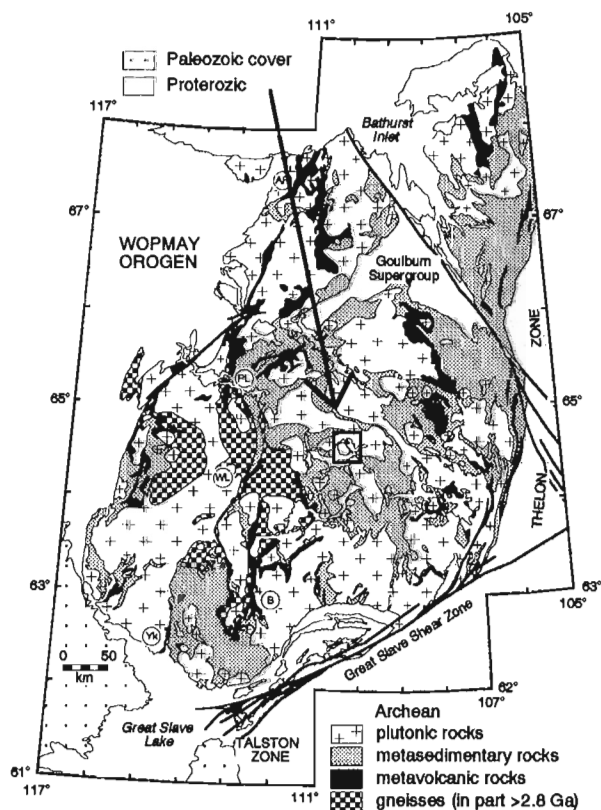


Figure 1. Location of map area in the central Slave Province.

Prior to this study, there has been no systematic regional mapping in the eastern part of the Lac de Gras sheet since the work of Folinsbee (1949).

## REGIONAL GEOLOGICAL SETTING

The Lac de Gras area is located in the central Slave Structural Province (Fig. 1). The Slave Province is an Archean craton thought to consist of accreted tectonostratigraphic terranes (the exact nature of terrane boundaries is obscure), derived from subduction-accretion of single (Kusky, 1989) or multiple (King et al., 1989) volcano-sedimentary arc complexes.

## DESCRIPTION OF MAP UNITS

All map units recognized are either Archean metasedimentary and granitoid rocks or younger intrusives (diabase, kimberlite). There is no evidence of basement to the above-mentioned units in the map area. A simplified compilation of mapping is presented in Figure 2. Lithological units in the legend of Figure 2 are described below in inferred stratigraphic order.

### Metasedimentary rocks

#### Greywacke

Green-brown to rusty brown weathering metagreywacke outcrops throughout the map area. Rocks of this unit are dominantly thin-bedded (1 - 10 cm beds; Fig. 3), although thicker beds (to 1 metre; e.g., Fig. 4) occur. The metagreywackes consist of massive psammitic beds and graded psammite-pelite sequences (e.g. Fig. 3). Bedding is preserved in porphyroblastic schists, although less so in migmatitic greywackes. Porphyroblasts of biotite, cordierite, and andalusite (var. chiastolite) are ubiquitous in pelitic layers. Garnet occurrence is variable, but its restriction to narrow, bedding-parallel zones, suggests its occurrence is a function of bulk composition, rather than metamorphic grade. Sillimanite (var. fibrolite) typically overgrows the porphyroblasts, and is ubiquitous. Migmatite (Fig. 5) occurs only in smaller rafts and panels (N.B. panel is a non-genetic term to describe narrow outcrops of greywacke which extend along-strike) of greywacke within hornblende+ biotite tonalites north of Eagle lake. No iron-formation was observed in the map area.

### Granitoid intrusive rocks

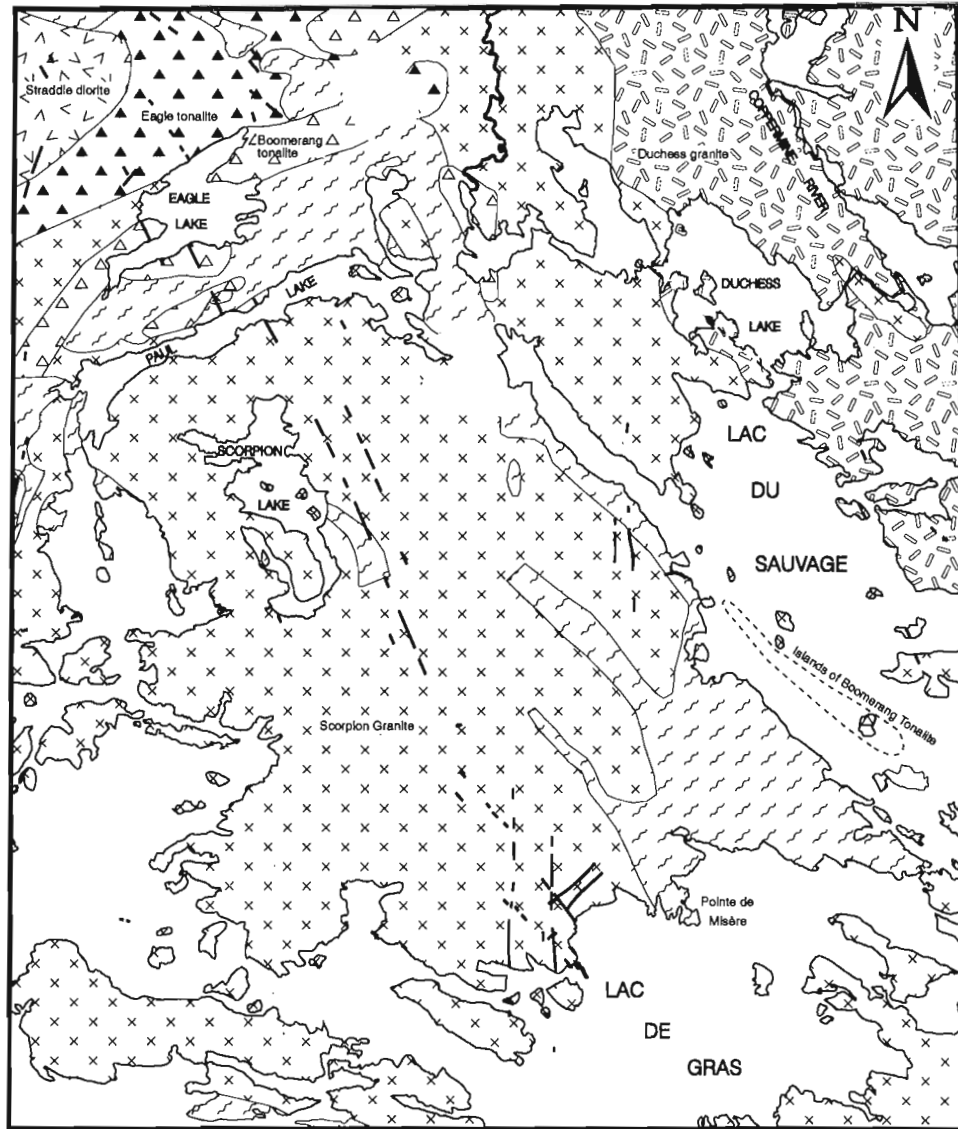
#### Hornblende+biotite quartz diorite

A large, homogeneous pluton of equigranular, medium grained quartz diorite (Straddle quartz diorite) occurs at the western margin of the map sheet. Preliminary petrographic studies illustrate that mineral assemblages consist principally of plagioclase+biotite+hornblende+quartz±epidote. The biotite and epidote are thought to be of magmatic origin. Inclusions of microdioritic cognate xenoliths are rare or absent in this body. This pluton is weakly deformed, with a poor to nonexistent foliation.

**Hornblende+biotite tonalite**

East of the Straddle quartz diorite, an extensive body of deformed tonalite outcrops north of Eagle lake (Eagle tonalite). The hornblende+biotite tonalites are distinguished in the field from the quartz diorites on the basis of lower modal hornblende, higher quartz+biotite contents and the presence of minor K-feldspar. Thin (10 cm - 10 m scale)

greywacke septae of variable length (tens to hundreds of metres) commonly occur in this body; good examples are found along the north shore of Eagle lake and also in association with the northwest-trending greywacke panel at the northwest margin of the map area. This suggests that the tonalite intruded the greywackes to form bedding concordant, sill-like bodies. The small, isolated outcrops of hornblende



**SIMPLIFIED GEOLOGY**

SCALE 5 0 10 km

- |  |                                   |  |                  |
|--|-----------------------------------|--|------------------|
|  | Hornblende-biotite quartz diorite |  | Two-mica granite |
|  | Hornblende-biotite tonalite       |  | Biotite tonalite |
|  | Porphyritic biotite granite       |  | Greywacke        |

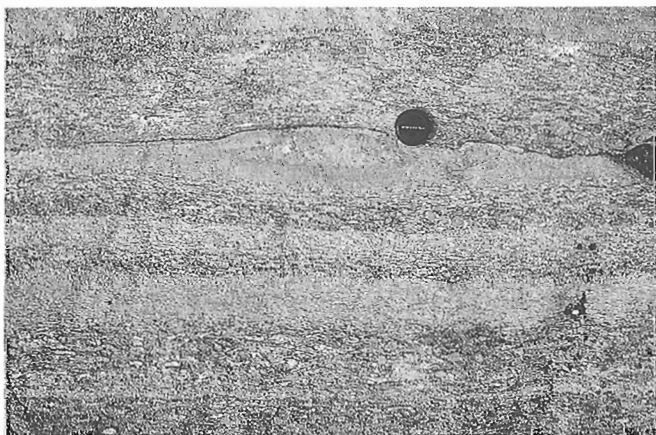
*Figure 2. Simplified geological map for the Paul Lake area, 76D19. Diabase dykes shown as heavy black lines.*



tonalite northeast of Paul Lake are also strongly foliated. In contrast to the Saddle quartz diorite, the Eagle tonalite is observed in places to contain abundant, hornblende-rich microdiorite enclaves (Fig. 6). The enclaves are typically boudinaged; the long axes lying parallel to  $S_1$ .

### Biotite tonalite

Biotite tonalite is exposed between Eagle lake and Paul Lake (in the west-central portion of the map sheet). Discontinuous biotite tonalite outcrops of variable size are also found following the trend of a lineament along the northwest arm of Lac du Sauvage. The biotite tonalite outcrops are inferred to have formed a continuous unit before intrusion of two mica granite. This map unit is termed the Boomerang tonalite. These rocks are light brown- to white-weathering, medium grained, and have weak to strong foliations (and are locally lineated). The Boomerang tonalite is distinguished in the field



**Figure 3.** Graded beds in greywacke (thin beds). Tops towards photo north. GSC 1993 251Y

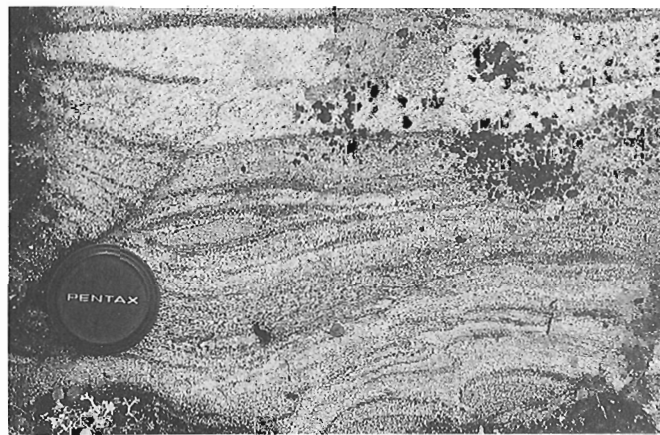


**Figure 4.** Thickly bedded turbidite intruded by two mica granite dyke. GSC 1993 251U

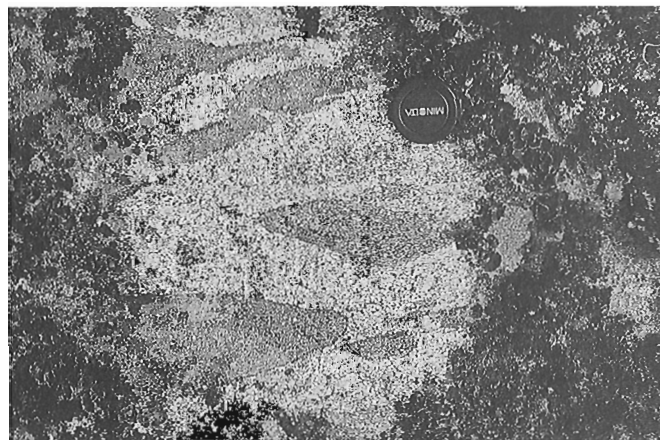
from the Eagle tonalite on the basis of hornblende-absent assemblages and a lower colour index. Rocks of this unit are observed to intrude the greywackes.

### Two mica granite

A distinctive white- to light grey-weathered surface and abundant primary muscovite characterizes these granites. Rocks typically consist of equal proportions of quartz, plagioclase, and K-feldspar, with 5-10% of both muscovite and biotite. Aquamarine apatite and tourmaline are common accessories; in places apatite comprises up to 5% of the rock. Garnet, cordierite, and sillimanite are also observed, but the latter is invariably found only in association with greywacke inclusions. These granites are fine- to coarse-grained and generally equigranular, but occasionally are weakly porphyritic. A very coarse grained, K-feldspar-rich, tourmaline-bearing pegmatitic phase forms dykes and small stocks up to 250 m



**Figure 5.** Migmatitic greywacke. Note schlieren formation in pelitic component. GSC 1993 251Q



**Figure 6.** Microdiorite enclaves in biotite tonalite. Enclaves are elongated parallel to the regional strain ellipsoid. GSC 1993 251M

in diameter. These pegmatites are widespread in the map area and occur both internal and external to the two mica granite plutons.

The majority of the central and southern portion of the map sheet consists of two-mica granite (Scorpion granite). These granites are observed to intrude greywacke, biotite tonalite, and hornblende tonalite. All intrusive contacts are sharp. Larger outcrops of two mica granite consist of multiple intrusions. Where there is good three-dimensional exposure, the two mica granites are observed to form shallowly dipping sheets of variable thickness (less than ten metres to greater than 100 metres). At outcrop-scale, the upper parts of a sheet are usually free of greywacke. Towards the base, greywacke rafts, septae, and inclusions are more abundant.

Subhorizontal contacts between the base of the two mica granite sheets and steeply bedded greywackes are observed (Fig. 7). Granite sills (concordant to bedding) seen in the greywackes are interpreted as feeder conduits to the overlying sheets (Fig. 7); magma emplacement in a passive environment (postdeformation) is consistent with a lack of penetrative fabrics in these rocks.

West of Lac du Sauvage, and north of Point de Misère, two narrow zones of greywacke form panels separating the two-mica granite into distinctive, lozenge-shaped bodies. The long axis of these lozenges lies parallel to the regional strain ellipse. Felsenmeer and surficial deposits limit exposure and have hindered attempts to further determine the continuity of these greywacke panels along strike.

### Porphyritic biotite granite

Light red- to pinkish-white-weathering, medium- to coarse-grained, K-feldspar porphyritic granite forms a distinctive pluton in the northeast part of the map sheet. K-feldspar phenocrysts range from 1-3 cm in length and display a preferred orientation. Rocks consist of 5-10% biotite, with primary muscovite usually absent, or present only in trace amounts (<1%). One large body (Duchess granite) of this unit is found in the region of the Coppermine River and east of Duchess Lake. Due to limited exposures of this unit, it is not possible to map out recognizable subunits of the body (as seen in grain size and modal mineralogy variations). Lack of penetrative deformation is consistent with these rocks being emplaced after the main regional metamorphism and deformational event(s). Although a small body of two mica granite occurs within the Duchess granite, thick surficial deposits obscure the contact relationship.

### Diabase dykes

Diabase dykes, ranging in width from 15 to 100 m are common in the area, and postdate granite intrusion. The dykes are distinguished on the basis of orientation, and are correlated with known dyke swarms in the Slave Province (Fahrig and West, 1986). Four (and possibly five) dyke swarms are represented; all interpreted to be of Proterozoic age. Field relationships are consistent with available age data.

### MacKay (080° trend)

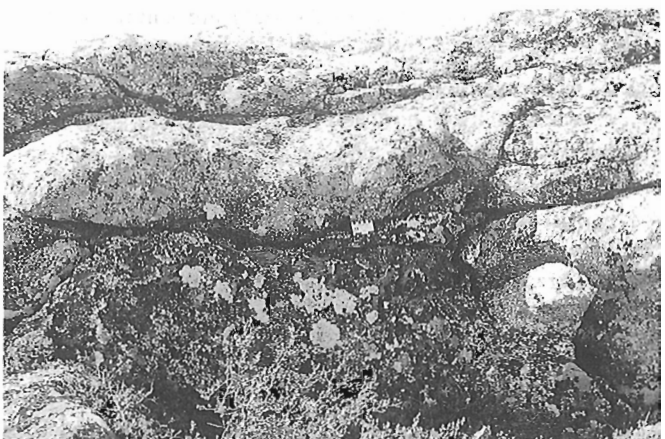
A single dyke, 50 metres wide and trending approximately 080°, is exposed intermittently across the central part of the map sheet. An estimated age of 2.4 Ga (K/Ar whole-rock; Fahrig and West, 1986) for this swarm suggests it is the oldest dyke in the map area. At two localities (both two mica granite/greywacke contacts) the dyke is observed to refract from 080° to approximately 125°. One possible explanation for this phenomena is that the dyke intrudes a pre-existing structure, and records stress refraction at the rheological boundary. Evidence for faulting at 080° is found in a parallel fracture 3 km to the southwest, in which slickensides are recorded. The slickensides indicate dextral movement, raking 20° on a fracture plane which lies at 075/85.

### Contwoyto (045° trend)

Three dykes, 20-40 m wide and trending approximately 045° were noted in the map area. These dykes were not observed to crosscut any other Proterozoic dykes. Preliminary U-Pb baddeleyite studies yield an age of 2.23 Ga (A. LeCheminant and O. van Breemen, pers. comm., 1993) A single dyke north of Eagle lake is found within, and concordant to, a greywacke/tonalite zone of moderate strain (trending 220°). In contrast, however, there is no evidence for a similar relationship between Contwoyto dyke orientation and regional structure in the Point de Misère area.

### Lac de Gras (190° trend)

Three dykes, 35-60 m wide, trending approximately 190°, outcrop intermittently in the map area. These dykes are easily distinguished by their well-developed ophitic texture. The Lac de Gras dykes are observed in the field to cut Contwoyto dykes. Preliminary U-Pb baddeleyite studies give an age of 2.02 Ga,



**Figure 7.** Cliff face (vertical surface) showing granite-greywacke contact. Granite sheet is overlying steeply dipping greywacke beds. Note feeder conduit on right side, concordant to  $S_0$  in the greywackes. GSC 1993 251P

suggesting these dykes are potentially correlative with rocks of the Booth River Igneous Complex 200 km to the north (A. LeCheminant and O. van Breemen, pers. comm., 1993).

### Mackenzie (335° trend)

Six dykes of the Mackenzie swarm, with trends of 330°-340° and up to 100 m wide, occur in the map area. Crosscutting relationships observed in the field suggest the Mackenzie dykes are younger than the Lac de Gras, Contwoyto, and MacKay dykes; consistent with their U-Pb baddeleyite age of 1.27 Ga (LeCheminant and Heaman, 1989).

### "305" dyke

A single dyke, 15-20 m wide, trending 300° to 310° can be traced intermittently over a distance of 25 km in the northeast part of the map sheet. The age of this dyke is unknown and its relationship to the other swarms (specifically the Mackenzie) is equivocal.

### Kimberlite

More than twenty kimberlite pipes, many diamondiferous (Northern Miner, 1993a) occur in the area. At this time the exact locations remain proprietary information. A Rb/Sr three point isochron yielded an Eocene age of  $52 \pm 1.2$  Ma (Northern Miner, 1993b), however the exact location of the specific kimberlite dated (other than being in the Dia Met/BHP claim block) is unknown. Kimberlite-derived mudstones with Cretaceous to Paleocene dinoflagellate, pollen, and spores (Northern Miner, 1993b) potentially suggest two periods of kimberlite emplacement.

## STRUCTURAL GEOLOGY

### Fabric elements

Fabric elements measured in the field are summarized as follows and described more completely below:

$S_0$  is primary compositional layering in metagreywacke. It is defined by textural and mineralogical variation at the outcrop scale.

$S_i$  (internal cleavage) occurs as inclusion trails in andalusite and cordierite poikiloblasts. The relationship between  $S_i$  and  $S_1$  is unknown.  $S_i$  could be a relict of an earlier cleavage, or alternatively, it may record the earliest stages of  $S_1$  development.

$S_1$  is the main or dominant "regional" cleavage, generally oriented parallel or subparallel to  $S_0$  in the metagreywackes.

$S_2$  is a locally observed, symmetric crenulation cleavage.

$F_1$  folds are isoclinal. Frequent changes in younging direction of  $S_0$  are observed at the mesoscale and  $S_1$  verges both clockwise and counter-clockwise. Fold closures are not observed due to pervasive lichen cover and shoreline exposures that parallel the regional strike of  $S_0$ .

$F_2$  is an open fold with limbs that extend beyond the limits of the map area, and a wavelength of  $>20$  km. The crenulation cleavage ( $S_2$ ) is believed to be genetically related to  $F_2$  folding, as it lies parallel to the axial trace (see Fig. 9 below).

### Structural development

The deformation history of the Paul Lake sheet is polyphase. Tectonic fabrics exhibit varying degrees of development and heterogeneity.  $S_0$  is dominantly steeply dipping, becoming moderate in the  $F_2$  hinge zone. The main cleavage ( $S_1$ ) is associated with cryptic isoclinal folds ( $F_1$ ) in metagreywacke.  $S_1$  forms a discrete, spaced cleavage in metagreywackes and is oriented subparallel to  $S_0$  (Fig. 8).

Large, idioblastic porphyroblasts, wrapped by  $S_1$  suggests that  $D_1$  deformation is preceded by static porphyroblastesis of cordierite, andalusite, staurolite, and biotite. These porphyroblasts contain straight inclusion trails, suggesting a relict cleavage related to either a previous, but unrecognized folding event, or the early stages of  $S_1$  fabric development. A more locally developed crenulation cleavage ( $S_2$ ) appears to be genetically related to the large, open fold ( $F_2$ ) in the map area.

Moderately-dipping stretching lineations trending approximately 020, C and S fabric in granitoids, local transposition of  $S_1$  and the presence of sheath folds suggest the development of localized high strain zones in the limbs of the  $F_2$  fold. Further evidence can be found in folded pegmatite veinlets, bedding-parallel shearing and localized ramping of greywackes. Strain partitioning is only observed within the greywackes, close to rheological interfaces with synkinematic granitoids. High strain fabrics parallel regional lineaments observed on Landsat 5 Thematic Mapper (TM) imagery.

### Geometry

One area of nearly continuous metagreywacke outcrops and a number of smaller, discontinuous metagreywacke panels occur in the map area (Fig. 2). The main outcrops lie in a

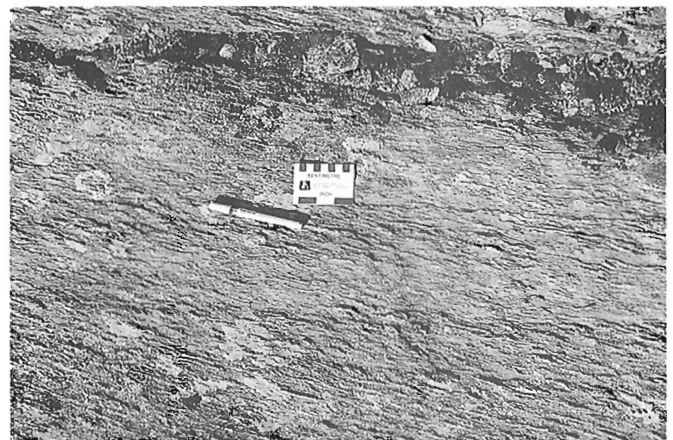
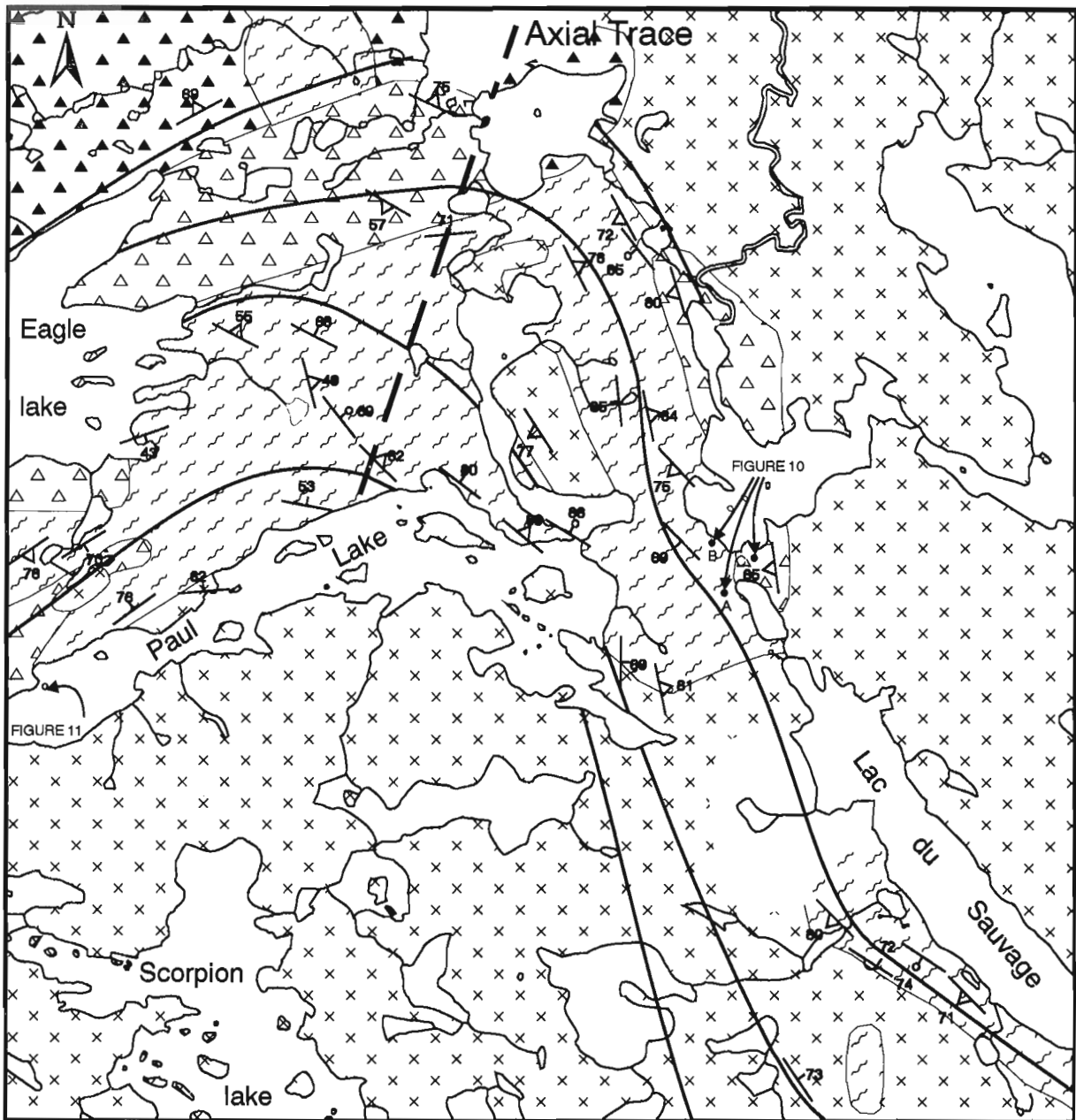


Figure 8. Relationship between  $S_0$  and  $S_1$ . Scale card lies parallel to  $S_0$  while pen outlines trace of  $S_i$ . GSC 1993 251T



**LEGEND**

SCALE 0 1 km

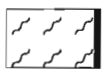

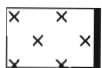
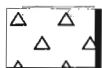

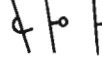

- |   |                             |   |  |
|---|-----------------------------|---|--|
|  | Greywacke                   |  | Hornblende-biotite tonalite            |
|  | Two-mica granite            |  | Biotite tonalite                       |
|  | Porphyritic biotite granite |  | Bedding; overturned, upright, inclined |
|   |                             |  | Foliation                              |

Figure 9. Detail of Paul Lake area, with form-surface traces.

folded belt that parallels the northwest arm of Lac de Sauvage, passes through the closure, and follows the long axis of Paul Lake (Fig. 9). In the Lac du Sauvage limb, the dominant bedding orientation is about 135/70. In the Paul Lake limb, it is 255/75. Bedding orientations between Lac du Sauvage and Paul Lake are consistent with ductile folding. The statistical mean fold axis for  $S_0$  trends 008° and plunges 70°.

Two panels of greywacke within the Scorpion granite have structural trends parallel to the Lac du Sauvage limb of the main belt (Fig. 2). A third greywacke panel (islands in the north arm of Lac de Gras), is of similar orientation. Limited exposure and intrusion of two mica granite obscures relationships between the latter panel and greywackes in the Paul Lake limb of the  $F_2$  fold.

The two dominant orientations of  $S_0$  (135° and 255° trends), are not observed in all greywackes in the map area. A panel of greywackes on the islands in the southwest corner of the map sheet is part of a larger belt that crosses Lac de Gras to the northwest and swings around to north/south as it enters sheet 76D/10. This change in orientation may be related to the Paul Lake  $F_2$  fold.

Granitoid rocks (Eagle and Boomerang tonalites) are observed to be foliated and/or lineated in the study area. Dominantly planar fabrics are found in the Eagle tonalite at the northern margin of the map sheet, but a lineation (defined by hornblende+plagioclase+quartz) is evident along the north shore of Eagle lake. In the Boomerang tonalite, the exposure between Eagle lake and Paul Lake has a weak planar fabric. Strong linear fabrics (defined by quartz+plagioclase) are found in this unit along the northwest arm of Lac du Sauvage and the region of the  $F_2$  fold culmination. These consistent lineation trends suggest stretching lineations associated with areas of high strain.

Fabrics recorded in the Scorpion and Duchess granites are discontinuous and poorly defined. They are not penetrative and usually only observed near the margins. While these fabrics could be interpreted to be magmatic in origin, it is possible that these granites were emplaced during the waning stages of deformation.

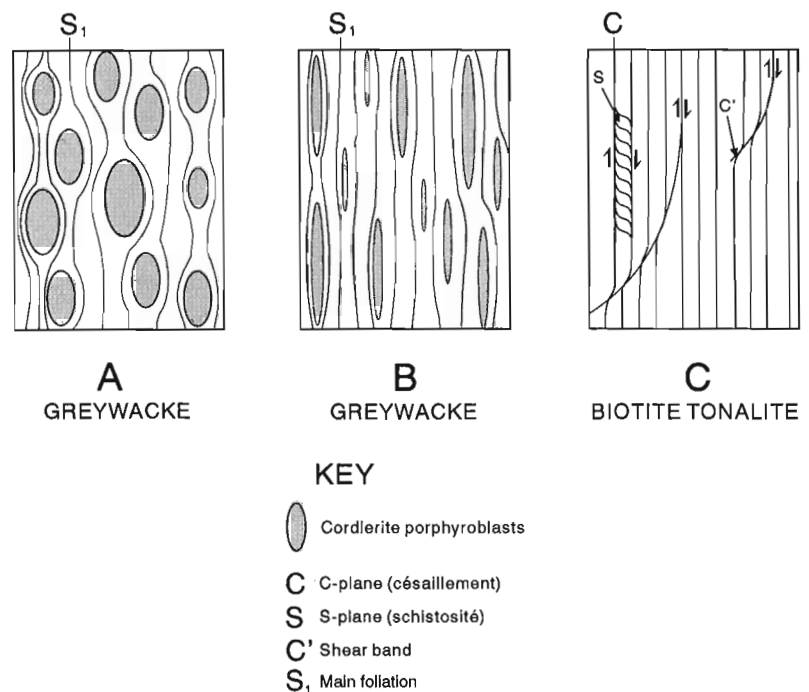
**Zones of high strain**

Three areas of high strain (Paul Lake; north shore Eagle lake; northwest arm Lac du Sauvage) are evident from field and structural studies. All occur within or adjacent to areas of metagreywacke outcrop and regional lineaments, but are also observed in the adjacent granitoids (Fig. 10).

One, and possibly two generations of high strain structures are observed in the limbs of the regional  $F_2$  fold. The two high strain zones (HSZ) in the northwest part of the map sheet at Eagle lake and Paul Lake, appear to have an overprinting relationship to one another. The Paul Lake high strain zone is associated with transposition of  $S_1$  and development of sheath folds (Fig. 11), oriented subparallel to the long axis of Paul Lake.

The Eagle Lake high strain zone is oriented parallel to an asymmetric crenulation cleavage that cuts the sheath folds in the Paul Lake area. The zone itself has a consistent stretching lineation (defined by hornblende+plagioclase+quartz) oriented at about 020/60. The regional significance of the overprinting fabric is currently equivocal in the absence of solid kinematic evidence to link the crenulation cleavage with the Eagle lake high strain zone.

A third high strain zone lies in the northwest arm of Lac du Sauvage. It is indicated by progressive strain of porphyroblasts and development of C and S and shear bands in rocks adjacent to the lineament (Fig. 10). Ramping of  $S_0$  and folding of pegmatite veinlets in greywackes are consistent with dextral kinematics.



**Figure 10.**

Scale drawings of three samples across the Lac du Sauvage high strain zone (see Fig. 9 for outcrop locations). A) Greywacke with weakly strained cordierite porphyroblasts (aspect ratio 2:1). B) Greywacke with highly strained cordierite porphyroblasts (aspect ratio 10:1). C) Boomerang tonalite with C-S fabric and shear bands ( $C'$  fabric).





**Figure 11.** Sheath folds in greywacke, on washed island outcrop in Paul Lake (see Fig. 9 for outcrop location). Note the typical eye-type interference pattern, and the presence of granitic leucosomes (white). GSC 1993 251Z

The high strain zones are thought to have occurred as a result of strain partitioning in the metagreywackes, due to their strong planar anisotropy ( $S_0$  and  $S_1$ ). The presence of phyllosilicates would also contribute to development of planar fabrics. In contrast, granitoids adjacent to the greywackes display stronger linear fabric elements. The high strain zones are associated with regional lineaments on aerial photographs and satellite imagery.

### Faulting

Mapping in 76D/10 has revealed evidence for shearing and faulting along a major lineament which extends into 76D/9 and trends  $080^\circ$ . The evidence is indirect, but consists of an echelon dextral shear zone in greywackes, and a parallel fracture surface in Scorpion granite with slickenside lineations (see MacKay dykes previous). The timing of movement on this fault zone is unconstrained at present, but lies between emplacement of two mica granite and the oldest mafic dykes (Late Archean to Early Proterozoic).

## METAMORPHISM

In pelitic rocks, there is a subtle variation in mineral assemblages suggesting that metamorphic grade increases slightly northward. All pelites contain andalusite±cordierite porphyroblasts. Fibrolite is common throughout the region. Occasional blades of accicular sillimanite are also observed. Greywackes are generally sillimanite-bearing in the main contact zones with granitic rocks, whereas those found in narrow panels within tonalite tend to be sillimanite-absent and migmatitic in character. The metamorphic assemblages observed in the greywackes are similar to those observed in other areas of the Slave Province (Thompson, 1978) and are consistent with low-P, high-T metamorphism.

## DISCUSSION

### Geology

Re-mapping of the Lac de Gras-Lac du Sauvage area has allowed for improved discrimination of geological units. The original two granitic map units have been subdivided into five distinct lithologies. Kimberlite outcrops were found in the course of mapping the regional geology. Additional exposures of greywacke define four discrete panels in the granitoids. Passive emplacement (post-deformation) of two mica granite through feeder conduits to overlying sheets is consistent with the discontinuous, poorly defined fabrics in these rocks. This style of emplacement precludes models in which 'ballooning plutons' affect greywacke geometry. Consideration of style of granite intrusion along with structural data are consistent with the interpretation that the bend in the greywackes at Paul Lake is a large, open  $F_2$  fold. Three zones of high strain are associated with the limbs of this fold.

Subdivision of the granites into five lithological units allows comparisons with granitoid rocks studied in other areas of the Slave Province. The most recent (and comprehensive) studies are those of Davis (1991) and King et al. (1991, 1992) in the Contwoyto-Nose Lakes area to the north. Utilizing the relative plutonic age classification scheme for this area, potential correlatives with plutonic units in the Lac de Gras-Lac du Sauvage area (from oldest to youngest) are: the Straddle quartz diorite and Eagle lake hornblende tonalite with the ca. 2604 Ma C4 suite; the Boomerang tonalite with the ca. 2616 Ma C5 suite; the Scorpion granite with the ca. 2592 Ma C6a suite; and the Duchess granite with the ca. 2582 Ma C6b suite. Therefore, the granitic rocks in the map area likely correspond to the 'younger granites' of the Slave Province (van Breemen et al., 1992).

The greywackes in the map area are dominantly thin-bedded and lack iron formation. They may be correlative to the Ichen Formation (Bostock, 1980; King et al., 1991), part of the Yellowknife Supergroup (Henderson, 1970). However, it is important to note the complete lack of volcanic rocks in an approximate 75 km radius around the map area (see Fig. 1). This suggests that the region may represent a discrete sedimentary basin.

### Kimberlite

Numerous kimberlites have recently been discovered in the central Slave Province. The Lac de Gras area is part of a larger (ca. 200 km wide) region dominated by greywackes and intrusive rocks of the younger Slave granitoid suite (intruded at 2625-2580 Ma; van Breemen et al., 1992). Based on presently available mapping, volcanic rocks as well as their inferred plutonic equivalents (the older Slave granitoid suite, intruded at 2695-2650 Ma; van Breemen et al., 1992) appear to be absent from this region. Approximate boundaries of this region are: to the east, the Clinton-Colden Lake/Hackett River volcanic belts, and to the west, the Courageous-Desteffany-Winter lakes volcanic belts.

Interestingly, kimberlites with diamond grades that have warranted continued drilling and/or bulk sampling all lie in the region in which the older Slave volcanic rocks (and their inferred plutonic equivalents) are absent and there is also a significant Bouguer gravity low (Goodacre et al., 1987). The region of the Bouguer gravity low approximately lies to the southwest of a line from north Yamba Lake (in NTS 76E) to Pellat Lake (in NTS 76F) to Tarpon Lake and the Outram Lakes (in NTS 76C), encompassing the Lac de Gras area. Combining the Bouguer gravity data with the known geology strongly suggests that the Lac de Gras area may represent a unique region within the Slave Province.

Controls on the spatial distribution of kimberlite emplacement in Archean cratons are poorly understood, however a variety of models have been presented. Two recent models relate kimberlite spatial distribution to: 1) structural trends (e.g., Coopersmith, 1993); and 2) mafic dyke swarms (e.g., Schiller, 1993). The Lac de Gras region has the potential to provide important insights into this problem as the area is cut by dykes from four different swarms, and detailed mapping has defined the regional structural trends, including zones of high strain.

Geological mapping has indicated that one dyke of the MacKay swarm and one of the Contwoyto swarm dykes may be intruding pre-existing, regional structures. The absence of diabase dykes adjacent to the Point Lake kimberlite pipe, coupled with a preliminary analysis (based on a limited number of kimberlite localities) suggests a stronger relationship to structural control rather than the diabase dyke swarms. Release of proprietary information in the future will greatly assist in developing this model.

## ACKNOWLEDGMENTS

Discussions with Jack Henderson, Bill Davis, Peter Thompson, and Janet King provided helpful insights about the geology of the Slave Province. Critical reviews by J. King and B. Davis clarified numerous points in the manuscript. Sergio Alvarado greatly assisted with the mapping in 1993. Tony LeCheminant, Tony Peterson, Ken Buchan, Pauline Orr, and Tara Sagriff contributed to the mapping in 1992. The Dia Met/BHP joint venture is thanked for casual helicopter charter in 1992 and 1993. Additional helicopter support in 1993 was provided by Polar Continental Shelf Project.

## REFERENCES

**Bostock, H.H.**  
1980: Geology of the Itchen Lake area, District of Mackenzie; Geological Survey of Canada, Memoir 391, 101 p.

- Coopersmith, H.**  
1993: Diamond mine discovery; in *Diamonds: Exploration, Sampling and Evaluation, Prospectors and Developers Association of Canada, Short Course notes, Toronto*, p. 73-108.
- Davis, W.J.**  
1991: Granitoid geochemistry and Late Archean crustal evolution in the central Slave Province; Ph.D. thesis, Memorial University of Newfoundland, St. John's, Newfoundland, 323 p.
- Fahrig, W. and West, T.D.**  
1986: Diabase dyke swarms of the Canadian Shield; Geological Survey of Canada, Map 1627A.
- Folinsbee, R.F.**  
1949: Lac de Gras, District of Mackenzie, Northwest Territories; Geological Survey of Canada, Map 977A.
- Goodacre, A.K., Grieve, R.A.F., and Halpenny, J.F.**  
1987: Bouguer Gravity Anomaly Map of Canada; Geological Survey of Canada, Canadian Geophysical Atlas, Map #3.
- Henderson, J.B.**  
1970: Stratigraphy of the Yellowknife Supergroup, Yellowknife Bay-Prosperous Lake area, District of Mackenzie; Geological Survey of Canada, Paper 70-26, 12 p.
- King, J.E., Davis, W.J., and Relf, C.**  
1989: Comment on "Accretion of the Archean Slave Province"; *Geology*, v. 17, p. 963-964.
- King, J.E., van Nostrand, T., Bethune, K.M., Wingate, M.T., and Relf, C.**  
1991: Final field report on the Contwoyto-Nose Lakes map area, central Slave Province, District of Mackenzie, N.W.T.; in *Current Research, Part C*; Geological Survey of Canada, Paper 91-1C, p. 99-108.
- King, J.E., Davis, W.J., and Relf, C.**  
1992: Late Archean tectono-magmatic evolution of the central Slave Province, Northwest Territories; *Canadian Journal of Earth Sciences*, v. 29, p. 2156-2170.
- Kusky, T.M.**  
1989: Accretion of the Archean Slave Province; *Geology*, v. 17, p. 63-67.
- LeCheminant, A.N. and Heaman, L.M.**  
1989: Mackenzie igneous events, Canada: Middle Proterozoic hotspot magmatism associated with ocean opening; *Earth and Planetary Science Letters*, v. 96, p. 38-48.
- Lord, C.S.**  
1952: Aylmer Lake, District of Mackenzie, Northwest Territories; Geological Survey of Canada, Map 1031A.
- Northern Miner**  
1993a: Economic pipes indicated at BHP-Dia Met project; *Northern Miner*, v. 79, no. 30, p. 1.  
1993b: BHP-Dia Met age date kimberlites; *Northern Miner*, v. 79, no. 29, p. 1.
- Schiller, E.**  
1993: Diabase dykes and kimberlites - A new link to diamond?; *The Canadian Mining and Metallurgical Bulletin*, v. 86, no. 968, p. 71.
- Thompson, P.H.**  
1978: Archean regional metamorphism in the Slave Province - a new perspective on some old rocks; in *Metamorphism of the Canadian Shield*, (ed.) J.A. Fraser and W.W. Heywood; Geological Survey of Canada, Paper 78-10, p. 85-102.
- Thompson, P.H., Ross, D., Froese, E., Kerswill, J.A., and Peshko, M.**  
1993: Regional geology in the Winter Lake-Lac de Gras area, central Slave Province, District of Mackenzie, Northwest Territories; in *Current Research, Part C*; Geological Survey of Canada, Paper 93-1C, p. 61-70.
- van Breemen, O., Davis, W.D., and King, J.E.**  
1992: Temporal distribution of granitoid plutonic rocks in the Archean Slave Province, northwest Canadian Shield; *Canadian Journal of Earth Sciences*, v. 29, p. 2186-2199.

# Glacial geology and implications for drift prospecting in the Lac de Gras, Winter Lake, and Aylmer Lake map areas, central Slave Province, Northwest Territories

L.A. Dredge, B.C. Ward, and D.E. Kerr  
Terrain Sciences Division

*Dredge, L.A., Ward, B.C., and Kerr, D.E., 1994: Glacial geology and implications for drift prospecting in the Lac de Gras, Winter Lake, and Aylmer Lake map areas, central Slave Province, Northwest Territories; in Current Research 1994-C; Geological Survey of Canada, p. 33-38.*

---

**Abstract:** As a contribution to the Slave Province NATMAP, Terrain Sciences mapped three 1:250 000 map areas (NTS 86A, 76D, and 76C) in the Lac de Gras area with the objective of providing a regional framework for geological interpretation and drift prospecting. This report documents the preliminary results from the first field season. Till is the most common surficial sediment and only one till sheet was identified. This till sheet represents several different directions of transport, including southwest, west, and northwest. Three broad zones of dominant flow were defined throughout the area, each requiring a different approach for drift prospecting. As well, glacial transport distances were evaluated, based on the lithology of pebbles in the till which indicated both local and distant transport.

**Résumé :** Comme contribution au projet CARTNAT de la Province des Esclaves, la Division de la science des terrains a cartographié trois régions au 1/250 000 (SNRC 86A, 76D et 76C) dans la région du lac de Gras, avec l'objectif de fournir un cadre régional pour l'interprétation géologique et pour faciliter la prospection minérale. Cet article porte sur l'interprétation préliminaire de la première saison sur le terrain. Le till est le dépôt meuble le plus commun et une seule unité de till a été identifiée. Cette unité est associée à plusieurs directions de transport glaciaire, telles que sud-ouest, ouest et nord-ouest. Trois zones principales d'écoulement glaciaire ont été identifiées dans la région, chacune exigeant une méthode d'échantillonnage différente pour la prospection minérale. Les distances de transport glaciaire, déterminées d'après des analyses lithologiques de cailloux dans le till, indiquent un transport variant de local à régional.

## INTRODUCTION

The Slave Structural Province is in the northwest Canadian Shield (Fig. 1). The Slave Province National Mapping (NATMAP) Program is a multi-disciplinary project whose aim is to enhance geological mapping and knowledge of this part of the craton. The discovery of diamonds by drift prospecting in the Lac de Gras region has resulted in frenzied diamond exploration and increased interest in the glacial geology of the area. Stimulated by this interest and the fact that detailed knowledge of the glacial geology of the area was lacking, Terrain Science Division carried out intensive fieldwork in three 1:250 000 map areas: Winter Lake (86A), Lac de Gras (76D), and Aylmer Lake (76C) (Fig. 1, 2). This work involves interpretation of 1:60 000 scale airphotos, ground mapping, striation sequencing, pebble lithology analysis, and mineralogical and geochemical analysis of till samples, with the aim of providing a regional framework for geological interpretation and drift prospecting. The objective of this report is to give a preliminary overview of the results of this first field season as an aid to current drift prospecting.

Fieldwork was carried out in collaboration with Peter Thompson and Bruce Kjarsgaard of the GSC who were mapping the bedrock geology in Winter Lake and Lac de Gras map areas, as well as W.A. Padgham (INAC) while working in the Winter Lake area.

## METHODS

Helicopter supported traverses were undertaken to verify airphoto interpretation and to collect samples for grain size, provenance studies and geochemical and mineralogical analysis. Preliminary airphoto interpretation was extensively verified by ground checks, short ground traverses and low level helicopter surveys. Because Quaternary materials are exposed at the surface, these controls allow us to extrapolate surface conditions using airphotos to produce accurate maps

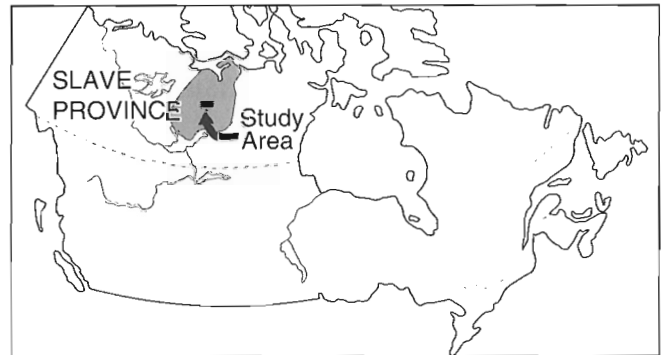


Figure 1. Location of Slave Province and study area.

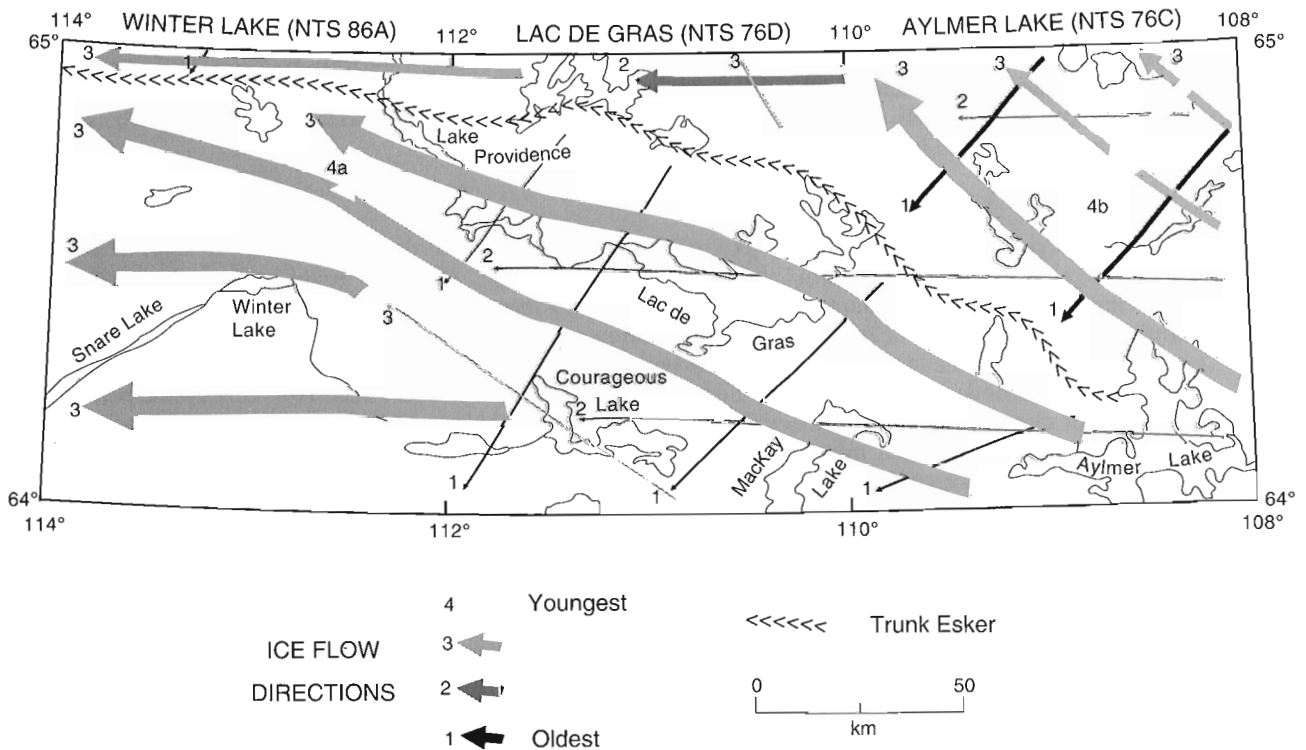


Figure 2. Summary ice flow diagram for the study area. The flow directions are numbered in order of decreasing age. The thickness of the line gives the relative affect of the flow on transport of debris and on modifying the landscape; the thickest arrows represent the dominant flow, most responsible for the transport of glacial debris.

at a scale down to 1:60 000. Approximately 500 till samples of 3 kg were taken for grain size and trace element geochemical analysis. At each site, 50 to 100 pebbles were collected for provenance investigations, and the nature of the bedrock was noted. As well, 160 samples of 10 kg were taken for analysis for kimberlite indicator minerals to document the range and background concentrations. Striations were measured and where possible, relative ages were determined to elucidate the history of ice movement.

## **BEDROCK**

Regional investigations of the bedrock geology of the area have been carried out by Fraser (1969) for Winter Lake (86A), Folinsbee (1949) for Lac de Gras (76D), and Lord and Barnes (1954) for Aylmer Lake (76C). Thompson et al. (1993) are currently remapping the eastern half of Winter Lake and the western half of Lac de Gras map areas. Although very complex, for the purposes of this report the bedrock can be subdivided into two broad categories: granitoid rocks of various affinities; and metasedimentary and metavolcanic rocks of the Yellowknife Supergroup. The metamorphic grade of the Yellowknife Supergroup ranges from very low grade schists and phyllites to migmatites. Some very low grade sediments were found in till and suggest the possibility of a younger unit being present.

## **NATURE AND DISTRIBUTION OF SURFICIAL DEPOSITS**

Till is the most extensive deposit in the area. Only one stratigraphic unit of till has been recognized and is attributed to Late Wisconsinan Laurentide Ice. The till consists of a matrix-supported diamicton, with the matrix ranging from silty sand to sand. Grain size appeared to vary according to bedrock source and amount of meltwater associated with deposition. Till derived from granitoid rocks was sandier than that derived from the Yellowknife Supergroup. Meltwater associated with till deposition also results in till with a very sandy matrix. In extreme cases, syn- and postdepositional reworking resulted in an openwork pebble-cobble lag. The clast content varied from 5 to 40% but was generally 25%. The upper 0.5 to 1 m of the till has been extensively modified by cryoturbation and solifluction. Surficial organics have been incorporated to depths of 70-80 cm, and primary deposition features such as layers or lenses have commonly been destroyed.

The till sheet has been divided into 3 units based on thickness and surface morphology: veneer, blanket, and hummocky. Till veneers are generally < 2 m thick, contain exposures of bedrock and conform to the underlying bedrock morphology. They are generally loose and their surfaces are characterized by high concentrations of cobbles and boulders (Fig. 3A); bedrock structures are usually visible on the air-photos. Till blankets are generally >2 m thick and either drape the underlying bedrock, often as gently undulating till plains (Fig. 3B), or form low relief drumlinoid features. They tend to be relatively compact and contain fewer boulders than veneers. Hummocky till deposits are >5 m thick and form

hummocky topography with relief up to 30 m which totally obscures bedrock (Fig. 3C). They range from firm to loose and bouldery. Till veneers and blankets are pervasive throughout the area; hummocky till is widespread in the Lac de Gras and Aylmer Lake map areas but occurs in only a few isolated localities in the Winter Lake map area.

Meltwater has variably affected all three map units and is especially evident in some zones of the hummocky topography. Ice stagnation features such as gravelly rim and ridge areas, often associated with till plateaus, and ablation boulder pits in the low areas characterize some hummocky moraine. Other areas are extensive boulder fields, regardless of the till type (Fig. 3D).

Glaciofluvial deposits are geographically widespread but limited in extent and are dominantly in the form of eskers and related kames; proglacial outwash is very limited. Eskers form a large network which feeds into a large trunk esker that runs across the area (Fig. 2). Associated with the eskers are washed zones occurring on either side of large eskers or connecting esker segments that contain little, if any, surface sediment. The eskers range from small, sinuous ridges to large, more linear features up to 45 m high, forming the major topographic relief in the area (Fig. 3E). Abundant nodes are present along their length and the ridges vary from sandy and flat topped to bouldery and sharp crested. Sediments exposed in rare sections are dominantly immature sand, containing subangular grains and large mica flakes, with a thin capping of gravel. Much of the sand is very fine- to fine-grained. Sedimentary structures consist dominantly of ripple and ripple drift bedding, commonly draped, and planar bedding (Fig. 3F); large scale crossbedding was rarely observed. Foot traversing revealed abrupt changes in surface sediment from fine sand to boulder gravel. These eskers can provide large volumes of aggregate.

The relative timing of esker development and till deposition is variable. Eskers are observed to have cut down into the till, to drape the till, and to be completely obscured by overlying till. As well, some eskers appear to be streamlined and molded by the passage of ice.

Associated with the esker systems, either adjacent to or on the washed zones, are small kame features. They range from streamlined forms parallel to meltwater flow, to slightly elongate forms perpendicular to flow, to irregular shapes. Their surfaces are strewn with abundant boulders associated with a very sandy till, but consist dominantly of sand. Other isolated bodies of sand which drape the till were observed and appear to have no relationship to the esker systems.

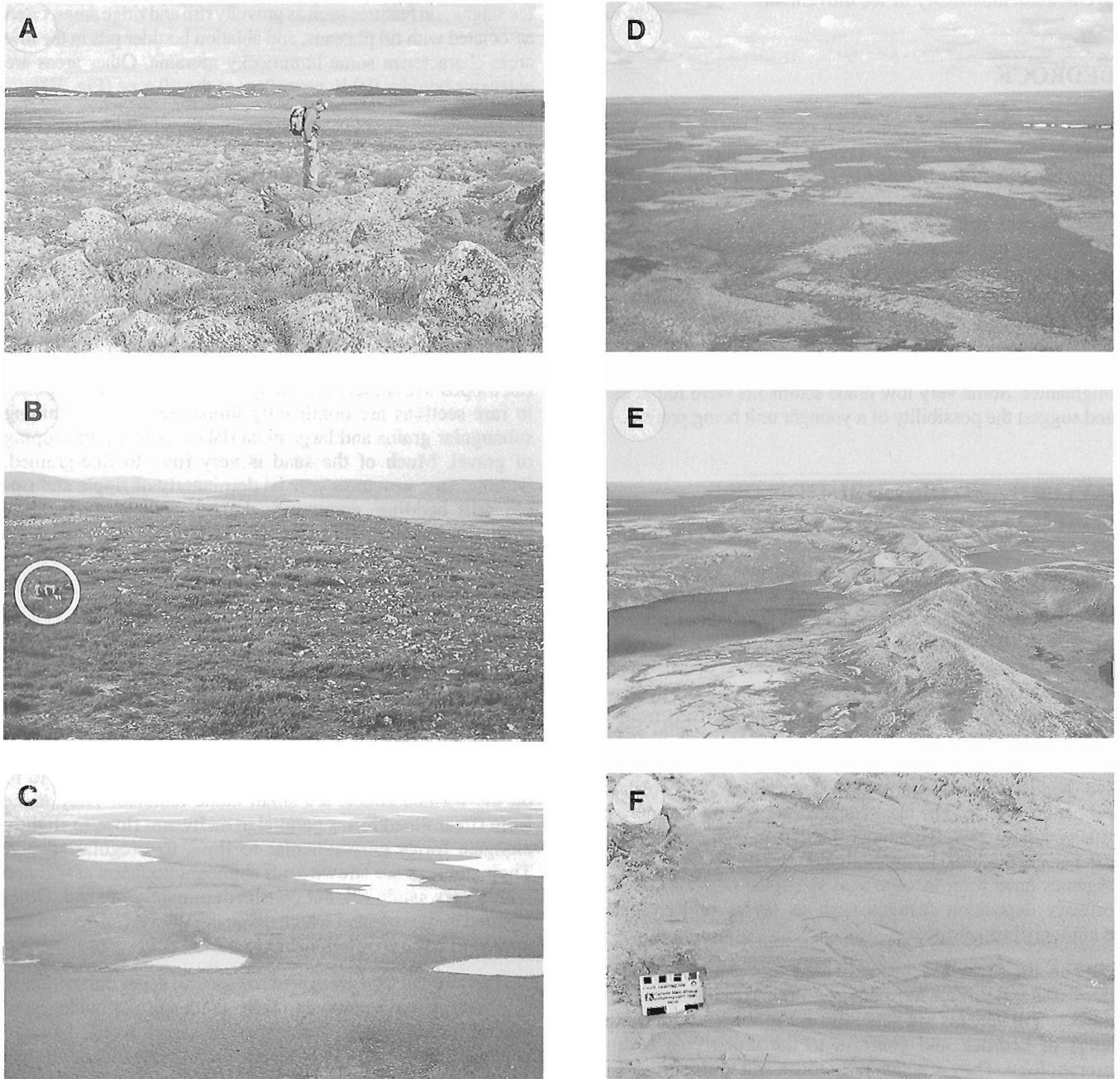
Despite the fine grain size suggesting esker deposition in low energy environments, little evidence for widespread glacial lakes exists. Evidence for short lived, isolated deglacial lakes or ponds occurs throughout the three map areas in the form of raised beaches, especially well developed on the flanks of eskers. However in the Lac de Gras and Aylmer Lake map areas, lake sediments were only identified in a few localities and these were thin and very sandy. In the Winter Lake map area, along the Snare Lake-Winter Lake-Snare River valley, isolated deposits of rhythmically bedded silt and clay attest to a relatively long lived ice-dammed glacial lake up to 35 m higher than the present Winter Lake.



## STRIATION DATA

Some aspects of the glacial history and the dominant direction of glacial transport can be determined by the relative age and strength of striations. Figure 2 is a summary diagram of flow direction and strength based on over 500 observation points. Throughout the central and eastern regions of the study area,

the earliest flow was to the southwest, followed by flow to the west and then by flow to the northwest. In the northeast corner of Aylmer Lake there is also evidence of a strong, younger southwest flow. In the Winter Lake map area, flow was generally towards the west-northwest in the northern and central regions and towards the west in the southern region. In the northeast part of the map area, west of Lake Providence,



**Figure 3.** *A) Very bouldery till veneer from the northwest corner of the Lac de Gras map area; B) Typical till blanket found throughout the study area, from north of Snare Lake (GSC 1993-278B); C) Typical hummocky till from west of Aylmer Lake (GSC 1993-278D); D) Ablation area where meltwater has washed the glacial debris leaving zones or boulders near Aylmer Lake (GSC 1993-278A); E) Large esker with bouldery sharp crested ridge and sandy aprons, from the central portion of the Aylmer Lake map area (GSC 1993-278C); F) Typical sedimentary structures from an esker section on Courageous Lake.*

a younger, westward set of striations crosscuts an older, northwestward set. Striations indicating local flow towards the trunk esker were also observed. All these striations are thought to represent the same glaciation.

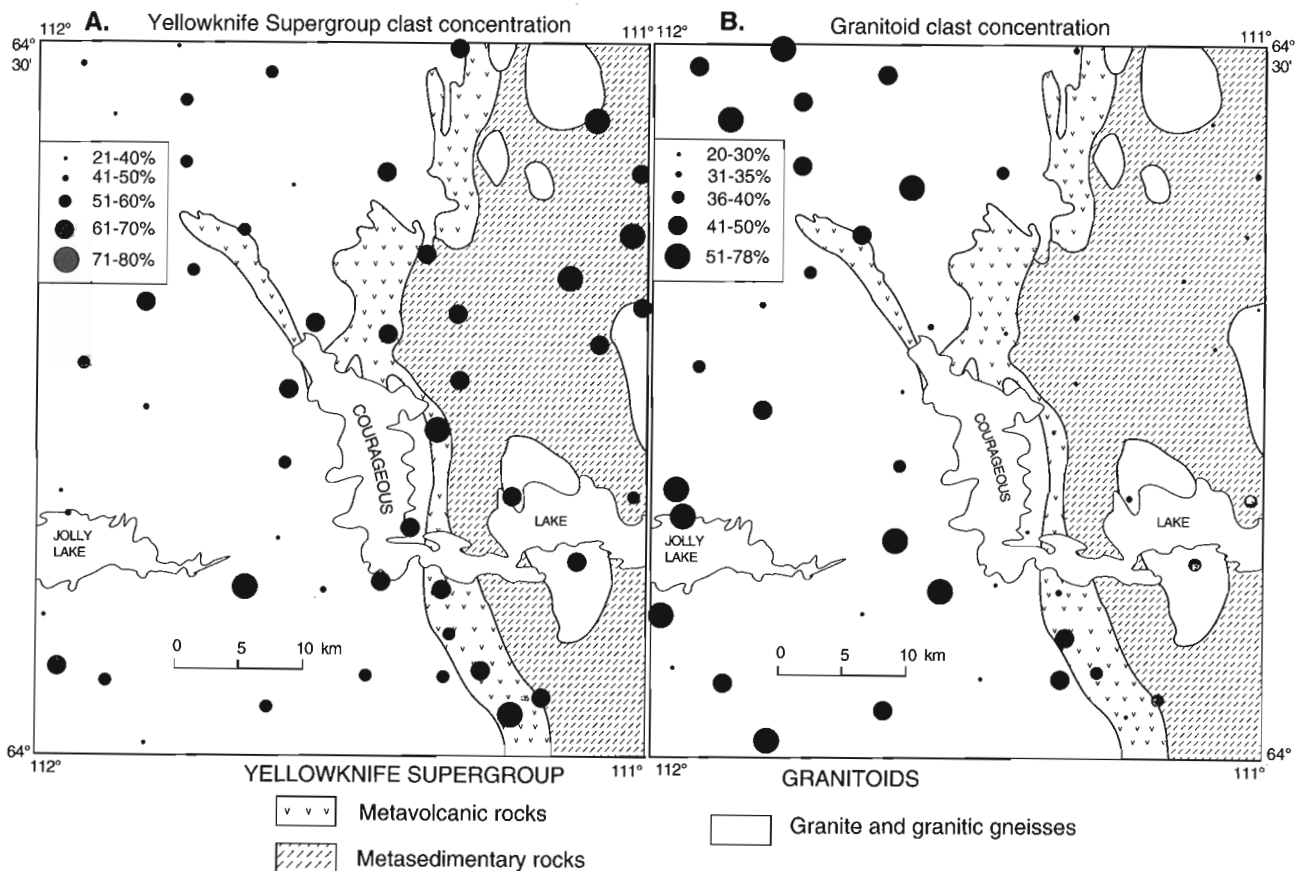
This striation arrangement is thought to represent the following sequence of events (Fig 2): 1) in the central and eastern region of the study area, southwestward flow as ice built up over the area; 2) a shift to a predominantly westward flow; 3) northwestward flow over much of the area with westward flow in the southern portion of Winter Lake map area; 4a) westward flow near Lake Providence, likely during deglaciation; and 4b) a southwestward flow in the northeast corner of Aylmer Lake, attributed to the last stages of active deglaciation.

The 'dominant' flow is the flow direction that is most responsible for transport of till and usually corresponds to the most prominent and frequent striae and the orientation of drumlins and crag and tails. The direction of dominant flow varies throughout the area with three broad zones being recognized (Fig. 2): 1) westward flow to the south of a line running through Winter, Courageous, and Aylmer lakes; 2) northwestward flow north of zone 1 and south of the main

trunk esker; and 3) northwestward and southwestward flow to the northeast of the trunk esker. Although the dispersal trains from exploration targets will be slightly modified by other flows, knowledge of the dominant flow is vital for planning a drift prospecting program. The most difficult area for drift prospecting is in the northwest corner of the study area where the latest southwestward flow has overprinted the northwestward flow, likely resulting in a more complicated dispersal pattern.

## TRANSPORT DISTANCES

Figures 4A and B show the distribution of Yellowknife Group metasedimentary and volcanic rocks, and granitoid rocks, chiefly granite and gneiss, in the vicinity of Jolly Lake. Because the main rock contact runs perpendicular to the principal east-west ice flow direction, the area affords an opportunity to determine patterns of drift transport. Lithological pebble counts from till samples, and field observations on boulder lithologies, were used to explore glacial transport distances. Figure 4A shows the distribution of Yellowknife



**Figure 4.** Lithological clast concentration from till near Jolly and Courageous lakes. Dominant ice flow is from east to west. **A)** Concentration of Yellowknife Supergroup clasts; **B)** Concentration of granitoid clasts. Bedrock geology modified from Thompson et al. (1993).

Group pebbles (2-8 cm) in till over these bedrock types. Yellowknife Group pebbles are found at all sites, including those underlain by granitoid rocks. Although the highest concentrations are found in areas underlain by Yellowknife Group bedrock, sites more than 20 km west of the contact commonly retain more than 40% Yellowknife clasts, indicating a considerable distance of glacial transport.

The expected pattern of Yellowknife clasts was one of consistently and rapidly decreasing Yellowknife Group pebbles down-ice (i.e., west) of the rock contact. The distribution map shows that the pattern of clast-content attenuation is more complicated. Several factors may contribute to the poor definition of a dispersal train here.

1. The lowest Yellowknife Group pebble count in the area is 21%. The lack of a rapid decrease of Yellowknife Group pebbles west of the rock contact may reflect differences in the break-down habits of metasedimentary and granitoid rocks. The metasediments fracture readily into thin segments that are prone to break quickly into pebble-sized components, whereas granitoid rocks are coarsely jointed and break initially into blocks and boulders before comminution to pebble sizes.
2. Different till thicknesses may have an effect on the concentration of travelled pebbles. We expected that till veneer areas would have relatively high concentrations of locally derived pebbles, and relatively low concentrations of travelled clasts. In till veneer areas, local rock types predominate in the boulder fraction of the till, and the veneers are texturally immature, and have coarser and more angular clasts than similar blanket tills. Although differences in till thickness were considered as a factor, we found that this did not account consistently for the observed pebble distribution; although, at a given distance west of the rock contact, till veneers generally carried less Yellowknife Group pebbles than till blankets.
3. Some sites lying between Jolly Lake and Courageous Lake show no attenuation of Yellowknife Group pebble concentration. These sites lie along a valley, and may be a locus of stronger ice flow.
4. The striation record suggests that there was an old southwestward ice flow across the region. The effects of this ice flow may have obscured the pebble dispersal pattern generated by the later and predominant east-west flow.

The distribution of granitoid rocks (Fig. 4B) shows the inverse situation, with a definite increase in granitic and gneissic pebbles westward of the Yellowknife Group bedrock. The very low granitoid pebble content in tills overlying the volcanics and metasediments strongly suggests that there was never an eastward ice flow in this area during the last glacial episode.

## CONCLUSION

We have presented a preliminary description of materials, striation patterns, and transport distances resulting from field work in 1993. Maps, comprehensive databases, more intensive assessment of glacial transport patterns, and geochemical analyses for trace element geochemistry and kimberlite indicator minerals are in progress. Although regional ice flows have been reported, more detailed orientation surveys would be needed to accurately determine surficial sediment types and local ice flow patterns for effective drift prospecting.

## ACKNOWLEDGMENTS

Murray Gingras, Roger Paulen, and Barb Pierna were field assistants on this project. Peter Thompson and his bedrock crew provided new information on bedrock types shown on our figures. Polar Continental Shelf Project provided helicopter support, and DIAND maintained radio contact and expediting facilities based out of Yellowknife.

## REFERENCES

- Folinsbee, R.E.**  
1949: Lac de Gras, District of Mackenzie, Northwest Territories; Geological Survey of Canada, Map 977A, scale 1" to 4 miles.
- Fraser, J.A.**  
1969: Winter Lake, District of Mackenzie; Geological Survey of Canada, Map 1219A, scale 1" to 4 miles.
- Lord, C.S. and Barnes, F.Q.**  
1954: Aylmer Lake, District of Mackenzie; Geological Survey of Canada, Map 1031A, scale 1" to 4 miles.
- Thompson, P.H., Ross, D., Froese, E., Kerswill, J.A., and Peshko, M.**  
1993: Regional geology in the Winter Lake-Lac de Gras area, central Slave Province, District of Mackenzie, Northwest Territories; in Current research, Part C; Geological Survey of Canada, Paper 93-1C, p. 61-70.

# The sedimentology and provenance of the Et-Then Group as a record of deformation on the McDonald fault zone, East Arm, Great Slave Lake, Northwest Territories

Bradley D. Ritts<sup>1</sup>

Continental Geoscience Division

*Ritts, B.D., 1994: The sedimentology and provenance of the Et-Then Group as a record of deformation on the McDonald fault zone, East Arm, Great Slave Lake, Northwest Territories; in Current Research 1994-C; Geological Survey of Canada, p. 39-48.*

---

**Abstract:** The Proterozoic Et-Then Group of the East Arm of Great Slave Lake, is a sequence of non-marine clastic rocks and minor basaltic volcanics with a maximum thickness of at least 4000 m. The alluvial fan conglomerates of the older Murky Formation fine gradationally into the braided fluvial sandstones of the younger Preble Formation. Physical relationships between Et-Then Group strata and structures related to the McDonald fault system indicate that Et-Then Group sedimentation was concurrent with deformation on that system. Stratigraphic relationships, sediment provenance and facies proximity show that Et-Then Group sedimentary rocks are a direct result, and record the history of deformation associated with the McDonald fault. Description and interpretation of the sedimentology, depositional systems, and three-dimensional lithostratigraphy of the Et-Then Group are used to suggest possible models for tectonic, climatic and/or source rock controls on Et-Then sedimentation.

**Résumé :** Le groupe protérozoïque d'Et-Then du Bras Est du Grand lac des Esclaves est une séquence de roches clastiques non marines, renfermant des quantités mineures de roches volcaniques basaltiques, dont l'épaisseur maximale est d'au moins 4 000 m. Selon l'ordre stratigraphique, les conglomérats de cône alluvial de la Formation de Murky deviennent plus fins et passent progressivement aux grès de cours d'eau anastomosés de la Formation de Preble. Les relations physiques entre les strates du Groupe d'Et-Then et les structures liées au système de failles de McDonald indiquent que la sédimentation du Groupe d'Et-Then a eu lieu en même temps que la déformation le long de ce système. Les liens stratigraphiques, la provenance des sédiments et le caractère proximal des faciès montrent que les roches sédimentaires du Groupe d'Et-Then sont le produit direct de la déformation associée à la faille de McDonald et qu'elles témoignent de l'évolution de cette déformation. On utilise une description et une interprétation de la sédimentologie, des systèmes de dépôt et de la lithostratigraphie tridimensionnelle du Groupe d'Et-Then pour proposer des modèles possibles du contrôle exercé par la tectonique, le climat et les roches mères sur la sédimentation du Groupe d'Et-Then.

---

<sup>1</sup> Department of Earth, Atmospheric, and Planetary Science, Massachusetts Institute of Technology, Cambridge, Massachusetts, U.S.A. 02139

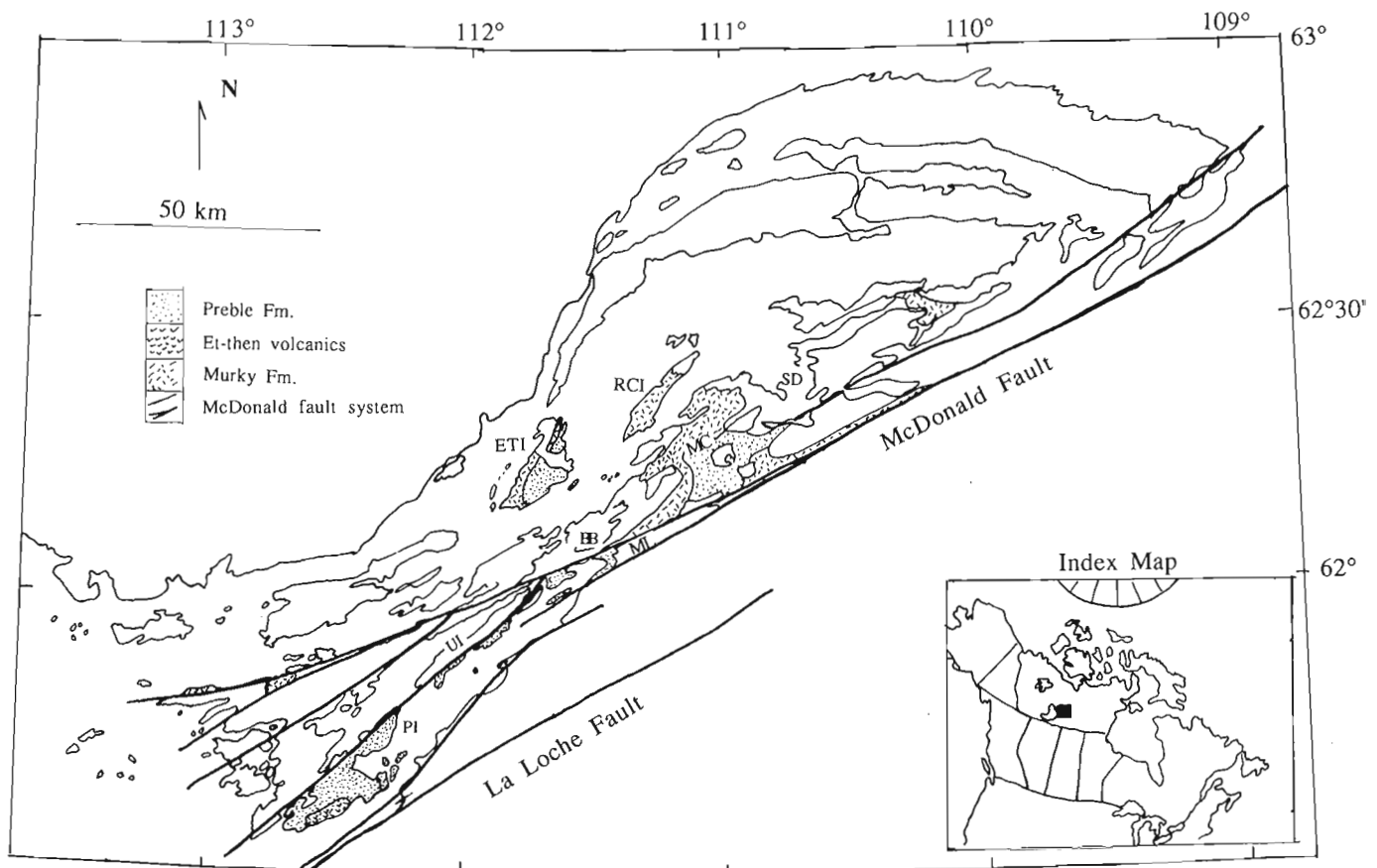
## INTRODUCTION

The Paleoproterozoic Et-Then Group is a thick sequence of coarse, non-marine siliciclastic rocks, with minor basaltic volcanics. It is subdivided into the older, conglomeratic Murky Formation, which grades into the younger, sandstone-dominant Preble Formation. The age of the Et-Then Group is constrained by 1865 Ma Compton laccoliths (Bowring et al., 1984), that lie unconformably below the Et-Then Group, and the 1270 Ma Mackenzie dyke swarm (LeCheminant and Heaman, 1989) that intrudes the Et-Then Group.

Previous workers (Hoffman, 1969, 1981; Hoffman et al., 1977) have correctly interpreted the Et-Then Group as an alluvial depositional system associated with motion on the transcurrent McDonald fault system. The McDonald Fault is believed to have been active during continental transform deformation associated with post-collisional indentation on the Thelon Tectonic Zone, perhaps driven by collision in the Wopmay orogen (Henderson et al., 1990; Hoffman, 1987). This suggests an age between 1735 and 1840 Ma (Henderson et al., 1990).

## METHODS

Outcrops of the Et-Then Group were examined throughout the East Arm for sedimentological, stratigraphic, petrological and structural data. Detailed stratigraphic sections were measured in the following areas (Fig. 1): 1) south shore of Et-Then Island (Fig. 2, 4); 2) north shore of Redcliff Island (Fig. 2, 3); southeast side of Preble Island and adjacent small islands; 4) south shore of the large island south of Basile Bay; 5) north side of Murky Channel and Murky Lake; 6) south side of Murky Channel and Murky Lake; and 7) on the mainland north of Murky Channel. Sedimentological, stratigraphic and structural data were collected, but sections were not measured (due to lack of exposure) on traverses in the following areas: 1) west side of Et-Then Island; 2) northeast peninsula of Preble Island; 3) the mainland south of Murky Channel; 4) three small islands northwest of Snowdrift (about 8 km, next to an island informally referred to as "Tomato Island"); 5) peninsula south of Basile Bay; 6) south shore of Preble Island; 7) south shore of Redcliff Island.



**Figure 1.** Geological and location map of the East Arm. This map shows the distribution of the Et-Then Group and major splays of the McDonald Fault System in the East Arm. Geographic names referred to in this report are labeled as follows: ETI = Et-Then Island; RCI = Redcliff Island; MC = Murky Channel; PI = Preble Island; SD = Snowdrift; BB = Basile Bay; UI = Union Island; ML = McDonald Lake. For more detailed geological mapping or geographic information see Hoffman, 1988 or Hoffman, 1968 (map adapted from Bowring et al., 1984; Hoffman, 1978).



## SEDIMENTOLOGY AND DEPOSITIONAL SYSTEMS

### Murky Formation

#### Description

The Murky Formation, with a maximum thickness of over 1000 m, consists of one dominant and four subordinate lithofacies assemblages (Fig. 2, 3, 4).

The dominant Gmm lithofacies assemblage (see Table 1 for facies codes) is a massive, matrix-supported (with varying degrees of clast-support), very poorly sorted, sub-angular to well rounded, cobble to boulder conglomerate. Clasts within typical beds average 25 to 50 cm in maximum diameter, with some clast diameters extending to over 1 m. Bed thicknesses range from 50 cm to more than 5 m. Beds have sharp, or

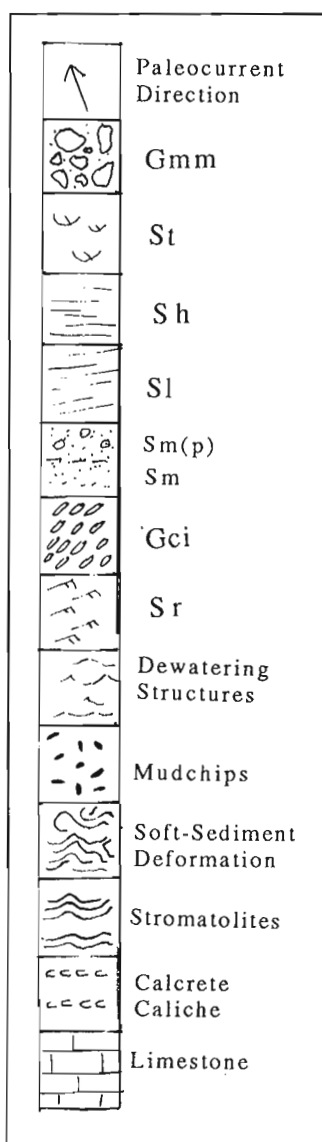


Figure 2. Key to measured sections. Symbols used in Figures 3 and 4 are shown. Facies codes are listed in Table 1.

poorly defined bases, and often have reworked tops (better sorting, small, anabranch channels). Individual beds can be strongly lenticular to tabular on outcrop scale. No primary sedimentary structures are found, and only uncommon coarsening- or fining-upward trends. There are very few clast-supported, pebble to cobble, imbricated conglomerates associated with the Gmm lithofacies assemblage. These beds are strongly lenticular, have erosional bases and show atbi imbrication (long axis transverse to flow). Few silty mud layers, some with calcrete and/or desiccation cracks, are present.

Subordinate lithofacies assemblages, in terms of abundance, are the St/Sh, Sm/Sh/Sl, Gcm, and carbonate lithofacies assemblages. The St/Sh lithofacies assemblage consists of 50 cm to 2 m thick beds of coarse to very coarse, poor to medium sorted sandstone. Primary sedimentary structures include trough crossbeds, upper regime plane beds and low-angle crossbedding. Beds have sharp or erosional bases and are lenticular on outcrop scale. coarsening- and fining-upward sequences are both present. Mud chips are present in most beds, and few beds are capped by green, silty mudstone layers, sometimes with desiccation cracks.

The Sm/Sh/Sl lithofacies assemblage consists of decimetre-scale plane-bedded and low-angle crossbedded, medium- to very coarse-grained, medium sorted sandstone; and metre-scale beds of massive, very coarse, very poorly sorted sandstone with floating pebbles. Beds are tabular on outcrop scale and have sharp, non-erosional bases. Primary sedimentary structures are absent from the massive sandstone, but primary current lineation and current ripples are found in the plane-bedded and low-angle crossbedded sandstones.

The Gcm lithofacies assemblage consists of angular, very poorly sorted, pebble to boulder, monolithological, clast supported conglomerate. There are no observable primary sedimentary structures or grain-size trends, and bedding is very poorly developed.

The carbonate lithofacies assemblage consists of metre-scale beds of limestone or dolomite. Beds are fine grained and show no physical structures, but many are stromatolitic (Hoffman, 1976) or otherwise show wavy laminations.

#### Interpretation

The Gmm lithofacies assemblage is interpreted as sub-aerial debris flow deposits, commonly with tops reworked by late-stage run-off. Many of the debris flows were channelized, whereas others were not. Some of the debris flows may have ultimately been deposited in lakes associated with the few carbonate horizons. Calcrete is taken to indicate pedogenesis which, with the desiccation cracks, strongly suggests subaerial exposure. The imbricated conglomerates are believed to be channelized traction deposits. These deposits would be typical of an inner-alluvial fan, with both entrenched and dispersed phases.

The St/Sh lithofacies assemblage is interpreted to be channelized, sub-aqueous traction deposits with unsteady paleo-flow between 0 and 140 cm/s, with typical velocities around 100 cm/s, based on grain size and primary sedimentary

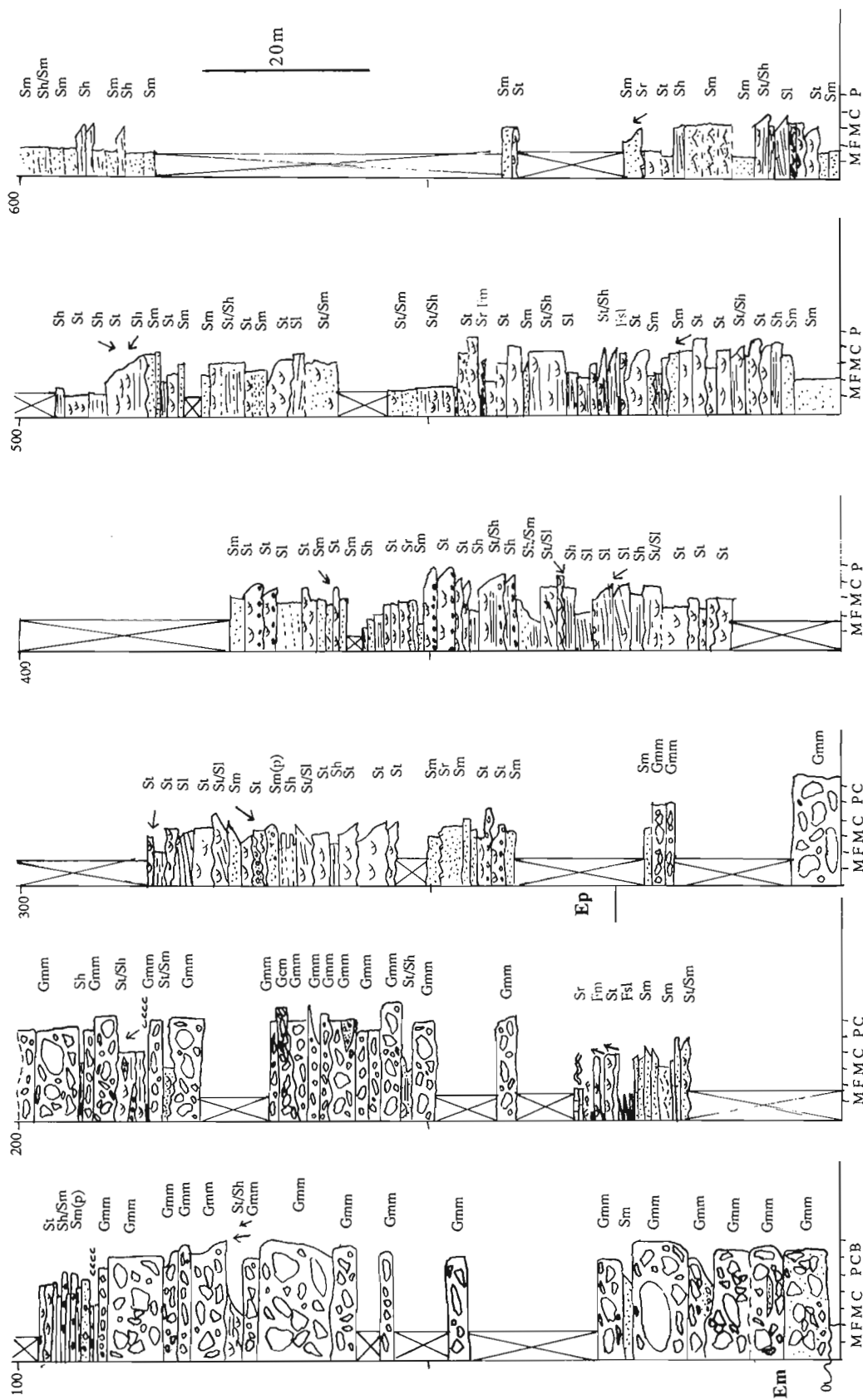


Figure 3. Measured section from Redcliff Island. Measured section located on the north side of Redcliff Island through most of the Murky Formation. Based on grain size characteristics, it is likely that less than 100 m are missing from the base. An unknown thickness is missing from the top of the section. For descriptions of facies codes and symbols see Table 1 and Figure 2.

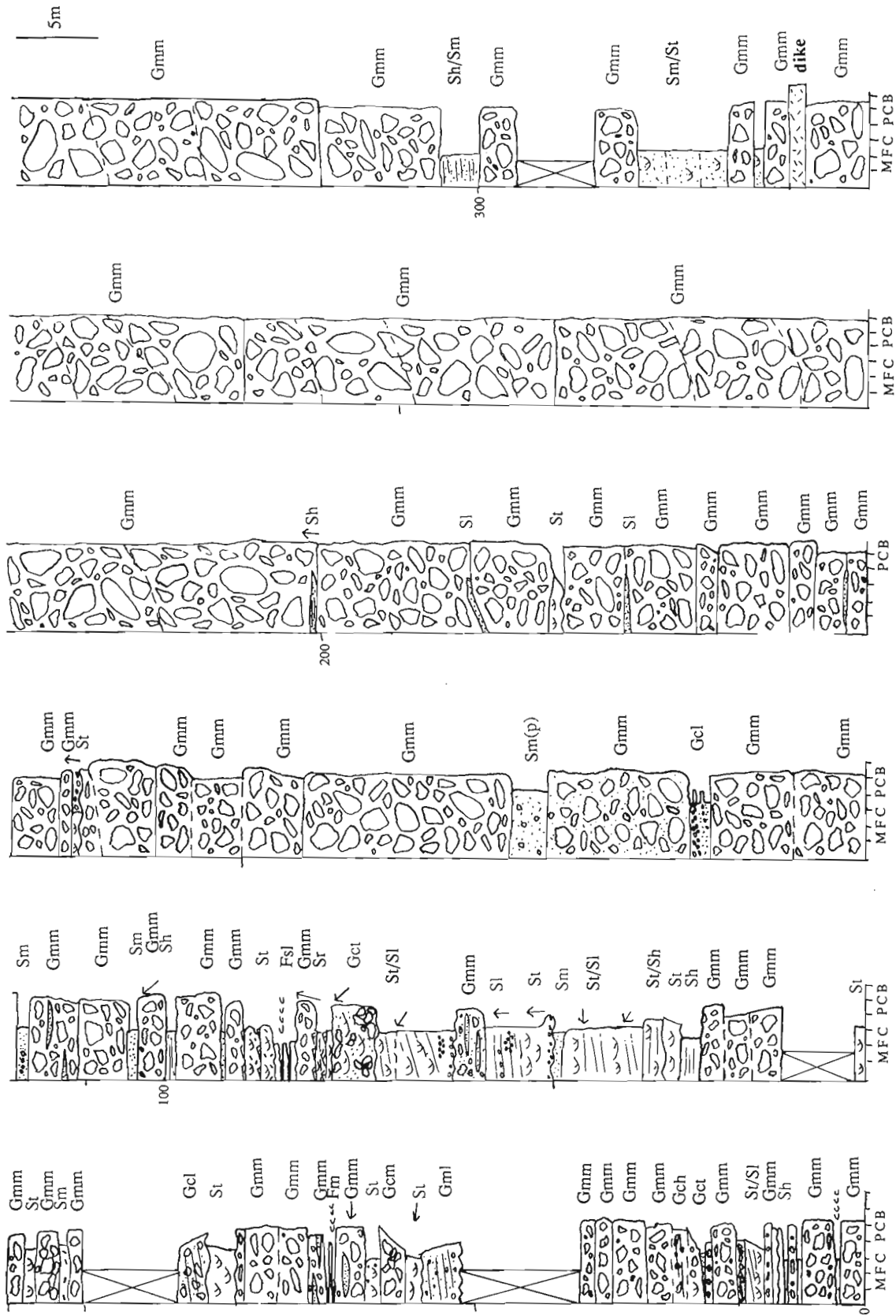


Figure 4. Measured Section from Et-Then Island. Measured section located on south shore of Et-Then Island through the entire Murky Formation and the exposed Preble Formation. For descriptions of facies codes and symbols, see Table 1 and Figure 2.

structures (Harms et al., 1982). Both channel and macroform elements are present, indicating that this lithofacies assemblage is deposited by sandy, braided channels on an alluvial fan surface, or at the toe of a fan lobe.

The Sm/Sh/SI lithofacies assemblage is interpreted to represent two depositional processes. The plane-bedded and low-angle crossbedded deposits result from episodic, unchanneled, shallow, sub-aqueous sheetfloods. The shallow nature of the flows accounts for the very high apparent flow velocities. The massive sandstone was deposited by mud flows. These depositional processes are interpreted to have been active on mid- to outer-alluvial fans.

The Gcm lithofacies assemblage is interpreted as talus, deposited directly adjacent to a fault scarp. Grain flow is probably the dominant depositional process.

The carbonate lithofacies assemblage is interpreted as lacustrine. These deposits are found at the base of the section, near the sub-Et-Then unconformity or at the most distal part of the outer-alluvial fan.

## ***Preble Formation***

### **Description**

The Preble Formation has a maximum thickness of over 3000 m and has one dominant and one subordinate lithofacies assemblage.

The dominant St/Sh/SI lithofacies assemblage consists of fine to very coarse, moderately to very well sorted sandstone. Primary sedimentary structures include trough crossbedding, upper-regime plane-beds with primary current lineations, low-angle crossbedding, and, to a lesser degree, asymmetric and symmetric, small-scale, two-dimensional ripples and interference ripples. Beds are 30 cm to over 2 m thick with sharp, erosional bases and lenticular geometry. Mudchips occur in many of the sandstones, and pebble to cobble lags, not thicker than the diameter of the largest clast, occur at the bases of many of the beds. Both coarsening- and fining-upward sequences are present, the former more common at the bottom of the formation, the latter more common towards the top. There are minor millimetre- to centimetre-scale red

**Table 1.** Facies codes, descriptions and general interpretations. Facies codes used in Figures 2, 3 and 4, and the text are shown with descriptions and general interpretations.

<u>Code</u>	<u>Description</u>	<u>Interpretation</u>
Gmm	massive, matrix-supported conglomerate	debris flow
Gcm	massive, clast-supported conglomerate	talus or hyperconcentrated flow
Gci	clast-supported conglomerate; imbricated clasts	gravel bars or channelized, sub-aqueous traction flow
Gch	horizontally bedded, clast-supported conglomerate	channelized, sub-aqueous traction flow
Gct	very sandy, faintly trough cross-bedded pebble conglomerate	channelized, sub-aqueous traction flow
St	trough cross-bedded sandstone	channelized, sub-aqueous migration of 3D dunes
Sh	plane-bedded sandstone, some PCL	channelized, sub-aqueous upper regime flow or sheetflood
Sl	low angle cross-bedded sandstone	sheetflood or fluvial macroform
Sm	massive sandstone, structureless	sub-aqueous or mud flow
Sm(p)	massive sandstone with floating pebbles	mud flow
Sr	rippled sandstone (asymmetric, symmetric, interference)	overbank, bar top or sheetflood migration of small ripples
Fm	massive mudstone (Fsm = massive siltstone)	overbank, paleosol
Fl	laminated mudstone (Fsl = laminated siltstone)	overbank flood, slack water settling

and green mud interlayers, some with desiccation cracks. The mean grain-size of the formation decreases upward from medium to very coarse at the base to very fine to medium higher in the formation.

The Gmm/Sh/SI/Sm lithofacies assemblage consists of two sub-lithofacies assemblages. The first sub-lithofacies assemblage contains two lithologies. The first is a pebble to cobble, very poorly sorted, rounded, matrix-supported conglomerate. Beds are 50 to 150 cm thick and have sharp, non-erosional bases and a tabular geometry on the outcrop scale. The beds lack primary sedimentary structures and grain size trends, although many show organized upper surfaces. The second lithology is similar to the first, only finer grained. It consists of massive, coarse to very coarse, poorly sorted sandstone with floating pebbles and cobbles. The beds, in the order of 1 m thick, have sharp, non-erosional bases and tabular geometry on outcrop scale. There are no discernible grain size trends or primary sedimentary structures.

The second sub-lithofacies assemblage consists of plane-bedded to low-angle crossbedded, well sorted, fine to medium sandstone with primary current lineations, and asymmetric and symmetric, two-dimensional, straight to sinuous, small-scale ripples. Bedding is on the centimetre to decimetre scale and is tabular on outcrop scale with sharp, non-erosional bases, commonly with preserved bedforms on bed tops.

### Interpretation

The St/Sh/SI lithofacies assemblage is interpreted as channelized, sub-aqueous, traction deposits. Flow velocities ranged from 0 to 140 cm/s, but were typically between 80 and 110 cm/s based on grain size and sedimentary structures (Harms et al., 1982). Deposition occurred in sandy, braided rivers, with both downstream-accreting and laterally accreting macroforms present, the latter increasing in abundance high in the formation. The upper regime plane beds and trough crossbedding are interpreted as channel elements. The mudstones, rippled fine sandstones and desiccation-cracked mudstones are interpreted as waning stage bar top or overbank deposits. The symmetric ripples, produced by oscillatory currents, are taken to indicate ponding in the system.

The Gmm/Sh/SI/Sm lithofacies assemblage represents two depositional processes occurring in proximity to each other. The massive conglomerate and sandstones are interpreted as sub-aerial debris flows and mudflows, respectively. Deposition occurred on a mid-alluvial fan. The horizontally and low-angle crossbedded sandstones are believed to be very shallow sheetflood deposits on a mid- to outer-alluvial fan. The shallow nature of the flow accounts for the very high apparent flow velocities. The symmetric ripples are produced by oscillatory currents and are taken to indicate ephemeral ponding.

### Summary

The Et-Then Group is interpreted as an alluvial system consisting of talus fan, inner-, mid-, and outer-alluvial fan or bajada, and sandy braided fluvial deposits. Broadly, the

alluvial fan/fluvial transition occurs at the transition from the Murky Formation to the Preble Formation, although distal alluvial fan deposits are found in the Preble Formation and fluvial deposits are found in the Murky Formation.

## STRATIGRAPHY AND BEDROCK PROVENANCE

The Et-Then Group has a two-part stratigraphy, defined by the formation designations, based on grain size. This section will address the internal stratigraphy and lateral variability in the Murky Formation. The data presented for the Preble Formation sandstones are based on cursory examination in the field with a 10X hand lens.

The clearest internal stratigraphy for the Murky Formation is seen in the Murky Channel area. The Murky Formation can be divided into an older, shale clast conglomerate and a younger, quartzite clast conglomerate. The shale clasts are mostly derived from the Kahochella and Wilson Island groups. In the Murky Channel area this division is apparently several hundred metres thick (only the lowest 450 metres are well exposed, presenting the danger of unrecognized faults higher in the section). Beds of differing composition occur within the shale clast conglomerate, but the package as a whole is dominantly shale clast conglomerate. The quartzite clast conglomerate has a sharp contact with the shale clast conglomerate although all physical characteristics besides dominant clast composition remain constant over the contact. The quartzite clasts are derived primarily from the Sosan Group, particularly the Kluziai Formation, but also the Wilson Island Group and the Hornby Channel Formation. The quartzite clast conglomerate persists vertically for several hundred metres, with some local composition variation, to the contact with the Preble Formation. This contact coincides with a change from the sedimentary bedrock provenance of the Murky Formation to a granitoid bedrock provenance for the Preble Formation sandstones. Pebbles and cobbles in channel lags within the Preble Formation consist of granitoid mylonites as well as undeformed granitoids, further supporting the change in provenance inferred from sandstone composition. This Murky Formation internal stratigraphy is valid for all Murky Formation exposures east of 112° longitude.

West of 112° longitude, in the Preble Island area, the Murky Formation has a mixed sedimentary (Great Slave Supergroup) and granitoid (Great Slave Lake shear zone) bedrock provenance. Unlike the sedimentary clasts in the Murky Formation east of 112° longitude, the sedimentary clasts in the Murky Formation in the Preble Island area are dominantly dolomite and limestone. The dominant clast type in the Murky Formation around Preble Island is of granitoid composition. Mylonitic rocks are about equal in proportion to non-foliated granitoids. No internal, clast-lithology-based, stratigraphy could be worked out and tested in the Preble Island area. The Preble Formation in the Preble Island area is also of granitoid provenance (including mylonitic and non-foliated varieties), as seen in the sandstones and in pebble and cobble channel lags.



The eastern Murky Formation stratigraphy can also be traced away from the McDonald fault system to the northwest, into the basin. Along this transect, the Murky Formation as a whole, and the shale clast conglomerate, in particular, thins and fines dramatically. On Redcliff Island the shale clast conglomerate is just over 100 m thick and has a higher proportion of fluvial and sheetflood deposits than the shale clast conglomerate at Murky Channel. The very thick, massive, poorly bedded debris flow conglomerates, typical of the Murky Formation in the proximal areas do not become extensive until deposition of the quartz clast conglomerate. Even more distally, on Et-Then Island, the shale clast conglomerate is not present, the quartz clast conglomerate lies directly on the Stark Formation of the Great Slave Supergroup. The Murky Formation on Et-Then Island is only about 200 m thick, including a 45 m thick fluvial sequence.

The three-dimensional lithostratigraphy is marked by several features. Across structural strike, thinning and fining of the Murky Formation and pinching out of the shale clast conglomerate into the basin is notable. Along the trend of the McDonald Fault, at about 112° longitude, the change in Murky Formation bedrock provenance, but not depositional system, is another interesting feature. Lastly, the coincidental change from a sedimentary to crystalline bedrock provenance at the Murky-Preble boundary demands attention.

## PALEOCURRENTS

Paleocurrent data were collected primarily by measuring trough limb sets (DeCelles et al., 1983) and trough axes. Primary current lineations were the next most common paleocurrent indicator measured, followed by small-scale asymmetric and symmetric ripple crests and clast imbrication in conglomerates. In all settings paleocurrents measured from trough axes, trough limb sets, clast imbrication and primary current lineation were consistent.

Paleocurrent indicators are sparse in the Murky Formation. Paleocurrents are only available from trough crossbedded units, plane-bedded sandstones with primary current lineations, and rare imbricated conglomerates. Paleocurrent data for the Murky Formation, where available show paleoflow to the northwest, away from a line trending 052° (Fig. 5A). Most of the paleocurrent indicators show flow between 282° and 001°.

This drainage configuration is consistent with the interpretation for the Murky Formation as being an alluvial fan or bajada system filling the basin from a paleohigh on the McDonald fault system. The agreement between the paleocurrent divide (052°) and the McDonald Fault trend (approximately 060°) is further evidence for this.

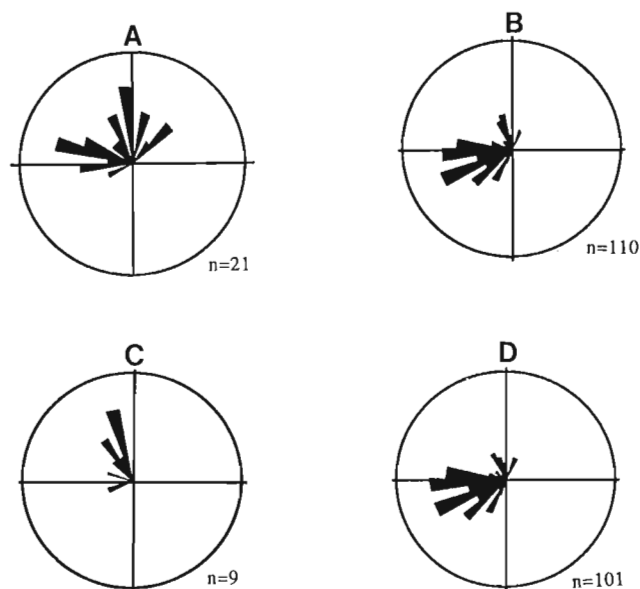
Paleocurrent indicators in the Preble Formation are more common. Dominant paleoflow directions are to the west-southwest, but some indicators show paleoflow to the north, or even east of north by as much as 20 or 30° (Fig. 5B). Upon further inspection, most of the northward paleocurrents are derived from the proximal Gmm/Sh/SI/Sm lithofacies assemblage (Fig. 5C), which was interpreted as a distal fan lobe,

and thus would be expected to give northward paleocurrent directions. The trough axis paleocurrents from the fluvial sandstones in the Preble Formation have a very dominant paleocurrent direction between 230° and 284° (Fig. 5D). This indicates that during Preble Formation deposition the regional drainage had reorganized into a longitudinally draining system subparallel to the trend of the McDonald Fault (approximately 240°).

## FACIES TRENDS

Along the length of the East Arm, Et-Then Group facies become more proximal toward the southeast, closer to the McDonald fault system. However, the proximity of facies and facies relationship are best seen between 111° and 111°30' longitude on a transect extending from the McDonald fault trace in the southeast (proximal) through Murky Channel and the last splays of the McDonald fault system (proximal) out to Redcliff Island and Et-Then Island (distal).

The most proximal deposits, talus breccias, are found only directly adjacent to fault strands. Occurrences are documented near McDonald Lake (Hoffman 1969), on Basile Bay Peninsula and at Murky Channel. Sheetflood deposits, interpreted as mid- to outer-fans, with debris flow and mud flow deposits, interpreted as mid-fan, are the most proximal facies within the Preble Formation. These features are seen only



**Figure 5.** Paleocurrent data from the Et-Then Group. **A)** Murky Formation paleocurrent data (trough axes). **B)** Preble Formation paleocurrent data (trough axes and primary current lineation). **C)** Preble Formation paleocurrent data from the Gmm/Sh/SI/Sm lithofacies assemblage near Murky Channel. **D)** Preble Formation paleocurrent data, excluding data from the proximal Gmm/SI/Sh/Sm lithofacies assemblage recorded near Murky Channel. Circle equals 20% for (A), (B), (D), and 50% for (C).

near splays of the McDonald fault system, most notably along the south shore of Murky Channel. The Murky Formation in proximal areas such as Murky Channel and near McDonald Lake are virtually all debris flow conglomerate with virtually no sandstone. However the Murky Formation in more distal areas, such as Redcliff Island and Et-Then Island, have substantial thicknesses of fluvial sandstone and sheetflood sandstones. In particular, the lower shale clast conglomerate of the Murky Formation at Redcliff Island is finer than at Murky Channel, and composed mostly of sheetflood and fluvial sandstone, with only thin debris flow conglomerates developed toward the top of the division. Thick, poorly bedded, massive debris flow deposits are not dominant until the upper quartzite clast conglomerate of the Murky Formation. This likely occurred in response to progradation of the alluvial fan into the basin. Furthermore, the thinning and pinching out of units to the northwest, as discussed earlier, indicates a proximal to distal transition from southeast to northwest.

## SEDIMENT/STRUCTURE RELATIONSHIPS

Physical relationships between strata of the Et-Then Group and structures associated with the McDonald fault system demonstrate synchronicity between Et-Then Group sedimentation and McDonald fault system deformation. On map scale, strands of the McDonald fault system can be seen to crosscut strata of the Murky Formation, Preble Formation, and the Et-Then volcanics (Hoffman et al., 1977; Hoffman, 1978, 1981). Furthermore, mesoscopic faults with offsets in the order of millimetres to at least 2 m examined in the Murky Formation and up to several hundred metres in the Preble Formation show right- and left-lateral strike-slip faults (rake of slickensides on fault plane are in the order of 7°), as well as oblique-slip faults (rake of slickensides on fault plane between 27° and 45°). This indicates that during Et-Then Group deposition strike-slip faulting occurred along the McDonald fault system, as well as faults with primarily oblique motion. These motions could account for abrupt thickness changes described in the Et-Then Group (Hoffman et al., 1977).

The presence of faults within the Et-Then Group indicates that these Et-Then Group strata were deposited and lithified prior to faulting. On map scale, however, sandstones of the Preble Formation overstep strands of the McDonald fault system (Hoffman et al., 1977; Hoffman, 1988), indicating that motion had ceased on these faults prior to final Et-Then Group deposition. These data prove the synchronicity between McDonald fault system deformation and Et-Then Group sedimentation.

## DISCUSSION

Sediment/structure relationships in the Et-Then Group indicate synchronicity between sedimentation and deformation. Therefore, the Et-Then group is a syntectonic deposit and should record the history of deformation along the McDonald fault zone, as suggested by (Hoffman, 1969, 1981; Hoffman et al., 1977). Several lines of evidence support this interpretation.

First, alluvial fan and braided fluvial systems require substantial relief, abundant sediment supply, and high gradient, all of which are provided in tectonically active areas. The second line of evidence is the change of facies from proximal to distal to the northwest, away from the McDonald fault system. In addition, paleocurrents in the Murky Formation show transport away from the McDonald fault system to the northwest, and Preble Formation paleocurrents also appear to be tectonically organized into a longitudinal drainage system (paleocurrents for both the Preble and Murky formations show direct relationships with the trend of the McDonald Fault). The stratigraphic trends discussed in the earlier section support the evidence listed above in terms of facies, paleocurrents, and thickness (both formational thickness and intra-formational thicknesses).

### *Significance of the Murky Formation-Preble Formation contact*

At the Murky Formation-Preble Formation contact the lithology fines dramatically over only tens of metres from cobble to boulder conglomerate to coarse sandstone; depositional system changes from a side-filling alluvial fan system to a longitudinally draining braided fluvial system; bedrock provenance changes from sedimentary or mixed sedimentary-granitoid provenance to a granitoid provenance. With the coincidental change in so many parameters at the same stratigraphic level, it is hard to demonstrate a single cause for the changes. Possibilities include various combinations of extrinsic controls, such as climate and tectonics, and intrinsic controls.

The best interpretation of the changes at the Preble Formation-Murky Formation boundary is that the source terrane changed from the local East Arm/Great Slave Lake shear zone to the Thelon Tectonic Zone. This would explain the change to a granitoid bedrock provenance, the change to west-southwest directed paleocurrents, and the change to a more distal facies. Furthermore, Henderson et al. (1990) suggests that considerable relief must have existed in the Thelon Tectonic Zone, at the apex of the McDonald and Bathurst faults during this time.

## SUMMARY

The Et-Then Group is a thick, non-marine clastic sequence, deposited contemporaneously with faulting on the McDonald fault system. The nature of the sediments and internal organization of the Et-Then group suggest strong tectonic controls on sedimentation were exerted by the McDonald fault system in terms of sediment supply, drainage organization, stratigraphic architecture and facies distribution.

Future research on the sedimentary rocks of the Et-Then Group (especially the provenance of the Preble Formation) should attempt to constrain tectonic or climatic influences on the stratigraphic changes within the Et-Then Group. In addition, a thorough treatment of the structural geology of both the Et-Then Group and the McDonald fault system in general is needed. Geochemical work on the volcanics may prove

illuminating. Finally, any successful geochronology attempt would serve to constrain the history recorded in the Et-Then Group.

## ACKNOWLEDGMENTS

W.A. Padgham and the NWT Geology Division, DIAND generously provided considerable support for fieldwork during 1993. P. Hoffman is thanked for illuminating discussions, particularly concerning regional geology and the significance of the Murky-Preble contact. S. Pratt provided field assistance. This material is based on work supported under a National Science Foundation Graduate Research Fellowship. Partial support was provided by National Science Foundation EAR-9058199.

## REFERENCES

- Bowring, S.A., Van Schmus, W.R., and Hoffman, P.F.**  
1984: U-Pb zircon ages from Athapuscow Aulacogen, East Arm of Great Slave Lake, N.W.T., Canada; *Canadian Journal of Earth Sciences*, v. 21, p. 1315-1324.
- DeCelles, P.G., Langford, R.P., and Schwartz, R.K.**  
1983: Two new methods of paleocurrent determination from trough cross-stratification; *Journal of Sedimentary Petrology*, v. 53, p. 629-642.
- Harms, J.C., Southard, J.B., and Walker, R.G.**  
1982: Structures and sequences in clastic rocks; *Society of Economic Paleontologists and Mineralogists Short Course No. 9*, p. 2-13.
- Henderson, J.B., McGrath, P.H., Thieriant, R.J., and van Breeman, O.**  
1990: Intracratonic identification of the Archean Slave Province into the Early Proterozoic Thelon Tectonic Zone of the Churchill Province, northwestern Canadian Shield; *Canadian Journal of Earth Science*, v. 27, p. 1699-1713.
- Hoffman, P.F.**  
1968: Stratigraphy of the Lower Proterozoic (Aphebian), Great Slave Supergroup, East Arm, Great Slave Lake, District of MacKenzie; *Geological Survey of Canada, Paper 68-42*.  
1969: Proterozoic paleocurrents and depositional history of the East Arm Fold Belt, Great Slave Lake; *Canadian Journal of Earth Science*, v. 6, p. 441.  
1976: Environmental Diversity of Middle Precambrian Stromatolites; in *Stromatolites*, M.R. Walter (ed.), Elsevier Scientific Publishing Co., p. 599-611.  
1981: Autopsy of Athapuscow Aulacogen: a failed rift affected by three collisions; in *Proterozoic Basins of Canada*, F.H.A. Campbell, (ed.); *Geological Survey of Canada, Paper 81-10*, p. 97-102.  
1987: Continental transform tectonics: Great Slave Lake shear zone (ca. 1.9 Ga), northwest Canada; *Geology* v. 15, p. 785-788  
1988: Geology and tectonics, East Arm of Great Slave Lake, Northwest Territories; *Geological Survey of Canada, Map 1628*, scale 1:250 000 and 1:500 000.
- Hoffman, P.F., Bell, I.R., Hildebrand, R.S., and Thorstad, L.**  
1977: Geology of the Athapuscow Aulacogen, East Arm, Great Slave Lake, District of MacKenzie; in *Report of Activities, Part A*; *Geological Survey of Canada, Paper 77-1A*, p. 117-128.
- LeCheminant, A.N. and Heaman, L.M.**  
1989: Mackenzie igneous events, Canadian Middle Proterozoic hotspot magmatism associated with ocean opening; *Earth and Planetary Science Letters*, v. 96, p. 38-48.

Geological Survey of Canada Project 820010

# Contact relationships between the Anialik River volcanic belt and the Kangguyak gneiss belt, northwestern Slave Province, Northwest Territories<sup>1</sup>

C. Relf<sup>2</sup>, A. Chouinard<sup>3</sup>, H. Sandeman<sup>4</sup>, and M.E. Villeneuve  
Continental Geoscience Division

*Relf, C., Chouinard, A., Sandeman, H., and Villeneuve, M.E., 1994: Contact relationships between the Anialik River volcanic belt and the Kangguyak gneiss belt, northwestern Slave Province, Northwest Territories; in Current Research 1994-C; Geological Survey of Canada, p. 49-59.*

---

**Abstract:** Mapping in the northwest part of the Hepburn Island map area examined a major fault separating the ca. 2.69 Ga Anialik River volcanic belt from ca. 3.1 Ga gneissic tectonites of the Kangguyak gneiss belt. Evidence for at least two periods of displacement along the fault were observed; early movement is marked by a 200 m wide zone of straight gneisses recrystallized under amphibolite facies conditions, and later movement is marked by a narrower zone (less than 10 m) of chlorite schist containing quartz veins, local C-S fabrics, and breccia zones. Kinematic indicators associated with the later displacement record oblique (dextral) west-over-east movement. Early movement is more ambiguous, but a steep lineation associated with the straight gneisses implies predominantly dip-slip movement. Contrasting ages, bulk compositions, deformation histories, and metamorphic grades across the fault suggest that the Kangguyak gneisses and the Anialik River volcanic belt represent two distinct terranes.

**Resumé :** Une cartographie de la partie nord-ouest de la région de l'île Hepburn a révélé une faille majeure séparant la ceinture volcanique de la rivière Anialik des tectonites de la ceinture gneissique de kangguyak. Le long de la faille des évidence pour au moins deux épisodes de déformation ont été observées. Le déplacement précoce est caractérisé par une zone de 200 m de large de "gneiss droits" recrystallisés au faciès amphibolite. Le déplacement tardif se retrouve dans une zone étroite (moins de 10 m) de schiste à chlorite comportant des veines de quartz, localement des fabriques C/S et des zones de brèches. Les indicateurs cinématiques associés avec le déplacement tardif enregistrent un déplacement oblique dextre chevauchant vers l'est. La superposition des fabriques tardives rend l'interprétation du déplacement Précoce ambiguë, par contre une linéation fortement plongeante associée avec les "gneiss droits" impliquerait un déplacement essentiellement vertical. Le contraste de lithologie, de style de déformation, de conditions métamorphique et d'âge de part et d'autre de la faille suggère que les gneiss de Kangguyak et les volcanites de la rivière Anialik représente deux terranes distincts.

---

<sup>1</sup> NATMAP Slave Province Project

<sup>2</sup> Canada-Northwest Territories Mineral Initiatives Office, Department of Energy, Mines and Petroleum Resources, Government of the N.W.T., Box 1320, Yellowknife, Northwest Territories X1A 2L9

<sup>3</sup> Department of Earth Sciences, Carleton University, Ottawa, Ontario K1S 5B6

<sup>4</sup> Geological Sciences, Queen's University, Kingston, Ontario K7L 3N6

## INTRODUCTION

An Archean fault separating the Anialik River volcanic belt from a unit of mixed gneisses was recognized recently in the northwestern Slave Province by Jackson (1989) and Relf et al. (1992). Based on contrasts in metamorphic grade and rock type across it, the potential of the fault to represent a tectonic boundary separating two distinct terranes was recognized and pursued by the Slave Province NATMAP Project (McEachern, 1993). The rocks west of the fault, informally named the Kangguyak gneiss belt (McEachern, 1993), consist of intensely deformed and recrystallized gneisses containing a component of older (>ca. 3.0 Ga) continental crust. To the east lies the ca. 2.69 Ga Anialik River volcanic belt and related intrusive rocks. Variably deformed granitoid plutons intrude rocks on both sides of the fault. During the 1993 field season, structural, metamorphic, and geochronological studies were undertaken to examine the possible origin of the gneisses, to document the movement history of the fault, and to compare the deformation histories of rocks on either side of the fault.

This paper summarizes the results of mapping and presents some preliminary U-Pb geochronological data from a quartzite unit within the gneisses. Fieldwork was carried out under the auspices of the Canada-NWT Mineral Initiatives Office (Yellowknife), and financial support by the NATMAP Slave Province Project allowed mapping to be extended into the Kangguyak gneisses. Geochronological studies are also funded through NATMAP.

## PREVIOUS WORK

Previous mapping in the area includes the regional (1:500 000) mapping of Fraser (1964), and a summary map of 1:50 000 field mapping by Tirrul and Bell (1980). Easton et al. (1982), Yeo et al. (1983), Jackson et al. (1985), and Abraham (1987, 1989) mapped parts of the area at 1:30 000 to 1:50 000, and Jackson (1989) produced a compilation of previous mapping at 1:125 000 scale. More recent work, focused on the Kangguyak gneisses, includes that of Relf et al. (1992), Barrie (1993), and McEachern (1993).

## ANIALIK RIVER VOLCANIC BELT

### Geology

The Anialik River volcanic belt is dominated by mafic to felsic volcanic and related volcanoclastic sedimentary rocks of the Yellowknife Supergroup (Hrabi et al., 1993; Padgham, 1993). These include pillowed and massive mafic flows, abundant felsic to intermediate volcanoclastic rocks, and minor quartz-feldspar porphyritic rhyolite (Tirrul and Bell, 1980; Jackson, 1989; Relf, 1992). Semi-pelitic sedimentary rocks, iron-formation, and exhalative carbonate rocks comprise a small portion of the belt. A large, composite tonalitic body – the Anialik River igneous complex – underlies the north end of the volcanic belt and is exposed in the core of a kilometre-scale antiform (Fig. 1). Current radiogenic age data

indicate that emplacement of the igneous complex (between ca. 2703 and 2682 Ma; Abraham et al., 1991) predated and overlapped with volcanism (ca. 2686 to 2678 Ma; Bowring and van Schmus in Easton, 1982; Abraham et al., 1991; and M. Villeneuve, unpub. data, 1993).

Numerous lenses of polymictic conglomerate occur within the volcanic belt. Detrital zircons from two of the lenses indicate that the conglomerates are younger than ca. 2600 Ma (M. Villeneuve, unpub. data, 1992), implying an unconformable contact between the volcanic belt and the conglomerates, as proposed by Tirrul and Bell (1980).

Metamorphic assemblages in the volcanic rocks range from lower greenschist to mid-amphibolite facies. Greenschist facies assemblages dominate the central part of the volcanic belt, and amphibolite facies assemblages occur in close proximity to the granitoid plutons that bound the belt. This metamorphic pattern is consistent with regional contact metamorphism related to late plutonism.

### Structure sets

The deformation history of the Anialik River volcanic belt is discussed in detail elsewhere (Relf, 1992), and is therefore only summarized briefly here. The main structure sets are shown on Figure 1, and are listed in Table 1. In the following discussion, the subscript "v" denotes structures found in the volcanic belt and related rocks.

The earliest tectonic fabric recognized in the volcanic belt ( $S_{1v}$ ) is a penetrative chlorite foliation that is only preserved locally in microlithons between  $S_{2v}$ , the second foliation in the area. The tectonic significance of  $S_{1v}$  is not understood.  $S_{2v}$ , which is generally the dominant tectonic fabric in outcrop, is defined by chlorite±biotite below the hornblende isograd, and aligned amphiboles above the isograd. In most outcrops,  $S_{2v}$  is bedding-parallel, but locally it parallels the axial surface of isoclinal folds of bedding; these folds are interpreted as  $F_{2v}$  folds. Although  $S_{2v}$  dominates most outcrops, the regional map pattern is controlled largely by a kilometre-scale antiform which deforms  $S_{2v}$  and all earlier fabrics. The antiform exposes the underlying Anialik River igneous complex in its core. This fold, designated  $F_{3v}$ , is associated with a subvertical, north-northeast-striking axial planar foliation defined by chlorite in greenschist facies rocks and by hornblende within the amphibolite facies. Numerous outcrop-scale folds of bedding and  $S_{2v}$ , particularly abundant near the north and south ends of the Anialik River igneous complex, are interpreted as parasitic  $F_{3v}$  folds. They plunge south-southwest near the south end of the complex, and north-northeast in the north, implying the structure is a doubly-plunging antiform. Foliated tonalite veins that both crosscut and are folded about  $S_{3v}$  occur near the northeast part of the volcanic belt, and are interpreted to overlap in age with  $D_{3v}$ . A sample from one of these veins yielded a preliminary U-Pb zircon age of ca. 2.61 Ga (M. Villeneuve, unpub. data, 1993).

Subsequent deformation in the volcanic belt produced at least two sets of brittle-ductile faults associated with lower greenschist facies mineral assemblages and quartz-carbonate



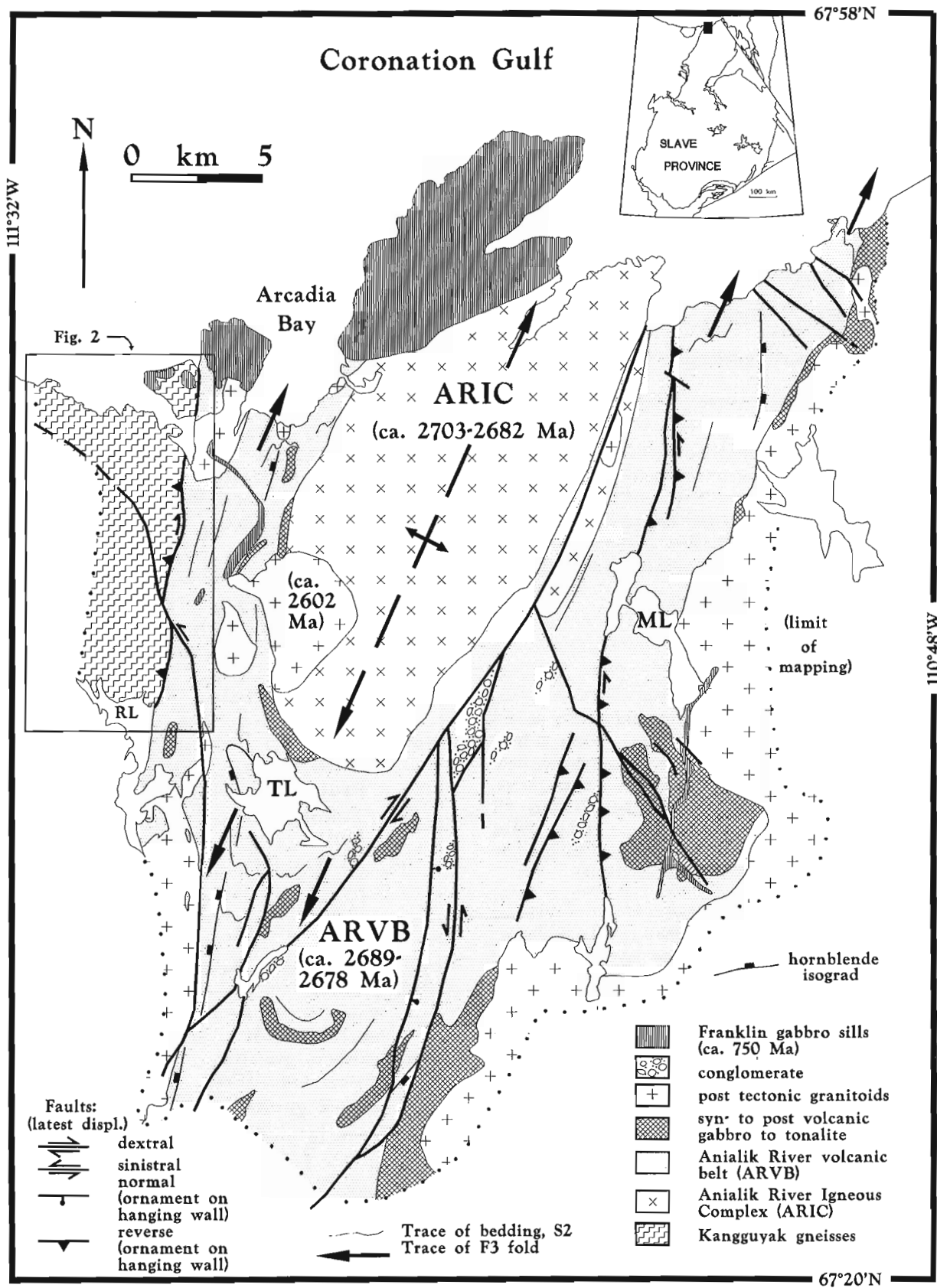


Figure 1. Simplified geology map of the northern Anialik River volcanic belt and the Kangguyak gneiss belt. Location in Slave Province shown on inset. Abbreviations: ML - Mistake lake; RL - Rhino lake; TL - Turtle lake (informal lake names).

**Table 1.** Summary of structure sets in the Anialik River volcanic belt (east) and Kangguyak gneiss belt (west).

Kangguyak gneisses			Anialik River volcanic belt		
Archean	D5	NE, NW transcurrent faults	↑ shared tectonic history   ?	D5	NE, NW transcurrent faults
	D4	oblique W-over-E reactivation of Tokhokatak fault		D4	oblique E-over-W faults
	D3	NNE upright folds, gneissosity, shearing along Tokhokatak fault		D3	NNE upright folds, cleavage
	D2	SW-dipping gneissosity, folds		D2	dominant cleavage, isoclinal folds
	D1	early gneissosity		D1	rare cleavage
				Prof?   Archean	

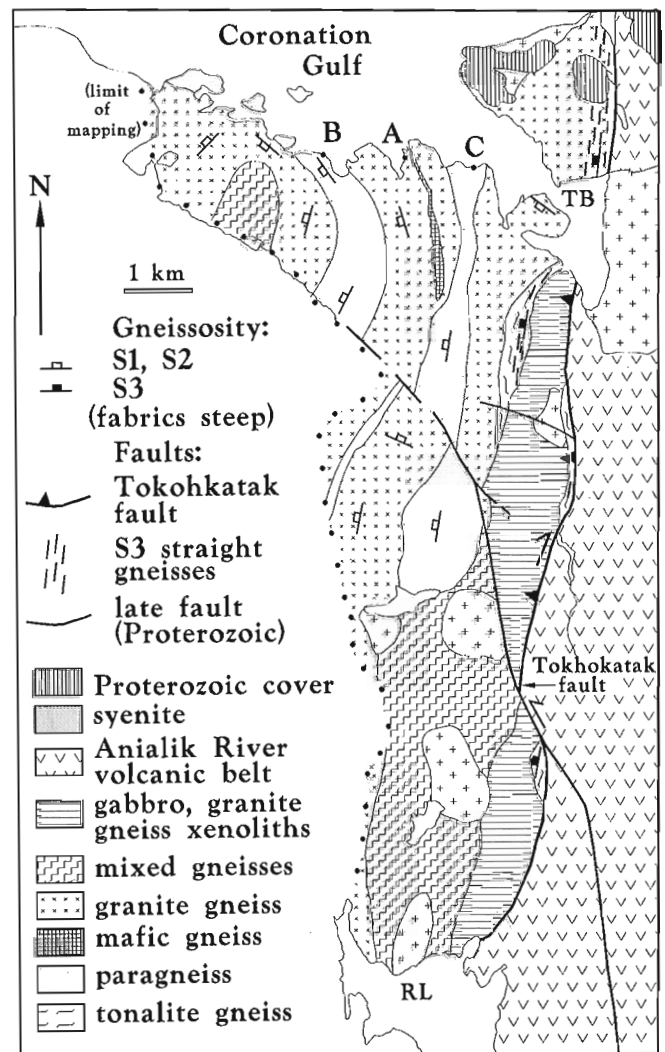
veins (Relf, 1992). These faults have similar orientations and displacement histories to Proterozoic faults further west, to which they have been correlated (Relf, 1992). Nevertheless, several of these faults appear to have had an earlier Archean displacement history, based on the local occurrence of cross-cutting granitoid dykes and amphibolite facies shear fabrics.

## KANGGUYAK GNEISSES

### Geology

A belt of mixed gneisses and migmatites, informally named the Kangguyak gneisses (McEachern, 1993), occur in fault contact with the west side of the Anialik River volcanic belt. The gneisses are here subdivided into four units: paragneiss, tonalitic gneiss, granitic gneiss, and mafic gneiss (Fig. 2). All four units are crosscut by numerous massive gabbro dykes and a variety of granitoid rocks that range from strongly foliated biotite monzonite to massive leucogranite.

The paragneiss, which corresponds to unit 2 (quartz-plagioclase-biotite gneiss) of McEachern (1993), is characterized by biotite±garnet-rich schistose layers, commonly intruded by veins and irregularly shaped pods of muscovite syenogranite and associated pegmatite. In addition, conglomerate (W.A. Padgham, pers. comm., 1993) and thinly bedded quartzite have been recognized in coastal exposures. The conglomerate (see locality A on Fig. 2) contains pebble to cobble-sized clasts of granite, quartz, quartzite and both fine- and coarse-grained amphibolite in a biotite+hornblende-rich matrix (Fig. 3). The unit is up to 30 m wide, and has been traced inland along strike for at least 150 m, where it is obscured by heavy lichen cover. Quartzite was observed in two localities along the coast. At one locality (see B on Fig. 2) the quartzite is about 5 m wide and consists of 80-90% quartz with accessory biotite and feldspar. This unit was sampled for detrital zircons. The second quartzite (locality C on Fig. 2) is less than a metre wide and contains about 70-75% quartz and 25-30% feldspar, biotite, and other minerals.



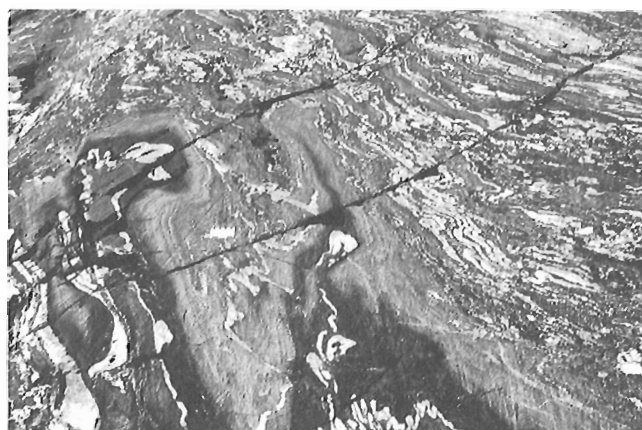
**Figure 2.** Simplified geology map of the Kangguyak gneisses in the Tokhokatak Bay area. Abbreviations: RL - Rhino lake; TB - Tokhokatak Bay (informal names). Location of Figure 2 outlined in Figure 1.



**Figure 3.** *a) Polyolithic conglomerate unit in the Kangguyak gneisses. Scale is 9 cm. For location see "A" on Figure 2. b) Thinly-bedded quartzite unit in the Kangguyak gneisses. Lens cap is 5 cm across. For location see "B" on Figure 2.*

Metamorphic assemblages in the paragneisses include biotite-garnet, biotite-garnet-hornblende, hornblende-garnet-orthopyroxene, and biotite-cordierite-garnet (plagioclase and quartz present in all assemblages), compatible with upper amphibolite to lower granulite facies conditions. Lenses of pegmatitic granite in the paragneiss are interpreted as anatectic melt, since mineral assemblages indicate temperatures compatible with a granite melt phase. Despite the degree of metamorphism and recrystallization, a compositional layering defined by varying abundance of biotite, the presence or absence of garnet±orthopyroxene±hornblende, or abundance of clasts (in conglomerate) is commonly present. This layering ranges in scale from a few millimetres to tens of centimetres, and is interpreted as relict bedding (Fig. 4).

The tonalitic gneiss corresponds to unit 1 (tonalite orthogneiss) of McEachern (1993), and appears to be confined mainly to the east part of the gneiss belt. However, as much of the area has been pervasively intruded by syntectonic monzogranite to syenogranite, it is commonly difficult to distinguish between a true granite gneiss and a tonalitic gneiss that has been "soaked through" with granitic melt. This problem is particularly pronounced where K-feldspar-rich layers



**Figure 4.** *Relict bedding (folded) preserved in pelitic paragneiss. Scale (centre left of photo) is 9 cm.*

do not show a clearly discordant relationship but are transposed into the gneissosity. As a result, tonalitic orthogneiss may be more extensive than shown in Figure 2. Contact relationships between the tonalitic gneiss and other units are not well defined, but the local presence of biotite±garnet-rich schleiren suggests that the tonalite may be intrusive into the paragneiss unit.

Granitic gneiss, in part correlative to McEachern's (1993) unit 3 (granodiorite orthogneiss) and in part to unit 2 (quartz-plagioclase-biotite gneiss) is widespread throughout the gneiss belt. The change in nomenclature is based on compositional and textural variations in McEachern's unit 2; where the quartz-plagioclase-biotite gneiss contains less than 20% biotite or lacks accessory minerals, such as garnet, which suggest a sedimentary origin, it was mapped as a granitic gneiss. As a result, the large area mapped by McEachern (1993) as quartz-plagioclase-biotite gneiss has been subdivided into areas interpreted as paragneiss, and areas classified as granitic gneiss. The origin of the granitic gneiss (igneous vs. sedimentary) is not known; it could be a mixed unit of ortho- and paragneiss. Leucocratic monzogranite and pegmatite veins are locally abundant in the granitic gneiss; veins both transect and parallel the gneissosity.

The fourth gneiss unit, the mafic gneiss, is characterized by hornblende amphibolites, locally containing garnet. This unit is interlayered with both paragneiss and granitic gneiss, and occurs as thin (up to 50 m thick), discontinuous layers that generally cannot be traced for more than a few hundred metres along strike. The origin of the mafic gneiss is uncertain, as no primary features such as pillows, bedding, or intrusive relationships are preserved. Nevertheless, the spatial association of mafic gneiss and paragneiss, and the hornblende-rich matrix of the conglomerate suggest that some of the mafic rocks may have been exposed during sedimentation. A supracrustal origin is therefore possible for at least some of the mafic gneisses.

Based on the mineral assemblages and textures observed in the gneisses, it appears that the Kangguyak gneisses have, in large part, a supracrustal origin.

**Geochronology**

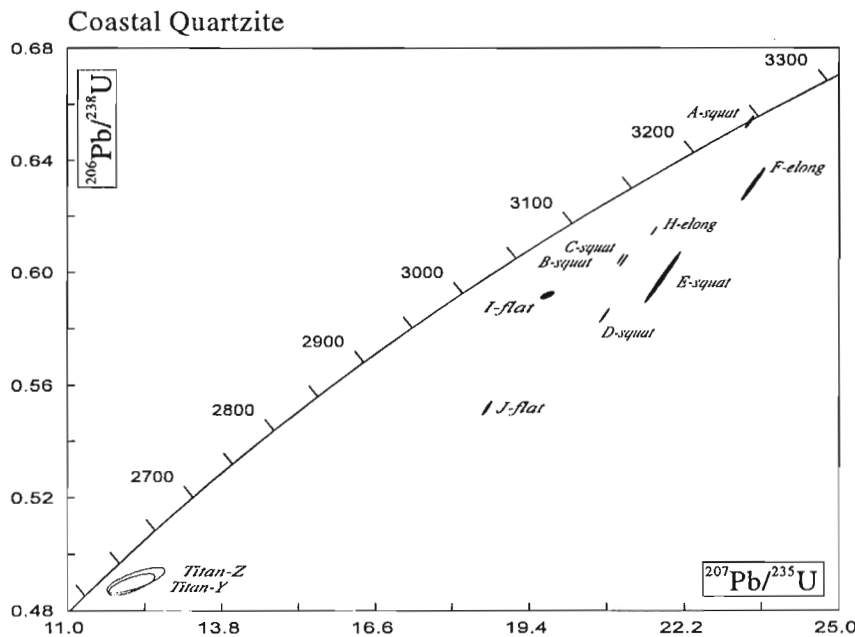
The quartzite at locality B (Fig. 2) was sampled for detrital zircon geochronology. The sample contained 0.1-1 cm thick biotite-rich beds interlayered with 1-1.5 cm thick quartz-rich (quartz ≥85%) beds. Nine single zircons with three distinct morphologies – squat (L:W<2:1); elongate (L:W>3:1); and flat (L:W=1:1; W:H>10:1) - were analyzed using U-Pb methods outlined in Villeneuve (1993) (Table 2). Polished grain

mounts revealed 1-5 μm zircon overgrowths truncate pre-existing growth structures in the core material. The truncation of the internal structure is interpreted to result from sedimentary processes having operated on the cores. Later zircon growth occurred during metamorphism, forming the overgrowths. All the crystals analyzed were larger than 75 μm in diameter and were heavily abraded to remove 10-20 μm of surface material, thereby eliminating as much late overgrowth as possible.

**Table 2.** U-Pb analytical data.

Fraction <sup>a</sup>	Wt. <sup>b</sup> μg	U ppm	Pb <sup>c</sup> ppm	Th <sup>d</sup> U	<sup>206</sup> Pb <sup>e</sup> <sup>204</sup> Pb	Pb <sup>f</sup> pg	Radiogenic ratios (±1σ, in %) <sup>g</sup>			Age (Ma, ±2σ) <sup>h</sup>	Discord. <sup>i</sup>
							<sup>206</sup> Pb/ <sup>238</sup> U	<sup>207</sup> Pb/ <sup>235</sup> U	<sup>207</sup> Pb/ <sup>206</sup> Pb	<sup>207</sup> Pb/ <sup>206</sup> Pb	
<b>COAST QUARTZITE (UTM Zone: 12 Easting: 473675 Northing: 7512688)</b>											
Titanite-Y	136	45	27	0.796	67	22.4	0.4892±0.39	12.161±1.8	0.18028±1.5	2655.5±50.1	4.02
Titanite-Z	145	35	21	0.973	60	19.7	0.4908±0.47	12.237±2.2	0.18083±1.8	2660.5±61.3	3.94
A-squat	3	274	214	0.497	1521	2.3	0.6537±0.17	23.381±0.18	0.25941±0.07	3243.1±2.1	0.02
B-squat	3	322	233	0.506	2660	0.8	0.6048±0.14	21.045±0.15	0.25237±0.03	3199.7±1.1	5.90
C-squat	1	674	488	0.515	1623	3.5	0.6043±0.17	21.098±0.17	0.25320±0.04	3204.9±1.2	6.17
D-squat	2	308	226	0.748	1482	1.3	0.5846±0.21	20.748±0.22	0.25739±0.05	3230.8±1.6	10.15
E-squat	2	75	55	0.620	407	1.2	0.5981±0.76	21.795±0.76	0.26427±0.11	3272.4±3.5	9.56
F-elong	1	221	166	0.425	410	6.9	0.6315±0.47	23.443±0.47	0.26925±0.09	3301.7±2.9	5.59
H-elong	3	407	299	0.501	3704	0.7	0.6149±0.13	21.645±0.14	0.25532±0.03	3218.0±1.0	5.03
I-flat	2	1333	981	0.750	227	186.5	0.5920±0.12	19.726±0.34	0.24168±0.28	3131.1±8.8	5.34
J-flat	1	857	549	0.384	607	23.6	0.5520±0.23	18.630±0.24	0.24479±0.08	3151.4±2.5	12.45

<sup>a</sup>All fractions are abraded except those marked with <sup>u</sup>; <sup>b</sup>Error on weight =±1 μg; <sup>c</sup>Radiogenic Pb; <sup>d</sup>Th/U from <sup>208</sup>Pb\*/<sup>206</sup>Pb\* and <sup>207</sup>Pb/<sup>206</sup>Pb age; <sup>e</sup>Measured ratio corrected for spike and Pb fractionation of 0.09±0.03/AMU; <sup>f</sup>Total common Pb on analysis corrected for fractionation and spike; <sup>g</sup>Corrected for blank Pb and U and common Pb (Stacey-Kramers model Pb composition at <sup>207</sup>Pb/<sup>206</sup>Pb age), 1 sigma error, in percent; <sup>h</sup>Corrected for blank and common Pb; <sup>i</sup>Discordance along a discordia to origin



**Figure 5.**

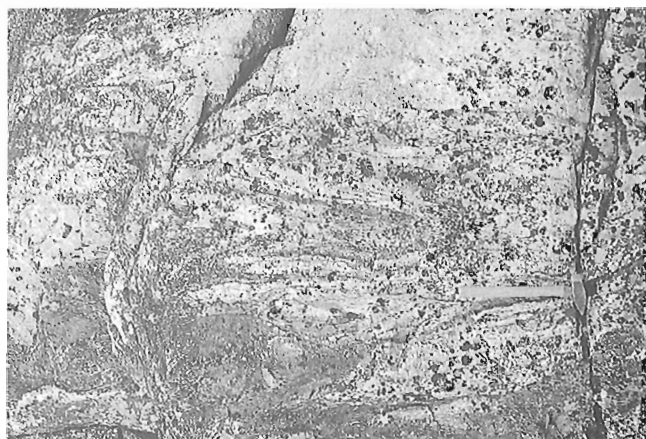
Concordia plot of detrital zircons and metamorphic titanite from quartzite in the Kangguyak gneiss belt.

All three zircon morphologies yielded  $^{207}\text{Pb}/^{206}\text{Pb}$  ages between 3.13 and 3.27 Ga (Table 2, Fig. 5). The grains range from concordant to 10% discordant (Table 1, Fig. 5). The large discordance shown by fraction J may result from remnant overgrowths on this crystal, as the flat crystals were the most difficult to abrade. Alternatively, some crystals had high U contents, possibly indicating late Pb loss as an additional factor. Although the data do not reveal the age of the overgrowths, they do indicate that the quartzite had its source in rocks greater than 3.1 Ga.

In addition to detrital zircons, metamorphic titanite was dated in order to determine the timing of metamorphism. Large dark red to brown titanite crystal fragments from within the biotite-rich layers of the quartzite were analyzed using methods summarized by Parrish et al. (1992). Two multigrain fractions gave  $^{207}\text{Pb}/^{206}\text{Pb}$  ages of ca 2.66 Ga (Fig. 5). These ages are about 4% discordant, and have large errors due to a high common Pb component in the crystals. Although no definitive titanite age can be assigned without better control on the composition of the common Pb, an estimate derived from the two  $^{207}\text{Pb}/^{206}\text{Pb}$  ages of  $2660 \pm 40$  Ma can be used. This age is in agreement with titanite ages from elsewhere in the northern Slave Province (Abraham et al., 1991; M. Villeneuve, unpub. data).

### Structure sets

Tectonic fabrics in the Kangguyak gneisses, summarized in Table 1, have been modified from McEachern (1993). The earliest foliation ( $S_{1g}$ ; "g" indicates a fabric within the Kangguyak gneisses) is a centimetre-scale gneissic layering defined by alternating quartzofeldspathic and mafic layers.  $S_{1g}$  is isoclinally folded about  $S_{2g}$  (Fig 6), an overprinting gneissosity with a mean orientation of 154/74. Locally  $S_{2g}$  defines 5 to 10 m wide zones of straight gneiss in which  $S_{1g}$  is transposed into  $S_{2g}$  and compositional layering is very straight and sharply defined. These zones of straight gneiss, which have gradational contacts with gently to tightly folded



**Figure 6.** Refolded gneissosity in granitic gneiss. Hammer handle is 30 cm. (GSC 1993-283)

gneisses of the same composition, are associated with a strong down-dip mineral lineation, and were interpreted as recrystallized mylonites by McEachern (1993).

The third set of structures in the gneisses consists of folds of gneissosity about a subvertical, north-northeast-striking axial surface ( $F_{3g}$ ). The majority of these folds plunge steeply to moderately southwest, with a few subhorizontal northeast and southwest plunges, implying that they deform a previously folded surface,  $S_{1g}$ . Throughout most of the gneiss belt,  $S_{3g}$  occurs in anastomosing domains with  $S_{1g}$  (folded) and  $S_{2g}$  (southeast-striking) preserved in low-strain windows between  $S_{3g}$  (McEachern, 1993). Within a few hundred metres of the east margin of the gneiss belt the intensity of  $S_{3g}$  increases, and  $F_{3g}$  fold limbs are commonly truncated by  $S_{3g}$ , implying shearing along fold limbs (McEachern, 1993) (Fig. 7). A zone of steeply west-dipping, strongly developed gneissosity associated with a down-dip mineral lineation transposes all earlier fabrics adjacent to the contact with the volcanic belt. This straight gneiss zone is up to about 200 m wide, and is interpreted as a recrystallized shear zone



**Figure 7.**  $F_{3g}$  fold truncated by  $S_{3g}$ , interpreted to indicate that shearing along  $S_{3g}$  accompanied folding. Pen is 20 cm.



(McEachern, 1993). Based on the greater intensity of  $S_{3g}$  near the fault, the parallelism of  $S_{3g}$  and the straight gneisses, and the presence of sheared  $F_{3g}$  fold limbs, folding is interpreted to have overlapped with shearing.

Metamorphic conditions during deformation of the Kangguyak gneisses were consistently high;  $S_{1g}$ ,  $S_{2g}$ , and  $S_{3g}$  are all defined by amphibolite facies assemblages. Orthopyroxene-bearing paragneisses suggest that metamorphism peaked within the granulite facies, although from textural relationships exposed in outcrop it is not clear whether the growth of peak assemblages accompanied  $D_{1g}$ ,  $D_{2g}$ , or  $D_{3g}$ . Ongoing thermobarometric studies will address the question of the metamorphic history of the gneisses.

## THE TOKHOKATAK FAULT

The contact between the Anialik River volcanic belt and the Kangguyak gneisses is marked by the Tokhokatak fault, after the local name for the bay through which the fault runs ("Tokhokatak" is Inuinaktun for "narrow channel"). The Tokhokatak fault preserves evidence of a protracted displacement history. Evidence for early fault movement is preserved in a 200 m wide zone of  $S_{3g}$  straight gneisses, interpreted as a recrystallized shear zone. Reactivation of the shear zone is marked by a narrow (10-20 m) zone of low-grade brittle-ductile fault fabrics along the volcanic belt-gneiss belt contact. Two intrusive phases showing cross cutting relationships with these fabric sets have been recognized, and their isotopic ages will help to bracket the timing of fault movement.

### Early Fault Movement

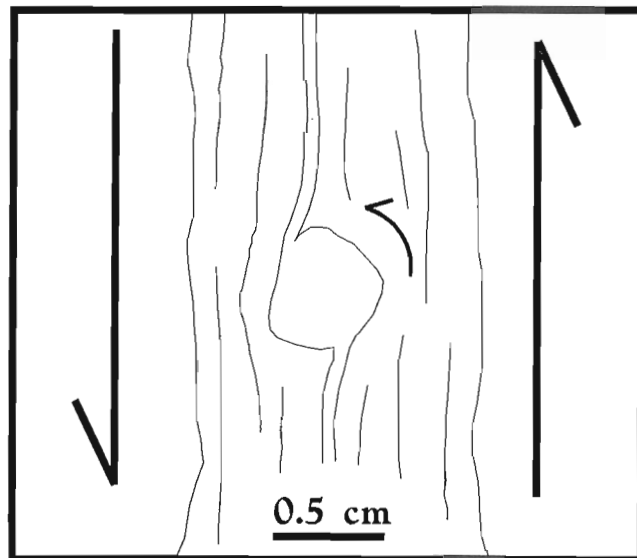
As described above, approximately 100-200 m west of the Anialik River volcanic belt  $S_{3g}$  defines a zone of steeply west-dipping straight gneisses interpreted as a recrystallized shear zone (Fig. 2). A steep mineral stretching lineation in these gneisses implies a predominantly dip-slip component of displacement during shearing. McEachern (1993) reported shallow-plunging lineations locally within  $S_{3g}$ ; it is not clear whether these lineations are related to shallowly plunging  $F_{3g}$  folds, or are related to later strike-slip movement along the fault (see below).

Although the straight gneisses are interpreted as a recrystallized shear zone, kinematic indicators are rare. A single rotated K-feldspar porphyroclast in granitic gneiss was observed near the north end of the straight gneiss zone (Fig. 8). The gneiss has a  $70^\circ N$  pitching lineation, and the asymmetry of the porphyroclast suggests a component of east-side-up displacement. In addition to this rotated porphyroclast, local folds of gneissosity with an asymmetry compatible with east-side-up movement were observed in the area, although the timing of these folds relative to porphyroclast rotation is not known.

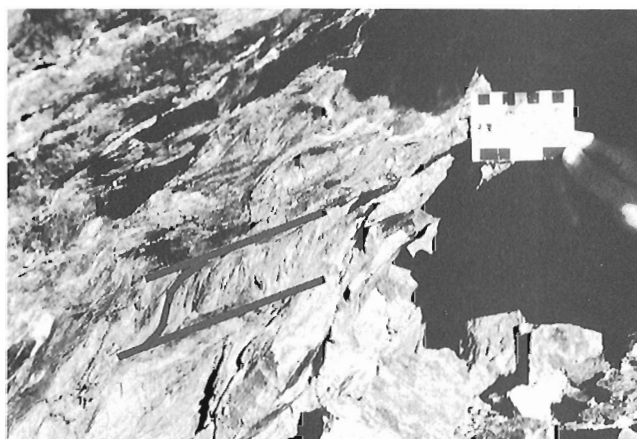
A complex unit consisting of gabbro to quartz diorite, crosscut by granitoid dykes, transects the gneisses and obscures  $S_{3g}$  along most of the remainder of the Tokhokatak

fault (Fig. 2). The unit, which ranges from massive to strongly foliated, truncates gneissosity and therefore is interpreted to postdate early shearing. Isolated rafts of mafic and tonalite gneiss occur locally within this unit, but they may be rotated, and thus cannot be used to determine shear sense.

Due to the paucity of clear kinematic indicators, the early fault history is not well documented. Nevertheless, the width of the high strain zone, the high metamorphic grade, and the steep lineation suggest dominantly dip-slip displacement across a ductile shear zone.



**Figure 8.** Sketch of rotated K-feldspar porphyroclast from straight gneisses near north end of Tokhokatak fault. View is looking north at vertical outcrop face; stretching lineation is steeply down-dip.



**Figure 9.** West-over-east C-S fabric in chlorite schist, hanging wall of Tokhokatak fault. View is looking north at vertical outcrop face; stretching lineation is plunges steeply south. Scale is 9 cm.



### Late Fault Movement

Chlorite-grade fault fabrics overprint the east margin of the straight gneisses adjacent to the Anialik River volcanic belt, overprinting the earlier structures on the Tokhokatak fault. These fabrics include C-S fabrics defined by chlorite, mineral stretching lineations, and slickensides on fracture surfaces coated by quartz veins. In addition, brecciated wall rock occurs commonly along the fault. These greenschist facies fabrics are confined to a zone generally less than 20 m wide along the volcanic-gneiss contact. Most stretching lineations within this zone plunge 50-70°S. C-S fabrics and minor offsets of quartz veins along the fault suggest west-side-up displacement with a dextral component (Fig. 9).

Slickensides, observed only in the south part of the area near Rhino lake, plunge both steeply south and subhorizontally. Overprinting relations between these two orientations have not been observed, and the sense of displacement associated with the subhorizontal slickensides is not known; however, the horizontal slickensides suggest that late, brittle faulting may have involved more than one episode of displacement.

### Timing of Fault Displacement

Early ductile shearing and late, brittle-ductile faulting are most easily distinguished in the northern part of the map area. Here, early faulting is marked by a zone of straight gneisses up to 200 m wide, crosscut by a biotite quartz monzonite. The quartz monzonite has a weakly to moderately developed foliation of uncertain age that parallels, and may be correlative to,  $S_{3g}$ . As the body transects the straight gneisses, it is interpreted to postdate shearing, however, the foliation in the quartz monzonite may have formed during late  $D_{3g}$  shortening. The age of this pluton will allow a minimum age to be assigned to the high grade, ductile displacement on the fault.

Along the east margin of the straight gneisses adjacent to the volcanic rocks, a narrow (up to 20 m) zone of brecciated, brick- red-weathering, mixed gneisses and quartz monzonite occurs. Here a small, massive hornblende syenite is dextrally offset about 300 m across the Tokhokatak fault. A 65°

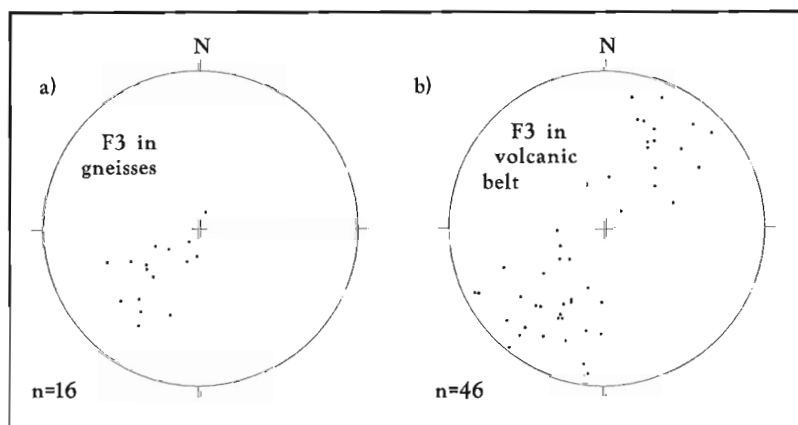
south-plunging mineral stretching lineation in the syenite implies oblique west-over-east dextral displacement. The age of this syenite will provide a maximum age for late faulting.

About 4 km north of Rhino lake, the Tokhokatak fault is sinistrally offset by 2 km across a late, northwest-striking transcurrent fault (Fig. 1, 2). This late fault, characterized by a 2 to 5 m wide zone of quartz and hematite veining and brecciated host rock, has an orientation and sense of displacement similar to 1.84-1.66 Ga transcurrent faults in the Wopmay Orogen 10 km to the west (Hoffman, 1987).

### Correlation of structures across the Tokhokatak fault

Correlation of structure sets in the Anialik River volcanic belt with those in the Kangguyak gneisses is difficult, as the only deformation so far to be assigned an absolute age is late upright folding in the volcanic belt ( $D_{3v}$ ; ca. 2.61 Ga). As a result, tentative correlation is based on strain state, metamorphic grade, and orientation of folds and fabrics on both sides of the Tokhokatak fault.

The youngest regional fabric-forming events on either side of the fault are  $D_{3v}$  and  $D_{3g}$  in the volcanic belt and the gneisses, respectively. Both of these structure sets involved upright folding of pre-existing fabrics, and the formation of a subvertical, north-northeast-striking foliation. Although the plunges of  $F_3$  folds differ in the two terranes – they range from about 50° northeast to 30° southwest in the volcanic belt, whereas in the gneisses most are 20° to 80° southwest (Fig. 10) – this does not preclude their correlation; it merely reflects variable orientations of pre- $D_3$  fabrics. The absolute age of structures associated with  $D_{3g}$  is not presently known. However, as the maximum temperatures associated with Proterozoic overprinting in the area correspond to biotite growth in pelites (about 400°C; Hoffman et al., 1984), and  $S_{3g}$  is defined by amphibolite facies assemblages,  $D_{3g}$  must be Archean. Crosscutting relationships along the north end of the Tokhokatak fault will allow a minimum age to be assigned to  $S_{3g}$  (see above). Based on the orientations of  $F_3$  axial surfaces, structures associated with  $D_{3v}$  and  $D_{3g}$  are tentatively interpreted to be correlative.



**Figure 10.**

*a) Equal area projection showing orientations of  $F_{3g}$  fold hinges in the Kangguyak gneisses.  $n=16$ . b) Equal area projection showing orientations of  $F_{3v}$  fold hinges in the Anialik River volcanic belt.  $n=46$ .*

Possible relationships between fabrics that predate  $D_{3g}/D_{3v}$  are more difficult to assess, as the original orientations of these fabrics are not well preserved. In the Anialik River volcanic belt,  $F_{3v}$  folds plunge shallowly, suggesting that  $S_{2v}$  was originally subhorizontal. The doubly plunging nature of the regional  $F_{3v}$  antiform may be a result of strain partitioning around the igneous complex, possibly combined with a component of diapiric uplift. In contrast,  $F_{3g}$  folds of  $S_{2g}$  in the Kangguyak gneisses have a consistent southwest plunge, implying a moderate to steep southwest dip for  $S_{2g}$  before  $D_{3g}$ . Although it is not conclusive evidence, the apparent difference in orientation of  $S_2$  on either side of the Tokhokatak fault – subhorizontal to the east; steeply southwest-dipping to the west – suggests that pre- $D_3$  fabrics in the two terranes formed separately.

Based on the above arguments, we suggest that the Kangguyak gneisses and the Anialik River volcanic belt share only part of their deformation histories; pre- $D_3$  structures may represent different, unrelated deformation events in the two terranes.

## DISCUSSION

Rocks of the Kangguyak gneiss belt are distinct from those of the Anialik River volcanic belt in two important ways. First, the proportion of mafic to felsic rocks and the abundance of paragneiss with a pelitic to semipelitic bulk composition suggest that the gneisses are not simply high grade equivalents of the Anialik River volcanic rocks, but represent a separate supracrustal terrane. Second, U-Pb zircon and titanite ages presented above show that the quartzite within the Kangguyak gneisses was deposited between ca. 3.15 and 2.66 Ga. Detrital zircons of synvolcanic age (ca. 2.69 Ga) are conspicuous by their absence in the quartzite. In fact the paragneiss component of the Kangguyak gneisses may have close affinities with ca. 3.15 Ga volcanic rocks in the Napaktulik Lake area about 60 km to the south (Jackson, 1991; Villeneuve et al., 1993). Further geochronological work will determine whether the paragneisses are part of a pre-Yellowknife Supergroup sequence.

The Tokhokatak fault, which separates the two terranes, preserves evidence of early, ductile dip-slip movement (possibly east-side-up displacement) under amphibolite facies metamorphic conditions, and subsequent, brittle-ductile reactivation marked by dextral west-over-east movement. Although the magnitude of early displacement is unknown, the width of the shear zone and the juxtaposition of two terranes suggest that this could be a major tectonic boundary.

The shared portion of the geological histories of the two terranes appears to consist of late Archean (ca. 2.61 Ga) upright folding, and subsequent (Proterozoic) brittle-ductile faulting (Table 1), indicating that the terranes were amalgamated prior to 2.61 Ga. Earlier fabrics on either side of the Tokhokatak fault may represent two unrelated tectonic histories that predate juxtaposition of the terranes. Future mapping, geochronological studies, and geothermobarometry will provide quantitative constraints on the relationships between these two terranes.

## ACKNOWLEDGMENTS

Doug Axani and Kari Pollock provided very competent and enthusiastic field assistance. This paper benefitted from discussion and critical reviews by J. King (Geological Survey of Canada), and M. Stublely and V. Sterenburg (Canada-Northwest Territories Mineral Initiatives Office, Energy, Mines and Petroleum Resources, GNWT). M. Hutcheson and T. LaRiviere of Polar Continental Shelf Project are thanked for logistical support in the field.

## REFERENCES

- Abraham, A.P.G.**  
1987: Preliminary report on the geology of the Arcadia Bay property, Coronation Gulf, NWT: a granitoid-hosted gold deposit; Department of Indian Affairs and Northern Development, NWT Geology Division, EGS 1987-8.  
1989: Tonalite-hosted Au-quartz vein/shear zone mineralization in the Arcadia Bay area, Slave Province, NWT, parts of 76M/11; Department of Indian Affairs and Northern Development, NWT Geology Division, EGS 1989-6.
- Abraham, A.P.G., Kamo, S.L., Davis, D.W., and Spooner, E.T.C.**  
1991: Geochronological constraints on magmatic evolution and gold mineralization in the Anialik River area, Slave Province; Geological Association of Canada-Mineralogical Association of Canada Joint Annual Meeting; Program with Abstracts, p. A1.
- Barrie, C.T.**  
1993: Initial observations on Archean and early Proterozoic deformation in the granitoid-migmatite terrane of Hepburn Island map area, northwestern Slave Province, Northwest Territories; in *Current Research, Part C*; Geological Survey of Canada, Paper 93-1C, p. 115-124.
- Easton, R.M., Ellis, C.E., Dean, M., Bailey, G., Bruneau, H.C. and Walroth, J.**  
1982: Geology of the Typhoon Point area, High Lake Greenstone Belt, District of Mackenzie, NWT; Department of Indian Affairs and Northern Development, NWT Geology Division, EGS 1982-6.
- Easton, R.M.**  
1982: Preliminary geology compilation of the Hepburn island map area, NTS 76 M; Department of Indian Affairs and Northern Development, NWT Geology Division, EGS 1982-7.
- Fraser, J.A.**  
1964: Geological notes on northeastern District of Mackenzie; Geological Survey of Canada, Paper 63-40 (with map 45-1963).
- Hoffman, P.F.**  
1987: Continental transform tectonics: Great Slave Lake shear zone (ca. 1.9 Ga), northwest Canada; *Geology*, 15, p. 785-788.
- Hoffman, P.F., Tirrul, R., Grotzinger, J.P., Lucas, S.B., and Erikson, K.A.**  
1984: The externides of Wopmay orogen, Takijuk Lake and Kikerk Lake map areas, District of Mackenzie; in *Current Research, Part A*; Geological Survey of Canada, Paper 84-1A, p. 383-395.
- Hrabi, R.B., Helmstaedt, H., and King, J.E.**  
1993: Supracrustal rocks of the Winter Lake belt, central Slave Province: Implications for stratigraphic subdivision of Archean rocks in the Slave Province; in Geological Association of Canada-Mineralogical Association of Canada Joint Annual Meeting, Program with Abstracts, p. A45.
- Jackson, V.A.**  
1989: Preliminary geological compilation of Hepburn Island Map Area (76M) with marginal notes; Department of Indian Affairs and Northern Development, NWT Geology Division, EGS 1989-11.  
1991: Geology of part of the Napaktulik Lake area, NWT, parts of NTS areas 86 I/7,8,9 with marginal notes; Department of Indian Affairs and Northern Development, NWT Geology Division, EGS 1991-10.
- Jackson, V.A., Crux, J., Ellis, C.E., Howson, S., Padgham, W.P., and Relf, C.**  
1985: Geology of the Mistake Lake area, Anialik River Greenstone Belt, NWT, NTS 76M/11; Department of Indian Affairs and Northern Development, NWT Geology Division, EGS 1985-5.

**McEachern, S.J.**

1993: Structural reconnaissance of gneissic tectonites in the western Hepburn Island map area, northernmost Slave Province, Northwest Territories; in *Current Research, Part C*; Geological Survey of Canada, Paper 93-1C, p. 103-113.

**Padgham, W.A.**

1993: Repeated shallow-water sedimentation in the Slave Province; in Geological Association of Canada-Mineralogical Association of Canada Joint Annual Meeting, Program with Abstracts, p. A80.

**Parrish, R.R., Bellerive, D., and Sullivan, R.W.**

1992: U-Pb chemical procedures for titanite and allanite in the Geochronology Laboratory, Geological Survey of Canada; in *Radiogenic Age and Isotope Studies; Report 5*; Geological Survey of Canada, Paper 92-2, p. 187-190.

**Relf, C.**

1992: Two distinct shortening events during Archean orogeny in the west-central Slave Province, Northwest Territories, Canada; *Canadian Journal of Earth Sciences*, v. 29, p. 2104-2117.

**Relf, C., Jackson, V.A., Lambert, M.B., Stuble, M., Villeneuve, M., and King, J.E.**

1992: Reconnaissance studies in the Hepburn Island Map area, northern Slave Province, Northwest Territories; in *Current Research, Part C*; Geological Survey of Canada, Paper 92-1C, p. 201-208.

**Tirrul, R. and Bell, I.**

1980: Geology of the Anialik River Greenstone Belt, Hepburn Island Map Area, District of Mackenzie; in *Current Research, Part C*; Geological Survey of Canada, Paper 80-1A, p. 157-164.

**Villeneuve, M.E.**

1993: Preliminary geochronological results from the Winter Lake-Lac de Gras Slave province NATMAP project, NWT; in *Radiogenic Age and Isotope Studies; Report 7*; Geological Survey of Canada, Paper 93-2 p. 29-38

**Villeneuve, M.E., Jackson, V.A., and Thompson, P.H.**

1993: Geochronological evidence for the existence of pre-Yellowknife Supergroup supracrustal sequences in the Slave Province; in Geological Association of Canada-Mineralogical Association of Canada Joint Annual Meeting, Program with Abstracts, p. A107.

**Yeo, G.M., Bailey, G., Crux, J., Fisher, B., Jackson, V., Relf, C., and Walroth, J.**

1983: Preliminary geology of western Hepburn Island map area, NWT (NTS 76M/3, M/4, M/5, M/11, M/12, M/13, M/14); Department of Indian Affairs and Northern Development, NWT Geology Division, EGS 1983-8.

---

Geological Survey of Canada Project 820010



# The Shaler Supergroup and revision of Neoproterozoic stratigraphy in Amundsen Basin, Northwest Territories<sup>1</sup>

Robert H. Rainbird, Charles W. Jefferson<sup>2</sup>, Robert S. Hildebrand, and John K. Worth<sup>3</sup>

Continental Geoscience Division

*Rainbird, R.H., Jefferson, C.W., Hildebrand, R.S., and Worth, J.K., 1994: The Shaler Supergroup and revision of Neoproterozoic stratigraphy in Amundsen Basin, Northwest Territories; in Current Research 1994-C; Geological Survey of Canada, p. 61-70.*

---

**Abstract:** Elevation of the Shaler Group to supergroup status and the following internal revisions are proposed in order to more properly reflect rock units of the Amundsen Basin. The names Escape Rapids, Mikkelsen Islands, Nelson Head and Aok are proposed to replace the lower clastic, cherty carbonate, upper clastic, and orange-weathering stromatolite members of the Glenelg Formation in Minto and Cape Lambton inliers, informal map units 19 to 21, 22, 23, and 24 in the Coppermine area and informal map units P1, P2, P3, and P4a in Brock Inlier, respectively. Collectively these are to be known as the Rae Group; the name Glenelg Formation is abandoned. The former Reynolds Point Formation is raised to group status and comprises the Grassy Bay, Boot Inlet, Fort Collinson and Jago Bay formations, which replace the lower clastic, lower carbonate, upper clastic and upper carbonate members in Minto Inlier and informal map units P4b, P4c, lower P4d and upper P4d in Brock Inlier, respectively.

**Résumé :** On propose d'élever le Groupe de Shaler au rang de Supergroupe, et d'apporter les modifications internes suivantes pour offrir une meilleure image des unités lithologiques du bassin d'Amundsen. Les appellations de formations d'Escape Rapids, de Mikkelsen Islands, de Nelson Head et d'Aok sont proposées afin de remplacer : le membre clastique inférieur, le membre de carbonate chertueux, le membre clastique supérieur et le membre stromatolitique à altération orange, respectivement, de la Formation de Glenelg dans les boutonnières de Minto et de Cape Lambton; les unités cartographiques 19-21, 22, 23 et 24, respectivement, dans le secteur de Coppermine; et les unités cartographiques P1, P2, P3 et P4a, respectivement, dans la boutonnière de Brock. Ensemble, ces formations constituent le Groupe de Rae; l'appellation de Formation de Glenelg est abandonnée. L'ancienne Formation de Reynolds Point est élevée au rang de groupe et comprend les formations de Grassy Bay, de Boot Inlet, de Fort Collinson et de Jago Bay qui remplacent : le membre clastique inférieur, le membre carbonaté inférieur, le membre clastique supérieur et le membre carbonaté supérieur, respectivement, dans la boutonnière de Minto; et les unités cartographiques P4b, P4c, la partie inférieure de P4d et la partie supérieure de P4d, respectivement, dans la boutonnière de Brock.

---

<sup>1</sup> Contribution to Canada-Northwest Territories Mineral Initiatives (1991-1996), an initiative under the Canada-Northwest Territories Economic Development Cooperation Agreement.

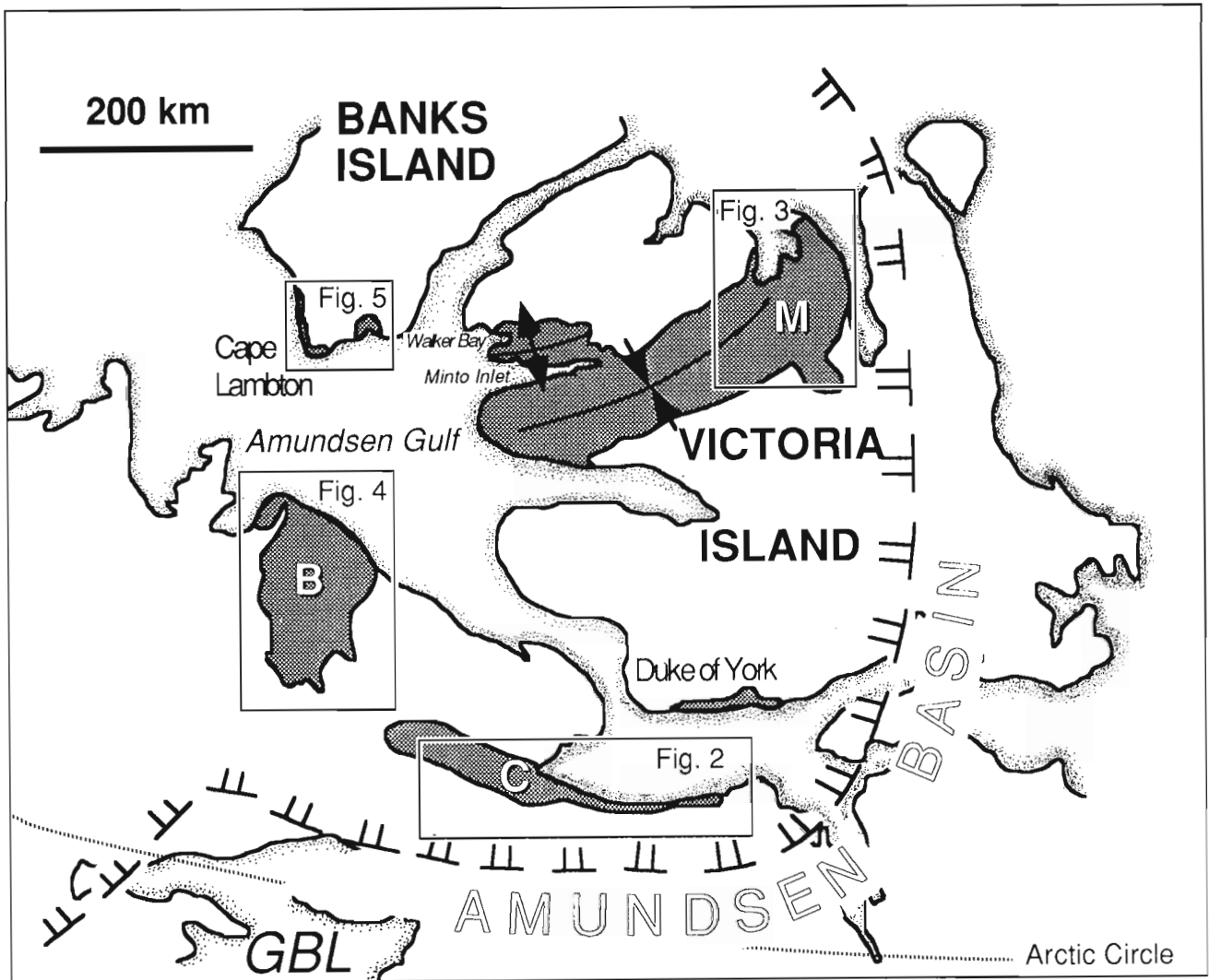
<sup>2</sup> Mineral Resources Division

<sup>3</sup> Department of Earth Sciences, Carleton University (deceased)

**INTRODUCTION**

The first complete geological reconnaissance of Victoria and Banks Islands was that of Washburn (1947), who recognized the similarity of Proterozoic strata of the Coppermine area and the Duke of York Inlier on the south shore of Victoria Island. Later, Thorsteinsson and Tozer (1962), proposed the name "Shaler Group" and its original formational subdivisions for the thick sequence of Proterozoic sedimentary strata that are exposed in Minto and Cape Lambton inliers (Fig. 1). Shaler Group strata were later recognized on the adjacent northern mainland coast in Brock Inlier (Cook and Aitken, 1969) and the Coppermine area where they are called Rae Group (Baragar and Donaldson, 1973). Stratigraphic correlation and sedimentological studies indicate that the inliers were part of the formerly contiguous intracratonic Amundsen Basin (Fig. 1).

Jefferson (1985) realized the need for further subdivision of the upper Shaler Group in southwest Minto Inlier and proposed the name Kuujjua Formation for a prominent quartzarenite unit, originally defined as an upper member of the Kilian Formation (Thorsteinsson and Tozer, 1962). Rainbird (1993) included the Natkusiak Formation, a basaltic succession which conformably overlies the Kuujjua Formation, with the Shaler Group. In this paper and henceforth we prefer to exclude the Natkusiak Formation from the proposed Shaler Supergroup, because of its contrasting lithological character and its partly unconformable relationship with underlying sedimentary strata (Table 1). Furthermore, the 723 Ma age of the Natkusiak Formation (Heaman et al., 1992) places it in Sequence C of Young et al. (1979), equivalent to the Windermere Supergroup in the Cordillera. It is generally accepted that sedimentary strata of the Shaler Supergroup, described herein, are equivalent to Sequence B of the Mackenzie Mountains Supergroup in the Cordillera (see Young et al., 1979).



*Figure 1. Location of Neoproterozoic inliers comprising Amundsen Basin of northwestern Canada. B=Brock Inlier, C=Coppermine area, M=Minto Inlier, GBL=Great Bear Lake.*



Numerous sills and dykes, equivalents of the Natkusiak Formation basalts, intrude the Shaler Supergroup throughout Amundsen Basin. These were dated by U-Pb method on baddeleyite providing a minimum age for the Shaler Supergroup of 723 Ma (Heaman et al., 1992). A maximum age of 1077 Ma was determined from U-Pb analysis of detrital zircon from the Nelson Head Formation in Minto Inlier (Rainbird and McNicoll, unpub. data, 1993).

Field studies by ourselves and other workers over the past 25 years have established that formations and members of the Shaler Group are similar throughout the Amundsen Gulf region. Presently, the nomenclature used to describe packages of rocks within the region does not properly reflect these similarities, largely because the original mapping was done by different geologists who concentrated their studies in single areas and therefore did not recognize the regional consistency of rock units. The intent of this paper is to revise stratigraphic nomenclature in Amundsen Basin.

## THE SHALER SUPERGROUP: PROPOSED GROUP AND FORMATIONAL SUBDIVISIONS

Formational status is proposed for informal members of the former Glenelg and Reynolds Point formations on the basis that they are mappable at 1:50 000 scale and was traced

throughout Amundsen Basin (Thorsteinsson and Tozer, 1962; Rainbird et al., 1992; Morin and Rainbird, 1993; see Table 1). Therefore, we propose elevating the Glenelg Formation and Reynolds Point Formation to group status and Shaler Group to supergroup status.

Field studies in 1993 confirmed that the Rae Group in the Coppermine area contains the same rock units as does the Glenelg Formation in Minto Inlier and map units P1, P2, P3, and P4a in Brock Inlier (Table 1). Therefore, we propose retention of the name Rae Group for these strata throughout Amundsen Basin and abandonment of the name Glenelg. Retention of more than one name for the same rocks would be confusing, particularly since we propose the same formation names in all areas. Although we acknowledge that use of the word Glenelg is well established in previous publications, so is the Rae Group, and rather than abandon Rae Group and raise the Glenelg to group status, we prefer to discard the term Glenelg.

### Rae Group

The Rae Group (Baragar and Donaldson, 1973) as herein defined, includes strata of Proterozoic age above rocks of the Coppermine River Group in the Coppermine area (Fig. 2) and rocks of Goulburn Supergroup in Minto Inlier (Fig. 3). Elsewhere the base is not exposed. The group is conformably

**Table 1.** Proposed revisions to stratigraphic nomenclature in Amundsen Basin. These revisions apply also to Cape Lambton and Duke of York inliers (Fig. 1).

Minto Inlier				Brock Inlier				Coppermine Area			
existing <sub>1</sub>		proposed		existing <sub>2</sub>		proposed		existing <sub>3</sub>		proposed	
Shaler Group	Natkusiak	Natkusiak	1100m								
	Kuujjua	Kuujjua	120m								
	Kilian	Kilian	550m								
	Wynniatt	Wynniatt	550m								
	Minto Inlet	Minto Inlet	260m	Unit P5	Minto Inlet	200m					
	Reynolds Point Fm. upper carbonate member	Jago Bay	65m	Unit P4d	Jago Bay	50m					
	Reynolds Point Fm. upper clastic member	Fort Collinson	170m	Unit P4c	Fort Collinson	50m					
	Reynolds Point Fm. lower carbonate member	Boot Inlet	500m	Unit P4b	Boot Inlet	500m					
	Reynolds Point Fm. lower clastic member	Grassy Bay	200m	Unit P4a	Grassy Bay	100m					
	Glenelg Fm. orange-weathering stromatolite mbr.	Aok	40m	Unit P3	Aok	50m					Aok
Glenelg Fm. upper clastic member	Nelson Head	>300m	Unit P2	Nelson Head	460m			Unit 23		Nelson Head	90m
Glenelg Fm. cherty carbonate member	Mikkelsen Islands	400m		Mikkelsen Islands	240m			Unit 22		Mikkelsen Islands	260m
Glenelg Fm. lower clastic member	Escape Rapids	>500m		Escape Rapids	910m			Unit 21		Bloody Fall Mbr.	635m
								Unit 20		Nipartoktuak Mbr.	150m
								Unit 19		Hihotok Mbr.	200m

1. Thorsteinsson and Tozer 1962, Young and Long 1977b, Rainbird et al. 1992
2. Cook and Aitken 1969, Jones et al. 1992
3. Baragar and Donaldson 1973

overlain by rocks of the Reynolds Point Group in Minto and Brock inliers (Fig. 4); unconformably overlain by rocks of Tertiary age in Cape Lambton Inlier (Fig. 5); and unconformably overlain by strata of Cambrian age in the Coppermine area. There has been some controversy as to the stratigraphic position of the basal Paleozoic unconformity within the Coppermine area (Baragar and Donaldson, 1973; Dixon, 1979; Campbell, 1983; 1985). However, fieldwork in 1991 and 1993 indicates that strata above a conspicuous brown-weathering stromatolitic unit within map unit 24 (Baragar and Donaldson, 1973) contain vermiform trace

fossils, arthropod tracks, and scratch marks: they are Cambrian rather than Proterozoic. The confusion arose because there are more than ten metres of paleotopography on the Proterozoic-Phanerozoic unconformity (Baragar and Donaldson, 1973; Dixon, 1979; Campbell, 1983; Jefferson and Young, 1989). As a result, it is easy to get the impression that Cambrian sedimentary rocks, deposited in paleovalleys, are stratigraphically below paleohills of the brown-weathering stromatolitic unit. Our 1993 field studies indicate that the same relationships exist in the western part of the Duke of York Inlier (Fig. 1), where paleohills of Proterozoic

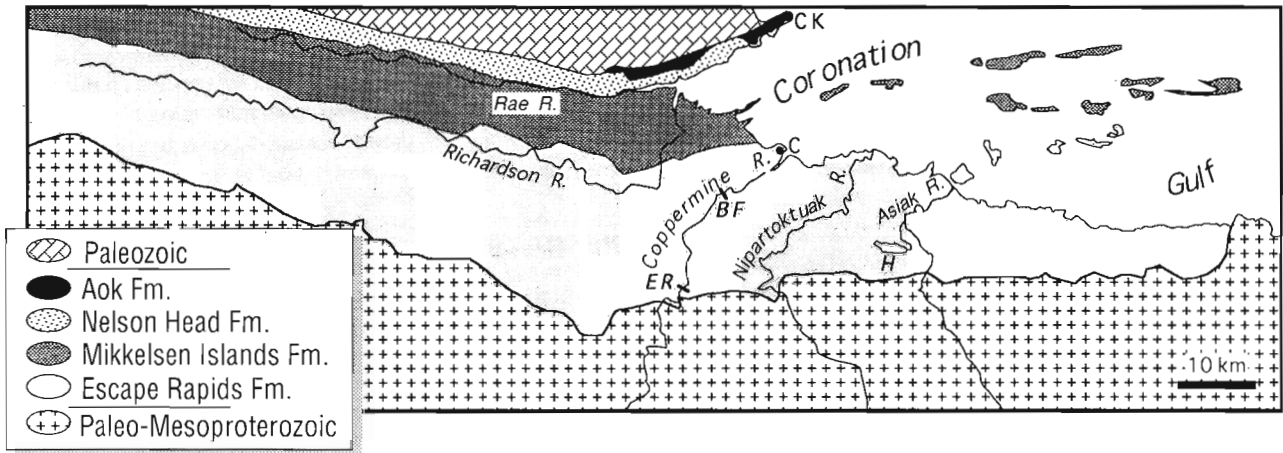


Figure 2. Generalized geology and geographic features in the Coppermine area (Fig. 1). C=Coppermine, BF=Bloody Fall, ER=Escape Rapids, H=Hihotok Lake, CK=Cape Kendall.

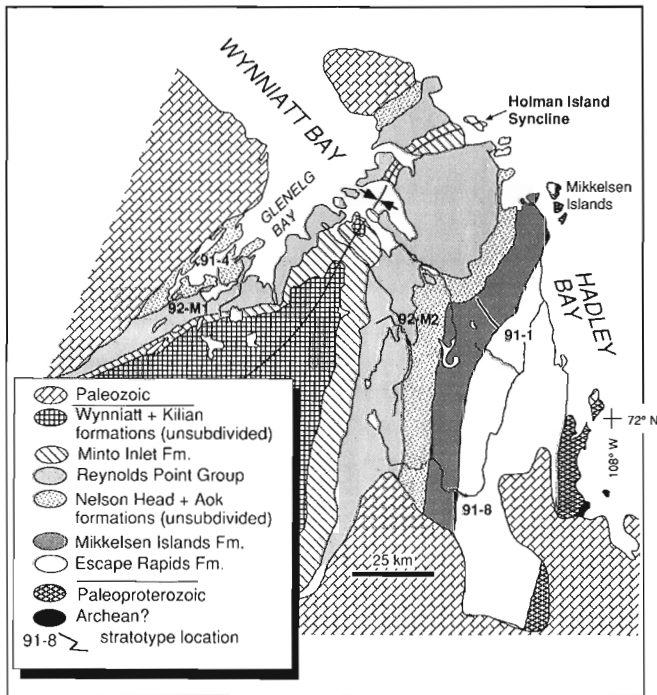


Figure 3. Geology, location of stratotypes and geographic features in northeast Minto Inlier, Victoria Island (Fig. 1).

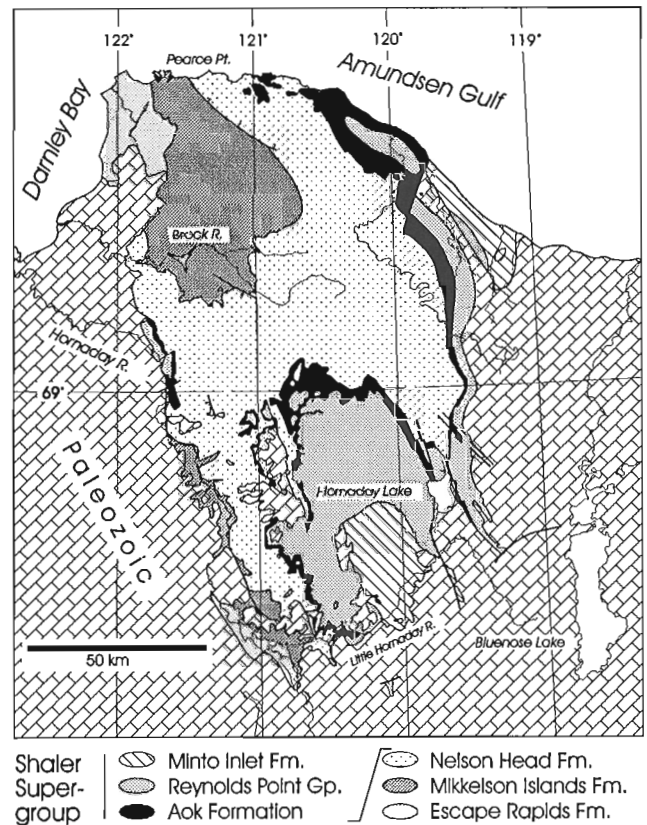
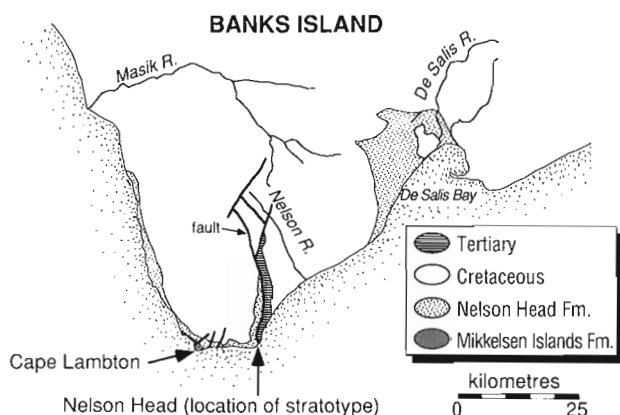


Figure 4. Geology and geographic features in Brock Inlier (Fig. 1).



**Figure 5.** *Geology and geographic features in Cape Lambton Inlier, southern Banks Island (after Miall 1976; Fig. 1).*

quartzarenite and one prominent paleohill of brown-weathering stromatolite protrude above recessive sandstones and carbonates of the Cambrian Old Fort Island Formation (Campbell, 1985). Identical stratigraphic problems were resolved by Jones et al. (1992) in Brock Inlier.

We propose to replace informal map units throughout Amundsen Basin with formations. The names Escape Rapids, Mikkelsen Islands, Nelson Head, and Aok are suggested for the lower clastic, cherty carbonate, upper clastic, and orange-weathering stromatolite members of the Glenelg Formation in Minto and Cape Lambton inliers (Rainbird et al., 1992), map units 19 to 21, 22, 23, and 24 in the Coppermine area (Baragar and Donaldson, 1973), and map units P1, P2, P3, P4a in Brock Inlier (Jones et al., 1992), respectively (Table 1). Wherever possible, names were chosen from geographic features in areas where rock units are well-exposed; however, due to lack of geographic names this could not always be adhered to.

### **Escape Rapids Formation**

The Escape Rapids Formation forms the base of the Rae Group and the Shaler Supergroup and is named for Escape Rapids in the Coppermine River (67°37'N, 115°44'W; Fig. 2). The lower boundary stratotype of the Escape Rapids Formation is about 3 km upstream from Escape Rapids, where drab-coloured sandstone and siltstone of the Hihotok Member overlies red sandstone and volcanoclastic conglomerate of the Husky Creek Formation (Coppermine River Group) with low angular erosional unconformity. The stratotype section was not measured in detail, but is exposed along the cutbank of the Coppermine River between Escape Rapids and Bloody Fall (Fig. 2).

As defined here, the Escape Rapids Formation includes map units 19, 20, and 21 of Baragar and Donaldson (1973) in the Coppermine area; these subdivisions were not recognized elsewhere in Amundsen Basin. Descriptions of the Rae Group in the Coppermine area (e.g., Baragar and Donaldson, 1973; Dixon, 1979; Campbell, 1983) and our field studies reveal

that units 19 and 21 are lithologically comparable and according to Campbell (1983), unit 20 pinches out east of the Coppermine River. For this reason we think a tripartite formational subdivision is unwarranted; however, member status for these rock units in the Coppermine area is suggested as in Table 1. The Hihotok Member is applied to map unit 19 and is named for a lake that drains into the Asiak River (67°40'N, 114°40'W; Fig. 2). It is exposed in a belt approximately 225 km long extending from about 50 km east of the Asiak River to the headwaters of the Richardson River (Baragar and Donaldson, 1973; Table 2 for description and interpretation).

The Nipartoktuak Member (map unit 20) conformably and gradationally overlies the Hihotok Member, and is named after outcrops along the Nipartoktuak River (67°42'N, 115°06'W; Fig. 2), southeast of Coppermine, and overlies the Hihotok Member along the Asiak River, along the Coppermine River immediately below Escape Rapids, and along the south branch of the Richardson River (Baragar and Donaldson, 1973; Table 2 for description and interpretation).

The Bloody Fall Member (map unit 21) sharply, but conformably, overlies the Nipartoktuak Member and is exposed from the mouth of the Asiak River (67°45'N, 114°25'W; Fig. 2) westward about 175 km to the headwaters of the Rae River. The name derives from Bloody Fall on the Coppermine River (67°44'N, 114°22'W; Fig. 2; lithological description in Table 2).

In Minto Inlier, the name Escape Rapids Formation is applied to the lower clastic member of the former Glenelg Formation (Dixon, 1979; Rainbird et al., 1992; Table 1). It outcrops only in northeast Minto Inlier, in isolated outcrops along the west coast of Hadley Bay and in creeks that drain into it from uplands to the east (Fig. 3).

In Brock Inlier, the name Escape Rapids Formation is applied to map unit P1 of Cook and Aitken (1969) (Table 1; description and interpretation in Table 2). It is exposed sporadically along the north shore of the Amundsen Gulf; thicker and more continuous sections occur in the upper reaches of the Brock River (Fig. 4). cursory descriptions are given by Cook and Aitken (1969), Balkwill and Yorath (1971), and Jones et al. (1992), but the formation is quite similar to other occurrences in Amundsen Basin.

### **Mikkelsen Islands Formation**

The Mikkelsen Islands Formation is named for a group of islands in Hadley Bay in northeast Minto Inlier (72°35'N, 108°25'W; Fig. 3). It is applied to the cherty carbonate member of the former Glenelg Formation in Minto and Cape Lambton inliers, map unit P2 in Brock Inlier and map unit 22 in the Coppermine area (Table 1). The composite stratotype proposed here comprises sections 91-8 and 91-1 of Rainbird et al. (1992), located on the east limb of the Holman Island Syncline (Fig. 3). The lower boundary stratotype is within section 91-8; the boundary is also exposed along the upper reaches of the Brock River (Fig. 4), and just west of the town of Coppermine (Fig. 2).

**Table 2. Lithological description and inferred depositional environments of new formations in the Rae and Reynolds Point groups, Shaler Supergroup, Amundsen Basin.**

Unit	Thicknesses (m)	Description	Interpretation
<b>Reynolds Point Group</b>			
Jago Bay Formation	<65 in NE Minto Inlier stratotype (text); >200 in SW Minto Inlier; ~100 undivided Jago Bay / Ft. Collinson in Brock Inlier (P44f <sup>2</sup> ).	Interbedded yellow-weathering, cross-bedded dolomitic quartzarenite, microbial laminate & dololunite. A distinctive, yellow-weathering stromatolite within 10 m of base <sup>1,3</sup> is columnar, laterally linked (cf. <i>Acaciaella</i> ) with abundant intercolumnar quartz. Upper part is recessive, yellow to pale grey parallel-laminated & mudcracked dolostolite & magnesiolite.	Marine intertidal to lagoonal, evolved upward into supratidal & restricted intertidal environment of the overlying Minto Inlet Formation
Fort Collinson Formation	65 at stratotype (see text); 170 at section near head of Gleneig Bay (92-M1 of <sup>4</sup> ; 50 in SW Minto Inlier (section 4 of <sup>1</sup> ); see above for Brock Inlier.	Lower part is quartzose sandstone rhythmic interbedded with medium bedded, fine-to-medium-grained dolomitic quartzarenite with ubiquitous herringbone cross-bedding & subordinate sub-horizontal planar stratification to low-angle cross-bedding. Upper part is medium bedded, medium-grained quartzarenite with abundant trough to planar, mainly tabular cross-beds. Paleocurrents from cross-bedding in lower part of formation are bimodal-bipolar; paleocurrents in upper part indicate unidirectional to polydirectional flow. <sup>1,4</sup>	Deposition by rivers in lower part & reworking by marine currents in upper part.
Boot Inlet Formation	350 to >500 in NE Minto Inlier <sup>4</sup> ; only upper 250 exposed in SW Minto Inlier <sup>4</sup> ; <500 in Brock Inlier <sup>2</sup> .	Cyclically alternating ooid graustone, stromatolite & dolostolite rhythmic magnafacies. Quartzarenite absent by definition from the gradational base of the formation (part of Grassy Bay Formation), quartzarenite gradually more abundant toward the top. <sup>1,3,4</sup> . Thickest & most prominent formation of Reynolds Point Group.	Prograding & shoaling, storm-dominated ramp (graustone = inner; stromatolite = mid; rhythmite = outer).
Grassy Bay Formation	60 at stratotype (see text); >200 in Gleneig Bay, NE Minto Inlier <sup>4</sup> ; 50-100 in Brock Inlier <sup>2</sup> . This & above removed by pre-Cambrian erosion in Coppermine area.	Basal 1/3 is mudstone (similar to basal Nelson Head Fm.); coarsens upward to quartzarenite with mainly unidirectional planar-tabular cross-bedding; intraformational erosional unconformity; fining-upward succession of HCS-bedded quartzarenite & planar bedded dolostolite/dololunite <sup>3,4</sup> . Exposed only in ravines; forms low talus-covered bench above the Aok Formation; in Brock Inlier forms recessive marker between two orange-weathering stromatolitic dolostones (Aok & Boot Inlet formations) <sup>2</sup> .	Marine-deltaic at base; fluvial in middle; marine transgression (erosion) & storm reworking of top; gradual basin deepening; clastic starvation; carbonate development.
Aok Formation	30 at type locality (see text); 20-30 in NE Minto Inlier; 0 at Cape Lambert; <20 in Coppermine area; 3-50 in Brock Inlier. Thicknesses from <sup>1r</sup> & <sup>2</sup> .	Cream-coloured & orange-brown weathering, sideritic to ankeritic dolostone hosting stromatolite biostrome composed of juxtaposed bioherms of fanning digitate columnar (elongate in plan) stromatolites. Generally two biostromes separated by maroon & green shale. Magnetite or siderite iron formation is associated in Duke of York Inlier & Brock Inlier. Basal unit is intraformational dolostolite-clast conglomerate in a matrix of medium grained glauconitic quartzarenite.	A remarkably extensive carbonate shelf deposit extending to Mackenzie Mountains <sup>2</sup> ; suggestion of shaling out to north of Brock Inlier.
Nelson Head Formation	25 basal shale + >275 quartzarenite in NE Minto Inlier <sup>4</sup> ; 110 shale + 530 quartzarenite at Nelson Head <sup>1</sup> ; see also <sup>6</sup> ; 90 in Coppermine Area <sup>2</sup> ; 460 in Brock Inlier <sup>2</sup> .	Basal: laminated black carbonaceous pyritic mudstone has sharp lower contact; laterally equivalent in NE Minto Inlier & Coppermine area to thin chert breccia & carbonaceous quartzarenite with unimodal trough crossbeds over paleokarst highs <sup>5</sup> . Basal members grade upward through laminated red siltstone & ripple-cross-laminated quartzarenite, to fine-to-medium-grained, white-to-light-pink quartzarenite with thin-intercalations of red ripple-cross-laminated to parallel-bedded siltstone & very fine quartzarenite. Top is planar parallel hummocky cross-bedded glauconitic quartzarenite with wavy-lenticular interbeds of very fine sandstone, parallel-laminated green siltstone, & <50% carbonaceous mudstone <sup>6,8,9</sup>	Mudstone-grading to quartzarenite; regionally prograding marine delta. Thin quartzarenites on paleokarst breccia; varied local fluvial systems; Upper thick arenites: NNW fluvial transport from distal to prox. craton.
Mikkelson Islands Formation	400-450 in NE Minto Inlier <sup>2</sup> ; 260 <sup>7</sup> or 460 <sup>10</sup> in Coppermine Area; 240 in Brock Inlier <sup>2</sup> ; >200 in Cape Lambert Inlier <sup>1</sup> .	Typically laminated reddish to cream-coloured pale grey cherty aphanitic dolostone with stromatolites, intraformational flar-chip conglomerate, local dolarenite. Cherts are white to frothy black preserving abundant microfossils. Basal member is 3- to 4-m-thick pink & green stromatolitic dolostolite & intraformational conglomerate interbedded with dark green-grey siltstone & mudstone. Basal contact is gradational in Coppermine area & locally unconformable elsewhere <sup>2,12</sup> .	Breccia & columnar stromatolites; sub-intertidal; cherts, tepee structures, beachrock & laminated stromatolites; upper intertidal to supratidal.
Escape Rapids Formation	200 + 150 + 635 <sup>7</sup> in Coppermine area; 550 in NE Minto Inlier <sup>1</sup> ; >900 in Brock Inlier <sup>2</sup> .	Three distinct members in Coppermine River area <sup>7</sup> . <b>Hihotok (lower)</b> Member: fine-to-medium-grained, cross-bedded to ripple cross-laminated quartzarenite & litharenite interbedded with ripple cross-laminated to plane-laminated siltstone. <b>Nipartoktuak (middle)</b> Member: maroon to red & grey-green variegated plane-laminated mudstone & siltstone with less common interbeds of dark grey-brown ripple cross-laminated to small-scale-cross-bedded sandstone. <b>Bloody Fall (upper)</b> Member: sharply conformable base, lithology similar to Hihotok except that up to 20 cm interbeds of argillaceous, concretionary limestone & stromatolitic dolostone are common near the top. This member is most representative of Escape Rapids Formation in Brock Inlier & NE Minto Inlier <sup>1,2,12</sup> .	Hihotok: scours & HCS suggest storm activity in marine environment. Nipartoktuak: deeper marine (below wave base to shallow subtidal). Bloody Fall: subtidal to intertidal, shoaling upward.

1. Young & Jefferson, 1975; 2. Jones et al., 1992; 3. Young & Long, 1977b; 4. Morin & Raubird, 1993; 5. Jefferson & Young, 1989; 6. Miall, 1976; 7. Worth, unpublished manuscript, 1973; 8. Conly, 1993; 9. Raubird et al., 1992; 10. Baragar & Donaldson, 1973; 11. Dixon, 1979; 12. 1993 fieldwork.

In Minto Inlier, the Mikkelsen Islands Formation is exposed along a 15-20 km wide belt extending southward from Mikkelsen Islands approximately 100 km (Fig. 3). In Brock Inlier it is well exposed along the northern coastal mainland at Pearce Point, in the Brock River Canyon and near the junction of the Hornaday and Little Hornaday rivers (Cook and Aitken, 1969; Balkwill and Yorath, 1971; Jones et al., 1992; Fig. 4). In the Coppermine area it is exposed in an outcrop belt extending from the eastern part of the Duke of York Inlier (Fig. 1), across islands in the Coronation Gulf southwestward through uplands between the Richardson and Rae rivers for about 300 km (Fig. 2). The Mikkelsen Islands Formation has been correlated with map unit H1 of the Mackenzie Mountains Supergroup in the Mackenzie Mountains (Young et al., 1979).

### Nelson Head Formation

The Nelson Head Formation derives its name from an impressive promontory in Cape Lambton Inlier on the southern tip of Banks Island (Fig. 5). It is applied to the upper clastic member of the former Glenelg Formation in Cape Lambton and Minto inliers (Thorsteinsson and Tozer, 1962; Young and Long, 1977b), map unit P3 in Brock Inlier (Cook and Aitken, 1969) and map unit 23 in the Coppermine area (Baragar and Donaldson, 1973). We propose that the unit stratotype be located at Nelson Head, where the thickest known continuous exposure is preserved. This corresponds to section 74-MLA-36 of Miall (1976), located at 71°05'N, 122°53'W (Fig. 5). The lower boundary is not exposed at Nelson Head so the lower boundary stratotype is placed in the Brock River Canyon of Brock Inlier (69°19'N, 122°52'W; Fig. 4) where it is well exposed. The Mikkelsen Islands Formation is abruptly and conformably overlain by interbedded red siltstone and fine grained quartzarenite. In Minto Inlier and the Coppermine area, a paleokarst unconformity separates the Mikkelsen Islands Formation from shales and quartzarenite of the Nelson Head Formation (Rainbird et al., 1992).

The Nelson Head Formation is exposed on both limbs of the Holman Island Syncline in northeast Minto Inlier; the thickest and best exposures are in the Glenelg Bay area (Fig. 3). In the Coppermine area it occurs to the west and northeast of Johansen Bay on southern Victoria Island (Duke of York Inlier; Fig. 1) and along a several kilometre-wide belt on the north side of the Rae River that stretches from Cape Kendall approximately 80 km westward (Fig. 2). It outcrops extensively in central Brock Inlier and throughout Cape Lambton Inlier. The Nelson Head Formation has been described in detail by Young and Jefferson (1975), Miall (1976), Rainbird et al. (1992), and Conly (1993) (summary in Table 2). Correlative strata to the Nelson Head Formation are the Tzesotene Formation and Katherine Group (units K1-K5) from the Mackenzie Mountains Supergroup (Young et al., 1979).

### Aok Formation

The Aok Formation is a new name proposed for an informal unit referred to throughout Amundsen Basin as the orange weathering stromatolite biostrome (Jefferson and Young, 1989). The name was chosen from the Inuit word for the colour red

or blood, as there are no geographic names in the type area and because an Inuit word for the colour orange does not exist. The Aok Formation is applied to the uppermost member of the former Glenelg Formation in Minto Inlier (Rainbird et al., 1992), map unit P4a in Brock Inlier (Jones et al., 1992) and the lower part of map unit 24 in the Coppermine area (Baragar and Donaldson, 1973; Table 1). The Aok Formation and succeeding strata of the Shaler Supergroup are not preserved in Cape Lambton Inlier.

The proposed unit stratotype is on a butte; the highest point on a large peninsula in the centre of Glenelg Bay, in northeast Minto Inlier (72°23'N, 111°24'W; Fig. 3 and 6). The lower boundary stratotype is in the same location (see Table 2 for description and interpretation). The Aok Formation is exposed on both limbs of the Holman Island Syncline in northeast Minto Inlier (Fig. 3), where it typically forms broad bench-like outcrops that can be traced for up to 100 km. In the Coppermine area, it occurs in one small outcrop at the west end of Johansen Bay on southern Victoria Island (Duke of York Inlier; Fig. 1) and along several isolated benches about 1 km north of the Rae River, near its mouth (Fig. 2). It occurs throughout Brock Inlier. According to Jefferson and Young (1989) the Aok Formation covers a depositional area of greater than 90,000 km<sup>2</sup> in Amundsen Basin.

The Aok Formation biostrome has been used as a marker for stratigraphic studies and regional mapping throughout Amundsen Basin and also in the Mackenzie Mountains area where it has been correlated to unit K-6 of the Katherine Group (Jefferson and Young, 1989). The biostrome may have

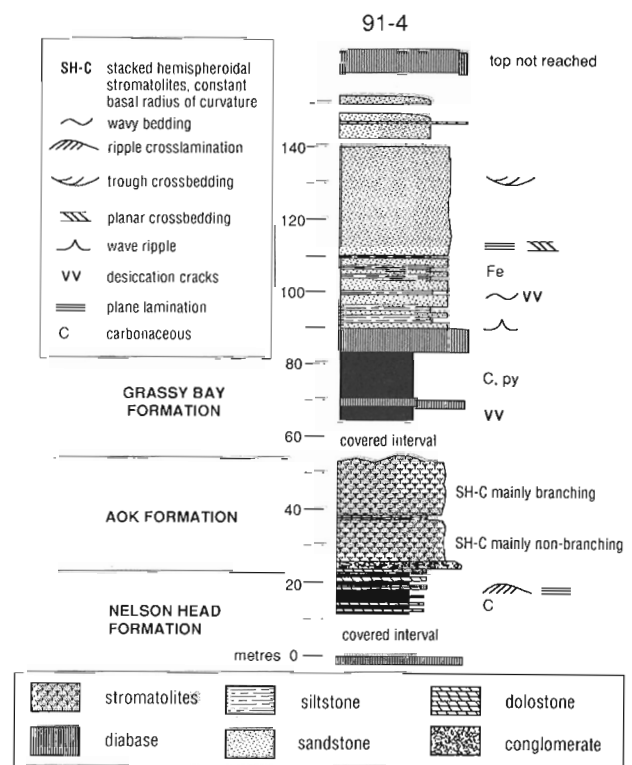


Figure 6. Stratotype for the Aok Formation, northeast Minto Inlier (see Fig. 3 for location).



been continuous between the two regions, and if so, would have been one of the most extensive stromatolitic buildups known.

### ***Reynolds Point Group***

The former Reynolds Point Formation of Thorsteinsson and Tozer (1962) is herein elevated to group (see Table 1). We propose the names Grassy Bay, Boot Inlet, Fort Collinson, and Jago Bay to replace the lower clastic, lower carbonate, upper clastic, and upper carbonate members of the former Reynolds Point Formation, as originally described by Young and Long (1977a, b) in Minto Inlier, and informal map units P4b, P4c, and P4d in Brock Inlier (Jones et al., 1992; Table 1). The Reynolds Point Group is not known to be exposed elsewhere within Amundsen Basin, but does appear to correlate with the Little Dal Group of the Mackenzie Mountains Supergroup (cf. Aitken, 1981). All geographic features for which these formations are named are located at the western end of Minto Inlier between Minto Inlet and Walker Bay (1:250 000 NTS 87G/7; Fig. 1).

### ***Grassy Bay Formation***

The Grassy Bay Formation is applied to the lower clastic member of the Reynolds Point Formation in Minto Inlier and map unit P4b in Brock Inlier (Table 1), and is named after an inlet of Fish Bay on the northwest side of Minto Inlet, in southwest Minto Inlier (71°19'N, 117°42'W).

The proposed composite stratotype is in a narrow canyon at the head of one of the main tributaries draining into Wynniatt Bay, in northeast Minto Inlier (72°13'N, 109°50'W; Fig. 3). The lower half of the section is at the south end of the canyon and the upper half is near the north end. The section has been described and illustrated by Morin and Rainbird (1993, section 92-M2) and is chosen as the stratotype because it is probably the only locality where the basal contact is exposed and thus it also represents the lower boundary stratotype. The contact is characterized by stromatolitic dolostone overlain by thin parallel-laminated red mudstone, separated by 30 cm of interbedded wavy dolosiltite and red mudstone. A reference stratotype is located in the same section as the Aok Formation stratotype (Fig. 6), although the upper contact with the overlying Boot Inlet Formation is not exposed there (see Table 2 for description and interpretation). The Grassy Bay Formation appears to correlate with unit K-7 of the Katherine Group and the Mudcracked formation of the overlying Little Dal Group in the Mackenzie Mountains (cf. Aitken, 1981).

### ***Boot Inlet Formation***

The Boot Inlet Formation is applied to the lower carbonate member of the Reynolds Point Formation in Minto Inlier (Young and Long, 1977b) and map unit P4c in Brock Inlier (Jones et al., 1992; Table 1), and is named after a large inlet on the north side of Minto Inlet, in southwest Minto Inlier (71°25'N, 117°25'W).

The proposed stratotype is a continuation of the Grassy Bay Formation composite stratotype (Morin and Rainbird, 1993; section 92-M2). It begins at the junction of two main branches of the unnamed tributary, described above, that drains into Wynniatt Bay, in northeast Minto Inlier (72°16'N, 108°55'W; Fig. 3), and continues through a deep dry gorge that is about 1.5 km to the northwest. The lower boundary stratotype is located at the top of the Grassy Bay Formation stratotype and is a gradational contact between a ~2 m thick unit of parallel laminated carbonaceous mudstone and siltstone and an overlying coarsening upward succession of parallel laminated dolosiltite and wavy bedded dolarenite. A reference lower boundary stratotype is located in the canyon of the Hornaday River in Brock Inlier (69°00'N, 122°39'W), where the contact is much more gradational and the mudstone and siltstone unit at the top of the Grassy Bay Formation is more than 10 m thick (Table 2 for description and interpretation).

The Boot Inlet Formation correlates with the Platform /Basinal assemblage and overlying Grainstone formation of the Little Dal Group in the Mackenzie Mountains (Aitken, 1981), although the rhythmite magnafacies generally is thinner and less well developed than it is in the Basinal assemblage.

### ***Fort Collinson Formation***

The Fort Collinson Formation derives its name from an abandoned Hudson's Bay Company trading post in Walker Bay (71°37'N, 117°50'W; Fig. 1), and is applied to the upper clastic member of the Reynolds Point Formation (Young and Long, 1977b) and the lower quartzose part of map unit P4d in Brock Inlier (Jones et al., 1992; Table 1).

The proposed stratotype is a continuation of the Boot Inlet Formation stratotype (Morin and Rainbird 1993, section M2). It begins near the bottom of a valley above a deep dry gorge (72°16'N, 110°00'W, Fig. 3). The lower boundary stratotype is at the same location and is at the top of the uppermost ooid grainstone bed, where there is a gradational change over ~50 m between sandy ooid grainstone of the Boot Inlet Formation upward into medium grained quartzarenite and sandstone rhythmite of the Fort Collinson Formation (Morin and Rainbird, 1993; Table 2 for description and interpretation). The Fort Collinson Formation may correlate with the upper part of the Grainstone formation of the Little Dal Group in the Mackenzie Mountains (cf. Aitken, 1981).

### ***Jago Bay Formation***

The Jago Bay Formation is applied to the upper carbonate member of the former Reynolds Point Formation (Young and Long, 1977b) and the upper carbonate-rich part of map unit P4d in the Brock Inlier (Jones et al., 1992; Table 1). It is named after an inlet on the north side of Walker Bay, in southwest Minto Inlier (Fig. 1).

The stratotype of the Jago Bay Formation is near the south end of Glenelg Bay in northeast Minto Inlier (section 92-M1 of Morin and Rainbird, 1993; 72°17'N, 111°25'W; Fig. 3). The lower boundary stratotype occurs at the same location and is gradational over about 10 m between parallel-laminated



to thinly bedded, fine- to medium-grained, dolomitic quartzarenite of the Fort Collinson Formation and interbedded yellow-weathering, crossbedded dolomitic quartzarenite, microbial laminite and dololite of the Jago Bay Formation. The Jago Bay Formation may correlate with the uppermost Grainstone formation of the Little Dal Group in the Mackenzie Mountains, although it has no lithological counterpart there.

### *Ungrouped formations*

Formations above the Jago Bay Formation remain ungrouped and unrevised, except that the Minto Inlet Formation from Minto Inlier (Thorsteinsson and Tozer, 1962; Young, 1981; Phaneuf, 1993) is applied to map unit P5 of Brock Inlier (cf. Cook and Aitken, 1969; Jones et al., 1992; Table 1). Within Amundsen Basin, the overlying Wynniatt, Kilian, and Kuujjua formations have no counterparts beyond Minto Inlier (Table 1).

### SUMMARY

Because we recognize that Neoproterozoic rock units are the same throughout Amundsen Basin, we propose the formation names Escape Rapids, Mikkelsen Islands, Nelson Head, and Aok to replace the lower clastic, cherty carbonate, upper clastic, and orange-weathering stromatolite members of the Glenelg Formation in Minto and Cape Lambert inliers, informal map units 19 to 21, 22, 23, and 24 in the Coppermine area and informal map units P1, P2, P3, and P4a in Brock Inlier. Collectively these are to be known as the Rae Group; the name Glenelg Formation is abandoned. The former Reynolds Point Formation is raised to group status and comprises the Grassy Bay, Boot Inlet, Fort Collinson, and Jago Bay formations, which replace the lower clastic, lower carbonate, upper clastic, and upper carbonate members in Minto Inlier and informal map units P4b, P4c, lower P4d, and upper P4d in Brock Inlier. These revisions require elevation of the Shaler Group to Shaler Supergroup.

### ACKNOWLEDGMENTS

Thanks are due to the Polar Continental Shelf Project for logistical support, to Unocal Canada Exploration Ltd. and Noranda Exploration Co. Ltd. for sharing ideas and logistics, and to Midwest Drilling and Mr. Adam Ruben for accommodation. We are grateful to J.B. Henderson and D.G. Cook for critically reviewing the manuscript. Studies in Brock Inlier were funded by the MERA process, cost shared among Canadian Parks Service, DIAND, and NRCan.

### REFERENCES

- Aitken, J.D.**  
1981: Stratigraphy and sedimentology of the upper Proterozoic Little Dal Group, Mackenzie Mountains, Northwest Territories, in *Proterozoic Basins of Canada*, (ed.) F.H.A. Campbell; Geological Survey of Canada, Paper 81-10, p. 47-71.
- Balkwill, H.R. and Yorath, C.J.**  
1971: Brock River map area, District of Mackenzie; Geological Survey of Canada, Paper 70-32, 25 p.
- Baragar, W.R.A. and Donaldson, J.A.**  
1973: Coppermine and Dismal Lakes map areas; Geological Survey of Canada, Paper 71-39, 20 p.
- Campbell, F.H.A.**  
1983: Stratigraphy of the Rae Group, Coronation Gulf area, District of Mackenzie; in *Current Research, Part A*; Geological Survey of Canada, Paper 83-1A, p. 43-52.  
1985: Stratigraphy of the upper part of the Rae Group, Johansen Bay area, northern Coronation Gulf, District of Franklin; in *Current Research, Part A*; Geological Survey of Canada, Paper 85-1A, p. 693-696.
- Conly, A.G.**  
1993: Sedimentology and stratigraphy of the upper clastic member, Glenelg Formation: Victoria Island, N.W.T.; B.Sc. thesis, Carleton University, Ottawa, Ontario, 59 p.
- Cook, D.G. and Aitken, J.D.**  
1969: Erly Lake (97A), District of Mackenzie; Geological Survey of Canada, Map 5-1969, scale 1:250 000.
- Dixon, J.**  
1979: Comments on the Proterozoic stratigraphy of Victoria Island and the Coppermine area, Northwest Territories; in *Current Research, Part B*; Geological Survey of Canada, Paper 79-1B, p. 263-267.
- Heaman, L.M., LeCheminant, A.N., and Rainbird, R.H.**  
1992: Nature and timing of Franklin igneous events, Canada: implications for a late Proterozoic mantle plume and the break-up of Laurentia; *Earth and Planetary Science Letters*, v. 109, p. 117-131.
- Jefferson, C.W.**  
1985: Uppermost Shaler Group and its contact with the Natkusiak Basalts, Victoria Island, District of Franklin; in *Current Research, Part A*; Geological Survey of Canada, Paper 85-1A, p. 103-110.
- Jefferson, C.W. and Young, G.M.**  
1989: Late Proterozoic orange-weathering stromatolite biostrome, Mackenzie Mountains and western Arctic Canada; in *Reefs, Canada and adjacent areas*, (ed.) H.H.J. Geldsetzer, N.P. James, and G.E. Tebbutt; Canadian Society of Petroleum Geologists, Memoir 13, p. 72-80.
- Jones, T.A., Jefferson, C.W., and Morrell, G.R.**  
1992: Assessment of the mineral and energy resource potential in the Brock Inlier-Bluenose Lake Area, N.W.T.; Geological Survey of Canada, Open File 2434, 95 p.
- Miall, A.D.**  
1976: Proterozoic and Paleozoic geology of Banks Island; Geological Survey of Canada, Bulletin 258, 77 p.
- Morin, J. and Rainbird, R.H.**  
1993: Sedimentology and sequence stratigraphy of the Neoproterozoic Reynolds Point Formation, Minto Inlier, Victoria Island, N.W.T.; in *Current Research, Part C*; Geological Survey of Canada, Paper 93-1C, p. 7-18.
- Phaneuf, S.M.**  
1993: Stratigraphy and sedimentology of the Neoproterozoic Minto Inlet Formation, Minto Inlier, Victoria Island, N.W.T.; B.Sc. thesis, Ottawa University, Ottawa, Ontario, 39 p.
- Rainbird, R.H.**  
1993: The sedimentary record of mantle plume uplift preceding eruption of the Neoproterozoic Natkusiak Flood Basalt; *Journal of Geology*, v. 101, p. 305-318.
- Rainbird, R.H., Darch, W., Jefferson, C.W., Lustwerk, R., Rees, M., Telmer, K., and Jones, T.**  
1992: Preliminary stratigraphy and sedimentology of the Glenelg Formation, lower Shaler Group and correlatives in the Amundsen Basin, Northwest Territories: relevance to sediment-hosted copper; in *Current Research, Part C*; Geological Survey of Canada, Paper 92-1C, p. 111-119.
- Thorsteinsson, R. and Tozer, E.T.**  
1962: Banks, Victoria and Stefansson Islands, Arctic Archipelago; Geological Survey of Canada, Memoir 330, 85 p.
- Washburn, A.L.**  
1947: Reconnaissance geology of portions of Victoria Island and adjacent regions, Arctic Canada; Geological Society of America, Memoir 22, 142 p.
- Young, G.M.**  
1981: The Amundsen Embayment, Northwest Territories; relevance to the upper Proterozoic evolution of North America; in *Proterozoic Basins of Canada*, (ed.) F.H.A. Campbell; Geological Survey of Canada, Paper 81-10, p. 203-211.

**Young, G.M. and Jefferson, C.W.**

1975: Late Precambrian shallow water deposits, Banks and Victoria Islands, Arctic Archipelago; Canadian Journal of Earth Sciences, v. 12, p. 1734-1748.

**Young, G.M. and Long, D.G.F.**

1977a: A tide-influenced delta complex in the upper Proterozoic Shaler Group, Victoria Island, Canada; Canadian Journal of Earth Sciences, v. 14, p. 2246-2261.

**Young, G.M. and Long, D.G.F. (cont.)**

1977b: Carbonate sedimentation in a late Precambrian shelf sea, Victoria Island, Canadian Arctic Archipelago; Journal of Sedimentary Petrology, v. 47, p. 943-955.

**Young, G.M., Jefferson, C.W., Delaney, G.D., and Yeo, G.M.**

1979: Middle and late Proterozoic evolution of the northern Canadian Cordillera and Shield; Geology, v. 7, p. 125-128.

---

Geological Survey of Canada Project 890011

# Geology of the Wijinnedi Lake area – a Paleoproterozoic(?) asymmetric uplift of Archean rocks in the southwestern Slave Province, District of Mackenzie, Northwest Territories

John B. Henderson  
Continental Geoscience Division

*Henderson, J.B., 1994: Geology of the Wijinnedi Lake area – a Paleoproterozoic(?) asymmetric uplift of Archean rocks in the southwestern Slave Province, District of Mackenzie, Northwest Territories; in Current Research 1994-C; Geological Survey of Canada, p. 71-79.*

---

**Abstract:** The area occurs at the north end of an 80 km long uplift bounded by a north-trending low-grade cataclastic shear zone exposing Archean low, high grade and ultimately granulite grade rocks in a series of mylonite separated domains. A large, deformed, dacitic volcanic breccia dome mantled by a relatively minor unit of mafic volcanic rocks occurs in the lowest grade Wijinnedi domain. It is intruded by a gabbro to anorthositic gabbro intrusion of a type known elsewhere in the Slave Province to be synvolcanic, and at one locality by a greenschist-grade, deformed diatreme containing abundant, very coarse garnet pseudomorphs. The rocks of the highest grade Ghost domain occur in an asymmetric antiform in which the rocks of the lower grade limb are more deformed than those of the higher grade limb where some granulite grade granitoid plutons are unfoliated. The antiformal axis is cored by large, coarsely megacrystic, granite plutons.

**Résumé :** Le secteur se trouve à l'extrémité nord d'un soulèvement de 80 km de longueur, limité par une zone de cisaillement cataclastique faiblement métamorphisée, où affleurent des roches archéennes montrant un métamorphisme faible, un métamorphisme élevé et un métamorphisme du faciès des granulites, dans une série de domaines séparés par des mylonites. Un grand dôme déformé de brèches volcaniques dacitiques enveloppé par une unité relativement mineure de roches volcaniques mafiques apparaît dans le domaine de Wijinnedi, qui a subi le métamorphisme le moins intense. Il est traversé par une intrusion de composition variant du gabbro au gabbro anorthositique, d'un type reconnu ailleurs dans la Province des Esclaves comme synvolcanique, et dont un représentant en un endroit est traversé par un diatème déformé, métamorphisé au faciès des schistes verts, renfermant en abondance des pseudomorphes de grenats très grossiers. Les roches du domaine de Ghost, le plus fortement métamorphisé, se trouvent dans un antiforme asymétrique où les roches du flanc présentant le degré de métamorphisme le plus faible ont subi une déformation plus intense que celles du flanc plus métamorphisé, dans lequel certains plutons de granitoïde du faciès des granulites ne sont pas foliés. La zone axiale de l'antiforme est constituée de grands plutons granitiques à très gros cristaux.

## INTRODUCTION

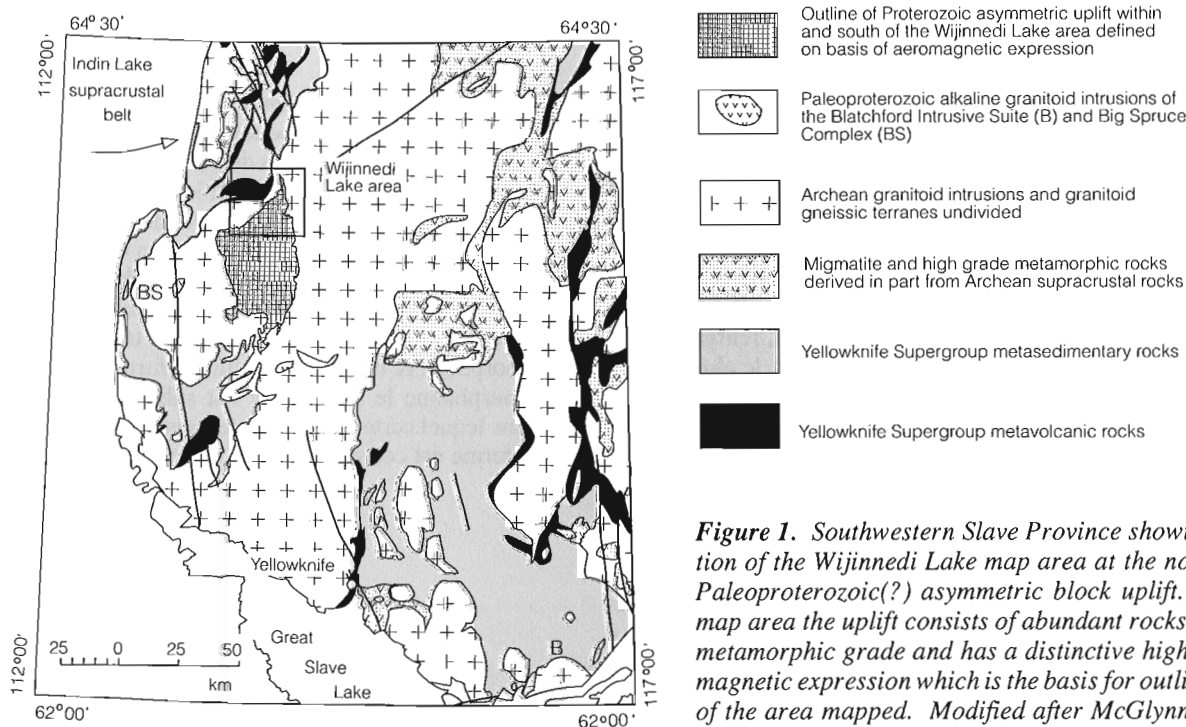
The Wijinnedi Lake area is situated near the southwestern margin of the Slave Province at the southern end of the Indin Lake supracrustal terrane (Frith, 1993) and at the northern end of an asymmetric block uplift (Fig. 1). Geological mapping of the area, for eventual publication at 1:50 000 scale, was started in 1992 (Henderson and Schaan, 1993) and completed during the 1993 field season. Parts of the area and surrounding region were previously mapped by Lord (1942) and Wright (1954) at 1" = 4 mi. and 1" = 1 mi. scale respectively. The rationale for the remapping of the area is discussed in Henderson and Schaan (1993).

The uplift has brought an extensive area of Archean granulite grade mid-crustal rocks to the present erosion level along a sharply defined cataclastic fault zone at its east side. As most of the uplift remains unmapped, its extent south of the map area and its asymmetric character is based largely on its aeromagnetic expression. The cataclastic shear zone that defines its eastern margin and along which most of the uplift took place, coincides with a pronounced aeromagnetic low that separates the higher magnetic relief terrane of the uplift from the magnetically more flat terrane to the east. The high magnetic relief of the eastern part of the uplift gradually grades into the typical flat aeromagnetic topography of the surrounding southwesternmost Slave Province (Geological Survey of Canada, 1969) suggesting that no sharp break defines the western side of the uplift.

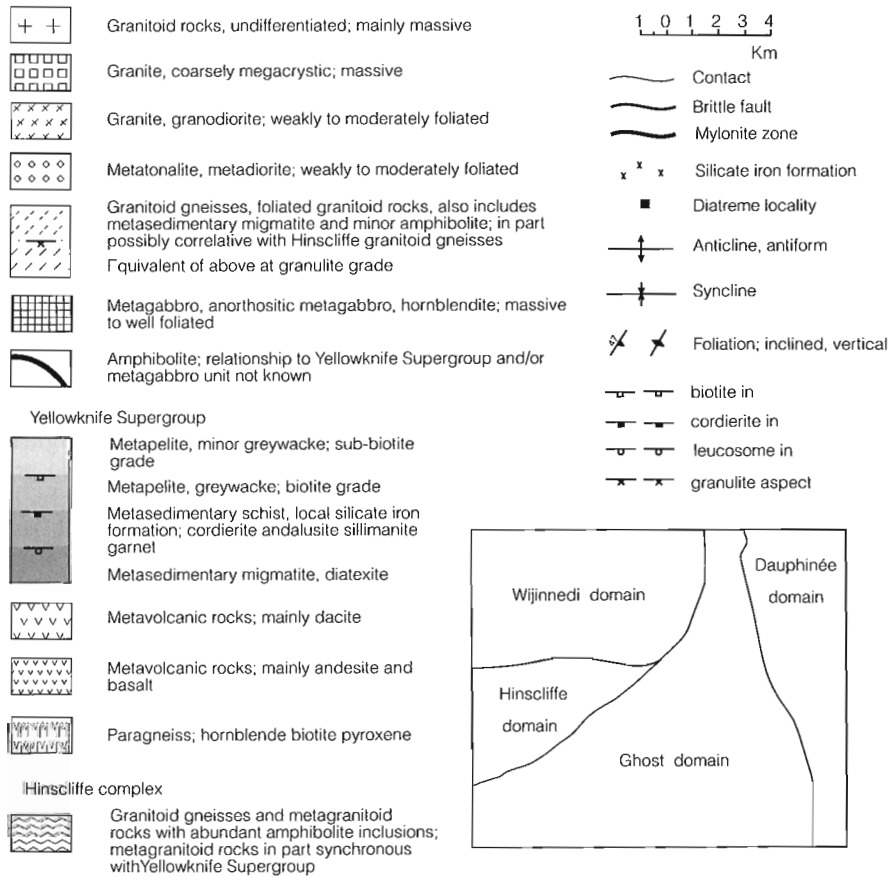
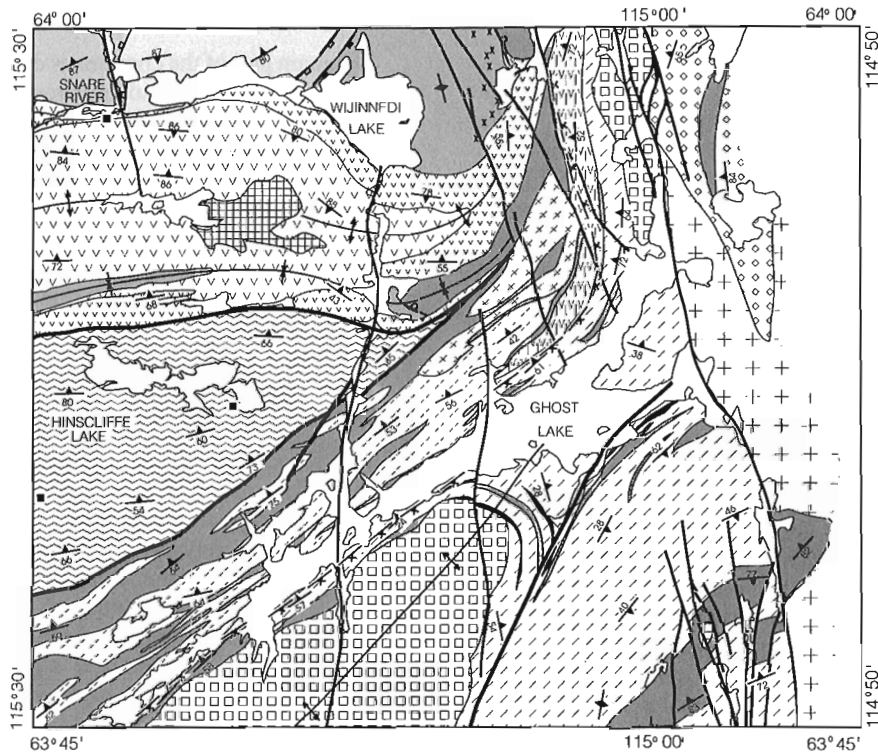
The age of the uplift event is unknown. However diabase dykes of the Indin set are deformed and broken in the cataclastic shear zone and associated brittle faults at the eastern margin of the uplift. The precise age of the Indin dykes is not

known but K-Ar whole rock data have been interpreted as possibly suggesting a 1.8 -2.0 Ga intrusive event (Leech, 1965) but as Alice Payne Leech pointed out in reference to K-Ar whole rock dating of dykes: "Updating and uplifting have the same effect; old dykes and old ladies give young ages". More easily interpretable U-Pb (baddeleyite) analyses are currently being attempted (O. van Breemen, pers. comm., 1993) which may more accurately constrain a maximum age for the uplift event. The minimum age is unconstrained. Previously it was speculated that the uplift may have been related to the indentation of the eastern Slave Province into the western Churchill Province at about 1.80 Ga (Henderson and Schaan, 1993). On the other hand, if the more-or-less

**Figure 2.** General geology of the Wijinnedi Lake area. The area has been divided into four shear zone bounded lithotectonic domains. The lowest grade, least deformed rocks, consisting mainly of the Archean Yellowknife Supergroup, occur in the Wijinnedi domain in the northwest. It is structurally underlain by complex granitoid and granitoid gneiss of the Hinscliffe domain, part of which may be pre-Yellowknife Supergroup in age. To the southeast, structurally underlying the previous two domains, is the Ghost domain, consisting mainly of higher grade, more deformed equivalents of units of those domains, as well as deformed and metamorphosed intrusive rocks. The metamorphic grade rises to granulite towards the southeast. In the east, the Dauphinée domain, consisting of massive granite, as well as metamorphosed and foliated granitoid and high grade Yellowknife units, is separated from the Ghost domain by a major greenschist cataclastic shear zone. Only the largest structural elements are illustrated to show the basic structural framework.



**Figure 1.** Southwestern Slave Province showing the location of the Wijinnedi Lake map area at the north end of a Paleoproterozoic(?) asymmetric block uplift. Within the map area the uplift consists of abundant rocks at granulite metamorphic grade and has a distinctive high relief aeromagnetic expression which is the basis for outlining it south of the area mapped. Modified after McGlynn (1977) and Geological Survey of Canada (1969).



symmetrical disposition of the Big Spruce alkalic intrusion west of the uplift (Fig. 1) is more than coincidental, it may be related to the uplift event. The Big Spruce intrusion was emplaced at about 2.19 Ga (Cavell and Baadsgaard, 1986).

As a result of the 1992 mapping, the area was divided into four distinct lithotectonic domains (Fig. 2). The domains within the uplift are separated by major wide mylonite zones. In the northwest, the least deformed and lowest grade metavolcanic and metasedimentary rocks of the Archean Yellowknife Supergroup together with a major mafic intrusive complex occur in the Wijinnedi domain. To the south and structurally below the Wijinnedi are granitoid gneisses and granitoid rocks of the Hinscliffe domain. The gneisses commonly contain blocks of amphibolite that may represent dismembered mafic dykes. The rocks of this domain are considered to be in part potentially older than the Yellowknife Supergroup (Henderson and Schaan, 1993) but at least one foliated granitoid phase has a synvolcanic age (M.E. Villeneuve, unpub. data, 1993). Of the four domains, the Hinscliffe is the only one that does not contain any Yellowknife Supergroup rocks. To the southeast and structurally below both the Wijinnedi and Hinscliffe domains is the Ghost domain. It consists of highly deformed and metamorphosed Yellowknife Supergroup rocks as well as variably deformed and metamorphosed granitoid intrusive phases, granitoid gneisses in part possibly derived from the Hinscliffe domain and a major suite of megacrystic granite. The southeastern two thirds of the domain are at granulite metamorphic grade. The Dauphinée domain occurs along the eastern margin of the map area and is outside the uplifted terrane. It is separated from the uplifted Ghost domain to the west by the low grade cataclastic shear zone which contrasts with the ductile shear zones that separate the other domains. The rocks of the Dauphinée domain consist mainly of massive granite but also include a metamorphosed mafic granitoid phase and high grade Yellowknife Supergroup rocks. Fieldwork during the 1993 field season was concentrated in the Wijinnedi domain and in the eastern Ghost and western Dauphinée domains along their mutual contact.

## **WIJINNEDI DOMAIN**

### ***Yellowknife Supergroup metavolcanic rocks***

The Wijinnedi domain consists largely of a dominantly dacitic volcanic complex situated in an east-trending elongate dome-like structure that extends about 4 km to the west beyond the map area (Fig. 2). This volcanic complex contrasts strongly with the generally linear, northerly trending and largely mafic volcanic units typical of the rest of the Indin supracrustal basin to the north (Frith, 1993; Fig. 1). Planar structures within the volcanic complex are steeply dipping to the north or south and lineations plunge steeply. This structural pattern contrasts with that of the Hinscliffe and northwestern Ghost domains where structural features consistently dip or plunge moderately to steeply to the northwest. Primary features are best preserved in the northern and

western parts of the volcanic complex but become more obscure with increasing metamorphic grade and deformation to the east and southeast.

The main part of the complex is dominated by grey dacitic volcanic breccia with no apparent primary stratification (Fig. 3). The clasts at any locality, ranging in composition within the dacite class, are commonly sparsely feldspar phyric and less commonly contain quartz phenocrysts. Locally the dacite is amygdaloidal. Also present, but much less abundant, are units of finer grained dacite that in some cases contain volcanoclastic textures. Elsewhere, where such textures are not present, similar fine dacite units might also represent synvolcanic sills. In the southern part of the complex, light pink, metre scale or less sills of rhyolite occur locally. Minor mafic volcanic units occur within the dacite unit, particularly in the southern part.

The felsic core of the volcanic complex is mantled by more mafic volcanic rocks that dominate its eastern end. These are grey-green to dark green rocks of presumed andesitic to basaltic composition. Both volcanoclastic units and flows are present, some containing pillows that are best preserved immediately south and southeast of Wijinnedi Lake. The southern margin of the complex along the tectonic contact between the Wijinnedi and Hinscliffe domains is dominated by amphibolitic mylonite. However, due to the increasingly higher metamorphic grade and degree of deformation towards the south, it is commonly difficult to differentiate between mafic volcanic units and mafic sills related to the major metagabbroic intrusion emplaced into the volcanic complex that is described below.

In the mafic volcanic unit on the north side of the complex just west of the sharp bend in the Snare River (Fig. 2) is a diatreme-like structure approximately 35 m long and 20 m across. It consists of a dark grey-green altered matrix of feldspar, chlorite, epidote, carbonate, and quartz containing up to 50% altered crystals, which were originally garnet. The matrix is weakly foliated and its metamorphic mineral assemblage is compatible with the regional medium greenschist grade. The garnet pseudomorphs are up to 8 cm in size and vary from rounded equidimensional to euhedral dodecahedral forms (Fig. 4). The smaller garnet pseudomorphs are white, while the coarser forms, that appear to be monomineralic in hand specimen, have a white marginal zone and dull mauve-pink, finely crystalline core. No primary garnet has been recognized and the pseudomorphs now consist mainly of strongly altered plagioclase with lesser amounts of a fine white mica and carbonate. The original garnet was clearly out of context with metamorphic grade of the matrix in which it presently occurs suggesting it was generated at greater depths under more extreme conditions.

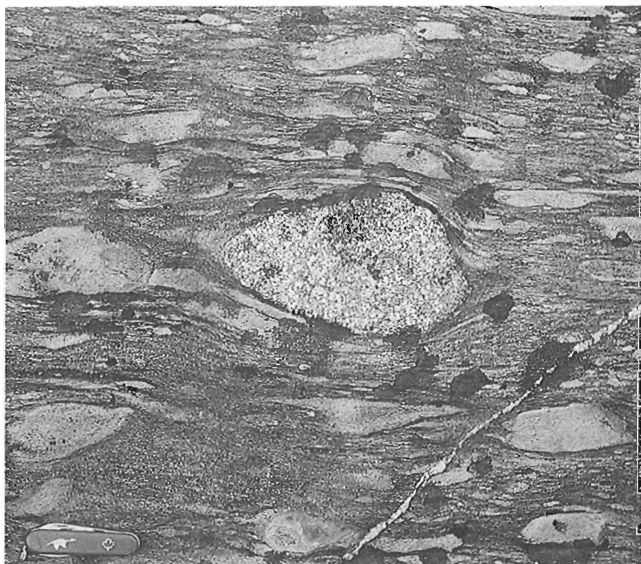
Two diatreme-like bodies also occur in the granitoid gneisses of Hinscliffe domain to the south (Fig. 2; Henderson and Schaan, 1993). These bodies have a dyke-like form and contain clasts of granite. Other diatremes occur in the Kam Group volcanic rocks at Yellowknife, one containing 3 Ga tonalitic clasts (Nikic et al., 1980). As no rocks of this age are known at the surface, a deep source is also implied.



### ***Yellowknife Supergroup metasedimentary rocks***

The metasedimentary rocks of the Wijinnedi domain conformably overlie the volcanic complex. As elsewhere in the Slave Province, the metasediments are turbidites but differ in that the pelite proportion strongly dominates and true greywacke is very rare. Bedding in general conforms to the trend of the volcanic rocks and is east-west with beds facing both north and south in the lower grade rocks west of Wijinnedi Lake but becomes northeasterly to northerly trending at higher metamorphic grades to the east. The dominant cleavage is most commonly subparallel to bedding. Steeply-plunging fold closures with axial planar cleavage occur only locally. This suggests a fold pattern consisting of older, shallow-plunging isoclinal folds locally refolded by steeply plunging folds. This is similar in general to the fold pattern of Yellowknife metasedimentary rocks elsewhere in the province (Fyson, 1993).

The pelite commonly occurs as up to metre-scale units without primary structures. Thinner, coarser grained units are typically siltstone but rare fine grained, quartz poor greywacke occurs locally in centimetre-scale units. Rare siltstone beds are as much as four metres thick and lack evidence to suggest that they are amalgamated. Iron-formation was not recognized in the low grade metasedimentary rocks in contrast to the abundant silicate iron-formation that occurs in the higher grade equivalents to the east of Wijinnedi Lake (Fig. 2; Henderson and Schaan, 1993). However on an island in the lake west of Wijinnedi Lake samples of arsenopyrite-bearing silicate iron-formation that assayed over 2500 ppb Au (John Brophy, DIAND, pers. comm., 1993) were found at an old camp. This material may have been originally collected in the region.



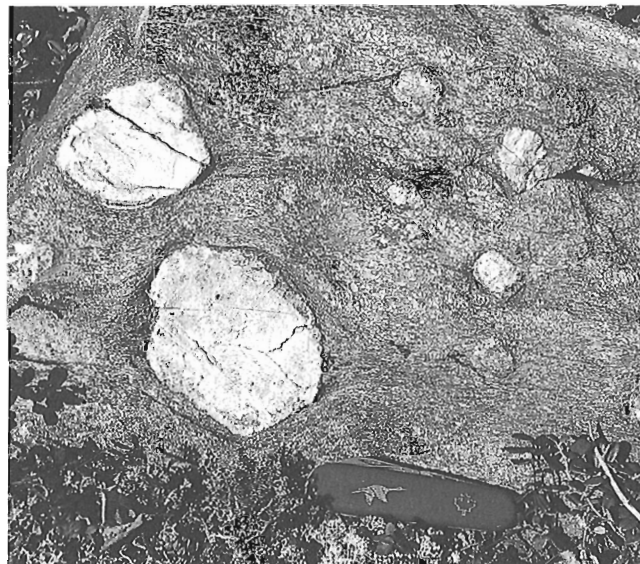
**Figure 3.** Representative example of the deformed dacitic volcanic breccias that dominate the volcanic complex in the Wijinnedi domain. The light coloured, less deformed clast in the centre of the photograph is a granitoid and is extremely unusual in the complex as a whole. Knife for scale is 10 cm long. GSC 1993-2370

The lack of quartz-bearing greywacke in these metasedimentary rocks has implications for the nature of the source terrane. Typical Yellowknife greywacke contains more-or-less equal parts of quartz, feldspar, and fine grained lithic clasts, at least some of which are considered to be of volcanic, mainly felsic, origin. Because coarse quartz and feldspar are abundant, it has been suggested that a granitoid and or granitoid gneiss terrane was a major component of the source (Schau and Henderson, 1983). This would not appear to hold in the Wijinnedi domain metasedimentary rocks which lack coarse quartz and feldspar. The volcanic complex to the south, on the other hand, may have been a major source, given its dominantly felsic composition but relatively minor content of feldspar and particularly quartz, contributing mainly felsic volcanic rock fragments to the nonpelitic component of the sediment.

The dominance of the pelitic component in these rocks and the rarity of quartzofeldspathic psammitic layers provide a strong linkage between these low metamorphic grade sediments and the migmatitic to diatexitic metasedimentary rocks of the Ghost domain to the south and southeast. There, the metasedimentary migmatites also contain few or no psammitic restite layers, in contrast to their common occurrence in Yellowknife metasedimentary migmatites elsewhere in the Slave Province.

### ***Mafic igneous complex***

A large mafic igneous complex with associated sills and dykes, occurs at the core of the metavolcanic complex dome (Fig. 2). The intrusion is everywhere metamorphosed to the



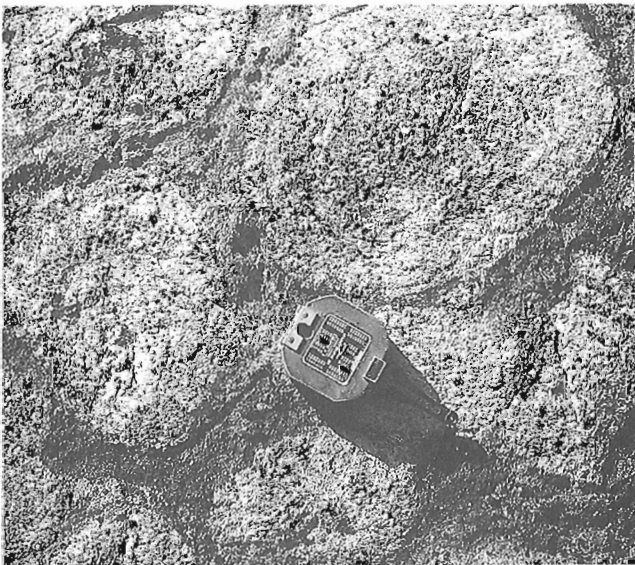
**Figure 4.** Part of a metamorphosed and deformed diatreme-like body within greenschist grade intermediate to mafic metavolcanic rocks containing coarse, euhedral to subhedral, altered garnets. Knife for scale is 10 cm long. GSC 1993-237N

regional grade. Deformation is expressed by shearing along its contacts and in the main complex by spaced ductile shear zones up to 10 m wide that separate unfoliated metagabbro.

The complex appears to consist of a series of plutonic lobes separated by screens of felsic volcanic inclusions. The dominant lithology in the western part of the complex is dark green to black, medium- to fine-grained, massive, recrystallized metagabbro, composed of hornblende and plagioclase and typically with metamorphic textures. The eastern parts of the complex are more heterogeneous with compositions ranging from metamagabbro to leucocratic anorthositic metagabbro. These variations are gradational over a few centimetres to abrupt through several intrusive phases. Primary textures are locally well preserved in the northeastern part of the complex where coarse plagioclase megacrysts and orbicular structures occur locally (Fig. 5).

Sills up to several metres wide and, less commonly, dykes, occur throughout much of the metavolcanic complex. They are particularly abundant south and east of the main intrusive complex but also occur to the north in both the metavolcanic and metasedimentary rocks. Most sills are medium- to fine-grained metagabbro but in a few cases consist of centimetre scale texturally and compositionally graded layers (Fig. 6). This suggests that the sills were originally horizontal when emplaced and would be a constraint on the time of their emplacement. However, a subvertical Paleoproterozoic Indin diabase dyke in the area contains similar features (Fig. 7) suggesting that this interpretation may not be unequivocal.

Parts of the intrusion have strong, positive aeromagnetic expression that are particularly prominent in the otherwise generally flat magnetic field over the Wijnnedi domain. The most prominent anomaly is a curvilinear feature in the western



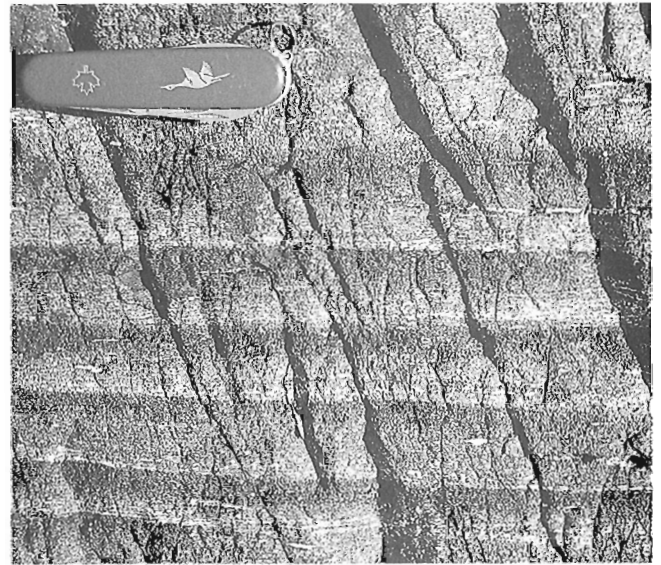
**Figure 5.** Coarse orbicular structures over 20 cm in diameter in a more leucocratic phase from an unusually well preserved part of the metamafic igneous complex in the northeastern part of the intrusion. Photograph by Susan E. Schaan. GSC 1993-237P

part of the complex that extends several kilometres to the west beyond the mapped extent of the complex. Although not identified in the field, it is thought to represent a dyke, unusually rich in magnetite associated with the complex.

Similar mafic intrusions occur elsewhere in the Slave Province. These include the anorthositic gabbro body in the Chan mafic volcanic sequence north of Yellowknife (Padgham, 1987), the gabbro-anorthositic gabbro at Camsell Lake south of MacKay Lake in the south central Slave Province (Johnstone, 1992), and the anorthositic gabbro bodies east and southeast of Clinton-Colden Lake in the eastern Slave Province (Macfie, 1987). All are intimately associated with Yellowknife volcanic rocks. The complex at Clinton-Colden Lake has a U-Pb (zircon) age of  $2686 \pm 3$  Ma (Macfie et al., 1990), about midway within the range of Yellowknife volcanic ages (van Breemen et al., 1992) throughout the Slave Province. If this correlation is correct, it would suggest that the mafic intrusive complex in the Wijnnedi Lake area is synvolcanic.

## GHOST DOMAIN

Most of the Ghost domain was mapped in 1992 and previously described by Henderson and Schaan (1993). In brief, the Ghost domain is the most heterogeneous domain and contains the highest grade rocks. The rocks occur in an asymmetric, northeasterly trending, antiformal structure with moderate to steep dips on the northwest limb and more gentle dips to the southeast (Fig. 2). The domain is dominated by metamorphosed and foliated granitoid rocks and granitoid gneisses. Migmatitic to diatexitic metasedimentary and, less commonly, metavolcanic rocks that are considered to be high



**Figure 6.** Deformed and metamorphosed mafic sill consisting of texturally and compositionally graded layers, within Yellowknife dacitic metavolcanic rocks. These structures might imply the sill was emplaced when the volcanic sequence was in a subhorizontal position, however see Figure 7. GSC 1993-237E



**Figure 7.** Subvertical and nondeformed Paleoproterozoic Indin diabase dyke containing texturally and compositionally graded layers adjacent to chilled contact with country rocks. Compare with similar structures in Figure 6. GSC 1993-237R



**Figure 8.** Small scale brittle faults in Archean migmatitic granitoid gneiss related to deformation associated with main cataclastic shear zone that separates the Ghost and Dauphinée domains. Location is within a few tens of metres of the main structure. GSC 1993-237C

grade equivalents of the Yellowknife Supergroup rocks of the Wijnnedi domain, occur throughout the Ghost domain but are most abundant on the northwest limb. The rocks of the central part and southeast limb of the structure are at granulite grade and, aside from a single locality about 100 km to the north (Thompson, 1978), is the only significant area at granulite grade known within the Slave Province. At the core of the antiform is a coarsely megacrystic granite that is not at granulite grade and appears to have retrograded its originally granulite grade host rocks. Mapping in 1993 was concentrated in the eastern parts of the domain, near the northern and southern margins of the map area.

The east side is bounded by the cataclastic shear zone along which uplift of the high grade rocks has taken place. It is largely covered by lakes or Quaternary deposits along much of its length. However, it is particularly well exposed locally in the southern part of the area where granulite grade granitoid rocks of the Ghost domain become increasingly redder on their weathered surface and increasingly fractured but not foliated as the shear zone is approached. Pyroxene (mantled by hornblende) is recognizable within 50 m of the fault zone. The exposed fault zone is about 5 m wide and consists of broken granitic clasts that become finer and darker toward the centre of the zone, where the rocks are black and aphanitic with no foliation. The Dauphinée domain rocks to the east appear to be altered to grey to greenish grey over a greater distance from the fault zone. In the central part of its extent within the map area, the fault has a bend with a wider fracture zone including dilatant features. To the north the main strand of the structure splays and shifts to the east. Beyond the map area it appears to swing into a more north-northeasterly direction, passing through Daran Lake and into Ranji Lake

(Tremblay et al., 1953). Small scale, epidote-bearing, brittle fractures are common, largely subparallel to the main fault (Fig. 8). Several northerly trending faults occur to the west (Fig. 2), some of which have evidence of a major vertical component of movement (Henderson and Schaan, 1993) and are believed to be related to the main domain boundary zone.

The widest zone of metasedimentary rock in the domain occurs near the southeastern corner of the map area and is possibly correlative with compositionally similar metasedimentary rocks across the antiformal structure along the northwest margin of the domain. This is the region where Folinsbee (1940) originally reported the occurrence of gem quality cordierite. The zone has a prominent and anomalously low aeromagnetic expression (Geological Survey of Canada, 1963a, b) and consists mainly of Yellowknife metasedimentary migmatite with distinct paleosome and leucosome. Compared to the rocks of metasedimentary origin in the northwestern part of the domain, metasedimentary diatexite is less common. As elsewhere in most of the domain, psammitic restite layers in the migmatite are rare. Garnet, typically very coarse, is ubiquitous and cordierite, in places also very coarse, is less common. Coarse blocky crystals of sillimanite, presumably pseudomorphic after andalusite, are rare. The biotite-rich metasedimentary migmatites are commonly bounded by narrow zones up to a few tens of metres in width of typically fine grained, quartzofeldspathic to mafic, thinly layered and finely laminated gneisses. James Farquhar is currently doing a detailed study of the metamorphism of these metasedimentary rocks and the bounding gneisses and granitic rocks in this zone and has reported preliminary temperature and pressure estimates of 780-870°C and 3.8-5.2 kbar (Farquhar et al., 1993).

In the northern part of the domain, supracrustal gneisses, originally interpreted as metavolcanic rocks by Lord (1942) and Wright (1954), were traced to the northern margin of the map area. They are olive green to rusty brown, medium- to fine-grained, finely laminated, mafic, quartzofeldspathic to amphibolitic paragneisses that are commonly finely laminated. They typically contain centimetre scale, pyroxene-bearing leucosome layers, anastomosing veinlets and wispy lenses. Locally they grade into metasedimentary migmatites through gneisses with layers that are texturally graded from medium grained quartzofeldspathic psammite to finer grained more biotite-rich semipelitic compositions. The mineralogy of these transitional rocks varies from pyroxene-bearing assemblages characteristic of the metavolcanic gneisses to garnet-bearing assemblages more characteristic of the pelite dominated metasedimentary migmatites. The thin units of gneiss marginal to the major metasedimentary gneiss zone near the south east corner of the area (Fig. 2) are similar in many respects to these more mafic gneisses of probable volcanogenic origin.

Intruding the granulite grade supracrustal gneisses is an extensive granitoid complex, also at granulite grade, that is up to 4 km wide and occurs in most places along the western margin of the domain. The leucocratic granitoid rocks are massive to weakly foliated, weather yellow to white to pinkish red near the domain bounding cataclastic shear zone, but always have the greenish to brownish fresh surface colour and presence of pyroxene characteristic of granulite grade rocks. In most areas these rocks are recrystallized from original coarser textures and only rarely are primary igneous textures preserved. The granitoid rocks are generally homogeneous except in local marginal phases where they contain inclusions of the supracrustal gneisses. The adjacent gneisses contain dykes and sills of the granitoid rocks, displaying unequivocal intrusive relationships. The generally massive, homogeneous nature of these granitoid bodies on the east margin of the domain contrasts strongly with the typically smaller, compositionally more heterogeneous and generally strongly foliated intrusions abundant in the northwest limb of the domain.

A pink, biotite-rich megacrystic granite consisting mainly of very coarse, densely packed, K-feldspar megacrysts intrudes the granulite grade granitoid plutons at the east side of the domain at the northern margin of the map area (Fig. 2). The megacrystic granite is not at granulite grade although it does have a somewhat recrystallized metamorphic texture. To the east it is cut off by the domain bounding cataclastic shear zone. The intrusion is, for the most part, massive with local marginal foliation. It is identical to the much larger megacrystic granite south of Ghost Lake and may well occupy a similar structural position in the antiformal axis of the domain. A somewhat similar but much smaller pluton of megacrystic granite occurs in centre of the wide zone of metasedimentary rocks near the southeastern corner of the area. It contains ubiquitous aggregates of fine grained garnet and as such is similar to the marginal phases of the main megacrystic granite at Ghost Lake where it is hosted by metasedimentary rocks.

## DAUPHINÉE DOMAIN

The Dauphinée domain, on the western edge of the map area, is separated from the Ghost domain by the throughgoing cataclastic shear zone and contrasts with the eastern Ghost domain in that its rocks are at subgranulite metamorphic grade.

The most abundant unit is a pale pink to light grey, massive to weakly foliated, biotite poor granite to granodiorite, in most areas with small, sparse K-feldspar megacrysts. In the northwestern part of the domain, presumably intruded by the granite, is a tonalite to quartz diorite body. It is a dark grey, medium grained, even grained biotite hornblende rock that most commonly has a metamorphic texture and is weakly to moderately foliated. Somewhat more mafic, smoothly elliptical inclusions of the same plutonic suite are common and are oriented in the foliation. The body is cut by pervasive sets of narrow dykes of white granite to pegmatite that are variably deformed, even within the same outcrop. Intrusions very similar in composition and texture to this suite occur northwest of the southwest part of Ghost Lake, within the Ghost domain.

Two units of metasedimentary migmatite that are assumed to have been derived from the Yellowknife Supergroup occur within the domain. One occurs within the tonalite-quartz diorite unit (Fig. 2). The second occurs in the southern part of the domain within the leucocratic granites. The second metasedimentary unit along strike from the major belt of metasedimentary migmatite in the adjacent southeastern Ghost domain (Fig. 2) and as such may represent a lithological linkage across the cataclastic shear zone.

## ACKNOWLEDGMENTS

Steven Bauke provided efficient and enthusiastic field assistance. Kevin Chiasson and Rob Brown provided expediting service. John Brophy, Indian and Northern Affairs, Canada provided the gold assay data for a silicate iron-formation sample. The paper was critically reviewed by J.R. Henderson and J.A. Percival.

## REFERENCES

- Cavell, P.A. and Baadsgaard, H.**  
1986: Geochronology of the Big Spruce Lake alkaline intrusion; Canadian Journal of Earth Sciences, v. 23, p. 1-10.
- Farquhar, J., Stavely, J.A., and Chacko, T.**  
1993: Granulite facies metamorphism near Ghost Lake, Slave Province, N.W.T.; Program and Abstracts, Geological Association of Canada/Mineralogical Association of Canada, 1993, p. A28.
- Folinsbee, R.E.**  
1940: Gem cordierite from the Great Slave Lake area, N.W.T., Canada; American Mineralogist, v. 25, p. 216.
- Frith, R.A.**  
1993: Precambrian geology of the Indin Lake map area, District of Mackenzie, Northwest Territories; Geological Survey of Canada, Memoir 424, 63 p.



- Fyson, W.K.**  
1993: Identification of structures in the Slave Province; N.W.T. Geology Division, Indian and Northern Affairs Canada, EGS 1993-07, 16 p.
- Geological Survey of Canada**  
1963a: Dauphinée Lake, District of Mackenzie, Northwest Territories; Geological Survey of Canada, Geophysics Paper 2956, Map 2956G.  
1963b: Ghost Lake, District of Mackenzie, Northwest Territories; Geological Survey of Canada, Geophysics Paper 2955, Map 2955G.  
1969: Wecho River, District of Mackenzie, Northwest Territories; Geological Survey of Canada, Geophysics Paper 7196, Map 7196G.
- Henderson, J.B. and Schaan, S.E.**  
1993: Geology of the Wijnnedi Lake area: a transect into mid-crustal levels in the western Slave Province, District of Mackenzie, Northwest Territories; *in* Current Research, Part C; Geological Survey of Canada, Paper 93-1C, p. 83-91.
- Johnstone, R.M.**  
1992: Preliminary geology of the Camsell Lake area, parts of NTS 75M/6, 10, 11; Indian and Northern Affairs Canada, Northern Affairs Program, EGS-1992-2.
- Leech, A.P.**  
1965: Potassium-argon dates of basic intrusive rocks of the District of Mackenzie, N.W.T.; Canadian Journal of Earth Sciences, v. 3, p. 389-412.
- Lord, C.S.**  
1942: Snare River and Ingray Lake map-areas, Northwest Territories; Geological Survey of Canada, Memoir 235, 55 p.
- Macfie, R.I.**  
1987: The Clinton-Colden hornblende gabbro-anorthosite intrusion, Artillery Lake map area, District of Mackenzie; *in* Current Research, Part A; Geological Survey of Canada, Paper 87-1A, p. 681-687.
- Macfie, R.I., van Breemen, O., and Loveridge, W.D.**  
1990: U-Pb zircon age of the Clinton-Colden gabbro-anorthosite intrusion, eastern Slave Province, N.W.T.; *in* Radiogenic Age and Isotopic Studies: Report 3, Geological Survey of Canada, Paper 90-2, p. 45-48.
- McGlynn, J.C.**  
1977: Geology of the Bear-Slave Structural Provinces, District of Mackenzie; Geological Survey of Canada, Open File 445.
- Nikic, Z., Baadsgaard, H., Folinsbee, R.E., Krupicka, J., Payne-Leech, A., and Saasaki, A.**  
1980: Boulders from the basement, the trace of ancient crust?; Geological Association of America, Special Paper 182, p. 169-175.
- Padgham, W.A.**  
1987: Access to anorthosite and sheeted dykes in the Chan Formation; *in* W.A. Padgham (ed.), Yellowknife Guidebook, a guide to the geology of the Yellowknife volcanic belt and its bordering rocks; Mineral Deposits Division, Geological Association of Canada, p. 41-42.
- Schau, M. and Henderson, J.B.**  
1983: Archean weathering at three localities on the Canadian Shield; Precambrian Research, v. 20, p. 189-224.
- Thompson, P.H.**  
1978: Archean regional metamorphism in the Slave Structural Province - a new perspective on some old rocks; *in* Metamorphism in the Canadian Shield, (ed.) J.A. Fraser and W.W. Heywood; Geological Survey of Canada, Paper 78-10, p. 85-102.
- Tremblay, L.P., Wright, G.M., and Miller, M.L.**  
1953: Ranji Lake, District of Mackenzie, Northwest Territories; Geological Survey of Canada, Map 1022A.
- van Breemen, O., Davis, W.J., and King, J.E.**  
1992: Temporal distribution of granitoid plutonic rocks in the Archean Slave Province, northwest Canadian Shield; *in* The Tectonic Evolution of the Superior and Slave Provinces of the Canadian Shield, (ed.) K.D. Card and J.E. King; Canadian Journal of Earth Sciences, v. 29, p. 2186-2199.
- Wright, G.M.**  
1954: Ghost Lake, District of Mackenzie, Northwest Territories; Geological Survey of Canada, Map 1021A.

---

Geological Survey of Canada Project 870008





# Geology and mineral occurrences of the central part of High Lake greenstone belt, Archean Slave Province, Northwest Territories: a preliminary account of an unconformity between two volcanic sequences<sup>1</sup>

J.R. Henderson, M.N. Henderson<sup>2</sup>, and J.A. Kerswill<sup>2</sup>

Continental Geoscience Division

*Henderson, J.R., Henderson, M.N., and Kerswill, J.A., 1994: Geology and mineral occurrences of the central part of High Lake greenstone belt, Archean Slave Province, Northwest Territories: a preliminary account of an unconformity between two volcanic sequences; in Current Research 1994-C; Geological Survey of Canada, p. 81-90.*

---

**Abstract:** Supracrustal rocks in the central part of the High Lake belt are interpreted to comprise an intermediate to felsic sequence of volcanic and volcanoclastic rocks that is unconformably overlain by a mafic to felsic sequence of volcanic, volcanoclastic, and sedimentary rocks.

The area contains many gossans, and numerous base and precious metal occurrences, including the synvolcanic polymetallic mineralization at High Lake which is tentatively assigned to the older sequence. Metamorphism is chlorite grade, and locally abundant cordierite in felsic volcanic rocks of the older sequence possibly resulted from synvolcanic hydrothermal alteration.

The older sequence predates the earliest deformation (D<sub>1</sub>). In the younger sequence, earliest structures (D<sub>2</sub>) are upright subhorizontal folds that apparently strike at a large angle to the dominant northerly trend of the belt; these are overprinted by a north-northeasterly trending vertical foliation and steeply-plunging folds (D<sub>3</sub>). Granitoid batholiths surround the belt, and are late syn- to post-D<sub>3</sub>.

**Résumé :** Les roches supracrustales de la partie centrale de la ceinture de roches vertes de High Lake sont interprétées comme comprenant une suite de roches volcaniques et volcanoclastiques intermédiaires à felsiques recouvertes de manière discordante par une suite de roches volcaniques et volcanoclastiques mafiques à felsiques et de roches sédimentaires.

La région comprend de nombreuses zones d'altération ferrugineuse et plusieurs gisements de métaux de base et de métaux précieux, y compris la minéralisation synvolcanique polymétallique de High Lake qui est temporairement attribuée à la suite ancienne. Le métamorphisme est de la zone à chlorite et la cordiérite abondante localement dans les roches volcaniques felsiques de la suite plus âgée résulte probablement d'altération hydrothermale synvolcanique.

La suite plus âgée précède la première déformation (D<sub>1</sub>). Dans la suite plus jeune, la première déformation (D<sub>2</sub>) consiste en plis droits subhorizontaux apparemment d'orientation très divergente de l'orientation principalement nord de la ceinture; sur ces plis sont superposés une foliation verticale d'orientation nord-nord-est et des plis à plongée forte (D<sub>3</sub>). Des batholites granitoïdes entourent la ceinture et sont syn- ou post-D<sub>3</sub>.

---

<sup>1</sup> Contribution to Canada-Northwest Territories Mineral Initiatives (1991-1996), an initiative under the Canada-Northwest Territories Economic Development Cooperation Agreement.

<sup>2</sup> Mineral Resources Division

## INTRODUCTION

Mapping of High Lake greenstone belt continued in 1993 as a Federal Government component of the 1991-1996 Canada-NWT Mineral Initiatives Agreement. Mapping was concentrated in the central part of the belt (Fig. 1) in parts of NTS map sheets 76M/6 and 7 (Hepburn Island). Padgham et al. (1973) mapped 76M/7 at 1:50 000. The southern part of the belt (Fig. 1) in 76L/14, 15, 16, and 76M/1, 2, 3 was most recently mapped in 1992, and published at 1:100 000 (Henderson et al., 1992). Relf (1992) mapped the Anialik River volcanic belt northwest of the area discussed in this report, Jackson et al. (1986) mapped to the east of the area of our mapping (76M/1, 2, 8, 9, and 15), and Easton et al. (1982) mapped to the north in 76M/10 and 11. A compilation of the geology and mineral occurrences in the Hepburn Island sheet by Jackson (1989) is an excellent summary of earlier work in the region.

In this paper we present a preliminary interpretation of field and geochronological data, and suggest that an unconformity separates two volcanic-dominated rock sequences in the High Lake greenstone belt.

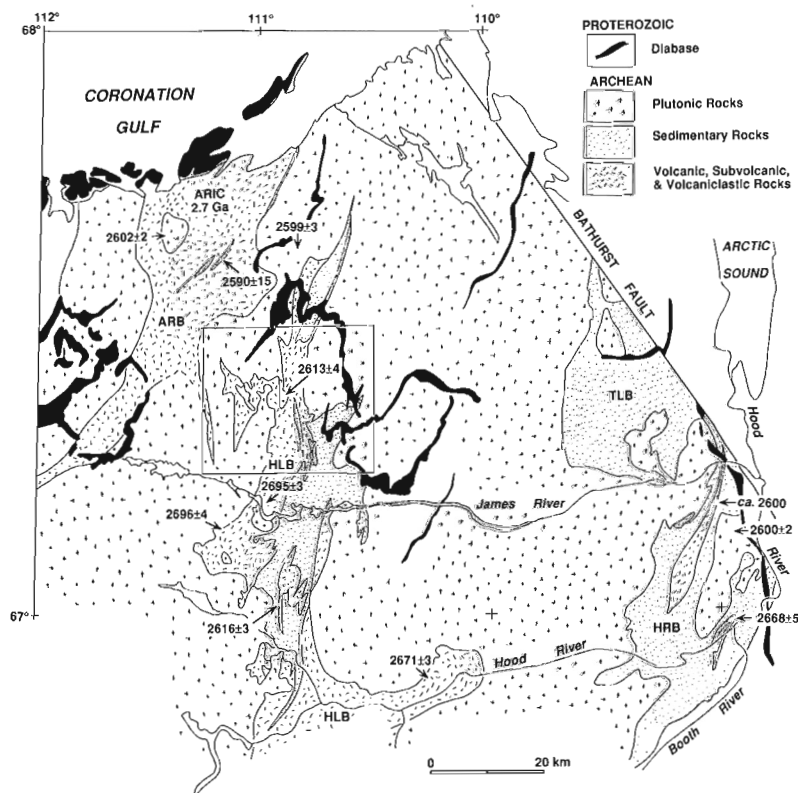
## REGIONAL STRATIGRAPHIC RELATIONSHIPS

In the northwestern Slave structural province (Fig. 1), the oldest rocks identified by U-Pb zircon dating are  $2702 \pm 2$  Ma rocks of the Anialik River Igneous Complex (Abraham et al., 1991) which are interpreted to be subvolcanic. This age is nearly coeval with felsic volcanism identified in the High Lake

greenstone belt at  $2696 \pm 4$  and  $2695 \pm 3$  Ma (Mortensen et al., 1988), and is about 25 Ma older than  $2671 \pm 3$  Ma (M. Villeneuve, pers. comm., 1993) volcanism along the Hood River in the High Lake belt. These U-Pb zircon dates indicate a time of "early" volcanism and sedimentation in the northwestern Slave Province ranging from ca. 2702 to 2671 Ma – similar to 2.71-2.65 Ga age range of Yellowknife Supergroup turbidite sedimentation and volcanism evident in other parts of the Slave Province (van Breemen et al., 1992).

In the Anialik River greenstone belt, an angular unconformity was mapped by Tirrul and Bell (1980) between older (ca. 2702 Ga, see above) volcanic rocks and a polymict conglomerate with flattened granitic boulders at String Lake. Zircons from a boulder collected from this conglomerate gave a  $2590 \pm 15$  Ma U-Pb zircon age (M. Villeneuve, pers. comm., 1992), indicating a maximum age for the conglomerate. In the Hood River and Torp Lake belts (Fig. 1), Henderson et al. (1991) mapped an angular unconformity between turbidites with a minimum age of  $2668 \pm 5$  Ma (O. van Breemen, pers. comm., 1992), and an overlying succession of conglomerates, arenites, flows, and tuffs. Zircons from a rhyolite boulder in the supracrustal sequence above the unconformity date volcanism at  $2604 \pm 2$  Ma (C.W. Jefferson and O. van Breemen, pers. comm., 1993), and indicate the maximum age of sedimentation. Within the High Lake belt south of the James River, zircons from rhyolite have been dated at  $2616 \pm 3$  Ma (M. Villeneuve, pers. comm., 1993).

Although the data cited above are preliminary and sparse, the 75 Ma minimum range in volcanic zircon ages, and the limited documentation by mapping of unconformities



**Figure 1.**

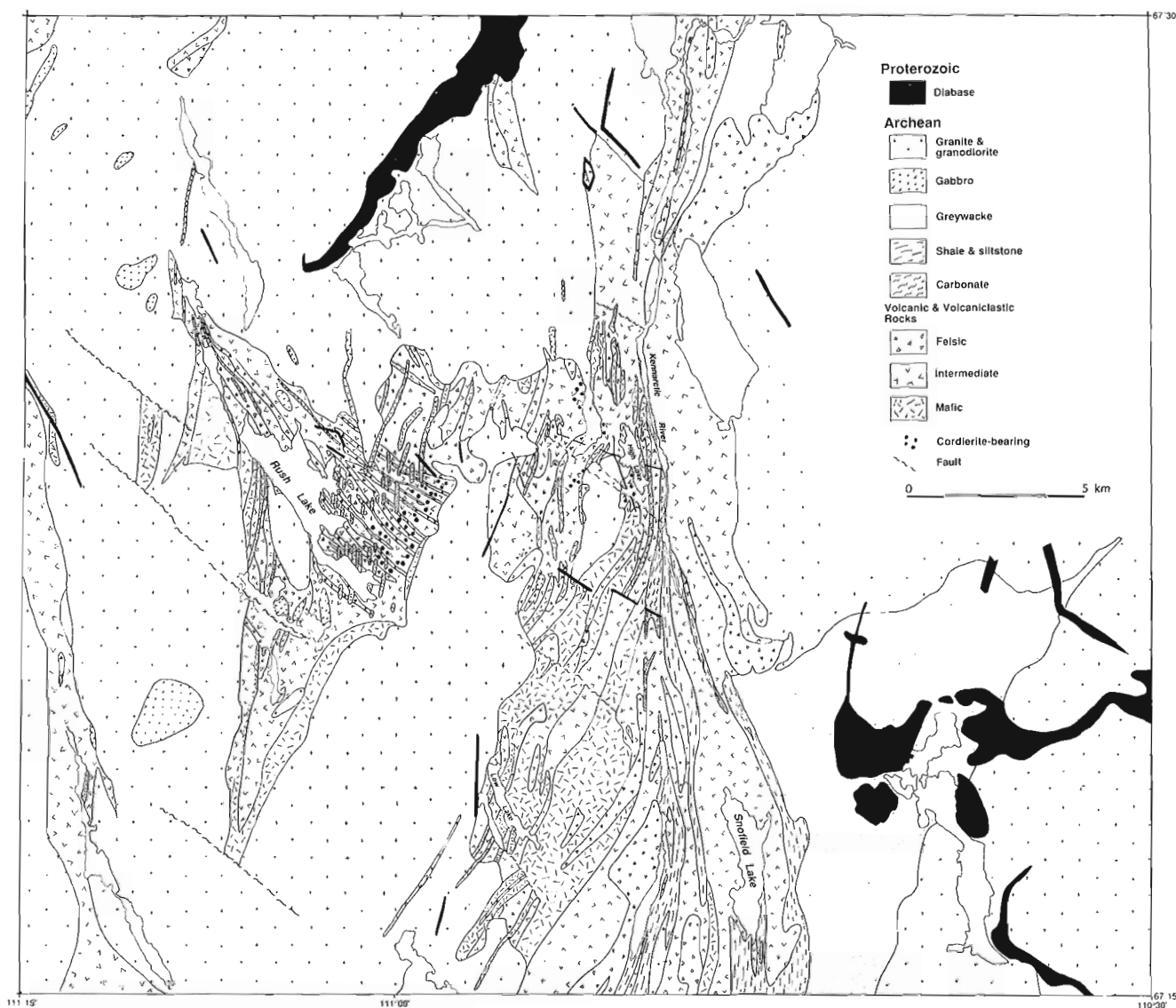
Geological sketch map of northwestern Slave structural province with the area mapped in 1993 outlined. U-Pb zircon dates (Ma) from Abraham, 1991; Mortensen et al., 1988; van Breemen et al., 1992; M. Villeneuve and O. van Breemen, pers. comm., 1992, 1993). Key to supracrustal belt abbreviations: **ARB** is Anialik River belt, **HLB** is High Lake belt, **HRB** is Hood River belt, **TLB** is Torp Lake belt. **ARIC** is ca. 2.7 Ga (Abraham et al., 1991) Anialik River intrusive complex. See text for discussion.

indicate the presence of at least two sequences of supracrustal rocks separated by an angular unconformity within the Yellowknife Supergroup in the northwestern Slave Province.

### LITHOLOGICAL SEQUENCES IN THE CENTRAL PART OF THE HIGH LAKE BELT

Interpretation of map patterns from geological mapping completed in 1993 (Fig. 2) suggests the presence of two compositionally distinct supracrustal sequences that are separated by an angular discordance in the vicinity of Rush Lake (Fig. 3). The discordance has not been observed in outcrop, and its presence is detected on the basis of a marked change in structural trend between two compositionally different

volcanic successions. In the Rush Lake area, as well as the Canoe Lake area mapped in 1992 (Henderson et al., 1992, 1993), the contact between felsic-intermediate and mafic volcanic rocks is abrupt and coincides with a change in strike which is not easily explained by folding or faulting. Southeast of Rush Lake (Fig. 3) the angular discordance is interpreted to be an unconformity based on the occurrence of eastward-younging pillowed basalt flows which are assigned to the base of a younger volcanic sequence. In this interpretation, an older felsic volcanic sequence in the Rush Lake-High Lake area is overlain unconformably by a mafic to felsic volcanic and sedimentary sequence that occurs mainly to the east of Rush Lake in the area of Low Lake and Snofield Lake (Fig. 4). Regionally, the younger sequence of rocks youngs eastward. In this paper, the supracrustal rocks are tentatively assigned to two informal sequences: an older Rush Lake sequence, and a younger Snofield Lake sequence. Additional



**Figure 2.** Generalized lithological map of the central part of High Lake greenstone belt (76M16 east & 76M17). Regional metamorphism within the area shown is chlorite grade (after Henderson et al., 1994).

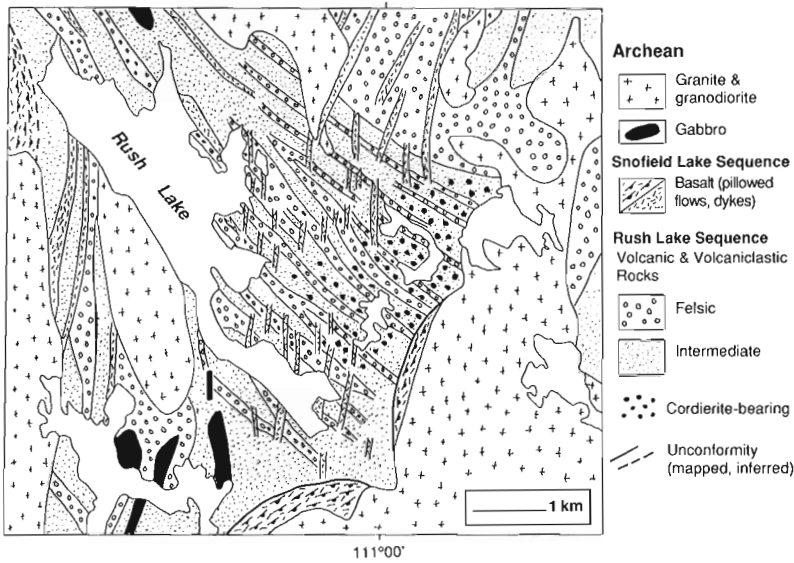


Figure 3.

Lithological sketch map of the Rush Lake area showing the trace of the apparent unconformity separating the Rush Lake and Snofield Lake sequences of supracrustal rocks. See text for discussion.

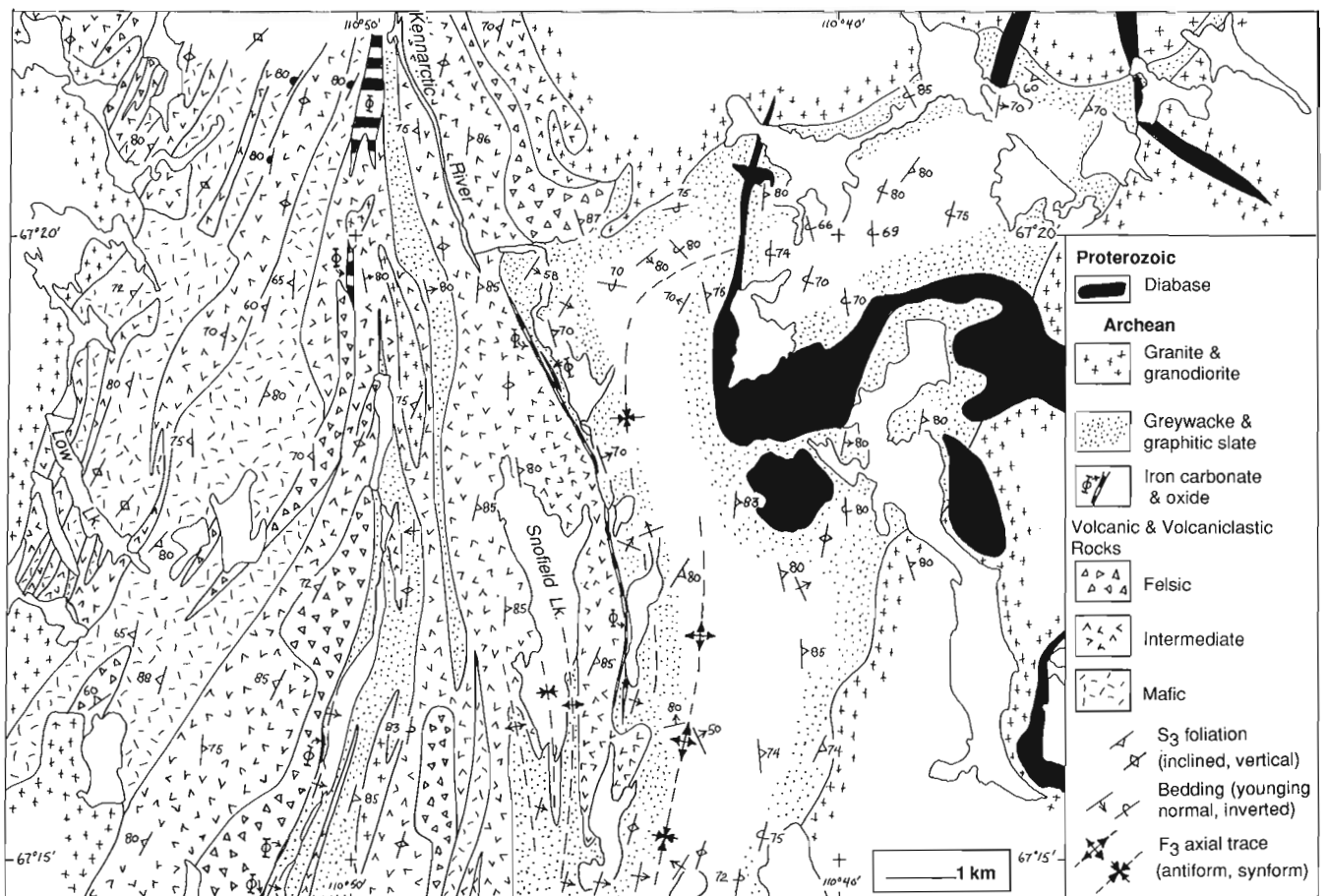


Figure 4. Geological sketch map of the Snofield Lake area. Note the regional eastward-younging of the Snofield Lake sequence of volcanic, volcanoclastic and sedimentary rocks, and the dome-and-basin fold interference pattern in the greywacke turbidites east of Snofield Lake. See text for discussion.

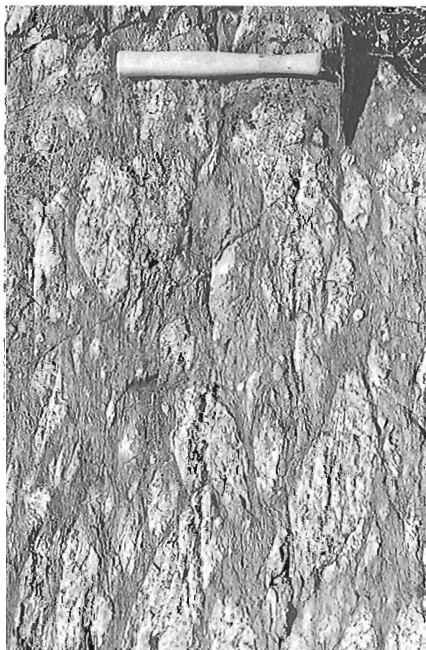
mapping and U-Pb zircon geochronology is required to verify the stratigraphy and confirm the presence of a regional unconformity.

Late Archean plutonic rocks of diorite, granodiorite, and granite composition intruded the volcanic and sedimentary sequences ca. 2.6 Ga, late in the tectonic history. The Archean rocks are intruded by numerous undeformed Proterozoic diabase, some of which appear to be feeders to extensive subhorizontal sheets (Fig. 1, 2). Diabase has not been dated, and probably includes both Franklin and Mackenzie components.

### ***Rush Lake sequence***

Mainly felsic flows and volcanoclastic rocks comprise the Rush Lake sequence (Fig. 3). The volcanoclastic rocks are not bedded, and lapilli to breccia sized clasts are variably flattened parallel to the vertical north-northeast-trending regional foliation (Fig. 5). No bedded sedimentary rocks have been recognized in the Rush Lake sequence, and contacts between flows and volcanoclastic rocks are sharp. The map units generally are discontinuous.

In the vicinity of Rush Lake and High Lake, felsic volcanic and volcanoclastic rocks contain centimetre-size cordierite porphyroblasts ("dalmatianite") believed to result from hydrothermal alteration (L. Covello, pers. comm., 1993). Regionally, the contacts mapped between formational



**Figure 5.** Photograph of felsic volcanic breccia on a subhorizontal surface exposed at the southwest shore of High Lake. Clasts are moderately flattened parallel to the north-striking regional cleavage (hammer scale is 35 cm). In nearby cleavage-parallel exposures, clasts are vertically elongated ca. 2:1. GSC 1993-249D

units in the Rush Lake area strike northwest, at a large angle to the foliation, and are cut by vertical northerly striking mafic dykes. The mafic dykes are weakly to strongly foliated, and have finer grained margins. They may be feeder dykes to pillowed basalts interpreted to unconformably overlie the Rush Lake felsites (Fig. 3), and they are tentatively assigned to the younger Snofield Lake sequence.

### ***Snofield Lake sequence***

Pillowed basalt and andesite form the base of the Snofield Lake sequence (Fig. 4). Less-deformed pillows indicate that the sequence youngs to the east, and the proportion of felsic volcanic and volcanoclastic rocks increases eastward in the succession. South of Snofield Lake, intermediate composition volcanic rocks grade into poorly-bedded and unsorted volcanic sandstones and conglomerates in the James River area (Henderson et al., 1992, 1993). Two horizons of iron-rich chemical sedimentary rocks occur within the Snofield Lake sequence. A lower horizon of mainly carbonate and minor magnetite-chert iron-formation trends discontinuously from the east side of High Lake (Fig. 2) to south of the James River (Canoe Lake area; Henderson et al., 1992, 1993). An upper carbonate horizon with several occurrences of stromatolites (Henderson, 1975), occurs in two discontinuous bands at the top of the intermediate to felsic volcanic rocks in the Snofield Lake sequence east of Snofield Lake. Black, graphitic slate and psammitic to pelitic, graded turbidite beds overlie the upper carbonate horizon as well as the black slate. Graphitic slate and siltstone lenses commonly are found within felsic volcanic and volcanoclastic rocks comprising the upper part of the Snofield Lake sequence. These rocks extend as a continuous band in the Kennarctic River valley east of High Lake for about six kilometres to the south, and they occur as numerous smaller lenses in the intermediate to felsic volcanic rocks west of Snofield Lake (Fig. 2).

East of Snofield Lake, psammitic to pelitic greywacke turbidites overlie black slate and carbonate beds and include the youngest rocks of the Snofield Lake sequence (Fig. 2, 4). The greywacke turbidites are truncated by granitic rocks that define the eastern margin of the High Lake greenstone belt.

## **DEFORMATION, PLUTONISM, AND METAMORPHISM**

The structural history of central High Lake greenstone belt is polyphase, and structural fabrics are heterogeneously developed. In places the rocks exhibit an early deformation defined by folds with limbs that are transected by the main regional cleavage (Fig. 6). This cleavage is axial-planar to steeply-plunging tight to isoclinal folds. Batholith margins are commonly parallel with and overprinted by the regional cleavage, and they are therefore believed to be mainly syntectonic. Solid-state fabrics are uncommon in most batholith interiors, suggesting that crystallization outlasted deformation. Metamorphic grade in the greenstones is low (chlorite) throughout the central part of the belt, and higher-grade contact metamorphic aureoles were not observed. Anomalous local

occurrences of cordierite porphyroblasts in felsic volcanic and volcanoclastic rocks (Fig. 2, 3) may result from hydrothermal alteration, and are a subject of current study.

### ***Structural fabric elements and deformation sequence***

Structural fabric elements, and the deformation sequence are defined as follows.

Bedding in sedimentary rocks and primary flow layering in volcanic rocks is  $S_0$ . It is defined by differences in mineral composition and texture observed on the mesoscale.

The first deformation,  $D_1$ , is responsible for the vertical angular unconformity between the Rush Lake sequence and the Snofield Lake sequence. Aphanitic felsites in the Rush Lake sequence do not preserve a mesoscopic foliation associated with this event, but a premetamorphic foliation is preserved in cordierite porphyroblasts which are flattened in the regional foliation ( $S_3$ , see below).

Within the younger Snofield Lake sequence, noncylindrical folds in bedding that are transected by the regional cleavage are defined as  $F_2$  (Fig. 5). The  $F_2$  folds are distinguished also by noting changes in structural facing on regional cleavage surfaces (i.e., the direction that graded beds young when observed on the cleavage; cf. Borradaile, 1976). These early folds do not appear to have an associated axial-planar cleavage, nor does there appear to be a bedding-parallel foliation in the rocks. However, Henderson et al. (1993) described a locally developed bedding-parallel  $S_1$  tectonic fabric south of the James River in the Ulu Lake area that is folded in the core of the  $F_2$  Ulu anticline. The early folds in the Snofield Lake sequence formed during the second regional deformation,  $D_2$ , and, where they are best developed east of Snofield Lake (Fig. 4), apparently are upright, subhorizontal folds at a moderate angle to the main regional folds and cleavage.

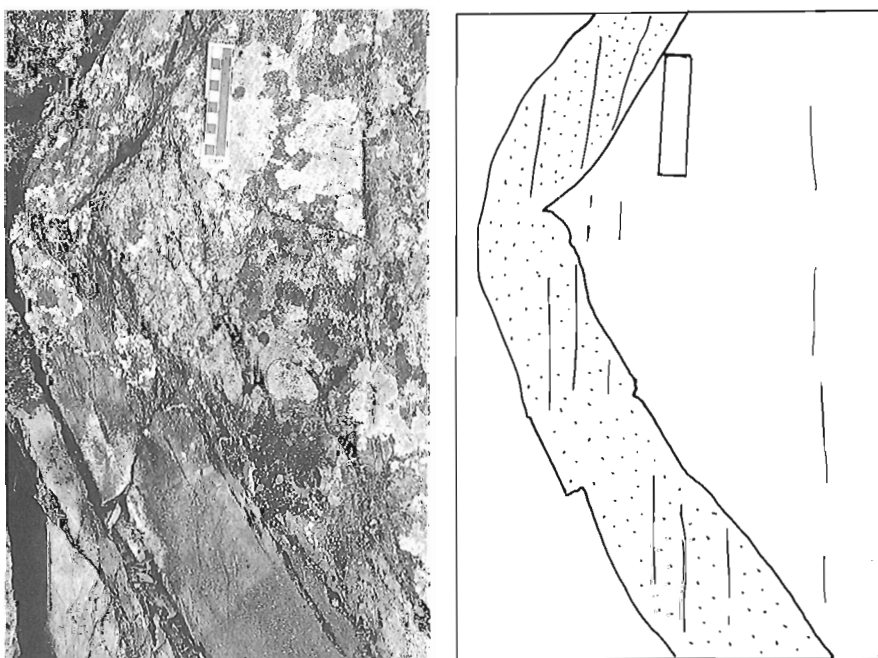
The regional cleavage is designated  $S_3$ , and is related to the third deformation in the belt,  $D_3$ . The  $S_3$  foliation is a slaty and spaced cleavage, defined by aligned muscovite and chlorite in pelitic and psammitic rocks. Most commonly, the  $S_0 \times S_3$  intersection lineation is steeply-plunging. Finite or bulk strain is defined by ellipsoidal fragments in tuffaceous rocks that also are aligned parallel to the  $S_3$  cleavage. Rarely, elongated fragments define a down-dip lineation in the cleavage. Locally developed cordierite porphyroblasts are aligned in  $S_3$ , and the cleavage is deflected around the porphyroblasts. By comparison, in the southern part of the belt, Henderson et al. (1993) observed that regional cordierite porphyroblastesis predates the  $S_3$  cleavage.

The major folds in the region generally are north-trending, steeply-plunging and tight to isoclinal. They are defined as  $F_3$ . The  $S_3$  cleavage is axial-planar to these folds where they are best developed around the south end of Snofield Lake (Fig. 4).

### ***Structural geometry and kinematics***

The absence of bedded rocks in the felsic Rush Lake sequence (as well as in the lower volcanic part of the Snofield Lake sequence) makes it difficult to define the geometry of the rocks. However, careful mapping indicates that contacts between volcanic and volcanoclastic rocks in the Rush Lake sequence (Fig. 3) are steeply inclined, and the formational (i.e. mappable) units strike northwesterly, in contrast to the north-northeasterly regional trend of the belt (Fig. 2). Mafic dykes in the area of Rush Lake, which are correlated with the pillowed flows at the base of the Snofield Lake sequence, appear to be coincidentally subparallel to the  $S_3$  cleavage.

All formational contacts appear to bend progressively into parallelism with the  $S_3$  cleavage as the Kennarctic River is approached, and this defines a zone of relatively strong,



***Figure 6.***

*Photograph and sketch of an open (?)  $F_2$  fold in greywacke beds transected by the north-striking regional  $S_3$  cleavage (10 cm scale). Horizontal outcrop located ca. 2 km northeast of Snofield Lake. GSC 1993-249B*



apparently coaxial flattening, and moderate vertical extension. Subhorizontal lenticular calcite veins are abundant along the Kennarctic River east of High Lake (Fig. 2) in the zone of high D<sub>3</sub> strain, and a shallowly-dipping crenulation of S<sub>3</sub> is weakly developed in this zone. The increment of vertical extension recorded by the flat veins is less than five per cent, but the bulk vertical extension could be much greater. The subhorizontal crenulation is developed best in slates with strong S<sub>3</sub> fabrics, and is an expression of a very weak vertical shortening strain increment.

In the area southwest and south of Snofield Lake, macroscale steeply plunging isoclinal F<sub>3</sub> folds (Fig. 4) with S<sub>3</sub> cleavage parallel to their axial surfaces were mapped in graded siltstone and sandstone beds. East of the upper carbonate horizon, outcropping to the east of Snofield Lake, several kilometre-scale domes and basins are defined by progressive changes in structural facing in low-grade greywacke turbidite and slate beds. This dome-and-basin interference pattern appears to be a combination of easterly

striking upright horizontal F<sub>2</sub> folds, and north-striking F<sub>3</sub> folds. The suggestion that F<sub>2</sub> folding was about easterly, subhorizontal axes needs additional documentation by mapping of systematic F<sub>3</sub> plunge reversals. The F<sub>3</sub> folds bend to the east, parallel to the north margin of the area of greywacke turbidites. This may be due in part to the competent intermediate and felsic volcanic rocks, and to the discordant granite at the north margin of the turbidite basin (Fig. 4). The effect of late granite intrusions on their wall rock structure is a subject of ongoing research.

The main D<sub>3</sub> deformation in the central part of High Lake belt is due to heterogeneously developed coaxial east-west shortening. In the zone of high bulk strain along the Kennarctic River east of High Lake, some vertical extension is also indicated. The granites surrounding the greenstone belt seem to be less strained than the supracrustal rocks, and whether they played an active role in the deformation of the belt, or whether they were emplaced passively relatively late in D<sub>3</sub> is a subject of continuing research. However, areas

**Table 1.** Table of mineral occurrences. Status: (1) current producer, (2) past producer, (3) extensively drilled, (4) drilled occurrence, (5) trenched occurrence, (6) showing.

ID	NTS	Principal Commodities	Occurrence Name	Host Rock (Map Unit)	Status	References
1	76M/6	Cu	Kennarctic Showing #7	felsic volcanic rocks near granitoid	6	DIAND AR 017159
2	76M/6	Cu	Kennarctic Showing #6	mixed volcanic rocks near granitoid	6	DIAND AR 017159
3	76M/6	Cu-Zn-Pb	Rush	felsic to intermediate volcanic rocks	4	DIAND AR 080485; MIR 1975, p. 75
4	76M/6	Cu-Zn-Fe	Nite	intermediate to felsic volcanic rocks	5	DIAND AR 080485; MIR 1975, p. 75
5	76M/6	Cu	Pie	felsic to intermediate volcanic rocks	6	DIAND AR 080482; MIR 1975, p. 70
6	76M/7	Cu-Zn	Chichi Lakes	mixed felsic and basaltic volcanic rocks	6	DIAND AR 080187
7	76M/7	Cu-Zn	Bow Lake	intermediate volcanic rocks	6	DIAND AR 080187
8	76M/7	Cu	SW of Gossan Lake	mixed volcanic rocks	6	DIAND AR 080187
9	76M/7	Cu-Zn	S of Low Lake	mixed volcanic rocks	6	DIAND AR 080187
10	76M/7	Cu	And Lake	mixed volcanic rocks	4	DIAND AR 080187
11	76M/7	Cu	SW end of Low Lake	mixed volcanic rocks	6	DIAND AR 080187
12	76M/7	Cu	Gossan Lake	mixed volcanic rocks	6	DIAND AR 080187
13	76M/7	Cu	NW end of Arrow Lake	mixed volcanic rocks	6	DIAND AR 080187
14	76M/7	Zn	NE end of Arrow Lake	mixed volcanic rocks	6	DIAND AR 080187
15	76M/7	Cu	Fog Lake	mixed volcanic rocks	6	DIAND AR 080187
16	76M/7	Cu-Zn	N end of Fog Lake	mixed volcanic rocks	6	DIAND AR 080187
17	76M/7	Cu-Zn	unnamed lake	mixed volcanic rocks	6	DIAND AR 080187
18	76M/7	Cu-Zn-Au-Ag-Pb	High Lake AB Zone	intermediate to felsic volcanic rocks	3	GSC Open File 239; GSC Paper 70-17, p. 84
19	76M/7	Cu-Zn-Pb	High Lake C Zone	intermediate to felsic volcanic rocks	3	GSC Open File 239
20	76M/7	Zn-Cu-Pb-Ag-Au	High Lake D Zone	intermediate to felsic volcanic rocks	3	GSC Open File 239
21	76M/7	Cu-Zn-Pb	High Lake E Zone	intermediate to felsic volcanic rocks	3	GSC Open File 239
22	76M/7	minor Cu	DC	intermediate volcanic rocks	6	DIAND AR 080626; MIR 1975, p.73
23	76M/7	minor Cu	FM	felsic volcanic rocks	6	DIAND AR 080626; MIR 1975, p. 75
24	76M/7	Cu	King (Chill) Grid A	intermediate volcanic rocks	5	DIAND AR 080399, 017140; MIR 1976, p. 91
25	76M/7	Cu	King (Chill) Grid B	felsic volcanic rocks	6	DIAND AR 080399, 017140; MIR 1976, p. 91
26	76M/7	Cu-Zn	Hi (980 Lake)	intermediate volcanic rocks	4	DIAND AR 080558; MIR 1976, p. 91
27	76M/7	Zn-Ag	Pan	intermediate volcanic rocks	4	DIAND AR 080551; MIR 1976, p. 92
28	76M/7	Au-Zn-Pb-Ag-Cu	Cairo	intermediate to felsic volcanic rocks	6 (??)	DIAND AR 082986

where the supracrustal belt narrows appear also to show the highest strain, and the regional cleavage appears to bend into parallelism with the batholith margins.

Northwesterly-striking faults are common in the area. Several sets of northerly- or northwesterly-striking mafic dykes were emplaced during the Late Proterozoic. Remnants of flat-lying diabase sheets are probably related to fissure eruptions or sills emplaced during the 723-718 Ma (Heaman et al., 1992) Franklin igneous event.

### ECONOMIC GEOLOGY

The High Lake greenstone belt contains many gossans as well as numerous occurrences, prospects, and deposits, including the synvolcanic massive sulphide and stringer zone mineralization

at High Lake (Johnson, 1974), and the epigenetic vein-controlled gold mineralization of the Flood Zone on the Ulu property (Flood, 1991; Henderson et al., 1992, 1993).

Information in the public domain has yielded data on 70 occurrences and 39 gossanous areas (Kerswill et al., 1993) in that portion of the High Lake greenstone belt which extends from south of the Hood River (76L/15 and 16) to the Arctic coast (76M/10). Twenty-eight occurrences in 76M/6 and 7 have been classified on the basis of their metal inventory into base metal, gold, or mixed types (Table 1). All of the occurrences are hosted by intermediate to felsic volcanic and volcanoclastic rocks, and the sulphide mineralization examined in the Rush Lake and High Lake areas appears to be synvolcanic, and can be assigned to either a conformable, massive to disseminated style or to a discordant, fracture controlled style. The mineral occurrences are located on Figure 7, which also shows a preliminary boundary between

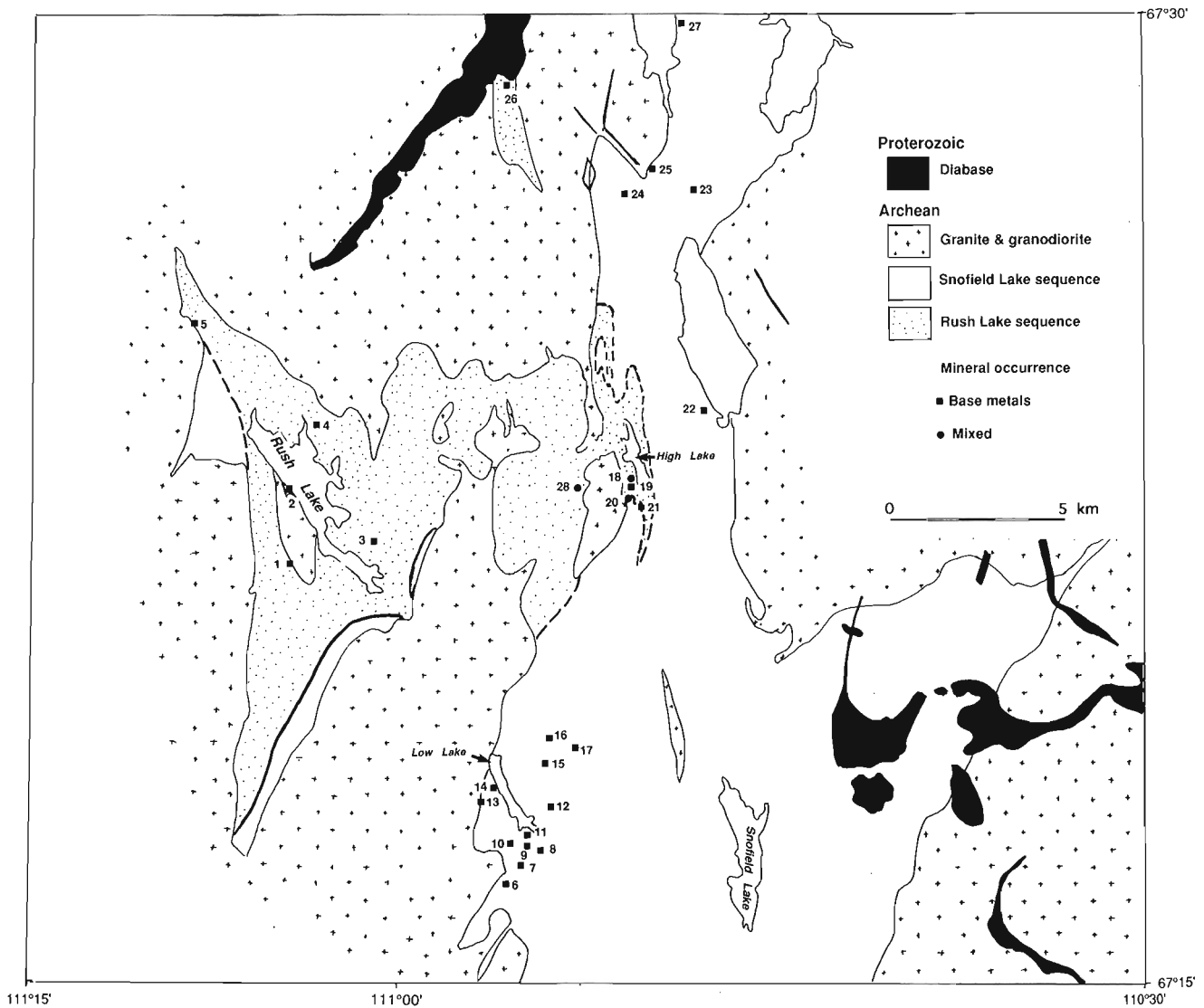


Figure 7. Map of the central part of High Lake greenstone belt showing the apparent distribution of the Rush Lake and Snofield Lake sequences with locations of principal mineral occurrences listed in Table 1.

the Rush Lake and Snofield Lake sequences. Twenty-five of the occurrences are of the base metal type. The High Lake AB and D deposits, and the nearby Cairo occurrence are of mixed character. The High Lake deposit is tentatively assigned to the Rush Lake sequence.

Detailed petrographic and lithochemical studies on samples from the High Lake belt, including those from six occurrences and several gossans in 76M/6 and 7, are currently underway to better define the distributions of sulphide minerals, gold, and associated alteration products. This information, combined with data on the geological settings of mineralization, may help define metallogenic zoning and identify new exploration targets.

Several cordierite-rich zones ("dalmatianite") of apparent hydrothermal alteration similar to those which occur at High Lake (Johnson, 1974) were identified during bedrock mapping and mineral occurrence sampling in 1993 (Fig. 2, 3, and 7). An extensive area near Canoe Lake (NTS 76M/3), which was mapped as metagreywacke because of the presence of cordierite porphyroblasts (Henderson et al., 1992, 1993), probably should be reconsidered as hydrothermally-altered intermediate and felsic volcanoclastic rocks because they are not bedded and regionally the metamorphic grade is low. The Canoe Lake "alteration" zone occurs adjacent to an area of known mineralization, but the "alteration" extends considerably beyond the known sulphide occurrences.

## SUMMARY AND CONCLUSION

Preliminary interpretation of geological map patterns suggests that two sequences of volcanic rocks separated by an angular unconformity attributed to an enigmatic D<sub>1</sub> can be defined in the central part High Lake greenstone belt. Volcanoclastic rocks are not bedded in the older Rush Lake sequence, but lithological contacts trend northwesterly relative to north-northeasterly striking S<sub>3</sub> cleavage. The Rush Lake sequence consists of felsic-intermediate flows and tuffs that apparently are hydrothermally altered in places as indicated by cordierite porphyroblasts. The Rush Lake sequence northeast of Rush Lake is cut by cleavage-parallel mafic dykes, and is overlain by pillowed basalt flows forming the base of the Snofield Lake sequence. The Snofield Lake sequence youngs to the east, and the volcanic rocks become more felsic towards the top of the succession. Chemical sedimentary rocks occur at two horizons within the sequence; the lower is mainly iron-rich carbonate with minor magnetite and chert beds, and the upper is carbonate with some stromatolite occurrences. Graphitic slate occurs in proximity to the carbonate horizons and also in proximity to felsic-intermediate volcanic and volcanoclastic rocks. Psammitic turbidites tend to occur above the black slates, and comprise the youngest part of the Snofield Lake sequence.

The structural sequence comprises three events. D<sub>1</sub> brought the Rush Lake sequence to the vertical before the emplacement of mafic dykes and pillowed flows, and apparently imposed an early cleavage on the volcanic rocks that is preserved within cordierite porphyroblasts. F<sub>2</sub> folds appear to be upright subhorizontal structures transected by S<sub>3</sub>

cleavage that is axial-planar to vertical north-trending F<sub>3</sub> folds. Regional metamorphism is chlorite grade, and predates S<sub>3</sub>. Granite emplacement is coeval with D<sub>3</sub>, and S<sub>3</sub> is a flattening foliation in the central part of the High Lake belt. The tectonic relationship between S<sub>3</sub> and granite intrusion is subject to continuing study. Local development of cordierite porphyroblasts in the greenschist regional metamorphic terrane due to early hydrothermal alteration of felsic volcanic and volcanoclastic rocks is being investigated.

The Rush Lake sequence is lithologically very similar to rocks in the Canoe Lake area dated at  $2696 \pm 4$  Ma and at  $2695 \pm 3$  to the north of the James River. The Snofield Lake sequence may be correlative with volcanic and sedimentary rocks in the vicinity of the rhyolite midway between the James and Hood rivers dated at  $2616 \pm 3$  Ma (Fig. 1).

In the High Lake greenstone belt it may be possible to determine which of several volcanic/sedimentary sequences of significantly different ages has the greatest potential to host synvolcanic mineralization.

## ACKNOWLEDGMENTS

Zaira Arias, John Dehls, Hendrik Falck, Tom Wright, and Matt O'Keefe made significant contributions to the mapping. We thank Covello, Bryan and Associates for casual helicopter charters, and sharing of logistical support at their High Lake camp. We also thank BHP Minerals Canada for casual helicopter charters, and for many courtesies at their Crown Lake camp. We greatly benefitted from the insights of Lou Covello and members of the High Lake Geological Discussion Group on High Lake belt geology. Bob Bretzlaff compiled much of the information on mineral occurrences. Otto van Breemen and Mike Villeneuve generously provided preliminary age dates. John B. Henderson and Karen Connors reviewed the manuscript.

## REFERENCES

- Abraham, A.P.G., Kamo, S.L., Davis, D.W., and Spooner, E.T.C.  
1991: Geochronological constraints on magmatic evolution and gold mineralization in the Aniak River area, Slave province; Geological Association of Canada-Mineralogical Association of Canada, Program with Abstracts, v. 16, p. A1.
- Borradaile, G.J.  
1976: "Structural facing" (Shakleton's rule) and the Paleozoic rocks of the Malaguide Complex near Vélez Rubio, SE Spain; Proceedings, Koninklijke Nederlandse Akademie van Wetenschappen, Series B, v. 79, p. 330-336.
- Easton, R.M., Ellis, C.E., Dean, M., and Bailey, G.  
1982: Geology of the Typhoon Point map area, High Lake greenstone belt (76M/10 and 76M/15 south-half); Indian and Northern Affairs Canada, NAP, Geology Division Yellowknife EGS 1982-6, scale 1:31 680.
- Flood, E.  
1991: BHP-UTAH Mines Ltd. Ulu gold property; in Exploration Overview 1991, (ed.) J.A. Brophy; Indian and Northern Affairs Canada, Geology Division, Yellowknife, p. 22.
- Heaman, L.M., LeCheminant, A.N., and Rainbird, R.H.  
1992: Nature and timing of Franklin igneous events, Canada: Implications for a Late Proterozoic mantle plume and the break-up of Laurentia; Earth and Planetary Science Letters, v. 109, p. 117-131.

**Henderson, J.B.**

1975: Archean stromatolites in the northern Slave province, Northwest Territories; *Canadian Journal of Earth Sciences*, v. 12, p. 1619-1630.

**Henderson, J.R., Arias, Z., Henderson, M.N., Lemkow, D., Wright, T.O., Rice, R., and Kerswill, J.A.**

1992: Geology and mineral occurrences of the central High Lake greenstone belt Slave Province, Northwest Territories; Geological Survey of Canada, Open File 2547, scale 1:100 000.

**Henderson, J.R., Henderson, M.N., Kerswill, J.A.**

1994: Preliminary geological map of north central High Lake greenstone Belt; N.W.T., NTS 76M/6 East, 76M/7; Geological Survey of Canada, Open File 2782, scale 1:50 000.

**Henderson, J.R., Henderson, M.N., Kerswill, J.A., Arias, Z., Lemkow, D., Wright, T.O., and Rice, R.**

1993: Geology and mineral occurrences of the southern part of High Lake greenstone belt, Slave Province, Northwest Territories; *in* Current Research, Part C; Geological Survey of Canada, Paper 93-1C, p. 125-136.

**Henderson, M.N., Henderson, J.R., Jefferson, C.W., Wright, T.O., Wyllie, R., and Schaan, S.**

1991: Preliminary geological map of the Hood River belt; Geological Survey of Canada, Open File 2413.

**Jackson, V.A.**

1989: Preliminary geological compilation of Hepburn Island map area (76M); Indian and Northern Affairs Canada, Geology Division, Yellowknife, EGS 1989-11, 1:125 000 scale map with marginal text and figures.

**Jackson, V.A., Bell, R., Bishop, S., Daniels, A., Howson, S., Kerr, D.E., and Treganza, M.**

1986: Preliminary geology of the eastern Hepburn Island area, NTS 76M/1, 2, 8, 9, 15, 16; Indian and Northern Affairs Canada, Geology Division, Yellowknife, EGS 1986-6, six 1:50 000 scale maps with notes.

**Johnson, W.**

1974: Geology of two base metal deposits of the Slave structural province; Geological Survey of Canada, Open File 239, 16 p.

**Kerswill, J.A., Brophy, J.A., Henderson, J.R., Henderson, M.N., Thompson, P.H., Bretzlaff, R., Arias, Z., and Garson, D.G.**

1993: Recent developments in the metallogeny of Slave province with emphasis on the Courageous Lake and High Lake greenstone belts, Northwest Territories; *in* Exploration Overview 1993, (ed.) S. Goff; Indian and Northern Affairs Canada, Geology Division, Yellowknife.

**Mortensen, J.K., Thorpe, R.I., Padgham, W.D., King, J.E., and Davis, W.J.**

1988: U-Pb zircon ages for felsic volcanism in the Slave province, N.W.T.; *in* Radiogenic Age and Isotopic Studies: Report 2, Geological Survey of Canada, Paper 88-2, p. 85-95.

**Padgham, W.A., Jefferson, C.W., Hughes, D.R., and Shegelski, R.J.**

1973: Geology of the High Lake area N.W.T. (76M7); Geological Survey of Canada, Open File 208, 1:50 000 scale geological map with marginal notes.

**Relf, C.**

1992: Preliminary geology of the northeastern Anialik River volcanic belt, N.W.T., parts of NTS 76M/10, 11, 12, 14, and 15; NWT Geology Division-NAP, EGS 1992-19, 1: 50 000 scale map and report.

**Tirru, R. and Bell, I.**

1980: Geology of the Anialik River greenstone belt, Hepburn Island map area, District of Mackenzie; *in* Current Research, Part A; Geological Survey of Canada, Paper 80-1A, p. 157-164.

**van Breemen, O., Davis, W.J., and King, J.E.**

1992: Temporal distribution of granitoid plutonic rocks in the Archean Slave province, northwest Canadian Shield; *Canadian Journal of Earth Sciences*, v. 29, p. 2186-2199.

---

Geological Survey of Canada Project 870008

# Preliminary report on the geology of the Indin Lake supracrustal belt, western Slave Province, Northwest Territories<sup>1, 2</sup>

S.J. Pehrsson and C. Beaumont-Smith<sup>3</sup>  
Continental Geoscience Division

*Pehrsson, S.J. and Beaumont-Smith, C., 1994: Preliminary report on the geology of the Indin Lake supracrustal belt, western Slave Province, Northwest Territories; in Current Research 1994-C; Geological Survey of Canada, p. 91-102.*

---

**Abstract:** Preliminary study of the Indin Lake area has identified two spatially restricted turbidite units; one coarser bedded containing felsic volcanogenic debris flows and a finer unit with iron-formation. They are intercalated with spatially separated volcanic belts characterized by mafic pillowed volcanic rocks or intermediate to felsic volcanoclastic rocks.

Four main structural sets have been recognized. The first set includes isoclinal folds without associated cleavage and foliations parallel to the volcanic belt contacts. The second set which controls the geometry of the belt includes a cleavage axial planar to meso- to macro-scale folds, and interference folds. The remaining sets are more locally developed. Repetition of the intercalated units is in part a function of third phase or later regional refolding.

The supracrustal belt is in contact with a heterogeneously deformed granodiorite-tonalite igneous complex to the east. Deformation of the complex is pre-intrusion of hornblende-biotite-granodiorite plutons.

**Résumé :** L'étude préliminaire de la région du lac Indin a permis de reconnaître deux unités turbiditiques spatialement restreintes : une unité stratifiée plus grossière contenant des coulées de débris felsiques d'origine volcanique et une unité plus fine à formation de fer. Elles sont intercalées avec des ceintures volcaniques spatialement séparées, caractérisées par des volcanites mafiques en coussins ou par des volcanoclastites intermédiaires à felsiques.

Quatre ensembles structuraux principaux ont été établis. Le premier ensemble comprend des plis isoclinaux sans schistosité associée et des foliations parallèles aux contacts de la ceinture volcanique. Le deuxième ensemble, qui contrôle la géométrie de la ceinture, comprend des plis à schistosité de plan axial d'échelle intermédiaire à grande et des plis d'interférence. Les autres ensembles sont plus localement développés. La répétition des unités intercalées est en partie fonction d'une troisième phase de déformation ou d'un replissement régional tardif.

La ceinture de roches supracrustales est en contact à l'est avec un complexe igné de granodiorite-tonalite déformé de façon hétérogène. La déformation du complexe est antérieure à la mise en place de plutons de granodiorite à hornblende-biotite.

---

<sup>1</sup> Contribution to Canada-Northwest Territories Mineral Initiative (1991-1996), an initiative under the Canada-Northwest Territories Economic Development Cooperation Agreement.

<sup>2</sup> NATMAP Slave Province Project

<sup>3</sup> University of New Brunswick, Fredericton, New Brunswick E3B 5A3

## INTRODUCTION

The Indin Lake project was undertaken to update the present understanding of the geology of the Indin Lake supracrustal belt and to provide a geological context for mineral showings in the area through 1:50 000 scale mapping and associated stratigraphic, structural, and metamorphic studies. Project funding is provided by the Canada-Northwest Territories Mineral Initiative with additional support from NATMAP.

The Indin Lake supracrustal belt is located near the western margin of the Slave Province (NTS 86B; Fig. 1). It is bounded to the west by Archean granitoid plutons and migmatites thought to be derived from the Yellowknife Supergroup. To the east it is in contact with gneissic rocks which were proposed as structural basement to the belt by Frith (1992). Previous work in the area includes 1:250 000 and 1:125 000 scale regional mapping by Lord (1942), Fortier (1949), and Frith et al. (1974). More detailed mapping at 1:50 000 scale focused on the greenstone belt (Tremblay et al., 1953; Stanton et al., 1954). Mapping in 1993 concentrated on an west-east transect through the supracrustal belt and proposed basement rocks to the east in order to establish a structural framework for the belt (Fig. 2).

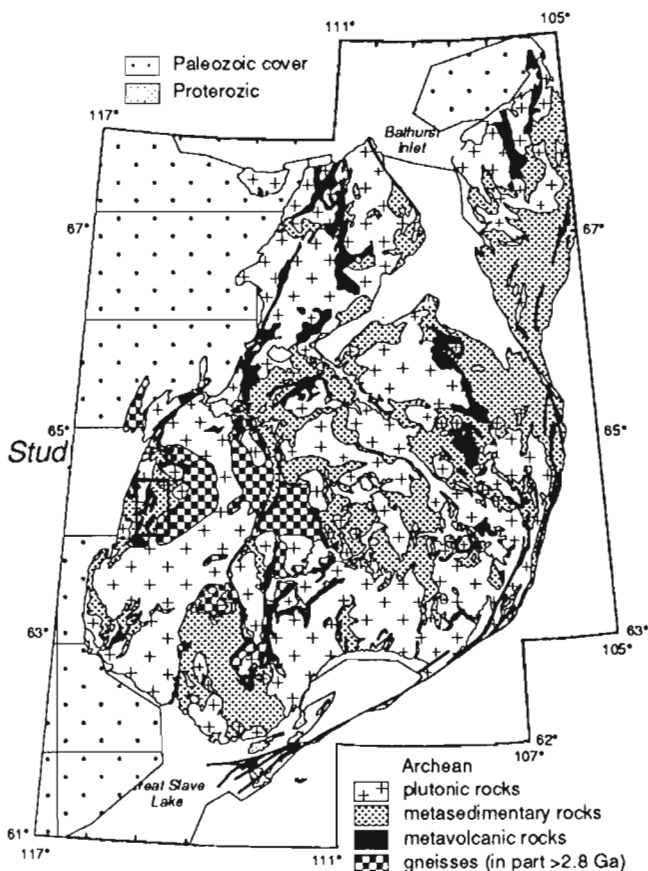


Figure 1. Location map of the study area within the Slave Province.

This preliminary report presents: (1) an overview of the lithological units of the supracrustal belt and adjacent igneous complex, including syn-turbidite deposition, felsic volcanic debris flows, and an unusual, siliceous gneiss unrecognized elsewhere in the Slave Province; (2) a preliminary description of structural elements; and (3) a discussion of the nature of the supracrustal belt stratigraphy. All rock units under consideration are metamorphosed to lower greenschist to amphibolite facies conditions. For clarity the prefix "meta" has been omitted from the lithological names.

## SUPRACRUSTAL ROCKS

Supracrustal rocks of the area include a variety of volcanic and volcanoclastic units, greywacke-mudstone turbidites, and iron-formation. Previous workers have correlated the supracrustal rocks at Indin Lake with the Yellowknife Supergroup (Frith, 1992). Volcanic and volcanoclastic rocks comprise a number of large north-northeast-trending belts, 12 to 30 km long and 2 to 5 km wide, which are intercalated with sedimentary rocks. The major belts are informally named the Hewitt Lake, Leta Arm, Burn Inlet, Snare River, Baton Lake, Chalco Lake, and Gamey Lake belts (Fig. 2). Their contacts with adjacent turbidite domains coincide with zones of very strong foliation development and attenuation of primary volcanic features. Variation in younging directions from pillowed flows and graded bedding across and along strike in the supracrustal belt indicates that the intercalated sequence is not in conformable contact. Consequently the volcanic belt-turbidite contacts are interpreted as being tectonically modified.

### Mafic volcanic rocks (unit 1)

Mafic volcanic rocks occur within major north-northeast-trending volcanic belts and smaller lenses surrounded by greywacke-mudstone turbidites. Typically they comprise amygdaloidal, green-weathering pillowed flows with local interflow breccias. Associated coarse grained, massive units are interpreted as subvolcanic gabbro intrusions. Mafic rocks comprise the bulk of the Hewitt Lake, Burn Inlet, Chalco Lake, and Gamey Lake belts (Fig. 2) within which the unit ranges from 250-500 m wide bands to a maximum thickness of 3800 m. Mafic volcanic rocks, are also interstratified with felsic and intermediate volcanic rocks in the Leta Arm and Baton Lake belts, where the proportion of mafic breccias is greater. The volcanic packages marginal to the supracrustal belt are dominated by the pillowed mafic flows and are termed Hewitt Lake type belts. Those in the central part of the belt are more heterogeneous and volcanoclastic dominated and are termed Leta type. The presence of reversed pillow facing directions in the Gamey Lake belt and ductile high strain zones in the Hewitt Lake belt suggest that the mafic pile has been thickened by folding and/or faulting.



### *Intermediate volcanic rocks (unit 2)*

Intermediate volcanic rocks are light green- to grey-weathering and typically occur as breccias, fine grained volcanoclastic units, or as plagioclase-phyric pillowed flows. Quartz diorite sills are found within the pillowed, intermediate composition flows of the Baton Lake belt. Their spatial association and similar composition suggest that they may be genetically related to the volcanic rocks. Volcanoclastic rocks comprise greater than 60% of the intermediate volcanic rocks within the Leta Arm belt and less 30% of the Baton Lake belt (Fig. 2). The unit is typically 1000 m thick or less. Other intermediate composition volcanoclastic rocks are found as thin horizons near the margins of the mafic-dominated belts.

### *Felsic volcanic rocks (unit 3a, b, c)*

Felsic volcanic rocks can be divided into 3 main subunits. Unit 3a comprises pale pink- to white-weathering felsic breccias, fine grained volcanoclastic rocks, and associated quartz porphyritic intrusive bodies which occur in discontinuous, lenticular segments up to 1000 m thick (Fig. 3a). Where adjacent to mafic pillowed flows, the unit contains mafic fragments, a relationship which strongly indicates conformable or disconformable contacts. The unit is typically moderately foliated. This assemblage occurs within the Leta Arm and Baton Lake belts.

Unit 3b comprises distinctive, matrix-supported felsic debris flows found within unit 4a turbidites in the western part of the map area (Fig. 2). Clasts within the flows are subrounded to angular, predominantly buff- to white-weathering, aphanitic felsic volcanic rock. The matrix is siliceous and aphanitic. Some fragments have an internal banding, possibly flow banding, and may be derived from rhyolite flows. Texture is seriate and clast size ranges from lapilli to bomb size. These flows are preserved as tabular to irregular pod-like bodies, 0.5-5 m thick and up to 25 m long. At its contact with the turbidites, the debris flow matrix is sandy to shaley, while within the flow it is composed of very fine grained to aphanitic felsic material, possibly ash (Fig. 3b). Local blocks of turbidite occur within the flows. Contacts with the turbidites are interpreted as conformable or disconformable.

Unit 3c comprises buff- to pale yellow-weathering, felsic clast-supported breccias, finer volcanoclastic rocks, and quartz phenocrystic massive aphanitic units (possibly flows). The main occurrence of unit 3c is as a dome-shaped body on the south shore of Indin Lake (Fig. 2). Its margins are characterized by volcanoclastic rocks which include angular tuffaceous and carbonate fragments, several centimetres in diameter, in a fine grained felsic matrix. Towards the interior of the body the clast size increases and the unit becomes a clast-supported breccia with equant to tabular blocks up to 0.5 m long. Clast alignment in the breccias may be primary. The complex could represent a felsic volcanic centre. White-weathering porphyritic felsic dykes, spatially associated with this subunit, and possibly feeders to it, intrude the adjacent Gamey Lake belt.

### *Greywacke-mudstone turbidites (unit 4a, b)*

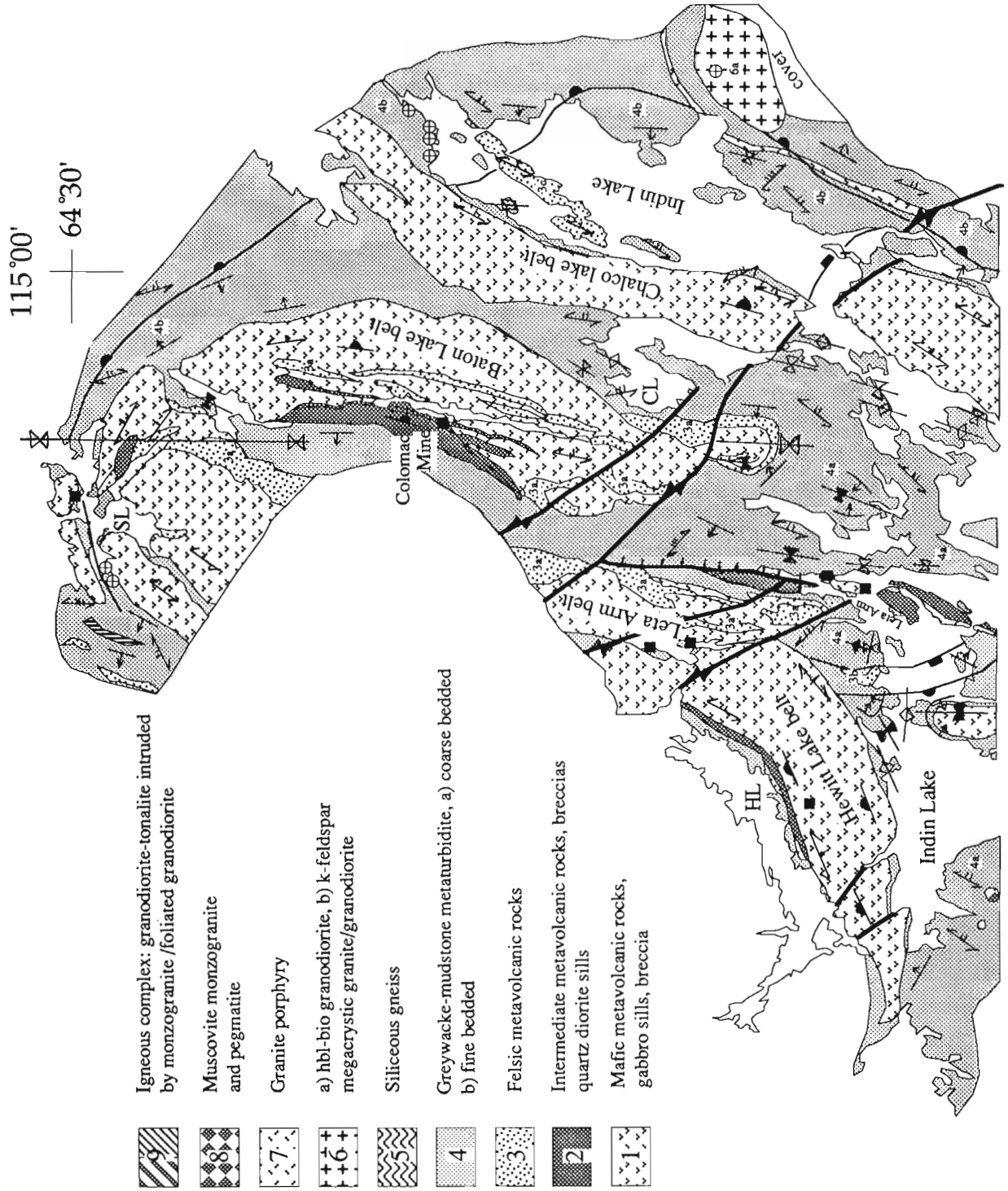
Two facies of greywacke-mudstone turbidites were distinguished. One, here designated unit 4a, outcrops in the central and western part of the map area and is characterized by relatively thick bedded (15-100 cm thick) greywacke-mudstones (Fig. 3c). The proportion of greywacke to mudstone is generally 3:2. Coarse sand horizons, up to several metres thick, are common and may represent amalgamated beds. Primary structures such as flames, graded bedding, ball and pillow structures, mud rip-ups, and calcareous concretions typify this sequence. West of Leta Arm at least five felsic, volcanogenic debris flows are interstratified with unit 4a turbidites (Fig. 3b). Greywacke-mudstone turbidites within 1-2 m of the debris flow contacts contain synsedimentary slumps, isoclinal, and faults, possible evidence for a tectonically active environment during deposition (Fig. 3d).

In contrast, greywacke-mudstones in the eastern part of the map area, designated unit 4b, are predominantly finely bedded rhythmites, often laminated with graded beds 1 cm or less thick (Fig. 3e). The proportion of greywacke to mudstone is generally less (1:1) and primary sedimentary features other than graded bedding are rare. Minor fine grained felsic horizons, possibly of volcanoclastic origin, are locally present. The mudstones are locally pyritic and weather rusty, and silicate or oxide facies iron-formation occurs as mappable horizons and lenses within the fine bedded turbidities (Fig. 3f). Iron-formation is presently found only within the unit 4b turbidites. Occurrences are restricted to the eastern and northern margins of the supracrustal belt (Fig. 2). The iron-formation is banded (BIF) with alternating chert and grunerite-garnet-pyroxene rich beds or chert nodules in the silicate facies banded iron-formation, and chert and magnetite beds in the oxide facies banded iron-formation. Sulphides occur locally with the silicate facies banded iron-formation. The iron-formation is typically found as thin, less than 1 m thick, continuous bands or irregular pods. Occurrences generally have three or more such bands separated by rusty turbidites. Locally the iron-formation is thicker, up to 6 m or more wide. Where examined in detail to date the thicker exposures are tightly refolded.

Occurrences of unit 4a and 4b turbidites appear to be spatially restricted, unit 4a to the western and central parts of the map area and unit 4b to the eastern and northern parts (Fig. 2). The two units are separated by the major volcanic segments, whose contacts with the turbidites are tectonically modified. Contact and temporal relationships between units 4a and 4b are not yet known.

### *Siliceous gneiss (unit 5)*

A siliceous gneiss of uncertain origin occurs as a 20-70 m, continuous unit along the west shore of the Snare River (Fig. 2). It is quartz-rich, white- to buff-weathering granoblastic rock characterized by a 1 cm wide anastomosing compositional layering, outlined by alternating quartz-rich



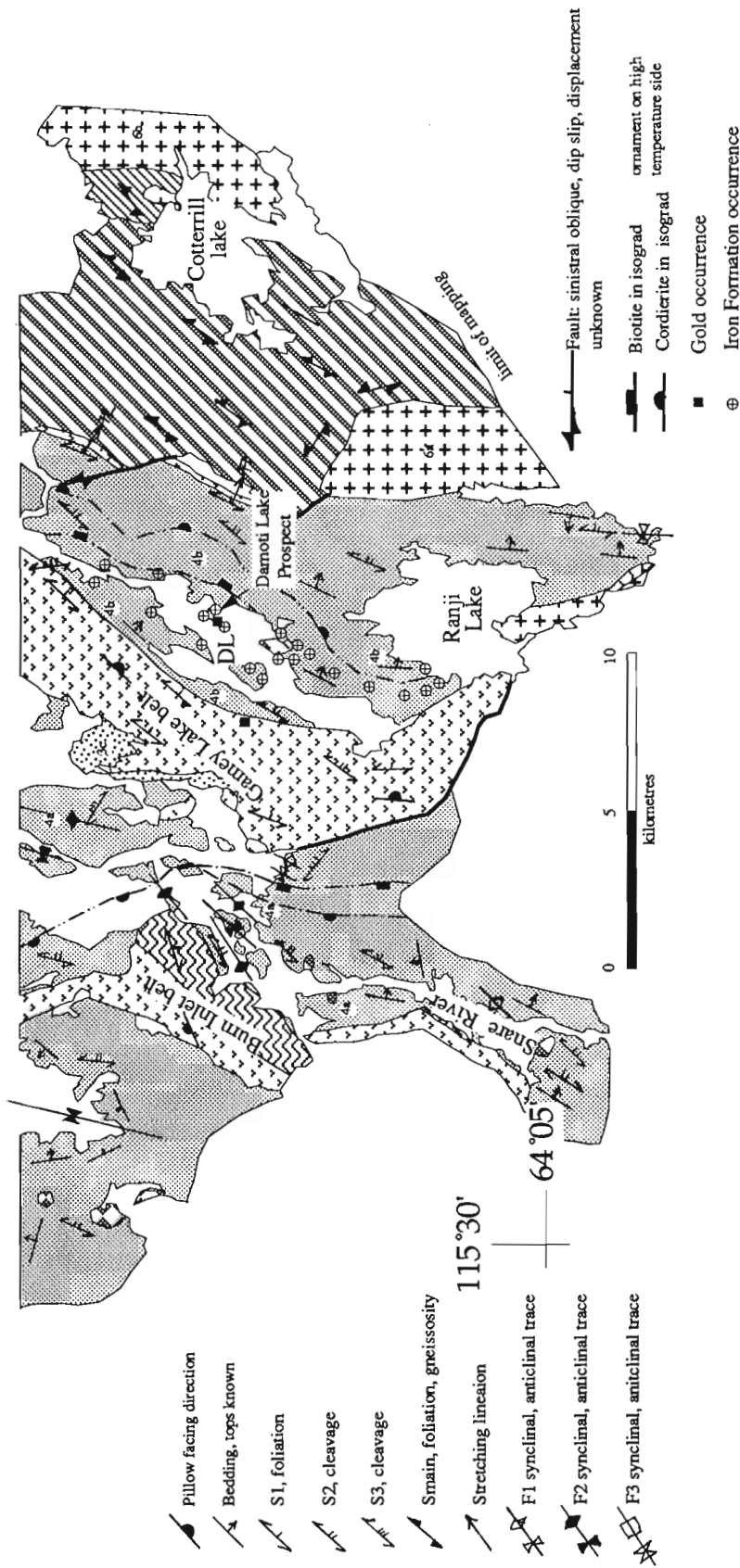
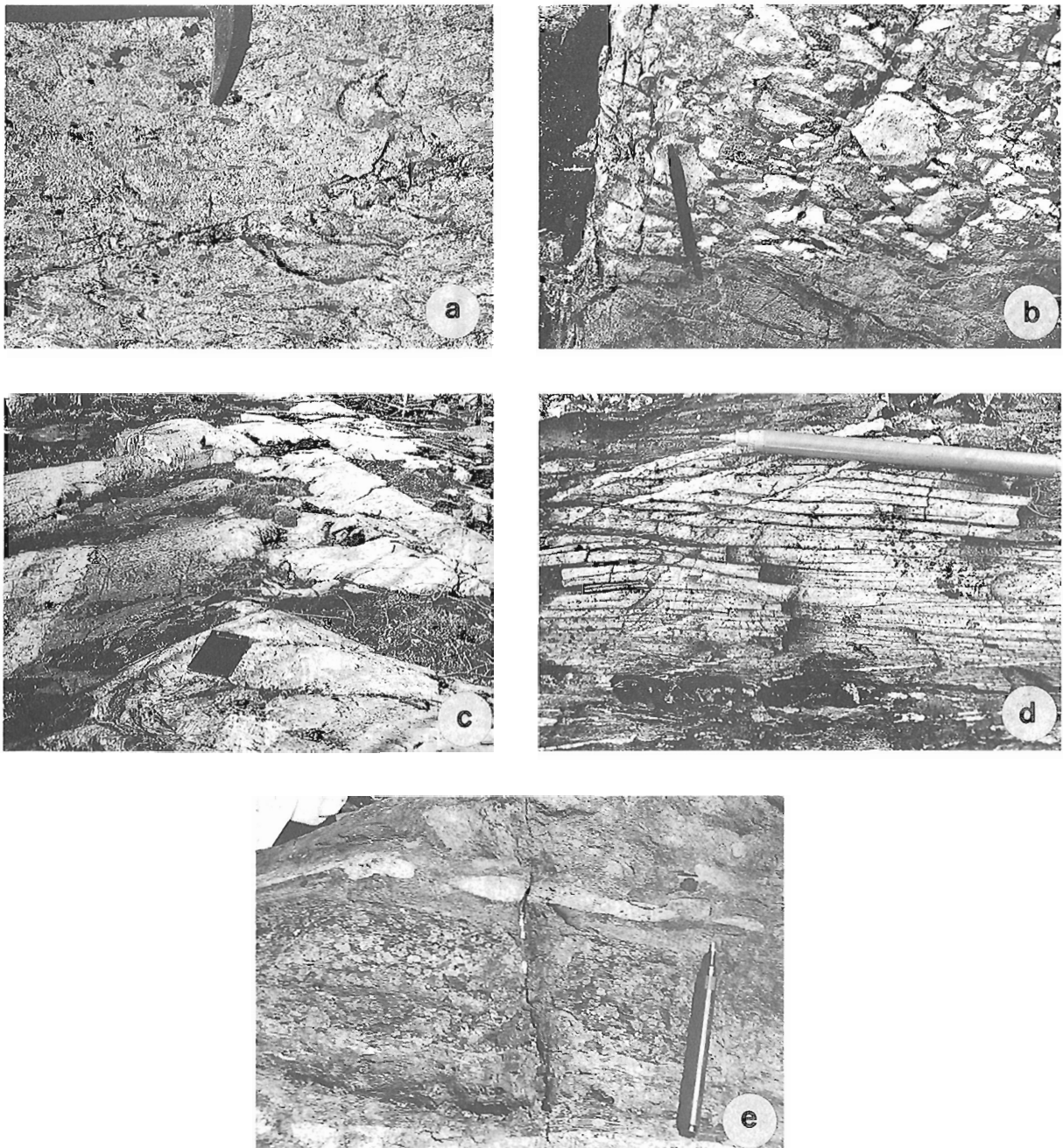
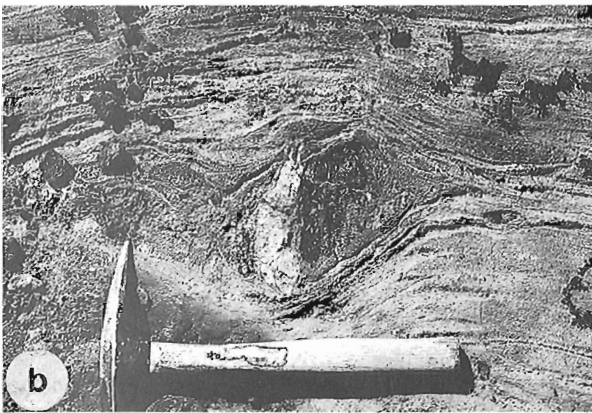


Figure 2. Simplified geological map of the Indin Lake area. SL = Spider Lake, DL = Damoti Lake, CL = Chalco Lake, HL = Hewitt Lake. Geological contacts are approximate.



**Figure 3.** *a) Felsic volcaniclastic rock with fiamme (dark grey). Hammer is 40 cm long. b) Felsic volcanogenic debris flow (unit 3b) in contact with unit 4a turbidites. Felsic clasts (white to light grey) are surrounded by a matrix of mudstone (dark grey). Graded bedding in turbidite below the contact indicates younging up into the debris flow. Pen is 15 cm long. c) Unit 4a: coarsely bedded greywacke-mudstone turbidites with massive sandy horizons. Notebook (foreground) is 25 cm long. d) Unit 4b: finely bedded to laminated greywacke-mudstone turbidites. Pencil is 15 cm long. e) Metamorphosed silicate-sulphide iron-formation within cordierite-andalusite grade turbidites. Light bands are recrystallized chert and central band is comprised of grunerite and garnet (medium-grey porphyroblasts). Outcrop exposed on the north shore of Indin Lake, northeast arm. Pen is 15 cm long.*



**Figure 4.** *a*) Compositional banding in siliceous gneiss (unit 5) defined by quartz rich and biotite (dark grey) zones. Small medium grey ovoids in biotite bands are garnets. Lens cap is 5 cm wide. *b*) Deformed mafic boudin (dark grey) in siliceous gneiss. Lighter, slightly recessed weathered zones in the mafic inclusion are quartz-carbonate filled fractures. Hammer is 40 cm long.

and narrower biotite-rich laminae (Fig. 4a). The biotite laminae contain abundant garnets and hornblende or diopside. Sphene occurs as small honey-brown crystals locally entirely replacing the biotite-rich laminae. Possible felsic volcanic and carbonate fragments in the gneiss were identified at one locality. Medium grained felsic horizons up to 1 m wide occur with margins subparallel to the gneissic foliation and may be transposed felsic dykes or sills. Horizons comprising 10-40% mafic blocks within gneiss matrix occur near the western contact with the Burn Inlet mafic volcanic belt. The mafic blocks are boudined and/or folded as well as pervasively fractured and cut by quartz-carbonate veining (Fig. 4b). The long axes of the blocks are parallel to the gneissic foliation. They range from 10 cm to several metres long. Fractured and folded tabular mafic units which obliquely cut across compositional banding may represent mafic dykes. The siliceous gneiss also contains isolated inclusions of dark grey-weathering mudstone. The nature of the contact with turbidites on the southeast side of the unit is not yet known, however, there is a general concordance between bedding in the turbidites and compositional layering

in the gneiss. The presence of strongly deformed mafic material within the gneiss, increasing in proportion to the west, and flattened mafic pillowed flows at its western margin suggest that its contact with the volcanic segment is sheared. The origin of this unit is uncertain at the present time.

## INTRUSIVE ROCKS

Intrusive rocks occur locally in the supracrustal belt, but form the largest component of an igneous complex at Cotterill Lake proposed by Frith (1992) as basement to the supracrustal belt.

### *Cotterill Lake igneous complex (unit 6)*

The oldest intrusive unit is the Cotterill Lake complex, a heterogeneously deformed igneous complex comprised of coarse, well-foliated hornblende-biotite granodiorite to tonalite intruded by fine grained, hornblende monzogranite and later syenogranite dykes and veins. The granodiorite contains xenoliths of foliated amphibolite whose internal fabric is locally discordant with the granodiorite fabric (Fig. 5a). An increase in the proportion of hornblende-monzogranite to granodiorite is noted westward. On the north and east side of Cotterill Lake the complex is intruded by massive to very weakly foliated K-feldspar megacrystic monzogranite to granodiorite which may be correlative with monzogranite found west of Indin Lake (unit 9).

### *Hornblende-biotite granodiorite (unit 7)*

Several plutons of a grey-weathering, coarse grained, hornblende-biotite granodiorite intrude the supracrustal belt along its eastern margin (Fig. 2). The plutons are internally homogeneous and have a weak foliation. The largest body intrudes the Cotterill Lake igneous complex. In plan view it is a tabular, sheet-like intrusion, internally very weakly foliated to massive. The two smaller plutons east of Indin Lake are more equant to elliptical bodies. They have sharp contacts with their host rocks and their margins are more strongly foliated.

### *Granite porphyry and dykes (unit 8)*

Small, fine- to medium-grained felsic intrusions occur within the greywacke-mudstone turbidites on the shore and islands of south-central Indin Lake (Fig. 2). They are typically cream- to buff-weathering, quartz and feldspar porphyritic granite that contain 1-3% muscovite. Similar, locally porphyritic, felsic dykes which intrude the adjacent turbidites and mafic volcanic rocks may be genetically related to the intrusions.

### *Muscovite monzogranite and pegmatite (unit 9)*

This unit comprises muscovite-bearing, pale pink-weathering, medium grained monzogranite-syenogranite stocks and pegmatite dykes. Typically the monzogranite is massive and equigranular. The unfoliated pegmatite dykes contain radiating



muscovite rosettes and tourmaline. Dykes of this unit intrude the previously described units. The granite occurs as dykes and 500-1000 m wide, tabular intrusions in turbidites on the southwest shore of Indin Lake. Outcrop in this region includes up to 50% crosscutting dykes of pegmatite and monzogranite. Only those areas of >50% plutonic material are designated unit 9 on the map.

## STRUCTURE

The deformation history of the Indin Lake area is polyphase and the distribution of structures, particularly in the turbidites, is heterogeneous. The dominantly observed structures in outcrop vary with lithology and locality. Five sets of structures have been recognized in the supracrustal belt. The sets are termed  $D_1$  through  $D_4$  based on their relative timing, determined by observations of fabric overprinting, relationship to metamorphism, and refolding. Set  $D_4$  is subdivided into shallow and steep structures which have not been observed together and whose relative timing cannot yet be determined. Regional orientations of the main structures are depicted on stereonet in Figures 5a-c. Structures within the Cotterrill Lake igneous complex will be described separately.

### Structural sets

#### $D_1$

$S_1$  is the first planar fabric recognized in outcrop. In the volcanic belts it is a foliation defined by flattening or attenuation of primary textures (e.g., pillows). In the sedimentary rocks,  $S_1$  parallels bedding and is only very locally developed. It is defined by amphiboles and biotite in the higher and lower metamorphic grade volcanic rocks, amphiboles in iron-formation, and muscovite or biotite in metagreywacke. Muscovite-inclusion trails which are oblique to a second fabric wrapping cordierite porphyroblasts may be relict  $S_1$  cleavage. Thermal peak mineral assemblages in the central part of the belt overprint these fabrics but are synchronous with fabric development in the higher grade margins. A down-dip mineral or stretching

$L_1$  lineation is best developed in the volcanic rocks. Meso- to macroscale isoclinal folds of bedding lacking an axial planar cleavage are the first observed folds (Fig. 6c). Ubiquitous bedding reversals in the turbidites, which occur without cleavage vergence, change within limbs of  $F_2$  folds are inferred to be  $F_1$  isoclines.  $S_1$  is interpreted as the main regional fabric within the volcanic rocks as it is crenulated by a second fabric which is axial planar to northeast-striking infolds of the turbidites.

#### $D_2$

$S_2$  is a finely spaced to weakly differentiated steep north to northeast cleavage which is the most obvious fabric recognized regionally in outcrop. It deforms metamorphic peak mineral assemblages throughout the area (Fig. 6b).  $L_2$  is a moderately to steeply plunging intersection lineation formed by  $S_2$  on bedding or  $S_1$ .  $S_2$  is axial planar to meso- to regional-scale open to moderately tight folds ( $F_2$ ) (Fig. 6c).  $F_2$  fold axes are northeast-striking and steeply plunging. Large-scale  $F_2/F_1$  interference folds are transitional between type 3 and type 1 (Fig. 6d, e).  $D_2$  structures are the predominant set observed in the turbidites and particularly control geometry through the central part of Indin Lake.

#### $D_3$

$S_3$  is a generally northwest-trending, steep, spaced cleavage which transects  $F_1$  and  $F_2$  folds south and west of Leta Arm without an associated fold phase. In the central Indin Lake area it is commonly preferentially developed in mudstone beds, forming a herringbone cleavage pattern. In the Damoti Lake area it is a differentiated northwest-trending cleavage. Rare meso-scale, moderate to open  $F_3$  folds are associated with the  $S_3$  cleavage. Based on the observation that  $S_2$  cleavage follows around the map-scale fold hinge at Spider Lake with no change in vergence, this structure is interpreted to be  $F_3$  or later (Fig. 2). Metamorphic isograds are also folded around this structure suggesting that  $D_3$  occurred after peak regional metamorphism.

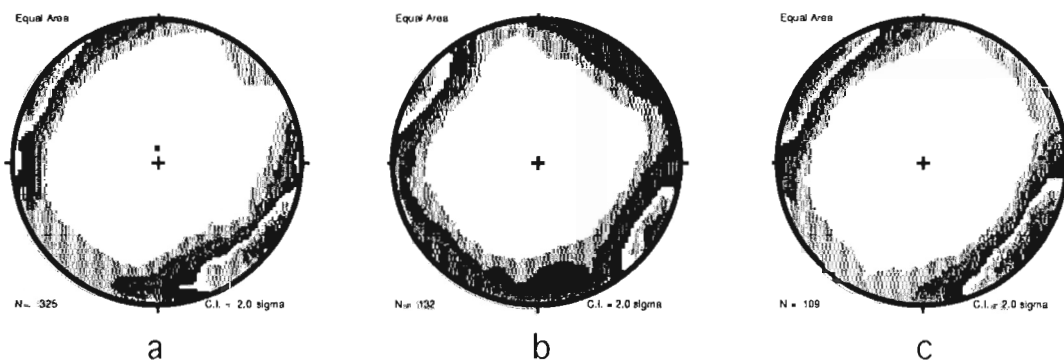


Figure 5. Contoured equal area stereonet projections of fabric elements in study area. a) poles to bedding,  $S_0$ , b) poles to foliation,  $S_1$ , c) poles to foliation,  $S_2$ .

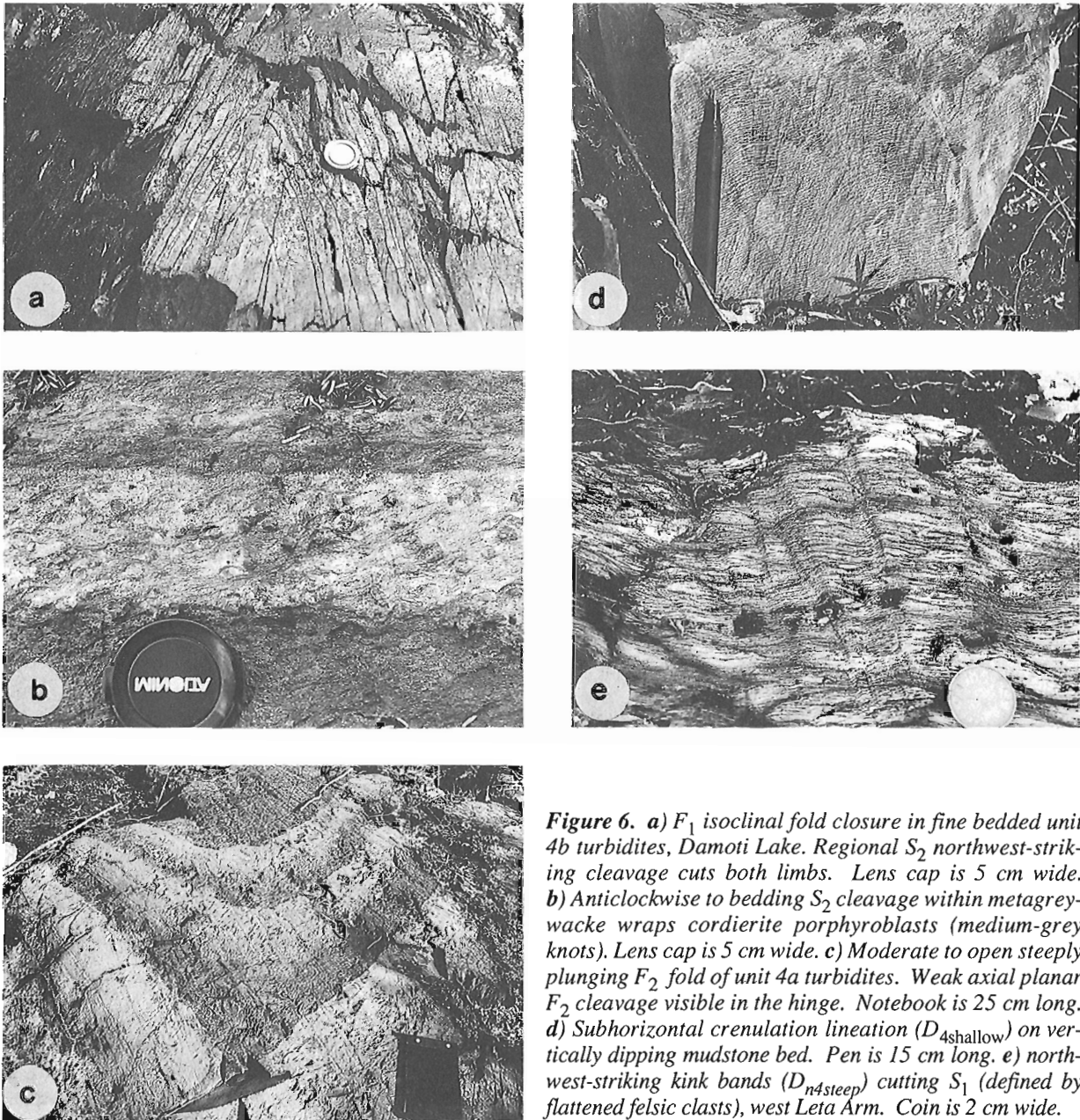


**D<sub>4shallow</sub>**

This set includes flat lying, shallowly plunging  $S_4$  kink bands and megakinks of variable orientation and a subhorizontal crenulation lineation only observed on vertical mudstone beds (Fig. 7a). These structures are observed to cut all other structure sets, except for  $D_{4steep}$ . Their orientation is indicative of late vertical compression within the belt.

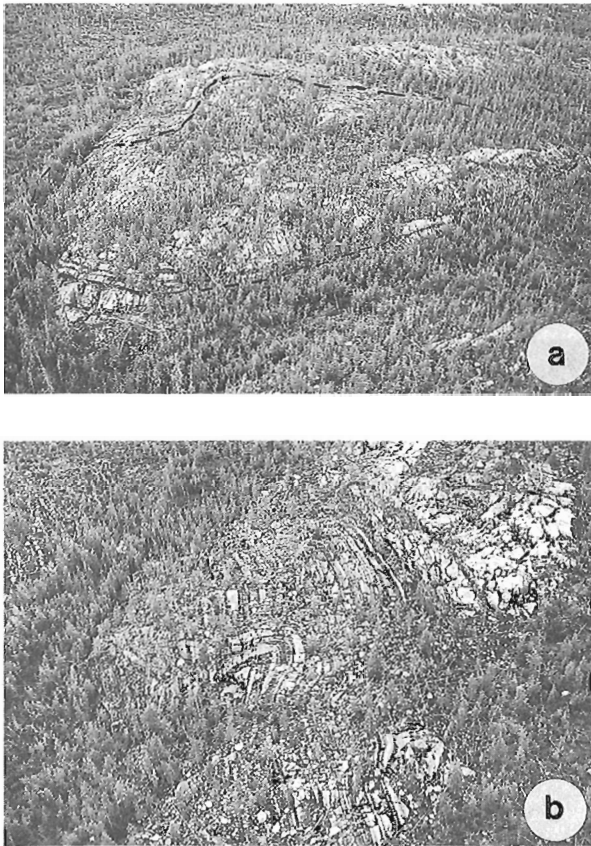
**D<sub>4steep</sub>**

$S_4$  in this set includes a moderately plunging northwest- and northeast-striking crenulation cleavage and northwest- or northeast-striking vertical kink bands (Fig. 7b).  $S_4$  is axial planar to minor-scale moderately to steeply plunging box to chevron folds and open to moderate meso- to minor-scale angular folds designated  $F_4$ . Grouped with this set are



**Figure 6.** a)  $F_1$  isoclinal fold closure in fine bedded unit 4b turbidites, Damoti Lake. Regional  $S_2$  northwest-striking cleavage cuts both limbs. Lens cap is 5 cm wide. b) Anticlockwise to bedding  $S_2$  cleavage within metagreywacke wraps cordierite porphyroblasts (medium-grey knots). Lens cap is 5 cm wide. c) Moderate to open steeply plunging  $F_2$  fold of unit 4a turbidites. Weak axial planar  $F_2$  cleavage visible in the hinge. Notebook is 25 cm long. d) Subhorizontal crenulation lineation ( $D_{4shallow}$ ) on vertically dipping mudstone bed. Pen is 15 cm long. e) northwest-striking kink bands ( $D_{n4steep}$ ) cutting  $S_1$  (defined by flattened felsic clasts), west Leta Arm. Coin is 2 cm wide.

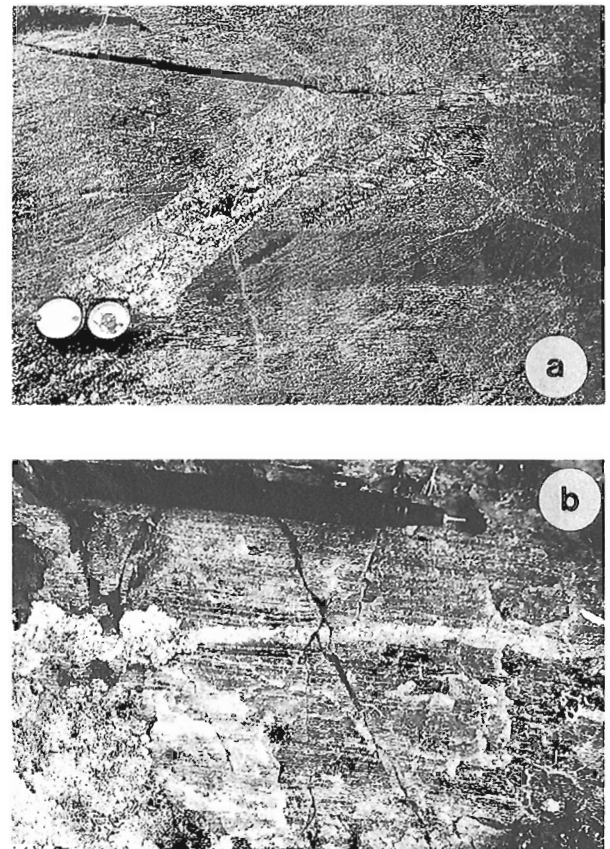
predominantly northwest-trending brittle-ductile faults which commonly carry moderately oblique stretching lineations, and sinistrally offset units (Fig. 2). Rare east-trending steep reverse faults of generally more minor offset were also noted. The  $S_4$  vertical kink bands and box folds are predominant in the western part of the map area while the crenulation cleavage and chevron folds are more common in the eastern part. In both regions these structures were observed to cut all other fabrics, except for  $D_{4\text{shallow}}$  structures. Overall this set is consistent with a component of horizontal compression across the supracrustal belt.



**Figure 7.** Oblique aerial photographs of  $F_1/F_2$  interference folds within unit 4a turbidites, looking north-northwest, west of Leta Arm, Indin Lake. **a)** Heart-shaped type 1-3 interference between east-striking  $F_1$  fold and more northerly striking  $F_2$ . Upper limb contains a smaller scale-doubly plunging  $F_1/F_2$  basin. All sections of the fold pattern are transected by the main  $300^\circ$  striking  $S_3$  cleavage which postdates the folding. **b)** 'S' asymmetric  $F_2$  fold with a weak axial planar cleavage visible in the hinge. Both limbs are transected by the main west-northwest-striking  $S_3$ . Younging reversal in graded and scoured beds infers the presence of an  $F_1$  isocline and indicates this is type 3 coaxial refolding. White unit in upper right is folded felsic debris flow.

### Distribution of structures

Throughout the belt, bedding in the turbidites is steeply dipping except for the north east arm of Indin Lake and in the west adjacent to the monzogranite intrusions (Fig. 2). West of the Leta Arm,  $S_3$  is the predominant fabric seen in the turbidites, while east of Leta Arm and south through the Snare River area,  $S_2$  is the main fabric with locally strong development of  $S_3$ . We note that this transition is spatially associated with the north-trending dip-slip Leta fault. In the east arm area of Indin Lake and Damoti Lake,  $S_2$  is the main fabric but moderately plunging  $F_4$  folds and  $S_4$  fabrics locally control the outcrop-scale geometry. The volcanic belts are internally folded or faulted and increasing  $D_1$  strain gradients are noted along their contacts with the sedimentary rocks. Regionally,  $D_2$  structures and interference with  $D_1$  control the overall geometry of the belt.



**Figure 8.** **a)** Strongly foliated and sheared granodiorite (dark grey) with augen trails of K-feldspar and foliated amphibolite xenolith (black) cut by late syenogranite dyke (whitellight grey), Cotterill Lake igneous complex. **b)** Mylonitic granodiorite of Cotterill Lake igneous complex cut by syenogranite vein (centre). Pen for scale is 15 cm long.

### Structures in Plutonic Rocks

The Cotterrill Lake igneous complex is heterogeneously deformed. An overall increasing strain gradient is noted toward the west, defined by a decrease in grain size of the foliated granodiorite-tonalite, and development of strongly foliated gneissic to mylonitic fabrics designated  $S_{\text{main}}$  (Fig. 8a, b). Zones of higher strain are typically several metres wide and anastomose, with the development of K-feldspar porphyroclasts and augen gneiss texture due to the disaggregation of the hornblende-monzogranite which intrudes the granodiorite. The discordant foliation of the amphibolite xenoliths in the granodiorite becomes transposed parallel to  $S_{\text{main}}$  in these zones. The high strain zones are characterized by a strong down-dip stretching lineation designated  $L_{\text{main}}$ . The late syenogranite dykes and veins crosscut the  $S_{\text{main}}$  fabric but are themselves locally boudined and/or folded. The orientation of the  $S_{\text{main}}$  fabric in the igneous complex is subparallel to that of a very strongly foliated, down-dip lineated mafic volcanic band found along its contact with the supracrustal belt.

The hornblende-biotite granodiorite plutons on the east side of the supracrustal belt are weakly internally foliated. This fabric is subparallel to  $S_2$  of the supracrustal rocks. Their margins are moderately to strongly foliated subparallel to their contacts with host rocks. Bedding or fabric in the host rocks deflects around the margin of the intrusions. The gneissic foliation of the Cotterrill Lake igneous complex is reoriented parallel to the margins of the granodiorite pluton intruding it (Fig. 2). Late syenogranite which is massive in the igneous complex is mylonitized adjacent to the pluton contact, possibly defining a contact strain aureole to the pluton.

### ECONOMIC POTENTIAL

Occurrences of gossan, commonly in association with quartz veining, were noted along the contacts of the volcanic segments, in particular along the east sides of Chalco Lake, Leta Arm, and Snare River belts. In addition, a number of gold occurrences are found along the Leta Arm belt. Of greatest potential economic interest is the recognition of iron-formation in the Indin Lake area (Fig. 2). Iron-formation at Damoti Lake, noted by H. Helmstede during a 1973 GSC mapping project, and first assayed by J. Brophy (1991) has yielded up to 16 g/t gold (The Northern Miner, v. 79, no. 32, October 1993, p. 1). Mapping this summer has extended known iron-formation south to the shore of Ranji Lake, north along the east shore of Damoti Lake and at the north shore of Indin Lake (Fig. 2). Banded iron-formation has also been found as >0.5 m long xenoliths in the granodiorite pluton on the east shore of Indin Lake and as an isolated 3 m lens south of Truce Lake. Oxide-facies iron-formation has been mapped west of Spider Lake. To date occurrences of iron-formation have been restricted to the unit 4b finer bedded turbidites found marginal to the supracrustal belt. A reconnaissance search of the north

shore of Daran Lake did not yield iron-formation to link the along strike occurrences at Ranji Lake and east of Wijinnedi Lake (Henderson, 1993). Mapping this summer suggests that localized significant thickening of the iron-formation can be accounted for by refolding of early isoclines ( $F_1$ ) by steeply plunging  $F_2$  folds.

### DISCUSSION

Mapping to date in the Indin Lake supracrustal belt has identified two distinct sequences of greywacke-mudstone turbidites separated by a number of volcanic belts. As the contacts between the sedimentary units and volcanic belts are strongly sheared there are no present constraints on the relationship of volcanism to sedimentation. Radiometric dating of the felsic volcanogenic debris flows within unit 4a turbidites will provide a direct test of the link between turbidite deposition and volcanism within the belt.

The distribution of the turbidites and compositionally distinct volcanic belts is spatially restricted. The coarser unit 4a turbidites with debris flows are restricted to the central part of the map area, while the finer turbidites with iron-formation are found at the eastern and northern margins of the supracrustal belt. The mafic pillow-dominated Hewitt Lake type volcanic belts occur around the margins of the belt while the more volcanoclastic, intermediate to felsic composition Beta type belts occur in the centre of the supracrustal belt. The present repeated distribution of intercalated sediment-volcanic packages is thought to be in part a function of late  $D_3$  or later regional-scale refolding. Removal of this fold pattern leaves an intercalated sequence of predominantly mafic, submarine volcanic rocks and intermediate to felsic dominated, submarine to subaerial volcanic rocks separated by coarser and finer turbidites. More work is required to investigate the significance of the  $D_1$  strain gradients in the volcanic belts and their tectonically modified contacts to the intercalated stratigraphy of the belt.

The Cotterrill Lake igneous complex has been proposed as basement to the supracrustal belt on the basis of its multiple intrusive phases and heterogeneous strain state (Frith, 1992). Mapping this summer has determined that the deformation within the complex is likely prior to intrusion of the hornblende-biotite granodiorite plutons. The link between this deformation and similar fabrics at the supracrustal belt contact cannot yet be evaluated. Radiometric dating of the tonalite phase of the complex will establish if it contains older crustal material.

Work in future will focus on further refining distribution of units and stratigraphy, evaluating the nature of the contact between the igneous complex and the supracrustal belt and the strained contacts between the sedimentary and volcanic segments, and better delineating the regional geometry of structures and their link to mineralization.

---

## ACKNOWLEDGMENTS

Adrienne Jones and Paul Graham are thanked for their skillful assistance in the field and independent mapping contributions. We gratefully acknowledge the hospitality and logistical assistance of Covello, Bryan and Associates and Southern Era Resources Ltd. at their Indin Lake camp. In particular we thank Joe Lariviere, Howard Bird and Lee Barker. Todd Brough, Steve Heskamp and Charlie Croal of Great Slave Helicopters are thanked for set-outs, hot coffee, and aerial photography. Discussions in the field with Herb Helmstaedt, Janet King, Tom Chacko and John Brophy were particularly helpful.

---

## REFERENCES

### **Fortier, Y.O.**

1949: Geology, Indin Lake, E 1/2, District of Mackenzie; Geological Survey of Canada, Preliminary map 49-10a, scale 1:125 000.

### **Frith, R.A.**

1992: Geology, Indin Lake, District of Mackenzie; Northwest Territories; Geological Survey of Canada, Map 1662A, scale 1:125 000.

### **Frith, R.A., Frith, R., Helmstaedt, H., Hill, J.D., and Leatherbarrow, R.**

1974: Geology of the Indin Lake area (NTS 86B), District of Mackenzie; in Current Research, Part C; Geological Survey of Canada, Paper 74-1A, p. 165-171.

### **Henderson, J.B.**

1993: Geology of the Wijnmedi Lake area: a transect into mid-crustal levels in the western Slave Province, District of Mackenzie, Northwest Territories; in Current Research, Part C; Geological Survey of Canada, Paper 93-1C, p. 83-92.

### **Hoffman, P.F.**

1989: Precambrian geology and tectonic history of North America; in The Geology of North America — An Overview (ed.) A.W. Bally and A.R. Palmer; Geological Society of America, p. 442-512.

### **Lord, C.S.**

1942: Snare River and Ingray Lake map areas, Northwest Territories; Geological Survey of Canada, Memoir 235, 55 p.

### **Stanton, M.S., Tremblay, L.P., and Yardley, D.H.**

1954: Chalco Lake, District of Mackenzie, Northwest Territories; Geological Survey of Canada, Map 1023A, scale 1:63,360.

### **Tremblay, L. P., Wright, G. M., and Miller, M.L.**

1953: Ranji Lake, District of Mackenzie, Northwest Territories; Geological Survey of Canada, Map 1022A, scale 1:63 360.

---

Geological Survey of Canada project 870008

# Disseminated gold mineralization in the Stewart River area, La Ronge Domain, Saskatchewan

K. Howard Poulsen and François Robert

Mineral Resources Division

*Poulsen, K.H. and Robert, F., 1994: Disseminated gold mineralization in the Stewart River area, La Ronge Domain, Saskatchewan; in Current Research 1994-C; Geological Survey of Canada, p. 103-112.*

---

**Abstract:** Disseminated gold mineralization in the Stewart River area occurs in sillimanite-bearing, quartzofeldspathic gneisses, derived from conglomerate, arenite, and minor tuff, and cut by monzodiorite dykes and younger pegmatite bodies. Zones of disseminated native gold occur mainly within more extensive lenses of quartz-feldspar-muscovite schist that contain less than 5% disseminated pyrrhotite and pyrite and traces of chalcopyrite, molybdenite, sphalerite, and galena. The lenses are approximately parallel to the regional strike of their host rocks, but, in detail, are discordant to primary lithological contacts. The para-concordant nature of the predeformational and premetamorphic sulphide bodies is the result of their transposition parallel to a strong northwest dipping  $S_1$  foliation, axial planar to a reclined intrafolial  $F_1$  anticline. The host rocks were further folded to occupy the overturned northwest limb of a southward-closing, reclined regional  $F_2$  fold.

**Résumé :** La région de la rivière Stewart contient de la minéralisation d'or disséminé dans des gneiss quartzo-feldspathiques à sillimanite, dérivés de conglomérat, d'arénite et d'un peu de tuf, recoupés par des dykes de monzodiorite et des corps plus jeunes de pegmatite. Des zones d'or natif disséminé occupent principalement des grandes lentilles de schiste à quartz, à feldspath et à muscovite contenant moins de 5% de pyrrhotine et de pyrite disséminées et des traces de chalcopyrite, de molybdénite, de sphalérite et de galène. Ces lentilles sont à peu près parallèles à l'orientation régionale des roches encaissantes mais, en détail, elles sont discordantes aux contacts lithologiques primaires. La nature paraconcordante des lentilles de sulfures antérieures métamorphisme et à la déformation résulte de leur transposition parallèlement à une intense foliation  $S_1$  et au plan axial penté vers le nord-ouest d'un anticlinal incliné  $P_1$  de nature intrafoliale. Les roches encaissantes ont été replissées pour occuper le flanc déversé vers le nord-ouest d'un pli régional incliné  $P_2$  fermant vers le sud.



## INTRODUCTION

The gold deposits and occurrences of the Stewart River area are located approximately 90 km northeast of La Ronge, Saskatchewan. They occur in the southern part of the La Ronge-Lynn Lake Domain of the juvenile Reindeer Zone of the Early Proterozoic Trans-Hudson Orogen. Gold in the La Ronge-Lynn Lake Domain occurs in five belts that have been interpreted to be the surface expressions of westerly dipping, easterly directed thrust sheets (Lewry et al., 1990). The most productive gold deposits occur within the Central Magmatic Belt, a granite-greenstone terrane. They are mainly quartz vein deposits hosted by shear zones that transect granitoid rocks. By contrast, gold occurrences in the Wapassini Belt are hosted by intravolcanic sedimentary rocks and lean iron-formation, and are disseminated and stratabound, if not stratiform (Coombe et al., 1986). The Kyaska (McLean Lake) Belt was not noted for its gold deposits until recent discoveries were made in the North Lake (Thomas, 1990) and Stewart River areas. This belt includes meta-arkosic rocks of the McLennan Group, the McLean Lake quartzofeldspathic gneisses, amphibolitic calc-silicate units, and locally abundant pegmatitic granite (Lewry and Slimmon, 1985; Thomas, 1986).

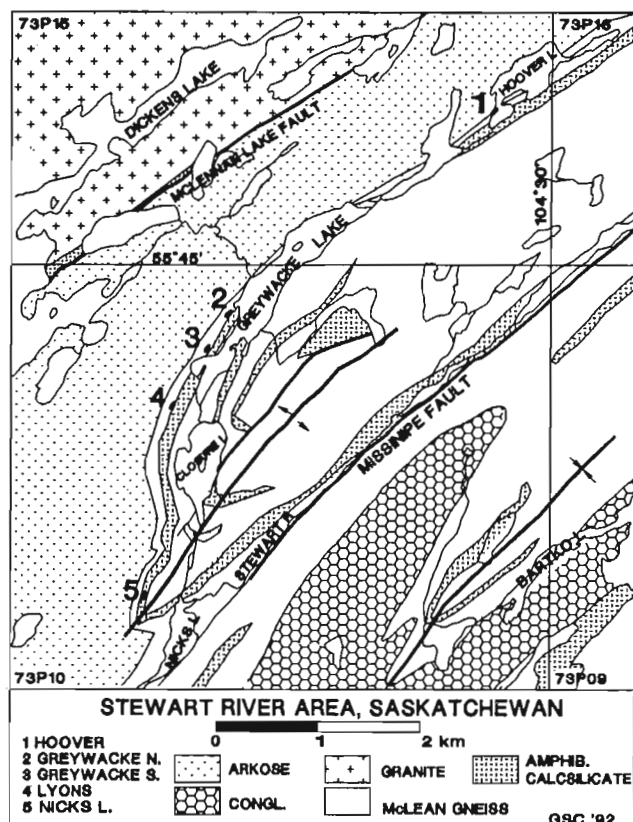


Figure 1. Simplified compilation map of the general geology of the Stewart River area, showing the locations of significant gold occurrences. (Adapted mainly from Padgham, 1963, 1966).

The gold occurrences in the Stewart River area occur in gneissic metasedimentary rocks (Fig. 1) and are of a disseminated style that is unlike any of the others in the La Ronge-Lynn Lake Domain. They were discovered by Cameco Corporation between 1987 to 1988 during follow-up of anomalous gold concentrations in lake sediments. In 1989, a large area covering the Greywacke Lake and Lyons occurrences was stripped of overburden and, in 1989-91, diamond drill programs tested these and other zones and outlined a small, as yet not fully defined, geological reserve at Greywacke Lake. In 1992 and 1993 we mapped the area including the North, Centre, and South zones (Fig. 2) and logged available drill core with emphasis on establishing the nature and setting of the mineralization.

## REGIONAL GEOLOGY

The Stewart River area (Fig. 1) has been previously mapped by the Saskatchewan Geological Survey at a scale of one inch to the mile: NTS 73P 9 (Padgham, 1966), 73P 10 (Padgham, 1963), 73P 15 (Pearson and Froese, 1959) and Morris (1961). Recent re-mapping (Thomas, 1986) extended into the north-western part of this area. Lucid accounts of the geology of the Stewart River area are found in reports, maps, and sections by Padgham (1963, 1966) and these are the primary sources for the compilation map shown in Figure 1. Some modifications have been made to reconcile older and current regional terminology (Lewry and Slimmon, 1985).

The McLennan Lake Fault (Lewry and Slimmon, 1985; Thomas, 1986) marks the tectonic boundary between the Central Magmatic Belt on the west and the Kyaska (McLean Lake) Belt on the east and defines the western limit of meta-arkosic rocks of the McLennan Group in this area. The Missinipe Fault (Lewry and Slimmon, 1985) coincides with the southeastern limb of a major southward-closing reclined fold in McLean Lake gneisses between the Stewart River and Bartko Lake. Both the dip of the fold axial surface and the plunge of the fold axis are to the northwest. Narrow hornblende-bearing calc-silicate units help to define this structure (Fig. 1) as many of the units correspond to aeromagnetic anomalies (Padgham, 1963). Padgham (Map 56A, 1963; Map 78A, 1966) also attempted a more detailed subdivision of the quartzofeldspathic gneisses between Greywacke Lake and Bartko Lake. There is, however, considerable uncertainty in the correlation of these rocks (McLean Lake gneiss) with the more distinctive rocks of the McLennan Group to the west and north of Greywacke Lake (Lewry and Slimmon, 1985; Thomas, 1986).

## STRATIGRAPHY

Although most rocks are thoroughly recrystallized to gneiss and schist, locally well preserved primary structures prompted us to subdivide them on the basis of inferred protolith (Fig. 2).



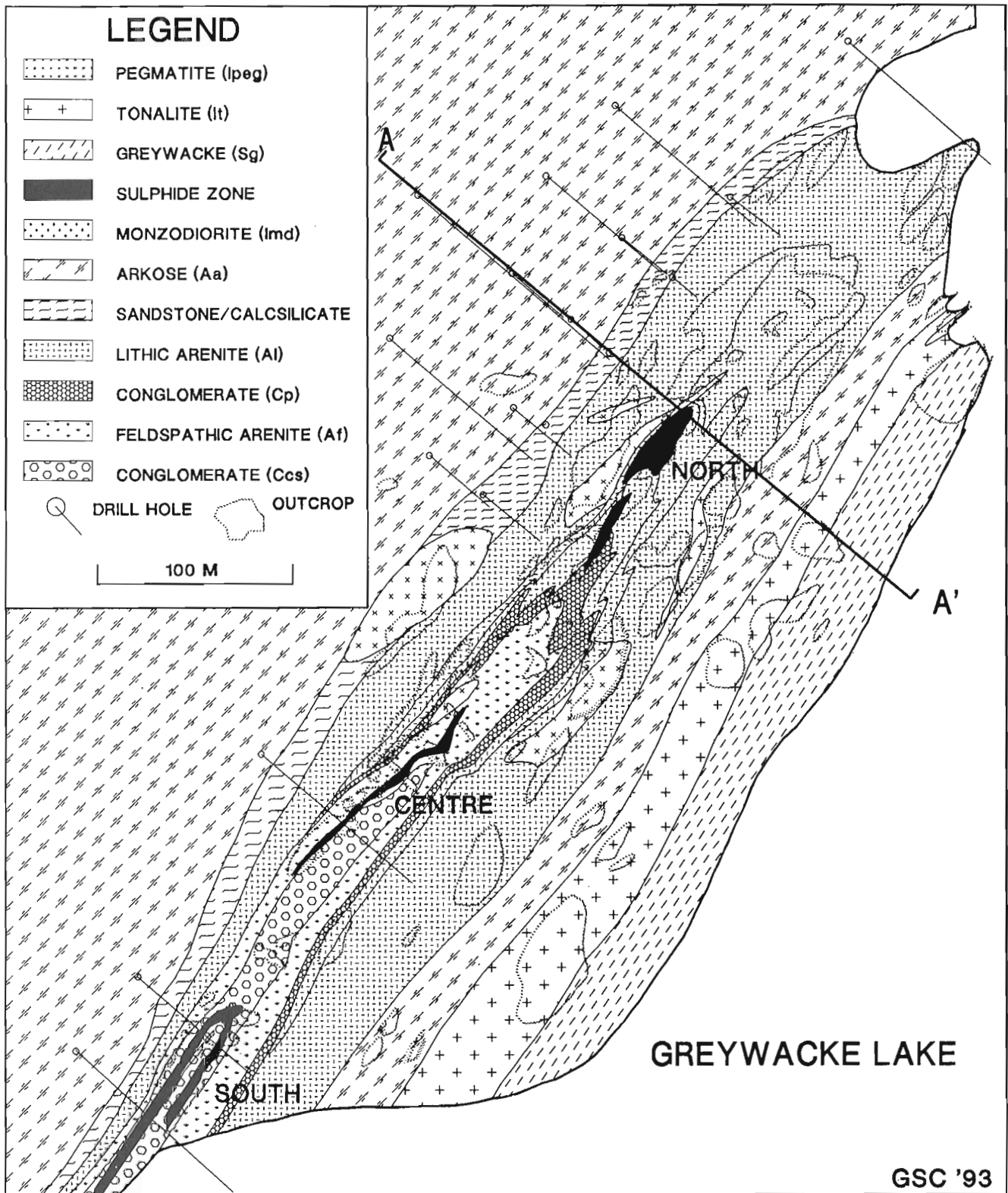
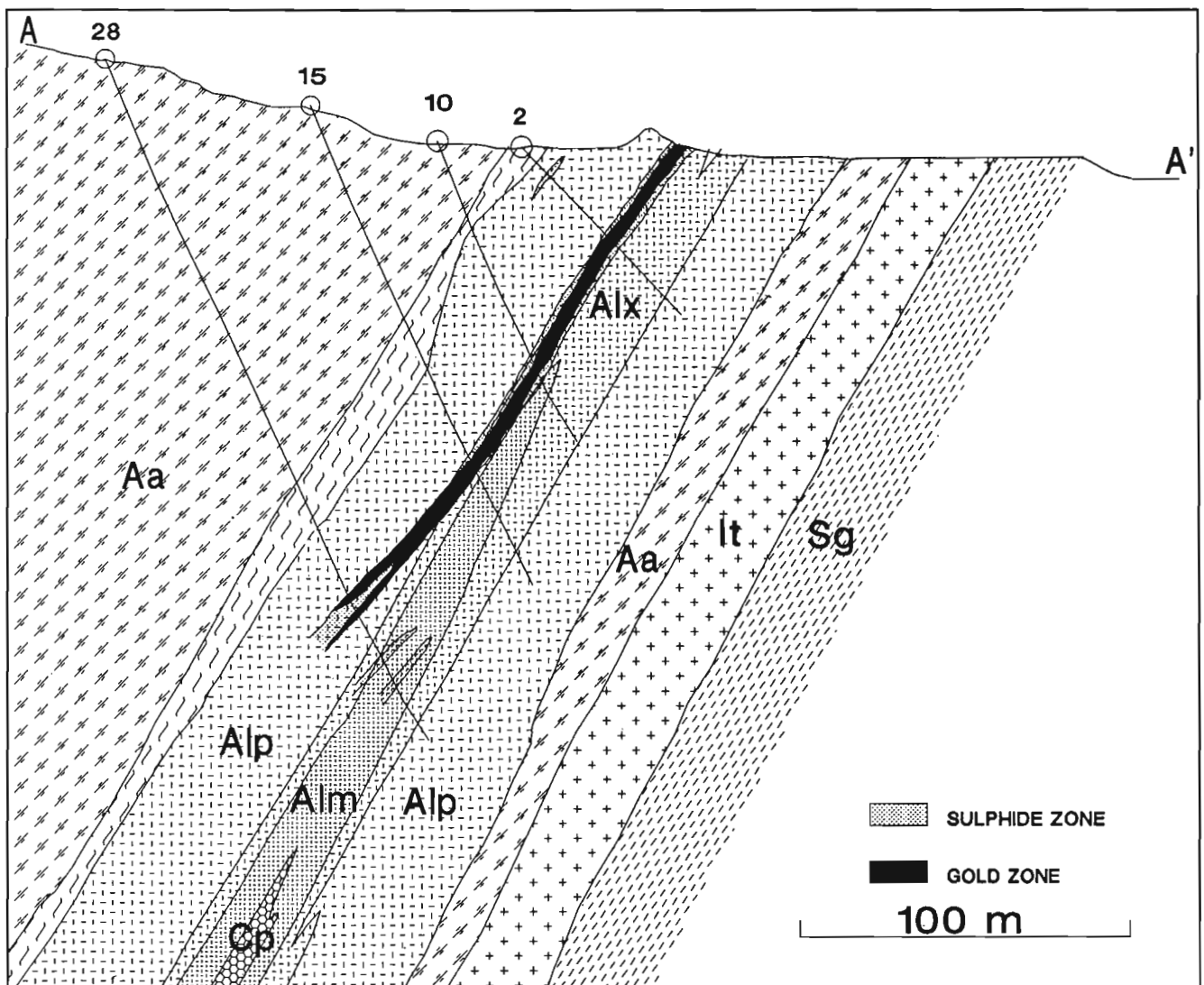


Figure 2. Geological map of the Greywacke Lake area showing the positions of the main gold-bearing sulphide zones.

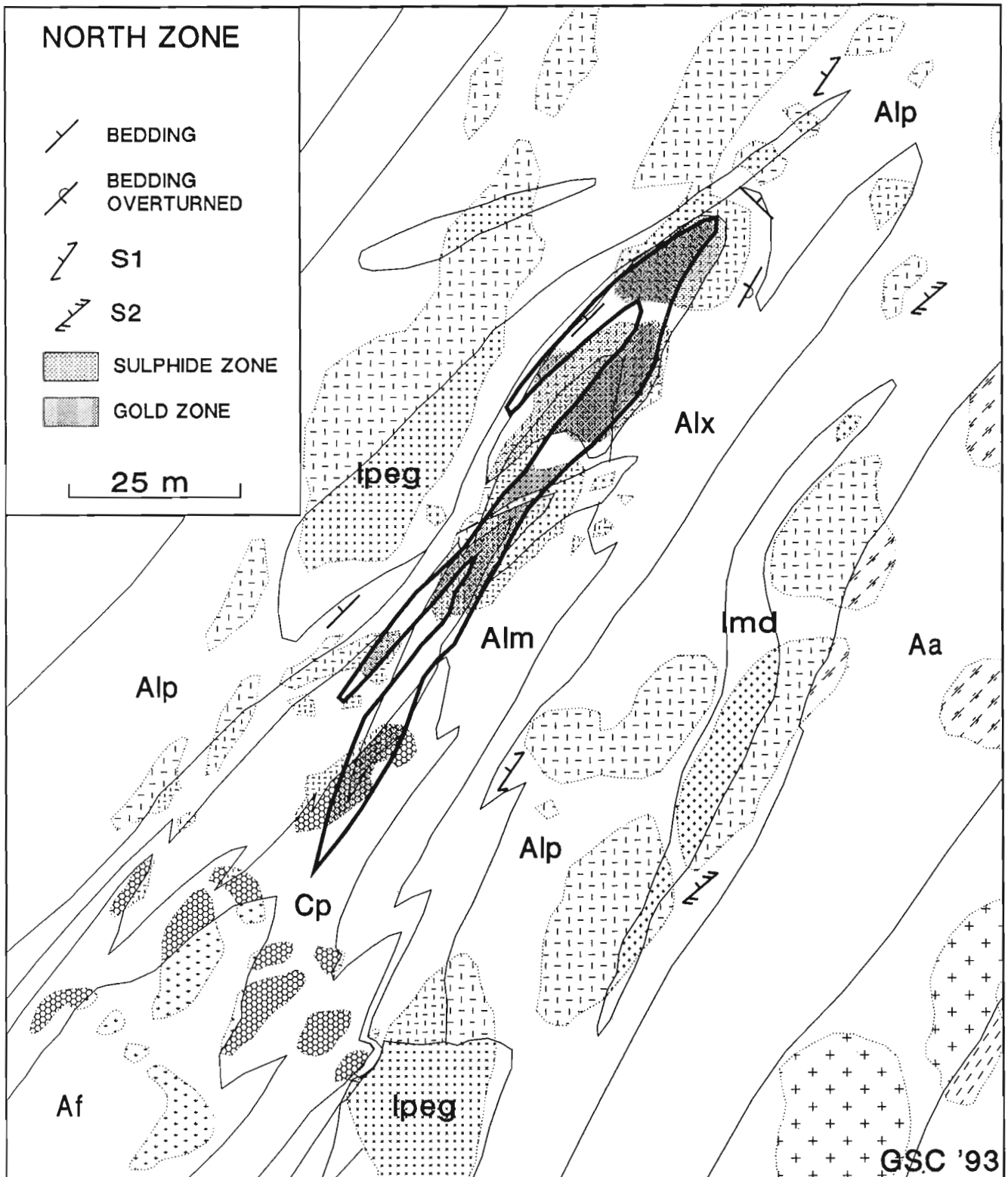
Stratigraphic way-up was determined from the shapes of trough crossbeds in one arenite unit. Although lithologic nomenclature and interpretation of protoliths are tentative at this stage, most of the mapped supracrustal units are meta-sedimentary. Intrusions, including numerous irregular pegmatite masses, are also present. The lithological contacts that were established in outcrop were extrapolated through intervening areas with the aid of drill sections (Fig. 3) leading to recognition of a first generation isoclinal anticline (Fig. 2, 4). Primary features in the supracrustal rocks are best preserved in the core of this fold. The supracrustal rock units are described below in order, from the interior of the fold outward, which with some notable exceptions, is also the inferred stratigraphic order.

**Metaconglomerate and conglomeratic metasandstone (Ccs)**

This unit is exposed at the Greywacke South zone (Fig. 2). It comprises mainly strongly banded, flaggy rock containing pink and dark grey-green bands 3 to 5 cm thick. Part of the light-coloured banding is caused by the presence of matrix-supported quartzofeldspathic clasts. These are predominantly of a single composition, although a few exotic mafic and highly altered siliceous clasts were observed. Locally the conglomerate contains 20 to 100 cm thick feldspathic arenite beds and has a transitional contact with overlying sandstone. It is highly strained in comparison with other units, as is indicated by the common occurrence of rotated "pseudo-clasts" that clearly have formed by boudinage of narrow pegmatite dykes.



**Figure 3.** Geological cross-section through the Greywacke North Zone. Note that the details portrayed on the section are constrained both by diamond drill information and by down-plunge projection of surface features. See Figure 2 for the location of the line of section. Patterns for rock units as in Figures 2 and 4.



*Figure 4. Enlarged plan view of the outcrop geology of the Greywacke North Zone. Note that the mineralized zone is both discordant to bedding in the host rocks and, like the host rocks, is locally folded. Patterns for rock units as in Figure 2 with added subdivision of the arenite subunits.*

### ***Feldspathic meta-arenite (Af)***

This unit is made up of massive, light-coloured sandstone beds, 10 to 50 cm thick, with local intercalated conglomerate. Major constituent minerals are plagioclase, microcline, muscovite, and quartz, with minor biotite. Faserkeisel (egg-shaped muscovite-sillimanite knots) and relict pressure solution seams composed of coarse muscovite are moderately common in more deformed portions of this unit but are generally confined to selected beds. Some weakly strained beds contain amoeboid lithic clasts of a single composition distributed homogeneously throughout a pink quartzofeldspathic matrix (Fig. 5). The clasts, which are darker than the matrix, exhibit re-entrant angles suggesting a greater pre-strain angularity suggestive of lapilli and, overall, the rock has the appearance of a welded lapilli tuff. Thick, massive bedded units are commonly separated by 2 to 10 cm thick bands of fine grained, laminated (tuffaceous?) rock, the laminations being accentuated by millimetre-thick quartz segregations parallel to bedding.

### ***Polymictic metaconglomerate (Cp)***

This unit comprises clast-supported conglomerate that grades locally into conglomeratic arenite. Both the lower and upper contacts of the conglomerate with adjacent units are sharp. The conglomerate contains a variety of distinctive clast types (Fig. 6) including coarse quartzofeldspathic (plutonic?), fine quartzofeldspathic (felsic volcanic), and most commonly mafic (volcanic?) types. The abundance of mafic clasts (>20%) is probably visually underestimated owing to their extreme flattening compared to the more felsic varieties but their presence distinguishes this unit from the lower conglomerate. Aluminosilicates and garnet were observed to overprint certain clasts of appropriate composition.



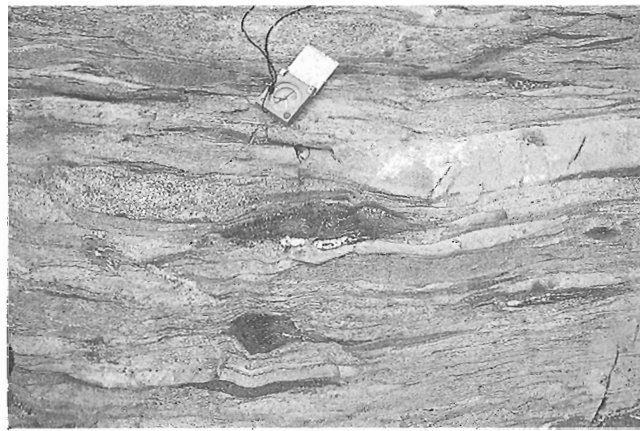
**Figure 5.** Photograph of darker amoeboid clasts in an outcrop of the feldspathic meta-arenite unit. The rock is possibly a welded lapilli tuff. Pencil is 12 cm long. GSC 1993-2201

### ***Lithic arenite (Al)***

Lithic arenite is a relatively featureless biotitic quartzofeldspathic rock containing 10-20% quartz, 30-40% feldspar (mainly plagioclase), and abundant biotite. Garnet and magnetite are particularly abundant in the outcrops north of the Greywacke North deposit where the unit is also overprinted by hornblende porphyroblasts. The lower contact between the lithic arenite and underlying conglomerate is sharp. Locally the arenite is difficult to distinguish from the feldspathic meta-arenite but can generally be identified by its greater biotite content, rare microcline, and fewer faserkeisel.

The lower part of the lithic arenite unit was subdivided in the area of exceptional exposure around the Greywacke North zone. These subunits and the underlying conglomerate outline the hinge of the isoclinal fold (Fig. 4).

Massive lithic arenite, (Alm) containing only rare crossbeds and local pebbly intervals, forms the base of the lithic arenite unit. It is overlain by crossbedded lithic arenite (Alx) composed of poorly defined beds ranging from 0.2 to 1 m thick. Trough crossbeds ranging from 10 to 50 cm in amplitude show the asymmetric merging of foresets at the base (Fig. 7) and are commonly truncated at the top contact with overlying troughs. The trough crossbeds are accentuated by the presence of 0.5 to 1 cm pebbles on the foresets. The crossbedded arenite also locally contains lenses of pebbly arenite and massive arenite that assist in defining the macroscopic orientations of beds. Pebbly lithic arenite (Alp) overlying the crossbedded unit is distinguished by the presence of variable proportions of white-weathering clasts that are from 1 to 10 cm long (average 5 cm) and 0.5 to 1 cm wide. It also contains rare mafic clasts similar in size and shape to the felsic ones. The presence of local poorly developed crossbeds and beds of massive pebble-free arenite suggest gradational facies transitions into the other arenite varieties.



**Figure 6.** Photograph of polymictic meta-conglomerate. Note the presence of mafic clasts (centre), fined grained felsic clasts (centre right), and granitoid clasts (centre left). Long axes of clasts are parallel to  $S_1$ . Compass face is 7 x 7 cm. GSC 1993-220N

The upper part of the arenite unit is not as well exposed as the lower part. Local exposures and good sections of drill core suggest, however, that conglomeratic lithic arenite and local calc-silicate (diopside-tremolite-grossular garnet) intervals distinguish it from the lower part.

### ***Meta-arkose (Aa)***

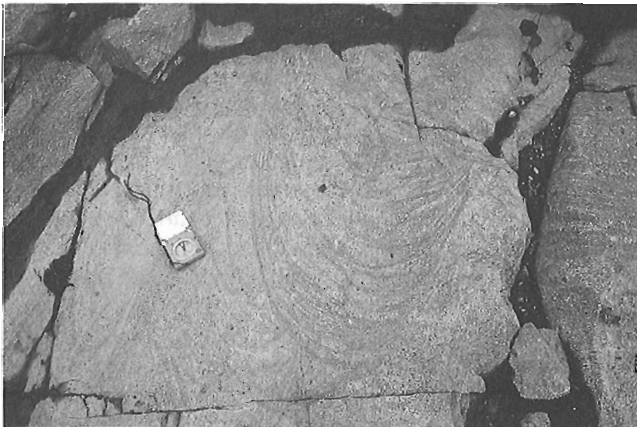
Lithic meta-arenite is in contact with meta-arkose on opposing limbs of the anticline (Fig. 2). This distinctive pink to brick-red rock contains little biotite but abundant rounded quartz grains that are unevenly distributed. The rock is further typified by abundant flaggy surfaces coated by coarse muscovite. Similar rocks characterize the "McLennan Group" elsewhere in the La Ronge Domain (Lewry, 1983) but the nature of its contacts with adjacent arenites is suspect.

### ***Metasandstone and calc-silicate rocks***

A diffuse sheared contact was observed in outcrop on the eastern limb of the fold and several sections of drill core show the western contact to be a highly foliated metasandstone and calc-silicate zone from 10 to 20 m thick in which lithic arenite, arkose, and calc-silicate units are irregularly intercalated. We provisionally view these contacts as early ductile fault zones.

### ***Metagreywacke (Sg)***

A unit of pelitic schist and gneiss extends along the shore of Greywacke Lake in the southeastern part of the map area. It contains much more biotite than any of the meta-arenites and is locally intercalated with leucocratic orthogneiss. We have not been able to establish a direct stratigraphic relationship between this metagreywacke and any of the arenite/conglomerate units.



**Figure 7.** Photograph of trough crossbeds in the hinge of a mesoscopic  $F_1$  anticline, viewed down its plunge. The amplitude of the trough is exaggerated in part by transverse shortening ( $S_1$ ). Compass face is 7 x 7 cm. GSC 1993-220K

## **INTRUSIONS**

Three distinctive varieties of intrusive rocks are present. Pegmatites, which appear to be of several different generations, are most common, metatonalite forms a single large body, and monzodiorite occurs as rare dykes only in the meta-arenite and metaconglomerate units (Fig. 2).

### ***Pegmatite (Ipeg)***

Simple pegmatite bodies, composed of quartz-plagioclase-microcline and biotite occur as irregular masses and dykes that cut all supracrustal lithologies. Some of the irregular masses comprise interconnected steep (dyke) and flat (sill) segments. Where the latter cap outcrops, pegmatite appears to be more extensive than it actually is. Several generations of pegmatite are present. All are locally folded and commonly boudinaged, and the younger ones contain screens of foliated supracrustal rocks.

### ***Metatonalite (It)***

A thick unit of quartz-plagioclase-hornblende-biotite gneiss outcrops between the lithic arenite and metagreywacke in the southeastern part of the map area. Similar in composition to smaller bodies within the metagreywacke, this coarse grained leucocratic rock contains centimetre-long prismatic hornblende grains commonly replaced by biotite. In places, the rock is banded and hornblende commonly is parallel to the gneissosity but, in local patches, is randomly oriented. It is suggested to be a tonalitic orthogneiss.

### ***Monzodiorite (Imd)***

Massive, homogeneous, medium grained, semi-concordant intrusive units 1 to 10 m wide occur locally within the arenite and conglomerate sequence. One such transposed dyke, of relict granitoid texture, is composed of altered plagioclase, hornblende, and interstitial potassium feldspar and hence is likely a monzodiorite. Other examples appear to be hydrothermally altered and contain abundant epidote, quartz, and sphene. Locally, football-shaped lenses, up to 50 cm long and 20-30 cm wide, composed of coarse grained, epidote-rich quartzofeldspathic rock occur at a single horizon within the feldspathic arenite unit. They are thought to represent boudins of a transposed, hydrothermally altered monzodiorite dyke.

## **STRUCTURE**

The nature and orientations of mesoscopic deformational fabric elements were recorded systematically across the mapped area. Coupled with the map distribution of lithological units and observed overprinting relationships, three deformational events  $D_1$ ,  $D_2$ , and  $D_3$  were identified; these are in agreement with the regional structural nomenclature of Lewry et al. (1990) and Coombe et al. (1986).



### First deformation ( $D_1$ )

$D_1$  deformation dominates the map-scale structure at Greywacke Lake (Fig. 2, 3, 4). The prominent anticline, defined in outcrop, is a reclined, intrafolial  $F_1$  fold that plunges approximately 55 degrees to the north-northwest ( $L_1$ :340-55). The plunge was deduced mainly from correlating the prominent closure of the distinctive polymictic metaconglomerate in plan (Fig. 4) with its position in successive drill sections. Note that the effects of folding are not as pronounced in the cross-section (Fig. 3) which is more nearly parallel to the fold hinge.

The strongest penetrative planar fabric in most outcrops is  $S_1$  which is axial planar to  $F_1$  folds and is displayed mainly as a micaceous pressure solution cleavage (now recrystallized) and extreme flattening of clasts. Careful examination of arenite units in mesoscopic  $F_1$  antiformal hinges confirmed that  $S_1$  does not overprint earlier planar elements other than bedding (Fig. 8). The shapes of trough crossbeds in the lithic arenite unit (Fig. 7) confirm that small  $F_1$  folds are anticlinal and synclinal in a stratigraphic sense and that they face upwards (i.e., younger units are encountered upwards and northeastward along  $S_1$ ).

### Second deformation ( $D_2$ )

$D_2$  deformation is less intense than  $D_1$  in most outcrops.  $S_2$  cleavage ( $S_2$ :240-65) is commonly marked by elongate faserkeisel, clearly crenulates  $S_1$ , and transects  $F_1$  folds (Fig. 9). S-shaped  $F_2$  folds are common minor structures. Locally, mineral and stretching lineations were recorded; most plunge down-dip in  $S_1$ , parallel to the intersection of  $S_1$  and  $S_2$  and also parallel to  $F_2$  fold hinges. Similar lineations are closer in orientation to the  $F_1$  hinge and may be related to  $D_1$ .



**Figure 8.** Photograph of transposed contact (solid line) between feldspathic meta-arenite and polymictic metaconglomerate. Note the elongation of clasts parallel to  $S_1$  (dashed line). Compass face is 7 x 7 cm. GSC 1993-220Q



**Figure 9.** Stripty  $S_1$  foliation in feldspathic arenite accentuated by muscovite seams (dark) overprinted by faserkeisel parallel to  $S_2$ . Pencil is 12 cm long. GSC 1993-220P

### Third deformation ( $D_3$ )

$F_3$  upright, open folds, up to 10 m in wavelength and trending 340°, deflect and overprint both  $S_1$  and  $S_2$  but have limited effect on the map-scale distribution of units. Local, small sinistral strike-slip faults, also with 340° strikes may be another manifestation of  $D_3$  deformation.

In addition to the mesoscopic folds described above, others of similar size were observed in the outcrops at Greywacke Lake. These folds lack systematic axial plane orientations and invariably are associated with margins of pegmatitic intrusions. They appear to be of  $D_2$  and/or  $D_3$  generation in that they refold  $S_1$  but their formation and the irregularity of their orientations is attributable to their common occurrence as indentations into necks of boudins in the pegmatite bodies.

## METAMORPHISM

All of the rock types, with the possible exception of some of the later generations of pegmatite, have a granoblastic texture. Nonetheless, ubiquitous shape fabrics of clasts and mineral aggregates, as well as relict pressure solution foliation, attest to an earlier dynamothermal recrystallization synchronous with deformation. Quartz, plagioclase, microcline, muscovite, biotite, garnet, and hornblende are stable and are present in abundances that reflect host rock compositions. Hornblende and garnet are poikiloblastic and sillimanite occurs both as a matrix mineral and in abundance within muscovitic faserkeisel that are parallel to  $S_2$ . Cordierite was tentatively identified in drill core from Greywacke South. Preliminary observations constrain metamorphic temperatures between 550°C (coexisting biotite-garnet-sillimanite) and 650°C (coexisting quartz-muscovite-plagioclase). Pressure constraints are poor (2-7 kbar) although results of recent geobarometric studies elsewhere in the McLean Lake belt (Abbas-Hasanie et al., 1992) would favour the higher end of this range.



## MINERALIZATION AND ALTERATION

The disseminated sulphide zones at Greywacke Lake are expressed in outcrop by weak gossans. Three subparallel sulphide-bearing lenses are exposed: Greywacke South, Centre, and North (Fig. 2). They all locally contain anomalous gold concentrations but the most continuous gold grades are in the Greywacke North zone where ore-grade material (approximately 12 g/t) is concentrated mainly in the arenite units and also clearly transgresses primary lithological contacts (Fig. 4). Outcrop-scale evidence also suggests that the sulphide zones have been folded with their enclosing rocks. The auriferous zone now has an irregular shape (Fig. 4) which reflects both the original form and the  $D_1$  folding of the zone. With reference to bedding, it originally comprised both discordant and concordant segments so that the concordant northern end of the auriferous zone was folded in sympathy with the crossbedded arenite.

The mineralized rocks are composed mainly of quartz-plagioclase-muscovite±biotite schist containing disseminated sulphide minerals (on average 1 to 5% by weight), magnetite, and locally, fine grained native gold. Sulphides and oxides occur as discontinuous, irregularly shaped trains of elongate grains and grain aggregates interstitial to granoblastic silicate minerals but, on average, parallel to  $S_1$ . The sulphide-oxide segregations take on the negative grain shapes of their silicate hosts but are in textural equilibrium with them. Pyrrhotite and pyrite are the most common sulphide phases. Triple-junctions among adjacent grains in pyrrhotite aggregates suggest metamorphic recrystallization of the sulphides. Chalcopyrite and magnetite occur as smaller grains on the edges of pyrrhotite grains and aggregates and are also in textural equilibrium with both sulphides and silicates. Rare idiomorphic pyrite grains overgrow pyrrhotite, and molybdenite, sphalerite, and galena are rare accessories. Sulphides also commonly occur as tiny inclusions in silicate minerals. Discrete grains of native gold are common in well mineralized areas; at the microscopic scale they are not directly associated with sulphide grains and, at the macroscopic scale, many portions of the sulphide zones contain no gold (Fig. 3, 4).

The problem of recognizing the effects, if any, of hydrothermal alteration at Greywacke Lake is particularly difficult because of the complete recrystallization during amphibolite facies metamorphism. A limited number of mineral phases (quartz, biotite, muscovite, microcline, and plagioclase) are common to all rocks and textural evidence of overprinting of one phase by another will likely have been destroyed. There are nonetheless indications, at a variety of scales, that metasomatism has affected the rocks at Greywacke Lake although, at this stage, it is uncertain how it relates to gold mineralization. At the microscopic scale, the sulphides at the Greywacke North zone are associated with leucocratic silicate segregations in the host arenite. Aggregates of quartz and microcline grains commonly envelope sulphides and it is possible that these represent fossil microfractures into which sulphides (and gold?) were originally emplaced.

At the mesoscopic scale, siliceous rocks containing abundant quartz, green mica, and albite correlate well with the presence of sulphides at the Greywacke South zone and likely reflect precursor hydrothermal alteration. Mineralized zones within the normally biotitic lithic arenite at Greywacke North are also characterized by a bleached appearance and anomalous quantities of muscovite, including a bright green variety (roscoelite or fuchsite?). Where monzodiorite dykes occur in mineralized zones they are rich in quartz, epidote, and sphene along with sulphides, likely as a result of precursor hydrothermal alteration. Dykes of this type containing abundant pyrrhotite are also prominent at the Lyons zone to the south of Greywacke Lake (Fig. 1). At the larger scale, magnetite and, locally, hornblende porphyroblasts are common in several of the rock units at Greywacke Lake but these minerals do not appear to be directly related to the presence of sulphides or gold.

## DISCUSSION

The host rocks to the gold mineralization at Greywacke Lake and the Lyons zone to the south are inferred to represent a coarse clastic sequence of shallow water origin. These rocks appear to comprise three distinct sedimentary facies. The lowermost sequence of conglomerate, conglomeratic sandstone, and feldspathic arenite is thought to be of possible epiclastic origin. It includes probable lapilli tuff and conglomerate of volcanic and hypabyssal provenance, and resembles shallow water, if not subaerial, rocks of volcanic derivation. It is in sharp contact with overlying polymictic conglomerate containing both volcanic and plutonic clasts. The conglomerate, although deformed, appears to be clast-supported and resembles subaerial alluvial-fluvial conglomerate. Even accounting for folding and inhomogeneous strain, the conglomerate at Greywacke Lake varies substantially in thickness from place to place suggesting that it was originally a lenticular depositional unit. The uppermost host rock unit, lithic arenite, is locally pebbly and crossbedded and likely is of fluvial origin. It is distinguishable from arkose of the McLennan Group to the west mainly by its low content of potassium feldspar.

The mean orientation of  $S_2$  and the S-shaped asymmetry of  $F_2$  folds at Greywacke Lake suggest a sympathetic relationship to a major ( $F_2$ ) fold that closes approximately one kilometre to the east (Fig. 1). During this event, the mineralized sequence which was first transposed into  $S_1$  and folded by local  $F_1$  intrafolial folds, was refolded into a steeper orientation by  $D_2$  folds. As a point of regional interest, this implies that, prior to  $D_2$ , the  $F_1$  folds likely had shallow dipping axial surfaces and were westward facing. The mineralization at Greywacke Lake falls into the broad category of disseminated sulphidic gold deposits. Although stratabound at the property-scale, it occurs in concordant and discordant lenses at the local scale. We have noted that the sulphide mineralization post-dates the emplacement of monzodiorite dykes into the supracrustal sequence but predates regional deformation and metamorphism, as well as the intrusion of pegmatitic dykes and sills. The alignment of sulphide mineral aggregates with  $S_1$  foliation and the macroscopic alignment of the sulphide-bearing lenses with  $F_1$  fold axial surfaces strongly suggests

that mineralization was at least synchronous with, if not earlier than,  $D_1$ . We prefer the latter interpretation, not only because we have observed folded sulphide lenses, but also because we could find no evidence of anomalous  $D_1$  deformation (higher strain zones for example) that correlates directly with mineralization. The fact that the mineralized zones are now parallel to the axial surface of  $F_1$  folds is likely the result of their transposition, along with their host rocks, into the  $S_1$  orientation. The mineralized zones were certainly originally much more discordant to their host units than they are now.

Greywacke Lake shares a number of geological attributes with deposits elsewhere in Canada such as Hemlo, Bousquet, Madsen Red Lake, Montauban, and Chetwynd where similar problems of interpretation exist. Common features include disseminated sulphide mineralization, occurrence at volcanic-sedimentary interfaces, aluminous and potassium-rich alteration, polyphase deformation involving strong transposition, and elevated metamorphic grade. Current views on the primary origin of these deposits run the gamut from shear zone replacement to deformed magmatic hydrothermal systems. At Greywacke Lake, we see no evidence of a shear zone relationship and can also rule out a paleoplacer origin on the basis of the discordance of mineralization, the immaturity of the host rocks, and the clear evidence of mineralization and alteration overprinting monzodiorite dykes. The nature of the host rocks and their subaerial stratigraphic setting are atypical of volcanogenic massive sulphide systems. A closer comparison exists with disseminated sedimentary-hosted epithermal deposits (e.g., Cannon Mine, Washington) that are commonly located in subaerial volcano-sedimentary sequences but the mineralization at Greywacke Lake lacks a typical epithermal metal suite. The best analogues are deeper, intrusion-related, noncarbonate replacement deposits or "mantos" (Sillitoe, 1991); such deposits are typically composed of gold associated with disseminated sulphides, are stratabound to discordant to sedimentary/volcanic host rocks, and are commonly associated with igneous dykes. The key question surrounding a manto origin for mineralization at Greywacke Lake is whether there is a related intrusion in the rocks underlying the metaconglomerate that forms the lowermost stratigraphic unit. Our structural interpretation implies either that the mineralized units may be detached from their original infrastructure or that the underlying rocks will be found in the core of the  $F_1$  fold farther to the south. The only concrete links between magmatism and mineralization preserved at Greywacke Lake are the monzodiorite dykes.

## CONCLUSIONS

Gold mineralization in the Stewart River area is a unique type in the La Ronge-Lynn Lake Domain. It is disseminated with sulphides in rather ordinary, isoclinally folded, sillimanite-bearing quartzo-feldspathic gneisses that are mainly of meta-sedimentary origin. Given that most rocks of the McLean Lake Belt are of similar type and that manifestations of the presence of gold is extremely subtle, further exploration for this unique style of mineralization is warranted.

## ACKNOWLEDGMENTS

Cameco Corporation and, in particular, Rick Kusmirski, Dave Chan, and Ted Herman are thanked for their co-operation in providing access to the properties and for relevant background information for this project. Tom Sibbald and Pam Schwann of Saskatchewan Energy and Mines are thanked for their support of the project as well as valuable advice and discussions in the field. D.C. Harris, GSC, provided supporting X-ray diffraction analyses. Critical reviews by Tom Sibbald, Don Harris, Al Sangster, and Dave Sinclair improved the manuscript.

## REFERENCES

- Abbas-Hasanie, S.A.F., Lewry, J.F., and Perkins, D.**  
1992: Metamorphism of high-grade pelites in the Brabant Lake area, eastern La Ronge Domain, northern Saskatchewan; *Canadian Journal of Earth Sciences*, v. 29, p. 1686-1700.
- Coombe, W., Lewry, J.F., and Macdonald, R.**  
1986: Regional geological setting of gold in the La Ronge Domain, Saskatchewan; in *Gold in the Western Shield*, (ed.) L.A. Clark; Canadian Institute of Mining and Metallurgy, Special Volume 38, p. 26-56.
- Lewry, J.F.**  
1983: Character and structural relations of the 'McLennan Group' meta-arkoses, McLennan-Jaysmith Lakes area; in *Summary of Investigations 1983*, Saskatchewan Geological Survey, Miscellaneous Report 83-4, p. 49-55.
- Lewry, J.F. and Slimmon, W.L.**  
1985: Compilation bedrock geology, Lac La Ronge, NTS Area 73P/73I; Saskatchewan Energy and Mines, Report 225, 1:250 000 scale map with marginal notes.
- Lewry, J.F., Thomas, D.J., Macdonald, R., and Chiarenzelli, J.**  
1990: Structural relations in accreted terranes of the Trans-Hudson Orogen, Saskatchewan: telescoping in a collisional regime?; in *The Early Proterozoic Trans-Hudson Orogen of North America*, (ed.) J.F. Lewry and M.R. Stauffer; Geological Association of Canada, Special Paper 37, p. 75-94.
- Morris, A.**  
1961: The Geology of the Settee Lake Area (West Half); Saskatchewan Department of Mineral Resources, Report no. 55, 27 p., accompanied by Map 55A, scale 1 inch = 1 mile.
- Padgham, W.A.**  
1963: The Geology of the Otter Lake Area (East Half), Saskatchewan; Saskatchewan Department of Mineral Resources, Report no. 56, 52 p., accompanied by Map 56A, scale 1 inch = 1 mile.  
1966: The Geology of the Guncoat Bay Area, Saskatchewan; Saskatchewan Department of Mineral Resources, Report no. 78, 143 p., accompanied by maps 78A, B, C, D, E.
- Pearson, W.J. and Froese, E.**  
1959: The Geology of the Forbes Lake Area, Saskatchewan; Saskatchewan Department of Mineral Resources, Report no. 34, 28 p., accompanied by Map 34A, scale 1 inch = 1 mile.
- Sillitoe, R.H.**  
1991: Intrusion-related gold deposits; in *Gold Metallogeny and Exploration* (ed.) R.P. Foster; Blackie, Glasgow and London, p. 165-209.
- Thomas, D.J.**  
1986: Bedrock geological mapping, Esmay Lake area (Part of NTS 73P-10 and -15); in *Summary of Investigations 1986*, Saskatchewan Geological Survey; Saskatchewan Energy and Mines, Miscellaneous Report 86-4, p. 19-31.  
1990: North Lake Gold Deposit: a model for arenite-hosted gold; in *Summary of Investigations 1990*, Saskatchewan Geological Survey; Saskatchewan Energy and Mines, Miscellaneous Report 90-04, p. 21-24.

# Structural relationships across the Tabbernor Fault, Nielson Lake area, Trans-Hudson Orogen, Saskatchewan

C.G. Elliott<sup>1</sup>

Continental Geoscience Division

*Elliott, C.G., 1994: Structural relationships across the Tabbernor Fault, Nielson Lake area, Trans-Hudson Orogen, Saskatchewan; in Current Research 1994-C; Geological Survey of Canada, p. 113-120.*

---

**Abstract:** Detailed mapping across the Tabbernor Fault in the Nielson Lake area reveals brittle, strike-slip movement on the fault that crosscuts the Nielson ductile strain zone. Shear on the Nielson strain zone east of the Tabbernor Fault was sinistral-oblique with moderate to steep, S-plunging extension lineations. Sinistral kinematic indicators postdate dextral shear structures with S-plunging lineations. Shear west of the Tabbernor Fault was sinistral with moderate north-plunging extension lineations. The north-striking Nielson strain zone splays to the west into north-dipping reverse faults across which stratigraphy is repeated and has a frontal- and lateral-ramp geometry. Movement on the Nielson strain zone postdates an angular unconformity between metasedimentary rocks, mafic metavolcanic rocks and tonalites, and overlying intermediate volcanogenic rocks. Correlation with dated units in the Glennie Domain suggests that pre-unconformity deformation, uplift, erosion, and deposition above the unconformity occurred between 1850 and 1840 Ma.

**Résumé :** La cartographie détaillée du secteur traversé par la faille de Tabbernor dans la région du lac Nielson révèle un mouvement de coulissage de type fragile associé à la faille qui recoupe la zone de déformation ductile de Nielson. Le cisaillement dans la zone de déformation de Nielson, à l'est de la faille de Tabbernor, était senestre-oblique et a produit des linéations d'étirement plongeant vers le sud selon un angle modéré à abrupt. Les indicateurs cinématiques du mouvement senestre sont postérieurs aux structures de cisaillement dextre accompagnées de linéations plongeant vers le sud. Le cisaillement, à l'ouest de la faille de Tabbernor, était senestre et a produit des linéations d'étirement plongeant vers le nord selon un angle modéré. La zone de déformation de Nielson, de direction nord, s'amortit vers l'ouest sous forme de failles inverses à pendage nord, qui produisent une répétition de la stratigraphie, et la zone présente dans l'ensemble une géométrie de rampes frontale et latérale. Le mouvement dans la zone de déformation de Nielson est postérieur à une discordance angulaire au contact de roches métasédimentaires, de roches métavolcaniques mafiques et de tonalites avec une succession sus-jacente de roches volcaniques intermédiaires. La corrélation avec les unités datées dans le domaine de Glennie indique que la déformation antérieure à la discordance, le soulèvement, l'érosion et la sédimentation des unités sus-jacentes à la discordance ont eu lieu entre 1 850 et 1 840 Ma.

---

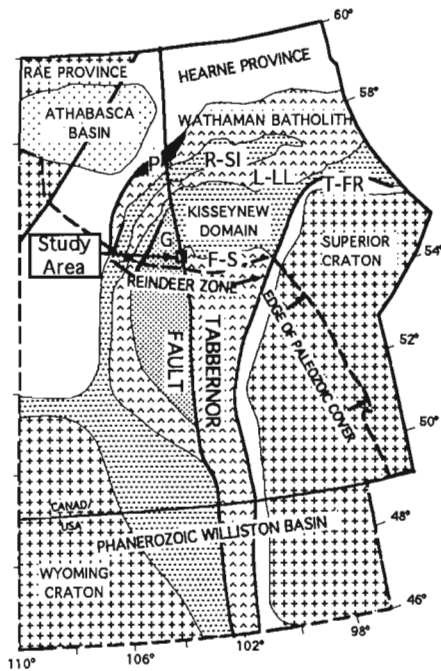
<sup>1</sup> Geology Department, Concordia University, 7141 Sherbrooke St. W, Montreal, Quebec H4B 1R6

## INTRODUCTION AND BACKGROUND

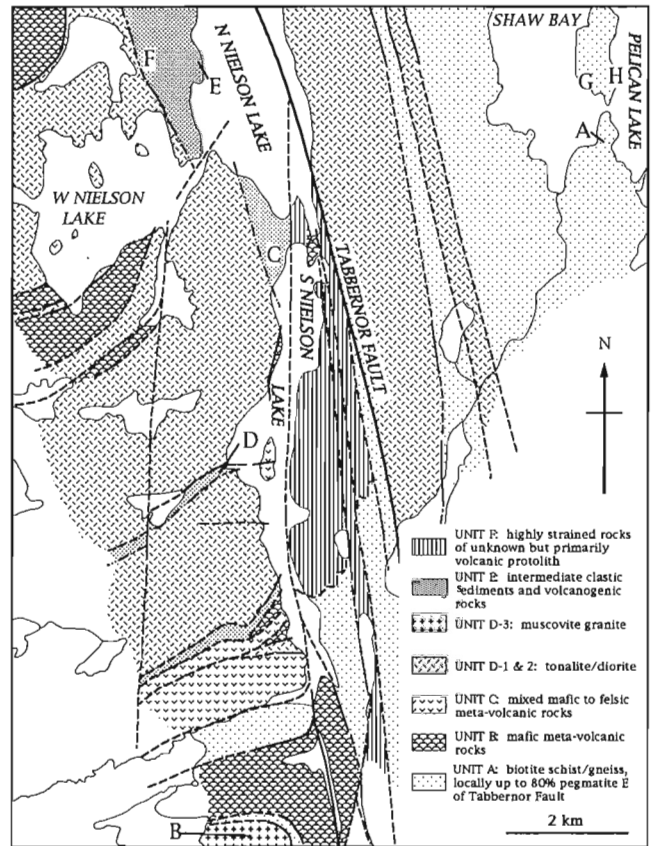
The Tabbernor Fault is a prominent, north-striking feature at the boundary between the Glennie Domain and Hanson Lake Block of the Proterozoic Trans-Hudson Orogen (Lewry, 1981) (Fig. 1). The fault can be traced on surface from small, brittle splays in the Northwest Territories to topographic lineaments in Ordovician dolomite south of the Shield margin. On the basis of geophysical data, Green et al. (1985) traced the fault as far south as 46°N (Fig. 1).

The part of the Tabbernor Fault under investigation during the summer of 1993 (Fig. 2) lies immediately west of the Sahli-Hanson Lake dome (Lewry et al., 1990) and coincides with a wide zone of ductile deformation and a region in which metamorphic grade increases abruptly towards the east (Sibbald, 1978). The shorelines of the north, south, and west lobes of Nielson Lake (N Nielson, S Nielson, and W Nielson Lake) and adjacent Shaw Bay of Pelican Lake expose a complete section across and beyond the walls of the Tabbernor Fault. The 1:20 000 form surface map of Nielson Lake resulting from the summer's fieldwork is published in the 1993 Summary of Investigations of the Saskatchewan Geological Survey (Elliott, in press).

Earlier descriptions of the southern end of the exposed, Proterozoic part of the Tabbernor Fault are reviewed in Wilcox (1990a, b, 1991). The previous studies most relevant



**Figure 1.** The location of the study area on the Tabbernor Fault. The fault trace shown is derived from surface mapping and topographic and geophysical lineaments (modified after Green et al., 1985, Lewry et al., 1990). F-S = Flin Flon-Snow Lake Domain; G = Glennie Domain; L-LL = La Ronge-Lynn Lake Domain; P = Peter Lake Domain; R-SI = Rottenstone-South Indian Lake Domain; T-FR = Thompson and Fox River belts.



**Figure 2.** Distribution of rock types in the Nielson Lake area. The known and inferred relative ages of rock units are as shown with unit A oldest and unit F (mylonites) youngest. Locations A to H are discussed in the text.

to the present study are Sibbald (1978) which reports 1:63 360 mapping of western Pelican Lake and surrounding regions, and Wilcox (1990a, 1991) which describes the Tabbernor Fault from Wood Lake to Nielson Lake. The current study is a continuation of work initiated by K. Wilcox on the kinematic history and significance of the Tabbernor Fault.

A sinistral sense of displacement on the Tabbernor Fault and adjacent ductile strain zone has long been recognized (Budding and Kirkland, 1956), but the kinematic history, timing of motion, and tectonic significance of the fault are still debated (Lewry, 1981; Green et al., 1985; Lewry et al., 1990; Wilcox, 1990a, 1991). The field work reported here indicates that motion of the Tabbernor Fault *sensu stricto* was purely strike-slip, at least over the area examined, and that deformation was primarily brittle. Ductile shearing adjacent to the Tabbernor Fault was also sinistral but was oblique and need not have been related to movement on the Tabbernor Fault. The brittle Tabbernor Fault, therefore, is here distinguished from the ductile Nielson strain zone on the basis of overprinting relationships. Movement vectors in ductilely sheared rocks of the Nielson strain zone change orientation across the Tabbernor Fault and are overprinted by brittle strike-slip faulting.

## ROCK UNITS AND STRATIGRAPHY

The distribution of rock types and interpreted tectono-stratigraphic sequence for the Nielson Lake area are shown in Figure 2.

### *Unit A: biotite schists and gneisses*

Fine- to medium-grained metasedimentary schists and gneisses exposed on both sides of the Tabbemor Fault have been described by Sibbald (1978) and Wilcox (1990a). They are dark to light grey with both coarse and fine compositional layering defined by grain size and composition. Coarse layering (centimetres to 10's of centimetres) is easily recognized as bedding west of the Tabbemor Fault but is less obvious to the east. The millimetre- to centimetre-scale layering of alternating quartz-rich and mica-rich layers is metamorphic.

West of the Tabbemor Fault these rocks contain: quartz+felspar+biotite+amphibole(hornblende)+garnet+staurolite + andalusite±sillimanite±magnetite. They are retrogressed to white mica and chlorite rocks adjacent to the Tabbemor Fault.

East of the Tabbemor fault the rocks vary from schists in the west to granoblastic and migmatitic gneisses in Shaw Bay. They become increasingly rich in cordierite towards the east and there is clear separation of leucosomatic and melanosomatic layers.

Pegmatites are abundant and have locally been attenuated through ductile deformation into strings of feldspar porphyroclasts within the gneissic foliation. Towards the east margin of the map area the biotite gneiss is inter-mixed with as much 80% pegmatite and leucocratic granite.

Both Sibbald (1978) and Wilcox (1990a, b) mapped steep, north-striking isograds based on assemblages within the biotite schists and gneisses. Garnet, andalusite, sillimanite, and cordierite, however, are more widespread than previously noted, bringing into question the validity of the isograds. The distribution of metamorphic minerals appears to be more closely related to lithology than to recognizable pressure-temperature transitions. There is an increase in metamorphic grade from west to east, but it is not clear whether isograds trend parallel to the Tabbemor Fault or whether they are as close together as previously mapped.

### *Unit B: mafic metavolcanic rocks*

Fine- to medium-grained hornblende schists and gneisses are exposed in belts west of the Tabbemor Fault. They vary from black to dark green, weather to rusty browns, and commonly contain: hornblende+plagioclase+biotite+chlorite+pyrite±actinolite. Primary structures were not observed in these rocks, but based on observations north of the map area Wilcox (1990a) concluded that they range from subvolcanic intrusive rocks to basaltic flows and pillow lavas. In the Nielson Lake area, mafic metavolcanic rocks are highly deformed and locally mylonitic to ultramylonitic.

Mafic rocks are common inclusions within the Nielson Lake granodiorite/tonalite that clearly intrudes unit B.

### *Unit C: mixed mafic to felsic metavolcanic rocks*

This unit contains intermixed volcanic rocks ranging from pillow basalts to amygdaloidal andesitic flows to rhyolites and cherts (based on field examination). The best exposures of this unit are near the west shore of S Nielson Lake. Elsewhere the unit is generally highly sheared and primary structures were not observed. It was not possible to distinguish between units B and C near the Tabbemor Fault where ductile deformation is most intense.

The age of unit C relative to other rock types is not clear. Contacts with other units are either not exposed or are faulted. To the northwest of S Nielson Lake a number of narrow lenses of granodiorite/tonalite in the mixed volcanic unit parallel a strong tectonic foliation and may be either fault slices or intrusions. Dykes of the muscovite granite (unit D-3, location B, Fig. 2) at the south end of the map area intrude units A and B right up to the southern edge of unit C but were not observed in the mixed volcanic unit. The interpretation favoured here is that unit C is younger than the structurally lower units A and B.

### *Unit D: intrusive rocks*

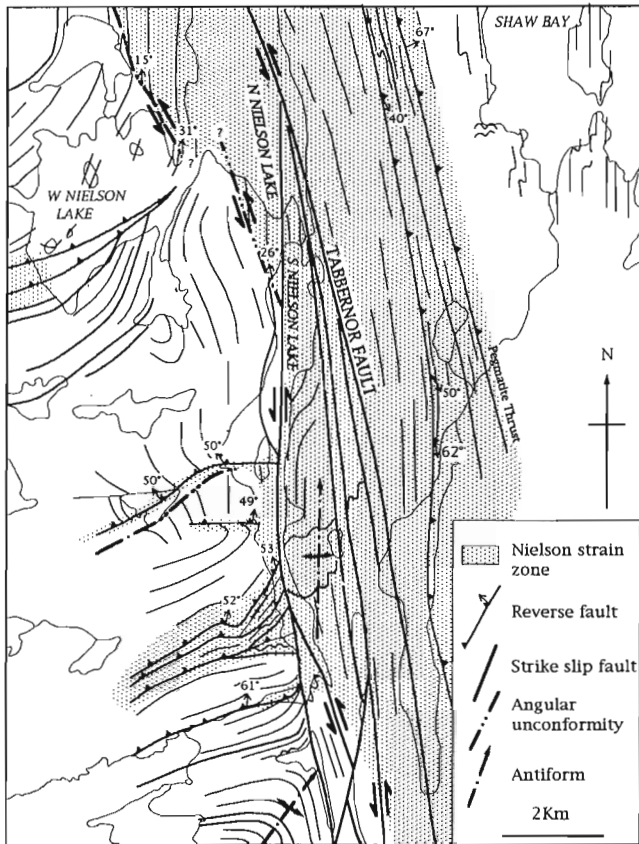
The main felsic intrusion in the map area is unit D-1, the Nielson Lake tonalite (unit 8 of Sibbald, 1978; unit 5 of Wilcox, 1990b). The tonalite is medium-grained, pinkish- to white-weathering to pale orange. The common mineral assemblage is: quartz+plagioclase+K-feldspar+hornblende+chlorite±epidote. The unit is generally well foliated, the foliation increasing in intensity towards the Tabbemor Fault. In places two foliations can be seen and field relationships suggest that the unit contains at least three. The first foliation ( $S_1$ ) predates unit E (below), and is defined by a preferred orientation of quartz aggregates and hornblende aggregates with annealed, recrystallized internal textures. A strong mylonitic foliation in the tonalite unit within the Nielson strain zone is a second and/or third generation foliation.

Mafic inclusions are common and locally quite abundant. They are elliptical to strongly elongate and are generally a few centimetres to a few ten's of centimetres long. They are composed predominantly of hornblende, feldspar, and epidote.

Unit D-2 is a medium- to coarse-grained diorite and quartz diorite associated with unit D-1. It varies in composition from almost pure hornblende to: hornblende+plagioclase+quartz+chlorite. It is locally complexly intermixed with unit D-1 and is interpreted to be a mafic phase of that body. Wilcox (1990a) suggested that it represents mafic contamination of the tonalite where it intruded mafic metavolcanic rocks. However, no spatial association between mafic metavolcanic rocks and the diorite/quartz diorite was noted during the present study.

Unit D-3 (unit 10 of Sibbald, 1978) is a pink, medium- to coarse-grained, muscovite-bearing granite south of S Nielson Lake (location B, Fig. 2). Dykes of the granite and granitic pegmatites intrude the mafic metavolcanic (unit B) and metasedimentary rocks (unit A) south of S Nielson Lake, but not other units. The granite is weakly foliated and this foliation is folded about the northeast-closing fold at the southernmost extent of the map sheet (Fig. 3, 4).





**Figure 3.** Structural interpretation map of the Nielson Lake area showing structural form lines, the Tabbernor Fault, the Nielson strain zone, the angular unconformity beneath unit E, and the "Pegmatite Thrust" of Wilcox (1990a).

The muscovite granite is unique to the west side of the Tabbernor Fault in the map area. However, muscovite-bearing pegmatites and leucogranites are abundant in the biotite schists (unit A) east of the Tabbernor Fault. There are many generations of these pegmatites, and they vary from mylonitic to very weakly deformed. The muscovite granite does not differ significantly from leucogranites and pegmatites east of the Tabbernor Fault.

#### **Unit E: intermediate metavolcanogenic rocks**

The youngest supracrustal rocks are fragmental metavolcanic rocks of dacitic composition and interlayered volcanogenic meta-arenites. They are salmon pink or white to dark gray and tend to be so fine grained that mineralogy is difficult to assess in hand specimen. The representative mineral assemblage of the unit is: quartz+plagioclase+micas+magnetite (locally altered to hematite)+hornblende+chlorite+epidote±garnet. The distinctive features of the unit include a high abundance of magnetite and the presence of monocrystalline quartz 'eyes' which have the iridescent blue tinge characteristic of volcanic quartz.

The rock is locally arenaceous (e.g., locations C, D, E, and F, Fig. 2) and contains crossbedding accentuated by thin laminae of black sand. At location F it contains, along with dacitic fragments, irregular clasts of foliated tonalite varying

in length from 10 cm to 50 cm. A belt of unit E extending west from location D (Fig. 2) varies from coarse sandstone to conglomerate, contains clasts of quartz, chlorite, quartz sandstone, and intermediate volcanic rocks, and contains garnets that appear to be abraded and may be detrital as well.

Elsewhere (e.g., between locations E and F, Fig. 2) the unit is composed of fine grained clasts or lenses elongate parallel to the main foliation. The clasts vary from light to dark grey, are variably quartz-rich, and may be amphibole- and/or feldspar-phyric. Blue quartz 'eyes' are abundant. Light green acicular amphibole crystals may be actinolite. This part of the unit appears to be homogeneous over tens of metres and is well foliated. It is interpreted to be of extrusive origin.

Unit E is the youngest unit in the map area and overlies the Nielson Lake tonalite with angular unconformity west of N Nielson Lake and west of the island in S Nielson Lake (locations D and F, Fig. 2; see also Fig. 3, 4). Just above a ductilely sheared contact between unit E and tonalite at location F, a large outcrop contains rounded clasts of foliated tonalite (described above) in a magnetite-rich matrix. The foliation orientation in the tonalite varies from clast to clast and is locally perpendicular to the penetrative fabric of unit E. Some fragments in that and adjacent outcrops contain a foliation that is crenulated by the penetrative fabric of unit E.

At location D (Fig. 2) Wilcox (1990a, b) mapped a grit horizon unconformably overlying the Nielson Lake tonalite. Here, coarse magnetite-rich quartz arenite is strongly foliated parallel to its contact with tonalite to the south. The contact is neither well exposed or clearly erosive, but the tonalite below the contact has a strong north-striking foliation that is abruptly terminated against the base of the grit. During 1993 the grit unit and unconformity were traced more than 1 km to the west where the grit becomes conglomeratic. The east-west foliation of the basal arenite/conglomerate locally overprints a north-striking foliation in the tonalite.

#### **Unit F: mylonites with uncertain protolith**

At the isthmus between N Nielson Lake and S Nielson Lake and in the zone west of the Tabbernor Fault is a belt of very fine grained, highly strained and foliated silicic to mafic rocks of uncertain protolith. Local occurrences of iridescent blue quartz grains suggest derivation from unit E, but elsewhere the absence of quartz and occurrence of rusty weathering suggests derivation from units B or C. It is inferred that the mylonites represent a tectonic mixture of units B, C, E, and possibly others.

### **STRUCTURE**

The structure of the Nielson Lake area is dominated by three features: 1) The Tabbernor Fault, 2) the Nielson strain zone, and 3) the angular unconformity at the base of unit E (described above) (Fig. 3). Also notable is an isolated north-east-closing fold at the south end of the map area (location B, Fig. 2).



The Tabbenor Fault is here defined as the narrow zone of brittle-ductile to brittle deformation that forms the distinct topographic lineament striking south-southeast through N Nielson Lake. Associated brittle splays, also marked by topographic lineaments, pass through S Nielson Lake (Fig. 3).

The Nielson strain zone is a new name that refers to the zone of intense ductile strain that extends for approximately 800 m either side of the main trace of the Tabbenor Fault. Wilcox (1990a, 1991) used the term "Tabbenor Strain Zone" for "the area adjacent to the Tabbenor Fault where early fabrics are deformed and overprinted and newly formed features

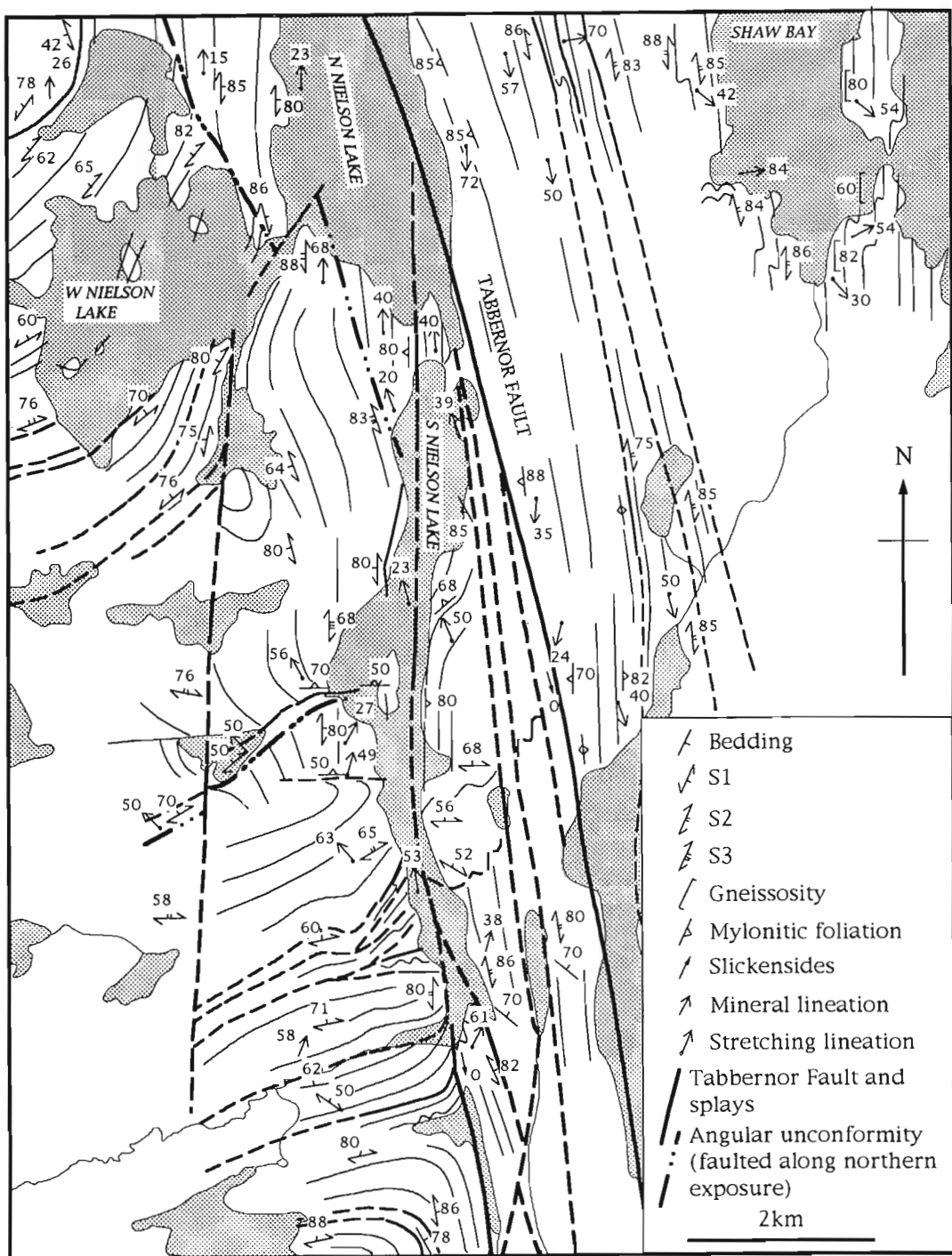


Figure 4. Form surface map of the Nielson Lake area. Due to difficulties in correlating foliations between units, the cleavage generations indicated (S<sub>1</sub>, S<sub>2</sub>, and S<sub>3</sub>) are specific to each unit. Thus S<sub>1</sub> in unit A need not be the same age as S<sub>1</sub> in unit B.

are confined"; However, overprinting fabrics are not confined to a zone parallel to the Tabbernor Fault, there is no evidence that the ductile strain zone and the Tabbernor Fault are more than just locally coincident, and the two have separate kinematic histories.

### ***The Tabbernor Fault***

A scarp up to 50 m high marks the trace of the Tabbernor Fault in the Nielson Lake area and separates granodioritic rocks on the east from metasedimentary and metavolcanic rocks on the west. The fault rocks are foliated cataclasite to variably brecciated tonalite. Fault lineations are subhorizontal slickensides and quartz-chlorite fibres, the latter indicating sinistral strike-slip movement. Unfilled sigmoidal extension gashes also indicate sinistral motion. Horizontal slickensides overprint older, plunging, feldspar and quartz aggregate lineations of the Nielson strain zone.

At the south end of S Nielson Lake a 50 m scarp marks a brittle splay of the Tabbernor Fault that cuts through the eastern limb and hinge of the northeast-closing fold at location B (Fig. 2, 3, and 4). The hinge zone of the fold appears to be sinistrally displaced by at least 2 km up the east shore of S Nielson Lake.

The magnitude of displacement on the Tabbernor Fault at the latitude of the study area is not known. Steep isograds mapped by Sibbald (1978) and Wilcox (1990a, b) have separations of 6-8 km; however, there is uncertainty about the locations of isograds, as discussed above. The 2 km minimum displacement on the Tabbernor splay suggests that displacement across the main trace of the Tabbernor Fault was greater than 2 km.

Conjugate crenulations trending approximately 125° and 040° have a vertical intersection and are roughly symmetric about the trend of the Tabbernor Fault. The crenulations overprint S-C and mylonitic foliations, are most abundant within the 200 m either side of the fault, and are tentatively inferred to have formed during strike-slip movement on the Tabbernor Fault.

### ***The Nielson strain zone***

In the Nielson Lake area a zone of ductile strain with well-developed mylonitic foliations straddles the Tabbernor Fault. The mylonitic foliation of the Nielson strain zone generally has the same trend and steep dip on either side of the Tabbernor Fault: However, the fault scarp marks an abrupt transition from moderate to steep south-plunging extension lineations on the east to moderate north-plunging extension lineations on the west (Fig. 4). (In this paper extension lineations are those in which extension is indicated by small-scale boudinage of the lineated material, larger scale boudinage perpendicular to the lineation, and/or smearing of mineral aggregates parallel to the lineation.)

The Nielson strain zone is described in two parts corresponding to lineation plunge domains separated by the Tabbernor Fault.

### **East Nielson strain zone**

The East Nielson strain zone includes all of the tonalite east of the Tabbernor Fault and extends into the adjacent biotite schists and gneisses (Fig. 2, 3). In the tonalite the penetrative mylonitic/ultramylonitic foliation is steeply-dipping to vertical and trends north to north-northwest, which is generally slightly clockwise from the trend of the Tabbernor Fault.

The tonalite is everywhere sheared, with S-C fabrics, shear bands, and extension lineation defined by elongate aggregates of quartz, feldspar, and chlorite (after hornblende?). Towards the eastern margin of the tonalite there is an increase in abundance of centimeter thick to tens of centimetres thick bands of strongly lineated and foliated tonalite in which grain size is below resolution with the naked eye. Lineations have the same moderately south-plunging orientations within and outside these ultramylonite bands. Kinematic indicators are uniformly sinistral oblique, with the east side moved up and northwards relative to the west.

Wilcox (1990a) described a 15 m wide high strain zone in which metasedimentary rocks to the east were transported up and to the north over tonalite to the west. He named this the "Pegmatite Thrust" (Fig. 3), and suggested that higher grade rocks had been emplaced over lower grade rocks. Though the fault would better be called a reverse fault, this kinematic interpretation fits well with observations reported here. It is further suggested that this is the locus of maximum strain in the East Nielson strain zone. Movement on this zone post-dates peak metamorphism.

To the east of the "Pegmatite Thrust" indicators of sinistral-oblique ductile shear are confined to narrow zones that decrease in abundance towards Pelican Lake. On Shaw Bay, zones of sinistral-oblique ductile shear overprint an earlier gneissosity that is pervasively Z-folded and contains rotated porphyroclasts and boudins, all of which indicate dextral shear along steep S-plunging extension lineations. On the east shore of Shaw Bay indicators of sinistral shear are all but absent, and the migmatitic gneisses with dextral kinematic indicators have a granoblastic texture.

At locations G and H (Fig. 2) the gneissosity and sheared, transposed pegmatites are intruded at right angles by younger pegmatite dykes in which the only signs of deformation are small, oblique, sinistral, ductile offsets. These offsets are believed to represent deformation at the easternmost limit of influence of the East Nielson strain zone.

### **West Nielson strain zone**

The West Nielson strain zone is defined by strongly sheared to mylonitic rocks with foliations that are steep to vertical where they trend subparallel to the Tabbernor Fault, and moderately to steeply north-dipping where they bend towards the west along the west shore of S Nielson Lake (Fig. 3, 4). Extension lineations defined by quartz, feldspar, and hornblende aggregates plunge moderately north. Kinematic indicators such as shear bands, rotated boudins, s porphyroclasts, and rotated tension gashes all indicate sinistral oblique motion on steep north-trending foliations. On east-trending foliations, the kinematic indicators and repetition of the

unconformity and units C, D, and E west of S Nielson Lake indicate south-directed reverse faulting. This deformation overprints a dominantly north-south foliation in the Nielson Lake tonalite ( $S_1$ ).

It is inferred that the sinistral oblique and reverse components of movement were synchronous and represent thrust faults and an adjacent lateral ramp or tear fault. This is because a) extension lineations have the same style and orientation regardless of the orientation of the foliation, and kinematic indicators all show south-directed transport, and b) the high-strain foliation varies continuously from north-south to east-west with no overprinting. North-south crenulations do exist but they are neither strong nor abundant, nor are they spatially related to the areas in which the foliation changes orientation. The crenulations are believed to be late and related to strike-slip movement on the Tabernor Fault.

### ***Northeast-southwest folding***

The northeast-closing fold at the south end of the map area (location B, Fig. 2) has muscovite granite in its core and overprints an earlier cleavage in the granite and in the metasedimentary and metavolcanic rocks on the flanks (Fig. 3, 4). Granitic and pegmatitic dykes radiating from the muscovite granite also appear to have been folded. The fold has no axial plane cleavage. Symmetric folds in the nose of the fold are upright and plunge moderately towards the northeast.

There are no other folds with this style or orientation in the map area, nor are there other structures with related orientations. The absence of geometrically related structures in units C, E, and F, suggests that folding may have occurred prior to the deposition/formation of those units. This possibility is supported by the fact that the granitic dykes emanating from unit D-3 occur right up to, but not across, the contact between units B and D at southwestern S Nielson Lake. Folds of a similar orientation in similar rocks were mapped by Sibbald (1978) east of the Tabernor Fault and about 10 km to the north of the present map area. If these fold axes correlate with that mapped south of Nielson Lake, this suggests at least 10 km of sinistral displacement along the Tabernor Fault.

## **GEOCHRONOLOGY AND TIMING OF DEFORMATION**

Because there are no published geochronological data for the rocks of the Nielson Lake area, no absolute time frame has been established for depositional and deformational events in the study area. Correlations can be made with adjacent areas for which age data have been published.

### ***Units A and C***

Most dated volcanic rocks in the Hanson Lake Block and Glennie Domain lie within a 1890-1875 Ma or 1845-1838 Ma range (Slimmon, 1992), although the dated rocks are

primarily rhyolites. It is tentatively assumed that the volcanic rocks in the Nielson Lake area that predate the Nielson Lake tonalite (units A and C) lie in the older age range.

### ***Unit D-1 and D-2***

Tonalites and granodiorites from the Glennie Domain yield ages in two ranges: 1859-1832 Ma, and 2343-2487 Ma (Slimmon, 1992; McNicoll et al., 1992). Van Schmus et al. (1987), Delaney et al. (1988) and McNicoll et al. (1992) refer to a major tonalitic magmatic event between 1846-1859 Ma, which included intrusion of the adjacent Wood Lake Batholith and Deschambault Narrows tonalite. The Nielson Lake tonalite is probably best correlated with the postvolcanic tonalite from Deschambault Narrows (20 km southwest of the study area) which has a U-Pb zircon age of  $1850 \pm 4$  Ma (Van Schmus et al., 1987). The mafic volcanic rocks of unit B would then be older than 1850 Ma, and perhaps older than 1875 Ma as discussed above.

### ***Unit E***

The magnetite-rich arenites of unit E may correlate with similar arkosic arenites of the Ourom Lake and Wapawekka Lake formations of the Glennie Domain which through U-Pb analysis of detrital zircons and felsic intrusive bodies have been dated as between 1848-1838 Ma old (McNicoll et al., 1992). Though these units differ in provenance from the molassic metasedimentary rocks of the Missi Formation east of the Tabernor Fault, they are similar in age and may indicate a widespread episode of molasse sedimentation in the Trans-Hudson Orogen (Delaney et al., 1988).

### ***Angular unconformity***

Deformation, uplift, and erosion occurred between the intrusion of the Nielson Lake tonalite and deposition of unit E. The ages for these units suggested by the above correlations narrowly constrain the timing of these events to between approximately 1850 and 1840 Ma.

### ***Nielson strain zone***

The East Nielson strain zone overprints and thus postdates high-grade dextral strain fabrics in biotite schists to migmatitic gneisses of the Sahli-Hanson Lake dome. The West Nielson strain zone postdates angular unconformity and deposition of intermediate volcanic and arenaceous supracrustal rocks. Both sides of the strain zone have sinistral ductile shear fabrics that are oblique in opposite directions. To the east of the Tabernor Fault, transport was east-side up and to the north. To the west, transport was west side up and to the south. In their present positions, the kinematics of the East and West strain zones are therefore not compatible.

Timing of movement on the West Nielson strain zone is constrained only by the age of unit E (1848-1838 Ma?), with no crosscutting lithology to provide a minimum age. Movement on the East Nielson strain zone is constrained by the age of unit B (unknown) and the age of late pegmatites which

crosscut the gneissosity in Shaw Bay and show evidence of minor deformation in the East Nielson strain zone. The late pegmatites, which are believed to have been deformed during latest shear in the East Nielson strain zone or at the easternmost reaches of the strain zone, are tentatively correlated with the Hanson Lake and Jan Lake pegmatite suites and pegmatitic granites in the Hanson Lake Domain. These rocks have an age range of 1780-1750 Ma (Slimmon, 1992). Pegmatites of a similar age are common in the Glennie domain (Slimmon, 1992).

U-Pb geochronology is presently underway to test the tentative correlations made here and to place absolute time constraints on depositional and deformational events.

## ACKNOWLEDGMENTS

Field work was funded by the NATMAP Shield Margin project of the Geological Survey of Canada. Logistic assistance was provided by the Saskatchewan Geological Survey and the Manitoba Department of Energy and Mines. I thank Steve Lucas (GSC) and Tom Sibbald (SGS) who initiated this project and made sure I had what I needed to get it done. I especially thank Chris Gammons (McGill University) who volunteered his time to help me map and who contributed to the ideas presented here.

## REFERENCES

- Budding, A.J. and Kirkland, S.J.T.**  
1956: The geology and mineral deposits of the Hanson Lake area; Saskatchewan Department of Mineral Resources, Report 30, 42 p.
- Delaney, G., Carr, S.D., and Parrish, R.R.**  
1988: Two U-Pb zircon ages from eastern Glennie Lake Domain, Trans-Hudson Orogen, Saskatchewan; in Radiogenic Age and Isotopic Studies: Report 2; Geological Survey of Canada, Paper 88-2, p. 51-58.
- Elliott, C.G.**  
in press: Structural study of the Tabbernor FAult, Nielson Lake area; in Summary of Investigations 1993, Saskatchewan Geological Survey, Saskatchewan Energy and Mines, Miscellaneous Report.
- Green, A.G., Hajnal, Z., and Weber, W.**  
1985: An evolutionary model of the western Churchill Province and western margin of the Superior Province in Canada and the north-central United States; Tectonophysics, v. 116, p. 281-322.
- Lewry, J.F.**  
1981: Lower Proterozoic arc-microcontinent collisional tectonics in the western Churchill Province; Nature, v. 294, p. 69-72.
- Lewry, J.F., Thomas, D.J., Macdonald, R., and Chiarenzelli, J.**  
1990: Structural relations in accreted terranes of the Trans-Hudson orogen, Saskatchewan: Telescoping in a collisional regime?; in The Early Proterozoic Trans-Hudson Orogen of North America, (ed.) J.F. Lewry and M.R. Stauffer; Geological Association of Canada, Special Paper No. 37, p. 75-94.
- McNicol, V.J., Delaney, G.D., Parrish, R.R., and Heaman, L.M.**  
1992: U-Pb age determinations from the Glennie Lake Domain, Trans-Hudson Orogen, Saskatchewan; in Radiogenic Age and Isotopic Studies: Report 6; Geological Survey of Canada, Paper 92-2, p. 57-72.
- Sibbald, T.I.I.**  
1978: Geology of the Sandy Narrows (East) area Saskatchewan (NTS area 63M-3E); Department of Mineral Resources, Saskatchewan Geological Survey, Precambrian Geology Sector, Report No. 170.
- Slimmon, W.L.**  
1992: Saskatchewan Precambrian Geochronology Chart: Version 1.2; Saskatchewan Geological Survey, Saskatchewan Energy and Mines publication.
- Van Schmus, W.R., Bickford, M.E., Lewry, J.F., and Macdonald, R.**  
1987: U-Pb Geochronology in the Trans Hudson Orogen, northern Saskatchewan, Canada; Canadian Journal of Earth Sciences, v. 24, p. 407-424.
- Wilcox, K.H.**  
1990a: Bedrock Geological Mapping, Nielson Lake Area, Tabbernor Fault zone; in Summary of Investigations 1990, Saskatchewan Geological Survey, Saskatchewan Energy and Mines, Miscellaneous Report 90-4, p. 74-83.  
1990b: Bedrock Geology, Nielson Lake Area, Tabbernor Fault Zone (NTS 63M3); in Summary of Investigations 1990, Saskatchewan Geological Survey, Saskatchewan Energy and Mines, Miscellaneous Report 90-4.  
1991: Geological relationships in the Wood Lake area, Tabbernor fault zone, Saskatchewan; in Summary of Investigations 1991, Saskatchewan Geological Survey, Saskatchewan Energy and Mines, Miscellaneous Report 91-4, p. 135-143.

Geological Survey of Canada Project 910035

# Structural investigation of high-grade rocks of the Kramanituar complex, Baker Lake area, Northwest Territories

M. Sanborn-Barrie<sup>1</sup>

Continental Geoscience Division

*Sanborn-Barrie, M., 1994: Structural investigation of high-grade rocks of the Kramanituar complex, Baker Lake area, Northwest Territories; in Current Research 1994-C; Geological Survey of Canada, p. 121-133.*

---

**Abstract:** The Kramanituar complex comprises granulite-grade gabbro, gabbroic anorthosite, and paragneiss and is hosted by amphibolite-grade plutonic and supracrustal wall rock. Its northern boundary coincides with a granulite-grade shear zone, 60 km long and up to 6 km wide, across which sinistral, south-side-up displacement is recorded. Its southern boundary appears to coincide with an amphibolite-grade shear zone, 30 km long and up to 2 km wide, across which dextral, north-side-up movement has occurred. Preliminary observations suggest that the complex represents a high-grade, crustal-scale tectonic lens, or boudin, which was rapidly exhumed during noncoaxial, southwest-directed shortening.

**Résumé :** Le complexe de Kramanituar est composé de gabbro, d'anorthosite gabbroïque et de paragneiss du faciès des granulites, encaissés dans des roches supracrustales et plutoniques du faciès des amphibolites. La limite nord du complexe coïncide avec une zone de cisaillement du faciès des granulites mesurant 60 km de longueur et jusqu'à 6 km de largeur, qui a été le siège d'un déplacement senestre avec soulèvement du compartiment sud. Sa limite sud semble coïncider avec une zone de cisaillement du faciès des amphibolites, mesurant 30 km de longueur et jusqu'à 2 km de largeur, dans laquelle s'est produit un déplacement dextre avec soulèvement du compartiment nord. Les premières observations indiquent que le complexe représente une lentille tectonique (ou boudin) d'échelle crustale fortement métamorphisée qui a été mise à nu rapidement durant un épisode de raccourcissement non coaxial à vergence sud-ouest.

---

<sup>1</sup> Ottawa-Carleton Geoscience Centre, Department of Earth Sciences, Carleton University, Ottawa, Ontario K7S 5B6

## INTRODUCTION

The Kramanituar complex comprises granulite-grade gabbroic anorthosite and gabbroic rocks (Schau and Hulbert, 1977; Schau and Ashton, 1980; Schau et al., 1982; Sanborn-Barrie, 1993) and is hosted by amphibolite-grade plutonic and supracrustal wall rock. The complex coincides with a regional geophysical anomaly, designated the Snowbird tectonic zone (Hoffman, 1988), along which discontinuously exposed rocks of similar composition, structural style, and metamorphic grade also occur (Gordon, 1988; Hanmer et al., 1992; Hanmer and Kopf, 1993; Tella and Annesley, 1988; Tella et al., 1993). This study is part of a collaborative effort to unravel the tectono-metamorphic history of these complexes and, in turn, that part of the Churchill Province transected by the Snowbird tectonic zone (Fig. 1). Well-constrained structural, petrological, and geochronological studies of the individual complexes will reveal whether each possesses a distinct history; or alternately, whether their histories are similar and reflect regional-scale crustal processes.

The Kramanituar complex is an ideal setting in which to undertake magmatic, structural, and metamorphic studies. It preserves several generations of fabric elements. It displays strain of variable intensity which, where low, preserves lithological relationships and, where high, results in regional-scale shear zones up to 60 km long and 6 km wide. It is characterized by high-grade, generally unannealed metamorphic mineral assemblages. Two significant structural interpretations that evolved from 1992 mapping were:

1. that the northern boundary of the granulite-grade complex coincides with a steep, curvilinear, regional-scale shear zone across which sinistral, south-side-up displacement has occurred. This shear zone may have had a major role in juxtaposition of granulite-grade rocks with amphibolite-grade rocks to the north.
2. that the southern boundary of the complex coincides with an east-striking, moderately dipping shear zone across which dextral, north-side-up displacement may, similarly, have been responsible for juxtaposition of the granulites with amphibolite-grade rocks to the south.

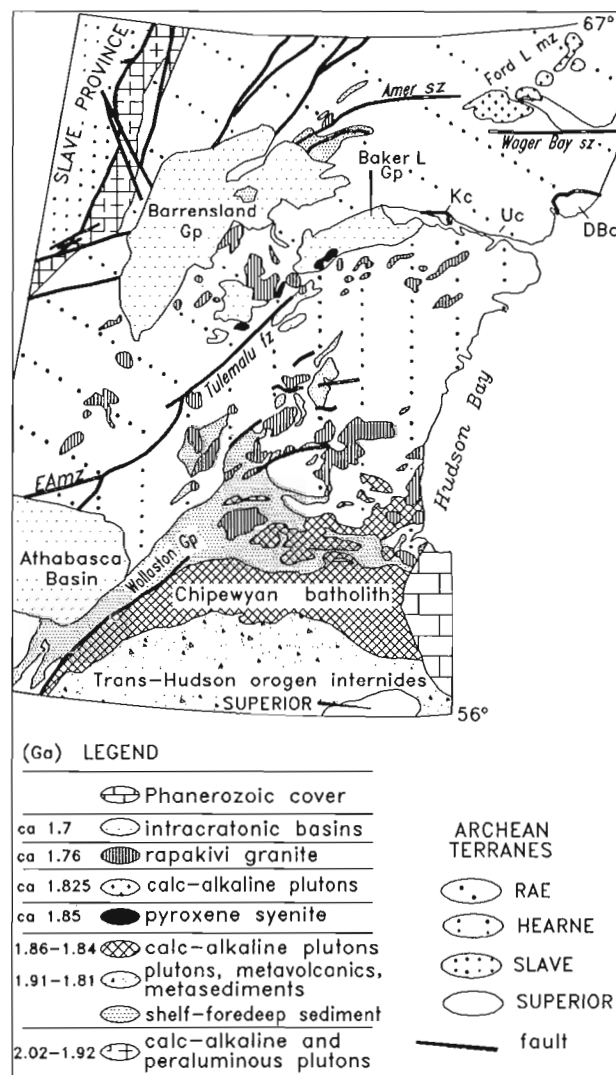
A primary goal of 1993 fieldwork was to further delineate the geometry, kinematics, and metamorphic character of these two bounding shear zones. Their character and the temporal relationship between them are critical to understanding uplift mechanisms involved in exhuming this granulite-grade complex, and may pertain to others along the Snowbird tectonic zone, and elsewhere. Emphasis was also placed upon documenting metamorphic mineral assemblages across the granulite complex and into its amphibolite-grade wall rocks to establish the relationship between metamorphism and both magmatism and structure.

This report emphasizes structural aspects of the Kramanituar complex based on 1992 and 1993 field observations. A preliminary description of its metamorphic character is also provided. Ongoing studies will integrate the structural and metamorphic aspects of these rocks to gain a better

understanding of their evolution, their relationship with similar complexes, and their role in the evolution of the central Churchill Province.

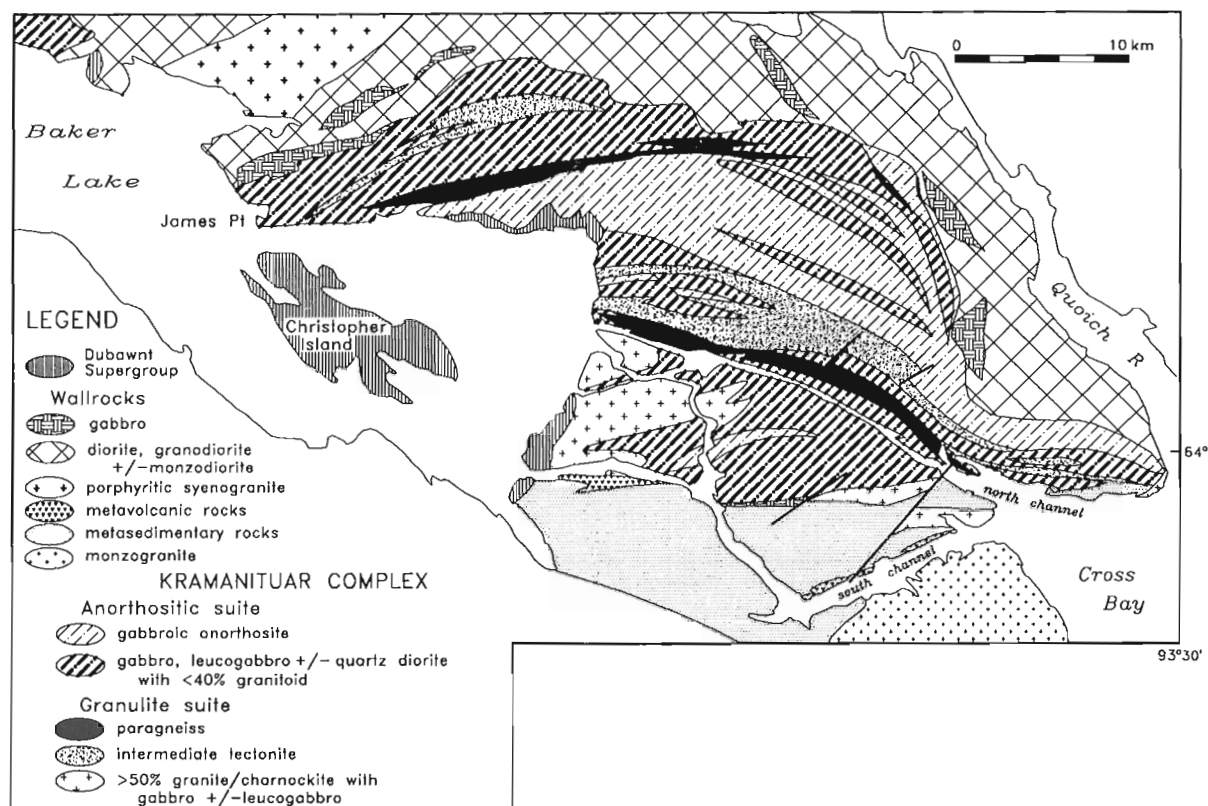
## LITHOLOGICAL UNITS WITHIN THE COMPLEX

Comprehensive descriptions of the principal lithological units of the map area are provided in Sanborn-Barrie (1993). In general, the Kramanituar complex comprises a gabbroic-anorthosite suite with minor interlayered paragneiss, orthogneiss, and granite-charnockite (Fig. 2). Where less deformed, gabbroic anorthosite is composed of phenocrysts



**Figure 1.** Geology of the western Canadian Shield after Hoffman (1988). Segments of the proposed Snowbird tectonic zone, at the interface between the Rae and Hearne provinces, include the East Athabasca mylonite zone (EAmz), the Tulemalu fault zone, the Kramanituar complex (Kc), the Uvauk complex (Uc) and the Daly Bay complex (DBc).





**Figure 2.** General geology of the Kramanituur complex and adjacent units. Modified from Schau and Ashton (1980).

of plagioclase±orthopyroxene in a groundmass of plagioclase, orthopyroxene, and clinopyroxene±magnetite. Metre-scale layers of gabbro and leucogabbro commonly occur with gabbroic anorthosite. These generally appear to represent intrusive dykes or sills owing to their uniform composition and abrupt contacts with gabbroic anorthosite. Magmatic layering, defined by systematic decrease in the percentage of mafic minerals across adjacent metre-scale layers is observed locally (Sanborn-Barrie, 1993). Anorthosite comprises <10% of the suite, occurring as continuous, tabular, 10 m wide horizons (sills?) in gabbro and paragneiss immediately north of gabbroic anorthosite. Gabbro and leucogabbro (±quartz diorite) are regionally extensive, occurring north and south of gabbroic anorthosite (Fig. 2). These consist of 25 to 60% mafic minerals, generally with clinopyroxene > garnet > orthopyroxene, with plagioclase and minor magnetite. These rocks typically display subtle metre-scale layering owing mainly to variations in colour index and are cut by parallel, centimetre-scale veinlets or sheets of granitic-charnockitic rock (described below).

Rocks interpreted as paragneiss occur immediately north of gabbroic anorthosite and along the north channel of Chesterfield Inlet (Fig. 2). These well-layered rocks contain 5-25% quartz, with biotite, plagioclase, and garnet±sillimanite±graphite. Two narrow panels of kyanite-bearing paragneiss occur in the northeast part of the complex, and rare sapphirine-bearing panels occur in the southeast (see Fig. 10).

A texturally distinctive unit designated intermediate tectonite occurs northwest and south of gabbroic anorthosite (Fig. 2). This pale buff- to rust-weathering unit, previously described as diatexite (Sanborn-Barrie, 1993), is compositionally similar to paragneiss in that these rocks contain 10-20% quartz, plagioclase, 2-10% garnet, and biotite±orthopyroxene. In contrast to paragneiss, these rocks do not contain sillimanite, kyanite, graphite, or sapphirine. A texture distinctive to this unit is created by garnet porphyroblasts (1 mm to 2 cm) which are draped by sigmoidal ribbons of quartz and feldspar. Layering within intermediate tectonite is much more nebulous than in paragneiss, and observed contacts with paragneiss and gabbroic rocks are subtle and diffuse. The descriptive term intermediate tectonite was assigned to these rocks since it remains unclear from field relationships whether they represent homogeneous diatexite derived through advanced anatexis of paragneiss. Alternate origins may include anatexis of an intermediate plutonic protolith, or single-stage crystallization at granulite-grade conditions of a peraluminous plutonic body of quartz dioritic composition.

Granitic rocks are a minor but widespread component of the complex and occur as centimetre- to metre-scale veins and panels that cut gabbro, paragneiss, and intermediate tectonite. These pink- to white-weathering rocks are of leucogranodioritic composition with 10 to 35% quartz, 10 to 15% K-feldspar, plagioclase, up to 5% garnet, 2-10% mafic minerals, and minor magnetite±pyrite. Mafic minerals are generally orthopyroxene in the southern part of the complex and

clinopyroxene in the north, a distribution which reflects increasing pressure conditions toward the north (see Metamorphism).

## UNITS EXTERNAL TO THE COMPLEX

North and east of the complex, foliated to gneissic hornblende- and/or biotite-bearing plutonic rocks are widespread (Fig. 2). These vary in composition from gabbro-diorite and quartz diorite with a colour index of 25 to 45, to granodiorite with 25% quartz and a colour index of 5 to 20. Gabbroic to dioritic host rocks are commonly cut by centimetre-scale veins and metre-scale panels of biotite±hornblende granodiorite. Northwest of the complex, foliated K-feldspar porphyritic syenogranite is exposed (Fig. 2).

South of the complex, metasedimentary rocks dominated by lithic wacke with lesser feldspathic wacke, pelites, and rare magnetite-ironstone occur. Amphibolite-facies metamorphism is reflected by the widespread occurrence of biotite+garnet. Sillimanite occurs locally as coarse grained porphyroblasts or fine grained fibrolite (see Fig. 10). In general, metasedimentary rocks display a strong foliation, transposition, and show incipient partial melt textures. In spite of this, primary lithological variations are recognized locally (Sanborn-Barrie, 1993); however, stratigraphic younging or structural facing could not be established.

Metavolcanic rocks are exposed in a restricted zone along the south channel of Chesterfield Inlet (Fig. 2) where they are tightly folded with metasedimentary rocks. Isolated occurrences of volcanics are compositionally and texturally diverse. Garnet-bearing amphibolites display remnant 2 cm wide selvages and are interpreted as pillowed mafic flows. Possible flow top breccia (Fig. 3a) occurs at the interface between pillowed and massive flows. Intermediate pyroclastic breccias with up to 40% buff-weathering rhyodacite fragments in a grey-weathering dacitic groundmass (plagioclase+biotite+garnet) also occur (Figure 3b). Fine grained, layered, tuffaceous rocks of andesitic to dacitic composition appear to be gradational with the metasedimentary rocks.

Early Proterozoic sedimentary and volcanic rocks of the Dubawnt Supergroup unconformably overlie the Kramanitar complex (Fig. 2). The lowermost part of this succession is the Baker Lake Group which includes the basal South Channel conglomerate and red-weathering Kazan sandstone.

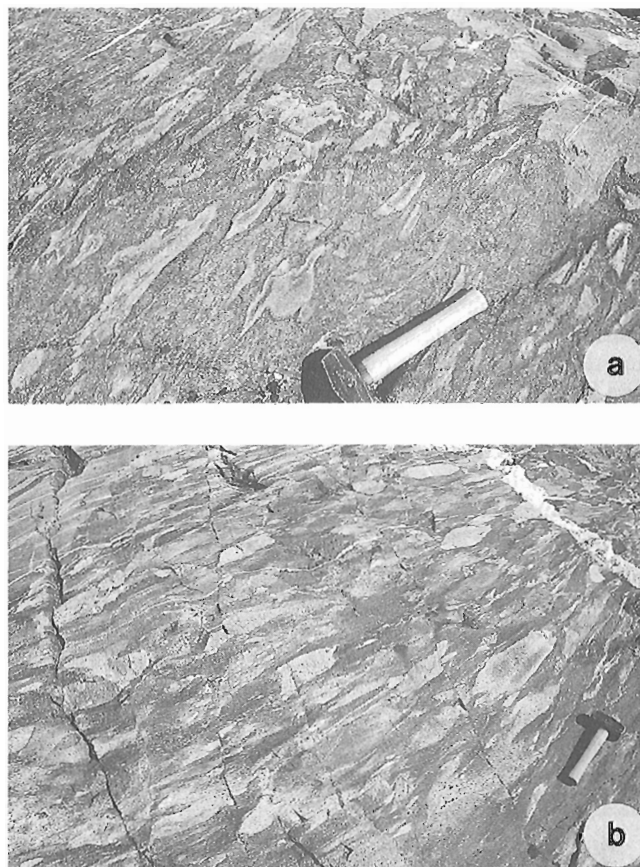
## STRUCTURE

### *Planar and linear elements within the complex*

Most localities within the Kramanitar complex display a single, strong to intensely developed planar fabric with an associated strong linear fabric. A number of localities, however, display two generations of planar fabrics, and at these localities, relative timing relationships (i.e.,  $S_1$ ,  $S_2$ ) can be discerned on the basis of overprinting relationships. In exposures where only one fabric is observed, it is then generally

feasible to identify it as  $S_1$  or  $S_2$  on the basis of its character and attitude (described below). Resultant patterns of  $S^1$  and  $S^2$  are shown in the foliation trajectory map of Figure 4a.

The character of  $S_1$  is dependent to some extent upon rock type. In relatively unstrained gabbroic anorthosite in the central part of the complex,  $S_1$  occurs as a weak to moderately developed foliation. More typically, and well exemplified in the southern part of the complex,  $S_1$  is defined by parallel, centimetre-wide sheets of granitic/charnockitic material cutting gabbro and leucogabbro. This imparts a compositional layering (Fig. 5) to much of the southern part of the complex, although this layering is essentially intrusive in nature. A shape fabric defined by the elongation of individual mineral constituents is only locally observed to be parallel to  $S_1$  layering (Fig. 5c). The general absence of a shape fabric parallel to  $S_1$  layering (Fig. 5d) is attributed to penetrative realignment of mineral constituents during later deformation. Throughout the complex, a characteristic feature of  $S_1$  is its moderately to shallowly dipping attitude (Fig. 4a). Locally  $S_1$  is subhorizontal.  $S_1$  strikes southeast or southwest, defining folds and monoclinical panels throughout the southern half of the complex (Fig. 4a).



**Figure 3.** Metavolcanic rocks. **a**) Possible flow-top breccia at interface between pillowed and massive flows. (GSC 1993-260I) **b**) Intermediate pyroclastic breccia, bedding (not shown) is subparallel to fragment elongation direction due to transposed nature of these tightly folded rocks. (GSC 1993-260H)

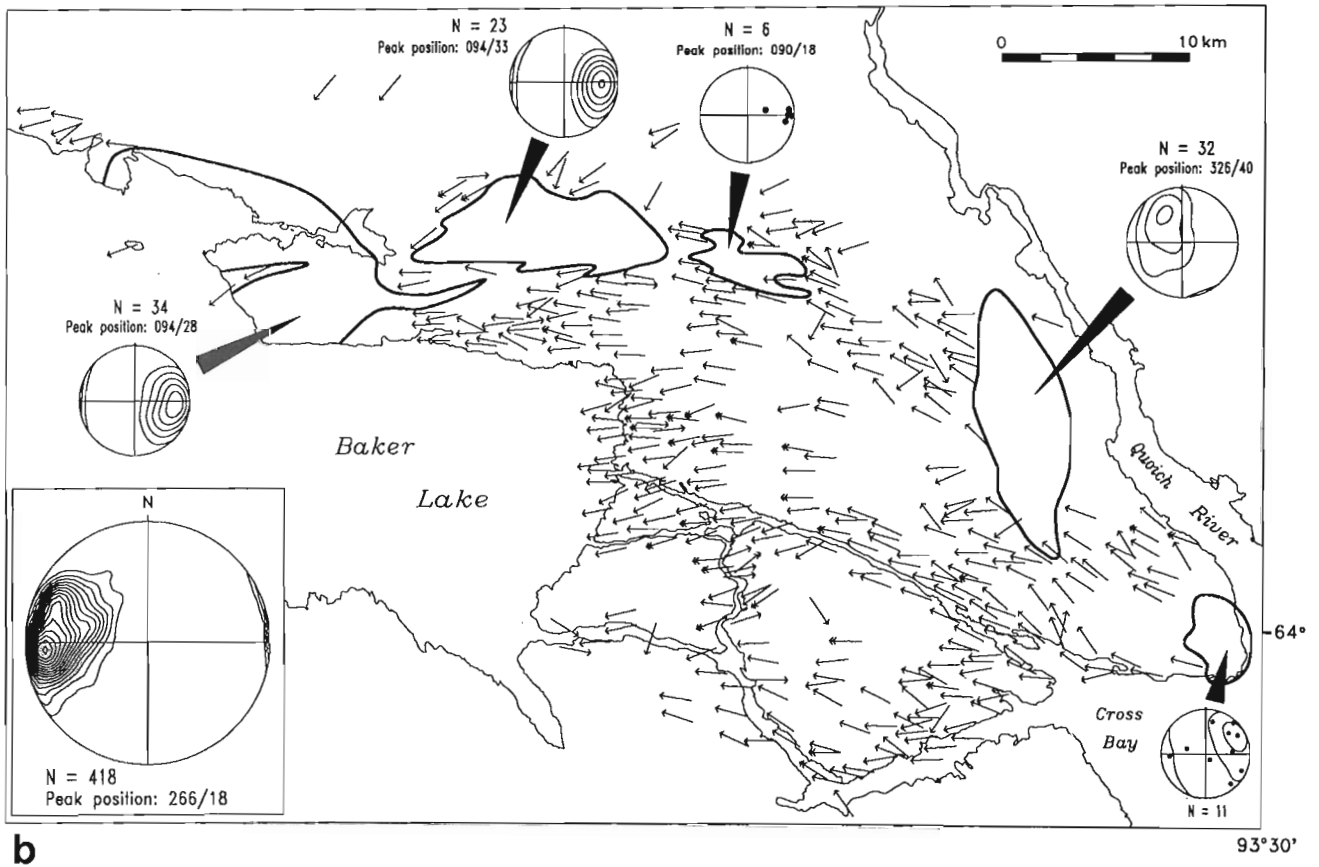
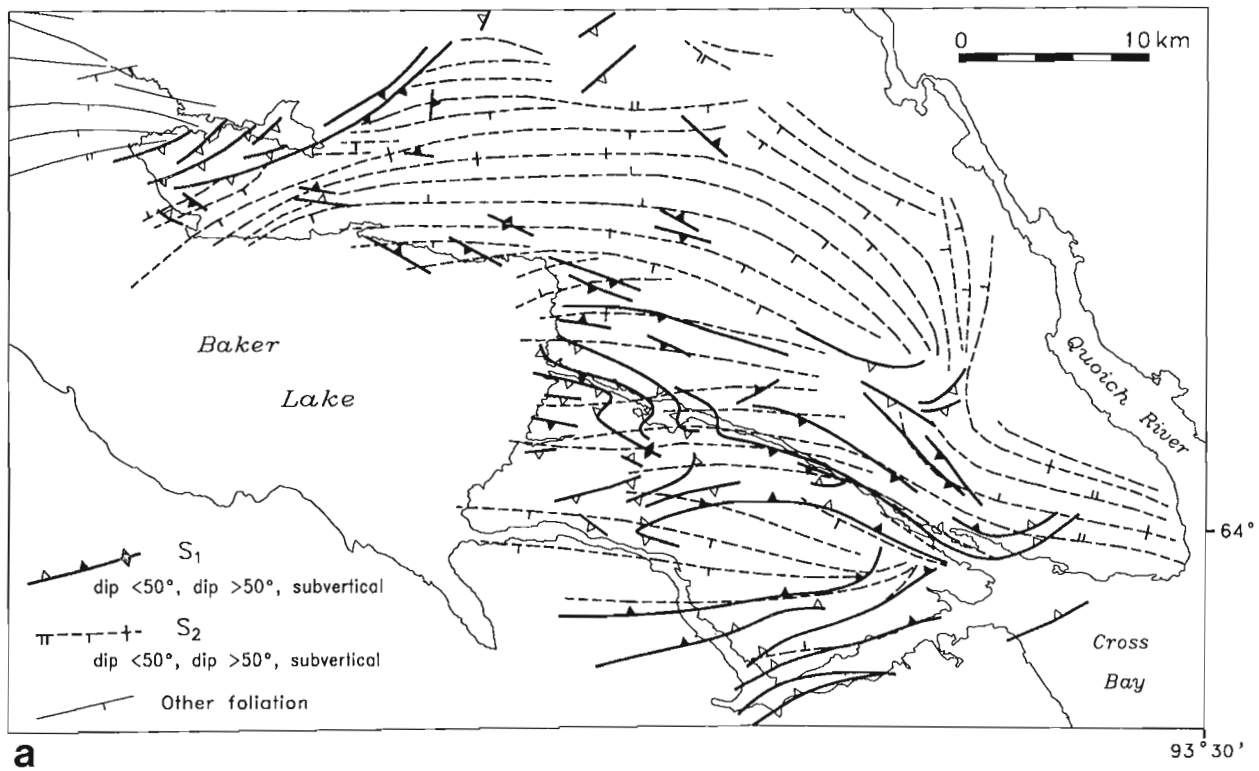
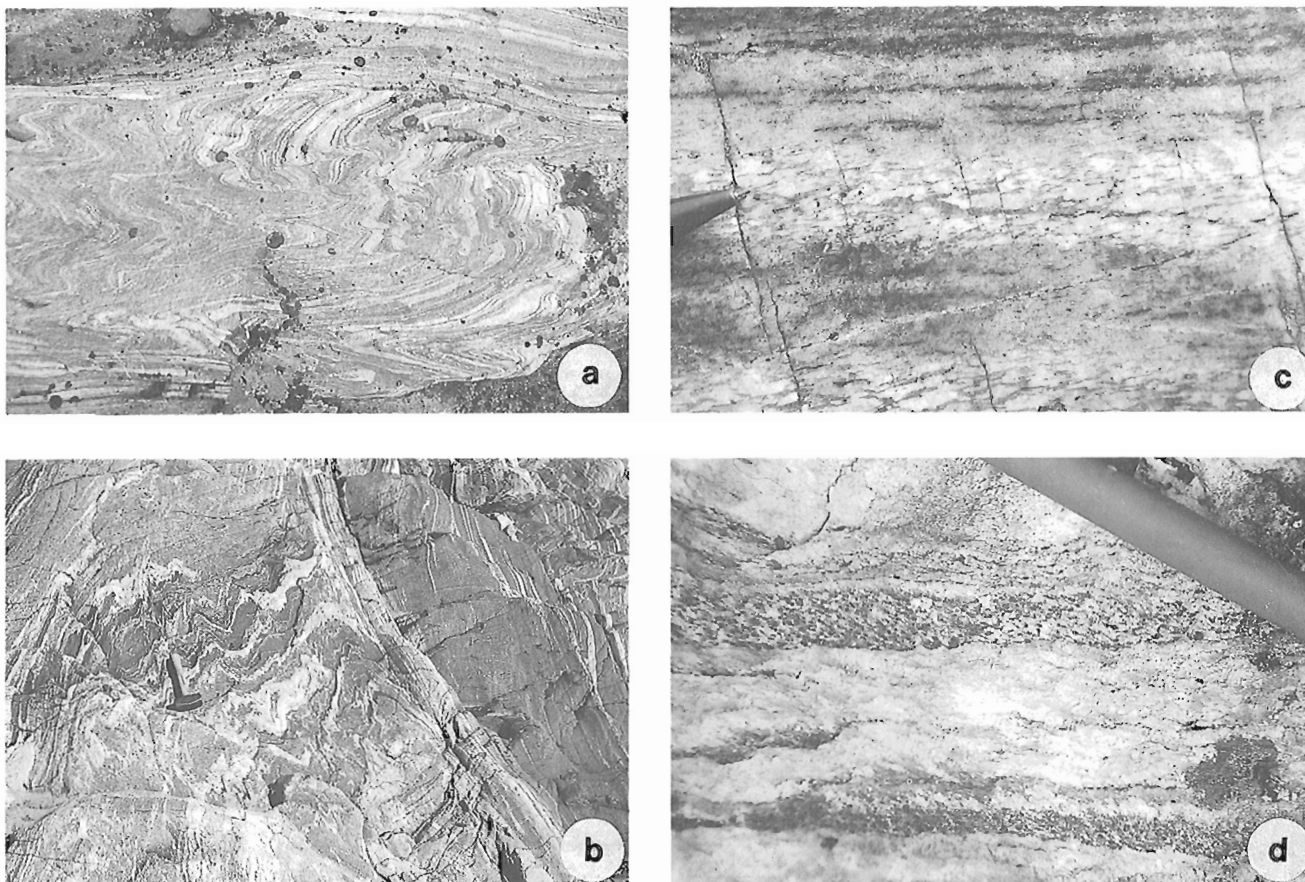


Figure 4. Planar and linear tectonic elements; a) foliation trajectory map. b) mineral lineation data.



**Figure 5.**  $S_1/S_2$  fabric elements. **a)** panel of folded  $S_1$  layering enveloped by straight gneisses thoroughly transposed parallel to  $S_2$ . (GSC 1993-260J) **b)** folded  $S_1$  layering with an axial planar foliation ( $S_2$ ) which is parallel to the shear fabric throughout the right half of the photo. (GSC 1993-260U) **c)**  $S_1$  layering which preserves an  $S_1$  shape fabric and carries an  $S_2$  shape fabric oblique to layering (parallel to pencil tip). (GSC 1993-260L) **d)**  $S_1$  layering with a penetrative  $S_2$  shape fabric oblique to layering (parallel to pencil). (GSC 1993-260M)

Metasedimentary rocks south of the complex generally possess a single foliation defined by both layering and a shape fabric. The attitude of this fabric, which strikes southwesterly and dips moderately northwest (Fig. 4a), is consistent with that of  $S_1$  within the complex. As such, it is tentatively interpreted as  $S_1$  also. The presence of a preferred shape fabric parallel to layering in these amphibolite-grade rocks is interpreted to be a function of their higher structural level, the absence of later penetrative strain, or both. In metasedimentary rocks south of the complex, attitudes of  $S_1$  define a shallow north-dipping homocline (Fig. 4a).

The dominant penetrative planar fabric within the complex is a strong to intensely-developed, east- to east-south-east-striking foliation (Fig. 4a). On the basis of overprinting relationships this foliation is designated  $S_2$ . These relationships include the widespread occurrence of mesoscopic folds defined by  $S_1$  layering to which  $S_2$  is axial planar, and of panels of folded  $S_1$  layering with intervening straight, transposed gneisses whereby the transposition foliation parallels the axial planar  $S_2$  (Fig. 5a, b). Since an  $S_1$  shape fabric is

rarely observed within the complex, a less common relationship is the partial realignment of the  $S_1$  shape fabric by  $S_2$  (Fig. 5c). In contrast to  $S_1$ ,  $S_2$  is subvertical to steeply south-dipping, with only local moderately ( $38-52^\circ$ N) dipping zones (Fig. 4a). The axial planar relationship of  $S_2$  to folded  $S_1$  layering is well displayed in the field and is reflected in the trajectory map (Fig. 4a) in which  $S_2$  trajectories symmetrically bisect folds defined by the trace of  $S_1$ .

Mineral lineations throughout most of the Kramanitar complex show a remarkably consistent pattern which reflects shallow to moderate ( $5-35^\circ$ ) westward extension (Fig. 4b). This extension direction is observed on all  $S_2$  planar fabrics and as such is interpreted as  $L_2$ . Discrete domains of east-plunging lineations are recognized in the northwest, north-central, and southeast parts of the complex (Fig. 4b). The northwest domain is characterized by shallow to moderate ( $10-55^\circ$ ) east-plunging lineations; the north-central domain by subhorizontal to shallow ( $5-20^\circ$ ) east-plunging lineations; and the extreme southeast part of the complex by a moderate east plunge. A domain of variably plunging mineral lineations

coincides with the eastern boundary of the complex (Fig. 4b). Lineations within this domain show a preferred moderate plunge (25-58°) to the north. This domain is interpreted to be associated with a bend in the northern shear zone (Sanborn-Barrie, 1993) and this is discussed below.

### ***Ductile shear zones***

Mappable zones of intensely deformed rock or ultramylonite transect both the northern and southern parts of the complex (Fig. 6a). These deformation zones were initially described by Sanborn-Barrie (1993) and a summary of their structural elements with additional observations from 1993 field work are provided below.

#### **Northern shear zone**

Granulite-grade mylonites of gabbroic and gabbroic anorthosite composition delineate the northern shear zone throughout an exposed strike length of approximately 60 km, from James Point in the northwest to the Quoich River in the southeast (Fig. 6a). This anastomosing, 3 to 6 km wide shear zone is complex. It has a curvilinear geometry: from James Point in the northwest, the zone strikes northeast to east across the northern part of the complex, and then bends southeast to south around its eastern margin. Its southeast segment which is east-striking, is separated from the rest of the zone by a right-handed step, or jog (locality j in Fig. 6a). All parts of the northern shear zone, except the gap at the dextral jog, comprise mylonites with granulite-grade assemblages, planar and linear fabric elements of similar intensity, and generally consistent shear-sense indicators (discussed below). The northern shear zone separates the Kramanitar complex from its amphibolite-grade wall rocks.

Throughout the zone, shear fabrics dip steeply. Steep southeast-dipping fabrics are observed in the James Point area in the northwest, whereas steep north- and northwest-dipping fabrics prevail across its central and northeast regions, respectively (Fig. 6a). The southeast segment of the shear zone possesses moderate to steep (40-88°) north-dipping shear fabrics. Mineral lineations on shear planes show patterns that parallel those of L<sub>2</sub> on the S<sub>2</sub> foliation. Shallow to moderate west-plunging mineral lineations are dominant; however, discrete domains of moderate, east-plunging lineations characterize the northwest (and locally north-central) part of the zone. The similar attitude and metamorphic grade of S<sub>2</sub>/L<sub>2</sub> fabric elements and those of the northern shear zone suggest that shearing throughout the northern part of the Kramanitar complex is an integral part of D<sub>2</sub> deformation and metamorphism, rather than an unrelated, superimposed event.

Regardless of lithology, rocks within the northern shear zone are characterized by continuous, evenly-spaced, millimetre- to centimetre-scale layering (Fig. 7a) and a marked absence of porphyroclasts, folds, and boudins. The uniform nature of ribbon mylonites of gabbroic, gabbroic anorthosite, and anorthositic protolith (Fig. 7b), as well as of paragneiss and leucogranodiorite attests to the absence of rheological contrasts between these rock types and the remarkably homogeneous strain along the northern margin of the complex

during D<sub>2</sub>. Preliminary thin section observations suggest that unannealed textures and equilibrium mineral assemblages (clinopyroxene+garnet±orthopyroxene+plagioclase gabbro and quartz+plagioclase+kyanite+garnet paragneiss) are preserved throughout much of the northern shear zone.

In spite of the remarkably symmetrical ribbon structure of the ultramylonites, shear-sense indicators although rare are widespread and reveal south-side-up, sinistral movement parallel to west-plunging lineations (Sanborn-Barrie, 1993). If the present attitude of shear planes approximate their position during displacement, then shearing appears to have taken place in an extensional regime across the north-central part of the zone where shear fabrics dip steeply north; and in a contractional regime across the restraining bend in the northeast (locality b in Fig. 6a) where shear fabrics dip steeply west.

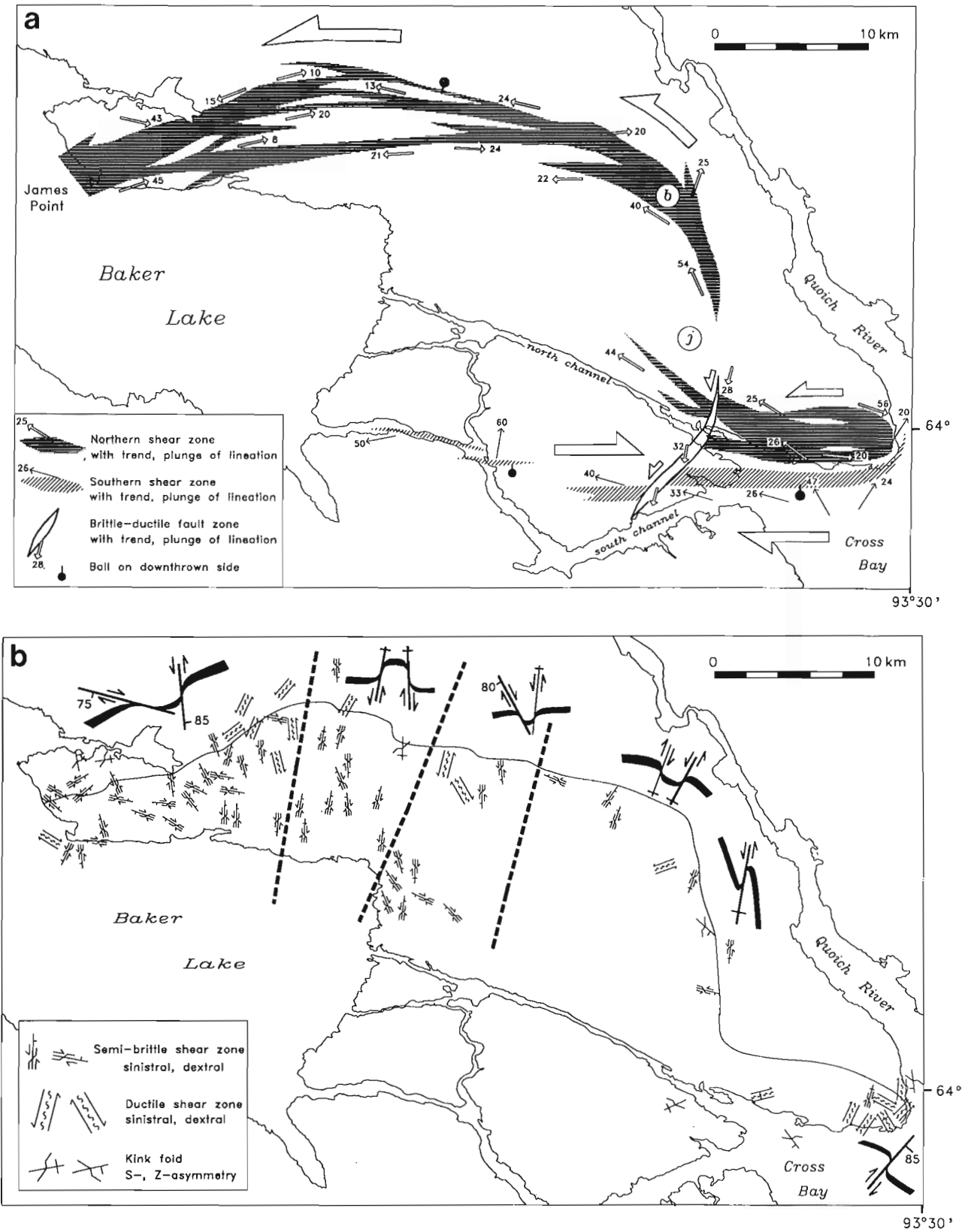
Portions of the northern shear zone examined during 1993 include the northwest sector near James Point, and the southeast sector near the Quoich River (Fig. 6a). In the James Point area, spectacular granulite-grade ultramylonites, well-exposed along the shores of Baker Lake, are compositionally and texturally similar to rocks elsewhere in the northern shear zone; however, two aspects of their fabrics are noteworthy. Firstly, these mylonites are characterized by moderately (20-50°) east-plunging mineral lineations. Secondly, they display an S>L fabric, such that the degree of fabric intensity parallel to XZ is virtually identical to that parallel to YZ (Fig. 7c). Generally rocks in the northern shear zone display L=S and less commonly, L>S fabrics. Kinematic indicators are generally ambiguous in terms of shear sense in these highly flattened rocks, but rarely garnet porphyroblasts show anticlockwise rotation which suggests at least local zones of sinistral displacement. Sinistral transcurrent movement coupled with moderate east-plunging mineral lineations may reflect local sinistral, south-side-down movement in the James Point area.

The southeast sector of the shear zone comprises subvertical, east-striking mylonites which display similar "anomalous" attributes: east-plunging mineral lineations and S>L fabrics. Asymmetrical structures reflecting shear sense are rare. Megascopic structural heterogeneities are, however, prevalent in this restricted domain and include tight folds, branching mafic layers and symmetrical boudinage consistent with significant flattening.

#### **Southern shear zone**

The southern shear zone is an east-striking ductile deformation zone that transects the southern part of the Kramanitar complex (Fig. 6a). This zone extends roughly 30 km along strike, maintains a width of 0.5 to 2 km, and has been referred to previously as a segment of the Chesterfield fault zone (Schau and Ashton, 1979). Within this zone, granitoid and amphibolite-grade metasedimentary rocks possess strong to intense, north-dipping (55-65°) shear fabrics. Strongly-developed mineral lineations generally plunge 25-50° to the northwest and, locally, are down-dip. In contrast to the northern shear zone, shear-sense indicators are well displayed (Sanborn-Barrie, 1993) and include asymmetric Z-folds,





**Figure 6.** Deformation zones. **a)** regional-scale shear zones that transect the complex. Restraining bend at **b**, antidilational jog at **j**. **b)** distribution and schematic representation of late-stage conjugate structures ( $S_3$ ).

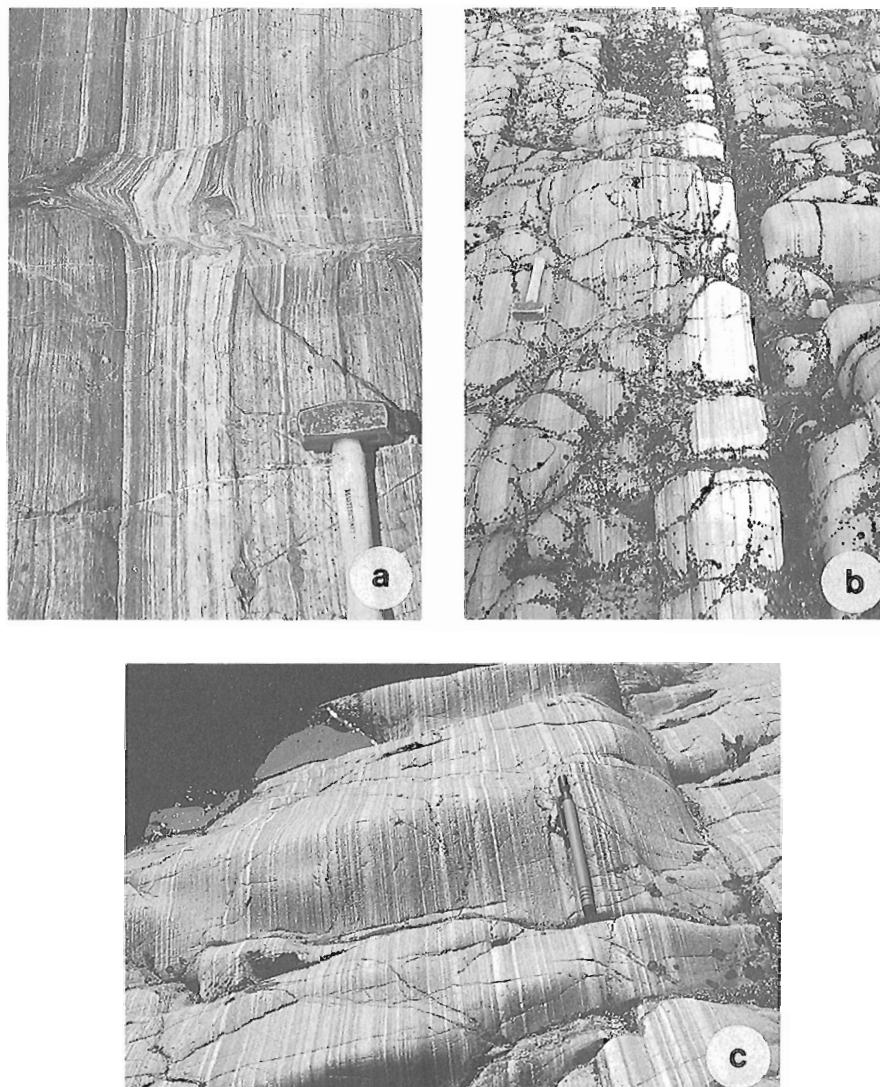


dextral shear bands, back-rotated boudins, and asymmetrical winged porphyroclasts which consistently reveal north-side-up, dextral displacement.

Two additional aspects of the southern shear zone were recognized during 1993. Toward the eastern end of the exposed zone, apparent curvature of the shear zone is recorded by a progressive change in the strike of mylonitic foliation from  $270^{\circ}$  to  $230^{\circ}$  over approximately 7 km of strike length (Fig. 6a). Shear-sense indicators consistent with dextral displacement are commonly recognized in  $250^{\circ}$ - to  $230^{\circ}$ -striking segments. Zones of sinistral displacement and flattening are

also recognized by asymmetrical winged porphyroclasts and symmetrical, conjugate extensional shear bands, respectively. The southeast part of the complex thus records flattening strains across both the northern and southern shear zones.

Toward its western extremity the southern shear zone appears to narrow and at several localities could not be mapped as a throughgoing structure (Fig. 6a). These observations suggest either that this part of the shear zone is discontinuous; that the structure steps successively to the right as echelon segments; or that the scale of mapping in this area was not adequate to delineate the structure.



**Figure 7.** Ultramylonite of the northern shear zone. *a)* millimetre-scale tectonic layering in mylonitized gabbro anorthosite. (GSC 1993-260C) *b)* layer of anorthosite mylonite (white) and adjacent gabbro mylonite. Note ribbon texture of both units and the absence of boudins or folds, reflecting similar rheological behaviour. (GSC 1993-260Q) *c)* S>L gabbro ultramylonite near James Point. (GSC 1993-260B)

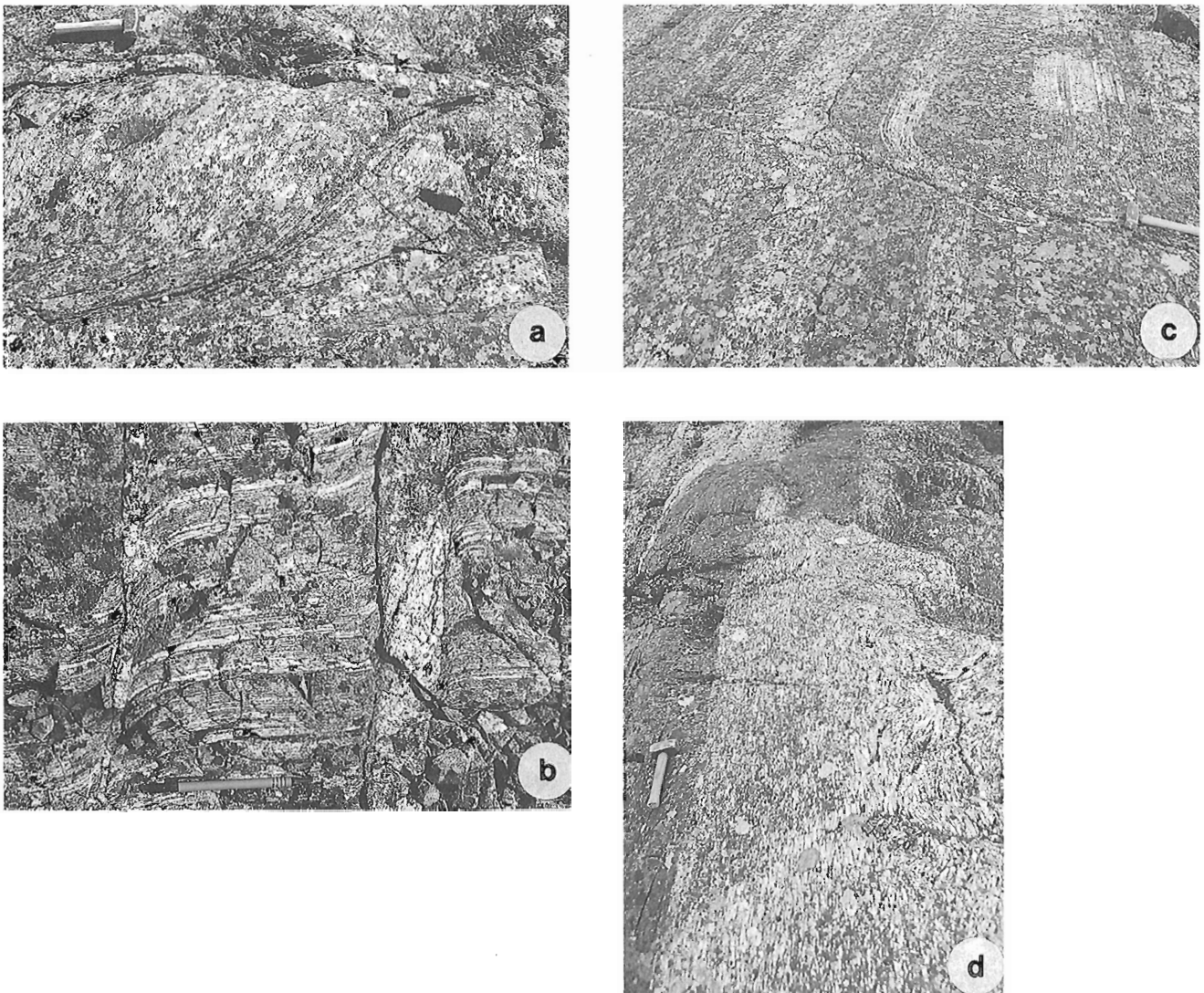
### ***Semi-brittle shear zones and kink folds***

Spaced, metre-scale structures cut ultramylonitic layering of the northern shear zone. Such structures include ductile shear zones (Fig. 8a), semi-brittle shear zones (Fig. 8b), and kink folds (Fig. 8c, d). These structures, which generally occur at a high angle to mylonitic layering (Fig. 6b), overprint and offset this fabric and are therefore designated  $S_3$ . Granulite-grade mineral assemblages within  $S_3$  structures reveal that P-T conditions during movement on the northern shear zone were maintained during formation of these later structures. An apparent sense of displacement across these structures is consistently provided by sigmoidal curvature of  $S_2$  into these zones as schematically illustrated in Fig. 6b. Curvature consistent with both sinistral and dextral offset is observed (Fig. 8), although typically only one structure of a conjugate set is observed at an outcrop scale. At different localities

either extensional or contractional conjugate structures occur. Extensional structures may be infilled with granitic material (Fig. 8a, b) which commonly carries a weakly to moderately developed foliation. The obliquity of this foliation with the walls of  $S_3$  structures is consistent with injection of granitic material synchronous with, but late, in their development.

### ***Regional-scale brittle-ductile fault***

A discrete, northeast-striking brittle-ductile fault zone cuts the southeast part of the complex (Fig. 6a). In general, planar fabrics within this zone strike northeast ( $010-035^\circ$ ), dip steeply east, and possess moderately south-plunging mineral lineations. Deformation style varies along the 10 km exposed strike length of this fault zone. South of the north channel, the zone is characterized by brittle-ductile deformation with associated greenschist-grade alteration. Composite fabrics



**Figure 8.**  $S_3$  structures. **a)** dextral extensional shear zones. (GSC 1993-260FF) **b)** sinistral, extensional, semi-brittle shear zones infilled with granitoid rock. (GSC 1993-260R) **c)** kink fold of S-asymmetry in tectonized gabbro anorthosite. (GSC 1993-260D) **d)** kink fold of Z-asymmetry, gabbro dyke cutting gabbro anorthosite. (GSC 1993-260F)

reflect sinistral displacement (Fig. 9) which, in conjunction with moderately south-plunging lineations, suggests sinistral, east-side-up movement. Rocks exposed along the north channel and further northeast reveal an increasingly brittle component to the deformation and attenuation of the fault zone (Fig. 6a). Centimetre-scale sinistral shear zones are, however, still locally observed. A sinistral transcurrent component of displacement on this fault zone is consistent with left-lateral offset of metasedimentary rocks (Fig. 2) and the southern



Figure 9. Composite fabrics in greenschist-grade brittle-ductile fault zone, consistent with sinistral movement.

shear zone (Fig. 6a) across this structure. Continuity of gabbroic anorthosite along the northeast margin of the Kramanitar complex (Fig. 2) is consistent with attenuation of this fault toward the northeast.

Timing of this fault zone relative to other deformation zones is clearly established on the basis of overprinting structural and metamorphic relationships. In the south, east-striking fabrics associated with the southern shear zone wrap into the fault zone in a sense consistent with sinistral movement on the latter. In the north, brittle fracturing and cataclasis of mylonitic rocks of the northern shear zone is restricted to this fault zone. Throughout its length, greenschist assemblages reflect retrograde alteration not associated with the other shear zones.

**METAMORPHISM**

Across the Kramanitar complex, variations in metamorphic assemblages with strain intensity appear to reflect a close relationship between deformation and metamorphism. In the southern part of the complex, gabbroic units that best preserve S<sub>1</sub> are characterized by the assemblage plagioclase+orthopyroxene > clinopyroxene. Toward the north, increasing strain is clearly demonstrated by the increasingly penetrative nature of S<sub>2</sub> which culminates in ultramylonitic rocks of the northern shear zone. A metamorphic reaction reflecting increasing pressure appears to track the increase in strain intensity. The

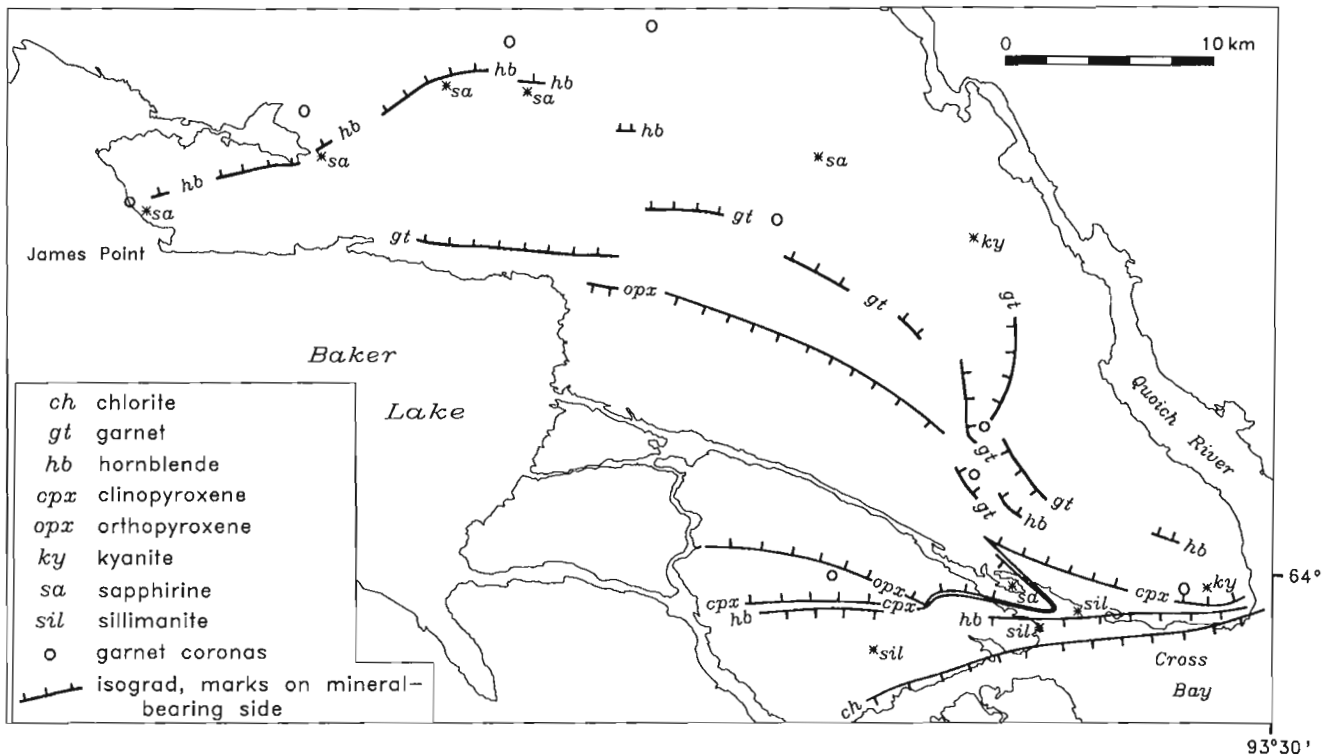


Figure 10. Preliminary metamorphic isograds and isolated metamorphic mineral occurrences based on field observation only.

reaction: orthopyroxene + plagioclase  $\rightarrow$  garnet + clinopyroxene + quartz is reflected by an orthopyroxene-out isograd located north of Chesterfield Inlet, and the garnet-in isograd parallel to, and roughly 3.5 km south of the northern shear zone (Fig. 10). The relationship between strain intensity and metamorphic grade is also mirrored in paragneiss, whereby sillimanite-bearing rocks are prevalent throughout the central part of the complex, while kyanite is restricted to the northern shear zone (Fig. 10).

Field observations pertaining to the transition from granulites to amphibolite-grade wall rocks are as follows. Across the north margin of the complex, the transition appears to occur across a 1 km wide zone. Lower metamorphic grade appears to be indicated initially by the occurrence of sapphirine in clinopyroxene+garnet+plagioclase gabbro and gabbroic dykes. Sapphirine-bearing mafic rocks delineate an isograd which extends from James Point to the northeastern part of the complex (Fig. 10), parallel to, and immediately north of, the northern shear zone. North of this, hornblende porphyroblasts occur in clinopyroxene+garnet gabbro and intermediate tectonite. Hornblende content increases progressively northward with systematic decrease of clinopyroxene and garnet. Plutonic rocks with hornblende $\pm$ biotite $\pm$ epidote are widespread north of the complex.

In the south, the granulite-amphibolite transition appears to occur at, or immediately north of, the southern shear zone. Hornblende-bearing mafic rocks occur immediately north of the southern shear zone (Fig. 10). Within the shear zone, semipelitic rocks contain biotite, lavender garnet and fibrolite sillimanite (Fig. 10). Further south, biotite and garnet persist throughout much of the exposed metasedimentary succession. Coarse-grained sillimanite porphyroblasts are locally observed. Retrograde chlorite after garnet is present along the south channel of Chesterfield Inlet and in gabbroic anorthosite mylonite in the extreme southeast part of the complex (Fig. 10).

## DISCUSSION

The field relationships described above are consistent with the Kramanituak complex as a crustal-scale, granulite-grade tectonic lens, or boudin, bound by asymmetrical shear zones generated upon uplift during southwest-directed shortening. The following structural chronology is preliminary, and based on the observed field relationships. Rare  $S_1$  shape fabrics in gabbroic anorthosite are consistent with southwest-directed shortening during  $D_1$ . Granitic sheets that define  $S_1$  compositional layering may have been injected during  $D_1$ , or may have utilized  $D_1$  anisotropies during magmatic injection prior to  $D_2$ . A second deformation event,  $D_2$ , resulted in folding of  $S_1$  layering; the development of discrete zones of transposition in the southern part of the complex; and the increasingly penetrative development of  $S_2$  toward the northern part of the complex. Highest  $D_2$  strains are recorded by anastomosing ultramylonites of the northern shear zone which delineate the northern margin of the Kramanituak complex. South-side-up and sinistral shear along much of the

northern shear zone is consistent with uplift of granulite-grade rocks relative to their amphibolite-grade wall rocks during southwest-directed shortening. Extensional shear across steeply dipping shear planes in the north-central part of the zone is contemporaneous with contractional shear across a restraining bend in the northeast part of the zone.

Anomalous east-plunging mineral lineations and marked flattening strains in the northwest and southeast sectors of the northern shear zone may reflect local strains in these quadrants during uplift and sinistral shear. A local dextral regime, reflected by attitudes of conjugate extensional  $S_3$  structures (Fig. 6b) in the northwest sector, may have been imposed on the high-temperature, low yield-strength mylonites by the stiffer, colder wall rocks which envelop them. In the southeast sector of the northern shear zone, contractional  $S_3$  structures generated by layer-parallel shortening similarly may reflect the localized effect of wall rocks near the southeast tip of this crustal-scale boudin.

Along the south boundary of the complex, highest strains are observed in the east-striking southern shear zone. The relative timing of the northern and southern shear zones could not be resolved during field mapping. Granulite-grade assemblages of the northern shear zone, relative to amphibolite-grade assemblages of the southern shear zone demonstrate that these deformation zones were operative at different crustal levels, but does not preclude contemporaneous movement. This problem, which is critical to understanding the uplift history of the Kramanituak complex may be resolved petrologically, if P-T conditions in the northern shear zone approach those of the southern shear zone in this area. Progressive curvature of the southern shear zone to a trend of  $230^\circ$  is consistent with wrapping of the southern shear zone around the attenuated southeast tip of a crustal-scale boudin.

## ACKNOWLEDGMENTS

I thank Julie Watson who provided cheerful and reliable assistance in all aspects of field work; Ralph Kownak who assisted us in August and shared with us the special experience of living on the land; Boris and Liz Kotelewetz, Peter Tapatai, and many other people from Baker Lake for assistance with equipment, transportation, radio communication, and supplies; and Thomas Iksiraq of the Jessie Oonark Centre for help with rock samples. Support from the Polar Continental Shelf Project and the Northern Careers Program is gratefully acknowledged. This research continues to benefit from discussions with Simon Hanmer (GSC), who is also thanked for critically reading this manuscript.

## REFERENCES

- Gordon, T.M.  
1988: Precambrian geology of the Daly Bay area, District of Keewatin; Geological Survey of Canada, Memoir 422, 21 p.
- Hanmer, S.K. and Knof, C.  
1993: The Snowbird tectonic zone in District of Mackenzie, Northwest Territories; in Current Research, Part C; Geological Survey of Canada, Paper 93-1C, p. 41-52.

**Hanmer, S., Darrach, M., and Kopf, C.**

1992: The East Athabasca mylonite zone: an Archean segment of the Snowbird tectonic zone in Northern Saskatchewan; in *Current Research, Part C*; Geological Survey of Canada, Paper 92-1C, p. 19-29.

**Hoffman, P.F.**

1988: United plates of America, the birth of a craton: Early Proterozoic assembly and growth of Laurentia; *Annual Review of Earth and Planetary Sciences*, v. 16, p. 543-603.

**Sanborn-Barrie, M.**

1993: Structural investigation of high-grade rocks of the Kramanituar complex, Baker Lake area, Northwest Territories; in *Current Research, Part C*; Geological Survey of Canada, Paper 93-1C, p. 137-146.

**Schau, M. and Ashton, K.E.**

1979: Granulites and plutonic complexes northeast of Baker Lake; District of Keewatin; in *Current Research Part A*; Geological Survey of Canada, Paper 79-1A, p. 311-316.

1980: Geological map of the granulite and anorthosite complex at the southeast end of Baker Lake, 56D1, 56C4, parts of 55M16 and 55N13; Geological Survey of Canada, Open File 712.

**Schau, M. and Hulbert, L.**

1977: Granulites, anorthosites and cover rocks northeast of Baker Lake, District of Keewatin; in *Report of Activities, Part A*; Geological Survey of Canada, Paper 77-1A, p. 399-407.

**Schau, M., Tremblay, F., and Christopher, A.**

1982: Geology of the Baker Lake map area, District of Keewatin: a progress report; in *Current Research, Part A*; Geological Survey of Canada, Paper 82-1A, p. 143-150.

**Tella, S. and Annesley, I.R.**

1988: Hanbury Island Shear Zone, a deformed remnant of a ductile thrust, District of Keewatin, Northwest Territories; in *Current Research, Part C*; Geological Survey of Canada, Paper 88-1C, p. 283-289.

**Tella, S., Schau, M., Armitage, A.E., and Loney, B.C.**

1993: Precambrian geology and economic potential of the northeastern parts of the Gibson Lake map area, District of Keewatin, Northwest Territories; in *Current Research, Part C*; Geological Survey of Canada, Paper 93-1C, p. 197-208.

---

Geological Survey of Canada Project 830008





# Geology of the Early Proterozoic gold metallotect, Hurwitz Group in the Cullaton-Griffin lakes area, central Churchill Structural Province, Northwest Territories<sup>1</sup>

A.R. Miller, M.J. Balog<sup>2</sup>, B.A. Barham<sup>3</sup>, and K.L. Reading<sup>4</sup>

Mineral Resources Division

*Miller, A.R., Balog, M.J., Barham, B.A., and Reading, K.L., 1994: Geology of the Early Proterozoic gold metallotect, Hurwitz Group in the Cullaton-Griffin lakes area, central Churchill Structural Province, Northwest Territories; in Current Research 1994-C; Geological Survey of Canada, p. 135-146.*

---

**Abstract:** Remnants of northeast-trending sediment-dominated fold and thrust belts are distributed across the Churchill Structural Province, north of 60°. These belts record early Proterozoic transpression across the entire Churchill Province. The early Proterozoic Hurwitz Group in the southern half of the Churchill Province is host to one past-producing gold mine and numerous gold prospects. Vein-type lode gold is confined to thrusts, imbricate thrust stacks, and coeval extensional faults associated with surge zones in para-autochthonous lower Hurwitz Group strata. Zoned hydrothermal alteration assemblages are temporally and spatially related to the earliest phase of basement-cover infolding. Hydrothermal fluids are interpreted to have been generated in the Archean basement and focused along Proterozoic thrusts and related faults. Regional variation of alteration assemblages in metasomatised Proterozoic rocks reflect hydrothermal fluid reaction with lithologically distinct Archean basement domains.

**Résumé :** Des vestiges de zones de plissement et de chevauchement de direction nord-est, composés principalement de roches sédimentaires, sont présents un peu partout dans la Province structurale de Churchill, au nord de 60°N. Ces zones révèlent une transpression ayant affecté l'ensemble de la Province de Churchill au Protérozoïque précoce. Le Groupe de Hurwitz du Protérozoïque précoce, dans la partie sud de la Province de Churchill, renferme une ancienne mine d'or et de nombreux prospects aurifères. Les gisements d'or filoniens sont confinés à des chevauchements, des zones d'écaillage et des failles de distension contemporaines du chevauchement associées à des zones d'introduction de fluides dans des couches paraautochtones de la partie inférieure du Groupe de Hurwitz. La zonation des assemblages d'altération hydrothermale est chronologiquement et spatialement liée à la phase la plus précoce d'involution du socle et de la couverture. Les fluides hydrothermaux sont interprétés comme ayant été formés dans le socle archéen et se sont concentrés le long des chevauchements protérozoïques et des failles associées. La variation régionale des assemblages d'altération dans les roches protérozoïques métasomatisées reflète la réaction des fluides hydrothermaux avec des domaines de socle archéen à lithologie distincte.

---

<sup>1</sup> Contribution to Canada-Northwest Territories Mineral Initiative (1991-1996), an initiative under the Canada-Northwest Territories Economic Development Cooperation Agreement.

<sup>2</sup> Comaplex Minerals Corp., 901, 1015 - 4th St., Calgary, Alberta T2R 1J4

<sup>3</sup> M.M. Dillon Ltd., 6 Donald St. South, Winnipeg, Manitoba R3L 0K6

<sup>4</sup> 11 Colbourne St., Thornhill, Ontario L3T 1Z4

## INTRODUCTION

This report outlines the critical lithological, structural, and alteration features that characterize a newly identified early Proterozoic gold metallogene in the Cullaton-Hawk Hill-Griffin lakes area, NTS 65G/west half and 65H/east half (Fig. 1). Data were assembled during field mapping and drill core logging in 1988 and 1992, complimented by petrographic studies, whole rock geochemistry, and detailed microprobe analyses. It focuses on the Shear Lake gold deposit and gold prospects in the Griffin Lake area, both contained in the early Proterozoic Hurwitz Group. The report is organized into four parts: 1) update on the geology of the Shear Lake deposit, 2) gold prospects in the Griffin Lake area, 3) comparison between the Shear Lake deposit and prospects in the Griffin Lake area, and 4) model for the Proterozoic gold metallogene. The reader is referred to the following publications in order to follow developments in regional geology, tectonics, stratigraphy, and sedimentology of the Hurwitz Group in the Cullaton-Hawk Hill-Griffin lakes area: Eade (1974), Eade and Chandler (1975), Miller (1989), Aspler and Bursey (1990), Patterson and Heaman (1991), Aspler et al. (1992), Aspler et al. (1993), Miller and Reading (1993), and Aspler et al. (1994). This report is a product of the "Metallogeny of

the Churchill Structural Province" project and was funded under the Canada-Northwest Territories Mineral Development Agreements, 1987-1991 and 1991-1996.

## EXPLORATION HISTORY

The earliest recorded indication of gold within strata now recognized as part of the early Proterozoic Hurwitz Group, dates to the late 1940s. Exploration during the 1960s and 1980s focused on Archean iron-formation and culminated in the development of the Cullaton B-Zone gold deposit, which is hosted in Archean iron-formation. During mining of the B-Zone, the Shear Lake gold deposit, located approximately 5 km north of the B-Zone deposit, was developed and mined. Raman et al. (1986) suggested a link between Archean and Proterozoic gold deposits and speculated on the origin of gold within stratigraphically higher units in the Hurwitz Group. The discovery of gold in the Griffin Lake area and in Hurwitz strata other than the basal orthoquartzite (Aspler and Bursey, 1990) stimulated gold exploration and led to the discovery of additional occurrences between 1990 and 1992 (Reading, 1990, 1991).

## UPDATE ON THE GEOLOGY OF THE SHEAR LAKE DEPOSIT

Re-examination of early exploration drill core and identification of significant structural and alteration features indicated that the Shear Lake deposit was contained in a thrustured Hurwitz section and that mineral zoning was comparable to epithermal-like precious metal deposits (Miller, 1989). Additional research has focused on the chemical compositions of hydrothermal minerals and evaluation of the structural setting.

### Structural setting

The Shear Lake gold deposit (Fig. 2) is hosted within Hurwitz Group Kinga orthoquartzite, ~3 km southwest of Cullaton Lake. This distinctive basal rock unit of the Hurwitz Group forms an arcuate to linear pattern from north of Cullaton Lake southeast to Otter Lake and marks the western edge of a regional north-northwest-trending D<sub>1</sub> synclinorium (Eade 1974, Map 1364A). The geology of the Hurwitz Group in the Shear Lake area has been reinterpreted (Fig. 2) based on surface mapping in 1988 and 1992, diamond-drill hole data and discussions with W. Hamilton, formerly of Corona Corp., in 1988 and 1993.

The structural reinterpretation of the Shear Lake area is based entirely on the distribution of asymmetrical ripple marks, having crest-to-crest distances of 3-4 cm, in the resistant Kinga Formation and shallowly dipping schistosity and joints commonly developed in orthoquartzite near the tectonized Archean-Proterozoic contact. Very poorly exposed, stratigraphically higher lithological units include a vari-coloured black to gray to orange slate, possibly Ameto Formation, overlain by silty dolostone, stromatolitic dolostone, and magnetite-bearing dolostone of the Watterson Formation.

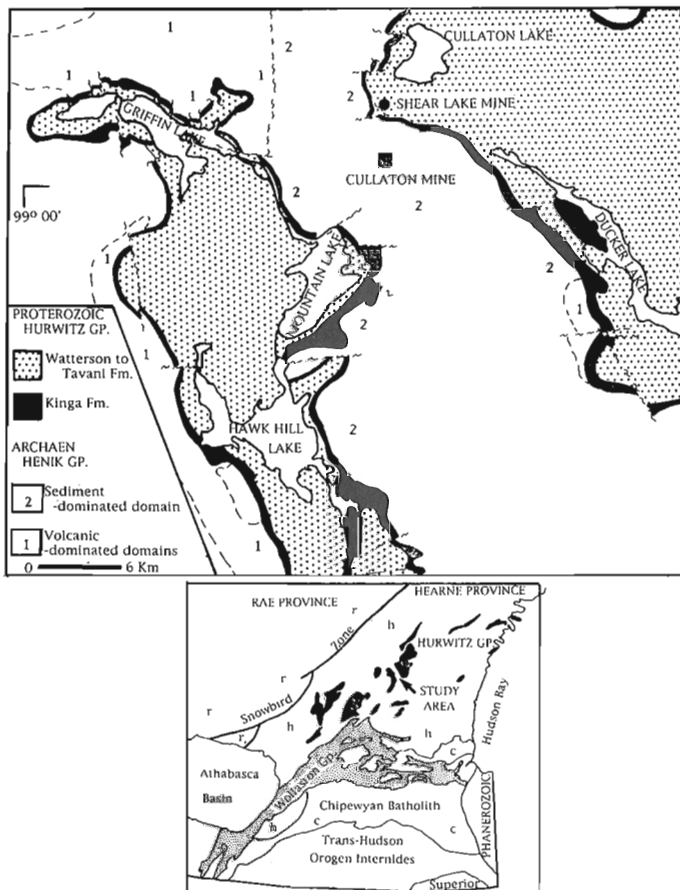


Figure 1. Regional setting of the Proterozoic gold metallogene (after Eade, 1974; Hoffman, 1987)

Northwest of the airstrip, schistose Henik Group meta-greywacke is interleaved with east-dipping, ripple-marked Kinga quartzite (Fig. 2, section A-A'). Deformation intensity increases from east to west across these orthoquartzite outcrops and is best observed on steep-sided, west-facing slopes. The strain gradient in white orthoquartzite is manifested by the transition from east-dipping, ripple-marked bedding planes into east-dipping, well jointed orthoquartzite. With increasing strain, an east-dipping, schistose orthoquartzite grades into mylonitic orthoquartzite. The mylonite is distinctive and recognized by grey to blue-grey hues, and a dense, foliated appearance with a ribbon quartz fabric (Fig. 3). Recognition of these fabrics in orthoquartzite, at and near the basement-cover interface in the Shear Lake area, confirms the presence of a high-strain detachment zone along the Archean-Proterozoic contact and identifies the western margin of the Hurwitz strata in the Shear Lake area to be para-autochthonous. These detachment surfaces are interpreted to be associated with  $D_1$  flexural slip folding of the Hurwitz Group.

The shallow east-dip to the para-autochthonous sheet of Hurwitz strata in the Shear Lake area is based on ripple-marked bedding planes in orthoquartzite along the western edge of the Hurwitz Group (Fig. 2) and structural sections through the Shear Lake gold deposit (Miller, 1989). Dip reversal is restricted to the orthoquartzite ridge that contains the Shear Lake discovery outcrop and mine portal. Bedding plane reversals are interpreted to result from a north-plunging anticline in the hanging wall above the ductile detachment zone. This fold in orthoquartzite is structurally similar to the doubly plunging anticline on the west side of Ducker Lake area, 15 km southeast of the mine (Eade, 1974, Map 1364A). The absence of orthoquartzite west of the airstrip may be due to the north plunge. Alternatively the orthoquartzite may be truncated by a west-trending, north-side down subvertical fault near section B-B'.

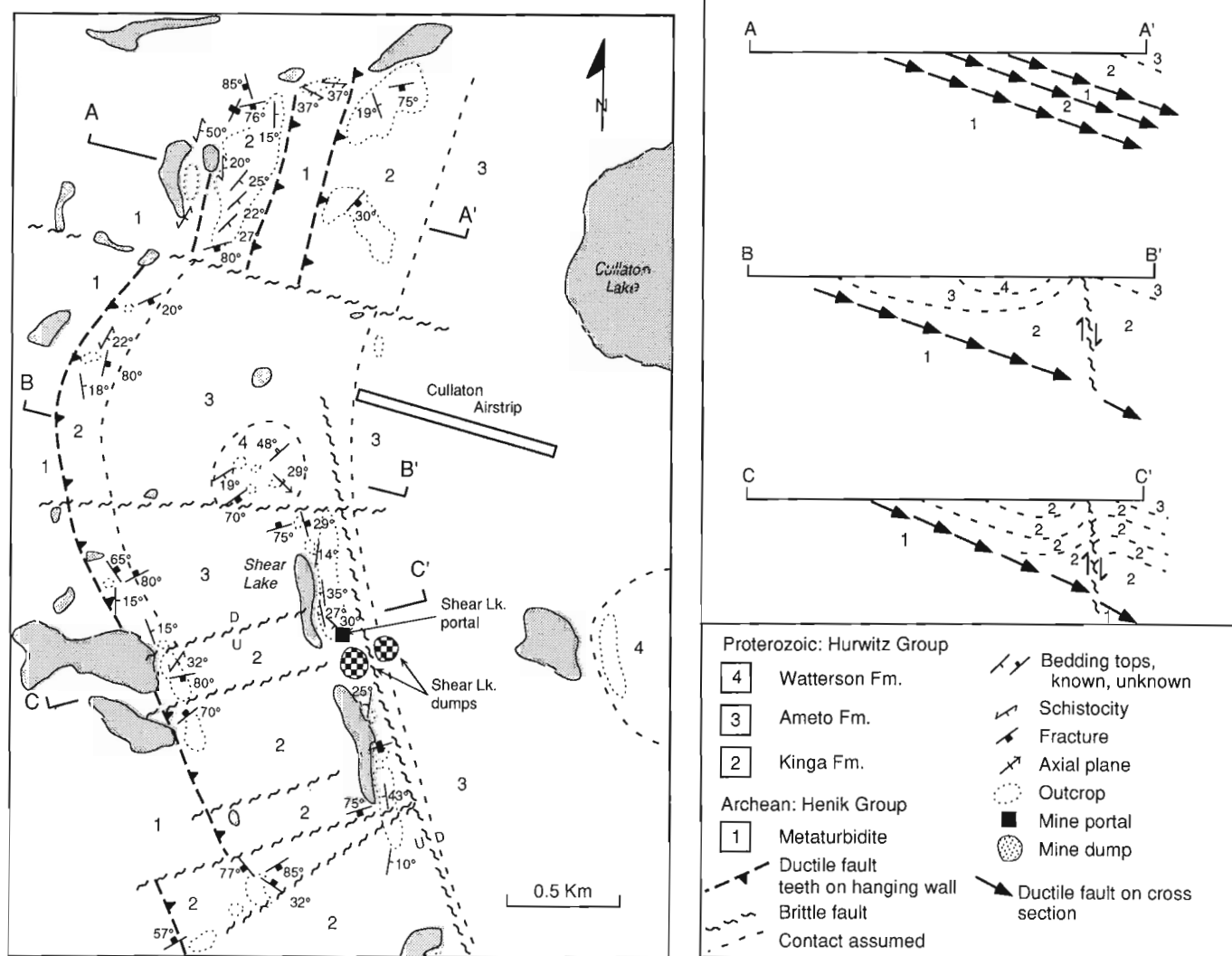


Figure 2. Geology of the Shear Lake gold deposit.



**Figure 3.** Outcrop of mylonitic orthoquartzite northwest of the airstrip. The mylonite, located at the snow edge and having an exposed width of 50-60 cm (hammer for scale), is dense, very fine grained and grades upward into foliated to well-jointed orthoquartzite. GSC 1993-253J

A cluster of subvertical to south-dipping,  $255^{\circ}$  to  $285^{\circ}$  trending faults transect the Hurwitz Group. These faults are perpendicular to the trace of the outer margin of Hurwitz Group rocks (Fig. 2; Miller, 1989, Fig. 2). The absence of slate-carbonate in the mine area and the displacement of the basement-orthoquartzite contact northwest of the airstrip confirms a consistent north-side down sense of motion across these faults. Within the Shear Lake mine, smaller-scale block rotations indicate both north- and south-side down motion (Miller, 1989, Fig. 2). Faults and related zones of closely spaced fracture represent extension around the outer margin of the para-autochthonous sheet. These faults-fractures display a geometry similar to local fracture patterns developed around fold hinges in the Griffin-Hawk Hill area (Aspler and Bursey, 1990).

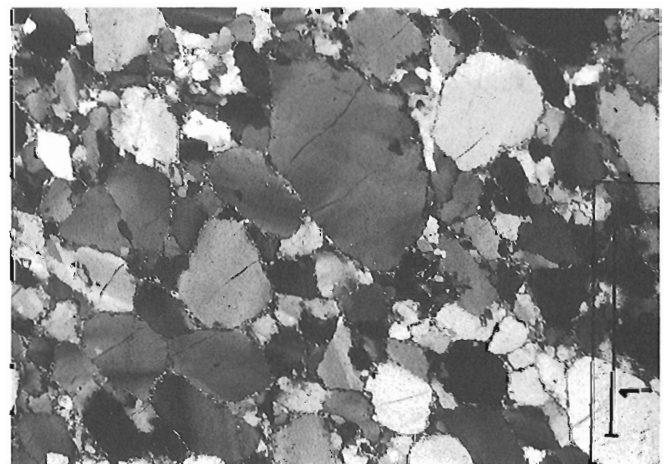
The interpreted genetic and temporal relationship between trusts and subvertical faults are critical components of the Shear Lake gold deposit. Partial to total metasomatism in and about the east-dipping ductile high strain zone represents a zone of semi-concordant alteration whereas the subvertical veins, fractures, and faults represent a discordant zone. Subvertical gold-bearing fracture zones penetrate the metasomatic albite zone and extend upward through the overlying orthoquartzite (Miller, 1989). A gold-bearing zone is comprised of closely spaced parallel to subparallel vein-fracture systems with subordinate brecciated orthoquartzite separated by weakly veined or unfractured orthoquartzite.

The metasomatic semiconcordant zone characterized by ochre to pale pink to red hues contrasts with white unaltered orthoquartzite. Contacts with unaltered orthoquartzite are gradational. White remnants of partially replaced, weakly recrystallized to mylonitic orthoquartzite are present within zones of intense replacement. Textural variations displayed by albite, the most abundant replacement mineral in this zone, indicate a protracted metasomatic deformational history. Crushed and polygonalized grains, through to weakly and unstrained albite and discordant albite veinlets indicate alkali metasomatism was at least synchronous with  $D_1$  ductile strain.

A  $345^{\circ}$ -trending, east-dipping subvertical fault with east-side down motion is contained in orthoquartzite immediately east of the mine outcrop ridge (W. Hamilton, pers. comm., 1988, 1993). The sense of motion on this fault implies that it is unrelated to, and later than the anticline in the hanging wall of the detachment plane. The absence of sulphide-bearing veins in this structure (W. Hamilton, pers. comm., 1988, 1993) supports the interpretation that this fault is later than the Shear Lake gold lodes. Displacement of the detachment plane at depth (Fig. 2) is based entirely on interpreted fault motion. The stratigraphic section east of the outcrop ridge is upright and similar to the stratigraphic sequence in section B-B'. This is based on exploration drill holes east of the mine portal, which collared in slate, as well as the presence of Watterson magnetite-bearing dolostone on the eastern edge of the map area (Fig. 2).

#### **Alteration and metasomatism**

Continuing studies on alteration assemblages and mineral compositions in conjunction with limited whole rock chemical analyses have refined the deposit zonation and better defined the relationship between the discordant veins and the



**Figure 4.** Photomicrograph (crossed nicols) of preserved clastic texture from a weakly recrystallized orthoquartzite, drill core from the Shear Lake deposit.

semiconcordant replacement zone. Mineralogical similarities between the metasomatized high strain zone and subvertical fractures strongly support a temporal and genetic link between detachment, metasomatism along the decollement plane, and the subvertical gold-bearing fracture zones.

The semiconcordant metasomatic zone near the Archean-Proterozoic contact is comprised essentially of albite and is similar to metasomatic albitite associated with Proterozoic uranium deposits (Turpin et al., 1988) and some Archean gold deposits (Witt, 1992). The mineral assemblage in the semiconcordant albitite zone and peripheral weakly replaced

orthoquartzite is presented in Table 1. Fine grained pyrite with trace chalcopyrite is disseminated throughout the phlogopite-bearing albitite.

The vertical mineralogical zonation in the discordant vein systems (Miller, 1989) has been refined and is presented in Table 1. It is noteworthy that quartz and iron-bearing dolomite are essential phases within each zone. Sulphides, almost exclusively pyrite with trace chalcopyrite and sphalerite, are contained in veins. Sulphides are rarely present in the wall rock to veins. However, in zones of high fracture or vein density, disseminated sulphide occurs in wall rock orthoquartzite.

**Table 1.** Comparison between the Shear Lake deposit and Griffin Lake prospects.

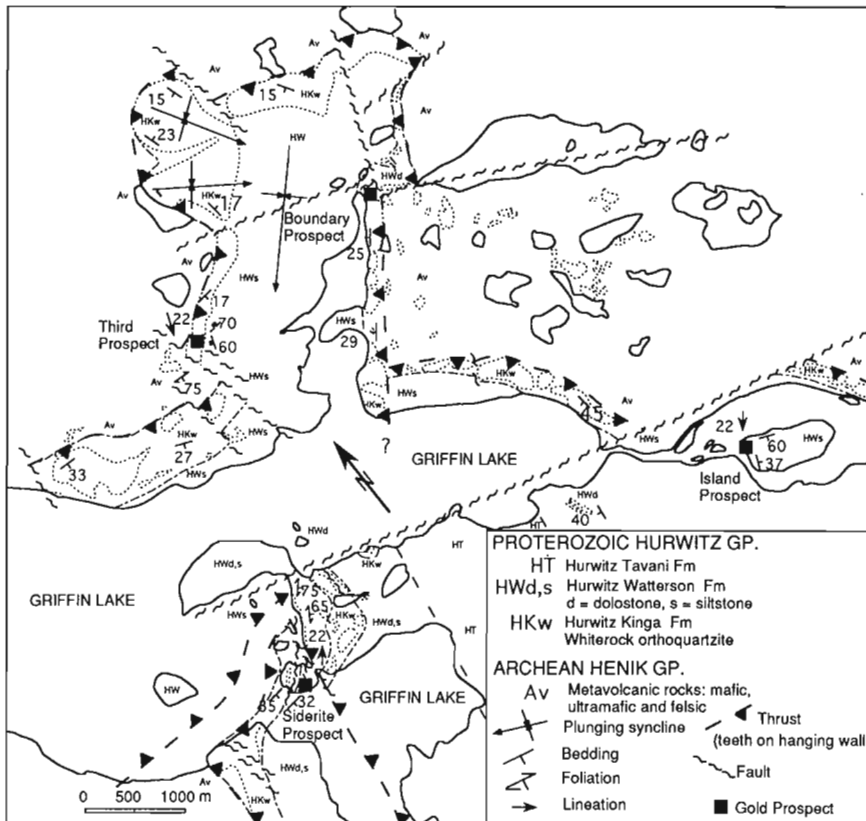
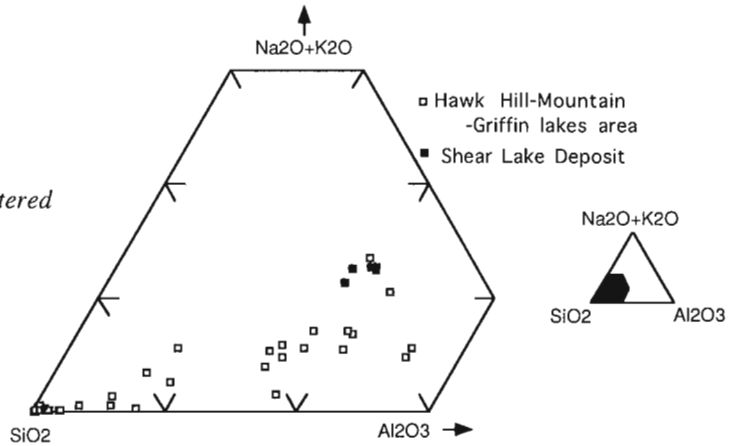
Area	SHEAR LAKE AREA	GRIFFIN LAKE AREA	GRIFFIN LAKE AREA	GRIFFIN LAKE AREA	GRIFFIN LAKE AREA
Deposit/Prospect	Shear Lake deposit	Boundary Zone	Siderite Zone	Island Zone	Island Zone
Host rock	Kinga quartzite & minor Henik Group	Kinga quartzite and very minor Henik Group metabasalt	Lower sulphide zone Kinga orthoquartzite	Upper sulphide zone Watterson Formation aluminous siliceous dolostone	Watterson Fm: calcareous arkose, siltstone and hematitic iron formation
Basement	Henik Group metaturbidite	Henik Group high-iron tholeiitic metabasalt & metakomatiite	talc schists and quartz-muscovite schists of Henik Group; komatiite and felsic volcanic rocks	Henik Group high-iron tholeiitic metabasalt & komatiite	no data
Hurwitz/basement metamorphism	regional greenschist grade, biotite zone in basement	Archean basement upper greenschist to lowest amphibolite, retrograded to lower greenschist at and near Archean-Proterozoic tectonic boundary; no diagnostic minerals in Hurwitz quartzite	no diagnostic minerals in Hurwitz quartzite	lower greenschist facies in Watterson Fm.	lower greenschist facies
Nature of Archean-Proterozoic boundary	mylonite having irregular width developed in quartzite and minor basement	mylonite zone developed in Henik metabasalt and adjacent King orthoquartzite; narrow high strain zones within orthoquartzite; orthoquartzite thickened due to imbricate thrust stacking	interpreted high strain zone near the base of the Kinga Fm.	not applicable	not applicable
Alteration along Archean-Proterozoic boundary	albitization: albite, subordinate K-feldspar, Fe-Mg tri-octahedral mica, pyrite, anomalous gold	albitization not as profound and thick as at Shear Lake deposit; phlogopite, rare biotite, chlorite, tourmaline, pyrite, trace chalcopyrite	no exposure nor was the Archean-Proterozoic boundary cut in drill hole.	not applicable	not applicable
Geometry of deposit/prospect	subvertical vein-breccia-fracture filling	predominantly as disseminated and vein sulphides in altered quartzite near detachment surface. Veins and alteration are sub-parallel to foliation. Minor sub-vertical fractures.	vein-filling and disseminated sulphides in altered orthoquartzite.	veins in a zone of intensely foliated Watterson Fm; deformation related to high strain zone near Kinga-Watterson contact.	veins in a subvertical fracture zones
Structural association	paraautochthonous thrust associated with D <sub>1</sub> ; Positioned in the outer arc of thrust; outer arc extension accompanied by faults perpendicular to the outer arc	in tight F <sub>2</sub> southwest-plunging box fold, imbricate thrust stacking interpreted as D <sub>1</sub> and refolded during D <sub>2</sub> ; positioned near an inflection point in D <sub>2</sub> fold	interpreted paraautochthonous section; near the Archean-Proterozoic detachment plane thrust; imbricate thrust stack; outer arc of D <sub>1</sub> thrust?	high strain zone near the base of the Watterson Fm; possibly related to D <sub>1</sub> imbricate thrust stacking	related to a NNE-trending fault transects stratigraphy
Orientation of sulphide zones	multiple parallel to subparallel subvertical east-west trending fracture & fault zones	irregularly shaped zone of disseminated sulphides near the base of the quartzite	disseminated sulphides near the base of the orthoquartzite	veins	veins
Gangue/alteration assemblages	quartz + kaolinite +/- anhydrite; chlorite + Fe-dolomite + kaolinite + muscovite +/- barite +/- scheelite; phlogopite + Fe-carbonate + barite +/- chlorite +/- muscovite	phlogopite, rare biotite, clinocllore to talc-chlorite, muscovite, tourmaline, albite, K-feldspar, low Fe-dolomite, clay (illite/hydromuscovite), anatase-rutile, rare apatite	phlogopite, chlorite, muscovite, dolomite & Fe-dolomite, tourmaline, minor albite, orthoclase	talc, talc-chlorite, magnesitic siderite, sideritic magnesite, magnetite, rare biotite	carbonate (sideritic to magnesitic based on rusty weathering), albite, sericite,
Sulphides	pyrite, trace chalcopyrite, very rare sphalerite	pyrite; minor to trace cobaltite, ullmannite, sphalerite, chalcopyrite	pyrite; minor to trace chalcopyrite, cobaltite, pyrrhotite, rare sphalerite	pyrite; trace pyrrhotite, chalcopyrite, rare cobaltite group minerals	pyrite, possibly cobaltite group minerals (interpretation based on geochemistry of Aspler & Bursey, 1990)
Deposit zoning	three mineralogical zones: 1) kaolinite 2) chlorite 3) phlogopite	two zones: 1) phlogopite + chlorite +/- muscovite in lower quartzite, 2) with talc + chlorite +/- clay +/- muscovite in upper quartzite	no zoning observed	no zoning observed	no data
Metasomatism	ALBITITE ZONE- Major: Na, K, Al, S, CO <sub>2</sub> ; Minor: S, Fe, Mg, Ca; Trace: Au VEINS- Major: Si, CO <sub>2</sub> , Na, Al, S, Fe, Au; Minor: Mg, Ca, K; Trace: Zn, B	Major: Na, Mg, K, B, Al, Ti Minor: S, Au, Ca, CO <sub>2</sub> Minor to trace: Au, Co, Sb, Ni, As, Zn	Major: Mg, K, Fe, S, Al Minor: B, Na, Ca, CO <sub>2</sub> Trace: Co, As, Zn, Au?	Major: Mg, CO <sub>2</sub> , Fe, S, H <sub>2</sub> O Trace: Au	Major: CO <sub>2</sub> , S, Au, K? Trace: Ni, As
Gold composition Au:Ag	average Au/Ag ~ 93.7/6.3	data unavailable at this time	no data	no data	Gold in pyrite, no data on composition.
Wall rock reaction	massive albite replacement in the ductile high strain zone. No wallrock alteration zones adjacent to quartz+carbonate veins in orthoquartzite; narrow selvages in Henik metaturbidite	interaction of hydrothermal fluid with orthoquartzite produces phyllosilicate+ albite altered orthoquartzite. Quartz-bearing vein systems are absent. Dissolution cavities imply silica undersaturated hydrothermal fluid and disequilibrium.	interaction of fluid with orthoquartzite produces phyllosilicate+carbonate altered hostrock.	cryptic alteration halo in Watterson metadolstone; resetting of Fe/Fe+Mg ratio in mafic metamorphic minerals	sericite in wallrocks to carbonate + quartz veins may define alteration halo?
Mechanism for Au deposition	D <sub>1</sub> thrust and fracture propagation related to outer arc extension. Hydrothermal fluid that 'greases' the thrust is bled off via subvertical fractures. Decreasing T-P and possibly second boiling initiates gold deposition.	dynamic metamorphism and fluid migration along the zones of high strain; fluid reaction extensive with orthoquartzite and minor with high Fe-tholeiite of basement Fe-sulphides precipitated in and adjacent to mylonite.	same mechanism as at Boundary	oxidizing CO <sub>2</sub> -rich hydrothermal system may have contained very little Au in solution	Fluid migration along faults that truncate stratigraphy near margin of structural basin (possibly a F <sub>1</sub> fault???)

Textural (Fig. 4) and chemical (greater than 99.5 wt.% SiO<sub>2</sub>, Fig. 5) maturity are two unique regional features of the snow white unaltered Kinga orthoquartzite. Subtle indications of Shear Lake-type mineralization in the Shear Lake area are clay+pyrite-bearing fractures and limonitic-hematitic hues in orthoquartzite due to oxidized sulphides. Colour variations from snow white to tan, ochre, and pink hues in the orthoquartzite indicate proximity of semi-concordant zones of alkali metasomatism near the base of the orthoquartzite. Alkali metasomatism is a regional, but unevenly distributed, alteration process localized along the detachment plane in the Cullaton-Griffin-Hawk Hill Mountain lakes area. With

progressive alkali metasomatism, the homogeneous composition of the orthoquartzite moves away from the SiO<sub>2</sub> apex along a line that trends towards the composition of albite (Fig. 5).

Sulphur, represented primarily by pyrite in the albitite, correlates with anomalously gold contents, to 2400 ppb compared with 1-2 ppb in unaltered Kinga orthoquartzite. Anomalous enrichments of Zr to 248 ppm, Sr to 117 ppm, Ba to 1140 ppm, and Ti to 2800 ppm in alkali metasomatized orthoquartzite contrast with <10 ppm Zr, <10 ppm Sr, <126 ppm Ba, and <130 ppm Ti in unaltered orthoquartzite. The contents of

**Figure 5.**  
*Compositional variation of altered Hurwitz Group rocks.*



**Figure 6.**  
*Geology of the gold prospects, eastern Griffin Lake.*



these trace elements are similar to albitite associated with gold and uranium deposits (Witt, 1992; Gatzweiler et al., 1989). U-Pb geochronology on zircon from the albitite will be used in an attempt to date metasomatism and deformation in the Hurwitz Group.

Alteration envelopes adjacent to subvertical discordant veins in orthoquartzite are either not present or insignificant. The lack of reaction envelopes adjacent to veins coupled with the stability of vein quartz throughout the vertical extent of the Shear Lake system indicates that the hydrothermal fluid was saturated in silica and therefore in equilibrium with quartz in the wall rock orthoquartzite. The presence of phyllosilicates in the uppermost zone coupled with barite in sulphide-bearing veins and Ca-sulphate, possibly anhydrite, as inclusions in pyrite, indicate that the Shear Lake hydrothermal system became oxidized and acidified, during ascent through the Kinga Formation. In contrast, thin, bleached sericitic alteration envelopes mantling veins hosted in the basement Henik Group metaturbiditic sedimentary rocks indicate disequilibrium between host rocks and hydrothermal fluid.

## GOLD PROSPECTS, GRIFFIN LAKE AREA

Gold prospects in the Griffin Lake area are hosted in the Kinga and Watterson formations. The Archean basement consists of an upper greenschist facies basalt-komatiite sequence in the Griffin Lake area and a middle greenschist facies sedimentary rocks in the Cullaton Lake area (Eade, 1974). Aspler and Bursey (1990) refined the geology in this area by focusing on stratigraphic and facies relationships and by deciphering the  $D_1$  and  $D_2$  fold geometry, interference patterns, and fault systems associated with each folding event. Fold patterns in the Griffin Lake area are dominated by upright  $D_2$  folds, a doubly plunging open syncline traversing the axis of Griffin Lake, and a tight southwest-plunging syncline. Associated

with folding are discordant and concordant faults. An inferred slip plane along the basement-cover contact and oblique-slip cross faults are important structural features in the southwest-trending syncline.

### Boundary prospect

The tight southwest-plunging syncline on the northeastern side of Griffin Lake contains two gold prospects, Boundary and Third (Fig. 6). The Boundary prospect is hosted in orthoquartzite which forms the eastern limb of the syncline. The Archean basement immediately beneath the orthoquartzite is dominated by middle greenschist pillowed and massive basalt, derived schists, and very minor gabbro, iron-formation, and greywacke. The metabasalt assemblage, outside the zone of Proterozoic strain, consists of quartz+plagioclase+chlorite+biotite+epidote+carbonate with accessory magnetite and anatase. Mafic metavolcanic rocks straddle the compositional field of high-iron tholeiite to Mg-basalt (Fig. 7). Spinifex-textured flows interfinger with mafic volcanic flows approximately 12 km to the west and north of the western end of Griffin Lake (Eade, 1974; Miller, unpub. data 1990). The plotting of samples in compositional fields other than the high-iron tholeiite field results from metasomatic processes associated with gold mineralization (Fig. 7; see Alteration and metasomatism).

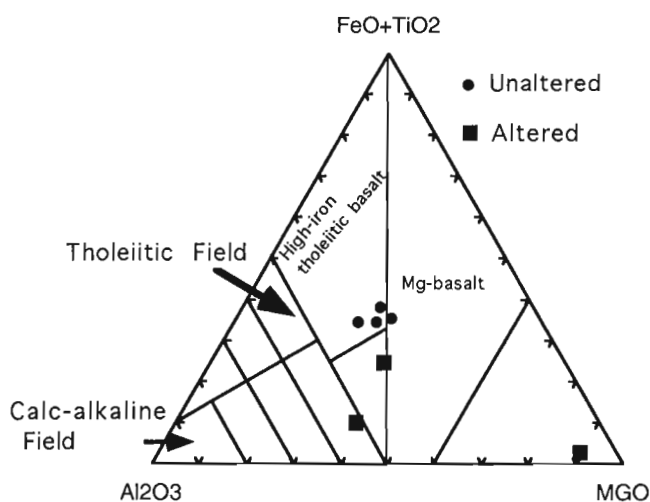


Figure 7. Jensen cation plot of metavolcanic rocks, Boundary prospect.

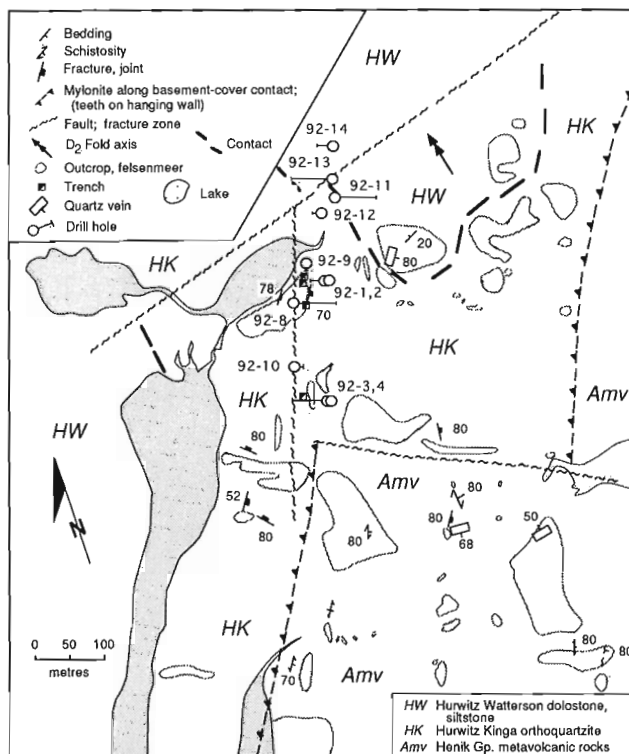


Figure 8. Geology of the Boundary prospect, eastern Griffin Lake.

**Structural setting**

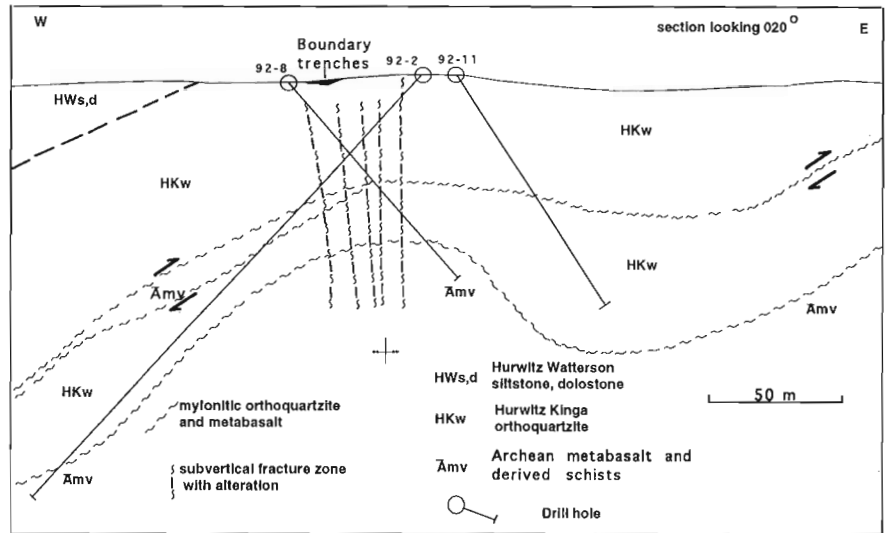
Three structural features are identified at the Boundary prospect: 1) 070° and 120° faults, 2) a 020° mineralized fracture zone, and 3) ductile slip zones along the basement-cover contact and within the Hurwitz orthoquartzite (Fig. 8, 9). Oblique faults trending ~070° and 120°, belong to the fault array that fans around the tight D<sub>2</sub> syncline (Aspler and Bursey, 1990). These faults displace the basement-cover contact and truncate or possibly displace the 020° phyllosilicate-gold-sulphide-bearing fracture zone.

Mylonites along the basement-cover interface and within the Hurwitz orthoquartzite, the latter bounding an allothonous sliver of Archean basement, are the most important structural

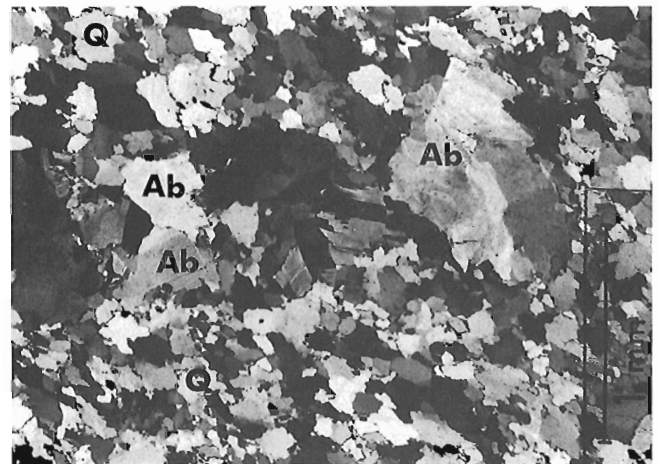
features in the Boundary prospect (Fig. 9). The slice of Archean basement bounded by mylonitic orthoquartzite dictates that the Kinga Formation has been tectonically thickened by imbricate thrust stacking and that thrusts, at this local scale, root to the west in Archean basement. Using the Boundary prospect as an example, tectonic thickening of the orthoquartzite in the Kognak River area may account for anomalously thick orthoquartzite sections in an area with regionally uniform shallow to moderate dips (Eade, 1974). The thick Kinga sections, southwest of Montgomery Lake, southeast of Oftedal Lake, and northeast of Ameto Lake, suggest imbricate stacking along the margin of the regional synclinorium. In some of these areas, thickened sections contain kyanite-bearing orthoquartzite.

**Figure 9.**

*Interpreted composite drill section through the Boundary prospect, Griffin Lake.*



**Figure 10.** *Solution cavities in orthoquartzite, Boundary prospect. GSC 1993-274*



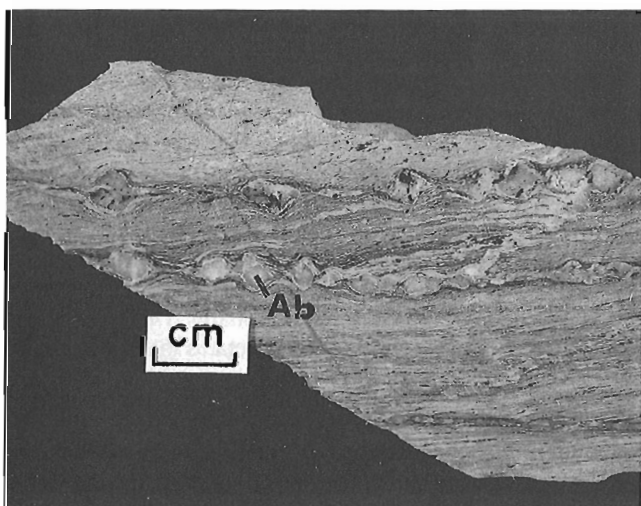
**Figure 11.** *Photomicrograph of moderately recrystallized orthoquartzite. Host rock consists of a fine grained interlocking mosaic of quartz (Q) with weakly strained metasomatic albite (Ab).*

The mylonites display a marked sinusoidal form which contrasts with the planar geometry of the mylonite in the Shear Lake area (Fig. 2; Miller, 1989). Folding of the imbricate thrust stack during  $D_2$  accounts for the observed sinusoidal form of the mylonites and basement (Fig. 9). Depth to basement drill data in the Boundary area indicate that the anticline plunges shallowly north-northeast. Since  $D_1$  and  $D_2$  are regionally orthogonal (Eade, 1974; Aspler and Bursey, 1990), subparallelism between the axial trace of this anticline and the regional southwest-plunging  $D_2$  syncline suggests these folds are coaxial  $D_2$  structures. A  $020^\circ$ -trending fracture zone is located along the hinge of this anticline. Decreasing fracture intensity away from the hinge suggests the fracture zone may represent a  $D_2$  axial plane cleavage.

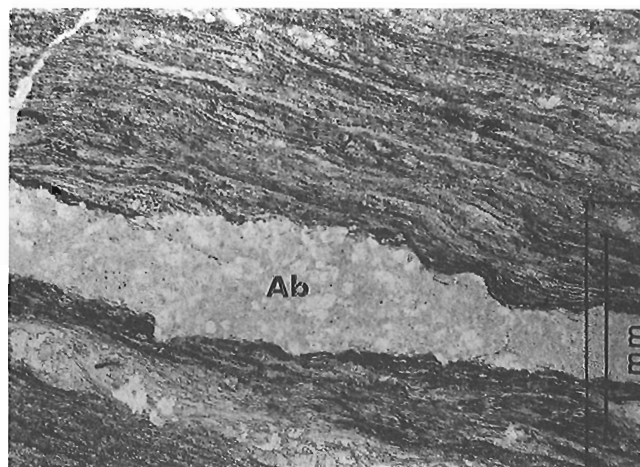
### Alteration and metasomatism

The Boundary occurrence and outcrops trending southwestward for approximately 250 m display weak hydrothermal alteration. Orthoquartzite exhibits an irregular mottled or dappled brown through tan to limonitic yellow discolouration resulting from oxidation of sulphides. White to green phyllosilicates coat fracture planes and partially fill ragged solution cavities, as large as 2 cm, in the orthoquartzite (Fig. 10).

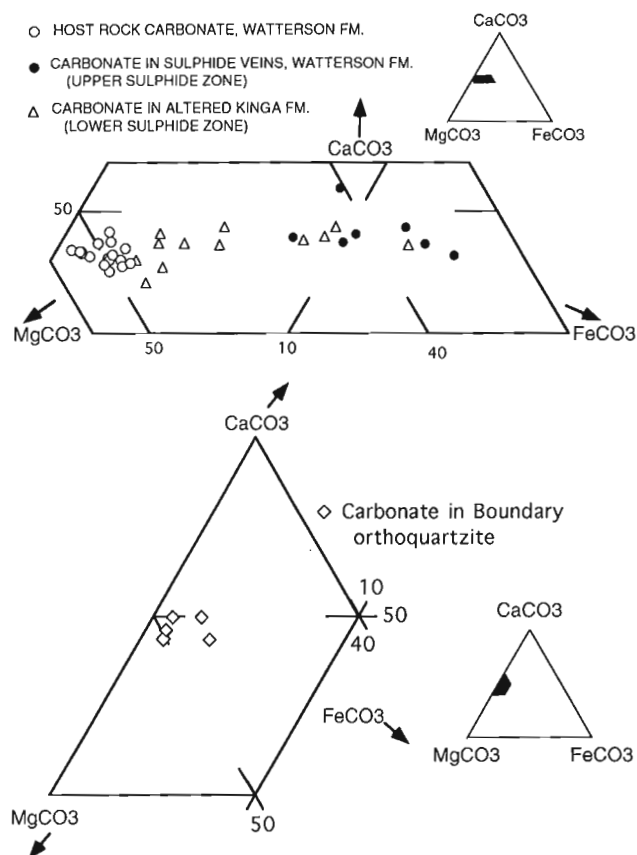
Alteration minerals occur most frequently as replacement and subordinately as veins and films on fracture walls. Partial to complete replacement of the Boundary orthoquartzite is principally confined to high strain zones within the orthoquartzite and along the Archean-Proterozoic interface (Fig. 11, 12). Vein-filling and fracture coatings are confined to brittle deformation zones peripheral to mylonites. Albite textural variations, particularly within mylonite zones, indicate a protracted metasomatic history. Fractured, polygonalized, and boudinaged albite grains indicate metasomatism is synkinematic, probably  $D_1$  (Fig. 13). These textures are comparable to textures within the basal replacement zone at Shear Lake.



**Figure 12.** Drill core specimen of mylonitic orthoquartzite with synkinematic boudinaged albite (Ab) aggregates, Boundary prospect.



**Figure 13.** Photomicrograph of fine grained ribbon textured mylonite, Figure 12. Boudinaged band of granulated albite (Ab) in foliation.



**Figure 14.** Composition of carbonate alteration minerals in the Siderite and Boundary prospects, Griffin Lake area.

Boundary and Shear Lake alteration zones are linked by the textural and compositional similarity of albite, carbonate (Fig. 14), and phlogopite (Table 1). However, increased abundances of phyllosilicates, decreased albite, orthoclase, and dolomite and the lack of quartz indicate that Boundary metasomatism, characterized by Mg-K-CO<sub>2</sub> with subordinate Na, is significantly different than metasomatism at Shear Lake. The dissolution of host rock by the hydrothermal fluid is recorded by solution cavities in the Boundary orthoquartzite record, the instability between this host rock and the Boundary hydrothermal system (Fig. 10). In Figure 7, the altered metavolcanic rocks are depleted in FeO+TiO<sub>2</sub> component and trend toward extremely Mg-rich altered equivalents.

Disseminated sulphides, more common than sulphide-bearing veinlets and sulphide+phyllosilicate coatings on fracture walls, are preferentially distributed in and peripheral to highly strained orthoquartzite. Trace sulphides are present in mylonitized and altered metavolcanic rocks. Euhedral pyrite is the ubiquitous sulphide and can be accompanied by trace sphalerite with exsolved chalcopyrite and rare fine grained cobaltite and ullmannite. The latter phases, which are diagnostic indicator minerals common to prospects in the Griffin-Mountain lakes area, have implications regarding source rocks (see Model for the Proterozoic gold metallogeny).

### *Siderite prospect*

Two structurally-controlled gold prospects, Siderite and Island, are hosted in the Watterson Formation, stratigraphically above the better explored Kinga orthoquartzite (Fig. 6). Similarities in fault geometry and alteration link these to prospects in the Boundary area and regionally to the Proterozoic gold metallogeny.

### **Structural setting**

From a regional perspective, the Siderite prospect is located near the intersection of the north-trending D<sub>1</sub> syncline and an east- and west-plunging D<sub>2</sub> syncline (Aspler and Bursey, 1990). Faults associated with each folding event and probable reactivation have complicated the geometry of basement-cover rocks.

In the Siderite prospect area, two sections of east-dipping Kinga-Watterson strata are separated by a sliver of east-dipping Archean basement composed of talc and quartz+muscovite schists. The north-northwest-trending fault that juxtaposes basement against Watterson is interpreted as a possible D<sub>1</sub> thrust. This repetition is identical to the imbricated Henik-Hurwitz section north of the Cullaton airstrip (Fig. 2) and suggests that the Hurwitz Group in the Siderite area is also para-autochthonous.

Two structurally-controlled sulphide zones constitute the Siderite Prospect. The upper sulphide zone is hosted in east-dipping, sheared to strongly foliated Watterson aluminous siliceous dolostone near the gradational contact with Kinga orthoquartzite. The lower sulphide zone is localized in highly strained orthoquartzite and is inferred to be near the Hurwitz-basement contact.

### **Alteration and metasomatism**

The upper sulphide zone is composed of sulphide-bearing veins, locally anastomosing and forming a breccia-like texture. Sulphide-bearing veins are enveloped by strongly foliated and chloritized aluminous siliceous dolostone. Silicate-carbonate veins are characterized by magnesium-rich minerals (Table 1) particularly the siderite-magnesite (Fig. 14). Pyrite is the most abundant sulphide and occurs as coarse grained aggregates of subhedral to euhedral grains. Rare cobaltite and sphalerite associated with pyrite is similar to the Boundary sulphide assemblage (Table 1); however, pyrite is stable with coarse grained magnetite, which has not been observed at other prospects. This suggests the Mg- and CO<sub>2</sub>-dominated hydrothermal system was more oxidized than at Boundary and the lower sulphide zone at Siderite (Table 1). The apparent difference of the upper sulphide zone at Siderite suggests that it may overlap in space but not in time with the Boundary and lower sulphide zone at Siderite.

### **COMPARISON BETWEEN SHEAR LAKE DEPOSIT AND GRIFFIN LAKE PROSPECTS**

Table 1 summarizes structural, mineralogical, and metasomatic features that characterize the past-producing Shear Lake deposit and prospects in the Griffin Lake area. These occurrences represent a single lode gold deposit-type within this new Proterozoic gold metallogeny. The Island Zone is included for comparison and the description is based on limited petrography and interpretation of geochemical data presented by Aspler and Bursey (1990).

### **MODEL FOR THE PROTEROZOIC GOLD METALLOGENY**

Accompanying D<sub>1</sub> shortening, the Kinga Formation acted like a rigid slab compared to overlying Hurwitz formations and underlying Archean basement. Differential slip associated with basement-cover flexural slip folding was focused along the rheologically weak boundaries of the slab, the basement-Kinga and Kinga-Watterson contacts. Intense strain along the Archean-Proterozoic interface created a regionally extensive mylonite. The Hurwitz Group is para-autochthonous with respect to basement. Imbricate thrust stacking is developed in both the Shear and Griffin lakes areas and may be even more common regionally. The presence of basement in imbricate thrust stacks dictates that thrust faults must root into basement.

Metasomatism in and adjacent to high strain zones indicates that thrust faults served as conduits for hydrothermal fluid. A pronounced curvature on a thrust sheet and the series of associated extensional and contractional faults are termed a surge zone (Coward, 1983; Fischer and Coward, 1982). Shortening of the surge zone, indicated by the formation of imbricate thrust stacks, folds within the thrust sheet and crosscutting faults, represented areally extensive domains of

enhanced hydrothermal fluid influx. Areas of enhanced hydrothermal fluid fluxing are potentially more prospective for gold exploration. In the Cullaton Lake area, a 11 km wide, convex westward para-autochthonous sheet, interpreted as a surge zone, may demonstrate that significant out-of-syncline thrusting with hydrothermal fluid influx are responsible for formation of the Shear Lake deposit.

This relationship between hydrothermal influx and structural anomalies can account for the temporal and genetic relationships common to the Proterozoic gold deposit and prospects. The migration and reaction of hydrothermal fluid along shallowly dipping mylonite, the Archean-Proterozoic detachment plane, accounts for the association of highly strained rocks with semiconcordant metasomatic zones and related alteration minerals. Protracted episodic fault movement with introduction of the hydrothermal fluid, may explain multiple generations of alteration minerals and their syn- to postkinematic timing. The mineralogical continuity between auriferous concordant alteration and discordant sulphide-gold lodes is accounted for by brittle failure in the hanging wall of the thrust. Extension along the outer margin of the arcuate para-autochthonous thrust sheet generates a family of faults that radiate around the arc. These faults breach the hydrostatically overpressured semiconcordant alteration zone and bleed-off the hydrothermal fluid along subvertical fractures and faults.

Hydrothermal fluids were generated in Archean greenstone basement and migrated into the overlying supracrustal sequence via Proterozoic thrusts that rooted in the Archean basement. Although the gold mineralization is structurally and mineralogically similar, distinct mineralogical differences exist between eastern (Shear Lake deposit) and western (Griffin Lake prospects) portions of the metalotect. Variations are attributed to regional differences in the Archean basement lithologies. In the east, the synclinorium that extends from Cullaton Lake eastward to Montgomery Lake is dominated by middle greenschist facies metasedimentary rocks. In the west, middle to upper greenschist mafic-ultramafic rocks floor the greater portion of the synclinorium in the Griffin-Hawk Hill-Mountain lakes area.

Similar metasomatic-hydrothermal minerals, notably albite, phlogopite, talc, carbonates, and pyrite, link the deposit/prospects in these two areas and suggest a common source of the hydrothermal fluid. However, fluid migration through and reaction with domains possessing marked lithological differences accounts for the subtle, but distinctive fingerprints that identify different mineralogical members in this Proterozoic lode gold deposit-type. The ubiquitous presence of carbonate as an alteration mineral suggests a CO<sub>2</sub>-rich hydrothermal fluid. In both the Shear and Griffin lake areas, this hydrothermal fluid intersected the same supermature Kinga orthoquartzite but produced strikingly different alteration assemblages. If a common origin for the hydrothermal fluid is accepted, the evolution towards different end members is attributed to fluid reaction with locally different rocks.

At Shear Lake, the hydrothermal fluid would have reacted with metatubidite having the assemblage biotite+muscovite+chlorite+quartz. Assuming metamorphic conditions of ~380°C and 2kbar in the lower to middle greenschist Hurwitz Group (Miller and Reading, 1993), this fluid would be saturated with respect to quartz and be neutral to slightly alkaline. The principal reason for the deposit-scale zoning may be conductive cooling of the fluid in the subvertical fracture systems.

In the Griffin Lake area, the magnesium-rich but quartz-poor alteration assemblage, similar to the assemblage in middle greenschist ultramafic volcanic rock, strongly suggests this fluid mixed with a metamorphic fluid derived from mafic-ultramafic rocks. Elements such as Ni, Co, Sb, and As are consistent with this source rock. Ragged solution cavities in orthoquartzite and the lining of these cavities with Mg-rich phyllosilicates records reaction between this modified highly alkaline fluid and orthoquartzite.

## ACKNOWLEDGMENTS

The first author expresses his gratitude to: Comaplex Minerals Corp. and Melinga Resources Ltd. for permission to research and publish data on the Griffin Lake area; Homestake Canada Ltd. for permission to research and publish data on the Shear Lake deposit; W. Hamilton, formerly of Corona Corp, for discussions on the geology of the Shear Lake area; Jack Henderson, GSC, for many useful discussions on thrust tectonics; R. Lancaster for computer graphics support and John Sterling for electron microprobe support. The first author is most grateful to John Kerswill for his critical review, editorial advice and computer assistance without which the publication deadline would have not been met.

## REFERENCES

- Aspler, L.B. and Bursey, T.L.**  
1990: Stratigraphy, sedimentation, dome and basin basement-cover infolding and implications for gold in the Hurwitz Group, Hawk Hill-Griffin-Mountain lakes area, District of Keewatin; in *Current Research, Part C; Geological Survey of Canada, Paper 90-1C*, p. 219-230.
- Aspler, L.B., Bursey, T.L., and LeCheminant, A.N.**  
1992: Geology of the Henik, Montgomery Lake and Hurwitz groups in the Bray-Montgomery-Ameto lakes area, southern District of Keewatin, Northwest Territories; in *Current Research, Part C; Geological Survey of Canada, Paper 92-1C*, p. 157-170.
- Aspler, L.B., Chiarenzelli, J.R., and Bursey, T.L.**  
1993: Geology of Archean and Proterozoic supracrustal rocks in the Padlei belt, southern District of Keewatin, Northwest Territories; in *Current Research, Part C; Geological Survey of Canada, Paper 93-1C*, p. 147-158.
- Aspler, L.B., Chiarenzelli, J.R., Ozarko, D.C., and Powis, K.B.**  
1994: Geology of Archean and Proterozoic supracrustal rocks in the Otter and Ducker lakes area, southern District of Keewatin, Northwest Territories; in *Current Research 1994-C, Geological Survey of Canada*.

**Coward, M.P.**

1983: The thrust and shear zones of the Moine thrust zone and the NW Scottish Caledonides; *Journal of the Geological Society of London*, v. 140, p. 795-811.

**Eade, K.E.**

1974: Geology of Kognak River Area, District of Keewatin, Northwest Territories; Geological Survey of Canada, Memoir 377, 66 p.

**Eade, K.E. and Chandler, F.C.**

1975: Geology of Watterson Lake (west half) map area, District of Keewatin, Northwest Territories; Geological Survey of Canada, Paper 74-64, 10 p.

**Fischer, M.W. and Coward, M.P.**

1982: Strains and folds within thrusts sheets: an analysis of the Heilam sheet, Northwest Scotland; *Tectonophysics*, v. 88, p. 291-312.

**Gatzweiler, R., Von Pechmann, E., Loewer, R., Strnad, G., and Fritsche, R.**

1989: Albitite-type uranium mineralization in the Nonacho Basin area, Northwest Territories, Canada; in *Uranium Resources and Geology of North America*, IAEA Technical Document 500, p. 491-518.

**Hoffman, P.F.**

1987: Subdivision of the Churchill Province and extent of the Trans-Hudson Orogen in The Early Proterozoic Trans-Hudson Orogen of North America, (ed.) J.F. Lewry and M.R. Stauffer; Geological Association of Canada, Special Paper 37, p. 15-39.

**Miller, A.R.**

1989: Highlights of gold studies in the Churchill Structural Province, Kaminak greenstone belt and Hurwitz Group, District of Keewatin, N.W.T.; in *Current Research, Part C*; Geological Survey of Canada, Paper 89-1C, p. 127-134.

**Miller, A.R. and Reading, K.L.**

1993: Iron-formation, evaporite, and possible metallogenetic implications for the Lower Proterozoic Hurwitz Group, District of Keewatin, Northwest Territories; in *Current Research, Part C*; Geological Survey of Canada, Paper 93-1C, p. 179-185.

**Patterson, J.G. and Heaman, L.M.**

1991: New geochronologic limits on the depositional age of the Hurwitz Group, Trans-Hudson hinterland, Canada; *Geology*, v. 19, p. 1137-1140.

**Raman, S., Kruse, J., and Tenney, D.**

1986: Geology, geophysics and geochemistry of the Cullaton B-zone gold deposit, NWT, Canada; in *Gold in the Western Shield*, (ed.) L.A. Clark; Canadian Institute of Mining and Metallurgy, Special Volume 38, p. 307-321.

**Reading, K.L.**

1991: Further prospecting reconnaissance of parts of two Hurwitz basins located in the Cullaton Lake area, District of Keewatin, Northwest Territories, during the 1990 summer season; confidential report submitted to Comaplex Minerals. Corp.

1990: A prospecting reconnaissance of sectors of two Hurwitz basins located in the Cullaton Lake area, Keewatin, Northwest Territories, during the 1991 summer season; confidential report submitted to Comaplex Minerals. Corp.

**Turpin, L., Maruejol, P., and Cuney, M.**

1988: U-Pb, Rb-Sr and Sm-Nd chronology of granitic basement, hydrothermal albitites and uranium mineralization (Lagoa Real, South-Bahia, Brazil); *Contributions to Mineralogy and Petrology*, v. 98, p. 139-147.

**Witt, W.K.**

1992: Porphyry intrusions and albitites in the Bardoc-Kalgoorlie area, Western Australia and their role in Archean epigenetic gold mineralization; *Canadian Journal of Earth Sciences*, v. 29, p. 1609-1622.

---

Geological Survey of Canada Project 810024



# Geology of the Sandhill Zn-Cu showing in the Gibson Lake area, District of Keewatin, Northwest Territories<sup>1</sup>

A.E. Armitage<sup>2</sup>, A.R. Miller, and N.D. MacRae<sup>2</sup>

Mineral Resources Division

*Armitage, A.E., Miller, A.R., and MacRae, N.D., 1994: Geology of the Sandhill Zn-Cu showing in the Gibson Lake area, District of Keewatin, Northwest Territories; in Current Research 1994-C; Geological Survey of Canada, p. 147-155.*

---

**Abstract:** The Gibson Lake area is underlain by a polydeformed amphibolite grade Archean sequence of mafic and felsic volcanic rocks, wacke with lesser arenite and minor oxide facies iron-formation, and orthogneiss. Proterozoic pyroxenite, gabbro, lamprophyre, and diabase dykes are common. Stratabound Zn-Cu mineralization at the Sandhill showing occurs within a concordant envelope of hydrothermally altered felsic tuff. Disseminated to massive, fine- to medium-grained sphalerite occurs as multiple bands (4 mm to 8 cm wide) associated with muscovite+pyrite+gahnite+staurolite+garnet-bearing assemblages, and within quartz veins as coarse grained, discontinuous blebs, associated with fine grained, disseminated chalcopyrite. The Sandhill showing is approximately 1400 m long and as much as 70 m wide, however the associated alteration assemblage persists eastward along strike for 12 km. A possible second, but discordant, alteration zone is inferred from brecciated and altered mafic and felsic volcanic rocks and a staurolite schist that lies structurally below the Sandhill zone.

**Résumé :** La région du lac Gibson renferme une séquence archéenne polydéformée, métamorphisée au faciès des amphibolites et composée de roches volcaniques mafiques et felsiques, de wackes avec des arénites en quantité moindre et un peu de formation de fer à faciès oxydé, ainsi que d'orthogneiss. Des dykes de pyroxénite, de gabbro, de lamprophyre et de diabase du Protérozoïque sont nombreux. À l'indice de Sandhill, une minéralisation stratoïde de Zn-Cu est encaissée dans des tufs felsiques présentant une altération hydrothermale formant une enveloppe concordante. De la sphalérite disséminée à massive, à grain fin à moyen, forme des bandes multiples (de 4 mm à 8 cm de largeur) en association avec muscovite+pyrite+gahnite+staurotide+grenat et est présente dans des filons de quartz, sous forme d'inclusions discontinues à grain grossier associées à de la chalcopyrite disséminée à grain fin. L'indice de Sandhill mesure 1 400 m de longueur environ et jusqu'à 70 m de largeur; cependant, l'assemblage d'altération associé persiste vers l'est parallèlement aux couches sur 12 km. Une deuxième zone d'altération possible mais discordante est déduite de la présence de roches volcaniques mafiques et felsiques bréchifiées et altérées et d'un schiste à staurotide qui s'étendent au-dessous (base structurale) de la zone de Sandhill.

---

<sup>1</sup> Contribution to Canada-Northwest Territories Mineral Initiatives (1991-1996), an initiative under the Canada-Northwest Territories Economic Development Cooperation Agreement.

<sup>2</sup> Department of Earth Sciences, University of Western Ontario, London, Ontario N6A 5B7

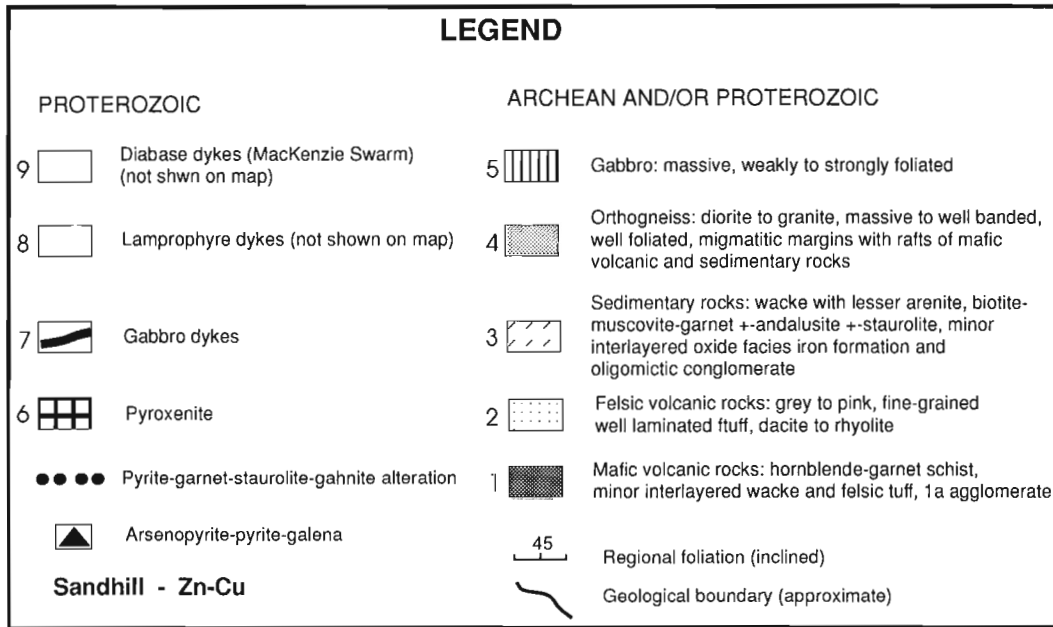
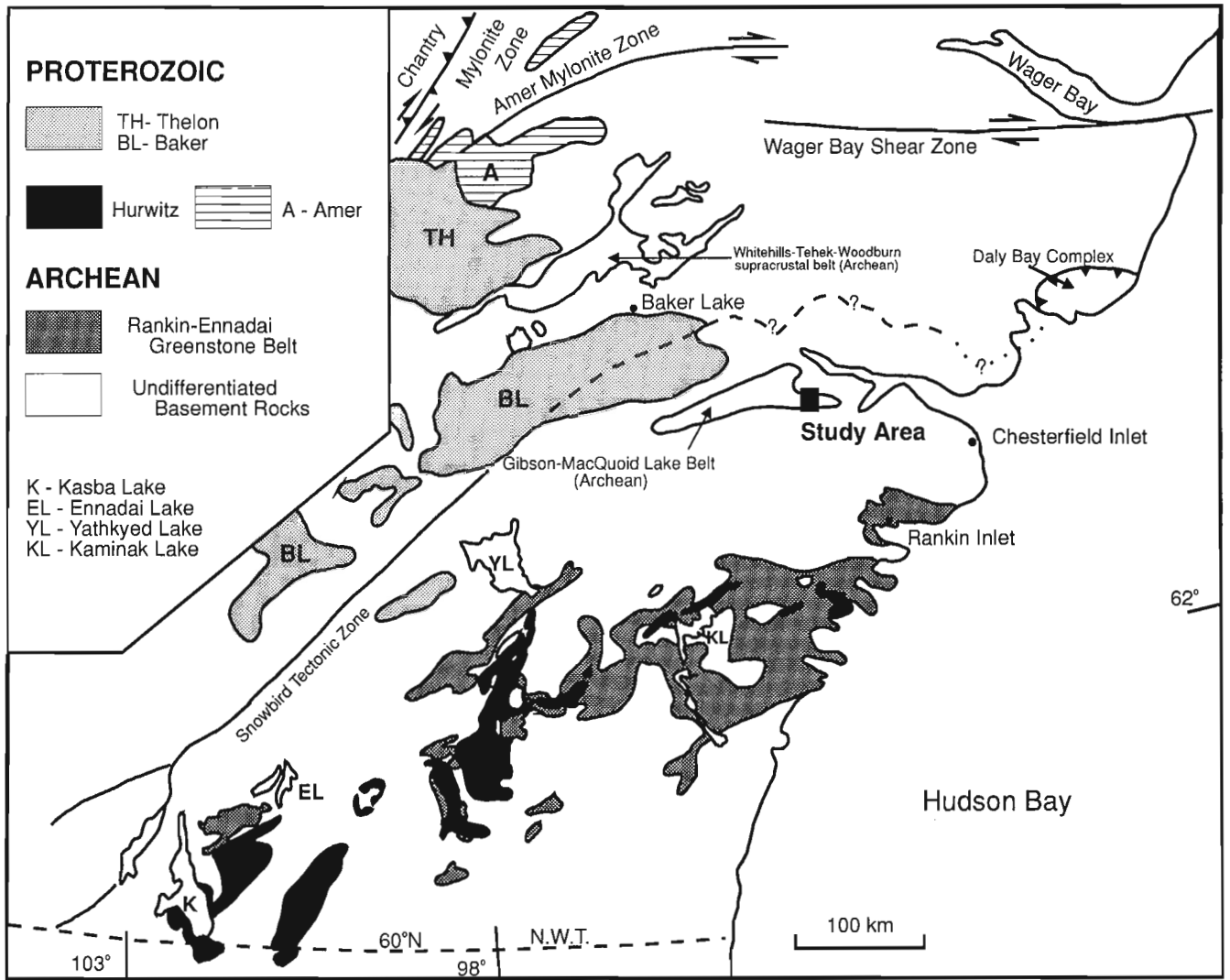


Figure 1. Map showing the location of the major supracrustal belts in the central part of the Churchill Structural Province.

## INTRODUCTION

Bedrock mapping (1:30 000 scale) in the Gibson Lake area, approximately 120 km northwest of Rankin Inlet (Fig. 1) covered part of the Gibson Lake (55N/12) map sheet. The study area straddles an inadequately mapped and poorly understood belt of Archean(?) metamorphosed interlayered volcanic and sedimentary rocks in the central part of the Churchill Structural Province of the Canadian Shield. Despite the limited database in this area, preliminary investigations indicate a good potential for future mineral exploitation. The objectives of this project are to map and document the geological, mineralogical, and structural features in and around the Sandhill massive sulphide prospect, in the Gibson Lake area. This project will enhance the limited database available on this area and provide useful guidelines for further exploration for base and precious metals in this greenstone belt.

Field data was processed using field-based portable PC and pocket computers with FIELDLOG (Brodaric and Fyon, 1989) v2.83 and AutoCAD software applications compatible with FIELDLOG's AutoCAD interface.

## REGIONAL GEOLOGY

Subsequent to the regional mapping by Wright (1967), results of more recent mapping in and around the Gibson Lake area were summarized in reports by Reinhardt and Chandler (1973), Reinhardt et al. (1980), LeCheminant et al. (1976, 1977), Tella and Annesley (1987), and Tella et al. (1986, 1989, 1990, 1992, 1993). This area is underlain by a predominantly west-trending Archean/Proterozoic granite-greenstone-gneiss terrane, which extends to the west into the MacQuoid Lake map area (55M). An extensive greenstone Belt, herein referred to as the Gibson-MacQuoid Lake belt, comprises a polydeformed sequence of interbedded mafic volcanic rocks and clastic and chemical sediments, with lesser proportions of intermediate to felsic volcanic rocks, all metamorphosed to the amphibolite facies. Smaller gabbro and syenite bodies of uncertain age intrude the volcanic and sedimentary rocks. The supracrustal sequence is bounded to the north and south by granite gneiss, migmatite and younger granitoids. The lithological and structural pattern in the Gibson-MacQuoid Lake belt is similar to the better understood Archean Rankin-Ennadai Greenstone Belt south of the study area (Fig. 1).

The Gibson-MacQuoid Lake belt was first investigated for its economic potential in 1986 by Comaplex Minerals Corporation in association with Asamera Minerals Inc. In the spring of 1988, an extensive reconnaissance and detailed exploration program (Staargaard, 1988), identified a major base metal massive sulphide prospect, termed Sandhill. Zinc-copper minerals are enclosed in a highly altered sequence of intermediate to felsic tuffs. The Sandhill showing is approximately 1400 m long and 70 m wide; representative samples contain up to 2% each of Zn and Cu, Pb to 0.25%, gold to 0.15 g/t and silver to 15 g/t (Staargaard, 1988).

## GEOLOGY OF THE GIBSON LAKE AREA

The study area (Fig. 2) is underlain by a predominantly west-trending interlayered sequence of mafic (unit 1) and felsic (unit 2) volcanic rocks, and sedimentary rocks (unit 3), all of the Gibson-MacQuoid Lake belt. The sedimentary rock unit includes wacke with lesser arenite and minor oxide facies iron-formation and oligomictic conglomerate. Syntectonic gabbro sills (unit 5) occur within the mafic volcanic rocks. Granitic gneiss (unit 4) is interlayered with the volcanic and sedimentary rocks, and forms the northern and southern boundaries of the greenstone belt. Pyroxenite (unit 6), an east-trending swarm of gabbro intrusions (unit 7), lamprophyre (unit 8), and diabase dykes (unit 9) are common throughout the map area. Outcrop is good to excellent with 60-70% exposure in most areas.

### *Volcanic rocks (units 1, 2)*

Mafic volcanic rocks (unit 1), with minor interlayered sedimentary and felsic volcanic rocks, form linear, continuous to discontinuous bands to 500 m thick throughout the central part of the map area (Fig. 2). They are strongly foliated to banded and consist of fine- to medium-grained hornblende-plagioclase-garnet (Fig. 3); banding is defined by variable hornblende and plagioclase content. Garnet is 0.1-4 mm in diameter, in places partially to completely replaced by plagioclase, and occurs in the more massive rocks and in the plagioclase-rich bands; it may form up to 30% of the rock. Remnant pillow structures were identified at one locality west of 'Thirsty Lake'; flow top breccias, recognized at several localities in the western part of the map area, are characterized by light to dark brown-weathering bands that border more massive dark green-weathering flows (Tella et al., 1986). Minor agglomerate (unit 1a; Fig. 2) in the northwest corner of the map area contains felsic to intermediate clasts as large as 30-50 cm long in a fine- to medium-grained matrix of hornblende and plagioclase. The clasts are aligned parallel to foliation.

Felsic volcanic rocks (unit 2) consist of crystal tuff, dacitic to rhyolitic in composition, and form a linear, continuous zone in the northern part of the map area (Fig. 2). The felsic tuff is fine grained, light grey to pink on fresh and weathered surface, well laminated to layered on a millimetre to centimetre scale (Fig. 4). The tuff consists predominantly of quartz, feldspar, biotite, and chlorite with minor 1-2 cm thick hornblende-rich bands. Throughout this unit, discontinuous lenses, 5-10 cm thick, contain angular 2-5 mm feldspar grains in a fine grained felsic matrix. Garnet, 1-5 mm in diameter, may form as much as 5% in some layers.

### *Sedimentary rocks (unit 3)*

Sedimentary rocks (unit 3) are the most abundant rocks in the map area (Fig. 2). Wackes, psammitic to semipelitic in composition, dominate this unit in the southern and central part of the map area. They are grey to red-brown, gritty, fine- to medium-grained (Fig. 5A) and consist of quartz-biotite-plagioclase-garnet±andalusite. Compositional layering in the

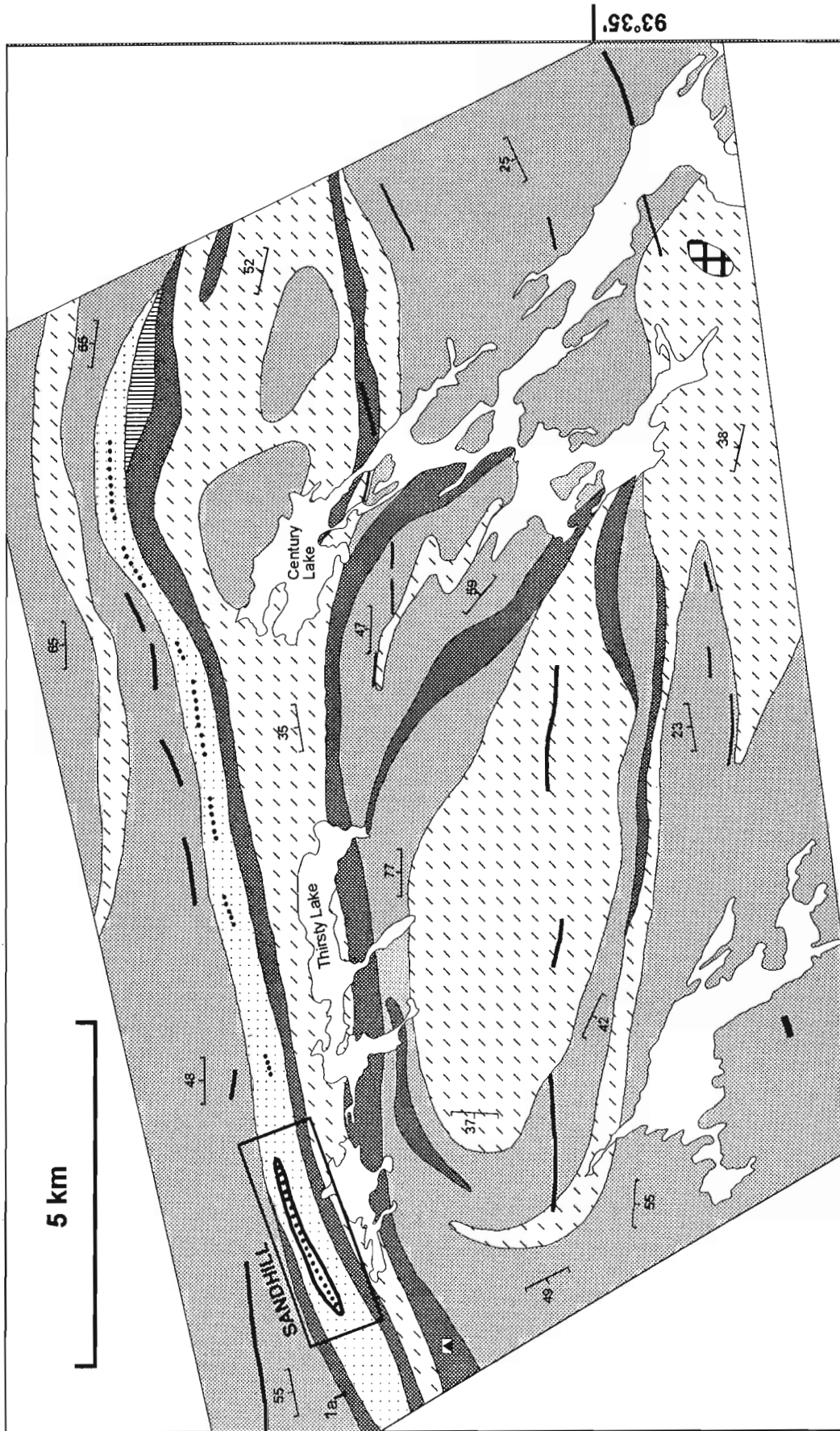


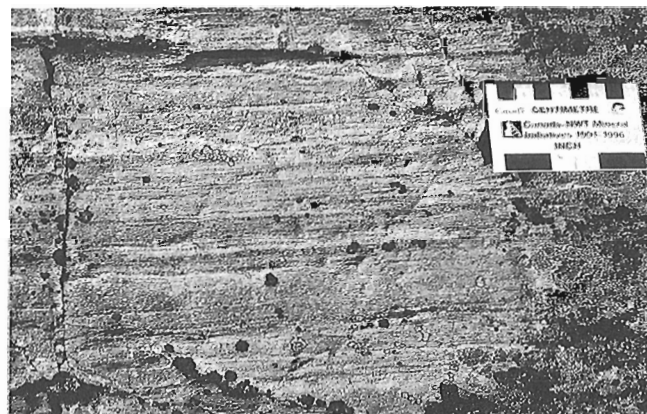
Figure 2. Geological map of the Gibson Lake map area.

wackes is indicated by biotite-rich (15-20%) and garnet-rich (to 20%) bands 5-20 cm wide. Bands, 20-30 cm wide, containing 0.5-1 cm plagioclase porphyroclasts (Fig. 5B) with coarse grained biotite±garnet, are common in the northern parts (Fig. 2). They are rare in the southern parts of the map area. Staurolite±andalusite porphyroblasts with coarse biotite characterize the wacke in the northwestern part of the map area.

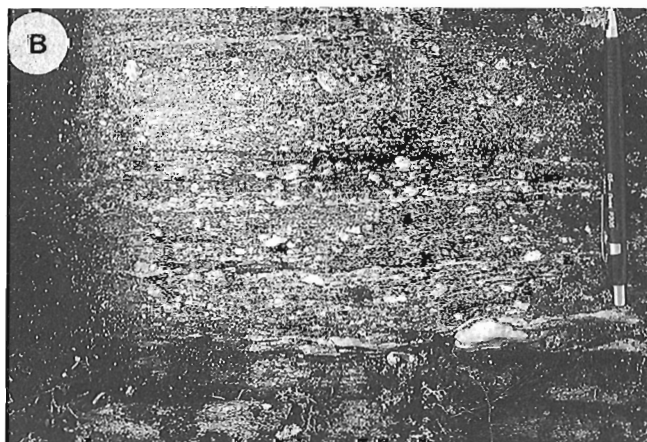
In the northern part of the map area, wackes grade into light grey, fine- to medium-grained arenite which consists predominantly of quartz, plagioclase, and muscovite. At two localities, in the southern and western parts of the map area, white-weathering quartz arenite forms thin discontinuous bands up to 8 m thick structurally below mafic volcanic rocks. Primary sedimentary structures are poorly preserved because of the strong to intense foliation present in supracrustal rocks. However, crossbedding was identified in quartz arenite at one locality in the western part of the map area. Within the arenite



**Figure 3.** Mafic volcanic (hornblende-plagioclase-garnet schist; unit 1) southwest of 'Thirsty Lake'. Garnets are partially replaced by plagioclase. GSC 1993-253B



**Figure 4.** Fine grained light grey to pink well laminated felsic tuff (unit 2).



**Figure 5.** A) Wacke (unit 3) from the central part of the map area. GSC 1993-253A. B) Wacke (unit 3) containing coarse feldspar clasts from the northern part of the map area. GSC 1993-253D



with a minor diorite component is the more dominant composition of the orthogneiss in the northern and southern parts of the map area. These rocks are grey to pink, massive to well banded, well foliated and consist of plagioclase-quartz-biotite±garnet±amphibole. Garnet (5-10%) forms in more biotite-rich (20-25%) bands. Medium grained, massive to weakly banded and foliated white- to grey-weathering granite gneiss in the central part of the map area consists of plagioclase, quartz, and K-feldspar with 2-10% biotite and muscovite. Medium- to coarse-grained, well foliated granodiorite is in sharp contact with the felsic volcanics (unit 2) and well banded granite gneiss along the northern boundary of the study area.

Foliated and boudinaged white pegmatite dykes are common in the diorite to granodiorite gneiss (unit 4), sedimentary rocks (unit 3), and mafic volcanic rocks (unit 1) in the southern and central part of the map area. However, dykes are absent in the felsic volcanic rocks and gneiss in the northern part of the map area. The pegmatite dykes predominantly consist of plagioclase and quartz. In the sedimentary rocks immediately south of the felsic volcanic rocks, the pegmatite dykes typically contain millimetre- to centimetre-long tourmaline crystals.

### ***Gabbro (unit 5)***

Gabbro sills (unit 5), most of which are not shown on the map (Fig. 2), are common within the northern volcanic rocks. The gabbro is dark green, massive, weakly to strongly foliated and contain medium- to coarse-grained hornblende, plagioclase, and chlorite.

### ***Mafic and felsic intrusions (units 6-9)***

Relatively undeformed mafic and felsic intrusions of probable Proterozoic age are common throughout the map area. In the southeast part of the map area, a 750 m long elliptical plug of pyroxenite (unit 6) intrudes the sedimentary rocks (unit 3). It consists of randomly oriented pyroxene phenocrysts, partially altered to amphibole, in a pyroxene-plagioclase matrix.

Numerous east-trending gabbro dykes (unit 7) form prominent topographic ridges, to 300 m wide, throughout the map area. These rocks are dark green, massive, and contain medium- to coarse-grained pyroxene-plagioclase-bearing assemblages. Several of the gabbro intrusions contain 1-2% disseminated, fine grained pyrrhotite.

Light to dark brown-weathering, northwest-trending lamprophyre dykes (unit 8), up to 2 m wide, are scattered throughout the map area. Two mineralogically distinct types of alkaline dykes are present. The most abundant type is a porphyritic dyke with phlogopite±pyroxene phenocrysts set in a fine grained matrix consisting of amphibole-feldspar-apatite-bearing assemblages. Two lamprophyre dykes from the west end of the map area consist of K-feldspar oikocrysts containing biotite (30-40%) and apatite (10-15%), and carbonate inclusions and trace titanite, rutile, zircon, pyrite, and chalcopyrite. Several dykes contain inclusions of country rock including granite, orthogneiss, and metasediments.

Lamprophyres are related to the 1.85 Ga alkaline igneous province that is defined by the distribution of Christopher Island Formation, Lower Dubawnt Group. The compositional range of volcanic rocks is lamproitic through to mafic and felsic minettes (Peterson and Rainbird, 1990; LeCheminant et al., 1987).

In the eastern part of the map area, three northwest-trending diabase dykes (unit 9), up to 1 m wide, cut the volcanic and sedimentary rocks. They are fine grained, massive, fresh, and contain hornblende and plagioclase; they are probably related to the  $1267 \pm 2$  Ma Mackenzie dyke swarm (LeCheminant and Heaman, 1989).

White to pink pegmatite dykes are common in the north-western part of the map area. These dykes contain muscovite books to 6 cm thick, tourmaline crystals to 10 cm long, and beryl to 6 cm in diameter. These pegmatites may correlate with mica+topaz-bearing pegmatites in the western half of the MacQuoid Lake map area (LeCheminant et al., 1976).

## **STRUCTURE AND REGIONAL METAMORPHISM**

Bedding ( $S_0$ ) is indicated by compositional layering in the sedimentary and felsic volcanic rocks. Facing directions are poorly preserved; however, west of 'Thirsty Lake', rare pillow structures with lava shelves in the mafic volcanic rocks and crossbedding in a quartz arenite indicate a younging to the north. Regional foliation ( $S_1$ ) is parallel to bedding ( $S_0=S_1$ ) and is defined by the micas in the sedimentary, felsic volcanic rocks and orthogneiss, and by amphibole in the mafic volcanic rocks. In the eastern and central parts of the map area (Fig. 2),  $S_1$  foliation strikes consistently west and dips moderately to the north. This structure defines moderate to steep east- and west-plunging isoclinal folds ( $F_1$ ) in the mafic and felsic volcanic rocks.

Shallow to moderate northwest- to northeast-plunging  $F_2$  folds show both S and Z asymmetry. In the western part of the map area,  $S_1$  foliations are folded by a regional northwest plunging  $F_2$  fold. Broad, open, north-plunging mesoscopic folds ( $F_3$ ) resulted in the reversals in both  $F_1$  and  $F_2$  plunge directions.

Moderate north- to northeast-plunging hornblende mineral lineations, quartz rodding, and crenulation lineation are related to post- $F_2$  deformation. These lineations are best developed in the northern part of the map area, along the mafic volcanic-sedimentary contact directly south of 'Thirsty Lake' (Fig. 2) and along the felsic volcanic-orthogneiss contact. Late north- to northwest-trending brittle faults, interpreted to be part of the Baker Lake cataclastic zone (Schau et al., 1982), display limited offset of both sinistral or dextral movement. Deformation associated with these faults has affected all rocks including the east-trending gabbro intrusions and northwest-trending lamprophyre dykes; local epidote and K-feldspar alteration is associated with these late faults.

Lower amphibolite facies metamorphism is indicated by biotite+garnet±andalusite±staurolite in sedimentary rocks, hornblende+garnet in mafic volcanic rocks, and biotite+garnet



in orthogneiss. An estimate of the P-T conditions for regional metamorphism are in the order of 2-3 kbar and 520-580°C based on the stability of Fe-staurolite and the aluminosilicate triple point (Yardley, 1989).

## MINERALIZATION AND ALTERATION

Stratabound Zn-Cu minerals of the Sandhill zone (Fig. 2) occur within an envelope of hydrothermally-altered felsic tuffs (unit 2). The strike length of the concordant mineralization and alteration envelope is 1400 m and the maximum width is approximately 120 m. However, altered felsic volcanic rocks, similar to those that enclose the Sandhill showing, persist for up to 12 km eastward along strike. The Sandhill zone comprises medium- to coarse-grained sphalerite which occurs as discontinuous 2-8 cm wide bands within coarse grained, white weathering pyritic

muscovite-quartz±gahnite±garnet±staurolite schist (Fig. 6A, B). Tourmaline is a common accessory mineral with this assemblage. To the south, structurally and stratigraphically below the muscovite-quartz schist, fine grained disseminated sphalerite occurs within well laminated, fine- to medium-grained quartz-pyrite-garnet-muscovite-gahnite-staurolite schist (Fig. 7). In the mineralized zone, subconcordant quartz-pyrite veins contain discontinuous blebs of coarse grained sphalerite±galena associated with 2-5% disseminated fine- to medium-grained chalcopyrite. A cherty pyrite-rich (10-15%) unit containing as much as 10-15% sulphides, is present at the upper contact between the muscovite-quartz schist and altered tuffs. This unit may represent a siliceous exhalite.

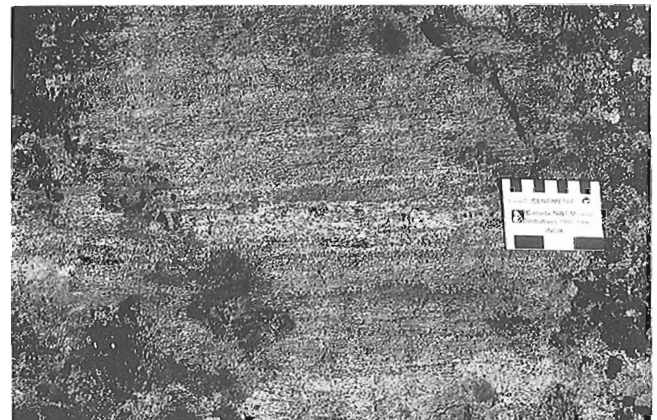
Eastward along strike, pyritic muscovite-quartz schist contains intermittent, fine- to medium-grained garnet-staurolite-gahnite-kyanite assemblages. Although sphalerite and/or chalcopyrite were rarely observed within the



**Figure 6.** A) Massive, coarse grained, white-weathering pyritic muscovite-quartz schist which hosts Sandhill Zn-Cu mineralization. B) Sphalerite in pyritic muscovite-quartz-gahnite-garnet-staurolite schist from the west end of the Sandhill zone.



**Figure 7.** Well laminated to banded fine- to medium-grained quartz-pyrite-garnet-muscovite-gahnite-staurolite schist with disseminated fine grained sphalerite.



**Figure 8.** Grey to red-brown, laminated to banded, hydrothermally altered felsic tuff structurally above the sulphide zone. It is characterized by a highly aluminous assemblage containing biotite, muscovite, garnet, staurolite, and gahnite along with pyrite and magnetite.

hydrothermally-altered equivalents of the Sandhill prospect, the presence of gahnite as well as staurolite is a good indicator of massive sulphide mineralization (Spry, 1986; Spry and Scott, 1986).

Hydrothermally altered felsic tuff enclosing the Sandhill zone (Fig. 8), is grey to red-brown, laminated and contrasts with grey to pink unaltered equivalents. Altered tuff contains the highly aluminous assemblage biotite, muscovite, garnet, staurolite, and gahnite along with pyrite and magnetite. In the western part of the map area, below the mineralized zone, felsic and mafic volcanic rocks are typically brecciated and replaced by epidote and chlorite. Staurolite±andalusite porphyroblasts with coarse biotite in the wacke to the south and southwest of the Sandhill zone may indicate the presence of another, but possibly discordant, alteration zone.

Numerous pyritic gossans within the mafic volcanic and sedimentary rock units are sporadically distributed throughout the map area. These gossans are related to the late north-west-trending brittle faults. In the western part of the map area, a 10 m wide sulphide horizon is located within a band of wacke, which is interlayered with mafic volcanic rocks. Massive arsenopyrite (30%), with pyrite (10-15%) and pyrrhotite (2-4%) and trace chalcopyrite, galena, and graphite occur within vuggy quartz veins. The sulphide-bearing quartz veins and graphite alteration can be traced for more than 1 km eastward along strike. This sulphide mineralization appears to be structurally controlled and formed later than zinc-copper sulphides in the Sandhill zone.

## SUMMARY AND DISCUSSION

In the Gibson Lake area, the west-trending, polydeformed Archean metavolcanic belt that hosts the Sandhill zinc-copper showing has been metamorphosed under lower amphibolite facies conditions, estimated to be in the order of 520-580°C and 2-3 kbar.

From south to north, the lithological succession in the area of the Sandhill showing is interpreted to face and dip north at moderate to steep attitudes. It comprises interlayered semipelitic to arenaceous metasedimentary units overlain by a mafic volcanic unit and, in turn, by a felsic volcanic unit. The finely laminated felsic unit and the absence of coarse fragmental rock, even though brecciated rocks are recognized stratigraphically below the showing, suggest this felsic unit may represent a distal subaqueous tuff to ash deposit.

The Zn-Cu Sandhill showing, hosted in felsic tuff, is stratabound and enveloped by hydrothermally-altered felsic tuff. This concordant alteration envelope is highly aluminous and bears the mineral assemblage muscovite+quartz+gahnite+garnet+staurolite. In addition, similarly altered felsic rocks persist eastward along strike for 12 km. The areal extent of aluminous altered felsic tuff represents regional metasomatism and is interpreted to be the metamorphosed product of advanced argillic hydrothermal alteration. The felsic volcanic host rock and aluminous alteration assemblage with disseminated and massive base metal sulphides are

features that draw the comparison to metamorphosed alteration assemblages associated with volcanogenic massive sulphide deposits.

The Snow Lake area, part of the early Proterozoic Flin Flon volcano-sedimentary belt Trans-Hudson orogen, is host to numerous Cu-Zn and Zn-Cu volcanogenic massive sulphide deposits. Some of these deposits are hosted in thick sequences of felsic volcanic rocks and are accompanied by extensive alteration zones (Walford and Franklin, 1982; Studer, 1982; Zaleski, 1989). On a district scale, large volumes of supracrustal rocks in the stratigraphic footwall to the deposits have been subjected to hydrothermal alteration (Bailes, 1987). Synvolcanic alteration zones, discordant pipes below exhalative massive sulphide lenses, and semi-conformable zones contain diagnostic metamorphic mineral assemblages that result from lower to upper almandine-amphibolite facies regional metamorphism. Metamorphism of synvolcanic alteration minerals produced an aluminous assemblage that includes quartz, muscovite, pyrite, zircon, staurolite, kyanite, biotite, chlorite, and sphalerite with gahnite (Zaleski, 1991).

The Sturgeon Lake massive sulphide camp lies within the Archean Wabigoon volcano-sedimentary greenstone belt of the Superior Province. Volcanogenic massive sulphide deposits and numerous base metal prospects are associated with a submarine caldera complex and in particular to felsic pyroclastic sequences (Morton et al., 1990; Osterberg et al., 1987). Local discordant alteration zones proximal to massive sulphide lenses and broader semi-concordant zones record corridors of hydrothermal fluid-rock interaction. Regional metamorphic grades range from greenschist to lower amphibolite. Aluminosilicate-bearing mineral assemblages containing pyrophyllite, andalusite, or kyanite in metamorphosed discordant pipes identify corridors of high fluid flow and reaction between modified sea water and volcanic rocks.

A direct relationship exists between base metal concentrations and exceptionally aluminous lithological compositions in the Sandhill showing and eastern extension. These features in other well studied volcanogenic massive sulphide districts are attributed to submarine sea-floor alteration related to synvolcanic hydrothermal systems. Microprobe studies are in progress to determine the chemistry of metamorphic minerals in order to evaluate the hydrothermal alteration, relative importance of concordant and discordant alteration zones, and the role of exhalative versus replacement processes associated with synvolcanic hydrothermal alteration.

## ACKNOWLEDGMENTS

We would like to thank the following agencies for additional financial support for this project: Indian and Northern Affairs Canada (Contract No. YK-93-94-314), UWO-VP Research (Grant No. FAB A 3291-000-989), and Natural Sciences and Engineering Research Council of Canada (Grant No. OGP 0005539). We thank Dean Besserer for field assistance; Subhas Tella, Continental Geoscience Division, for his advice and support in the field, specifically on the structural aspects of

this study; Boyan Brodaric, Continental Geoscience Division, for his assistance with FIELDLOG and AutoCAD applications; John Sterling, GSC, for electron microprobe support; P. Mudry and M. Pyke of Comaplex Minerals Corp. for making available unpublished reports and maps from the Sandhill area and logistical support; and Melinda and Peter Tatty of M&T Enterprises Ltd., Rankin Inlet for excellent expediting services.

## REFERENCES

- Bailes, A.H.**  
1987: Chisel-Morgan Lake project; in 1987 Report of Field Activities, Manitoba Energy and Mines, p. 70-80.
- Brodaric, B. and Fyon, J.A.**  
1989: OGS FIELDLOG: A Microcomputer-based Methodology to Store, Process and Display Map-related data; Ontario Geological Survey, Open File Report 5709, 73 p. and 1 diskette.
- Geological Survey of Canada**  
1971:  
Sheet 55N/12; Geophysical Series (Aeromagnetic) Map 6800G.
- LeCheminant, A.N. and Heaman, L.M.**  
1979: Mackenzie igneous events, Canada: Middle Proterozoic hot spot magmatism associated with ocean opening; Earth and Planetary Science Letters, v. 96, p. 38-48.
- LeCheminant, A.N., Hews, P.C., Lane, L.S., and Wolff, J.M.**  
1976: MacQuoid Lake (55 M west half) and Thirty Mile Lake (65 P east half) map-areas, District of Keewatin; in Report of Activities, Part A; Geological Survey of Canada, Paper 76-1A, p. 383-386.
- LeCheminant, A.N., Blake, D.H., Leatherbarrow, R.W., and deBie, L.**  
1977: Geological studies: Thirty Mile Lake and MacQuoid Lake map-areas; in Report of Activities, Part A; Geological Survey of Canada, Paper 77-1A, p. 205-208.
- LeCheminant, A.N., Roddick, J.C., and Henderson, J.R.**  
1987: Geochronology of Archean and Early Proterozoic magmatism in the Baker Lake-Wager Bay region, N.W.T.; in Geological Association of Canada/Mineralogical Association of Canada, Program with Abstracts, v. 12, p. 66.
- Morton, M.L., Hudak, G.J., Walker, J.S., and Franklin, J.M.**  
1990: Physical volcanology and hydrothermal alteration of the Sturgeon Lake caldera complex; in Mineral Deposits in the Western Superior Province, Ontario, (ed.) J.M. Franklin, B.R. Schneiders, and E.R. Koopman; 8th IAGOD Field Trip Guidebook, Geological Survey of Canada, Open File 2164, p. 77-94.
- Osterberg, S.A., Morton, R.L., and Franklin, J.M.**  
1987: Hydrothermal alteration and physical volcanology of Archean rocks in the vicinity of the Headway-Coulee massive sulphide occurrence, Onaman area, northwestern Ontario; Economic Geology, v. 82, no. 6, p. 1505-1521.
- Peterson, T.D. and Rainbird, R.H.**  
1990: Tectonic and petrological significance of regional lamproite-minette volcanism in the Thelon and Trans-Hudson hinterlands, Northwest Territories; in Current Research, Part C; Geological Survey of Canada, Paper 90-1C, p. 69-79.
- Reinhardt, E.W. and Chandler, F.W.**  
1973: Gibson-MacQuoid Lake map area, District of Keewatin; in Report of Activities, Part A; Geological Survey of Canada, Paper 73-1A, p. 162-165.
- Reinhardt, E.W., Chandler, F.W., and Skippen, G.B.**  
1980: Geological map of the MacQuoid Lake (NTS 55M, E1/2) and Gibson Lake (NTS 55N, W1/2) map area, District of Keewatin; (comp.) G.B. Skippen; Geological Survey of Canada, Open File 703.
- Schau, M., Tremblay, F., and Christopher, A.**  
1982: Geology of Baker Lake map area, District of Keewatin: a progress report; in Current Research, Part A; Geological Survey of Canada, Paper 82-1A, p. 143-150.
- Spry, P.G.**  
1986: The stability of zincian spinels in sulfide systems and their potential as exploration guides for metamorphosed massive sulfide deposits; Economic Geology, v. 81, p. 1446-1463.
- Spry, P.G. and Scott, S.D.**  
1986: Zincian spinel and staurolite as guides to ore in the Appalachians and Scandinavian Caledonides; Canadian Mineralogist, v. 24, p. 147-163.
- Staargaard, C.F.**  
1988: Report on a 1988 program of reconnaissance exploration on permits 1108, 1109, 1128-1138 along with detailed exploration in selected areas in the Parker Lake-MacQuoid Lake areas, District of Keewatin, N.W.T.; Confidential report submitted to Comaplex Minerals Corp., Calgary, Alberta.
- Studer, R.D.**  
1982: Geology of the Stall Lake copper deposit, Snow Lake, Manitoba; Canadian Institute of Mining and Metallurgy Bulletin, v. 75, no. 837, p. 66-72.
- Tella, S. and Annesley, I.R.**  
1987: Precambrian Geology of parts of the Chesterfield Inlet map area, District of Keewatin; in Current Research, Part A; Geological Survey of Canada, Paper 86-1A, p. 25-36.
- Tella, S., Annesley, I.R., Borradaile, G.J., and Henderson, J.R.**  
1986: Precambrian geology of parts of Tavani, Marble Island and Chesterfield Inlet map areas, District of Keewatin, N.W.T.; Geological Survey of Canada, Paper 86-13, 20 p.
- Tella, S., Roddick, J.C., Bonardi, M., and Berman, R.G.**  
1989: Archean and Proterozoic tectonic history of the Rankin Inlet-Chesterfield Inlet region, District of Keewatin, N.W.T.; Geological Society of America, Abstracts with Programs, v. 21, no. 6, p. 22.
- Tella, S., Roddick, J.C., Park, A.F., and Ralsler, S.**  
1990: Geochronological constraints on the evolution of the Archean and Early Proterozoic terrane in the Tavani-Rankin Inlet region, Churchill Structural Province, N.W.T.; Geological Society of America, Abstracts with Programs, v. 22, no. 7, p. A174.
- Tella, S., Schau, M., Armitage, A.E., and Loney, B.C.**  
1993: Precambrian geology and economic potential of the northeastern parts of the Gibson Lake (55N) map area, District of Keewatin, Northwest Territories; in Current Research, Part C; Geological Survey of Canada, Paper 93-1C, p. 197-208.
- Tella, S., Schau, M., Armitage, A.E., Seemayer, B.E., and Lemkow, D.**  
1992: Precambrian geology and economic potential of the Meliadine Lake-Barbour Bay region, District of Keewatin, Northwest Territories; in Current Research, Part C; Geological Survey of Canada, Paper 92-1C, p. 1-11.
- Walford, P.C. and Franklin, J.M.**  
1982: The Anderson Lake Mine, Snow Lake, Manitoba; in Precambrian Sulphide Deposits, (ed.) R.W. Hutchinson, C.D. Spence and J.M. Franklin; Geological Association of Canada, Robinson Symposium Volume, Special Paper 25, p. 481-524.
- Wright, G.M.**  
1967: Geology of the southeastern barren grounds, Parts of the Districts of Mackenzie and Keewatin; Geological Survey of Canada, Memoir 350.
- Yardley, B.W.D.**  
1989: An Introduction to Metamorphic Petrology; Longman, England, 248 p.
- Zaleski, E.**  
1991: Metamorphic petrology of Fe-Zn-Mg-Al alteration at the Linda volcanogenic massive sulphide deposit, Snow Lake, Manitoba; Canadian Mineralogist, v. 29, p. 995-1017.  
1989: Metamorphism, structure and petrogenesis of the Linda volcanogenic massive sulphide deposit, snow Lake, Manitoba; Ph.D. thesis, University of Manitoba, Winnipeg, Manitoba, 344 p.



# Archean and Lower Proterozoic geology of western Dubawnt Lake, Northwest Territories

T.D. Peterson and P. Born<sup>1</sup>  
Continental Geoscience Division

*Peterson, T.D. and Born, P., 1994: Archean and Lower Proterozoic geology of western Dubawnt Lake, Northwest Territories; in Current Research 1994-C; Geological Survey of Canada, p. 157-164.*

---

**Abstract:** The bedrock of western Dubawnt Lake consists of: (1) Archean, migmatized metasedimentary rocks comprised mainly of biotite-quartz-feldspar-garnet schist, including sulphide iron-formation; (2) a mafic-to-felsic intrusive suite (the Snow Island suite), dominated by granites (2605 Ma), which accompanied the migmatization; and (3) orthoquartzite plus minor schists assigned to the Lower Proterozoic Amer Group. A pervasive, shallowly south-southwest-plunging extension lineation (L2) developed at upper greenschist facies during thrusting (D2) which involved the Amer Group and older basement rocks. L2 was folded (D3) by east-west-trending folds. D2 and D3 must predate brittle deformation at 1.84 Ga leading to Dubawnt Supergroup deposition, during the Trans-Hudson orogeny. Deformation of the Amer Group probably accompanied the east-west collision between the Slave and Churchill cratons at 2.0-1.9 Ga.

**Résumé :** Le substratum rocheux de la partie ouest de la région du lac Dubawnt se compose : (1) de roches métasédimentaires archéennes, migmatisées, principalement composées de schiste à biotite-quartz-feldspath-grenat, avec notamment une formation de fer à faciès sulfuré; (2) d'une suite intrusive mafique à felsique (suite de Snow Island) qui contient en majorité des granites (2 605 Ma), et dont la mise en place a accompagné la migmatisation; et (3) d'un orthoquartzite et de quantités secondaires de schiste attribués au Groupe d'Amer (Protérozoïque inférieur). Une linéation d'étirement (L2) répandue, qui plonge légèrement vers le sud-sud-ouest, s'est formée dans des conditions du faciès des schistes verts supérieur pendant l'épisode de chevauchement (D2) qui a affecté les roches du Groupe d'Amer et les roches plus anciennes du socle. L2 a été déformée (D3) par des plis d'orientation est-ouest. D2 et D3 doivent être plus anciens que la déformation fragile survenue à 1,84 Ga, qui a abouti à la sédimentation du Supergroupe de Dubawnt, pendant l'orogénèse transhudsonienne. La déformation du Groupe d'Amer a probablement accompagné la collision est-ouest survenue entre le craton des Esclaves et le craton de Churchill à 2-1,9 Ga.

---

<sup>1</sup> Department of Earth Sciences, Carleton University, Ottawa, Ontario K1S 5B6

## INTRODUCTION

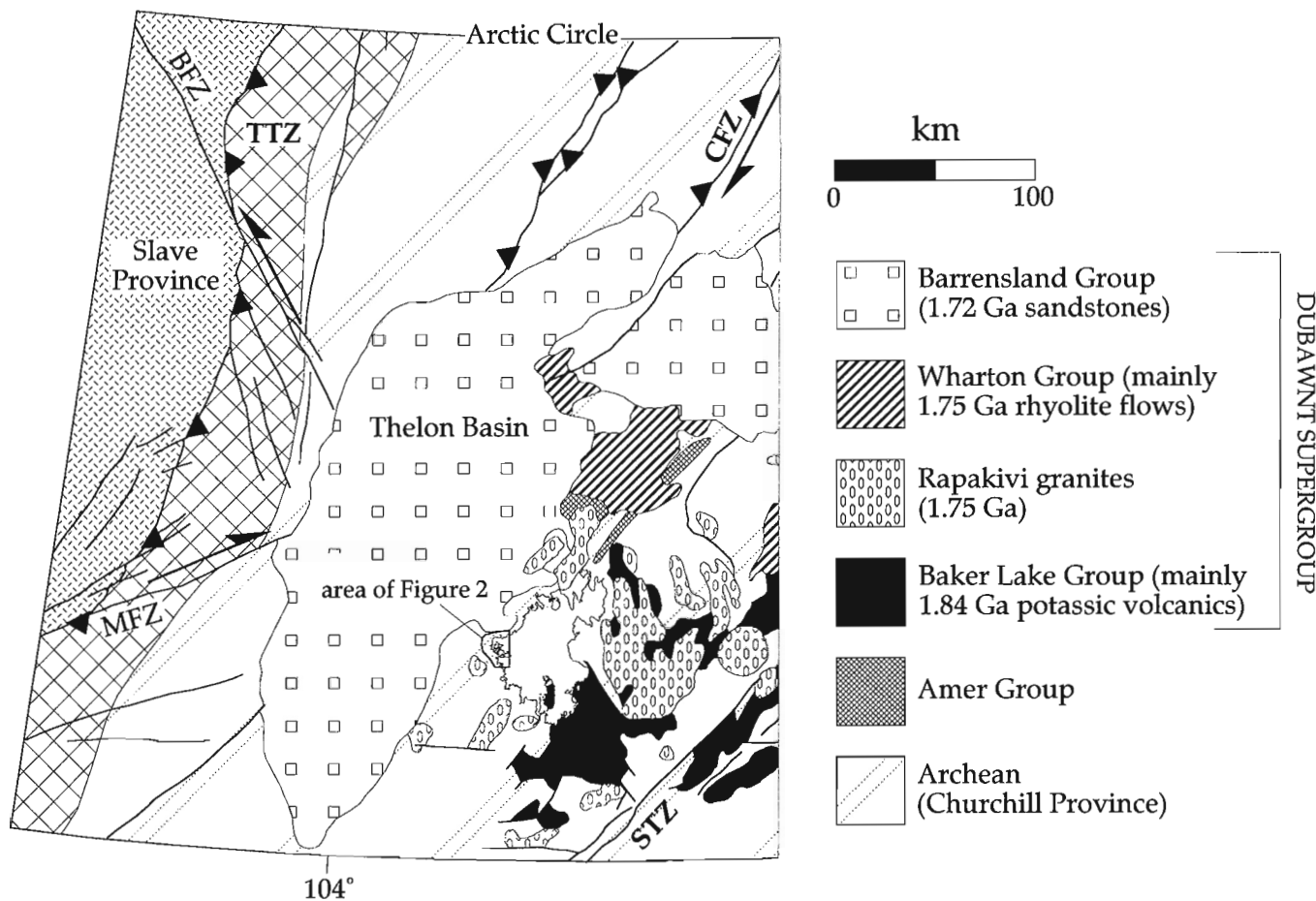
Previous reports summarizing the results of mapping at Dubawnt Lake (Fig. 1) have emphasized the 1.85-1.72 Ga volcanism and sedimentation of the Dubawnt Supergroup, and Archean (2.6 Ga) granitic plutonism (Peterson et al., 1989; Peterson and Rainbird, 1990; Rainbird and Peterson, 1990). Outcrops of these rocks are well exposed in the area. Less well exposed are older Archean rocks that are intruded by the granites, as well as deformed metasedimentary rocks assigned to the Lower Proterozoic Amer Group (quartzite and minor schists). Peterson (1992a) noted that quartzites of the Amer Group in the Dubawnt Lake area commonly display a strong south-southwest-plunging stretching lineation, developed at greenschist to lower amphibolite facies, which is also prominent in the underlying Archean gneisses. This lineation reflects a deformation event older than the very low-grade, brittle faulting which produced the basins of the lower Dubawnt Supergroup, formed during the Trans-Hudson orogeny (Hoffman and Peterson, 1991). Mapping at 1:50 000 scale of a large bay on the west side of Dubawnt Lake (NTS 65M/1, 65N/4) (Fig. 2) in July-August 1993 has clarified: (1) the style and intensity of Proterozoic, pre-Dubawnt Supergroup deformation, (2) the intrusive mechanisms and sequences of

the voluminous 2.6 Ga granitoid suite (the Snow Island intrusive suite), and (3) the nature of the pre-2.6 Ga metasedimentary rocks.

## DESCRIPTION OF THE AREA

The geology of western Dubawnt Lake was first described by Tyrrell (1897), who recognized "Athabasca-type" sandstones (the Thelon Formation) overlying Archean gneisses. Reconnaissance mapping during Operation Thelon (Wright, 1967) identified the Archean metasedimentary unit in the present field area (Fig. 2), subdivided the Archean intrusive suite, and defined the Dubawnt Group (redefined as the Dubawnt Supergroup by Gall et al., 1992). Donaldson (1965, 1969) obtained sedimentological data on the Thelon Formation and the underlying paleosol. The Thelon Basin, which covers the intersection of the Mackenzie and Bathurst fault systems west of Dubawnt Lake, outcrops near the western shore of Dubawnt Lake and at the north end of the map area.

Excellent shoreline access is available in the field area during the short ice-free interval, although caution is needed in many of the shallow inlets. Outcrop varies from excellent in the north, to poor or nonexistent in the south. Poor outcrop



**Figure 1.** Location of Dubawnt Lake (grey) and the map area. TTZ=Thelon tectonic zone; BFZ, MFZ, CFZ=Bathurst, Mackenzie, and Chantry fault zones; STZ=Snowbird tectonic zone.



here and elsewhere in the Dubawnt Lake area commonly coincides with Archean leucogranite or Nueltin suite granite (ca. 1.75 Ga), both of which are medium grained rocks which break up into boulder fields.

## DESCRIPTION OF THE ROCK UNITS

### *Pre-2.6 Ga metasedimentary rocks*

The 1:500 000 geology compilation by Eade (1981) shows that the Archean metasedimentary belt is surrounded on all sides by the Snow Island intrusive suite. This study divides the metasedimentary rocks into two mappable units (Fig. 2). The biotite schists, consisting of biotite + quartz + feldspar  $\pm$  muscovite  $\pm$  garnet, are usually intensely deformed and migmatized. No aluminosilicate minerals were noted in the field. Many outcrops contain dismembered 10-cm bands of sulphide-facies iron-formation (now consisting of garnet + biotite + pyrite  $\pm$  quartz). The biotite schist can be subdivided locally into a muscovite-bearing variant, and thin bands of muscovite-rich, biotite-absent schist were noted. However, these proved impossible to trace out over any significant distance. The schists display a strong foliation, but no mineral lineation.

The second metasedimentary unit is a grey, psammitic to quartzofeldspathic gneiss which is never migmatized, and in which a foliation is usually difficult to discern due to the absence of phyllosilicates. Iron-formation is scarce in this unit, and is restricted to enclosed schistose bands. Within the metasomatic aureole of the leucogranite (below), this unit strongly resembles nonfoliated, fine grained granite. In the south half of the map area, this unit is host to a small body of chlorite-amphibolite schist which is probably of volcanic origin.

### *Snow Island intrusive suite*

The Snow Island suite is named after Snow Island (named by Tyrrell, 1897), in western Dubawnt Lake. Descriptions of individual lithologies in this suite are given by Peterson et al. (1989). The most voluminous rock types are a Kspar-megacrystic granite, dated by U-Pb (zircon) at 2605 Ma (LeCheminant and Roddick, 1991), and a biotite leucogranite, dated at  $2606 \pm 2$  Ma (C. Roddick, unpublished data). Field relations demonstrate that the leucogranite, which forms dykes crosscutting the megacrystic granite, must be the youngest member of the suite. The megacrystic granite intrudes biotite-hornblende diorite, which in turn intrudes rare bodies of cumulate peridotite (olivine + orthopyroxene + clinopyroxene + chromite). Thus, there was a mafic-to-felsic intrusive sequence within the Snow Island suite, which strongly resembles groups 2 and 3 of the 2.6 Ga granitoids of the Slave Province (Davis et al., in press).

Rocks of the Snow Island suite are commonly weakly deformed. The exceptions are: (1) a strong relict foliation is present in megacrystic granite and leucogranite adjacent to migmatized paragneiss, and (2) a strong mineral stretching lineation, and a weak to strong schistosity, are localized within thrust faults and shear zones which also affect the Amer Group. Mafic schlieren in megacrystic granite were

formerly interpreted as a result of mafic-felsic magma mingling (Peterson et al., 1989); however, the present work has shown that some of these may be melted, mafic gneisses. Much of the variation in the colour index of the megacrystic granite in the present field area is due to contamination by Fe-rich paragneisses or metavolcanic rocks.

### *Metasomatized gneisses*

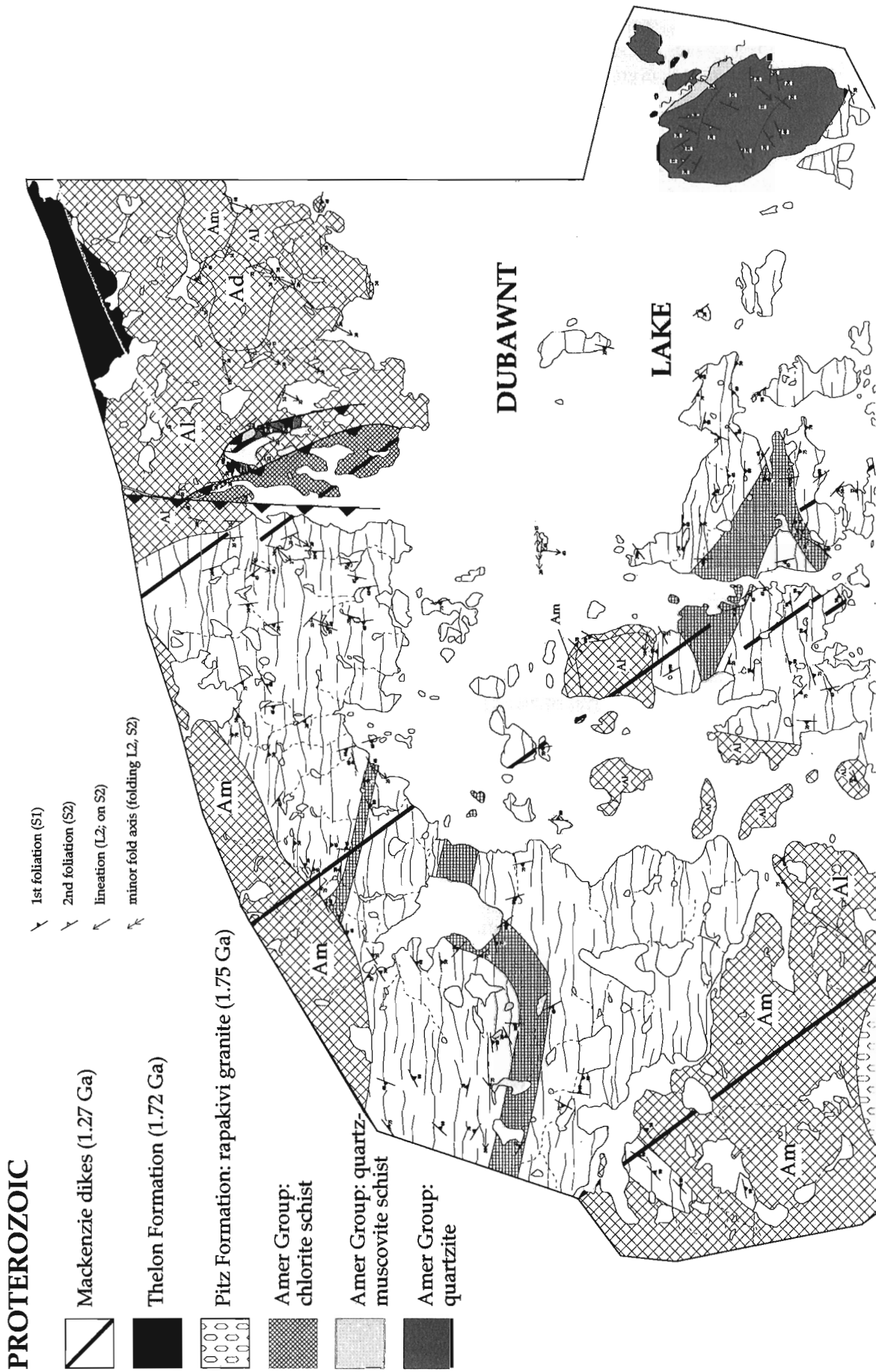
A striking contact phenomenon of the leucogranite is reminiscent of alkali metasomatism around silica-undersaturated alkaline complexes (see for example Peterson and Currie, 1994). Some Archean metasedimentary rocks (particularly the psammitic gneisses) near leucogranite bodies were observed to grade continuously, with no intervening migmatite zone, into fine grained granitic rocks bearing a relict foliation. These rocks were very difficult to distinguish from igneous leucogranite deformed in D2 shear zones, but were occasionally cut by sharp, nonfoliated leucogranite dykes which made their origin clear. The metasomatism did not involve partial melting or melt injection, and must have been mediated by subsolidus fluids. This phenomenon was not observed near the megacrystic granite, which is invariably surrounded by a migmatite aureole. Similar metasomatism, described as resembling fenitization around carbonatite intrusions, is associated with alkaline granites in Niger and Nigeria (Bowden et al., 1987).

### *Amer Group*

The term Amer Group was first used by Heywood (1977) in reference to a belt of Aphebian metasedimentary and minor metavolcanic rocks near Amer Lake, in the northeastern Churchill Province. Patterson (1986) described the group as consisting mainly of orthoquartzite, quartz-muscovite schist, carbonate, and greenstone exposed in mostly southwest-trending synclinoria. The age constraints on the Amer Group are poor; it unconformably overlies Archean rocks throughout the Churchill Province, and is older ( $>1.84$  Ga) than nondeformed rocks of the Dubawnt Supergroup. However, its lithostratigraphy and metamorphic grade are very similar to the Hurwitz Group (Aspler, 1989), which is older than 2111 Ma, the age of gabbro sills that intrude it (Heaman and LeCheminant, in press).

Orthoquartzites north of Dubawnt Lake were mapped as Amer Group by Operation Thelon (Wright, 1967). Identical quartzites occur on a 3-km long island at the east edge of the map area. The contact with Archean migmatite at the south end of the island is not well exposed and may be faulted. Bedding in the quartzites was usually obtained from pelitic and heavy mineral bands, and infrequently from truncated crossbeds. Minor exposures of quartz-muscovite schist occur on the northeast corner of this island, stratigraphically above the quartzite. This schist was also observed in stratigraphic contact with quartzite at the north end of the map area.

A dark green-brown weathering, slaty, chlorite-rich schist is in fault contact with quartzite in the north (Fig. 3, 4). It is assumed to be part of the Amer Group due to its low (greenschist)



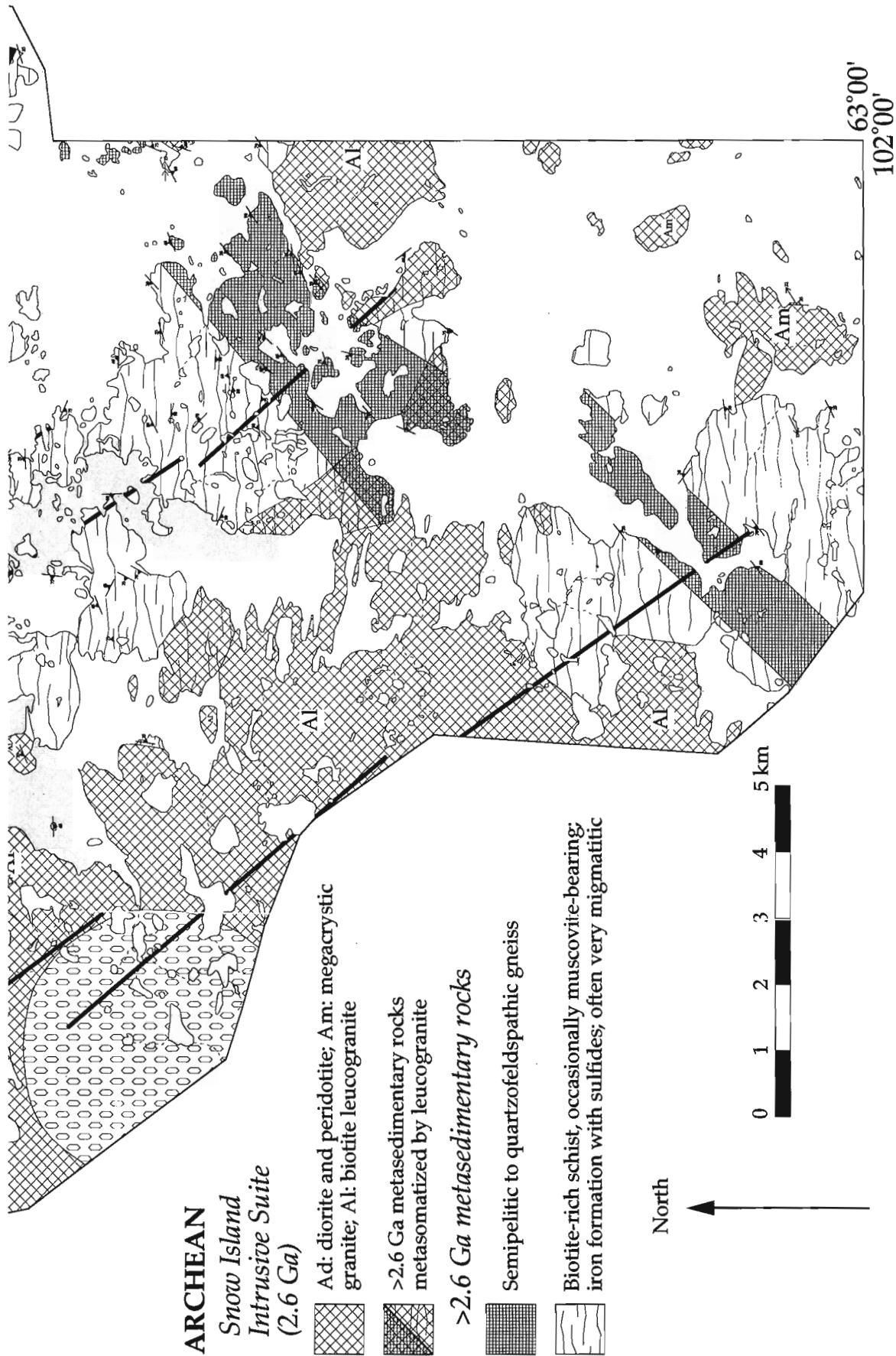


Figure 2. Geological map of west-central Dubawnt Lake (NTS 65M/1, N/4).

grade of metamorphism, and the presence of D2 structures (below). However, there is no stratigraphic control for the chlorite schist and it could even be older than the Amer Group.

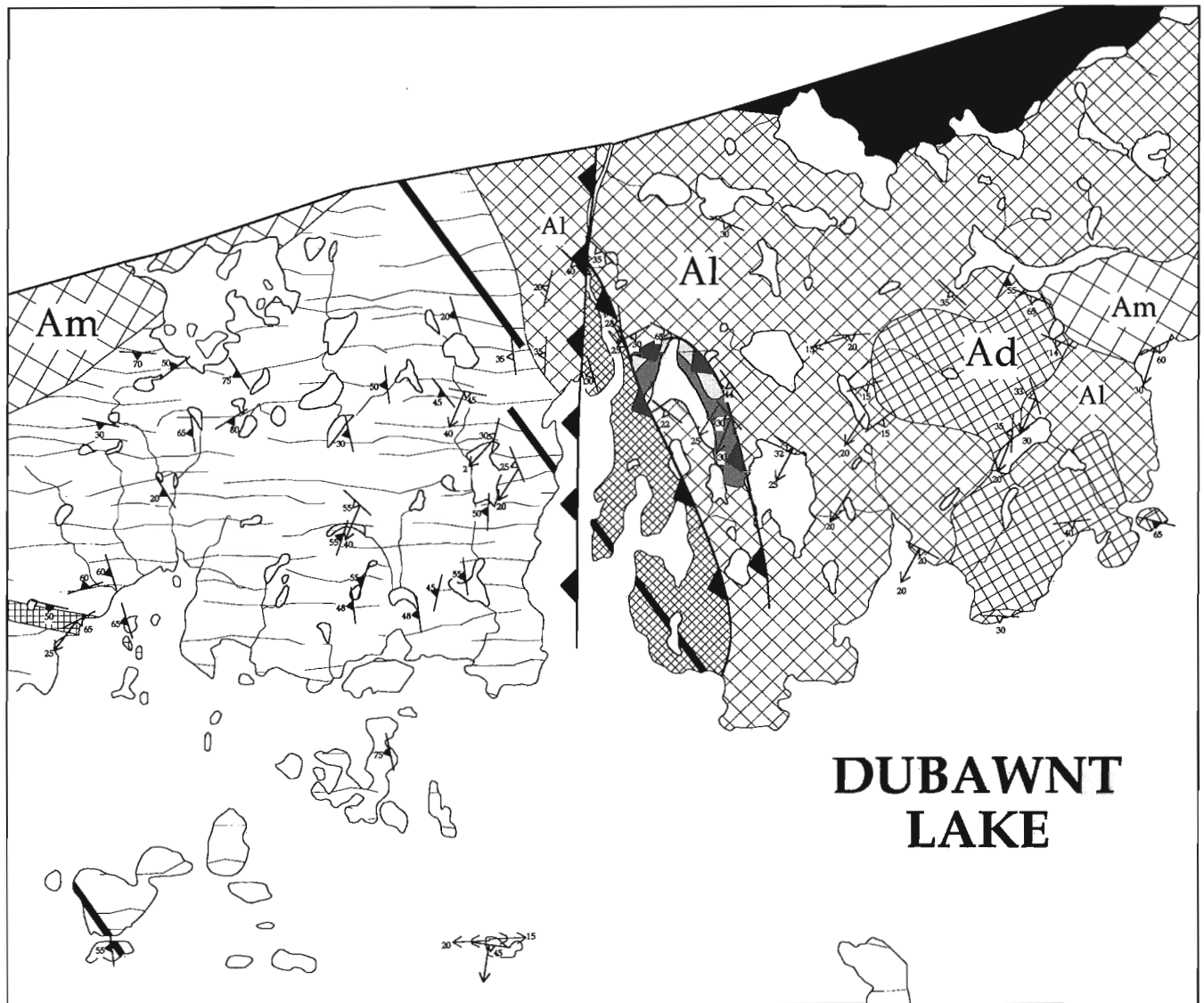
## DESCRIPTION OF THE STRUCTURES

### *Archean (D1) structures*

Three Archean phases of deformation were recognized: (1) a pre-2.6 Ga foliation (S1) and isoclinal folding in biotite schist, (2) regional deflection of S1 near granite plutons, and extreme small-scale deformation associated with migmatization, and (3) late to post-igneous extension. Because these may have been very closely spaced in time, all Archean deformation is considered as D1.

Bedding could rarely be determined in the Archean metasedimentary rocks. Kilometre-scale bands of psammitic gneiss generally parallel the regional schistosity, suggesting bedding has been rotated close to the foliation, but locally this was directly observed to be untrue. The bands probably have a more complex geometry than depicted in Figure 2, but are inadequately exposed for more detailed mapping.

The contacts between the Snow Island granites and the biotite schists typically consist of injection zones, with sills in migmatite grading into regions of contaminated granite bearing a relict foliation picked out by unmelted biotite. Partial melts of the schists are readily distinguished from the granites by the presence of muscovite (+Kspar+quartz). Locally, S1 is deflected parallel to the contacts of plutons (D1'), and strongly flattened septa of schist can occur between adjacent plutons.



**Figure 3.** North end of map area, showing the fault zones affecting Amer Group rocks. See Figure 2 for legend.

Evidence for late or post-igneous extension occurs as boudinaged and rotated dykes of leucogranite (Fig. 5) and shear bands in the schists (D1''). No apparent retrograde metamorphism accompanied formation of these minor structures, and they are considered to have formed very shortly after peak metamorphism.

### *Proterozoic (D2, D3) structures*

A strong, shallowly south-southwest-plunging mineral lineation (L2) is present in Amer Group and older rocks along much of the west shore of Dubawnt Lake north of the map area (Peterson et al., 1989). The metamorphic grade of this deformation is upper greenschist/lower amphibolite facies, as indicated by staurolite + biotite in Fe-rich semipelitic bands of Amer quartzite, and retrograde chlorite + biotite after biotite in leucogranite.

The L2 lineation was observed on a shallowly west-dipping schistosity (S2) at the north end of the map area (Fig. 4). The schistosity, present as muscovite-rich planes, is

developed in leucogranite and Amer quartzite, which are either imbricated or intensely infolded at the quartzite/granite contact. S2 is also present in a chlorite-rich schist (Fig. 4), exposed in a river gorge which follows a fault trace. Both L2 and S2 are measurable in the Archean rocks within a kilometre of the fault zone. The deformation zone is interpreted as a series of thrust faults (minimum of 3). The easternmost fault plane is folded at its north end (where it forms a tight syncline with its fold axis roughly parallel to L2) and cut off by the next fault to the west. Assuming the thrusts have not been overturned, the easternmost fault places younger (Amer Group) over older (leucogranite) rocks. This fault may represent a décollement beneath the Amer Group, with piggy-backing thrusts to the west transporting older Archean metasedimentary rocks over the Proterozoic cover rocks.

A strong L2 lineation in Archean schist is folded by east-west folds (amplitude about 20 cm) in the central part of the bay. These folds are themselves weakly transversely folded and plunge shallowly both east and west. This folding is assigned to D3.



**Figure 4.**

*Photo (facing northeast) of slaty chlorite schist showing S2 foliation; the outcrop is interpreted as the footwall of a thrust fault within the river. GSC 1993-224*

**Figure 5.**

*Dyke of 2.6 Ga leucogranite in migmatitic biotite schist, showing extension and rotation (followed by minor shortening); compass pointing north. GSC 1993-225*





## DISCUSSION

The deformational history and metamorphic grade of Amer Group rocks near Amer Lake suggested by Patterson (1986) is similar to that deduced in this study. Early thrusts and folds (her *D1* event; *D2* of this paper) were refolded by *D2* (*D3* in this paper), followed by extensional normal faulting (*D3*) (possibly corresponding to formation of lower Dubawnt Supergroup basins). The mean trend of Patterson's *D1* fold axes of 250°, plunging 12° at Amer Lake, is close to the pervasive southwest-plunging *L2* (230° at 20°) of the Dubawnt Lake area. However, the direction of thrusting deduced by Patterson was northwesterly. Kinematic data from southwest-trending *D2* shear zones in northwestern Dubawnt Lake indicate mainly dextral shear; some sinistral slip in conjugate northwest faults is indicated by offsets in magnetic anomalies (Peterson, 1992a, b). A plausible explanation for the structures at Dubawnt Lake is that oblique north-east-vergent thrusting accompanied east-west shortening and formation of the southwest-plunging extension lineation.

Previous workers (see Patterson, 1986, and references therein) generally associated deformation of the Amer Group with ca. 1900-1800 Ma convergent tectonics in the Trans-Hudson orogen. However, near 1850 Ma, deformation in the Dubawnt Lake area involved extension, subsidence, and brittle faulting at low metamorphic grade (Peterson, 1992b), inconsistent with the grade and structural style of *D2* metamorphism. A more likely scenario would associate *D2* with the Thelon orogeny, the Slave-Churchill collision which occurred from ca. 2.0-1.9 Ga (Theriault, 1992). Ductile deformation of this age range has been noted well into the central Churchill Province, notably in the Snowbird tectonic zone (Fig. 1). For example, southwest dextral shear at granulite facies affected syntectonic granites at ca. 1.9 Ga in the Wholdaia Lake area, 200 km south-southwest of Dubawnt Lake (S. Hanmer and R. Parrish, pers. comm.). The pre-1.84 Ga structures at Dubawnt Lake are consistent with a regional scenario involving east-west shortening, and dextral shear on northeast-southwest-trending faults. This scenario coincides well with the collision between the Slave and Churchill Provinces along the Great Slave Lake shear zone (Hanmer et al., 1992).

## REFERENCES

- Aspler, L.B.**  
1989: Sedimentology, structure, and economic geology of the Poorfish-Windy thrust-fold belt, Ennadai Lake area, District of Keewatin, and the shelf to foredeep transition in the foreland of Trans-Hudson Orogen; in *Current Research, Part C*; Geological Survey of Canada, Paper 89-1C, p. 143-155.
- Bowden, P., Black, R., Martin, R.F., Ike, E.C., Kinnaird, J.A., and Batchelor, R.A.**  
1987: Niger-Nigerian alkaline ring complexes: a classic example of African Phanerozoic anorogenic mid-plate magmatism; in *Alkaline Igneous Rocks*, (ed.) J.G. Fitton and B.G.J. Upton; Geological Society of London, Special Publication 30, p. 357-379.
- Davis, W.J., Fryer, B.J., and King, J.E.**  
in press: Geochemistry and evolution of late Archean plutonism and its significance to the tectonic development of the Slave craton; Precambrian Research.
- Donaldson, J.A.**  
1965: The Dubawnt Group, Districts of Keewatin and Mackenzie; Geological Survey of Canada, Paper 64-20.
- Donaldson, J.A. (cont.)**  
1969: Descriptive notes (with particular reference to the Late Proterozoic Dubawnt Group) to accompany a geological map of central Thelon Plain, Districts of Keewatin and Mackenzie; Geological Survey of Canada, Paper 68-49.
- Eade, K.E.**  
1981: Geology of Dubawnt Lake (NTS 65NW, NE) map area, District of Keewatin, N.W.T.; Geological Survey of Canada, Open File 771, geological map, scale 1:500 000 with legend.
- Gall, Q., Peterson, T.D., and Donaldson, J.A.**  
1992: Early Proterozoic stratigraphy of the Thelon and Baker Lake basins, District of Keewatin: a proposed revision; in *Current Research, Part C*; Geological Survey of Canada, Paper 92-1C, p. 19-29.
- Hanmer, S., Bowring, S., van Breemen, O., and Parrish, R.**  
1992: Great Slave Lake shear zone, NW Canada; mylonitic record of early Proterozoic continental convergence, collision and indentation; *Journal of Structural Geology*, v. 14, p. 757-773.
- Heaman, L.M. and LeCheminant, A.N.**  
in press: Paragenesis and U-Pb systematics of baddeleyite (ZrO<sub>2</sub>); *Chemical Geology*.
- Heywood, W.W.**  
1977: Geology of the Amer Lake map-area; in *Report of Activities, Part A*; Geological Survey of Canada, Paper 77-1A, p. 139-142.
- Hoffman, P.F. and Peterson, T.D.**  
1991: Tectonic evolution of the Keewatin Hinterland during the consolidation of Laurentia (1.8-1.6 Ga); *Geological Association of Canada, Abstracts with Program*, v. 16, A57.
- LeCheminant, A.N. and Roddick, J.C.**  
1991: U-Pb zircon evidence for widespread 2.6 Ga magmatism in the central District of Keewatin, NWT; in *Radiogenic Age and Isotopic Studies, Report 4*; Geological Survey of Canada, Paper 90-2, p. 91-99.
- Patterson, J.**  
1986: The Amer Belt: remnant of an Aphebian foreland fold and thrust belt; *Canadian Journal of Earth Sciences*, v. 23, p. 1012-2023.
- Peterson, T.D.**  
1992a: Geology, Dubawnt Lake; Geological Survey of Canada, Open File 2551.  
1992b: Early Proterozoic ultrapotassic volcanism of the Keewatin Hinterland, Canada; *Proceedings, 5th International Kimberlite Conference*; v. 1, Kimberlites, related rocks and mantle xenoliths, (ed.) H.O.A. Mayer and O.H. Leonardos; CPRM, Brasilia, p. 221-235.
- Peterson, T.D. and Currie, K.L.**  
1994: The Ice River complex; in *Current Research 1994-A*; Geological Survey of Canada, p. xx-yy.
- Peterson, T.D. and Rainbird, R.H.**  
1990: Tectonic and petrological significance of regional lamproite-minette volcanism in the Thelon and Trans-Hudson hinterlands, Northwest Territories; in *Current Research, Part C*; Geological Survey of Canada, Paper 90-1C, p. 69-79.
- Peterson, T.D., LeCheminant, A.N., and Rainbird, R.H.**  
1989: Preliminary report on the geology of northwestern Dubawnt Lake area, District of Keewatin, N.W.T.; in *Current Research, Part C*; Geological Survey of Canada, Paper 89-1C, p. 173-183.
- Rainbird, R.H. and Peterson, T.D.**  
1990: Physical volcanology and sedimentology of lower Dubawnt Group strata, Dubawnt Lake, District of Keewatin, N.W.T.; in *Current Research, Part C*; Geological Survey of Canada, Paper 90-1C, p. 207-217.
- Theriault, R.J.**  
1992: Nd isotopic evolution of the Taltson Magmatic Zone, Northwest Territories, Canada: insights into Early Proterozoic accretion along the western margin of the Churchill Province; *Journal of Geology*, v. 4, p. 465-475.
- Tyrrell, J.B.**  
1897: Report on the Dubawnt, Kazan, and Ferguson rivers and the north-west coast of Hudson Bay and on two overland routes from Hudson Bay to Lake Winnipeg; Geological Survey of Canada, Annual Report 1897, v. 9, Part F, p. 1-218.
- Wright, G.M.**  
1967: Geology of the southeastern barren grounds, parts of the districts of Mackenzie and Keewatin; Geological Survey of Canada, Memoir 350.



# Geology of Archean and Proterozoic supracrustal rocks in the Otter and Ducker lakes area, southern District of Keewatin, Northwest Territories<sup>1</sup>

Lawrence B. Aspler<sup>2</sup>, Jeffrey R. Chiarenzelli<sup>3</sup>, Diana L. Ozarko<sup>4</sup>,  
and Kelli B. Powis<sup>5</sup>

Continental Geoscience Division

*Aspler, L.B., Chiarenzelli, J.R., Ozarko, D.L., and Powis, K.B., 1994: Geology of Archean and Proterozoic supracrustal rocks in the Otter and Ducker lakes area, southern District of Keewatin, Northwest Territories; in Current Research 1994-C; Geological Survey of Canada, p. 165-174.*

---

**Abstract:** The local stratigraphy of the Archean Henik Group, part of the Ennadai-Rankin greenstone belt, consists of a siliciclastic turbidite sequence and a sequence of interlayered mafic and felsic volcanic rocks with magnetite iron-formation-bearing turbidites. Both sequences are intruded by Archean granitic plutons. Early Proterozoic Hurwitz Group granulestone, subarkose and quartz arenite (Kinga Formation) were deposited in fluvial, eolian and lacustrine environments in a radially expanding intracontinental basin developed on Archean basement. The abrupt appearance of mudstone and arkose (Ameto Formation) is attributed to sudden basin deepening and marine flooding. Upper Hurwitz Group strata define an offlap sequence including a carbonate ramp (Watterson Formation), local lagoons (Ducker Formation semi-pelites) and a coastal facies (Tavani Formation subarkose with evaporite-bearing dolostone). Map patterns are controlled by the interference between basement-involved northwest- and east-trending D1 folds and antithetic thrusts and northeast- and north-trending D2 folds.

**Résumé :** La stratigraphie locale du Groupe de Henik de l'Archéen, qui fait partie de la ceinture de roches vertes d'Ennadai-Rankin, est définie par une séquence de turbidites silicoclastiques et une séquence de roches volcaniques mafiques et felsiques interstratifiées contenant des turbidites renfermant des formations de fer à magnétite. Les deux séquences sont recoupées par des plutons granitiques de l'Archéen. Un granulestone, un grès arkosique et une quartzarénite (Formation de Kinga) du Groupe de Hurwitz du Protérozoïque inférieur se sont déposés dans des milieux fluviaux, éoliens et lacustres dans un bassin intracontinental à expansion radiale formé sur un socle archéen. L'apparition rapide de mudstone et d'arkose (Formation d'Ameto) est attribuée à un approfondissement soudain du bassin et à une crue marine. Les couches de la partie supérieure du Groupe de Hurwitz définissent une séquence de progradation incluant une rampe carbonatée (Formation de Watterson), des lagunes locales (semi-pélites de la Formation de Ducker) et un faciès littoral (subarkose avec dolomie à minéraux évaporitiques de la Formation de Tavani). La configuration des unités sur la carte est le produit d'une interférence entre les plis D1 de direction nord-ouest et est et des chevauchements antithétiques affectant le socle et les plis D2 de direction nord-est et nord.

---

<sup>1</sup> Contribution to Canada-Northwest Territories Mineral Initiative (1991-1996), an initiative under the Canada-Northwest Territories Economic Development Cooperation Agreement.

<sup>2</sup> 23 Newton Street, Ottawa, Ontario K1S 2S6

<sup>3</sup> 5339 Brick Schoolhouse Road, North Rose, New York, USA 14516

<sup>4</sup> Carleton University, Ottawa, Ontario K1S 5B6

<sup>5</sup> Department of Geology, University of Ottawa, Ottawa, Ontario K1N 6N5

## INTRODUCTION

This paper summarizes the initial results of 1:50 000-scale mapping in the Otter and Ducker lakes area (Fig. 1, Table 1). It extends work south from Bray and Montgomery lakes (Aspler et al., 1992) and represents the continuation of a project designed to better understand Archean and Proterozoic supracrustal rocks in the south-central District of Keewatin, with a focus on the stratigraphy of the Henik Group (Archean, part of the Ennadai-Rankin greenstone belt), the stratigraphy, depositional setting, original geometry and tectonic significance of the Hurwitz Group (Early Proterozoic), the structure

of the Hurwitz Group and the extent to which Archean rocks were affected by Proterozoic deformation (Aspler et al., 1989; 1993a; Aspler and Bursey, 1990). Results of mapping in the Watterson Lake area 75 km to the west, also completed in 1993, are reported elsewhere (Aspler et al., 1993c).

## HENIK GROUP

The Henik Group is inferred to be Archean on the basis of U-Pb zircon ages reported from other parts of the Ennadai-Rankin greenstone belt: Tavani area (2660-2680 Ma, Park

**Table 1.** Description and preliminary interpretation of map units, Otter-Ducker lakes area.

UNIT		DESCRIPTION	COMMENT/INTERPRETATION	
Mackenzie Diabase		Northwest-trending diabase dykes, non-foliated, unmetamorphosed	1267+/- 2 Ma baddeleyite: LeCheminant and Heaman, 1989	
GROUP	GABBRO HG	Discontinuous gabbro sills; coarse-grained, poikilitic. Local crude layering concordant with bedding in adjacent units. Chloritic shear zones common. Typically within Ameto Formation; locally within Watterson Formation or at Watterson-Ducker contact. In Watterson Lake area, contain Ameto Formation xenoliths that display sharp, angular borders (Aspler et al. 1993 c).	Evidence of injection pre- Hurwitz Group lithification or of multiple injection episodes is lacking; pre folding of Hurwitz Group. Baddeleyite 2094 +26/-17 Ma (Patterson and Heaman, 1991); 2111+/- 0.6 Ma (Heaman and LeCheminant in press).	
	TAVANI FORMATION	HT3	Microbial laminated dolostone with metre-scale interbeds consisting of arkose to mudrock fining-upward sequences	Marine flooding of coastal plain; development of carbonate flats; extreme desiccation. Enterolithic folds likely from gypsum to anhydrite transformation; breccias from solution collapse.
		HT2	In structural depression north of Ducker Lake, interbedded microbial laminated and stromatolitic dolostone; subarkose and mudrock. Abundant gypsum pseudomorphs to 3 cm; local salt hoppers (see Fig. 3 in Miller and Reading, 1993). Common intraformational breccia, with m-scale dolostone clasts; enterolithic folds (Fig. 6).	
		HT1	Tan and grey weathering subarkose, local parallel and cross-stratified heavy mineral bands; rare interbeds of green shale and mudchip breccia.	
	DUCKER FM HD	Discontinuous unit with cm to dm-scale fining-upward cycles of grey and tan arkose to blue argillite (Fig. 5); discrete beds of arkose with parallel-stratification. Dm-m-scale interbeds of orange microbial laminate at base. Forms wedges with abrupt thickness changes; where absent, Watterson passes directly and conformably to Tavani.	Local lagoons between Tavani coastal plain and Watterson carbonate ramp. Below wave-base mass flows alternating with arkose sheetfloods and algal mounds.	
	WATTERSON FORMATION	HW3	Orange weathering microbial laminated dolostone; local m-scale siltstone to mudstone fining upward sequences.	Intertidal to supratidal carbonate ramp
		HW2	Mixed siliciclastic/carbonate unit in which siltstone to mudstone fining-upward sequences are predominant (typically 80%). Brown massive and microbial laminated dolostone forms cm-dm-scale interbeds. In northern and eastern part of map area, pelite-rich W2 is absent and the Watterson Formation forms a single unit.	Below wave base mass flows alternating with subtidal carbonate flats.
		HW1	Rose, flesh and orange stromatolitic and microbial laminated dolostone; local intraclastic breccia. Stromatolites close, laterally-linked, bulbous to nodular hemispheroids (Fig. 4). Mixed carbonate and siliciclastic intervals of grey arkose with angular carbonate intraclasts grading to orange microbial laminate; arkose to slate fining-upward sequences interbedded with orange microbial laminate.	Intertidal to supratidal carbonate ramp; tidal channel breccias. Punctuated (storm?) and facies mixing of arkose (see Mount, 1984); below wave base mass flows alternating with shallow subtidal to intertidal carbonate flats.
	AMETO FM HA	At base: red, blue, green slate with mm-cm-scale parallel-stratified arkose. Up-section: cm-dm-scale arkose to slate fining-upward cycles. At top: 0.1-2m microbial laminates.	Below wave-base sedimentation interrupted by turbidity currents; shoaling-upward to Watterson carbonate ramp.	
	KINGA FM	Hawk Hill Mbr HKh	Discontinuous unit of bedded white chert, maroon chert and chert breccia conformably between the Whiterock Member and Ameto Formation. Discordant hematitic breccias at top of Whiterock Member.	Previously considered silcretes; re-interpreted as sinters formed by surface discharge of hot springs (Aspler et al., 1992)
Whiterock Mbr HKw		Supermature quartz arenite. Lower part of section commonly massive, upper 200 m with ubiquitous wave ripples. Paleodepth calculations based on symmetric, vortex orbital ripples indicates depths of 2 cm to 2 m for the entire sequence (Aspler et al., in press).	Vast, hydrographically-open, tide-free, fresh-water lake or series of lakes.	
Maguse Mbr HKm		Maroon, pink, grey subarkose to quartz arenite; interbeds of white quartz arenite at top. Local black parallel and cross stratified heavy mineral bands. At base, pebbly sandstone and grit with clasts of well rounded spherical white quartz, jasper, blue and grey chert.	High energy unchanneled sheet floods draining low-relief paleotopography. Conformable pinchout beneath Whiterock Member southeast of Otter Lake.	
Agd	Granodiorite	Well-foliated granodiorite intrusive into Henik Group. Border zone of Henik Group xenoliths in granodiorite and granodiorite sills within the Henik Group.	2512+/- 112 ma; Rb/Sr whole rock; Wanless and Eade, 1975.	
Agn	Gneissic diorite/Granodiorite	Diorite-granodiorite-feldspar/biotite gneiss. With garnet-bearing pegmatites that engulf gneissic xenoliths.	Deep-level equivalent to Agd; but possibility of being basement to Henik Group cannot be precluded	
HENIK GP	Avs	Volcanic/Sedimentary Sequence	Avsm: mafic flows (in part pillowed) mafic tuffs and gabbro sills. Avsf: feldspar-quartz tuffs; porphyries (in part sills?) Avsi: Dm-scale graded sandstone to mudstone and mm to cm-scale sandstone to magnetite iron formation rhythmites; abundant soft sediment deformation structures (Fig. 2). Silimanite and garnet-bearing near Kognak River.	
	As	Sedimentary Sequence	Massive sandstone and dm-m-scale sandstone to mudstone fining-upward sequences (Fig. 3)	

and Ralser, 1991); Kaminak Lake ( $2697 \pm 14$ ;  $2692 \pm 1$  Ma, Mortensen and Thorpe, 1987;  $2681 \pm 3$  Ma, Patterson and Heaman, 1990); and northeastern Saskatchewan ( $2682 \pm 6$  Ma, Chiarenzelli and Macdonald, 1986,  $2708 \pm 3/2$  Ma, Delaney et al., 1990).

In the vicinity of Montgomery Lake, a ca. 11 km thick section of Henik Group supracrustal rocks is exposed in a northeast-dipping homocline. The lowest sub-unit, a sequence of interlayered mafic and felsic volcanic, volcanoclastic and siliciclastic rocks (unit **A1**, Aspler et al., 1992) was traced south into the present map area (unit **Avs**, Table 1; Fig. 1). Near the base of the unit, mafic volcanic rocks, in part pillowed, are predominant. Up section are lenses of magnetite iron-formation-bearing turbidites (Fig. 2) and, toward the top, magnetite-jasper iron-formation. The number and thickness of iron-formation-bearing lenses diminishes southward such that at the Kognak River, iron-formation-bearing turbidites form a single 50-metre-thick bed within felsic and mafic tuffs. Overlying unit **Avs** in the Montgomery Lake area is a unit of jasper-white chert-magnetite iron-formation and quartz-eye tuff that lacks the siliciclastic and mafic rocks characteristic of unit **Avs** (unit **A2** of Aspler et al., 1992). This unit appears to pinch out southward into the present map area. South of the Kognak River, a unit of massive sandstone and decimetre- to metre-scale sandstone to mudstone fining-upward sequences underlies unit **Avs** (unit **As**, Table 1; Fig. 3). Previously we speculated that lenses of rhyolite and rhyolite breccia exposed on the northwest side of the Padlei belt were part of unit **A1** (unit **As**, this paper; Aspler et al., 1992, 1993a). Similar rocks (Fig. 2A) were found within unit **A1** during a reconnaissance traverse across the centre of the large east-trending basement-cored anticline between Montgomery and North Henik lakes (Eade, 1974) lending support to this suggestion.

South of the Kognak River the Henik Group is intruded by a well-foliated granodiorite pluton (unit **Agd**, Fig. 1). The pluton is assumed to be co-magmatic with similar bodies exposed northeast of the Henik lakes that have a Rb-Sr whole rock age of  $2512 \pm 112$  Ma (Wanless and Eade, 1975). Large granodiorite sills intrude the Henik Group close to the contact with the pluton; at the margins of the pluton are abundant Henik Group xenoliths up to several metres across. Northeast of the Kognak River is a dioritic-granodioritic-feldspar/biotite gneiss body with garnet-bearing pegmatites that engulf gneissic xenoliths (map unit **Agn**). Large areas of overburden obscure contact relationships with the Henik Group. We tentatively suggest that this unit is a deep-level equivalent to unit **Agd** although we cannot rule out that it may represent basement to the Henik Group emplaced along faults.

## HURWITZ GROUP

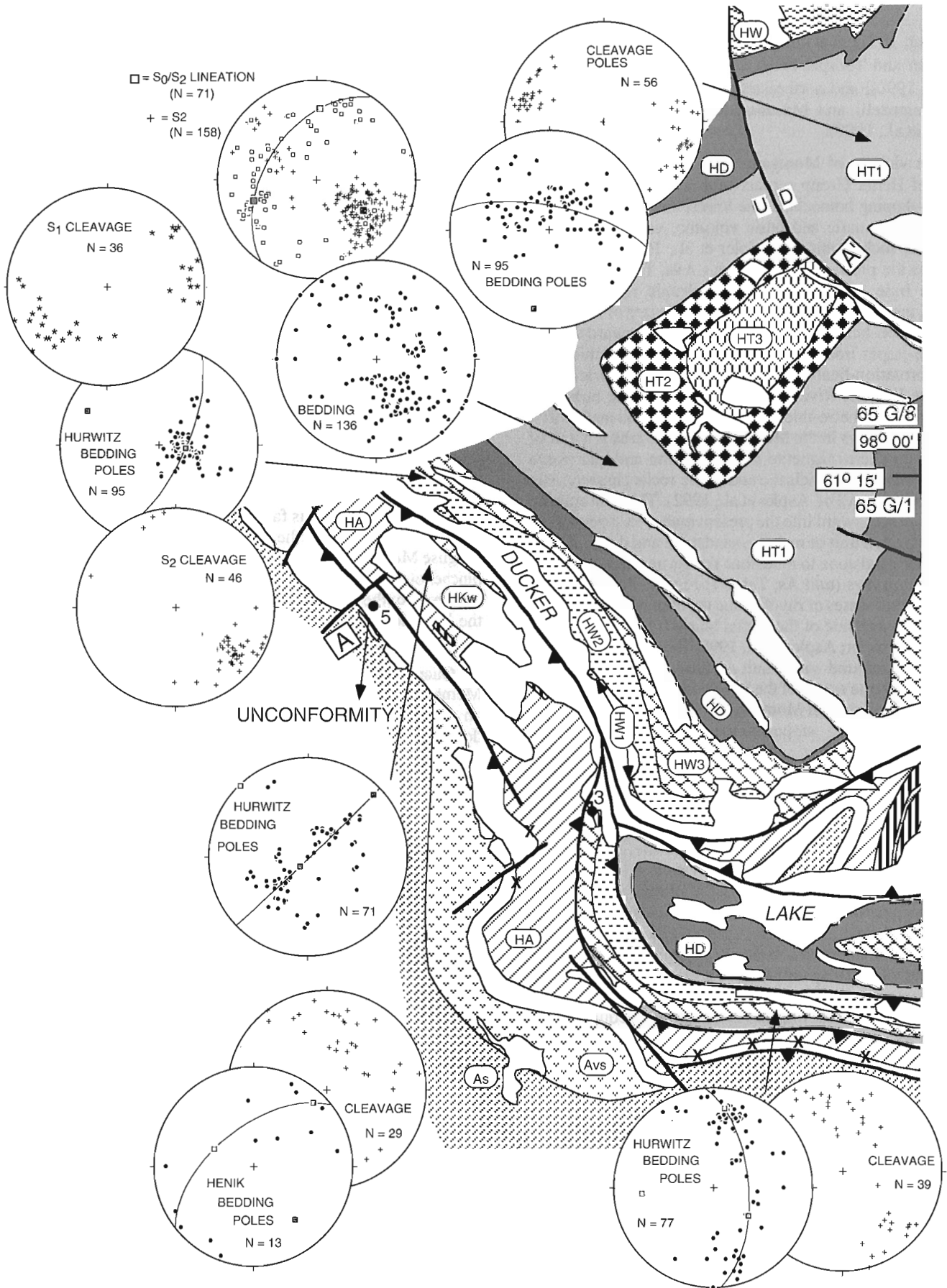
The Early Proterozoic Hurwitz Group is preserved in a north-east-trending belt of outliers that represent the remnants of a large intracratonic basin thought to have formed due to compressive intraplate stress arising from the ca. pre-2.1 Ga convergence of the Buffalo Head terrane (Ross et al., 1991) with the western margin of the Churchill Province (Fig. 1; Aspler et al., 1993a). It unconformably overlies the Archean

supracrustal and plutonic rocks. Close coincidence between rocks of the Ennadai-Rankin greenstone belt and the Hurwitz Group may indicate that initiation of basin subsidence was due to structural reactivation of Archean basins during the Proterozoic, with stress-induced viscosity decreases in the lower crust allowing the relatively high-density Archean rocks to sink (uncompensated excess mass in the upper crust; see de Rito et al., 1983; Howell and van der Pluijm, 1990; Shaw et al., 1991).

Lower Hurwitz Group strata are arranged in a conformable onlap sequence of radial basin expansion. The Maguse Member is the lowest unit exposed in the present map area (Table 1). The unconformity between the Henik Group and the Maguse Member is exposed southwest of Ducker Lake (65 G/1; UTM: 386867; Fig. 1). Like other examples of the sub-Hurwitz unconformity, the contact is sharp and lacks features indicative of a paleosol (Aspler et al., 1992, 1993a). Bell (1970a, b; 1971) originally defined the Maguse Member as a distinctive sequence of varicoloured subarkose, quartz arenite, granulestone and conglomerate at the base of the Kinga Formation in the Henik Lakes (east half) map sheet. The present study has shown the Maguse Member to be a useful regional marker as far west as Watterson Lake (Aspler et al., 1993c). North of the map area, in The Grey Hills, the Maguse Member is about 320 m thick. It thins southward and pinches out conformably beneath quartz arenite of the Whiterock Member southeast of Otter Lake (Fig. 1); farther to the west the Maguse Member is represented by rare lenses less than 5 m thick.

Quantitative analysis of wave-ripples within the Whiterock Member indicate average water depths of 2 cm to 2 m over an area of about 100 000 km<sup>2</sup>. The Whiterock Member was deposited in a large, hydrographically open, tide-free lake or series of lakes that overlapped fluvial and eolian deposits of the Maguse Member within a low relief continental depression (Aspler et al., in press). Several new exposures of Hawk Hill Member chert and chert breccia, likely sinter deposits (Aspler et al., 1992) were mapped as thin (<10 m) discontinuous lenses above the Whiterock Member east and south of Otter Lake (Fig. 1).

The upper Hurwitz Group stratigraphy defines a marine to terrestrial offlap sequence. The abrupt change from shallow lacustrine sedimentation of Whiterock Member quartz arenites to deep water mudrock and arkose of the Ameto Formation is attributed to sudden basin deepening induced by intraplate stress (see Cloetingh, 1991) and marine waters flooding through gaps in basement arches. This may be analogous to Lake Chad Basin (Burke, 1976) in which a modest rise in sea level would cause marine waters to breach the discontinuous ring of uplifts that surround the basin, and cause a change from lacustrine to marine sedimentation even though the basin is ca. 500 km away from the Atlantic Ocean. With the source of quartz sand effectively cut off by drowning, the compositional maturity of arenites overlying the Whiterock Member decreased and carbonate rocks of the Watterson Formation accumulated on ramps that prograded away from low-relief arches. Accordingly, mudrocks of the Ameto Formation are considered a distal ramp facies, carbonate rocks of the Watterson Formation an inner ramp facies,



**Figure 1.** Simplified geological map Otter-Ducker lakes area (see Aspler et al., 1993b for details). Map units as in Table 1. See Figure 7 for structure sections. Stereonets are equal area, lower hemisphere projections. See Table 2 for analyses of numbered gossans. Index map after Hoffman (1990).

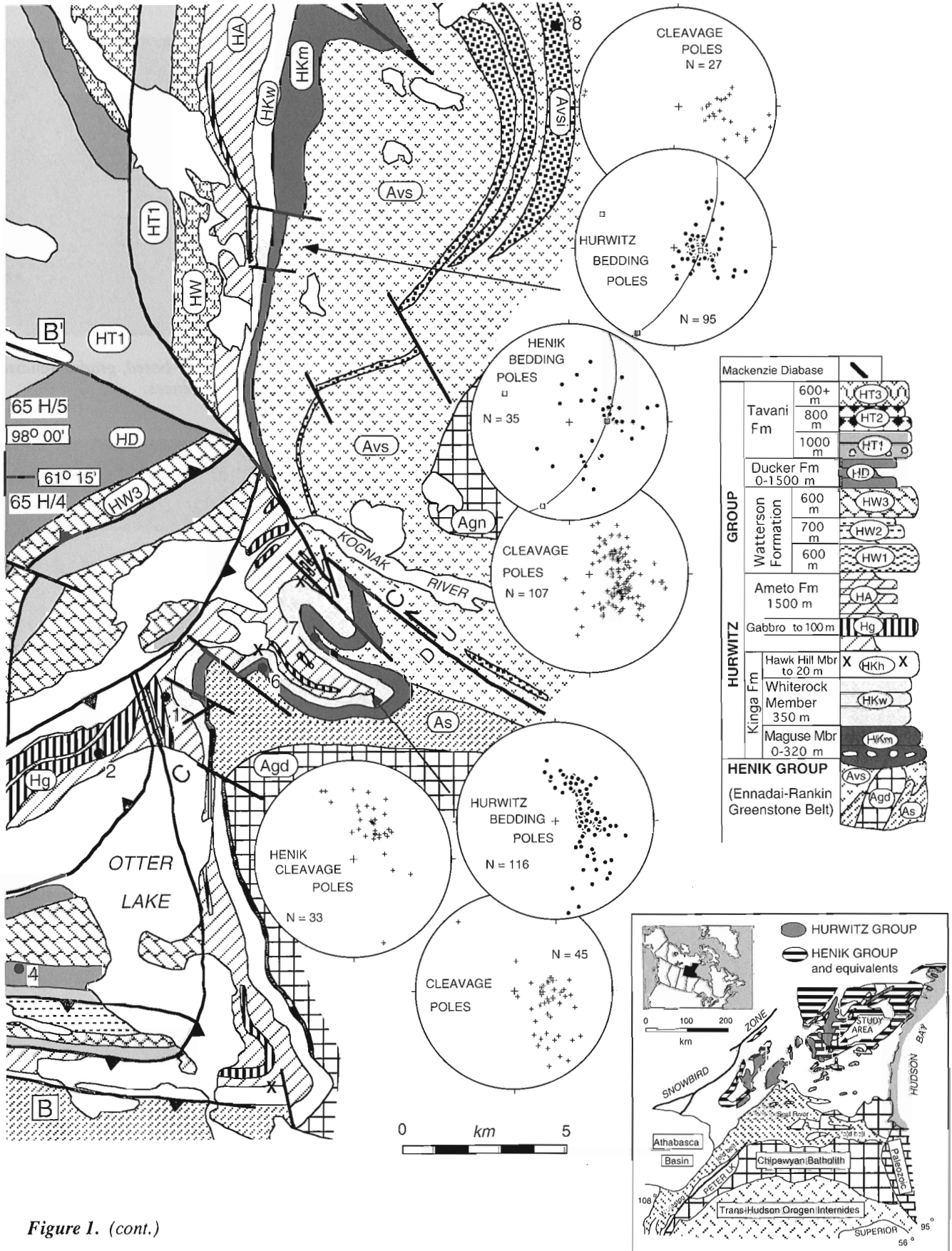
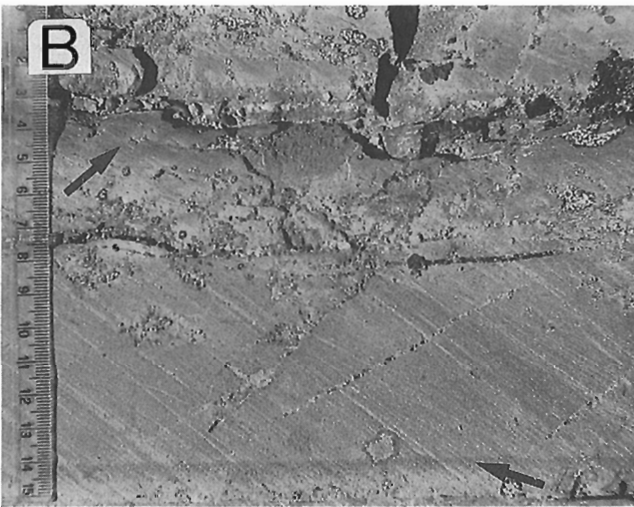
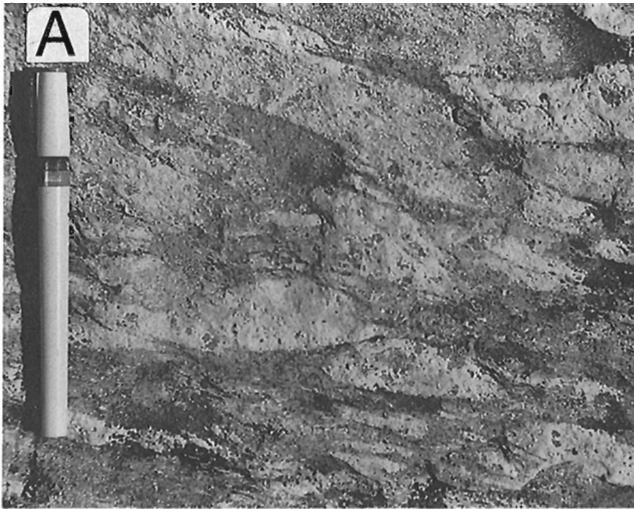
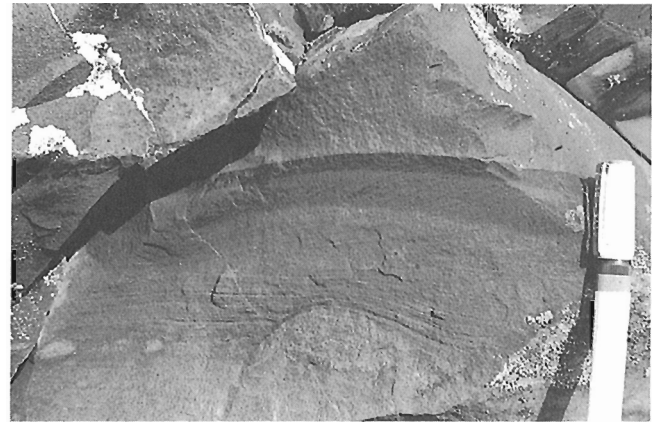


Figure 1. (cont.)

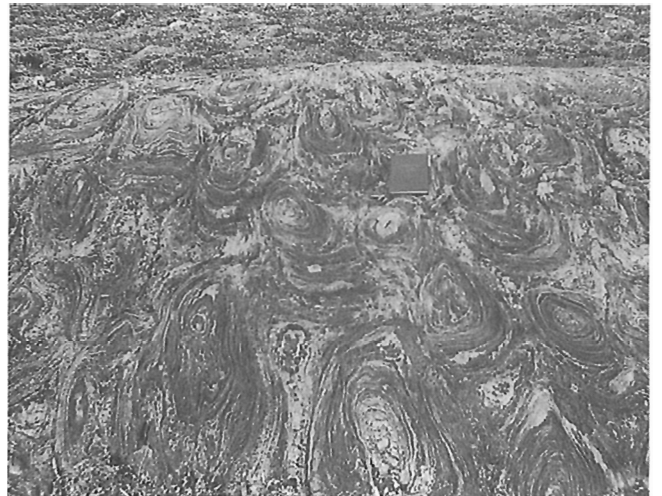




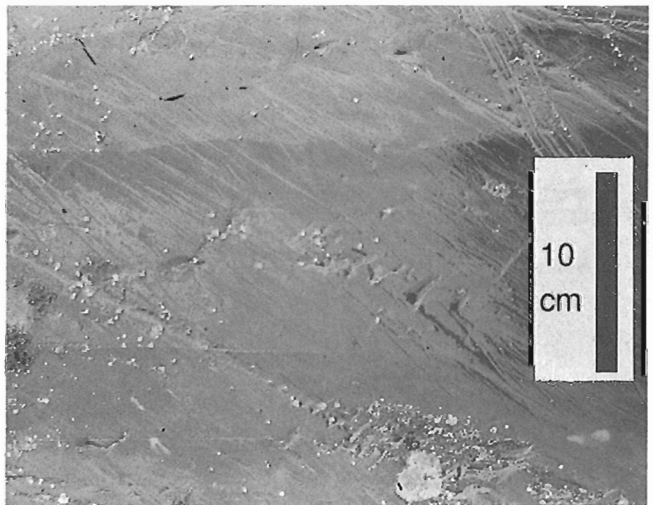
**Figure 2.** Map unit Avs: **A)** rhyolitic agglomerate; **B)** sandstone to mudstone fining-upward sequences; arrows point to magnetite-rich zones (unit Avsi); **C)** soft sediment folds/faults, magnetite and white chert iron-formation-bearing turbidites (unit Avsi).



**Figure 3.** Map unit As: sharp-based, graded sandstone to mudstone fining-upward sequences.



**Figure 4.** Watterson Formation bulbous stromatolites (bedding-plane view; stromatolites elongate along cleavage).



**Figure 5.** Ducker Formation; sharp-based, graded sandstone to mudstone fining-upward sequences.

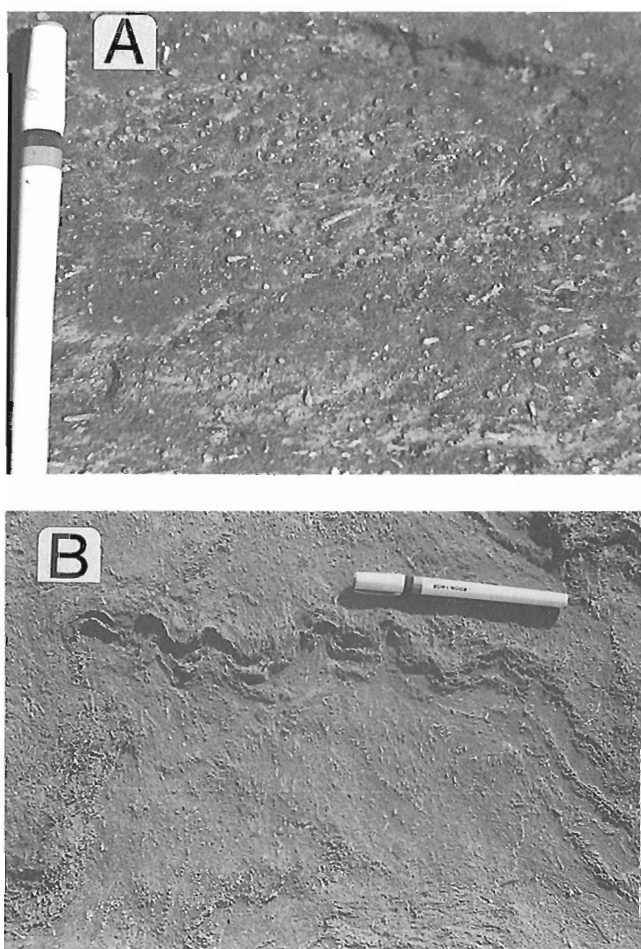


isolated lenses of semi-pelite ( $\pm$ carbonate) of the Ducker Formation local lagoons, and arkose and subarkose of the Tavani Formation a coastal sand complex.

In the northern and eastern part of the map area, the Watterson Formation (Fig. 4) forms a single unit of stromatolitic and microbial laminated dolostone, with mixed carbonate-siliciclastic interbeds and local intraformational breccia. In the southern part, a ca. 700 m thick semipelite ( $\pm$  carbonate) unit ( $HW_2$ ) separates the formation into lower ( $HW_1$ ) and upper ( $HW_3$ ) carbonate-rich members, similar to the type area at Watterson Lake (Eade and Chandler, 1975; Aspler et al., 1993c) and the Hawk Hill Lake area (Aspler and Bursey, 1990). One of the regional characteristics of the Ducker Formation is its lateral impersistence (Eade, 1974). Hence carbonate rocks of the Watterson Formation can pass directly upsection to subarkoses of the Tavani Formation (such as in the eastern part of the map area) or wedges of Ducker Formation semi-pelite (Fig. 5) may intervene (such as in the southern and

western parts of the map area). Although lenses of microbial laminate and intraformational conglomerate are found in the basal portions of the Tavani Formation, the remainder of the unit, as exposed elsewhere in the basin, lacks carbonate rocks. In the present map area, a structural depression preserves rocks at higher stratigraphic levels. These include microbial laminated and stromatolitic dolostones and mudrocks similar to those of the Watterson Formation, within which are evaporite pseudomorphs, enterolithic-like folds and intraformational breccias (solution collapse?) and conglomerates (map unit  $HT_2$ ; Fig. 6) and an overlying subunit of microbial laminated dolostone and mudrock (map unit  $HT_3$ ).

A set of discontinuous gabbro sills in the Hurwitz Group extend for a strike length of about 350 km, from the Tavani area southwest to the Watterson Lake area. The gabbros are typically within weak pelitic rocks of the Ameto Formation, but form local pods within the Watterson Formation. The stratigraphically highest sills are at the contact between the Watterson and Ducker formations in the Griffin Lake area (Aspler and Bursey, 1990) and at the contact between the Whiterock Member and Tavani Formation in the Tavani area (Park and Ralsler, 1991). In the present map area, the gabbros form multiple sheets, up to 100 m thick, within the Ameto Formation; on the west shore of Ducker Lake one small body is within the Watterson Formation (Fig. 1). The gabbros are folded with sedimentary rocks of the Hurwitz Group and thus were intruded before Hurwitz Group deformation. Bell (1968) suggested that the gabbros were coeval with the Happotiyik Member, a mafic volcanic unit exposed in the Kaminak Lake area, on the basis of possible sill-flow feeder relations. Yet the gabbros locally contain angular Ameto Formation xenoliths that display sharp, well-defined boundaries. Furthermore, thinly interbedded sandstones, siltstones and mudrocks adjacent to the gabbros lack soft sediment deformation structures; when wet, such rocks are highly susceptible to load or shock-induced strain. Hence we infer that the Hurwitz Group was well lithified before gabbro emplacement. It is uncertain if there was more than one episode of gabbro injection; baddeleyite ages of  $2094 \pm 26$ -17 Ma from the Kaminak Lake area (Patterson and Heaman, 1991) and of  $2111 \pm 0.6$  Ma from the Montgomery Lake area, 180 km to the southwest (Heaman and LeCheminant, in press) are consistent with a single episode.



**Figure 6.** Tavani Formation, map unit  $HT_2$ . **A)** Massive and microbial laminated dolostone with randomly oriented prismatic gypsum pseudomorphs (light-toned, weather in positive relief). **B)** Enterolithic-like folds in microbial laminated dolostone with siliciclastic sand-rich layers and scattered gypsum pseudomorphs.

## STRUCTURAL GEOLOGY

Similar to other Hurwitz Group outliers, the distribution rocks in the Otter-Ducker lakes area is controlled largely by Early Proterozoic dome and basin basement-cover infolds. In the western and southern part of the area, northwest- and east-trending  $D_1$  structures are predominant. Basement and cover are deformed together in a series of open, in part box-like, concentric folds and high angle thrusts (Fig. 7). The folds (in part overturned) and thrusts display an opposing vergence and define a geometry similar to the "pop-up" and "triangle" zones of Butler (1982; section B-B', Fig. 7). In the northern part of the map area, northeast- and north-trending  $D_2$  structures are predominant; northwest-trending  $D_1$  folds are refolded by open, concentric  $D_2$  folds with moderately to steeply dipping

axial surfaces; the variation in  $S_0/S_2$  lineations (Fig. 1) reflects the pre-existing  $D_1$  fold geometry. The structural depression cored by uppermost Tavani Formation rocks in the western part of the map area defines a Type I (Ramsay and Huber, 1987) interference pattern. Both sets of structures are cut by variably oriented minor oblique-slip faults, particularly around the periphery of the outlier where such faults likely reflect outer arc extension due to flexural slip folding. The Hurwitz Group was deformed before ca. 1.75 Ga, the age of

the Nueltin granite (U/Pb, Loveridge et al., 1988; cf. Rb/Sr, Wanless and Eade, 1975). How long before is uncertain; a preliminary metamorphic zircon determination of ca. 1.83 Ga (L. Heaman, pers. comm., 1992) suggests that deformation of the Hurwitz Group may be related to collisional events in Trans-Hudson Orogen, signifying a large time gap between sedimentation (pre- 2111 Ma; Heaman and LeCheminant, in press) and deformation.

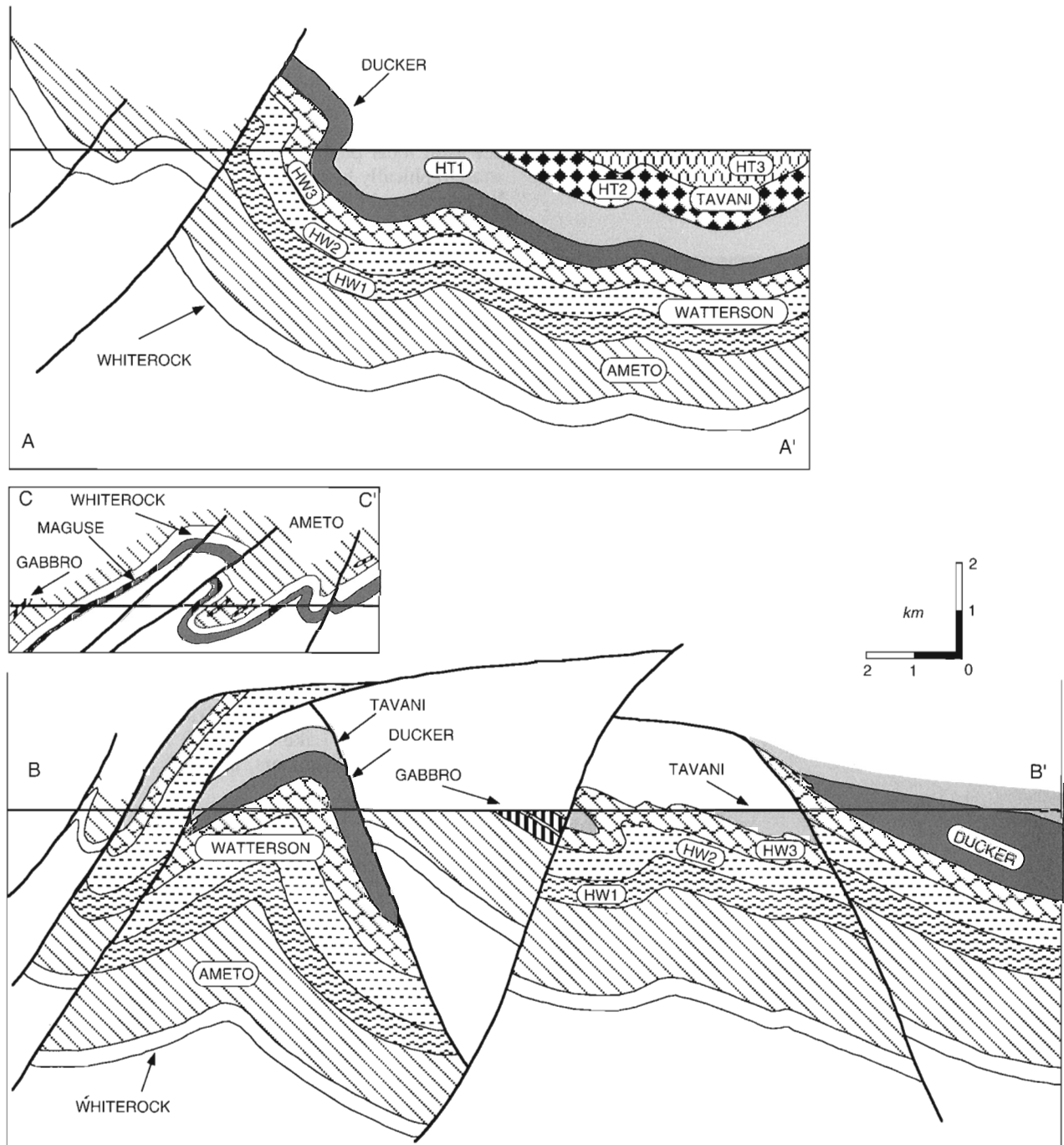


Figure 7. Structure sections; see Figure 1 for locations; Table 1 for unit descriptions.

**Table 2.** Geochemistry of grab samples. Gossan numbers are plotted in Figure 1. All analyses by X-Ray Assay Laboratories, Don Mills, Ontario.

			ELEMENT	Au	Co	Ni	Cu	Zn	As	Mo	Ag	Cd	Sb	W	Pb
			METHOD	NA	ICP	ICP	ICP	ICP	NA	ICP	ICP	ICP	NA	NA	ICP
			DETECTION LIMIT	5 ppb	1 ppm	1 ppm	.5 ppm	.5 ppm	2 ppm	1 ppm	.5 ppm	1 ppm	.5 ppm	2 ppm	2 ppm
GOSSAN	SAMPLE	UTM	LITHOLOGY / UNIT												
1	93-12-4B	65H/4; 578847	py/cpy quartz vein Hurwitz gabbro	13	5	8	3900	37.6	2	<1	3.2	2	<.5	<2	3
	93-12-4D		py/cpy quartz vein Hurwitz gabbro	190	4	<1	16600	80.7	6	<1	14.9	<1	1.5	<2	6
2	93-12-17A	65H/4; 564831	py/cpy quartz vein Hurwitz gabbro	9	4	11	1990	27.6	3	<1	2	2	<.5	2	5
3	93-37-1	65G/1; 447818	py in Hurwitz gabbro	8	70	86	26.6	14	7	<1	<0.5	<1	1.5	2	9
4	93-2-12	65H/4; 539774	py in Ducker arkose	36	26	141	48.5	66.4	13	<1	<0.5	<1	1.3	<2	<2
5	93-30-40	65G/1; 586875	py in Whiterock quartz arenite	43	23	16	53.6	2.5	30	<1	<.5	<1	<.5	2	4
6	93-13-30	65H/4; 605856	py in Maguse subarkose	380	<1	<1	47.4	<.5	3	<1	<.5	<1	7.9	13	<2
7	93-15-67A	65H/4; 623884	py in Maguse subarkose	29	1	<1	13	<.5	<2	106	<.5	<1	1.1	66	<2
8	93-42-13A	65H/5; 694034	sulphides in magnetite BIF	49	41	52	143	65.9	89	10	1.9	<1	9.4	2	39
	93-42-13B		sulphides in magnetite BIF	52	40	26	31.4	18.2	210	12	2.3	<1	23	<2	109
9	93-52-8	65H/12; 620234	py in mafic volcanic	16	26	33	972	37.3	<2	9	1	<1	<.5	<2	2
10	93-52-14	65H/12; 615245	py/cpy in rhyolitic agglomerate	9	<1	<1	102	6	170	2	1.3	<1	<.5	6	<2
11	93-52-21	65H/12; 610233	py in magnetite BIF	<5	46	34	28.6	11.7	24	<1	1.8	<1	5.1	2	43

On the east side of the map area, a major north- and northwest-trending, Proterozoic, east-side up, sinistral-oblique fault was traced for about 40 km, south from Bray Lake and across the Kognak River (Fig. 1). Archean rocks east of the fault are part of a moderately to steeply dipping package that extends south from Montgomery Lake (Aspler et al., 1992). The strike of this package follows the outline of the west-plunging, west-facing synclinorium defined by Hurwitz Group rocks centred at The Grey Hills, yet the Archean rocks are east-plunging and east-facing, indicating pre-Hurwitz Group tilting. Close to the Kognak River, the northeast trends of the Archean rocks deflect into coincidence with the fault. West of the fault, Archean rocks are tightly infolded with the Hurwitz Group (Fig. 7, section C-C').

Elsewhere around the margins of the outlier, cleavage trends in the Henik Group are broadly coincident with those of the Hurwitz Group, presumably due to both deflection of Archean cleavage during basement-cover infolding and to the generation of Proterozoic cleavage in the Archean rocks.

## ECONOMIC GEOLOGY

Mineral occurrences are plotted in Figure 1; UTM co-ordinates and available analyses are given in Table 2. The highest gold value in this study is from subarkoses of the Maguse Member that contain pyrite-quartz veinlets (380 ppb Au, Gossan 6). Quartz veins in Hurwitz gabbros display elevated gold (to 190 ppb Au; Gossan 1) and silver (14.9 ppm Ag; Gossan 1). One sample of Maguse Member (Gossan 7) yielded elevated Mo (106 ppm) and W (66 ppm).

## ACKNOWLEDGMENTS

This project is funded by the Canada-NWT Minerals Initiative 1991-1996. We appreciate the continued support and encouragement given by C.W. Jefferson and W.A. Padgham. Logistical support was from Treeline Lodge (Nueltin Lake); we thank Gary Gurke, Ingrid Brooks and Boyd Jackson for

expediting and radio contact, pilots Ron Last, Hap Bednarek and Richard Olson for efficient camp moves and set outs and B. Bental, T. Hip and T. Petty for their contribution. Critical comments by F.W. Chandler, C.W. Jefferson and A.N. LeCheminant helped to improve the manuscript.

## REFERENCES

- Aspler, L.B. and Bursey, T.L.  
1990: Stratigraphy, sedimentation, dome and basin basement-cover infolding and implications for gold in the Hurwitz Group, Hawk Hill-Griffin-Mountain Lakes area, District of Keewatin; in Current Research, Part C; Geological Survey of Canada, Paper 90-1C, p. 219-230.
- Aspler, L.B., Bursey, T.L., and LeCheminant, A.N.  
1992: Geology of the Henik, Montgomery Lake, and Hurwitz groups in the Bray-Mongomery-Ameto lakes area, southern District of Keewatin, Northwest Territories; in Current Research, Part C; Geological Survey of Canada, Paper 92-1C, p. 157-170.
- Aspler, L.B., Bursey, T.L., and Miller, A.R.  
1989: Sedimentology, structure and economic geology of the Poorfish-Windy thrust-fold belt, Ennadai Lake area, District of Keewatin, and the shelf to foreland transition in the foreland of Trans Hudson Orogen; in Current Research, Part C; Geological Survey of Canada, Paper 89-1C, p. 143-155.
- Aspler, L.B., Chiarenzelli, J.R., and Bursey, T.L.  
1993a: Archean and Proterozoic geology of the Padlei belt, District of Keewatin, Northwest Territories; in Current Research, Part C; Geological Survey of Canada, Paper 93-1C, p. 147-158.
- in press: Ripple marks in quartz arenites of the Hurwitz Group, Northwest Territories, Canada: Evidence for sedimentation in a vast, Early Proterozoic, shallow, fresh-water lake; *Journal of Sedimentary Petrology*.
- Aspler, L.B., Chiarenzelli, J.R., Ozarko, D.L., and Powis, K.B.  
1993b: Geological map of the Otter-Ducker lakes area, District of Keewatin, Northwest Territories; Geological Survey of Canada, Open File 2766, scale: 1:50 000.
- 1993c: Geological map of the Watterson Lake area, District of Keewatin, Northwest Territories; Geological Survey of Canada, Open File 2767; scale: 1:50 000.
- Bell, R.T.  
1968: Preliminary notes on the Proterozoic Hurwitz Group, Tavani (55K) and Kaminak Lake (55L) areas, District of Keewatin; Geological Survey of Canada, Paper 68-36, 17 p.
- 1970a: Preliminary notes on the Hurwitz Group, Padlei map area, Northwest Territories; Geological Survey of Canada, Paper 69-52, 13 p.

- Bell, R.T. (cont.)**  
 1970b: The Hurwitz Group—a prototype for deposition on metastable cratons; in A.J. Baer (ed.) Symposium on basin and geosynclines of the Canadian Shield; Geological Survey of Canada, Paper 70-40, p. 159-169.  
 1971: Geology of Henik lakes (east half) and Ferguson Lake (east half) map-areas, District of Keewatin; Geological Survey of Canada, Paper 70-61, 31 p.
- Burke, K.**  
 1976: The Chad Basin: An active intra-continental basin; *Tectonophysics*, v. 36, p. 197-206.
- Butler, R.W.H.**  
 1982: The terminology of structures in thrust belts; *Journal of Structural Geology*, v. 4, p. 239-245.
- Chiarenzelli, J.R. and Macdonald, R.**  
 1986: A U-Pb zircon date for the Ennadai Group; in Summary of Investigations 1986, Saskatchewan Geological Survey, Miscellaneous Report 86-4, p. 112-113.
- Cloetingh, S.**  
 1991: Tectonics and sea-level changes: a controversy?; in *Controversies in Modern Geology*, D.W. Muller, J.A. McKenzie, and H. Weissert (ed.); Academic Press, London, p. 249-277.
- Delaney, G.D., Heaman, L.M., Kamo, S., Parrish, R.R., Slimmon, W.L., and Reilly, B.A.**  
 1990: U-Pb sphene/zircon geochronological investigations; in Saskatchewan Geological Survey, Miscellaneous Report 90-4, p. 54-57.
- de Rito, R., Cozzarelli, F.A., and Hodge, D.S.**  
 1983: Mechanism of subsidence of ancient cratonic rift basins; *Tectonophysics*, v. 94, p. 141-168.
- Eade, K.E.**  
 1974: Geology of Kognak River area, District of Keewatin, Northwest Territories; Geological Survey of Canada, Memoir 377, 66 p.
- Eade, K.E. and Chandler, F.W.**  
 1975: Geology of Watterson Lake (west half) map-area, District of Keewatin; Geological Survey of Canada, Paper 74-64, 10 p.
- Heaman, L.M. and LeCheminant, A.N.**  
 in press: Paragenesis and U-Pb systematics of baddeleyite (ZrO<sub>2</sub>); *Chemical Geology*.
- Hoffman, P.F.**  
 1990: Subdivision of the Churchill Province and extent of the Trans-Hudson orogen; in *The Early Proterozoic Trans-Hudson Orogen of North America*, J.F. Lewry and M.R. Stauffer (ed.); Geological Association of Canada, Special Paper 37, p. 15-39.
- Howell, P.D. and van der Pluijm, B.A.**  
 1990: Early history of the Michigan Basin: subsidence and Appalachian tectonics; *Geology*, v. 18, p. 1195-1198.
- LeCheminant, A.N. and Heaman, L.M.**  
 1989: Mackenzie igneous events, Canada: Middle Proterozoic hotspot magmatism associated with ocean opening; *Earth and Planetary Science Letters*, v. 96, p. 38-48.
- Loveridge, W.D., Eade, K.E., and Sullivan, R.W.**  
 1988: Geochronological studies from Precambrian rocks from the southern District of Keewatin; Geological Survey of Canada, Paper 88-18, 36 p.
- Miller, A.R. and Reading, K.L.**  
 1993: Iron-formation, evaporite, and possible metallogenetic implications for the Lower Proterozoic Hurwitz Group, District of Keewatin, Northwest Territories; in *Current Research, Part C*; Geological Survey of Canada, Paper 93-1C, p. 179-185.
- Mortensen, J.K. and Thorpe, R.I.**  
 1987: U-Pb zircon ages of felsic volcanic rocks in the Kaminak Lake area, District of Keewatin; in *Radiogenic Age and Isotopic Studies, Report 1*; Geological Survey of Canada, Paper 87-2, p. 123-128.
- Mount, J.F.**  
 1984: Mixing of siliciclastic and carbonate sediments in shallow shelf environments; *Geology*, v. 12, p. 432-435.
- Patterson, J.G. and Heaman, L.M.**  
 1990: Geochronological constraints on the depositional age of the Hurwitz Group, N.W.T.; Geological Association of Canada, Program With Abstracts, v. 5, p. A102.  
 1991: New geochronologic limits on the depositional age of the Hurwitz Group, Trans-Hudson hinterland, Canada; *Geology*, v. 19, p. 1137-1140.
- Park, A.F. and Ralsler, S.**  
 1991: Structure of the early Proterozoic Hurwitz Group in the Tavani area, Keewatin, N.W.T.; *Canadian Journal of Earth Sciences*, v. 28, p. 1078-1095.
- Ramsay, J.G. and Huber, M.I.**  
 1987: *The techniques of modern structural geology, V. 2. Folds and Fractures*; Academic Press, London, 462 p.
- Ross, G.M., Parrish, R.R., Villeneuve, M.E., and Bowring, S.A.**  
 1991: Geophysics and geochronology of the crystalline basement of the Alberta Basin, western Canada; *Canadian Journal of Earth Sciences*, v. 28, p. 512-522.
- Shaw, R.D., Etheridge, M.A., and Lambeck, K.**  
 1991: Development of the Late Proterozoic to Mid-Paleozoic, intracratonic Amadeus Basin in central Australia: a key to understanding tectonic forces in plate interiors; *Tectonics*, v. 10, p. 688-721.
- Wanless, R.K. and Eade, K.E.**  
 1975: Geochronology of Archean and Proterozoic rocks in the southern District of Keewatin; *Canadian Journal of Earth Sciences*, v. 12, p. 95-114.

# Ice flow events in the Cormorant Lake- Wekusko Lake area, northern Manitoba<sup>1</sup>

Isabelle McMartin  
Terrain Sciences Division

*McMartin, I., 1994: Ice flow events in the Cormorant Lake-Wekusko Lake area, northern Manitoba; in Current Research 1994-C; Geological Survey of Canada, p. 175-182.*

---

**Abstract:** Surficial mapping in the Cormorant Lake-Wekusko Lake area indicates that numerous and complex ice flow events occurred near the Shield margin area. On the Shield and west of The Pas moraine, which represents a major glacial landform on the Paleozoic cover, the dominant ice flow trend is south-southwestward, and till composition reflects a northern provenance (Keewatin ice), closely related to the local bedrock. East of the moraine, major ice flow events trend westerly, and till composition indicates an eastern and distal provenance (Hudson ice). A major late readvance in glacial Lake Agassiz was recorded west of the moraine. Along the Shield margin east of the moraine, this readvance caused a confluent and parallel ice flow between the two lobes. These events were followed by minor readvances of Hudson ice in glacial Lake Agassiz and against Keewatin ice within a large ice-contact zone at the Shield edge.

**Résumé :** La cartographie des matériaux de surface dans la région des lacs Cormorant et Wekusko indique qu'il y a eu de nombreux écoulements glaciaires complexes près de la bordure du Bouclier. Sur le Bouclier et à l'ouest de la moraine de The Pas, qui est un important modelé glaciaire reposant sur les roches de couverture du Paléozoïque, la direction d'écoulement glaciaire prédominante est sud-sud-ouest; d'après sa composition, le till provient du nord (glaces du Keewatin) et est étroitement associé au substratum rocheux local. À l'est de la moraine, les écoulements glaciaires majeurs ont une direction ouest, et le till provient d'une source distale à l'est (glaces d'Hudson). Il y a des indications d'une réavancée majeure tardive dans le Lac glaciaire Agassiz à l'ouest de la moraine. En bordure du Bouclier à l'est de la moraine, cette réavancée a provoqué un écoulement glaciaire confluent et parallèle entre les deux lobes. Ces événements ont été suivis par des réavancées mineures des glaces d'Hudson dans le Lac glaciaire Agassiz et contre les glaces du Keewatin dans une vaste zone de contact glaciaire en bordure du Bouclier.

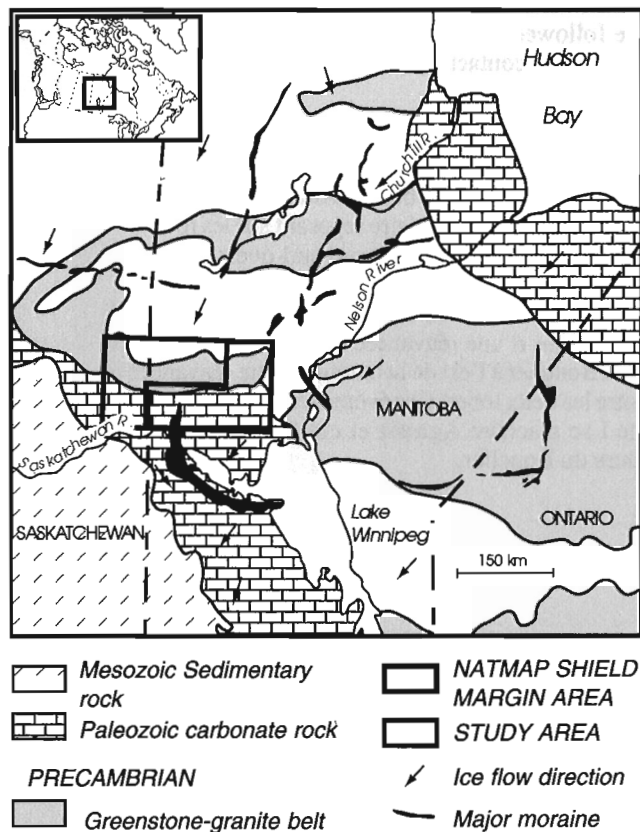
---

<sup>1</sup> Contribution to NATMAP Shield Margin Project

## INTRODUCTION

Quaternary geology investigations in the Cormorant Lake-Wekusko Lake area were initiated in 1991 under the NATMAP Shield Margin Project with the following objectives: (1) to map surficial deposits and compile maps at 1:100 000 scale in digital form, (2) to study the Quaternary stratigraphy and to interpret the paleoenvironmental history of the area, and (3) to systematically sample the drift. The project was designed to provide basic knowledge related to mineral exploration (mainly base metals, gold, and diamonds), environmental protection, and land use planning. This report outlines the glacial history of the central and eastern parts of the project area (Fig. 1).

The study area encompasses the Paleozoic/Precambrian contact near the Manitoba-Saskatchewan border (Fig. 1). The Shield portion is underlain by the Flin Flon-Snow Lake greenstone belt in the south and by the Kisseynew metasedimentary gneiss belt in the northeast (Bailes, 1971). Several sites of gold and base metal mineralization have been reported (Manitoba Mineral Resources Division, 1980), particularly in the Flin Flon and Snow Lake areas, where a few base metal mines are still in operation (mostly for Cu and Zn). The Proterozoic rocks are overlain by a Phanerozoic platform composed of subhorizontal Paleozoic carbonate rocks (Fig. 1).



**Figure 1.** Location map of study area within the NATMAP Shield Margin Project area showing regional ice flow trends and major moraines (taken, in part, from Klassen, 1983).

On the Shield, relief is low to moderate, and drift cover is generally thin (<2 m) and discontinuous, with thickest till accumulations occurring on the lee-side of bedrock highs. South of the Shield margin, the drift cover is thick in places, up to 80 m on The Pas moraine (Pedersen, 1973), and commonly forms fluted landforms 15 m high east of the moraine. In general though, the drift is relatively thin (<5 m), or absent in large areas, namely south of Talbot Lake and around Cormorant Lake, Rocky Lake, and Namew Lake. A large paleobasin filled with laminated sediments forms a north-south trending belt east of Hargrave Lake, masking both Shield and Paleozoic terrane.

## PREVIOUS WORK

The early observations of Pleistocene features by Tyrrell (1902) and McInnes (1913) roughly outlined the limits of two glaciations in the area, named *Keewatin* and *Patrician* glaciations, and described the limits of glacial Lake Agassiz. Antevs (1931) examined laminated sediments from the last stages of Lake Agassiz in the Grass River Basin, which led to regional correlations of late glacial recession events. Preliminary reconnaissance work was done by Craig (1965) to the south in The Pas area and by Klassen (1967) to the southeast in the Grand Rapids area. Bell (1978) proposed a sequence of glacial and deglacial events in the Wekusko Lake area, based on observations of surficial sediments and striae collected while mapping the bedrock. In the eastern part of the study area, Klassen (1983, 1986) described the surficial sediments and outlined the history of deglaciation, as part of a regional study of north-central Manitoba. Nielsen and Groom (1987, 1989) provide the most comprehensive study of the Quaternary geology history of The Pas-Flin Flon area, by documenting ice flow events and till provenance. Current studies conducted within the NATMAP Project area have concentrated on drift prospecting and understanding till provenance (Gobert and Nielsen, 1991; Henderson and Campbell, 1992; McMartin, in press; McMartin et al., 1993a; Nielsen, 1992, in press). Other studies were aimed at providing information for use in aggregate resources and land use planning activities (Groom, 1989; Pedersen, 1973; Singhroy and Werstler, 1980).

Surficial geology mapping was completed in the Cormorant Lake area (63K) at the scale of 1:250 000 as part of the 1983-1989 Canada-Manitoba Development Agreement (Clarke, 1989). The Saskatchewan part of this area was also mapped on a reconnaissance scale (1:250 000) by Schreiner (1984). The surficial geology of the Wekusko Lake area (Klassen, 1980a) and the Nelson House area (Klassen, 1980b) was compiled at a regional scale (1:250 000). Preliminary surficial geology and aggregate resources maps have been completed for different parts of NTS 63K and 63J, primarily at a scale of 1:50 000 (Groom, 1989; Mihychuk, 1988; Singhroy, 1977; Singhroy and Werstler, 1980). As part of the NATMAP Shield Margin Project, The Talbot Lake area (NTS 63J/3 to J/6) was compiled at a scale of 1:100 000 (McMartin, 1993; NATMAP Shield Margin Group, 1993).



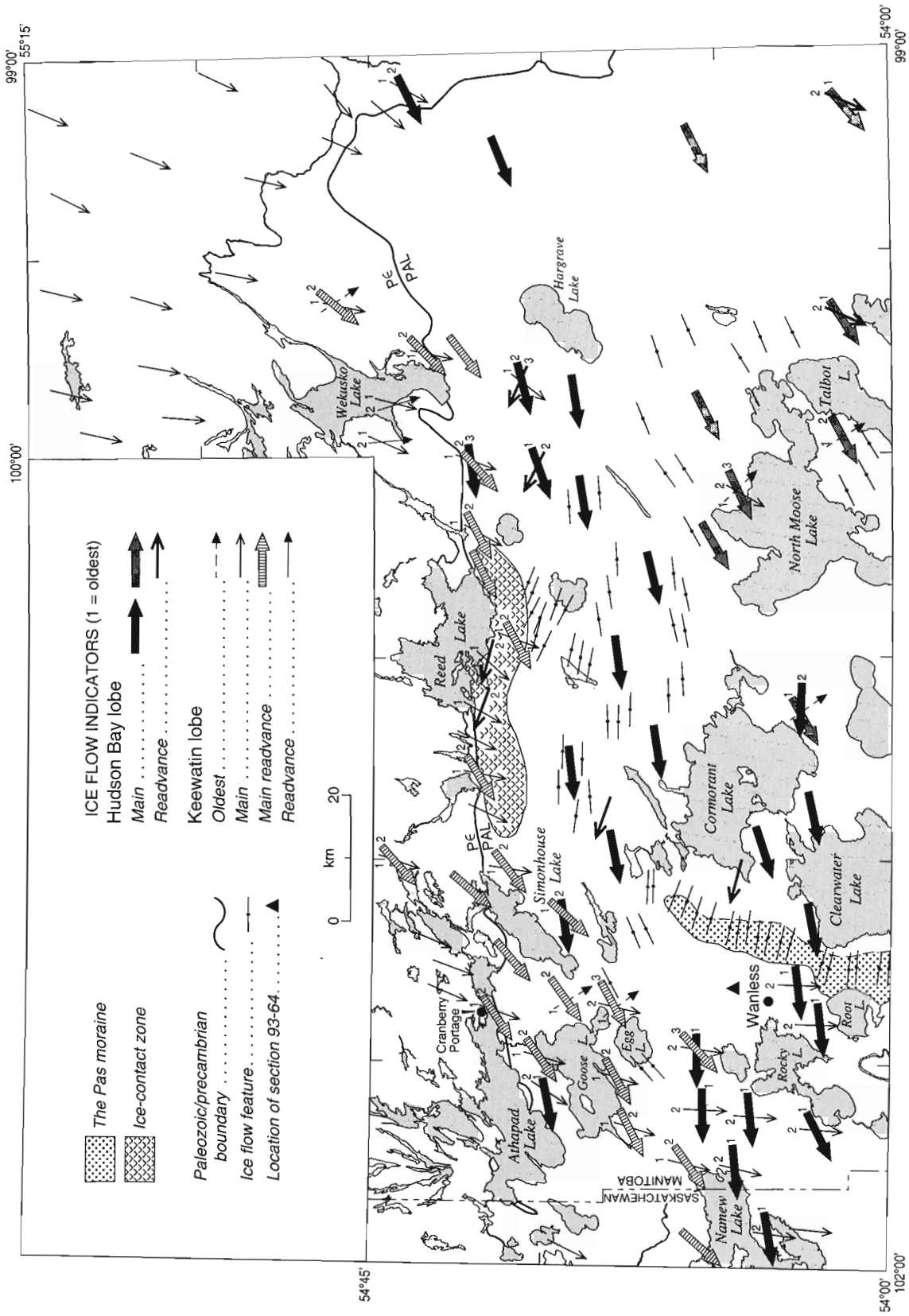
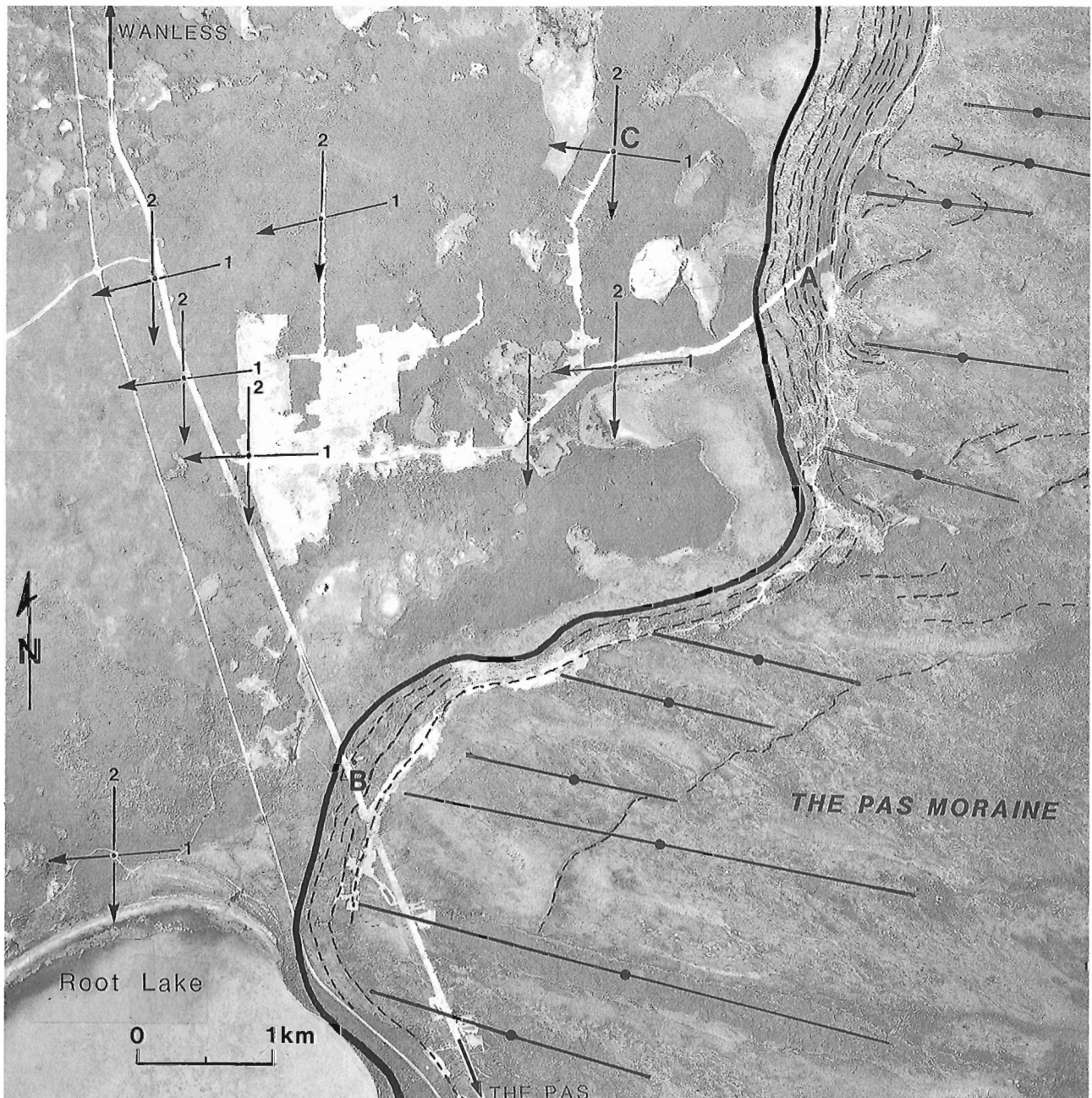


Figure 2. Map of the study area showing major ice contact deposits and ice flow trends associated to Hudson and Keewatin ice lobes. Major ice flow trends were compiled from detailed mapping of ice flow indicators (350 sites).

### DRIFT COMPOSITION AND REGIONAL ICE FLOW TRENDS

The study area is located in the zone of confluence of two major Late Wisconsinan ice lobes (Prest, 1983), where ice flowing from the Keewatin Sector of the Laurentide Ice Sheet (northern provenance) competed with ice flowing out of Hudson Bay from the Labrador Sector (northeastern provenance). Major ice-contact landforms consist of end,

lateral, or interlobate moraines deposited by the retreating ice lobes in glacial Lake Agassiz, which formed as both ice masses were pushing up the regional gradient (Fig. 1). The northern tip of The Pas moraine, which represents a major glacial landform in northern Manitoba, lies within the study area (Fig. 2). This moraine was formed during a halt in the general recession of the Hudson ice lobe, approximately 11 000 years BP (Christiansen, 1979; Klassen, 1983).



**Figure 3.** *Striation trends and relative ages (1 = oldest) in front of The Pas moraine in the Wanless area. Flutings are shown on top of the moraine and beach ridges are indicated with a dashed line. Note the difference in orientation between the flutings and the oldest ice flow trend on the west side of the moraine. Letters refer to sites mentioned in the text. NAPL A24477-52*

## Keewatin Sector provenance

### Southeastward flow

The oldest ice low event from the Keewatin Sector was towards the southeast, as recorded by isolated deep striae trending  $135^{\circ}$  to  $144^{\circ}$  found sporadically in the study area (Fig. 2). This southeasterly flow was documented throughout north-central Manitoba by Nielsen and Groom (1987) and attributed to the Late Wisconsinan by Klassen (1983). No till unit associated to this movement outcrops in the study area. A reddish cream-brown till found at depth under The Pas moraine below a clayey grey till (Pedersen, 1973) and a highly calcareous pink-brown till unit found extensively west of The Pas moraine and in southeasterly trending drumlins in the Pasquia basin southwest of The Pas were both associated with the early southeastward advance (Singhroy and Werstler, 1980). Nielsen and Groom (1987) also associated the lowest red till found under The Pas moraine with this early advance. However, their interpretation of the red till found in the drumlins of the Pasquia basin contrasts greatly from that of the previous authors. On the basis of till composition and crosscutting striae relationships in front of The Pas moraine, Nielsen and Groom (1987) interpreted the drumlins as having been formed by a minor late readvance of Keewatin ice over a previously deposited red till by Hudson ice (Arran till named by Klassen, 1979). From 1993 fieldwork, two reddish till units have been recognized, but as discussed below, none of them can be absolutely correlated with the early flow towards the southeast.

### Main south-southwestward flow

Keewatin ice was deflected towards the southwest either as a result of shifts in centres of outflow (Clayton and Moran, 1982) or from a widespread change in glacier bed conditions at the Shield edge (Dyke and Prest, 1987). On the Shield portion of the study area, dominant striae and roche moutonnée trend  $190^{\circ}$  to  $214^{\circ}$ , indicating ice flow toward the south-southwest (Fig. 2). A noncalcareous sandy till is found and is correlated with this main event. In this area, major dispersal trains parallel the dominant flow (McMartin et al., 1993a; Nielsen, 1992).

East of The Pas moraine, evidence for this southwestward flow is rare, except in a fringe area directly south of the Shield boundary. It is unknown whether this is related to the increasing influence of Hudson ice over Keewatin ice or to the poor preservation of the striae. Within a large 25 km belt south of the Shield margin, a Precambrian derived sandy-silty calcareous till related to this event is found, commonly overlying striated bedrock toward  $206^{\circ}$  to  $214^{\circ}$ . This till is variably enriched in Shield clasts (22% to 95%), relative to the distance of transport down-ice from the Paleozoic-Precambrian contact.

West of The Pas moraine, this dominant flow curves progressively from  $210^{\circ}$  immediately south of the Shield margin to  $179^{\circ}$  at the southern edge of the study area (Fig. 2). A thin pink-brown (10YR to 7.5YR, 8/3) till sheet outcropping as far north as Atik Lake is correlated with this event. This unit is found on bedrock in most sites, constantly overlying southwesterly to southerly trending striae (Fig. 3). The till is highly compact, pebbly and highly calcareous (87 to 99% carbonate pebbles), reflecting a local provenance. On the basis of its position on top of south-southwesterly trending

striae, this reddish till unit can not be associated to the southeasterly flow. Furthermore, it cannot be differentiated from the till found in the southeasterly trending drumlins of the Pasquia basin, which may in fact represent the continuation of this curving ice flow from the northeast. In that respect, the possibility of a minor readvance of Keewatin ice moulding a previously deposited red till into drumlins (Nielsen and Groom, 1987) remains a valuable hypothesis, only it is regarded now as a major advance that followed a west-southwestward flow of Hudson ice.

### Southwestward readvance

During deglaciation, as the Keewatin ice margin receded north-northeastward, the influence of Hudson ice over Keewatin ice increased in intensity, and the ice shifted to a more southwesterly trend. West of the moraine, the Keewatin lobe readvanced from the northeast to a position no further south than Rocky Lake and Namew Lake (Fig. 2). In that area, a till unit commonly overlies glaciolacustrine laminated sediments, indicating a readvance in glacial Lake Agassiz (Fig. 4, Unit A). The composition and texture of this till vary from a calcareous, clayey, clast poor diamicton when found overlying laminated sediments to a weakly calcareous, sandy Precambrian derived till (13% to 95% Shield clasts) overlying striated bedrock ( $228^{\circ}$  to  $235^{\circ}$ ). At several sites on the Shield and east of Simonhouse Lake, this southwesterly advance was also recorded, with striae trending  $218^{\circ}$  to  $224^{\circ}$ . South of Wekusko Lake, a zone of extensive parallel and confluent ice flow has been associated with this deglacial event (McMartin et al., 1993b).

### Minor deglacial event

A late minor event towards the south-southeast was recorded on the Shield at one site in the Elbow Lake area with striae trending  $156^{\circ}$  (Nielsen, 1992) and sporadically in the Wekusko Lake area ( $160^{\circ}$  to  $178^{\circ}$ ). No till unit can be related to this minor deglacial event.

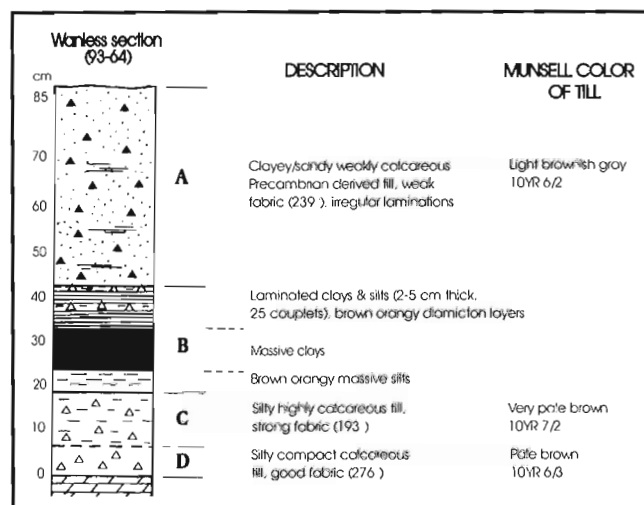


Figure 4. Hand dug section exposed immediately east of the railway, 5 km north of Wanless (Fig. 2). Striae measurements on underlying bedrock trend due west.

## Labrador Sector provenance

### Main westerly flow

West of The Pas moraine, the oldest ice flow recorded was towards the west and west-southwest ( $254^{\circ}$  to  $275^{\circ}$ ), indicating ice flowing out of Hudson Bay (Fig. 2). This early event is commonly preserved on protected outcrop surfaces, truncated by the dominant south-southwesterly ice flow direction for that area (Fig. 5a). Future fieldwork west of Namew Lake will probably help define the western extension of Hudson lobe ice.

East of the moraine, westerly trending striae ( $254^{\circ}$  to  $270^{\circ}$ ) roughly parallels the mean orientation of numerous drumlins and flutings (Fig. 5b), which are associated to a lobe originating in Hudson Bay on the Glacial map of Canada (Prest et al., 1968). Within the moraine (Singhroy and Werstler, 1980), east of Simonhouse Lake and generally east of the moraine, the till unit consists of a grey to white (10YR, 7/2 to 8/2) calcareous relatively clast-poor till. This till is silty to silty-sandy and is variably enriched in carbonate debris (59 to 97% in 4-8 mm). The presence of Omarolluck greywacke in the till and the relatively high carbonate content (up to 15%) of tills sampled on the Shield immediately east of the study area confirm the Hudson Bay provenance of this unit.

Southeast of Cormorant Lake and in the North Moose Lake area, an earlier southwesterly flow ( $240^{\circ}$  to  $248^{\circ}$ ) appears to predate the dominant, more westerly flow (Fig. 2). East of Talbot Lake, this southwesterly flow shifted toward the south, presumably related to the last glacier advance observed by Klassen (1967) in the Grand Rapids area to the south.

A red-brown (10YR to 7.5YR, 6/3) calcareous silty and pebbly till outcrops at several sites northwest and southeast of Cormorant Lake. At one site in that area it overlies southwesterly striae and underlies the grey silty calcareous till. It also outcrops in the slope of The Pas moraine east of Wanless (Fig. 3, Site A). West of the moraine, this unit is difficult to differentiate on the basis of colour and composition from the southwestward deposited pink till described above. At the base of the Wanless section (Fig. 4, Unit D), it is very thin and rests on bedrock striated by the westward flow. This unit appears to have been intensely redistributed and redeposited on either side of the moraine, either by the dominant southwesterly flow on the west side or by the westerly flow east of the moraine. Probably because of poor exposure, this red till unit was first interpreted as having been deposited by the southeasterly flow (Singhroy and Werstler, 1980). This study suggests that it was deposited during an Hudson ice advance preceding the main westerly flow, possibly in a west-southwestward direction.

### Main readvance

Directly on top of The Pas moraine and along the Shield margin south of Reed Lake, a glacial readvance occurred toward the west-northwest, with flutings and fine striae trending  $270^{\circ}$  to  $285^{\circ}$ . The till found in the flutings can not be distinguished from the till unit that forms the numerous drumlins located further east of the moraine. This late

readvance, interpreted as glacial overriding of The Pas moraine, was first noted by Craig (1965) and Klassen (1967), and documented by Nielsen and Groom (1987). In the study area, the flutings terminate at the moraine and do not trend parallel to the oldest striae recorded in front of the moraine (Fig. 3). Since the flutings have commonly been associated to the Arran readvance on both sides of the moraine (Nielsen and Groom, 1987), this observation is significant. At the distal end of a fluted landform in the slope of the moraine (Fig. 3, Site B), a grey calcareous till was found overlying massive glaciolacustrine fine sediments. From these observations, it is suggested that the ice lobe that moulded the previously deposited till into flutings, became a floating ice shelf and flowed into a lake and over lake deposits to a position in front of the moraine. The general lack of striae parallel to the flutings and the absence of an associated till unit in front of the moraine support this hypothesis.



**Figure 5.** a) Cross-cutting striae in front of The Pas moraine (Fig. 3, Site C). Main ice flow trends parallel to the moraine (southward) and postdates the westward flow preserved on the lee-side of the outcrop. Note the pink-brown till deposited by southward flowing ice. GSC 1993-264B. b) Truncated striated surfaces south of Simonhouse Lake indicating southerly striae postdated by dominant westerly trending striae. A grey calcareous till of eastern provenance covers the outcrop. GSC 1993-264A





**Figure 6.** Hummocky terrain south of Reed Lake. Small hills (up to 10 m high) are composed of ice contact material, highly enriched in carbonate debris. Depressions are filled with peat and clay underlain by till, commonly more derived from Shield lithologies. GSC 1993-264C

### Ice contact zone

Near the Shield margin, the ice flow record is particularly abundant and complex, associated with the presence of a large east-west trending ice-contact zone between Keewatin ice and Hudson Bay ice (Fig. 2). In that zone, main ice flow directions trend 210°, 230°, 250°, and 280°, with variable age relationships. The area is characterized by a hummocky topography (Fig. 6), with knobs of material composed of boulders, pebbly gravels, and a very cobbly, highly calcareous beige till (88 to 99% carbonates). The depressions are filled with peat and clay overlying a till commonly enriched in Shield lithologies. This hummocky morainic material appears to have been deposited during the last glacier advance by a stagnant portion of the Hudsonian ice lobe at a time when Hudson ice encroached upon Keewatin ice. Part of the Reed Lake interlobate moraine, first described by Antevs (1931), lies within this hummocky terrain. The southwestern extension of this moraine, inferred by Nielsen and Groom (1987) from photointerpretation, was not recognized from fieldwork in the area.

### SUMMARY

Surficial mapping in the Cormorant Lake-Wekusko Lake area since the last two summers has documented a complex ice flow history. The presence of confluent Late Wisconsinan ice lobes in the study area resulted in ice flow directions and till composition differing on either side of The Pas moraine. In addition, at the Shield edge, contrasting glacier bed conditions from nondeforming to deforming beds (Fisher et al., 1985) were possibly reflected by abrupt ice flow direction changes. These variations in flowline trends along the Shield boundary, as well as contrasting bedrock lithologies, significantly influence till composition.

The Keewatin Sector events and associated till units dominate the Shield portion and the area west of The Pas moraine. The dominant curving southwestward flow around the moraine and the associated till unit indicate that this glacier advance occurred at a time when Hudson ice had probably retreated back to The Pas moraine, hence delimiting a major ice contact zone between the two lobes during deglaciation. The extension of The Pas moraine towards Reed Lake and further north to the Leaf Rapids interlobate moraine (Kaszycki and DiLabio, 1986) as suggested by Nielsen and Groom (1987) was not confirmed. The presence of westerly striae in the Namew Lake area also suggests that the limit of Hudson lobe ice extended further west than previously interpreted.

As the Keewatin lobe margin retreated further north, glacial Lake Agassiz inundated the low areas west of the moraine where a thin glaciolacustrine sequence was deposited. Keewatin ice, deflected by the dominant Hudson ice flow, shifted to a more southwesterly direction and readvanced into the lake, forming in places a Shield derived clayey till. East of the moraine, this readvance caused a confluent and parallel ice flow directly south of the Shield, as recorded by rapidly curving striae to which no till unit can be differentiated. Hudson ice apparently lost contact with Keewatin ice before readvancing to a position near Simon-house Lake, which marks the western extension of white-grey calcareous till of eastern provenance. This position also indicates the limit of westerly trending striae postdating the southwestward flow. In the Reed Lake area, Hudson ice abutted against Keewatin ice, forming a large east-west trending ice-contact zone where Hudson ice stagnated and deposited hummocky material.

The till composition of flutings and drumlins located on top and east of The Pas moraine can not be differentiated from the generally thin till sheet found throughout this area, indicating a similar provenance for these westerly events. The latest minor readvance which formed the flutings on top of The Pas moraine was that of a relatively thin glacier flowing into glacial Lake Agassiz near Wanless and against Keewatin ice south of Reed Lake.

It is hoped that this study will aid mineral exploration by establishing the glacial history for interpreting regional till geochemical data.

### ACKNOWLEDGMENTS

I am grateful to Robert Boucher, Simon Gautrey, Patrick Rummel, Jocelyn Rutherford, Julie Watson, and Stephen Warner for their invaluable field assistance, to Erik Nielsen and Penny Henderson for discussions and comments, and to Annie Roy and Tracy Barry for preparing the diagrams.

### REFERENCES

- Antevs, E.  
1931: Late-glacial correlations and ice recession in Manitoba; Geological Survey of Canada, Department of Mines, Memoir 168, 76 p.

**Bailes, A.H.**

1971: Preliminary compilation of the geology of the Snow Lake-Flin Flon Sherridon area; Manitoba Department of Mines and Natural Resources, Mines Branch, Geological Paper 1/71, 27 p.

**Bell, C.K.**

1978: Geology, Wekusko Lake map-area, Manitoba; Geological Survey of Canada, Memoir 384, 84 p.

**Clarke, M.D.**

1989: Surficial geology, Cormorant Lake, Manitoba-Saskatchewan; Geological Survey of Canada, Map 1699A, scale 1:250 000.

**Clayton, L. and Moran, S.R.**

1982: Chronology of Late Wisconsin glaciation in middle North America; Quaternary Science Reviews, v. 1, p. 55-82.

**Christiansen, E.A.**

1979: The Wisconsinan deglaciation of southern Saskatchewan and adjacent area; Canadian Journal of Earth Sciences, v. 16, p. 913-939.

**Craig, B.C.**

1965: Preliminary reconnaissance of the surficial geology of The Pas area; in Report of Activities, Geological Survey of Canada, Paper 66-1, p. 139-140.

**Dyke, A.S. and Prest, V.K.**

1987: Late Wisconsinan and Holocene history of the Laurentide Ice Sheet; Géographie Physique et Quaternaire, v. 41, p. 237-263.

**Gobert, G. and Nielsen, E.**

1991: Till geochemistry of the Snow Lake-File Lake area (NTS 63K/16, J/13); in Manitoba Energy and Mines, Report of Activities, 1991, p. 47-48.

**Groom, H.D.**

1989: Sand and gravel resources in the Flin Flon-Cranberry Portage area; Manitoba Energy and Mines, Aggregate Report AR88-13, 34 p.

**Fisher, D.A., Reeh, N., and Langley, K.**

1985: Objective reconstructions of the Late Wisconsinan Laurentide Ice Sheet and the significance of deformable beds; Géographie Physique et Quaternaire, v. 49, p. 229-238.

**Henderson, P.J. and Campbell, J.E.**

1992: Quaternary studies in the Annabel Lake-Amisk Lake area (NTS Areas 63L-9 and -16, and Part of 63K-12 and -13); in Summary of Investigations, Saskatchewan Geological Survey, p. 172-176.

**Kaszycki, C.A. and DiLabio, R.N.W.**

1986: Surficial geology and till geochemistry, Lynn Lake-Leaf Rapids region, Manitoba; in Current Research, Part B; Geological Survey of Canada, Paper 86-1B, p. 245-256.

**Klassen, R.W.**

1967: Surficial geology of the Wterhen-Grand Rapids area, Manitoba (63B, 63G); Geological Survey of Canada, Paper 66-36, 6 p.

1979: Pleistocene geology and geomorphology of the Riding Mountain areas, Manitoba-Saskatchewan; Geological Survey of Canada, Memoir 396, 52 p.

1980a: Surficial geology, Wekusko Lake, Manitoba; Geological Survey of Canada, Map 4-1979, scale 1:250 000.

1980b: Surficial geology, Nelson House, Manitoba; Geological Survey of Canada, Map 17-1978, scale 1:250 000.

1983: Lake Agassiz and the late glacial history of northern Manitoba; in Glacial Lake Agassiz, (ed.) J.T. Teller and L. Clayton; Geological Association of Canada, Special Paper 26, p. 97-115.

1986: Surficial geology of North-Central Manitoba; Geological Survey of Canada, Memoir 419, 57 p.

**Manitoba Mineral Resources Division**

1980: Mineral Map of Manitoba, Map 80-1, scale 1:1 000 000.

**McInnes, W.**

1913: The basins of Nelson and Churchill rivers; Geological Survey of Canada, Memoir 30, 146 p.

**McMartin, I.**

in press: Highlights of Quaternary geology investigations in the Cormorant Lake area (NTS 63K); in Report of Activities, Manitoba Energy and Mines.

**McMartin, I. (cont.)**

1993: Surficial geology of the Talbot Lake area, Manitoba (NTS 63J3 to J6); Geological Survey of Canada, Open File 2744, 1 sheet, scale 1:100 000.

**McMartin, I., Bélanger, J.R., and Rummel, P.**

1993a: Quaternary Geology Studies in the Eastern NATMAP Shield Margin Project Area; in Program with Abstracts, Geological Survey of Canada Forum '93, Ottawa, p. 15.

**McMartin, I., Nielsen, E., and Henderson, P.**

1993b: Quaternary geology studies and drift prospecting in the NATMAP Shield Margin Project area; in Program with Abstracts, A special meeting of the Flin Flon-Creighton Canadian Institute of Mining and Metallurgy Branch, "New Perspectives on the Flin Flon-Snow Lake-Hanson Lake Belt from the NATMAP Shield Margin Project", Flin Flon, p. 10.

**Mihychuk, M.**

1988: Surficial geology and aggregate resources in the Snow Lake area; in Report of Activities, Manitoba Energy and Mines, Map 1988 SL-2 and SL-3, scale 1:50 000.

**NATMAP Shield Margin Group**

1993: Preliminary release of selected geoscience data for the NATMAP Shield Margin Project, Manitoba and Saskatchewan; Geological Survey of Canada, Open File 2743, 1 CD-ROM.

**Nielsen, E.**

1992: Surficial geology mapping and glacial dispersion studies as aids to geochemical exploration and mineral tracing in the Elbow Lake area (NTS 63K/15); in Report of Activities, Manitoba Energy and Mines, p. 52-55.

in press: Surficial geology and till geochemical sampling in the Naosap Lake area (63K/14); in Report of Activities, Manitoba Energy and Mines.

**Nielsen, E. and Groom, H.D.**

1987: Glacial and late glacial history of The Pas area; in The Quaternary between Hudson Bay and the Rocky Mountains, (ed.) B.T. Schreiner; XIIIth INQUA Congress, Ottawa, Excursion Guide C-13, National Research Council of Canada, NRC 27533, 45 p.

1989: Trace element geochemistry and till provenance in The Pas-Flin Flon area, Manitoba; Manitoba Energy and Mines, Open File Report OF89-3, 20 p.

**Pedersen, A.**

1973: Ground water availability in The Pas area; Manitoba Resources Branch, Report #9, Winnipeg, Manitoba.

**Prest, V.K.**

1983: Canada's heritage of glacial features; Geological Survey of Canada, Miscellaneous Report 28, 120 p.

**Prest, V.K., Grant, D.R., and Rampton, V.N.**

1968: Glacial map of Canada; Geological Survey of Canada, Map 1253A, scale 1:5 000 000.

**Schreiner, B.T.**

1984: Quaternary geology of the Amisk Area (63-L,K) Saskatchewan; Saskatchewan Geological Survey, Open File Report 84-2, scale 1:250 000.

**Singhroy, V.**

1977: Quaternary Geology of The Pas area; Manitoba Energy and Mines, Preliminary Map Series 1977-S/PAS-1 to 9, scale 1:50 000.

**Singhroy, V. and Werstler, R.**

1980: Sand and gravel resources and Quaternary geology of The Pas region; Manitoba Energy and Mines, Geological Report GR80-2, 60 p.

**Tyrrell, J.B.**

1902: Report on explorations in the northeastern portion of the District of Saskatchewan and adjacent parts of the District of Keewatin; Geological Survey of Canada, Annual Report, v. XIII, pt. F, 218 p.



# Transition between the Flin Flon and Kisseynew domains of the Trans-Hudson Orogen, File Lake-Limestone Point Lake area, northern Manitoba<sup>1</sup>

Karen A. Connors and Kevin M. Ansdell<sup>2</sup>

Continental Geoscience Division

*Connors, K.A. and Ansdell, K.M., 1994: Transition between the Flin Flon and Kisseynew domains of the Trans-Hudson Orogen, File Lake-Limestone Point Lake area, northern Manitoba; in Current Research 1994-C; Geological Survey of Canada, p. 183-192.*

---

**Abstract:** The tectonothermal evolution of the File Lake-Limestone Point Lake area, which includes part of both the Flin Flon and Kisseynew domains of the Trans-Hudson Orogen, involved early bedding parallel faulting, two generations of isoclinal folds (F1, F2), and two generations of upright folds (F3, F4). Prograde metamorphism occurred syn- or post-F1 and peaked post-F1/S1, pre-S2. Metamorphic conditions remained sufficient for biotite recrystallization during F4. Map units and early isoclinal folds can be traced from greenschist grade rocks to uppermost amphibolite grade gneisses. S1 and S2 vary progressively from near vertical in greenschist to amphibolite grade rocks to gently dipping in upper amphibolite gneisses. This transition from steep to shallow structures with increasing metamorphic grade may reflect: i) changing rheology; ii) increasing shear strain; and/or iii) a buttress effect at the northern margin of the Flin Flon Domain.

**Résumé :** L'évolution tectonothermique du secteur des lacs File et Limestone Point, qui comprend des portions du domaine de Flin Flon et du domaine de Kisseynew dans l'orogène transhudsonien, comprend la formation de failles initiales parallèles à la stratification, et celle de deux générations de plis isoclinaux (P1, P2) et de deux générations de plis droits (P3, P4). Le métamorphisme prograde a eu lieu lors de phases contemporaines de P1 ou postérieures à P1 et a culminé postérieurement à P1/S1 et antérieurement à S2. Les conditions du métamorphisme sont demeurées adéquates pour la recristallisation de la biotite pendant P4. On peut tracer les unités cartographiques et les plis isoclinaux initiaux depuis les roches du faciès des schistes verts jusqu'aux gneiss du faciès des amphibolites sommital. S1 et S2 passent progressivement d'une position presque verticale dans les roches allant du faciès des schistes verts au faciès des amphibolites, à une position légèrement inclinée dans les gneiss du faciès des amphibolites supérieur. Cette transition de structures fortement inclinées à des structures peu inclinées, en fonction de l'accroissement du degré de métamorphisme, peut indiquer: i) une variation de la rhéologie; ii) un accroissement de la déformation par cisaillement; et/ou iii) un effet de butée de la part de la marge nord du domaine de Flin Flon.

---

<sup>1</sup> Contribution the NATMAP Shield Margin Project.

<sup>2</sup> Department of Geological Sciences, University of Saskatchewan, Saskatoon, Saskatchewan S7N 0W0

## INTRODUCTION

The Flin Flon and Kisseynew domains lie within the Paleoproterozoic Trans-Hudson Orogen, west of the Archean Superior Province (Fig. 1). The low grade Flin Flon Domain consists largely of arc-related mafic to felsic volcanic rocks of the Amisk Group which are intruded by calc-alkaline granitoids (Bailes, 1980). These arc-related rocks are unconformably overlain by fluvial molasse deposits of the Missi Group at Flin Flon (Stauffer, 1990) and just west of the study area (Zwanzig, 1990). In the study area, the arc-related rocks are structurally overlain by File Lake formation turbidites of the Burntwood River Group (Fig. 2). The high grade gneisses of the southern Kisseynew Domain (Fig. 1) are considered metamorphosed equivalents of these three units (Froese and Moore, 1980; Bailes, 1980; Zwanzig, 1990).

The traditional boundary between the Flin Flon and Kisseynew domains was defined as the Kisseynew lineament (Harrison, 1951; Fig. 3). More recently, however, Bailes (1980) and Froese and Moore (1980) have suggested that the lineament does not exist and that the boundary is gradational and is marked by a rapid increase in metamorphic grade (Fig. 3) and/or a facies change from volcanism to sedimentation. The boundary is commonly defined as the sillimanite-biotite-garnet isograd (Froese and Moore, 1980; Fig. 3).

The File Lake-Limestone Point Lake area straddles the "boundary" between the Flin Flon and Kisseynew domains and thus presents an excellent opportunity to evaluate the structural and metamorphic transition. Recent studies have documented the northward increase in metamorphic grade, correlated the principal map units (Amisk, Burntwood River and Missi groups) between low and high grade rocks, and examined the structural history (Bailes, 1980; Zwanzig and Schledewitz, 1992). However, the detailed maps of Bailes (1980) and Zwanzig and Schledewitz (1992) are separated by a 3-4 km wide strip north of Loonhead Lake (Fig. 2). Reconnaissance mapping was carried out in this strip, in order to

join the existing maps. The principal aims of this project are to: i) document the structural history in the File Lake area; ii) determine the nature of contacts between Missi, Burntwood River and Amisk groups; and iii) evaluate the significance of the structural and metamorphic transition between the Flin Flon and Kisseynew domains (Fig. 3). Note that although all rocks in this area have been metamorphosed, the prefix meta has been omitted.

## ROCK UNITS

The File Lake-Limestone Point Lake area is dominated by three lithostratigraphic units: i) Missi Group quartzo-feldspathic sedimentary rocks, ii) Burntwood River Group turbidites, and iii) Amisk Group volcanic and intrusive rocks, all of which are cut by both felsic and mafic intrusions (Fig. 2).

### *Amisk Group*

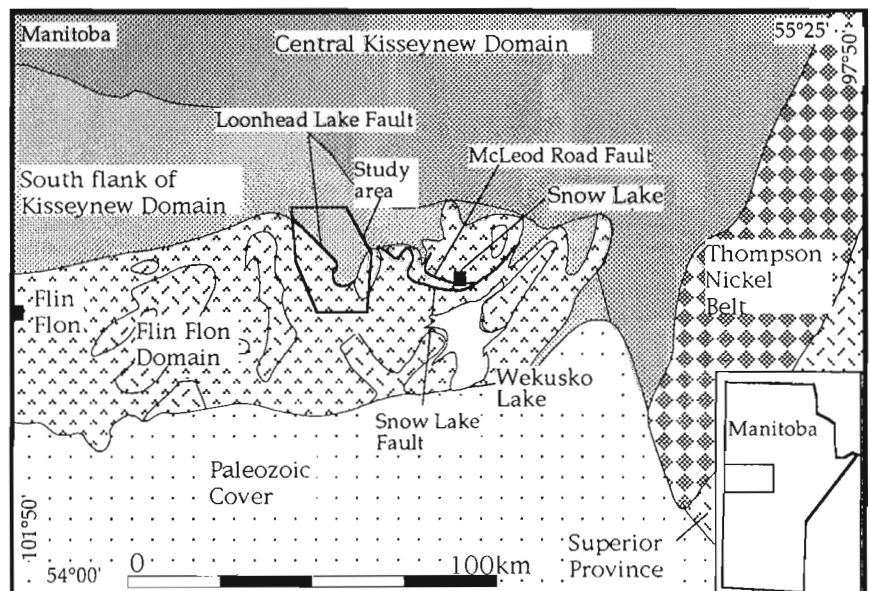
The Amisk Group comprises subalkaline basalt to rhyolite (<20%) flows and fragmental rocks (Bailes, 1980). Zircon U-Pb geochronology from other parts of the Flin Flon Domain indicates ages in the range of 1904-1885 Ma (David and Machado, 1993; Stern et al., 1993). Amisk Group rocks grade north into amphibolitic gneisses with primary structures largely obliterated (Zwanzig and Schledewitz, 1992).

### *Josland Lake Gabbro*

The Josland Lake Gabbro occurs as concordant, differentiated and zoned bodies (Bailes, 1980) throughout the Amisk Group and along the contact with the Burntwood River Group (Fig. 2). It is uncertain whether the large bodies of Josland Lake Gabbro intrude the Burntwood River Group because the contacts are typically faulted (Fig. 2), but smaller bodies interpreted as Josland Lake Gabbro by Bailes (1980) intrude the turbidites.

**Figure 1.**

*Simplified map of the Manitoba part of the Trans-Hudson Orogen depicting the Flin Flon and Kisseynew domains.*

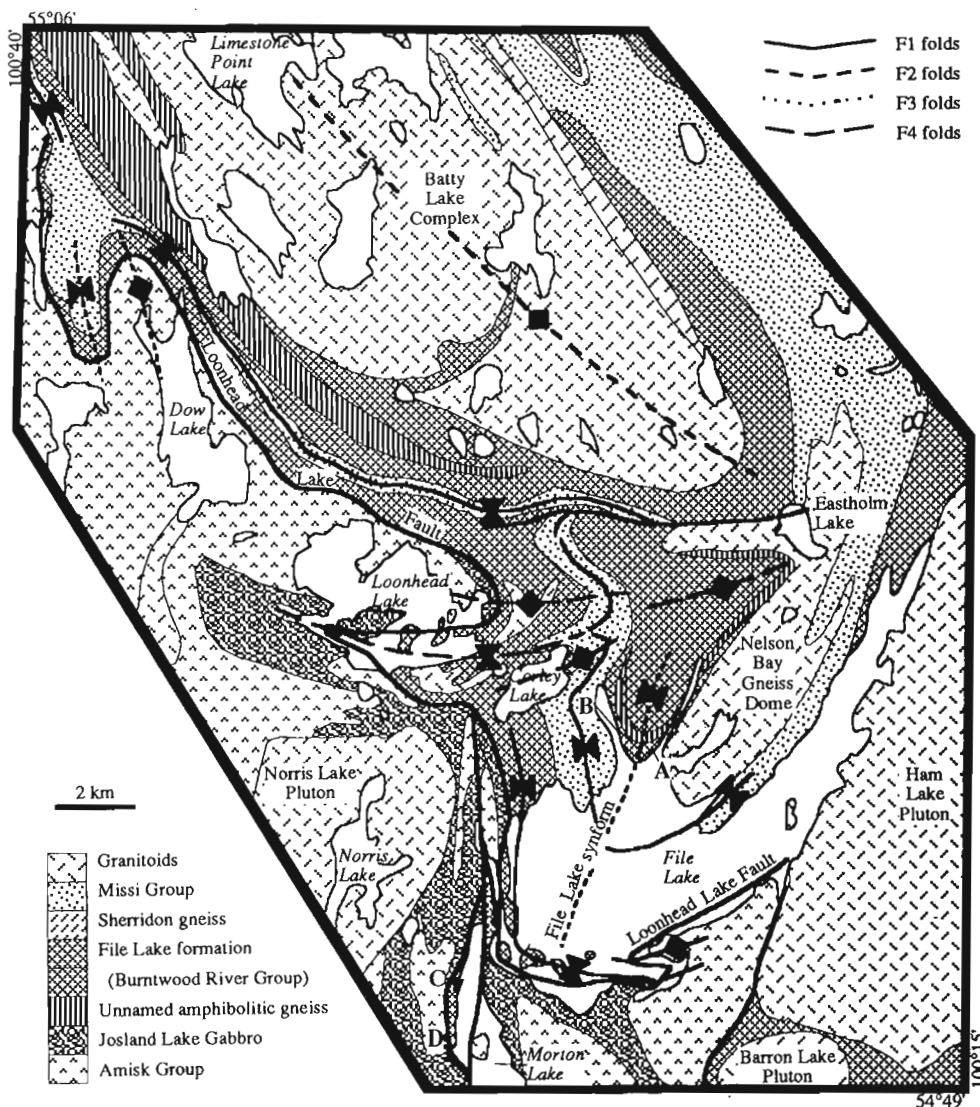


### File Lake formation / Burntwood River Group

Amisk Group rocks are structurally overlain (Fig. 2) by the Burntwood River Group which is dominated by the File Lake formation turbidites in this area. The File Lake formation turbidites consist largely of felsic to intermediate volcanic detritus (Bailes, 1980). This unit can be traced from Morton Lake where primary structures are preserved (Bailes, 1980), to north of File and Loonhead lakes where it is recrystallized and partially melted (Fig. 4). Although the File Lake formation has been interpreted as part of the Amisk Group (Bailes, 1980), U-Pb geochronology of detrital zircons from File, Morton, and Wekusko lakes (Fig. 1, 2) indicates the turbidites are younger than ~1850 Ma (David and Machado, 1993).

### Amphibolitic gneiss

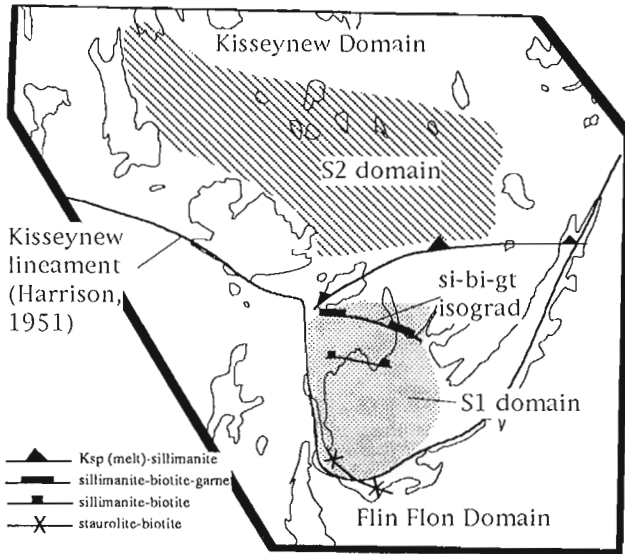
An unnamed unit of mafic to intermediate gneiss occurs within the File Lake formation (Fig. 2). South of the Batty Lake Complex, Zwanzig and Schledewitz (1992) have suggested this unit includes metamorphosed gabbro, basalt, and locally, ultramafic rocks and silicate iron-formation. In the File Lake synform (Fig. 2), this unit consists largely of fine grained banded gneisses which contain thin discontinuous felsic bands within a mafic host (Fig. 5a). This unit also includes mafic flows with deformed pillow selvages (Fig. 5b) suggesting a volcanic origin. Whether these gneisses represent part of the stratigraphy or a fault-bounded package is uncertain as their contacts are not exposed.



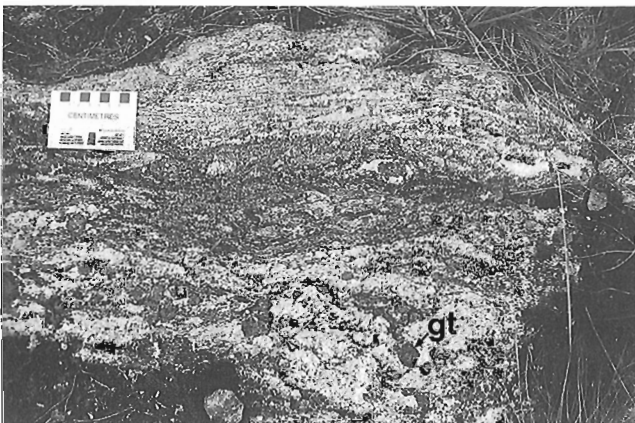
**Figure 2.** Simplified geology of the File Lake-Limestone Point Lake area (based on Zwanzig and Schledewitz (1992), Bailes (1980) and this study).

**Missi Group**

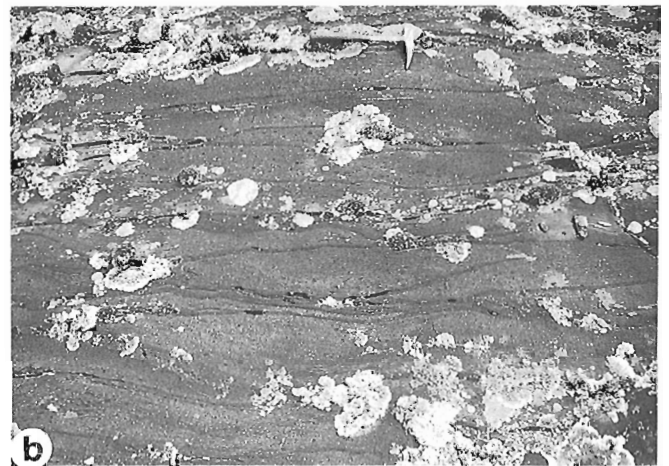
Missi Group quartzo-feldspathic paragneisses overlie the File Lake formation. The nature of this contact in the study area is uncertain due to poor exposure. Zwanzig and Schledewitz (1992) reported a deformed conglomerate ~12 km west of Dow Lake and interpreted the contact as an unconformity. In contrast, the only contact between these two units on Wekusko Lake (Fig. 1) is an early fault (Ansdell and Connors, 1994). The Missi Group rocks are typically magnetite-rich and parallel laminated (Fig. 6). Low-angle truncations are locally preserved indicating younging direction. Age of the Missi Group at Flin Flon (Fig. 1) is bracketed by an  $1842 \pm 3$  Ma cross cutting intrusion and the youngest detrital zircon



**Figure 3.** Schematic map highlighting the distribution of isograds and Harrison's (1951) Kiskeynew lineament. The patterned areas indicate zones where S1 or S2 are the dominant fabric. The dominant fabric in the intervening area may be either S1 or S2.



**Figure 4.** Garnet-bearing leucosome in the File Lake formation. (GSC 1993-280D)



**Figure 5.** a) Discontinuous felsic lenses within the unnamed mafic gneisses. b) Possible deformed pillow selvages in the mafic gneisses. (GSC 1993-280F)



**Figure 6.** Typical Missi Group gneisses with, locally magnetite-rich, parallel laminations. (GSC 1993-280A)

analyzed to date which is  $1847 \pm 2$  Ma (Ansdell, 1993). East of Wekusko Lake (Fig. 1), however, felsic volcanic rocks interpreted as Missi Group are dated at  $1832 \pm 2$  Ma (Gordon et al., 1990).

The interpreted continuity of Missi Group gneisses from File Lake to Dow Lake (Fig. 2) is based on magnetic data and limited mapping, due to poor exposure. Magnetite-bearing Missi Group rocks stand out against File Lake formation rocks on magnetic maps, and a fairly consistent magnetic high joins known Missi outcrops north of File Lake to those at Dow Lake.

### **Felsic intrusive rocks**

The calc-alkaline Ham Lake, Norris Lake and Barron Lake plutons postdate the File Lake formation and the Missi Group (Bailes, 1980). Deformation state of these intrusions is variable. Overprinting relationships and geochronological data are generally insufficient to accurately determine their timing with respect to deformation. The Ham Lake Pluton (Fig. 2) yielded a zircon U-Pb age of  $1830 \pm 27$ -19 Ma (Gordon et al., 1990).

The Nelson Bay gneiss dome (Fig. 2) forms a doubly plunging, north-northeast-trending antiform of oligoclase-quartz-biotite $\pm$ microcline orthogneiss. The local presence of 2-4 mm feldspar phenocrysts confirms an igneous origin. Sills of these felsic gneisses can be traced into the Missi Group paragneisses. This may reflect intrusion, felsic volcanism during Missi Group deposition, or juxtaposition by low-angle faulting. East of Wekusko Lake (Fig. 1), Missi Group rocks unconformably overlie felsic volcanic rocks and are faulted against a felsic to mafic volcanic package, but interbedded volcanics within the Missi Group have not been documented (Ansdell and Connors, 1994).

The Batty Lake Complex (Fig. 2) forms a doubly plunging dome of well-foliated and lineated quartz-rich tonalitic orthogneiss (Zwanzig and Schledewitz, 1992). Tonalitic sills similar to the Batty Lake Complex intrude the File Lake formation near the contact, suggesting that although the contact may be sheared, it is primarily intrusive.

## **FOLD/CLEAVAGE GENERATIONS AND THEIR TIMING WITH RESPECT TO METAMORPHISM**

The increasing metamorphic grade from greenschist at File Lake to uppermost amphibolite with extensive anatexis to the north is well documented (Bailes and McRitchie, 1978). P-T conditions are estimated at  $550^\circ\text{C}$  and 3.5-5 kbar in the sillimanite field and  $750 \pm 50^\circ\text{C}$  at  $5.5 \pm 1$  kbar in gneisses just north of the map area (Gordon, 1989). Briggs and Foster (1992) estimated a peak temperature of  $560$ - $625^\circ\text{C}$  at 3.3-4.6 kbar between File and Corley lakes. The age of metamorphism is estimated as  $\sim 1815$  Ma (the age of antectic gneisses in the Kiskeynew; Gordon et al., 1990) and  $\sim 1807$  Ma (the age of metamorphic zircon overgrowths in the Herblet Lake gneiss dome (north of Snow Lake; Fig. 1); David and Machado, 1993).

### **Early structures (F1-F2 folds)**

The oldest recognized generation of structures are F1 isoclinal folds and the S1 axial planar cleavage which is largely parallel to layering. F1 hinges are rarely exposed and the folds are identified by changes in younging. In the File Lake formation staurolite, garnet and faserkiesel (sillimanite-quartz nodules) overgrow S1, and porphyroblast inclusion trails are continuous with the matrix fabric, suggesting that the metamorphic peak postdates F1/S1.

A steep, south-southwest-plunging extension lineation, defined by aligned micas and faserkiesels, and stretched clasts, is developed on S1. This lineation locally forms the dominant fabric on the limbs of F1 folds within the File Lake formation. The lineation and S1/S0 intersection lineation are sub-parallel where both are exposed on the western half of File Lake. F1 fold traces can be followed for more than 10 km (Fig. 2), suggesting that either the axes are steep and the folds are very high amplitude, or the fold hinges are subhorizontal on a regional scale and have not rotated toward the extension direction. It is also possible that the extension lineation postdates F1 (see below).

Regional metamorphism resulted in extensive anatexis north of File Lake. Bailes (1980) mapped a roughly east-striking "melt" isograd near the south of Corley Lake (Fig. 2), but possible indications of melting occur  $\sim 2$  km south (i.e. down grade; A Fig. 2) where leucocratic segregations occur around garnet porphyroblasts (Fig. 7a), similar to those reported by Bailes and McRitchie (1978). In addition, larger melt segregations occur  $\sim 1.5$  km south of Bailes' (1980) isograd (B Fig. 2). The segregations at this location contain blue cordierite up to 3 cm diameter (Fig. 7b), which is a common leucosome phase (Bailes and McRitchie, 1978; Bailes, 1980).

F1, S1 and peak metamorphic assemblages are overprinted by S2 which is developed at a small angle to bedding and S1 throughout the File Lake area. S2 shows a consistent angular relationship with bedding that indicates antiform to the north or east (i.e. toward the core of an overprinting F3). Staurolite and garnet contain straight inclusion trails, despite S2 crenulations in the matrix, suggesting that S2 postdates peak metamorphism. S2 forms a biotite cleavage, which is similar to and thus difficult to distinguish from S1. Although no F2 folds have been identified in the File Lake area, folds of this generation are interpreted to occur in the Kiskeynew gneisses (see below).

The S2/S1 and S2/S0 intersection lineations both plunge steeply south-southwest parallel to the L1 extension lineation. This suggests several possible interpretations: i) F1/S1 and F2/S2 structural generations developed during progressive deformation and the extension lineation is related to both generations of structures; ii) the older extension lineation and S1/S0 intersection lineation may have influenced orientation of the S2/S1 intersection lineation; or iii) the extension lineation developed during F2/S2 and overprints F1/S1 structures. Although studies in the Kiskeynew favour the first hypothesis (e.g. Norman and Williams, 1993), F1/S1 may substantially predate F2/S2 at File Lake (see below).



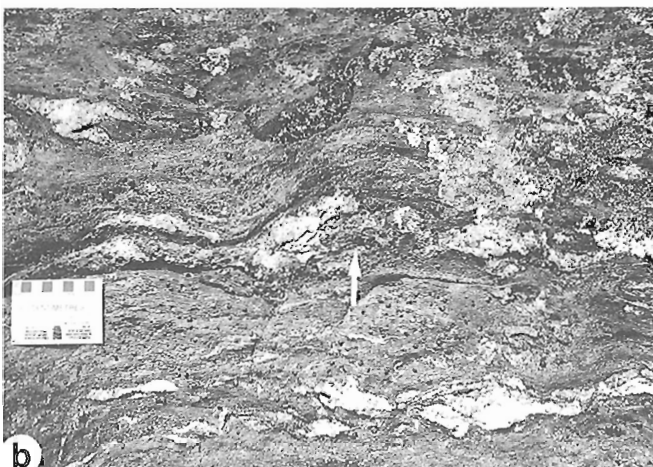
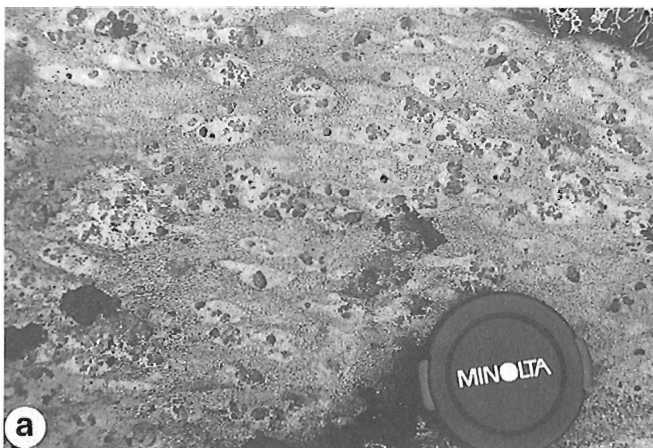
It is difficult to trace cleavages from low grade rocks into the gneisses due to lack of well-exposed outcrop, problems distinguishing S2 from S1 north of File Lake (Fig. 3), and paucity of overprinting relationships. S1 forms the dominant fabric in the File Lake area, but the dominant foliation north of Loonhead Lake is a crenulation cleavage suggesting that it is at least the second cleavage (Fig. 3). In addition, this cleavage contains flattened faserkiesel and is axial planar to folded leucosome suggesting that it postdates peak metamorphism and anatexis. This fabric is therefore correlated with S2 in the lower grade rocks.

**Late folds (F3-F4)**

F1/S1 and S2 are overprinted by the north-northeast-trending F3 File Lake synform (Fig. 2). Mesoscopic structures are dominated by asymmetric folds (Fig. 8) and by crenulations in mica-rich rocks. The steep, axial planar S3 crenulation cleavage is only developed within F3 hinge zones and is locally defined by aligned biotite. The trend of F3/S3 structures varies from north-northeast to east-northeast. In thin section, S3 crenulations deform faserkiesel and therefore postdate

peak metamorphism. Nevertheless biotite, and locally sillimanite, are recrystallized in S3 crenulation hinges, indicating conditions close to the sillimanite stability field during S3.

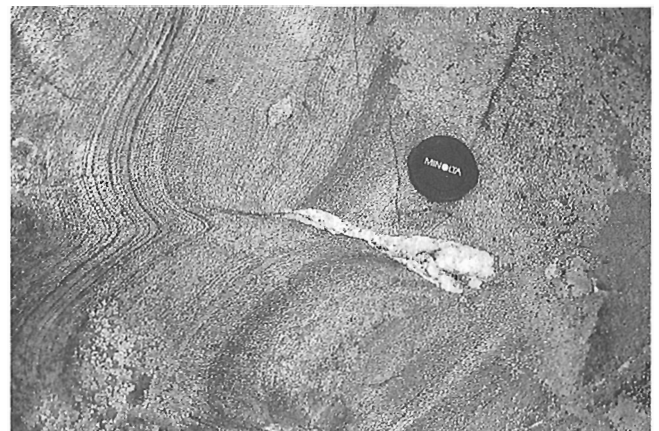
Tight to open F4 folds plunge moderately east to east-northeast and are best developed north of File Lake (Fig. 2). The steep S4 cleavage is only developed within hinge zones of F4 folds and is defined by crenulations in micaceous units and aligned micas in quartzo-feldspathic gneisses. Biotite laths in the S4 crenulations are recrystallized. A generation of centimetre to metre thick pegmatites is associated with F4/S4. Some pegmatites cross-cut F4 folds, some are folded by F4, and some are associated with offset along F4 axial planes (Fig. 9), indicating emplacement during F4 folding. F4 folds appear to overprint the limbs of the F3 File Lake synform (Fig. 2), however, F4 and F3 show similar microstructures and locally have the same orientation (i.e. west of the nose of the File Lake synform), suggesting that they may represent the same generation, or closely associated generations.



**Figure 7.** a) Felsic segregations around garnet porphyroblasts in File Lake formation. b) Cordierite porphyroblast (arrow) in leucosome in File Lake formation. (GSC 1993-280H)



**Figure 8.** Asymmetric, steeply plunging F3 folds near core of File Lake synform. (GSC 1993-280C)



**Figure 9.** Pegmatite associated with offset parallel to F4 axial plane. (GSC 1993-280E)



## EARLY LOW-ANGLE FAULTING

### Loonhead Lake Fault

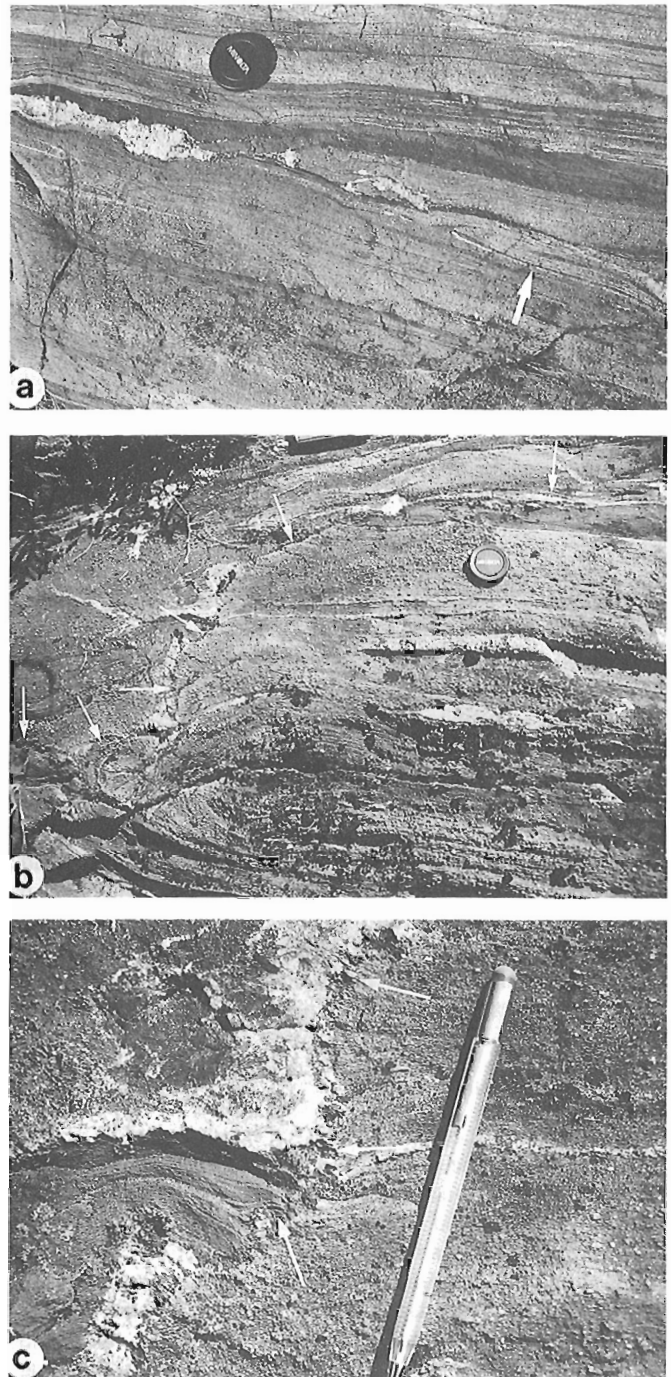
The ~35 Ma age difference between Amisk Group and File Lake formation has prompted re-evaluation of the contact between these units. The contact is poorly exposed and overprinting relationships with the fold/cleavage generations were not observed. There is intense cleavage development, boudinage, disruption of units and alteration in units adjacent to this contact (Fig. 10), suggesting that it is faulted. Furthermore, this contact can be traced northwards (Harrison, 1949) to Dow Lake where Zwanzig (1992) interpreted it as a fault. The File Lake formation-Amisk Group contact in the File Lake area is therefore interpreted as a fault, and is here referred to as the Loonhead Lake Fault which is partly equivalent to the File Lake fault of Harrison (1949). West of Dow Lake this fault is truncated at the base of the Missi Group (Fig. 2; Zwanzig and Schledewitz, 1992) by either an unconformity or a low-angle fault.

East of the Ham Lake Pluton, the apparently same File Lake formation – Amisk Group contact is interpreted as the Snow Lake Fault (Fig. 1; Harrison, 1949). If the Loonhead Lake and Snow Lake faults represent the same structure, this implies a strike length of >80 km and possibly substantial displacement. Kinematic analyses in the Kisseynew Domain suggest south or southwest transport of high grade rocks toward the Flin Flon domain (Zwanzig, 1990; Norman and Williams, 1993).

This faulted contact between the Amisk Group and File Lake Formation appears to be truncated on both sides of the Ham Lake Pluton (Fig. 1) based on Harrison's (1949) map and recent magnetic data. Although, it is possible that the fault postdates the pluton and is localized along its margin, the angle between the Loonhead Lake Fault and pluton margin (Fig. 2) suggests truncation. This possible truncation of the Loonhead Lake ( $\pm$ Snow Lake) Fault (Fig. 2) warrants further investigation.



**Figure 10.** Boudinaged quartz and carbonate veins in intensely deformed and altered mafic volcanic rocks along the faulted contact with File Lake formation. (GSC 1993-280B)



**Figure 11.** a) Bedding-parallel fault truncating F1 fold. Note boudinage of quartz-feldspar veins along fault surface. b) Flat and ramp structure of early fault. Arrows highlight fault trace. c) Enlargement of 11b showing S1 alignment of coarse micas (arrows) on margins of quartz-feldspar veins which define the fault. S1 is overgrown by staurolite and garnet porphyroblasts to right of pencil. (GSC 1993-280I)

Bailes (1980)	Zwanzig and Schledewitz (1992; pers. comm. 1993)	This study
F1 isoclinal folds	early faulting D1 fold nappes, faults	low-angle faulting (pre- to syn-F1) F1 isoclinal folds
F2 NNE upright folds	D2 out-of-sequence fold nappes	S2 cleavage
F3 E-W folds	D3 NNW-trending upright to recumbent folds	F3 NNE upright folds
	D4 ENE to NNE-trending, upright folds	F4 E- to NE-trending, upright folds

Figure 12. Correlation of structural generations and metamorphism.

The Amisk Group and File Lake formation are also in contact west of Morton Lake (locations C and D) and west of the Barron Lake Pluton (Fig. 2). At location C, File Lake formation turbidites and Amisk Group basalts are exposed within ~2 metres, but the contact is covered. Both units are extensively silicified (± feldspathic alteration) 10-25 m from the contact. This alteration, which is overprinted by a north-to northeast-striking cleavage (S1 or S2), is similar to that along parts of the Loonhead Lake Fault. The File Lake formation – Amisk Group contact on Morton Lake is interpreted as a fault and may be the same age as the Loonhead Lake Fault. The faulted File Lake formation – Amisk Group contact west of the Barron Lake Pluton was interpreted as a post-F4 structure by Bailes (1980). Harrison (1949) suggested this fault merged with the Loonhead Lake Fault. This fault was not examined during this study.

**Small scale faults**

Numerous mesoscopic faults at a low-angle to bedding were identified along the northwest shore of File Lake. Some of these structures truncate F1 folds (Fig. 11a), whereas other faults are folded and overprinted by the S1 cleavage especially where ramps are developed (Fig. 11b, c). Many of these small faults are filled by quartz-feldspar veins which are symmetrically boudinaged both in horizontal and vertical planes, suggesting flattening perpendicular to the faults and S1. The mutually overprinting relationships suggest that these low-angle faults formed during F1/S1.

**Other possible low-angle faults**

The mafic gneisses within the File Lake formation are of probable volcanic origin and form a relatively continuous unit within the File Lake formation north of the Missi Group syncline, but are absent in the southern band of File Lake formation (Fig. 2). This suggests either low-angle faulting in the northern band of File Lake formation or mafic volcanism during deposition of the File Lake formation turbidites. It is

also uncertain whether the contact between Missi Group and File Lake formation is stratigraphic or faulted as discussed above.

**DISCUSSION AND CONCLUSIONS**

**Timing of low-angle faulting**

If the Loonhead Lake Fault is truncated by the ~1830 Ma Ham Lake Pluton (Fig. 2), it may substantially predate peak metamorphism (1815-1807 Ma; Gordon et al., 1990; David and Machado, 1993), and therefore also predate S2, F3/S3, and F4/S4. However, this relationship requires further investigation. If the other possible faults discussed above actually exist (i.e. between File Lake formation and the mafic gneisses or between File Lake formation and Missi Group), then they must predate the S2 cleavage. S2 has a consistent orientation and vergence across all of these possible faults suggesting that it postdates them. These early faults may represent the initial stages of collision and shortening within the volcanic arcs and intervening sedimentary basins.

**Timing of metamorphism**

Several stages of deformation in the File Lake area occurred during regional metamorphism which postdates F1/S1 and outcrop scale low-angle faults. Metamorphic conditions peaked pre-S2 within the sillimanite-garnet-biotite field, and remained near the sillimanite stability field through to F3/S3. S4 microstructures indicate that conditions were sufficient for biotite recrystallization during F4.

Bailes (1980) suggested peak metamorphism postdated F3 folding because his isograds (Fig. 2) appear largely unaffected by the F3 File Lake synform. We argue that the staurolite-biotite isograd is folded by the synform (Fig. 3) and suggest that the detailed trace of the three higher grade isograds may not be well constrained due to limited exposure of suitable rock types. Evidence presented above suggests

that the "melt" isograd may curve to the south toward locations A and B and therefore be folded by the File Lake synform.

### *Correlation of structural generations*

The syncline of Missi Group at Dow Lake has been tentatively traced through to the F1 syncline of Missi Group at File Lake (Fig. 2), therefore providing a basis for structural correlations between low grade rocks at File Lake and high grade gneisses (Fig. 12). Although we did not identify map scale folds in the File Lake area which correlate with D2 folds in the high grade rocks (i.e. Batty Lake complex antiform; Fig. 2), we did identify a cleavage (S2) which postdates F1 isoclinal folds and is folded by north-northeast-trending, upright folds, and is tentatively interpreted as equivalent age (Fig. 12). The S2 cleavage in the File Lake area shows a consistent angular relationship to bedding/S1 indicating antiform approximately to the north (after removing the effects of F3 folding). This suggests that the File Lake area occurs on the southern limb of a F2 antiform which may correlate with the antiform of the Batty Lake Complex.

Further support for the interpreted correlation of structural generations between the low and high grade rocks is provided by the timing of metamorphism. Zwanzig and Schledewitz (1992) suggested that metamorphism peaked after their first generation of fold nappes (Fig. 12), similar to the post-F1/S1, pre-S2 timing for peak metamorphism determined for the File Lake area.

### *Structural / metamorphic transition*

The structural correlations outlined in Figure 12 highlight variations in structural style from the low grade Flin Flon Domain into the high grade gneisses north of Loonhead Lake. The S1 and S2 cleavages and extension lineation of the File Lake area are consistently steep, whereas equivalent age structures to the north dip/plunge gently northeast (~30° or less; Zwanzig and Schledewitz, 1992). This change occurs in pre- to syn-metamorphic structures, therefore suggesting that the transition to gently dipping structures occurred with paleodepth at the time the structures formed. No overprinting structures which could account for the systematic change in dip/plunge have been identified. There are several factors which may have been partly responsible for this structural transition. These include: i) differences in rheology at higher temperature; ii) increasing shear strain with depth (cf. Sanderson 1982); and iii) the influence of the more rigid domain of arc-related volcanic and intrusive rocks to the south. It is likely that all three factors influenced the structural transition between the Flin Flon and Kiseynew domains.

### *The boundary between the Kiseynew and Flin Flon domains*

Defining the boundary between the Flin Flon and Kiseynew domains has been a long-standing problem (e.g. Harrison, 1951). Harrison (1951) defined the boundary as the Kiseynew lineament which largely followed faults, including the Snow Lake

and Loonhead Lake faults, (Fig. 1, 3) and allowed for low and high grade rocks in both domains. In contrast, Bailes (1980) and Froese and Moore (1980) suggested that the "boundary" is gradational and is defined by a rapid increase in metamorphic grade and/or a facies change. The only boundary provided by this interpretation is a metamorphic isograd which is not always obvious in outcrop and cannot be defined in areas where suitable rock types are absent. If the Loonhead Lake and Snow Lake faults define the main boundary between the arc-related rocks and marine turbidites, as proposed here and by Harrison (1951), then perhaps this structure provides a more tangible definition of the boundary between the Flin Flon and Kiseynew domains, at least in this area.

### **ACKNOWLEDGMENTS**

We would like to thank Sue Schaan and Ian Russell for pleasant and efficient assistance in the field; Neil Brandson for logistical services; Alan Bailes for providing thin sections and location maps, and for showing us around the File Lake area; Steve Lucas, Terry Gordon, and Alan Bailes for numerous geological discussions; and Steve Lucas, Simon Hanmer, Edgar Froese, Alan Bailes, and Herman Zwanzig for reviewing the manuscript.

### **REFERENCES**

- Ansdell, K.M.**  
1993: U-Pb constraints on the timing and provenance of fluvial sedimentary rocks in the Flin Flon and Athapapuskow basins, Flin Flon Domain, Trans-Hudson Orogen, Manitoba and Saskatchewan; in *Radiogenic Age and Isotopic Studies: Report 7*; Geological Survey of Canada, Paper 93-2.
- Ansdell, K. M. and Connors, K.A.**  
1994: Lithological and structural relationships in Paleoproterozoic rocks in the east Wekusko Lake area, Trans-Hudson Orogen; in *Current Research 1994-C*; Geological Survey of Canada.
- Bailes, A.H.**  
1980: Geology of the File Lake area; Manitoba Energy and Mines, Geological Report, 78-1, 134p.
- Bailes, A.H. and McRitchie, W.D.**  
1978: The transition from low to high grade metamorphism in the Kiseynew sedimentary gneiss belt, Manitoba; *Metamorphism in the Canadian Shield*, Geological Survey of Canada, Paper 78-10, p. 155-178.
- Briggs, W.D. and Foster, C.T.**  
1992: Pressure-temperature conditions of Early Proterozoic metamorphism during the Trans-Hudson Orogen as determined from rocks straddling the Flin Flon – Kiseynew boundary at Niblock and File Lakes, Manitoba; *Canadian Journal of Earth Sciences*, v. 29, p. 2497-2507.
- David, J. and Machado, N.**  
1993: U-Pb geochronology of the Flin Flon - Snow Lake Belt: New results; in *New Perspectives on the Flin Flon – Snow Lake – Hanson Lake Belt from the NATMAP Shield Margin Project*; Conference Proceedings, CIM meeting Flin Flon, June 1993.
- Froese, E. and Moore, J.M.**  
1980: Metamorphic petrology of the Snow Lake area, Manitoba; Geological Survey of Canada, Paper 78-27.
- Gordon, T.M.**  
1989: Thermal evolution of the Kiseynew sedimentary gneiss belt, Manitoba: metamorphism at an early Proterozoic accretionary margin; in *Evolution of Metamorphic Belts*, (ed.) J.S. Daly, R.A. Cliff, and B.W.D. Yardley; Geological Society Special Publication, v. 43, p. 233-243.

**Gordon, T.M., Hunt, P.A., Bailes, A.H., and Syme, E.C.**

1990: U-Pb ages from the Flin Flon and Kiseynew Belts, Manitoba: chronology of crust formation at an Early Proterozoic accretionary margin; Geological Association of Canada, Special Paper 37, p. 177-199.

**Harrison, J.M.**

1949: Geology and mineral deposits of the File-Tramping Lakes area, Manitoba; Geological Survey of Canada, Memoir 250, 92 p.

1951: Precambrian correlation and nomenclature, and problems of the Kiseynew gneisses in Manitoba; Geological Survey of Canada, Bulletin 20, 53 p.

**Norman, A.R. and Williams, P.F.**

1993: Early Proterozoic progressive deformation along the southern margin of the Kiseynew gneiss belt; Lithoprobe Trans-Hudson Orogen Transect Report.

**Sanderson, D.J.**

1982: Models of strain variation in nappes and thrust sheets: a review; Tectonophysics, v. 88, p. 201-233.

**Stern, R., Lucas, S., Syme, E., Bailes, A., Thomas, D., Leclair, A., and Hulbert, L.**

1993: Geochronological studies in the Flin Flon Domain, Manitoba-Saskatchewan, NATMAP Shield Margin Project area: results for 1992-1993; in Radiogenic Age and Isotopic Studies: Report 7; Geological Survey of Canada, Paper 93-2.

**Stauffer, M.R.**

1990: The Missi Formation: an Aphebian molasse deposit in the Reindeer Lake Zone of the Trans-Hudson Orogen, Canada; in The Early Proterozoic Trans-Hudson Orogen of North America, (ed.) J.F. Lewry and M. R. Stauffer; Geological Association of Canada, Special Paper 37, p. 121-141.

**Zwanzig, H.V.**

1990: Kiseynew Gneiss Belt in Manitoba: stratigraphy, structure, and tectonic evolution; in The Early Proterozoic Trans-Hudson Orogen of North America, (ed.) J. F. Lewry and M. R. Stauffer; Geological Association of Canada, Special Paper 37, p. 95-120.

1992: Geological investigations in the Walton Lake – Evans Lake area (Parts of NTS 63N/2); in Manitoba Energy and Mines, Minerals Division, Report of Activities, 1992, p. 4-7.

**Zwanzig, H.V. and Schledewitz, D.C.**

1992: Geology of the Kississing-Batty Lakes Area: Interim Report; Manitoba Energy and Mines, Open File, OF92-2, 87 p.

---

Geological Survey of Canada Project 910035

# Lithological and structural relationships in Paleoproterozoic rocks in the east Wekusko Lake area, Trans-Hudson Orogen, Manitoba<sup>1</sup>

Kevin M. Ansdell<sup>2</sup> and Karen A. Connors  
Continental Geoscience Division

*Ansdell, K.M. and Connors, K.A., 1994: Lithological and structural relationships in Paleoproterozoic rocks in the east Wekusko Lake area, Trans-Hudson Orogen, Manitoba; in Current Research 1994-C; Geological Survey of Canada, p. 193-203.*

---

**Abstract:** Distinct lithological packages, largely fault-bounded, have been defined east of Wekusko Lake in the Flin Flon Domain, Trans-Hudson Orogen. Packages of sedimentary rocks include the File Lake formation turbidites and two packages of Missi Group sandstones and conglomerates. The packages of volcanic rocks include the North Roberts Lake mafic volcanics, the Herb Lake fold rhyolites, andesites and basalts, a heterogeneous package of felsic volcanic rocks, and the McCafferty Lifter mafic to intermediate lavas and tuffs. The main stage of deformation involved isoclinal F2 folding, and associated faulting which resulted in juxtaposition of lithological packages. Metamorphism occurred during this stage of deformation. Local preservation of an older cleavage indicates an earlier phase of deformation (D1) which may have been responsible for initial thickening and tectonic burial. F2 folds and associated faults are overprinted by F3 folds which postdate peak metamorphism and may represent the terminal stages of this event.

**Résumé :** On a défini des ensembles lithologiques distincts, limités dans une grande part par des failles, à l'est du lac Wekusko dans le domaine de Flin Flon, dans l'orogène transhudsonien. Les ensembles de roches sédimentaires comprennent les turbidites de la formation de File Lake et deux ensembles de grès et conglomérats du Groupe de Missi. Les ensembles de roches volcaniques comprennent les roches volcaniques mafiques de North Roberts Lake, les rhyolites, andésites et basaltes de Herb Lake fold, un ensemble hétérogène de roches volcaniques felsiques, et les laves et tufs intermédiaires à mafiques de McCafferty Lifter. Le principal stade de déformation a été marqué par la formation de plis isoclinaux P2 et le jeu de failles associées qui ont permis la juxtaposition des ensembles lithologiques. Le métamorphisme s'est produit pendant ce stade de déformation. La conservation locale d'une schistosité ancienne révèle une phase initiale de déformation (D1), qui a peut-être causé l'épaississement initial et l'enfouissement tectonique. Aux plis P2 et aux failles associées se surimposent des plis P3 plus récents que la culmination du métamorphisme et pouvant représenter les stades terminaux de cet épisode.

---

<sup>1</sup> Contribution to the NATMAP Shield Margin Project

<sup>2</sup> Department of Geological Sciences, University of Saskatchewan, Saskatoon, Saskatchewan S7N 0W0

## INTRODUCTION

Wekusko Lake occurs in the eastern Flin Flon Domain of the Paleoproterozoic Trans-Hudson Orogen (Fig. 1). The regionally recognized units within this domain include Amisk Group island-arc and ocean-floor rocks (Syme, 1990) which are unconformably overlain by Missi Group fluvial sedimentary rocks (Stauffer, 1990) and structurally overlain (Connors and Ansdell, 1994) by File Lake formation marine turbidites (Bailes, 1980). The supracrustal rocks are intruded by 1875-1835 Ma gabbroic to granitic plutons (Gordon et al., 1990; Ansdell and Kyser, 1991). This domain is bounded by the southern flank of the Kisseynew Domain (Fig. 1) which contains metamorphosed equivalents of Flin Flon Domain rocks (Bailes, 1980; Froese and Moore, 1980). The boundary between the two domains is generally defined as the garnet-biotite-sillimanite isograd (e.g. Zwanzig, 1990).

Previous mapping east of Wekusko Lake examined the distribution of volcanic and sedimentary rocks (Armstrong, 1941; Frarey, 1950), and focused on the gold occurrences (Stockwell, 1937; Galley et al., 1986). The contact relationships between the lithological packages were unclear, based on previous mapping, and lead to complex structural and stratigraphic interpretations. This integrated stratigraphic, structural and geochronological study was therefore initiated. Preliminary lithological and structural observations and interpretations are summarized in this report. This study focused on the stratigraphy, the contact relationships between different rock types, and the relative timing of folding and faulting. The most significant result to date is the identification of several lithologically distinct, fault-bounded packages which were juxtaposed by bedding-parallel faults during isoclinal folding and metamorphism. All rocks are deformed and metamorphosed, but the prefix "meta" is omitted for clarity.

## ROCK UNITS/PACKAGES

This study focused in part on the rock types to define the stratigraphy and the distinct lithological packages. The stratigraphic and lithological data formed the basis for geochronological sampling which will help define age relationships between the fault-bounded packages.

### *File Lake formation package*

Sedimentary rocks west of the Crowduck Bay Fault (Fig. 1) consist of fine grained sandstones, siltstones and mudstones (Fig. 3a). These sedimentary rocks mainly consist of AE Bouma graded beds and were likely deposited by turbidity currents. Changes in younging direction indicate isoclinal folding. Similar rocks on Wekusko Lake have been described by Bailes and Galley (1992), and together are considered to be equivalent to the File Lake formation (e.g. Bailes, 1980).

### *Missi Group packages*

Missi Group rocks (Frarey, 1950) outcrop in two main packages (Fig. 1, 2). Although rock types are similar there are no unambiguous marker horizons, and no direct correlation can be made between these packages.

#### **Eastern package**

The eastern Missi Group package includes lower, middle and upper conglomerates (Fig. 1, 4), which are typically massive, clast-supported, polymictic pebble to boulder conglomerates with similar clast types (Fig. 4). The base of the lower conglomerate is not exposed, but is interpreted as a fault (Fig. 2). The proportion of grits, and crossbedded sandstones increases up sequence, and these lithologies occur as lensoid layers within conglomerates, or more laterally extensive layers with channel scours and pebble lags (Fig. 3b).

Overlying the lower conglomerate are medium- to coarse-grained, tabular and trough crossbedded sandstones. Mud drapes are common on the foresets, and locally define centimetre-scale ripples. The consistent dip direction of crossbedding suggests a unidirectional paleocurrent and supports the interpretation of a fluvial environment. Correlation between these sandstones and parallel-laminated sandstones and siltstones, conglomerates, pebbly sandstones and grits along strike on the southeastern shore of Stuart Lake is unclear, but may indicate facies variations within these fluvial rocks (Fig. 4).

The sandstones above the middle conglomerate are shallow crossbedded to parallel-laminated, and were likely deposited in a quieter environment than underlying sandstones. The crossbed foresets are commonly magnetite-rich (Fig. 3c). Above the upper conglomerate are pebbly sandstones, grits and sandstones in which scour surfaces, graded bedding and rip-up clasts are sometimes observed.

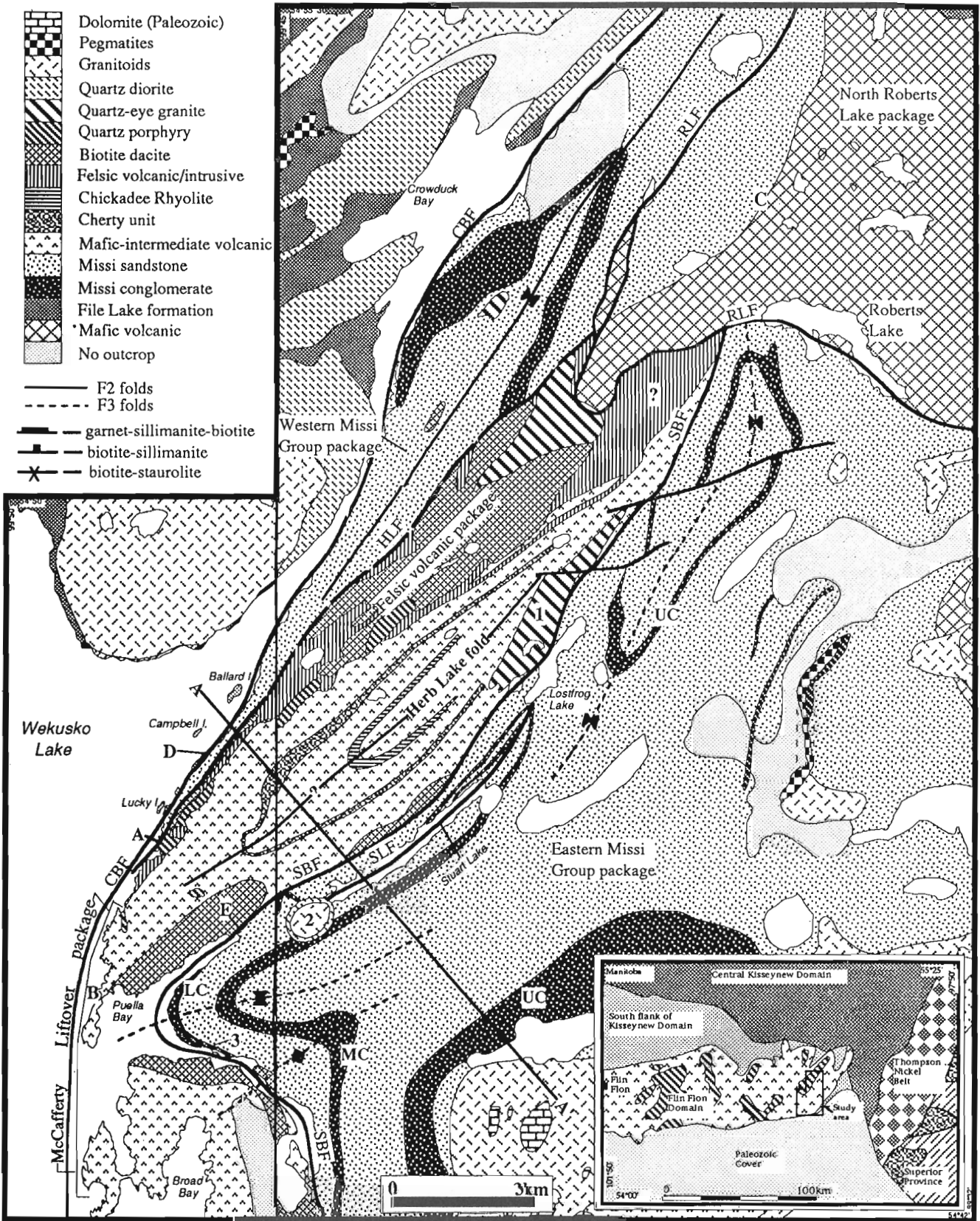
#### **Western package**

At the southernmost outcrops of the western Missi Group package (A, Fig. 1) bedding strikes 090-106°, perpendicular to the regional orientation. At this outcrop conglomerates unconformably overlie a package of rhyolite and felsic tuff (Fig. 5). Approximately 6 m of felsic volcanic rocks have

---

**Figure 1 (opposite).** Simplified geological map of the east Wekusko Lake area (based on Armstrong, 1941; Frarey, 1950; Gordon and Gall, 1982, and this study). Locations A to E are referred to in the text. Intrusions sampled for geochronology are labeled (1, 2, 3). The cross-section A-A' is shown in Figure 8. Abbreviations: CBF – Crowduck Bay Fault, HLF – Herb Lake Fault, SBF – Stuart Bay Fault, SLF – Stuart Lake Fault, RLF – Roberts Lake Fault, LC – Lower conglomerate, MC – Middle conglomerate, UC – Upper conglomerate. Inset shows the location of the study area within the Manitoba part of the Trans-Hudson Orogen.





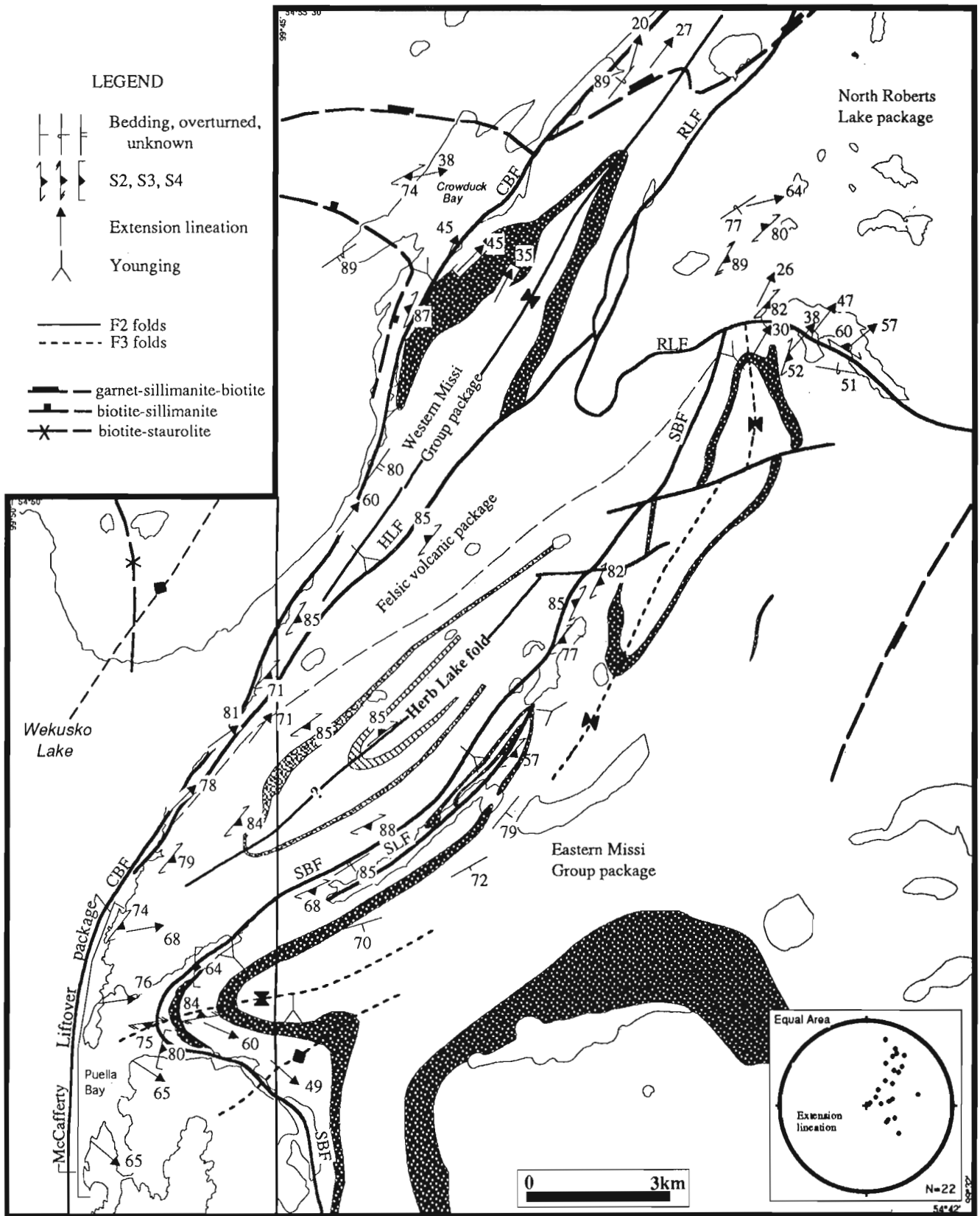
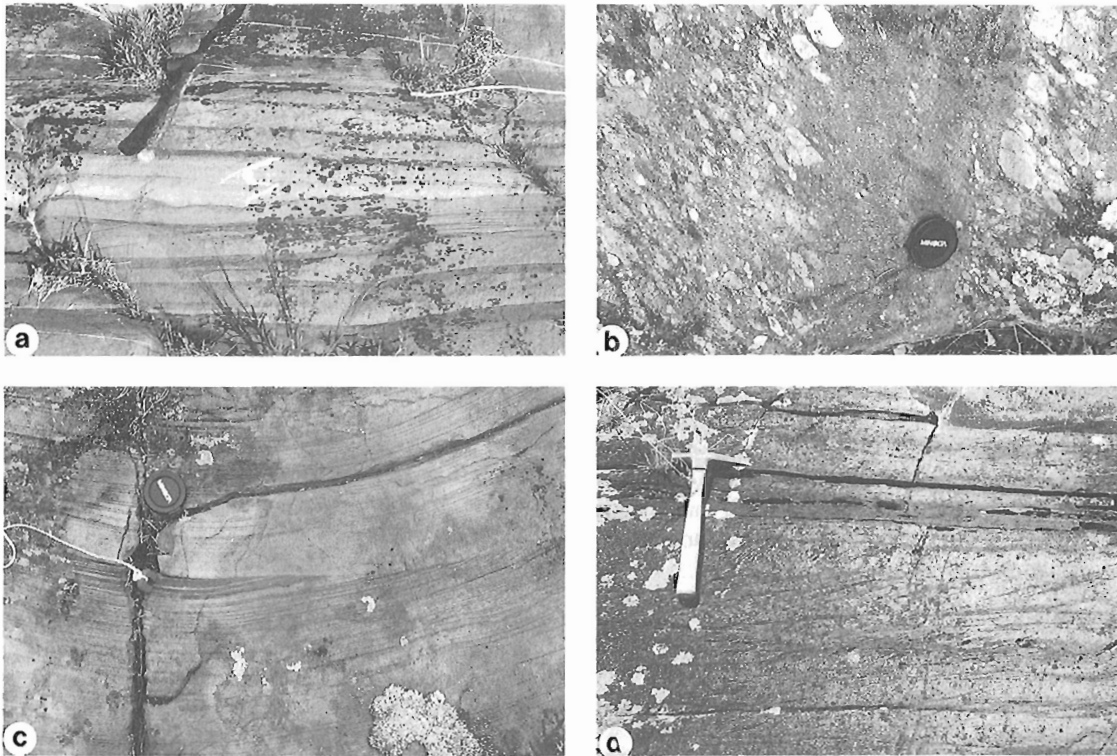
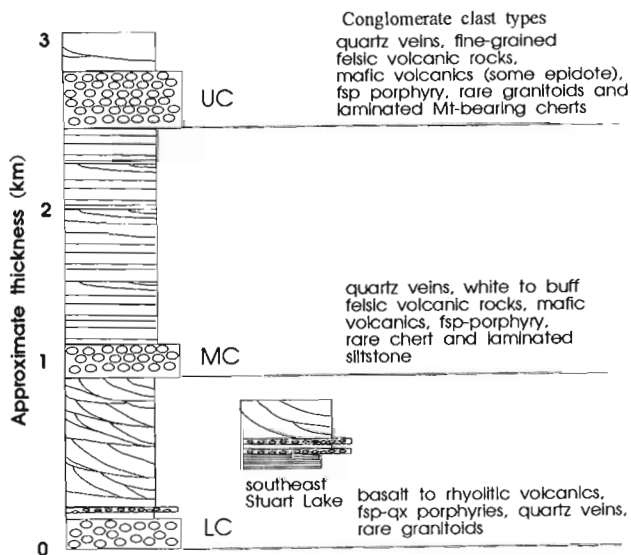


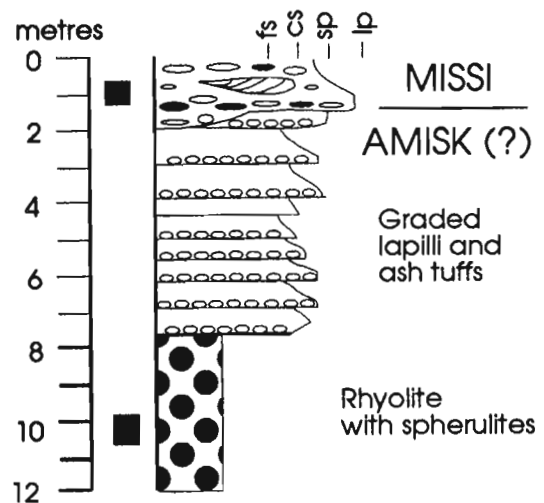
Figure 2. Simplified map of the east Wekusko Lake area showing limited structural data, lithological packages, and major faults. Inset shows stereographic projection of the extension lineation measurements.



**Figure 3.** Outcrop photographs of sedimentary rocks. *a*) Graded turbidites, File Lake formation (GSC 1993-218E). *b*) Interbedded conglomerates and grits, eastern Missi Group. Pebbles are aligned in S4 (GSC 1993-218M). *c*) Shallow crossbedded to parallel laminated, magnetite-rich sandstones, eastern Missi Group (GSC 1993-218Z). *d*) Tabular crossbedded sandstones and interbedded mudstones, western Missi Group (GSC 1993-218T).



**Figure 4.** Simplified stratigraphic section through the sandstones and conglomerates of the eastern Missi Group (based on Shanks and Bailes (1977) and this study). Shown is the inferred correlation between the rocks on the southeast shore of Stuart Lake, and the east shore of Puella Bay. Abbreviations: LC, MC, UC - lower, middle and upper conglomerates, respectively.



**Figure 5.** Stratigraphic section at location A (Fig. 1), emphasizing the unconformable relationship between Missi sedimentary rocks and underlying volcanic rocks. Black squares indicate geochronology samples. Abbreviations: fs - fine sand; cs - coarse sand; sp - small pebbles; lp - large pebbles.

been eroded over a lateral distance of ~20 m. The basal sedimentary rocks consist of polymictic clast-supported conglomerates, gravel and coarse sandstone lenses, sometimes crossbedded. Pebble lags occur within the sandier units. Scour surfaces indicate the sediments stratigraphically overlie the volcanic rocks. Sub-angular to rounded clasts in the conglomerates include quartz veins, felsic volcanic rocks, and chert with magnetite-bands. Magnetite is also present in the matrix. In one portion of the outcrop the conglomerates and sandstones grade laterally into a breccia, consisting of angular clasts of porphyritic to vesicular volcanic rocks, which might suggest a local volcanic source.

The sedimentary rocks farther north along the shoreline have a faulted base, although they may stratigraphically overlie the rocks at location A. The crossbedded sandstones consist of trough and tabular sets of gently dipping foresets with intermittent millimetre to centimetre thick mud seams (Fig. 3d). These rocks grade upwards into coarse sandstones, grits and conglomerates.

This western package widens northward (up plunge) where it includes a conglomerate band within a thick sequence of sandstones (Fig. 1). Magnetite- or mica-rich laminations occur throughout the sandstones, but only locally define crossbeds or low angle truncations. These rocks are similar to the Missi Group sandstones east of the interpreted Roberts Lake Fault (Fig. 1).

### ***North Roberts Lake package***

Volcanic rocks north of the Roberts Lake Fault (Fig. 1, 2) consist of pillowed and massive mafic lavas, tuffs and associated dykes and sills, which have been metamorphosed to amphibolites (Gordon and Gall, 1982). Frarey (1950) recorded younging directions, however, relict primary features have been strongly deformed and no unambiguous younging directions were obtained from limited observations during this study. These rocks are considered to belong to the Amisk Group because they are in stratigraphic contact with west-younging Missi sedimentary rocks to the west (Fig. 1). Although this contact between the mafic volcanic rocks and Missi sedimentary rocks has been interpreted as a fault (Gordon and Gall, 1982), it is exposed over ~40 m and is interpreted here as a stratigraphic contact. Parallel laminated sandstones overlie well-layered mafic volcanics. Relief on this sharp contact averages 1-2 cm, but locally reaches ~20 cm.

### ***Herb Lake fold package***

The Herb Lake fold package of volcanic rocks consists of a complex sequence of massive basaltic flows, andesites, dacites, rhyolites, thinly laminated chert and high-level intrusions (Fig. 1, 2). The Chickadee Rhyolite (Fig. 1), a welded rhyolitic tuff, has been dated at  $1832 \pm 2$  Ma using discordant zircons (Gordon et al., 1990). Younging directions from structurally underlying Missi sedimentary rocks, coupled with the 1832 Ma age, have been used to suggest that the volcanic rocks are Missi in age. However, our results suggest that the volcanic and sedimentary rocks are in fault contact (Fig. 1). High Zr, Y, and

TiO<sub>2</sub> (Gordon and Lemkow, 1987) distinguish the basaltic rocks from typical Amisk Group mafic rocks (Stern et al., in press), although Ta-Nb troughs on element variation diagrams still imply a subduction zone component in their generation. The lack of pillowed mafic volcanic rocks, the presence of welded felsic rocks, and their apparent association with fluvial sedimentary rocks has been used to suggest that these volcanic rocks are dominantly subaerial (Shanks and Bailes, 1977; Gordon and Gall, 1982).

### ***Felsic volcanic package***

On the western edge of the Herb Lake fold package is a heterogeneous package of feldspar-phyric rhyolitic lavas, quartz-feldspar porphyritic intrusions, felsic tuffs and heterolithic debris flows (Fig. 1, 2, 6a). These rocks were identified as "greywacke, arkose, and conglomerate" by Frarey (1950). Stockwell (1937) distinguished these rocks from the more obvious sedimentary rocks along the shore, but identified many of the rocks as arkoses. Our identification of many of the finer grained rocks as felsic volcanic is based on the presence of pink-weathering feldspar crystals (to 5 mm) and local quartz eyes in the fine groundmass. This bimodal grain size distribution is not consistent with even a poorly sorted arkosic rock.

The felsic volcanic rocks exposed at A (Fig. 1) consist of spherulitic rhyolite, overlain by ash and lapilli tuffs exhibiting graded bedding (Fig. 5). These rocks are unconformably overlain by the western Missi package. Geochronology samples have been taken to determine the age of these felsic volcanic rocks, and their correlation with the Chickadee Rhyolite and other felsic volcanic rocks described above.

### ***McCafferty Liftover package***

The McCafferty Liftover package of mafic and intermediate volcanic and volcanoclastic rocks is well-exposed along the east shore of Wekusko Lake (Fig. 1, 2). This succession is distinct from the Herb Lake fold package, but the contact relationships are unknown due to lack of outcrop. Aphyric, plagioclase-phyric, and amygdaloidal basaltic rocks, which are commonly pillowed and have recrystallized hyaloclastite matrices (Fig. 6b), are typically deformed and provide no unambiguous evidence of younging directions. At B (Fig. 1) a sequence of intermediate agglomerates and turbiditic crystal tuffs is exposed. Agglomerates intimately associated with the turbiditic tuffs are usually monomict, comprising angular to sub-rounded blocks, up to 20 cm in length, which contain up to 3 mm plagioclase crystals in a fine grained dark matrix (Fig. 6c). The turbiditic tuffs consist of graded beds, up to 10 cm in thickness, consisting of plagioclase crystal-rich bases and finer grained laminated, and rare cherty, tops (Fig. 6c). Erosive bases and graded bedding indicate eastward younging. These rocks are cut by plagioclase-phyric dykes which are compositionally similar to the volcanic rocks. The agglomerates may represent pyroclastic flows related to the climactic stage of a submarine volcanic eruption, with later reworking by turbidity currents as volcanic activity waned (e.g. Fiske and Matsuda, 1964). Overlying these volcanoclastics is a heterogeneous package of dacitic volcanic rocks

(Armstrong, 1941). They consist of massive lavas or intrusions, heterolithic debris flows (Fig. 6d), and volcanic breccias, and outcrop on Puella Bay (Fig. 1).

Shoreline outcrops of the McCafferty Lifter package suggest it is a compositionally evolving package of submarine mafic to intermediate volcanic and volcanoclastic rocks. This contrasts with the subaerial depositional environment inferred for volcanic rocks in the Herb Lake fold package (Fig. 1), indicating a complex volcanic paleogeography, faulting, and/or significant age variations which have not been identified.

### ***Intrusive rocks***

In the Wekusko Lake area, there are several types of felsic intrusions, some of which are associated with the volcanic rocks (Fig. 1), and numerous small (up to a few metres wide) coarse grained gabbro and diorite bodies, aphyric and sometimes plagioclase-phyric, banded mafic dykes, and feldspar-porphyrific felsic dykes. Three distinct intrusive bodies (numbered in Fig. 1) have been sampled for geochronology with the aim of providing minimum age constraints on deposition of sedimentary and volcanic rocks:

1. The Lostfrog Lake quartz-porphyrific granite cuts the volcanic rocks in the Herb Lake fold package, and is cut by the Stuart Bay Fault;

2. The Stuart Lake biotite-granodiorite, which is rimmed by a coarse grained gabbro, intrudes the older portions of the eastern package of Missi sedimentary rocks; and
3. The Puella Bay quartz-feldspar porphyry intrudes the lower Missi conglomerate and is cut by the Stuart Bay Fault.

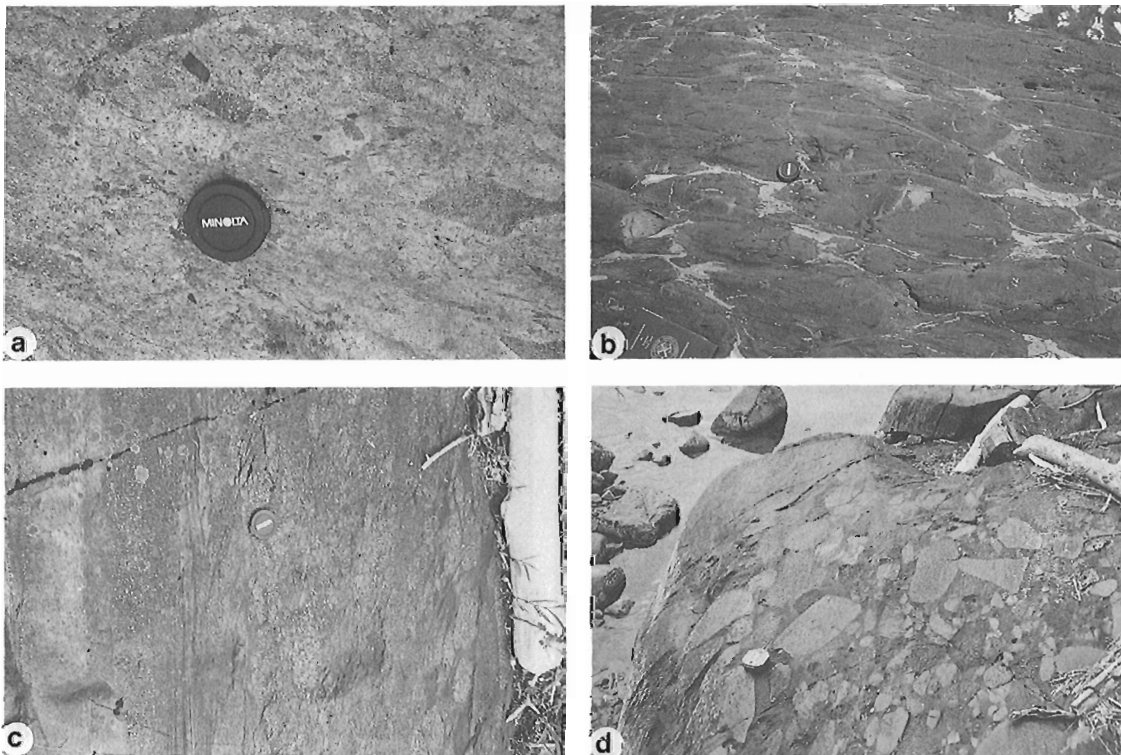
## **METAMORPHISM**

Metamorphic grade east of the Crowduck Bay Fault ranges from biotite to sillimanite grade and increases northward and eastward (Fig. 2). Gordon and Gall (1982) mapped several isograds, but the paucity of suitable rock types hampered their work. Briggs and Foster (1992) estimated P-T conditions of 525-625°C and 2.5-5 kbar in andalusite- and sillimanite-bearing rocks in the Niblock Lake area, northeast of Roberts Lake.

## **FOLD AND CLEAVAGE GENERATIONS**

### ***Syn-depositional folding***

Syn-sedimentary folds occur within the sandstones of the Missi Group at the north end of Stuart Lake (Fig. 1). These disharmonic, non-cylindrical folds occur between planar horizons of thinly bedded sandstones (Fig. 7a). The slump-folded layers range from 10 to ~50 cm thick. Although some



**Figure 6.** Outcrop photographs of volcanic rocks. **a)** Felsic heterolithic debris flow (felsic volcanic package; GSC 1993-218S). **b)** Pillowed mafic lavas (GSC 1993-218U). **c)** Graded crystal turbiditic tuffs underlying a compositionally similar agglomerate (GSC 1993-218R). **d)** Intermediate heterolithic debris flow (GSC 1993-218L). (b, c and d are from McCafferty Lifter package).



slump folds are recumbent and have axial planes sub-parallel to the bedding-parallel (S2) cleavage, most of these folds are overprinted by the cleavage.

### Early deformation

The oldest cleavage (S1) has been identified at a few localities, however no F1 folds have been recognized. In the core of the F2 syncline at location A (Fig. 1) some pebbles in the Missi conglomerate preserve an east-west, bedding parallel fabric which is overprinted by S2. In the File Lake formation, S1 has been locally observed sub-parallel to bedding. S2 and F2 also overprint boudinaged gabbro sills and quartz veins (Fig. 7b). These boudins are generally symmetrical in both the horizontal and vertical planes indicating a flattening strain. The S1 cleavage may have developed during this phase of flattening, or during a separate, pre-S2 deformation phase.

### Pervasive F2/S2/L2 development

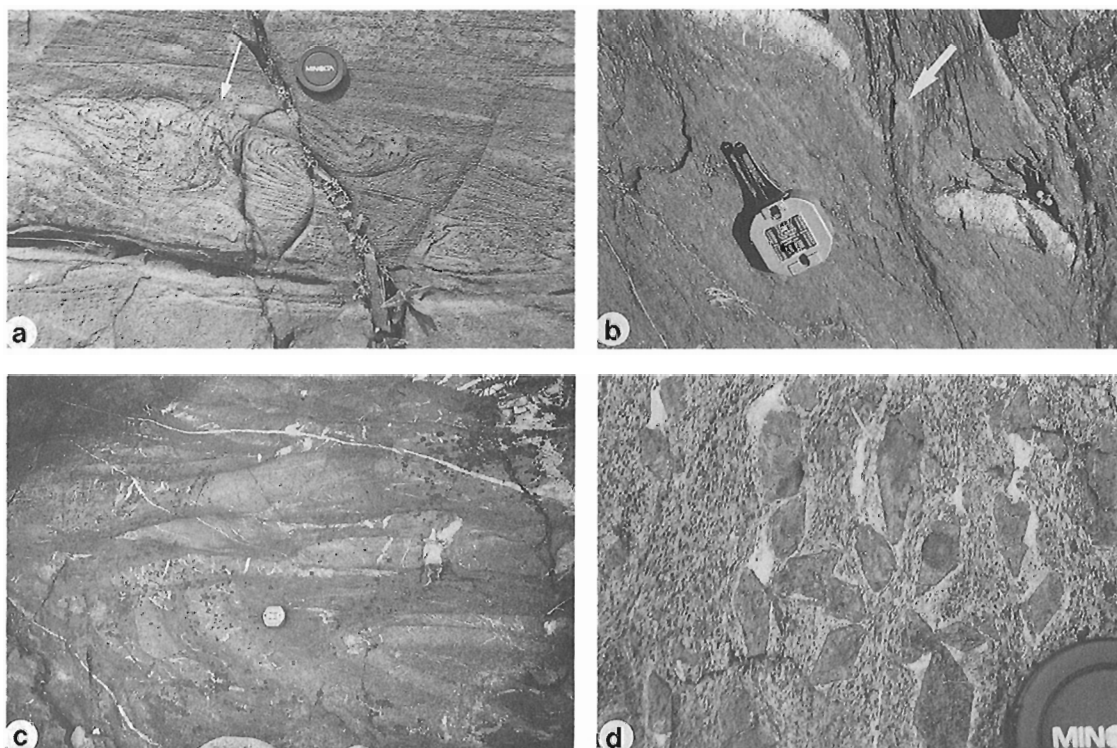
The dominant northeast-striking S2 foliation is largely parallel to layering and is axial planar to tight to isoclinal folds. Isoclinal folds with thickened hinges and thinned limbs occur throughout the File Lake formation. F2 fold hinges are commonly truncated by cleavage-parallel faults (Fig. 7c).

Correlation of S2 from the File Lake formation to the Missi Group suggests that several map scale folds in the Missi Group are F2 (Fig. 1).

Outcrop-scale matrix-porphyroblast relationships suggest that metamorphism occurred during F2/S2. In biotite-grade rocks, S2 is defined by phyllosilicates which have crystallized or recrystallized syn- to post-S2. In the staurolite-garnet zone, S2 is deflected around staurolite porphyroblasts (Fig. 7d), but garnet overgrows the cleavage.

The Herb Lake fold (Fig. 1) is interpreted as F2 based on similarities in the style of mesoscopic folds and the timing of cleavage development with respect to metamorphism, between it and other F2 folds. It is uncertain, however, whether this structure is synformal or antiformal because the limbs are sub-parallel and the hinge is poorly exposed. This fold has been interpreted as synclinal based on younging directions in structurally underlying Missi Group rocks (Frarey 1950), however our observations suggest that the volcanic package is fault-bounded (see below).

The L2 extension lineation is developed in all units and is defined by elongate minerals and by stretched clasts in conglomerates, agglomerates and breccias. The L2 lineation is the dominant fabric in some conglomerates, breccias and fine grained felsic intrusions. In the south, the lineation plunges steeply (70-80°) north-northeast, but shallows to ~20° in the



**Figure 7.** a) Synsedimentary folds in the Missi Group sandstones on the north shore of Stewart Lake (GSC 1993-230N). b) F2 fold (arrow) and S2 overprinting boudinaged quartz vein in File Lake formation (GSC 1993-229H). c) S2-parallel faults on the limb of an F2 fold in the File Lake formation (GSC 1993-229S). d) Deflection of S2 cleavage (defined by biotite) around staurolite porphyroblasts (GSC 1993-229K).



north (Fig. 2). F2 fold axes parallel the extension lineation in the File Lake formation, but are doubly plunging in Missi Group rocks (Fig. 1).

### F3 folds and S3 cleavage

F3 folds and a weak S3 cleavage are developed within the eastern package of Missi rocks (Fig. 1). The anticline-syncline pair overprint a strong bedding-parallel fabric and appear to plunge steeply northeast. The variation in orientation of the extension lineation around Puella Bay may be related to folding by the F3 syncline (Fig. 2). S3 is poorly developed in the core of the syncline.

### S4 cleavage

A well-developed, northerly-striking cleavage (S4) overprints F3 folds at Puella Bay. Although this fabric is not recognized elsewhere, it is locally quite intense at Puella Bay (Fig. 3b). The origin of this fabric is unknown; it could be related to unrecognized cross-folds or faulting in Wekusko Lake.

## FAULTING

Although previous workers interpreted most contacts between lithological packages as stratigraphic, our observations suggest that these packages are fault-bounded. These faults are described from west to east.

### Crowduck Bay Fault

The contact between the File Lake formation and the western Missi package was interpreted as sedimentary by Frarey (1950), and as a fault (Crowduck Bay Fault) by Gordon and Gall (1982). There is 1-10 m of no outcrop along most of the contact. Faulting is suggested by truncation of Missi conglomerates east of Crowduck Bay (Fig. 1). At location D (Fig. 1), both units are exposed within about 1 m and an intense, S2-parallel fabric is developed. The possible S2 strain gradient and consistent orientation of S2 and L2 across the fault, suggest syn-S2/F2 faulting. This timing relationship, along with the syn-S2 timing of metamorphism, argues against substantial post-metamorphic movement. This suggests that the apparent deflection of the isograds (Gordon and Gall, 1982; Fig. 2) results from insufficient exposure of suitable rock types or offset on a separate, younger fault.

### Herb Lake Fault

The eastern contact of the western Missi Group package with the felsic volcanic rocks has been interpreted as stratigraphic (Armstrong 1941; Frarey 1950). However, at location A (Fig. 1) where Missi conglomerates unconformably overlie felsic volcanic rocks, these rocks are folded by a F2 syncline and the hinge is truncated against the felsic volcanic package. This truncation is attributed to a syn- to post-F2 fault (Herb Lake Fault). This fault is extrapolated to the northeast (Fig. 1), although it is not exposed.

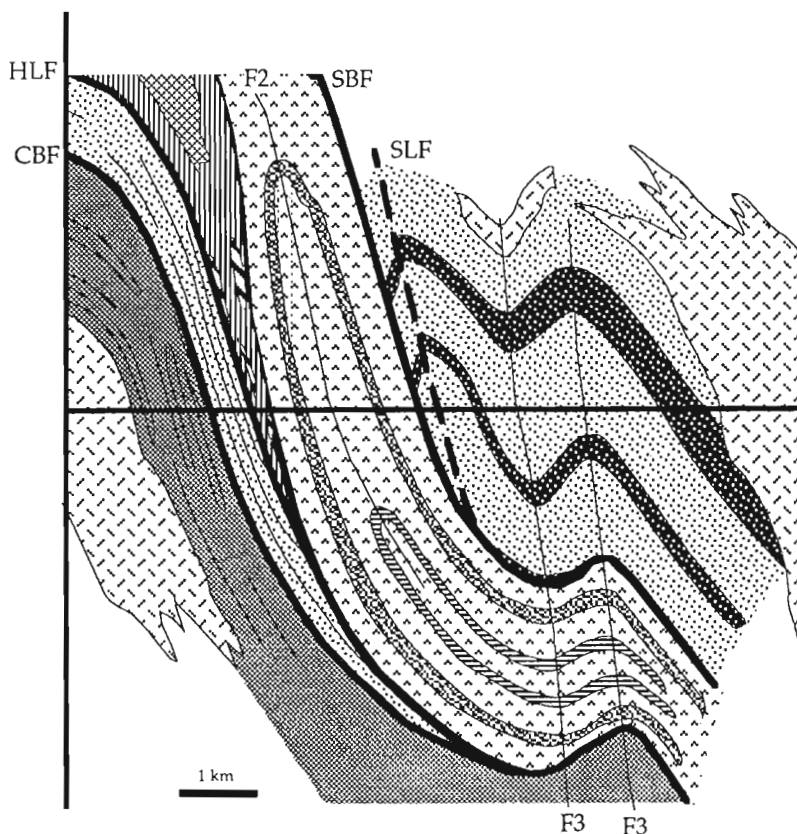


Figure 8.

Preliminary cross-section (A-A', Fig. 1) indicating the possible fold and thrust geometry. Note that the Herb Lake fold may be either a synform or an antiform, although it is depicted as an antiform here.

### **Stuart Bay Fault**

The contact between the Herb Lake fold volcanic package and the eastern Missi package has similarly been interpreted as stratigraphic (Frarey, 1950). The contact is exposed along the shore of Lostfrog Lake (Fig. 1) where mafic to intermediate tuff is juxtaposed with sandstones. Both units are intensely silicified and there is evidence of millimetre-scale brecciation. The alteration is overprinted by S2, suggesting alteration and brecciation, possibly related to faulting, occurred pre- to syn-S2/F2. At location E (Fig. 1) an aphanitic felsic igneous rock within the volcanic package, is brecciated near the contact with Missi sandstones. The breccia fragments in a quartz matrix are stretched parallel to L2, supporting pre- to syn-S2/L2 faulting. Furthermore, absence of the lower Missi conglomerate suggests the contact is faulted (Stuart Bay Fault; Fig. 1). This fault is interpreted to extend from Roberts Lake, where it is apparently truncated by the Roberts Lake Fault (Fig. 1), south to Puella Bay where it is folded by F3 structures (Fig. 1, 2).

### **Stuart Lake Fault**

Stuart Lake Fault occurs within the eastern Missi Group rocks and disrupts the hinge of the F2 anticline between Stuart and Lostfrog lakes (Fig. 1). This fault was first interpreted by Shanks and Bailes (1977). The continuation of this fault south of Stuart Lake or north of Lostfrog Lake is uncertain due to poor outcrop.

### **Roberts Lake Fault**

Roberts Lake Fault (Frarey, 1950; Bailes, 1985) juxtaposes the North Roberts Lake mafic volcanic package with the eastern Missi Group package (Fig. 1, 2). Frarey (1950) interpreted this fault to die out west of the Stuart Bay Fault, but absence of the lower Missi Group and truncation of the Stuart Bay Fault suggest substantial movement. Based on existing mapping, it appears most likely that the fault changes orientation and continues north (Fig. 1) rather than dying out. Although the most likely location for the fault is along the north-striking section of the contact between mafic volcanic rocks and Missi Group, this contact is stratigraphic, not faulted (as discussed above). The Roberts Lake Fault is therefore interpreted to cut up section into the Missi sedimentary rocks and juxtapose this sequence of mafic volcanic and Missi sedimentary rocks with the western Missi package along a fault mapped by Frarey (1950) (Fig. 1). The change in orientation of this fault (Fig. 1) may result from intersection of a curving fault (due to ramping or folding) with the erosion surface.

## **PRELIMINARY TECTONIC INTERPRETATION**

Overprinting relationships indicate that the Crowduck Bay and Stuart Bay faults formed pre- to syn-S2, but syn-S2/F2 development is favoured because both are subparallel to S2.

Furthermore, the association of faulting with this fold/cleavage forming event is supported by the commonly sheared/faulted limbs on mesoscopic folds (Fig. 7c). Although the Herb Lake and Stuart Lake faults cut F2 hinges, they are subparallel to S2, and may have formed during the same period of folding and faulting.

This temporal association between F2 folding and faulting suggests development in either a fold and thrust belt or a terrain dominated by steep strike-slip or reverse faults with significant shortening perpendicular to these faults (i.e. transpression). The fold and thrust belt hypothesis is favoured due to the progressive northward shallowing of F2 and L2 plunges (Fig. 2) which appears to be primary, suggesting that F2 folds (and associated faults) originated as steep structures in the south and as shallow structures in the north (cf. Murphy, 1987). This geometry is consistent with thrusting of deeper structural levels southwest over low grade rocks. However, the axial trace of the F2 folds and fault traces trend north-northeast parallel to the stretching lineation, and the F2 anticline along Stuart Lake closes to the northwest (after removing F3 effects) favouring north-west-directed movement on the faults. The relationship between folds and the extension lineation requires further evaluation. It is possible that F2 folds formed parallel, or were rotated parallel, to the extension direction.

Pre- to syn-S2 porphyroblast growth indicates that metamorphism occurred during this stage of shortening/thickening. This also suggests that, in order to account for syn-F2/S2 metamorphism, substantial thickening must have occurred *prior* to this phase of deformation. It is likely that pervasive deformation during folding (F2/S2) and related faulting may have obliterated most pre-existing structures.

This study presents some of the first evidence of fold-thrust belt tectonics in the Trans-Hudson Orogen. This is significant in a collisional orogen where relatively few low-angle faults have been recognized, and provokes questions regarding the structural geometry throughout the region. The association between increasing metamorphic grade and shallowing of structures (as in the File Lake area; Connors and Ansdell, 1994) has implications for the transition between the Flin Flon and Kiseynew domains elsewhere. Although further work remains to be done, this model may have significant implications for tectonic interpretations throughout the Trans-Hudson Orogen.

## **CONCLUSIONS**

1. The east Wekusko Lake map area is dominated by a series of lithologically distinct, fault-bounded packages.
2. These rock packages were juxtaposed by bedding-parallel (and S2-parallel) faults which formed in association with the F2 folds, and may represent a fold-thrust belt.
3. Metamorphism was contemporaneous with F2 folding and associated faulting.

## ACKNOWLEDGMENTS

The enthusiastic and competent assistance of Ian Russell and Sue Schaan made fieldwork easy. Neil Brandson provided logistical support. Geological discussions with Al Bailes, Terry Gordon, Dan Ziehlke, and Al Galley are appreciated. Constructive reviews were made by Steve Lucas and Jack Henderson.

## REFERENCES

- Ansdell, K.M. and Kyser, T.K.**  
1991: Plutonism, deformation, and metamorphism in the Proterozoic Flin Flon greenstone belt, Canada: limits on timing provided by the single-zircon Pb-evaporation technique; *Geology*, v. 19, p. 518-521.
- Armstrong, J.E.**  
1941: Wekusko, Manitoba; Geological Survey of Canada, Map 665A.
- Bailes, A.H.**  
1980: Geology of the File Lake area; Manitoba Energy and Mines, Geological Report, 78-1, 134 p.  
1985: Geology of the Saw Lake area; Manitoba Energy and Mines, Geological Report GR83-2, 47 p.
- Bailes, A.H. and Galley, A.G.**  
1992: Geology of the Kormans Lake area (63J/13SW); Manitoba Energy and Mines, Mineral Division, Report of Activities, 1992, p. 65-74.
- Briggs, W.D. and Foster, C.T.**  
1992: Pressure-temperature conditions of Early Proterozoic metamorphism during the Trans-Hudson Orogen as determined from rocks straddling the Flin Flon – Kiseynew boundary at Niblock and File Lakes, Manitoba; *Canadian Journal of Earth Sciences*, v. 29, p. 2497-2507.
- Connors, K.A. and Ansdell, K.M.**  
1994: Transition between the Flin Flon and Kiseynew Domains of the Trans-Hudson Orogen, File Lake-Limestone Point Lake area, northern Manitoba; Geological Survey of Canada, *Current Research* 1994-C.
- Fiske, R.S., and Matsuda, T.**  
1964: Submarine equivalents of ash flows in the Tokiwa Formation, Japan; *American Journal of Science*, v. 262, p. 76-106.
- Frarey, M.J.**  
1950: Crowduck Bay, Manitoba; Geological Survey of Canada, Map 987A.
- Froese, E. and Moore, J.M.**  
1980: Metamorphic petrology of the Snow Lake area, Manitoba; Geological Survey of Canada, Paper 78-27.
- Galley, A.G., Ziehlke, D.V., Franklin, J.M., Ames, D.E., and Gordon, T.M.**  
1986: Gold mineralization in the Snow Lake-Wekusko Lake region, Manitoba; in *Gold in the Western Shield*, (ed.) L.A. Clark; The Canadian Institute of Mining and Metallurgy, Special Volume 38, p. 379-398.
- Gordon, T.M. and Gall, Q.**  
1982: Metamorphism in the Crowduck Bay area, Manitoba; *Current Research, Part A*; Geological Survey of Canada, Paper 82-1A, p. 197-201.
- Gordon, T.M. and Lemkow, D.**  
1987: Geochemistry of Missi Group volcanic rocks, Wekusko Lake, Manitoba; Geological Survey of Canada, Open File 1442.
- Gordon, T.M., Hunt, P.A., Bailes, A.H., and Syme, E.C.**  
1990: U-Pb ages from the Flin Flon and Kiseynew Belts, Manitoba: chronology of crust formation at an Early Proterozoic accretionary margin; Geological Association of Canada, Special Paper 37, p. 177-199.
- Murphy, D.C.**  
1987: Suprastructure/infrastructure transition, east-central Cariboo Mountains, British Columbia: Geometry, kinematics and tectonic implications; *Journal of Structural Geology*, v. 9, p. 13-30.
- Shanks, R.J. and Bailes, A.H.**  
1977: "Missi Group" rocks, Wekusko Lake area; Report of Field Activities, Manitoba Mineral Resources Division, p. 83-87.
- Stauffer, M.R.**  
1990: The Missi Formation; Geological Association of Canada, Special Paper 37, p. 121-142.
- Stern, R., Syme, E.C., and Bailes, A.H.**  
in press: Geochemical and isotopic synthesis of Amisk Group mafic metavolcanic rocks, Flin Flon belt; Lithoprobe Trans-Hudson Orogen Transect, Annual Workshop Report.
- Stockwell, C.H.**  
1937: Gold Deposits of Herb Lake area, Northern Manitoba; Geological Survey of Canada, Memoir 208.
- Syme, E.C.**  
1990: Stratigraphy and geochemistry of the Lynn Lake and Flin Flon metavolcanic belts, Manitoba; Geological Association of Canada, Special Paper 37, p. 143-161.
- Zwanzig, H.V.**  
1990: Kiseynew Gneiss Belt in Manitoba: stratigraphy, structure, and tectonic evolution; Geological Association of Canada, Special Paper 37, p. 95-120.



# Glacial dispersal and drift composition, Rice Lake Greenstone Belt, southeastern Manitoba<sup>1</sup>

P.J. Henderson

Terrain Sciences Division

*Henderson, P.J., 1994: Glacial dispersal and drift composition, Rice Lake Greenstone Belt, southeastern Manitoba; in Current Research 1994-C; Geological Survey of Canada, p. 205-214.*

---

**Abstract:** Quaternary geology mapping and till sampling in the Rice Lake Greenstone Belt is oriented toward understanding the major factors influencing mineral exploration using drift prospecting. These factors include: the nature of glacial dispersal, bedrock composition, and the extent of postglacial weathering. Ice flow indicators and patterns of glacial dispersal of clasts from known sources indicate the area was glaciated predominantly by ice flowing southwest during the last glaciation. Near Lake Winnipeg, the striation record is more complex. Older striae indicate ice flow toward the south-southwest, southeast, and south, although relative ages are unclear. Trace element concentrations in the <0.063 mm fraction of till reflect bedrock composition, and anomalous gold values are directly related to known occurrences or zones of gold mineralization. In vertical profiles, variations in trace element values show patterns related to postglacial weathering. These effects are minimized at depths over 0.6 m, which suggests the zone below may provide the most consistent sample medium.

**Résumé :** La cartographie des dépôts meubles et l'échantillonnage des tills dans la ceinture de roches vertes de Rice Lake ont pour but de nous renseigner sur les facteurs principaux qui influencent l'application des méthodes de la géologie du Quaternaire à l'exploration minérale. Ces facteurs comprennent : la nature de la dispersion glaciaire, la composition de la roche en place et le degré d'altération postglaciaire. Les indicateurs d'écoulement glaciaire et le mode de dispersion glaciaire de cailloux à partir d'une source connue indiquent que la région a été englacée par des glaciers s'écoulant vers le sud-ouest durant la dernière glaciation. Près du lac Winnipeg, les stries indiquent un patron plus complexe. Des stries antérieures indiquent un écoulement glaciaire vers le sud-sud-ouest, le sud-est et le sud. Cependant, leurs âges relatifs demeurent incertains. La concentration d'éléments traces dans la fraction inférieure à 0,063 mm du till reflète la composition de la roche en place et les valeurs anormales d'or sont reliées directement à la présence d'or dans la roche en place. Dans les profils verticaux, les variations des valeurs des éléments traces indiquent des patrons associés à l'altération postglaciaire. Ces effets sont réduits à des profondeurs supérieures à 0,6 m, ce qui suggère que cette zone pourrait représenter la matière d'échantillonnage la plus consistante.

---

<sup>1</sup> Contribution to Canada-Manitoba Partnership Agreement on Mineral Development (1990-1995), a subsidiary agreement under the Canada-Manitoba Economic and Regional Development Agreement.

## INTRODUCTION

During 1993, surficial geology mapping and drift sampling continued in the westernmost part of the Rice Lake Greenstone Belt, southeastern Manitoba (Henderson, 1993). This study is oriented toward developing drift prospecting methods specific to the area as part of the joint Canada-Manitoba Partnership Agreement on Mineral Development. The main objectives are to establish a regional geochemical database and provide a geological framework for interpreting the glacial dispersal of components of till derived from mineralized bedrock. The greenstone belt has a high potential for gold and base metal mineralization, with many reported occurrences dating back from the first gold discovery in 1911 (Theyer, in press).

Prior to this study, the Quaternary geology was mapped at 1:100 000 scale based on air photo interpretation with limited ground observations (Nielsen, 1980). Local studies relating to aggregate resources (Berssenbrugge, 1986) and placer gold deposits of the Manigotagan area (NTS 62P/1) have been published (Nielsen, 1986; Nielsen and Dilabio, 1987). Relevant Quaternary geology studies in the interlake district west and south of the study area concentrated on assessing aggregate reserves and defining ice flow history (Groom, 1985), and till geochemistry and glacial stratigraphy (Nielsen, 1989).

This paper is based on the results of field investigations during the summers of 1992 and 1993. It summarizes glacial dispersal as indicated by ice flow measurements and glacial transport of specific lithologies from known outcrop areas. Till geochemistry will also be examined to determine lateral and vertical variation in drift composition. All these aspects of the project are fundamental to drift prospecting. They provide a means of determining the extent of glacial erosion and transport, provenance control on till geochemistry, and the effectiveness of the sampling methodology.

## REGIONAL SETTING

The study area is located in southeastern Manitoba, within the Superior structural province of the Canadian Shield and near the margin of Phanerozoic cover (Fig. 1). It is underlain primarily by Archean supracrustal and intrusive rocks of the southeasterly trending Rice Lake Greenstone Belt, which is in fault contact to the north and south with plutonic and gneissic rock types (McRitchie and Weber, 1971). Paleozoic quartz sandstone and dolomite outcrop along the western margin of the study area, on the shore and some islands of Lake Winnipeg.

The area was glaciated by ice flowing primarily from the northeast (Manitoba Mineral Resources Division, 1981). During ice retreat, the entire area was inundated by glacial Lake Agassiz resulting in extensive deposition of glacio-lacustrine sediments within topographic lows (Nielsen, 1980). These deposits are up to 10 m thick and consist of glaciolacustrine rhythmically bedded sand, silt, and clay and glaciolacustrine ice-contact deposits modified by lacustrine processes. At higher elevations, drift deposits are generally

thin and discontinuous, with thicker accumulations of till occurring in depressions or on the down-ice side of bedrock knobs. In most of the area, only one till is recognized.

On Black Island and the mainland adjacent to Lake Winnipeg, overlying lithologically distinct tills have been observed that may represent a multiple ice flow history. In these sections, till composed predominantly of clasts derived from Paleozoic sources overlies Precambrian derived till. Striation patterns are also more complex near the lake, with older striae indicating ice flow towards the south, south-southwest, and southeast. This complexity may be related to the interaction between southwesterly ice flow and southeasterly flowing ice (the Red River Lobe) recognized west and south of the lake (Groom, 1985; Nielsen, 1989) (Fig. 1). In both these areas,

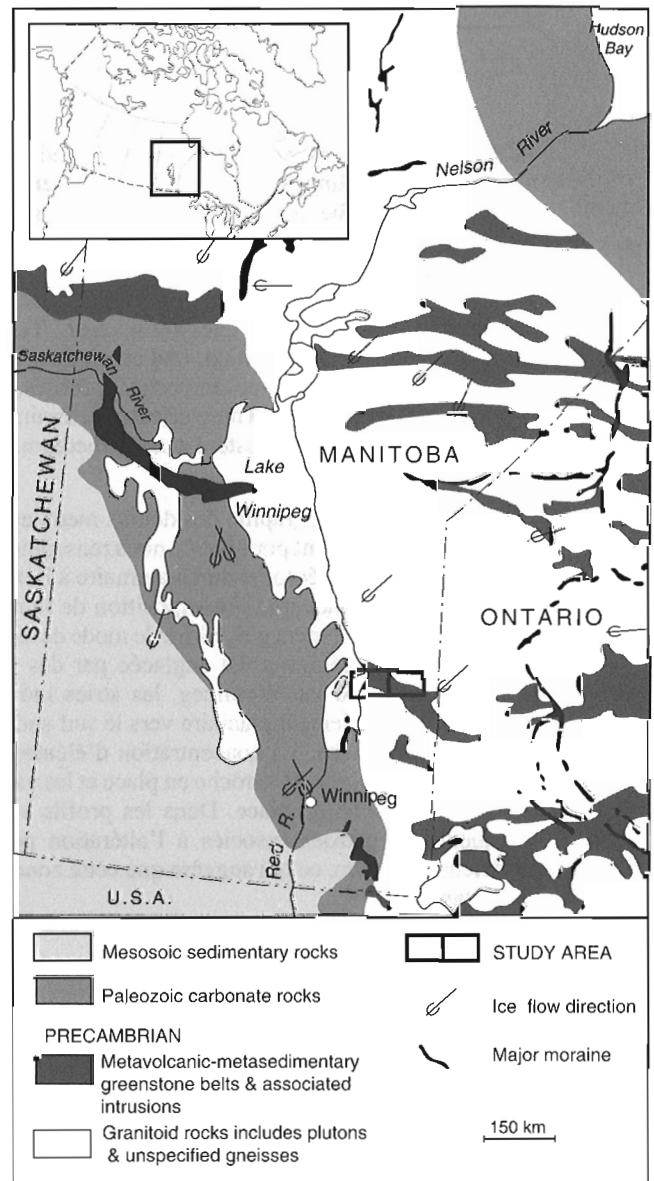


Figure 1. Location map for the study area showing major moraines and regional ice flow trends (after Prest et al., 1968).



ice flow toward the southwest was found to predate ice flow toward the southeast. Till associated with the younger flow has been interpreted as a late glacial deposit formed by the readvance of an ice lobe into glacial Lake Agassiz (Groome, 1985).

## BEDROCK GEOLOGY AND GOLD MINERALIZATION

The Archean Rice Lake Greenstone Belt trends east-southeast across the study area (Stockwell, 1938; Russell, 1949; Davies, 1950; Ermanovics, 1970; McRitchie and Weber, 1971). It consists of a sequence of folded and faulted metavolcanic and metasedimentary rocks of the Rice Lake Group which is intruded by quartz diorite plutons, mafic sills and dykes, and ultramafic plugs, and is unconformably overlain by metasedimentary rocks of the San Antonio Formation, primarily feldspathic quartzite. Margins of the greenstone belt are in fault contact with plutonic and gneissic rocks of the Wanipigow River plutonic complex and the Manigotagan gneissic belt to the north and south, respectively. Ultramafic intrusions occur as discontinuous serpentized lenses within the Wanipigow River plutonic complex (Scoates, 1971).

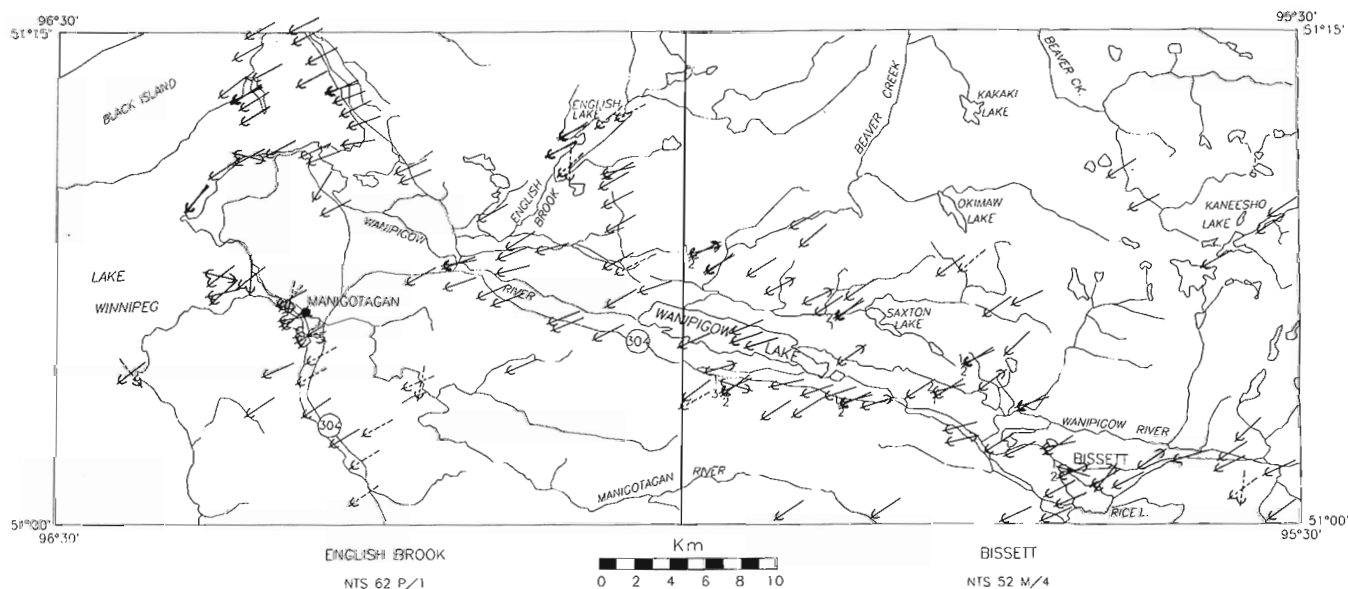
Known mineralization is largely limited to gold, although mafic and ultramafic bodies in the area have been examined as potential environments for massive sulphide and/or platinum group mineralization (Theyer, 1987; Weber, 1991). In other areas of Manitoba, a relationship has been recognized between nickel sulphide deposits and discrete ultramafic intrusions (e.g., Lynn Lake Gabbro); however the relevant

minerals are rare in the Rice Lake area (Scoates, 1971). Hydrothermal alteration in the mafic metavolcanic rocks near English Brook does indicate a potential for volcanogenic massive sulphide deposits (Weber, 1991).

Gold mineralization in the area is structurally controlled. It is confined predominantly to auriferous quartz veins in shear zones hosted by mafic intrusions. Gold occurs as particles in micro-crystalline quartz or disseminated in sulphide minerals, particularly pyrite, arsenopyrite, and chalcopyrite, occurring as small inclusions or brecciated veinlets. Gold content of the veins varies widely depending on the chemical and mineralogical composition of the enclosing wall rock (Amukum and Turnock, 1971). Occurrences are erratically distributed and, in several places, have exhibited high grade with small tonnage. Over 1.5 million oz. gold have been produced from the region with 80% coming from the San Antonio mine in Bissett, which is no longer in production (Stephenson, 1971).

## ICE FLOW INDICATORS

Throughout the area, exposed bedrock surfaces are commonly striated, polished, and glacially moulded. There is a continuum in the dominant striation direction which ranges from 227° to 260°, indicating regional ice flow toward the southwest. The more westerly measurements (250°-260°) are concentrated within the Wanipigow River valley and near Lake Winnipeg (Fig. 2a). On faceted outcrops, where relative ages are preserved, these trends predate the more widespread 238°-244° striation orientations, although this relationship is



**Figure 2a.** Map of the study area showing striation trends and relative ages (1 = oldest), where possible. Dashed striae indicate poor definition; double-sided striae signify ice flow direction unknown.

not consistent throughout the area. Toward Lake Winnipeg, more south-southwesterly ( $227^{\circ}$ - $233^{\circ}$ ) oriented striae are present and, where relationships are preserved, these appear older than both southwesterly trends (Fig. 2b).

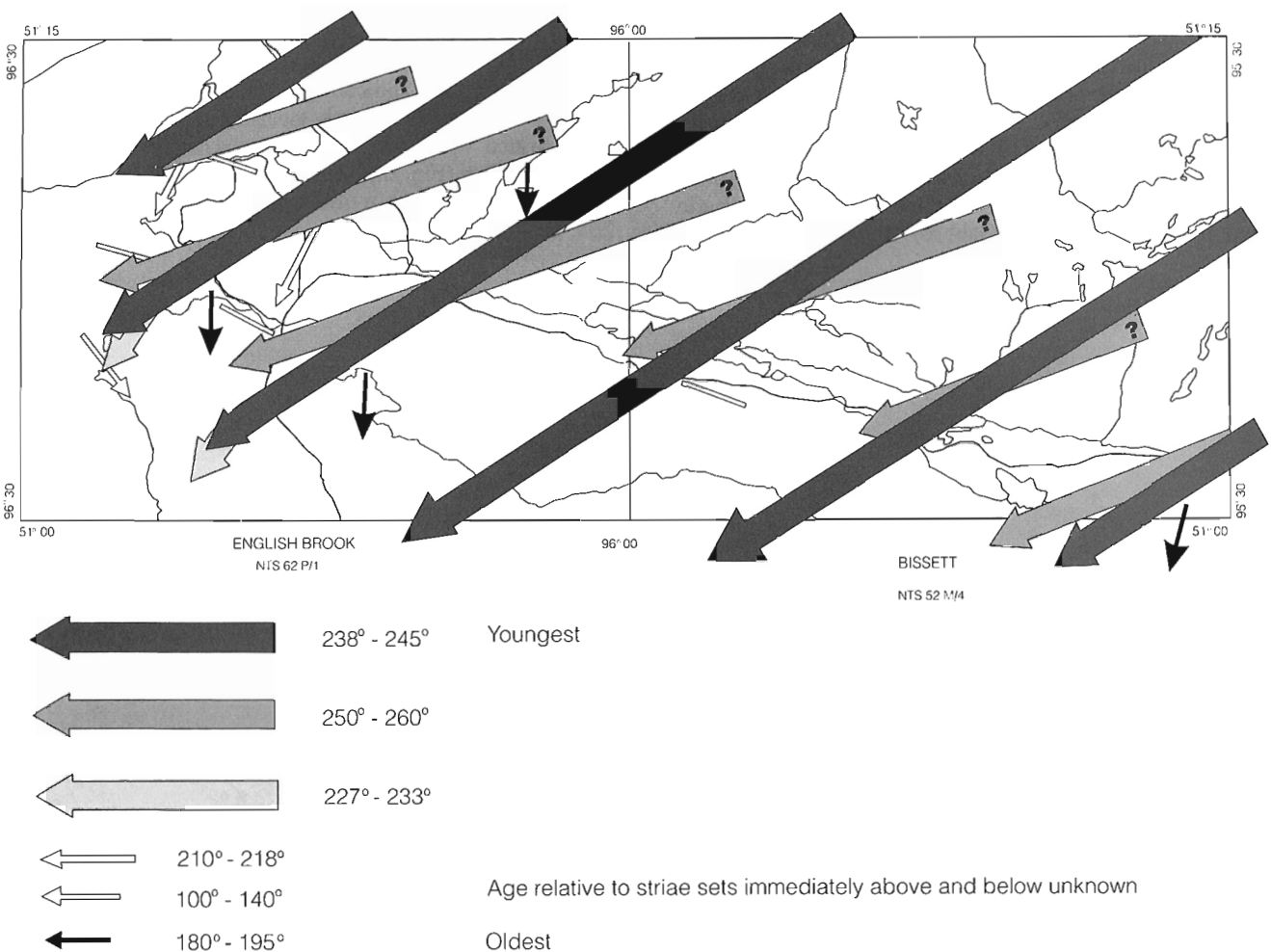
In the English Brook area (NTS 62P/1), near Lake Winnipeg, the striation record is more complex. Along the shore and at the mouth of the Manigotagan River, older striae indicating ice flow toward the south-southwest ( $210^{\circ}$ - $218^{\circ}$ ), and southeast ( $140^{\circ}$ - $100^{\circ}$ ) have been recognized. Southerly trending striae ( $180^{\circ}$ - $195^{\circ}$ ) have also been measured near the mouth of the Manigotagan River, at English Lake, and the southeastern margin of the study area. These orientations are all older than the regional southwesterly trend; where preserved, ice flow to the south appears to postdate flow to the south-southwest. The relative age of southeasterly and southerly trending striae is unknown.

The significance of these relative ages is not fully understood. The wide range in striae orientations and inconsistencies in relative ages in the Rice Lake area may result, in part,

from local variation in striae directions related to outcrop shape. More likely, however, this striae pattern was developed through the repetition of several similar ice flow events through time such as, several glaciations, and/or the interaction of ice lobes, and/or a fluctuating ice margin during deglaciation. Although southerly and southeasterly striation orientations are similar to those in the interlake area (Groom, 1985; Nielsen, 1989), the relative ages are opposite to those observed in this study.

### GLACIAL DISPERSAL AND DRIFT COMPOSITION

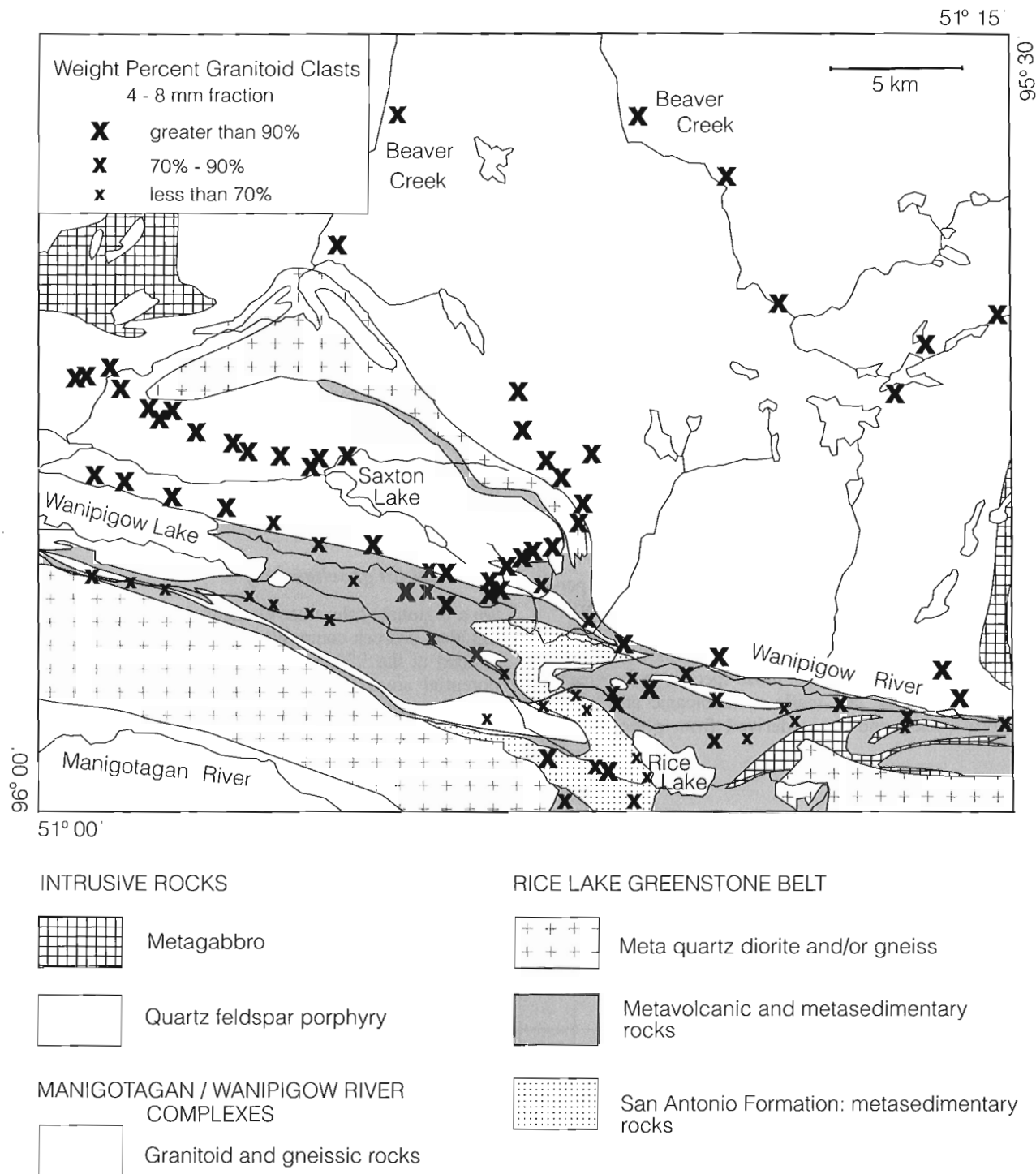
The following discussion is based on data from samples collected in 1992 from the western half of the study area (NTS 52M/4). Glacial dispersal in that area is influenced solely by ice flow to the southwest.



**Figure 2b.** Generalized interpretation of the ice flow history in the region. Symbols lacking arrowheads indicate trends.

The till is characteristically a grey to grey-brown sandy diamicton (40-80% sand), noncalcareous, commonly stoney, massive to poorly stratified with sandy lenses and/or stringers, and generally loose. In highland areas dominated by bedrock, it forms a single discontinuous veneer with thicker accumulations occurring in depressions or as tails on the

down-ice side of bedrock knobs. It is commonly capped by a bouldery mantle of unsorted debris, or a veneer of fine grained to sandy glaciolacustrine sediment. In the major river valleys, till occurs on the down-ice side of bedrock-controlled topographic highs, where overlying glaciolacustrine sediments thin. These lee-side deposits are commonly complex,



**Figure 3.** Distribution of granitoid clasts (4-8 mm fraction) in till. Geology is simplified from Theyer (in press). As expected, concentrations generally decrease from north to south across the greenstone belt. Ice flow is toward the southwest.

comprising interbedded diamicton, sand, and gravel, however, there is no evidence to suggest that they represent stratigraphic sequences deposited by multiple flow events.

### Procedure

Approximately 110 sediment samples have been collected from the area (NTS 52M/4) at approximately 1-5 km spacing depending on access. Samples were obtained primarily from pits hand dug to bedrock or 1.0 m depth and, in nearly all cases, were collected below the A and B soil horizons. Occasionally, where sections were exposed, samples were collected in vertical profile in order to assess weathering effects and local variability. Till is the preferred sample medium, although this material may be extensively reworked so that texturally it approaches a poorly sorted sandy gravel, lacking the fine grain sizes characteristic of till.

The <0.002 mm (clay) and <0.063 mm (silt and clay) fraction of tills has been analyzed for trace metal content. In addition, the carbonate content, texture, and pebble composition (4-8 mm fraction) have been determined. Clay was separated by centrifuge and decantation; silt and clay by dry sieving. Both fractions were analyzed using standard ICP-AES multi-element packages by Chemex, Inc. after nitric-aqua regia digestion. Gold platinum, and palladium were analyzed using the <0.063 mm fraction by ICP-AES fire assay techniques. Pebble counts were done by Consorminex Inc.

### Pebble composition

Because the greenstone belt is oriented approximately perpendicular to ice flow direction, analysis of the pebble fraction (4-8 mm) of till provides a direct method of assessing the extent of glacial transport in the area. Pebble lithologies were broadly divided into two groups: those specific to the greenstone belt (e.g., felsic and mafic metavolcanic and meta-sedimentary rocks) and those derived from plutonic and

gneissic sources. The relative proportion of each group was determined by weight based on 250 pebbles. The distribution of plutonic and gneissic pebbles in till is shown in Figure 3.

As expected, the pebble fraction of tills overlying granitoid terrane north of the greenstone belt is composed almost entirely of these rock types. Within the greenstone belt, the proportion of granitoid pebbles drops to about 50% about 2 km down-ice from the contact due to the incorporation of metavolcanic and metasedimentary rocks. Where small intrusions are present within the greenstone belt, concentrations of granitoid clasts are commonly elevated slightly. In other areas, specifically southeast of Saxton Lake, granitoid percentages exceed 90% up to 1 km down-ice from the granitoid/greenstone contact. This implies that in this area, at least, rocks of the greenstone belt were not subjected to glacial erosion when the till was deposited, or greenstone lithologies broke down to clast sizes finer than pebbles.

The northern contact between the granitoid terrane and greenstone belt is coincident with the Wanipigow River valley. Discontinuous deposits of interbedded glaciofluvial sand and gravel interpreted as subaqueous outwash are present along the valley margin. Therefore, one possible explanation for observed undiluted granitoid transport across the contact may be the presence of subglacial meltwater streams along the valley floor. This would cause the glacier to essentially ride over the contact area and deposit its load further down-ice, without eroding local bedrock or previously deposited glaciofluvial debris.

### Regional till geochemistry

On a regional scale, trace element concentrations in till tend to reflect bedrock composition. Anomalous values, commonly defined at the 95th percentile, have been used to delineate potential areas of mineralization. When the geochemical database is treated as a single population, however, anomalous values defined internally may, in some instances, be

**Table 1.** Summary statistics of trace element concentrations with bedrock lithology (<0.063 mm fraction).

Lithology	Sample size	Au (ppb)			Cr (ppm)			Cu (ppm)			Ni (ppm)			Pb (ppm)			Zn (ppm)		
		A.M.	S.D.	95th	A.M.	S.D.	95th	A.M.	S.D.	95th	A.M.	S.D.	95th	A.M.	S.D.	95th	A.M.	S.D.	95th
Total Population (all lithologies combined)	85	3.7	3.3	18	34.2	12.6	121	24.5	11.4	66	18.7	8.6	52	7.1	3.3	16	30.6	12.6	70
Granitoid Rocks	43	4.6	2.8	14	34.4	15.2	255	22.2	16.0	110	17.3	14.1	90	7.4	2.9	14	24.7	12.4	84
Greenstone Lithologies (combined)	42	4.8	4.3	26	34.3	9.5	121	26.9	9.8	63	21.6	7.6	51	8.7	4.4	22	34.9	12.0	66
Total Volcanics (Mafic/Felsic)	28	3.7	2.2	14	34.5	8.6	64	28.6	11.0	66	21.8	6.0	40	7.7	3.6	20	37.6	10.8	60
San Antonio Fm. (Metasedimentary Rocks)	8	12.0	15.1	64	30.7	6.4	-	21.4	7.6	-	16.9	3.8	-	8.6	4.1	-	31.3	11.5	-

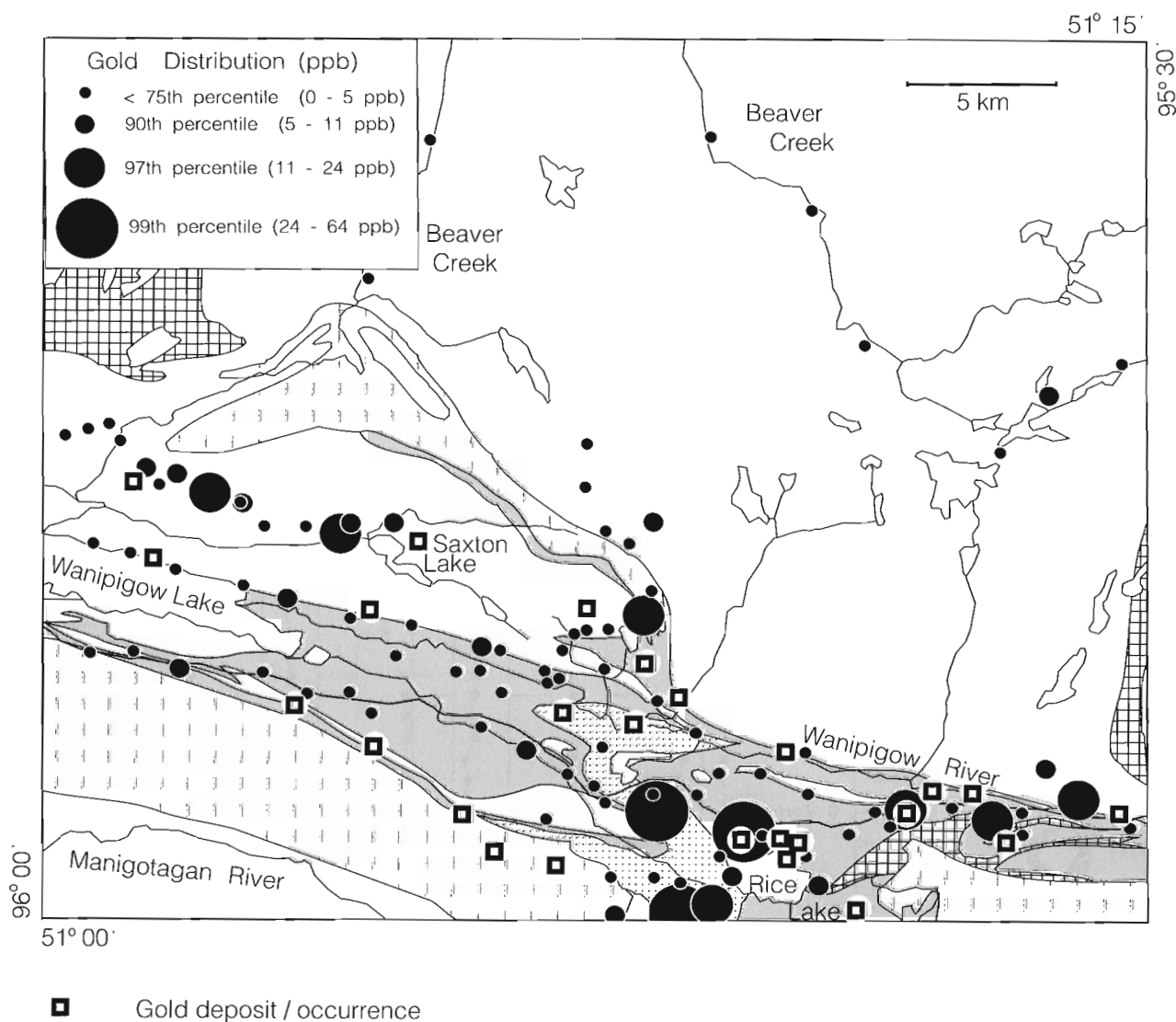
A.M. = Arithmetic Mean      S.D. = Arithmetic Standard Deviation      95<sup>th</sup> = 95<sup>th</sup> percentile

more representative of high background levels pertaining to specific bedrock types or geological settings than part of a dispersal train from a mineralized zone.

In order to evaluate the variation in background levels related to regional variation in bedrock lithology in the Rice Lake area, statistics were calculated for Au, Cr, Cu, Ni, Pb, and Zn using the total population and several subpopulations related to the bedrock lithology associated with the till sample (Table 1). Chosen elements reflect the main types of mineralization in the area. Subpopulations represent broad lithological groups: one representing gneissic and plutonic (granitoid) sources, the other sources related to the greenstone belt itself. Concentrations greater than the 95th percentile or less than the 5th percentile were eliminated from calculations since these extreme values distort background concentrations.

For some elements, differences in mean values are related to differences in gross lithology (Table 1). Results suggest that background concentrations of base metals in the greenstone belt, particularly Cu, Ni, and Zn (shown in bold type), are elevated compared to those of the granitoid terrane and the total population. The geochemical signature is undoubtedly diluted to some extent by glacial transport of debris derived from granitoid sources north and within the greenstone belt, as indicated from examination of the pebble fraction, however, differences are not so great as to affect the recognition of anomalous values.

Although the background levels for base metals are depressed in granitoid lithologies, the standard deviations are high and indicate that the range in values for this subpopulation exceeds that of any other lithological group. In fact, the 95th



**Figure 4.** Gold distribution in till (<0.063 mm fraction). Highest concentrations are generally associated with areas or zones of known gold occurrences. High concentrations are also present down-ice from the San Antonio mine on the north shore of Rice Lake. Bedrock geology legend is shown in Figure 3.

percentile is much greater for granitoid rocks (i.e., Cu – 110 ppm in granitoids, 66 ppm in total population, 63 ppm in greenstone lithologies). Because of the low background in granitoid terrane, the anomalies in this area are very significant and indicate areas for more detailed follow-up studies.

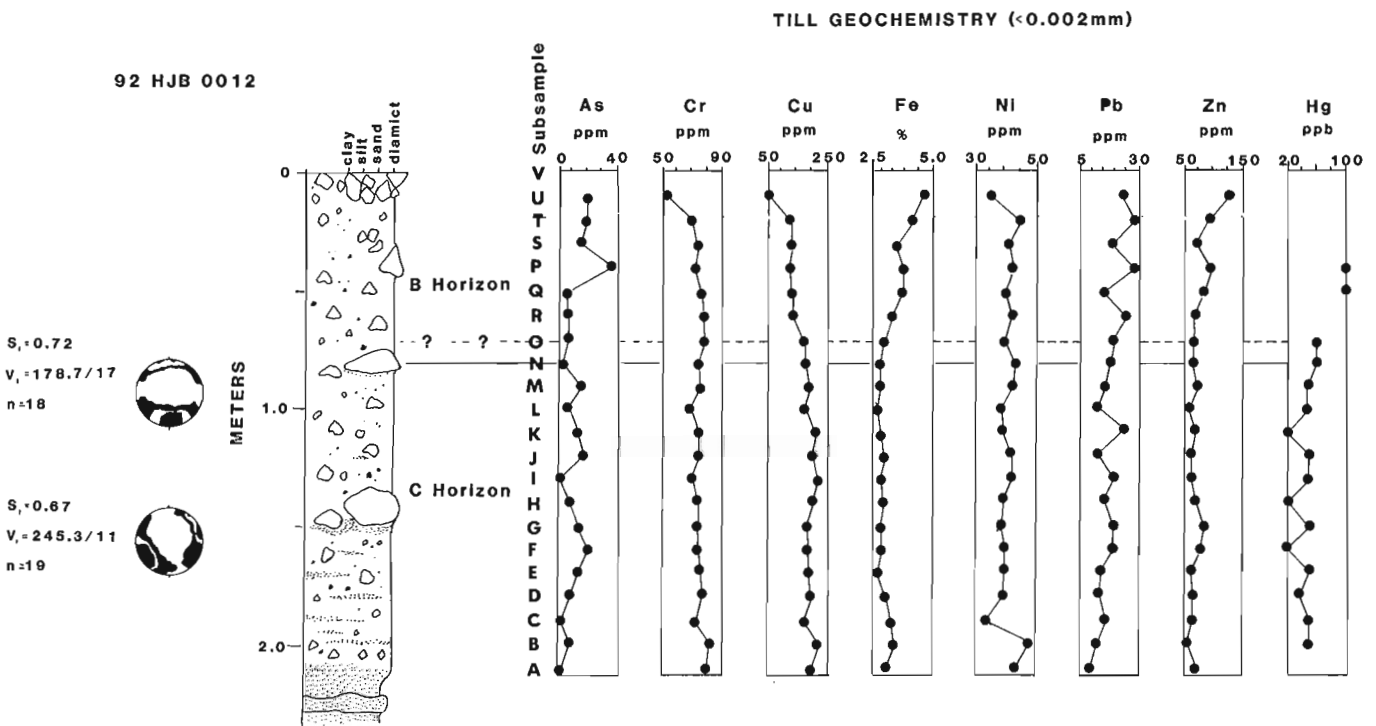
There is very little difference in Cr and Au background levels between groups, with the significant exception of gold values associated with the San Antonio Formation (although the sample number is small; Table 1). The regional distribution of gold in till is shown in Figure 4. Abundances exceeding 10 ppb in soil are considered significant (Dilabio, 1982). Highest values are west and southwest of Rice Lake. Those to the southwest are directly down-ice from the San Antonio mine, the former major gold producer in the area, as well as several other known occurrences. Other samples with high concentrations east of Rice Lake and west of Saxton Lake are located along a zone of known gold mineralization but cannot be directly related to particular occurrences. In general, gold appears to be erratically distributed and mirrors the localized nature of gold mineralization in the Rice Lake Greenstone Belt (Stephenson, 1971).

**Till geochemical profiles**

In order to determine postglacial weathering effects and local variation in trace element composition, samples were collected from vertical profiles in till. In most cases, the till appeared massive with no, or little, variation in texture

or sedimentary structures indicative of facies changes. The B horizon is generally thin, averaging 30 cm. At several sites, particularly in lee-side situations, diamictons may overlie or interfinger with stratified sediments. An example is shown in Figure 5 which represents a section exposed along a logging road at a well drained site on the northern margin of the Wanipigow River valley (east of Saxton Lake) at the northern contact between the greenstone belt and the granitoid terrane.

The section consists of a sandy diamicton with clasts up to 30 cm diameter. The humus is thin (approximately 2 cm). It is underlain by 10-15 cm of light grey brown, fine sandy diamicton containing rounded to subangular cobbles, representing the upper B horizon. It is underlain by 55 cm of the more Fe-stained material characteristic of the lower B horizon, a red-brown, loose, homogeneous sandy diamicton; clasts appear slightly more angular. The contact with the underlying grey-brown, sandy diamicton is gradational. This unit is approximately 140 cm thick and is characteristic of the C horizon. It is fairly compact with sand stringers or laminations and a strong subhorizontal fissility near the base of the unit. A basal contact with sand is sharp and has a red colouration indicative of Fe-oxide accumulation. Till fabrics are moderately well developed with preferred orientations in the lower part of the unit parallel to the regional ice flow (245°) (Fig. 5). In the upper part of the unit, the fabric is oriented north-south (179°) which is more likely a response to the local topography than the southerly ice flow recognized near Lake Winnipeg. Based on the fabrics and sedimentology, the diamicton probably represents a subglacial till.



**Figure 5.** Till sedimentology and vertical variation in trace element concentration. Section located on the northern margin of the Wanipigow River valley near the contact between the greenstone belt and granitoid terrane to the north.



Till geochemistry (<0.002 mm) throughout the section shows definite patterns which can primarily be related to the postglacial soil forming processes. Cr, Cu, Ni and Pb concentrations are depressed near the top and increase down-section, while Fe and Zn are elevated in the upper part of the section and decrease downward. At approximately 0.7 m from the surface, trace element concentrations appear to stabilize, and the diamicton becomes more grey. This zone represents the B/C soil horizon transition and material collected below this zone, although oxidized, would provide a consistent sampling medium for hand dug samples.

Throughout the section, As, Pb, and Hg concentrations show more variability than other elements. It is also noteworthy that near the base of the diamicton unit Cr, Cu, Fe, Ni, and Zn concentrations in the clay fraction are all elevated to varying degrees. This may be a result of textural differences in the lower part of the unit (i.e., increased sand content which would result in increased porosity and increased mobility of ions) or part of a glacial dispersal train and indicative of mineralization.

## DISCUSSION

During glaciation, bed material (either bedrock or previously deposited sediment) is eroded and deposited down-ice from source. Therefore, an understanding of glacial dispersal and other factors affecting till composition is fundamental to drift prospecting for mineralization. Drift composition results from the interplay of many variables including:

1. The ice flow history of the area, particularly the direction or directions of ice flow and the number of events.
2. The response of the glacier to local variables such as topography, and bed composition during glaciation and deglaciation. This affects ice flow and the way debris is eroded, transported, and deposited by the glacier.
3. The type, size, and erodibility of the bedrock and the effects of regional variation in bedrock lithology on till composition. The type of mineralization will also influence dispersal patterns of relevant trace elements or minerals.
4. Postglacial weathering effects on till composition.

Within the study area, striations indicate a consistent direction of glacial transport toward the southwest which appears to be related to events associated with the last glaciation (Late Wisconsin). Minor variations in trends may be a response of the glacier to local topographic irregularities. Interbedded diamicton and sand deposits occurring on the lee-side of bedrock knobs are interpreted as subglacial deposits, and are not indicative of multiple flow events. Toward Lake Winnipeg, the ice flow patterns are more complex with striations recorded that indicate ice flow toward the south, southeast, and south-southwest, although the relative ages are unclear. Stratigraphy and ice flow indicators observed within this region suggest the interaction of several glacial events or, more likely, ice lobes.

The general direction of sediment transport, as indicated by the distribution of granitoid lithologies in till, is from north to south across the greenstone belt. This is consistent with the observed ice flow in the area, but is not detailed enough to define specific dispersal trains. The pattern of glacial dispersal suggests that topography may have influenced the ability of the glacier to erode bedrock at a local scale.

On a regional scale, trace element concentrations in till reflect bedrock composition. For some elements, particularly base metals, background values are elevated compared to those of the granitoid terrane and the total population. These differences do not affect the recognition of anomalous values defined at the 95th percentile, however. The regional distribution of gold in till appears to be related to known gold occurrences or zones of known mineralization.

Postglacial weathering effects and local variation in till geochemistry was assessed from vertical profiles in till. The observed geochemical variation with depth indicates that, on a detailed scale, postglacial processes and textural variation in till could be important in mineral exploration. On a regional scale, however, trace element values stabilize after approximately 0.6 m depth, at most, indicating that material collected below this level would provide a consistent sampling medium for till sampling programs.

## ACKNOWLEDGMENTS

Field assistance was provided by Barbara Pierna during the 1992 season, and Martin Roy, Chris Zdanowicz, and Adrienne Hanly, in 1993. Erik Nielsen and Peter Theyer of the Manitoba Geological Survey shared their knowledge of the Quaternary geology and mineral deposits of the area, respectively. G. Walker and the staff of the regional office of the Manitoba Department of Natural Resources provided helpful advice about access to the area. Richard Laframboise of the Terrain Sciences Division prepared the striation diagram and John Henderson assisted with the remaining computer-generated figures.

## REFERENCES

- Amukum, S.E.O. and Turnock, A.C.**  
1971: Composition of the gold-bearing quartz vein rocks, Bissett area, Manitoba; in *Geology and Geophysics of the Rice Lake Region, Southeastern Manitoba*, (ed.) W.D. McRitchie and W. Weber; Manitoba Department of Mines and Natural Resources, Mines Branch Publication 71-1, p. 325-336.
- Bressenbrugge, G.**  
1986: Granular investigation: Report on Hollow Water Indian Reserve no. 10; Indian and Northern Affairs Canada, Internal Report, 20 p.
- Davies, J.F.**  
1950: Geology of the Wanipigow Lake area; Manitoba Mines and Natural Resources, Mines Branch, Publication 49-3, 21 p.
- DiLabio, R.N.W.**  
1982: Drift prospecting near gold occurrences at Onaman River, Ontario and Oldham, Nova Scotia; in *Geology of Canadian Gold Deposits*, Canadian Institute of Mining and Metallurgy, Special Volume 24.
- Ermanovics, I.F.**  
1970: Precambrian geology of Hecla-Carroll Lake map-area, Manitoba-Ontario (62P E1/2, 52M W1/2); Geological Survey of Canada, Paper 69-42, 33 p.

**Groom, H.D.**

- 1985: Surficial Geology and Aggregate Resources of the Fisher Branch Area: Local Government District of Fisher and Rural Municipality of Bifrost; Manitoba Energy and Mines, Aggregate Report AR84-2, 33 p.

**Henderson, P.J.**

- 1993: Quaternary geology of the Bissett area, southeastern Manitoba: applications to drift prospecting; in Current Research, Part B; Geological Survey of Canada, Paper 93-1B, p. 63-69.

**Manitoba Mineral Resources Division**

- 1981: Surficial Geological Map of Manitoba, Map 81-1, scale 1:1 000 000.

**McRitchie, W.D. and Weber, W.**

- 1971: Geology and Geophysics of the Rice Lake Region, Southeastern Manitoba. (Project Pioneer); Manitoba Department of Mines and Natural Resources, Mines Branch Publication 71-1, 430 p.

**Nielsen, E.**

- 1980: Quaternary Geology of a part of southeastern Manitoba; Manitoba Department of Energy and Mines, Map GR 80-6.

- 1986: A preliminary investigation of Quaternary placer gold in the Manigotagan area; in Report of Field Activities, Manitoba Energy and Mines, p. 131-134.

- 1989: Quaternary stratigraphy and overburden geochemistry in the Phanerozoic terrane of southern Manitoba; Manitoba Energy and Mines, Geological Paper GP87-1, 78 p.

**Nielsen, E. and DiLabio, R.N.W.**

- 1987: Investigations of Quaternary placer gold occurrences in the Manigotagan area; in Report of Field Activities, Manitoba Energy and Mines, p. 111-115.

**Prest, V.K., Grant, D.R., and Rampton, V.N.**

- 1968: Glacial Map of Canada; Geological Survey of Canada, Map 1253A, scale 1:5 000 000.

**Russell, G.A.**

- 1949: Geology of the English Brook Area; Manitoba Department of Mines and Natural Resources, Mines Branch, Preliminary Report and Map 48-3, 22 p.

**Scoates, R.F.J.**

- 1971: Ultramafic rocks of the Rice Lake Greenstone Belt; in Geology and Geophysics of the Rice Lake Region, Southeastern Manitoba, (ed.) W.D. McRitchie and W. Weber; Manitoba Department of Mines and Natural Resources, Mines Branch Publication 71-1, p. 189-202.

**Stephenson, J.F.**

- 1971: Gold deposits of the Rice Lake-Beresford Lake Greenstone Belt, Manitoba; in Geology and Geophysics of the Rice Lake Region, Southeastern Manitoba, (ed.) W.D. McRitchie and W. Weber; Manitoba Department of Mines and Natural Resources, Mines Branch Publication 71-1, p. 337-375.

**Stockwell, C.H.**

- 1938: Rice Lake-Gold Lake area, southeastern Manitoba; Geological Survey of Canada, Memoir 210, 79 p.

**Theyer, P.**

- 1987: Platinum group elements in southeastern Manitoba; in Manitoba Energy and Mines, Minerals Division, Report of Field Activities 1987, p. 115-118.

- in press: Mineral deposits and occurrences in the Bissett area, NTS 52M/4; Manitoba Energy and Mines, Mineral Deposit Series.

**Weber, W.**

- 1991: Geology of the English Brook area, southeastern Manitoba (NTS 62P/1); in Manitoba Energy and Mines, Minerals Division, Report of Activities 1991, p. 49-52.

---

Geological Survey of Canada Project 920070

# Regional geology and geophysics of the sub-Phanerozoic Precambrian basement south of the Flin Flon-Snow Lake-Hanson Lake Belt, Manitoba-Saskatchewan<sup>1, 2, 3</sup>

A.D. Leclair, S.B. Lucas, R.G. Scott<sup>4</sup>, D. Viljoen, and J. Broome  
Continental Geoscience Division

*Leclair, A.D., Lucas, S.B., Scott, R.G., Viljoen, D., and Broome, J., 1994: Regional geology and geophysics of the sub-Phanerozoic Precambrian basement south of the Flin Flon-Snow Lake-Hanson Lake Belt, Manitoba-Saskatchewan; in Current Research 1994-C; Geological Survey of Canada, p. 215-224.*

---

**Abstract:** Regional geological mapping of the sub-Phanerozoic segment of the Flin Flon-Snow Lake-Hanson Lake Belt (Trans-Hudson Orogen) involved the interpretation of potential field data combined with relogging of industry drill core. This approach has permitted the subdivision of the buried Precambrian basement into eight principal domains which are defined by their distinct lithostructural characteristics and aeromagnetic-gravity anomaly patterns. The Amisk Lake, Athapapuskow, and Clearwater domains are characterized by northerly trending positive gravity anomalies and correlate with volcanic assemblages (Amisk Group) on the exposed shield. The Namew Gneiss Complex and Cumberland Domain are marked by complexly distributed orthogneiss and paragneiss packages. Late-tectonic granite of the Cormorant Batholith and Windy Lake Pluton are centred over low-intensity aeromagnetic and gravity anomalies. The sub-Phanerozoic portion of the Hanson Lake Block, bounded by the Sturgeon-weir Shear Zone and Tabernor Fault Zone, is subdivided into two volcano-plutonic subdomains by the Suggi Lake Fault.

**Résumé :** La cartographie régionale du segment subphanérozoïque de la ceinture de Flin Flon-Snow Lake-Hanson Lake (orogène trans-hudsonien) a impliqué l'interprétation de données de champs de potentiel jumelée au réexamen de carottes de forage recueillies par l'industrie. Cette approche a permis la subdivision de la partie enfouie du socle précambrien en huit domaines principaux, définis par leurs caractéristiques lithostructurales et leurs patrons d'anomalies aéromagnétiques et gravimétriques. Les domaines d'Amisk Lake, d'Athapapuskow et de Clearwater se caractérisent par des anomalies gravimétriques positives de direction générale nord et peuvent être corrélés avec les assemblages volcaniques (Groupe d'Amisk) de la partie affleurante du bouclier. Le complexe gneissique de Namew et le domaine de Cumberland se distinguent par des unités d'orthogneiss et paragneiss présentant une répartition complexe. Les granites tarditectoniques du batholite de Cormorant et du pluton de Windy Lake sont centrés sur des anomalies aéromagnétiques et gravimétriques de basses intensités. La portion subphanérozoïque du bloc d'Hanson Lake, limité par la zone de cisaillement de Sturgeon-weir et la zone de faille de Tabernor, est subdivisée en deux sous-domaines volcano-plutoniques par la faille de Suggi Lake.

---

<sup>1</sup> Contribution to Canada-Manitoba Partnership Agreement on Mineral Development (1990-1995), a subsidiary agreement under the Canada-Manitoba Economic and Regional Development Agreement.

<sup>2</sup> Contribution to Canada-Saskatchewan Partnership Agreement on Mineral Development (1990-1995), a subsidiary agreement under the Canada-Saskatchewan Economic and Regional Development Agreement.

<sup>3</sup> NATMAP Shield Margin Project

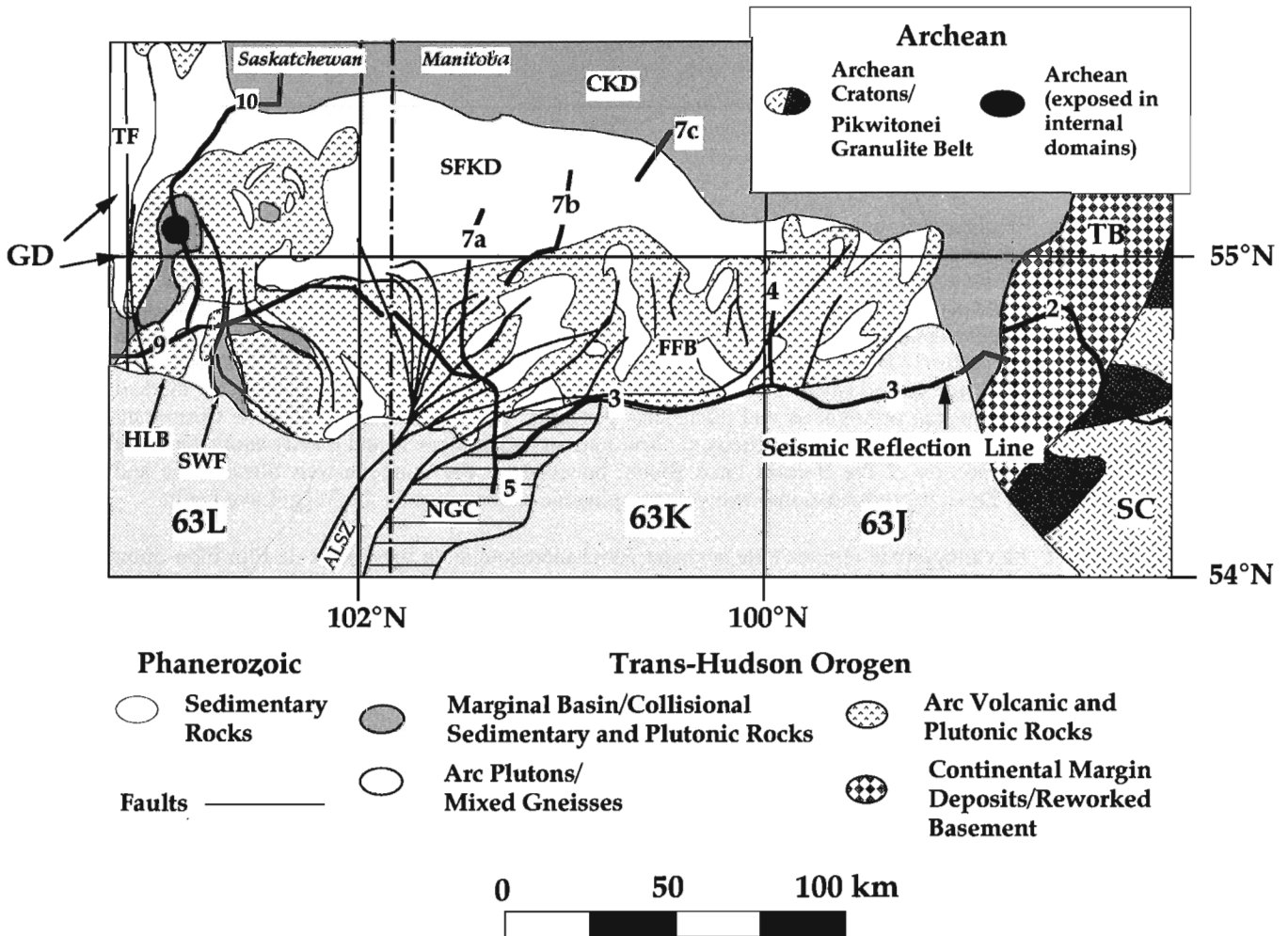
<sup>4</sup> Ottawa-Carleton Geoscience Centre, Department of Geology, University of Ottawa, Ottawa, Ontario K1N 6N5

**INTRODUCTION**

Regional geological mapping of the sub-Phanerozoic Precambrian basement south of the Flin Flon-Snow Lake-Hanson Lake Belt represents one of the fundamental geoscientific components of the NATMAP Shield Margin Project (Lucas, 1992). Sub-Phanerozoic interpretation studies span across parts of three 1:250 000 scale map areas (99°-103°30'W in 63J, 63K, and 63L; Fig. 1). They involve the integration of results from interpretation of aeromagnetic and gravity data with systematic regional mapping of industry drill core (see Leclair et al., 1993a), and have been supported by a diamond drilling program (Leclair and Weber, in press). The principal goal of these studies is to develop a series of interpretive geological maps at 1:100 000 scale for the sub-Phanerozoic Precambrian basement. The results of the initial work carried out in the Cormorant Lake area, 63K (Leclair et al., 1993a) have been incorporated in a 1:250 000 scale bedrock compilation map of

both exposed and sub-Phanerozoic Precambrian geology (Lucas and NATMAP Shield Margin Project Group, 1993). The following paper complements this work and presents the outcome of regional mapping in the Amisk Lake area, 63L, to the west.

South of the shield margin, the coverage of high resolution vertical gradient and residual total field aeromagnetic data encompasses most of the project area (Geological Survey of Canada, 1993). A Bouguer gravity image derived from ~1000 gravity stations also covers the same area (Broome et al., 1993). The interpretation of these data combined with drill core data from more than 700 diamond drillholes has led to the recognition of several geological-geophysical elements in the sub-Phanerozoic Precambrian basement (Leclair et al., 1993a, b, c). In this report, we briefly describe the geophysical and interpreted geological characteristics of each of these distinct elements.



**Figure 1.** General geological map showing the principal elements of the Flin Flon-Snow Lake-Hanson Lake Belt and the location of the Cormorant Lake (63K) and Amisk Lake (63L) areas. ALSZ – Athapapuskow Lake Shear Zone; CKD – Central Kisseynew Domain; FFB – Flin Flon Belt; GD – Glennie Domain; HLB – Hanson Lake Block; NGC – Namew Gneiss Complex; SC – Superior Craton; SFKD – South Flank of Kisseynew Domain; SWF – Sturgeon-weir Fault; TB – Thompson Belt; TF – Tabernor Fault.

## GENERAL GEOLOGICAL AND GEOPHYSICAL FRAMEWORK

The Flin Flon-Snow Lake-Hanson Lake Belt of the Trans-Hudson Orogen, well known for its volcanogenic massive Cu-Zn sulphide deposits, comprises juvenile arc, oceanic, basinal sedimentary, and plutonic rocks. Arc magmatism and accretion occurred in the interval between 1.91 and 1.83 Ga and were accompanied by multiphase deformation and sub-greenschist- to amphibolite-facies regional metamorphism (Gordon et al., 1990; Lewry et al., 1990). These rocks are structurally overlain to the north by gneisses of the Kisseynew Domain, and are covered unconformably by Phanerozoic sedimentary rocks to the south (Fig. 1). To the west, they are separated from the Glennie Domain, a similar 1.91-1.83 Ga juvenile volcano-plutonic belt, by the Tabbemor Fault Zone. The regional along-strike continuity of prominent aeromagnetic and gravity anomaly patterns indicates that the Flin Flon-Snow Lake-Hanson Lake Belt extends beneath the south-dipping Phanerozoic cover (Blair et al., 1988; Leclair et al., 1993a, b), possibly to 46°N latitude (Green et al., 1985). The diminishing amplitude of the aeromagnetic anomalies towards the south correlates with increasing Phanerozoic cover thickness, and suggests that the causative bodies for the anomalies lie in the Precambrian basement.

## MAJOR GEOLOGICAL-GEOPHYSICAL ELEMENTS OF THE BURIED PRECAMBRIAN BASEMENT

The regional structural grain of the buried Precambrian basement rocks trends north-northeast, as indicated by the aeromagnetic anomaly patterns (Fig. 2). This mimics structural trends on the exposed shield and implies that lithological and structural correlations exist between certain exposed geological elements and their inferred sub-Phanerozoic counterparts. The structure of the buried basement can be depicted from the trend of striated magnetic anomaly patterns combined with drill core data (see Fig. 4). The strike and dip direction of basement structures were derived from the azimuth and inclination of over 1000 industry drillholes which have diametric orientations with respect to the down-dip direction of the structures.

### *Cormorant Lake area (63K)*

The sub-Phanerozoic Precambrian basement in 63K has been subdivided into the Athapapuskow Domain, Clearwater Domain, Namew Gneiss Complex, and Cormorant Batholith (Leclair et al., 1993a, c) (Fig. 2). Six main rock units and three subunits have been delineated within these geological-geophysical entities (Fig. 3).

### **Clearwater Domain**

The Clearwater Domain is a broad, south-southwest-trending volcano-plutonic domain with a corrugated aeromagnetic pattern, which is abruptly truncated against the Cormorant

Batholith (Fig. 2). This domain is represented by layered sequences of intercalated, amphibolite-facies, mafic meta-volcanic and metasedimentary rocks (unit **Aa**) which are intruded by felsic and mafic plutons (units **T**, **Ta**, **G**, **Ga**, and **Um**) (Fig. 3). Mafic to ultramafic plutons are typically centred on coincident high-intensity positive aeromagnetic and gravity anomalies. The overall structure has a predominant east-southeast dip and appears to be essentially homoclinal (Leclair et al., 1993b) (Fig. 4). The Clearwater Domain is interpreted to represent the subsurface extension of the Flin Flon Assemblage as exposed in the Snow Lake area. This interpretation is supported by the continuity of gravity and linear aeromagnetic anomalies across the shield margin.

### **Cormorant Batholith**

The 60 x 25 km Cormorant Batholith is characterized by a smooth aeromagnetic signature and a regional gravity low (Fig. 2; units **G**, **Gm** on Fig. 3; Leclair et al., 1993a). Limited drill core data indicate a predominance of monzogranite. A gentle gradient in the gravity field (~20 mGal over 25 km) over the southwestern half of the batholith might be related to a gently northeast-dipping contact with metavolcanic rocks of the Clearwater Domain. In contrast, the steep gradient along the northeastern margin implies a near-vertical contact. The obvious truncation of magnetic anomaly patterns at the margins of the Cormorant Batholith indicate that its emplacement was late tectonic (Leclair et al., 1993a). A biotite monzogranite core sample from the batholith has an age of 1831 ± 5/-4 Ma (Blair et al., 1988; Stern et al., 1993), corresponding with the youngest phase of plutonism in the belt.

### **Namew Gneiss Complex**

The Namew Gneiss Complex is a heterogeneous domain of variably-deformed granitoid rocks (unit **Ta**) with enclaves of mafic, psammitic and pelitic gneisses (unit **Aag**; Fig. 3). The complex has intermediate to low gravity values (-40 to -60 mGal) and displays curvilinear aeromagnetic highs which outline a north- to northwest-dipping structural pattern (Fig. 2). In the southeastern part of the complex, interlayered orthogneiss and paragneiss delineate tight northeast-trending folds that are overturned to the east (Leclair et al., 1993b; Fig. 4).

Initial epsilon Nd values and U-Pb ages for the Namew Gneiss Complex (minimum age of 1880 ± 2 Ma, Stern et al., 1993) are similar to those obtained north of the Shield margin. This implies that initial magmatism in the complex may have occurred soon after the development of the volcanic arc assemblages. The highly deformed nature and upper amphibolite grade of the complex further suggests that it may have been built up from multiple intrusion of tonalite-diorite sheets at mid-crustal levels, and possibly represents a deeper portion of the magmatic arc than the rest of the belt (Leclair et al., 1993c).

The nature of the boundary between the Namew Gneiss Complex and Clearwater Domain is uncertain. On the LITHOPROBE seismic reflection profile (line 3, Fig. 1), this boundary coincides with a moderately east-dipping reflective



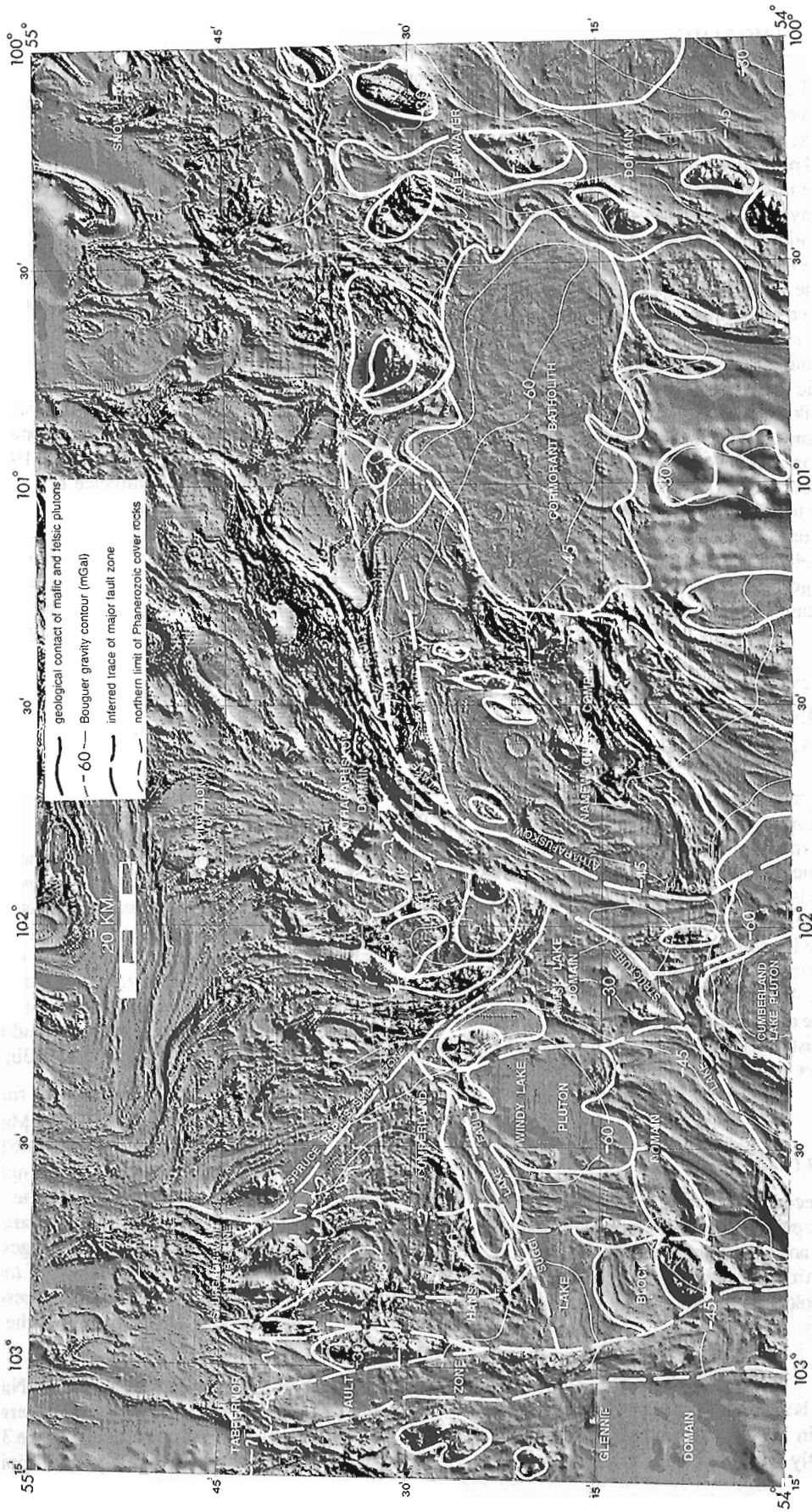


Figure 2. Shaded relief image of aeromagnetic data showing major geological-geophysical elements of the sub-Phanerozoic Precambrian basement south of the Flin Flon-Snow Lake-Hanson Lake Belt. The outlines of some mafic (high relief) and felsic (low relief) plutons are shown.



zone which has been interpreted as a major décollement that floors upper-crustal arc rocks (Lucas et al., 1993), separating them from the footwall orthogneisses.

### Athapapuskow Domain

The Athapapuskow Domain is a fault-bounded belt of strongly foliated metavolcanic/volcaniclastic rocks (unit Av; Fig. 3) with a striated magnetic anomaly pattern (Fig. 2). The rocks are metamorphosed predominantly to greenschist facies. They are separated from amphibolite-facies gneisses of the Namew Gneiss Complex by the South Athapapuskow Lake Fault which accommodates a component of north-side-down displacement as implied by the difference in the metamorphic grade between the two domains. On the west, the Athapapuskow Domain is bounded by the Namew Lake Structure. The continuity across the shield margin of the striated magnetic anomaly patterns with the exposed ocean floor assemblage suggests that some rocks of the Athapapuskow Domain correlate with this assemblage (Leclair et al., 1993c).

### Amisk Lake area (63L)

The sub-Phanerozoic Precambrian basement in the eastern part of 63L is dissected into five principal domains by major fault zones, each with distinct lithostructural character and aeromagnetic-gravity anomaly pattern (Fig. 2 and 3).

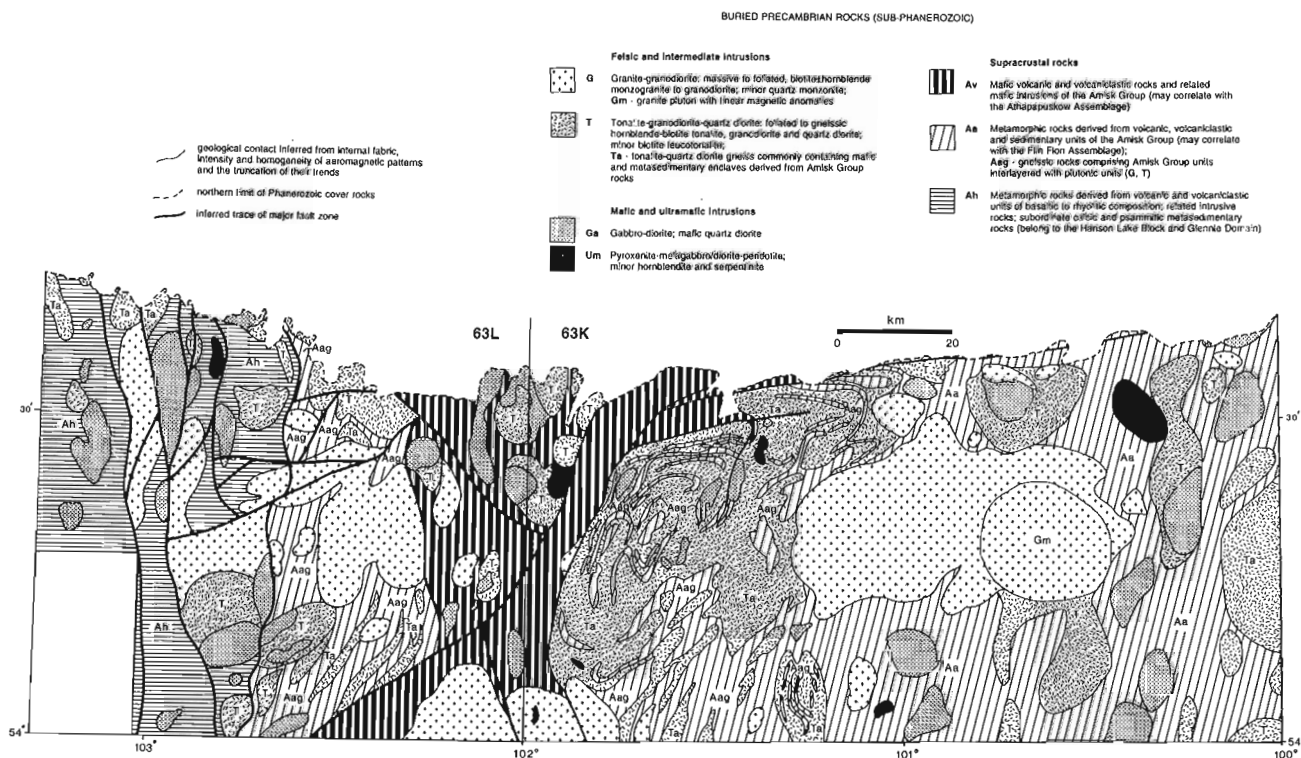
### Southwestern extension of the Athapapuskow Domain

The Athapapuskow Domain, as described above, continues into the Amisk Lake area. Drill core data indicate a steeply-dipping sequence of mainly low-grade metabasalts and associated diorite-gabbro. These rocks are bounded to the west by the Namew Lake Structure, which stretches north of an elliptically-shaped, low-amplitude aeromagnetic anomaly considered to be the northern margin of a granitoid intrusion (Cumberland Lake Pluton; Fig. 2 and 3). A large negative gravity anomaly with a minimum value at -79 mGal coincides with this pluton.

The Athapapuskow Domain forms the eastern flank of a positive gravity anomaly which is centred over the Amisk Lake Domain (Fig. 2). The steep gradient (amplitude of -15 to -25 mGal) displayed on gravity profiles (Thomas et al., 1993) is typical of a change in rock density across a planar boundary with moderate dip. This is compatible with a fault contact, defined by the South Athapapuskow Lake Fault, between orthogneisses to the east and dense metavolcanic rocks to the west.

### Amisk Lake Domain

The Amisk Lake Domain is characterized by a prominent north-south gravity high (-45 to -25 mGal), and coincides with a north-striking, corrugated aeromagnetic anomaly pattern (Fig. 2). This composite gravity-magnetic pattern appears to be



**Figure 3.** Simplified geological compilation map of sub-Phanerozoic Precambrian basement rocks in the Cormorant Lake area (63K) and eastern part of the Amisk Lake area (63L).

sinistrally offset across the Spruce Rapids Shear Zone. Similar anomaly patterns have been attributed to Amisk Group rock sequences consisting of mafic to intermediate metavolcanic-volcaniclastic rocks (Leclair et al., 1993a). The correlation is supported by widely distributed drillholes which intersected basalt, andesite, dacite, and associated mafic to felsic tuff/wacke (unit Av; Fig. 3). In addition, diorite-gabbro, felsic porphyry, and graphitic argillite were identified locally in drill core. North of the Windy Lake Pluton, a high-amplitude positive aeromagnetic anomaly is composed of magnetite-bearing quartz diorite to diorite which is variably sheared and cut by brittle faults. These structures may be related to the boundary with the Cumberland Domain to the west.

The Amisk Lake Domain is interpreted as the subsurface continuation of the volcanic-volcaniclastic rock package exposed in the vicinity of Amisk Lake (see Byers and Dahlstrom, 1954; Ashton, 1992; Slimmon, 1991; Syme et al., 1993; Reilly, 1992). This interpretation is based on similarity in rock type between drill core samples and units in the exposed shield, and on the continuity of aeromagnetic and gravity anomaly patterns across the shield margin (Fig. 2). The gravity high of the Amisk Lake Domain extends over the adjacent Athapapuskow Domain, both eastward and southward of the intervening Namew Lake Structure. Although the Amisk Lake and Athapapuskow Domains are similar lithologically (Fig. 3), they may not belong to the same tectonostratigraphic assemblage.

**Spruce Rapids Shear Zone**

The exposed segment of the southeast-striking Spruce Rapids Shear Zone parallels the shield edge over a distance of about 25 km, and abuts with the Sturgeon-weir Shear Zone to the northwest (Fig. 2). It juxtaposes predominantly supracrustal rocks to the north with plutonic rocks to the south. Well-developed kinematic indicators related to this moderately north-east-dipping shear zone suggest a sinistral movement sense (Ashton, 1992).

The Spruce Rapids Shear Zone continues south-eastward beneath the Phanerozoic sedimentary cover, as indicated by truncations and perturbations of aeromagnetic anomaly patterns associated with the Amisk Lake Domain (Fig. 2). It terminates sharply against the Namew Lake Structure, and thus has a total strike length of >60 km (Leclair et al., 1993b). The north-trending anomalies are clearly rotated counterclockwise into the trace of the shear zone, indicating a sinistral map-view separation.

**Cumberland Domain**

The Cumberland Domain is defined by linear, north-east-trending, moderate-intensity positive aeromagnetic highs which are truncated against the

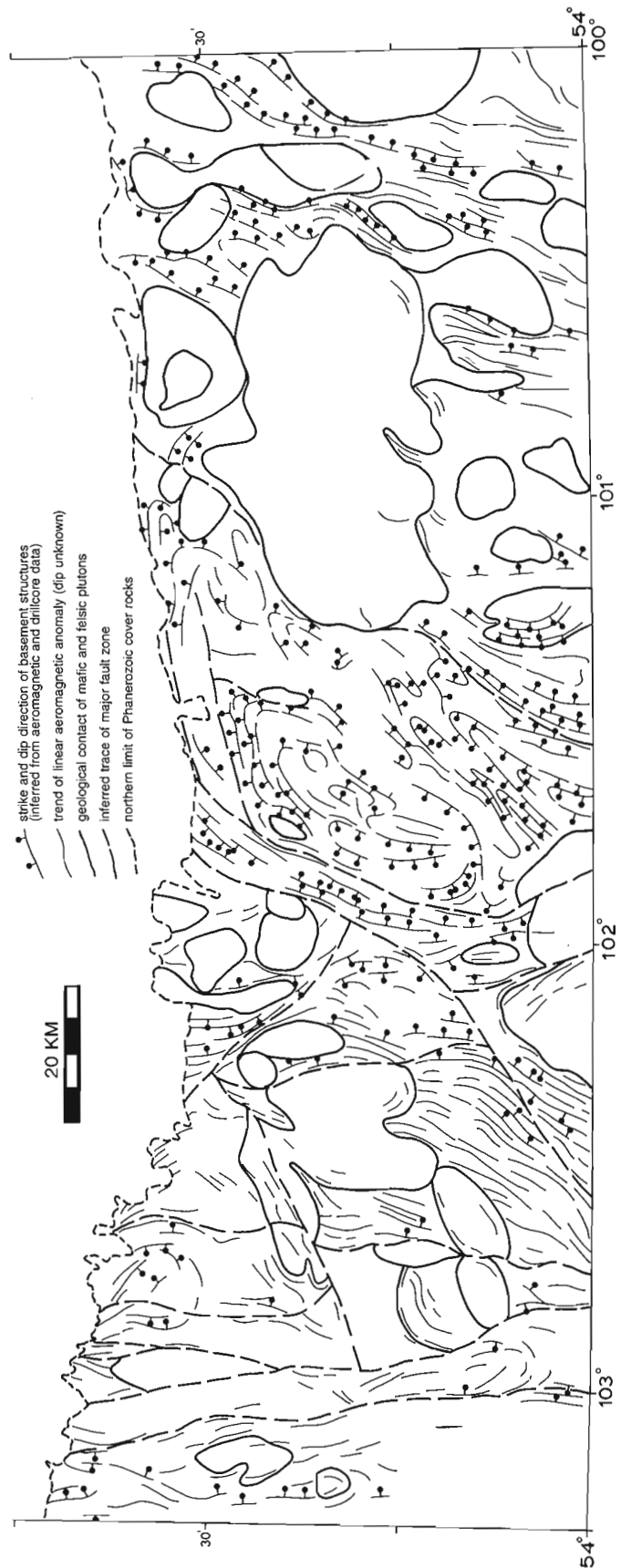


Figure 4. Interpreted structure map showing strike and dip direction of major structures and the trend of aeromagnetic anomalies in the buried Precambrian basement.

Windy Lake Pluton (Fig. 2 and 4). North of the Suggi Lake Fault, a similar aeromagnetic anomaly pattern is deflected northwestward into the Spruce Rapids Shear Zone, presumably due to transposition by intense shear deformation. The Bouguer gravity field over the Cumberland Domain varies in intensity from -45 and -60 mGal.

Limited drill core data from the Cumberland Domain indicate the presence of amphibolite-facies metasedimentary gneisses (unit **Aag**; Fig. 3). These rocks have calcic, mafic, psammitic or pelitic compositions and contain a wide variety of mineral assemblages. The heterogeneity of the gneisses suggests that they were derived from a compositionally-diverse sequence, possibly including "turbiditic" wackes and volcanoclastic sediments. A subordinate volcanic component may also exist; however, the combined effects of high-grade metamorphism and deformation preclude definite characterization of precursor lithologies. The gneisses of the Cumberland Domain have some lithological affinities with Amisk Group metasedimentary rocks mapped north of the Spruce Rapids Shear Zone (cf. Ashton, 1992; Reilly, 1992), and with some gneisses of the Namew Gneiss Complex (cf. Leclair et al., 1993a).

Another important lithological component of the Cumberland Domain is inferred to be felsic and mafic plutonic rocks (Fig. 3), based on potential field data. North of the Suggi Lake Fault, granitoid rocks are responsible for a low-amplitude northwest-trending ridge in the gravity contours from -55 to -60 mGal (Fig. 2). These rocks may represent the subsurface continuation of variably-deformed granitoid rocks mapped along the Shield margin (see Ashton, 1992).

The Cumberland Domain is bounded on the west by the sub-Phanerozoic extension of the Sturgeon-weir Shear Zone (Fig. 2). However, the nature of the boundary between the Cumberland and Amisk Lake Domains is uncertain. Local brittle-ductile deformation fabrics and an abrupt westward increase in the metamorphic grade, may indicate a fault zone.

### Windy Lake Pluton

The Windy Lake Pluton occupies more than 400 km<sup>2</sup> in the centre of the Cumberland Domain. It is the source of a prominent gravity low (<-55 to -60 mGal) and a neutral aeromagnetic anomaly (Fig. 2). This combination of gravity and magnetic lows suggests that this pluton consists of relatively low density and low magnetic susceptibility granitoid rocks (unit **G**; Fig. 3). The pluton clearly crosscuts the structural trend of the Cumberland Domain and is faulted by the Suggi Lake Fault. Its eastern contact with the Amisk Domain is tentatively interpreted to be tectonic. The geophysical characteristics of this intrusive body are comparable to those for the Cormorant Batholith. This may suggest a similar late emplacement age in the magmatic history of the area.

### Sturgeon-weir Shear Zone

The Sturgeon-weir Shear Zone is generally thought to separate the Flin Flon Belt to the east from the Hanson Lake Block to the west (Macdonald, 1981; Ashton, 1992; Slimmon,

1992). Structural studies demonstrate oblique dextral-reverse displacement on this moderately east-dipping structure, implying southwestward overthrusting of the Flin Flon Belt (Ashton, 1992). The sub-Phanerozoic extension of this shear zone is marked by a weak aeromagnetic lineament which is generally concordant with or obliquely crosscutting with respect to the trend of anomaly patterns (Fig. 2). Some segments of the shear zone are largely inferred, because of their lack of definitive expression.

### Suggi Lake Fault

The Suggi Lake Fault is a northeast-trending structure that has been mapped on the basis of both a marked change in the character of aeromagnetic anomaly patterns and the deflection and truncation of their trends (Fig. 2). Although this fault is buried beneath the Phanerozoic cover over its entire strike length (>45 km), it is considered to be a fundamental structure that subdivides the sub-Phanerozoic portion of the Hanson Lake Block into two subdomains. The Suggi Lake Fault roughly coincides with a regional gravity low and appears to be truncated by the Spruce Rapids Shear Zone to the northeast and the Tabbornor Fault Zone to the southwest. The clockwise deflection of anomaly patterns into the Suggi Lake Fault implies dextral separation in map-view.

### Hanson Lake Block

The Hanson Lake Block is bounded by the Sturgeon-weir Shear Zone on the east and the Tabbornor Fault Zone on the west (Lewry et al., 1990). It consists of a wide variety of supracrustal and plutonic rocks which have a north-south structural trend (cf. Byers, 1957; Macdonald and Posehn, 1976; Macdonald, 1981; Slimmon, 1992; Maxeiner et al., 1992). The aeromagnetic anomaly patterns produced by these rocks can be traced below the Phanerozoic cover to the Suggi Lake Fault (Fig. 2). The drill core data indicate that the sub-Phanerozoic basement includes amphibolite-facies volcanic and volcanoclastic rocks of basaltic to rhyolitic composition (unit **Ah**; Fig. 3). These rocks appear to correlate with the Hanson Lake metavolcanics as they are dominated by dacitic compositions (see Maxeiner et al., 1992). They are intercalated with calcic and psammitic metasedimentary rocks. The supracrustal rocks are intruded by diorite, gabbro, quartz-feldspar porphyry, and peridotite bodies. This part of the Hanson Lake Block is typically associated with a positive gravity anomaly (-35 to -55 mGal). The slightly less positive gravity expression compared to the Amisk Lake Domain (-45 to -25 mGal) can be attributed to its relatively large proportion of less dense felsic to intermediate volcanic rocks.

Further south, a gentle gravity gradient of -50 to -60 mGal suggests the presence of plutonic rocks such as tonalite, diorite, quartz diorite, granodiorite, and granite (units **T** and **G**; Fig. 3). A high-amplitude positive aeromagnetic anomaly is interpreted as gabbro. The rest of the basement displays aeromagnetic patterns that resemble those expressed by the metavolcanic package to the north. The single drillhole for this area penetrated intercalated metabasalt and mafic metatuff, coinciding with a striated aeromagnetic anomaly pattern that extends from the shield margin.

A gravity high with a peak value of -28 mGal and a matching high-intensity positive aeromagnetic anomaly occur along the western edge of the Hanson Lake Block (Fig. 2). Correlation with similar types of geophysical expression suggests a mafic pluton of gabbro-pyroxenite (see Leclair et al., 1993a).

The aeromagnetic signature of the Hanson Lake Block changes markedly south of the Suggi Lake Fault, where it can be divided into four main geological-geophysical elements (Fig. 2):

1. The northernmost element is characterized by an aeromagnetically low-relief neutral pattern without internal fabric and a gravity low (<-55 mGal). These geophysical traits correlate with those for felsic intrusive bodies (unit G; Fig. 3), such as the Cormorant Batholith and Windy Lake Pluton.

2. A dome-shaped magnetic boundary to the south may represent the margin of a granitoid intrusion, possibly belonging to unit T (Fig. 3). This element is associated with a negative aeromagnetic anomaly featuring a weak semi-concentric internal fabric, and gravity values between -45 and -55 mGal (Fig. 2 and 4).

3. Further south, gravity and magnetic highs (Fig. 2) coincide with a subcircular gabbro-diorite pluton (unit Ga; Fig. 3). This gabbro-diorite is coarse grained and massive, and contains 60-85% combined hypersthene, clinopyroxene, biotite, olivine, and magnetite.

4. Within the southernmost element, a few drillholes intersected amphibolite, heterogeneous mafic, calcic and psammitic gneisses and gabbro. The amphibolite and some of the gneisses are thought to be derived from volcanic and volcanoclastic rocks of mafic to intermediate composition. Gneisses composed of alternating garnet-, magnetite-, and quartz-rich layers may be derived from oxide-facies iron-formation and chert. These gneisses are considered to produce the narrow high-amplitude positive aeromagnetic anomalies which are sharply truncated against the gabbro-diorite pluton.

### Tabbemor Fault Zone

The north-trending Tabbemor Fault Zone separates the Hanson Lake Block to the east from the Glennie Domain to the west (Lewry et al., 1990). The exposed north-striking Tulabi Brook and Sarginson Lake faults, which are part of the fault array

**Table 1.** Summary of density measurements.

LITHOLOGY	NUMBER OF SAMPLES	RANGE	STANDARD DEVIATION	MEAN DENSITY
Mafic Volcanic Rock	206	2.45-3.22	0.13	2.96
Intermediate Volcanic Rock	115	2.23-3.10	0.14	2.82
Felsic Volcanic Rock	82	2.41-2.97	0.07	2.73
Amphibolite	125	2.84-3.19	0.07	3.03
Mafic gneiss	78	2.73-3.44	0.12	2.99
Intermediate gneiss	88	2.34-3.10	0.12	2.83
Felsic gneiss	42	2.40-2.98	0.10	2.73
Calcic gneiss	57	2.76-3.14	0.11	2.94
Pelitic metasediment	32	2.63-3.06	0.09	2.83
Semipelitic metasediment	49	2.06-3.06	0.14	2.81
Psammitic metasediment	60	2.55-3.11	0.11	2.85
Wacke, Mudstone	50	2.24-3.44	0.19	2.81
Graphitic Argillite	42	1.33-3.24	0.30	2.76
Iron Formation	15	2.71-3.57	0.23	2.93
Mafic Intrusive Rock	163	2.18-3.21	0.14	2.95
Felsic Intrusive Rock	268	2.57-3.08	0.07	2.73
Ultramafic Intrusive rock	31	2.67-3.18	0.12	2.99

comprising the Tabbemor Fault Zone (Macdonald and Posehn, 1976; Lewry et al., 1991), have been traced south as two prominent aeromagnetic lineaments (Leclair et al., 1993b) (Fig. 2). The eastern lineament obliquely truncates the aeromagnetic anomaly patterns in the Hanson Lake Block lying to the east. Patterns west of the fault zone appear to extend across the western lineament. This supports the suggestion that the Tabbemor Fault Zone is a late feature across which there is general continuity of lithotectonic elements (Lewry et al., 1991).

On the basis of the character of potential field anomalies and limited drill core data, it is suggested that the sub-Phanerozoic segment of the Tabbemor Fault Zone is dominated by granitoid rocks in the north and supracrustal rocks in the south (Fig. 3). The continuity of anomalies with exposed rocks indicates that the zone includes amphibolite-facies mafic volcanic and mixed volcanoclastic rocks of the Northern Lights Volcanics (see Macdonald and Posehn, 1976; Lewry et al., 1991). One drillhole in the northern part intersected massive granite coinciding with a region of low aeromagnetic relief with little internal fabric (Fig. 2). Near the southern edge of 63L, closely-spaced drillholes revealed a remarkable section of volcanic and volcanoclastic rocks with transitional greenschist-amphibolite facies metamorphic assemblages. This section comprises basalt and andesite flows, heterolithic mafic to intermediate debris flows, and felsic to intermediate tuffs associated with minor iron-formation and cherty interbeds. Locally, these rocks are interbedded with siltstone and argillite and intruded by massive gabbro-diorite, diabase, and quartz-plagioclase porphyry.

### West of the Tabbemor Fault Zone

Exposed rocks west of the Tabbemor Fault Zone have been assigned to the Glennie Domain and comprise mainly mafic and metasedimentary gneisses intruded by granitoid plutons. The mafic gneisses have been interpreted as highly strained metagabbro and metavolcanic rocks belonging to the Northern Lights and Hanson Lake volcanics (Macdonald and Posehn, 1976; Lewry et al., 1991). The sub-Phanerozoic continuity of these rocks is indicated by a well-striated aeromagnetic anomaly pattern striking north (Fig. 2).

### DENSITY MEASUREMENTS

Density measurements were done on 1503 drill core samples using a high-precision digital balance. The samples have been grouped into seventeen rock types (Table 1) on the basis of mafic content and general composition. Variations within a particular rock type reflect degrees of alteration, mineralization, and the percentage of mafic minerals present. The results have been incorporated into the digital geoscience database of the NATMAP Shield Margin Project, where they are being used in ongoing sub-Phanerozoic interpretation and GIS analysis studies.

### SUMMARY

The integrated interpretation studies of potential field and drill core data represent an important component of the coordinated efforts by the federal and provincial geological surveys to map and understand the geology of the sub-Phanerozoic continuation of the Flin Flon-Snow Lake-Hanson Lake Belt. To date the results of these studies have opened a window (>14 000 km<sup>2</sup>) on the sub-Phanerozoic Precambrian basement in parts of the Cormorant (63K) and Amisk Lake (63L) areas. Numerous geological-geophysical elements of the buried basement have been mapped and characterized, including major fault zones that separate distinct lithotectonic domains. The result is a new regional framework for the geology and structure of a large portion of the sub-Phanerozoic basement in the project area.

### ACKNOWLEDGMENTS

The following exploration companies are acknowledged for granting permission to examine confidential drill core and reports: Cameco Corp., Cominco Ltd., Esso Ltd., Granges Inc., Hudson Bay Exploration and Development Co. Ltd., Inco Inc., and Parres Ltd. Rod MacQuarrie, Stephen Masson, John Pearson, Jim Pickell, Dave Price, and Tony Pryslak provided stimulating discussions. We thank Warner Miles for the shaded relief aeromagnetic map. Critical reviews by Robert Macdonald and Richard Stern improved the presentation.

### REFERENCES

- Ashton, K.E.  
1992: Geology of the Snake Rapids area: Update; in Summary of Investigations 1992, Saskatchewan Geological Survey, Saskatchewan Energy Mines, Miscellaneous Report 92-4, p. 97-113.
- Blair, B., Weber, W., Kornik, L.J., and Gordon, T.M.  
1988: Project Cormorant: Interpretations of sub-Paleozoic geology of the Cormorant Lake map area from geophysical and drill core data; Geoscience Canada, v. 15, p. 98-100.
- Broome, J.H., Lucas, S.B., and Thomas, M.D.  
1993: Bouguer gravity map of the sub-Phanerozoic portion of the Flin Flon Belt, Manitoba and Saskatchewan; Geological Survey of Canada, Open File 2657, scale 1:250 000.
- Byers, A.R.  
1957: Geology and mineral deposits of the Hanson Lake area, Saskatchewan; Saskatchewan Department of Mineral Resources, Report 30, 47 p.
- Byers, A.R. and Dahlstrom, C.D.A.  
1954: Geology and mineral deposits of the Amisk-Wildnest lakes area, Saskatchewan; Saskatchewan Department of Mineral Resources, Report 14, 177 p.
- Geological Survey of Canada  
1993: Aeromagnetic (Residual Total Field and Vertical Gradient) maps, Manitoba and Saskatchewan; NTS 63J, 63K and 63L map areas, scale 1:50 000.
- Gordon, T.M., Hunt, P.A., Baines, A.H., and Syme, E.C.  
1990: U-Pb zircon ages from the Flin Flon and Kisseynew belts, Manitoba: Chronology of crust formation at an Early Proterozoic accretionary margin; in The Early Proterozoic Trans-Hudson Orogen of North America, (ed.) J.F. Lewry and M.R. Stauffer; Geological Association of Canada, Special Paper 37, p. 177-199.

- Green, A.G., Hajnal, Z., and Weber, W.**  
1985: An evolutionary model of the western Churchill Province and western margin of the Superior Province in Canada and the north-central United States; *Tectonophysics*, v. 116, p. 281-322.
- Leclair, A.D. and Weber, W.**  
1993: NATMAP diamond drilling program: additional insights on the sub-Phanerozoic geology south of the Flin Flon-Snow Lake Belt; in *Manitoba Energy and Mines, Report of Activities, 1993*, p. 112-116.
- Leclair, A.D., Broome, H.J., Lucas, S.B., Stern, R.A., and Thomas, M.D.**  
1993c: A new interpretation of the sub-Paleozoic bedrock geology of the Flin Flon Belt from integrated drillcore and potential field data, Manitoba and Saskatchewan; *Geological Association of Canada, Program with Abstracts*, v. 18, p. A57.
- Leclair, A.D., Broome, H.J., Lucas, S.B., and Viljoen, D.**  
1993b: Development of interpretive sub-Phanerozoic maps for NTS 63K and 63L, Manitoba and Saskatchewan; (extended abstract) *Canadian Institute of Mining and Metallurgy, Special meeting of Flin Flon-Creighton Branch, Flin Flon*.
- Leclair, A.D., Scott, R.G., and Lucas, S.B.**  
1993a: Sub-Paleozoic geology of the Flin Flon Belt from integrated drillcore and potential field data, Cormorant Lake area, Manitoba and Saskatchewan; in *Current Research, Part C; Geological Survey of Canada, Paper 93-1C*, p. 249-258.
- Lewry, J.F., Sibbald, T.I.I., and Hayward, N.**  
1991: Revision bedrock geological remapping of the Southeast Arm, Deschambault Lake-Northern Lights area (parts of NTS 63L-10, -11 and 14); in *Summary of Investigations 1991, Saskatchewan Geological Survey, Saskatchewan Energy Mines, Miscellaneous Report 91-4*, p. 57-65.
- Lewry, J.F., Thomas, D.J., Macdonald, R., and Chiarenzelli, J.**  
1990: Structural relations in accreted terranes of the Trans-Hudson Orogen, Saskatchewan: telescoping in a collisional regime?; in *The Early Proterozoic Trans-Hudson Orogen of North America*, (ed.) J.F. Lewry and M.R. Stauffer; *Geological Association of Canada, Special Paper 37*, p. 75-94.
- Lucas, S.B.**  
1992: NATMAP Shield Margin Project: new results from multidisciplinary studies in the Flin Flon-Snow Lake Belt and its sub-Paleozoic continuation; in *Report of Activities 1992, Manitoba Energy Mines*, p. 103-105.
- Lucas, S.B. and NATMAP Shield Margin Project Group**  
1993: Geology of the Cormorant Lake sheet (NTS 63K), Manitoba and Saskatchewan; *Geological Survey of Canada, Open File 2581*, 3 sheets, scale 1:250 000.
- Lucas, S.B., Green, A., Hajnal, Z., White, D., Lewry, J., Ashton, K., Weber, W., and Clowes, R.**  
1993: Deep seismic profile across a Proterozoic collision zone: surprises at depth; *Nature*, v. 363, p. 339-342.
- Macdonald, R.**  
1981: Compilation bedrock geology: Pelican Narrows and Amisk Lake areas; (NTS 63M, 63L, part of 63N and 63K); Preliminary geological map, 1:250,000 scale; in *Summary of Investigations 1981, Saskatchewan Department of Mineral Resources, Miscellaneous Report 81-4*, p. 16-23.
- Macdonald, R. and Posehn, G.A.**  
1976: Re-investigation of the Pickereel River and Limestone-Tulabi Lakes area; in *Summary of Investigations 1976, Saskatchewan Department of Mineral Resources*, p. 44-52.
- Maxeiner, R.O., Watters, B.R., and Sibbald, T.I.I.**  
1992: New implications for geochemistry and metamorphism in the Hanson Lake area; in *Summary of Investigations 1992, Saskatchewan Geological Survey, Saskatchewan Energy Mines, Miscellaneous Report 92-4*, p. 72-78.
- Reilly, B.A.**  
1992: Revision bedrock geological mapping, Neagle Lake-Errington Lake area (parts of NTS 63L-9 and -16); in *Summary of Investigations 1992, Saskatchewan Geological Survey, Saskatchewan Energy Mines, Miscellaneous Report 92-4*, p. 16-22.
- Slimmon, W.L.**  
1991: Revision bedrock geological mapping, Table Lake area (part of NTS 63L-9); in *Summary of Investigations 1991, Saskatchewan Geological Survey, Saskatchewan Energy Mines, Miscellaneous Report 91-4*, p. 16-20.
- 1992: Bedrock geological mapping, Hanson Lake-Sturgeon-weir River area (part of NTS 63L-10 and -15); in *Summary of Investigations 1992, Saskatchewan Geological Survey, Saskatchewan Energy Mines, Miscellaneous Report 92-4*, p. 23-29.
- Stern, R.A., Lucas, S.B., Syme, E.C., Bailes, A.H., Thomas, D.J., Leclair, A.D., and Hulbert, L.**  
1993: Geochronological studies in the Flin Flon Domain, Manitoba-Saskatchewan, NATMAP Shield Margin Project Area: Results for 1992-1993; in *Radiogenic Age and Isotopic Studies: Report 7; Geological Survey of Canada, Paper 93-2*, p. 59-70.
- Syme, E.C., Thomas, D.J., Bailes, A.H., Reilly, B.A., and Slimmon, W.L.**  
1993: Geology of the Flin Flon area, Manitoba and Saskatchewan (parts of NTS 63K and 63L); *Geological Survey of Canada, Open File 2658*, 1 sheet, scale 1:50 000.
- Thomas, M.D., Williamson, B.L., Williams, R.P., and Miles, W.**  
1993: Progress report on gravity surveys in Cormorant Lake map area, Manitoba-Saskatchewan; in *Current Research, Part C; Geological Survey of Canada, Paper 93-1C*, p. 239-247.



# Geological, geochemical, and age constraints on base metal mineralization in the Manitouwadge greenstone belt, northwestern Ontario<sup>1</sup>

E. Zaleski, V.L. Peterson, and O. van Breemen  
Continental Geosciences Division

*Zaleski, E., Peterson, V.L., and van Breemen, O., 1994: Geological, geochemical, and age constraints on base metal mineralization in the Manitouwadge greenstone belt, northwestern Ontario; in Current Research 1994-C; Geological Survey of Canada, p. 225-235.*

---

**Abstract:** The Cu-Zn deposits of the Manitouwadge greenstone belt lie within an upper amphibolite-facies, highly deformed remnant of supracrustal rocks adjacent to the Wawa-Quetico subprovince boundary. In the primary depositional setting, two independent and geochemically distinct, coeval volcanic centres (circa 2720 Ma) erupted calc-alkaline felsic rocks onto a substratum of tholeiitic shield basalt. Metasedimentary rocks were deposited in a basin between the volcanic centres. The northern felsic domain, associated with extensive synvolcanic alteration, subvolcanic intrusion and iron-formations, hosts massive sulphide mineralization including the Geco mine. Original relationships were modified during D1 and D2 thrust imbrication and folding. The regional structure of the belt is dominated by the D3 Manitouwadge synform, interpreted to be a refolded fold. Metamorphic grade increases continuously across the Wawa-Quetico boundary, but peak conditions developed later in the Quetico subprovince (2670 to 2650 Ma) than in the Manitouwadge belt (2675 Ma).

**Résumé :** Les gisements de Cu-Zn de la ceinture de roches vertes de Manitouwadge se situent dans un vestige intensément déformé de roches supracrustales du faciès des amphibolites supérieur jouxtant la limite des sous-provinces de Wawa et de Quetico. Le milieu de mise en place des volcanites est caractérisé par deux centres de volcanisme contemporains l'un de l'autre, indépendants et géochimiquement distincts (âgés d'environ 2 720 Ma), ayant épanché des laves felsiques calco-alkalines sur un substratum de basalte tholéiitique issu de volcan en bouclier. Des roches métasédimentaires se sont déposées dans un bassin entre les centres volcaniques. Le domaine felsique du nord, auquel sont associés une altération synvolcanique de grande étendue, des intrusions hypovolcaniques et des formations de fer, contient des minéralisations de sulfures massifs, dont le gisement de la mine Geco. Les relations originelles se sont modifiées pendant les phases D1 et D2 d'imbrication par chevauchement et de plissement. La structure régionale de la ceinture est dominée par le synforme de Manitouwadge associé à D3, qui serait un pli ayant subi un replissement. Le degré de métamorphisme augmente continuellement d'un côté à l'autre de la limite des sous-provinces de Wawa et de Quetico, mais le métamorphisme a culminé plus tardivement dans la sous-province de Quetico (2 670 à 2 650 Ma) que dans la ceinture de Manitouwadge (2 675 Ma).

---

<sup>1</sup> Contribution to Canada-Ontario Subsidiary Agreement on Northern Ontario Development (1991-1995), under the Canada-Ontario Economic and Regional Development Agreement.

## INTRODUCTION

The Manitouwadge greenstone belt and its Cu-Zn deposits, including the Geco mine, have seen a complex magmatic, metamorphic and structural history. Our objective in this field-based project is to gain an understanding of the origin, setting and subsequent modification of the mineralization and alteration, and their host rocks. Observations during the 1993 field season, presented here and in a companion paper (Peterson and Zaleski, 1994), have resulted in reinterpretation of the volcanic and structural setting of the belt and its attenuated and dismembered extensions. Detailed mapping (1:5000) in 1992 encompassed the past and present Cu-Zn producers, the Geco, Willroy, Nama Creek and Willecho mines (Fig. 1) (Zaleski and Peterson, 1993a). In 1993, mapping was directed toward more extensive coverage of the belt, its extensions and enclosing plutonic rocks (Zaleski and Peterson, 1993b). Detailed mapping (1:10 000) was pursued in key areas, in particular, in the hinge regions of map-scale folds that determine the geometry of the Manitouwadge belt.

## REGIONAL SETTING

The Manitouwadge belt lies in the volcano-plutonic Wawa subprovince of the Superior Province, near its boundary with the metasedimentary-migmatitic Quetico subprovince (Fig. 1). The belt is a remnant of metavolcanic and metasedimentary rocks, highly deformed and metamorphosed to upper amphibolite facies. The supracrustal rocks are bounded to the west and south by foliated multiphase plutonic rocks, mostly tonalitic, of the Black Pic batholith. Within the batholith to the northwest of the Manitouwadge belt, screens of supracrustal rocks and aeromagnetic lineaments trend southwest toward the Schreiber-Hemlo greenstone belt (Fig. 1, inset), suggesting dismemberment of an originally continuous greenstone terrane (Williams et al., 1991). Both belts host massive sulphide mineralization interpreted to be of synvolcanic origin (Suffel et al., 1971; Friesen et al., 1982; Severin et al., 1990). To the east and possibly continuous with the Manitouwadge belt, the Moshkinabi belt comprises supracrustal rocks intruded by a layered complex including gabbro, leucogabbro, anorthosite and peridotite (Williams and Breaks, 1989; 1990).

Five phases of ductile deformation, some of which involve the Wawa-Quetico subprovince boundary, are recognized in the Manitouwadge belt (Peterson and Zaleski, 1994). D1 and D2 are based on the interpretation of pre- to syn-metamorphic ductile thrust faults and, in the case of D2, associated folds. D2 was the main fabric-forming event, producing the dominant foliations and lineations (Fig. 1). The regional geometry of the belt is largely shaped by the D3 Manitouwadge synform, with the greatest thickness of supracrustal rocks in the hinge region of the fold. The synform folds D2 foliations and lineations, and is refolded and deformed by D4 and D5 structures (ibid.).

In the Schreiber-Hemlo belt, felsic volcanism ranges in age from  $2772 \pm 2$  Ma near the Hemlo gold camp to  $2695 \pm 2$  Ma for the Heron Bay volcanic complex (Corfu and Muir, 1989a).

Felsic metavolcanic rocks associated with the Winston Lake Zn-Cu mine near Schreiber, and muscovite schist (altered rhyolite) at the Geco Cu-Zn mine, Manitouwadge, contain zircons of the same age,  $2723 \pm 2$  Ma (Schandl et al., 1991) and  $2720 \pm 2$  Ma (Davis et al., in press), respectively. Monazites, interpreted as synmetamorphic, gave ages of  $2675 \pm 1$  Ma at Geco and  $2677 \pm 1$  Ma at Winston Lake (ibid.). Tonalitic rocks of the Black Pic batholith apparently were intruded during or somewhat before D2 deformation in the Manitouwadge belt (Peterson and Zaleski, 1994), and probably contributed to metamorphic heating. South of the Schreiber-Hemlo belt, marginal rocks of the Pukaskwa batholith were intruded at  $2719 \pm 6/-4$  Ma (Corfu and Muir, 1989a), broadly coeval with felsic volcanism at Winston Lake and Manitouwadge. Near Hemlo, several granodiorite plutons cluster closely around 2687-2688 Ma, but amphibolite-facies metamorphism dated by titanite, peaked around 2676-2678 Ma, coeval with the late tectonic Gowan Lake pluton at  $2678 \pm 2$  Ma (Corfu and Muir, 1989b). These ages suggest synchronous metamorphism throughout most of this part of the Wawa subprovince. Younger monazite ( $2661 \pm 1$  Ma) in biotite schist at Geco was interpreted to date late K-metasomatism (Davis et al., in press).

The metagreywackes of the Quetico subprovince have been interpreted as an accretionary complex, contiguous with the Wawa subprovince at least since 2689-2684 Ma, and possibly since 2696-2689 Ma (Percival, 1989). Provenance studies show a dominance of felsic volcanogenic sources with ages  $<2750$  Ma (ibid.) and, in western Ontario, detrital zircons defining an age of  $2698 \pm 3$  Ma constrain the maximum age of sedimentation (Davis et al., 1990). Along most of its length, the Quetico is metamorphically zoned from low grade margins adjacent to the Wawa and Wabigoon subprovinces, to high grade central migmatites (see Percival, 1989). Percival (1989) suggested that metamorphism was approximately coeval with granitic intrusion from 2670-2650 Ma, and that this generally post-dated plutonism in the Wawa and Wabigoon subprovinces. The Wawa-Quetico boundary in the vicinity of the Manitouwadge greenstone belt is unusual in that there is a continuous metamorphic gradient, from amphibolite facies in the region of the Schreiber-Hemlo greenstone belt (Corfu and Muir, 1989b), through upper amphibolite at Manitouwadge, to upper amphibolite and granulite facies in the southern Quetico subprovince (Williams and Breaks, 1989).

## LOCAL GEOLOGY

The Manitouwadge greenstone belt comprises felsic to mafic metavolcanic rocks, metamorphosed iron-formation, metasedimentary rocks and foliated intrusive rocks (Fig. 1). The main lithological units were described in Zaleski and Peterson (1993a), and are summarized in Table 1 (see also GSC Open File 2753). Several Cu-Zn mines, including the Willroy and Geco mines, lie along the north side of the southern limb and toward the hinge region of the Manitouwadge synform. A laterally persistent unit of orthoamphibole-cordierite-garnet gneiss, interpreted as metamorphosed synvolcanic altered

rocks, lies to the north of most of the deposits. Zones of straight gneiss (annealed mylonite), associated with truncation of units and repetition of sequences, have been interpreted as the loci of D1 and D2 ductile thrust faults (Zaleski and Peterson, 1993a; Peterson and Zaleski, 1994). Thrust imbrication, folding, and the likely presence of additional cryptic early faults, complicates recognition of a stratigraphic sequence and relationships between massive sulphide deposits. Nevertheless, interpretation of the general sequence: mafic metavolcanic rocks, felsic metavolcanic rocks, and metagreywackes, as a stratigraphic succession has been supported, based on comparison to typical successions in other greenstone belts (Suffel et al., 1971; Friesen et al., 1982).

Away from the hinge region of the D3 Manitouwadge synform, supracrustal units are attenuated and invaded by foliated plutonic rocks. Along the northern limb, orthoamphibole-garnet gneisses outcrop along the inner margin of the synform as far as Rabbitskin Lake (Fig. 1). Mafic rocks and iron-formation extend east of Rabbitskin Lake, mainly as screens engulfed by plutonic rocks. North of Thompson Lake, the zone of supracrustal screens is folded by the Blackman Lake antiform (D4), and the Jim Lake synform (D4) south of the Quetico boundary (Peterson and Zaleski, 1994). The general paucity of identifiable screens of felsic to intermediate composition is probably due to their susceptibility to digestion by intrusive rocks, and to their compositional similarity to the dominantly tonalitic plutonic suite.

Along the southern limb of the Manitouwadge synform, two belts of metavolcanic rocks diverge eastward (Fig. 1). The southern belt of mafic metavolcanic rocks can be traced as screens within foliated plutonic rocks. South of Thompson Lake, the Banana Lake antiform (D5) is poorly exposed and no supracrustal rocks outcrop in the hinge region. Foliations in plutonic rocks are folded, and supracrustal rocks are exposed in the southern part of the short limb (as screens) and in the Moshkinabi belt (Fig. 1, inset) where they are intruded by layered gabbroic, anorthositic and ultramafic rocks (Williams and Breaks, 1990).

Orthoamphibole-cordierite-garnet gneisses and iron-formation (locally referred to as the Geco horizon), and associated straight gneisses are exposed as far east as the Hucamp zone of subeconomic mineralization near Wowun Lake (Fig. 1). To the north, orthoamphibole-cordierite-garnet gneisses are in contact with foliated quartz-rich tonalite (Table 1), identified to the north of the Willroy and Geco deposits as a synvolcanic intrusion (Zaleski and Peterson, 1993a; also Geochemistry and Geochronology). The straight gneisses (annealed mylonites), lying between orthoamphibole-cordierite-garnet gneisses to the north and iron-formation to the south, are interpreted as the lateral extension of an early ductile thrust fault that caused imbrication of quartz-phyric felsic rocks in the Willroy area (ibid. and Fig. 3). East of the Hucamp zone (Fig. 1), the Geco horizon forms a prominent aeromagnetic anomaly and has been intersected by drilling as far as the Falconbridge zone of subeconomic mineralization (H. Lockwood, pers. comm., 1993). In the East One Otter and Banana grid areas, semicontinuous screens of orthoamphibole-garnet gneisses, mafic rocks and, in one area, iron-formation, define complex folding (D4) with a northerly striking enveloping surface (fig. 6 in Peterson and Zaleski, 1994).

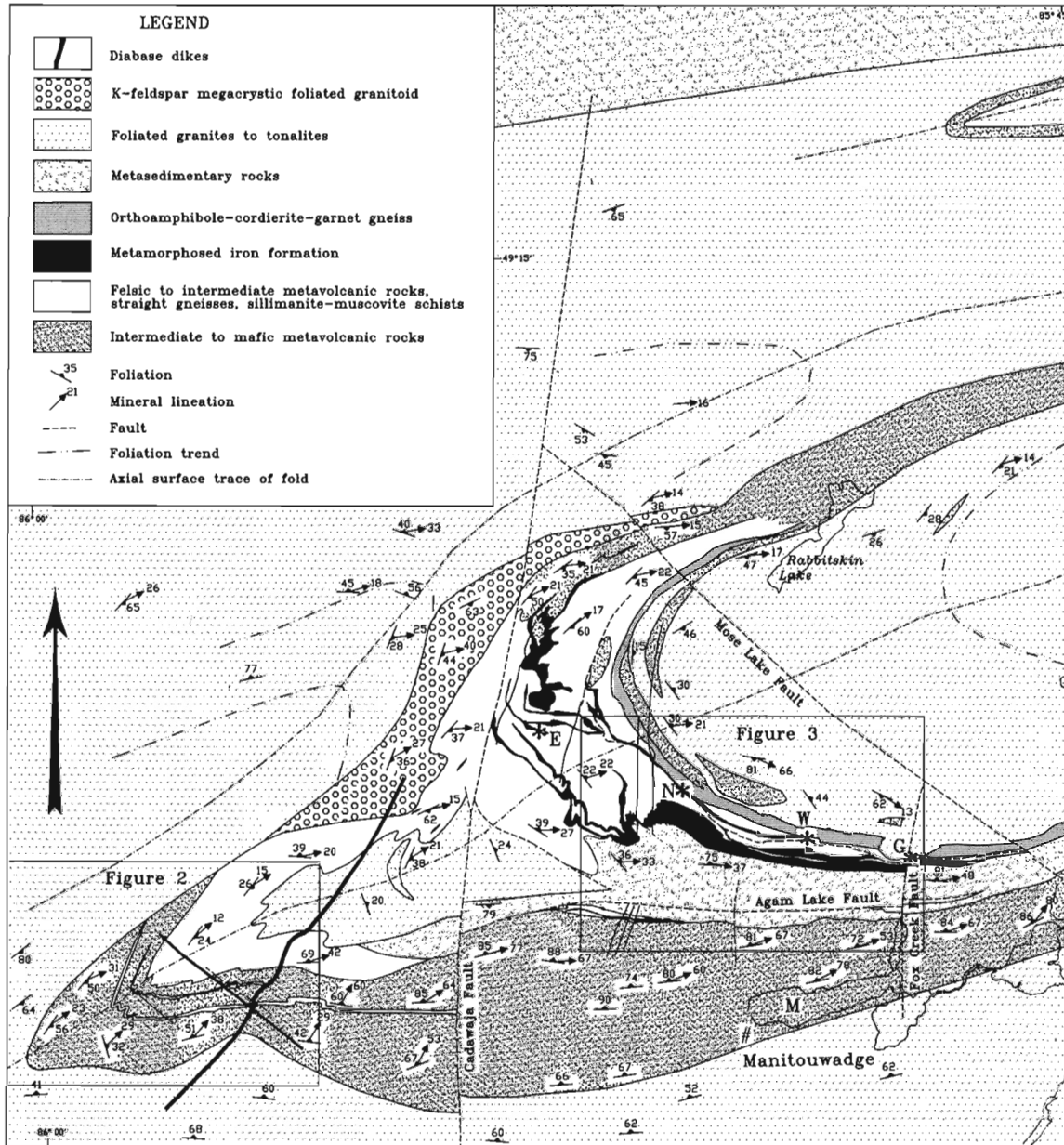
Orthoamphibole-garnet gneisses are associated with a distinctive rock composed of abundant medium grained quartz in a matrix of fine grained garnet and magnetite; an origin as digested iron-formation has been suggested (H. Lockwood, pers. comm., 1993). Much of the enclosing rock is foliated quartz-rich tonalite similar in texture and mineral proportions to the synvolcanic intrusion to the west. The supracrustal/altered suite is tentatively correlated with the Geco horizon (Falconbridge zone), separated by an interpreted sinistral shear zone (Peterson and Zaleski, 1994).

Within the core of the Manitouwadge synform, there is a transition from foliated quartz-rich tonalite (synvolcanic) to more potassic foliated granitoids in the centre. Both quartz-rich tonalite and granitoids are consistently medium- to coarse-grained, quartz-rich and typically contain disseminated magnetite porphyroblasts (Table 1). Supracrustal screens, including mafic rocks, iron-formation and quartz-rich rocks with a fine grained garnet-magnetite matrix, occur well within the central plutonic area (to the central foliation trend in fig. 1 which corresponds to an aeromagnetic trend in Fig. 3 of Peterson and Zaleski, 1994). The extent of the synvolcanic intrusion is not known; but given these observations, it is possible that between the main sequence of supracrustal rocks and the innermost screens, most of the foliated plutonic rocks are synvolcanic. An alternative interpretation for the supracrustal rocks in the East One Otter and Banana areas would correlate them with the inner zone of screens.

Rocks of the Black Pic batholith, outside the supracrustal belt, differ from those of the plutonic core. The Black Pic batholith comprises a multiphase suite of foliated tonalites, with subordinate foliated diorites, granodiorites, granites and cross-cutting aplitic to pegmatitic dykes. In general, intrusive relationships indicate that the more mafic phases are older, although all phases are foliated. Near the Blackman Lake antiform, weakly foliated to massive leucocratic tonalite is commonly present on the short limbs of minor and map-scale folds and outcrop-scale shear zones. Contacts with the foliated host rocks are diffuse. The relationships suggest that these are anatectic mobilizates that migrated into dilational zones. Evidence of migmatization increases northward toward the Quetico boundary (also Peterson and Zaleski, 1994). In the Quetico subprovince, metasedimentary rocks south of the granulite-facies isograd locally contain cordierite-bearing leucosome.

### *Swill Lake hinge region of the Manitouwadge synform*

In the Swill Lake area, the southern domain of mafic and felsic metavolcanic rocks is folded in the hinge region of the D3 Manitouwadge synform (Peterson and Zaleski, 1994) (Fig. 2). The southernmost unit is a thick sequence of mafic metavolcanic rocks, varying from homogeneous schists, to laminated and layered schists (tuffaceous?), to pillowed flows. Foliated gabbroic rocks, interlayered with the fine grained mafic schists, may be massive flows, massive bases of flows, or sills. Fine grained, high strain zones in the gabbro resemble homogeneous mafic schists. Strain is generally high, but in one location, pillow shapes suggest southerly



**Figure 1.** Generalized geology of the Manitowadge greenstone belt, based on mapping and compilation of existing maps and aeromagnetic data (see Peterson and Zaleski, 1994, Fig. 3 for a corresponding aeromagnetic map). G-Geco mine, W-Willroy mine, N-Nama Creek mine, E-Willecho mine, H-Hucamp zone, F-Falconbridge zone, B-Banana grid area, O-East One Otter grid area, M-Manitowadge Lake. The inset shows the location of the Manitowadge belt, and the Schreiber-Hemlo greenstone belt to the southwest, in the Wawa subprovince. G-Geco mine, Z-Winston Lake Zn-Cu mine, A-Hemlo gold camp, Mb-Moshkinabi belt, PC-Port Coldwell alkalic complex. Adapted from Williams et al. (1991).

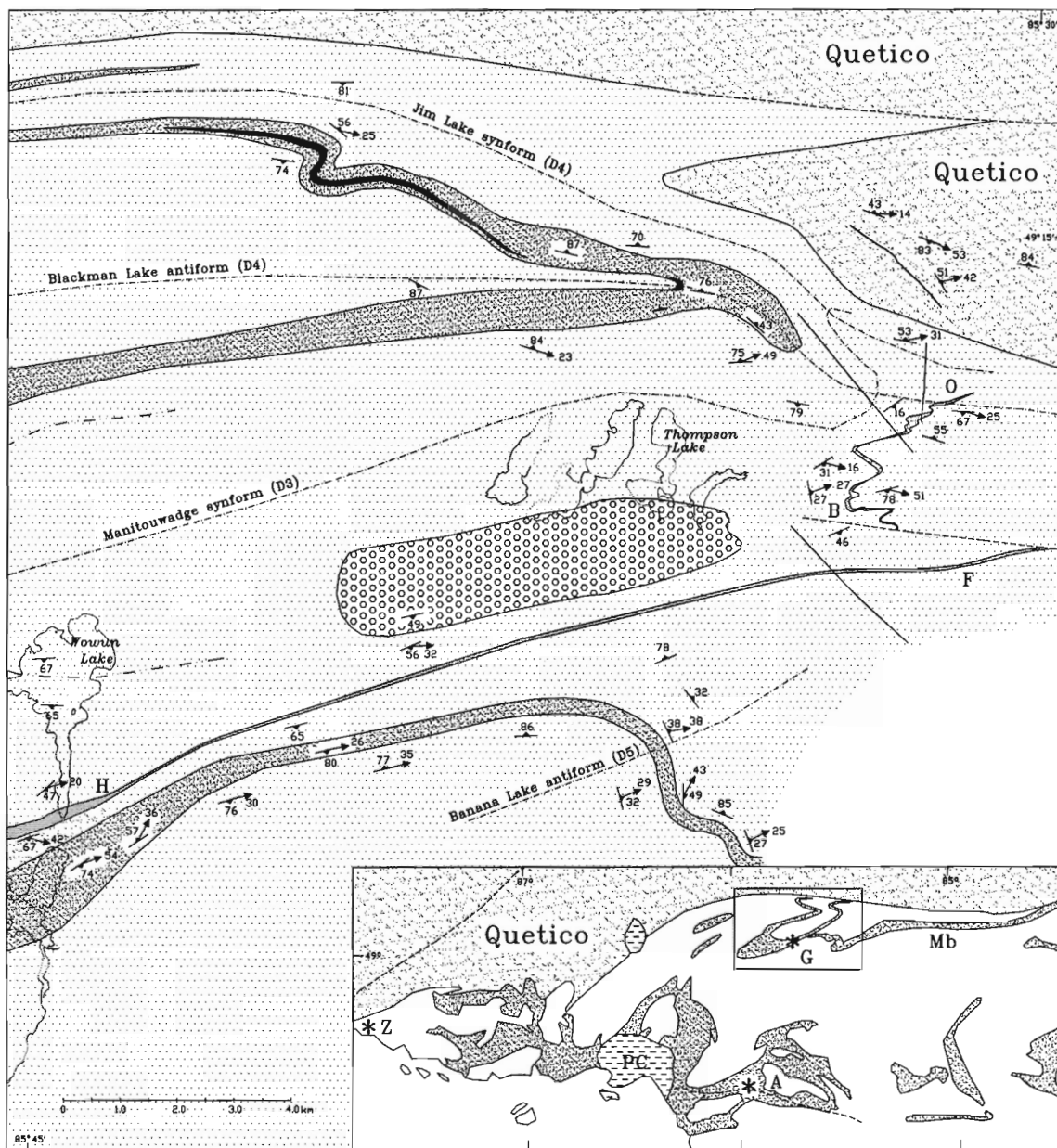


Figure 1. (cont.)



**Table 1.** Summary of Units.

Unit	Description
<b>INTRUSIVE ROCK UNITS</b>	
Diabase	Dikes of probable Proterozoic age
Pegmatites, aplites	Massive to foliated, locally porphyroclastic or with lineated Sil on shear surfaces and transitional to straight gneiss
Undifferentiated foliated intrusive rocks	Diorite, tonalite, granodiorite, granite, mostly multiphase intrusions (e.g. Black Pic batholith) enclosing supracrustal rocks, also semiconcordant bodies within supracrustal rocks
Foliated K-feldspar porphyritic granitoid	In two main bodies: 1) west between Black Pic batholith and supracrustal rocks - Hbl-Bt-rich (to 25%) matrix, sparse (1-25%) 1 cm phenocrysts, involved in Nama Creek shear zone, 2) east between limbs of Manitouwadge synform - Kfs megacrystic (to 15 cm) augen
Foliated quartz-rich tonalite	Synvolcanic intrusion locally with Grt-Oam alteration seams (Fig. 7 in Zaleski and Peterson, 1993a), transitional to more potassic variants toward synform core, leucocratic, medium to coarse grained, Qtz-rich (30-45%), typically Mag porphyroblasts
<b>TECTONIC ROCK UNITS</b>	
Straight gneiss	Laminated annealed mylonite, mappable units of felsic composition
<b>SUPRACRUSTAL ROCK UNITS</b>	
Metasedimentary rocks	Mainly monotonous metagreywackes and Bt schists $\pm$ Grt-Sil, locally with tuffaceous component (Qtz and Pl crystal clasts), locally bedded and showing soft-sediment deformation (Fig. 4 in <i>ibid.</i> )
Metamorphosed iron formation	3 main types: 1) Qtz-Mag - alternating Qtz-rich and Mag-Gru $\pm$ Grt layers commonly folded or brecciated (Fig. 3 in <i>ibid.</i> ), 2) Silicate facies - homogeneous intergrowth of Mag-Gru $\pm$ Grt-Hd, 3) Sulphidic - Qtz-rich with disseminated Py-Po, locally transitional to massive sulphide bodies
Quartz-phyric felsic metavolcanic rocks	3 mappable bodies in northern volcanic belt, varies from homogeneous to fragmental with both monolithologic and heterolithic breccias, typically some Ms or calc-silicate minerals, patchy distribution of Mc
Aphyric felsic meta-volcanic rocks	Monolithologic (proximal) and heterolithic breccias in southern volcanic belt, typically with abundant Grt-Hbl matrix
Felsic to intermediate metavolcanic rocks	Subtly heterogeneous and transitional breccias, schists, straight gneisses, incipient calc-silicate and Sil-Ms alteration and foliated tonalites without useful marker units
Intermediate to mafic metavolcanic rocks	Heterogeneous and transitional Hbl-Bt schists, gneisses, layered rocks and foliated diorites, commonly with Grt-Hbl-rich patches
Mixed mafic and felsic metavolcanic rocks	Interlayered mafic, felsic and leucofelsic schists, transitional to Grt-Oam gneisses
Mafic metavolcanic rocks	Dark laminated to schistose Hbl-rich, locally pillowed (Fig. 5 in <i>ibid.</i> ), intercalated with medium to coarse grained foliated gabbros and Hbl-augen schists, locally Grt-rich zones $\pm$ Oam
<b>METASOMATICALLY ALTERED ROCK UNITS</b>	
Orthoamphibole-garnet $\pm$ cordierite gneiss	Coarse grained, typically layered with Qtz-rich layers or lenticules overgrown by Ged-Grt porphyroblasts (Fig. 6 in <i>ibid.</i> ), intercalated (on a scale of 0.5 to several metres) with Sil-Grt-Bt schist, also contains Mag, Bt and St mantled by Crd, local Bt pseudomorphs of Oam
Sillimanite-muscovite-quartz felsic gneiss/schist	Includes interlayered similar or transitional rock types characterized by abundant Ms and/or Sil-Qtz $\pm$ Pl-Bt-Kfs-Grt-Crd-Mag; associated with Willroy and Geco - Qtz-Ms-Sil schist varies from finely interlayered Qtz and Ms to abundant Sil knots; hinge region north of Willecho - mainly large (1-8 cm) zoned Sil knots dispersed in schistose Qtz-Pl-Mc-Bt $\pm$ Grt matrix, local Qtz-Grt-Ep patches



younging (Fig. 2). In view of the folding in the area, the younging determination probably does not have regional significance.

Within the mafic units, two semicontinuous felsic units are useful as markers defining map-scale symmetrical and asymmetrical folds (Fig. 2). The southern unit, up to 50 m wide, locally is recognizable as highly deformed monolithological felsic breccia, with fine grained to aphanitic felsic clasts in a matrix of biotite or garnet-hornblende schist. The breccia resembles a lapilli tuff. The southern felsic unit is associated with minor exposures of iron-formation, and locally hosts disseminated pyrite and pyrrhotite. Garnetiferous zones, less than 15 m thick, are common in mafic rocks along the northern contacts of felsic units. In some areas, garnet is concentrated in pillow selvages. The garnetiferous zones are interpreted to be the result of metamorphism superimposed on minor seafloor alteration.

North of the mafic metavolcanic rocks, felsic to intermediate rocks are strongly deformed, fine grained and commonly laminated. The dominance of hornblende over biotite suggests that they had a metavolcanic protolith. Toward the core of the Manitowadge synform, a transition to biotite schists

suggests metasedimentary rocks. Felsic to intermediate metavolcanic and metasedimentary rocks are extensively invaded by foliated tonalite, that becomes dominant to the northeast.

The supracrustal rocks are enclosed by foliated intrusive rocks of the Black Pic batholith. The western contact is sheared and both plutonic and supracrustal rocks are characterized by strong linear fabrics (D4 Nama Creek shear zone, Peterson and Zaleski, 1994). In the Manitowadge area, foliations in the Black Pic batholith mimic the orientations of those in the supracrustal rocks, wrapping around the Manitowadge synform (Fig. 1). Screens of mafic rock and minor iron-formation that are present on the north side of the Blackman Lake antiform may represent an extension of mafic units in the southern Manitowadge belt (*ibid.*).

### Central area of the southern limb

The Geco, Willroy and Nama Creek massive sulphide deposits lie along the north side of the southern limb of the Manitowadge synform (Fig. 3). Most of the deposits are associated with quartz-magnetite iron-formation that grades laterally to sulphidic iron-formation and to massive sulphide

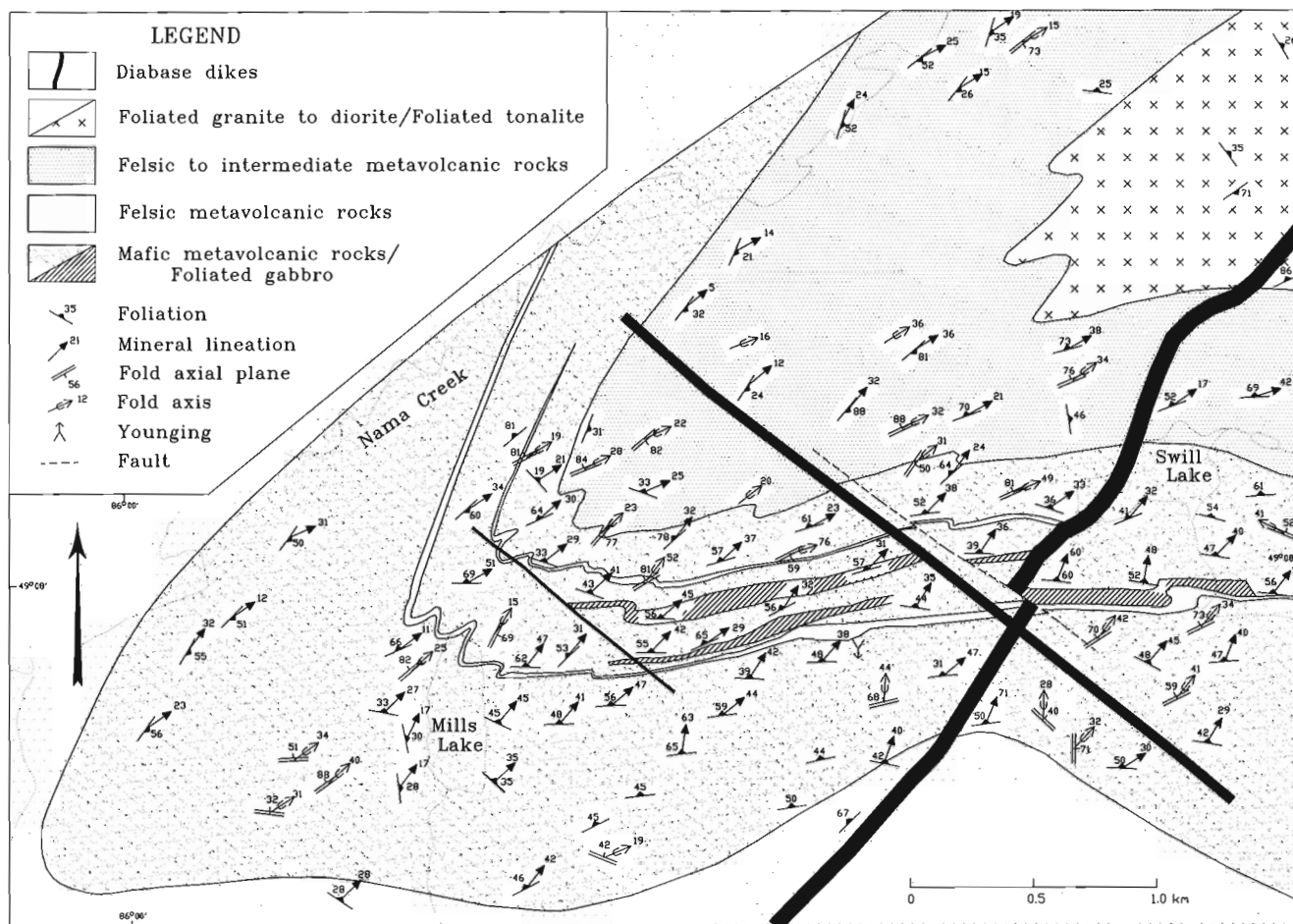


Figure 2. Geology of the hinge region of the Manitowadge synform near Swill Lake.

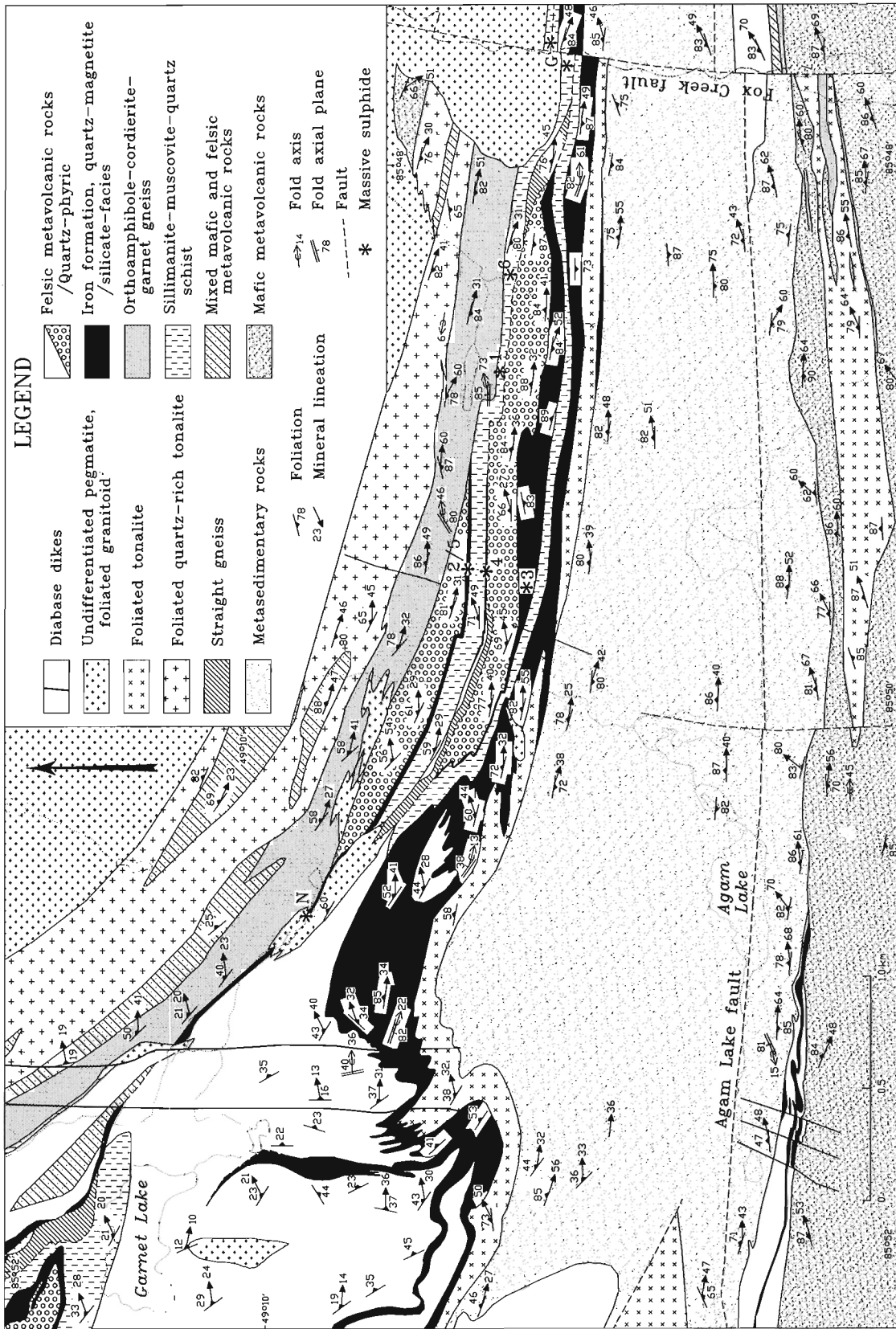
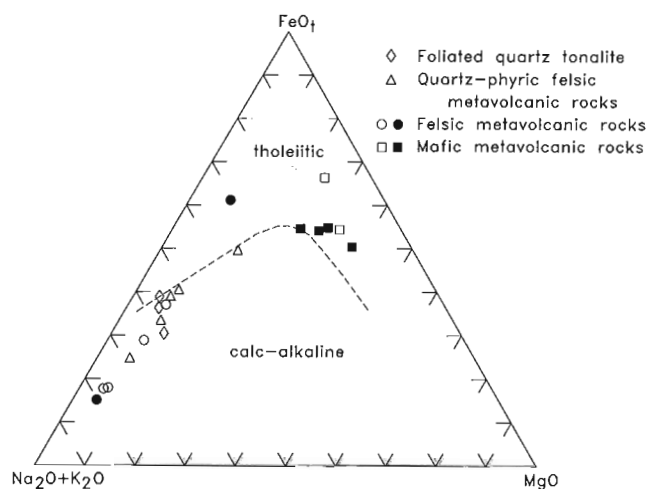


Figure 3. Geology of the central part of the southern limb of the Manitowadge synform showing the symmetry of the two metavolcanic belts separated by metasedimentary rocks. The Geco (G), Willroy (1 to 6 ore lenses) and Nama Creek (N) massive sulphide deposits lie in the northern metavolcanic belt. Note the low angle early faults. The D1 fault and iron formation in the northwest are folded by a D2 map-scale S-fold (Zaleski and Peterson, 1993a; Peterson and Zaleski, 1994).

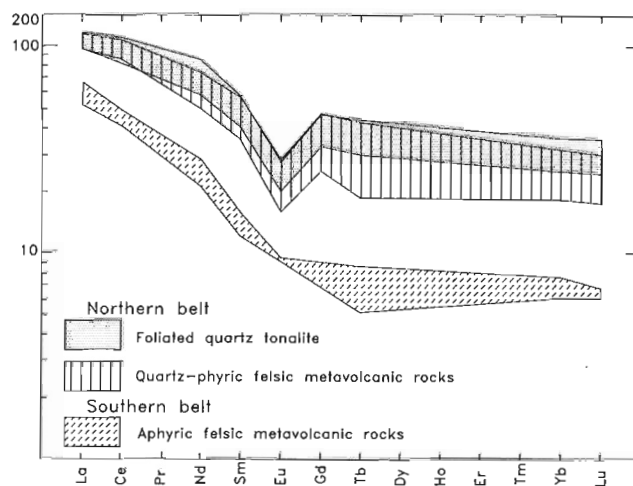
mineralization (Timms and Marshall, 1959). The Nama Creek, Geco and Willroy 1 and 6 deposits lie immediately south of altered rocks characterized by orthoamphibole, cordierite, garnet, staurolite and magnetite. The Willroy 2, 3, 4 and 5 deposits lie on iron-formation horizons farther to the south, intercalated with quartz-phyric felsic metavolcanic rocks and breccias, and sillimanite-muscovite schists. A low angle ductile thrust fault truncates some iron-formations and repeats the sequence: quartz-phyric felsic rock, iron-formation (and sulphide mineralization), sillimanite-muscovite schists. Additional cryptic faults may be present in the area, complicating the primary relationships.

A general symmetry of lithological units across the southern limb of the synform is defined by the sequence (from margin to centre): mafic metavolcanic rocks, orthoamphibole-bearing rocks, felsic metavolcanic rocks interlayered with iron-formation, and metasedimentary rocks. However, there are important differences between the northern and southern belts. Alteration (orthoamphibole-cordierite-garnet gneiss and sillimanite-muscovite schist) is much more extensive and intense in the north, and the main protolith, still recognizable in less altered areas, is a unit of thinly inter-layered mafic and felsic metavolcanic rocks. In the south, thin semicontinuous zones of orthoamphibole-garnet occur in mafic metavolcanic rocks near the contact with metasedimentary rocks.

Felsic rocks in both belts include volcanoclastic and epiclastic (heterolithic) breccias. Some of the southern breccias resemble proximal deposits having coarse (50 cm scale) angular monolithologic clasts. The matrix commonly contains abundant garnet and hornblende porphyroblasts, interpreted to have crystallized during metamorphism of synvolcanic calc-silicate alteration. Breccias with an epiclastic component contain



**Figure 4.** AFM diagram (after Irvine and Baragar, 1971) for mafic and felsic metavolcanic rocks from the northern (open symbols) and southern (filled symbols) volcanic belts.



**Figure 5.** Ranges of chondrite-normalized REE abundances in felsic rocks from northern and southern volcanic belts. Gd abundance is interpolated.

garnet-hornblende-bearing clasts that resemble the matrix of the monolithologic breccias, thus supporting syngenetic calc-silicate alteration. Breccia facies in the north are harder to identify, both because alteration (muscovite-sillimanite and calc-silicate) is more advanced and because the rocks are more deformed. Southern felsic rocks are aphyric, whereas the northern rocks, especially near the Geco and Willroy deposits, are quartz-phyric. There is a much larger volume of felsic metavolcanic rocks and intercalated iron-formation in the north, and quartz-rich tonalite (synvolcanic) has been found only in the north.

## GEOCHEMISTRY AND GEOCHRONOLOGY

A suite of 30 samples, representing unaltered or 'least' altered metavolcanic, intrusive and metasedimentary rocks, was collected in 1992, mainly in the area of Figure 3. Preliminary results show that mafic metavolcanic rocks and foliated gabbro from the northern and southern belts are chemically indistinguishable, in the field of tholeiitic basalt and basaltic andesite (Fig. 4). Felsic metavolcanic rocks and quartz-rich tonalite generally follow a calc-alkaline trend, the presence of minor garnet and hornblende (a result of incipient alteration) causing one incursion into the tholeiitic AFM field.

In contrast to mafic rocks, felsic metavolcanic units from north and south are markedly different, especially in trace element composition (Fig. 5). The northern quartz-phyric rocks and quartz-rich tonalite have moderately sloping rare earth element (REE) patterns, with La/Yb from 4-8, pronounced negative Eu anomalies ( $\text{Eu}/\text{Eu}^* = 0.43-0.55$ ), and low Zr/Y from 4-10. Southern felsic rocks (2 samples) have a lower abundance of REE, a steeper slope from light to heavy REE with La/Yb of 13, small negative Eu anomalies ( $\text{Eu}/\text{Eu}^* = 0.69-0.94$ ), and high Zr/Y from 32-44. In comparison to geochemical analyses

compiled by Leshner et al. (1986) for felsic metavolcanic rocks in the Superior Province, the southern felsic rocks in the Manitouwadge belt are typical of barren rocks not associated with mineralization. The northern felsic rocks and quartz-rich tonalite, are geochemically similar to felsic rocks known to host massive sulphide deposits, in particular, to those in the Sturgeon Lake area of the Wabigoon subprovince (Type FII, *ibid.*). The quartz-rich tonalite is indistinguishable from northern quartz-phyric felsic rocks and could have been a reservoir for extrusive volcanic activity.

Preliminary U-Pb dates on zircon from a sample of the southern felsic suite give a volcanic age of  $2722 \pm 2$  Ma, within error of zircon from muscovite schist at Geco ( $2720 \pm 2$  Ma, Davis et al., in press). The age of zircon (circa  $2720 \pm 3$  Ma) from foliated quartz-rich tonalite north of Willroy and Geco confirms our field interpretation of synvolcanic intrusion. Volcanism was coeval in the northern and southern parts of the belt, but produced felsic rocks with different geochemical signatures.

A sample of foliated tonalite dyke, interpreted to be a syn-D2 intrusion on the basis of field relationships, did not contain zircon. However, monazite of igneous morphology gave an age of  $2671 \pm 3$  Ma.

## DISCUSSION

The general sequence – tholeiitic metabasalt, felsic metavolcanic rocks and iron-formation, and metasedimentary rocks – suggests a stratigraphic succession in which the youngest rocks lie in the centre of the southern limb of the Manitouwadge synform. This raises the possibility of an early fold (see discussion in Zaleski and Peterson, 1993a); however, we have not found conclusive supporting evidence (such as a fold closure) for this. The divergence of northern and southern metavolcanic rocks to the east (near the Banana Lake antiform) and, possibly, to the west (near the Blackman Lake antiform) argues against repetition by an early fold. The simplest explanation for the observed sequence, taking into account the significant differences between northern and southern felsic rocks and their associations, is that they developed as two independent coeval volcanic centres on a substratum of tholeiitic shield basalt. In this scenario, the central metasedimentary rocks were deposited in a basin between the felsic centres. The original configuration has been imbricated and shortened during early deformation related to accretion of the Wawa subprovince or the Wawa and Quetico belts (Peterson and Zaleski, 1994).

Despite the complications imposed by deformation and metamorphism, massive sulphide deposits in the Manitouwadge belt still preserve primary relationships that support a synvolcanic origin. The rock types are generally consistent with a subaqueous setting (pillowed mafic flows, iron-formation, volcanic breccias, metasediments). The geochemistry of the northern felsic rocks is typical of felsic rocks associated with

mineralization. Leshner et al. (1986) postulated that geochemical signatures of this type indicate plagioclase fractionation in a high level magma chamber, and that the same magma chamber might have been instrumental in driving hydrothermal activity. Franklin et al. (1981) have also stressed the role of subvolcanic intrusions as heat sources for hydrothermal systems. In the Manitouwadge belt, the close association of massive sulphide deposits with altered rocks (orthoamphibole-cordierite-garnet gneiss and sillimanite-muscovite schist), felsic volcanic rocks of appropriate composition, synvolcanic quartz-rich tonalite and chemical precipitates (iron-formation), supports a syngenetic model.

In the syngenetic model, orthoamphibole-cordierite-garnet rocks originated as alkali-depleted alteration, and sillimanite-muscovite rocks as aluminous-potassic alteration. In most volcanogenic deposits, these alteration types would be localized in a discordant subvolcanic pipe and in a broad near-surface halo enveloping the upper pipe, respectively. The Manitouwadge altered rocks do not fit comfortably into this scheme; the orthoamphibole-cordierite-garnet rocks are crudely strat-abundant, as noted by James et al. (1978), and form a laterally continuous unit that cannot be simply attributed to intense deformation. Sillimanite-muscovite schists envelop or 'cap' the Geco and Willroy 1 and 6 deposits, but elsewhere they are separated from the alkali-depleted alteration by felsic rocks and iron-formation. However, these rocks are locally associated with straight gneisses (annealed mylonites) and were zones of focussed deformation during D1/D2 thrusting. Undoubtedly, primary relationships were significantly modified. In addition, the synvolcanic quartz-rich tonalite intrudes orthoamphibole-cordierite-garnet rocks and, hence, it is likely that part of the deeper level of the original hydrothermal system was obliterated.

Regional metamorphism was broadly synchronous with D2 deformation (Zaleski and Peterson, 1993a). Based on field observations, the intrusion of the Black Pic batholith was pre- to syn-D2 and may have been directly involved in heat transfer. Metamorphism in the Wawa subprovince was essentially coeval from the amphibolite-facies Schreiber-Hemlo belt, to the upper amphibolite Manitouwadge belt, at 2678-2675 Ma. Our preliminary age of  $2671 \pm 3$  Ma for a syn-D2 tonalite dike is slightly younger; however, at this stage, the significance of the minor discrepancy is unknown. It is still possible that metamorphism was diachronous from south to north. Within the Manitouwadge belt, metamorphic grade increases toward the north; muscovite-sillimanite-quartz schists near Geco and Willroy give way to sillimanite-microcline-quartz schists north of Willecho. Folded and cross-cutting leucosomes in Quetico metasedimentary rocks suggest that migmatization occurred during D4 (Peterson and Zaleski, 1994). These observations are consistent with diachronous development of peak metamorphism between the Quetico and Wawa subprovinces, and with peak metamorphism in the Quetico coeval with granitic magmatism at 2670-2650 Ma (Percival, 1989). By this time, the Wawa subprovince near Manitouwadge may have been undergoing slow cooling, during which ductile deformation (D3 to D5) continued.

## ACKNOWLEDGMENTS

Noranda Minerals Inc. (Geco Division), Granges Inc., Minnova Inc. and Al Turner contributed to this project by providing access to unpublished maps and reports. Noranda Minerals released data acquired during a high resolution aeromagnetic survey (contracted to Dighem Inc.) to Joan Tod, Geophysics Division. The data were compiled by Warner Miles, Geophysics Division, and the resulting aeromagnetic maps (GSC Open Files 2754, 2755) were valuable aids to mapping and interpretation. Our special thanks go to Hugh Lockwood, Noranda Minerals Inc., for discussions, ideas, and all around support of our efforts during the field season. Thanks also go to Rob Reukl, Jody Hache, Al Turner and Neil Poster. We benefited from field trips and/or discussions with Doug McKay, Mark Smyk and Bernie Schnieders, Ontario Geological Survey. Our field work was greatly aided by the mapping of Katherine Boggs, and the assistance of Joanne Treidlinger and Andrea Dorval. The manuscript was improved by comments from Ingo Ermanovics and John Percival.

## REFERENCES

- Corfu, F. and Muir, T.L.**  
1989a: The Hemlo-Heron Bay greenstone belt and Hemlo Au-Mo deposit, Superior province, Ontario, Canada 1. Sequence of igneous activity determined by zircon U-Pb geochronology; *Chemical Geology (Isotope Geology Section)*, v. 79, p. 183-200.
- 1989b: The Hemlo-Heron Bay greenstone belt and Hemlo Au-Mo deposit, Superior province, Ontario, Canada 2. Timing of metamorphism, alteration and Au mineralization from titanite, rutile and monazite U-Pb geochronology; *Chemical Geology (Isotope Geology Section)*, v. 79, p. 201-223.
- Davis, D.W., Pezzutto, F., and Ojakangas, R.W.**  
1990: The age and provenance of metasedimentary rocks in the Quetico subprovince, Ontario, from single zircon analyses: implications for Archean sedimentation and tectonics in the Superior Province; *Earth and Planetary Science Letters*, v. 99, p. 195-205.
- Davis, D.W., Schandl, E.S., and Wasteneys, H.A.**  
in press: U-Pb dating of minerals in alteration halos of Superior province massive sulphide deposits: syngensis vs. metamorphism; *Contributions to Mineralogy and Petrology*.
- Franklin, J.M., Lydon, J.W., and Sangster, D.F.**  
1981: Volcanic-associated massive sulphide deposits; in *Economic Geology, 75th Anniversary Volume*, (ed.) B.J. Skinner, p. 485-627.
- Friesen, R.G., Pierce, G.A., and Weeks, R.M.**  
1982: Geology of the Geco base metal deposit; *Geological Association of Canada, Special Paper 25*, 343-363.
- Irvine, T.N. and Barager, W.R.A.**  
1971: A guide to the chemical classification of the common volcanic rocks; *Canadian Journal of Earth Sciences*, v. 8, p. 523-548.
- James, R.S., Grieve, R.A.F., and Pauk, L.**  
1978: The petrology of cordierite-anthophyllite gneisses and associated mafic and pelitic gneisses at Manitouwadge, Ontario; *American Journal of Science*, v. 278, p. 41-63.
- Leshner, C.M., Goodwin, A.M., Campbell, I.H., and Gorton, M.P.**  
1986: Trace-element geochemistry of ore-associated and barren, felsic metavolcanic rocks in the Superior Province, Canada; *Canadian Journal of Earth Sciences*, v. 23, p. 222-237.
- Percival, J.A.**  
1989: A regional perspective of the Quetico metasedimentary belt, Superior Province, Canada; *Canadian Journal of Earth Sciences*, v. 26, p. 677-693.
- Peterson, V.L. and Zaleski, E.**  
1994: Structure and tectonics of the Manitouwadge greenstone belt and Wawa/Quetico subprovince boundary, Superior Province, northwestern Ontario; in *Current Research 1994-C*; Geological Survey of Canada.
- Schandl, E.S., Davis, D.W., Gorton, M.P., and Wasteneys, H.A.**  
1991: Geochronology of hydrothermal alteration around volcanic-hosted massive sulphide deposits in the Superior Province; Ontario Geological Survey, *Miscellaneous Paper 156*, p. 105-120.
- Severin, P.W.A., Balint, F., and Sim, R.**  
1990: Geological setting of the Winston Lake massive sulphide deposit; in *Mineral Deposits in the Western Superior Province, Ontario*, (ed.) J.M. Franklin, B.R. Schneiders, and E.R. Koopman, Geological Survey of Canada, Open File 2164, p. 58-73.
- Suffel, G.C., Hutchinson, R.W., and Ridler, R.H.**  
1971: Metamorphism of massive sulfides at Manitouwadge, Ontario, Canada; *Society of Mining Geologists of Japan, Special Issue 3*, p. 235-240.
- Timms, P.D. and Marshall, D.**  
1959: The geology of the Willroy mines base metal deposits; *Proceedings, Geological Association of Canada*, v. 11, p. 55-65.
- Williams, H.R. and Breaks, F.W.**  
1989: Geological studies in the Manitouwadge-Hornpayne area; Ontario Geological Survey, *Miscellaneous Paper 146*, p. 79-91.
- 1990: Geology of the Manitouwadge-Hornpayne area; Ontario Geological Survey, Open File Map 142, scale 1:50 000.
- Williams, H.R., Stott, G.M., Heather, K.B., Muir, T.L., and Sage, R.P.**  
1991: Wawa subprovince; in *Geology of Ontario*, Ontario Geological Survey, Special Volume 4(1), p. 485-539.
- Zaleski, E. and Peterson, V.L.**  
1993a: Lithotectonic setting of mineralization in the Manitouwadge greenstone belt, Ontario: preliminary results; in *Current Research, Part C*; Geological Survey of Canada, Paper 93-1C, p. 307-317.
- 1993b: Geology of the Manitouwadge greenstone belt; Geological Survey of Canada, Open File 2753.

Geological Survey of Canada Project 910033





# Structure and tectonics of the Manitouwadge greenstone belt and Wawa-Quetico subprovince boundary, Superior Province, northwestern Ontario<sup>1</sup>

V.L. Peterson and E. Zaleski  
Continental Geoscience Division

*Peterson, V.L. and Zaleski, E., 1994: Structure and tectonics of the Manitouwadge greenstone belt and Wawa-Quetico subprovince boundary, Superior Province, northwestern Ontario; in Current Research 1994-C; Geological Survey of Canada, p. 237-247.*

---

**Abstract:** We propose a revised structural geometry and deformation history for the Manitouwadge greenstone belt of the northern Wawa subprovince adjacent to the Quetico subprovince. Early folding and thrusting with a possible sinistral component produced D<sub>1</sub> and D<sub>2</sub> structures. The dominant D<sub>2</sub> foliation and lineation were produced during peak metamorphism. The Manitouwadge synform resulted from D<sub>3</sub> deformation, possibly progressive from D<sub>2</sub>, following peak metamorphism. Dextral oblique shear during D<sub>4</sub>, possibly synchronous with migmatization in the Quetico subprovince, produced broad to focussed shear strain and refolded the Manitouwadge synform. Evidence for refolding, based on detailed mapping and aeromagnetic interpretation, is suggested by northeastward extension of the 'Geco horizon' through a series of folds. D<sub>5</sub> structures reflect continued dextral oblique shear, focussed along the Wawa-Quetico boundary. The Manitouwadge belt and its mineral deposits appear to have shared a common structural history with the adjacent Quetico subprovince since D<sub>2</sub>/D<sub>3</sub>.

**Résumé :** Nous proposons une révision de la géométrie structurale et de l'évolution de la déformation dans la ceinture de roches vertes de Manitouwadge, qui se trouve dans le nord de la sous-province de Wawa, à proximité de la sous-province de Quetico. Les plis et chevauchements initiaux, qui possèdent peut-être une composante senestre, ont produit des structures D<sub>1</sub> et D<sub>2</sub>. La foliation et la linéation dominantes associées à D<sub>2</sub> sont apparues pendant la culmination du métamorphisme. Le synforme de Manitouwadge a été produit par une déformation D<sub>3</sub>, qui a peut-être progressivement dérivée de l'épisode de déformation D<sub>2</sub>, après la culmination du métamorphisme. Un cisaillement dextre oblique associé à une déformation D<sub>4</sub>, peut-être synchrone de la migmatisation survenue dans la sous-province de Quetico, a produit des zones de cisaillement étendues à concentrées et replissé le synforme de Manitouwadge. La cartographie détaillée et l'interprétation des données aéromagnétiques permet d'identifier un replissement dont l'existence est confirmée par la reconnaissance du prolongement vers le nord-est de l'«horizon de Geco» à travers une série de plis. Les structures D<sub>5</sub> traduisent un cisaillement continu à composante oblique et à déplacement dextre, concentré le long de la limite entre les sous-provinces de Wawa et de Quetico. La ceinture de Manitouwadge et ses gîtes minéraux ont sans doute connu une évolution structurale commune avec la sous-province adjacente de Quetico depuis D<sub>2</sub>/D<sub>3</sub>.

---

<sup>1</sup> Contribution to Canada-Ontario Subsidiary Agreement on Northern Ontario Development (1991- 1995), under the Canada-Ontario Economic and Regional Development Agreement.

## INTRODUCTION

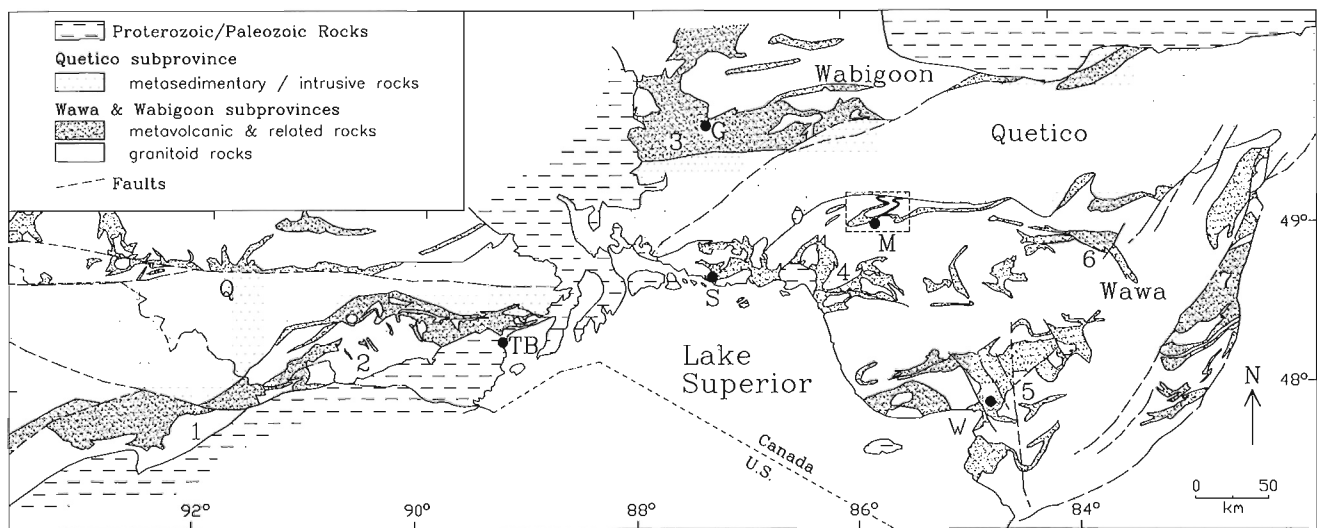
The Manitowadge greenstone belt is an upper amphibolite-facies remnant of supracrustal rocks with a complex deformation history. It lies within the Wawa subprovince of the Archean Superior Province, adjacent to the Quetico subprovince boundary (Fig. 1). Previous detailed mapping (Pye, 1957; Milne, 1974) revealed the deformed geometry of the Manitowadge belt and regional studies (Williams and Breaks, 1989, 1990b) delineated a protracted structural history. We are building on these previous studies by applying detailed mapping, structural and petrogenetic analysis toward an understanding of 1) the evolution of the belt; 2) the influence of primary setting, deformation and metamorphism on the present geometry of its mineral deposits; and 3) the relationship of the belt to the adjacent Wawa-Quetico boundary. In addition, the structural history of the Manitowadge greenstone belt and the Wawa-Quetico boundary records part of the evolution of this major lithotectonic contact and of the construction of the Superior Province.

This study is based primarily on observations made during detailed mapping (1:5000 and 1:10 000) of the Manitowadge greenstone belt during 1992 and 1993. A high-resolution aeromagnetic survey flown by Dighem for Noranda, Inc. and released to the Geological Survey of Canada was useful for directing our mapping and extrapolating lithological units in areas of poor exposure. The overall geological setting of the belt is discussed more fully in Zaleski and Peterson (1993) and in a companion paper in this volume by Zaleski et al. (1994).

## STRUCTURAL AND TECTONIC SETTING

Subdivision of the Superior Province into east-west-trending linear volcano-plutonic (granite-greenstone), meta-sedimentary, and high grade gneiss subprovinces was based on lithological, structural, metamorphic, geochronological, and geophysical criteria (Card and Ciesielski, 1986). The supracrustal belts within the volcano-plutonic subprovinces resemble arc-type deposits in modern orogenic belts (Card, 1990). In the southwestern Superior Province, the Wawa and Wabigoon volcano-plutonic subprovinces are separated by the metasedimentary Quetico subprovince (Fig. 1). Among recent tectonic models for these southern subprovinces, an arc-accretionary model has been favoured by Percival (1989), Percival and Williams (1989), and Williams (1990). In this scenario, the Quetico subprovince represents an accretionary complex built southward from the margin of the Wabigoon arc above a northerly dipping subduction zone. Collision of the Wawa arc from the south amalgamated the three subprovinces. Relatively high temperature/low pressure metamorphism preserved within the Quetico and northern Wawa subprovinces may be explained by subduction of a ridge or by post-subduction thermal relaxation (see Percival, 1989).

Comparison of structural studies within the Quetico subprovince and along the subprovince boundaries reveals not only many differences in structural history and style of deformation, but also important similarities. The differences may reflect variations in metamorphic grade, rock type (i.e. competency contrasts) or the dominant trend of the major structures (cf. Bauer et al., 1992). One recurrent feature in these



**Figure 1.** Tectonic map showing the Wawa, Quetico, and southern Wabigoon subprovinces of the southwestern Superior Province. Rectangular outline (in vicinity of M) shows area of Figures 2 and 3. 1 = Vermilion district, Minnesota; 2 = Shebandowan greenstone belt; 3 = Geraldton-Beardmore belt; 4 = Hemlo-Schreiber greenstone belt; 5 = Michipicoten greenstone belt; 6 = Kabinakagami greenstone belt; 7 = Kapuskasing structural zone; Q = Quetico fault; TB = Thunder Bay; M = Manitowadge; W = Wawa. Adapted from Williams et al. (1991) and Percival (1989).

studies is the presence of structures produced by dextral transcurrent motion. These include both ductile and brittle structures, typically found in shear zones or deformation zones near subprovince boundaries, for example, the Quetico fault (Borradaile et al., 1988), Vermilion district (Hudleston et al., 1988), Beardmore-Geraldton belt (Devaney and Williams, 1989), Shebandowan belt (Corfu and Stott, 1986), Shebandowan-Quetico boundary (Borradaile and Spark, 1991), and Hemlo-Schreiber belt (Williams, 1989). Zones of distributed dextral motion in the western Quetico subprovince (Bauer et al., 1992) and dextral shear zones far from subprovince boundaries, as in the Kabinakagami belt (Leclair, 1990) have also been noted (Fig. 1). Corfu and Stott (1986) constrained timing of dextral transcurrent motion in the Shebandowan Belt (local D<sub>2</sub>) between 2689±3/-2 and 2684±6/-3 Ma, however temporal correlation with dextral motion elsewhere in the Wawa-Quetico-Wabigoon region is uncertain. Although timing and style of dextral motion appears to vary widely across this region, in several places it is associated with the later phases of deformation (e.g. Bauer et al., 1992; Devaney and Williams, 1989; Hudleston et al., 1988). In the western Quetico subprovince, dextral motion has been attributed to dextral transpression produced by oblique arc collision (e.g. Hudleston et al., 1988; Borradaile and Spark, 1991; Bauer et al., 1992).

Several studies within the region of Figure 1 have noted features indicative of thrusting prior to dextral transcurrent motion. In the Beardmore-Geraldton belt (Fig. 1), Devaney and Williams (1989) identified stratigraphic packages separated by dip-slip faults, which they attributed to thrust stacking in an accretionary wedge. Jirsa et al. (1992) presented evidence for early (D<sub>1</sub>) thrusting and nappe formation in the western Wawa subprovince (Vermilion district), possibly associated with accretion. Along the Wawa-Quetico boundary near Schreiber (Fig. 1), Williams (1989) identified structures possibly related to early dip-slip thrusting. In the Michipicoten greenstone belt, early thrust structures (D<sub>2</sub> and earlier) have been described by Arias and Helmstaedt (1990) and McGill (1992). There is also evidence of early thrusting along ductile shear zones in the Manitouwadge greenstone belt (Zaleski and Peterson, 1993).

## LOCAL GEOLOGICAL SETTING

The supracrustal sequence within the Manitouwadge belt was previously mapped by Pye (1957) and Milne (1974). Various theses (e.g. Robinson, 1979; Watson, 1970), and maps produced by mining companies and prospectors have focussed on areas of economic interest. The regional setting of the Manitouwadge greenstone belt was studied by Williams and Breaks (1989, 1990a, b). Rock types are described by Zaleski and Peterson (1993) and Zaleski et al. (1994). Within the supracrustal package, these include: mafic metavolcanic rocks, felsic metavolcanic rocks, metasedimentary rocks, and metamorphosed quartz-magnetite-garnet-grunerite iron-formation. Orthoamphibole-garnet-cordierite gneiss and quartz-muscovite-sillimanite schist are interpreted as metamorphosed synvolcanic alteration zones (ibid.). The Geco Cu-Zn mine and several formerly producing deposits lie south

of the main belt of synvolcanic alteration and in most areas are associated with iron-formation. Intrusive rocks include foliated diorites to granites, gabbro, K-feldspar-megacrystic granodiorite and strongly foliated to massive pegmatites (ibid.). Intrusive rocks outside the belt of supracrustal rocks, collectively referred to as the Black Pic Batholith (Williams and Breaks, 1990a), are distinctly different from those inside the belt (Zaleski et al., 1994). Mineral assemblages and geothermobarometry suggest that the metamorphic grade reached upper amphibolite facies (600-700°C and 3-6 kbar) in the Manitouwadge belt (Petersen, 1984; Pan and Fleet, 1992) and granulite facies (>700°C and 5.4 kbar) in the Quetico metasediments to the north (Percival, 1989).

A number of previous studies have contributed to our understanding of the structure and petrogenesis of the Manitouwadge belt. Pye (1957) first recognized the synformal shape of the belt, which folds the dominant foliation, and observed that lineations are parallel to local fold axes. Timms and Marshall (1959) noted that orebodies have a shallow easterly plunge, parallel to the dominant mineral lineations. Pye (1957) and Milne (1974) identified the major map-scale folds and late faults within the belt, and Milne interpreted belts of quartz-muscovite schist as shear zones. Touborg (1973) and Robinson (1979), among others, suggested that the crude symmetry of units, most evident across the southern limb of the synform, may be the result of an early synclinal structure cored by metasediment. Williams and Breaks (1989, 1990b) described a 5-phase sequence of deformation in which D<sub>2</sub> was the dominant fabric-forming event. D<sub>2</sub> planar and linear fabrics were deformed by nearly coaxial D<sub>3</sub> structures, including the Manitouwadge synform (ibid.). D<sub>4</sub> structures include Z-shaped folds and extensional crenulation cleavage. A compatible three-phase structural sequence is described by Nichol (1991) based on detailed studies in supracrustal and gabbroic rocks southeast of the Manitouwadge belt.

## STRUCTURAL FEATURES

We identify five phases of ductile deformation in the Manitouwadge belt, generally comparable to the regional deformation sequence of Williams and Breaks (1989, 1990b). Significant differences are based on detailed mapping and interpretation of aeromagnetic data (Fig. 2, 3). Heterogeneity of deformation across the belt complicated construction of a cross section for the whole belt, however, down-plunge projection for a limited area in the inner hinge region of the synform helped to elucidate the complex relationships in that area (Fig. 4).

Map-scale triple points of lithological units, truncation of units and repetition of sequences, particularly in the inner hinge and southern limb regions of the synform are interpreted as resulting from D<sub>1</sub> faults or shear zones (Fig. 4, A-E). Dynamic structural fabrics are not preserved; however, local occurrences of finely laminated straight gneisses were interpreted to be annealed mylonites (Zaleski and Peterson, 1993). Fault B is a probable D<sub>1</sub> structure folded by D<sub>2</sub> folds (Fig. 4 and ibid.). Fault C (Fig. 4) could be interpreted as a

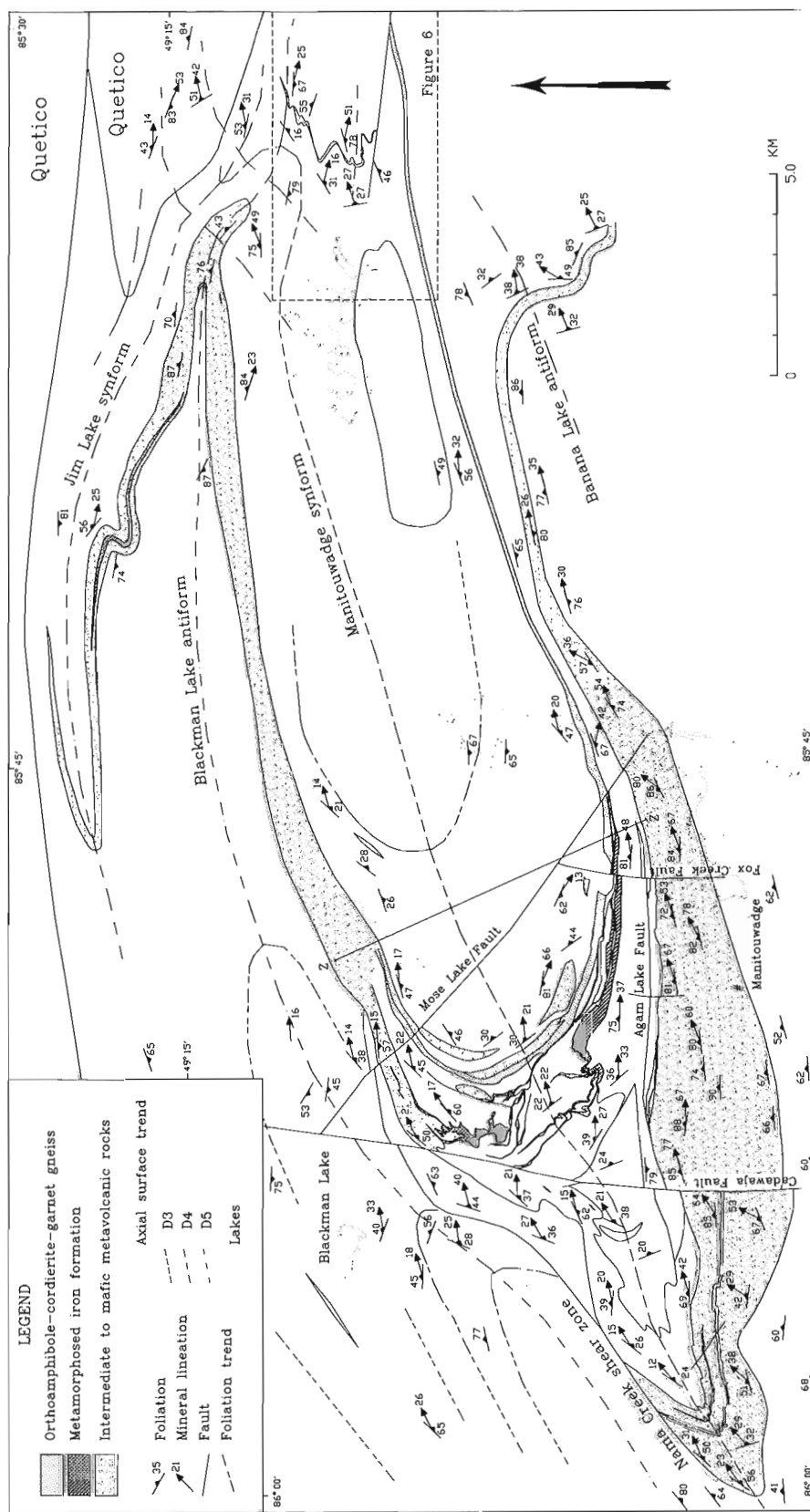


Figure 2. Simplified geological map of the Manitowadge region showing map-scale structural features. Z-Z' is the trace of projection plane in Figure 4.



**Figure 3.** Shaded relief, total field aeromagnetic map for the same area as Figure 2. Illumination from 180°. Prominent northwest- and northeast-trending linear features are diabase dykes. Data flown by Digheem, Inc. for Noranda, Inc. and compiled by the Geophysics Division, Geological Survey of Canada (note: visible seams between data blocks not removed).

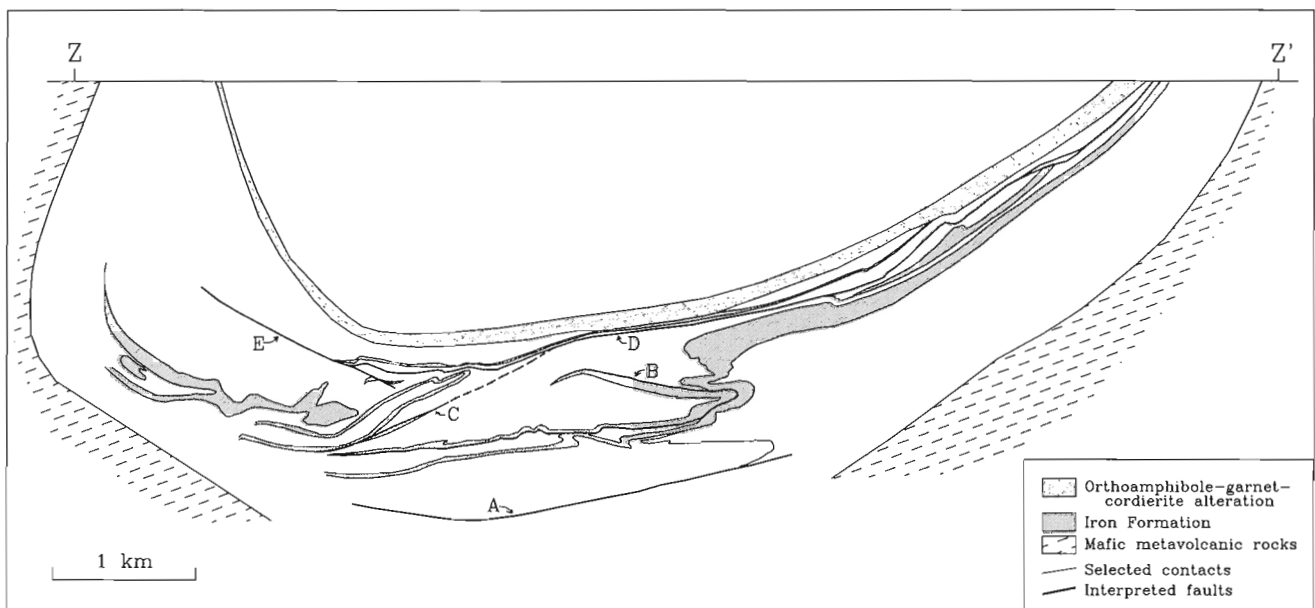
short-limb thrust related to the formation of the isoclinal fold to the north. Foliations in the hinge region of the fold, north of fault C, do not appear to be folded and are locally oblique to folded contacts. Both the fold and fault are possible early structures truncated by fault D. The kinematics of possible D<sub>1</sub> structures is unknown. D<sub>1</sub> fabrics, including annealed mylonitic or gneissic layering, can be distinguished only in the hinge regions of some D<sub>2</sub> folds (ibid.).

The dominant planar fabrics, mineral lineations and outcrop-scale folds, as well as some map-scale folds within the supra-crustal belt were interpreted as D<sub>2</sub> structures (Zaleski and Peterson, 1993). D<sub>2</sub> foliations and east-northeast-plunging mineral/stretching lineations are parallel to axial surfaces and axes of local D<sub>2</sub> folds, respectively, and are folded by the D<sub>3</sub> Manitouwadge synform. The map-scale S-shaped folds in iron-formation (Fig. 2, 4) are well documented as D<sub>2</sub> folds (ibid.). New mapping in 1993 suggests that fault D (Fig. 4), previously interpreted as a D<sub>1</sub> structure (ibid.), extends into the hinge region of the synform and is not folded by major D<sub>2</sub> folds. Hence, fault D is re-interpreted as a relatively late D<sub>2</sub> ductile shear zone that juxtaposed the continuous sequence of altered rocks to the northeast with the more complex region to the southwest. Fault A truncates the southern limb of a possible D<sub>2</sub> fold and could be similar in age to fault D. Both faults A and D are identified on the basis of map-scale geometry and do not preserve dynamic fabrics, although map-view offsets along fault D indicate a component of westward vergence (ibid.). Fault E forms a pronounced lineament and truncates belts of iron-formation and fault D (Fig. 2, 4) with apparent map-view sinistral offset. The fault zone is characterized locally by grain-size reduction and slivers of various rock units. The zone is deflected around the Manitouwadge synform, suggesting that it is a late D<sub>2</sub>

structure. D<sub>2</sub> structures were produced by folding and ductile thrusting at upper amphibolite facies (near peak metamorphic conditions, ibid.). An oblique sinistral component of motion is suggested by the S-asymmetry of the map-scale D<sub>2</sub> folds, by possible westward motion on fault D, and by sinistral offset along fault E.

The D<sub>3</sub> Manitouwadge synform dominates the regional structure of the belt, folding D<sub>2</sub> foliations and lineations. The synform has a moderate to gentle northeast plunge, nearly coaxial with D<sub>2</sub> folds. An axial planar fabric is not apparent in the hinge region of the synform and few other outcrop- or map-scale features can be unambiguously assigned to D<sub>3</sub>. Smaller map-scale Z-folds on the south limb of the synform with Z-asymmetry may be parasitic D<sub>3</sub> folds, or they may be D<sub>4</sub> folds. Outcrop-scale folds ( $\approx 0.1 - 1$  m amplitude) with curving hinge lines, which deform the dominant (D<sub>2</sub>) lineation and are cut by a later crenulation cleavage, are tentatively interpreted as D<sub>3</sub> structures. The absence of a pervasive D<sub>3</sub> fabric may indicate that the Manitouwadge synform formed after the local peak metamorphism.

Map-scale D<sub>4</sub> structures include the Nama Creek shear zone, Blackman Lake antiform, Jim Lake synform, and several minor folds shown in Figures 2 and 5. Both the Blackman Lake antiform and Jim Lake synform fold the D<sub>3</sub> Manitouwadge synform (Fig. 2). Outcrop-scale D<sub>4</sub> structures, typically associated with northeast-plunging linear fabrics, deform the dominant D<sub>2</sub> fabrics and, where kinematics can be inferred, they suggest a dextral oblique sense of motion. The style of deformation and characteristic D<sub>4</sub> structures are somewhat variable across the region, reflecting differences in rock type and, possibly, metamorphic grade.



**Figure 4.** Down-plunge projection of the inner hinge region of the Manitouwadge synform. The line of projection is the plunge of synform at  $065^{\circ}/125^{\circ}$ . Z - Z' (Fig. 2) is the line of intersection between the projection plane and the horizontal at 350 m elevation. Topographic relief ( $\approx 140$  m) is not shown.



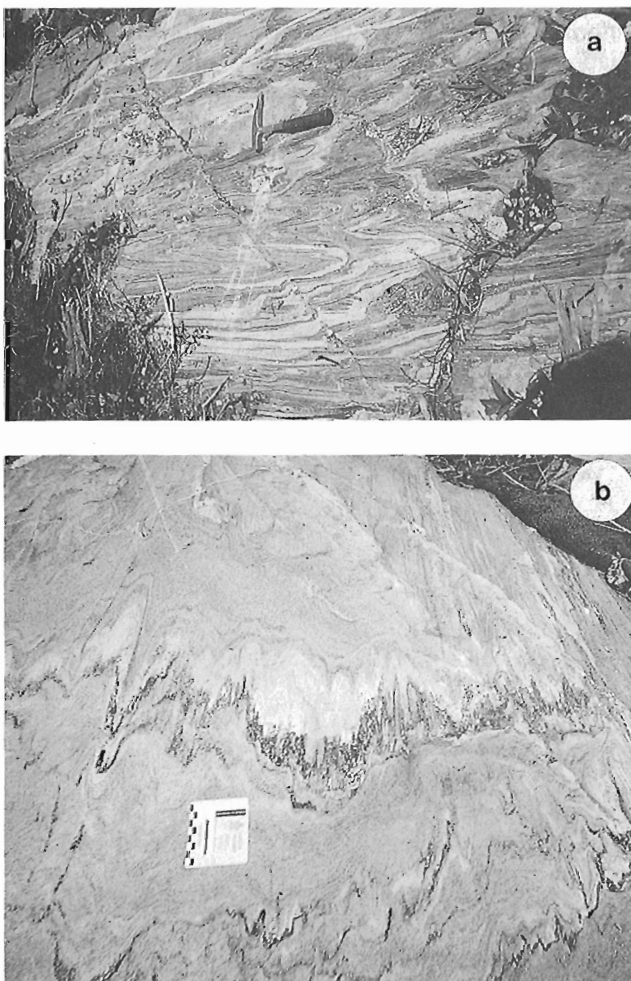
The Nama Creek shear zone along the northwest margin of the Manitouwadge synform (Fig. 2) is identified from a dramatic westward increase in strain toward the hinge region in the Swill Lake area (Fig. 2 in Zaleski et al., 1994), and from the northward curvature and truncation of aeromagnetic trends (Fig. 3). The zone of truncation is inferred to follow the Nama Creek valley and is not exposed. In the hinge region of the synform, spectacular L>S tectonites and folds with a moderate northeasterly plunge, parallel to lineations (Fig. 5), dominate exposures nearest to the shear zone. The pronounced stretching lineation is defined by hornblende, quartz rods (especially in folded quartz veins), and by streaky mafic lenses within intermediate volcanic rocks. All scales of folds typically have an M- or Z-symmetry with locally developed axial planar fabric and fold D<sub>2</sub> planar fabrics (Fig. 5; *ibid.*, fig. 3). The D<sub>4</sub> foliation has completely transposed all other fabrics; however, with decreasing

D<sub>4</sub> strain to the east, a D<sub>2</sub> planar fabric, locally axial planar to D<sub>2</sub> folds, is more evident. Both D<sub>2</sub> folds and foliation are deformed by the dominant Z-shaped D<sub>4</sub> folds.

North of the Nama Creek shear zone, the D<sub>2</sub> foliation is folded by the D<sub>4</sub> Blackman Lake antiform. On the north-trending part of the short limb of this fold, D<sub>2</sub> foliation in migmatitic rocks is reoriented in outcrop-scale shear zones ( $\approx$  1-3 m long) and convolute minor folds. The shear zones have northerly strikes and steep dips, and show either sinistral or dextral offset in plan view. The folds vary in style and orientation, but most have S-asymmetry and moderate northeasterly plunges. Locally they deform an earlier (D<sub>2</sub>?) mineral lineation. Along the east-trending long limb of the Blackman Lake antiform, south of Blackman Lake (Fig. 2), strongly foliated tonalites host pegmatites and granitic veins which may represent incipient migmatization. Z-shaped folds are common and plunge moderately east-northeast, parallel to a distinct stretching lineation. Locally, pegmatites and granitic veins are concentrated in the short limbs of folds; a geometry analogous to the apparent map-scale concentration of migmatitic rocks along the north-trending short limb of the Blackman Lake antiform. North of Blackman Lake, the concentration of migmatitic rocks and veins increases toward the Quetico boundary. Abundant screens of mafic volcanic rocks and, locally, iron-formation (see also Williams and Breaks, 1990a) could be an extension of the thick belt of mafic metavolcanic rocks on the southern margin of the Manitouwadge synform (Fig. 2).

The D<sub>4</sub> Blackman Lake antiform and the Jim Lake synform deform the D<sub>3</sub> Manitouwadge synform (Fig. 2, 3). The Blackman Lake antiform appears to extend southeastward to fold the northern limb, axial region and southern limb of the Manitouwadge synform (Fig. 2). Field mapping, aeromagnetic trends (Fig. 2, 3), and compilation of mining company maps and drilling data indicate the presence of the Jim Lake synform and suggest that it deforms the northern limb and axial region of the Manitouwadge synform.

The proposed extension and folding of the southern limb of the synform represents the most radical departure from previous interpretations. Field mapping of the eastern extension of this limb is frustrated by poor exposure. Noranda has traced the metamorphosed altered rocks associated with mineralization at the Geco mine (the 'Geco horizon') eastward as shown in Figure 2, through mapping and extensive drilling. The easternmost known extension of the 'Geco horizon' is referred to as the Falconbridge zone (Fig. 6). A second zone of metamorphosed alteration to the north, the East One Otter zone (Fig. 6), is characterized by garnet-orthoamphibole gneiss, iron-formation, and mafic metavolcanic rocks. Our mapping in 1993 (Fig. 6), combined with interpretation of the aeromagnetic data (Fig. 3), suggests that the East One Otter zone continues southward through a series of folds that also deform the dominant foliation. This map geometry suggests that the East One Otter and Falconbridge zones may be correlative and that the southern limb of the Manitouwadge synform continues northward from the Falconbridge zone toward the Quetico boundary through a series of minor folds. Extrapolating to the whole region (Fig. 2, 3), this interpretation is consistent with refolding of the D<sub>3</sub> Manitouwadge



**Figure 5.** Outcrop photos of northeast-plunging D<sub>4</sub> folds from the hinge region of Manitouwadge synform near Nama Creek shear zone in **a**) felsic to intermediate layers (GSC 1993-263A). **b**) streaky layers in intermediate host with pronounced stretching lineation parallel to fold axes (scale bar in centimetres). (GSC 1993-263C)

synform by the D4 Blackman Lake antiform and related folds. A definitive correlation between the Falconbridge zone and the East One Otter zone cannot be made yet, due to the limitations of poor exposure and north-south noise (flight lines?) in the aeromagnetic data. The two zones are tentatively shown separated by a fault with apparent sinistral offset (Fig. 6).

Structures observed in migmatitic rocks within, and adjacent to, the Quetico subprovince also reflect oblique dextral shear and are interpreted to be a product of D4 deformation. These include ubiquitous Z-shaped folds with northeast-plunging axes that fold the dominant planar fabric (D2?), shear bands, foliation fish, and rotated boudinage. All of these deform migmatitic layering but are transected by discordant migmatitic veins. North- to northwest-striking outcrop-scale ( $\approx$  1-2 m long) shear zones with dextral and sinistral offsets are also observed in the Quetico rocks.

Along the southern limb of the Manitouwadge synform, particularly north of the belt of metasediments, transposition of structures is more intense than in the hinge region, possibly reflecting a D4 high-strain zone. Focussed D4 shearing may have transposed earlier D2/D3? fabrics so that D2/D3/D4 are indistinguishable. Shear sense indicators in this area primarily reflect a dextral component of motion (fig. 6 in Zaleski and Peterson, 1993), although sinistral indicators are also present (ibid.).

In general, D4 structures reflect oblique dextral shear across the Manitouwadge region. In the northern part of the region, this deformation is expressed as broadly distributed

shear strain, generally synchronous with migmatization. The concentration of migmatites along the short limbs of some D4 folds and the presence of north-trending shear zones may indicate a component of layer-parallel extension during shearing. In the southern unmigmatized part of the belt steeper strain gradients may reflect slightly lower metamorphic grades.

The gentle deflection of the Blackman Lake antiform, Jim Lake synform, and Quetico boundary in the northeastern part of the map area (Fig. 2, 3) is ascribed to D5 deformation. The Banana Lake antiform, which folds the southern belt of mafic metavolcanic rocks, may be a similar structure. East of the area shown in Figure 3, arcuate magnetic anomalies in the northern Wawa belt are concave southward and appear to be truncated along a surface approximately corresponding to the Quetico boundary. This geometry is consistent with a dextral component of focussed shear along this boundary, reflecting either D4 or D5 deformation. Kink folds and crenulation cleavage are locally developed, particularly in micaceous rocks associated with mineralization on the south limb of the synform. The intersection of the crenulation cleavage with foliation produces an intersection lineation with a moderate east plunge. The cleavage has a variable, generally northeasterly, strike and both kinks and cleavage typically have a Z-asymmetry. At a few localities, D4(?) dextral asymmetric quartz lenses in quartz-muscovite schist are folded by these kinks. Crenulations are also present in biotite-rich zones of retrograde potassic metasomatism in the orthoamphibole-garnet-cordierite gneisses (Zaleski and Peterson, 1993). In some outcrops, a second crenulation produces an indistinct,

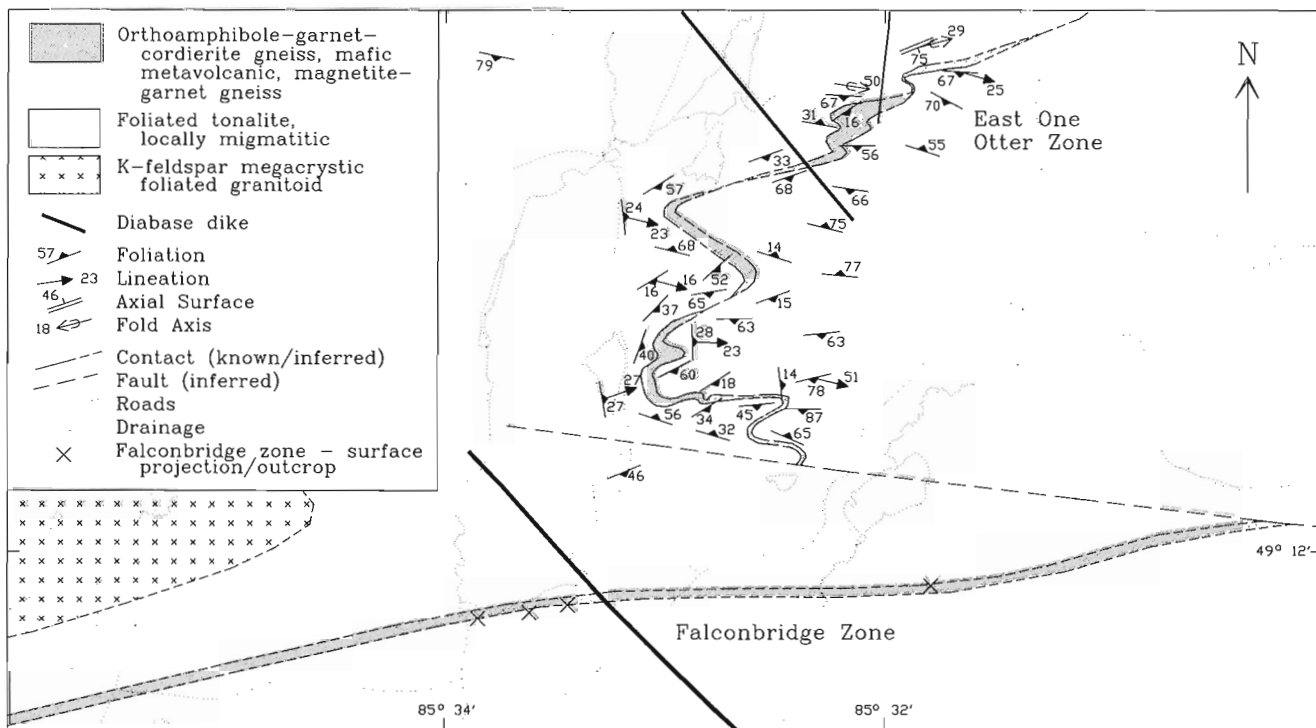
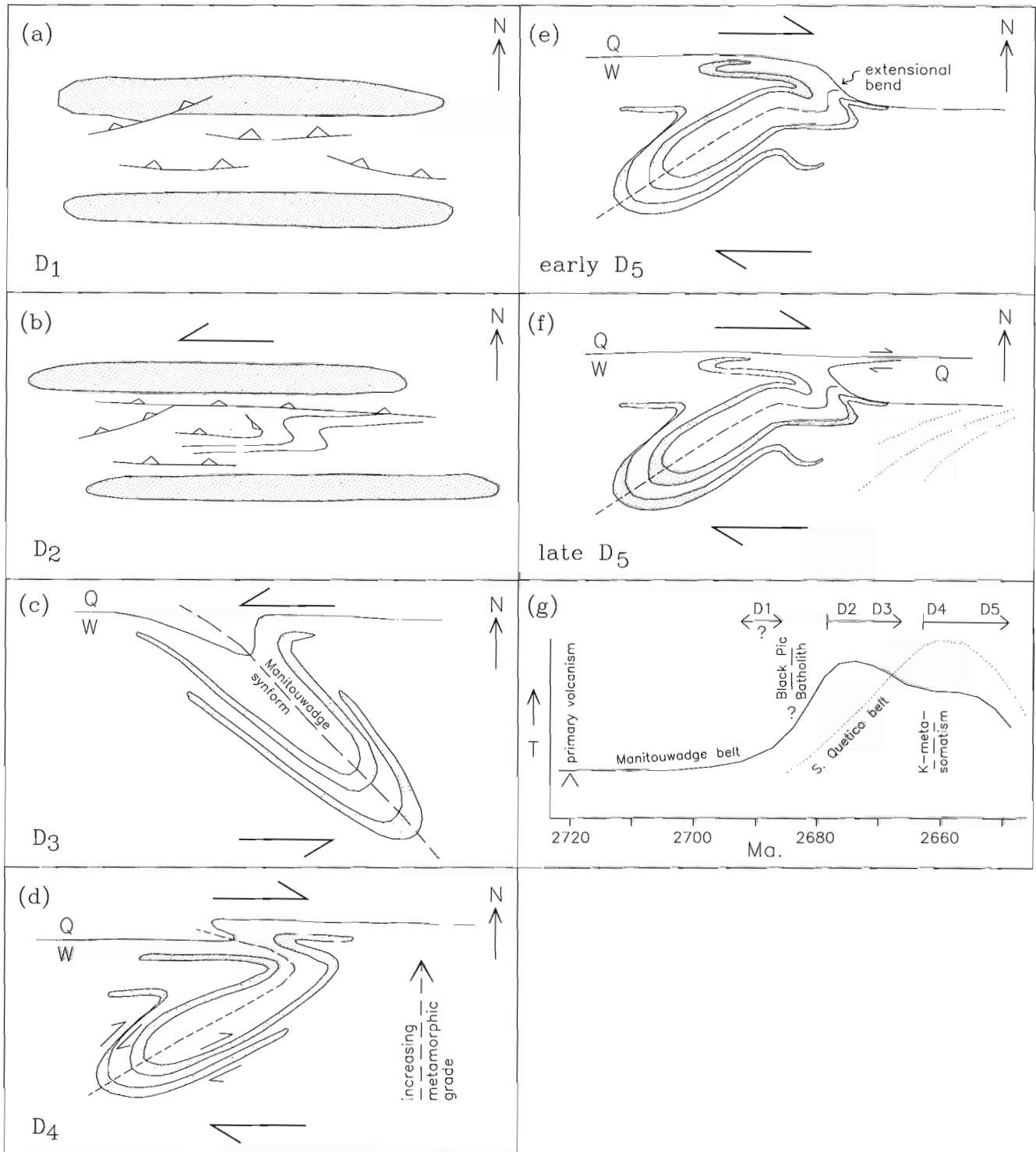


Figure 6. Geological map of the eastern extension of the supracrustal belt (see dashed rectangular outline, eastern Fig. 2).



**Figure 7.** Structural/tectonic synthesis of ductile deformation in the Manitowadge region. a) - f) are map-view sketches showing a possible deformation sequence. See text for discussion. Stippled areas represent volcanic centres. Q = Quetico subprovince. W = Wawa subprovince. Dotted lines in e) and f) represent concave south aeromagnetic anomalies. a) D1, b) D2, c) D3, d) D4, e) early D5, f) late D5, g) Time-temperature plot showing possible relationship between the proposed deformation sequence and the metamorphic evolution in the Manitowadge belt (solid line) and adjacent Quetico belt (dashed line). For discussion of absolute dates see Zaleski et al. (1994) and Percival (1989).

generally west-plunging intersection lineation on the foliation surface and a less distinct cleavage. The kinks and cleavages described above are tentatively assigned to D<sub>5</sub>.

Several late faults have been identified in the area, some of which are shown in Figure 2. The Agam Lake fault (Pye, 1957; Watson, 1970) forms a distinct strike-parallel lineament in the metasediments on the southern limb of the synform. It appears to be primarily a brittle fault, however localized L-tectonites suggest an earlier ductile history. Cross-cutting brittle faults include the Cadawaja fault, Mose Lake fault, and Fox Creek fault (Pye, 1957; Milne, 1974). These also form prominent lineaments and are associated with brittle structures at the surface and in some cases in underground localities.

## STRUCTURAL AND TECTONIC SYNTHESIS

The complex structural relationships observed in the Manitowadge greenstone belt and adjacent Wawa-Quetico boundary can be interpreted in the context of an accretionary arc setting (Percival, 1989). During primary volcanism, felsic rocks were erupted from two volcanic centres onto older tholeiitic shield basalts (Zaleski et al., 1994). The northern centre was associated with a hydrothermal system and now hosts orebodies within the Manitowadge belt. Volcanogenic sediments and greywackes accumulated in a basin between the felsic centres.

The earliest recognizable deformation, D<sub>1</sub>, may have resulted from thrust imbrication during the early stages of shortening between the Wawa and Quetico subprovinces (Fig. 7a). During D<sub>2</sub> deformation, folding and thrusting or shearing continued, possibly with an oblique sinistral component of motion, at conditions near the metamorphic peak in the supracrustal belt (Fig. 7b). D<sub>2</sub> structures deformed earlier D<sub>1</sub> thrusts and produced the dominant regional foliations and lineations. The Black Pic Batholith, in which most phases have D<sub>2</sub> fabrics, was intruded pre- to syn-D<sub>2</sub>. The Manitowadge synform was produced by D<sub>3</sub> deformation, which was nearly coaxial with earlier D<sub>2</sub> folds. In the structural synthesis presented here, the regional structural geometry requires that the synform originally closed eastward, suggesting D<sub>3</sub> folding in response to regional sinistral oblique shortening and shearing (Fig. 7c). More extreme folding of the supracrustal belt, compared to the enclosing tonalites, may reflect competency differences. D<sub>2</sub> and D<sub>3</sub> deformation may represent a continuous progression during and after the peak of metamorphism, so that the structures are essentially coaxial, but with little development of new fabrics during D<sub>3</sub>. D<sub>4</sub> may reflect a regional change from sinistral oblique deformation to broadly distributed dextral oblique shear (Fig. 7d). Refolding of the Manitowadge synform as shown in Figure 6d could be accomplished within a broad dextral shear zone with increasing strain toward the Wawa-Quetico boundary. The strain gradient may partly reflect a thermal gradient during metamorphism, with hotter conditions leading to partial melting in the north near the Quetico boundary. This scenario is consistent with more broadly distributed D<sub>4</sub> strain near the

Quetico boundary and more focussed high-strain zones to the south. Extension along the southern limb of the Manitowadge synform and shearing along the northwest limb (Nama Creek shear zone) may have been a by-product of D<sub>4</sub> refolding of the synform. During D<sub>5</sub>, continued oblique dextral motion during cooling may have focussed shear strain along the Wawa-Quetico boundary (Fig. 7e). D<sub>5</sub> may also be responsible for development of the open extensional bend in the boundary (Fig. 7e), and warping of nearby D<sub>4</sub> axial surfaces. Perhaps the proximity of the Manitowadge supracrustal rocks helped to localize this bend. During later D<sub>5</sub>, shear strain may have been transferred northward to a more linear zone, cutting off the southerly bend in the Quetico boundary (Fig. 7f).

The Quetico subprovince north of Manitowadge is unusual in that the hottest, granulite-facies rocks are near its southern boundary. From the Quetico, there appears to be a continuous metamorphic gradient across the boundary to upper amphibolite facies in the Wawa subprovince. Field relations and geochronology (Zaleski et al., 1994) suggest the possibility of slightly younger metamorphism in the Quetico subprovince than in the Manitowadge belt (Fig. 7g). This is consistent with our structural interpretation that supracrustal rocks in the Manitowadge belt remained relatively hot and ductile during post-peak metamorphic deformation.

## ACKNOWLEDGMENTS

We are indebted to those already acknowledged in Zaleski et al. (1994). In addition we wish to thank Warner Miles of the Geophysical Data Centre for prompt compilation, production, and assistance with aeromagnetic maps. Reviews by John Percival, Ingo Ermanovics, and Jonathan Burr improved the manuscript.

## REFERENCES

- Arias, Z.G. and Helmstaedt, H.**  
1990: Structural evolution of the Michipicoten (Wawa) greenstone belt, Superior Province: evidence for an Archean fold and thrust belt; in Geoscience Research Grant Program, Summary of Research, 1989-1990; Ontario Geological Survey, Miscellaneous Paper 150, p. 1107-114.
- Bauer, R.L., Hudleston, P.J., and Southwick, D.L.**  
1992: Deformation across the western Quetico subprovince and adjacent boundary regions in Minnesota; *Canadian Journal of Earth Sciences*, v. 29, p. 2087-2103.
- Borradaile, G.J. and Spark, R.**  
1991: Deformation of the Archean Quetico-Shebandowan subprovince boundary in the Canadian shield near Kashabowic, northern Ontario; *Canadian Journal of Earth Sciences*, v. 28, p. 116-125.
- Borradaile, G.J., Sarvas, P., Dutka, R., Stewart, R., and Stuble, M.**  
1988: Transpression in slates along the margin of an Archean gneiss belt, northern Ontario - magnetic fabrics and petrofabrics; *Canadian Journal of Earth Sciences*, v. 25, p. 1069-1077.
- Card, K.D.**  
1990: A review of the Superior Province of the Canadian Shield, a product of Archean accretion; *Precambrian Research*, v. 48, p. 99-156.
- Card, K.D. and Ciesielski, A.**  
1986: Subdivisions of the Superior Province of the Canadian Shield; *Geoscience Canada*, v. 13, p. 5-13.

- Corfu, F. and Stott, G.M.**  
1986: U-Pb ages for late magmatism and regional deformation in the Shebandowan belt, Superior Province, Canada; *Canadian Journal of Earth Sciences*, v. 23, p. 1075-1082.
- Devaney, J.R. and Williams, H.R.**  
1989: Evolution of an Archean subprovince boundary: a sedimentological and structural study of part of the Wabigoon - Quetico boundary in northern Ontario; *Canadian Journal of Earth Sciences*, v. 26, p. 1013-1026.
- Hudleston, P.J., Schultz-Ela, D., and Southwick, D.L.**  
1988: Transpression in an Archean greenstone belt, northern Minnesota; *Canadian Journal of Earth Sciences*, v. 25, p. 1060-1068.
- Jirsa, M.A., Southwick, D.L., and Boerboom, T.J.**  
1992: Structural evolution of Archean rocks in the western Wawa subprovince, Minnesota: refolding of precleavage nappes during D2 transpression; *Canadian Journal of Earth Sciences*, v. 29, p. 2146-2155.
- Leclair, A.D.**  
1990: Puskuta Lake shear zone and Archean crustal structure in the central Kapuskasing uplift, northern Ontario; *in* Current Research, Part C; Geological Survey of Canada, Paper 90-1C, p. 197-206.
- McGill, G.E.**  
1992: Structure and kinematics of a major tectonic contact, Michipicoten greenstone belt, Ontario; *Canadian Journal of Earth Sciences*, v. 29, p. 2118-2132.
- Milne, V.G.**  
1974: Mapledoram-Gemmell, Thunder Bay District, scale 1:12000; Ontario Division of Mines, Map 2280.
- Nichol, D.L.**  
1991: Deformation of layered rocks near the Wawa-Quetico subprovince boundary; unpublished M.Sc. thesis, Lakehead University, 76 p.
- Pan, Y. and Fleet, M.E.**  
1992: Mineralogy and genesis of calc-silicates associated with Archean volcanogenic massive sulphide deposits at the Manitouwadge mining camp, Ontario; *Canadian Journal of Earth Sciences*, v. 29, p. 1375-1388.
- Percival, J.A.**  
1989: A regional perspective of the Quetico metasedimentary belt, Superior Province, Canada; *Canadian Journal of Earth Sciences*, v. 26, p. 677-693.
- Percival, J.A. and Williams, H.R.**  
1989: The late Archean Quetico accretionary complex, Superior Province, Canada; *Geology*, v. 17, p. 23-25.
- Petersen, E.U.**  
1984: Metamorphism and geochemistry of the Geco massive sulphide deposit and its enclosing wall-rocks; Ph.D. thesis, University of Michigan, 195 p.
- Pye, E.G.**  
1957: Geology of the Manitouwadge area; Ontario Department of Mines, Annual Report 66, 144 p., map.
- Robinson, P.C.**  
1979: Geology and evolution of the Manitouwadge migmatite belt, Ontario, Canada; Ph.D. Thesis, University of Western Ontario, 367 p.
- Timms, P.D. and Marshall, D.**  
1959: The geology of the Willroy mines base metal deposits; *Proceedings, Geological Association of Canada*, v. 11, p. 55-65.
- Touborg, J.F.**  
1973: Structural and stratigraphical analysis of the Geco sulphide deposit in Manitouwadge, northwestern Ontario (abstract); 19th Annual Institute on Lake Superior Geology, p. 38-39.
- Watson, D.W.**  
1970: The geology and structural evolution of the Geco massive sulphide deposit at Manitouwadge, northwestern Ontario, Canada; Ph.D. thesis, University of Michigan, 272 p.
- Williams, H.R.**  
1989: Geological studies in the Wabigoon, Quetico and Abitibi-Wawa Subprovinces, Superior Province of Ontario, with emphasis on the structural development of the Beardmore-Geraldton belt; Ontario Geological Survey, Open File Report 5724, 188 p.  
1990: Subprovince accretion tectonics in the south-central Superior Province; *Canadian Journal of Earth Sciences*, v. 27, p. 570-581.
- Williams, H.R. and Breaks, F.W.**  
1989: Geological studies in the Manitouwadge-Hornpayne area; Ontario Geological Survey, Miscellaneous Paper 146, p.79-91.  
1990a: Geology of the Manitouwadge-Hornpayne area; Ontario Geological Survey, Open File Map 142, scale 1:50,000.  
1990b: Geological studies in the Manitouwadge-Hornpayne area; Ontario Geological Survey, Miscellaneous Paper 151, p.41-47.
- Williams, H.R., Stott, G.M., Heather, K.B., Muir, T.L. and Sage, R.P.**  
1991: Wawa Subprovince; *in* Geology of Ontario, Ontario Geological Survey, Special Volume 4, Part 1, p.485-539.
- Zaleski, E. and Peterson, V.L.**  
1993: Lithotectonic setting of mineralization in the Manitouwadge greenstone belt, Ontario: preliminary results; *in* Current Research, Part C; Geological Survey of Canada, Paper 93-1C, p. 307-317.
- Zaleski, E., Peterson, V.L., and van Breemen, O.**  
1994: Geological, geochemical and age constraints on base metal mineralization in the Manitouwadge greenstone belt, northwestern Ontario; *in* Current Research 1994-C; Geological Survey of Canada.

---

Geological Survey of Canada Project 910033





# Till composition in the vicinity of the Manitouwadge greenstone belt, Ontario<sup>1</sup>

Inez M. Kettles and Julian B. Murton<sup>2</sup>

Terrain Sciences Division

*Kettles, I.M. and Murton, J.B., 1994: Till composition in the vicinity of the Manitouwadge greenstone belt, Ontario; in Current Research 1994-C; Geological Survey of Canada, p. 249-257.*

---

**Abstract:** In 1991 and 1992, 286 till samples were collected for mineral exploration purposes in the vicinity of the Manitouwadge greenstone belt. Samples were analyzed for their content of clasts of distinctive Precambrian and Paleozoic lithologies and for trace elements in the <0.002 mm fraction. Variation in till composition can be related to glacial transport and local bedrock geology. In many areas, the till contains abundant Paleozoic carbonate clasts glacially transported southwestward from the Hudson Bay and James Bay lowlands. Where present in large quantities, Paleozoic carbonate tends to suppress the geochemical signature of till partially derived from local Precambrian bedrock, which contains higher trace element levels. Despite the effects of dilution, anomalously high concentrations of Cu, Pb, and Zn are found in till overlying and immediately down ice from the Geco and associated VMS deposits at Manitouwadge and, elsewhere, at a few sites overlying and away from the greenstone belt.

**Résumé :** En 1991 et 1992, 286 échantillons de till ont été prélevés à des fins de prospection minérale dans les environs de la ceinture de roches vertes de Manitouwadge. Ils ont été analysés pour déterminer leur teneur en clastes de lithologies distinctives du Précambrien et du Paléozoïque, ainsi que leur teneur en éléments traces dans la fraction <0,002 mm. La variation de la composition du till peut être liée au transport glaciaire et à la géologie du substratum rocheux local. Dans de nombreux secteurs, le till contient d'abondants clastes de roches carbonatées du Paléozoïque transportés par les glaces vers le sud-ouest à partir des basses terres de la baie d'Hudson et de la baie James. Là où ils sont présents en grandes quantités, les clastes de roches carbonatées du Paléozoïque ont tendance à supprimer la signature géochimique du till partiellement dérivé du socle précambrien local qui contient de fortes concentrations d'éléments traces. Malgré les effets de la dilution, des concentrations de Cu, de Pb et de Zn anormalement élevées ont été relevées dans le till sus-jacent au gisement de sulfures massifs volcanogènes de Geco et autres gisements associés de Manitouwadge et à l'aval glaciaire de ceux-ci, de même qu'ailleurs à quelques endroits situés dans la ceinture de roches vertes et à l'extérieur de celle-ci.

---

<sup>1</sup> Contribution to Canada-Ontario Subsidiary Agreement on Northern Ontario Development (1991-1995), under the Canada-Ontario Economic and Regional Development Agreement.

<sup>2</sup> Department of Earth Sciences and Ottawa-Carleton Geoscience Centre, Carleton University, Ottawa, Ontario K1S 5B6

**INTRODUCTION**

As part of the Northern Ontario Development Agreement (NODA), the Geological Survey of Canada carried out till sampling in 1991 and 1992 in the Manitowadge-Hornepayne area (Kettles, 1993a, b). The purpose was to provide information about Quaternary geology (e.g. ice flow directions and lithological and geochemical composition of glacial sediments) that would be valuable for drift prospecting. This survey included more detailed sampling in the vicinity of the Manitowadge greenstone belt, especially near the Geco and several abandoned Cu-Zn mines (Fig. 1). In 1992 additional till sampling, also relating to mineral exploration, was undertaken in the Manitowadge area by Carleton University. The two surveys collected 286 till samples. In this paper preliminary results of their analysis are presented. The paper has three objectives: (1) to describe physical and chemical properties of Manitowadge tills; (2) to interpret local ice flow directions; and (3) to identify areas where subsequent, detailed drift prospecting may locate new base metal deposits.

**Bedrock and glacial geology**

The study area is underlain by Archean greenstone belts and granitoid plutons of the Wawa subprovince of the Canadian Shield (Williams and Breaks, 1990; Zaleski and Peterson, 1993; Ontario Geological Survey, 1991; Fig. 2; Table 2). The Manitowadge greenstone belt, comprising highly deformed metavolcanic and metasedimentary rocks, hosts four known volcanogenic massive sulphide (VMS) deposits, the largest of which is the Geco Cu-Zn-Ag deposit (Fig. 1; Friesen et al., 1982).

All glacial sediments in the Manitowadge area are thought to have been deposited during the Late Wisconsinan (Kristjansson and Geddes, 1986; Geddes and Bajc, 1985;

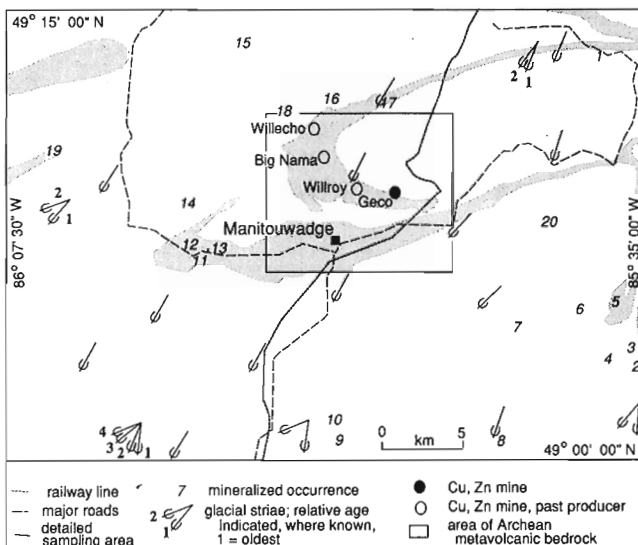
**Table 1.** Mineral occurrences shown in Figure 1 (after D.B. McKay, in prep.)

Table 1. Description of mineral occurrences; accompanies Figure 1.	
1 Cu	11 Cu, Zn, Au
2 Sulphides, Cu	12 Sulphides, Au
3 Sulphides	13 Sulphides
4 Sulphides	14 Base metals
5 Cu	15 Sulphides
6 Sulphides	16 Au, base metals
7 Cu	17 Zn
8 Sulphides	18 Sulphides
9 Sulphides, Mo	19 Sulphides
10 Au	20 Sulphides

Barnett et al., 1991). Striae measurements indicate that the predominant flow direction was 210-220° (Kristjansson and Geddes, 1985; Geddes and Bajc, 1985; Kettles, 1993a, b; Fig. 1). From striae on stoss and lee facets of glacially moulded bedrock and in grooves eroded during earlier flow events, earlier (southerly) and later (more westerly) flow events were determined.

The most widespread glacial deposits in the Manitowadge area are diamictons likely deposited either directly from, or in close association with, glacial ice. They have the physical and chemical characteristics that closely approximate those of the debris load carried by the last glacier to cross the project area, and are, therefore, collectively referred to as till. A single stratigraphic unit has been recognized (Kristjansson and Geddes, 1985; Geddes and Bajc, 1985). Till commonly forms a thin, discontinuous veneer (up to 1.5 m thick), but in places exceeds 10 m in thickness. On account of poor exposure it was difficult to distinguish between till facies. However, where till was better exposed three facies were observed and sampled:

1. Compact diamicton with 30-65% Paleozoic carbonate clasts. It is locally fissile, pale grey where unweathered and buff where weathered. Compact diamicton was observed on the down-ice (lee) slopes of certain hills and in some lowland sites. Thicknesses locally exceed at least a few metres.
2. Loose, sandy diamicton with low to high concentrations of Paleozoic carbonate clasts (8-40%); this material is light to dark grey where unweathered and tan to olive coloured where weathered. It is the most widespread till, commonly forming discontinuous sheets of variable thickness (0.5-3.0 m).
3. Loose, very sandy to clast-rich diamicton with few Paleozoic carbonate clasts (0-8%) and high concentrations of angular, generally large (up to boulder size) clasts derived from the local Precambrian bedrock. This unit is dark grey when unweathered and olive to tan coloured when weathered. It is common in areas of exposed bedrock.



**Figure 1.** Study area, Manitowadge area, Ontario. See Table 1 for mineral occurrences.

Glaciofluvial ice-contact and outwash sand and gravel are also present in the study area. Outwash deposits are common in the region east of Manitowadge, in low-lying areas above the maximum levels of glacial lake incursion (post-Lake Minong; Kristjansson and Geddes, 1986). Elsewhere, in low-lying areas, glaciolacustrine deposits consisting of sand, silt, and clay are widespread. In the Manitowadge area, lacustrine sediments have been observed as high as 325 m a.s.l. (R. Geddes, 1987, unpublished report). Eolian dunes are found in some areas where outwash or glaciolacustrine sediments predominate and alluvial sands and silts are well developed along major rivers and streams. Deposits of peat and organic muck are widespread, particularly in areas underlain by glaciolacustrine sediments.

## FIELD AND LABORATORY METHODS

Two hundred and eighty-six till samples were collected from hand-dug holes at off-road or shoreline sites or in roadside exposures. Care was taken to sample the least weathered till, most samples being collected below the B-horizon of the soil.

**Table 2.** Bedrock geology units accompanying Figures 2 to 6.

GEOLOGICAL LEGEND	
<b>ARCHEAN</b>	
<b>INTRUSIVE ROCKS</b>	
9	Massive granodiorite to granite
8	Diorite - monzonite - granodiorite suite
6	Gneissic tonalite suite
5	Mafic and ultramafic rocks
<b>SUPRACRUSTAL ROCKS</b>	
4	Migmatized supracrustal rocks
3	Metasedimentary rocks
2	Felsic to intermediate metavolcanic rocks
1	Mafic to intermediate metavolcanic rocks
	Iron formation
	Geological contact
	Mine site (current and past producer)
	1. Willecho
	2. Big Nama
	3. Willroy
	4. Geco

Pebbles (5.0-16.0 mm) were separated from most samples for lithological analysis. On average, 185 clasts were examined from each sample. The clasts were grouped into the following 6 classes and relative percentages (by number) calculated: 1) Paleozoic limestones and dolomites; 2) Paleozoic sandstones and siltstones; 3) Proterozoic greywackes and argillites (these clasts are characteristic of the Omarolluk Formation which outcrops in the Belcher Island Fold Belt and Sutton Inlier (e.g. Ricketts and Donaldson, 1981); 4) Precambrian metasediments of uncertain provenance; 5) Precambrian intrusive and high-grade metamorphic rocks; and 6) undifferentiated Archean metavolcanic rocks.

The <0.063 mm and <0.002 mm fractions of the samples were analyzed for 28 trace and minor elements (Ag, Al, As, Ba, Bi, Ca, Cd, Co, Cr, Cu, Fe, K, La, Mg, Mn, Mo, Na, Ni, Pb, Sb, Sc, Sr, Sn, Te, V, W, Y, and Zn) by Inductively Coupled Plasma and Atomic Emission Spectroscopy (ICP-AES) following a nitric acid-aqua regia partial extraction. The <0.063 mm fraction was further analyzed for Au, Pt, and Pd by fire assay and Direct Current Plasma (DCP) spectroscopy.

Results of analyses, with sample locations and descriptions, are stored on computer files. Geochemical and pebble lithology data for a representative sample from each of the 286 sites in the Manitowadge region were statistically analyzed using the computer software program Statview and was plotted using a computer program developed by Wyatt Geoscience, Ottawa. Data for 80 samples collected in the vicinity of the Manitowadge VMS deposits were later extracted from the above database, reanalyzed statistically, and plotted.

## RESULTS

### *Pebble composition*

The frequency distribution and dispersal patterns of pebbles in till samples from the Manitowadge area were studied to examine relationships between glacial transport and pebble lithology. Clasts in the Manitowadge tills were derived from two major bedrock terranes: 1) local Precambrian units and 2) Paleozoic and Proterozoic terranes of the Hudson Bay and James Bay Lowlands. Clasts derived from the latter must have been glacially transported at least 100 km.

The pebble fraction in more than 80% of the till samples contained at least 8% Paleozoic carbonate and 50% had greater than 25% Paleozoic carbonate. In addition, over 60% of the samples contained more than 7% clasts of Proterozoic metasedimentary rock. In the Manitowadge tills, the distribution of these distinctive lithologies are similar, the highest concentrations of each generally occurring in the eastern part of the study area. This local pattern of till distribution is consistent with the regional pattern (Sado and Carswell, 1987). Manitowadge lies on the western edge of a plume of thick till extending south from the James and Hudson Bay lowlands. This is one of several plumes in northern Ontario likely formed by late glacial ice streams in the Laurentide Ice Sheet (Hicock et al., 1989). In contrast to exotic Paleozoic and

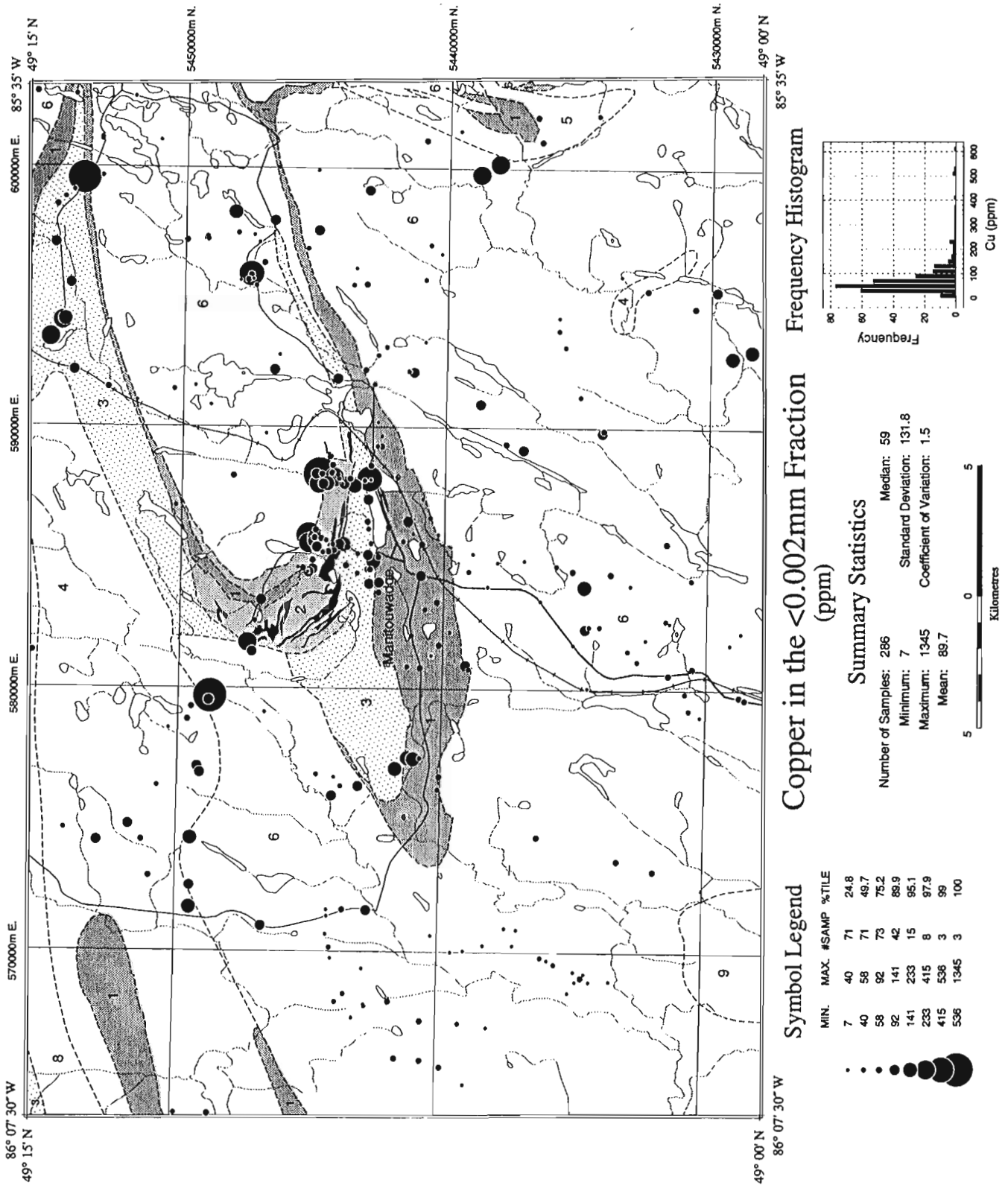


Figure 2a. Distribution of Cu in the clay-sized (<2 μm) fraction of Manitowadge tills. Bedrock geology legend shown in Table 2.

Proterozoic lithologies, the highest concentrations of local Precambrian lithologies (e.g. metavolcanics) were found in till overlying or within 1-2 km of their outcrops (Kettles, 1993a,b). The distribution pattern of local lithologies reflects the effects of glacial erosion and transport at a local scale.

**Trace element composition**

High concentrations of Paleozoic carbonate in till tends to suppress the geochemical signature of the fine fraction (see Kettles, 1993a, correlation matrix; Kaszycki, 1989), because unmetamorphosed carbonate bedrock contains low trace element concentrations with some exceptions (Mason, 1966, Table 6.5).

Despite the effects of dilution resulting from long-distance transport of Paleozoic carbonate, the distribution of trace and minor elements in the fine fractions of till may, in many areas,

be related to local bedrock composition. Anomalously high concentrations of Cu, Zn, and Pb were measured in till overlying and within 1-2 km of the Manitowadge VMS deposits (Fig. 2a, b, 3, 4a, b). These samples also contain numerous clasts of local Precambrian metavolcanic and metasediment lithologies. Away from the main VMS deposits, Cu, Zn, and Pb anomalies were noted at the following sites: (1) 1345 ppm Cu overlying the greenstone belt in the northeastern part of the study area; (2) 603 ppm Cu, 9 km northwest of Manitowadge; (3) 279 ppm and 352 ppm Cu, 16 km southeast of Manitowadge; (4) 549 ppm Pb and 570 ppm Zn, 9 km west northwest of Manitowadge; and (5) 444 ppm Zn, 16 km southwest of Manitowadge. The first site is known to overlie the greenstone belt and the third and fourth sites may also overlie metavolcanic bedrock, as yet unmapped, since in these samples this lithology is abundant. Subsequent mineral exploration in these areas may be profitable.

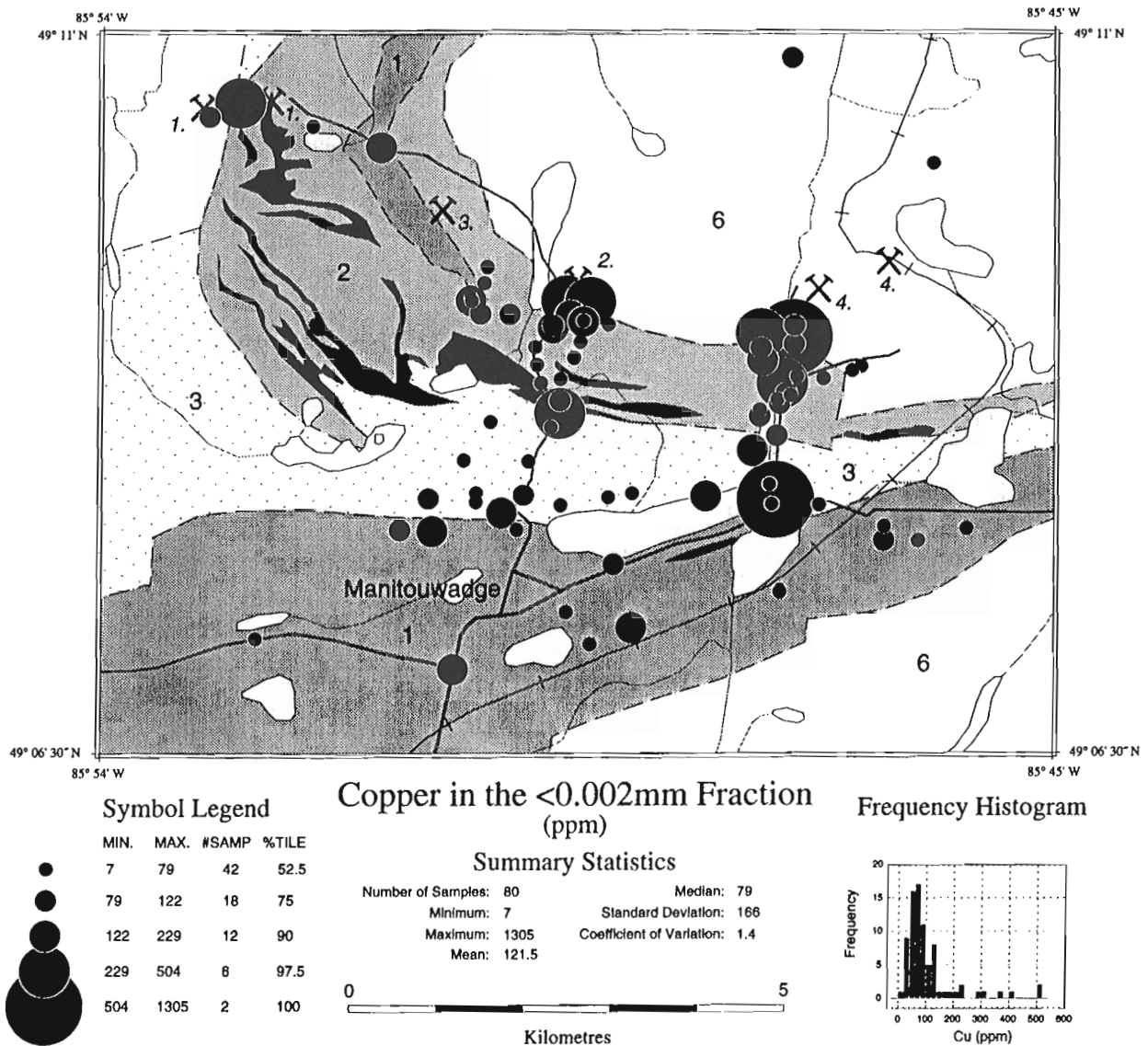


Figure 2b. Distribution of Cu in clay-sized (<2 μm) fraction of Manitowadge tills in the vicinity of the Geco and abandoned mines. Bedrock geology legend shown in Table 2.

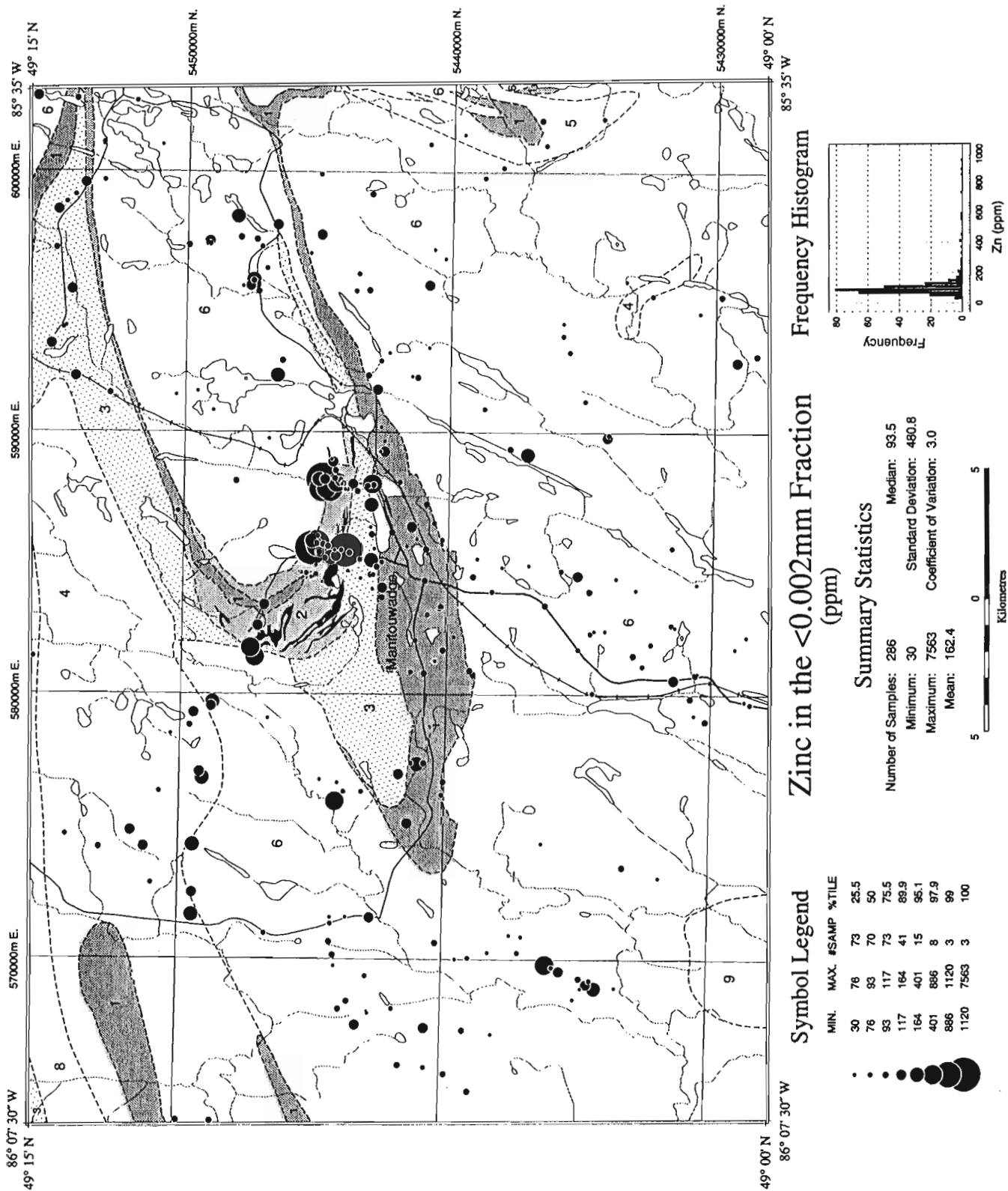


Figure 3. Distribution of Zn in the clay-sized (<2 μm) fraction of Manitowadge tills. Bedrock geology legend shown in Table 2.



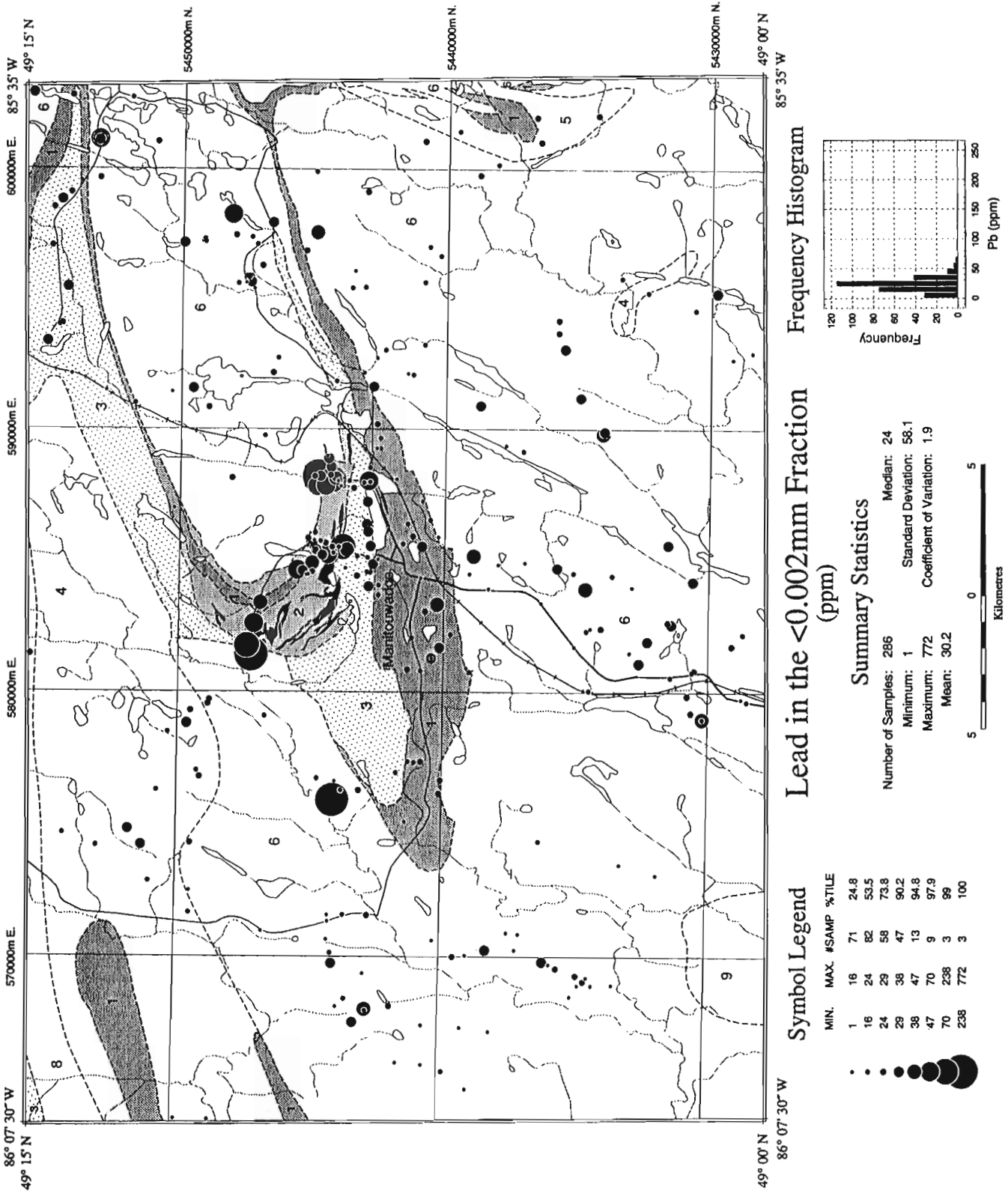


Figure 4a. Distribution of Pb in the clay-sized (<2 μm) fraction of Manitowadge tills. Bedrock geology legend shown in Table 2.

Another major factor which influences the geochemical signature of surficial till is weathering. In this study, the effects of weathering on composition have been minimized by sampling till below the A and B horizons of the postglacial solum. As a result, regional patterns of Cu, Pb, and Zn shown in Figures 2 to 4 are believed to primarily reflect the original composition of the till.

**CONCLUSIONS**

Variations in till composition are related to the effects of glacial transport and the composition of local bedrock. Manitowadge tills commonly contain large percentages of

Paleozoic carbonate debris, glacially transported more than 100 km from the Hudson and James Bay lowlands. They also contain local Precambrian lithologies, the highest concentrations of which were observed near their respective outcrops.

Although the geochemical signature of mineralized bedrock may be masked in some areas by dilution from Paleozoic carbonates, the signature generally does stand out in the fine fractions of till. Anomalously high concentrations of Cu, Pb, and Zn occur near the main Manitowadge VMS deposits. Elsewhere, at several sites not associated with known VMS deposits, concentrations of base metals in till are also anomalously high. Further exploration near these sites may prove worthwhile.

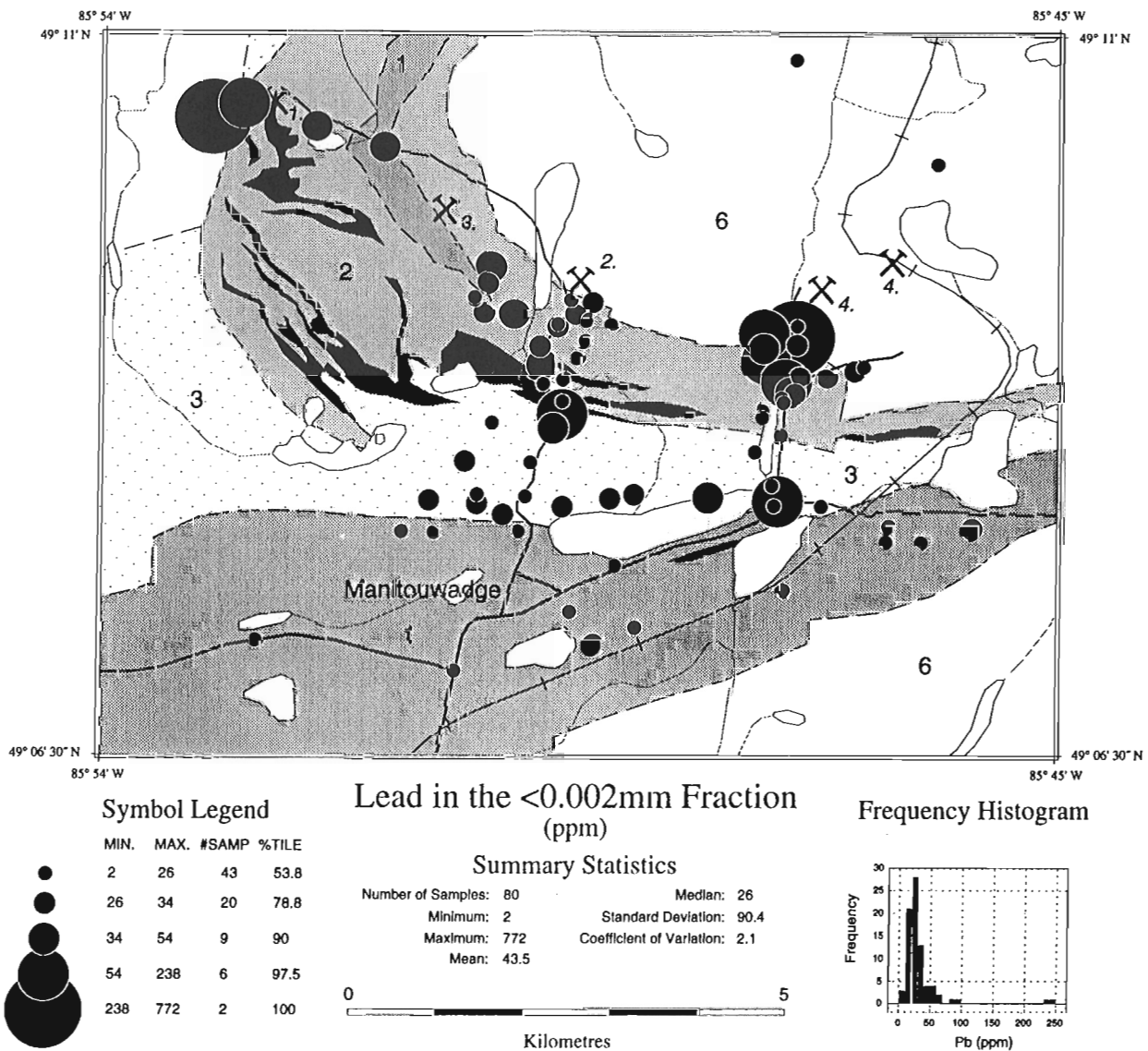


Figure 4b. Distribution of Pb in clay-sized (<2 μm) fraction of Manitowadge tills in the vicinity of the Geco and abandoned mines. Bedrock geology legend shown in Table 2.

## ACKNOWLEDGMENTS

The authors wish to thank the following: K. Bell, Carleton University, for permission to use samples collected for a project funded by an NSERC strategic grant; K. Laurus, S. Bauke, and S. Bayne for their able assistance in the field; D. B. McKay for helpful advice; the staff of the geology department of Noranda Geco mine for helpful discussions and permission to sample near the mine; M. Hebel for assistance with data compilation; Northwood Geoscience for plotting the proportional symbol maps; D. Pare, Consorminex Ltd., and K. Laurus for carrying out pebble counts; J. Card and P. Lindsay for technical assistance.

## REFERENCES

- Barnett, P.J., Henry, A.P., and Babuin, D.**  
1991: Quaternary geology of Ontario, east-central sheet; Ontario Geological Survey, Map 2555, scale 1: 1 000 000.
- Friesen, R.G., Pierce, G.A., and Weeks, R.M.**  
1982: Geology of the Geco base metal deposit; Geological Association of Canada, Special Paper 25, p. 343-363.
- Geddes, R.S.**  
1987: Quaternary geology of the Hemlo region, Districts of Thunder Bay and Algoma; Ontario Geological Survey, unpublished report.
- Geddes, R.S. and Bajc, A.F.**  
1985: Quaternary geology of the White Lake (Hemlo area), District of Thunder Bay, Ontario Geological Survey, Map P. 2849, Scale 1: 50, 000.
- Hicock, S.R., Kristjansson, F.J., and Sharpe, D.R.**  
1989: Carbonate till as a soft bed for Pleistocene ice streams on the Canadian Shield north of Lake Superior; Canadian Journal of Earth Sciences, v. 26, p. 2249-2254.
- Kaszycki, C.A.**  
1989: Surficial geology and till composition, northwestern Manitoba; Geological Survey of Canada, Open File 2118, 150 p.
- Kettles, I.M.**  
1993a: Reconnaissance geochemical data for till samples from the Manitouwadge area, Ontario; Geological Survey of Canada, Open File 2616, 197 p.  
1993b: Till geochemistry in the Manitouwadge area, Ontario; in Current Research, Part E; Geological Survey of Canada, Paper 93-1E, p. 165-173.
- Kristjansson, F.J. and Geddes, R.S.**  
1986: Quaternary geology of the Manitouwadge area, District of Thunder Bay; Ontario Geological Survey, Map P. 3055, Scale 1: 50, 000.
- Mason, B.**  
1966: Principles of geochemistry; Wiley, New York; 329 p.
- Ontario Geological Survey**  
1991: Bedrock geology of Ontario, east-central sheet; Ontario Geological Survey, Map 2534.
- Ricketts, B.D. and Donaldson, J.A.**  
1981: Sedimentary history of the Belcher Group of Hudson Bay; in Proterozoic Basins of Canada, (ed.) F.H.A. Campbell; Geological Survey of Canada, Paper 81-10, p. 235-254.
- Sado, E.V. and Carswell, B.F.**  
1987: Surficial geology of Northern Ontario; Ontario Geological Survey, Map 2518, scale 1: 1 200 000.
- Williams, H.R. and Breaks, F.W.**  
1990: Geology of the Manitouwadge-Hornpayne area; Ontario Geological Survey, Open File Map 142, scale 1: 50, 000.
- Zaleski, E. and Peterson, V.L.**  
1993: Lithotectonic setting of mineralization in the Manitouwadge greenstone belt, Ontario: preliminary results; in Current Research, Part C; Geological Survey of Canada, Paper 93-1C, p. 307-317.

Geological Survey of Canada Project 910017



# An interim report on geological, structural, and geochronological investigations of granitoid rocks in the vicinity of the Swayze greenstone belt, southern Superior Province, Ontario<sup>1</sup>

Kevin B. Heather and Otto van Breemen  
Continental Geoscience Division

*Heather, K.B. and van Breemen, O., 1994: An interim report on geological, structural, and geochronological investigations of granitoid rocks in the vicinity of the Swayze greenstone belt, southern Superior Province, Ontario; in Current Research 1994-C; Geological Survey of Canada, p. 259-268.*

---

**Abstract:** Lithological and structural mapping of granitoid rocks both within and surrounding the Swayze greenstone belt is described and preliminary U-Pb zircon geochronology presented (Swayze NODA project). There is a temporal progression, based on crosscutting relationships and supported by geochronology, from early, more mafic, hornblende-rich diorites through hornblende and biotite tonalites and granodiorites to more felsic, hornblende- and biotite-bearing granodiorites and granites. This progression can be documented within the Kenogamissi Batholith and the Ramsey-Algoma granitoid complex. The Kenogamissi Batholith consists of early, 2713  $\pm$  2/-3 Ma, foliated hornblende±biotite tonalites which are cut by 2697  $\pm$  3 Ma, foliated biotite tonalites. The northern and southern margins of the batholith consist of massive to foliated, potassium feldspar megacrystic, hornblende granodiorite to granite which crosscuts the earlier tonalite phases. The southern phase yielded an age of 2682  $\pm$  3 Ma while the northern phase is younger than 2695 Ma. Late, ca. 2665 Ma, massive, nonfoliated biotite granites with associated aplite and pegmatite dykes crosscut all of the tonalite and granodiorite phases. The 2740  $\pm$  2 Ma Chester biotite trondhjemite and the presence of a 2730-2740 Ma inherited zircon population within a ca. 2700 Ma felsic metavolcanic rock may indicate the presence of a more aerial extensive, older volcano-plutonic package of rocks.

**Résumé :** La cartographie lithologique et structurale des roches granitoïdes sises à l'intérieur et autour de la ceinture de roches vertes de Swayze est décrite, et leur datation préliminaire par la méthode U-Pb sur zircon est présentée (projet Swayze de l'EDNO). Il existe une progression chronologique, basée sur les relations de recoupement et appuyée sur la géochronologie, allant, des plus anciennes aux plus récentes, de phases plus mafiques (diorite à hornblende) à des phases plus felsiques (granodiorites et granites à hornblende et à biotite) en passant par des tonalites et granodiorites à hornblende et à biotite. Cette progression peut être documentée au sein du batholite de Kenogamissi et du complexe granitoïde de Ramsey-Algoma. Le batholite de Kenogamissi est composé d'une phase initiale de tonalites à hornblende-biotite foliées, âgées de 2 713  $\pm$  2/-3 Ma, qui sont recoupées par des tonalites à biotite foliées, datées à 2 697  $\pm$  3 Ma. Les bordures nord et sud du batholite sont composées de granodiorite-granite à hornblende à mégacristaux de feldspath potassique, massif à folié, qui recoupe les phases tonalitiques initiales. La phase méridionale a donné un âge de 2 682  $\pm$  3 Ma tandis que la phase septentrionale est plus récente que 2 695 Ma. Les granites à biotite, massifs et non foliés, mis en place tardivement autour de 2 665 Ma environ, et auxquels sont associés des dykes d'aplite et de pegmatite, recoupent toutes les phases de tonalite et de granodiorite. La trondhjemite à biotite de Chester de 2 740  $\pm$  2 Ma et la présence d'une population de zircons hérités de 2 730-2 740 Ma au sein d'une roche métavolcanique felsique d'environ 2 700 Ma peuvent indiquer la présence d'un ensemble de roches volcano-plutoniques plus ancien et plus étendu.

---

<sup>1</sup> Contribution to Canada-Ontario Subsidiary Agreement on Northern Ontario Development (1991-1995), under the Canada-Ontario Economic and Regional Development Agreement.

## INTRODUCTION

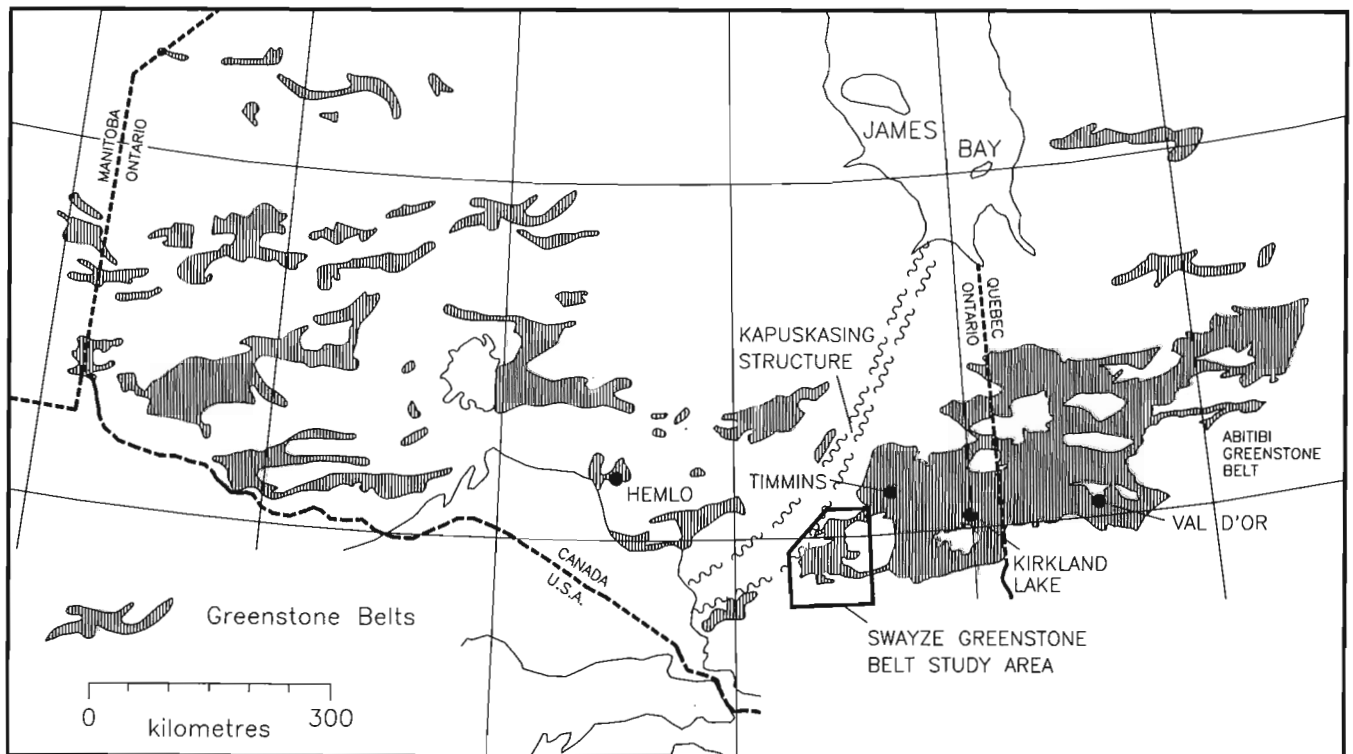
The Swayze project is a bedrock mapping program being conducted by the Geological Survey of Canada under the auspices of the Northern Ontario Development Agreement (NODA) for minerals. The project area encompasses approximately 12 000 km<sup>2</sup> southwest of Timmins, Ontario centred on the Swayze greenstone belt (SGB) and surrounding granitoid terranes (Fig. 1). The objectives and methodologies of the project are outlined in Heather (1993). The purpose of this report is to highlight the results of the 1993 field mapping. An overview of the regional geology and structure is provided by Heather (1993).

The Swayze greenstone belt (SGB) is located within the western Abitibi Subprovince of the Superior Province and is bounded to the: a) west by the Kapuskasing Structural Zone; b) east by the Kenogamissi Batholith; c) north by the Nat River granitoid complex; and d) south by the Ramsey-Algoma granitoid complex (Fig. 2). The Swayze greenstone belt is connected to the Abitibi greenstone belt by narrow septa of metavolcanic-metasedimentary rocks that wrap around the north and south margins of the Kenogamissi Batholith (Fig. 1, 2). Results reported here are from the Kenogamissi Batholith, the Ramsey-Algoma granitoid complex southeast of the Swayze greenstone belt, and from two granitoids internal to the Swayze greenstone belt. Rocks of the Nat River granitoid complex are not discussed, however Heather (1993) provides a basic description.

The granitoid rock names used in this report are consistent with Streckeisen (1976) and are based on field estimates of the proportions of quartz, plagioclase, potassium feldspar, and mafic minerals.

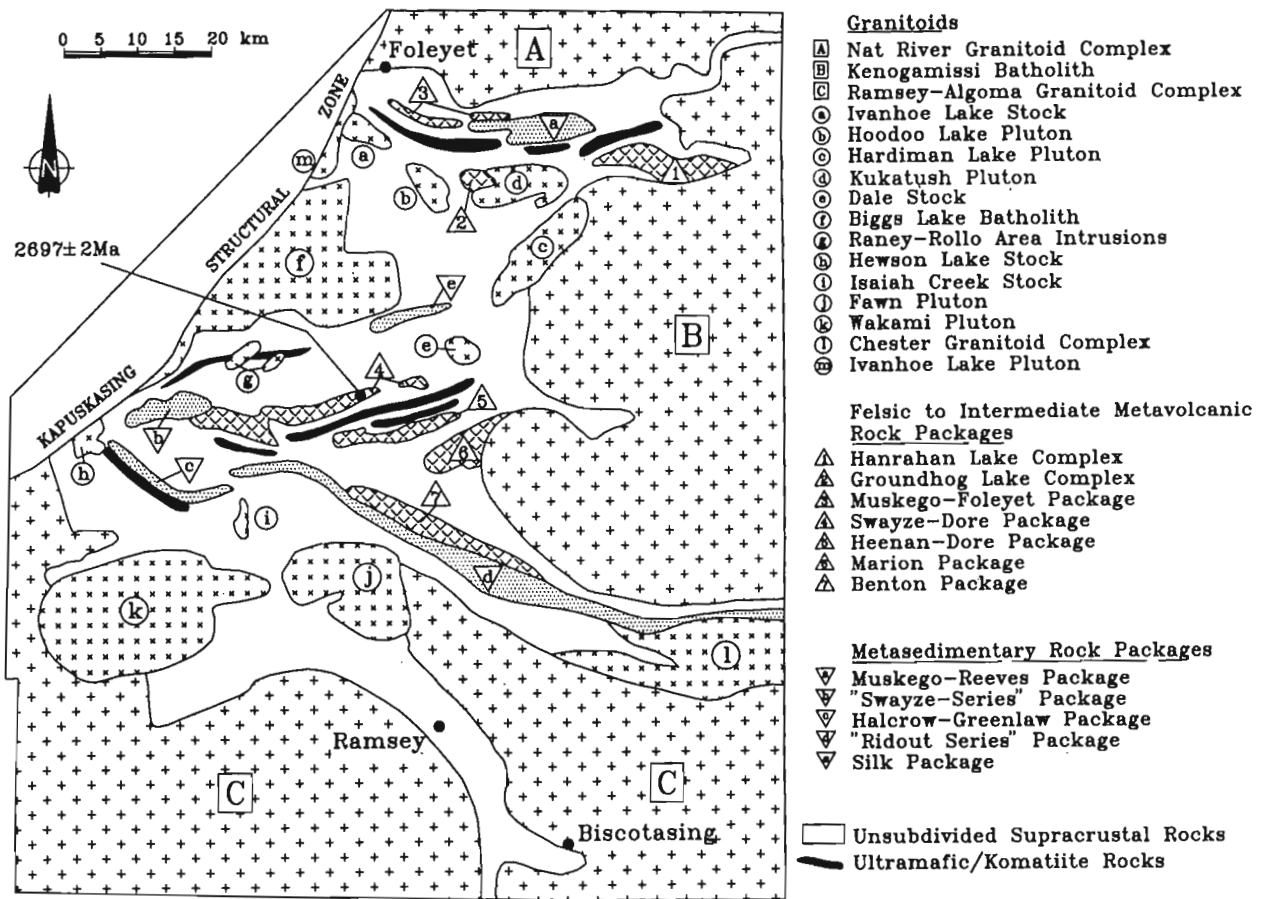
### *Kenogamissi Batholith*

The Kenogamissi Batholith is a large granitoid complex that separates the Swayze greenstone belt from the Abitibi greenstone belt to the east (Fig. 1, 2). A complex, yet systematic sequence of crosscutting intrusive rock phases has been documented within the batholith. From oldest to youngest these phases are: a) remnant xenoliths of foliated mafic amphibolite; b) foliated hornblende diorite to monzodiorite and hornblende monzonite to quartz monzonite; c) foliated hornblende ±biotite tonalite to granodiorite and associated pegmatite and aplite dykes; d) foliated biotite tonalite to granodiorite and associated pegmatite and aplite dykes; e) foliated mafic gabbroic dykes; f) massive to foliated, potassium feldspar megacrystic, hornblende granodiorite to granite and associated dykes; and g) massive, nonfoliated, biotite granite to granodiorite and associated pegmatite and aplite dykes. The main intrusive phases (i.e., c, d, f, and g above) within the western half of the Kenogamissi Batholith are described below and their general distribution depicted in Figure 3.



*Figure 1. Regional setting of the Swayze greenstone belt study area.*





**Figure 2.** Simplified geology of the Swayze project area. Only the major rock packages and intrusions are depicted. Late diabase dykes have been omitted for clarity. This figure is to be used in conjunction with Figure 3.

### Hornblende±biotite tonalite to granodiorite

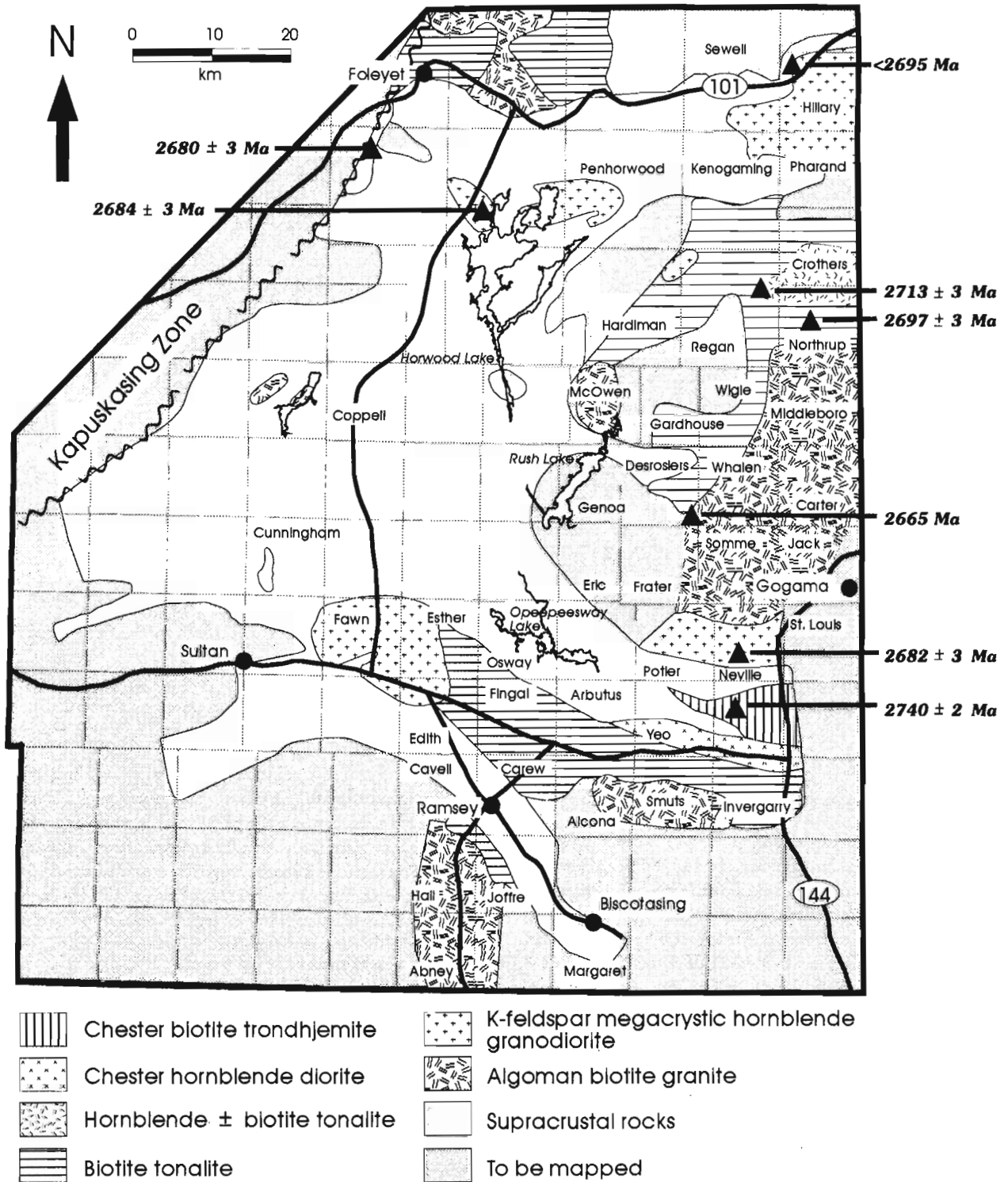
The foliated, hornblende±biotite tonalites, locally with an igneous layering/foliation, appear to be the oldest, mappable phase within the Kenogamissi Batholith (Fig. 3). The hornblende±biotite tonalites are spatially related to, but have a more restricted distribution than, the foliated biotite tonalites which crosscut them. The hornblende tonalites locally contain xenoliths of foliated mafic amphibolite and foliated hornblende diorite to monzodiorite (Fig. 4) and hornblende monzonite to quartz monzonite intrusive rocks. There appears to be a mappable correlation, both at the outcrop scale and the regional scale, between zones of mafic xenoliths and the hornblende tonalites versus the biotite tonalites. A variably developed tectonic foliation is oblique to the locally developed igneous layering/foliation within the hornblende tonalite (Fig. 5).

### Biotite tonalite to granodiorite

The foliated biotite tonalites to granodiorites are more regionally extensive than the early, hornblende±biotite tonalites (Fig. 3). Xenoliths of foliated/layered hornblende±biotite

tonalite are common within the foliated biotite tonalite. The biotite tonalites contain 10 to 25% disseminated biotite and locally are intimately interlayered with the hornblende±biotite tonalites. A tectonic foliation cuts the biotite tonalites and becomes more pronounced near the contacts with supracrustal rocks. Aplite and pegmatite dykes related to the biotite tonalite are foliated and buckle folded about the foliation. The foliation within the tonalites is of similar orientation to a strong tectonic foliation (local  $S_2$ ) within the supracrustal rocks which is axial planar to isoclinal folds (locally intrafolial and rootless) of an earlier tectonic foliation (local  $S_1$ ).

A narrow zone of strongly foliated biotite (±hornblende?) granodiorite to tonalite occurs along the western margin of the Kenogamissi Batholith in McOwen Township (Fig. 3). An early, strong foliation (local  $S_1 = 140/75$ ) within the tonalite is overprinted and crenulated by small Z-shaped folds accompanied by a second foliation (local  $S_2 = 116/81$ ). The mafic metavolcanic rocks adjacent to the batholith are amphibolitized, variolitic and amygdaloidal pillowed basalts with minor intermediate lapilli tuffs and feldspar crystal tuffs. The pillows are highly strained with their long axes parallel to a strong foliation (local  $S_1 = 138/82$ ) which is parallel to the batholith margin. Within the metavolcanic rocks the local  $S_1$

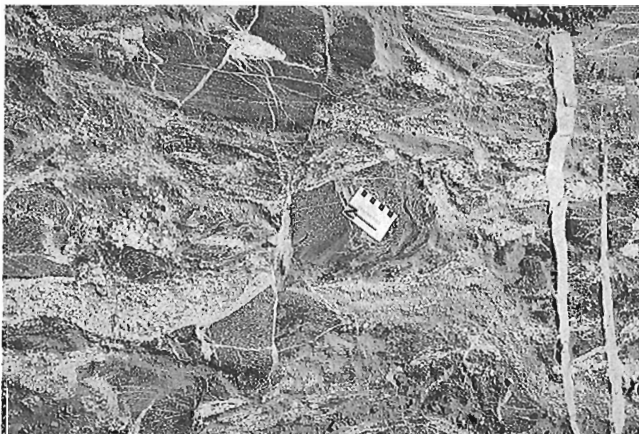


**Figure 3.** General distribution of granitoid rocks within the Swayze project area based on 1992 and 1993 mapping. This figure is to be used in conjunction with Figure 2.

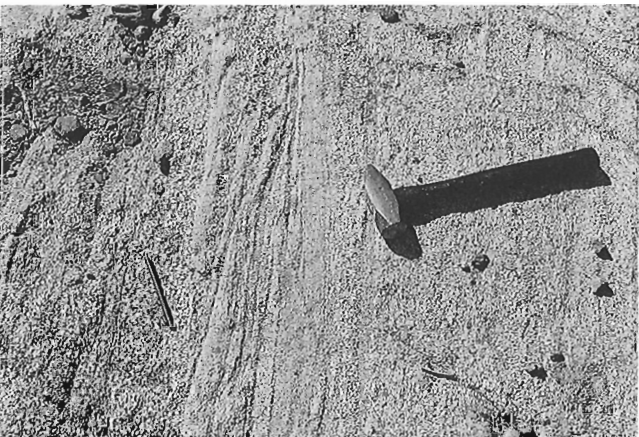
is overprinted and deformed into Z-shaped folds accompanied by a second foliation (local  $S_2 = 110/77$ ). The western margin of the Kenogamissi Batholith records a similar structural history as the adjacent supracrustal rocks.

### Potassium feldspar megacrystic hornblende granodiorite

The northern Kenogamissi Batholith consists of massive to variably foliated, potassium feldspar megacrystic (Fig. 6), hornblende granodiorite to granite (Fig. 3). This intrusive phase contains characteristic mafic to hornblende inclusions/autoliths (Fig. 7) which help to distinguish it from the later, nonfoliated, Algonian suite biotite granites.



**Figure 4.** Early, mafic hornblende diorite xenoliths within a matrix of hornblende tonalite. From the northern Kenogamissi Batholith, southeast Kenogaming Township. Scale card indicates north. (GSC 1993-279E)

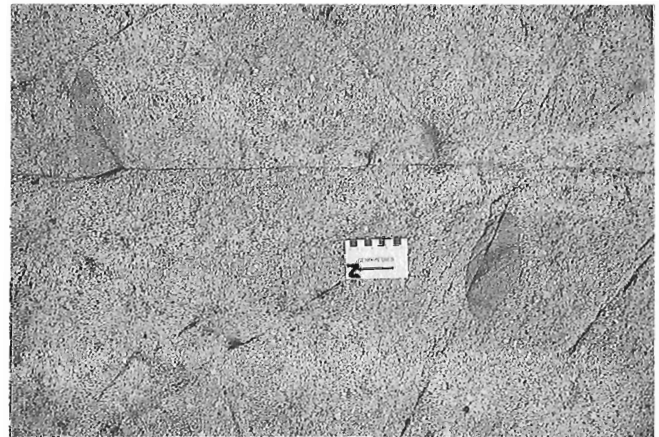


**Figure 5.** Hornblende-biotite tonalite exhibiting an igneous layering which is overprinted by a weak foliation (parallel to the pen magnet). From the northern Kenogamissi Batholith, southeast Kenogaming Township. Rock hammer handle indicates north.

A massive, biotite-hornblende, locally potassium feldspar megacrystic, granite to quartz monzonite characterized by abundant mafic inclusions, strong brittle fracturing, and hematite alteration occurs in northeast Hardiman Township (Fig. 3). This intrusive phase is similar to the potassium feldspar megacrystic, hornblende granodiorite to granite occupying the northern Kenogamissi Batholith (Fig. 3). The mafic inclusions vary from fine- to coarse-grained, are sub-rounded to rounded, and range in size from 2 cm to over 2 m. All of the inclusions contain potassium feldspar and acicular hornblende crystals. This phase is similar to the Kukatash Pluton, a hornblende quartz monzonite to granodiorite (Milne, 1972) which intrudes the supracrustal rocks (Fig. 3). Xenoliths of biotite-hornblende granite to quartz monzonite



**Figure 6.** Megacrystic potassium feldspar texture typical of the hornblende granodiorite occupying the northern margin of the Kenogamissi Batholith, Hillary Township. Scale card indicates north.



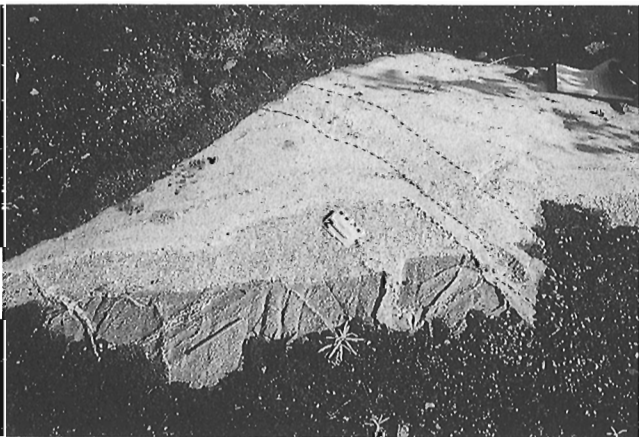
**Figure 7.** Hornblende inclusions/autoliths that are characteristic of the potassium feldspar megacrystic, hornblende granodiorite phases, Neville Township. Note the undeformed state of the inclusions and compare them to those in Figure 8. Scale card indicates north.

are found within dykes and bodies of massive, nonfoliated, locally potassium feldspar megacrystic, Algonian biotite granite.

The southern margin of the Kenogamissi Batholith (Fig. 3) consists of massive to foliated, potassium feldspar megacrystic, hornblende granodiorite to granite. Hornblende inclusions/autoliths are common within the hornblende granodiorite to granite and serve as strain markers (Fig. 7, 8). There is a marked increase in the deformation intensity (i.e., strain) within this phase as the contact with the supracrustal



**Figure 8.** Strongly foliated, potassium feldspar megacrystic, hornblende granodiorite from the southern margin of the Kenogamissi Batholith, Neville Township. Note the deformed hornblende inclusions/autoliths parallel to the strong foliation and compare them to those in Figure 7. Scale card indicates north. (GSC 1993-279A)



**Figure 9.** Early, foliated (parallel to the pen magnet) hornblende tonalite (dark grey) cut by a foliated biotite tonalite (light grey). Note the small biotite tonalite dyke cutting the hornblende tonalite. Both tonalite phases are cut by massive, nonfoliated Algonian biotite granite (white) and a late pegmatite dyke. From the Ramsey-Algoma granitoid complex, Abney Township. Scale card indicates north. (GSC 1993-279D)

rocks is approached. The strong foliation within the hornblende granodiorite to granite (Fig. 8) is parallel to the supracrustal contact and parallel to a strong foliation (local  $S_2$ ) that folds an earlier foliation (local  $S_1$ ) within the adjacent mafic metavolcanic rocks, and is axial planar to tight folds of bedding within the Timiskaming-type metasedimentary rocks. This phase is very similar to the hornblende granodiorite occurring along the northern margin of the batholith (Fig. 3).

#### Algonian biotite granite

A large body of late, massive, nonfoliated biotite granite and associated aplite and pegmatite dykes occurs north of Gogama in Northrup, Middleboro, Whalen, Carter, Somme, and Jack townships (Fig. 3). Xenoliths of hornblende tonalite, biotite tonalite are locally preserved, however they are too small to be depicted on Figure 3. The massive to foliated, potassium feldspar megacrystic, hornblende granodiorite to granite phase occurring along the southern margin of the batholith is intruded to the north by the late, biotite granite to produce a 3 km wide zone of transition. Numerous small dykes of Algonian biotite granite are found throughout the batholith (Fig. 9, 10) and although they are too small to be shown on Figure 3, they are volumetrically important.



**Figure 10.** A foliated biotite tonalite and associated pegmatite and aplite dykes (foreground) crosscut at a high angle by a large dyke of nonfoliated, Algonian biotite granite (background). From the Kenogamissi Batholith, Kenogaming Township. Rock hammer handle indicates north. (GSC 1993-279C)

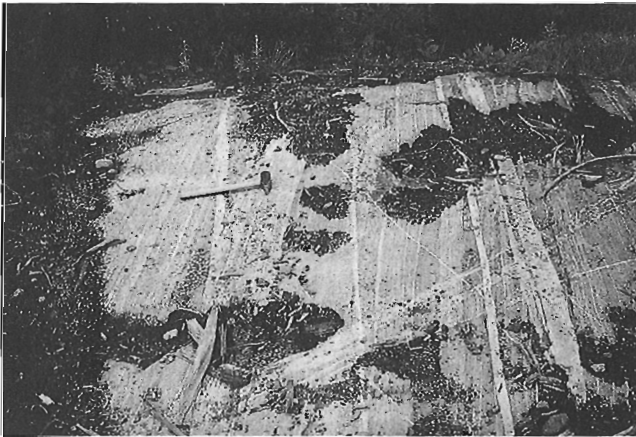


### Ramsey-Algoma granitoid complex

A complex chronology of crosscutting intrusive rock phases has been documented in the Ramsey-Algoma granitoid complex (Heather, 1993) which is similar to that documented within the Kenogamissi Batholith. Rocks mapped within the Ramsey-Algoma granitoid complex will be described by geographic areas using the township names shown on Figure 3.

#### Yeo, Alcona, Smuts, and Invergarry townships

The earliest phase recognized is a strongly foliated biotite±hornblende tonalite which is cut by biotite granodiorite and aplite dykes which are parallel to the strong foliation. The superposition of these dykes and the strong foliation parallel to a crude igneous layering within the tonalites produces a pseudo-gneissic appearance (Fig. 11). Larger bodies of foliated biotite granodiorite are more homogenous than the earlier tonalites and have few crosscutting dykes. The biotite granodiorites locally have a vague igneous layering defined by colour and compositional differences (i.e., mafic mineral content) and by grain size variations (i.e., fine to medium). Both the tonalite and granodiorite phases are cut by massive, nonfoliated biotite granites which are similar to the late, Algomian suite of intrusions documented elsewhere in the study area (Heather, 1993; this report). In southern Yeo and northern Invergarry townships the biotite granodiorite and late, biotite granite intrude the hornblende diorites and quartz diorites along the southern margin of the Chester granitoid complex (Fig. 2). There is locally an intrusion breccia developed along this contact with fragments of diorite and quartz diorite within a more granitic matrix.



**Figure 11.** Biotite tonalite exhibiting a pseudo-gneissic texture as a result of the superposition of abundant aplite dykes and a strong tectonic foliation subparallel to an igneous layering. Note the later aplite and pegmatite dykes that cut obliquely across the layering. From the Ramsey-Algoma granitoid complex. Rock hammer handle indicates north. (GSC 1993-279B)

#### Esther, Edith, Fingal, Arbutus, and Carew townships

The dominant phase in this portion of the Ramsey-Algoma granitoid complex (Fig. 3) is foliated biotite tonalite to granodiorite which contains xenoliths of foliated hornblende±biotite tonalite. The xenoliths are elongated parallel to a strong southeast-striking foliation. The biotite in the hornblende±biotite tonalite appears to be secondary after the hornblende, which is suggested by its abundance in the more strained domains (i.e., strongly foliated) whereas the hornblende is dominant in less strained domains (i.e., weakly foliated). Both phases of tonalite have associated aplite and pegmatite dykes that are folded about the tectonic foliation. The foliated tonalites are cut by massive, nonfoliated, equigranular biotite granite. The hornblende±biotite tonalites adjacent to the supracrustal rocks contain xenoliths of foliated, fine- to coarse-grained amphibolite and foliated hornblende tonalite to diorite. The hornblende tonalite to diorite xenoliths contain elongated xenoliths of mafic metavolcanic material. The mafic metavolcanic xenoliths contain feldspar porphyroblasts and numerous foliated and folded felsic intrusive dykes parallel to the foliation. Near the greenstone belt contact the foliated hornblende diorite is cut by dykes of foliated hornblende±biotite tonalite which is in turn cut by dykes of aplitic biotite tonalite to granodiorite. The hornblende diorite phase generally occurs near the greenstone belt contact and may represent a hybrid phase of the hornblende±biotite tonalite due to contamination by the supracrustal rocks. The deformation intensity (i.e., strain) recorded within the tonalites increases northward toward the greenstone belt contact. Within approximately 3 km of the greenstone belt contact the tonalites exhibit an early foliation (local  $S_1$ ) which is locally folded by a strong, roughly eastward-striking foliation (local  $S_2$ ). These tonalites also have a strong, near vertical mineral/stretching lineation which is parallel to the lineation developed within the adjacent supracrustal rocks.

#### Carew, Joffre, and Margaret townships

The Ramsey-Biscotasing belt of highly strained and metamorphosed supracrustal rocks and complex intrusive rocks extends southeastward, from the main Swayze greenstone belt, through Cavell, Carew, Joffre, and Margaret townships (Fig. 2). Previous mapping by Rogers (1962) delineated a mixed package of metavolcanic hornblende±quartz±feldspar±epidote gneisses and metasedimentary biotite±quartz±feldspar gneisses which are intruded by two distinctive suites of granitoids, the grey and pink granitic rocks. The recent Geology of Ontario map for the area (Ontario Geological Survey, 1991) divides the appendage of supracrustal rocks into a northern sequence of mafic to intermediate metavolcanic rocks and a southern sequence of migmatized supracrustal rocks.

Preliminary results presented here are from reconnaissance mapping during 1993 along the Ramsey-Biscotasing road. Highly strained, amphibolitized mafic pillowed metavolcanic rocks occur in central Carew Township, 300 m southeast of the Ramsey-Biscotasing road junction. The pillows exhibit approximately a 10:1 to 15:1 east-southeast

elongation in plan view, however the lack of vertical relief precluded the determination of the vertical elongation. The pillow rocks are cut by numerous feldspar-hornblende veinlets which have distinctive epidote alteration haloes associated with them. The altered pillowed rocks grade into strongly banded, hornblende-feldspar-epidote amphibolites in which the pillow selvages and epidote-rich pillow cores are strongly deformed and the alteration veinlets are pygmatically folded and transposed. Nonetheless, within the banded amphibolites the pillow terminations are still locally discernable in rocks exhibiting greater than 100:1 elongation in plan view, as are highly elongated and boudinaged epidote-rich cores.

The mafic metavolcanic amphibolites are intruded by a hornblende ( $\pm$ biotite) tonalite to diorite complex which contains abundant inclusions/xenoliths of melanocratic hornblende diorite and lesser amphibolitized mafic metavolcanic rock. The melanocratic diorite inclusions are texturally and mineralogically similar to the leucocratic tonalite to diorite host. The tonalite-diorite complex rocks are shown as mafic migmatite rocks on the Geology of Ontario map (Ontario Geological Survey, 1991). There is a moderate to strong foliation (local  $S_1$ ), defined by the alignment of hornblende, within most of the tonalite-diorite rocks which varies from 190/70 to 165/74. The inclusions are typically aligned parallel to this foliation. A second, weaker foliation (local  $S_2$ ), defined by biotite and quartz ribbons and ranges from 336/80 to 125/76 and locally overprints the earlier foliation. The angular difference in strike between the two foliations remains a consistent 30° to 40° despite variations in foliation orientation. Both the leucocratic and melanocratic phases of the tonalite-diorite complex are cut by nonfoliated granitic aplite and pegmatite dykes.

Locally, there are fine grained, grey-coloured, finely laminated paragneisses made up of quartz, feldspar, biotite, and hornblende. These metasedimentary rocks are also cut by the hornblende tonalite-diorite complex described above. Both the metasedimentary rocks and the tonalite-diorite complex are cut by foliated biotite tonalite dykes.

### **Cavell, Hall, and Abney townships**

Reconnaissance mapping has indicated that massive, nonfoliated, equigranular biotite granites of the Algonian suite predominate south of Ramsey (Fig. 2). The early, foliated hornblende tonalites are crosscut by foliated biotite tonalites and both are cut by the late, Algonian biotite granites (Fig. 9). Xenoliths of mafic amphibolite, hornblende tonalite, and biotite tonalite are locally present. The early tonalite phases are variably foliated and locally contain xenoliths of mafic amphibolite. The late, biotite granites locally exhibit a crude layering defined by grain size differences and biotite schlieren. These textures are similar to those documented within the Algonian biotite granites within the Kenogamissi Batholith. The percentage of hornblende and biotite tonalite increases, at the expense of the biotite granites, as the southern boundary of the Ramsey-Biscotasing supracrustal belt is approached.

### **Granitoids internal to the Swayze greenstone belt**

#### **Fawn Pluton**

The Fawn Pluton occupies Fawn and western Esther townships (Fig. 2) and consists of foliated, equigranular, medium grained, hornblende $\pm$ biotite granodiorite to granite with mafic and hornblendic inclusions/autoliths.

#### **Isaiah Creek Stock**

The Isaiah Creek Stock is located in Cunningham Township (Fig. 2) and consists of massive, nonfoliated, locally potassium feldspar megacrystic biotite granite. The stock contains up to 35% quartz phenocrysts which are locally large and exhibit square to rectangular cross-sections which may be inverted Beta quartz, consistent with a subvolcanic origin for this intrusion.

## **GEOCHRONOLOGY**

An integral component of the Swayze bedrock mapping project is a comprehensive program of geochronology within both the greenstone belt supracrustal rocks and the granitoid complexes surrounding the greenstone belt. The objectives of this work are to provide absolute ages for the various volcanic packages, principally the felsic to intermediate ones, as well as the various phases of granitoid rocks both within the greenstone belt and those in the extensive granitoid complexes outside the greenstone belt. Lithological and structural mapping augmented with lithogeochemical and geochronological data will be critical in constructing a more accurate tectonic history of the area.

### **1992 results**

Preliminary U-Pb zircon geochronological results are presented for seven samples collected during the 1992 field season (Fig. 3). Uranium concentrations in the zircons are low, and some problems were encountered in resolving inherited components. Five samples representing four regionally extensive granitoid phases within the Kenogamissi Batholith (Fig. 3) have yielded preliminary U-Pb zircon age results. One of the older hornblende tonalites (Fig. 3) yielded an age of 2713  $\pm$  2/-3 Ma. A foliated biotite tonalite to granodiorite was dated at 2697  $\pm$  3 Ma. This age is identical to the 2697  $\pm$  2 Ma (Cattell et al., 1984) felsic volcanoclastic rock from the Swayze-Dore rock package, in southeastern Coppel Township (Fig. 2). Both the hornblende- and the biotite-tonalite suites are crosscut, along the southern margin of the Kenogamissi Batholith (Fig. 3), by a massive to foliated, potassium feldspar megacrystic, hornblende granodiorite to granite dated at 2682  $\pm$  3 Ma. A similar phase occurring along the northern margin of the Kenogamissi Batholith (Fig. 3) has a less constrained age but is younger than 2695 Ma. All of the above intrusive phases are crosscut by the extensive, ca. 2665 Ma, Algonian suite of massive, nonfoliated, biotite granites to granodiorites (Fig. 3).



Within the southern Swayze greenstone belt the Chester granitoid complex, a composite trondhjemite (leucotonalite)-diorite intrusion (Fig. 2 and 3), can be subdivided into a northern leucocratic, trondhjemite-dominated zone and a southern melanocratic, diorite-dominated zone (Heather, 1993). Complex and enigmatic crosscutting relationships and textures suggestive of magma mixing have been observed between the trondhjemite and diorite phases. A sample of leucocratic, quartz-rich, biotite trondhjemite yielded an age of  $2740 \pm 2$  Ma. A massive, rhyolitic feldspar-quartz porphyry, spatially associated with volcanic breccias and lapilli tuffs, within the Heenan-Dore felsic rock package (Fig. 2), produced an age of circa 2700 Ma. However, there is also evidence of an inherited, 2730 to 2740 Ma, zircon population. The preliminary results from this sample, as well as the Chester trondhjemite suggest the presence of a ca. 2740 Ma metavolcanic rocks which have not been identified to date.

### 1993 sampling

A total of eight samples were collected for U-Pb zircon geochronology during the 1993 field season. The emphasis of the 1993 sampling program shifted from the external granitoids to the supracrustal rock packages within the Swayze greenstone belt. A sample of foliated, feldspar-phyric felsic metavolcanic rock immediately south of the Nat River iron-formation (Milne, 1972; Fig. 2) was collected, in Kenogaming Township, in order to date the Hanrahan Volcanic Complex (Milne, 1972; Hanrahan Assemblage of Jackson and Fyon, 1991). Due to the continued economic interest in base metal mineralization (e.g., Shunshby Zn-Pb-Cu occurrence; Brereton and Sobie, 1991) in the Cunningham Township area, four samples were collected to provide data on the age of felsic volcanism and possible associated plutonism (i.e., Isaiah Creek Stock), as well as provide some constraints on the timing of folding in the area.

A sample of "Ridout Series" Timiskaming-type (summarized in Heather (1993)), coarse grained sandstone, from northwest Osway Township (Fig. 3) was collected for detrital zircon dating to establish the maximum age of sedimentation. Nearby, a feldspar-quartz porphyry intrusion that cuts Timiskaming-type polymictic conglomerates was sampled to provide a minimum age for sedimentation and a maximum age for the deformation recorded in the metasedimentary rocks. The final sample taken during the 1993 sampling program is a strongly foliated and vertically lineated biotite tonalite, part of a larger tonalite body within the Ramsey-Algoma granitoid complex immediately south of the Swayze greenstone belt (Fig. 3).

## DISCUSSION

Systematic lithological and structural mapping, in concert with litho-geochemical and geochronological studies, within both the granitoid and supracrustal rocks is essential to the better understanding the regional tectonics of the Swayze

greenstone belt, and hence, the mineral deposits contained within. This report has highlighted important field and age relationships that are critical to achieving this goal (Fig. 3).

The  $2740 \pm 2$  Ma biotite trondhjemite (leucotonalite) of the Chester granitoid complex (Fig. 2), is one of the oldest intrusions identified in the southern Abitibi Subprovince. The 2730-2740 Ma inherited zircon population within a ca. 2700 Ma felsic metavolcanic rock of the Heenan-Dore package, along with the Chester trondhjemite result, may indicate the presence of an older volcano-plutonic package of rocks which may have formed local basement to some of the younger metavolcanic packages in the southern Swayze greenstone belt.

The Kenogamissi Batholith has been shown to be a composite intrusion made up of four regionally extensive phases of widely varying composition, strain state, and age. These phases share a spatial association but not necessarily a genetic one. Therefore the term batholith as applied to the Kenogamissi Batholith is strictly a description of its geometry. The  $2713 \pm 2/3$  Ma hornblende-biotite tonalite is similar in age to felsic metavolcanic rocks dated elsewhere in the southern Superior (Ontario Geological Survey, 1992; Jackson and Fyon, 1991), although metavolcanic rocks of this age have not yet been identified within the Swayze greenstone belt. The  $2697 \pm 3$  Ma biotite tonalite is coeval with the  $2697 \pm 2$  Ma (Cattell et al., 1984) felsic metavolcanic rocks of the Swayze-Dore package (Fig. 2). All of the above intrusive phases are thought to be synvolcanic.

The  $2682 \pm 3$  Ma potassium feldspar megacrystic, hornblende granodiorite is coeval with the  $2684 \pm 3$  Ma (Frarey and Krogh, 1986) potassium feldspar megacrystic, biotite quartz monzonite Hoodoo Lake Pluton and the  $2680 \pm 3$  Ma (Percival and Krogh, 1983) massive to weakly foliated dioritic phase of the Ivanhoe Lake pluton (Fig. 2). All of these intrusions are synchronous with Timiskaming-type sedimentation in the southern Abitibi greenstone belt (Corfu et al., 1991; Ontario Geological Survey, 1992). Both the 2682 Ma hornblende granodiorite and the Timiskaming-type, "Ridout Series" metasedimentary rocks in the Swayze greenstone belt have a strong tectonic foliation and are clearly not post tectonic. Percival and Krogh (1983) interpreted the dioritic phase of the 2680 Ma Ivanhoe Lake pluton to be post tectonic, however this now seems not to be the case. Contact relationships with the adjacent supracrustal rocks and structural information suggest that at least some of the strain experienced by many of the granitoid rocks post dates their emplacement. Further work is planned to better constrain the timing of fabric development within both the granitoid and supracrustal rocks. The ca. 2665 Ma, Algoman biotite granites are part of a regionally extensive suite of nonfoliated rocks that appears to be posttectonic.

Within the Kenogamissi Batholith there is a temporal progression, based on crosscutting relationships and supported by geochronology, from early, more mafic, hornblende-rich diorites through hornblende and biotite tonalites

and granodiorites to more felsic, hornblende- and biotite-bearing granodiorites and granites (i.e., Algoman). Granitoid rocks within the Nat River and Ramsey-Algoma granitoid complexes (Heather, 1993; this report) are of similar type, composition, strain state, and relative timing to one another as the phases documented within the Kenogamissi Batholith.

## ACKNOWLEDGMENTS

The author would like to thank Dave Bouwman for providing conscientious assistance during the field season. Once again the staff of the Timmins Resident Geologist office provided many essential services and logistical support. The support of S. Garner and D. Dedo of E.B. Eddy Forest Products Ramsey Division are gratefully acknowledged. Geological discussions with M. Houle, R. Gadzala, and B. Jeffery (Falconbridge Exploration), and R. Dahn, J. Wakeford, and T. Barrie (Noranda Exploration) have helped elucidate the geological concerns faced by explorationists in the Swayze belt and point out future areas for geological mapping. Discussions with J. Ayer and M. Bernier (Ontario Geological Survey) and visits to the field by Cees van Staal (Geological Survey of Canada) and Lorianne Wilkinson (University of Toronto) have been extremely beneficial to the author. John A. Percival and Cees van Staal provided constructive reviews of this report. Lorianne Wilkinson and Olga Ijewliw drafted Figure 3.

## REFERENCES

### Brereton, W.E. and Sobie, P.A.

1991: Report on 1991 exploration program on the Shunby base metal prospect, Swayze greenstone belt, Ontario, for Kirkton Resources Corp.; unpublished assessment file T3358, Timmins Resident Geologist's Office, Timmins, Ontario, 90 p.

### Cattell, A.C., Krogh, T.E., and Arndt, N.T.

1984: Conflicting Sm-Nd whole-rock and U-Pb zircon ages for the Archean lavas from Newton Township, Abitibi Belt, Ontario; *Earth and Planetary Science Letters*, v. 70, p. 280-290.

### Corfu, F., Jackson, S.L., and Sutcliffe, R.H.

1991: U-Pb ages and tectonic significance of late Archean alkalic magmatism and nonmarine sedimentation: Timiskaming Group, southern Abitibi belt, Ontario; *Canadian Journal of Earth Sciences*, v. 28, p. 489-503.

### Frarey, M.J. and Krogh, T.E.

1986: U-Pb zircon ages of late internal plutons of the Abitibi and eastern Wawa subprovinces, Ontario and Quebec; in *Current Research, Part A*; Geological Survey of Canada, Paper 86-1A, p. 43-48.

### Heather, K.B.

1993: Regional geology, structure, and mineral deposits of the Archean Swayze greenstone belt, southern Superior Province, Ontario; in *Current Research, Part C*; Geological Survey of Canada, Paper 93-1C, p. 295-305.

### Jackson, S.L. and Fyon, A.J.

1991: The western Abitibi subprovince in Ontario; in *Geology of Ontario, Ontario Geological Survey, Special Volume 4*, pt. 1, p. 405-482.

### Milne, V.G.

1972: Geology of the Kukatush-Sewell Lake area, District of Sudbury; Ontario Division of Mines, Geological Report 97, 116 p., accompanying Map 2230 and Map 2231, scale 1:31 680.

### Ontario Geological Survey

1991: Bedrock geology of Ontario, east-central sheet; Ontario Geological Survey, Map 2543, scale 1:1 000 000.

1992: Chart B-Archean tectonic assemblages, plutonic suites and events in Ontario; Ontario Geological Survey, Map 2580.

### Percival, J.A. and Krogh, T.E.

1983: U-Pb zircon geochronology of the Kapuskasing structural zone and vicinity in the Chapleau-Foley area, Ontario; *Canadian Journal of Earth Sciences*, v. 20, p. 830-843.

### Rogers, D.P.

1962: Geology of the Biscotasing area, District of Sudbury; Ontario Department of Mines, Geological Report No. 7, 35 p., accompanying Map 2013, scale 1:63 360.

### Streckheisen, A.

1976: To each plutonic rock its proper name; *Earth-Science Reviews*, v. 12, p. 1-33.

Geological Survey of Canada Project 850014

# Geology of the Levack gneiss complex, the northern footwall of the Sudbury structure, Ontario

K.D. Card

Continental Geoscience Division

*Card, K.D., 1994: Geology of the Levack gneiss complex, the northern footwall of the Sudbury structure, Ontario; in Current Research 1994-C; Geological Survey of Canada, p. 269-278.*

---

**Abstract:** Rocks of the Archean Levack gneiss complex that underlie the northern part of the Sudbury Structure comprise supracrustal and intrusive units that were deformed and metamorphosed under granulite facies conditions in the lower crust during the Archean. They were intruded by late Archean granite of the Cartier batholith and uplifted, either during the late Archean or early Proterozoic, by tectonic or impact processes. They were strongly affected by the shock and thermal metamorphism associated with the Sudbury impact event and probably contributed significantly to the formation of the Sudbury igneous complex and its ores. Structures imaged by seismic reflection profiles in the area are attributed to thrusts or deformation zones that are part of a regional system of south-dipping structures that cut and displace the Sudbury structure.

**Résumé :** Les roches du complexe gneissique archéen de Levack, que l'on rencontre dans la partie nord de la structure de Sudbury, comprennent des unités supracrustales et des unités intrusives, qui ont été déformées et métamorphosées à l'Archéen dans des conditions du faciès des granulites au niveau de la croûte inférieure. Elles ont été traversées par des granites de l'Archéen tardif appartenant au batholite de Cartier, et ont été soulevées à l'Archéen tardif ou au Protérozoïque précoce par des mécanismes tectoniques ou d'impact météoritique. Elles ont été profondément modifiées par le dynamométamorphisme et le thermométamorphisme associés à l'épisode d'impact météoritique de Sudbury et ont probablement contribué dans une mesure significative à la formation du complexe igné de Sudbury et de ses minerais. Les structures illustrées par les profils de sismique-réflexion de la région sont attribuées à des zones de chevauchement ou de déformation faisant partie d'un système régional de structures de pendage sud qui recoupent et déplacent la structure de Sudbury.

## INTRODUCTION

The Levack gneiss complex (LGC), consisting of high-grade gneisses and related intrusive rocks, forms a collar about the northern part of the 1850 Ma (Krogh et al., 1984) Sudbury structure (SS). In the south, the complex is intruded by the Sudbury igneous complex (SIC) and probably underlies the northern half of the Sudbury structure (Milkereit et al., 1992; McGrath and Broome, in press). To the north, the Levack gneiss complex is intruded by massive granite of the Cartier batholith. The Levack gneiss complex rocks are also cut by early Proterozoic mafic dykes, many of which probably belong to the 2450 Ma (Heaman, 1989) Matachewan swarm. Levack gneiss complex tonalitic gneiss has a U-Pb zircon age of 2711 Ma and a leucosome layer, presumably dating the age of high-grade metamorphism, is 2647 Ma old (Krogh et al., 1984).

The Levack gneiss complex includes migmatitic tonalite orthogneiss, biotite paragneiss, diatexitic granitoid rocks, mafic and intermediate gneiss, gabbroic, dioritic, and pyroxenitic intrusions and inclusions, and foliated granodiorite bodies. These rocks were deformed and metamorphosed under upper amphibolite to granulite facies conditions (James et al., 1991) during the Archean and were subsequently affected by amphibolite and greenschist facies events during the late Archean and early Proterozoic. They were also strongly affected by the Sudbury event, notably by shatter cones and Sudbury breccia dykes that occur throughout the complex, and by pyroxene and hornblende hornfels contact metamorphism near the Sudbury igneous complex contact (Dressler, 1984a).

Recent isotopic and geochemical studies by Faggart et al. (1985), Naldrett et al. (1986), Walker et al. (1991), and others have shown that the rocks and ores of the Sudbury igneous complex were contaminated by, and probably largely derived from, the older Archean and Proterozoic crustal rocks that surround and underlie the Sudbury structure. The rocks of the Levack gneiss complex could be a major source of this crustal contamination. Certainly many of the north range ore bodies are hosted by sublayer units consisting mainly of brecciated, remobilized Levack gneisses and there are several sulphide occurrences within the Levack gneiss complex well away from the Sudbury igneous complex contact.

The Levack gneiss complex represents rocks deformed and metamorphosed in the middle to lower crust that were uplifted either by late Archean or early Proterozoic tectonic processes prior to the Sudbury event (Card et al., 1984) or as a result of the meteorite impact event that formed the Sudbury structure (Grieve et al., 1991). Percival et al. (1992) have suggested that the complex represents the basal part of a crustal cross-section exposed as a result of impact. A better understanding of the Levack gneiss complex, the genesis of its rocks and structures, and the timing of its uplift relative to the Sudbury event, are essential to understanding the origin of the Sudbury structure and its rich ore deposits.

## PREVIOUS INVESTIGATIONS AND SCOPE OF THE PRESENT WORK

Rocks of the Levack gneiss complex were first mapped in the Levack area north of Sudbury as "Archean Levack granite and granite-gneiss" by W.H. Collins and his assistants (Geological Survey of Canada, 1947). Langford (1960) mapped the complex in Levack Township where he subdivided the gneisses into tonalitic, mafic, and biotitic varieties and described their contact relationships with the intrusive Cartier granite. Card and Meyn (1969) mapped part of the complex in Harty, Foy and Bowell townships and recognized the high-grade (granulite facies) metamorphic mineral assemblages in the gneisses. Other parts of the complex have been mapped by Dressler (1982) in the Lake Wanapitei area, by Muir (1981, 1983) in the Capreol-Morgan township area in the northeast, and by Lafleur and Dressler (1985) in the Levack-Trill township area in the southwest. Dressler (1984b) synthesized much of the foregoing work in a 1:50 000 scale geological compilation map of the Sudbury structure and environs.

Recent seismic reflection studies of the Sudbury structure by Milkereit et al. (1992), part of the Abitibi-Grenville Lithoprobe project, have revealed the presence of numerous, generally south-dipping reflectors. Some are attributed to lithological layers and others to thrust faults or shear zones that transect and telescope the structure. Several prominent reflectors project into the Levack gneiss complex and Cartier batholith. Other investigations include gravity modelling of the Sudbury structure utilizing new structural models based on the seismic results (McGrath and Broome, in press), thermobarometric studies of the Levack gneisses (James et al., 1991), and a structural transect across parts of the Levack gneiss complex and Cartier batholith (Feuten et al., 1992).

During the 1993 field season, geological observations were made along some twenty 1.5 to 7 km transects across the complex in the area between Lake Wanapitei in the east and Trill Township in the west. Over 400 samples were collected for petrographic, geochemical, geochronological, and physical properties studies and "in situ" magnetic susceptibility measurements were made at a number of sites. The data gathered will be integrated with existing geological and geophysical information in order to outline the major rock assemblages and structural elements of the Levack gneiss complex and to better define the tectonic evolution of these rocks and their relationships to the Archean evolution of the Superior Province and the early Proterozoic Sudbury event.

## GENERAL GEOLOGY

Gneisses and related intrusive rocks of the Levack gneiss complex are exposed in an arcuate belt 0.5 to 5 km wide about the northern and eastern limbs of the Sudbury structure (Fig. 1). At surface, they are bounded on the south by the

Sudbury igneous complex and on the north by the Cartier batholith. Recent geophysical studies (Milkereit et al., 1992; McGrath and Broome, in press) indicate that the gneisses probably extend beneath both the Sudbury igneous complex and the Cartier batholith. On the basis of deep drilling and mining, and geophysical modelling, the basal Sudbury igneous complex contact dips moderately (average 45°) southward. Modelling of the gravity data suggests that the Cartier batholith-Levack gneiss complex contact dips northward (McGrath and Broome, in press). Near the Sudbury igneous complex contact, the gneisses have a bleached appearance and a spotted hornfelsic texture, the results of contact metamorphism by the Sudbury igneous complex. The gneisses are also variably brecciated and remobilized and pods and disseminations of sulphide minerals are present. At many localities, the moderately south-dipping Sudbury igneous complex contact is at a high angle to the commonly subvertical gneissosity in the Levack gneiss complex (Fig. 2).

The northern contact with the Cartier batholith is also clearly intrusive, though contact thermal effects, if present, are not obvious. Massive intrusive rocks of the Cartier batholith transect gneissosity in the Levack gneiss complex at the contact. Within the complex, massive granite dykes similar to the batholith rocks cut across the foliation in the gneiss. The Levack gneiss complex-Cartier batholith contacts are hybrid zones several tens of metres wide consisting of Cartier granite littered with gneissic inclusions and Levack gneiss complex gneisses "soaked" with potassic granitic material.

There are also kilometre-scale rafts of paragneiss, orthogneiss, and foliated granodiorite isolated within the Cartier batholith.

The Levack gneiss complex consists of several lithologic assemblages including tonalitic orthogneiss with abundant layers and inclusions of mafic gneiss and diorite, gabbro, and pyroxenite. These rocks form a prominent, relatively continuous unit adjacent to the Sudbury igneous complex. Biotite paragneiss and related migmatitic and diatexitic rocks form less continuous, though sizeable, units farther away from the Sudbury igneous complex. Several large gabbroic bodies occur within tonalitic orthogneiss near the Sudbury igneous complex. The bodies, though mainly massive, do have foliated margins, are cut by granite dykes, and are similar to inclusions within the gneisses; they are considered to be part of the Levack gneiss complex. So too are numerous small and several large bodies of foliated to gneissic granodiorite that occur throughout the complex.

### *Tonalite gneiss and related diatexite*

Well-layered gneiss and more massive inhomogeneous and homogeneous diatexite of tonalitic, and less commonly quartz dioritic and granitic composition, form approximately 40% of the exposed Levack gneiss complex. The tonalite gneiss, consisting of alternating leucocratic and more mafic layers ranging from a few centimetres to several metres in

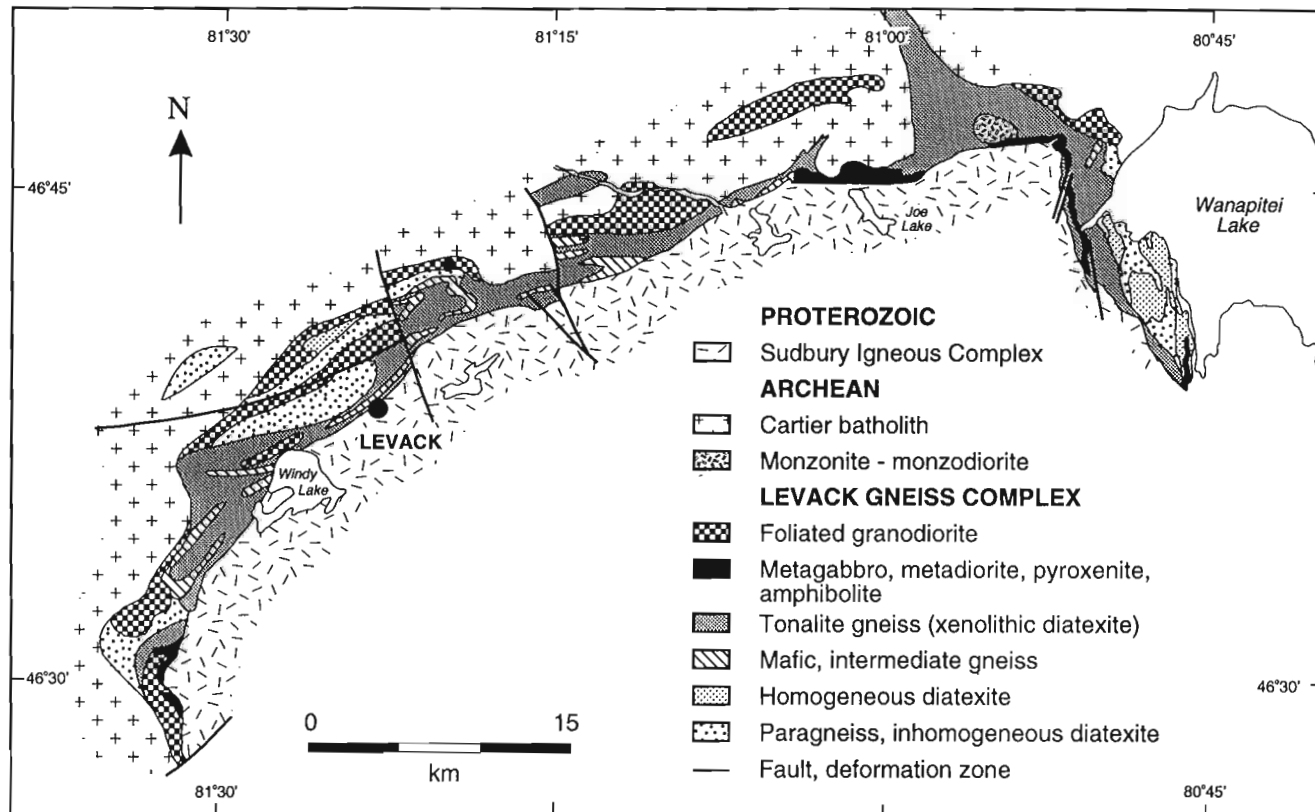


Figure 1. Major rock units of the Levack gneiss complex.

thickness (Fig. 3a) is a medium- to coarse-grained granoblastic to foliated rock consisting of plagioclase, quartz, pyroxenes, amphiboles, biotite, and rare garnet. The pyroxenes, both orthopyroxene and clinopyroxene, are commonly altered to amphibole. The gneisses are generally migmatitic with tonalitic mobilizate forming several generations of concordant and discordant bodies.

The associated diatexites, both homogeneous and inhomogeneous, are generally poorly layered and have granoblastic, variably fine- to coarse-grained textures (Fig. 3b). They are mineralogically similar to the gneisses. Leucotonalite and coarse anorthositic patches poor in quartz and mafic minerals are common.

Inclusions in the form of layers, diffuse schlieren, and sharp-bordered inclusions are abundant in the tonalite gneiss and diatexite commonly forming 10% and locally more than 30% of these units (Fig. 3c). Massive and foliated dioritic, amphibolitic, gabbroic, and pyroxenitic inclusions may represent remnants of older supracrustal rocks in part, but are probably mainly disrupted mafic intrusions.

### Intermediate and mafic gneiss

Dioritic, gabbroic, and amphibolitic gneisses form units up to several hundred metres wide, as well as numerous thinner enclaves within the tonalitic gneiss (Fig. 3d). Such rocks form approximately 15% of the complex. They are brown to black weathering, medium grained, massive to weakly foliated, layered rocks composed of plagioclase, hornblende,

pyroxenes, biotite, and quartz. Both orthopyroxene and clinopyroxene are present, though generally altered, and garnet is rare. The intermediate and mafic gneisses are migmatitic with several generations of tonalitic leucosome.

### Paragneiss and related diatexite

Dark grey, well-layered, migmatitic biotite gneiss, interpreted as paragneiss or metatexite of metasedimentary origin, forms several units in the northern part of the complex (Fig. 3e). The paragneiss is associated with diatexite, granitic rocks with blocky white feldspars in a biotite-rich matrix which are commonly littered with remnants of biotite gneiss in various stages of assimilation.

The paragneiss is composed mainly of biotite, plagioclase and quartz, with local garnet- and pyroxene-bearing assemblages. Several generations of migmatitic mobilizate of tonalitic to granitic composition are present.

Remnants of banded iron-formation occur at several localities within the Levack gneiss complex. Northeast of Levack, highly deformed remnants of finely laminated quartz-magnetite iron-formation occur within tonalitic and mafic gneisses (Sweeny and Farrow, 1990). A thin unit of similar quartz-magnetite iron-formation is present near the Onaping River northwest of Levack (Fig. 3f). West of Windy Lake there are occurrences of fine grained, siliceous gneiss with abundant pyrite that probably represent sulphide-facies iron-formation.

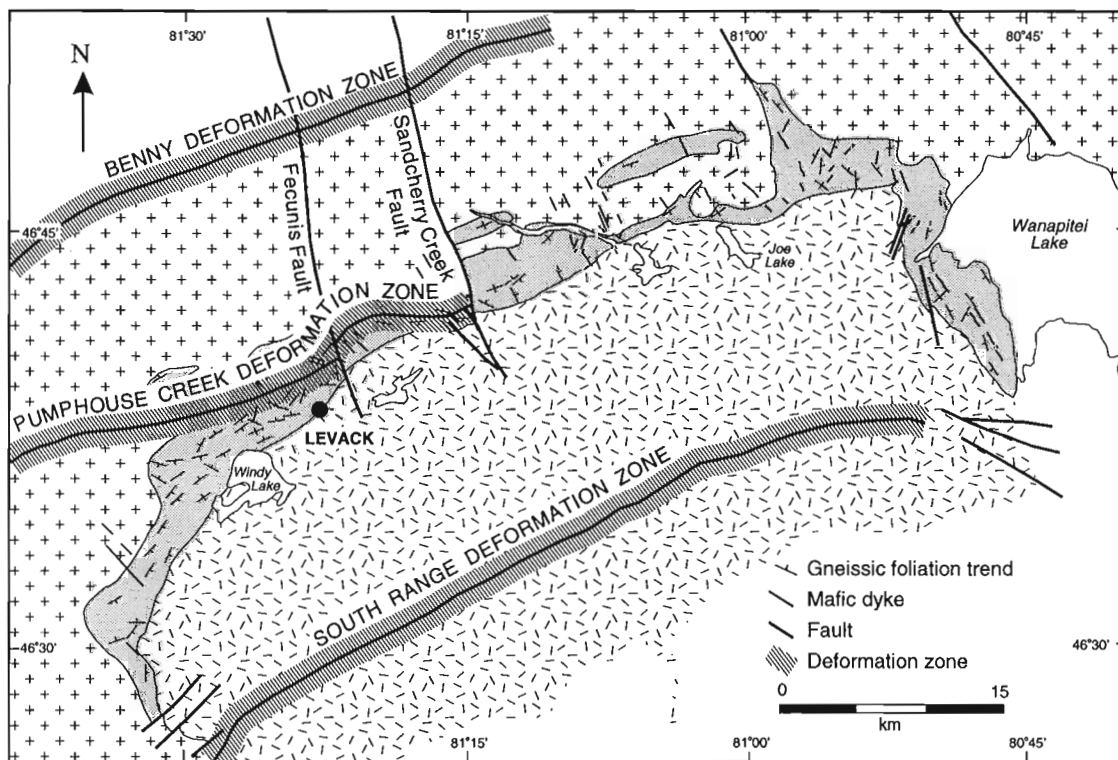


Figure 2. Structural elements and early Proterozoic mafic dykes in the Levack gneiss complex and Cartier batholith.



Diatexite associated with paragneiss is mainly inhomogeneous at outcrop scale, containing 25% to 30% paleosome as inclusions and schlieren. The diatexite is typically highly variable in composition from tonalitic to granitic, and in grain-size from aplitic to pegmatitic. Coarse, blocky, white feldspars floating in a dark, biotite-rich matrix are characteristic (Fig. 3g).

### **Gabbro**

In addition to metre-scale gabbroic inclusions present in tonalitic gneisses and diatexites, there are several larger gabbroic bodies within the complex. These include several elongate bodies near Lake Wanapitei in the east, a 1 x 7 km body north of Joe Lake, a small, 0.6 km diameter, body northeast of Levack, here named the Blue Diamond gabbro, and several bodies in the southwest (Fig. 1). All consist of variably metamorphosed, medium- to coarse-grained gabbro and leucogabbro and have foliated margins and generally massive interiors. The Joe Lake body has zones of igneous breccia consisting of fine grained, foliated gabbro enclosed in coarse grained, massive leucogabbro (Fig. 3h). The Joe Lake body is cut by granite. The Blue Diamond body is also cut by granite dykes and there are boudins of gabbro in the gneisses surrounding this body. It is possible that all of the gabbro bodies, like many of the smaller inclusions, represent boudins in the mobile gneisses. All are probably of Archean age although it is possible that some are Proterozoic, equivalent to either 2480-2490 Ma gabbro-anorthosite intrusions that occur in the region (Krogh et al., 1984) or to the Nipissing Diabase.

### **Foliated granodiorite**

Foliated granodiorite, in the form of several large bodies and numerous smaller intrusions, forms approximately 10% of the complex. The granodiorite is typically altered, commonly by epidote replacing feldspars, and is generally foliated to weakly gneissic. Amphibolitic and gneiss inclusions are common. The granodiorite intrusions were probably emplaced at a late stage in the tectonic-metamorphic evolution of the Levack gneiss complex prior to emplacement of the Cartier batholith.

### **Cartier batholith**

The Cartier batholith is a member of a suite of late Archean granitic intrusions, the Algoma plutons, that form several large batholiths in the southern Superior Province (Card, 1979). The Cartier batholith consists mainly of massive, medium- to coarse-grained, subporphyritic granite. The rock is fresh except for minor shear zones and alteration along late faults, has few inclusions except near contacts, and typically contains large titanite and allanite grains. It is unconformably overlain by Huronian rocks and is cut by mafic dykes and Sudbury breccia bodies. Judging from its textural and structural characteristics, and the foregoing field relationships, the Cartier batholith was probably emplaced at relatively high crustal levels (epizonal-mesozonal) in the late Archean.

### **Mafic Dykes**

Numerous mafic dykes ranging from approximately 1 to 10 m wide cut the rocks of the Levack gneiss complex and the Cartier batholith but not the Sudbury structure. Regionally, the dykes are weakly metamorphosed, possibly the result of late deuteritic alteration or of low-grade regional metamorphism that also affected the Huronian rocks north of the present map-area (Card and Innes, 1981). They are cut by Sudbury breccia bodies. Two dominant dyke sets are evident, one trending northwest, the other northeast (Fig. 2). Dykes of both sets transect the gneissic foliations of the Levack gneiss complex and display chilled contacts (Fig. 3i). Many dykes of the northwest set have coarse white plagioclase phenocrysts or glomerocrysts typical of the 2450 Ma Matachewan swarm.

### **Sudbury breccia**

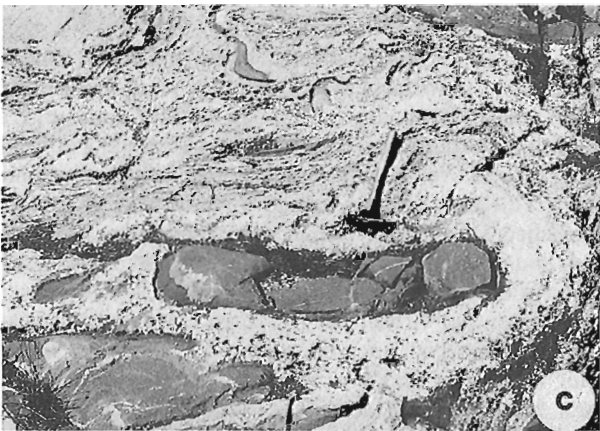
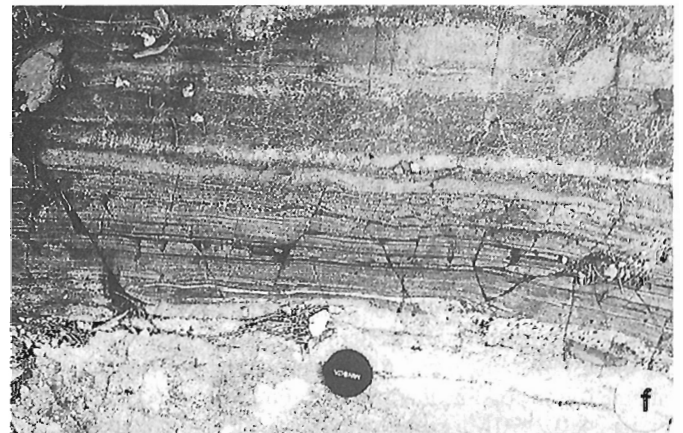
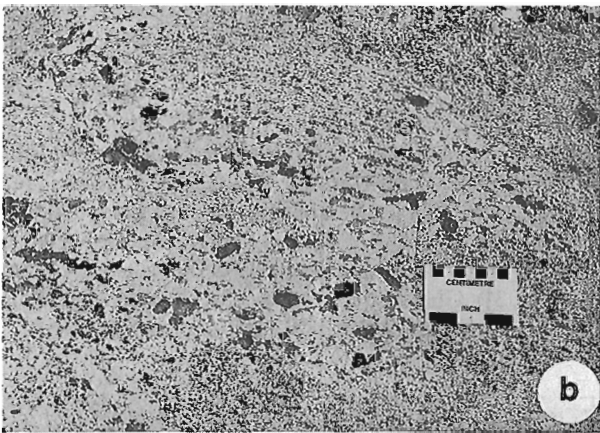
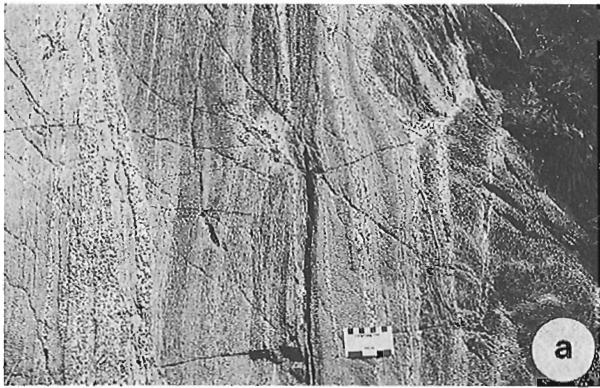
Sudbury breccia bodies occur throughout the area where they affect the Levack gneiss complex, the Cartier batholith, and the mafic dykes but not the Sudbury igneous complex. The breccia consists of blocks of country rock up to several metres in diameter in a very fine grained, dark, psuedotachylite matrix (Fig. 3j). Gneiss blocks within the breccias are rotated and, locally, flow-layering is present in the breccia matrix.

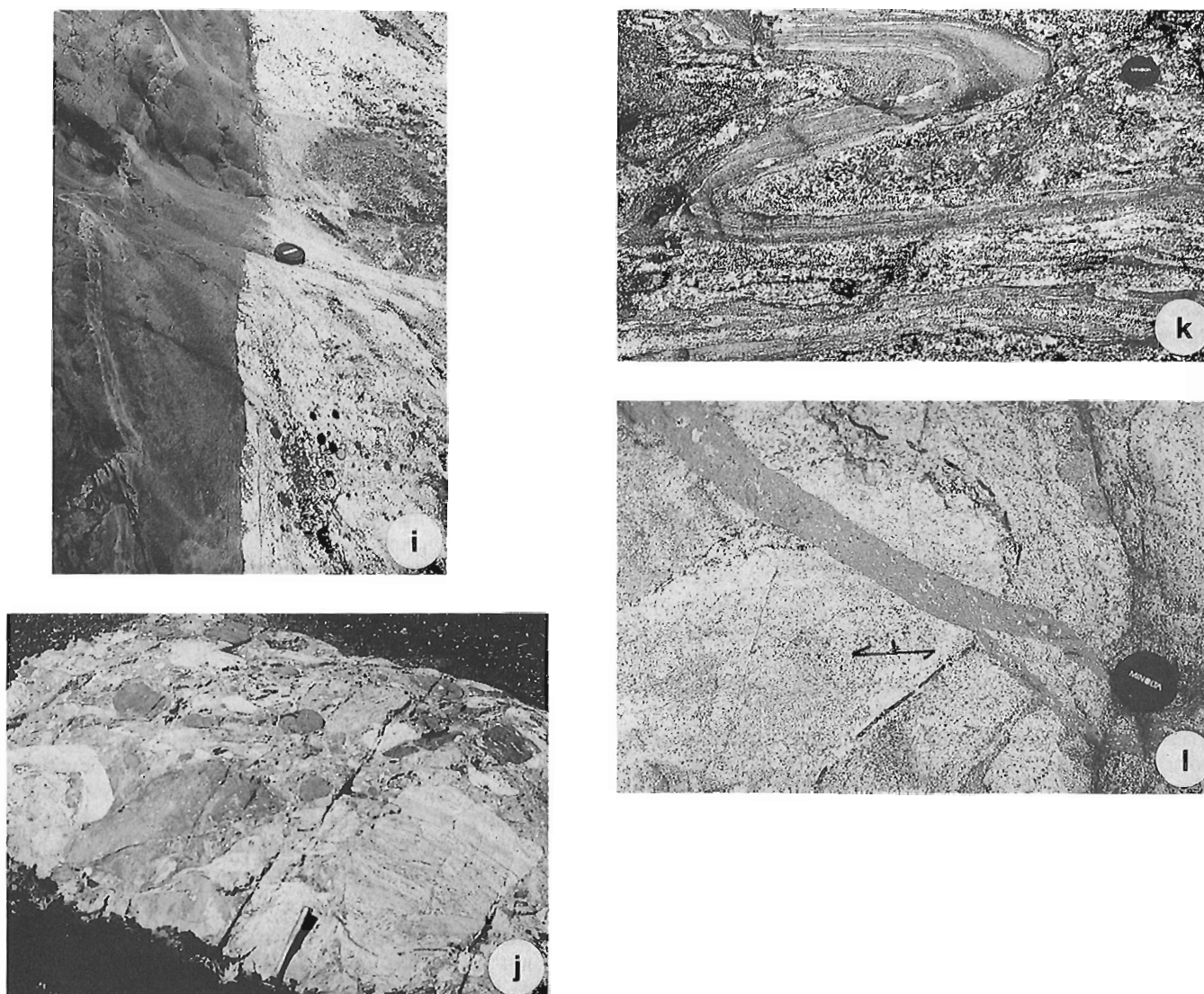
## **STRUCTURAL GEOLOGY**

### **Regional relationships**

The Sudbury structure is located along the main contact between Archean rocks of the Superior Province to the north and Proterozoic, Huronian Supergroup rocks of the Southern Province to the south. The contact is, in part, a major zone of faulting here referred to as the South Range deformation zone (Fig. 2). This zone corresponds to a major zone of reverse ductile shear, the South Range shear zone, described by Shanks and Schwerdtner (1990) as affecting part of the southern limb of the Sudbury igneous complex and adjacent rocks of the Whitewater Group and Huronian Supergroup. Rocks within the zone contain both a strong L-S fabric, south-dipping schistosity and accompanying stretching lineation, and a shear-plane (C-S) fabric. The South Range deformation zone is part of the Murray system, major south-dipping thrusts along which rocks of the Southern Province and the Sudbury structure were thrust northward onto the Superior Province Archean craton in the early Proterozoic.

Similar deformation zones probably exist north of the Sudbury structure. North of the Levack gneiss complex, the southern margin of the Benny greenstone belt, the adjacent Cartier batholith, and outliers of Huronian rocks are deformed along an east-northeast trending zone of faulting and ductile shearing here named the Benny deformation zone (Fig. 2). Coarse fragmental volcanic rocks in the southern Benny belt display prominent shallow south-dipping foliation and stretching lineation similar in style and orientation to the





**Figure 3.** *a.* Interlayered tonalitic, intermediate, and mafic gneiss with tonalitic mobilizate veins. (GSC 1993-242B). *b.* Vari-textured homogeneous tonalite diatexite with large clinopyroxenes partly altered to amphiboles. (GSC 1993-242C). *c.* Mafic inclusions, possibly fragments of a disrupted mafic dyke, in inhomogeneous tonalite diatexite. (GSC 1993-242F). *d.* Mafic gneiss with coarse grained orthopyroxene-bearing tonalitic mobilizate. (GSC 1993-242H). *e.* Biotite-plagioclase-quartz paragneiss. Lens cap in this and subsequent photographs is 5 cm in diameter. (GSC 1993-242E). *f.* Banded quartz-magnetite iron-formation bounded by mafic (mafic metavolcanic?) and granitic gneiss. (GSC 1993-242J). *g.* Inhomogeneous biotite-plagioclase-quartz±clinopyroxene±garnet diatexite. Note the coarse white feldspars in the leucosome. (GSC 1993-242A). *h.* Igneous breccia in the Joe Lake gabbro body. (GSC 1993-242D). *i.* Chilled contact of mafic dyke cutting foliation in Levack gneiss complex tonalite gneiss. (GSC 1993-242I). *j.* Sudbury breccia with blocks of gneiss, metagabbro, and porphyritic, Matachewan-type diabase. (GSC 1993-242G). *k.* Moderately plunging minor fold in inhomogeneous diatexite. (GSC 1993-242K). *l.* Late northeast-trending foliation that is axial planar to minor folds in gneissosity and is cut by a Sudbury breccia dyke. (GSC 1993-239B).



structures of the South Range deformation zone (Card and Innes, 1981). Shearing is expressed in the batholith by alignment of feldspar phenocrysts and quartz ribbons (Feuten et al., 1992).

A possible third zone, herein termed the Pumphouse Creek deformation zone, may be expressed by a topographic lineament along Pumphouse and Windy creeks west of Levack (Fig. 2). The Pumphouse Creek deformation zone may correlate with one of the seismic reflectors that project into this area (B. Milkereit, pers. comm., 1993). The structure is expressed by brecciation, shearing and quartz veining near the contact between the Levack gneiss complex and Cartier batholith (Feuten et al., 1992) and by offset of lithological units and abrupt changes in foliation trends within the Levack gneiss complex. The Pumphouse Creek deformation zone may have been displaced northward by sinistral movements on the north-northwest-trending Fecunis and Sandcherry Creek faults.

### *Structure of the Levack gneiss complex*

Although the Levack complex forms a continuous collar about the northern part of the Sudbury structure, trends of gneissic layering within the complex are highly variable at all scales, and, commonly, discordant to both the Sudbury structure and the Cartier batholith. The variable trends of the gneissosity are probably attributable in part to faulting and rotation of blocks within Sudbury breccia bodies. However, the gneissic layering has been folded and faulted. Minor and mesoscopic folds are prevalent (Fig. 3k) and many have detached, sheared-off limbs typical of ductile deformation at high metamorphic grade. At outcrop scale, inclusions with rotated internal fabrics and folds are common, as are deflections of the foliation around inclusions. Such deflections probably occur at larger scales as well.

In Figure 2, it can be seen that even though the gneissosity is subparallel to the Sudbury igneous complex contact in many areas, it is notably discordant in many others. Even where the gneissosity strikes subparallel to the Sudbury igneous complex, the dip is generally subvertical in contrast to the moderate southerly dip of the Sudbury igneous complex contact. The contact between the Levack gneiss complex and the Cartier batholith is probably more concordant, although strong discordances were observed at several localities.

The gneissic foliation is overprinted and locally offset by a later northeast-trending foliation. This foliation is generally weakly developed, is expressed either by a spaced cleavage or by oriented mafic minerals, and is axial planar to minor folds in the gneissic layering. It is cut by Sudbury breccia dykes (Fig. 3l) and is similar in style and orientation to the cleavage that affects the rocks of the Whitewater Group within the Sudbury structure. Lineations of several types and orientations were recorded, including slickensides plunging steeply north and south, minor folds with moderately northeast-plunging axes, and a few moderately northeast-plunging mineral lineations. No kinematic indicators were noted.

## **METAMORPHISM**

The Levack gneisses are polymetamorphic. Early high-grade (granulite facies) metamorphism at lower crustal depths (James et al., 1991) was followed by amphibolite facies metamorphism, probably accompanying uplift of these rocks, and by later, greenschist alteration, notably along Proterozoic faults and shear zones, and by contact metamorphism near the Sudbury igneous complex.

The high-grade regional metamorphism produced assemblages with quartz, plagioclase, perthitic feldspar, biotite, orthopyroxene, clinopyroxene, and hornblende in tonalitic and mafic gneisses and biotite, plagioclase, quartz, garnet, orthopyroxene, and clinopyroxene in paragneiss. Pyroxenes are commonly replaced by amphiboles, talc, and chlorite, plagioclase is saussuritized, and garnet is replaced by cordierite-orthopyroxene symplectites and chlorite.

Thermobarometric studies by James et al. (1991) on gt-opx-bi, gt-bi, and gt-cd-opx symplectites indicated that high-grade metamorphism occurred at pressures of 6 to 8 kb (depths of 21 to 28 km) and temperatures of 750°-800°C. Judging from the radiometric age data of Krogh et al. (1984), this high-grade metamorphism occurred about 2650 Ma ago.

The amphibolite facies metamorphism that overprints the earlier high-grade assemblages probably accompanied uplift of these rocks. This uplift may have been associated with emplacement of the late Archean Cartier batholith or with the early Proterozoic Sudbury event (James et al., 1991). Similarly, the greenschist alteration may have been associated with low-grade metamorphism that affected the Huronian outliers to the north, or to late, post-Sudbury igneous complex faulting, or both.

The contact metamorphism associated with the 1850 Ma Sudbury igneous complex has been described by Dressler (1984) as consisting of a narrow (100 m) inner zone of pyroxene hornfels (opx-plg-qz ± hb ± bi), a middle zone (200 m) of hornblende hornfels (hb-plg-qz ± bi), and an outer zone (1 km) in which only plagioclase was recrystallized. This metamorphism probably occurred at relatively shallow (5-10 km) crustal levels (James et al., 1991).

## **SUMMARY AND CONCLUSIONS**

The Levack gneiss complex is an Archean high-grade complex consisting of both intrusive and supracrustal rocks that were deformed and metamorphosed at lower crustal depths during the late Archean. In terms of rock types, structures, metamorphism, age, and tectonic relationships, the Levack gneiss complex resembles the Kapuskasing structural zone (Percival and Card, 1983). The Levack gneiss complex was uplifted, either during the late Archean or early Proterozoic, to upper crustal levels where it was strongly affected by the 1850 Ma Sudbury impact event. The complex underlies much of the northern part of the Sudbury structure and probably contributed significantly to the contamination or formation of the Sudbury igneous complex and the Sudbury ores (Faggart et al., 1985; Naldrett et al., 1986).

A major unresolved problem is the timing of uplift of the Levack gneiss complex relative to the Sudbury event. A possible key is the presence of Matachewan-type dykes cutting both the high-grade Levack gneiss complex and the relatively high-level Cartier batholith. Dyke widths, compositions, degree of alteration, and contact relationships are similar in both areas. If the dykes are members of the 2450 Ma Matachewan swarm, this would suggest that uplift occurred prior to 2450 Ma. This problem could be resolved by further geochronological, mineralogical, paleomagnetic and thermobarometric studies.

Preliminary measurements indicate that the rock units immediately beneath the Sudbury igneous complex, the tonalite-mafic gneiss assemblage and the gabbro bodies, have a relatively high (ca. 2.8-2.9 g/cm<sup>3</sup>) average density. This confirms the assumptions of gravity models by McGrath and Broome (in press). It does not, however, resolve the problem of whether or not a dense magnetic body exists at depth beneath the Sudbury structure (Gupta et al., 1984).

Seismic reflectors (Milkereit et al., 1992) in this area are probably not attributable to compositional layering within the Levack gneiss complex. The layering is generally steep, discontinuous, and commonly discordant to the Sudbury igneous complex, and therefore is not a good candidate to explain the prominent south-dipping reflectors. These are more likely attributable to thrusts or deformation zones that are part of a south-dipping regional system of post-Sudbury thrusts.

## ACKNOWLEDGMENTS

The writer was cheerfully and ably assisted in the field by Christopher Johns and Natasha Wodicka. Dr. Wodicka collected samples from the complex for geochronological studies that she will carry out at the geochronology laboratories of the Geological Survey of Canada.

The writer also wishes to thank the following persons and organizations for information and assistance; Falconbridge Limited (Exploration), Falconbridge, especially J.M. Sweeny; Inco Exploration and Technical Services Incorporated, Copper Cliff, especially G.G. Morrison; Ontario Geological Survey, Sudbury, especially B.O. Dressler; R.S. James and D. Peck, Laurentian University; and Ed O'Connor, Cartier.

The manuscript was critically reviewed by T. Skulski, P.H. Thompson, and J.A. Percival.

## REFERENCES

- Card, K.D. and Meyn, H.D.**  
1969: Geology of the Leinster-Bowell area; Ontario Department of Mines, Geology Report 65, 40 p.
- Card, K.D.**  
1979: Regional geological synthesis, central Superior Province; in *Current Research, Part A*; Geological Survey of Canada, Paper 79-1A, p. 87-90.
- Card, K.D. and Innes, D.G.**  
1981: Geology of the Benny area, District of Sudbury; Ontario Geological Survey, Report 206, 117 p.
- Card, K.D., Gupta, V.K., McGrath, P.H., and Grant, F.S.**  
1984: The Sudbury Structure: Regional Geological and Geophysical Setting; in *The Geology and Ore Deposits of the Sudbury Structure*, (ed.) E.G. Pye, A.J. Naldrett, and P.E. Giblin; Ontario Geological Survey, Special Volume 1, p. 25-43.
- Dressler, B.O.**  
1982: Geology of the Wanapitei Lake area, District of Sudbury; Ontario Geological Survey, Report 213, 131 p.  
1984a: The Effects of the Sudbury Event and Intrusion of the Sudbury Igneous Complex on the Footwall Rocks of the Sudbury Structure; in *The Geology and Ore Deposits of the Sudbury Structure*, (ed.) E.G. Pye, A.J. Naldrett, and P.E. Giblin; Ontario Geological Survey, Special Volume 1, p. 97-136.  
1984b: Sudbury Geological Compilation; Ontario Geological Survey, Map 2491, Precambrian Geology Series, Scale 1:50 000.
- Faggart, B.E., Basu, A.R., and Tatsumoto, M.**  
1985: Origin of the Sudbury complex by meteorite impact: Neodymium isotopic evidence; *Science*, v. 230, p. 436-439.
- Feuten, F., Seabright, R., and Morris, B.**  
1992: A structural transect across the Levack Gneiss Cartier Batholith complex, northwest of the Sudbury Structure; in *Lithoprobe, Abitibi-Grenville Project, Abitibi-Grenville Transect*, Report 33, p. 11-15.
- Geological Survey of Canada**  
1947: Chelmsford, Map 871A, scale 1 inch to 1 mile.
- Grieve, R.A.F., Stoffler, D., and Deutsch, A.**  
1991: The Sudbury Structure: Controversial or misunderstood?; *Journal of Geophysical Research*, v. 96, p. 22, 753-22, 764.
- Gupta, V.K., Grant, F.S., and Card, K.D.**  
1984: Gravity and Magnetic Characteristics of the Sudbury Structure; in *Geology and Ore Deposits of the Sudbury Structure*, (ed.) E.G. Pye, A.J. Naldrett, and P.E. Giblin; Ontario Geological Survey, Special Volume 1, p. 411-427.
- Heaman, L.M.**  
1989: U-Pb dating of mafic dyke swarms: what are the options?; *International Association Volcanology and Chemistry of the Earth's Interior, Congress Abstracts*, New Mexico Bureau Mines and Mineral Resources Bulletin 131, p. 125.
- James, R.S., Sweeny, J.M., and Peredery, W.**  
1991: Thermobarometry of the Levack Gneisses-Footwall rocks to the Sudbury Igneous Complex; in *Lithoprobe, Abitibi-Grenville Project, Abitibi Grenville Transect*, Report 32, p. 179-182.
- Krogh, T.E., Davis, D.W., and Corfu, F.**  
1984: Precise U-Pb zircon and baddeleyite ages for the Sudbury area; in *Geology and Ore Deposits of the Sudbury Structure*, (ed.) E.G. Pye, A.J. Naldrett, and P.E. Giblin; Ontario Geological Survey, Special Volume 1, p. 431-446.
- Lafleur, J. and Dressler, B.O.**  
1985: Geology of Cascaden, Dowling, Levack, and Trill Townships, District of Sudbury; Ontario Geological Survey, Open File Report 5533.
- Langford, F.F.**  
1960: Geology of Levack Township, District of Sudbury; Ontario Department of Mines, Preliminary Report 1960-5.
- McGrath, P.H. and Broome, H.J.**  
in press: A gravity model for the Sudbury Structure along the Lithoprobe seismic line; *Geophysical Research Letters*.
- Milkereit, B., Green, A., and Sudbury Working Group**  
1992: Deep geometry of the Sudbury structure from seismic reflection profiling; *Geology*, v. 20, p. 807-811.
- Muir, T.L.**  
1981: Geology of the Capreol area, District of Sudbury; Ontario Geological Survey, Open File Report 5344.  
1983: Geology of the Morgan Lake - Nelson Lake area, District of Sudbury; Ontario Geological Survey, Open File Report 5426.
- Naldrett, A.J., Rao, B.V., and Evensen, N.M.**  
1986: Contamination at Sudbury and its role in ore formation; in *Metallogeny of Basic and Ultrabasic Rocks*; London, Institute of Mining and Metallurgy, p. 79-91.
- Percival, J.A. and Card, K.D.**  
1983: Archean crust as revealed in the Kapuskasing uplift, Superior Province, Canada; *Geology*, v. 11, p. 323-326.

**Percival, J.A., Fountain, D.M., and Salisbury, M.H.**

1992: Exposed crustal cross sections as windows on the lower crust; in Continental Lower Crust, (ed.) D.M. Fountain, R.J. Arculus, and R.W. Kay; Elsevier, Amsterdam, p. 317-362.

**Shanks, W.S. and Schwerdtner, W.M.**

1990: Structural analysis of the central and southwestern Sudbury Structure, Southern Province, Canadian Shield; Canadian Journal of Earth Sciences, v. 28, p. 411-430.

**Sweeny, M. and Farrow, C.**

1990: Geology Report, Morgan West Project, Levack and Morgan Townships; Unpublished Report, Falconbridge Limited Exploration, 35 p.

**Walker, R.J., Morgan, J.W., Naldrett, A.J., Li, C., and Fassett, J.D.**

1991: Re-Os isotope systematics of Ni-Cu sulphide ores, Sudbury igneous complex, Ontario: evidence for a major crustal component; Earth and Planetary Science Letters, v. 105, p. 416-429.

---

Geological Survey of Canada Project 930028



# Acoustic velocity logging at the McConnell nickel deposit, Sudbury area, Ontario: preliminary in situ measurements<sup>1</sup>

K.A. Pflug, P.G. Killeen, and C.J. Mwenifumbo  
Mineral Resources Division

*Pflug, K.A., Killeen, P.G., and Mwenifumbo, C.J., 1994: Acoustic velocity logging at the McConnell nickel deposit, Sudbury area, Ontario: preliminary in situ measurements; in Current Research 1994-C; Geological Survey of Canada, p. 279-286.*

---

**Abstract:** An acoustic velocity logging probe has been used to acquire data on the seismic characteristics of the McConnell nickel deposit in the Sudbury area. Preliminary results indicate good velocity contrasts in the stratigraphic sequence associated with the massive sulphides. These velocity contrasts are related to the density and elastic properties of the rocks; density was measured in the same borehole with a density logging probe. One interesting observation is that the high density massive sulphides have low P-wave velocities relative to the host rocks. This is not a universally applicable condition because some massive sulphides in other areas being investigated have higher velocities. Full sonic waveforms were recorded and these will be further studied to extract S-wave velocities. The P- and S-wave velocity and amplitude logs will then be used to derive valuable geotechnical information.

**Résumé :** On a utilisé une sonde diagraphique de vitesse acoustique pour obtenir des données sur les caractéristiques sismiques du gisement nickélicifère de McConnell dans la région de Sudbury. Les résultats préliminaires indiquent que la séquence stratigraphique associée aux sulfures massifs présente des vitesses d'ondes nettement différentes. Ces différences sont liées à la densité et aux propriétés élastiques des roches; la densité a été mesurée dans le même trou à l'aide d'une sonde diagraphique de densité. On a relevé une observation intéressante, soit que la vitesse des ondes P est faible dans les sulfures massifs à densité élevée, comparativement à la vitesse dans les roches encaissantes. Cette caractéristique n'est pas universelle, car certains sulfures massifs à l'étude ailleurs présentent des vitesses plus élevées. Des trains d'ondes acoustiques complets ont été enregistrés et feront l'objet d'études plus détaillées visant à déterminer la vitesse des ondes S. Les diagraphies de la vitesse et de l'amplitude des ondes P et S serviront à dériver des renseignements géotechniques utiles.

---

<sup>1</sup> Contribution to Canada-Ontario Subsidiary Agreement on Northern Ontario Development (1991-1995), under the Canada-Ontario Economic and Regional Development Agreement.

## INTRODUCTION

An accurate knowledge of the acoustic velocity of P waves in the various lithologies encountered will aid the application of seismic methods (such as surface seismic reflection and hole to hole tomography) to base metal exploration.

Although acoustic velocities can be determined in the laboratory on rock samples or drill core, greater accuracy is possible with in-situ borehole measurements using an acoustic velocity logging tool. The Borehole Geophysics Section of the GSC has begun acoustic velocity logging using a tool with a piezoelectric transducer for an energy source, and two piezoelectric transducer receivers separated by 30 cm. The difference in arrival times of the transmitted pulses (P waves) at the two fixed receivers is converted to a velocity measurement. In addition, the amplitude of the first arrival is recorded as an amplitude log, which can be used to give a qualitative measurement of the attenuation factor (Q). The equipment, manufactured by Mount Sopris Instrument Co. of Colorado, records the full sonic waveform, making it possible to reprocess the field data to improve the precision of the first arrival picks, or in some cases, to pick the arrival time of the slower S waves which will provide additional information on the mechanical properties of the rocks.

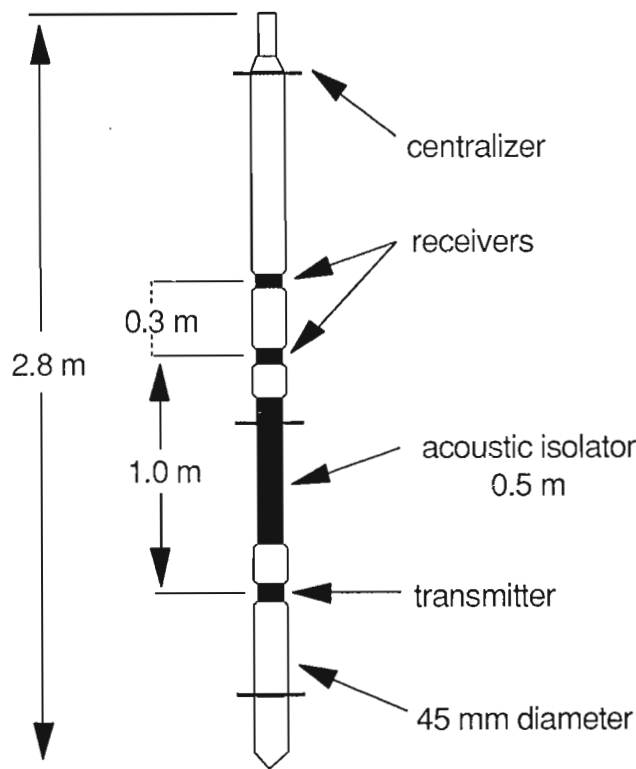
By pulsing the energy source every half second and recording alternately with the 2 receivers, an average velocity is obtained every second, which, at a logging speed of 3 m/min, represents a sample every 5 cm in the borehole.

The physical characteristics of the acoustic velocity probe are shown in Figure 1. The 45 mm diameter probe consists of 2 sections: the transmitter section, and the receiver section, separated by a flexible acoustic isolator 0.5 m long. The manufacturer recommends a logging speed of less than 40 ft/min (12 m/min).

Tests were run at the GSC's Bells Corners Borehole Geophysics Test Site near Ottawa (Killeen, 1986; Schock et al., 1991) to gain experience with recording at different logging speeds from 0.5 to 10 m/min. Two of the four preset gains in the probe were also tested. The probe should be centralized in the hole with suitable flexible rubber spacers (centralizers). This is a relatively simple matter in the NQ test holes (75 mm diameter) with the 45 mm diameter probe. However in inclined holes typical of Canadian shield mineral exploration, centralizing the probe is more difficult. In a BQ (60 mm diameter) borehole, there is little space for a centralizer around the probe. The logging data from the McConnell deposit discussed below were acquired without a centralizer.

## DATA PROCESSING METHODS

During data acquisition, the arrival time of the transmitted pulse at each receiver is determined when the signal crosses a threshold level selected by the operator. The thresholds of the two receivers can be set independently. As different rock types are traversed, the received signal amplitude may vary and sometimes not cross the threshold until the second (or later) cycle in the waveform. When this occurs at the far



**Figure 1.** Acoustic velocity probe; not to scale (model CLP-4681, Mount Sopris Instrument Co.).

receiver but not the near receiver the travel time between receivers appears anomalously long. This "cycle skipping" results in apparent low velocity spikes in the velocity logs. Spikes may also be generated in the logs if the system triggers early on noise at the front of the waveform; this can be a problem in inclined holes where the probe is subjected to vibrations as it moves along the borehole wall.

Reprocessing the data to remove these spikes generally requires locating the spikes in the log, examining individual waveform pairs and adjusting the thresholds such that the first arrivals are correctly picked. This can be tedious if the data are particularly noisy. Preliminary tests suggest that reprocessing the data by cross-correlating the near and far waveforms against each other (Scott and Sena, 1974) to determine the travel time of the first arrival removes most of the spikes in the velocity log. The method is simple to automate and may be useful in determining the velocities of later arrivals.

## THE McCONNELL NICKEL DEPOSIT

As part of a project within the Northern Ontario Development Agreement (NODA), the GSC is working to establish borehole geophysics test sites at major deposit-types in Ontario. The McConnell deposit (Garson Offset) represents the nickel (pentlandite, pyrrhotite, chalcopyrite) deposits of the Sudbury area. First described in a 1992-93 NODA summary report (Mwenifumbo et al, 1993), a fence of five holes intersecting

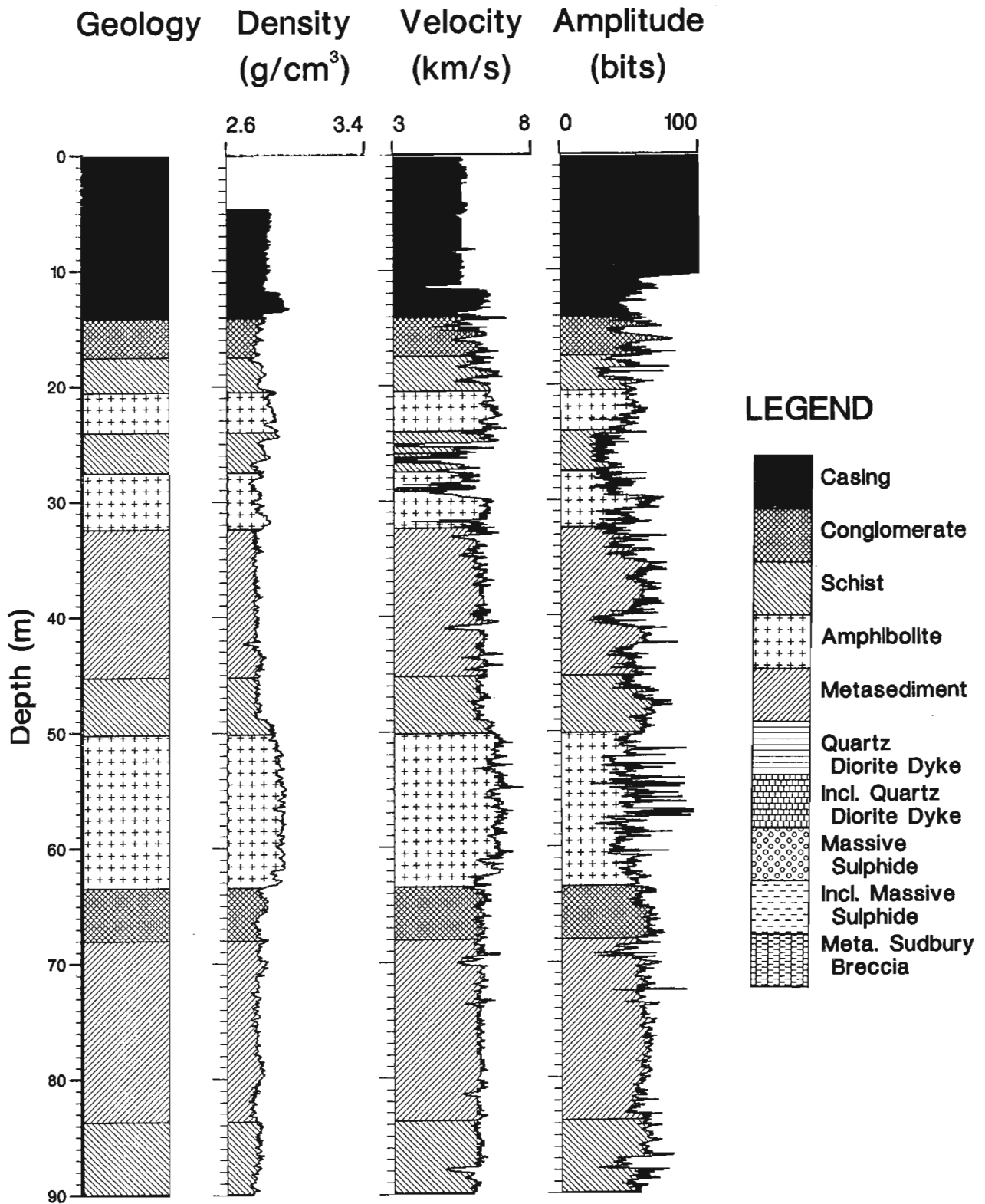


Figure 2. Density, acoustic velocity and amplitude (P wave) logs for the top half of hole 78930, McConnell deposit (Garson Offset), Sudbury, Ontario.

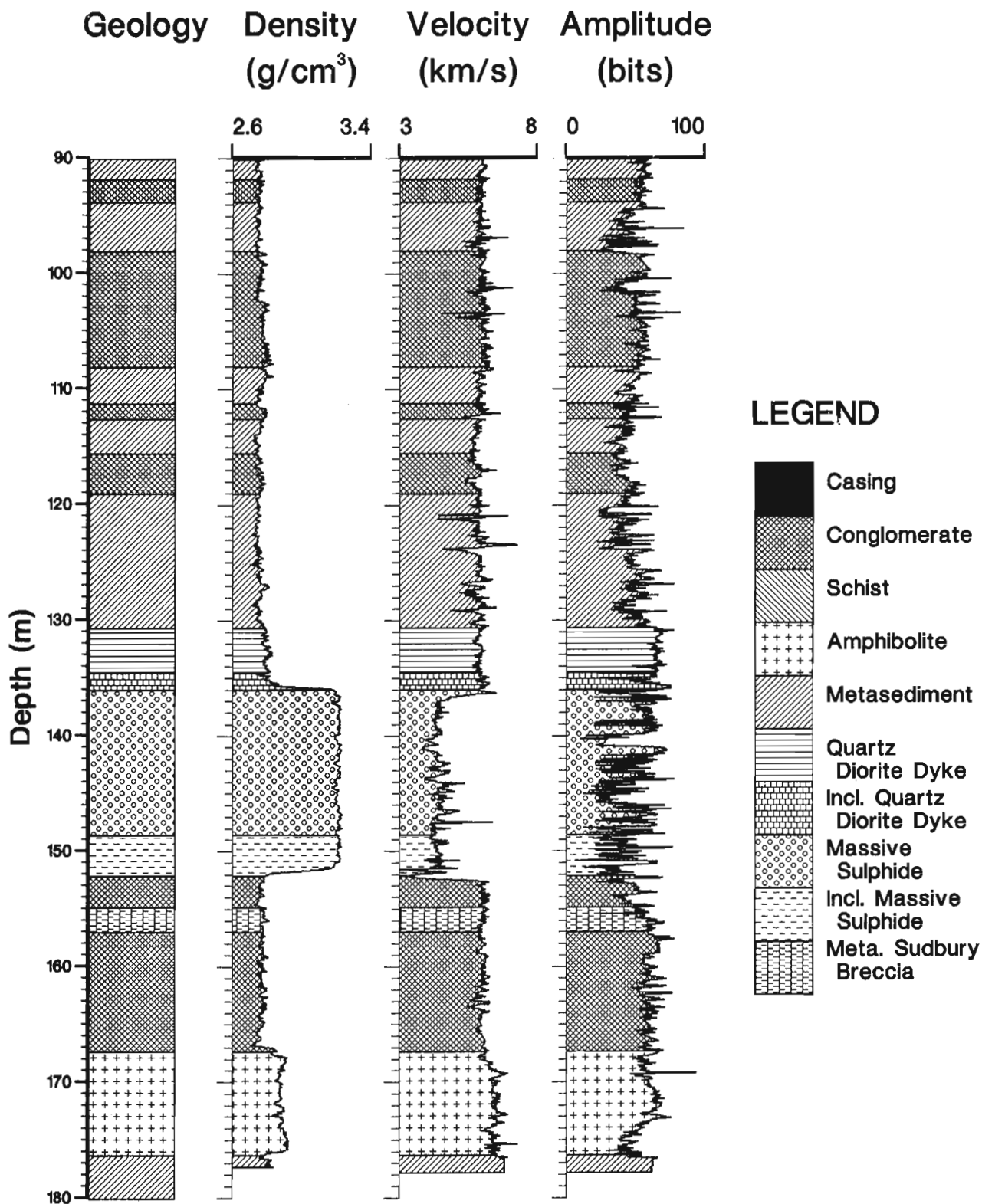


Figure 3. Density, acoustic velocity and amplitude (P wave) logs for the bottom half of hole 78930, McConnell Deposit (Garson Offset), Sudbury, Ontario.

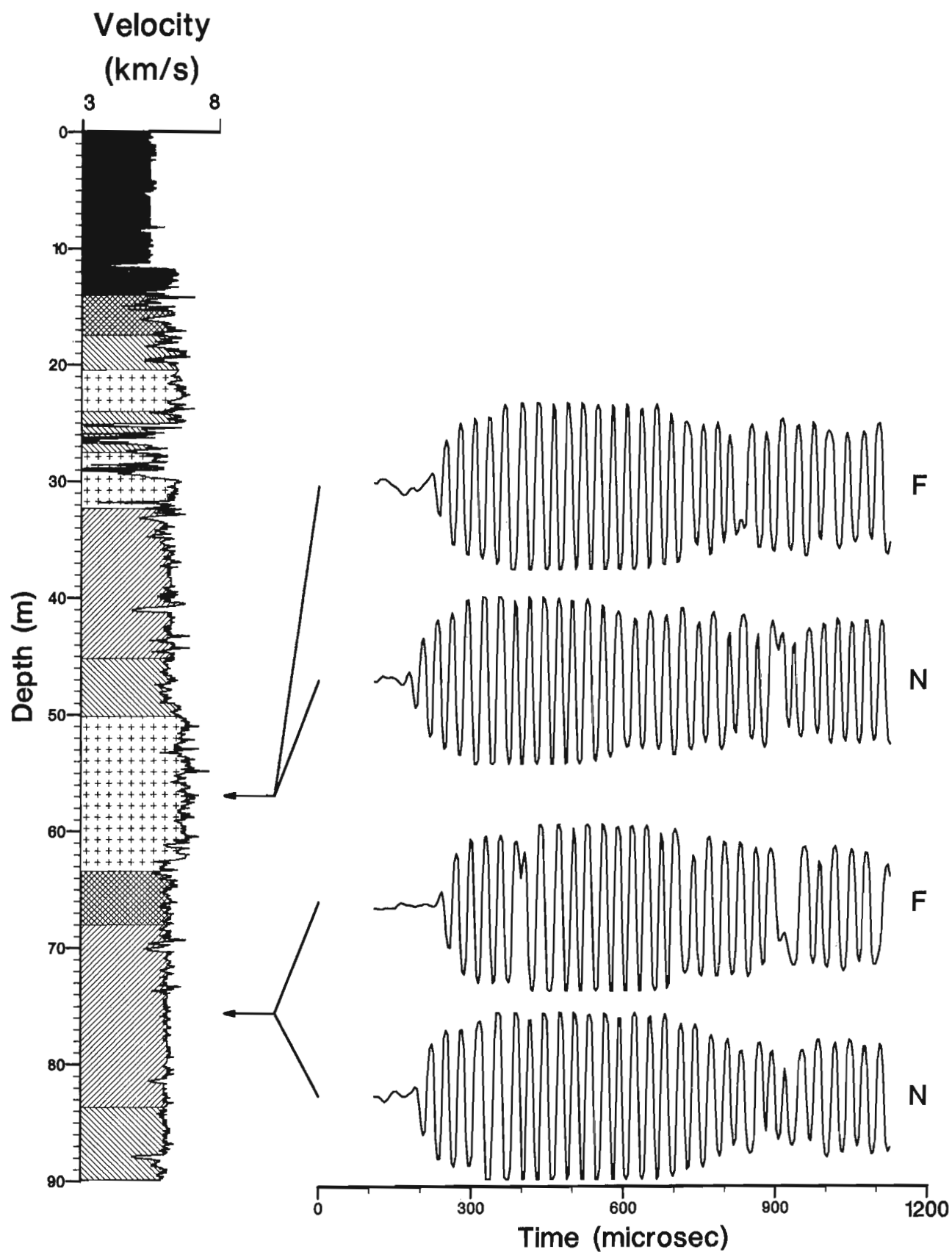


Figure 4. Typical waveforms recorded at the near (N) and far (F) receivers in the amphibolite (50-63 m) and metasediment (68-83 m) for the top half of hole 78930.

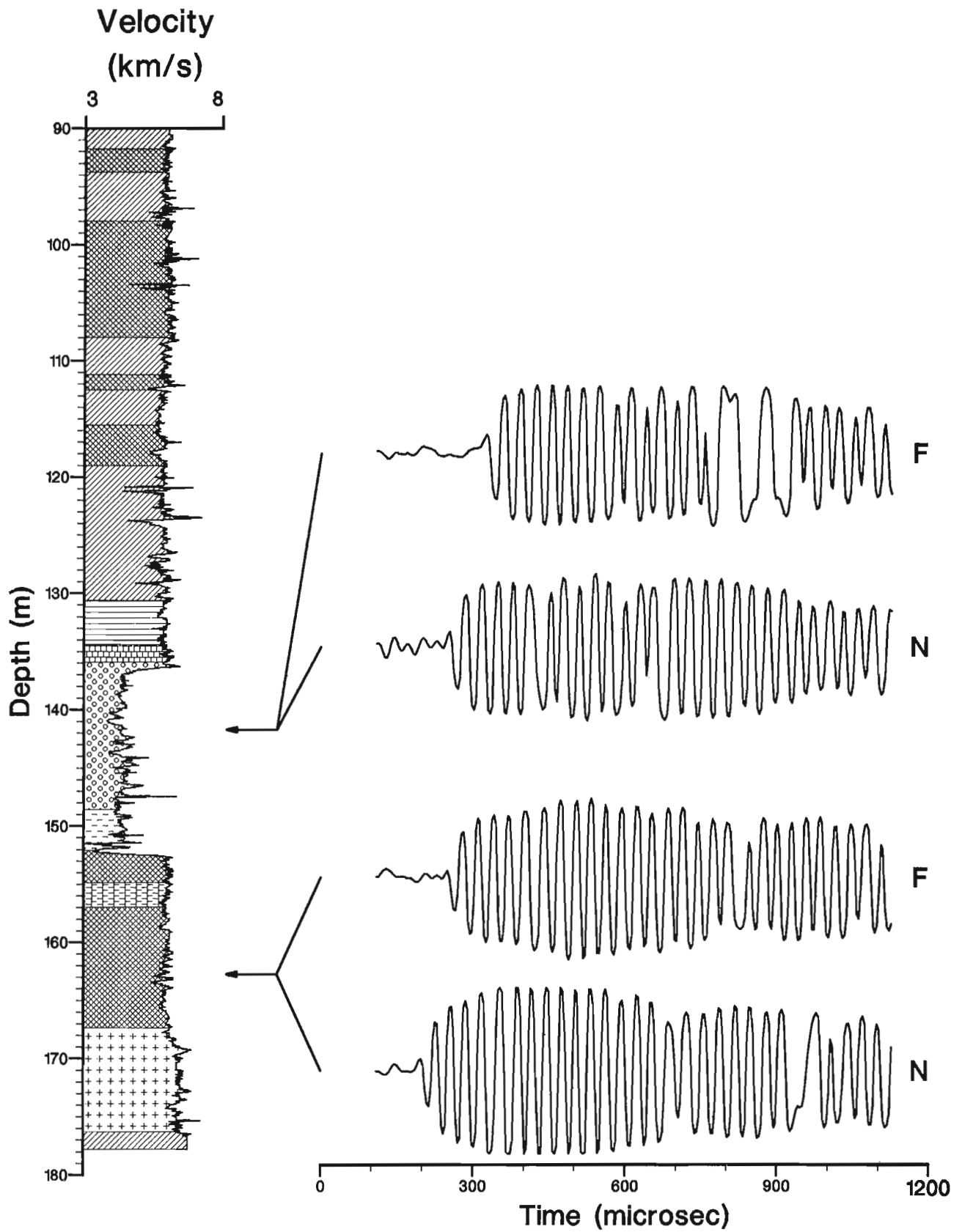


Figure 5. Typical waveforms recorded at the near (N) and far (F) receivers in the massive sulphides (136-148 m) and conglomerate (157-167 m) for the bottom half of hole 78930.



the ore body has now been logged with numerous geophysical parameters. The stratigraphic sequence which contains the massive sulphides consists of schists, amphibolites, conglomerates, metasediments, Sudbury breccia and quartz diorite dykes. The massive sulphides form a steeply dipping ore body which extends from the surface to a depth of about 350 m. The body is intersected at depths of 50 m in the shallowest hole, and about 300 m in the deepest hole.

The acoustic velocity probe was run in the middle hole in the fence, which intersected the massive sulphides at about 150 m. Figures 2 and 3 show the acoustic velocity and amplitude logs recorded in the borehole at 3 m/min, plotted with the density log. The density and acoustic velocity are related as follows:

$$V_p = \sqrt{(\lambda + 2\mu)/\rho} \quad (1)$$

where  $V_p$  is the P-wave velocity,  $\rho$  is the density,  $\lambda$  is Lamé's constant and  $\mu$  is the shear modulus. The velocity log has been edited to remove spikes due primarily to triggering on noise at the front of the waveform. The amplitude log has not been filtered in this way so it appears noisier.

A few selected recorded waveforms are shown with the acoustic velocity log in Figures 4 and 5. The amplitude variations in these waveforms (and in the P-wave amplitude logs) are suppressed because the acoustic signal is passed through a logarithmic amplifier in the probe. In the waveform displays, the signal that first crosses the preset threshold is the down-going motion evident at the front of the packet of seismic energy. This down-going pulse has a small amplitude relative to later arrivals in the wave train. The velocity logs and the amplitude logs refer to this signal as the first arrival (P wave).

The density log in Figure 2 shows that the density of the amphibolite from 50 to 63 m depth is relatively homogeneous and higher than the adjacent schist and conglomerate. The acoustic velocity is also higher (~6.7 km/s) than the schist (~6.0 km/s) or conglomerate (~6.1 km/s). Typical waveforms for the amphibolite zone for both the near and far receivers are shown in Figure 4. The velocity measured in the metasediment from 68 to 83 m is relatively constant at about 6.0 km/s. The first arrival amplitudes (Fig. 2) as exemplified by waveforms for near and far receivers (Fig. 4) are slightly higher on average (and less noisy) for the metasediment than for the amphibolite, suggesting the P waves are attenuated more by the amphibolite than the metasediment.

Figures 3 and 5 show the lower half of the hole from 90 to 180 m and include the massive sulphides between 136 and 148 m depth. Note the very high (and relatively constant) density within the sulphides. The acoustic velocity log indicates a velocity of less than 5.0 km/s in the ore and a sharp contrast between the velocity in the ore and in the host rocks. The ore is a low velocity zone. The amplitude log also shows a relatively low average value but this is mostly due to triggering on noise in front of the transmitted pulse. The correct value for the average amplitude lies between the values in the amphibolite and metasediment. Typical waveforms in the massive sulphides are shown in Figure 5. These were selected from a zone in which the amplitude of the first arrival was quite high. Below the ore zone, from

157 to 167 m, is a relatively homogeneous conglomerate zone with density about equal to the metasediments (Fig. 2), but a slightly lower velocity (5.9 km/s). The amplitude log in the conglomerate is about the same level as in the metasediment but more variable, implying the P-wave attenuation in the conglomerate is similar to but more variable than that in the metasediment. (See also the recorded waveforms for the near and far receivers, Fig. 5.)

## CONCLUSIONS

Acoustic logging can provide detailed measurements of compressional wave velocity as well as measurements of the attenuation of seismic energy in the immediate vicinity of a borehole. As well as being lithological indicators, these measurements provide valuable information for seismic reflection or tomographic surveys or modelling. Additionally, they can be used to determine physical properties of the rocks encountered. This will be the subject of more detailed investigation in the future. It is also possible to pick the arrival time of the slower S waves, which are hidden in the recorded waveform. The P wave is the first arrival in the wave train, and hence is reasonably easy to pick. Poisson's ratio which relates to the mechanical properties of the rocks, can be determined from the ratio of the velocities of the P and S waves. S-wave analysis will be investigated as further experience is obtained with acoustic logging in different ore environments. Methods of enhancing the data and improving the speed and ease of extracting information from the raw data are presently being tested.

We see this as a significant development leading to reliable determination of velocities in a wide diversity of rocks associated with base metal (and gold) deposits. These data will be extremely useful for practitioners of surface reflection seismic surveys, and for surface to borehole, or hole to hole seismic tomography. In addition, geotechnical engineering parameters of importance in mining operations may be determined more accurately (in situ) over larger and more representative volumes of rock (than laboratory samples), using acoustic logging techniques.

## ACKNOWLEDGMENTS

The authors wish to thank Barry Krause and Alan King of INCO Exploration and Technical Services Inc. for their help in establishing the McConnell deposit as a test site for borehole geophysics. We are grateful to Yves Blanchard for modifying the equipment to operate with our logging system. We thank Susan Pullan for critically reviewing the manuscript.

## REFERENCES

- Killeen, P.G.  
1986: A system of deep test holes and calibration facilities for developing and testing new borehole geophysical techniques; in *Borehole Geophysics for Mining and Geotechnical Applications*, (ed.) P.G. Killeen; Geological Survey of Canada, Paper 85-27, p. 29-46.

**Mwenifumbo, C.J., Killeen, P.G., and Bernius, G.R.**

1993: Ore deposit signatures by borehole geophysics; in Summary Report, 1992-93, Northern Ontario Development Agreement, minerals, (ed.) N. Wood, R. Shannon, L. Owsicki, and M. Walters; co-published by Energy, Mines and Resources Canada, p. 123-125.

**Schock, L.D., Killeen, P.G., Elliott, B.E., and Bernius, G.R.**

1991: A review of Canadian calibration facilities for borehole geophysical measurements; in Proceedings of the 4th International MGLS/KEGS Symposium on Borehole Geophysics for Minerals, Geotechnical and Groundwater Applications, Toronto 18-22 August, 1991, p. 191-202.

**Scott, J.H. and Sena, J.**

1974: Acoustic logging for mining applications; in Transactions of the Fifteenth Annual Logging Symposium; Society of Professional Well Log Analysts, Paper P, June 2-5, p. 1-11.

---

Geological Survey of Canada Project 880030

# Timing relationships between Cu-Au mineralization, dykes, and shear zones in the Chibougamau camp, northeastern Abitibi subprovince, Quebec<sup>1</sup>

François Robert  
Mineral Resources Division

*Robert, F., 1994: Timing relationships between Cu-Au mineralization, dykes, and shear zones in the Chibougamau camp, northeastern Abitibi subprovince, Quebec; in Current Research 1994-C; Geological Survey of Canada, p. 287-294.*

---

**Abstract:** The Chibougamau camp is characterized by the presence of porphyry copper-style mineralization and by that of shear zone-hosted Cu-Au mineralization, commonly associated with dykes apparently related to the neighboring Chibougamau pluton. The temporal relationships between the two styles of mineralization, dyke emplacement and shear zone development, are important in understanding the genesis and distribution of these styles of mineralization. Two outcrops exposing sulphide mineralization, shear zones, and dykes were mapped in detail. The mapping shows that fracture-controlled Fe-Cu sulphides predated the development of the shear zones and indicates that sericite alteration associated with these early mineralized fractures played an important role in localizing subsequent deformation. It also shows that dykes were emplaced before and after development of fracture-controlled Fe-Cu sulphides, but before shear zone development.

**Résumé :** Le camp minier de Chibougamau se distingue par la présence de minéralisation de style porphyre cuprifère et celle de minéralisation à Cu-Au dans des zones de cisaillement, communément associée à des dykes apparemment reliés au pluton de Chibougamau. L'établissement des relations temporelles entre les deux styles de minéralisation, l'emplacement des dykes et le développement des zones de cisaillement est un élément clé de la compréhension de la genèse et de la distribution de ces gisements. Deux affleurements exposant la minéralisation, des dykes et des zones de cisaillement ont été cartographiés en détail. La cartographie démontre qu'une minéralisation sulfurée de Fe-Cu associée à des fractures est antérieure au développement des zones de cisaillement et que la séricitisation enveloppant ces fractures a joué un rôle important dans la localisation d'incrément ultérieurs de déformation. Elle démontre, de plus, la présence de dykes plus anciens et plus jeunes que la minéralisation en Fe-Cu associée à des fractures, et qui sont tous affectés par les zones de cisaillement.

---

<sup>1</sup> Contribution to Special Assistance Program for the Mining Sector of the Chapais-Chibougamau Region (1992-1995), under the Canada-Quebec Subsidiary Agreement on the Economic Development of the Regions of Quebec.

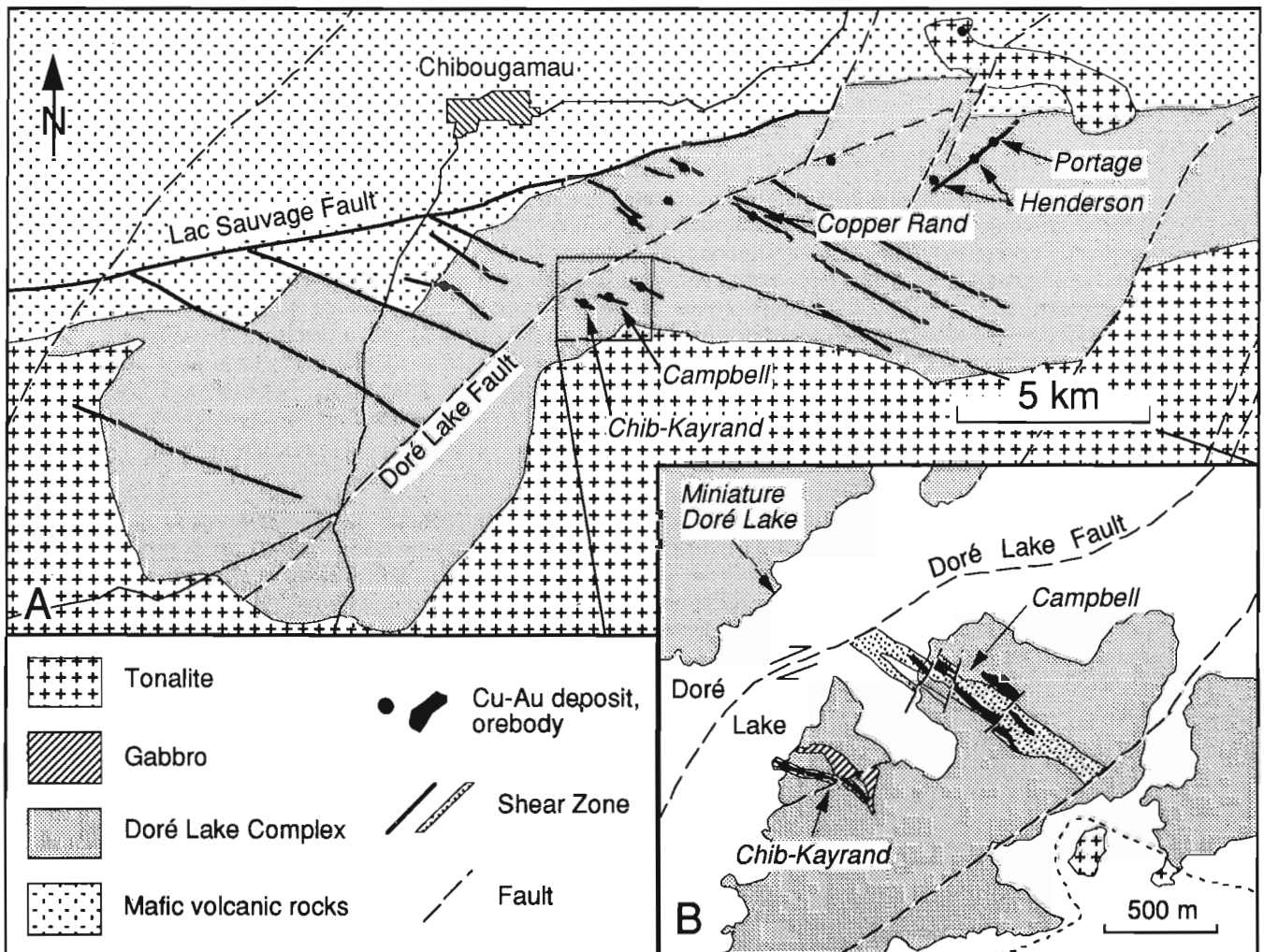
## INTRODUCTION

The Chibougamau area, located in the northeast corner of the Abitibi greenstone belt, possesses a wide diversity of ore deposit types (Guha et al., 1990). In particular, it is characterized by the presence of shear zone-hosted Cu-Au mineralization (Fig. 1), unique in Superior Province (Allard, 1976), and by that of low grade porphyry copper-type mineralization (Kirkham, 1972; Cimon, 1973). A joint project, involving the Ministère de l'Énergie et des Ressources du Québec, the Geological Survey of Canada, the Université du Québec à Chicoutimi, and industry, was initiated in the spring of 1993 to characterize better these two styles of mineralization and to explore their spatial, temporal, and genetic relationships (see Pilote et al., in press; Sinclair et al., 1994).

As part of this project, two key outcrops were mapped in detail to define the timing relationships between Cu-Au mineralization, dykes, and the shear zones in which they commonly occur. This document presents the results and interpretations of this mapping.

## GEOLOGICAL SETTING

Copper-gold deposits of the Chibougamau camp occur within the gabbroic Doré Lake Complex in an area approximately 15 by 5 km on the northwestern limb of the Chibougamau anticline (Fig. 1A). The geology of this area has been described in detail by Graham (1956), Allard (1976), and Daigneault and Allard (1990). In this area, the Doré Lake Complex intrudes mafic volcanic rocks of the Gilman Formation and is itself intruded by tonalite of the Chibougamau



**Figure 1.** A: Simplified geological map of the Chibougamau camp showing the distribution of Cu-Au deposits and of major shear zones and faults; adapted from Allard (1976). B: Enlargement of the area encompassing the two outcrops mapped in detail; adapted from Graham (1956).

pluton (Fig. 1). Abundant dykes of intermediate to felsic composition are present within the Doré Lake Complex and are generally considered to be related to the Chibougamau pluton (see for example Allard, 1976). Most Cu-Au deposits in the camp occur in southeast-trending shear zones although three deposits occur in a shear zone that trends northeast. The mineralized shear zones have steep dips, generally to the southwest, and have been interpreted as reverse-oblique structures (Guha et al., 1983; Archambault et al., 1984; Daigneault and Allard, 1990). These shear zones are truncated by the right-lateral Doré Lake fault, which strikes east-northeast (Fig. 1).

Most mineralized shear zones occur within meta-anorthosite of the Doré Lake Complex. Mineralization consists of lenses and veins of semi-massive to massive sulphides with variable proportions of quartz and carbonates (Allard, 1976; Guha et al., 1990). The sulphides consist mainly of chalcopyrite, pyrite, and pyrrhotite with minor amounts of sphalerite and galena; gold occurs as small grains associated with pyrite and chalcopyrite. The shear zone rocks consist of sericite-carbonate and chlorite ( $\pm$ chloritoid) schists derived from the Doré Lake meta-anorthosite. The mineralized shear zones also contain numerous dykes of intermediate to felsic compositions with which the orebodies are commonly spatially associated (Allard, 1976; Daigneault and Allard, 1990).

Several interpretations have been proposed for the origin and the timing of emplacement of the Cu-Au orebodies in the shear zones. Some authors have proposed sulphide emplacement during active development of the shear zones (e.g., Guha et al., 1983, 1988, 1990), whereas others consider the sulphide ores to be related to the Chibougamau pluton and to have subsequently been deformed (e.g., Duquette, 1970; Allard, 1976). Guha and Koo (1975) further presented textural evidence for metamorphism and deformation overprinting sulphide mineralization. A Proterozoic age has also been considered for Cu-Au mineralization on the basis of Pb isotopes (Thorpe et al., 1984).

The first outcrop examined in detail exposes mineralization of the Chib-Kayrand deposit, representative of the Cu-Au mineralization in southeast-trending shear zones, as well as a Fe-Cu sulphide stockwork. The other outcrop, locally referred to as the "Miniature Doré Lake Camp" (Allard, 1984), exposes mineralized fractures, shear zones, and faults of orientations typical of the larger structures in the camp. Each outcrop is described in detail below.

## **CHIB-KAYRAND OUTCROP**

The Chib-Kayrand deposit is located 800 m southwest of the important Campbell Main mine (Fig. 1B). Cu-Au mineralization follows and overprints a feldspar porphyry dyke which is coincident with a southeast-trending shear zone dipping 70° to the northeast (Graham, 1956). Orebodies were composed of chalcopyrite, pyrrhotite, and pyrite, with trace quantities of sphalerite and gold. The dyke, shear zone, and mineralization have been traced along strike for a distance of approximately 500 m. A left-lateral fault, striking east-northeast, offsets the deposit by about 50 m (Fig. 1B).

The outcrop mapped in detail represents the crown pillar of one of the orebodies; it exposes sulphide mineralization, a narrow continuous shear zone, and various intrusive rocks. Their distribution and age relationships are depicted in Figure 2 and described below.

## **Lithologies**

Three generations of intrusive rocks cut the host meta-anorthosite. The earliest consists of a medium- to coarse-grained gabbro which corresponds to an irregular body described by Graham (1956) and which occurs mostly in the hanging wall of the shear zone (Fig. 1B). The gabbro has an irregular shape in outcrop and occurs on both sides of the shear zone (Fig. 2). On the northeast side, intrusive contacts between the gabbro and the anorthosite are clearly truncated by the shear zone at several localities (Fig. 2). The second generation of intrusions is represented by a grey feldspar porphyry dyke, up to 5 m wide, that can be traced discontinuously across the outcrop. It contains 5-15% plagioclase phenocrysts, 2-8 mm in diameter, with rare quartz eyes of similar dimensions in a fine grained feldspathic matrix. This dyke likely corresponds to the feldspar porphyry dyke described by Graham (1956). The intrusive contact between this feldspar porphyry dyke and the gabbro is only locally preserved because it is obscured by a younger intrusion of diorite. At one locality (location A, Fig. 2), the dyke clearly cuts the gabbro.

The diorite is typically fine grained and forms an irregular dyke-like body that has intruded both the feldspar porphyry dyke and the gabbro (Fig. 2). The diorite is characterized by the presence of abundant subrounded gabbro xenoliths, 5-20 cm in diameter; it has well developed chilled margins around the xenoliths. Diorite contacts with the feldspar porphyry dyke are sharp, but those with the gabbro are commonly gradational due to a progressive increase in proportion of gabbro xenoliths. Such gradational contacts account in part for the irregular shape of this intrusion. Importantly, the fine grained diorite also contains large mineralized blocks of anorthosite (location B, Fig. 2) and of the feldspar porphyry dyke (Location C, Fig. 2; Fig. 3), up to 2 m in their longest dimension.

## **Shear zones and faults**

Several shear zones are present in outcrop and overprint all lithologies. The main shear zone exposed in the outcrop strikes southeast and dips steeply to the northeast. It reaches a few metres in thickness and approximately follows the northeast wall of the feldspar porphyry dyke (Fig. 2). The presence of a back-filled open stope in the northwest segment of this shear zone indicates that it contained Cu-Au mineralization. It is defined by an intense penetrative foliation developed in all rock types except the very competent feldspar porphyry dyke where it is weak to absent. Foliation dips 70-85° to the northeast and strikes more easterly than the boundaries of the shear zone; it contains a mineral lineation pitching at 60° to the northwest. These structural elements indicate reverse-dextral movement along the shear zone, consistent with interpreted movements along other southeast-trending shear zones in the area (Daigneault and Allard, 1990).

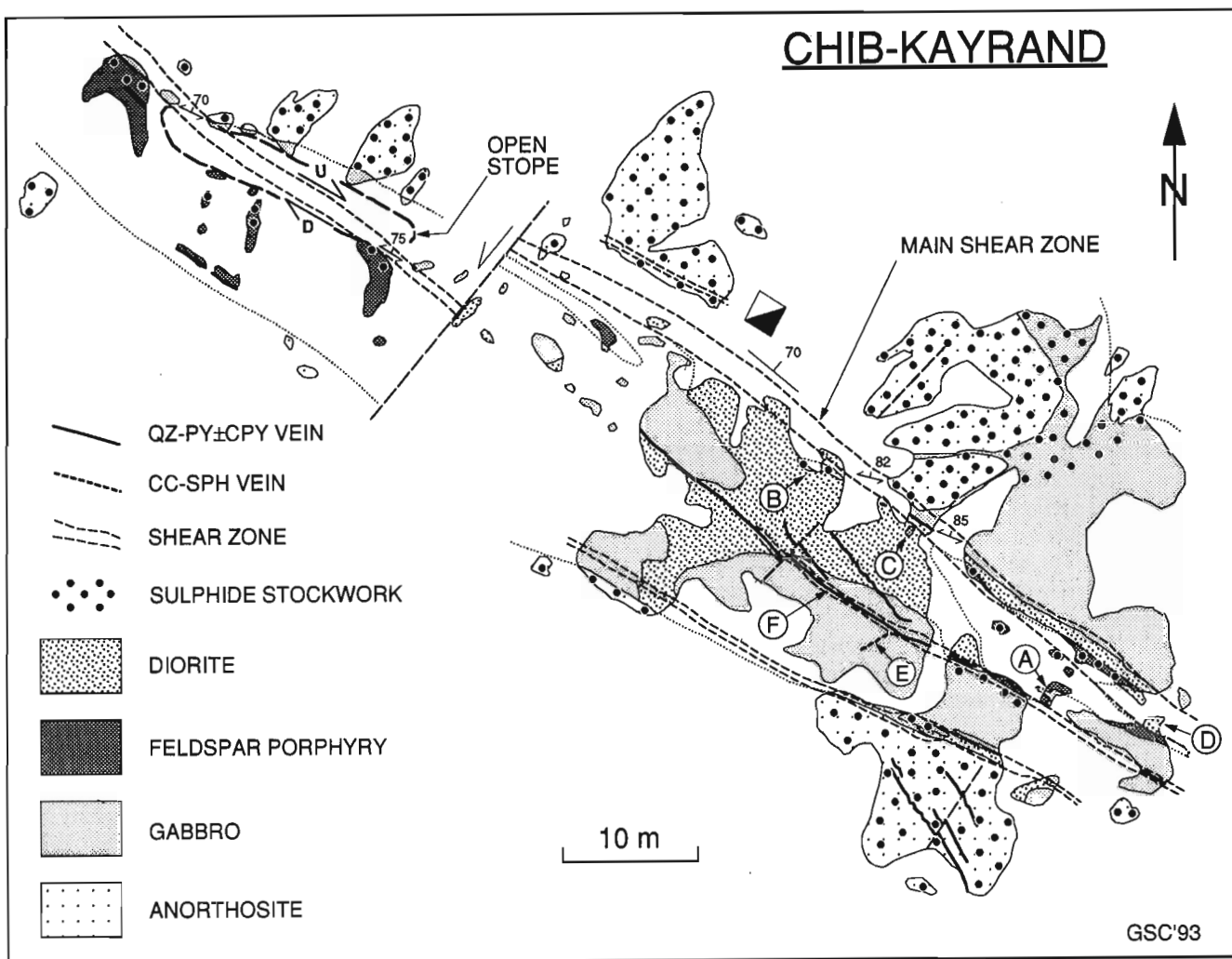


Figure 2. Detailed geological map of the Chib-Kayrand outcrop.

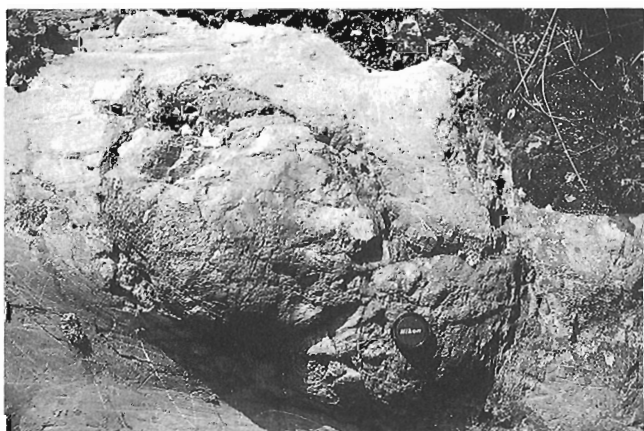


Figure 3. Large block of mineralized feldspar porphyry dyke in barren, fine grained diorite. Lens cap is 5 cm in diameter. Location C in Figure 2. GSC 1993-220F



Figure 4. Flattened gabbro xenoliths in fine grained diorite overprinted by the main shear zone. Location D in Figure 2. GSC 1993-220G



Other shear zones of smaller dimensions are parallel to the main one and display the same internal foliation geometries indicating similar movements. All of these shear zones clearly overprint and postdate all intrusive rock types. In the fine grained diorite, gabbro xenoliths are clearly flattened where overprinted by the main shear zone, as illustrated in Figure 4.

These shear zones also locally contain central quartz-sulphide veins which are described below. The shear zones and veins are further cut by a set of late vertical faults which strike northeast and have left-lateral offsets up to 10 m (Fig. 2). They may be part of the same set as the larger left-lateral fault that offsets the deposit (Fig. 1B).

### Mineralization

Three styles of sulphide mineralization are observed on the Chib-Kayrand outcrop: sulphide stockwork, semi-massive sulphide lenses, and sulphide-bearing veins. These styles of mineralization and their age relationships are presented below.

A Fe-Cu sulphide stockwork is heterogeneously developed in outcrop. It is centered approximately on the main shear zone and forms a halo extending up to 20 m away from it (Fig. 2). This style of mineralization consists of fine grained Fe-Cu sulphides distributed along, and adjacent to, fractures which may contain narrow quartz veinlets. Fractures comprising the stockwork are randomly oriented and range from planar to irregular in shape (Fig. 5). The sulphide stockwork is best developed in the anorthosite and, where the fracturing is most intense, the rocks may contain up to 10% sulphides by volume. Sulphides consist of chalcopyrite, pyrite, and pyrrhotite; in places, up to 10% disseminated sphalerite accompanies stockwork mineralization in the anorthosite.

The sulphide stockwork overprints the anorthosite, the gabbro, and the feldspar porphyry dyke, but is *not present* in the fine grained diorite dyke. The presence of stockwork mineralization in large blocks of anorthosite and feldspar porphyry dyke within barren diorite (Locations B and C, Fig. 2; Fig. 3) indicates unequivocally that the fine grained diorite postdates stockwork development.



Figure 5. Typical outcrop exposure of the stockwork sulphides in anorthosite. GSC 1993-220A

The second style of mineralization consists of discontinuous semi-massive sulphide lenses (up to 70% sulphides by volume), corresponding to the orebodies and spatially associated with the main shear zone (Graham, 1956). This style of mineralization is only preserved as scattered boulders excavated from a back-filled open stope in the northwestern part of the outcrop (Fig. 2). It consists of varying proportions of chalcopyrite and pyrrhotite with irregular and contorted layers of quartz and carbonate. Gold grains are reported to be associated with the semi-massive sulphides (Graham, 1956). In some samples, wall rock slivers and fragments, now transformed into sericite schist, are also interspersed with the sulphides. The relative timing between the semi-massive sulphide lenses and the shear zones cannot be established in outcrop, but the contorted nature of quartz and carbonate layers indicates that the semi-massive sulphide lenses have been overprinted by at least some shear zone deformation. The age relationships between the sulphide stockwork and the semi-massive sulphide lenses cannot be established at Chib-Kayrand; however, their similar mineral assemblages suggest that they may be genetically related.

The third style of mineralization is represented by two types of sulphide-bearing veins: calcite-sphalerite and quartz-sulphide veins. The only calcite-sphalerite vein present in outcrop is 15 cm thick and a few metres long, and strikes east-northeast (Location E, Fig. 2). This vein is cut by a quartz-sulphide vein, central to a southeast-trending shear zone, and is dextrally dragged by that shear zone. The age relationships of calcite-sphalerite veins with the Fe-Cu sulphide stockwork and with the diorite intrusion cannot be established from the available exposure, however, the presence of sphalerite in both the stockwork and the calcite-sphalerite vein suggests that they may be related.

Veins of the quartz-sulphide type, which consists of quartz, pyrite, and traces of chalcopyrite, are the most common and the best developed in outcrop. It is not known at present if they are auriferous. These veins reach several tens of centimetres in thickness and a few tens of metres in length. They occur in all rock types, including the diorite (Fig. 2), and they crosscut the sulphide stockwork fractures and the calcite-sphalerite vein.

Two sets of quartz-sulphide veins are observed. The first set consists of veins central to shear zones, such as the one exposed at location F in Figure 2. The second set of quartz-sulphide veins strikes at 320-330° and dips between 45 and 60° to the northeast (Fig. 2); these veins lack wall rock foliation and are slightly buckled. The age relations between shear zones and the quartz-sulphide veins are not clear. However, the quartz in veins central to shear zones is milky to vitreous, rather than having the cherty appearance of recrystallized quartz; this suggests that the veins were emplaced during or after shear zone development, rather than being overprinted by the shear zone. The nature and orientation of veins of the second set are compatible with, but do not necessarily imply, formation as extensional veins during development of the reverse-oblique shear zones.

## MINIATURE DORÉ LAKE CAMP OUTCROP

The second mapped outcrop is located on the shore of Doré Lake across from the Chib-Kayrand and Campbell deposits, on the opposite side of the the Doré Lake fault (Fig. 1B). It consists of anorthosite and gabbroic anorthosite, with small southeast-trending semi-massive sulphide zones, originally exposed in trenches that are now overgrown (Allard, 1984). In the mapped portion of the outcrop (Fig. 6), the anorthosite is cut by a metre-wide siliceous, porphyritic grey dyke striking north. The dyke consists of 1-5% feldspar phenocrysts in an aphanitic matrix, and as much as 5% pyrite, distributed along quartz-filled hairline fractures.

Abundant barren and mineralized fractures, shear zones, and faults overprint the anorthosite and the dyke. They are described in detail below.

### Mineralized and barren fractures

Three main sets of subvertical fractures and faults are observed in outcrop (Fig. 6). They are subdivided on the basis of their strikes into southeast, northeast, and east-northeast sets.

The southeast- and northeast-striking sets have similar characteristics and are described together, although the southeast-striking set is the best developed. The two sets comprise both barren and mineralized fractures and do not display any systematic crosscutting relationships. They are typically planar, 0.5-2 m long, and vary greatly in abundance. For example, the northeastern part of the outcrop is characterized by very closely spaced southeast-trending fractures (Fig. 6). The mineralized fractures are typically lined with fine grained Fe-Cu sulphides and locally contain a central quartz veinlet up to a few millimetres thick. They are similar to fractures defining the sulphide stockwork at Chib-Kayrand, except that they are here more planar and have more consistent orientations than at Chib-Kayrand. The mineralized fractures are also fringed by centimetre-wide sericite alteration haloes. The majority of the mineralized fractures and their sericitic haloes do not display any foliation; a certain number of these fractures, however, have well developed foliation in the adjacent sericitized wall rocks (see below).

The east-northeast-striking set consists of brittle faults and fractures concentrated in two main zones transecting the mapped outcrop (Fig. 6). These faults and fractures clearly cut and offset mineralized southeast-striking fractures

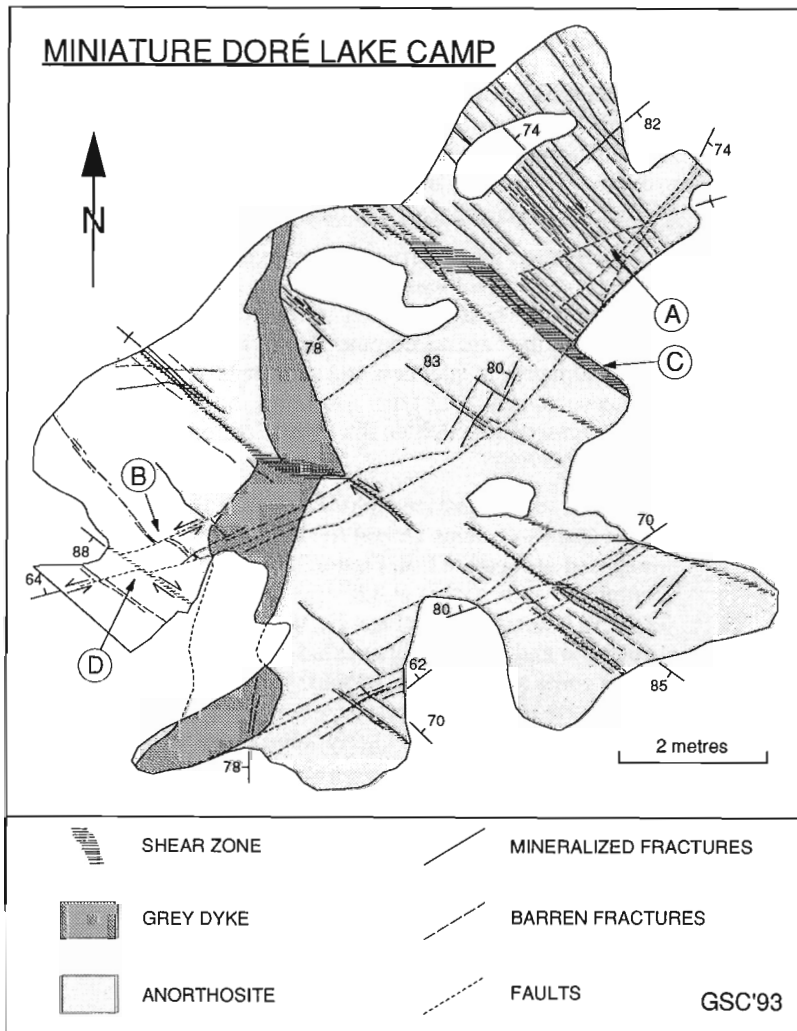


Figure 6.

Detailed geological map of a selected portion of the Miniature Doré Lake Camp outcrop.

(Fig. 7). A clear example of left-lateral offset of southeast-striking fractures is exposed at location B in Figure 6. For the most part, east-northeast-trending fractures are barren.

### Shear zones

Several narrow shear zones occur parallel to, and spatially coincident with, mineralized southeast-trending fractures (Fig. 6). The shear zones have a well developed internal foliation and range in width from <1 cm to 40 cm. The orientation of the internal foliation and the offset of the grey dyke (Fig. 6) indicate a dextral horizontal component of movement along these shear zones, similar to that observed on the Chib-Kayrand outcrop.

In the shear zones that are coincident with mineralized southeast-trending fractures (Fig. 6), the foliated zone is localized in the sericitic alteration halo around the fractures. In some cases, the shear zone is developed only along a segment of a given fracture. In addition, the widest shear zone on outcrop has sharp boundaries coincident with southeast fractures (Location C, Fig. 6), in contrast to the expected gradational nature of shear zone boundaries. All these relationships indicate that the southeast-trending shear zones overprint a pre-existing set of southeast fractures.

At several locations on the outcrop, the east-northeast fractures and faults are in turn clearly offset by the southeast shear zones (location C, Fig. 6; Fig. 8). The fact that the east-northeast faults cut the nonsheared mineralized southeast fractures elsewhere gives further support to the interpretation that the southeast shear zones overprint the early mineralized fractures and result from their reactivation during later deformation. The sericitic alteration haloes around these fractures likely played a major role in localizing foliation development given their incompetent nature. There is no evidence in outcrop for additional mineralization being introduced during development of the southeast shear zones.



**Figure 7.** Closely spaced mineralized southeast-striking fractures cut by a barren east-northeast-striking fault. Compass is 7 cm wide. Location A in Figure 6. GSC 1993-220B



**Figure 8.** East-northeast fault dextrally offset by a southeast shear zone. Location D in Figure 6. GSC 1993-220C

## DISCUSSION AND CONCLUSIONS

The Chib-Kayrand and Miniature Doré Lake Camp outcrops have in common the presence of dykes, of southeast-trending shear zones and of fracture-controlled Fe-Cu sulphides (see below). Both also contain semi-massive sulphide lenses typical of Cu-Au ores in Chibougamau but the poor exposure of these lenses did not permit documentation of their relationships with the other geological elements. The Chib-Kayrand outcrop further contains quartz-sulphide veins, not present in the Miniature Doré Lake Camp outcrop. In both cases, crosscutting and overprinting relationships indicate a rather complex structural and hydrothermal evolution of the mineralized structures, believed to be representative of those in the larger Cu-Au deposits.

In both outcrops, the earliest stage of mineralization is represented by fracture-controlled Fe-Cu sulphides, which takes the form of a stockwork at Chib-Kayrand and that of planar fracture arrays at Miniature Doré Lake Camp. Such fracture-controlled Fe-Cu sulphides overprint porphyritic dykes and they are, in turn, overprinted by the southeast-trending shear zones. Prior to development of southeast-trending shear zones, this style of mineralization was intruded by a diorite body at Chib-Kayrand and was offset by east-northeast-trending faults at Miniature Doré Lake Camp.

These fracture-controlled Fe-Cu sulphides represent an early stage of hydrothermal activity. At Chib-Kayrand, a later stage is indicated by the quartz-sulphide veins. These two stages are separated in time by at least the intrusion of diorite, which contains blocks of anorthosite and feldspar porphyry dyke with Fe-Cu stockwork, but which is cut by the quartz-sulphide veins. As indicated above, limited evidence also suggests that the quartz-sulphide veins may have formed during or after shear zone development, which would increase the time gap between the two hydrothermal stages. The relationships between the semi-massive sulphide lenses, which constitute the Cu-Au ores in the camp, and these two hydrothermal stages cannot be firmly established at present and will be the focus of further field studies.

This mapping also illustrates the role of sericite alteration haloes associated with Fe-Cu sulphide fractures in localizing shear zones, as indicated by the confinement of the shear zone foliation to such haloes on the Miniature Doré Lake Camp outcrop. The common spatial coincidence of shear zones, broad sericite alteration zones, and Cu-Au mineralization in the Chibougamau camp may reflect the role of "early" sericite alteration in localizing subsequent deformation and shear zone development. This role may not be readily apparent in the large Cu-Au deposits of the camp because of the greater magnitude of the effects of shearing.

Several workers in the area have noted that the Cu-Au deposits in the Chibougamau camp are closely associated with dykes and have proposed genetic links between mineralization and plutonism (see Allard, 1976). The presence of dykes both pre- and postdating fracture-controlled Fe-Cu sulphides at Chib-Kayrand suggests a close temporal relationship between hydrothermal activity and dyke emplacement and certainly supports such a hypothesis.

The presence in the camp of numerous dykes, fractures, and sulphide lenses in a southeast orientation strongly suggests the existence of an early fracture or fault set with that orientation which acted as a conduit for magma and hydrothermal fluids and which localized later shear zone development. As illustrated by the Miniature Doré Lake Camp outcrop, not all these early structures have been reactivated as shear zones. It could thus be expected that some structures, or segments of structures, have been spared from the superimposed shear zone deformation. Such preserved structures or segments would offer the best opportunity to document the primary characteristics of the sulphide mineralization. In this context, one could also expect that significant variations in structural character exist between areas of preserved mineralization and those dominated by the overprinting shear zones.

Finally, this mapping clearly indicates that the mineralized shear zones have undergone a complex structural and hydrothermal history which, apart from the two hydrothermal stages documented here, may well extend into Proterozoic time, as argued by Thorpe et al. (1984) and Guha et al. (1990).

## ACKNOWLEDGMENTS

Réal Daigneault, Rod Kirkham, Pierre Pilote, and Dave Sinclair are thanked for stimulating and enlightening discussions in the field; however, I remain solely responsible for any error of interpretation. Thanks also go to Benoît Dubé, Pierre Pilote, Howard Poulsen, Al Sangster, and Dave Sinclair for their critical review of the manuscript.

## REFERENCES

- Allard, G.O.**  
1976: Doré Lake Complex and its importance to Chibougamau geology and metallogeny; Ministère des Richesses Naturelles, Québec, DP-368, 466 p.  
1984: Mineralized outcrops and showings around Doré Lake; in Chibougamau – Stratigraphy and Mineralization: An Archean Belt with a Difference; CIM Geology Division, Field Trip Guidebook p. 62-66.
- Archambault, G., Guha, J., Tremblay, A., and Kanwar, R.**  
1984: Implications of the geomechanical interpretation of the Copper Rand deposit on the Doré Lake shear belt; in Chibougamau – Stratigraphy and Mineralization, (ed.) J. Guha and E.H. Chown; Canadian Institute of Mining and Metallurgy, Special Volume 34, p. 300-318.
- Cimon, J.**  
1973: Possibility of an Archean porphyry copper in Quebec; Canadian Mining Journal, v. 94, p. 57.
- Daigneault, R. and Allard, G.O.**  
1990: Le complexe du Lac Doré et son environnement géologique (région de Chibougamau-sous province de l'Abitibi); Québec, Ministère de l'Énergie et des Ressources, MM89-03, 275 p.
- Duquette, G.**  
1970: Stratigraphie de l'Archéen et relations métallogéniques dans la région de Chibougamau; Ministère des Richesses Naturelles, Québec, Étude Spéciale 8, 18 p.
- Graham, R.B.**  
1956: Moitié nord du canton d'Obalski, district Électoral d'Abitibi-est; Québec, Ministère des Mines, Québec, Rapport Géologique 71, 48 p.
- Guha, J. and Koo, J.**  
1975: Role of fluid state mobilization during metamorphism of the Henderson ore bodies, Chibougamau, Quebec, Canada; Canadian Journal of Earth Sciences, v. 12, p. 1516-1523.
- Guha, J., Archambault, G., and Leroy, J.**  
1983: A correlation between evolution of mineralizing fluids and the geomechanical development of a shear zone as illustrated by the Henderson 2 Mine; Economic Geology, v. 78, p. 1605-1618.
- Guha, J., Chown, E.H., Archambault, G., Barnes, S.J., Brisson, H., Daigneault, R., Dion, C., Dubé, B., Mueller, W., and Pilote, P.**  
1990: Metallogeny in relation to magmatic and structural evolution of an Archean greenstone belt: Chibougamau mining district; University of Western Australia, Geology Department, University Extension Publication 24, p. 121-166.
- Guha, J., Dubé, B., Pilote, P., Chown, E.H., Archambault, G., and Bouchard, G.**  
1988: Gold mineralization patterns in relation to the lithologic and tectonic evolution of the Chibougamau mining district, Quebec, Canada; Mineralium Deposita, v. 23, p. 293-298.
- Kirkham, R.V.**  
1972: Geology of copper and molybdenum deposits; Geological Survey of Canada, Report of Activities, Paper 72-1, Part A, p. 82-87.
- Pilote, P., Cimon, J., Dion, C., Kirkham, R.V., Robert, F., Sinclair, W.D., and Daigneault, R.**  
in press: Les gisements de type Cu-Au porphyrique de la région de Chibougamau. Ministère de l'Énergie et des Ressources du Québec, Rapport d'activité, D.V. 93-02.
- Sinclair, W.D., Pilote, P., Kirkham, R.V., Robert, F., and Daigneault, R.**  
1994: A preliminary report of porphyry Cu-Mo-Au and shear zone-hosted Cu-Au deposits in the Chibougamau area, Quebec; in Current Research 1994-C, Geological Survey of Canada.
- Thorpe, R.I., Guha, J., Franklin, J.M., and Loveridge, W.D.**  
1984: Use of Superior Province lead isotope framework in interpreting mineralization stages in the Chibougamau district; in Chibougamau – Stratigraphy and Mineralization, (ed.) J. Guha and E.H. Chown; Canadian Institute of Mining and Metallurgy, Special Volume 34, p. 496-516.

# Vein fields in gold districts: the example of Val d'Or, southeastern Abitibi subprovince, Quebec

François Robert

Mineral Resources Division

*Robert, F., 1994: Vein fields in gold districts: the example of Val d'Or, southeastern Abitibi subprovince, Quebec; in Current Research 1994-C; Geological Survey of Canada, p. 295-302.*

---

**Abstract:** Among abundant vein-type gold deposits in the Val d'Or district, quartz-tourmaline-carbonate veins are singled out as having a remarkable uniformity of hydrothermal and structural characteristics over an area 40 x 15 km. These veins are undeformed and are younger than other types of veins in the district. Quartz-tourmaline-carbonate veins are interpreted to be the product of a single, large hydrothermal system and to define a vein field. The recognition of at least two ages of veins and of the existence of a large vein field at Val d'Or has important implications for the understanding of the origin of these deposits and for their exploration.

**Résumé :** Parmi les nombreux gisements d'or filoniens du district de Val d'Or, les filons de quartz-tourmaline-carbonate se distinguent par la remarquable uniformité de leurs caractéristiques hydrothermales et structurales sur une superficie de 40 x 15 km. Ces filons ne sont pas déformés et sont plus jeunes que les autres types de filons du district. Les filons de quartz-tourmaline-carbonate sont interprétés comme étant le produit d'un seul système hydrothermal de grande dimension, et ils définissent un champ filonien. L'identification d'au moins deux âges de filons et l'existence d'un vaste champ filonien à Val d'Or ont des implications importantes pour la compréhension de la génèse de ces filons de même que pour leur exploration.



## INTRODUCTION

It has long been recognized that greenstone gold deposits in Superior Province and other Archean cratons occur in clusters that define gold camps, or districts, which are spatially associated with major, crustal-scale structures that commonly correspond to subprovince boundaries (Card et al., 1989; Eisenlohr et al., 1989). It is now recognized that different styles of gold deposits may be present within these districts, including, for example, quartz vein and sulphidic types of deposits (Card et al., 1989; Robert 1990a). However, quartz vein deposits represent the dominant style of gold mineralization in a large number of camps such as those of Bridge River, B.C., Yellowknife, N.W.T., Rice Lake, Manitoba, Timmins and Red Lake, Ontario, and Val d'Or, Quebec, among many others.

In addition, recent studies in the Rice Lake camp, Manitoba, demonstrate the existence of multiple ages of gold-quartz veins in the same district (Brommecker et al., 1989). This is also the case in the Val d'Or district, southeastern Abitibi Subprovince, where several seasons of field studies of gold-quartz veins have led to the recognition of different groups (and ages) of veins. One group with nearly identical hydrothermal (vein mineral assemblages and hydrothermal alteration) and structural characteristics form what is here referred to as a *vein field*. Recognition of vein fields, which may represent single, large hydrothermal systems within gold districts, has implications both for exploration and for the understanding of auriferous systems. In this report, gold-quartz veins of different types and ages and the existence of a vein field at Val d'Or are documented, along with a discussion of their implications.

## GEOLOGICAL SETTING

The Val d'Or district is located along the southeastern margin of the Abitibi greenstone belt (Fig. 1). The northern part of the area is underlain by ultramafic to felsic metavolcanic rocks of the Abitibi Subprovince; these rocks are separated from the clastic metasedimentary rocks of the Pontiac Subprovince to the south by the Larder Lake-Cadillac fault zone, locally designated as the Cadillac tectonic zone. Volcanic rocks of the Abitibi Subprovince are cut by a series of plutons, sills, and dykes including synvolcanic gabbro, diorite, and tonalite, and syn- to late-tectonic diorite, tonalite, and monzonite. All these rocks, including syntectonic intrusions, have been metamorphosed to greenschist grade.

The area has undergone a complex structural evolution involving at least three increments of penetrative deformation (Robert, 1990b; Desrochers et al., 1993). A dominant steep east-west foliation, overprinting both volcanic and sedimentary rocks, corresponds to a second increment of deformation. It is largely responsible for the overall east-west arrangement of most lithological units in southern Abitibi, and records important north-south shortening across the belt. An earlier increment of folding has been recognized in the western part of the area, west of the town of Val d'Or, which accounts, at least in part, for the northwest trend of lithological units in

this domain (Babineau, 1985; Sansfaçon and Hubert, 1990; Desrochers et al., 1993). A third increment of deformation, recording dextral strike-slip along the subprovince boundary, has been documented along the Cadillac tectonic zone (Robert, 1990b).

Abundant shear zones, parallel to the structural trend, are present in the district (Fig. 1) and have been grouped into three orders (Robert, 1990b). First-order shear zones are represented by the Larder Lake-Cadillac fault zone, a complex high strain zone reaching 1 km in thickness and at least 200 km long, which strikes overall east-west and dips steeply to the north (Green et al., 1990; Robert, 1990b). Second-order shear zones are typically 1-10 km long and 10-100 m wide; they have steep to subvertical dips and vary in strike from south-east in the western part of the district to east-west in the eastern part (Fig. 1). Third-order shear zones, which are the most abundant, are a few metres thick and reach 1 km in length. They strike between northwest and northeast and dip between 35 and 75° to the north or to the south. Based on field relationships and on the presence of similar alteration and auriferous quartz veins in shear zones of all orders, Robert (1990b) proposed that they formed a large-scale interconnected plumbing system at some stage in the structural evolution of the district.

Numerous gold deposits and occurrences are present in the Val d'Or district (Fig. 1) and account for in excess of 900 tonnes of gold (production plus reserves). Excellent summary descriptions of the significant gold deposits of the area are presented in Trudel and Sauv  (1992) and Sauv  et al. (1993), and an extensive study of the structural setting of gold-quartz veins is presented in Robert (1990b).

Two main descriptive classes of gold deposits have been distinguished in the area: "disseminated" and "vein-type" deposits (Fig. 1). Disseminated deposits comprise zones of disseminated sulphides in massive, fractured, or brecciated wall rocks, commonly with small quartz veinlets but without significant quartz veins; examples include the Camflo, Barnat, Sladen, Canadian Malartic, and Kiena deposits. In vein-type deposits, orebodies consist of gold-quartz veins and their adjacent altered wall rocks. As shown in Figure 1, vein-type deposits are the most abundant in the Val d'Or district and account for approximately 60% of the total gold production. Vein-type deposit are considered in more detail below.

## CHARACTERISTICS OF GOLD-QUARTZ VEINS

More than forty vein-type deposits and showings in the Val d'Or area have been studied or examined in detail by the author, with particular emphasis on their structural and kinematic aspects. Field observations indicate that, among all the veins present at Val d'Or, quartz-tourmaline-carbonate veins can be singled out as a group on the basis of their hydrothermal and structural attributes. The characteristics of quartz-tourmaline-carbonate veins are presented below and are contrasted with those of other veins at Val d'Or, as summarized in Table 1. The following synthesis is based on



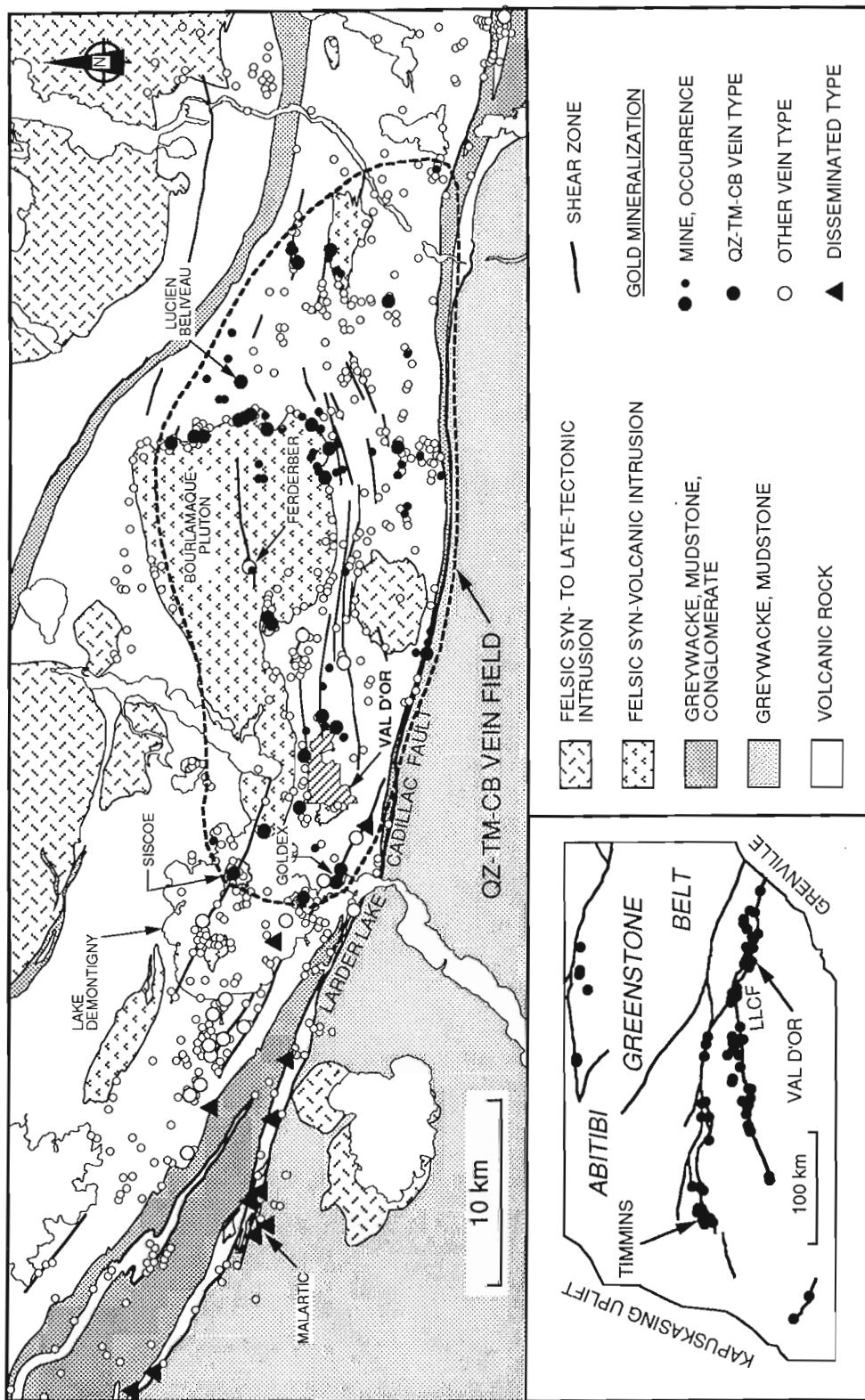


Figure 1. Simplified geological map of Val d'Or showing the distribution of different types of gold deposits; inset shows the location of the district within the Abitibi greenstone belt.

the author's observations and previous studies (in particular Robert and Brown, 1986a, b; Robert, 1990b), complemented by the deposit descriptions and summaries presented in Trudel and Sauvé (1992) and in Sauvé et al. (1993).

The majority of mined deposits in the district consist of one vein type or the other. Both types of veins were present and mined in only a small number of deposits, such as at Siscoe and Shawkey (Sauvé et al., 1993).

### Hydrothermal characteristics

Quartz-tourmaline-carbonate veins consist essentially of quartz, tourmaline (5-20 vol. %) and carbonate, with common scheelite and rare chlorite. In contrast, most other veins consist of quartz and carbonate, with variable but subordinate amounts of chlorite and, in a few cases, epidote. Pyrite is the dominant sulphide mineral in all vein types and it is accompanied in some deposits by chalcopyrite or pyrrhotite. The available data indicate that Au:Ag ratios have the same range of values for all types of veins, i.e. from 4:1 to about 10:1.

Hydrothermal alteration associated with the vast majority of veins involved carbonatization of the wall rocks over variable distances away from the veins, accompanied by progressive destruction of epidote and amphiboles (if present). Small quantities of sulphide minerals, generally pyrite, are present immediately adjacent to the veins. Hydrothermal alteration associated with quartz-tourmaline-carbonate veins systematically involved a generally abrupt and complete destruction of chlorite, giving the rock a typical bleached appearance (Fig. 2; Robert and Brown, 1986b). This is in contrast with alteration around other veins, where chlorite tends to be stable except close to the vein where it becomes progressively less abundant and in some cases completely destroyed. Altered wall rocks around quartz-tourmaline-carbonate veins may also contain variable amounts of tourmaline. Sauvé et al. (1993) have noted that sericite is an important alteration product in deposits ascribed to quartz-tourmaline-carbonate vein category, in contrast with other vein-type deposits, where albite is important.

### Structural characteristics

The majority of vein-type deposits at Val d'Or occur within, or are spatially associated with, shear zones. The veins form discontinuous lenses, reaching 100 m in length within the shear zones, and are typically subparallel to the local foliation. Quartz-tourmaline-carbonate veins are generally more continuous in shear zones than the other veins. In addition to those hosted in the shear zones, quartz-tourmaline-carbonate veins also commonly form a set of subhorizontal veins that



**Figure 2.** Undeformed quartz (white)-tourmaline (black)-carbonate veins with typical bleached alteration haloes, illustrating the typical association of subhorizontal extensional veins with steeply-dipping fault veins. Cross-section; field of view is 2 m wide; Goldex deposit. GSC 1993-275C

**Table 1.** Summary of characteristics of quartz-tourmaline-carbonate and other veins.

	QUARTZ-TOURMALINE-CARBONATE	OTHER VEINS
<b>MINERAL ASSEMBLAGES</b>	Quartz, tourmaline, carbonate, scheelite Pyrite ± chalcopyrite, pyrrhotite	Quartz, carbonate, chlorite, Pyrite ± chalcopyrite, pyrrhotite
<b>HYDROTHERMAL ALTERATION</b>	Carbonate, sericite ± albite, tourmaline Chlorite-destructive	Carbonate, albite ± sericite Chlorite generally stable
<b>DISTRIBUTION</b>	Mostly east of Lac Demontigny	Many deposits centered on Lake Demontigny
<b>STRUCTURAL SITES</b>	Associated with third-order shear zones	Associated with second-order shear zones
<b>GEOMETRY AND STRUCTURE</b>	Moderate to steep veins in shear zones and subhorizontal veins outside shear zones Undeformed	Steep veins parallel to foliation Commonly deformed (boudinaged, folded)
<b>TIMING CONSTRAINTS</b>	Only cut by Proterozoic diabase dykes	Commonly cut by dykes of variable composition

extend outside the shear zones (Fig. 2; see below); as indicated by Sauvé et al. (1993), these subhorizontal veins are not present west of Lake Demontigny (Fig. 1), where quartz-tourmaline-carbonate veins are absent. Quartz-tourmaline-carbonate veins are typically associated with small,



**Figure 3.** Quartz-carbonate vein overprinted by foliation. Cross-section looking east; Ferderber deposit. GSC 1993-275E



**Figure 4.** Quartz-carbonate vein cut by a narrow mafic dyke; note that the dyke itself is overprinted by the foliation. Steel plate in center of photo is 10 x 10 cm; Kierens deposit. GSC 1993-275B

third-order shear zones (Robert, 1990b), whereas a large number of the other vein-type deposits are spatially associated with shear zones of the second order.

Quartz-tourmaline-carbonate veins are very well preserved (Fig. 2) and display no evidence of significant overprinting deformation (Robert and Brown, 1986a; Robert, 1990b). In contrast, veins in several other deposits display evidence of deformation within the shear zones: they are commonly boudinaged, foliated (Fig. 3), and, in some cases, such as those of the Ferderber deposit (Vu et al., 1987), they are folded.

### **Distribution**

The geographical distribution of vein-type deposits and occurrences is represented in Figure 1. The distribution of all known quartz-tourmaline-carbonate veins, compiled from field observations and available documentation, is also shown. It is very clear that quartz-tourmaline-carbonate veins have a restricted distribution and represent a subset of the entire vein population at Val d'Or. All the known occurrences of quartz-tourmaline-carbonate veins occur within a well defined area, approximately 40 km by 15 km (Fig. 1).

### **Age relationships**

Several geological elements suggest that quartz-tourmaline-carbonate veins represent one specific hydrothermal event, distinct from those indicated by other types of veins, and of different age. These include their unique hydrothermal fingerprint (presence or absence of tourmaline and scheelite), their different spatial distribution, and the fact that quartz-carbonate veins are commonly deformed whereas quartz-tourmaline-carbonate veins are not, as described above.

As pointed out by Sauvé et al. (1993), a large number of vein deposits at Val d'Or, irrespective of type, are spatially associated with dykes of different compositions. However, not all veins show the same timing relationships with dykes. In all observed cases, quartz-tourmaline-carbonate veins systematically cut across all the dykes present, including mafic ones, except for Proterozoic diabase dykes (see also Robert and Brown, 1986a; Tessier, 1990). In contrast, mafic dykes clearly crosscutting quartz-carbonate veins, previously only reported at the Siscoe mine (Hawley, 1932; Backman, 1936), have been observed by the author at the Kierens, Siscoe and Norlartic mines, as illustrated in Figures 4 and 5. Some of the dykes cutting these veins are also foliated (Fig. 4), indicating that deformation has overprinted both the veins and the dykes.

In a few mines, two types of veins are present and allow further clarification of their relative ages. This is the case at the Siscoe mine (Fig. 6), where a set of quartz-carbonate veins are cut by an albitite dyke and a mafic dyke (Fig. 5), which are in turn cut by a set of quartz-tourmaline-carbonate veins, indicating that they are of different ages. The mafic dyke cutting the quartz-carbonate vein in Figure 5 is carbonatized, which is consistent with superimposed hydrothermal activity related to the emplacement of the younger quartz-tourmaline-carbonate veins. The absolute time gap between the formation

of the different types of veins is unknown at present. However, given the differences in their structural sites and their distribution, it is unlikely that all veins represent different stages within a single hydrothermal event. It is well established that the veins of the quartz-tourmaline-carbonate type are younger than 2685 Ma, the age of the diorite-tonalite stock hosting quartz-tourmaline-carbonate veins at the Lamaque mine (Jemielita et al., 1989).

**QUARTZ-TOURMALINE-CARBONATE VEIN FIELD**

The above observations indicate that at least two distinct major episodes of gold-quartz vein formation took place in the Val d'Or district, each resulting in a different distribution of veins. All the known quartz-tourmaline-carbonate veins are confined to an area 40 km by 15 km, located west of Lake Demontigny, on the north side of the Cadillac tectonic zone (Fig. 1). Across this entire area, they have identical mineral assemblages, associated hydrothermal alteration, and consistent geometric and structural characteristics, which are briefly reviewed below.

Two main groups of quartz-tourmaline-carbonate veins are observed: moderately to steeply dipping fault veins, central to shear zones or narrow faults (Fig. 7), and associated sub-horizontal extensional veins that extend outside the shear zones. As documented in detail by Robert and Brown (1986a) and Robert (1990b), the quartz-tourmaline-carbonate fault veins occupy reverse to reverse-oblique shear zones and faults, and they formed during, and as a result of, active reverse slip. The distribution and orientation of extensional gash veins at the

terminations of fault veins, as illustrated in Figure 7, are also consistent with this interpretation. The orientations of the fault veins and extensional veins are relatively uniform across the vein field, as is the slip direction along the fault veins. Local deviations in vein orientation or slip direction can be accounted for by local refraction of stress trajectories related to the presence of strength anisotropies such as lithological contacts and dykes (see Belkabit et al., in press).

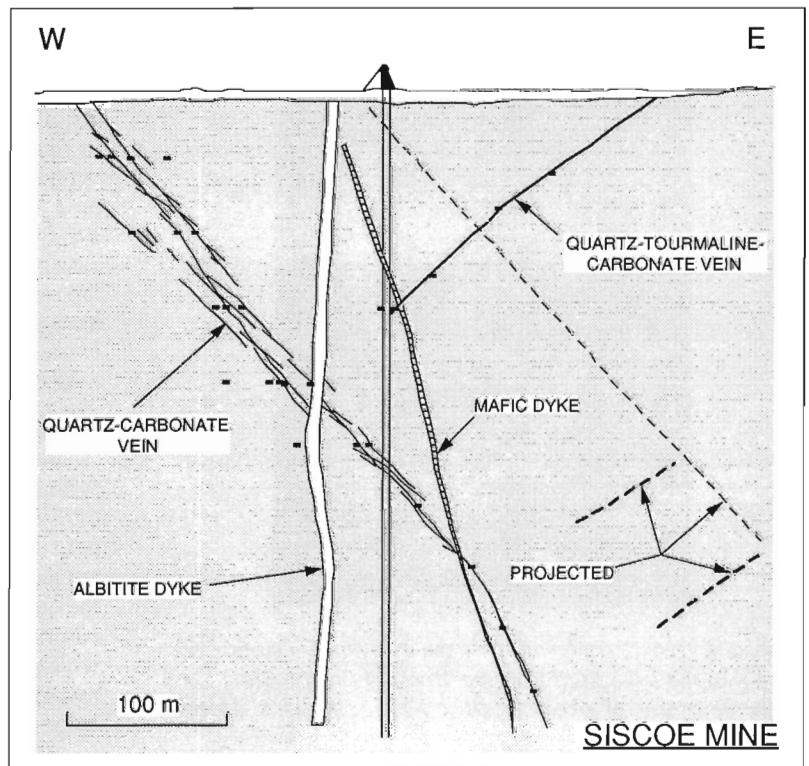
The nature and orientation of the two quartz-tourmaline-carbonate vein sets indicate that they developed in response to a horizontal, northerly-directed shortening (Robert, 1990b), consistent with that responsible for the D<sub>2</sub> regional increment of deformation. The quartz-tourmaline-carbonate



Figure 5. Quartz-carbonate vein cut at high angle by a fine grained mafic dyke. Siscoe deposit. GSC 1993-275A

Figure 6.

East-west cross-section through the Siscoe deposit illustrating crosscutting relationships between quartz-carbonate veins, albitite and andesite dykes, and younger quartz-tourmaline-carbonate veins. Adapted from Backman (1936).





**Figure 7.** Down-dip termination of a reverse fault vein with sigmoidal extensional veins also consistent with the reverse sense of motion. Cross-section looking east; field of view is 3 m wide; Lucien Beliveau deposit. GSC 1993-275F

veins and host structures overprint the  $S_2$  foliation and truncate  $F_2$  folds, but predate the  $D_3$  dextral strike-slip increment of deformation, which overprints and folds quartz-tourmaline-carbonate veins within the Cadillac tectonic zone (Robert, 1990b). The quartz-tourmaline-carbonate veins thus most likely formed during a late stage of the  $D_2$  deformation. The asymmetric folding of quartz-carbonate veins at the Ferderber deposit records reverse slip (Vu et al., 1987), and suggests that reactivation of existing quartz-carbonate veins and their host shear zones accompanied formation of the quartz-tourmaline-carbonate veins.

The remarkable hydrothermal and structural uniformity of the quartz-tourmaline-carbonate veins strongly suggests a single age for these veins. This, in turn, implies that they are related to the same hydrothermal event and that they are the manifestations of a single, large hydrothermal system. Given their outstanding uniformity of attributes over such an area, this group of quartz-tourmaline-carbonate veins should be referred to as a *vein field*. By analogy with pegmatite fields (Cerny, 1991), vein fields would be comprised of veins presenting nearly identical mineral assemblages, hydrothermal alteration, and structural setting, and that have formed approximately at the same time, over areas covering several tens to hundreds of square kilometres.

## DISCUSSIONS AND CONCLUSIONS

The recognition of at least two types of veins and the definition of a quartz-tourmaline-carbonate vein field have important implications for studies of vein-type gold deposits at Val d'Or. Because the veins are of at least two distinct ages and do not share a common origin, any geochemical, stable isotope, fluid inclusion, or geochronologic study of the Val d'Or deposits must be based on knowledge of which type (and age) of vein is being studied. The fact that some deposits can be comprised of two, unrelated generations of veins, and that in

some cases, quartz-tourmaline-carbonate veins could develop within, or along, pre-existing quartz-carbonate veins (Hawley, 1932), is another important point.

Considering the quartz-tourmaline-carbonate vein field, it appears that the individual deposits within the field are small components of a larger hydrothermal system, rather than representing isolated hydrothermal entities. This implies that any close spatial or temporal association between the veins and a particular geological element in one deposit (for example a particular type of intrusion; see Burrows and Spooner, 1989) loses its significance if it is not repeated in a number of other deposits within the same field. In addition, the dimensions of the vein field approximate the dimensions of the sink area of the hydrothermal system. In the case of the quartz-tourmaline-carbonate vein field at Val d'Or, the dimensions of the field require a crustal-scale hydrothermal system, as generally inferred from the close spatial association of gold deposits with crustal-scale fault zones (Eisenlohr et al., 1989; Kerrich and Wyman, 1990).

Another interesting implication of the presence of vein fields is that the distribution of veins within a field tracks the district-scale fluid flow at the time of mineralization. At Val d'Or, for example, the abundance of quartz-tourmaline-carbonate veins around the Bourlamaque pluton would suggest that the pluton margins were zones of enhanced fluid flow. This may also provide additional insight into the possible analogy between formation of quartz-tourmaline-carbonate veins and earthquake processes as proposed by Sibson et al. (1988) and more recently by Robert and Boullier (in press). The apparent centering of the quartz-tourmaline-carbonate vein field on the Bourlamaque pluton (Fig. 1) is either a coincidence or a reflection of the fluid flow pattern; there are no possible genetic links between the two, because the Bourlamaque pluton, dated at 2700 Ma (Wong et al., 1991), is at least 15 Ma older than the quartz-tourmaline-carbonate veins.

Kerrich et al. (1987) and Kerrich and Wyman (1990) pointed out the provinciality of O, C, Sr, and Pb isotopic composition of gold deposits between districts; they ascribed this provinciality to lithological differences in the source areas for these elements. It is possible that some of this provinciality also reflects the existence of different vein fields within and among gold districts.

Finally, it is not clear at present if all the other veins at Val d'Or define one or several coalescing vein fields of single or multiple ages; however, one can suggest that the dense cluster of vein within, and immediately west of, Lake Demontigny, where numerous dykes and intrusive bodies are also known to occur (Sauvé et al., 1993), represents one vein field or hydrothermal system. This illustrates that vein fields in gold districts can only be identified by a systematic documentation in the field of the types of veins present, including their distribution, their hydrothermal and structural relationships, as well as their timing relationships to other geological or structural events. Proper understanding of the genesis of vein-type gold deposits clearly requires consideration of *entire* hydrothermal systems; recognition of vein field represents an important step towards that goal.



## ACKNOWLEDGMENTS

I would like to thank Howard Poulsen and Dave Sinclair for their critical review of this document, and all the geologists who shared with me their knowledge of the Val d'Or gold deposits.

## REFERENCES

- Babineau, J.**  
1985: Géologie de la région de La Motte, Abitibi; Ministère de l'Énergie et des Ressources, Québec, ET 84-03, 17 p.
- Backman, O.L.**  
1936: Geology of Siscoe Mine; Canadian Mining Journal, v. 57, p. 467-475.
- Belkabit, A., Robert, F., Vu, L., and Hubert, C.**  
in press: The influence of dykes on auriferous shear zone development within granitoid intrusions: the Bourlamaque pluton, Val d'Or district, Abitibi greenstone belt; Canadian Journal of Earth Sciences, v. 30.
- Brommecker, R., Poulsen, K.H., and Hodgson, C.J.**  
1989: Preliminary report on the structural setting of gold at the Gunnar mine in the Beresford Lake area, Uchi Subprovince, southeastern Manitoba; in Current Research, Part C; Geological Survey of Canada, Paper 89-1C, p. 325-332.
- Burrows, D.R. and Spooner, E.T.C.**  
1989: Relationships between Archean gold quartz vein-shear zone mineralization and igneous intrusions in the Val d'Or and Timmins areas, Abitibi Subprovince, Canada; in The Geology of Gold Deposits: the Perspective in 1988, (ed.) R.R. Keys, W.R.H. Ramsay, and D.I. Groves; Economic Geology Monograph 6, p. 424-444.
- Card, K.D., Poulsen, K.H., and Robert, F.**  
1989: The Archean Superior Province of the Canadian Shield and its lode gold deposits; in The Geology of Gold Deposits: the Perspective in 1988, (ed.) R.R. Keys, W.R.H. Ramsay, and D.I. Groves; Economic Geology Monograph 6, p. 19-36.
- Cerny, P.**  
1991: Rare-element pegmatites. Part II: Regional to global environments and petrogenesis; Geoscience Canada, v. 18, p. 68-81.
- Desrochers, J.-P., Hubert, C., Ludden, J.N., and Pilote, P.**  
1993: Accretion of Archean oceanic plateau fragments in the Abitibi greenstone belt, Canada; Geology, v. 21, p. 451-454.
- Eisenlohr, B.N., Groves, D.I., and Partington, G.A.**  
1989: Crustal-scale shear zones and their significance to Archean gold mineralization in Western Australia; Mineralium Deposita, v. 24, p. 1-8.
- Green, A.H., Milkereit, B., Mayrand, L.J., Ludden, J.N., Hubert, C., Jackson, S.L., Sutcliffe, R.H., West, G.F., Verpaelst, P., and Simard, A.**  
1990: Deep structure of an Archean greenstone terrane; Nature, v. 344, p. 327-330.
- Hawley, J.E.**  
1932: The Siscoe gold deposit; Transactions of the Canadian Institute of Mining and Metallurgy, v. 35, p. 368-386.
- Jemielita, R.A., Davis, D.W., Krogh, T.E., and Spooner, E.T.C.**  
1989: Chronological constraints on the origin of Archean lode gold deposits in the southern Superior Province from U/Pb isotopic analyses of hydrothermal rutile and titanite; Geological Society of America, 1989 Annual Meeting, Abstracts with Programs, p. A351.
- Kerrich, R., Fryer, B.J., King, R.W., Willmore, L.M., and van Hees, E.**  
1987: Crustal outgassing and LILE enrichment in major lithosphere structures, Archean Abitibi greenstone belt: evidence on the source reservoir from strontium and carbon isotope tracers; Contributions to Mineralogy and Petrology, v. 97, p. 156-168.
- Kerrich, R. and Wyman, D.**  
1990: Geodynamic setting of mesothermal gold deposits: an association with accretionary tectonic regimes; Geology, v. 18, p. 882-885.
- Robert, F.**  
1990a: An overview of gold deposits in the Eastern Abitibi belt; in The Northwestern Quebec Polymetallic Belt, (ed.) M. Rive, P. Verpaelst, Y. Gagnon, J.-M. Lulin, G. Riverin, and A. Simard; Canadian Institute of Mining and Metallurgy, Special Volume 43, p. 93-105.  
1990b: Structural setting and control of gold-quartz veins of the Val d'Or area, southeastern Abitibi Subprovince; University of Western Australia, Publication No. 24, p. 164-209.
- Robert, F. and Boullier, A.-M.**  
in press: Mesothermal gold-quartz veins and earthquakes; in The Mechanical Involvement of Fluids in Faulting, USGS-Red Book Conference, United States Geological Survey, Open File Report.
- Robert, F. and Brown, A.C.**  
1986a: Archean gold-bearing quartz veins at the Sigma mine, Abitibi greenstone belt, Quebec. Part I: Geologic relations and formation of the vein system; Economic Geology, v. 81, p. 578-592.  
1986b: Archean gold-bearing quartz veins at the Sigma mine, Abitibi greenstone belt, Quebec. Part II: Vein paragenesis and hydrothermal alteration. Economic Geology, v. 81, p. 593-616.
- Sansfaçon, R. and Hubert, C.**  
1990: The Malartic gold district, Abitibi greenstone belt, Quebec: geological setting, structure and timing of gold emplacement at Malartic Goldfields, Barnat, East-Malartic, Canadian Malartic and Sladen mines; in The Northwestern Quebec Polymetallic Belt, (ed.) M. Rive, P. Verpaelst, Y. Gagnon, J.-M. Lulin, G. Riverin, and A. Simard; Canadian Institute of Mining and Metallurgy, Special Volume 43, p. 221-235.
- Sauvé, P., Imreh, L., and Trudel, P.**  
1993: Description des gîtes d'or de la région de Val d'Or; Ministère de l'Énergie et des Ressources, Québec, MM 91-03, 178 p.
- Sibson, R.H., Robert, F., and Poulsen, K.H.**  
1988: High angle reverse faults, fluid-pressure cycling, and mesothermal gold-quartz deposits; Geology, v. 16, p. 551-555.
- Tessier, A.C.**  
1990: Structural evolution and host rock dilation during emplacement of gold-quartz veins at the Perron deposit, Val d'Or, Quebec; M.Sc. thesis, Queen's University, Kingston, Ontario, 242 p.
- Trudel, P. and Sauvé, P.**  
1992: Synthèse des caractéristiques géologiques des gisements d'or du district de Malartic; Ministère de l'Énergie et des Ressources, Québec, MM 89-04, 113 p.
- Vu, L., Darling, R., Béland, J., and Popov, V.**  
1987: Structure of the Ferderber gold deposit, Belmoral Mines Ltd, Val d'Or, Quebec; Canadian Institute of Mining and Metallurgy Bulletin, v. 80, p. 68-77.
- Wong, L., Davis, D.W., Krogh, T.E., and Robert, F.**  
1991: U-Pb zircon and rutile chronology of Archean greenstone formation and gold mineralization in the Val d'Or region, Quebec; Earth and Planetary Science Letters, v. 104, p. 325-336.



# A preliminary report of porphyry Cu-Mo-Au and shear zone-hosted Cu-Au deposits in the Chibougamau area, Quebec<sup>1</sup>

W.D. Sinclair, P. Pilote<sup>2</sup>, R.V. Kirkham, F. Robert, and R. Daigneault<sup>3</sup>  
Mineral Resources Division

*Sinclair, W.D., Pilote, P., Kirkham, R.V., Robert, F., and Daigneault, R., 1994: A preliminary report of porphyry Cu-Mo-Au and shear zone-hosted Cu-Au deposits in the Chibougamau area, Quebec; in Current Research 1994-C; Geological Survey of Canada, p. 303-309.*

---

**Abstract:** The Chibougamau area, Quebec, has been important primarily for the production of copper and gold from sulphide-rich, shear zone-hosted deposits. Subeconomic porphyry deposits with minor amounts of molybdenum and gold also occur in the area. Preliminary observations suggest that both deposit types may be associated with intermineral felsic intrusions, and that intrusive and copper mineralizing events predated shear zone development; gold mineralization is more complex and, in part, postdates shearing. Future research will focus on the chronology of the intrusive, mineralization, and deformation events, and on the possible genetic links between the two types of deposits. The potential for economic porphyry-type deposits of copper, molybdenum, and gold will also be evaluated.

**Résumé :** La région de Chibougamau, au Québec, a surtout été importante pour la production de cuivre et d'or à partir de gisements logés dans des zones de cisaillement riches en sulfures. Des gisements porphyriques sous-économiques contenant de faibles quantités de molybdène et d'or sont également présents dans la région. Les observations préliminaires indiquent que ces deux types de gisements peuvent être associés à des intrusions felsiques mises en place pendant un épisode de minéralisation, ou entre deux épisodes minéralisateurs, et que les épisodes d'intrusion et de minéralisation en cuivre ont précédé la formation des zones de cisaillement; la minéralisation aurifère est plus complexe et est, en partie, postérieure au cisaillement. Les travaux futurs seront axés sur la chronologie des événements d'intrusion, de minéralisation et de déformation ainsi que sur les possibles liens génétiques entre les deux types de gisements. Le potentiel en gisements porphyriques de cuivre, de molybdène et d'or économiques sera également évalué.

---

<sup>1</sup> Contribution to Special Assistance Program for the Mining Sector of the Chapais-Chibougamau Region (1992-1995), under the Canada-Quebec Subsidiary Agreement on the Economic Development of the Regions of Quebec.

<sup>2</sup> Ministère de l'Énergie et des Ressources, 400 boul. Lamaque, Val d'Or, Québec J9P 3L4

<sup>3</sup> Université du Québec à Chicoutimi, Chicoutimi, Québec G7H 2B1

## INTRODUCTION

The Chibougamau area, Quebec, is one of the important but somewhat unique mining camps of the Abitibi greenstone belt. It contains typical volcanogenic massive sulphide deposits and mesothermal shear zone-hosted gold deposits, but has been important primarily for the production of copper and gold from sulphide-rich shear zones (Gobeil and Racicot, 1984). Sub-economic porphyry copper deposits with minor amounts of molybdenum and gold are also present (Kirkham, 1972; Cimon, 1973); some occur in close proximity to the metalliferous shear zones. In the Frotet Lake area, about 125 km to the north, a bulk tonnage deposit containing greater than 40 Mt averaging 1.4 g Au/t and 0.12% Cu, which might be mineable by open pit methods (The Northern Miner, November 16, 1992, p. 15), is a possible porphyry deposit (Falconbridge Ltd. geologists, pers. comm., 1992).

Initiated in the spring of 1993, this multidisciplinary research project is a collaborative effort by the Geological Survey of Canada, the Quebec Ministère de l'Énergie et des Ressources, the Université du Québec à Chicoutimi, and companies working in the area. It is directed at learning more about the porphyry and shear zone-hosted deposits and establishing any possible relationships between the two deposit types. This project is part of a larger concerted effort in the Chibougamau camp, which includes a Ph.D. research project on the Copper Rand deposit by M. Magnan at the Université du Québec à Chicoutimi, and a Ph.D. research project on the Portage deposit by A.C. Tessier at Queen's University. Copper Rand and Portage are the only operating mines in the area and provide excellent exposures of shear zone-hosted ore.

Our work is centred on the shear zone-hosted copper-gold deposits on Merrill Island and on the nearby Clark Lake porphyry copper-molybdenum deposit. The main objectives of this project are to document and correlate the geology of the Clark Lake porphyry deposit and the Merrill Island copper- and gold-bearing shear zones, and to establish a detailed chronology of intrusive, deformation, alteration, and metal deposition events. Within the framework of this research study, we also hope to evaluate the exploration potential for porphyry copper-molybdenum-gold deposits in the Chibougamau area, particularly the Clark Lake porphyry deposit. This paper presents results from the initial stage of fieldwork carried out in the summer of 1993.

## REGIONAL GEOLOGY

Archean rocks of the Chibougamau area consist of two mafic to felsic volcanic cycles (Roy Group) which are overlain by a volcanic-sedimentary sequence (Opemiska Group) (Daigneault and Allard, 1990; Daigneault et al., 1990; Chown et al., 1992). Roy Group volcanic rocks include, in ascending stratigraphic order, the Obatogamau Formation (mafic volcanic rocks), the Waconichi Formation (felsic volcanic rocks), the Gilman Formation (mafic volcanic rocks) and the Blondeau Formation (felsic volcanic, mafic volcanic, and

sedimentary rocks) (Daigneault and Allard, 1990). The Waconichi and Gilman formations have been intruded by the Doré Lake Complex, a major layered complex of gabbro and anorthosite (Allard, 1976; Daigneault and Allard, 1990; Fig. 1). The lowest exposed part of the Doré Lake Complex is composed of gabbroic and anorthositic rocks that form a massive unit as much as 2500 to 3600 m thick. These rocks are characterized by coarse grained, cumulus plagioclase crystals which are commonly replaced by albite and zoisite. They also contain most of the important copper-gold deposits of the Chibougamau camp. The central part of the Doré Lake Complex consists of layered rocks containing vanadium-rich magnetite layers. The upper part of the complex is represented by a thin border zone of anorthositic to gabbroic rocks or, in places, granophyric rocks. All rock units have been regionally deformed into broad north-south warps and isoclinally refolded about east-west axes (Daigneault and Allard, 1990); metamorphism produced greenschist facies assemblages (Allard, 1976). A few isolated remnants of relatively undeformed sedimentary rocks of Proterozoic age unconformably overlie the folded Archean rocks (outside the area shown in Fig. 1).

Felsic plutons, such as the Chibougamau pluton, occur in axial zones of major anticlines (Duquette, 1970; Daigneault and Allard, 1990). The Chibougamau pluton is a large body that lies to the south of the principal copper-gold deposits of the Chibougamau camp, mainly beneath Doré Lake and Lake Chibougamau (Fig. 1). It consists of four principal assemblages consisting of hornblende meladiorite, hornblende quartz diorite, biotite tonalite, and leucotonalite; however, compositional divisions are not distinct and intermediate compositions are also present (Racicot et al., 1984). Widespread foliation, particularly well developed in border phases, suggests that the pluton was emplaced prior to the main regional deformation. The age of the Chibougamau pluton, based on a single U-Pb analysis of zircon, is  $2718 \pm 2$  Ma (Krogh, 1982). Dykes of intermediate to felsic composition, at least some of which are likely related to the Chibougamau pluton, are associated with many of the copper-gold deposits (Jeffrey, 1959; Blecha, 1966; Maillet, 1978). A quartzfeldspar porphyry dyke northeast of Chibougamau, which has been dated at  $2711.7 \pm 9.4/-7.0$  Ma by U-Pb analysis of zircon, is probably comagmatic with the Chibougamau pluton (Mortensen, 1993).

Prominent structural features of the Chibougamau area include east- to northeast-trending faults or shear zones such as the Lac Sauvage Fault and the Doré Lake Fault, and southeast-trending shear zones (Fig. 1). The Lac Sauvage Fault is one of the most important fault systems in the area. It includes several east- to east-northeast-trending, anastomosing shear zones that form a belt of strongly foliated and deformed rocks about 20 km long and as much as 400 m wide. Iron carbonate alteration (ankerite and siderite) is a prominent feature along the fault system. Down-dip stretching lineations indicate a predominantly vertical component of movement; kinematic indicators suggest that the south side was down-dropped relative to the north (Daigneault and Allard, 1990).

The southeast-trending shear zones represent zones of ductile deformation as much as 300 m wide but limited in strike length, ranging from 2 to 5 km long. Most of these shear zones occur within the Doré Lake Complex, between the Chibougamau pluton and the Lac Sauvage Fault (Daigneault and Allard, 1990). Within these shear zones, anorthositic rocks of the Doré Lake Complex are strongly foliated and consist of sericite (paragonite)-chlorite schist, iron carbonate and, locally, chloritoid (Allard, 1956). Foliation generally dips steeply to the southwest. Although the relationships are not well understood, Daigneault and Allard (1990) suggested that the southeast-trending shear zones could be subsidiary deformation zones associated with the Lac Sauvage fault system. They are particularly important in the Chibougamau mining camp as they host most of the economically-important copper-gold deposits; exceptions are the Portage and Henderson deposits which are in northeast-trending shear zones (Allard, 1976; Guha, 1984; Daigneault and Allard, 1990; Fig. 1).

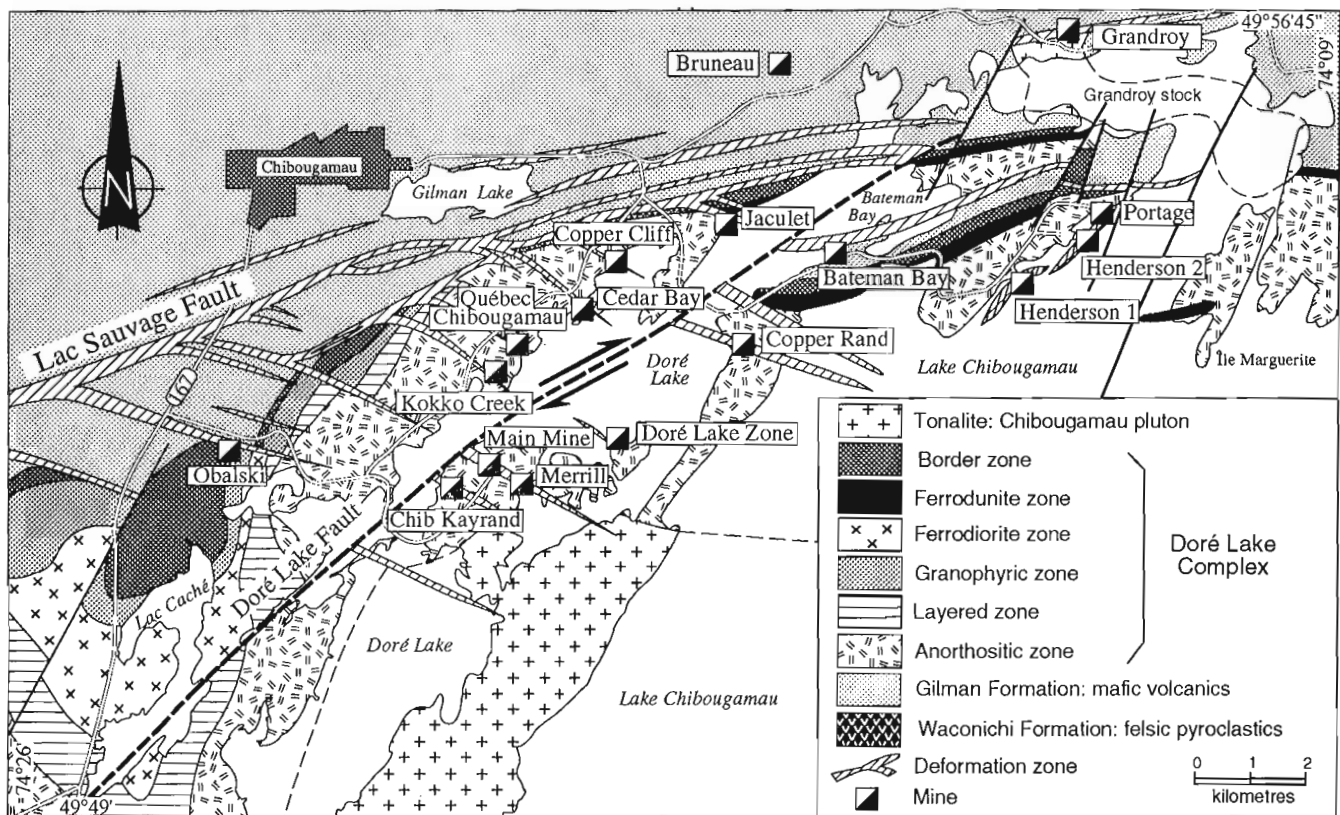
The Doré Lake Fault is a major east-northeast-trending fault more than 10 km long that lies mainly beneath Doré Lake. Where observed in underground workings and in surface outcrops, it varies from strongly foliated and mylonitized rocks to fault breccia in a zone 60 to 120 m wide (Malouf and Hinse, 1957; Jeffrey, 1959). It truncates, and thus postdates, the southeast-trending shear zones, including some of the

mineralized zones. Right-lateral displacement on the Doré Lake Fault is at least 1 km, based on lithological offset of the upper part of the Doré Lake Complex (Daigneault and Allard, 1990; Fig. 1).

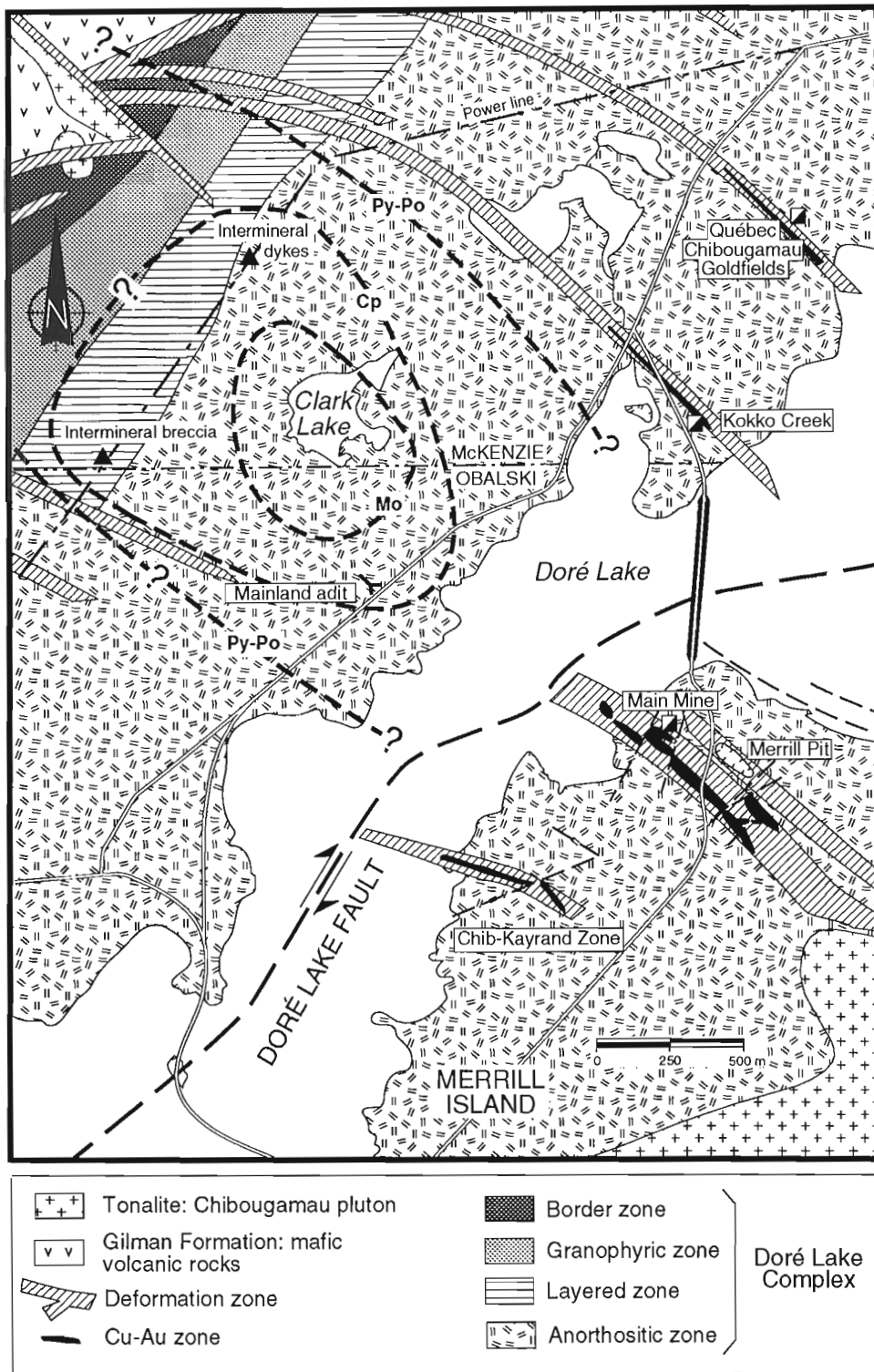
### SHEAR ZONE-HOSTED COPPER-GOLD DEPOSITS, MERRILL ISLAND

The main copper-gold deposits on Merrill Island occur within the Campbell Chibougamau-Merrill Island shear zone, which consists of an anastomosed mesh of smaller shear zones that form two subparallel branches (Fig. 2). The principal ore bodies in the Main mine on Merrill Island were confined to the southwestern branch of the Campbell Chibougamau-Merrill Island shear zone; ore bodies in the Merrill Pit occur in the northeastern branch. The Chib-Kayrand ore bodies are in a smaller, separate shear zone to the southwest (Fig. 2).

Overall, the Campbell Chibougamau-Merrill Island shear zone has a width of about 300 m and, on average, dips steeply to the southwest. Within the shear zone, the anorthositic host rocks range from massive, relatively undeformed to strongly foliated. Strongly foliated anorthosite typically consists of sericite-chlorite schist; massive anorthosite is generally altered to quartz, sericite, carbonate, and chlorite. Strongly



**Figure 1.** Simplified geological map of the Chibougamau area, showing the relationships between the Lac Sauvage Fault, the Doré Lake Fault, southeast-trending shear zones, and copper-gold deposits (modified from Daigneault and Allard, 1990).



**Figure 2.** Geology of the Clark Lake area and the northwestern part of Merrill Island; the distribution limits of chalcopyrite (Cp), molybdenite (Mo), and pyrite-pyrrhotite (Py-Po) at Clark Lake are indicated by the heavy dashed lines (geology modified from Ford, 1974; Daigneault and Allard, 1990).

foliated zones range from less than one metre to tens of metres wide. Contacts between the foliated and nonfoliated rocks vary from sharp to gradational.

Ore zones within the Main mine range from massive bodies consisting of more than 80% sulphides to diffuse bodies containing finely disseminated sulphide grains (Jeffrey, 1959). The massive bodies are confined mainly to zones of strong foliation; disseminated sulphides occur in both the foliated rocks and surrounding nonfoliated rocks. The main sulphide minerals are pyrrhotite, chalcopyrite, and pyrite; minor sulphide minerals include sphalerite, galena, cubanite, and valleriite (Jeffrey, 1959). Gold occurs mainly as discrete grains associated with chalcopyrite and pyrite.

Preliminary mapping in the Merrill Pit indicates that low-grade but more extensive mineralized zones, tens to hundreds of metres wide, surround the shear zone-hosted copper-gold deposits. These zones consist mainly of pyrite and/or pyrrhotite with minor amounts of chalcopyrite, as disseminated grains and in fractures cutting massive anorthosite. Minor but widespread molybdenite is also present, mainly in fractures and in late-stage quartz veinlets that crosscut pyrite- and chalcopyrite-bearing fractures. The gold content of these zones is not known at present. Overall sulphide content in the low-grade zones varies from <1% to 10%; the widespread and, to a large degree, fracture-controlled nature of the sulphides is similar to that in porphyry deposits.

Mapping in the Merrill Pit has confirmed the presence of several types of dykes, many of which have been described previously (e.g., Jeffrey, 1959; Blecha, 1966). One of the main types is a leucotonalite dyke that is medium grained equigranular to porphyritic and consists mainly of quartz and feldspar, with 2% chlorite (altered biotite?) and about 1% disseminated pyrite. Plagioclase is typically altered to sericite, giving the rock a pale, slightly yellowish-green colour. This dyke is well exposed in the southeast part of the pit where it forms a southeast-trending body as much as 50 m wide. It is similar in appearance and composition to the Chibougamau pluton to the southeast (Fig. 2) and is probably connected to it.

Also exposed in the Merrill Pit are 0.2 to 10 m wide dykes of feldspar porphyry. These dykes contain 30 to 40% phenocrysts, mainly white to yellowish, fine- to medium-grained feldspar; quartz phenocrysts are present in places. The matrix is a medium-grey, fine grained mixture of quartz, feldspar, and chlorite. At the southeastern end of the pit, feldspar porphyry dykes contain 1 to 2% pyrite and traces of chalcopyrite, mainly along fractures. Elsewhere in the southeastern part of the pit, similar feldspar porphyry dykes appear to be intermineral, i.e., they were emplaced during or between periods of mineralization: in places they truncate early pyrite- and chalcopyrite-bearing fractures and in turn are cut by later sulphide-bearing veinlets. One feldspar porphyry dyke, exposed on the northeastern side of the pit, contains traces of disseminated molybdenite.

Other dykes observed in the Merrill Pit include narrow (1 to 2 m wide) mafic dykes consisting mainly of fine grained quartz and chlorite. Some of these dykes are strongly foliated. Age relationships between the various dykes are not

clear. Near the southeast end of the pit, some mafic dykes cut the leucotonalite dyke; however, crosscutting relationships between the feldspar porphyry dykes and the leucotonalite dyke were not observed.

The leucotonalite dyke and the feldspar porphyry dykes are epizonal intrusions that appear to predate shear zone development. Although the larger dykes are in many places nonfoliated, smaller dykes and the margins of the larger dykes are commonly foliated. In other places, narrow shear zones crosscut the larger dykes. The relationship of the mafic dykes to shear zone development is less certain; they either predated or were synchronous with shear zone development.

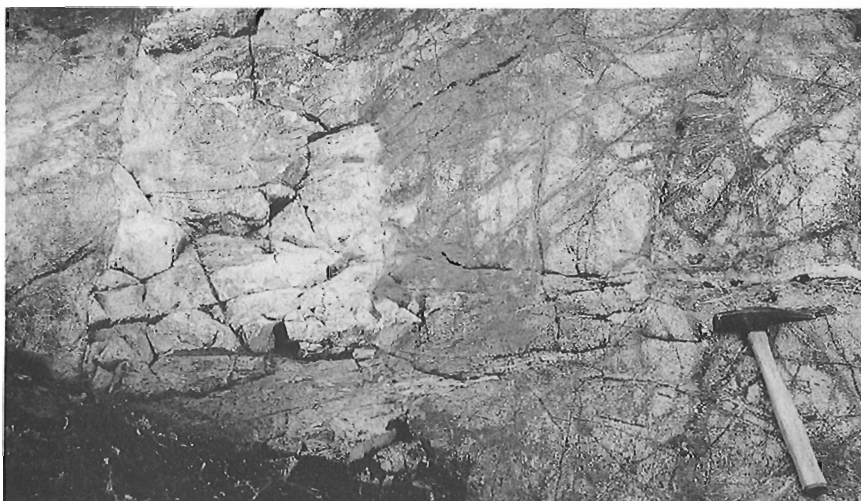
The association of the copper-gold deposits and the dykes in the Chibougamau camp is significant. Our preliminary observations on Merrill Island (see also Robert, 1994) suggest that copper-rich sulphide bodies within the foliated zones have been deformed, thus indicating that the main stages of sulphide deposition, as well as emplacement of the leucotonalite and feldspar porphyry dykes, predated the main penetrative deformation. These observations, plus the fact that some of the dykes are intermineral, support Duquette's (1970) conclusion that the copper deposits in the Doré Lake Complex may be genetically related to the Chibougamau pluton. Although gold is associated with copper in many places, the relationship between copper and gold is not necessarily simple. Some or all of the gold may have been emplaced originally at the same time as copper, but at least some was either introduced or remobilized later (e.g., Guha and Kanwar, 1987). As part of this project, we intend to examine closely the association of the dykes and the copper-gold deposits and to evaluate possible genetic relationships.

## **PORPHYRY COPPER-MOLYBDENUM-GOLD DEPOSITS, CLARK LAKE**

In the area surrounding Clark Lake, less than 2 km northwest of the copper-gold deposits on Merrill Island and about 1 km west of the Kokko Creek deposit (Fig. 2), massive anorthositic and gabbroic rocks of the Doré Lake Complex are highly fractured, sulphide-bearing, and pervasively altered over an area greater than 2 km<sup>2</sup>. The rocks are altered mainly to quartz, albite, and chlorite; pyrite, pyrrhotite, and locally, magnetite make up one to 10% of the rock. Pyrite is the main sulphide and is widespread in fractures and veinlets and as disseminated grains. Pyrrhotite is abundant in the eastern part of the area, and magnetite is abundant locally in the western part. Minor amounts of chalcopyrite and molybdenite are also present, especially in the area immediately surrounding Clark Lake.

Although the amounts of copper and molybdenum encountered in the Clark Lake area to date are minor, the nature of the occurrence and distribution of the sulphides and the presence of intermineral dykes are typical of porphyry-type deposits (Kirkham, 1971). For example, several stages of sulphide deposition are evident. An early stage, represented by magnetite veinlets, is cut by pyrite- and chalcopyrite-bearing fractures that form an extensive stockwork; late epidote-bearing





**Figure 3.**

*Pyritic stockworks cut by light-coloured intermineral feldspar porphyry dyke, Clark Lake area.*

veins cut the sulphide-bearing fractures locally. Molybdenite occurs with pyrite in sulphide-bearing fractures and in late-stage quartz veins that crosscut the pyritic fractures.

Distribution of pyrite-pyrrhotite, chalcopyrite, and molybdenite, based on unpublished company maps (Ford, 1974) and our own preliminary observations, are outlined in Figure 2. Chalcopyrite distribution may extend farther to the southeast, based on the presence of sparse chalcopyrite in outcrops along the northwestern side of Doré Lake; its extension to the northwest is uncertain due to lack of outcrop. The southwestern limit of pyrite and pyrrhotite is also poorly constrained due to lack of outcrop. Preliminary lithogeochemical data indicate that some areas are anomalous in zinc.

In the western part of the chalcopyrite zone, fragments of mineralized anorthosite occur in an intrusive breccia that is itself cut by mineralized veins. Farther to the north in the same zone, intermineral porphyry dykes crosscut the pyritic stockwork (Fig. 3). These and other related dykes in the Clark Lake area are similar to some of the porphyry dykes associated with the copper-gold deposits on Merrill Island, suggesting a possible temporal and genetic relationship between the shear zone-hosted copper-gold deposits and a porphyry deposit such as Clark Lake.

## **DISCUSSION**

Shear zone-hosted deposits of the Chibougamau camp have been an important source of copper and gold. From 1955 to 1992 they accounted for production of more than 40 Mt grading 1.5 to 2% Cu and 1 to 2 g Au/t (Gobeil and Racicot, 1984; Canadian Mines Handbooks, 1984-1992). Porphyry deposits generally have not been considered as desirable exploration targets in the Canadian Shield, primarily because they have been thought to occur only in young orogenic belts. Furthermore, exploration of porphyry deposits in the Chibougamau area to date has outlined deposits that are too low grade or too small to be economic. However, Precambrian

porphyry deposits are being mined at Malanjkhand in India, where estimated reserves are 789 Mt averaging 0.83% Cu, 0.004% Mo, 0.2 g Au/t, and 6 g Ag/t (Sikka et al., 1991), and at Tongkuangyu in China, where reserves are about 380 Mt grading 0.67% Cu (Kirkham and van Staal, 1990). At the Boddington Gold Mine in Western Australia, gold is recovered from a lateritic deposit derived from primary, porphyry-type copper-gold-molybdenum-bismuth-tungsten zones in Archean rocks (Roth et al., 1991). In view of these deposits, and the discovery of a possible economic gold-copper porphyry deposit in the Frotet Lake area to the north of Chibougamau, porphyry deposits in the Canadian Shield warrant more in-depth examination.

The Chibougamau area was selected for study because it contains several, albeit low-grade, porphyry-type deposits such as Clark Lake. Furthermore, these deposits may be genetically related to the shear zone-hosted copper-gold deposits in the area. Chronological relationships are not yet entirely clear, but our initial observations suggest that sulphide-rich copper mineralization predated shear zone development and was associated closely in time with the emplacement of felsic dykes. However, some stages of mineral deposition, particularly those involving gold, postdate deformation; others may have been synchronous with deformation. Future work will focus on documenting the geology and establishing the detailed chronology of intrusive, metal deposition, alteration, and deformation events in the study area.

## **ACKNOWLEDGMENTS**

We are grateful to SOQUEM geologists, particularly Daniel Bernard, for information and general co-operation, and to Jules Cimon (MERQ) for helpful discussions and guided visits to numerous localities. The Resident Geologist for the Ministère de l'Énergie et des Ressources in Chibougamau, Rémy Morin, provided accommodation and other logistic support. Howard Poulsen reviewed the manuscript and offered helpful comments.



---

**REFERENCES**


---

- Allard, G.O.**  
 1956: The geology of a portion of McKenzie township, Chibougamau district, Quebec; Ph.D. thesis, Johns Hopkins University, Baltimore, Maryland, 168 p.  
 1976: Doré Lake Complex and its importance to Chibougamau geology and metallogeny; Ministère des Richesses Naturelles; DP-368, 446 p.
- Blecha, M.**  
 1966: A study of the variation in chemical composition of certain dykes at the Campbell Chibougamau mine; M.Sc. thesis, McGill University, Montreal, Quebec, 65 p.
- Chown, E.H., Daigneault, R., Mueller, W., and Mortensen, J.K.**  
 1992: Tectonic evolution of the Northern Volcanic Zone, Abitibi belt, Quebec; Canadian Journal of Earth Sciences, v. 29, p. 2211-2225.
- Cimon, J.**  
 1973: Possibility of an Archean porphyry copper in Quebec; Canadian Mining Journal, v. 94, p. 57.
- Daigneault, R. and Allard, G.O.**  
 1990: Le Complexe du lac Doré et son environnement géologique, Région de Chibougamau; Ministère de l'Énergie et des Ressources du Québec, MM89-03.
- Daigneault, R., St-Julien, P., and Allard, G.**  
 1990: Tectonic evolution of the northeast portion of the Archean Abitibi greenstone belt, Chibougamau area, Quebec; Canadian Journal of Earth Sciences, v. 27, p. 1714-1736.
- Duquette, G.**  
 1970: Archean stratigraphy and ore relationships in the Chibougamau district; Quebec Department of Natural Resources, Special Paper 8, 16 p.
- Ford, G.M.**  
 1974: Mainland property, assessment report, Campbell Chibougamau Mines Ltd; Ministère de l'Énergie et des Ressources du Québec, filière des travaux statutaires, GM-30763.
- Gobeil, A. and Racicot, D.**  
 1984: Chibougamau: histoire et minéralisations; in Chibougamau, Stratigraphy and Mineralization, (ed.) J. Guha and E.H. Chown; The Canadian Institute of Mining and Metallurgy, Special Volume 34, p. 261-270.
- Guha, J.**  
 1984: Hydrothermal systems and correlations of mineral deposits in the Chibougamau mining district – an overview; in Chibougamau, Stratigraphy and Mineralization, (ed.) J. Guha and E.H. Chown; The Canadian Institute of Mining and Metallurgy, Special Volume 34, p. 517-534.
- Guha, J. and Kanwar, R.**  
 1987: Vug-brines – fluid inclusions: a key to the understanding of secondary gold enrichment processes and the evolution of deep brines in the Canadian Shield; in Saline Water and Gases in Crystalline Rocks, (ed.) P. Fritz and S.K. Frape; Geological Association of Canada, Special Paper 33, p. 95-101.
- Jeffrey, W.G.**  
 1959: The geology of the Campbell Chibougamau mine; Ph.D. thesis, McGill University, Montreal, Quebec, 185 p.
- Kirkham, R.V.**  
 1971: Intermineral intrusions and their bearing on the origin of porphyry copper and molybdenum deposits; Economic Geology, v. 66, p. 1244-1249.  
 1972: Geology of copper and molybdenum deposits; in Report of Activities, Part A: April to October, 1971, Geological Survey of Canada, Paper 72-1, p. 82-87.
- Kirkham, R.V. and van Staal, C.**  
 1990: Bizigou-type stratiform copper deposits, Zhongtiaoshan district, Shanxi, China: diagenetic and/or metamorphic concentration of copper?; Geological Association of Canada/Mineralogical Association of Canada Annual Meeting, Program with Abstracts, v. 15, p. A70.
- Krogh, T.E.**  
 1982: Improved accuracy of U-Pb zircon ages by the creation of more concordant systems using air abrasion techniques; Geochimica et Cosmochimica Acta, v. 46, p. 637-649.
- Maillet, J.**  
 1978: Pétrographie et géochimie des dykes du camp minier de Chibougamau; M.Sc. thesis, Université du Québec à Chicoutimi, Chicoutimi, Quebec, 150 p.
- Malouf, S.E. and Hinse, R.**  
 1957: Campbell Chibougamau Mines; in Structural Geology of Canadian Ore Deposits, Volume II, The Canadian Institute of Mining and Metallurgy, p. 441-449.
- Mortensen, J.K.**  
 1993: U-Pb geochronology of the eastern Abitibi Subprovince. Part 1: Chibougamau - Matagami - Joutel region; Canadian Journal of Earth Sciences, v. 30, p. 11-28.
- Racicot, D., Chown, E.H., and Hanel, T.**  
 1984: Plutons of the Chibougamau-Desmaraisville belt: A preliminary survey; in Chibougamau, Stratigraphy and Mineralization, (ed.) J. Guha and E.H. Chown; The Canadian Institute of Mining and Metallurgy, Special Volume 34, p. 178-197.
- Robert, F.**  
 1994: Timing relationships between Cu-Au mineralization, dykes, and shear zones in the Chibougamau camp, northeastern Abitibi Subprovince, Quebec; in Current Research 1994-C; Geological Survey of Canada.
- Roth, E., Groves, D.E., Anderson, G., Daley, L., and Staley, R.**  
 1991: Primary mineralization at the Boddington Gold mine, Western Australia: an Archean porphyry Cu-Au-Mo deposit; in Brazil Gold '91, The Economics Geology, Geochemistry and Genesis of Gold Deposits, (ed.) E.A. Ladeira; Proceedings of Gold '91, An International Symposium on the Geology of Gold, Belo Horizonte, 1991, A.A. Balkema, Rotterdam, p. 481-488.
- Sikka, D.B., Petruk, W., Cherukupalli, E.N., and Zhang, Z.**  
 1991: Geochemistry of secondary copper minerals from Proterozoic porphyry copper deposit, Malanjkhand, India; in Applied Mineralogy in Exploration, (ed) W. Petruk, A.H. Vassiliou, and D.H. Hausen; Ore Geology Reviews, v. 6, p. 257-290.

---

 Geological Survey of Canada Project 900019



# Oceanic allochthons in an Archean continental margin sequence, Vizien greenstone belt, northern Quebec

T. Skulski, J.A. Percival, and R.A. Stern  
Continental Geoscience Division

*Skulski, T., Percival, J.A., and Stern, R.A., 1994: Oceanic allochthons in an Archean continental margin sequence, Vizien greenstone belt, northern Quebec; in Current Research 1994-C; Geological Survey of Canada, p. 311-320.*

---

**Abstract:** The Vizien belt comprises tectonic panels of mature arc rocks, a continental rift sequence, and an oceanic allochthon. The 2.724 Ga arc sequence contains mafic to felsic calc-alkaline lavas and metasediments. The <2.718 Ga rift package comprises metasediments which rest unconformably on 2.9 Ga tonalite, overlain by mafic to felsic tholeiitic lavas. The allochthonous oceanic panel is floored by mélange or serpentinite, and comprises peridotite/gabbro sills intruded into submarine basalts and sediments. The arc lavas are LREE-enriched with  $\epsilon_{Nd}$  of +0.50; rift lavas have higher LREE abundances and lower  $\epsilon_{Nd}$  (0.33 to -0.47); whereas oceanic peridotite sills (to F<sub>087</sub>) have REE contents and  $\epsilon_{Nd}$  values (1.34 to 2.94) reflecting depleted mantle derivation. Early marine sediments in the Vizien arc sequence indicate an island arc setting. Later marginal basin formation may have produced juvenile oceanic crust. Subsequent orogeny involved oceanic crustal obduction, basement-cored nappe emplacement, isoclinal folding, high-T metamorphism, late folding and faulting.

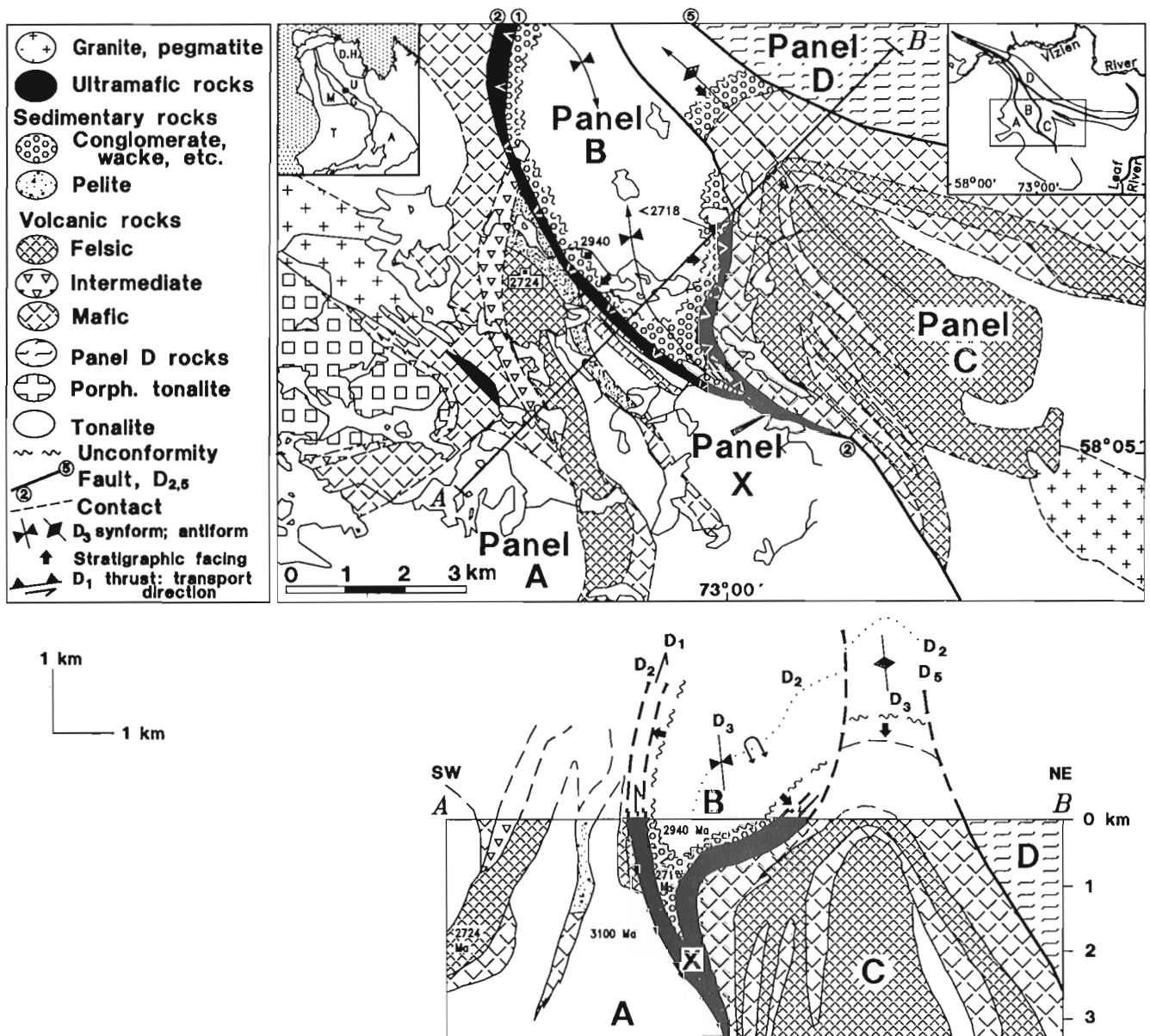
**Résumé :** La ceinture de roches vertes de Vizien englobe des panneaux tectoniques composés de roches d'arc mature, une séquence de rift continental et un allochtone océanique. La séquence d'arc, datée à 2,724 Ga, contient des laves calco-alkalines, mafiques à felsiques, et des métasédiments. L'ensemble de roches du rift, dont l'âge est de <2,718 Ga, englobe des métasédiments reposant en discordance sur une tonalite de 2,9 Ga, et est surmonté par des laves tholéiitiques, mafiques à felsiques. Le plancher du panneau de roches océaniques allochtones est constitué d'un mélange ou de serpentinite, et renferme des filons-couches de péridotite/gabbro mis en place dans des basaltes et sédiments sous-marins. Les laves d'arc sont enrichies en terres rares légères avec un  $\epsilon_{Nd}$  de +0,50; les laves de rift présentent des niveaux d'abondance des terres rares légères plus élevés et ont des valeurs de  $\epsilon_{Nd}$  moindres (0,33 à -0,47); les filons-couches de péridotite océanique (composition jusqu'à F<sub>087</sub>) ont des teneurs en terres rares et des valeurs de  $\epsilon_{Nd}$  (1,34 à 2,94) indiquant qu'elles sont dérivées d'un manteau appauvri. Les sédiments marins initiaux de la séquence d'arc de Vizien indiquent un milieu d'arc insulaire. Il est possible que la formation ultérieure d'un bassin marginal ait abouti à la formation d'une croûte océanique juvénile. L'orogénèse ultérieure s'est traduite par l'obduction de croûte océanique, la mise en place d'une nappe de charriage à noyau composé de roches du socle, la formation de plis isoclinaux, un métamorphisme de température élevée, et la formation de plis et failles tardifs.

**INTRODUCTION**

It has become increasingly evident that many Archean greenstone belts do not represent simple, thick cyclic accumulations of volcano-sedimentary rocks in synclinal basins. Various field-based studies have cited evidence of structural repetition involving recumbent folds and thrust faults (Coward et al., 1976; de Wit, 1982; Martyn, 1987; Kusky, 1990). Thrust repetition has also been documented through combined field and U-Pb geochronological studies (Ayles and Corfu, 1991) and is consistent with seismic reflection data (Green et al. 1990). Evidence of large-scale horizontal

displacement provides an attractive mechanism to explain the juxtaposition of oceanic terranes with continentally derived Archean sequences (Hoffman, 1991).

Current tectonic models of Archean granite-greenstone terranes in the Superior and Slave Provinces of the Canadian Shield emphasize the role of accretionary tectonics involving assembly of arc terranes (Card, 1990; Kusky, 1989) or fragments of oceanic plateaus (Desrochers et al., 1993). Recently described greenstone belts in the northeastern Superior Province (Moorhead, 1989; Percival and Card, 1992b) place new constraints on the assembly of the Archean craton (Percival et al., 1993a).



**Figure 1.** a) Geological map of the Vizien greenstone belt. Inset maps show location with respect to northern Ungava peninsula. Line of section (A-B) in (b) is shown. Numbers adjacent to faults refer to deformation sequence. b) Down plunge (D<sub>3</sub>) schematic cross section. An average plunge of 58°N was calculated on the basis of D<sub>3</sub> stretching lineations and minor folds over an area ~3 km northwest and southeast of the line of section.

The Vizien greenstone belt of the Minto block (Fig. 1) was revisited during the 1993 field season to investigate the structural context of a group of rocks recognized geochemically as oceanic in origin. This report builds on previous descriptions of the belt as a collage of fault-bounded terranes (Percival and Card, 1992a; Percival et al., 1993a), in assessing the tectonic setting of each lithotectonic panel, and establishing a structural chronology. The field observations are supported by whole-rock geochemical and Sm-Nd isotopic data.

## REGIONAL GEOLOGICAL SETTING

The Minto block, characterized by northwesterly structural and aeromagnetic trends, is composed mainly of plutonic rocks, divided into four lithotectonic domains (Fig. 1, inset A; Percival et al., 1991). The Vizien belt forms part of the Goudalie domain of tonalitic and metavolcanic rocks, the central spine of the Minto block. It is bordered to the west by the Lake Minto domain of orthopyroxene-bearing granitoid rocks containing enclaves of high-grade supracrustal rock. Both the Tikkerutuk domain to the west, and the Utsalik domain to the east consist of granodiorite and granite without supracrustal relicts.

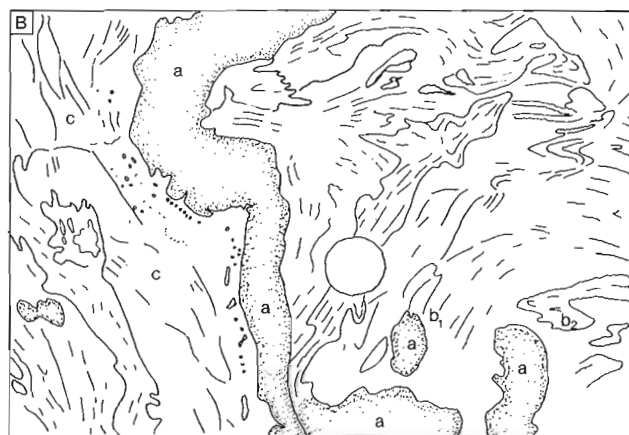
The Goudalie domain can be traced as an aeromagnetic low for 700 km, from the western Cape Smith belt to the northern Ashuanipi complex (Fig. 1; Percival et al., 1992). It consists of tonalitic rocks, with sparse relicts of metavolcanic and metasedimentary rock, including the well preserved Vizien greenstone belt (Fig. 1; Percival and Card, 1992a). Metamorphic grade is generally amphibolite facies, except for local greenschist facies in the Vizien belt and granulite facies along the eastern edge of Goudalie domain adjacent to pyroxene-bearing plutons of Utsalik domain. Tonalitic rocks have yielded U-Pb zircon ages between 3.1 Ga and 2.9 Ga, and late granodiorite plutons, 2702 Ma (Percival et al., 1992).

## VIZIEN GREENSTONE BELT

The 40 by 10 km Vizien belt consists of five discrete lithotectonic panels (Fig. 1; Percival et al., 1993b) separated by faults of different ages. On the west, panel A is a homoclinal, east-facing, moderately east-dipping assemblage of mafic to felsic volcanic rocks, intruded at its base by tonalite. The roof of the quartz-porphyritic tonalite has dacitic and andesitic chill margins and dykes, suggesting that it is a syn-volcanic intrusion. The base of the volcanic sequence contains plagioclase-phyric andesite, overlain by basalt with lenses of sulphidic iron-formation and intruded by ultramafic sills, with an overlying sequence of andesite, dacite,  $2724 \pm 1$  Ma rhyolite, pelitic schist, siltstone and minor conglomerate. Xenoliths of andesite in the dacite unit indicate that the stratigraphic sequence is normally facing to the northeast. Upward shoaling of the sequence is indicated by a change from banded iron-formation and hydrothermally altered basalt (cordierite-anthophyllite-cummingtonite) of probable submarine origin, to units of arkose and conglomerate of likely shallow marine origin near the top. Panel A is in fault contact with structurally overlying units of panel B/X (Fig. 1).

Panel B consists of a central core of tonalite, overlain unconformably (Percival et al., 1993b) by a thin autochthonous metasedimentary unit, including basal conglomerate. A granite cobble from the unit contains 2718 Ma zircon, providing a maximum age for deposition (Fig. 1). Mineral assemblages in the overlying schist indicate metamorphism to mid-amphibolite facies. In one location, a thin unit of mafic volcanic rocks and sills lies conformably on schist (Percival et al., 1993b).

A sheet of submarine ultramafic and mafic rocks, previously considered to be part of panel B (Percival and Card, 1992a; Percival et al., 1993a), was recognized as a discrete fault-bounded lithotectonic entity and called panel X (Fig. 1). The sheet wraps around and underlies panel B in synformal geometry (Fig. 1b). Its basal contact is tectonic, marked by a serpentinite layer up to 30 m thick, and local *mélange*. The <10-m-thick *mélange* pods consist of a serpentinitic matrix with angular and rounded fragments on the 1-50 cm scale of variably deformed gabbro, serpentinite and rare chert (Fig. 2). Blocks with massive to contorted or mylonitic internal structure have random orientation, giving a chaotic appearance to the *mélange* that contrasts with the simple layering of structurally lower and higher stratified units. Ultramafic rocks



**Figure 2.** Upper panel B *mélange* structurally underlying allochthonous panel X. Shown are gabbroic blocks (a) in a serpentinite matrix that shows local discordance between adjacent, folded domains (b1 vs b2), in contact with less deformed diorite (c). GSC 1993-246A

within panel X comprise peridotite sills and minor flows. Pillowed mafic units and layered sills indicate symmetrical outward facing with respect to the panel B unconformity. Closure of the unit in the south, together with north-plunging lineations which indicate regional plunge, suggest downward facing of the B/X assemblage, making the structure a synformal anticline (Fig. 1b).

Panel C to the east consists mainly of a mafic-felsic volcanic sequence exposed in a north-plunging antiform (Fig. 1). The volcanic rocks structurally overlie a unit of polymict conglomerate. Although not exposed, the contact between conglomerate, with large clasts of tonalite, and structurally underlying, weathered (sapolithic) tonalite is probably unconformable, based on its similarity to the basement-cover relationship well exposed in adjacent panel B (Percival et al., 1993a). The volcanic assemblage consists of a basal unit of massive basalt, overlain by a thin lens of south-facing, interbedded arkose and conglomerate, overlain by andesite with granitoid xenoliths, and a thick upper unit of rhyodacite

and massive rhyolite. The structurally highest unit, a fine grained felsic schist, is bordered to the south by tonalitic gneiss. A strong, steeply dipping axial planar foliation with parallel quartz veins and pegmatite dykes characterize panel C. In light of the northerly fold plunge and southward stratigraphic facing, the structure is interpreted as an antiformal syncline (Fig. 1b).

Panels B and C have common stratigraphic features, including tonalitic basement with muscovitic alteration near an exposed or inferred unconformity, and basal conglomerate overlain by sedimentary schist, suggesting a correlation at this stratigraphic level. The tonalite-conglomerate contact is off-set sinistrally less than 1 km along the B/X-C fault contact (Fig. 1a).

A cataclastic fault zone separates panels C and D, which is an east-dipping package of mafic and felsic schists with peridotite pods (Percival and Card, 1992a). Although it contains rock types common to panels B and C, an intense tectonic shear fabric renders stratigraphic correlation impossible.

**Table 1.** Representative chemical analyses.

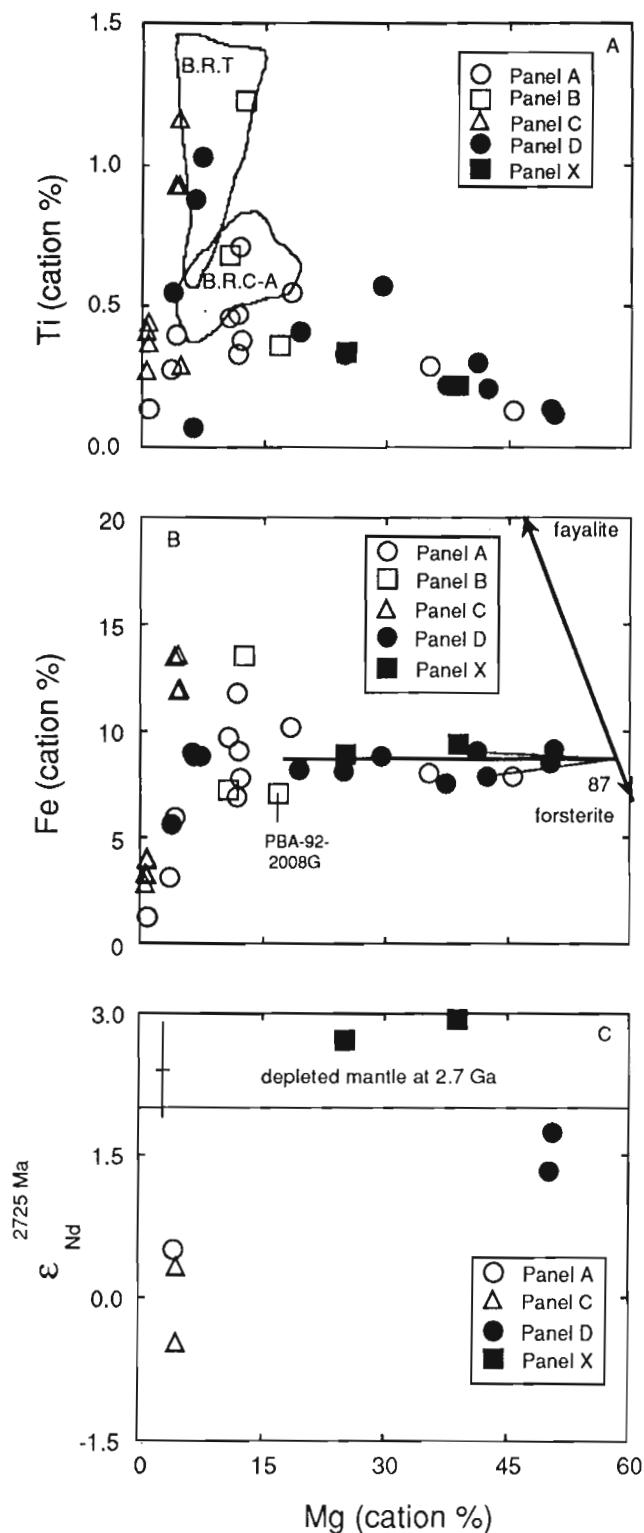
	MLB91002A		PBA91185		MLB91001		PBA2008G		PBA91188		PBA9166		PBA91107		PBA92011	
	MLB91004A		MLB91003B		PBA91100		PBA91187		PBA9169		PBA91170		PBA91104			
Panel	A	A	A	A	A	B	B	C	C	C	C	D	D	D	X	
Rock	PER	BAS	AND	DAC	RHY	BAS	BAS	BAD	AND	DAC	RHY	PER	BAD	AND	PER	
SiO <sub>2</sub>	43.20	51.60	55.95	65.00	73.30	50.90	52.40	53.25	56.20	69.80	73.40	42.36	53.10	60.90	24.80	
TiO <sub>2</sub>	0.19	0.99	0.57	0.37	0.20	1.67	0.52	1.61	1.29	0.52	0.38	0.21	0.10	0.76	0.31	
Al <sub>2</sub> O <sub>3</sub>	3.40	12.60	18.68	14.70	15.00	12.90	11.90	14.76	13.90	13.10	12.30	1.88	15.70	16.00	6.50	
MgO	32.90	8.43	2.98	2.33	0.65	8.67	12.10	3.27	3.28	0.57	0.38	39.14	4.48	2.65	27.20	
FeO	10.17	11.40	7.62	0.00	1.65	16.61	9.12	13.56	11.88	4.04	3.26	11.87	11.23	6.96	11.78	
MnO	0.17	0.19	0.11	0.06	0.03	0.02	0.18	0.18	0.15	0.08	0.05	0.20	0.18	0.11	0.22	
CaO	2.45	9.60	8.42	3.90	1.98	5.55	8.88	6.66	6.04	1.54	0.58	2.88	8.07	6.25	1.14	
Na <sub>2</sub> O	0.03	1.90	3.43	3.70	4.19	1.00	2.70	3.67	3.40	3.50	4.50	0.11	3.10	2.90	0.03	
K <sub>2</sub> O	0.05	0.93	1.23	2.19	1.94	0.05	0.06	1.17	2.29	4.87	2.93	0.00	1.35	1.22	0.05	
P <sub>2</sub> O <sub>5</sub>	0.03	0.09	0.14	0.11	0.07	0.11	0.04	0.36	0.25	0.10	0.06	0.02	0.19	0.14	0.03	
Rb	18	37	44	88	98	10	10	28	210	120	94		39	43	10	
Sr	25	190	350	560	520	34	120	500	390	160	95		180	190	20	
Ba	50	250	360	560	550	70	40	500	670	400	620		170	280	40	
Sc	11	28		8	3	42	30			6	5		25	15	19	
Y	5	18	20	10	11	28	11	22	27	26	23	4	24	16	5	
Zr	19	76	100	110	200	100	30	140	140	290	300	13	150	140	13	
V	54	210	96	45	5	290	180	300	260	5	5	46	170	110	110	
Nb	11	12		10	11	16	11			12	15		16	13	10	
Cr	1500	160	32	25	10	47	390	11	13	1010	10	1700	47	13	1400	
Ni	3600	320	62	66	10	66	460	25	25	2010	10	2000	26	10	2400	
La	4.4	7.3	16	26	26	6.7	1.9	32	29	48	37	0.80	15	16	0.80	
Ce	8.5	17	34	48	49	16	5.4	58	59	86	79	2.3	34	34	2.0	
Nd	3.7	10	17	19	18	11	4.1	31	31	41	31	1.8	17	15	1.6	
Sm	0.80	2.8	3.3	3.1	3.0	3.3	1.4	6.1	6.1	7.0	5.2	0.60	4.1	3.3	0.40	
Eu	0.20	0.90	0.90	0.7	0.40	1.6	0.50	1.7	1.6	1.4	0.80	0.20	1.20	1.0	0.10	
Gd	0.86	3.9	3.2	2.4	2.2	4.5	1.9	5.4	5.5	5.7	4.6	0.72	5.0	3.7	0.65	
Tb							0.35								0.12	
Dy	0.91	3.5	3.5	1.8	1.9	5.6	2.2	4.6	5.5	5.2	4.6	0.76	4.7	3.3	0.79	
Ho	0.19	0.75		0.38	0.40	1.2	0.48			1.0	1.1		0.90	0.72	0.18	
Er	0.54	2.0	2.2	1.0	1.2	3.3	1.4	2.3	2.9	2.7	2.8	0.49	2.8	1.9	0.54	
Tm	0.09	0.33		0.17	0.23	0.61	0.24			0.5	0.55		0.50	0.37	0.09	
Yb	0.50	1.9	2.2	1.0	1.4	3.5	1.4	2.0	2.8	2.9	3.0	0.46	2.8	1.8	0.58	

notes: Major elements and Rb, Sr, Zr and Nb determined by WDS XRF on fused disks at the Analytical Chemistry Laboratories, (GSC). Chromium, Ni, Sc, and V determined by ICP-ES, and the REE and Y were determined by ICP-MS at the GSC. Estimated precisions based on replicate determinations are ±1% for major elements, ±2% for P<sub>2</sub>O<sub>5</sub>, ±3-6% for Cr, V, Rb, Sr, Sc, Zr, and Ba, ±20-50% for Ni and Nb, and ±5% for the REE and Y. Rock types are PER peridotite, BAS basalt, BAD basaltic andesite, AND andesite, DAC dacite, and RHY rhyolite.



## GEOCHEMISTRY OF VIZIEN LAVAS AND PERIDOTITES

Panel A volcanic rocks include basalt, andesite, dacite and rhyolite (Table 1). The lavas have the low Ti and Fe contents characteristic of calc-alkaline lavas from the Abitibi belt (e.g. Blake River Group; Lafleche et al., 1992; Fig. 3a). As a whole,



the suite has lower Zr/Si values than lavas in panel C (Fig. 4). Low Zr/Si values, such as those found in panel A lavas, are characteristic of Phanerozoic arc magmas. Panel A volcanism at 2724 Ma is contemporaneous with emplacement of the widespread Leaf River granodiorite intrusions (Percival et al., 1992) and the two suites are geochemically similar. Both panel A lavas and Leaf River plutons have enriched light rare earth element (LREE) profiles (Fig. 5a), and andesite with an  $\epsilon_{Nd}$  of 0.50 (Table 2; Fig. 3c) overlaps  $\epsilon_{Nd}$  values of the Leaf River plutonic suite (Stern et al., in press). However, panel A lavas appear to have formed in a submarine setting and may represent the vestiges of an island arc, whereas the Leaf River suite comprises a continental plutonic arc.

Panel B basalts are tholeiitic and have Ti contents similar to those of tholeiitic basalts in the Blake River Group of the Abitibi belt (Lafleche et al., 1992; Fig. 3a). The basalts show flat (10-20x chondrites) to slightly LREE-enriched profiles. A high magnesium basalt within panel B (PBA-92-2008G, Table 1) is characterized by relatively high SiO<sub>2</sub> (52.4%), MgO (12.10%), Ni (390 ppm) and Cr (460 ppm), and has a slightly depleted LREE profile  $(La/Sm)_n = 0.8$ ; Fig. 5b).

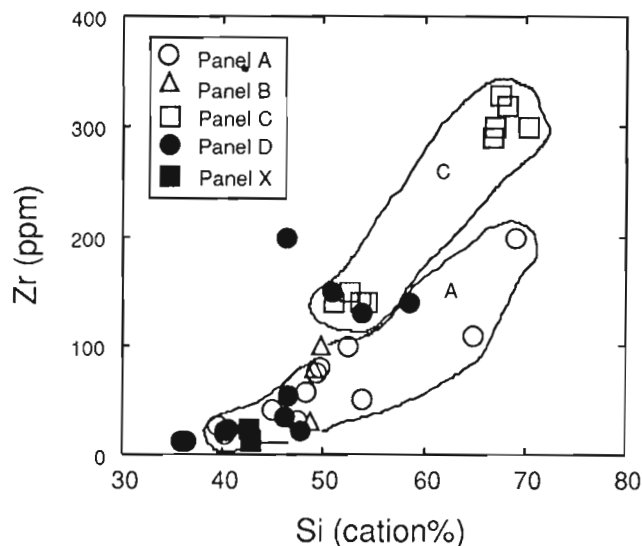


Figure 4. Si versus Zr diagram.

Figure 3 (opposite). **A**) Ti versus Mg diagram (cation % units). The fields of panel C and panel A lavas are emphasized. Blake River tholeiitic (B.R.T) and calc-alkaline (B.R.C-A.) lavas (Abitibi belt) are data from Lafleche et al. (1992). **B**) Fe-Mg diagram in cation % units. A mixing line (bold unadorned line) is shown between olivine of Fo<sub>87</sub> composition and peridotites in the Vizienz belt. Tie lines are drawn connecting individual peridotites to Fo<sub>87</sub> olivine determined by microprobe analysis. **C**) Mg versus  $\epsilon_{Nd}$  diagram. The field of depleted mantle  $\epsilon_{Nd}$  values is taken from studies of 2.7 Ga lavas in the Abitibi belt (Dupré et al., 1984; Machado et al., 1986; Walker et al., 1988; Barrie and Shirey, 1991). Line representing  $2\sigma$  uncertainty ( $\pm 0.5$  epsilon units) is shown in upper left.

**Table 2.** Sm and Nd isotopic compositions.

Sample#	Panel	Rock	Nd (ppm)	Sm (ppm)	$^{147}\text{Sm}/^{144}\text{Nd}$	$^{143}\text{Nd}/^{144}\text{Nd}$	$\epsilon_{\text{Nd}}(2725 \text{ Ma})$	
PBA91-185	* A	AND	15.409	3.098	0.12150	0.511313	0.50	
PBA91-188	* C	AND	25.073	5.147	0.12408	0.511310	-0.47	
PBA91-187	* C	BAD	30.795	5.957	0.11691	0.511222	0.33	
PBA91-170	* D	PER	1.499	0.507	0.20448	0.512848	1.34	
PBA91-125	* D	PER	1.251	0.390	0.18872	0.512586	1.76	
PBA92-2010	X	PER	3.63	1.55	0.19237	0.512701	2.73	
"	"	X	PER	3.567	1.35	0.19234	0.512701	2.74
PBA92-2011	X	PER	1.424	1.424	0.18906	0.512652	2.94	

notes: Samples marked (\*) are taken from Stern et al. (1994). Isotopic measurements were carried out on a Finnigan MAT 261 multicollector mass spectrometer at the GSC using the static mode. Over the course of the study, 29 analyses of the La Jolla standard gave  $^{143}\text{Nd}/^{144}\text{Nd}=0.511878$  ( $2\sigma=\pm 0.000015$ ;  $2\text{S.E.}=0.000003$ ) when normalized to  $^{146}\text{Nd}/^{144}\text{Nd}=0.7219$ . All  $^{143}\text{Nd}/^{144}\text{Nd}$  ratios have been bias corrected by  $-0.000018$ , to give La Jolla  $^{143}\text{Nd}/^{144}\text{Nd}=0.511860$ . Replicate reproducibility for the samples was within  $\pm 0.005\%$  for  $^{143}\text{Nd}/^{144}\text{Nd}$  ratios and  $\pm 0.05\%$  for  $^{147}\text{Sm}/^{144}\text{Nd}$  ratios. In general, there is an uncertainty of  $\pm 0.5$  epsilon units for individual rocks at their crystallization ages. Rock types are BAD basaltic andesite, AND andesite, and PER peridotite.

Modelling calculations (modified after Nielson, 1988) show that the liquidus phase of a melt of sample 2008G composition is  $\text{Fo}_{89}$  olivine at  $\sim 1355^\circ\text{C}$  where  $\text{XFe}^{3+}$  is buffered near Fe-FeO ( $\text{Fo}_{90}$  at QFM and  $1350^\circ\text{C}$ ). A primitive melt of this composition is unlikely to produce basalts typical of panel B, since they have lower  $\text{SiO}_2$  contents and flat to slightly enriched LREE patterns.

Siliceous high magnesian basalts are found in many Archean greenstone belts (Barnes, 1989; Sun et al., 1989), and samples with greater than 52%  $\text{SiO}_2$  are predominantly LREE-enriched. These LREE-enriched lavas have been interpreted as the products of crustal contamination of komatiitic magmas (Skulski et al., 1988; Barnes, 1989; Sun et al., 1989). However, the LREE-depleted character of sample 2008G is inconsistent with extensive crustal contamination.

Panel C volcanic rocks include basaltic andesite, andesite, dacite and rhyolite. The lavas have higher Ti and Fe contents than panel A rocks, with similar Mg abundances (Fig. 3a, b). Panel C mafic lavas have similar Ti contents to panel B tholeiitic basalts, but show a greater extent of LREE enrichment (Fig. 5c) and resemble Phanerozoic LREE-enriched, rift-related continental tholeiites (Basaltic volcanism study project, 1981). Panel C rocks have  $\epsilon_{\text{Nd}}$  values of 0.33 to -0.47 (Table 2, Fig. 3c), which along with the observations that they are LREE-enriched, contain granitic xenoliths, overlie continentally derived sediments, and consist largely of rhyolite, imply continental crustal assimilation in the production of panel C magmas.

Panel D consists of mafic to intermediate metavolcanic rocks and tonalite, with pods of peridotite. The volcanic rocks are geochemically similar to panel C tholeiites in terms of their Ti, Zr and LREE contents (Fig. 3a, 4, 5d). The peridotites range from slightly LREE-depleted to LREE-enriched (Fig. 5d) and have  $\epsilon_{\text{Nd}}$  values that overlap the field of depleted mantle compositions at 2.7 Ga (Fig. 3c). The most Mg-rich peridotite (A91170; Table 1) contains 80% cation normative

olivine ( $\text{Fo}_{85}$  where  $\text{XFe}^{3+}=0$ ). Collectively panel D peridotites define an olivine accumulation trend, which in Fe-Mg compositional space projects to  $\sim\text{Fo}_{87}$  (Fig. 3b); olivine relicts with this composition occur within the peridotites (B. Williamson, pers. comm., 1993). Primitive magmas that fractionate olivine have relatively constant  $\text{Fe}^{2+}$  abundances, and therefore, using Fe/Mg exchange equilibria (Roeder and Emslie, 1970) we calculate that a magma in equilibrium with  $\text{Fo}_{87}$  olivine, that has an  $\text{Fe}^{2+}$  content of 8.46% (olivine accumulation trend of panel D peridotites; Fig 3b), contains 17% Mg ( $\sim 12\%$  MgO).

Two samples of panel X peridotite were analyzed and both have compositions that lie close to an  $\text{Fo}_{87}$  accumulation trend characteristic of panel D peridotites (Fig. 3b). The rocks have generally flat REE chondrite-normalized profiles, with both positive and negative Eu anomalies (Fig. 5e). The latter may reflect mixing between olivine-rich cumulate and a range of basaltic intercumulus liquids which have either fractionated plagioclase (negative Eu anomaly) or accumulated plagioclase (positive anomaly). Panel X peridotites have high  $\epsilon_{\text{Nd}}$  values (2.73 and 2.94; Table 2 and Fig. 3c) similar to estimated depleted mantle at 2.7 Ga.

The flat REE element profiles and high  $\epsilon_{\text{Nd}}$  values of panel X peridotite suggest that these rocks may have formed by the ponding and crystallization of primitive, mid-ocean ridge-like basaltic magmas. An oceanic origin for panel X is supported by the presence of submarine basalts and lenses of sulphidic banded iron-formation, and conspicuous lack of continentally derived sediment. Peridotite cumulate sills with  $\text{Fo}_{87}$  olivine and flat REE profiles are common to panels B, D and X. The different peridotites may share a common origin, and magmas with  $\sim 12\%$  MgO (in equilibrium with  $\text{Fo}_{87}$ ) may have been widespread. Variations in LREE contents and  $\epsilon_{\text{Nd}}$  values amongst the peridotites may reflect the extent of crustal assimilation during emplacement into variably LREE-enriched host rocks.

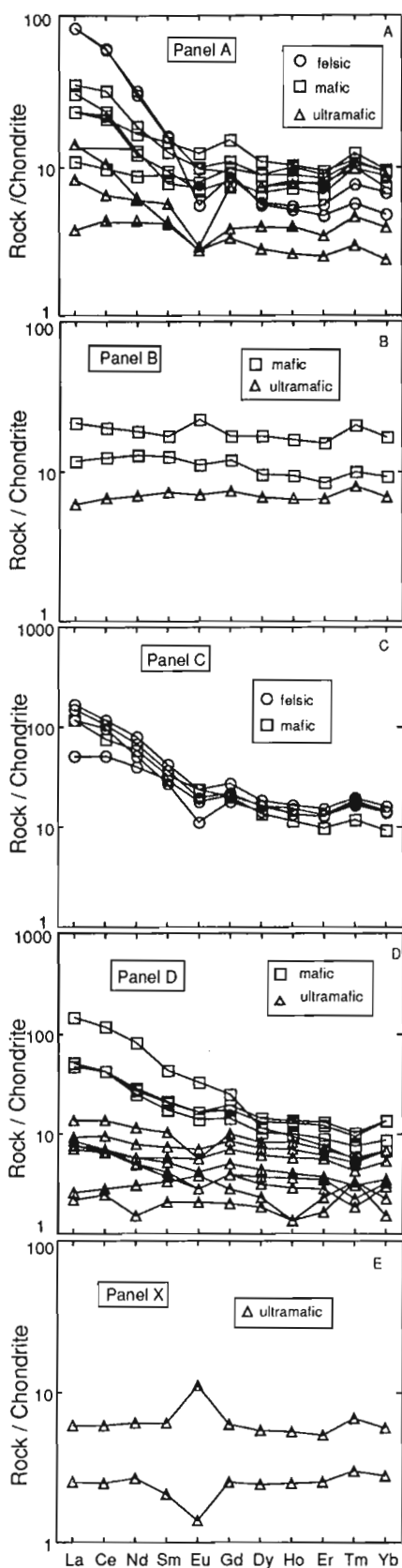


Figure 5. Chondrite normalized REE diagram of Vizien lavas.

## STRUCTURAL GEOLOGY AND INTERPRETATION

At least five sets of structures are recognized in the Vizien belt and are described below. The oldest thrust fault recognized ( $D_1$ ) juxtaposed panels X and B. Panels B/X and C were subsequently inverted onto panel A by a  $D_2$  nappe. Neither early event produced penetrative fabrics. The pervasive foliation of the belt is a  $D_3$  fabric associated with map-scale folds. West-northwest-plunging crenulation folds of  $D_3$  foliation and macroscopic warps are attributed to a  $D_4$  event. The latest structures in the area ( $D_5$ ) occur as brittle faults. All of the structural events post-date conglomerate deposition and are therefore younger than 2718 Ma.

The earliest ( $D_1$ ) structures recognized are related to thrust emplacement of panel X. They include a fault marked by map-scale truncation of panel B stratigraphy (Percival et al., 1993b), a strong schistosity in basal panel X serpentinite, and deformation fabrics preserved within blocks in mélangé (Fig. 2). The latter structures, including tight folds in serpentinite and gabbroic blocks, as well as mylonitic foliation in gabbro, are unique to the mélangé unit and inferred to have formed during thrust emplacement of panel X.

Structures of  $D_2$  generation are inferred from the geometry of panels B/X and C (Fig. 1b). Both panels have basement-cover relationships that establish stratigraphic facing as downward (Fig. 1a), requiring large-scale overturning. The basement-over-cover relationship resembles the geometry of the lower limb of a basement-cored nappe. Pervasive grain-scale fabrics associated with the stratigraphic inversion have not been recognized, however a zone of mylonite between panels A and B/X may represent a fault of  $D_2$  age. Units of panel A are truncated along this 30-m-wide zone of thinly laminated (<1 mm) felsic mylonite against a narrow (<2-m-wide) serpentinite schist zone developed at the western margin of panel X. With the exception of the mylonite, structures of  $D_1$  and  $D_2$  age are not recognized in panel A, which is normal facing, suggesting that the mylonite zone may have carried the B/X-C nappe.

A northwest-striking, moderately northeast-dipping  $D_3$  foliation and schistosity forms the pervasive fabric element of the belt (Percival and Card, 1992b). The foliation is generally parallel to lithological contacts and is axial planar to map-scale folds in panels B/X and C. A doubly plunging isoclinal synform with northeast-dipping axial surface characterizes panel B/X. Based on the orientation of minor fold axes, mineral and stretching lineations, the fold plunges  $\sim 60^\circ$  northwest in the south and  $\sim 75^\circ$  southeast in the north (op. cit.). A north-plunging isoclinal antiform with northeast-dipping axial surface dominates the structure of panel C. Its average plunge is  $58^\circ$  northwest based on a compilation of minor fold axes, mineral and stretching lineations. Throughout most of panel A,  $D_3$  is the only evident fabric element in this homoclinal, northeast-facing volcanic assemblage; macroscopic folds have not been recognized. Iron-formation of the basal mafic unit is highly contorted, perhaps indicating some pre- $D_3$  deformation, or a response to extreme competency contrasts. Intense shear fabrics that characterize panel D (Percival and Card, 1992a) are parallel to  $D_3$  foliations throughout the belt.

The relationship between structural elements and amphibolite-facies metamorphism is best illustrated in pelitic schists of panel B. Metamorphic minerals including garnet, staurolite and andalusite enclose biotite aligned in the  $D_3$  plane, and fibrolitic sillimanite is oriented randomly with respect to the biotite-defined foliation. These observations indicate that the peak of the ~2.5 kb, 580°C metamorphism occurred after  $D_3$ .

Structures of a fourth phase of ductile deformation ( $D_4$ ) are variably developed in the Vizien belt. These include open, map-scale (Fig. 1a) folds and crenulation folds and lineations of  $D_3$  foliation, with west-northwest axial planes and steep westerly plunges. The plunge reversal of the panel B/X  $D_3$  synform may be attributable to  $D_4$  deformation.

A set of dykes of white peraluminous pegmatite (garnet-muscovite-tourmaline granite) cuts cleanly across the ductile deformation fabrics. Zircon from one dyke gave highly discordant, uninterpretable results.

Fault rocks separating panels C and D are cataclastic in nature and therefore appear to be later than the ductile deformation fabrics. The black, aphanitic, structureless cataclasites are rarely exposed as sharp-walled, centimetre-scale veins in hematite-epidote altered rocks adjacent to a major topographic valley. These structures are tentatively assigned a  $D_5$  age.

## TECTONIC EVOLUTION

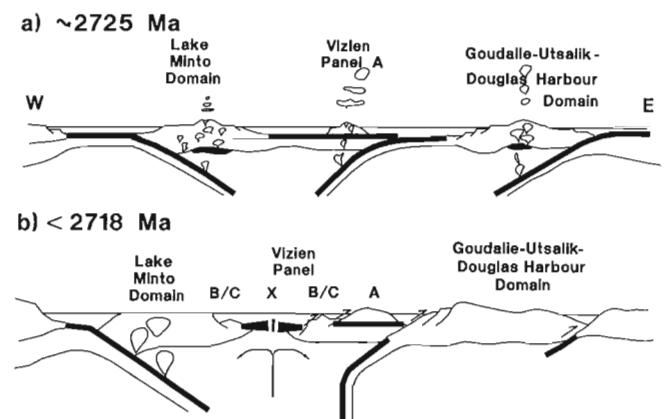
The diverse tectonic panels that make up the Vizien belt are characterized by distinct sets of structural, stratigraphic and geochemical attributes. Questions arise as to whether the panels developed independently, and how they fit into the tectonic framework of the Minto block. A number of observations are pertinent in this regard.

Sometime after 2718 Ma, tonalite basement was eroded and clastic sediments of lower panel B were deposited, followed by the eruption of mafic lavas including siliceous magnesian basalts. The drowning sequence may have been related to an extensional event in which the tonalitic basement and cover were down-dropped on rift-bounding normal faults. Ongoing geochronology will determine if panels B and C are coeval, as is inferred from the close proximity of their basal unconformities. Panel C volcanism, involving the eruption of basaltic andesites with continental tholeiitic affinities and contaminated andesites and rhyolites, probably occurred in response to rifting of arc crust and its continental foundation, driven by the upward migration of hot asthenosphere-derived magmas. The age of panel X is not known; if current geochronological investigations indicate an age <2718 Ma, it may represent the oceanic stage of Goudalie continental arc rifting; alternatively if panel X is older than 2725 Ma, it may represent a sliver of pre-arc oceanic crust.

Leaf River continental arc magmatism is broadly contemporaneous across most of the Minto block at  $\sim 2725 \pm 5$  Ma (Percival et al. 1992) and is characterized by water-undersaturated compositions and high crystallization temperatures (Stern et al., 1994). Within this wide continental arc terrane is the Goudalie domain, containing older tonalite (3.1,

2.9 Ga), a 2724 Ma upward-shoaling mature arc sequence (panel A), continental-derived sediments (<2718 Ma), tholeiitic basalts and ultramafic rocks (collectively within panels B and C), and a submarine sequence of basalts intruded by depleted mantle-derived peridotites (panel X). Evidence of pre 2.72 Ga continental crust is not restricted to the Goudalie domain, but includes >3.1 Ga tonalitic gneiss inclusions in eastern Lake Minto domain diatexite (Percival et al., 1992) and >2.8 Ga tonalite in the Douglas Harbour domain (Parrish 1989) and possible eastern equivalents in the hinterland of the New Quebec orogen (Machado et al., 1989). Unless panels B, C and X are exotic and are far travelled, the simplest model is that they formed either within a single broad 2725 Ma continental arc, or alternatively, were trapped between two colliding continental landmasses represented by Lake Minto domain in the west, and composite Goudalie-Utsalik domain in the east. Models in which the Minto block constitutes an assembly of arc terranes must still explain coeval, short-lived ( $2725 \pm 5$  Ma) magmatism over a large area on continental crust in the Lake Minto, Goudalie – Utsalik, and Douglas Harbour domains.

The main objections to a single continental arc model are its anomalous width (~500 km), and the fact that coeval panel A rocks appear to have formed in an island arc setting. Since the Goudalie and Utsalik domains appear to have been stitched by 2725 Ma (Percival et al., 1992), the panel A arc must have lain between the Lake Minto and Goudalie domains (Fig. 6a). The presence of an island arc within the Minto block can be explained by three subduction zones, which can account for the broad distribution of the Leaf River plutons, shown schematically in Figure 6b. Subduction beneath the island arc, and beneath the Goudalie composite



**Figure 6.** Possible tectonic model for the formation of the Minto block. **a)** Multiple arc segments involve subduction beneath the Lake Minto domain (M), a panel A island arc (A), and the Goudalie-Utsalik-Douglas Harbour domains. **b)** Ocean closure in the east ends arc activity beneath Goudalie-Utsalik-Douglas Harbour domains, while a marginal basin develops in the eastern Lake Minto domain (panels B, C and X). Subsequent collision in the western Lake Minto domain leads to marginal basin closure, obduction and widespread orogeny.

terranes ended around 2720 Ma. Slab drop-off beneath the panel A arc may have triggered asthenospheric rise and <2718 Ma back-arc rifting beneath the eastern Lake Minto continental margin (Fig. 6b). Arc detritus in the rift basin could reflect uplift of the island arc. Terminal collision prior to 2690 Ma, the age of posttectonic plutons, would have triggered back-arc basin collapse, D<sub>1</sub> overthrust tectonics and D<sub>2</sub> nappe formation.

The model presented above should satisfy a number of tests. If panel A represents a mature island arc, then both felsic lavas and synvolcanic plutons should have juvenile Nd isotopic compositions relative to coeval Leaf River granitoid plutons that intrude older continental crust. The provenance of upper panel A sediments as reflected in Nd model ages and U-Pb ages of detrital zircons, should be restricted to ~2725 Ma if they were deposited on the flanks of an island arc, and include older components if formed in a continental arc setting. Finally, the model predicts that a suture zone should lie between panel A (and possible northern correlatives), and the Goudalie domain. The suture, if present, may be delineated by oceanic crustal rocks.

## REGIONAL TECTONIC IMPLICATIONS

The northwesterly trends of the Minto block, the dominant history of arc magmatism, and evidence of thrust-nappe tectonics indicate prolonged orthogonal convergence along the northeastern Superior margin. Conversely, west-trending greenstone belts in the southern Superior with prominent dextral shear zones reflect an obliquely convergent margin at 2.7 Ga (Percival et al., 1993a). Formation of the Minto block by the amalgamation of multiple arc segments is similar to models advocated for the southern Superior Province (e.g. Card, 1990), but is distinct in the abundance of continental arc terranes. Accretion of multiple, short-lived, continental arcs of similar age (2725 Ma) requires that prior to 2725 Ma, a number of small, young ocean basins were present in the northeast. The vestiges of island arc terranes flanking these ocean basins, such as panel A in the Vizien greenstone belt, probably hold the greatest economic potential in the Minto block.

## ACKNOWLEDGMENTS

We thank Ken Card, Janet King and Bill Davis for thoughtful reviews of this paper and Olga Ijewliw for helping to draft some of the figures.

## REFERENCES

- Ayres, L.D. and Corfu, F.  
1991: Stacking of disparate volcanic and sedimentary units by thrusting in The Archean Favourable lake greenstone belt, central Canada; *Precambrian Research*, v. 50, p. 221-238.
- Barnes, S.J.  
1989: Are Bushveld U-type parent magmas boninites or contaminated komatiites?; *Contributions to Mineralogy and Petrology*, v. 101, p. 447-457.
- Barrie, C.T. and Shirey, S.B.  
1991: Nd- and Sr-isotope systematics for the Kamiskotia-Montcalm area: implications for the formation of Late Archean crust in the western Abitibi Subprovince, Canada; *Canadian Journal of Earth Sciences*, v. 28, p. 58-76.
- Basaltic volcanism study project**  
1981: *Basaltic volcanism on the terrestrial planets*; Pergamon Press, New York, 1268 p.
- Card, K.D.  
1990: A review of the Superior Province of the Canadian Shield, a product of Archean accretion; *Precambrian Research*, v. 48, p. 99-156.
- Coward, M.P., James, P.R., and Wright, L.  
1976: Northern margin of the Limpopo mobile belt, southern Africa; *Geological Society of America Bulletin*, v. 87, p.601-611.
- Desrochers, J.-P., Hubert, C., Ludden, J.N., and Pilote, P.  
1993: Accretion of Archean oceanic plateau fragments in the Abitibi greenstone belt, Canada; *Geology*, v. 21, p. 451-454.
- de Wit, M.J.  
1982: Gliding and overthrust nappe tectonics in the Barberton greenstone belt; *Journal of Structural Geology*, v. 4, p. 117-136.
- Dupré, B., Chauvel, C., and Arndt, N.  
1984: Pb and Nd isotopic study of two Archean komatiitic flows from Alexo, Ontario; *Geochimica et Cosmochimica Acta*, v. 48, p. 1965-1972.
- Green, A.G., Mikereit, B., Mayrand, L.J., Ludden, J.N., Hubert, C., Jackson, S.L., Sutcliffe, R.H., West, G.F., Verpaest, P., and Simard, A.  
1990: Deep structure of an Archean greenstone terrane; *Nature*, v. 344, p. 327-330.
- Hoffman, P.F.  
1991: On accretion of granite – greenstone terranes; in *Greenstone gold and crustal evolution*, (ed.) F. Robert, P.A. Shearan, and S.B. Green; Geological Association of Canada NUNA Conference volume p. 32-45.
- Kusky, T.M.  
1989: Accretion of the Archean Slave Province; *Geology*, v. 17, p. 63-67.  
1990: Evidence for Archean ocean opening and closing in the southern Slave province; *Tectonics*, v. 9, p. 1533-1563.
- Lafliche, M.R., Dupuy, C., and Dostal, J.  
1992: Tholeiitic volcanic rocks of the late Archean Blake River Group, southern Abitibi greenstone belt: origin and geodynamic implications; *Canadian Journal of Earth Sciences*, v. 29, p. 1448-1458.
- Machado, N., Brooks, C., and Hart, S.R.  
1986: Determination of initial <sup>87</sup>Sr/<sup>86</sup>Sr and <sup>143</sup>Nd/<sup>144</sup>Nd in primary minerals from mafic and ultramafic rocks: experimental procedure and implications for the isotope characteristics of the Archean mantle under the Abitibi greenstone belt, Canada; *Geochimica et Cosmochimica Acta*, v. 50, p. 2334-2348.
- Machado, N., Goulet, N., and Gariépy, C.  
1989: U-Pb geochronology of reactivated Archean basement and of Hudsonian metamorphism in the northern Labrador Trough; *Canadian Journal of Earth Sciences*, v. 26, p. 1-15.
- Martyn, J.E.  
1987: Evidence for structural repetition in the greenstones of the Kalgoorlie district, Western Australia; *Precambrian Research*, v. 37, p. 1-18.
- Moorhead, J.  
1989: Géologie de la région du lac Chukotat (fosse de l'Ungava); Ministère de l'Énergie et des Ressources ET87-10.
- Nielson, R.L.  
1988: TRACE.FOR: a program for the calculation of combined major and trace-element liquid lines of descent for natural magmatic systems; *Computers and Geosciences*, v. 14, p. 15-36.
- Parrish, R.R.  
1989: U-Pb geochronology of the Cape Smith belt and Sugluk block, northern Quebec; *Geoscience Canada*, v. 16, p. 126-130.
- Percival, J.A., Card, K.D., Stern, R.A., and Bégin, N.J.  
1991: A geologic transect of the Leaf River area, northeastern Superior Province, Ungava Peninsula, Quebec; in *Current Research, Part C*; Geological Survey of Canada, Paper 91-1C, p. 55-63.
- Percival, J.A. and Card, K.D.  
1992a: Vizien greenstone belt and adjacent high grade domains of the Minto block, Ungava Peninsula, Quebec; in *Current Research, Part C*; Geological Survey of Canada, Paper 92-1C, p. 69-80.

**Percival, J.A. and Card, K.D.**

1992b: Geology of the Vizion greenstone belt; Geological Survey of Canada, Open File 2495, scale 1:50 000.

**Percival, J.A., Mortensen, J.K., Stern, R.A., and Card, K.D.**

1992: Giant granulite terranes of northeastern Superior Province: the Ashuanipi complex and Minto block; Canadian Journal of Earth Sciences, v. 29, p. 2287-2308.

**Percival, J.A., Stern, R.A., Card, K.D., and Mortensen, J.K.**

1993a: Northeastern Superior province: missing link in describing tectonic assembly of the craton at 2.7 Ga; Geological Society of America, Abstracts with Programs, Annual Meeting, v. 25, p. A-236.

**Percival, J.A., Card, K.D., and Mortensen, J.K.**

1993b: Archean unconformity in the Vizion greenstone belt, Ungava Peninsula, Quebec; in Current Research, Part C; Geological Survey of Canada, Paper 93-1C, p. 319-328.

**Roeder, P.L. and Emslie, R.F.**

1970: Olivine-liquid equilibrium; Contributions to Mineralogy and Petrology, v. 29, p. 275-289.

**Skulski, T., Hynes, A., and Francis, D.**

1988: Basic Lavas of the Archean La Grande Greenstone belt: products of polybaric fractionation and crustal contamination; Contributions to Mineralogy and Petrology, v. 100, p. 236-245.

**Stern, R.A., Percival, J.A., and Mortensen, J.K.**

in press: Geochemical evolution of the Minto block: a 2.7 Ga continental magmatic arc built on the Superior proto-craton; Precambrian Research.

**Sun, S., Nesbitt, R.W., and McCulloch, M.T.**

1989: Geochemistry and petrogenesis of Archean and early Proterozoic siliceous high-magnesian basalts; in Boninites, A.J. Crawford (ed.); Unwin Hyman, London.

**Walker, R.J., Shirey, S.B., and Stecher, O.**

1988: Comparative Re-Os, Sm-Nd, and Rb-Sr isotope and trace element systematics for Archean komatiite flows from Munro Township, Abitibi belt, Ontario; Earth and Planetary Sciences, v. 87, p. 1-12.

---

Geological Survey of Canada Project 890009



# New results and summary of the Archean and Paleoproterozoic geology of the Burwell domain, northern Torngat Orogen, Labrador, Quebec, and Northwest Territories<sup>1</sup>

M.J. Van Kranendonk, R.J. Wardle<sup>2</sup>, F.C. Mengel<sup>3</sup>,  
L.M. Campbell<sup>4</sup>, and L. Reid<sup>5</sup>

Continental Geoscience Division

*Van Kranendonk, M.J., Wardle, R.J., Mengel, F.C., Campbell, L.M., and Reid, L., 1994: New results and summary of the Archean and Paleoproterozoic geology of the Burwell domain, northern Torngat Orogen, Labrador, Quebec, and Northwest Territories; in Current Research 1994-C; Geological Survey of Canada, p. 321-332.*

---

**Abstract:** The final summer of fieldwork on Project Torngat identified: 1) tectonic slivers of suspected Archean orthogneiss in the Tasiuyak gneiss, that were either melted in situ to form, or were extensively invaded by, homogeneous rocks of the Killinek charnockitic suite; 2) an extensive belt of Paleoproterozoic mafic supracrustal rocks within the southern part of the Komaktorvik shear zone; and 3) a complex history of deformation within the Komaktorvik shear zone, including higher-grade and lower-grade Paleoproterozoic events. Tectonic evolution is related to, in sequence: late Archean-Paleoproterozoic rifting of the Nain margin; deposition of platformal and extensive turbiditic metasediments on the Rae margin, coeval with, or postdated by, accretion; arc magmatism on both the Nain and Rae margins, with the possible development of a back-arc basin in the former; and Nain-Rae collision at ca. 1860 Ma. Subsequent deformation and cooling continued through several pulses, from ca. 1843-1710 Ma.

**Résumé :** Les travaux d'été sur le terrain dans le cadre de la dernière année du projet Torngat ont permis d'identifier : 1) des copeaux tectoniques d'orthogneiss, que l'on croit d'âge archéen, dans le gneiss de Tasiuyak, qui ont subi une fusion in situ pour former les roches homogènes de la suite charnockitique de Killinek ou ont été considérablement envahis par ces roches; 2) une vaste ceinture de roches supracrustales mafiques du Paléoprotérozoïque au sein de la partie méridionale de la zone de cisaillement de Komaktorvik; et 3) une histoire complexe de déformation au sein de la zone de cisaillement de Komaktorvik, incluant des épisodes de métamorphisme élevé et faible au Paléoprotérozoïque. L'évolution tectonique est définie, selon un ordre chronologique normal, par un rifting de la marge de Nain à l'Archéen tardif-Paléoprotérozoïque; par le dépôt de métasédiments de plate-forme et d'une vaste étendue de métasédiments turbiditiques sur la marge de Rae, concurrentement à l'accrétion ou suivi par celle-ci; par un magmatisme d'arc sur les marges de Nain et de Rae, accompagné de la formation possible d'un bassin d'arrière-arc dans le cas de la première marge; et par une collision Nain-Rae vers 1 860 Ma. La déformation et le refroidissement subséquents se sont poursuivis sous forme de nombreuses impulsions, de 1 843 à 1 710 Ma environ.

---

<sup>1</sup> Contribution to Canada-Newfoundland Cooperation Agreement on Mineral Development (1990-1994), a subsidiary agreement under the Canada-Newfoundland Economic and Regional Development Agreement.

<sup>2</sup> Geological Survey Branch, Newfoundland Department of Mines and Energy, 95 Bonaventure Ave., St. John's, Newfoundland A1B 4J6

<sup>3</sup> Geological Museum, University of Copenhagen, Østervoldgade 5-7, 1350 Copenhagen K, Denmark

<sup>4</sup> CIRES and the Department of Geological Sciences, Box 250, University of Colorado, Boulder, CO 80309-0250 U.S.A.

<sup>5</sup> Department of Geology, University of Ottawa, Ottawa, Ontario K1N 6N5

## INTRODUCTION

The Torngat project - aimed at mapping the Labrador peninsula north of 59°15'N at 1:100 000 scale - is funded through a Canada-Newfoundland Agreement on Mineral Development for mapping in Labrador, and A-base for mapping in north-eastern Quebec and the Northwest Territories (Killinek and Button islands: see Fig. 1). Mapping was successfully completed this summer in the southern part of the map area (Rae Province, interior Burwell domain, and Four Peaks domain) and on Killinek Island, through helicopter-supported traverses.

The Paleoproterozoic Torngat Orogen separates unreworked Archean rocks of the Nain and Rae provinces in the east and west, respectively, and affects rocks of both provinces as well as a variety of Paleoproterozoic rocks (inset, Fig. 1). In the map area, strong shear deformation splays into two distinct belts: the east-west trending portion of the Abloviak shear zone in the south, and the north-south trending Komaktorvik shear zone in the east (Fig. 2). These zones bound an elliptical region of relatively lower strain, known as the Burwell domain, which is composed of a heterogeneous and complex assemblage of granulite- to amphibolite-facies reworked Archean orthogneisses and deformed Paleoproterozoic metaplutonic and metamorphosed supracrustal rocks (Fig. 1).

In this report we present new discoveries from this summer and summarize the geology of the map area as gleaned from the past three field seasons. Readers are referred to Wardle et al. (in press) for a description of the Archean Nain Province and to previous reports by Van Kranendonk and Scott (1992), Van Kranendonk et al. (1993a, b) and Wardle et al. (1992, 1993) for more complete descriptions of lithology and structures in the map area. All radiometric ages in this report are from Scott et al. (1993) or D. Scott (pers. comm., 1993).

## PRINCIPAL SUBDIVISIONS OF THE MAP AREA

The geology of the map area is shown in Figure 1. This area is divided into a number of lithotectonic and structural elements, as shown in Figure 2 (Van Kranendonk et al., 1993b). Lithotectonic assemblages are defined on the basis of restricted associations between some rock units, a restricted geographic distribution, and their continuity along strike. Assemblages include: 1) reworked Archean gneisses of the Rae Province and deformed Paleoproterozoic supracrustal rocks of the Lake Harbour Group; 2) unreworked Archean gneisses of the Nain Province in the Four Peaks domain; 3) the Noodleook complex; and 4) the Tasiuyak gneiss complex. Rocks of the Killinek charnockitic suite form the dominant lithology in the northwestern part of the map area, but also occur throughout the Tasiuyak gneiss complex and in the Rae Province. Structural divisions of the map area include the Four Peaks domain, the Burwell domain, and the Abloviak, Komaktorvik and Katherine River shear zones (Fig. 2).

## LITHOTECTONIC ASSEMBLAGES

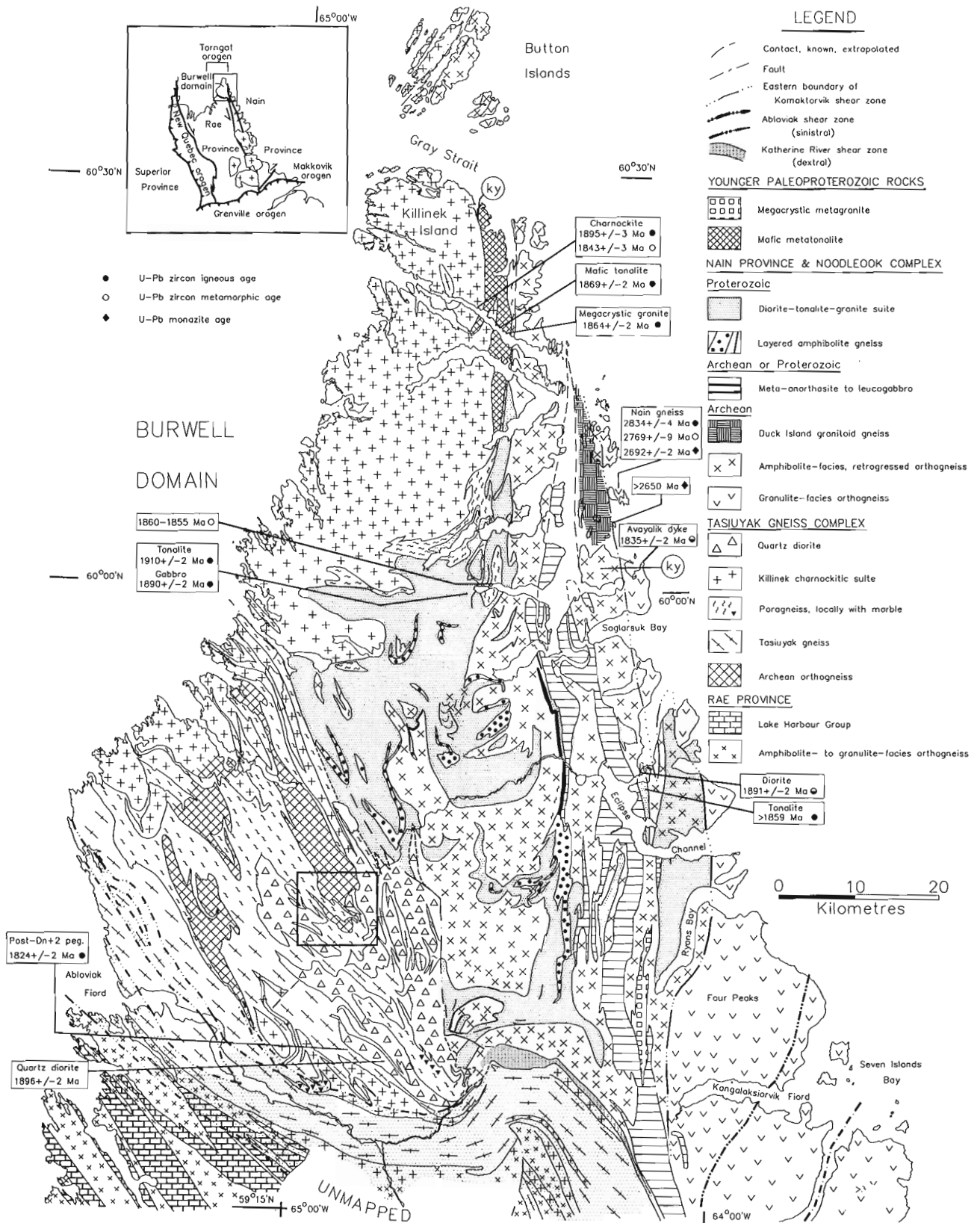
### *Four Peaks domain of the Nain Province*

The Four Peaks domain is located along the eastern part of the map area and is underlain by Archean gneisses of the Nain Province (Bridgwater and Wardle, 1992) that escaped penetrative Paleoproterozoic deformation (see Van Kranendonk et al., 1993a and Wardle et al., in press, for detailed descriptions).

The Archean history of the domain includes an early phase of tonalite intrusion into anorthositic-ultramafic metaplutonic rocks and supracrustal rocks, followed by deformation and high-grade metamorphism. Mafic dykes, locally preserved as disrupted amphibolite layers with round plagioclase megacrysts, intruded the migmatitic gneisses and are themselves cut by homogeneous, foliated to gneissic tonalites, dated in one locality as  $2834 \pm 4$  Ma (Fig. 1). All rocks were then deformed under granulite-facies metamorphic conditions, which is interpreted to have occurred at  $2769 \pm 5$  Ma, the age of metamorphic zircon overgrowths from the previous sample.

Archean gneisses and structures are cut by Paleoproterozoic Avayalik mafic dykes, and these rocks are themselves affected by Paleoproterozoic metamorphism which varies in grade across the map area. In the southeast, orthopyroxene-bearing Archean gneisses host east-west trending, subvertical Avayalik dykes that are undeformed and unmetamorphosed with chilled margins and black feldspar megacrysts, or cut by garnet-clinopyroxene-quartz veins (Fig. 3A). Locally the dykes have irregular, branching, or en echelon intrusion forms and shallow dips. Farther west, both Archean gneisses and Avayalik dykes are recrystallized to garnet-clinopyroxene assemblages (Fig. 3B and C) in the absence of associated deformation features, thus suggesting static Paleoproterozoic recrystallization. Dykes in this area trend north-east-southwest and dip moderately to the southeast, and may be deformed, but the change in orientation is interpreted to be primary. The metamorphic history is complicated by the fact that retrograde shear zones within Archean granulite-facies gneisses are locally cut by Avayalik dykes (D. Bridgwater, pers. comm., 1993), and that in metamorphosed dykes,

**Figure 1.** Geological compilation map of the northern part of the Torngat Orogen: data in part from Taylor (1979), and mapping by L. Godin, N. Goulet, and V. Bodycomb around Abloviak Fiord. Location of Figure 7 outlined by box. Ky = kyanite localities. Bold lines in Four Peaks domain = metamorphic isograds: right of dash-dot line = Archean orthopyroxene-bearing (opx) gneisses and Avayalik dykes that are unmetamorphosed or cut by garnet-clinopyroxene (gt+cpx) fractures; dash-dot to dash-double dot lines = relict Archean opx granulite-facies in Proterozoic gt+cpx granulite-facies; left of dash-double dot line = Proterozoic gt-cpx assemblages: north of Eclipse Channel = Archean opx gneisses with gt+cpx Avayalik dykes.



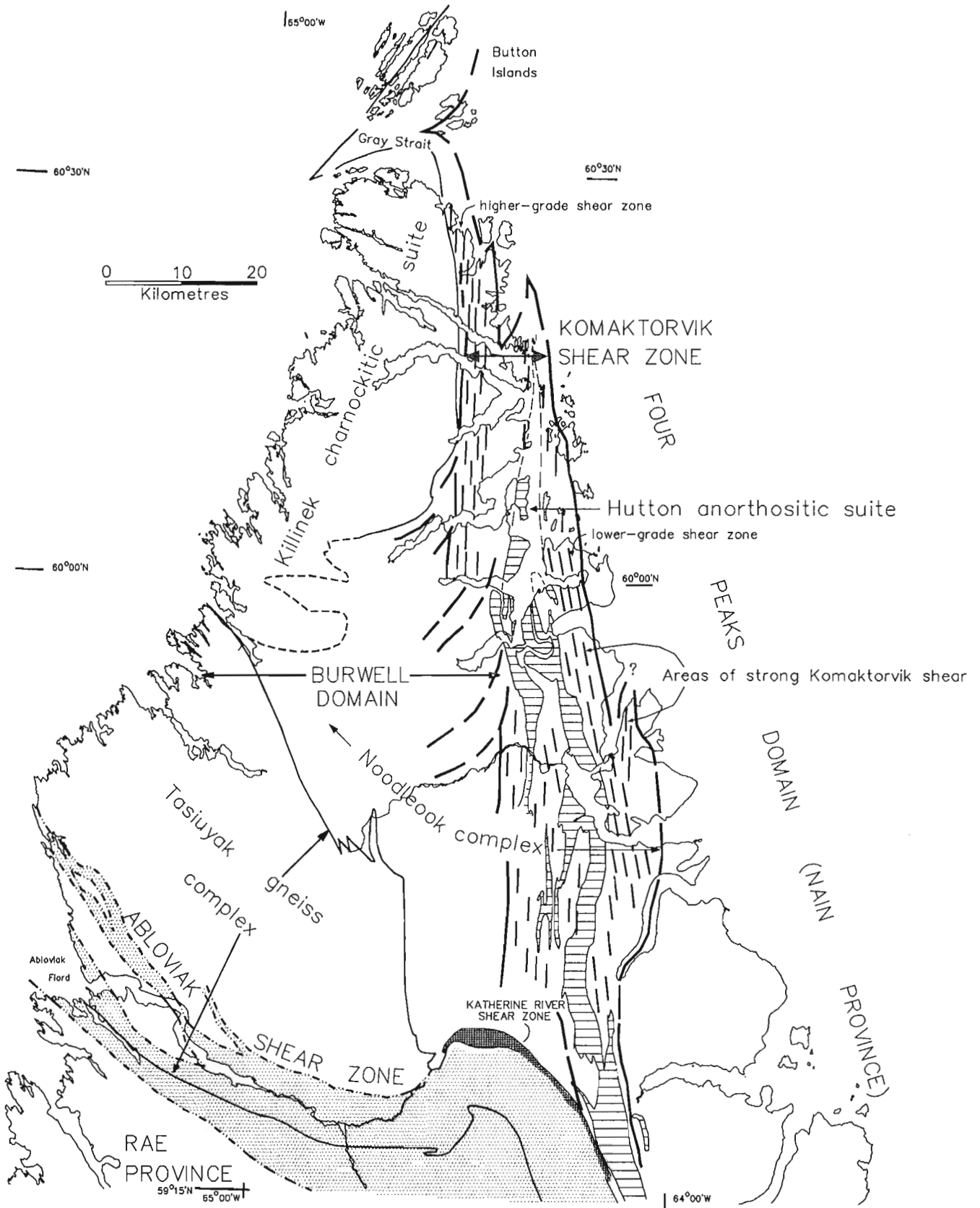


Figure 2. Structural (upper case: domains and shear zones) and lithotectonic (lower case: complexes) subdivisions of the map area (after Van Kranendonk et al., 1993b).

metamorphic garnet-clinopyroxene-quartz assemblages ( $T=660^{\circ}\text{C}$ : Mengel and Rivers, 1992) replace earlier hornblende-plagioclase assemblages (Fig. 3C).

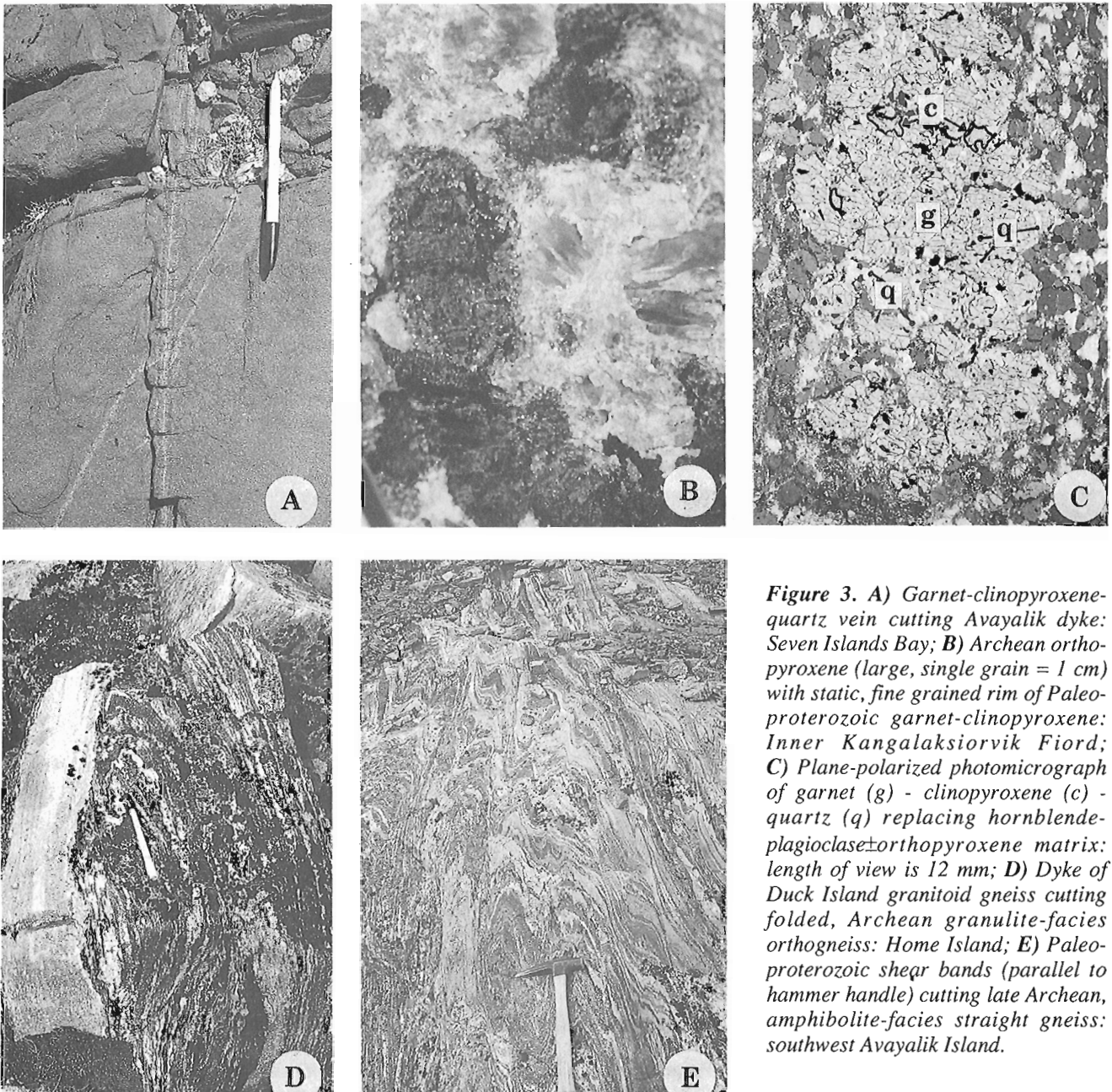
Avayalik dykes do not occur in Paleoproterozoic metaplutonic or metasedimentary rocks and are thus interpreted to be  $>1910$  Ma, the oldest dated Paleoproterozoic metaplutonic rock. However, euhedral zircon from an Avayalik dyke in the Four Peaks domain (see Fig. 1 for location) has yielded an upper intercept age of  $1835 \pm 2$  Ma, which can be interpreted as either the age of dyke emplacement and magmatic zircon crystallization, or zircon growth during metamorphism. The former interpretation would suggest the possibility of several

generations of Avayalik-type dykes (D. Scott, pers. comm.), whereas the latter interpretation – which we prefer – may indicate the time of formation of the garnet-clinopyroxene assemblages within the Four Peaks domain.

### *Noodleook complex*

#### **Archean and/or Paleoproterozoic gneisses**

In the Noodleook complex (Fig. 2), Archean Nain gneisses with deformed and metamorphosed Avayalik dyke remnants are partly to completely recrystallized under Paleoproterozoic amphibolite facies, contain a number of distinct units, and are



**Figure 3.** A) Garnet-clinopyroxene-quartz vein cutting Avayalik dyke: Seven Islands Bay; B) Archean orthopyroxene (large, single grain = 1 cm) with static, fine grained rim of Paleoproterozoic garnet-clinopyroxene: Inner Kangalaksiorvik Fiord; C) Plane-polarized photomicrograph of garnet (g) - clinopyroxene (c) - quartz (q) replacing hornblende-plagioclase±orthopyroxene matrix: length of view is 12 mm; D) Dyke of Duck Island granitoid gneiss cutting folded, Archean granulite-facies orthogneiss: Home Island; E) Paleoproterozoic shear bands (parallel to hammer handle) cutting late Archean, amphibolite-facies straight gneiss: southwest Avayalik Island.



interlayered and tectonically interleaved with a variety of Paleoproterozoic metamorphosed supracrustal and metaplutonic rocks (Fig. 1: Van Kranendonk et al., 1993a; Wardle et al., 1992, 1993).

In the eastern part of the complex, the amphibolite-facies Duck Island granitoid suite (>2650 Ma: Fig. 1) cuts older granulite-facies Archean gneisses (Fig. 3D). Within the suite, amphibolite-facies structures are cut by Avayalik dykes, indicating a period of late Archean or Paleoproterozoic deformation (Fig. 3E): the former is supported by the sole occurrence of late Archean U-Pb monazite dates from this area (see Fig. 1).

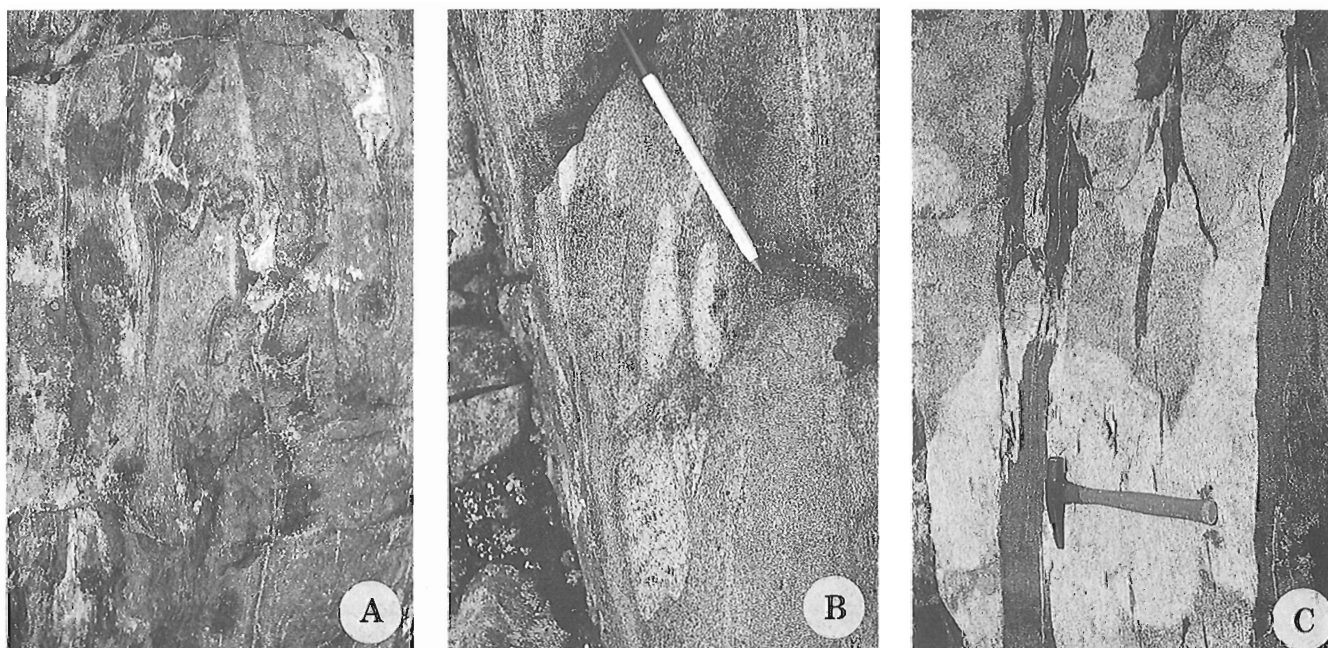
The Hutton anorthositic suite (Fig. 1) - of late Archean or Paleoproterozoic age - lies entirely within Archean gneisses and, in contrast with the area previously mapped to the north, was found to contain abundant relict igneous textures and to lack migmatitic textures throughout much of the southern part of the map area. The only rocks seen to clearly intrude anorthositic rocks are those of the diorite-tonalite-granite suite and (?) younger megacrystic granites (see below). These features, together with the remarkable continuity of the suite (>175 km long, from the northern tip of the map area to south of Nachvak fiord: Taylor, 1979; Wardle, 1983), suggest that an early Proterozoic age can not be ruled out. Direct attempts at dating the Hutton anorthositic suite have so far yielded only metamorphic zircons ( $1781 \pm 2$  Ma), but there is good field evidence for an older age because it is crosscut by: 1) a granitic pegmatite, dated as  $1804 \pm 3/-2$  Ma, which cuts migmatitic gneissosity in the suite; 2) Avayalik dykes, the age of which is discussed below; and 3) Paleoproterozoic metaplutonic rocks (diorite-tonalite-granite suite), the equivalents of which have been dated as 1910-1890 Ma.

Within the Komaktorvik shear zone, deformed, subvertical Avayalik dykes trend north-northwest, parallel to shear foliations. The dykes are thoroughly recrystallized to hornblende-garnet±epidote assemblages and commonly contain recrystallized white feldspar megacrysts. West of the Komaktorvik shear zone, mafic dyke remnants interpreted to be derived from Avayalik protoliths are a common feature in Archean gneisses. Dykes in the Noodleook complex are recrystallized to hornblende-plagioclase-epidote assemblages and locally contain white feldspar megacrysts. In Archean gneiss slivers in the Tasiuyak gneiss complex, granulite-facies dykes contain granoblastic garnet-pyroxene-hornblende assemblages.

### Paleoproterozoic supracrustal rocks

Numerous narrow units of garnet ± sillimanite paragneiss occur dominantly in the northern part of the Noodleook complex, particularly along the boundaries of the Killinek charnockitic suite and Archean Nain gneisses, but also as layers and rafts within Paleoproterozoic metaplutonic rocks (Fig. 1: Wardle et al., 1993).

South of 60°N, supracrustal rocks are dominated by narrow units of layered mafic gneiss, the largest of which includes a  $\leq 1.5$  km wide body located just west of, and parallel to the Hutton anorthositic suite (Fig. 1). The layered mafic gneisses are typified by centimetre-scale compositional layering (fig. 3a in Van Kranendonk et al., 1993a), but include feldspar porphyritic layers and homogeneous, unlayered units  $\leq 20$  m thick. Possible evidence for pillows was identified in one locality (Fig. 4A). Rare interlayers of paragneiss,



**Figure 4.** A) Possible relict pillow texture in thick unit of layered mafic gneiss; B) Elliptical felsic inclusions in hornblende diorite unit of layered mafic gneiss = possible fragmental andesite(?); C) Inclusions of mafic gneiss in tonalite. All from southwest of Eclipse Channel.



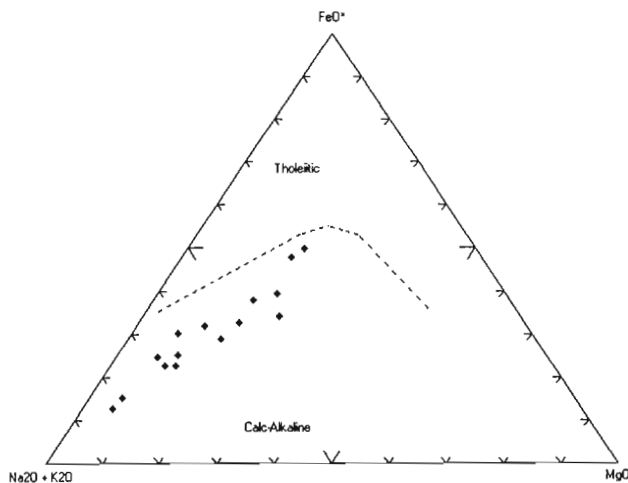
calc-silicate and possible fragmental andesites (Fig. 4B) suggest a dominantly supracrustal origin for these rocks, and the typical centimetre-scale layering of the mafic gneisses is interpreted to be original compositional layering in flows, and/or tuffs. Homogeneous mafic layers may represent massive volcanic flows or sills, whereas the occurrence of layers and discordant sheets of hornblende diorite and rare units of quartz-feldspar porphyry suggest that subvolcanic intrusions are also present.

In the east, mafic gneisses contain amphibolite-facies assemblages of hornblende-plagioclase-titanite-quartz-ilmenite and show no evidence of having been metamorphosed to granulite facies, other than they are locally cut by garnet- and clinopyroxene-bearing veins. Adjacent to the Killinek charnockitic suite, however, inclusions and rafts of mafic gneiss within Paleoproterozoic metaplutonic rocks are at granulite facies.

The supracrustal rocks of this complex are considered to be Paleoproterozoic in age because of their location along major lithological contacts, their continuity along strike, and the fact that they are not cut by Avayalik dykes. That the supracrustal gneisses are intruded by Paleoproterozoic tonalites (Fig. 4C) indicates a minimum age of  $\geq 1910$  Ma (see below).

#### Diorite-tonalite-granite (DTG) suite

Archean gneisses and Paleoproterozoic supracrustal rocks of the Noodleook complex were intruded by a suite of Paleoproterozoic metaplutonic rocks (Fig. 1: Van Kranendonk et al., 1993a). Dominated by tonalitic compositions, this suite displays a broad calc-alkaline trend (Fig. 5), in accord with the tentative interpretation that it represents a magmatic arc suite. Zircon dates from the suite lie in the range 1910–1890 Ma (Fig. 1). Sm-Nd results by L. Campbell on two samples of the suite show an  $\epsilon_{\text{Nd}}$  (@ 1.91 Ga) of 0.2 and -2, which fall below that of a depleted mantle source at the time of crystallization



**Figure 5.** A-F-M plot of diorite-tonalite-granite suite rocks (gabbro and diorite through tonalite to granite), showing distribution along a broad calc-alkaline trend.

and suggest the involvement of some Archean crustal material (Archean crust or Proterozoic sediments with an Archean detrital component).

Within the Komaktorvik shear zone, straight sheets of mildly foliated tonalite-granodiorite cut across folded migmatitic layering in older diorite-tonalite-granite suite rocks and Nain gneisses, suggesting a syn-tectonic emplacement for at least some of the diorite-tonalite-granite suite and a complex history for the zone (see below).

It is important to emphasize here that none of the Paleoproterozoic rocks in the Noodleook complex are cut by Avayalik dykes, whereas in occurrences of Archean gneisses, relict mafic dykes of presumed Avayalik parentage are commonly preserved.

#### Tasiuyak gneiss complex

Granulite-facies rocks of the Tasiuyak gneiss complex (cf. Van Kranendonk and Ermanovics, 1990) outcrop in the southwestern part of the map area and are characterized by large volumes of white garnet±sillimanite±graphite paragneiss and associated diatexite collectively known as the Tasiuyak gneiss (Wardle, 1983). In low-strain areas, the Tasiuyak gneiss has a subhorizontal compositional layering which varies from garnet quartzites and quartz arenites, through garnet-biotite-graphite quartzo-feldspathic gneiss (semi-pelite and diatexitic granite), to garnet-sillimanite-biotite-graphite metapelite, and that clearly represents transposed bedding.

Other rocks within the complex include Paleoproterozoic charnockitic rocks and quartz diorites of the Killinek charnockitic suite, garnet quartzo-feldspathic paragneisses with thin calc-silicate and marble units (described in Van Kranendonk et al., 1993a), and newly discovered tectonic slices of Archean gneiss (Fig. 1).

#### Killinek charnockitic suite

The Killinek charnockitic suite is the dominant lithology in the northwestern part of the map area (Fig. 1), where it consists primarily of homogeneous, medium- to coarse-grained, orthopyroxene-bearing granitoid rocks with a range in composition from tonalite-granodiorite-granite. These rocks contain rare xenoliths of ultramafic, anorthositic and mafic rocks, large rafts of Tasiuyak-like metasedimentary gneisses, and locally, orthogneiss inclusions with complex structures suggestive of an Archean protolith. A sample of this suite from Killinek Island is  $1895 \pm 3$  Ma.

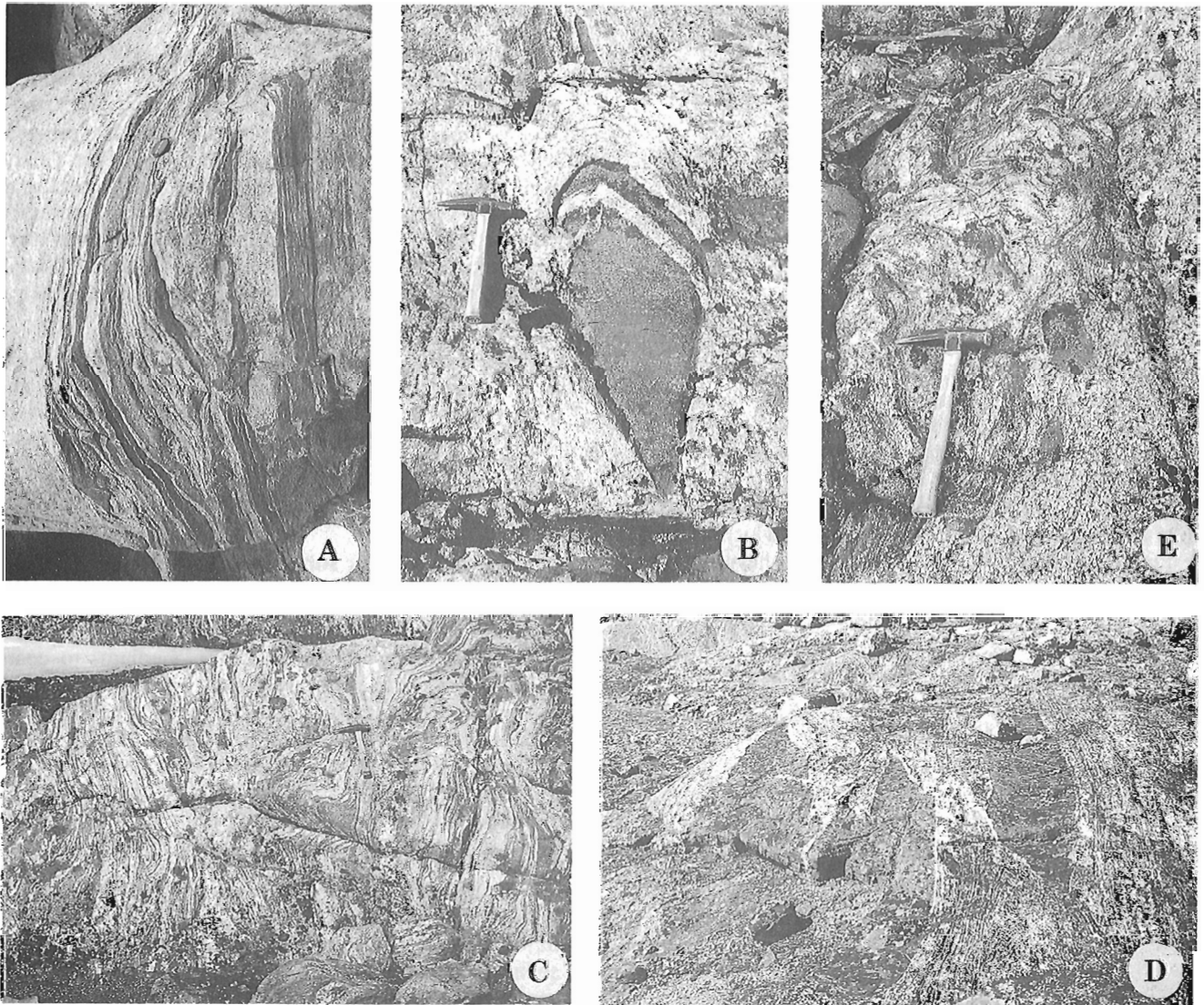
The Killinek charnockitic suite is in tectonic contact with Archean Nain gneisses and associated Paleoproterozoic rocks of the diorite-tonalite-granite suite across thin belts of meta-sediment in the northeastern part of the map area. In the central-western part of the area, however, the relationship between the charnockitic and diorite-tonalite-granite suites is less clear and occurs across a complex zone of heterogeneous metaplutonic gneisses with abundant mafic supracrustal enclaves. The transition, in part, coincides with the change from granulite facies in the west to retrogressed granulite facies in the east.

Orthopyroxene-bearing metaplutonic rocks, interpreted as the southerly continuation of the Killinek charnockitic suite, occur throughout the Tasiuyak gneiss complex and into the Rae Province. In the former, charnockitic rocks locally contain xenoliths of layered orthogneiss (Fig. 6A) and commonly of mafic granulite (Fig. 6B), and were extensively mapped as diatexite. These rocks grade into large areas of lithologically and structurally more complex orthogneiss of suspected Archean age (see below). A Sm-Nd result from a sample of homogeneous, orthopyroxene tonalite shows an  $\epsilon_{Nd}$  (@ 1.89 Ga) of -9.59, consistent with a large amount of contamination by an Archean crustal component, and significantly more negative than for samples of the diorite-tonalite-granite suite.

Mesocratic quartz diorite intrusions (CI = 20-30%) within the Tasiuyak gneiss complex are interpreted as part of the Killinek charnockitic suite (Fig. 1: see Van Kranendonk et al., 1993a). In contrast with the charnockitic rocks of the suite, however, the quartz diorites are interpreted to be juvenile intrusions since they commonly show intrusive relationships with surrounding paragneisses and contain cognate xenoliths of finer grained diorite but none of tonalite gneiss or mafic granulite. A sample of the quartz diorite is  $1896 \pm 2$  Ma.

### Suspected Archean orthogneiss

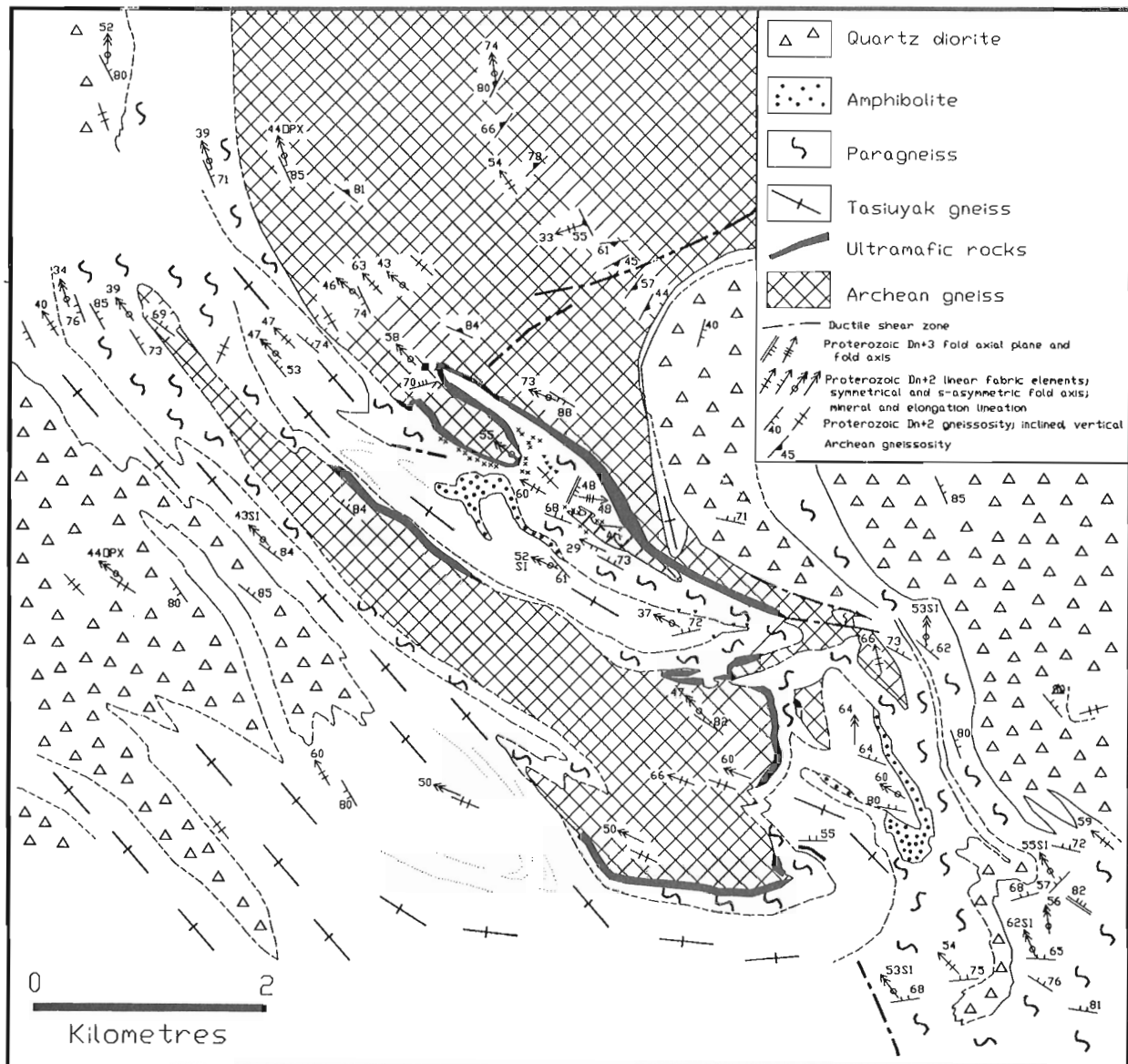
Migmatitic tonalite-granodiorite orthogneisses occur as tectonic slices within the Tasiuyak gneiss complex (Fig. 1). They preserve evidence of a complex structural and metamorphic



**Figure 6.** Orthogneisses in the Tasiuyak gneiss complex: **A)** Inclusion of mafic granulite (relict dyke?) in homogeneous orthopyroxene tonalite of the Killinek charnockitic suite; **B)** Inclusion of tonalite gneiss (Archean?) in homogeneous orthopyroxene tonalite; **C)** Heterogeneous orthogneiss of suspected Archean age; **D)** Folded and disrupted mafic dykes in suspected Archean gneiss; **E)** Suspected Archean gneiss and vein of homogeneous Paleoproterozoic tonalite (bottom right).

history and contain layers and rafts of mafic gneiss, anorthositic gneiss, and rare paragneiss (Fig. 6c). The orthogneisses display greater lithological and structural complexity than surrounding paragneisses and contain folded and disrupted remnants of granoblastic, equigranular mafic dykes which locally preserve discordant relationships with gneissic layering in the host rocks (Fig. 6D). The absence of such dykes in the adjacent paragneisses and the more complex fabrics in the orthogneisses suggest an Archean age for the latter.

The contact zone between Archean gneiss slivers and surrounding Paleoproterozoic paragneisses ranges from 0-500 m and is characterized by discontinuous units of ultramafic rocks, rusty, graphitic-rich paragneisses, blue-grey graphitic and/or red Fe-rich quartzites, rare layers of calc-silicate and/or impure marble, and migmatitic paragneiss (Fig. 7). The contacts are considered to be of tectonic origin and to represent early thrust faults as they truncate individual paragneiss and/or ultramafic units, but are themselves folded and deformed by regionally developed sets of structures.



**Figure 7.** Detailed map of tectonically bounded slices of suspected Archean gneiss in the Tasiuyak gneiss complex (see Fig. 1 for location). Units other than Archean gneiss are Paleoproterozoic in age. Note the thick units of folded and boudinaged ultramafic rocks and of paragneiss along the margins of Archean gneisses. In paragneiss: small x = occurrences of marble, calc-silicate and graphitic quartzite; small inverted triangles = rusty graphitic paragneiss.

Within Archean crustal slices, migmatitic orthogneisses are locally to extensively homogenized to an equigranular, wispy-textured orthopyroxene-bearing tonalite-granodiorite containing mafic layers and lenses derived from remnant mafic dykes and mafic granulite gneiss (Fig. 6E). The homogeneous rocks have an identical appearance to those of the Killinek charnockitic suite farther north, except that the former contain a greater proportion of mafic inclusions. Homogenization may have occurred either through assimilation of the older rocks by widespread intrusion of younger magmas, or through in situ partial melting of the Archean gneisses.

### ***Rae Province and Lake Harbour Group***

Rae Province orthogneisses of suspected Archean age vary from white-weathering, homogeneous, tonalitic gneiss to agmatitic and schlieric textured migmatites in which 40-50% of inclusions of grey gneiss and mafic - or less commonly anorthositic - rocks float in a granitic neosome of possible Proterozoic age. Rare mafic dykes have also been observed. Rae orthogneisses differ from their Nain counterparts and those in the Tasiuyak gneiss complex by having abundant granite and a general shortage of ultramafic inclusions.

The Paleoproterozoic Lake Harbour Group (Taylor, 1979) contains white marble, quartzite, garnet-sillimanite metapelite, rusty garnet-graphite-biotite±sillimanite paragneiss, hornblende-biotite-plagioclase-quartz dioritic gneiss, and rare sheets of hornblende-plagioclase±garnet±orthopyroxene mafic gneiss. The structurally lowermost unit in many of the folds is marble. Contact relationships between the group and Rae Province orthogneisses are sharp and strongly sheared near the Ablviak shear zone, but unshaped away from the zone, where they may represent stratigraphic contacts or the trace of pre-metamorphic thrusts.

Orthopyroxene-bearing tonalitic rocks with a single set of planar and linear fabric elements are interlayered with Rae orthogneisses and Lake Harbour Group metasedimentary rocks. These charnockitic rocks are similar in appearance and mineralogy to those of the Killinek charnockite suite, but are distinct from the migmatitic, heterogeneous gneisses of suspected Archean age in the Rae Province by virtue of their monocyclic character, the presence of coarse hypersthene crystals, and a buff weathering surface.

## **YOUNGER PALEOPROTEROZOIC ROCKS**

### ***Metaplutonic rocks***

Plagioclase-porphyrific mafic metatonalites (1869 ± 3/-2 Ma: C.I. = 30-40%) and megacrystic metagranites (minimum age of 1864 ± 2 Ma) within the northern part of the Komaktorvik shear zone represent a younger suite of Paleoproterozoic metaplutonic rocks than either the diorite-tonalite-granite or Killinek charnockitic suites (Fig. 1). The mafic metatonalites cut Nain gneisses and diorite-tonalite-granite suite rocks, but are in sharp (?) tectonic contact with the Killinek charnockitic suite. Megacrystic metagranites, however, were seen to

crosscut rocks of both the Killinek charnockitic suite and the Nain Province/diorite-tonalite-granite suite association, thus indicating a minimum age for the amalgamation of these units. Similar granites, though undated, occur as linear bodies south of Eclipse Channel (Fig. 1).

## **SYN-TECTONIC MAFIC DYKES**

Nain gneisses, Avayalik dykes, and rocks of the diorite-tonalite-granite suite are cut by a set of fine- to medium-grained, pale-green weathering, hornblende-plagioclase±garnet dykes. In general, these are not feldspar phyric, but some contain black feldspar megacrysts (≤ 5 cm), and/or round feldspar±quartz and K-feldspar (?) xenocrysts (< 1 cm). Pale green dykes trend north-south within the Komaktorvik shear zone, commonly have highly irregular intrusion forms, and are weakly deformed relative to strongly sheared country rocks; features which strongly suggest a syn-tectonic emplacement during Komaktorvik shear deformation.

Compositionally and texturally heterogeneous amphibolite dykes cut all previous sets of dykes. They vary from undeformed, equigranular, medium grained amphibolites and round plagioclase-phyric portions that cut across strongly sheared Archean gneisses, to thin (< 10 cm), foliated hornblendites which strike parallel to the shear foliation. These dykes are considered to be late tectonic with respect to the Komaktorvik shear zone.

## **POST-TECTONIC MAFIC DYKES**

Cambrian diabasic to gabbroic dykes (K-Ar age = 524 ± 78 Ma: Taylor, 1979) vary from a 50 m wide, subvertical body that can be traced for more than 40 km east-west across the central part of the map area, to flat-lying sheets, 0.2-10 m thick, which locally cover several 1000 m<sup>2</sup> farther south. These dykes were not recognized north of 60°N and are concentrated in the eastern half of the map area.

Rare, narrow (< 1 m), ultramafic lamprophyres of unknown age have been found along the Labrador Sea coast in areas of very good exposure (see Wardle et al., in press); the true extent of these bodies is not known. The dykes commonly contain numerous small xenoliths and/or xenocrysts of ultramafic and mafic material and phlogopite in a fine grained, soft, micaceous matrix. Some dykes display good compositional flow banding and lack xenoliths.

## **MINERALIZATION**

Two rusty-weathering gossans with massive pyrite and local chalcopyrite form linear belts, up to 50 m wide, that extend across the north-south width of Killinek Island along the contact between mafic metatonalite and rocks of the Killinek charnockitic suite (Fig. 1). Samples have been submitted for assay.



## TECTONIC AND STRUCTURAL EVOLUTION

The complex Archean histories of the Nain and Rae provinces in the map area are as yet incompletely understood and will not be further discussed. For simplicity, all Archean structures are referred to as  $D_n$ . The Paleoproterozoic structural evolution of the map area is described in Van Kranendonk et al. (1993a) and does not require significant modifications as the result of the 1993 fieldwork. However, the new field results and recent U-Pb age data have provided additional insight into the Paleoproterozoic evolution, which is briefly summarized below.

The age and origin of the Hutton anorthositic suite – whether late Archean or earliest Proterozoic (pre-1910 Ma) – are still unresolved. In the former scenario, the rocks are believed to form an integral part of the Nain gneiss complex, whereas in the latter, the anorthositic suite is envisaged to have been emplaced during rifting of the Nain Province margin after the end of late Archean tectonism.

The presence of tectonic slices of Archean gneiss and ultramafic rocks within the Tasiuyak gneiss complex is used to suggest that it represents an accretionary complex. The age of possible accretionary tectonics in the Torngat Orogen is unknown, but if the presence of monocyclic, orthopyroxene-bearing tonalites within the Rae Province represents the southern continuation of the Killinek charnockitic suite, then the Tasiuyak gneiss was clearly pinned to the Rae Province prior to ca. 1895 Ma.

The period from 1910-1890 Ma was one of extensive magmatism in both the Rae Province/Tasiuyak gneiss complex and Nain Province margin. The diorite-tonalite-granite suite is interpreted to represent a magmatic arc that resulted from easterly subduction beneath the Nain Province. The layered mafic supracrustal rocks may represent the remnants of a marginal (back arc?) basin which developed along the thinned western margin of the Nain Province during the early stages of subduction.

The Killinek charnockitic suite is also tentatively interpreted to represent a magmatic arc suite that resulted from westerly directed subduction beneath the Rae Province and Tasiuyak gneiss complex at ca. 1895 Ma. The relationship between the Killinek and diorite-tonalite-granite suites, and the implications that the presence of these broadly co-eval suites on either side of the orogen have for the tectonic evolution of the area, is yet to be fully established pending further geochemical and isotopic analysis.

$D_{n+1}$  structures include a migmatitic gneissosity in rocks of the Tasiuyak gneiss complex and a foliation or migmatitic textures in some rocks of the diorite-tonalite-granite suite. These structures, and tectonic intercalation of Archean rocks, diorite-tonalite-granite suite rocks, and layered mafic gneisses in the Noodleok complex, and of Lake Harbour Group metasediments with Rae basement gneisses, are believed to have resulted from Nain-Rae collision at ca. 1860 Ma, the age of the oldest metamorphic zircons in the map area (Fig. 1).

Granulite-facies  $D_{n+2}$  deformation resulted in the formation of the sinistral Abloviak shear zone and large-scale, northwest-southeast trending folds and shear zones throughout the Tasiuyak gneiss complex and Killinek charnockitic suite. An  $1824 \pm 2$  Ma pegmatite which crosscuts  $D_{n+2}$  mylonitic fabric elements and is affected by  $D_{n+3}$  dextral shear, provides a minimum age for  $D_{n+2}$  deformation (Fig. 1).

Amphibolite-facies  $D_{n+3}$  structures include the sinistral, east-side-up Komaktorvik shear zone, the Katherine River dextral mylonite zone, and large-scale, north-south trending folds in the Abloviak shear zone and Burwell domain (Van Kranendonk et al., 1993a). Dating of syn-tectonic pegmatites and of metamorphic zircons from rocks within  $D_{n+3}$  amphibolite-facies shear zones has shown that deformation occurred at between ca. 1798-1780 Ma, whereas titanite dates from 1774-1710 Ma indicate prolonged cooling and local deformation.

The Komaktorvik shear zone shows evidence of a complex and possibly long-lived deformational history. On Killinek Island, sheared metasedimentary rocks between the northeastern margin of the Killinek charnockitic suite and Archean gneisses contain kyanite-garnet-K-feldspar-biotite-quartz (in contrast to the regional development of sillimanite) and steeply north-plunging mineral lineations. These rocks are at a higher-grade and have a different orientation of linear fabric elements than the lower-grade Komaktorvik shear zone farther south and east (Fig. 2). Kyanite is also found north of Saglarsuk Bay (Fig. 1: B. Patey, Memorial University of Newfoundland, pers. comm., 1993), suggesting that this period of higher-grade deformation ( $D_{n+2}$ ?) occurred throughout the Komaktorvik shear zone.

If the kyanite-bearing mineral assemblages within the Komaktorvik shear zone are related to an earlier period of shear deformation (pre-1798-1780 Ma), we speculate that this may have occurred during  $D_{n+2}$  and correspond with a period of west-side-up uplift required to expose the high-grade Killinek charnockitic suite ( $P \leq 9.2$  kbars,  $T=800^\circ\text{C}$ : Mengel and Rivers, 1992). Uplift and concomitant depression of the Nain lithosphere may have resulted in the development of static garnet-clinopyroxene assemblages in Nain gneisses and Avayalik dykes, at ca. 1835 Ma, the age of zircon growth in an Avayalik dyke. Subsequent east-side-up, sinistral shear within the Komaktorvik shear zone at ca. 1798-1780 Ma, was then responsible for uplift of the high-grade Four Peaks domain.

## ACKNOWLEDGMENTS

Capable and cheerful field assistance was provided by Rod Churchill (Memorial U.) and Anders Haumann (U. of Copenhagen). A visit by J. Connelly (Memorial U.) and a tour of the Seven Islands Bay area by D. Bridgwater (Geological Museum, Copenhagen) were greatly appreciated. Twin Otter transportation by Air Inuit and excellent flying by Jeff Maloney and Boyd Summers of Universal Helicopters

(Goose Bay) made the field season a success. Reviews of a preliminary version of this report by Ingo Ermanovics, Garth Jackson and Dave Scott helped to clarify the ideas presented.

## REFERENCES

- Bridgwater, D. and Wardle, R.**  
1992: Whole rock Pb isotopic compositions of Archean and Proterozoic rocks from northern Labrador used to separate major units in the shield; Lithoprobe Report No.32, p.54-63.
- Mengel, F. and Rivers, T.**  
1992: 3-D architecture and thermal structure of deep crustal-scale transcurrent shear zones - Report 2: Preliminary results from the Komaktorvik Shear Zone north of 60°N; Lithoprobe Report No.32, p.64-73.
- Scott, D., Machado, N., Van Kranendonk, M., Wardle, R., and Mengel, F.**  
1993: A preliminary report of U-Pb geochronology of the northern Torngat Orogen, Labrador; *in* Current Research, Part C; Geological Survey of Canada, Paper 93-1C, p.341-348.
- Taylor, F.**  
1979: Reconnaissance geology of a part of the Precambrian Shield, northeastern Quebec, northern Labrador and Northwest Territories; Geological Survey of Canada, Memoir 393, 99p.
- Van Kranendonk, M. and Ermanovics, I.**  
1990: Structural evolution of the Hudsonian Torngat Orogen in the North River map area, Labrador: Evidence for east-west transpressive collision of Nain and Rae continental blocks; Geoscience Canada, v.17, p.283-288.
- Van Kranendonk, M. and Scott, D.**  
1992: Preliminary report on the geology and structural evolution of the Komaktorvik Zone of the Early Proterozoic Torngat Orogen, Eclipse Harbour area, northern Labrador; *in* Current Research, Part C; Geological Survey of Canada, Paper 92-1C, p.59-68.
- Van Kranendonk, M., Godin, L., Mengel, F., Scott, D., Wardle, R., Campbell, L., and Bridgwater, D.**  
1993a: Geology and structural development of the Archean to Paleoproterozoic Burwell domain, northern Torngat Orogen, Labrador and Quebec; *in* Current Research, Part C; Geological Survey of Canada, Paper 93-1C, p.329-340.
- Van Kranendonk, M., Wardle, R., Mengel, F., Ryan, B., and Rivers, T.**  
1993b: Lithotectonic divisions of the northern part of the Torngat Orogen, Labrador, Quebec and N.W.T.; Lithoprobe Report No.32, p.21-31.
- Wardle, R.**  
1983: Nain-Churchill Province cross-section, Nachvak Fiord, northern Labrador; *in* Current Research; Newfoundland Department of Mines and Energy, Mineral Development Division, Report 83-1, p.78-90.
- Wardle, R., Van Kranendonk, M., Mengel, F., and Scott, D.**  
1992: Geological mapping in the Torngat Orogen, northernmost Labrador: Preliminary results; *in* Current Research (1992); Newfoundland Department of Mines and Energy, Geological Survey Branch, Report 92-1, p.413-429.
- Wardle, R., Van Kranendonk, M., Mengel, F., Scott, D., Schwarz, S., and Ryan, B.**  
1993: Geological mapping in the Torngat Orogen, northernmost Labrador: Report 2; *in* Current Research (1993); Newfoundland Department of Mines and Energy, Geological Survey Branch, Report 93-1, p.77-89.
- Wardle, R., Bridgwater, D., Mengel, F., Campbell, L., Van Kranendonk, M.J., Haumann, A., Churchill, R., and Reid, L.**  
in press: Mapping in Torngat Orogen, northernmost Labrador: The Nain Craton; *in* Current Research (1994); Newfoundland Department of Mines and Energy, Geological Survey Branch, Report 94-1.

Geological Survey of Canada Project 910034



# Tholeiitic and weakly alkalic basaltic volcanism of the Mugford Group, northern Labrador: preliminary geochemical results<sup>1</sup>

M.A. Hamilton

Continental Geoscience Division

*Hamilton, M.A., 1994: Tholeiitic and weakly alkalic basaltic volcanism of the Mugford Group, northern Labrador: preliminary geochemical results; in Current Research 1994-C; Geological Survey of Canada, p. 333-342.*

---

**Abstract:** The Mugford Group, comprising basal siliciclastic sediments, deep-water euxinic shales, cherts, mudstones and dolostones overlain by pillowed and massive basalt, tuff and agglomerate, represent a Lower Proterozoic supracrustal succession deposited unconformably on listric normal faulted Archean gneisses of the Nain craton. Mugford Group volcanics share many physical and chemical properties of continental rift or plateau basalts. Initial volcanism (Calm Cove formation) is represented by pillowed and massive flows of relatively evolved, weakly alkaline to transitional basalts and then by more primitive tholeiitic basalts. Eruptive compositions in agglomerates and massive flows of the overlying Finger Hill formation show a comparable chemical evolution and bipartite division in alkalinity to those in the Calm Cove formation. Lavas in both sequences show strong enrichments in incompatible trace elements and the rare earths, similar to continental alkaline basalts as well as plume-influenced mid-ocean-ridge basalts.

**Résumé :** Le Groupe de Mugford, composé de sédiments silicoclastiques basaux, de shales euxiniques de mer profonde, de cherts, de mudstones et de dolomies, surmontés de basaltes en coussins et de basaltes massifs, de tufs et d'agglomérats, représente une succession supracrustale du Protérozoïque inférieur, qui s'est déposée en discordance sur des gneiss archéens du craton de Nain découpés par des failles listriques normales. Les roches volcaniques du Groupe de Mugford partagent un grand nombre des propriétés physiques et chimiques des basaltes de rift ou de plateau continentaux. Le volcanisme initial (formation de Calm Cove) est représenté par des coulées de laves massives ou de laves en coussins constituées de basaltes relativement évolués, légèrement alcalins à transitionnels, qui font ensuite place à des basaltes tholéiitiques plus primitifs. La composition des roches éruptives dans les agglomérats et dans les coulées massives de la formation de Finger Hill sus-jacente montrent une évolution chimique et une division bipartite de l'alcalinité, comparables à celles observées dans la formation de Calm Cove. Les laves des deux séquences montrent de forts enrichissements en éléments traces incompatibles et en terres rares, comme dans les basaltes alcalins continentaux et les basaltes de dorsale médio-océanique associés à des panaches.

---

<sup>1</sup> Contribution to Canada-Newfoundland Cooperation Agreement on Mineral Development (1990-1994), a subsidiary agreement under the Canada-Newfoundland Economic and Regional Development Agreement.

## **INTRODUCTION**

Contrasting models of Proterozoic crustal growth and contemporaneous mantle evolution continue to be the subject of considerable debate (Condie, 1992). Particularly important towards resolving these issues is a more complete knowledge of the nature and degree of the depletion of mantle source regions, which can be very heterogeneous. Sparse data currently exist for depleted mantle compositions during the earliest Proterozoic (e.g. 2.5 - 2.0 Ga). In this paper, preliminary geochemical data are presented for a suite of mafic volcanic rocks from the extremely well-preserved lower Proterozoic Mugford Group, and form part of a study aimed at characterizing aspects of crust-mantle evolution in the western North Atlantic (Nain) craton.

Geological mapping and sampling in the Kaumajet Mountains area (Fig. 1) continued in July and August 1993, and complements work initiated in 1992 initiated as part of Canada-Newfoundland Cooperation Agreement on Mineral Development.

## **GEOLOGICAL SETTING**

The stratigraphy and structure of the Mugford Group has been described in detail most recently by Smyth (1976), Smyth and Knight (1978), and Hamilton (1993). A collateral study was made by Barton (1975) on the geochemistry of part of the group.

The project area lies within the Nain Province of northern coastal Labrador. Much of this region is underlain by amphibolite- to granulite-facies quartzofeldspathic orthogneiss (and lesser supracrustal gneisses), typical of the northern Labrador segment of the North Atlantic craton which has elsewhere yielded U-Pb ages in excess of 3.8 Ga (Schjøtte et al., 1989).

The Mugford Group is preserved as a nearly flat-lying sequence in a graben-like structure bounded on its western side by a series of northwest-striking, brittle and ductile faults. Most Mugford Group rocks are preserved at low greenschist grade, reached in response to early Proterozoic Torngat orogenesis, whose front lay some 60 km to the west (Van Kranendonk, 1990). Visible best on Cod and Grimington Islands, multiple high-angle, listric normal faults with up to a few tens of metres of dip-slip displacement, and spaced at a few hundred metre intervals, are responsible for a locally irregular basement topography. As outlined in detail by Hamilton (1993), the age of Mugford Group volcanism is poorly constrained between 2.4 and 2.0 Ga. However, preliminary Sm-Nd isotopic results suggest a crystallization age close to 2.0 Ga (Hamilton, in prep.).

### ***Stratigraphic relationships***

Smyth (1976) divided the group into a lower sedimentary unit, a lower volcanic unit, a 'middle' sedimentary unit and an upper volcanic unit, and suggested a maximum thickness of 1225m for the entire group. Following a slight revision of the stratigraphy, Smyth and Knight (1978) suggested individual

formation names - the Sunday Run, Cod Island, Calm Cove, Shark Gut and Finger Hill formations, and these informal names are used in this report (Fig. 1). As this paper deals primarily with the chemistry of basaltic flows in the lower volcanic unit (Calm Cove formation) and the upper volcanic unit (Finger Hill formation), a brief lithological description is provided below.

### ***Calm Cove formation***

Calm Cove formation consists essentially of 400 m of inter-layered pillowed and massive basaltic flows, and pillow breccias. Flows may be predominantly either pillowed or massive or be compound in structure, with a massive base transitional into an overlying pillowed section with or without an amoeboid pillow breccia top. Most flows average between 5 and 15 m in thickness. The relative proportions of pillowed, massive, and breccia zones within individual flows vary unsystematically. Subaqueous volcanic extrusive activity persisted continuously throughout the deposition of the entire Calm Cove formation.

Fine- to medium-grained, dark- to light-grey and light-green, buff-weathering, massive basalts are generally blocky, or less commonly, columnar jointed. These units may be locally plagioclase-phyric, as are some pillowed counterparts in the lower sections of the formation. Many of the massive sections within pillowed flows were sampled for chemical analysis throughout the entire stratigraphy.

### ***Finger Hill formation***

Smyth (1976) estimated that the Finger Hill formation consists of at least 600 m of mafic agglomerates and breccias, minor tuffs and basaltic sills. The breccias are composed of thick individual flow units, are poorly sorted, and contain buff-weathering (at times vesicular) angular to rounded basaltic fragments that are less than 1 cm to over 2 m in size. Subordinate clasts and blocks of older breccia and agglomerate and white-weathering tuffaceous material are common. Minor pillowed flows are also present in lower sections of the formation. Sampling emphasis was placed on the interiors of volumetrically minor, but ubiquitous massive flows.

### ***Diabase dykes***

A number of fine- to medium-grained, grey, weakly deformed diabase dykes, probably components of the early Proterozoic Napaktok dyke swarm of Ermanovics et al. (1989), clearly intrude Archean orthogneiss in the study area (Fig. 1). These define a conjugate set oriented roughly west-northwest and north-northeast. These dykes typically carry grey to very pale green subequant plagioclase phenocrysts. The dykes are 5 to 15 m thick and can generally be traced along strike for several hundred metres. Although the Mugford Group and underlying basement are clearly separated by an unconformity, it is unclear whether all elements of the Napaktok swarm predate deposition of the group. The Mugford Group itself is cut in many places by similar, grey, two-pyroxene diabase dykes of

comparable size to the Napaktok dykes (Hamilton, 1993). These subvertical dykes are dominantly oriented north-south, with a minor conjugate set oriented approximately east-west. Their exact relationship to the main Napaktok dyke swarm and to Mugford Group magmatism is unknown. Locally, however, the east-west dykes can be seen feeding flows of the

Calm Cove formation, and can be traced to feldspar-phyric dykes mapped by Ermanovics (1992) as components of the Napaktok dyke swarm. Several samples have been analyzed in an attempt to compare dyke chemistries and to evaluate their relation to extrusive volcanism of the Calm Cove and Finger Hill formations.

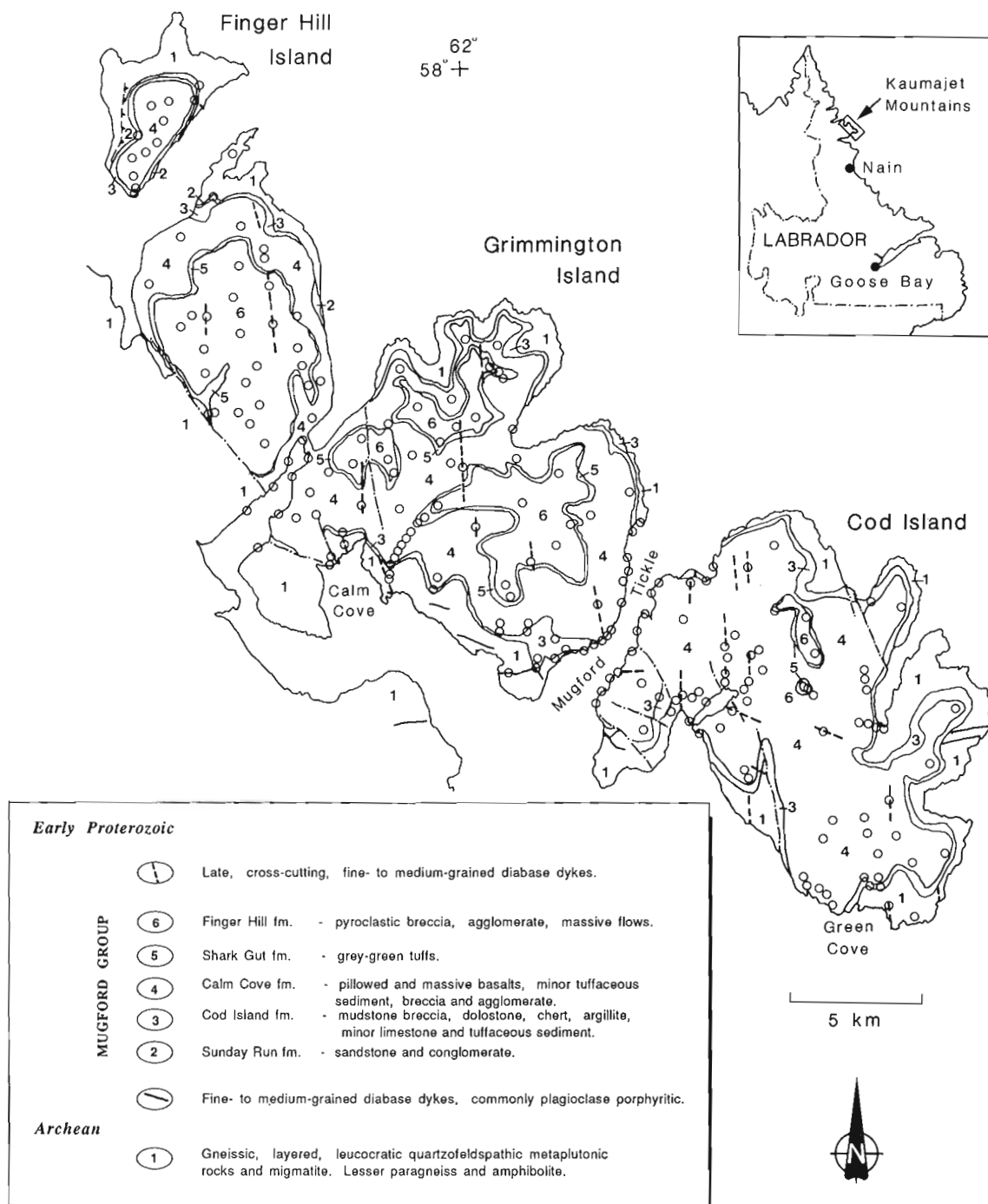


Figure 1. Geological sketch map of the Kaumajet Mountains area, Nain Province, Labrador. Geology of the Mugford Group modified after Smyth (1976). Principal 1992 and 1993 sampling areas shown in open circles.

## PETROGRAPHY

Massive and pillowed flows are dominantly either aphyric or sparsely plagioclase-phyric (up to 5%), and consist of a matrix of fine grained actinolite, chlorite, plagioclase microlites (variably replaced by albite or epidote), and locally pseudomorphs after olivine or clinopyroxene. Plagioclase phenocrysts may reach up to 2 cm in length as individual grains or as glomeroporphyritic clusters. Accessory minerals include ilmenite, magnetite, apatite, titanite (after oxide), and minor quartz. In all cases, samples with reported chemical analyses were taken from massive flow interiors.

Early Proterozoic (Napaktok) diabase dykes and the late-stage, two-pyroxene, diabase dykes which locally cut the entire Mugford Group volcanic series have comparable mineralogies and textures. These commonly have fine grained chilled margins and medium grained subophitic interiors consisting of (2-8%) porphyritic plagioclase laths (to 2 cm) set in an intersertal intergrowth of orthopyroxene, clinopyroxene, magnetite, pyrrhotite and apatite.

## GEOCHEMISTRY

Barton (1975) provided geochemical data for only the lower volcanics (Calm Cove formation) of the Mugford Group. These included all major element, but only few trace element data, most of which are either compatible in some ferromagnesian liquidus phases (e.g. Cr, Ni) or are now known to be variably mobile during low-grade metamorphism or low-temperature alteration (e.g. Rb, Ba, Sr). On this basis, he recognized two principal compositional types in the Mugford Group volcanics - tholeiites and 'greenstones' - and interpreted the latter as being the result of low-temperature alteration processes. Although the presence of relict grains of titanite was noted in occasional 'greenstone' samples, the overall enrichments in sodium, iron, titanium and phosphorus were ascribed to largely secondary alteration of the tholeiitic basalts.

Preliminary geochemical data for representative examples of the tholeiitic and weakly alkaline volcanic rocks of this study are presented in Table 1. Data are also presented for a

**Table 1.** Representative chemical analyses of Mugford Group lavas.

Sample	Calm Cove formation					Finger Hill formation				Diabase dykes		
	Subalkaline series		Alkaline series			Subalkaline series		RM-69 242A	Alkaline series		HMB92 005B	HMB92 050A
	HMB92 82	HMB92 94B	TA-69 230	HMB92 019A	HMB92 41	HMB92 078A	HMB92 77		HMB92 086A	HMB92 086A		
%												
SiO <sub>2</sub>	48.70	48.30	50.60	48.50	49.80	47.90	47.10	49.10	49.40	51.70	51.70	51.70
TiO <sub>2</sub>	1.01	1.31	2.46	2.88	2.27	1.55	1.58	1.54	2.19	1.64	1.59	1.59
Al <sub>2</sub> O <sub>3</sub>	15.40	14.60	13.20	14.30	12.80	13.20	13.70	12.30	12.50	14.50	15.00	15.00
Fe <sub>2</sub> O <sub>3</sub>	2.30	2.40	2.50	6.40	3.00	3.00	3.40	4.50	5.90	2.60	3.60	3.60
FeO	8.00	10.00	11.90	10.00	11.40	11.00	10.50	11.50	10.60	9.00	8.10	8.10
MnO	0.17	0.19	0.29	0.34	0.19	0.21	0.22	0.23	0.15	0.18	0.18	0.18
MgO	7.02	6.68	4.70	3.80	4.00	6.35	5.75	5.33	4.60	4.23	4.27	4.27
CaO	10.50	10.10	5.23	4.04	6.93	10.49	11.09	9.41	6.22	7.54	7.15	7.15
Na <sub>2</sub> O	2.60	2.20	2.80	4.80	4.10	2.00	2.00	1.60	4.30	3.20	3.30	3.30
K <sub>2</sub> O	0.41	0.30	2.10	0.56	1.14	0.37	0.28	0.76	1.15	2.07	1.78	1.78
P <sub>2</sub> O <sub>5</sub>	0.11	0.14	0.38	0.38	0.44	0.12	0.13	0.15	0.26	0.32	0.31	0.31
H <sub>2</sub> O	2.80	2.80	4.00	4.40	3.10	2.80	3.60	3.30	2.30	1.50	1.60	1.60
CO <sub>2</sub>	0.00	0.10	0.20	0.10	0.00	0.00	0.00	0.10	0.00	0.10	0.20	0.20
S	0.10	0.13	0.02	0.04	0.13	0.13	0.11	0.03	0.07	0.15	0.11	0.11
TOTAL	99.12	99.25	100.38	100.54	99.30	99.12	99.46	99.85	99.64	98.73	98.89	98.89
Mg# (molar)	61.0	54.4	41.3	40.4	38.5	50.7	49.4	45.2	43.6	45.6	48.4	48.4
ppm												
Rb	13	7	49	28	45	8.6	6.0	13.3	29	77	52	52
Sr	477	356	203	98	450	232	481	465	168	481	422	422
Ba	304	233	730	291	453	289	238	130	539	915	836	836
Zr	76	70	200	305	223	88	87	120	180	187	174	174
Nb	8.7	10	22	36	36	12	13	<10	23	9.3	9.3	9.3
U	0.20	0.18		0.72	0.92	0.21	0.22		0.46	1.1	1.1	1.1
Th	1.3	1.0		4.9	4.2	0.98	1.1		2.6	3.5	3.5	3.5
Pb	6.3	9.8		7	4.2	5.4	6.3		5.4	24	20	20
V	220	280	300	320	310	330	310	290	350	240	220	220
Sc	29	35	29	29	25	38	37	41	41	33	31	31
Co	63	66	45	46	50	65	57	57	56	49	52	52
Ni	140	100	45	28	28	68	62	57	37	19	23	23
Cr	190	140	64	25	24	74	68	45	34	68	64	64
Cu	100	100	170	240	67	100	85	310	110	53	50	50
Zn	78	79	140	130	110	85	67	130	90	110	99	99
Y	18	17	31	40	32	22	23	29	40	35	33	33
La	15.0	12.0	39.0	64.0	42.0	12.0	11.0	18.0	30.0	38.0	34.0	34.0
Ce	31.0	27.0	80.0	130.0	88.0	25.0	24.0	38.0	62.0	77.0	69.0	69.0
Nd	17.0	14.0	42.0	56.0	45.0	16.0	15.0	19.0	35.0	39.0	36.0	36.0
Sm	3.4	2.9	7.7	11.0	8.3	3.8	3.7	4.4	7.9	8.2	7.5	7.5
Eu	1.20	1.10	2.4	3.40	2.50	1.40	1.10	1.50	2.10	2.20	2.10	2.10
Gd	3.60	3.10	7.4	9.30	7.70	4.40	4.30	5.00	8.10	7.30	7.10	7.10
Tb	0.56	0.55		1.40	1.10	0.73	0.68		1.30	1.00	0.99	0.99
Dy	3.40	2.90	6.2	7.80	6.80	4.40	4.70	5.50	7.40	6.00	6.00	6.00
Er	1.90	1.70	3.1	3.70	3.10	2.50	2.40	3.20	4.40	3.50	3.40	3.40
Yb	1.70	1.60	2.9	3.60	2.70	2.20	2.30	3.30	3.90	3.30	3.10	3.10
Lu	0.28	0.26		0.49	0.40	0.36	0.35		0.68	0.48	0.47	0.47

Major and trace elements Sr, Ba, Zr were determined by wavelength dispersive XRF techniques and wet chemical methods. Data for other trace elements were obtained by ICP-ES and ICP-MS techniques. All analyses performed in the analytical chemistry laboratories of the GSC.

late east-west diabase dyke cutting the Calm Cove volcanics (005B) and an east-west diabase dyke interpreted to be a component of the Napaktok dyke swarm (050A).

### Major elements

The analyzed flows are predominantly basaltic in composition, with SiO<sub>2</sub> between 47 and 51%; most rocks are either weakly quartz- or olivine-normative. The major element composition of these rocks is quite comparable to that of many continental tholeiites (Macdougall, 1988). Compared with mid-ocean ridge basalts, most of the volcanics have lower Al<sub>2</sub>O<sub>3</sub> (12.3-15.7 wt%), CaO (4.0-11.8 wt%) and Mg# (64.7- 8.5), and higher FeO\* (9.8-15.8 wt%), TiO<sub>2</sub> (0.93-2.88 wt%) and P<sub>2</sub>O<sub>5</sub> (0.09-0.44 wt%) (Mg# = 100Mg/(Mg+Fe<sup>2+</sup>); FeO\* = total Fe). MgO ranges from 3.80 to 7.52 wt%. The subalkalic samples fall predominantly into the tholeiitic field on an AFM diagram, showing a weak iron-enrichment trend (Fig. 2). All samples plot in the tholeiitic field on a diagram of SiO<sub>2</sub> vs. FeO\*/MgO (Miyashiro, 1974); no samples define a calc-alkaline trend. On the basis of silica and total alkali contents, it is possible to classify Mugford Group lavas as subalkaline (tholeiitic) basalts, (weakly) alkaline basalts, or intermediate (transitional) basalts. Many of the earliest erupted lavas, in the lowest levels of the Calm Cove formation, described by Barton (1975) as 'greenstones', are either alkaline or transitional basalts by this classification. Despite the known mobility of the major elements, especially the alkali elements, this terminology will be continued below as it will be shown that consistent and identical classifications can be drawn from the distributions of immobile minor and trace elements.

Among Calm Cove and Finger Hill formation tholeiitic and weakly alkalic lavas, there is some overlap in SiO<sub>2</sub>, Al<sub>2</sub>O<sub>3</sub>, and FeO. However, relative to the tholeiitic lavas, the alkalic flows have higher abundances of alkali metals, TiO<sub>2</sub> and P<sub>2</sub>O<sub>5</sub>, and higher Al<sub>2</sub>O<sub>3</sub> at a given Mg#, but have lower CaO.

Most alkalic lavas are clearly more evolved than tholeiitic counterparts; Calm Cove weakly alkalic flows have Mg# between 38.5 and 41.3, whereas later tholeiites range from 54.4 to 64.7. Rocks classified as transitional fall between these groups in terms of most elements. Similarly, the one analyzed Finger Hill weakly alkaline flow (Mg# = 43.6) is more evolved than subalkaline members (Mg# = 45.2-50.7); this sample has slightly lower CaO/Al<sub>2</sub>O<sub>3</sub> than the latter (0.50 vs. 0.67-0.81), and may be related to them by clinopyroxene fractionation.

With decreasing Mg# (increasing differentiation) the oxides FeO\*, TiO<sub>2</sub> and P<sub>2</sub>O<sub>5</sub> increase steadily. Na<sub>2</sub>O and K<sub>2</sub>O also increase, but in a less regular fashion; undoubtedly, much of the scatter is due to mobility during submarine weathering. Al<sub>2</sub>O<sub>3</sub> and CaO both decrease in well-defined trends with falling Mg#.

The diabase dykes are compositionally quite uniform, with somewhat higher SiO<sub>2</sub> (~52 wt%), and lower CaO (~7-7.5 wt%), and have relatively low Mg# (43-48).

Figure 3 illustrates the systematic increase in TiO<sub>2</sub> with P<sub>2</sub>O<sub>5</sub> in all of the samples, with the earliest lavas of the Calm Cove formation showing the greatest concentrations (2.27-2.88 wt% TiO<sub>2</sub>, 0.38-0.44 wt% P<sub>2</sub>O<sub>5</sub>). The one alkaline basalt analyzed from the Finger Hill formation contains

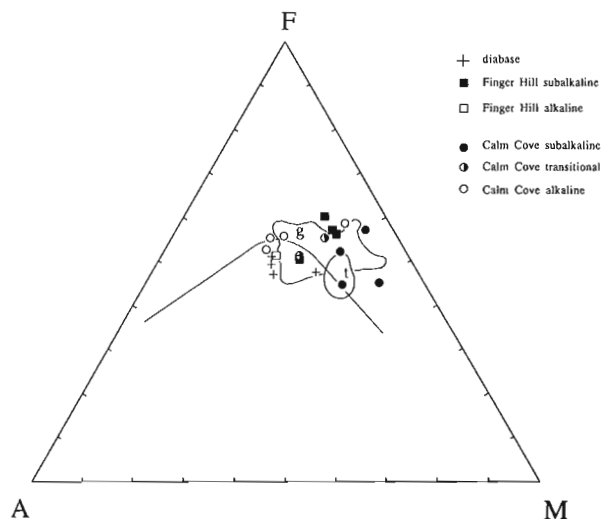


Figure 2. AFM diagram for Mugford Group basalts. Field outlined 'g' = 'greenstones', and 't' = tholeiites of Barton (1975). Dividing line of Irvine and Baragar (1971).

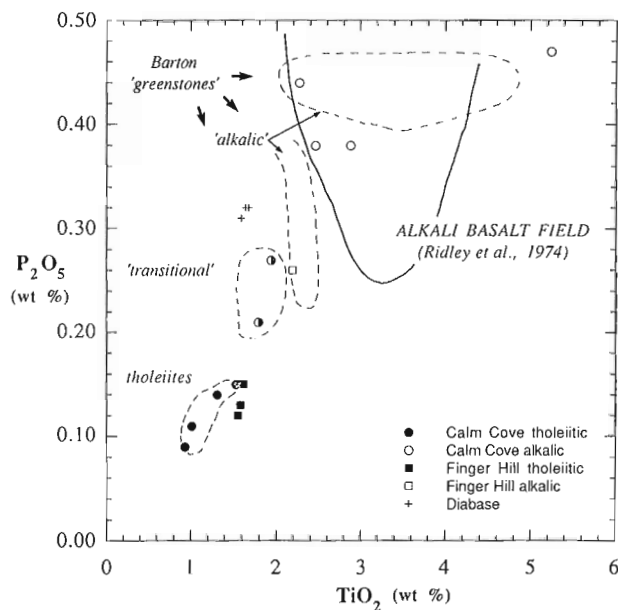


Figure 3. Plot of TiO<sub>2</sub> vs. P<sub>2</sub>O<sub>5</sub> for Mugford Group basalts. Additional dashed fields from Barton (1975), including 'greenstones' interpreted as transitional and alkaline members. Half-filled circles = 'transitional' basalt.

lower  $P_2O_5$  (0.26 wt%), but is not unlike several Calm Cove samples of Barton (1975), which are interpreted here to be weakly alkaline or transitional in composition.

### Transition metals (Sc, V, Cr, Co, Ni, Cu, and Zn)

Abundance of Cr decreases from 220 to 37 ppm in Calm Cove and Finger Hill tholeiites and from 160 to 24 ppm in the alkalic rocks, with decreasing Mg#. Together with a parallel decrease in Ni from 150 to 57 ppm (tholeiites) and 120 to 28 ppm (alkali basalts), the influence of Cr-spinel and/or clinopyroxene and olivine fractionation is suggested.

The concentration of Cu ranges with little systematic behaviour from 85 to 310 ppm in tholeiitic lavas and from 67 to 250 ppm in alkalic flows. Likewise, Zn varies from 59 to 130 ppm and 90 to 140 ppm in tholeiitic and alkali basalts, respectively. Sc (28-41 ppm) and V (190-320 ppm) both increase with decreasing Mg# in tholeiites of the Calm Cove formation and Sc also increases slightly (37 to 41 ppm) in Finger Hill lavas. Abundances of Sc in Calm Cove alkalic lavas are distinctly lower and decrease slightly from 32 to 25 ppm with falling Mg#, indicating the likely effect of clinopyroxene fractionation at some stage during their magmatic history.

In addition to their low Mg#, the diabase dykes show signs of extensive fractionation in having very low concentrations of Ni (15-23) and Cr (61-68).

The Ti/V ratio is nearly constant for Calm Cove (28-29) and Finger Hill (28-32) tholeiites, but is distinctly higher in transitional (34-47) and weakly alkalic basalts (38-54; Fig. 4). This is in good agreement with the findings of Shervais (1982) that modern-day mid-ocean ridge basalts (MORB) and

Miocene continental flood basalts typically have Ti/V ratios between 20-50, whereas alkali basalts are characterized by higher ratios (>50). The diabase dykes studied here have fairly uniform Ti/V ratios between 41-56, somewhat like the alkalic basalts, but with lower concentrations of both elements.

### Incompatible trace elements (Ba, Rb, Sr, Th, Nb, Zr, Y, and REE)

The abundances of the incompatible trace elements for the most part show consistent behaviour with rock type and degree of differentiation. In almost all cases, concentrations are higher in alkalic and evolved lava flows, compared to the tholeiites and rocks with higher Mg#. Less systematic behaviour is seen in Sr, which may be due to the influence of variable plagioclase fractionation (or accumulation) or to late alkali mobility.

Representative chondrite-normalized multielement diagrams for Calm Cove and Finger Hill lavas are presented in Figure 5. All of the samples are enriched relative to normal (N-type) or enriched (E-type) MORB for the large-ion-lithophile (LIL) and the light rare earth elements (LREE) but, with the exception of the alkalic rocks, have similar abundances of the high field strength (HFS) and heavy rare earth elements (HREE). For the subalkalic basalts of the Calm Cove and Finger Hill formations (Fig. 5a, b), the incompatible trace element patterns are comparable and show small negative P anomalies, and small positive or negligible Sr anomalies. The range of trace element concentrations for a Keweenaw olivine tholeiite (KEW-4; Basaltic Volcanism Study Project, 1981), which has a similar major element composition to these lavas, is shown for comparison. Large negative Nb anomalies, common in rocks with strong crustal signatures, are not present.

Weakly alkalic basalts are strongly enriched in LIL and LREE elements relative to the HFS and HREE (Fig. 5c, d). These rocks also display relatively strong negative anomalies for Sr, and less well-defined negative anomalies for P, probably as a consequence of low-pressure plagioclase and apatite fractionation. These flows have trace element abundances and distributions similar to those described in plume-affected basalts from the Southwest Indian Ridge (P-MORB; Le Roux et al., 1983), as well as in some continental alkali basalts reported from the southern Gregory Rift of Kenya (Baker et al., 1977; Fig. 5c, d).

The subalkaline tholeiites have low Zr/Nb ratios (6.7-8.8), and high ratios of Nb/Y (0.39-0.59) and Zr/Y (3.5-4.2), similar to incompatible trace element ratios in enriched (E-type) MORB (Zr/Nb $\approx$ 8.8, Nb/Y $\approx$ 0.38, Zr/Y $\approx$ 3.3). Compared to the tholeiites, alkaline lavas of the Mugford Group all show consistently higher ratios of Nb/Y (0.58 - 1.13), Zr/Y (4.5 - 7.6) and Zr/TiO<sub>2</sub> (69 - 106), analogous to plume-influenced (P-type) MORB (Nb/Y $\approx$ 0.95, Zr/Y $\approx$ 7.6, Zr/TiO<sub>2</sub> $\approx$ 74). They are not distinguished from tholeiitic rocks on the basis of Zr/Nb (6.2-9.2 for all rocks, excluding transitional basalts which have Zr/Nb = 5.2, 12.7).

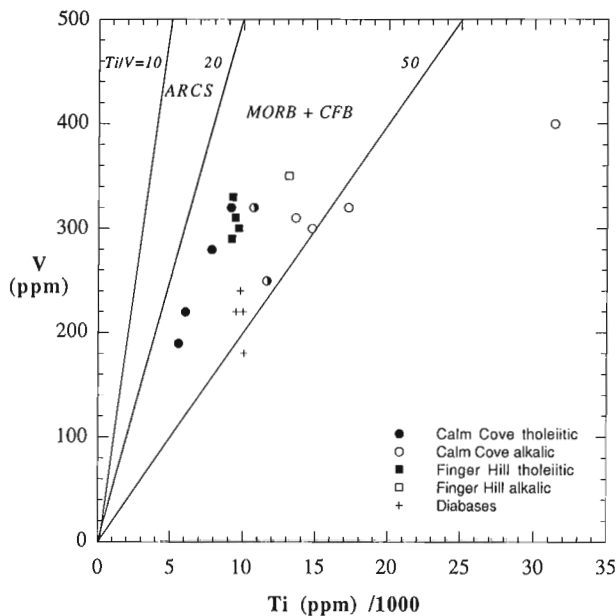


Figure 4. Ti-V diagram for Mugford Group basalts. Fields after Shervais (1982). Half-filled circles = 'transitional' basalt.



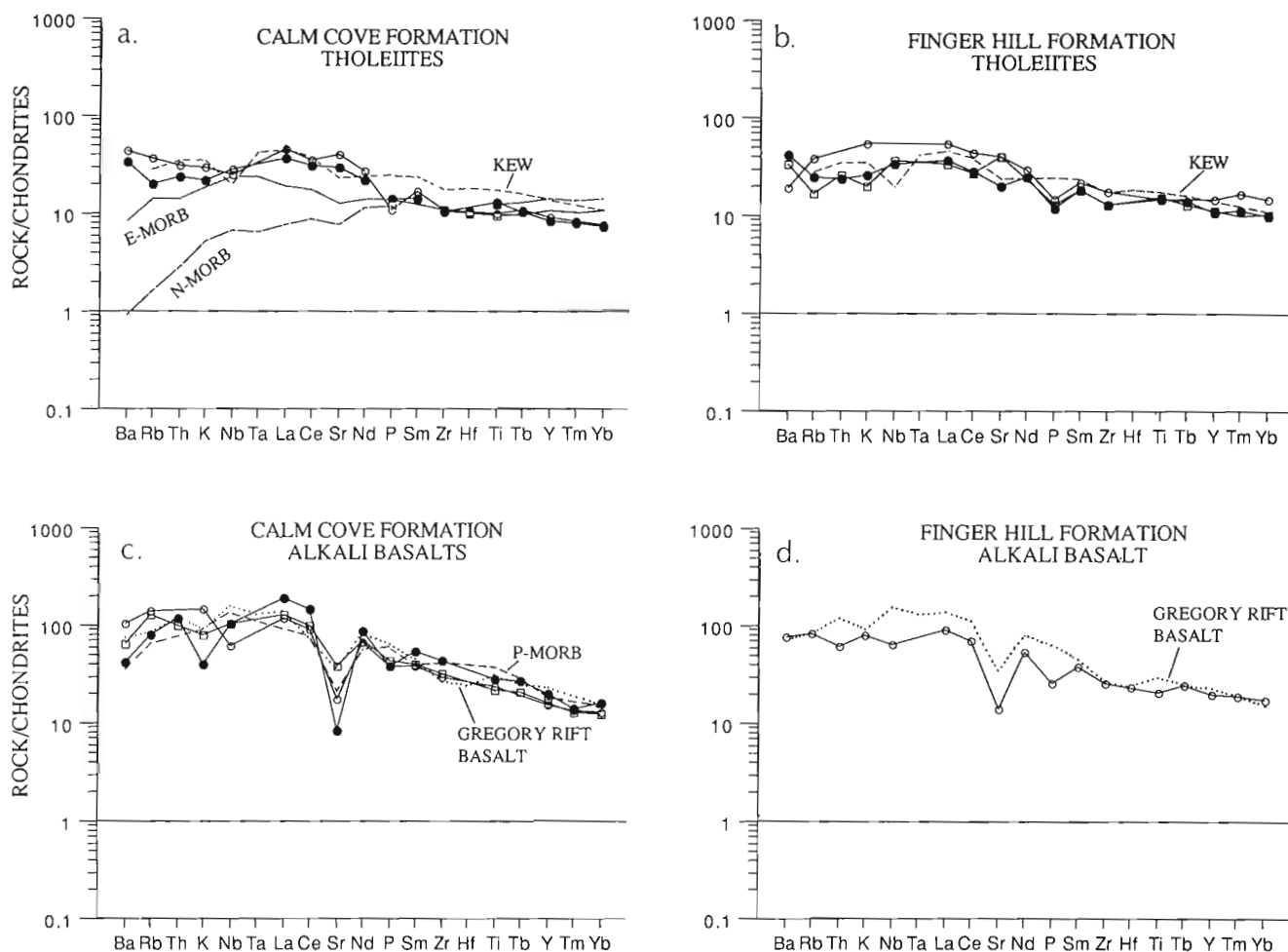
The diabase dyke suite has enriched trace element signatures, with notable positive Ba anomalies, strong negative anomalies for Nb, and lesser negative Sr, P and Ti anomalies. These are very similar to those described by Tarney (1992) for many other Proterozoic dyke swarms, but the rocks described here have generally higher abundances.

Figure 6 illustrates the overall REE enrichment and strong degree of REE fractionation observed in all Mugford Group basalts. Basalts of the Calm Cove formation can be divided into three groups based on REE abundance and chondrite-normalized pattern (Fig. 6a). Early, weakly alkaline flows have the highest LREE enrichment in the entire sequence, with La 125-206 x chondrites, and  $(La/Yb)_N = 9.0-12.6$ . These lavas are not characterized by any significant Eu anomaly ( $Eu/Eu^* = 0.96-1.11$ ), in contrast to the strong negative Sr anomalies noted earlier. It is possible that any reduction in  $Eu^{2+}$  from these liquids was offset by coprecipitation of another phase (pyroxene?). Tholeiitic Calm Cove formation basalts have distinctly lower abundances of LREE (La = 31-48x chondrites), flatter LREE/HREE slopes ( $(La/Yb)_N = 3.1-6.0$ ), and much less fractionated middle-to heavy-REE

patterns. These samples also have insignificant Eu anomalies ( $Eu/Eu^* = 0.97-1.12$ ). Rarer transitional basalts have patterns and abundances intermediate between these groups (La $\approx$ 80x chondrites;  $(La/Yb)_N \approx 7$ ).

Slightly less compositional spread is shown in overlying Finger Hill alkaline and tholeiitic lavas (Fig. 6b). Relative to Calm Cove equivalents, the single weakly alkaline flow is not as enriched in the LREE (La $\approx$ 100x chondrites), but has higher HREE (Yb $\approx$ 20x chondrites), lower  $(La/Yb)_N = 5.2$ , and a distinctly negative Eu anomaly ( $Eu/Eu^* = 0.80$ ). This is in general similar to patterns seen in subalkalic basalts of the same formation. Chondrite-normalized La abundances for Finger Hill tholeiites range from 35-58,  $(La/Yb)_N = 3.2-4.2$ , and there is a tendency towards flatter MREE - HREE profiles. Eu anomalies are variable ( $Eu/Eu^* = 0.84-1.05$ ).

The diabase dykes have a remarkably uniform REE distribution (not shown), with  $(La/Yb)_N = 6.3-7.8$ , and HREE concentrations similar to Calm Cove formation alkalic and Finger Hill basalts. There is only a very faint suggestion of a negative Eu anomaly ( $Eu/Eu^* = 0.87-0.96$ ).



**Figure 5.** Chondrite-normalized incompatible trace element diagrams for Mugford Group tholeiites (a, b) and weakly alkaline basalts (c, d). Normalizing factors after Thompson (1982). KEW = Keweenaw olivine tholeiite.

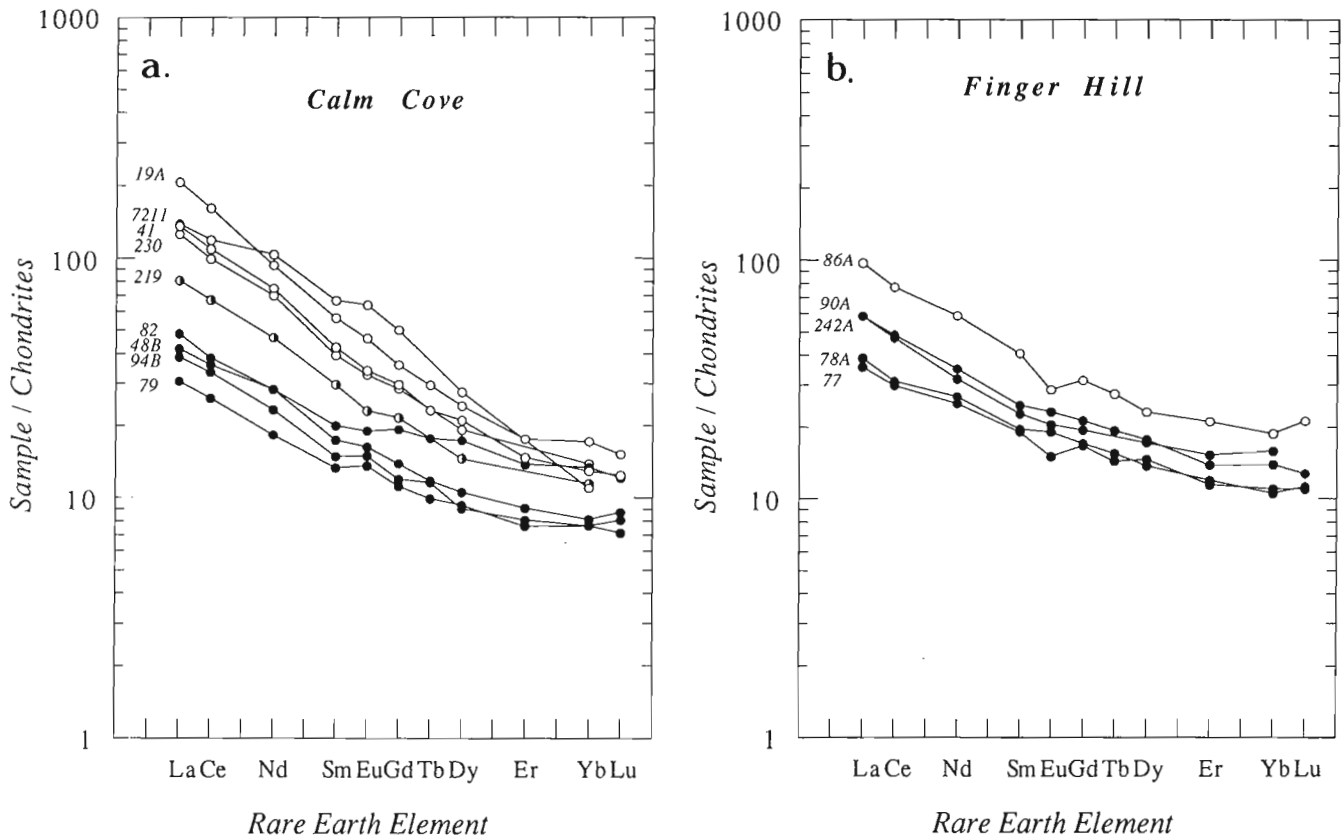


Figure 6. Chondrite-normalized REE patterns for mildly alkaline (open circles), transitional (half-filled circles), and subalkaline (filled circles) lavas of the a) Calm Cove, and b) Finger Hill formations.

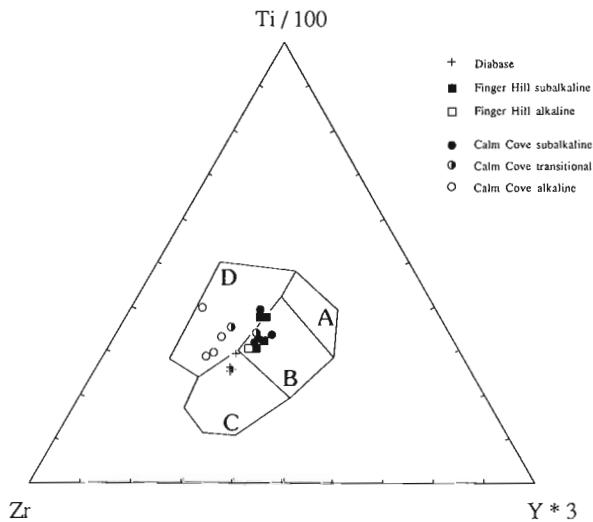


Figure 7. Tectonic setting of Mugford Group basalts, classified according to the Ti-Zr-Y discrimination diagram of Pearce and Cann (1973). Fields A+B = volcanic arc basalt (low-K tholeiites); B+C = calc-alkali basalt; B = ocean-floor basalt; D = within-plate basalt.

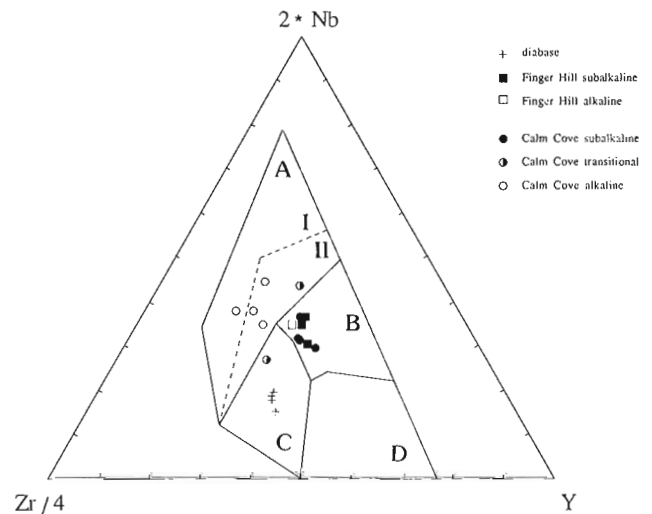


Figure 8. Tectonic setting of the Mugford Group basalts, using the trace element diagram of Meschede (1986). Field AI + AII = within-plate alkalic basalt; AII + C = within-plate tholeiite; B = P-type MORB; D = N-type MORB; C + D = volcanic arc basalt.

### *Magmatic and tectonic affinity diagrams*

Several incompatible trace elements, which are considered to be relatively immobile during greenschist facies metamorphism, are used here to distinguish primary magmatic and tectonic affinities. Numerous studies have shown that relative abundances of Ti, Y and Zr and many of the REE are changed little during metamorphism (Ludden et al., 1982). Because of the consistent and regular variations between these elements as well as with Nb and V, the latter are also interpreted as being unaltered in the Mugford Group lavas.

In terms of Zr-Y variations, the tholeiitic samples plot in the overlapping field of MORB and within-plate basalts of Pearce and Norry (1979), whereas all transitional and alkaline rocks have compositions which fall strictly in the field of within-plate basalts. On the Ti-Zr-Y tectonic characterization diagram (Fig. 7) of Pearce and Cann (1973), subalkalic tholeiites of the Calm Cove and Finger Hill formations plot predominantly in the field of MORB and volcanic arc compositions (calc-alkaline basalt and island arc tholeiite). A few samples (including the transitional basalts) straddle the boundary to the within-plate basalt field, and by comparison all of the early-erupted Calm Cove alkalic lavas have within-plate basalt characteristics, as is consistent with their high Zr/Y ratios. The diabases plot in Pearce and Cann's (1973) calc-alkaline basalt field, close to within-plate compositions, but distinct from most Mugford Group lavas.

Figure 8 shows the Mugford Group basalts in terms of Meschede's (1986) Zr-Nb-Y diagram. The early, weakly alkalic lavas of the Calm Cove formation plot entirely within the field of within-plate alkali basalts, whereas the subalkaline lavas of the Calm Cove and Finger Hill formations fall strictly in the field defined by P-type MORB. Diabase dykes cluster in a tight group in the field of within-plate tholeiites (and volcanic arc basalts).

### *Nd isotopic compositions*

Nd isotopic compositions have been determined on twelve of the freshest samples from the two principal suites. Calculated initial  $\epsilon_{Nd}$  values, determined for a crystallization age of 2100 Ma, range from +2.5 to -3.9 for Calm Cove alkalic lavas and -0.4 to -4.2 for transitional and tholeiitic flows. Samples of Finger Hill formation flows range from -3.3 (weakly alkalic) to -2.0 (subalkalic). The enriched nature of most of the initial ratios suggests a finite involvement of continental crust during the evolution of these magmas; calculated depleted mantle model ages ( $T_{DM}$ ) range between 2390 and 3180 Ma.

Several studies of tholeiitic and alkaline magmatic suites from areas of variably extended continental lithosphere have also illustrated the extreme isotopic compositions of projected mantle source regions (Farmer et al., 1989). Both suites from these studies have been shown to have either an isotopically depleted source (i.e. MORB asthenosphere), or a less-depleted lithospheric source similar to plume-contaminated asthenosphere (akin to an ocean-island basalt source). Although one Calm Cove alkalic sample ( $\epsilon_{Nd} = +2.5$ )

suggests derivation from a source having moderate long-term LREE depletion (like MORB-source), preliminary evaluation of melting models imply that this type of source must have been LREE-enriched shortly before derivation of the magmas parental to the Calm Cove alkalic lavas. Alternatively, the low positive initial  $\epsilon_{Nd}$  may reflect an ancient example of a plume-type source signature, analogous to what is observed from mantle supplying modern-day ocean-island basalts.

## **DISCUSSION**

Weakly alkaline, transitional and tholeiitic lavas of the Mugford Group share many physical and chemical properties of continental rift or plateau basalts. In many respects they resemble basalts from the Coppermine River area (Dostal et al., 1983), the Keweenaw rift, and early Iapetus rift system (Green, 1992); they are relatively evolved basalts and have elevated concentrations of incompatible trace elements and the REE. Subalkaline tholeiites consistently show within-plate, ocean-floor or P-MORB affinities on tectonic discriminant diagrams as well as trace element patterns and concentrations comparable to some Keweenaw olivine tholeiites. Similarly, alkalic basalts are uniformly distributed in within-plate alkali basalt classifications, and are somewhat analogous chemically to early rift basalts from the south Gregory Rift, Kenya, as well as P-MORB.

The transition from strongly LREE-enriched alkalic lavas of the Calm Cove formation to flows with lower  $(La/Yb)_N$  and higher overall Yb contents characteristic of the overlying Finger Hill formation may be indicative of a progressive depletion of residual garnet in the mantle source, or perhaps a reduction in the role of garnet fractionation due to melting at shallower levels. Scandium is also lower in the early Calm Cove alkalic rocks, probably because of the presence of residual clinopyroxene and garnet during the initial stages of melting. Additional data are required to more rigorously test these hypotheses.

The geochemical data are permissive of a model wherein early rifting of a stable Archean continent or development of a rifting continental margin is initiated (under plume-influence?) during the early Proterozoic. Earliest eruptive compositions (Calm Cove alkalic lavas) may have tapped deep (garnet-bearing) mantle source regions which were undergoing small degrees of melting. As lithospheric stretching continued, MORB-source asthenospheric mantle may have become involved in greater degrees of melting at shallower levels, and subsequent development of alkalic liquids might have been driven by high-level fractional crystallization processes.

## **ACKNOWLEDGMENTS**

The author gratefully acknowledges the careful and constructive reviews of W. R. A. Baragar and R. F. Emslie, which led to a much improved manuscript.

## REFERENCES

- Baker, B.H., Goles, G.G., Leeman, W.P., and Lindstrom, M.M.**  
1977: Geochemistry and petrogenesis of a basalt-benmoreite-trachyte suite from the southern part of the Gregory Rift, Kenya; *Contributions to Mineralogy and Petrology*, v. 64, p. 303-332.
- Barton, J.M., Jr.**  
1975: The Mugford Group volcanics of Labrador: age, geochemistry and tectonic setting; *Canadian Journal of Earth Sciences*, v. 12, p. 1196-1208.
- Basaltic Volcanism Study Project**  
1981: *Basaltic Volcanism on the Terrestrial Planets*; Pergamon Press, New York, 1286 p.
- Condie, K.C. (ed.)**  
1992: *Proterozoic Crustal Evolution; Developments in Precambrian Geology 10*, Elsevier, Amsterdam, 550 p.
- Dostal, J., Baragar, W.R.A., and Dupuy, C.**  
1983: Geochemistry and petrogenesis of basaltic rocks from Coppermine River area, Northwest Territories; *Canadian Journal of Earth Sciences*, v. 20, p. 684-698.
- Ermanovics, I.**  
1992: Geology of the North River - Nutak map area; Geological Survey of Canada, Open File 2443.
- Ermanovics, I.F., Van Kranendonk, M., Corriveau, L., Mengel, F., Bridgwater, D. and Sherlock, R.**  
1989: The boundary zone of the Nain-Churchill Provinces in the North River-Nutak map areas, Labrador; in *Current Research, Part C; Geological Survey of Canada, Paper 89-1C*, p. 385-394.
- Farmer, G.L., Perry, F.V., Semken, B. Crowe, B., Curtis, D., and DePaolo, D.J.**  
1989: Isotopic evidence on the structure and origin of sub-continental lithospheric mantle in southern Nevada; *Journal of Geophysical Research*, v. 94, p. 7, 885-7, 898.
- Green, J.C.**  
1992: Proterozoic rifts; in *Proterozoic Crustal Evolution; Developments in Precambrian Geology 10*, Elsevier, Amsterdam, p. 97-149.
- Hamilton, M.A.**  
1993: Preliminary report on the geology of the Mugford Group volcanics, northern coastal Labrador; in *Current Research, Part C; Geological Survey of Canada, Paper 93-1C*, p. 349-357.
- Irvine, T.N. and Baragar, W.R.A.**  
1971: A guide to the chemical classification of the common volcanic rocks; *Canadian Journal of Earth Sciences*, v. 8, p. 523-548.
- Le Roux, A.P., Dick, H.J.B., Erlank, A.J., Reid, A.M., Frey, F.A., and Hart, S.R.**  
1983: Geochemistry, mineralogy and petrogenesis of lavas erupted along the Southwest Indian Ridge between the Bouvet triple junction and 11 degrees East; *Journal of Petrology*, v. 24, p. 267-318.
- Ludden, J., Gélinais, L., and Trudel, P.**  
1982: Archean metavolcanics from the Rouyn-Noranda district, Abitibi greenstone belt, Quebec. 2. Mobility of trace elements and petrogenetic constraints; *Canadian Journal of Earth Science*, v. 19, p. 2276-2287.
- Maccougall, J.D. (ed.)**  
1988: *Continental Flood Basalts*; Kluwer Academic Publishers, Dordrecht, 341 p.
- Meschede, M.**  
1986: A method of discriminating between different types of mid-ocean ridge basalts and continental tholeiites with the Nb-Zr-Y diagram; *Chemical Geology*, v. 56, p. 207-218.
- Miyashiro, A.**  
1974: Volcanic rock series in island arcs and active continental margins; *American Journal of Science*, v. 274, p. 321-355.
- Pearce, J.A. and Cann, J.R.**  
1973: Tectonic setting of basic volcanic rocks determined using trace element analyses; *Earth and Planetary Science Letters*, v. 19, p. 290-300.
- Pearce, J.A. and Norry M.J.**  
1979: Petrogenetic implications of Ti, Zr, Y, and Nb variations in volcanic rocks; *Contributions to Mineralogy and Petrology*, v. 69, p. 33-47.
- Ridley, W.I., Rhodes, J.M., Reid, A.M., Jakes, P., Shih, C., and Bass, M.N.**  
1974: Basalts from Leg 6 of the Deep-Sea Drilling Project; *Journal of Petrology*, v. 15, p. 140-159.
- Schiøtte, L., Compston, W., and Bridgwater, D.**  
1989: Ion probe U-Th-Pb dating of polymetamorphic orthogneisses from northern Labrador, Canada; *Canadian Journal of Earth Sciences*, v. 26, p. 1533-1556.
- Shervais, J.W.**  
1982: Ti-V plots and the petrogenesis of modern and ohioitic lavas; *Earth and Planetary Science Letters*, v. 59, p. 101-118.
- Smyth, W.R.**  
1976: Geology of the Mugford Group, northern Labrador; in *Report of Activities for 1976*, R.V. Gibbons, (ed.); Newfoundland Department of Mines and Energy, Report 77-1, p. 72-79.
- Smyth, W.R. and Knight, I.**  
1978: Correlation of the Aphebian supracrustal sequences, Nain Province, northern Labrador; Newfoundland Department of Mines and Energy, Mineral Development Division, Report 78-1, p. 59-64.
- Tarney, J.**  
1992: Geochemistry and significance of mafic dyke swarms in the Proterozoic; in *Proterozoic Crustal Evolution; Developments in Precambrian Geology 10*, Elsevier, Amsterdam, p. 151-179.
- Thompson, R.N.**  
1982: Magmatism of the British Tertiary Volcanic Province; *Scottish Journal of Geology*, v. 18, p. 49-107.
- Van Kranendonk, M.V.**  
1990: Structural history and geotectonic evolution of the eastern Torngat Orogen in the North River map area, Labrador; in *Current Research, Part C; Geological Survey of Canada, Paper 90-1C*, p. 81-96.

Geological Survey of Canada Project 730044

# Combining field observations and remote sensing to map the Grenville Front along the Pascagama River, Quebec

D.F. Graham<sup>1</sup> and A. Ciesielski<sup>2</sup>  
Mineral Resources Division

*Graham, D.F. and Ciesielski, A., 1994: Combining field observations and remote sensing to map the Grenville Front along the Pascagama River, Quebec; in Current Research 1994-C; Geological Survey of Canada, p. 343-354.*

---

**Abstract:** A remote sensing analysis of part of the Grenville Front is presented, following previous work east of Val d'Or, Quebec using ground geology, satellite imagery and magnetic data to reveal the front. In the study area, 110 km east of Senneterre, Quebec, Landsat and magnetic data were supplemented with data from a new ERS-1 satellite imaging radar which is sensitive to terrain topography and surface roughness. The data were enhanced using contrast stretch, directional and median filtering, shaded relief and the IHS (Intensity, Hue and Saturation) transform. The Grenville Front was located using structural trends based on field observations and coinciding with the boundaries of magnetic anomalies, linear waterways and lineaments enhanced on TM and ERS-1 radar data. The position of the Front was extrapolated in unmapped and till covered areas using magnetic contrasts of the vertical gradient data.

**Résumé :** Une analyse par télédétection d'une partie du front de Grenville est présentée, qui fait suite à une étude à l'est de Val d'Or, Québec, utilisant la géologie de surface, l'image satellite et les données magnétiques pour mettre en évidence le front. Dans la région étudiée, 110 km à l'est de Senneterre, Québec, les données Landsat et les données magnétiques ont été complétées par les données d'un nouveau satellite radar image ERS-1, sensible à la topographie et aux rugosités du terrain. Les données ont été rehaussées en utilisant le filtrage directionnel et médian, le relief ombré, l'étalement des contrastes et les transformations d'intensité, de teintes et de saturation (IHS). Le front de Grenville a été localisé en utilisant les orientations structurales tirées des observations de terrain et coïncidant avec les limites des anomalies magnétiques, les voies d'eau rectilignes et les linéaments, rehaussées sur les données TM et radar ERS-1. La position du front a été extrapolée dans des zones non cartographiées et recouvertes de till, en utilisant les contrastes magnétiques du gradient vertical.

---

<sup>1</sup> Remote Sensing Office, Geological Survey of Canada, Ottawa

<sup>2</sup> Continental Geoscience Division

## INTRODUCTION

The Pascagama River is located 110 km east of Senneterre, Quebec and the study area covers 2500 km<sup>2</sup> straddling the Superior-Grenville boundary (see index map of Fig. 8). The region was previously mapped by Faessler (1935), Laurin (1965), Charbonneau (1969, 1973), Charre (1975) and compiled by Avramtchev and Lebel-Drolet (1981); more recent mapping south of the area was carried out by Girard et al. (1992).

The Superior-Grenville boundary, known as the Grenville Front, has not received attention in the area east of Senneterre because there is little information on highly strained rocks and thick overburden in much of the area making detailed geological work difficult (Grant, pers. comm., 1993). Neale (1952) projected a fault zone at the Superior-Grenville boundary in the study area from mapping in the Mistassini-Témiscamie River area to the northeast.

A recent study 100 km southwest of the study area using a Grenville Front structure composed of lineaments coinciding with aeromagnetic anomalies (Ciesielski et al., 1990). The use of Landsat TM data can assist regional mapping and provides information on the surface expression of bedrock fractures which can be related to regional subsurface magnetic lineaments. Regional structures inferred from these two types of information, supported by field observations located the Grenville Front structure with better accuracy. In thick overburden, where field observations are impeded, vegetation patterns and surface roughness were shown to enhance surface lineaments.

The objectives of this paper are (1) to evaluate the lineament enhancement capability of Landsat TM and aeromagnetic data for this study area, through specific enhancements, (2) to evaluate ERS-1, a new remotely sensed Synthetic Aperture Radar which began imaging in August 1991, (3) to document enhancement methodologies that were applied and to determine the factors that affected the enhancement performance of each data set, and (4) to locate the Grenville Front structure combining geological and remotely sensed data.

## GEOLOGICAL SETTING

### Regional setting

The Grenville Front is a 1100 km northeast-trending structure defining the Superior-Grenville boundary. The central segment of the front shows complex geological settings, and although it has been known since the thirties, few detailed studies were conducted on the subject, partly because of relatively poor exposures. The front was first investigated by Norman (1940) who noted major fault and thrust zones extending from Lake Mistassini to Georgian Bay, known as the Huron-Mistassini Fault Zone (see Neale, 1952 for complete references). The central segment of the front (index map of Fig. 8) separates the Superior Province from reworked

parautochthonous Archean rocks locally comparable to Superior sequences and uplifted, metamorphosed and eroded during Grenvillian Orogeny (c.f. Ar-Ar ages west of the Grenville Front in Baker, 1980). It is composed of fault zones and tectonic contacts showing pervasive deformation. Recent works confirmed the faulted nature of the central segment of the Grenville Front (Ciesielski et al., 1990; Ciesielski, 1992; Girard et al., 1992) and dominating cataclastic deformation and coexistence of minor mylonite and pseudotachylite along major faults forming the Front (Ciesielski, 1993; S. Ji, pers. comm., 1993).

### Local setting

In the study area, according to Charbonneau (1973), the Superior-Grenville boundary is designated as a transition zone, separating mainly granitic and minor mixed gneiss of the Superior from granitic and mixed gneiss of the Grenville Province. Hornblende and hybrid gneisses coincide with the Mégiscane magnetic anomaly (Geological Survey of Canada, Aeromagnetic Maps 7082G and 7083G, for NTS 32B and 32C) lying astride the Grenville Front boundary (Charbonneau, 1969, 1973). Charre (1975) did not mention a sharp Superior-Grenville contact in the Mégiscane – Mesplet Lakes area; the northwest part is dominated by granitic gneiss and is referred to as Temiscamian type; the southeast area is dominated by amphibole gneiss and is described as Grenvillian type. Charbonneau (1973) referred to a transition zone of some 20 km wide based mainly on K-Ar age dates. In the southern part of the study area, Girard et al. (1992) showed the Grenville Front as a fault zone separating massive and gneissic tonalites of the Superior Province from parautochthonous tonalitic gneiss, biotite paragneiss and metabasite of the Grenville Province. This fault zone parallels dykes older than 2 Ga on either side of the

Table 1. Data parameters.

Data	Imaging platform	Raw spatial resolution (m)	Wavelength range
Landsat TM	Satellite	30.0	Band 1 0.45 - 0.52* Band 2 0.52 - 0.60 Band 3 0.63 - 0.69 Band 4 0.76 - 0.90 Band 5 1.55 - 1.75 Band 6 10.3 - 12.5 Band 7 2.08 - 2.35
ERS-1 SAR	Satellite	12.5	C-band 5.66**
Magnetics	Airborne	200.0	N/A

\*Values are given in micrometres  
\*\*Value is given in centimetres



Grenville Front (Madore and Ciesielski, 1990; Buchan et al., 1993), suggesting that these structures have been reactivated along the front during the Grenvillian Orogeny.

### Remote sensing

In the study area, the Superior-Grenville boundary has not been precisely located (Charbonneau, 1969, 1973; Charre, 1975). Studies along the central segment of the Grenville Front showed that it can be designated by a narrow zone of dominating brittle deformation (Neale 1952; Ciesielski et al., 1990; Ciesielski, 1992, 1993; Girard et al., 1992). Accordingly, the Grenville Front was located using abrupt changes in structural trends on Charbonneau's and Charre's geological maps. However, in areas of thick Quaternary cover, there was inconclusive information to identify the fault. In order to overcome this limitation, a multiple remote sensing analysis was applied to the study area. These data are shown in Table 1.

## DATA PRE-PROCESSING

### Landsat TM

Two digital Landsat TM quadrants were acquired and processed for this project. The first TM data set was from June 22, 1984 (Path 17, Row 26) and the second was from August 2, 1984. The imaging geometry of this multispectral sensor is depicted in Figure 1a. These data were geometrically corrected to UTM co-ordinates, using ten 1:50 000 topographic maps. Only Landsat TM bands 3,4 and 5 were available for this study.

### ERS-1 SAR

ERS-1 Synthetic Aperture Radar (SAR) is a side looking satellite radar sensor which is depicted in Figure 1b. The pulsed C-band (5300 MHz) beam has a depression angle range between  $64^\circ$  and  $70^\circ$ . The detected backscatter response is a function of both terrain topography and surface roughness (CCRS, undated). SAR is an all-weather sensor, capable of night time imaging. These data, acquired on July 28, 1992, were compressed from 16 to 8 bits. The data were median filtered using a  $3 \times 3$  kernel to remove radar speckle (noise) and registered to the geocoded TM data. In the process the ERS-1 data were resampled to 30m pixels, further reducing radar image speckle.

### Total field magnetics

These data, acquired with a line spacing of 800 m at an altitude of 305 m were compiled by the Geophysical Data Centre (Geological Survey of Canada). Vertical gradient data which are a derived product, were used only for the recognition of magnetic lineaments. Magnetic gradient values are not quantified.

## DATA ENHANCEMENT METHODOLOGY

### Background on enhancement algorithms

These algorithms are designed to improve image contrast for the enhancement of geological features for easier visual interpretation. This is done by increasing the dynamic range of the image and/or by filtering the image which improves the ability to separate subtle variations in image tone.

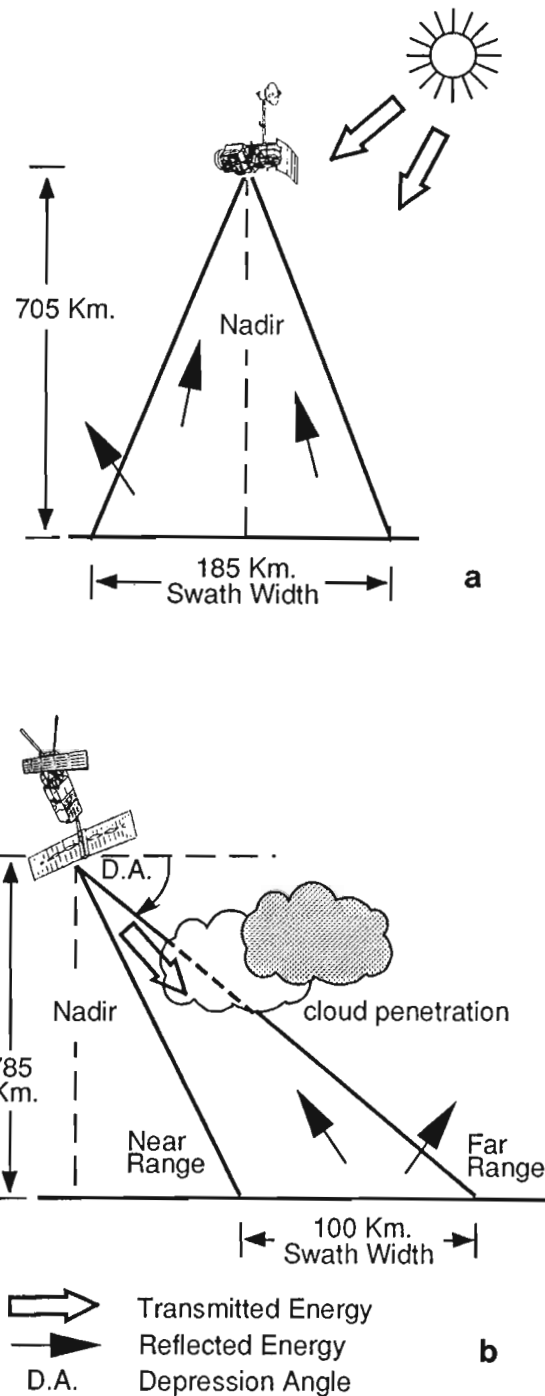


Figure 1. Satellite Imaging Geometries (not to scale). a) Landsat TM. b) ERS-1 SAR.

### Contrast stretch

Landsat data are typically received with a low dynamic range (poor image contrast). High and low end data limits are mapped to the full 8 bit dynamic range (0 to 255 DN). This produces an image with optimal image contrast.

### Median filtering

The filter is implemented by computing the median of the digital values within a user specified filter kernel. This kernel is normally square (i.e. 3 x 3) but can be designed as a rectangle. The output image is generated by convolving the filter within the input image (Wahl 1987). This filter was used to reduce image speckle inherent in the ERS-1 data.

### Directional filtering

Spatial domain filtering emphasizes the linearity of image features to aid in the identification of geological structures (Sabins, 1991). The directional filter algorithm is based on the design of a filter kernel (window) which is convolved over the image data. The filter kernel is designed using parameters of: filter direction, kernel size, central weighting of kernel, the proportion (A%) of the filtered image that is added to the unfiltered image (unfiltered image + A x filtered image), and an output image mean and standard deviation scaling adjustment (DIPIX, 1990; Gillespie, 1976; Jackson and Wagner, 1979).

Directional trends are determined by calculating the directional derivative or gradient of image pixel values, then replacing the image values with a magnitude of the gradient. In addition, the size of the kernel defines the resultant "smoothing" effect of the output image.

### Shaded relief

This enhancement employs a user-specified illumination direction to convert pixel height (digital number) to a shaded relief image. The grey level (digital number) of a pixel is calculated as the cosine of the angle between the normal vector to the surface (slope and aspect) and the illumination direction (PCI, 1993). Highlighting of slopes facing the light source and shadowing of slopes which face away enables lineaments to be enhanced.

The shaded relief algorithm is controlled by parameters of elevation step size and light source location. The elevation step size, gives the elevation corresponding to one grey level. A step size greater than one adds contrast to the enhancement. The light source location is specified by an azimuth angle and elevation angle in degrees. A light source azimuth angle of 360° shines from the top of the image and an elevation angle of 180° shines normal to the plane of the image. Illumination parameters are chosen to highlight terrain lineaments which are orthogonal to the illumination direction.

### IHS transform

Intensity, Hue and Saturation (IHS) is a colour transformation commonly used for data integration and image enhancement. In this transformation, colour is defined by three parameters: intensity (brightness), hue (colour) and saturation (purity of colour) (Gillespie, 1980). This technique is useful for combining various types of geological data and forming image map products (Harris et al., 1990).

### Data enhancement

Each algorithm is associated with another in a procedure with the goal of generating the optimum enhancement methodology for each data set. These procedures are presented as flow diagrams in Figures 2, 3, and 4. The filter kernels in these figures are shown before a central weighting and percentage add back to the image were applied.

### Landsat TM

Enhancements were prepared using band 5 after optimizing image contrast. To minimize the influence of glacial drift fluting but still enhance the lineaments oriented parallel to the front, a 5 x 5 directional filter kernel was used with a central weighting of 10. Ten percent of the original image is added to the filtered image and the mean and standard deviation of the data are fixed at 160 and 60 respectively to brighten the image for plotting.

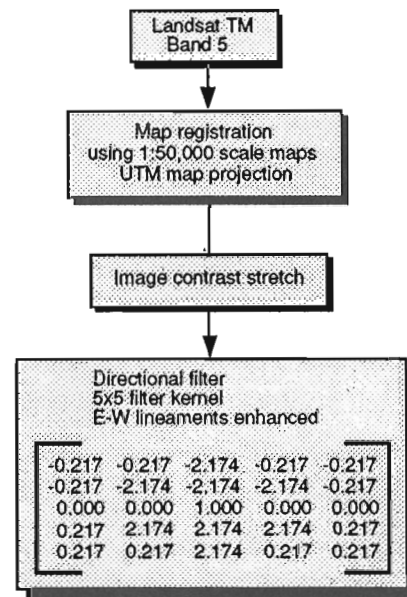


Figure 2. Enhancement Flow Diagram – Landsat TM.

Terrain 'noise' effects, which obscured lineaments characterizing the Grenville Front, were due to vegetation (forested vs. unforested, cultivated, forest burn) and cultural features (roads, powerlines, Fig. 5). The high frequency information associated with short lineaments evident in the shaded relief enhancement was suppressed in the directional filter enhancement forming a subtle image texture. This served as a background for the longer and more important lineaments. Lineaments extracted from the enhancement were defined using lines of high image tonal contrast or edges of marked image texture contrast. From all of the terrain surface 'noise' types, forest burn was the most problematic due to high homogeneous albedo response.

**ERS-1 SAR**

A contrast stretch of ERS-1 enhanced north-northeast structural lineaments. A second ERS-1 enhancement was generated by directional filtering of the contrast stretched enhancement (Fig. 6). A 3 x 3 filter was used with a central weighting of 5 and 7.5 per cent of the original image added to the filtered image. The ERS-1 enhancement is dominated by glacial fluting which reflects the depth of glacial material that masks the bedrock lineaments. The bright backscatter return from the water bodies stems from the vertical transmit and receive (VV) polarization, enhancing water roughness derived from wind action.

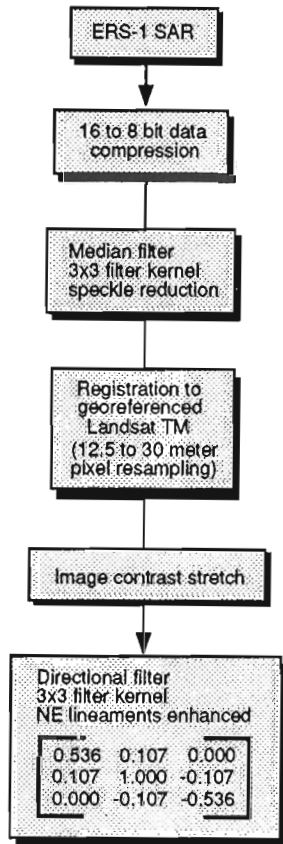


Figure 3. Enhancement Flow Diagram – ERS-1 SAR.

**Total field magnetics**

In this enhancement an azimuth of 360° and elevation of 50° was used to preferentially enhance linear features trending in a north-northwest direction. These data can be directly input into the shaded relief algorithm. To combine the information on magnetic textural patterns with this shaded relief image, the IHS transform was used.

The IHS transform was applied to the single channel of total field magnetics. A colour composite was generated to enhance the magnetic trends within the anomaly highs without

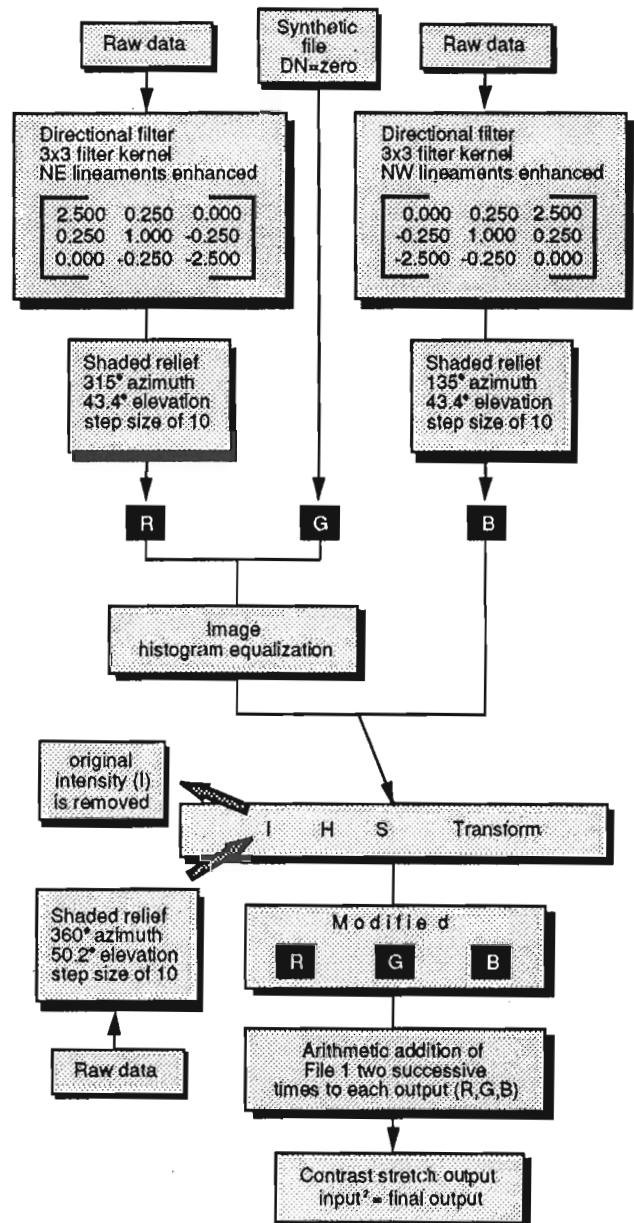


Figure 4. Enhancement Flow Diagram – Total field magnetics.



Figure 5. Landsat TM band 5 – 5 x 5 directional filter, enhancing east-west lineaments.



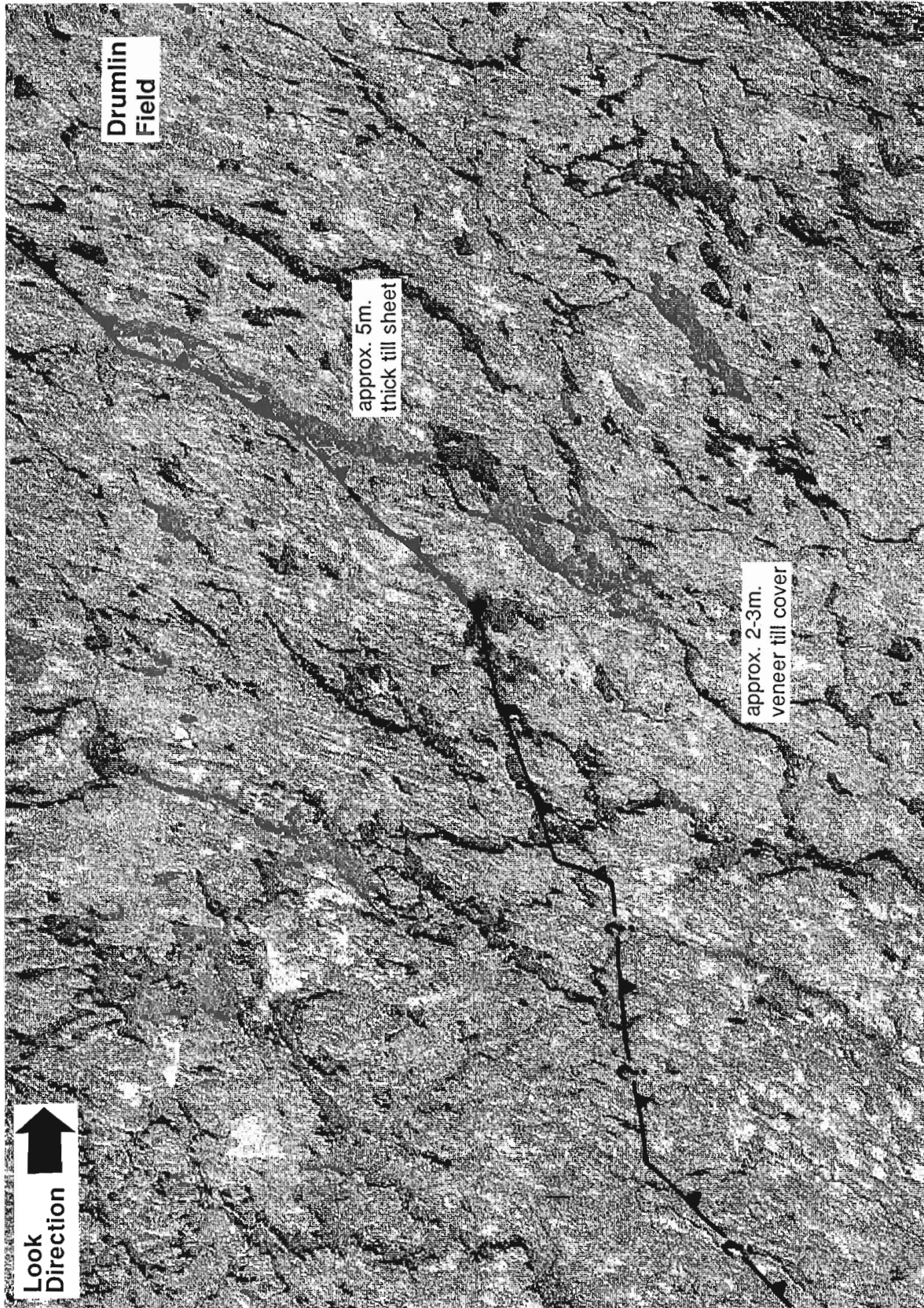


Figure 6. ERS-1 SAR - 3 x 3 directional filter, enhancing northeast-southwest lineaments.

loss of information in the rest of the image. The original (raw) magnetic data, input into IHS are generated in the following manner (see also Fig. 4).

The raw data are both northwest filtered to enhance magnetic lineaments oriented in a northeast direction and northeast filtered to enhance northwesterly trends. The 3 x 3 filter northwest and northeast kernels have a central weighting of 10. Three percent of the original image is added to the filtered image and no additional scaling was applied to the resultant image. To further enhance the magnetic lineaments the directional filtered images were enhanced by shaded relief. Raw magnetic data were further enhanced by histogram equalization, to bring out subtle textures in the magnetic anomaly highs.

In RGB space, red and green channels served as input along with a synthetic file consisting of zero values (blue). These three channels were converted into IHS space. The IHS enhancement reveals significant trends without sacrificing the details of minor trends, making it an effective way of enhancing the data. The hue information enhances the subtle lineament trends which are associated with the major lineaments and enhancing trends within the anomaly highs. The new intensity information presents the shaded relief image as an image base, which shows general lineament trends and delineates magnetic anomalies.

### Vertical gradient magnetics

As the data were received with an optimum distribution of data within the 8 bit range and there was good image contrast which enhanced magnetic lineaments, no enhancements were applied to the raw data (Fig. 7).

## DISCUSSION

In the study area, the Grenville Front had not been studied in detail and generally was considered as a transition zone following Wynne-Edwards (1972) model. However, recent studies show that Grenvillian deformation is limited in the Archean Parautochthon adjacent to the southeast side of the front (index map of Fig. 8) and that most of this deformation is located in narrow fault zones at the front. Accordingly, the Grenville Front was located using structural trends coinciding with magnetic anomalies, linear waterways and lineaments enhanced on TM and ERS-1 radar data. The position of the front was extrapolated in unmapped and till covered areas using magnetic contrasts and TM feature alignment and is indicated in Figure 8 by question marks. The vertical gradient magnetic data show numerous regional lineaments and apparent structural offsets of magnetic bodies. Such an approach needs confirmation by future field work in the region given local contradiction between structural trends and the Grenville Front orientation (Fig. 8).

The M $\acute{e}$ giscane anomaly (Fig. 7), is separated by a north-east-trending fault zone. The northeast part is elongated and shows a concentration of linear anomalies related to hornblende-pyroxene-magnetite orthogneiss (Charbonneau 1969, 1973,

pers. comm., 1993), and possibly gabbro and diabase dykes. The Grenville Front structure is located on the east side of the anomaly following linear rivers interpreted as fault zones (Fig. 5, 8). The southwest part is lozenge shaped and is related to the presence of pyroxene-hornblende-magnetite-bearing para- and orthogneiss. The Grenville Front structure is located on the west side of the southwest part of the anomaly following fault zones (Girard et al., 1992). Part of the front is interpreted to crosscut the northern part of the anomaly following an east-west trending magnetic contrast. Magnetic data thus permit interpretation of the trace of the Grenville Front from known locations of front-type sheared rocks to regions where field data are inconclusive.

Landsat TM band 5 data enhanced image features of powerlines and forest burn (Fig. 6). Powerline lineaments are localized and do not hinder the ability to interpret the image. Forest burn increases the reflectivity of the terrain surface in the mid-infrared which reduces the image contrast. Lineament interpretation in these areas is considered unreliable. A recommended choice of date for imaging should be at a time of minimum leaf cover (spring or fall time frame) during a year when cultural interference and forest burn is minimal. Landsat TM band 5 data enhanced a terrain lineament coincident with a vertical gradient lineament which prompted the tentative positioning of the front in an east-west orientation (question marks in Fig. 8).

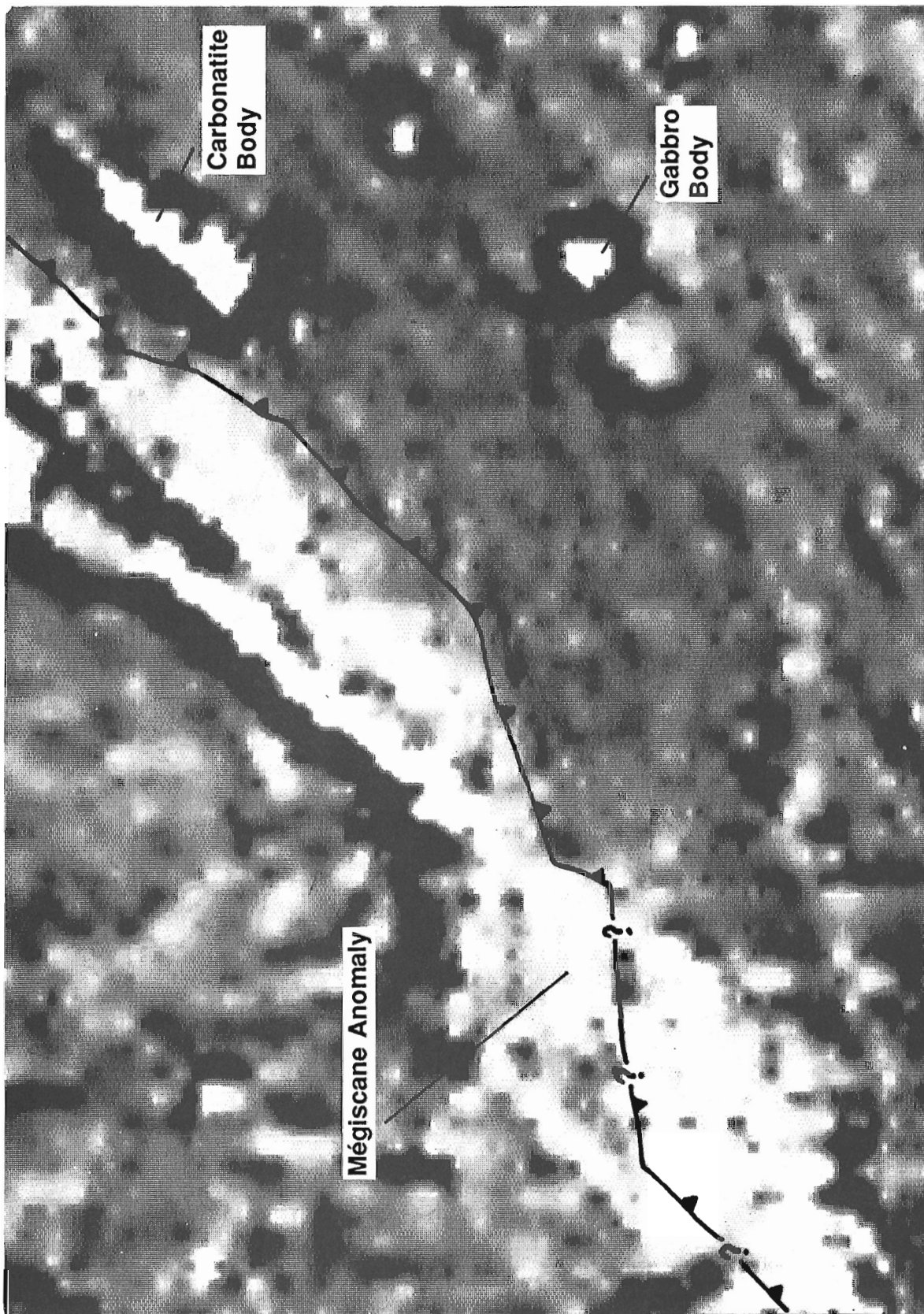
The ERS-1 enhanced alignment of small water bodies and useful to define the relative thickness and extent of till cover associated with a drumlin field producing a linear fabric in the image. The drumlin field is enhanced by the orthogonal orientation to the radar imaging or 'look' direction, as noted previously in SEASAT SAR imagery which has the same imaging geometry (fig. 6, Harris, 1987). In the radar image the high backscatter response of each drumlin is shown by a white lineament which collectively generates a linear fabric. ERS-1 information served as a first attempt in determining the regional extent and thickness of till in the study area. In general terms, a northwest-southeast imaginary diagonal line, which bisects Figure 8, separates 5 m thick till to the northeast from veneer till of less than 3 m to the southwest (Grant, pers. comm., 1993).

## CONCLUSIONS

Landsat TM band 5 and vertical gradient magnetics provided information for extrapolating field data to unexposed regions of the Grenville Front. Due to the complexity of the information content found in the enhancements, single file manipulation proved most useful.

The abundance of regional lineaments and apparent structural offsets of magnetic bodies on the vertical gradient magnetic data indicated a control by structural geological features. Using field geological data, predicted sections of the Grenville Front were extrapolated from the outcrop location. Directional filtered Landsat TM band 5 data were used to support the position of the predicted locations of the front.





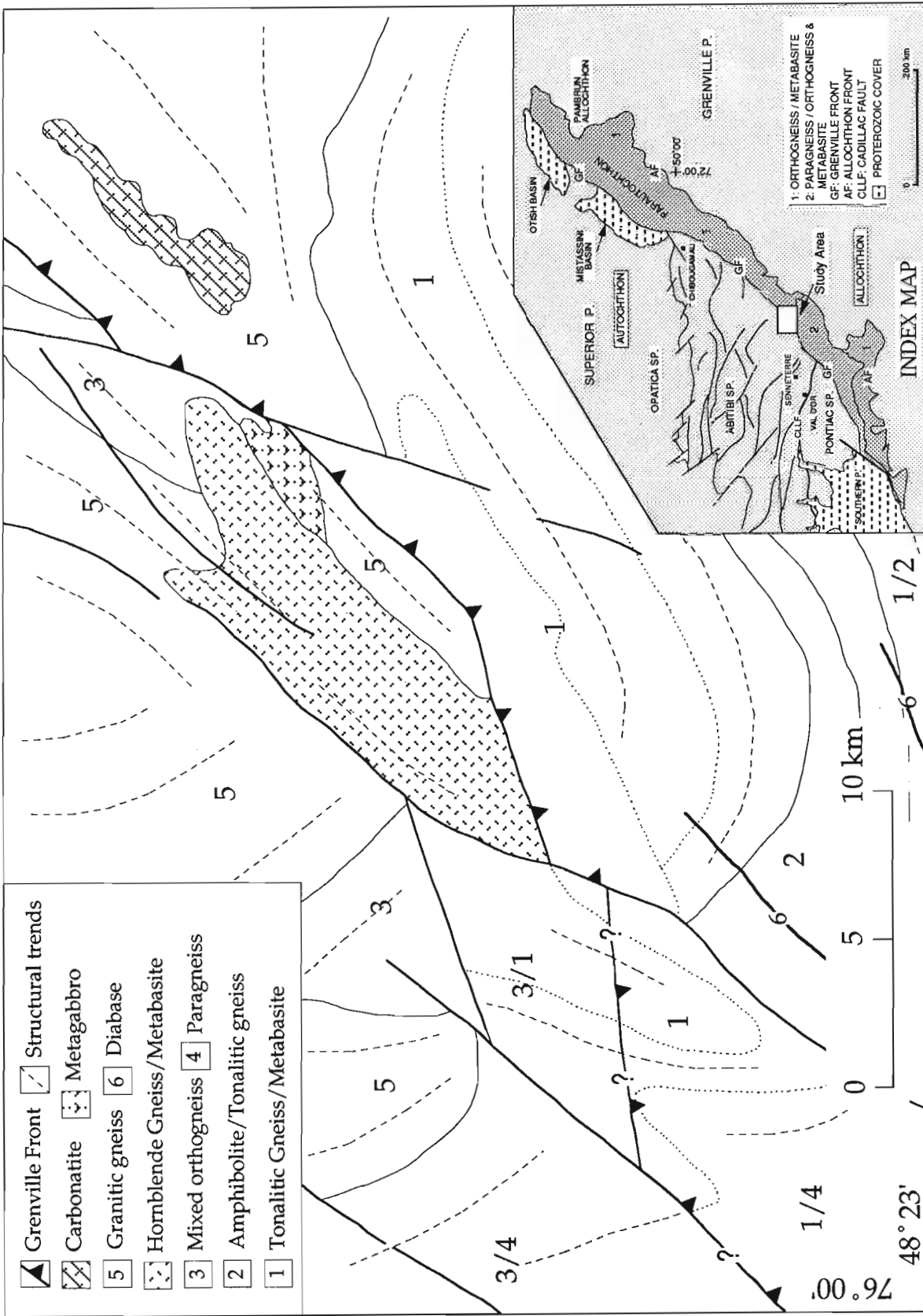


Figure 8. Index map (inset) showing the Grenville Front transecting the Abitibi Greenstone Belt and the adjacent parautochthonous Archean terrain of the Superior Province metamorphosed and uplifted during the Grenvillian Orogeny. Local geology showing the Grenville Front separating tonalitic orthogneiss, paragneiss and metabasite of the Grenville Parautochthon from granitic, tonalitic and mafic gneiss of the Superior Province. The front location uncertainty is outlined by question marks. Geology modified from Charbonneau (1973), Charre (1975), Girard et al., (1992). Dotted lines: transition from massive to gneissic texture.

The magnetic and TM data together were used to extend the continuity of this regional feature to recommend specific locations to be revised in further detail in future field activities.

Directional filtering of TM mid-infrared data were used to locate the Grenville Front southwest of the study area, primarily because of the contrast in terrain relief and bedrock lithology on either side of the front (Ciesielski et al., 1990). The extrapolation of field data for the present study area using TM band 5 data proved marginally useful due to: the homogeneity of rock type in either side of the front, the prevalence of glacial drift cover, and vegetational and cultural terrain "noise".

ERS-1 satellite SAR data preferentially enhanced glacial fluting in the drift cover for reconnaissance mapping of the Grenville Front on the terrain surface. The sensor's large far range depression angle of 64° and low resolution of 30 m made the data unsuitable for the extraction of geological structures but did provide information on the extent of thick till cover associated with a fluted terrain surface. Graham and Grant (1991) recommended that airborne SAR data be used as a more effective means of extracting bedrock and surficial lineament information.

Directional filtering, shaded relief and the IHS transform are algorithms used for the enhancement of lineament information. The utility of these techniques are site specific and require the geologist's knowledge of local primary structures, a knowledge of remotely sensed data acquisition and an awareness of how the digital enhancements are performed. Directional filtering of Landsat TM data proved more useful than shade relief for enhancing regional structural trends important in this study. Filtering suppressed high frequency lineament fabric information to allow the extraction of major lineament trends; it also allows the flexibility of changing the filter size as a function of study area scale.

In this study, remotely sensed data have been applied to interpret the structure of a segment of the Grenville Front in central Quebec to define the location more precisely. The outcome of this study is that the front has been located as a sharply defined line along which the deformation occurred. This interpretation requires further study and refinement in the field.

## ACKNOWLEDGMENTS

The project work by D.F. Graham was accomplished under a Geological Survey of Canada and Canada Centre for Remote Sensing contract with MIR Télédétection Incorporated.

We wish to thank the Canada Centre for Remote Sensing for the use of the Landsat TM and ERS-1 data. We wish to thank B.W. Charbonneau and D.R. Grant of the Geological Survey of Canada and S. Ji, Université de Montréal for their assistance. We would like to thank A. Rencz and B.W. Charbonneau for critically reviewing the paper.

## REFERENCES

- Avramtchev, L. and Lebel-Drolet, S.**  
1981: Cartes des gîtes minéraux du Québec 32 C et 32 B; Ministère de l'Énergie et des Ressources du Québec.
- Baker, D.J.**  
1980: The metamorphic and structural history of the Grenville Front near Chibougamau, Québec; Ph.D. Thesis, University of Georgia, Athens, 335 p.
- Buchan, K.L., Mortensen, J.K., and Card, K.D.**  
1993: Northeast-trending Early Proterozoic dykes of southern Superior Province: multiple episodes of emplacement recognized from integrated paleomagnetism and U-Pb geochronology; Canadian Journal of Earth Sciences, v. 30, p. 1286-1296.
- CCRS (Canada Centre for Remote Sensing)**  
undated: ERS-1, Canadian Users Guide; CCRS, Energy Mines Ressources Canada, Bilingual, 22p.
- Charbonneau, B.W.**  
1969: A Grenville Front magnetic anomaly, Mégiscane Lake area, Quebec; in Report of Activities, Part A; Geological Survey of Canada, Paper 69-1A, p. 70-77.  
1973: A Grenville Front magnetic anomaly, in the Mégiscane Lake area, Quebec; Geological Survey of Canada, Paper 73-29, 20 p.
- Charre, R.**  
1975: Région des lacs Mégiscane et Mesplet; Ministère des Richesses Naturelles du Québec, R.G. -166, 31 p.
- Ciesielski, A., Pouliot, G., and Rocheleau, M.**  
1990: The Grenville Front SE of Val D'OR, a multi-disciplinary analysis, in the Northwestern Quebec Polymetallic Belt: a summary of 60 years of mining exploration; The Canadian Institute of Mining and Metallurgy (CIM) Symposium, Poster Volume, Rouyn-Noranda, May 28 to June 1, p. 56-58.
- Ciesielski, A.**  
1992: The nature of the central Grenville Front: its implications for the Parautochthon tectonic evolution and uplift in Grenvillian time; Abitibi-Grenville Lithoprobe Workshop 1991, Report 25, p. 97-101.  
1993: The Archean Parautochthon in the Lake Temiscaming area, with reference to the Grenville Front & A-G Lithoprobe line 15; Abitibi-Grenville Lithoprobe Workshop 1992, Report 33, p. 3-6.
- DIPIX**  
1990: Aries Vstream Software User's Guide, Vstream 5.1+; Dipix Technologies, Ottawa, Ontario.
- Faessler, C.**  
1935: Mégiscane river headwaters area; Quebec Bureau of Mines Annual Report for 1935, part C, p. 27-38.
- Gillespie, A.R.**  
1976: Directional fabrics introduced by digital filtering of images; Basement Tectonics, v. 58, p. 500-507.  
1980: Digital techniques of image enhancement in remote sensing in geology; B.S. Siegal and A.R. Gillespie (ed.), Wiley, New York, p. 139-226.
- Girard, R., Birkett, T.C., Moorhead, J., and Marchildon, N.**  
1992: Carte géologique de la Province de Grenville à l'est de l'axe Louvicourt-Val d'Or-Senneterre; Ministère de l'Énergie et des Ressources du Québec, MB-92-15
- Graham, D.F. and Grant, D.R.**  
1991: A test of airborne, side-looking, Synthetic Aperture Radar in central Newfoundland for geological reconnaissance; Canadian Journal of Earth Sciences, Vol. 28, No. 2, February Issue, p. 257-265.
- Harris, J.R., Murray, R., and Hirose, T.**  
1990: IHS transform for the integration of Radar imagery with other remotely sensed data; Photogrammetric Engineering and Remote Sensing, v.56, p. 1631-1641.
- Harris, J.R., Graham, D.F., Newton, R., Yatabe, S., and Miree, H.**  
1987: Regional structural reconnaissance of the southwestern Grenville Province using remotely sensed imagery; 7th International Conference on Basement Tectonics, Paper no. 45, August 17-21, Queen's University, Kingston, Ontario. p. 441-463.
- Jackson, P.L. and Wagner, H.L.**  
1979: Gradient filtering for directional trends in images; 45th ASP-ACSM Annual Meeting Proceedings, Washington, DC, March 18-24, v. 2, p. 456-464.

**Laurin, A.F.**

1965: Gouin Reservoir Basin, Abitibi-East and Laviolette Counties, a geological outline; Quebec Department of Natural Resources, Geological Report 130, 14 p.

**Madore, C. and Ciesielski, A.**

1990: Petrology of some diabase dykes in the central Grenville Province, SE of Chibougamau, Quebec; Geological Association of Canada, Program with Abstracts, v. 15, p. A81.

**Neale, E.R.W.**

1952: Geology of the Bethoulat Lake area, Mistassini territory, Quebec; Ph.D. Thesis, Yale University, 345 p.

**Norman, G.W.H.**

1940: Thrust faulting of Grenville gneisses NWward against the Mistassini series of Mistassini lake, Quebec; Journal of Geology, v. 48, p. 512-525.

**PCI**

1993: User's manual, Version 5.1; PCI, Richmond Hill, Ontario.

**Sabins, F.F.**

1991: Digital processing of satellite images of Saudia Arabia; Presented at the SPE Middle East Oil Show, Bahrain, 16-19 November, p. 207-212.

**Wahl, F.M.**

1987: Digital image signal processing; Artech House Inc., 183 p.

**Wynne-Edwards, H.R.**

1972: The Grenville Province; in Variations in Tectonic Styles in Canada, R.A. Price and R.J.W. Douglas (ed.); Geological Association of Canada, Special Paper 11, p. 263-334.

---

Geological Survey of Canada Project 840016

# Géologie et cibles d'exploration de la partie centre est de la ceinture métasédimentaire du Québec, Province de Grenville

Louise Corriveau, David Morin<sup>1</sup> et Louis Madore<sup>2</sup>  
Centre géoscientifique de Québec

*Corriveau, L., Morin, D. et Madore, L., 1994 : Géologie et cibles d'exploration de la partie centre est de la ceinture métasédimentaire du Québec, Province de Grenville; dans Recherches en cours 1994-C; Commission géologique du Canada, p. 355-365.*

---

**Résumé :** La partie centre est de la ceinture métasédimentaire du Québec (Province de Grenville) comprend d'est en ouest :

(1) une zone de cisaillement ductile au faciès des amphibolites d'une puissance de 10 km, où des monzonites et des diorites se sont injectées en feuillets dans des paragneiss porphyroclastiques anormalement riches en pyrrhotine et en tourmaline;

(2) un dôme granulitique comprenant une masse tonalitique; et

(3) une séquence de métasédiments qui forme un synforme régional dans le coin sud-ouest du feuillet 31J/3.

Au cœur du dôme, la brèche ultrapotassique de Rivard forme un dyke non déformé et non recristallisé, d'orientation nord-sud. Environ le tiers des xénolites sont ultramafiques (clinopyroxénites à grenat, à spinelle ou à mica, webstérites, péridotites...). Ce dyke s'est mis en place dans des gneiss possiblement volcanogènes comprenant des lithofaciès alumineux et magnésiens avec localement de petits amas de sulfures. De tels lithofaciès sont considérés comme d'importants métallotectes dans la région de Montauban.

**Abstract:** The east-central portion of the Central Metasedimentary Belt of Québec (Grenville Province) consists from east to west of:

(1) a 10 km-wide shear zone at amphibolite facies with lit-par-lit injections of monzonite and diorite among porphyroclastic paragneiss with anomalous concentrations of pyrrhotite and tourmaline;

(2) a granulitic dome with a tonalitic component;

(3) a paragneiss sequence folded into a regional synform in the southwest corner of 31J/3.

Within the dome, the Rivard ultrapotassic breccia forms a north-south trending dyke that is neither deformed nor recrystallized. About one third of the xenoliths are ultramafic (garnet, spinel or mica clinopyroxenites, websterites, peridotites...). The dyke was emplaced in possibly volcanogenic gneisses with hyperaluminous and magnesian lithofacies locally with small sulphide clots. In the Montauban area such lithofacies represent important targets for mineral exploration.

---

<sup>1</sup> INRS-Géoressources, 2700 rue Einstein, C.P. 7500, Sainte-Foy, Québec G1V 4C7

<sup>2</sup> Université du Québec à Chicoutimi, 555 boul. de l'Université, Chicoutimi, Québec G7H 2B1

## INTRODUCTION

Les levés géologiques entrepris sur les feuillets 31J/3 et 31G/14 du SNRC dans la partie centre est de la ceinture métasédimentaire (Province de Grenville; fig. 1 et 2) confirment l'extension de la zone de cisaillement du lac Montjoie (Corriveau et Jourdain, 1992 et 1993) et font la lumière sur deux des complexes charnockitiques identifiés par Wynne-Edwards et al. (1966). La cartographie de la région avoisinant un gneiss siliceux et magnésien, semblable à un des métallotectes de la région de Montauban en Mauricie (Corriveau et al., 1993), a permis d'en préciser le contexte géologique. Ce gneiss fait partie d'une zone de dix kilomètres de longueur qui comprend toute une série de grenatites riches en magnétite (formation de fer silicatée) et des lithofaciès hyperalumineux renfermant localement de la chalcopryrite (fig. 2 et 3). Les travaux antérieurs remontent à Logan et al. (1912), dans la partie nord-ouest du feuillet 31G/4, et à Pollock (1957, 1960) et Wynne-Edwards et al. (1966), dans le feuillet 31J/3.

## GÉOLOGIE

La région centre est de la ceinture métasédimentaire recoupe deux domaines lithotectoniques (fig. 1 et 2), l'un riche en marbre à l'ouest qui s'étend jusqu'à la rivière Gatineau, l'autre riche en quartzite à l'est (Corriveau et Jourdain, 1992). Un dôme granulitique allongé avec des flancs fortement pentés (fig. 2 et 3) se retrouve au coeur du domaine riche en quartzite. Au sud-ouest, un autre dôme comprend un pluton de monzonite, de mangérite et de diorite avec des quartzites et des orthogneiss comme encaissant. Ces dômes sont mutuellement bordés d'une séquence de paragneiss riches en graphite avec localement des marbres dolomitiques à olivine. La marge est des feuillets de Duhamel (31J/3) et de Nominique (31J/6) consiste en une zone de cisaillement ductile au faciès des amphibolites où se sont mis en place syncinématiquement des injections lit-par-lit de monzonite et de diorite, ainsi que des dykes en filet de microdiorite et de syénite ou de granite.

Les grands éléments structuraux de la région comprennent : un dôme granulitique allongé occupant la partie nord-ouest du feuillet 31J/3 et la partie sud-ouest du feuillet 31J/6; un synforme dans le coin sud-ouest du feuillet 31J/3; et une zone de cisaillement dans la partie est des deux feuillets. Un boudin d'extension régionale est aussi apparent sur le feuillet 31J/3 à l'ouest du lac Gagnon. Le développement de ces structures est postérieur au métamorphisme régional. L'isograde de l'orthopyroxène est en effet plissée suivant un antiforme plurikilométrique qui plonge vers le nord et longe le pourtour du dôme dans sa partie nord (feuillet 31 J/6). Cet isograde quitte les flancs du dôme dans le feuillet 31J/3 et se poursuit vers le sud (fig. 2 et 3).

### Paragneiss du domaine quartzitique

Les paragneiss, dans la région de Duhamel, sont constitués principalement de quartzite et de gneiss siliceux avec des intercalations de métapélites, de gneiss quartzofeldspathiques à biotite, localement graphitiques ou avec sulfures de fer, de

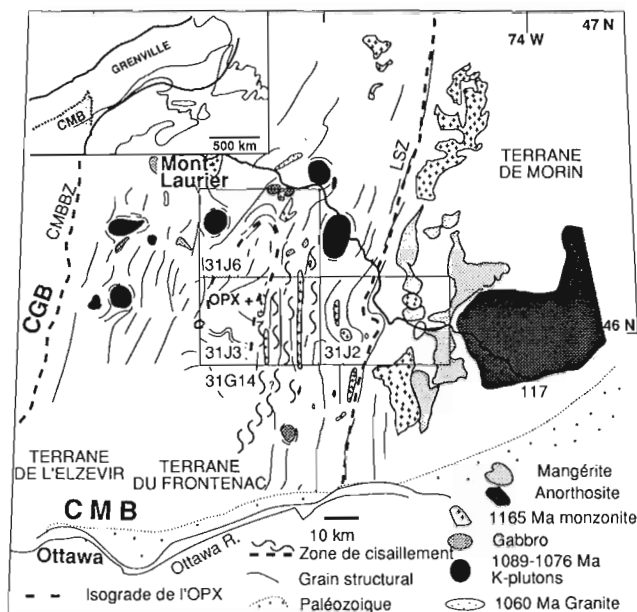


Figure 1. Localisation de la ceinture métasédimentaire du Québec (CMB) à l'intérieur de la Province de Grenville, dans le carton, et détails de ses suites plutoniques, de son grain structural et de ses terranes (subdivision préliminaire). Abréviations : CGB-Ceinture de gneiss centrale; CMBBZ-zone de bordure de la ceinture métasédimentaire; LSZ-zone de cisaillement de Labelle.

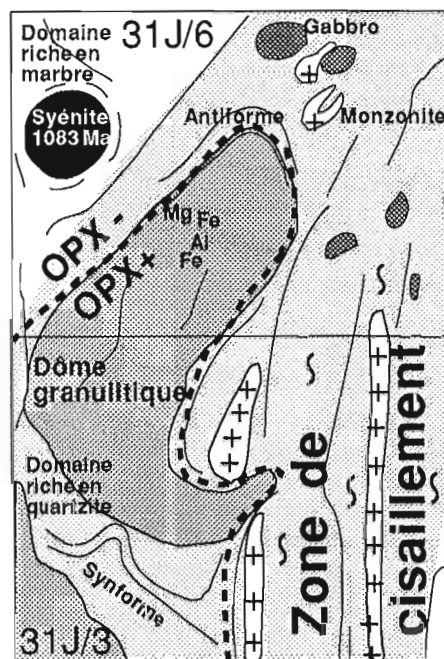


Figure 2. Grandes lignes de la géologie des feuillets 31J/3 et 31J/6.



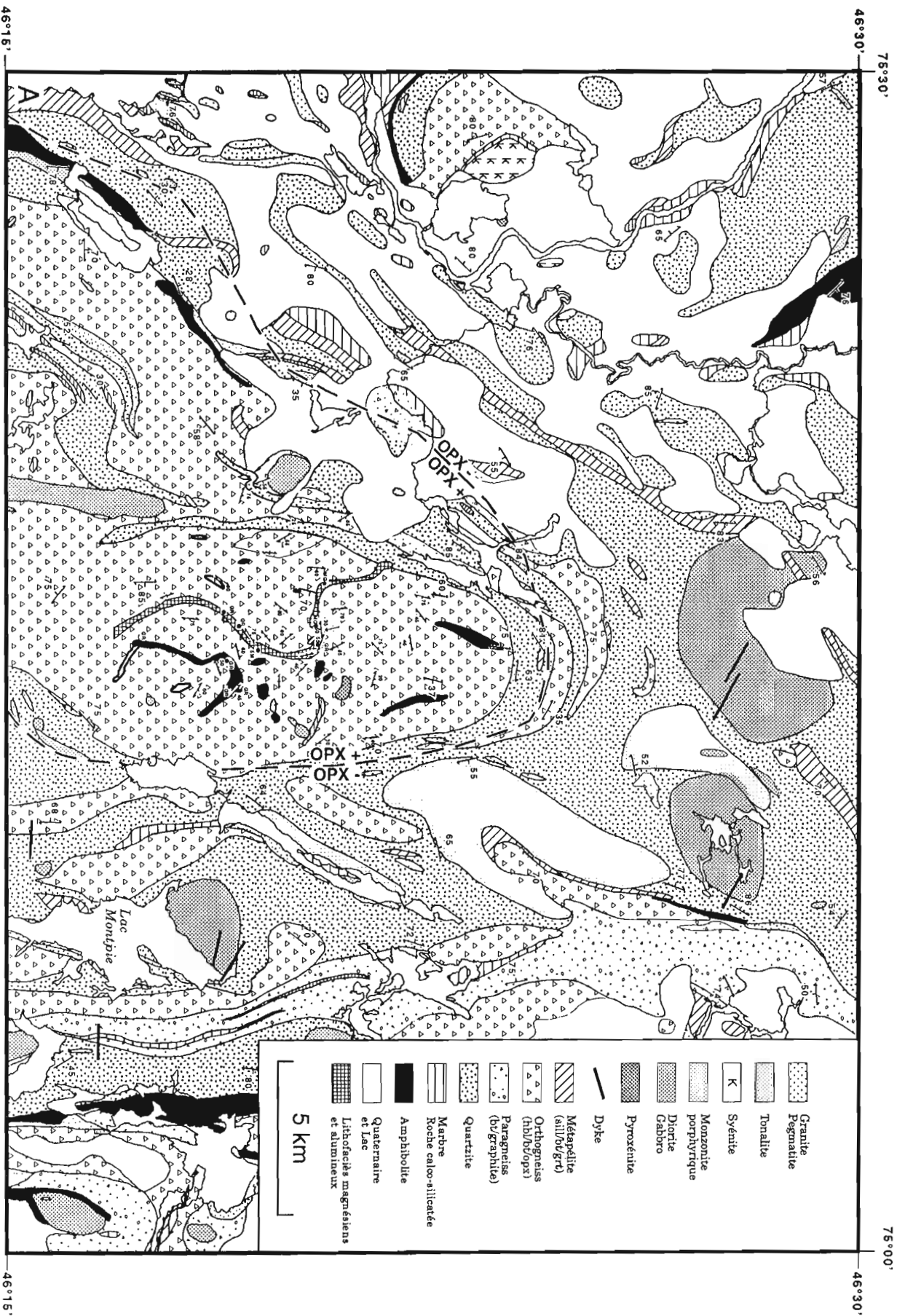


Figure 3. A) Géologie détaillée de la région de Nominique (feuille 31116), modifiée de Corriveau et Jourdain (1992 et 1993), montrant, au centre de la carte, la bande de gneiss possiblement volcanogènes et ses lithofaciès magnésiens et hyperalumineux. MG-gneiss siliceux et magnésien; SM-lithofaciès hyperalumineux de gneiss à quartz et sillimanite; GR-grenatites riches en magnétite.



Figure 3. B) Géologie détaillée de la région de Duhamel (feuillelet 31J13 au sud). Voir la légende en A.

marbres et de roches calcosilicatées. Ils sont similaires aux paragneiss des régions de Saint-Jovite et de Nominungue décrits par Martignole et Corriveau (1991, 1993) et Corriveau et Jourdain (1992, 1993).

La foliation régionale est marquée par la gneissosité, le rubanement compositionnel et l'orientation préférentielle des minéraux tabulaires et aciculaires. Les linéations, quant à elles, sont définies par l'orientation préférentielle des minéraux et agrégats de minéraux, tels que le quartz dans les veines granitiques et la sillimanite dans les métapélites. Elles sont très dispersées, sauf à l'est, dans la zone de cisaillement le long du lac Gagnon (fig. 3, 4 et 5B). La foliation est fortement pentée vers l'est ou l'ouest (fig. 3 et 5A). Le boudinage des unités est commun mais les textures de tectonites sont rares ou oblitérées par la recristallisation.

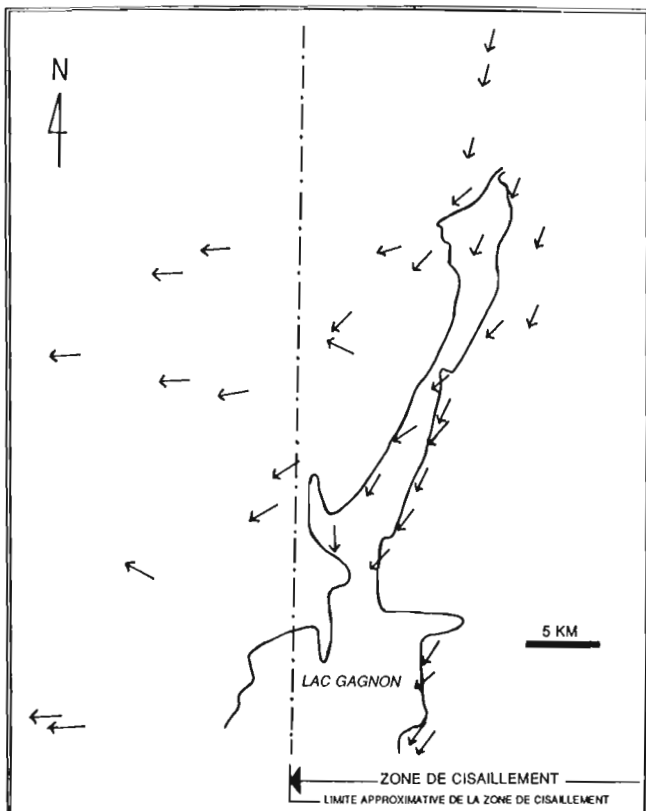
### Dôme granulitique

Le dôme granulitique consiste principalement en orthogneiss granitiques et tonalitiques intercalés avec des bandes de metabasites (dykes transposés?) d'épaisseur généralement inférieure à quelques mètres. Ces orthogneiss sont leucocrates, à grain fin, rubanés et foliés. Ils ont comme minéraux accessoires de l'orthopyroxène, du grenat, de la

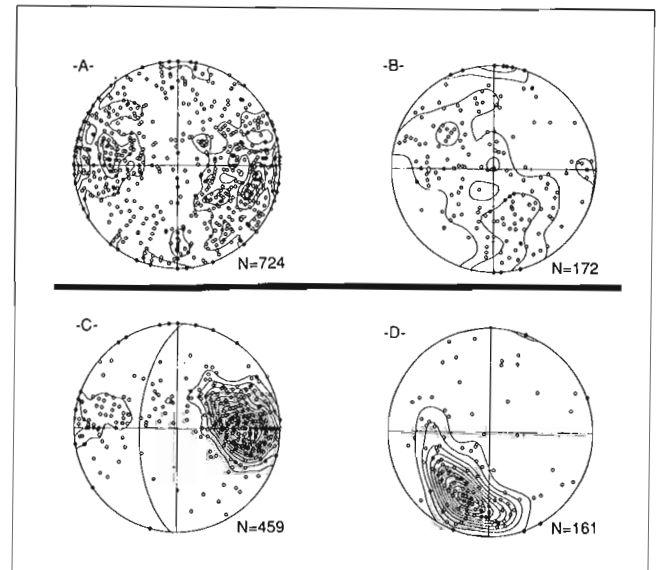
biotite ou de la hornblende. Les leucosomes granitiques à orthopyroxène y sont bien développés, parallèles à la foliation, massifs et à grain moyen.

Une masse tonalitique (30 km<sup>2</sup>), gneissique en bordure, affleure parmi les orthogneiss dans la partie sud du dôme. Cette tonalite est relativement homogène, blanche en surface altérée, leucocrate et granoblastique à faiblement foliée, avec de la biotite, de la hornblende ou de l'orthopyroxène. Les leucosomes sont granitiques à tonalitiques, massifs et à grain moyen. Aucun contact franc n'a été observé entre cette masse et les orthogneiss avoisinants; la présence d'orthopyroxène et d'une texture granoblastique suggère que cette masse a été métamorphosée, mais l'absence de gneissosité pénétrante suggère qu'elle a échappé en partie à la déformation régionale. Cette masse pourrait être un des protolites des orthogneiss.

Les orthogneiss (fig. 4E dans Corriveau et Jourdain, 1992) et la tonalite sont recoupés par des dykes lamprophyriques veinés en filet (net-veined) avec amphibole et pyroxène (fig. 6A) et localement avec des phénocristaux de biotite. Ces dykes sont constitués de masses arrondies, centimétriques à décimétriques, de lamprophyre dans une matrice granitique. Ces deux composantes sont localement séparées par des zones de réactions anhydres. Les dykes en filet sont injectés au coeur de dykes de pegmatite et ont des contacts lobés et très irréguliers avec celle-ci. Ils ont été boudinés avant leur solidification. Les pegmatites, par contre, ont des contacts francs avec l'encaissant.



**Figure 4.** Secteur nord de la zone de cisaillement du lac Gagnon illustrant la déviation de la linéation vers l'étranglement du boudin crustal (fig. 2 et 3). Les flèches indiquent la direction des linéations.



**Figure 5.** Projections stéréographiques équiales. Les contours sont effectués selon la méthode de Robin et Jowett (1986); N-nombre de données. **A)** Pôles des foliations dans les gneiss du feuillet 31J/3, à l'ouest de la zone de cisaillement. **B)** Linéations minérales dans les gneiss situés à l'ouest de la zone de cisaillement. **C)** Pôles des foliations dans les gneiss de la zone de cisaillement le long du lac Gagnon (le grand cercle à 183°/160° correspond au plan moyen de la foliation). **D)** Linéations minérales dans les gneiss situés dans la zone de cisaillement le long du lac Gagnon.

Des gneiss granitiques et des amphibolites grenatifères, localement rubanés et possiblement d'origine volcanogène (fig. 6B, C) affleurent au nord-ouest du dôme sur une dizaine de kilomètres de longueur et 200 m de largeur (fig. 3). Des lithofaciès hyperalumineux et magnésiens y sont associés (fig. 6D et E). Cette zone conserve localement des évidences de cisaillement ductile et les leucosomes y sont fréquents. Ces gneiss sont recoupés par la brèche ignée ultrapotassique de Rivard (fig. 6F). Ce dyke, ou un dyke apparenté, affleure également à 8 km plus au sud.

### *Lithofaciès magnésien et hyperalumineux*

Le lithofaciès magnésien est constitué d'un gneiss siliceux blanc (quartz et plagioclase) avec des niveaux très magnésiens (MgO : 10%) de quelques centimètres d'épaisseur de bronzite, de cordiérite magnésienne, de kornéropine et de tourmaline magnésienne avec accessoirement du zircon, de la magnétite, de la pyrite, de la pyrrhotine et des traces de chalcopryrite (fig. 6D; coordonnées de la projection transverse universelle de Mercator [UTM], zone 18 : 478250m E, 5131970m N, feuillet 31J/6; Corriveau et al., 1993). Ces niveaux sont parallèles à la gneissosité et s'étendent d'un bout à l'autre de l'affleurement. Les agrégats de tourmaline et de bronzite sont communément allongés dans la gneissosité, ce qui ne semble pas être le cas de la kornéropine et de la cordiérite. Des leucosomes à bronzite recoupent la gneissosité. Le zircon montre toujours une mince couronne et contient aussi parfois un coeur distinct, indiquant au moins trois épisodes de croissance.

Cette unité de gneiss siliceux affleure plus à l'est (UTM : 479750m E, 5131750m N) et est associée (1) à des grenatites riches en magnétite avec des amas de chalcopryrite et de pyrite, représentant peut-être des formations de fer silicatées (fig. 6E; UTM : 480200m E, 5131800m N), (2) à des gneiss à cordiérite, à hypersthène et à grenat, riches en zircon, (3) à des gneiss à sillimanite, à grenat, à cordiérite et à biotite, avec zircon et pyrrhotine, et enfin (4) à un gneiss granitique non porphyroclastique, au rubanement centimétrique et continu fort inhabituel, qui ne ressemble pas à un «straight gneiss» (fig. 6B; UTM : 480000m E, 5131850m N). Plus au sud, cet assemblage de gneiss passe à un lithofaciès hyperalumineux constitué essentiellement de sillimanite et de quartz avec accessoirement de la pyrrhotine et de la biotite et des traces de chalcopryrite et de pyrite (UTM : 480500m E, 5129850m N). Cet horizon, fortement rouillé, affleure sur deux mètres d'épaisseur; il est plissé isoclinalement et est recoupé par d'abondantes veines granitiques. Des grenatites riches en biotite et des gneiss à biotite, à grenat et à hypersthène (UTM : 479300m E, 5128800m N) affleurent à nouveau plus au sud parmi des amphibolites à grenat très hétérogènes, de plusieurs dizaines de mètres d'épaisseur.

De tels lithofaciès magnésiens et hyperalumineux représentent, dans la région de Montauban, des métallotectes pour l'or et les sulfures massifs (Gauthier et al., 1985; Bernier, 1992). À l'ouest de la ceinture métasédimentaire, des tourmalinites sont associées à des amas zincifères dans des séquences supracrustales riches en marbre (Lapointe et al., 1992). Dans la région d'étude, aucun marbre n'est associé à

la zone anormale, mais les paragneiss à graphite sont communs. Ces gneiss, de par leur grande conductivité, représentent un obstacle important à la prospection géophysique de la région pour les sulfures massifs.

### *La brèche de Rivard*

La brèche intrusive de Rivard (fig. 6F; UTM : 478420m E, 5131546m N) se présente sous la forme d'un dyke fortement penté vers l'ouest s'étendant selon une orientation nord-sud sur plus de 200 m avec une puissance variant de quelques centimètres à deux mètres (fig. 6F). Plus de 50 % du volume du dyke est occupé par des xénolites de taille, de forme et de composition diverses. Ces xénolites sont cimentés par un lamprophyre apparenté à la suite de plutons potassiques mis en place entre 1 090 et 1 076 Ma (Corriveau et al., 1990; Corriveau et Gorton, 1993). La brèche n'est ni déformée, ni métamorphosée et recoupe des orthogneiss et des amphibolites granulitiques, ainsi que des veines pegmatitiques irrégulières. La bordure du dyke est rectiligne lorsque parallèle à la gneissosité de l'encaissant et irrégulière, avec érosion différentielle de l'orthogneiss, lorsqu'elle recoupe la

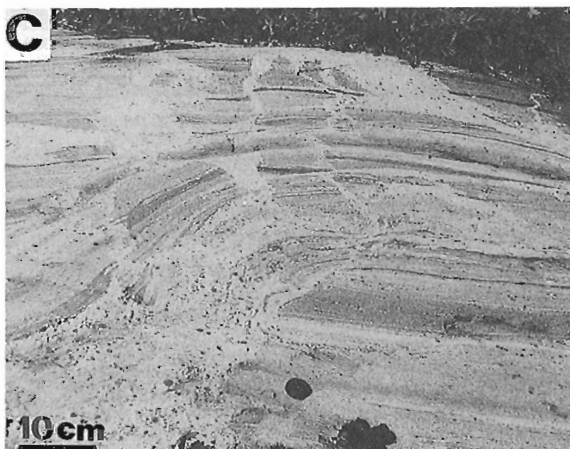
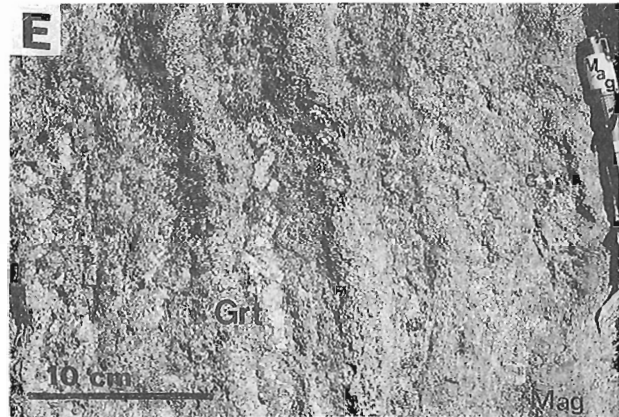
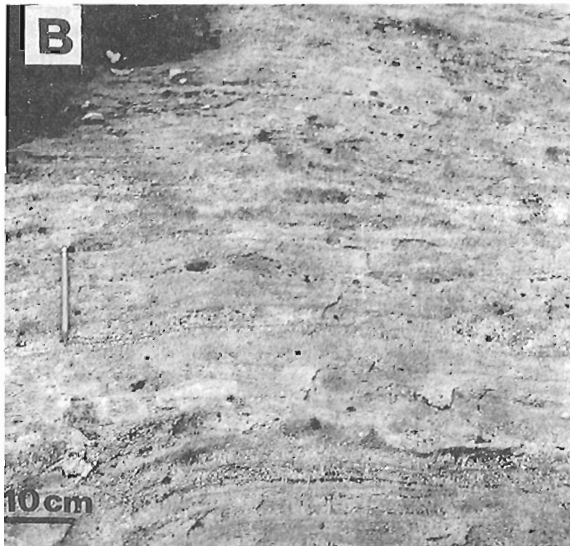
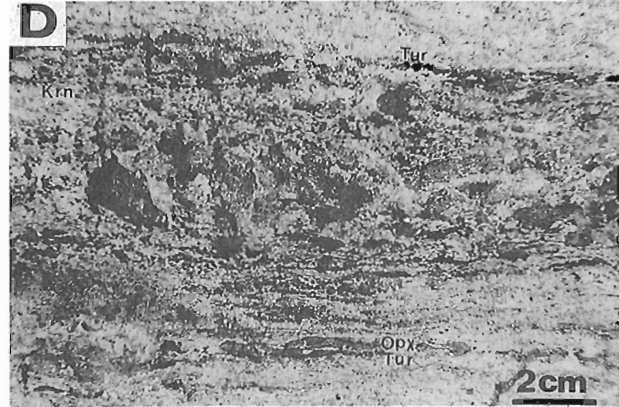
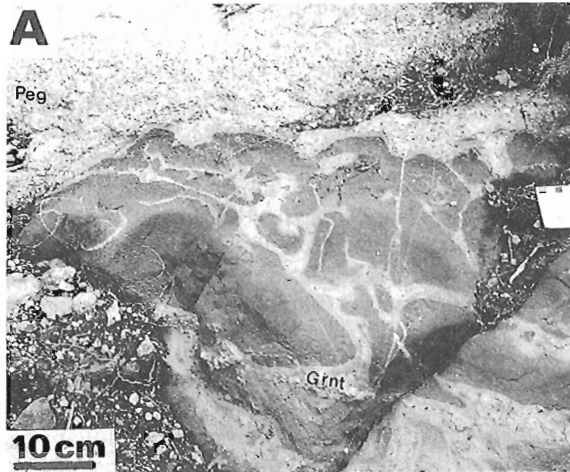
- 
- A) *Dyke veiné en filet mis en place dans un dyke de pegmatite (Peg). Ces dykes sont typiques de la partie sud-ouest du dôme granulitique. Le lamprophyre forme des coussins dans les veines granitiques (Grnt).*
  - B) *Gneiss granitique rubané : le rubanement est continu à la base structurale et très irrégulier dans le haut de la photo.*
  - C) *Amphibolite grenatifère rubanée, intercalée avec des gneiss à hornblende et recoupée par des veines granitiques. Une bande d'amphibolite, elle aussi rubanée, semble recouper les niveaux précédents, ce phénomène n'a pu être expliqué.*
  - D) *Niveau de tourmaline (tur) à grain fin et de bronzite (opx), de kornéropine (krn) et de cordiérite à grain moyen dans un gneiss siliceux riche en plagioclase. Les agrégats de bronzite et de tourmaline suivent la gneissosité, par contre la kornéropine semble y être superposée.*
  - E) *Horizon de grenatite riche en magnétite (à droite) avec localement des amas de pyrrhotine et de chalcopryrite et des traces de pyrite dans un gneiss rubané à biotite, à cordiérite, à grenat (Grt), à magnétite (Mag) (principalement dans les couches foncées) et à orthopyroxène ou à sillimanite.*
  - F) *Brèche ultrapotassique de Rivard : les xénolites ultramafiques (umf) sont concentrés le long de la bordure est (à gauche). Le dyke est fortement penté vers l'ouest. Ces xénolites représentent diverses parties de la lithosphère sous la ceinture métasédimentaire.*

**Figure 6.**



foliation. De nombreuses apophyses isolent plus ou moins complètement des fragments de la roche encaissante. L'orientation des apophyses semble contrôlée par celle de la gneissosité de l'encaissant et ne permet pas, à prime abord, de définir un sens d'écoulement. Le décalage dextre d'un niveau d'amphibolite sur un mètre indique une mise en place

dominée par l'extension. Toutefois, la présence d'irrégularités arrondies dans l'éponte et l'existence de bordures opposées non parallèles montre que l'encaissant a été partiellement démembré ou assimilé par le lamprophyre. Des bordures de trempe sont présentes à la marge d'apophyses centimétriques, mais sont absentes des sections les plus larges du dyke. La



mise en place s'est effectuée en plusieurs injections, distinctes par la granulométrie et la composition du lamprophyre et par l'abondance des xénolites.

Les xénolites sont arrondis à anguleux et leur dimension varie de 1 mm à 70 cm. Parmi les quelque 1 500 xénolites décrits, environ 30 % sont de composition ultramafique. Il s'agit de plusieurs types de clinopyroxénites (à grenat, à spinelle ou micacées), d'orthopyroxénites, de webstérites et de rares péridotites. Environ 30 % des xénolites sont de composition mafique à intermédiaire et comprennent des gabbros, des norites, des anorthosites, des metabasites, des roches calcosilicatées et possiblement des éclogites. Environ 40 % des xénolites sont felsiques et sont composés de gneiss (orthogneiss et paragneiss), avec une abondance anormalement élevée de grenat, de quartzites grises ou bleues et de granitoïdes. Quelques-unes de ces lithologies peuvent être observées dans les affleurements de la région. La minéralogie, la granulométrie et l'intensité de la déformation des xénolites sont très variables. Un exemple extrême de déformation inter-xénolites est illustré par un rentrant dans un gneiss quartzofeldspathique occupé par un xénolite anguleux de clinopyroxénite autour duquel la gneissosité a été déviée de manière ductile. La bordure des xénolites est nette ou résorbée et peut montrer une fine couronne de clinopyroxène, d'amphibole et/ou de biotite, ce qui suggère que certains xénolites ont partiellement réagi avec le magma ultrapotassique et que d'autres ont servi de sites de nucléation. La brèche contient en outre d'abondants mégacristaux de clinopyroxène pouvant atteindre 5 cm, de même que quelques xénocristaux de grenat rouge avec texture kélyphitique et de feldspaths gris communément résorbés.

Le lamprophyre qui cimente les xénolites est porphyrique avec des phénocristaux millimétriques à submillimétriques de clinopyroxène et de biotite formant environ 20 % du volume du lamprophyre. La matrice ignée est composée de clinopyroxène, de biotite, de feldspath potassique, de plagioclase, d'amphibole et d'apatite, avec des quantités mineures de quartz, de titanite, de zircon(?) et de sulfures. Les phénocristaux définissent localement une foliation magmatique dont la forme autour de certains xénolites montre un écoulement vers le haut.

### Marge ouest

La marge ouest du dôme granulitique (fig. 3) comprend une séquence de métasédiments riches en graphite avec sporadiquement des marbres dolomitiques et des marbres à olivine. Ces métasédiments forment dans le coin sud-ouest du feuillet 31J/3 un synforme régional plongeant vers le sud. Ces paragneiss forment la bordure est d'un autre complexe charnockitique comprenant des monzonites, des mangérites et des diorites et, au sud dans le feuillet 31G/14, des granites, des monzonites et des gabbros localement pegmatitiques et hétérogènes.

### Marge est

La partie est du feuillet 31J/3 comprend des paragneiss protomylonitiques et mylonitiques, cisailés (déplacement normal, senestre, bloc occidental abaissé) au faciès des

amphibolites et anormalement riches en pyrrhotine et en tourmaline (fig. 7E). Ces paragneiss sont intercalés sur plusieurs kilomètres d'épaisseur avec des feuillets concordants, centimétriques à kilométriques, de monzonite et de diorite foliées (foliations tectonique et magmatique; fig. 3 et 7A à C), de microdiorite et de dykes en filet (foliation magmatique) dont des exemples types sont décrits dans Corriveau (1991). Les évidences d'assimilation (fig. 7D), de mélange de magmas, d'emplacement syntectonique et de formation de skarn (fig. 7C) sont communes dans ce corridor. Là où la monzonite a été fortement cisailée, elle est transformée en gneiss à biotite et à grenat et contient des intercalations de roches calcosilicatées (fig. 7D) dont les protolites gabbroïques sont localement préservés. Des failles est-ouest tardives, pouvant atteindre un mètre d'épaisseur, recoupent la zone de cisaillement. Certaines de ces failles sont remplies de veines de quartz formant des géodes d'un volume de près de un mètre cube avec des cristaux limpides, souvent zonés, qui atteignent 10 cm de longueur (fig. 7E).

L'intensité et le moment de la déformation varient de l'est à l'ouest et du nord au sud. À l'ouest, une grande partie des feuillets et leurs dykes ont conservé leur foliation magmatique et les dykes de pegmatite sont rectilignes ou légèrement ondulés. À l'est, par contre, même les dykes de microdiorite et de pegmatite sont mylonitisés, ce qui suggère que le cisaillement s'est terminé plus tardivement dans cette région. Le plan moyen de la foliation est de 183°/60° (fig. 5C). Le

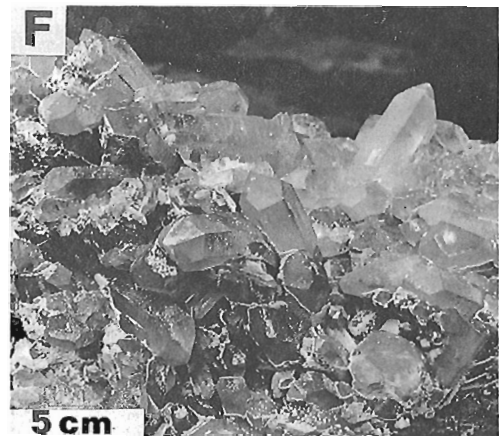
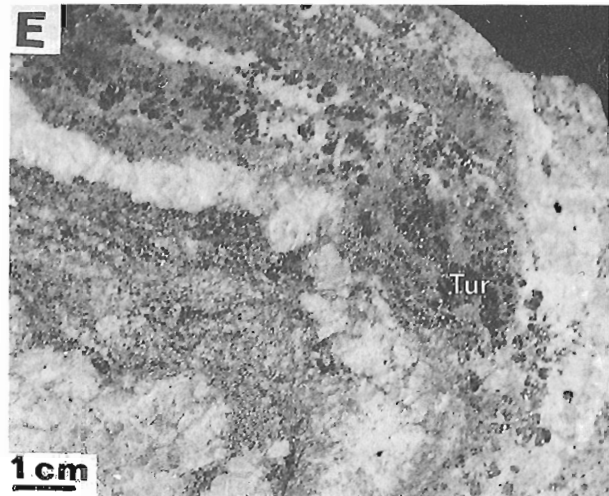
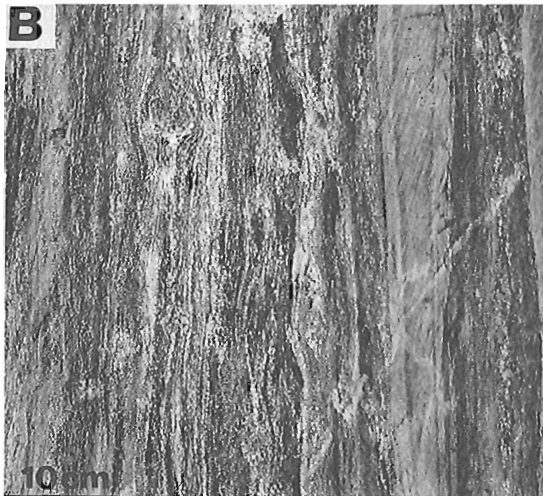
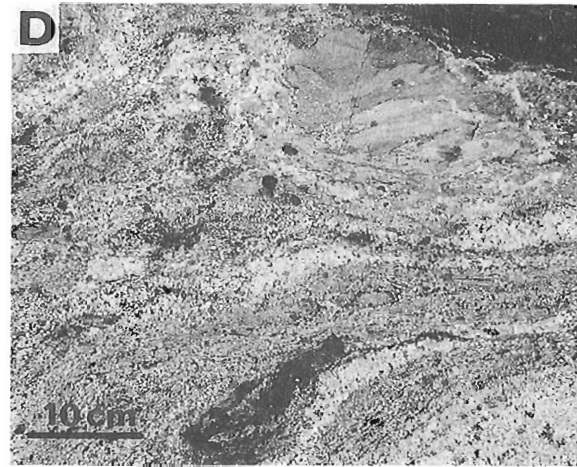
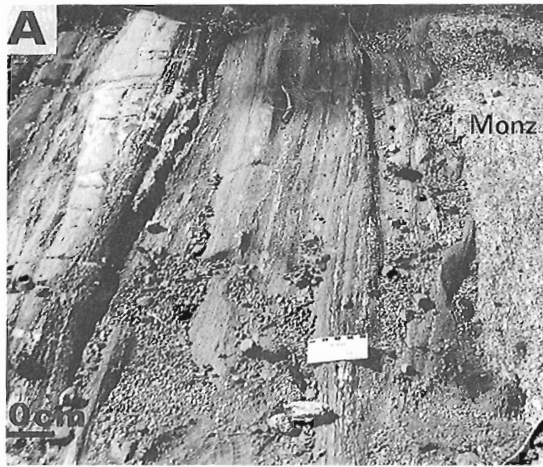
- 
- A) *Feuillet de monzonite porphyrique (Monz) intercalé avec des bandes de roches calcosilicatées mylonitiques, possiblement d'origine gabbroïque, et d'autres gneiss. Le feuillet est parallèle au plan de cisaillement de la mylonite hôte et les phénocristaux de la monzonite sont alignés selon une foliation ignée parallèle aux contacts du feuillet.*
  - B) *Vue rapprochée et*
  - C) *échantillon du même affleurement qu'en A montrant des feuillets de monzonite transformés par le cisaillement en gneiss à biotite et à grenat. Les roches calcosilicatées forment des bandes zonées à grain très fin. Des phénocristaux de la monzonite sont localement préservés dans les gneiss à biotite.*
  - D) *La roche encaissante est localement démembrée et digérée par des monzonites non porphyriques comagmatiques.*
  - E) *Paragneiss à biotite avec pyrrhotine et tourmaline (Tur), recoupés par des veines granitiques. Une nouvelle génération de tourmaline est formée aux dépens des veines et des paragneiss.*
  - F) *Cristaux de quartz formés dans des veines de quartz d'orientation est-ouest.*

Figure 7.



cisaillement s'est produit lors du métamorphisme rétrograde au faciès des amphibolites moyen, comme en témoigne l'apparition de la muscovite dans les gneiss à biotite. Les linéations passent d'une direction sud-ouest, le long du lac Gagnon, à une direction ouest à l'intérieur de la zone d'étranglement d'un boudin crustal (fig. 2 à 5). Le boudinage semble avoir entraîné l'extrémité sud du dôme granulitique et dévié les linéations de part et d'autre de la zone d'étranglement.

L'extension nord de ce corridor de déformation, à l'est du lac Montjoie dans le feuillet 31J/6, est marquée par du plissement pygmatique dysharmonique et quelques zones de cisaillement et est pauvre en intrusions monzonitiques (Corriveau et Jourdain, 1992, 1993; Tremblay et al., 1993). Ce corridor se poursuit vers le sud dans le feuillet 31G/14 (cette étude) et dans le feuillet 31 G/11 au nord de la rivière des Outaouais (Dupuis et al., 1989). La zone s'amincit graduellement vers le nord; sa puissance est de 10 km dans la partie



sud du feuillet 31J/3, de 6 km dans la partie nord et de 3 km dans la région du lac Montjoie. Cette zone montre un grade métamorphique plus faible (muscovite stable) que la zone de cisaillement de Labelle, plus à l'est.

## CONCLUSION

Les levés régionaux sur le feuillet 31J/3 à l'échelle de 1/50 000 en 1992 et les études thématiques en 1993 ont permis de suivre, du nord au sud (parallèlement au grain structural) et de l'est à l'ouest, les structures et les types de plutons observés lors de la cartographie des feuillets 31J/2 et 31J/6 (1990, 1991) et de tracer sur une dizaine de kilomètres une cible d'exploration comportant des lithofaciès hyperalumineux et magnésiens qui, dans la région de Montauban en Mauricie, sont considérés comme d'importants métalotectes. La brèche ultrapotassique de Rivard recoupe ces lithofaciès. Elle forme un dyke d'orientation nord-sud, non déformé et non recristallisé où 30 % des xénolites sont ultramafiques (p. ex., clinopyroxénites à grenat, périclites). Ces xénolites sont une fenêtre sur la lithosphère grenvillienne et sous-grenvillienne. Des études sont en cours afin de déterminer si la source de ce magma ultrapotassique du Protérozoïque est dans le champ de stabilité des diamants et si le craton archéen s'étend jusque sous la ceinture métasédimentaire.

La zone de déformation ductile identifiée en 1991 à la marge est de la ceinture se poursuit vers le sud dans les feuillets 31J/3 et 31G/14. Cette zone renferme des paragneiss porphyroclastiques et des mylonites, cisailés (déplacement normal, senestre, bloc occidental abaissé) au faciès des amphibolites où se sont intercalés des injections lit-par-lit décamétriques à kilométriques de monzonite, de diorite et des dykes en filet. Ces dykes peuvent être eux-mêmes très déformés au faciès des amphibolites. Les paragneiss et les veines qui les recoupent sont anormalement riches en pyrrhotine, en pyrite et en tourmaline le long de toute cette zone.

Une séquence de métasédiments, qui renferme des marbres dolomitiques, forme un synforme régional dans le coin sud-ouest de la région. Cette séquence borde deux des complexes charnockitiques identifiés par Wynne-Edwards et al. (1966). Le complexe du sud comprend des masses de monzonite, de mangérite, de diorite et de gabbro d'une étendue de quelques kilomètres carrés. Le dôme au nord consiste en orthogneiss granitiques à tonalitiques, et en une masse tonalitique homogène qui représente possiblement le protolite.

## REMERCIEMENTS

Nous avons été grandement aidés pour la cartographie et la numérisation des données de terrain sur FIELDLOG par Katherine Boggs (UQAC), Guillaume Couture (INRS), John Delhs (U. de Toronto), Nalini Mohan (U. de Toronto), Martin Simard (U. Laval) et Maxime Tellier (INRS). Nicolas Lepage (U. de Montréal) a numérisé les cartes sur COREL DRAW à partir de GÉNÉRIC CAD et Marco Boutin (CGQ) a produit la version finale des figures. Nous remercions aussi Otto van Breemen (CGC) et tout un groupe de

géologues de compagnies minières pour avoir partagé avec nous leurs visions de la géologie régionale et des cibles métallogéniques visitées, ainsi que Graphicor, KWG et la famille Forget pour avoir permis la publication de données sur leurs propriétés. Les fonds de recherche pour l'étude de la brèche de Rivard viennent en grande partie de Ressources KWG dans le cadre du Programme des partenaires industriels de la Commission géologique du Canada. Nous leurs en sommes extrêmement reconnaissants. Nous remercions aussi Tyson Birkett et Maxime Tellier pour leur critique constructive de ce rapport, ainsi que toute l'équipe de la Réserve faunique de Papineau-Labelle pour les milliers de services qu'ils nous ont rendus et pour nous avoir hébergés au refuge Héron. Salut Alain (Demers) et merci!

## REFERENCES

- Bernier, L.**  
1992: Caractéristiques géologiques, lithogéochimiques et pétrologiques des gîtes polymétalliques de Montauban et de Dussault; Ministère de l'Énergie et des Ressources du Québec, DV 92-03, p. 31-34.
- Corriveau, L.**  
1991: Lithotectonic studies in the Central Metasedimentary Belt of the southwestern Grenville Province: plutonic assemblages as indicators of tectonic setting; in Current Research, Part C; Geological Survey of Canada, Paper 91-1C, p. 89-98.
- Corriveau, L. and Gorton, M.P.**  
1993: Coexisting K-rich alkaline and shoshonitic magmatism of arc affinities in the Proterozoic: A reassessment of syenitic rocks in the southwestern Grenville Province; Contributions to Mineralogy and Petrology, v. 113, p. 262-279.
- Corriveau, L. and Jourdain, V.**  
1992: Terrane characterization in the Central Metasedimentary Belt of the southern Grenville orogen: the Lac Nominique map area; in Current Research, Part C; Geological Survey of Canada, Paper 92-1C, p. 81-90.
- Corriveau, L. et Jourdain, V.**  
1993: Géologie de la région de Lac Nominique, Québec (SNRC 31J/6); Commission géologique du Canada, Dossier public 2641, 1 carte annotée à l'échelle de 1/50 000.
- Corriveau, L., Heaman, L.M., Marcantonio, F., and van Breemen, O.**  
1990: 1.1 Ga K-rich alkaline plutonism in the southwestern Grenville Province - U-Pb constraints for the timing of subduction-related magmatism; Contributions to Mineralogy and Petrology, v. 105, p. 473-485.
- Corriveau, L., Morin, D. et Boggs, K.**  
1993: Cibles d'exploration dans la Ceinture métasédimentaire, province de Grenville, région de Mont-Laurier, Québec (SNRC 31J/2, 3 et 6); Commission géologique du Canada, Dossier public 2617, 8p.
- Dupuis, H., Sharma, K.N.M., Chidiac, Y. et Lévesque, J.**  
1989: Géologie de la région de Thurso-Papineauville; Ministère de l'Énergie et des Ressources du Québec, DP 89-08, 1 carte annotée à l'échelle de 1/20 000.
- Gauthier, M., Morin, G. et Marcoux, P.**  
1985: Minéralisations aurifères de la partie centrale de la Province de Grenville, Bouclier canadien; CIM Bulletin, vol. 78, p. 60-69.
- Lapointe, S., Nantel S. et Gauthier, M.**  
1992: Tourmalinites, amas sulfurés zincifères et formations de fer dans la région de Maniwaki-Gracefield, province de Grenville; Ministère de l'Énergie et des Ressources du Québec, DV 92-02, p. 13.
- Logan, W.E., Eills, R.W., Adams, F.D. et Giroux, N.J.**  
1912: Géologie du feuillet Grenville à l'échelle de 1/253440; Commission géologique du Canada, Carte n° 750.
- Martignole, J. and Corriveau, L.**  
1991: Lithotectonic studies in the Central Metasedimentary Belt of the southern Grenville Province: lithology and structure of the Saint-Jovite map area, Québec; in Current Research, Part C; Geological Survey of Canada, Paper 91-1C, p. 77-88.

**Martignole, J. et Corriveau, L.**

1993: Géologie de la région de Saint-Jovite, Québec (SNRC 31J/2); Commission géologique du Canada, Dossier public 2640, 1 carte annotée à l'échelle de 1/50 000.

**Pollock, D.W.**

1957: Rapport préliminaire sur la région de Preston-Gagnon, districts électoraux de Papineau et de Labelle; Ministère des Mines, Québec, RP 334, 6p., 1 carte à l'échelle de 1/63 360.

**Pollock, D.W.**

1960: Rapport préliminaire sur la région de Rocheblave, districts électoraux de Papineau et de Labelle; Ministère des Mines, Québec, RP 408, 8p., 1 carte à l'échelle de 1/63 360.

**Robin, P.-Y. and Jowett, C.E.**

1986: Computerized density contouring and statistical evaluation of orientation data using counting circles and continuous weighting functions; Tectonophysics, v. 121, p. 207-223.

**Tremblay, P., Corriveau, L. et Daigneault, R.-A.**

1993: Géologie de la Réserve faunique de Papineau-Labelle -Rallyes géologiques; INRS-Géoresources, 1 carte annotée à l'échelle de 1/100 000.

**Wynne-Edwards, H.R., Gregory, A.F., Hay, P.W., Giovanella, C.A., and Renhardt, E.W.**

1966: Mont-Laurier and Kempt lake map area, Quebec; Geological Survey of Canada, Paper 66-32, 32 p., 1 map, scale 1:253 440.

---

Projet 920002 de la Commission géologique du Canada.



# Comparison of trace element distributions in lake sediments and waters from the Florence Lake area, Labrador<sup>1</sup>

P.W.B. Friske, G.E.M. Hall, and S.J.A. Day  
Mineral Resources Division

*Friske, P.W.B., Hall, G.E.M., and Day, S.J.A., 1994: Comparison of trace element distributions in lake sediments and waters from the Florence Lake area, Labrador; in Current Research 1994-C; Geological Survey of Canada, p. 367-376.*

---

**Abstract:** As part of a detailed infill lake sediment survey in the Florence Lake area of Labrador, waters were collected from 131 sites for trace metal determination. The distribution of 15 elements in waters and accompanying lake sediments were compared. Results indicate a significant correlation between U, Ni, Ce, La, Sm, Tb, Cu, and Mn in the two media. Zn, Cd, Pb, F, V, Fe, and Co do not appear to have a sympathetic relationship.

Evaluation of the variance of the total data set as well as site and blind duplicate data suggests that the lack of correlation for some elements may be related to relatively high within-site variability, particularly for the water data.

The correlation in the distribution of sediment and water data suggests that the extensive National Geochemical Reconnaissance sediment database may be useful, in terms of environmental and public health concerns, for identifying areas in which naturally elevated concentrations of elements occur in surface waters.

**Résumé :** Dans le cadre d'un levé détaillé des sédiments de remplissage lacustres dans la région du lac Florence au Labrador, des échantillons d'eau ont été prélevés à 131 sites pour déterminer leur teneur en métaux traces. Les répartitions de 15 éléments dans les eaux et les sédiments lacustres associés ont été comparées. Les résultats indiquent une importante corrélation entre U, Ni, Ce, La, Sm, Tb, Cu et Mn dans les deux milieux. Zn, Cd, Pb, F, V, Fe et Co ne semblent pas présenter de corrélation.

L'évaluation de la variance dans l'ensemble des données totales ainsi que des données d'échantillons additionnels pour un même site et d'échantillons témoins indique que l'absence de corrélation de certains éléments peut être liée à une variabilité relativement élevée au sein d'un même site, en particulier en ce qui concerne les données sur les échantillons d'eau.

La corrélation entre la répartition des données sur les échantillons de sédiment et les échantillons d'eau révèle que l'importante base de données sur la composition des sédiments du sous-programme national de reconnaissance géochimique pourrait être utile, en ce qui a trait aux problèmes de santé publique et d'environnement, pour repérer les régions où les eaux de surface contiennent des concentrations d'éléments naturellement élevées.

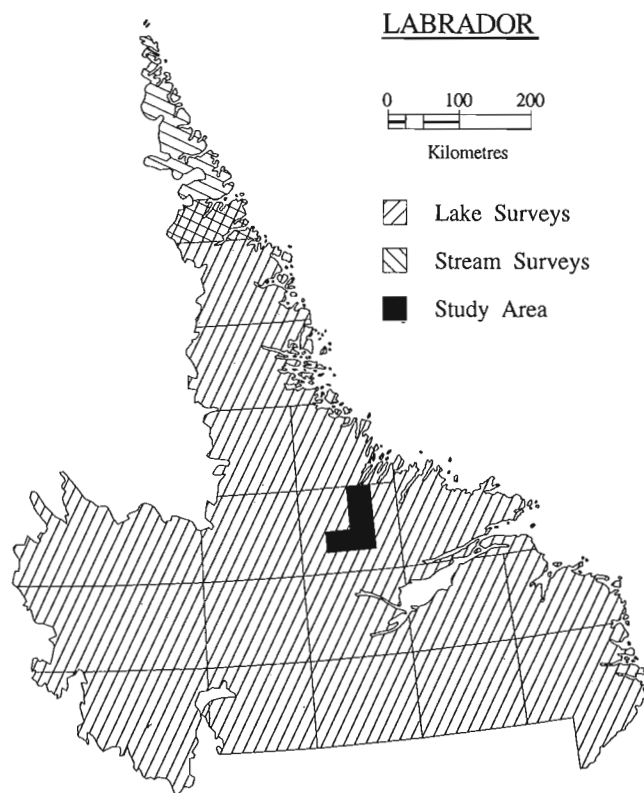
---

<sup>1</sup> Contribution to Canada-Newfoundland Cooperation Agreement on Mineral Development (1990-1994), a subsidiary agreement under the Canada-Newfoundland Economic and Regional Development Agreement.

## INTRODUCTION

National Geochemical Reconnaissance (NGR) surveys in Labrador commenced in 1976 and by 1988 the entire land-mass of Labrador had been covered. In total, sediment and coincident water samples were collected from 18 000 lakes and 2500 streams (Fig. 1), at an average sample density of approximately 1 per 13 km<sup>2</sup>. These reconnaissance surveys were funded through a series of Mineral Development Agreements between the Governments of Canada and Newfoundland and Labrador. Under the present Canada-Newfoundland Cooperative Agreement on Mineral Development (1990-1994), a reanalysis program is being undertaken on the entire Labrador lake and stream sediment sample set to expand the element suite (Davenport et al., 1991).

Also under this agreement a detailed infill lake sediment and water survey was completed in the Florence Lake area (Fig. 1). This region was selected based on: its favourable mineral potential; interesting results from the original NGR surveys; discussions with Newfoundland Geological Survey personnel; and, the mineral industries interest in the area. Although the primary objective of the survey was to assist mineral exploration activity, additional sampling was undertaken to evaluate the use of lake waters in both mineral exploration and environmental studies. Therefore, in addition to routine NGR sediment and water samples (Friske and Hornbrook, 1991), waters were collected from selected sites for trace metal determination.



**Figure 1.** Map of Labrador showing distribution of lake and stream coverage as well as the Florence Lake survey area.

Data from the routine sediment and water samples have already been released (Friske et al., 1993). It is the purpose of this paper to present the lake water data and compare it to data from concomitant lake sediments. Several other hydrogeochemical surveys have also been carried out recently in Newfoundland to evaluate waters in terms of exploration and environmental applications (Finch et al., 1992; Hall, 1992).

## DESCRIPTION OF SURVEY AREA

The Florence Lake study area covers four 1:50 000 scale NTS map sheets (13K/6, 7, 10, 15), an area of approximately 3700 km<sup>2</sup>. Located 140 km north of Goose Bay, the area is accessible only by helicopter or float plane, with the exception of the extreme northeast which can be reached from the shores of Ugjoktok Bay. Physiography of the area varies from the flat string bogs to sediment choked valleys to the rugged rolling hills of the uplands. Elevations range from sea level to near 700 m, with local relief up to 300 m. Vegetation reflects the varied terrain: bogs in the wet poorly drained areas, spruce and lichen sporadically blanket the predominantly barren bedrock hills. The climate of the area can be described as having harsh winters with abundant snow accumulations, and short cool summers. The area lies within a region of discontinuous permafrost.

### Geological setting

The study area is underlain by Archean rocks of the Nain Province and Makkovik Subprovince, and Proterozoic rocks of the Grenville Province. Ryan (1984) has mapped the area in detail and the following description of the bedrock geology and mineralization comes largely from his report.

The Archean rocks are concentrated in the northern part of the study area and consist of amphibolites (Weekes Amphibolite, unit 1), quartzofeldspathic gneisses (Maggo Gneiss, unit 2), mafic metavolcanics (Florence Lake Group, unit 3), and granitoid rocks (Kanaiiktok Intrusive Suite, unit 4). Together these rocks are referred to as the Kanairiktok Valley Complex. Similar rocks (referred to as equivalents in the geological legend), which have undergone retrogressive metamorphism, occur in the Makkovik Subprovince portion of the study area and are referred to as the Kaipokok Valley Complex. Mineral exploration within the Archean terrain has been directed primarily at the supracrustal rocks of the Florence Lake group, which has base metal and asbestos occurrences, and a potential for PGEs (Wardle, 1987). Several uranium occurrences have been noted in the intrusives.

The Archean basement is overlain unconformably by Aphebian rocks of the Moran Lake Group. It consists of a sedimentary assemblage (Warren Creek Formation, unit 5), capped by mafic volcanic rocks (Joe Pond Formation, unit 6). The most significant mineralization in the Moran Lake Group is the base metal occurrences in the supracrustal rocks. These occur as syngenetic sulphide-rich lenses and beds, and to later crosscutting Pb and Zn veins.



**Table 1.** Variables determined and methods used for Florence Lake lake sediment and water samples.

LAKE SEDIMENT	LAKE WATER
Ag, Cd, Co*, Cu, Fe, Mn, Mo, Ni*, Pb, V, Zn (atomic absorption spectrometry)	pH (glass calomel electrode and pH meter)
F (ion selective electrode)	F (ion selective electrode)
As, Au, Ba, Br, Ce, Co, Cr, Cs, Eu, Fe*, Hf, La, Lu, Mo, Na, Ni, Rb, Sb, Sc, Sm, Ta, Tb, Th, U, W, Yb (instrumental neutron activation analysis)	Al, Cd, Ce, Co, Cu, Dy, Eu, Er, Fe, Gd, Ho, In, La, Lu, Mn, Nd, Ni, Pb, Pr, Sm, Tb, Ti, Tm, U*, V, Yb, Y, Zn (ion chromatography-inductively coupled plasma-mass spectrometry)
Hg (cold vapour extraction-atomic absorption spectrometry)	U (laser-induced fluorescence)
LOI (gravimetry)	

Four Helikian bedrock units occur in the study area. The oldest (Bruce River Group, units 7 and 8) is a sedimentary-volcanic package that unconformably overlies the Moran Lake Group. Numerous base metal and uranium occurrences have been discovered throughout the group.

The Bruce River Group is intruded by two groups of Helikian rocks, the Nipishish Lake Intrusive suite (unit 9) and the Michael Gabbro (unit 10). The Nipishish Lake Intrusive suite is monzonitic to granitic in composition, forming wide northeast-trending linear igneous bodies. Small disseminated molybdenite occurrences and small veins of purple fluorite are known to occur in this unit. The Michael Gabbro is a semicontinuous series of olivine gabbro dykes. No appreciable mineralization has been noted for this unit.

The Seal Lake Group is the youngest supracrustal sequence of the area. Four formations (units 11 to 15) make up the sequence of deformed sedimentary, volcanic and associated intrusive rocks. Although the Seal Lake Group is host to over 250 copper showings none occur within the study area.

### *Surficial geology*

The entire study area was last glaciated by the Wisconsin continental ice sheet during the Pleistocene. Glacial direction was predominantly from west to northeast, with local variations. Batterson et al. (1988) identified, in the Moran Lake area, an eastward directed flow overprinting the ubiquitous northeast flow direction. Bedrock dominates the upland areas. Generally thin and discontinuous tills are draped across the intermediate elevations. At lower elevations eskers, drumlinoid ridges, and tills are common and subparallel the bedrock ridges. Post glacial outwash plains dominate the lower elevations of the Kanairiktok and Kaipokok river valleys.

### METHODS

During the summer of 1992, lake sediment and water samples were collected from 404 sites as part of the Florence lake infill survey. In addition to the routine NGR water and sediment samples (refer to Friske and Hornbrook, 1991, for a detailed description of the NGR methodology), 131 lake-water samples

were collected using 250 mL Nalgene™ linear polyethylene bottles that were immersed 10-20 cm below the lake surface. Within 12 hours of collection, the samples were filtered using 0.45 µm filter paper and acidified with 2 mL of 8 M HNO<sub>3</sub> (pH <2).

Lake sediment and water field duplicate samples were collected at 24 sites. Before chemical analysis blind duplicate splits were prepared from 25 sediment and 9 water samples.

Sediment and water samples were analyzed for a wide range of variables by a number of different techniques, summarized in Table 1. All the data, except for variables determined by ICP-MS on the waters, have been released along with detailed descriptions of the analytical procedures (Friske et al., 1993).

Transition and rare earth elements in waters were determined by a method, recently developed by Hall and colleagues at the GSC, which is based upon automated preconcentration using a chelating resin of iminodiacetate functionality. The combination of a 10 times preconcentration factor (50 mL to 5 mL) and analysis by ICP-MS achieves detection limits in the ppt range for most elements. Generally limitations in low-level detection capability derive not from the sensitivity of ICP-MS, but from random contamination introduced during the processes of filtration, acidification and bottling.

### RESULTS

The main objective of this paper is to evaluate the relationship between trace element distributions in lake sediment and associated water. Therefore, although numerous variables were determined, the following discussion is restricted to elements that were determined in both media. A further restriction is that for an element to be considered, at least 50 per cent of the determinations in both media are greater than the detection limit. Based on these criteria the following discussion focuses on data for Cd, Ce, Co, Cu, F, Fe, La, Mn, Ni, Pb, Sm, Tb, U, V, and Zn. For variables determined by more than one method in a given medium, an asterisk distinguishes which data set was used (Table 1). For example, lake sediment Co data by AAS rather than INAA are used because of the superior detection limit by AAS.

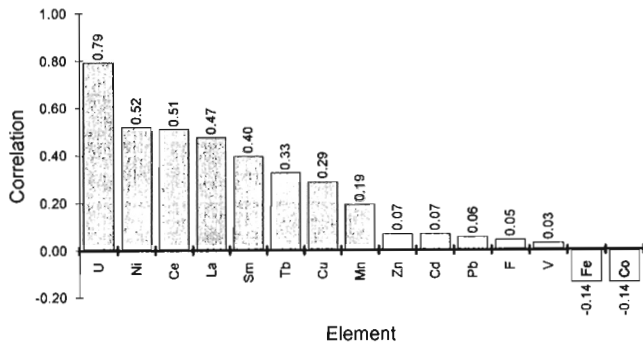


Figure 2. Summary of Pearson correlation coefficients between elements in lake sediment and water.

**Correlation of lake water and sediment data**

Pearson correlation coefficients were calculated as a first approach in evaluating whether there is a sympathetic relationship between element concentrations in lake sediment and lake water. The results are summarized in Figure 2. Values were calculated using log transformed data. The critical value for  $r$  at the 95% confidence level ( $N=131$ ) is 0.16. As shown in Figure 2, there is a significant correlation between U, Ni, Ce, La, Sm, Tb, Cu, and Mn in sediment and water, whereas Zn, Cd, Pb, F, V, Fe, and Co do not appear to have a sympathetic association. These relationships are corroborated by scatter plots, selected ones of which are shown in Figure 3. This figure also illustrates the importance of log transforming the data before calculating the correlation coefficients. The value of  $r$  for the raw Zn data is 0.36, which is clearly the effect of one or two "flyers".

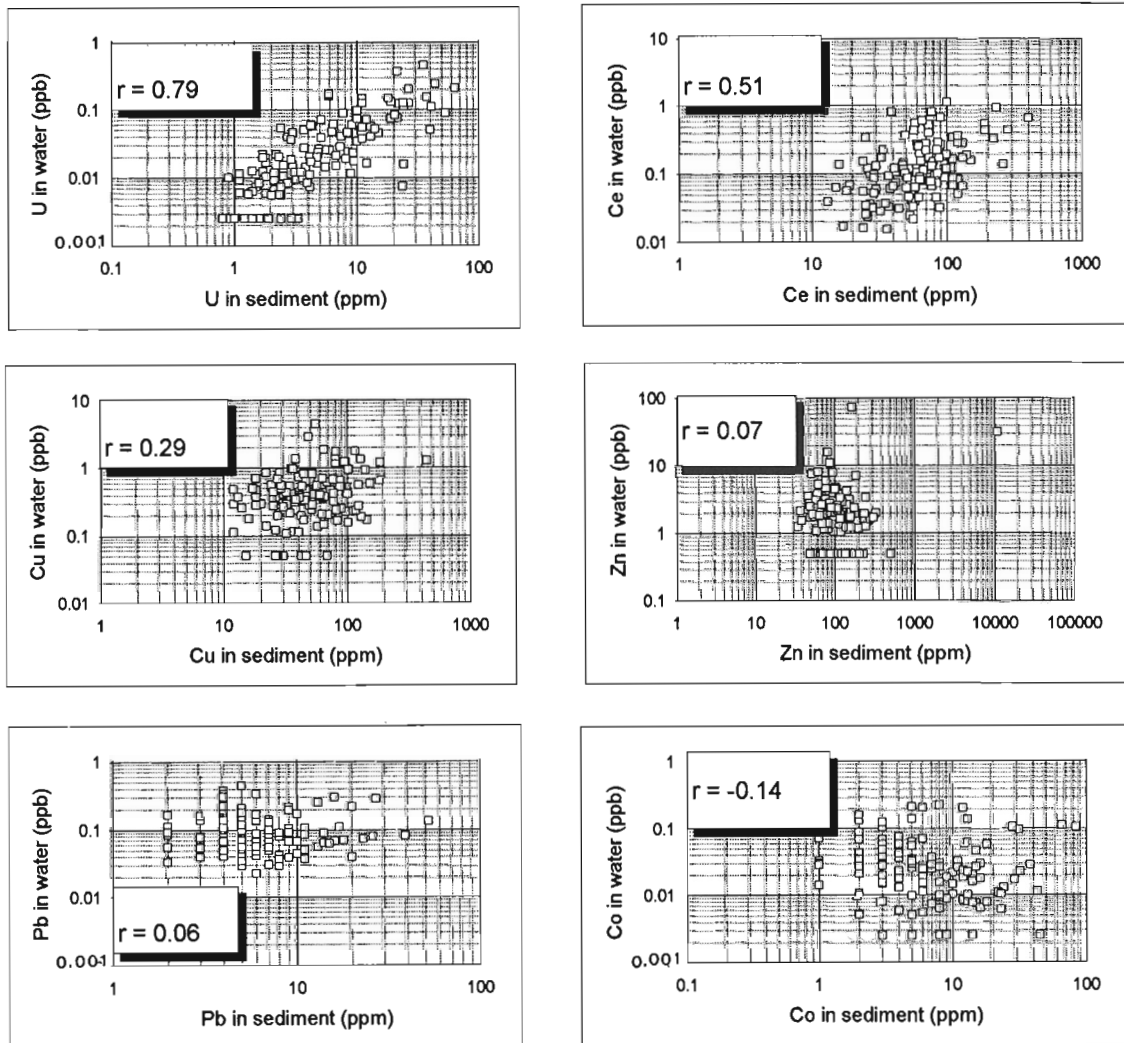


Figure 3. Scatter plots of selected elements in lake sediment and water.

Proportional circle plots were produced to evaluate the possibility that an element, although not correlating on a site basis, exhibits similar regional distribution patterns in lake sediment and water. To allow for direct visual comparison of an element in both media the raw data were normalized by converting them to percentiles. Therefore, regardless of data distribution, equivalent percentile values are represented by circles of equal size.

Figures 4 and 5 show the distribution of Zn and Co in sediment and water, superimposed on the bedrock geology. It is evident that these elements exhibit distinctly different patterns in the sediment and water media. Zn and Co in sediment display similar trends with elevated levels closely associated with areas underlain by mafic volcanics. In the study area there are three units (3, 6, and 12) dominated by mafic volcanics that are shaded to highlight their aerial distribution (Fig. 4 and 5).

The association of elevated Co in the sediment with mafic volcanics reflects elevated background levels of Co in mafic igneous rocks relative to most other lithologies. Cobalt concentrations in various rock types given by Kabata-Pendias and Pendias (1984) include: mafic igneous rocks, 35-50 ppm; felsic igneous rocks, 1-7 ppm; limestone, 0.4-1.0 ppm; sandstone, 0.3-10 ppm, and shale, 11-20 ppm. The distribution of Co in water, however, shows no obvious association with the bedrock geology.

Zn is not as strongly differentiated between the major rock types. Although there is some enrichment in the mafic volcanics relative to most other lithologies, the association of elevated Zn values (in lake sediment) with the mafic volcanics likely reflects a component related to mineralization. Batterson et al. (1988) indicated that base metal and precious metal showings are associated with volcanics of Moran Lake Group (unit 6), whereas within the Florence Lake Group (unit 3) asbestos and uranium showing and potential for PGEs are the main types of mineralization. Although elevated Zn levels occur over all three mafic units, the strongest signature is clearly over the area underlain by the Moran Lake Group rocks (unit 6). The distribution of Zn in water shows no obvious association with the bedrock geology.

### *Effect of data variability on observed relationships between sediment and water*

A cursory evaluation of the data indicated considerably more variability in the lake water data than in the sediment data for several elements. To confirm this and see what effect it might have on the observed relationship (correlation) between an element in sediment and water, closer examination was made of the variability of the total data sets as well as site and blind duplicate data. The site duplicates are two samples taken within a few metres of each other and are used to evaluate combined sampling and analytical variance (within-site variation). Blind duplicates represent laboratory splits of single samples and are used to evaluate analytical variance.

Variations were calculated based on the total data set and the site and blind duplicate pairs and are summarized in Table 2. Total data variability was determined by the usual statistical method. Variances for the field and blind duplicate pairs were calculated using the approach outlined by Garrett (1969, 1973);

$$S^2_{(SA \text{ or } A)} = \frac{1}{2N} \sum_{i=1}^N (X_{1i} - X_{2i})^2$$

where  $S^2$  is the variance of the field(SA) and blind(A) duplicate data

$X_{1i}$  is the logarithm of the first determination

$X_{2i}$  is the logarithm of the second determination

and N is the number of pairs.

As expected, the variance for a given element is greatest for the total data set, followed by the site duplicates (combined sampling and analytical variance) and blind duplicates (analytical variance).

<b>LEGEND (Figures 4 and 5)</b>	
<b>HELIKIAN</b>	
<i>Seal Lake Group (Units 11-15)</i>	
16	<i>Salmon Lake Formation: shale, basaltic flows, and diabase sills</i>
14	<i>Whiskey Lake Formation: shale, argillite, quartzite</i>
13	<i>Wuchusk Lake Formation: quartzite, shale, chert, limestone, minor diabase and gabbro sills</i>
12	<i>Bessie Lake Formation: amygdaloidal and vesicular basalt (12); quartzite, arkose, and conglomerate (11)</i>
11	
10	<i>Michael Gabbro: olivine gabbro, metagabbro</i>
9	<i>Nipishish Lake Intrusive Suite: granites, granodiorite, diorite, monzonite</i>
<i>Bruce River Group (Units 7-8)</i>	
8	<i>rhyolite to andesitic volcanic rocks, minor basalt</i>
7	<i>volcaniclastics, metasediments, conglomerates, sandstone, mudstone</i>
<b>APHEBIAN</b>	
<i>Moran Lake Group (Units 5-6)</i>	
6	<i>Joe Pond Formation: massive and pillowed basalt, pillow breccia, tuff, dolostone, and chert</i>
5	<i>Warren Creek Formation: mudstone, slate, siltstone, sandstone, limestone, dolostone, and chert</i>
<b>ARCHEAN</b>	
<i>Kanairiktok and Kaipokok Valley Complexes (Units 1-4)</i>	
4	<i>Kanairiktok Intrusive Suite and equivalents: granite, granodiorite, and tonalite</i>
3	<i>Florence Lake Group and equivalents: mafic volcanics and volcaniclastics</i>
2	<i>Maggo Gneiss and equivalents: layered quartzofeldspathic gneiss</i>
1	<i>Weekes Amphibolite and equivalents: layered amphibolite</i>

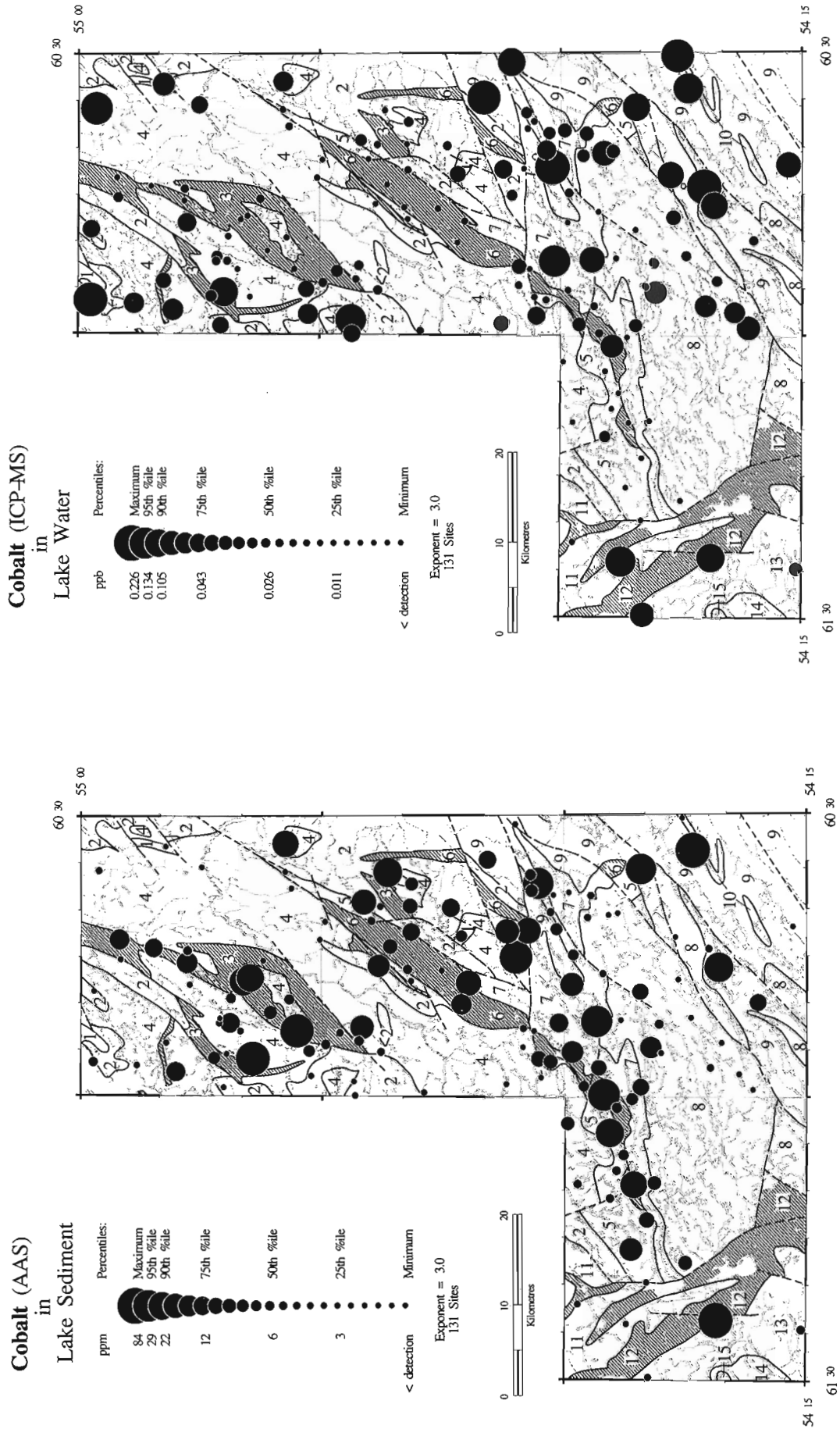


Figure 4. Proportional circle plots of cobalt in lake sediment and lake water. Raw data normalized to percentiles for plotting purposes. Units dominated by mafic volcanics (3, 6, and 12) are shaded to highlight their distribution.

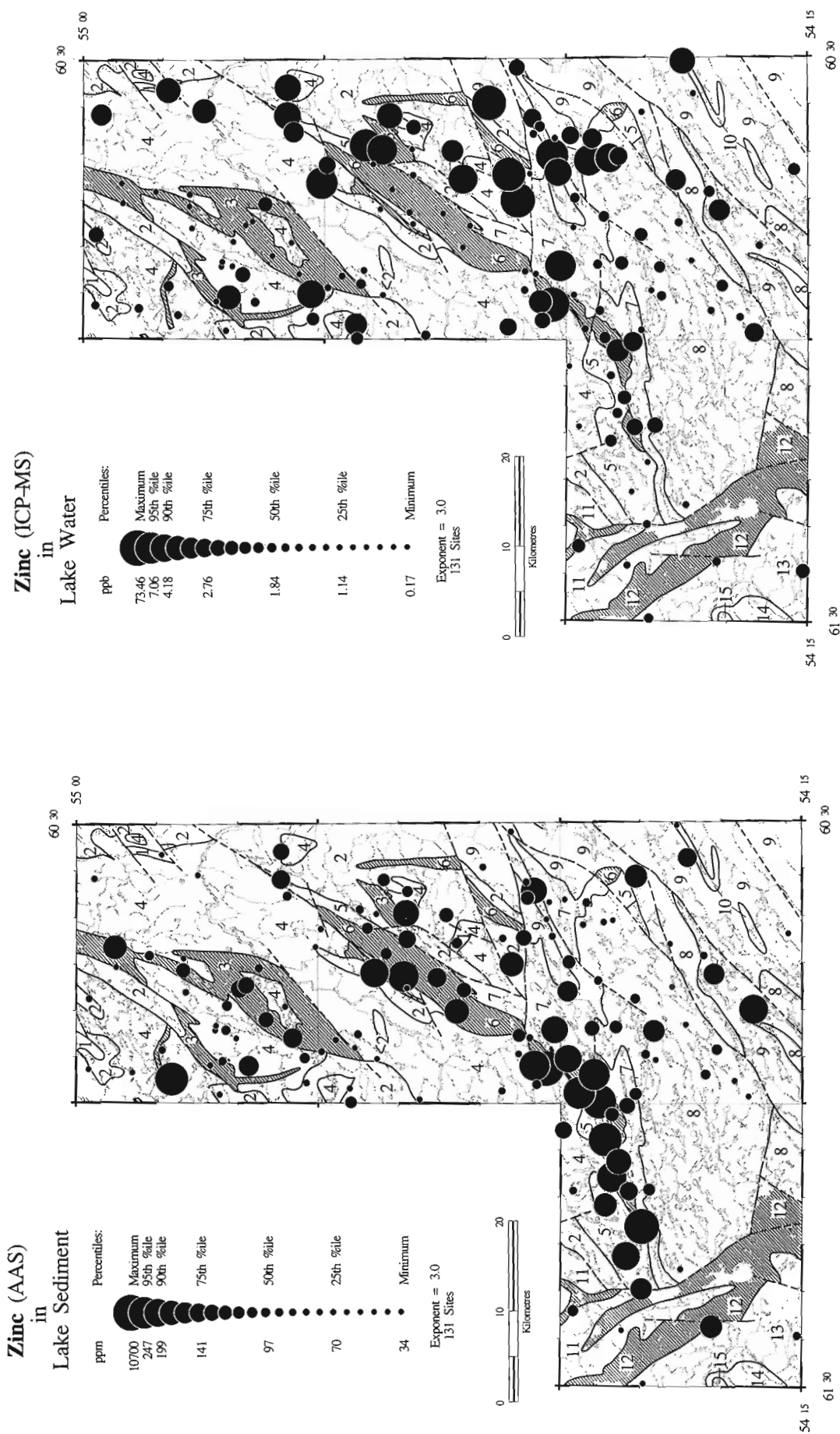
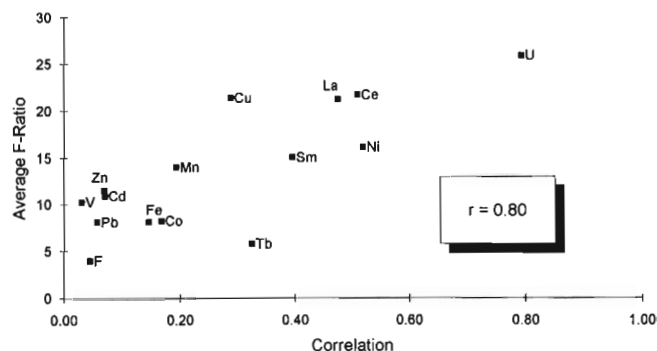


Figure 5. Proportional circle plots of zinc in lake sediment and lake water. Raw data normalized to percentiles for plotting purposes. Units dominated by mafic volcanics (3, 6, and 12) are shaded to highlight their distribution.

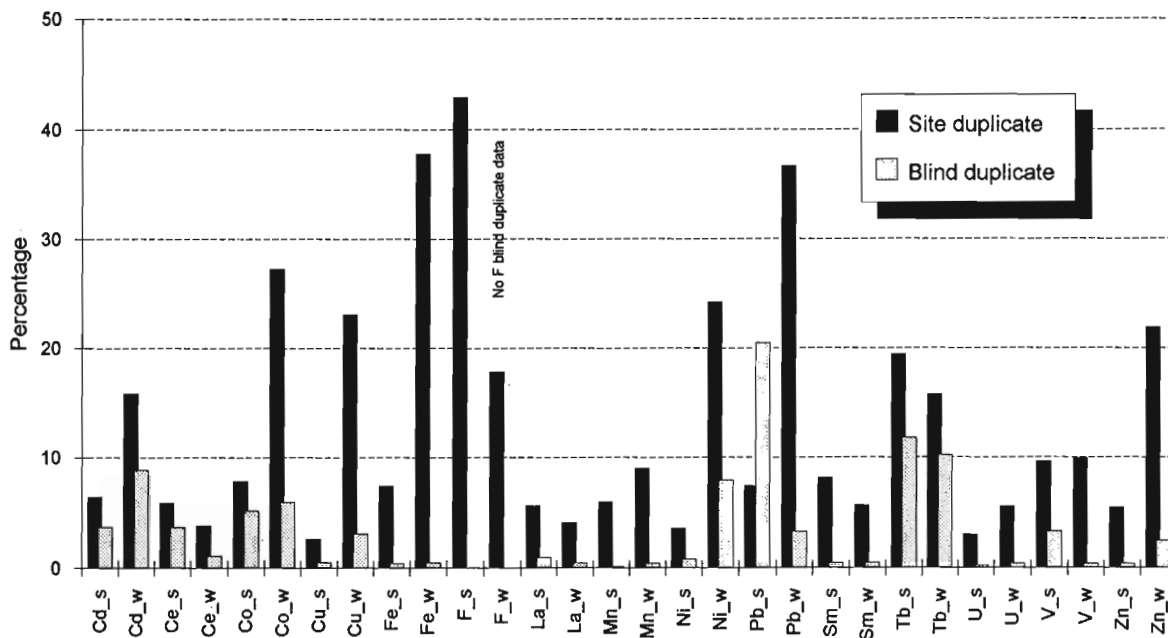
**Table 2.** Summary of variance for total, site and blind duplicate data.

Variable	Variance			F-Ratio $F = S^2_T / S^2_{SA}$
	Total Data $S^2_T$	Site Duplicate $S^2_{SA}$	Blind Duplicate $S^2_A$	
Cd_s	0.1545	0.0099	0.00571	15.6
Cd_w	0.1758	0.0279	0.01554	6.3
Ce_s	0.0752	0.0044	0.00276	17.0
Ce_w	0.1598	0.0061	0.00172	26.4
Co_s	0.1639	0.0128	0.00843	12.8
Co_w	0.2162	0.0589	0.01276	3.7
Cu_s	0.0815	0.0021	0.00040	38.4
Cu_w	0.1291	0.0297	0.00396	4.3
Fe_s	0.1951	0.0144	0.00080	13.6
Fe_w	0.1357	0.0514	0.00062	2.6
F_s	0.0518	0.0222	-	2.3
F_w	0.0132	0.0024	-	5.6
La_s	0.0582	0.0033	0.00055	17.9
La_w	0.1161	0.0047	0.00051	24.6
Mn_s	0.3594	0.0214	0.00050	16.8
Mn_w	0.2341	0.0210	0.00092	11.2
Ni_s	0.0842	0.0030	0.00067	28.0
Ni_w	0.1189	0.0288	0.00943	4.1
Pb_s	0.0691	0.0051	0.01417	13.5
Pb_w	0.0909	0.0333	0.00297	2.7
Sm_s	0.0499	0.0040	0.00023	12.3
Sm_w	0.1054	0.0059	0.00048	17.7
Tb_s	0.0744	0.0144	0.00878	5.2
Tb_w	0.1126	0.0177	0.01150	6.3
U_s	0.2088	0.0062	0.00045	33.6
U_w	0.2977	0.0164	0.00107	18.2
V_s	0.0459	0.0044	0.00150	10.4
V_w	0.1293	0.0128	0.00047	10.1
Zn_s	0.0780	0.0042	0.00029	18.4
Zn_w	0.1694	0.0370	0.00415	4.6

Also listed in Table 2 are the ratios of the total variance to the site variance (F-ratio). Garrett (1969, 1973) considered the relationship of these two variances and argued that the total variance (between-site variance) should be significantly greater than the site variance (combined within-site and analytical) if the data are to show clear spatial patterns. A similar approach was used by Davenport (1990) to evaluate the quality of regional lake sediment data from Newfoundland.



**Figure 6.** Scatter plot of average F-ratio versus correlation coefficient for an element in sediment and water.



**Figure 7.** Ratio (expressed as a percentage) of site and blind duplicate variance to total variance.



**Table 3.** Ratio of 50th percentile to detection limit for variables in water and sediment.

Variable	Units	D.L.	Values >D.L.	50th %tile	Ratio: 50th/D.L.
Cd_s	ppm	0.2	83%	0.5	2.5
Cd_w	ppb	0.01	81%	0.03	3.0
Ce_s	ppm	5.0	100%	63.0	12.6
Ce_w	ppb	0.01	100%	0.12	12.0
Co_s	ppm	2.0	83%	6.0	3.0
Co_w	ppb	0.005	92%	0.026	5.2
Cu_s	ppm	2.0	100%	44.0	22.0
Cu_w	ppb	0.1	89%	0.39	3.9
Fe_s	pct	0.2	99%	2.0	10.0
Fe_w	ppb	10.0	91%	30.6	3.1
F_s	ppm	40.0	96%	110.0	2.8
F_w	ppb	20.0	57%	30.0	1.5
La_s	ppm	2.0	100%	37.0	18.5
La_w	ppb	0.01	98%	0.09	9.0
Mn_s	ppm	5.0	100%	208	41.6
Mn_w	ppb	1.0	64%	2.2	2.2
Ni_s	ppm	2.0	100%	16.0	8.0
Ni_w	ppb	0.1	56%	0.16	1.6
Pb_s	ppm	2.0	95%	5.0	2.5
Pb_w	ppb	0.02	97%	0.08	4.0
Sm_s	ppm	0.1	100%	5.5	55.0
Sm_w	ppb	0.005	92%	0.015	3.0
Tb_s	ppm	0.5	67%	0.7	1.4
Tb_w	ppb	0.001	69%	0.002	2.0
U_s	ppm	0.2	100%	4.2	21.0
U_w	ppb	0.005	89%	0.02	4.0
V_s	ppm	5.0	100%	29.0	5.8
V_w	ppb	0.01	97%	0.06	6.0
Zn_s	ppm	2.0	100%	97.0	48.5
Zn_w	ppb	1.0	77%	1.8	1.8

A number of features of the F-ratio values are worth noting. On average, the between-site to within-site variation (F-ratio) is significantly greater for sediments compared to waters (average sediment F-ratio = 17.1; average water F-ratio = 9.6). There is also a clear association between the correlation coefficient of an element in sediment and water and the average F-ratio for the element in both media. Figure 6 shows the strong positive correlation ( $r=0.80$ ) between these two parameters. This suggests that the lack of correlation for some variables may be related to high within-site variability relative to overall variability. This would most likely be the case for Co, Pb, Fe, and F, which have the 4 lowest F-ratios (Table 2): Co, Pb, and Fe in the water data and F in the sediment data.

To make a more meaningful comparison of sediment and water data for some elements it is evident that a higher between-site (total variance) to within-site variance is required, particularly for the water data. To see where improvements might be made, Figure 7 shows the ratio (expressed as a percentage) of site duplicate and blind duplicate variance to total variance. Co, Cu, Fe, Pb, and Zn in water show considerable combined site and analytical variation (up to almost 40% of total variance) but relatively small analytical variation. Therefore, for these elements, sample collection

procedures need to be re-evaluated in order to identify the sources of the variability and thereby reduce them. Where analytical variability is relatively high, as indicated by the blind duplicate variance, concentrations measured are often close to the method's detection limit. For example, the data in Table 3 reveal that the ratio of the 50th percentile concentration to the detection limit is 3 or less for the following parameters which have relatively high blind duplicate variance: Cd, Ni and Tb in water; and Pb and Tb in sediment. Lowering the detection limits for these variables will likely reduce the blind duplicate variability and therefore the within-site variance.

## SUMMARY

Results of this study indicate that there is a significant correlation in the distribution of a number of elements in lake sediment and water. Of the 15 elements considered U, Ni, Ce, La, Sm, Tb, Cu, and Mn exhibit some degree of association. Zn, Cd, Pb, F, V, Fe, and Co do not appear to have a sympathetic relationship based on the available data. Plots of the sediment and water data indicate that, for those elements which do not correlate, the distribution of the sediment data is closely related to chemical composition of the underlying bedrock, whereas the water data show no obvious association.

Evaluation of the variance of the total data sets as well as site and blind duplicate data suggests that the lack of correlation for some elements may be related to relatively high within-site variability. This is particularly the case for the water data, where collection procedures need to be re-evaluated in order to identify, and if possible reduce, the source(s) of variability. The result could be an overall increase in the association between sediment and water data, some of which may presently be obscured due to erratic water data.

One implication of the observed correlation of some variables in sediment and water is the potential value of the NGR data in terms of environmental and public health concerns. Over one million square kilometres of Canada have been covered by lake surveys (plus an additional 0.9 million km<sup>2</sup> by stream surveys), sediments from which have been analyzed for up to 40 elements. When properly interpreted these data may be useful in outlining areas in which significantly elevated concentrations of elements occur in the surface waters, which in one form or another may be used for domestic needs.

## ACKNOWLEDGMENTS

The authors wish to thank John McConnell, of the Newfoundland Geological Survey, and his summer field crew for their assistance with logistics and collection of the samples. Chris Durham of the GSC is also thanked for his assistance in the field. Thanks to Martin McCurdy who helped prepare some of the figures and tables.

---

## REFERENCES

---

**Batterson, M., Simpson, A., and Scott, S.**

1988: Quaternary mapping and drift exploration in the Central Mineral Belt (13K/7 and 13K/10), Labrador; Newfoundland Department of Mines, Mineral Development Division, Report 88-1, p. 331-341.

**Davenport, P.H.**

1990: Techniques to determine the quality of geochemical data: examples from regional lake sediment geochemical surveys in Newfoundland; Newfoundland Department of Mines and Energy, Geological Survey Branch, Report 90-1, p. 95-105.

**Davenport, P.H., Friske, P.W.B., Hornbrook, E.H.W., and Nolan, L.W.**

1991: Geochemical mapping of Newfoundland and Labrador: Progress for 1991; Government of Newfoundland and Labrador, Department of Mines and Energy, Report of Activities 1991, p. 49-52.

**Finch, C., Hall, G., and McConnell, J.**

1992: The development and application of geochemical analyses of water; Newfoundland Department of Mines and Energy, Geological Survey Branch, Report 92-1, p. 297-307.

**Friske, P.W.B. and Hornbrook, E.H.W.**

1991: Canada's National Geochemical Reconnaissance programme; Transactions of the Institution of Mining and Metallurgy, Section B; Volume 100, p.47-56.

**Friske, P.W.B., McCurdy, M.W., Gross, H., Day, S.J., Lynch, J.J., and Durham, C.C.**

1993: Lake sediment and water geochemical infill survey data, Province of Newfoundland (Labrador) (NTS 13K/6, 13K/7, 13K/10, and 13K/15); Geological Survey of Canada Open File 2650; 44 maps, 90 p.

**Garrett, R.G.**

1969: The determination of sampling and analytical errors in exploration geochemistry; *Economic Geology*, v. 64, p. 568-569.

1973: The determination of sampling and analytical errors in exploration geochemistry—a reply; *Economic Geology*, v. 68, no. 2, p. 282-283.

**Hall, G.E.M.**

1992: Hydrogeochemical exploration in the Baie Verte area, Newfoundland; in Report of Activities 1992; Newfoundland Department of Mines and Energy, p. 53-54.

**Kabata-Pendias, A. and Pendias, H.**

1984: Trace elements in soils and plants; CRC Press Inc., Boca Raton, Florida, 315 p.

**Ryan, A.B.**

1984: Regional geology of the central part of the Central Mineral Belt, Labrador; Newfoundland Department of Mines and Energy, Mineral Development Division, Memoir 3, 185 p.

**Wardle, R.J.**

1987: Platinum-group-element potential in Labrador; in Current Research (1987); Newfoundland Department of Mines and Energy, Report 87-1, p. 211-223

---

Geological Survey of Canada Project 850047

## AUTHOR INDEX

Ansdell, K.M. . . . .	183, 193	Lucas, S.B. . . . .	215
Armitage, A.E. . . . .	147	MacRae, N.D. . . . .	147
Aspler, L.B. . . . .	165	Madore, L. . . . .	355
Balog, M.J. . . . .	135	McMartin, I. . . . .	175
Barham, B.A. . . . .	135	Mengel, F.C. . . . .	321
Beaumont-Smith, C. . . . .	91	Miller, A.R. . . . .	135, 147
Berclaz, A. . . . .	13	Morin, D. . . . .	355
Born, P. . . . .	157	Murton, J.B. . . . .	249
Broome, J. . . . .	215	Mwenifumbo, C.J. . . . .	279
Campbell, L.M. . . . .	321	Ozarko, D.L. . . . .	165
Card, K.D. . . . .	269	Pehrsson, S.J. . . . .	91
Ciesielski, A. . . . .	343	Percival, J.A. . . . .	311
Chiarenzelli, J.R. . . . .	165	Peterson, T.D. . . . .	157
Chouinard, A. . . . .	49	Peterson, V.L. . . . .	225, 237
Connors, K.A. . . . .	183, 193	Pflug, K.A. . . . .	279
Corriveau, L. . . . .	355	Pilote, P. . . . .	303
Daigneault, R. . . . .	303	Poulsen, K.H. . . . .	103
Davidson, A. . . . .	1	Powis, K.B. . . . .	165
Day, S.J.A. . . . .	367	Rainbird, R.H. . . . .	61
Dredge, L.A. . . . .	33	Reading, K.L. . . . .	135
Duquette, D. . . . .	13	Reid, L. . . . .	321
Elliott, C.G. . . . .	113	Relf, C. . . . .	49
Friske, P.W.B. . . . .	367	Ritts, B.D. . . . .	39
Graham, D.F. . . . .	343	Robert, F. . . . .	103, 287, 295, 303
Grant, J.W. . . . .	13	Ross, D. . . . .	1
Hall, G.E.M. . . . .	367	Sanborn-Barrie, M. . . . .	121
Hamilton, M.A. . . . .	333	Sandeman, H. . . . .	49
Heather, K.B. . . . .	259	Scott, R.G. . . . .	215
Henderson, J.B. . . . .	71	Sinclair, W.D. . . . .	303
Henderson, J.R. . . . .	81	Skulski, T. . . . .	311
Henderson, M.N. . . . .	81	Stern, R.A. . . . .	311
Henderson, P.J. . . . .	205	Thompson, P.H. . . . .	1
Hildebrand, R.S. . . . .	61	van Breemen, O. . . . .	225, 259
Hrabi, R.B. . . . .	13	Van Kranendonk, M.J. . . . .	321
Jefferson, C.W. . . . .	61	Viljoen, D. . . . .	215
Kerr, D.E. . . . .	33	Villeneuve, M.E. . . . .	13, 49
Kerswill, J.A. . . . .	81	Ward, B.C. . . . .	33
Kettles, I.M. . . . .	249	Wardle, R.J. . . . .	321
Killeen, P.G. . . . .	279	Worth, J.K. . . . .	61
Kirkham, R.V. . . . .	303	Wyllie, R.J.S. . . . .	23
Kjarsgaard, B.A. . . . .	23	Zaleski, E. . . . .	225, 237
Leclair, A.D. . . . .	215		



## **NOTE TO CONTRIBUTORS**

Submissions to the Discussion section of Current Research are welcome from both the staff of the Geological Survey of Canada and from the public. Discussions are limited to 6 double-spaced typewritten pages (about 1500 words) and are subject to review by the Chief Scientific Editor. Discussions are restricted to the scientific content of Geological Survey reports. General discussions concerning sector or government policy will not be accepted. All manuscripts must be computer word-processed on an IBM compatible system and must be submitted with a diskette using WordPerfect 5.0 or 5.1. Illustrations will be accepted only if, in the opinion of the editor, they are considered essential. In any case no redrafting will be undertaken and reproducible copy must accompany the original submissions. Discussion is limited to recent reports (not more than 2 years old) and may be in either English or French. Every effort is made to include both Discussion and Reply in the same issue. Current Research is published in January and July. Submissions should be sent to the Chief Scientific Editor, Geological Survey of Canada, 601 Booth Street, Ottawa, Canada, K1A 0E8.

## **AVIS AUX AUTEURS D'ARTICLES**

Nous encourageons tant le personnel de la Commission géologique que le grand public à nous faire parvenir des articles destinés à la section discussion de la publication Recherches en cours. Le texte doit comprendre au plus six pages dactylographiées à double interligne (environ 1500 mots), texte qui peut faire l'objet d'un réexamen par le rédacteur scientifique en chef. Les discussions doivent se limiter au contenu scientifique des rapports de la Commission géologique. Les discussions générales sur le Secteur ou les politiques gouvernementales ne seront pas acceptées. Le texte doit être soumis à un traitement de texte informatisé par un système IBM compatible et enregistré sur disquette WordPerfect 5.0 ou 5.1. Les illustrations ne seront acceptées que dans la mesure où, selon l'opinion du rédacteur, elles seront considérées comme essentielles. Aucune retouche ne sera faite au texte et dans tous les cas, une copie qui puisse être reproduite doit accompagner le texte original. Les discussions en français ou en anglais doivent se limiter aux rapports récents (au plus de 2 ans). On s'efforcera de faire coïncider les articles destinés aux rubriques discussions et réponses dans le même numéro. La publication Recherches en cours paraît en janvier et en juillet. Les articles doivent être envoyés au rédacteur en chef scientifique, Commission géologique du Canada, 601, rue Booth, Ottawa, Canada, K1A 0E8.



Geological Survey of Canada Current Research, is released twice a year, in January and July. The four parts published in January 1994 (Current Research 1994- A to D) are listed below and can be purchased separately.

Recherches en cours, une publication de la Commission géologique du Canada, est publiée deux fois par année, en janvier et en juillet. Les quatre parties publiées en janvier 1994 (Recherches en cours 1994-A à D) sont énumérées ci-dessous et sont vendues séparément.

Part A: Cordillera and Pacific Margin  
Partie A : Cordillère et marge du Pacifique

Part B: Interior Plains and Arctic Canada  
Partie B : Plaines intérieures et région arctique du Canada

Part C: Canadian Shield  
Partie C : Bouclier canadien

Part D: Eastern Canada and national and general programs  
Partie D : Est du Canada et programmes nationaux et généraux